TN
1
A5
Vol. 193
NIC

TRANSACTIONS

OF THE

AMERICAN INSTITUTE OF MINING AND METALLURGICAL ENGINEERS

(INCORPORATED)

American Institute of Mining, Metallurgical, and Petroleum Engineers,

Volume 193

MINING BRANCH

1952

Metal Mining, Minerals Beneficiation, Coal,
Industrial Minerals, Geology,
Mineral Industry Education,
Geophysics

THIS VOLUME IS MADE UP OF PAPERS AND DISCUSSIONS PRESENTED AT MEETINGS HELD AT CLEVELAND, OCT. 24-25, 1950; ST. LOUIS, FEB. 19-22, 1951; MEXICO CITY, OCT. 29-NOV. 4, 1951; NEW YORK, FEB. 18-21, 1952; LOS ANGELES, FEB. 16-19, 1953.

PUBLISHED BY THE INSTITUTE
AT THE OFFICE OF THE SECRETARY
29 WEST 39TH STREET
NEW YORK 18, N. Y.

COPYRIGHT, 1953, BY THE
AMERICAN INSTITUTE OF MINING AND METALLURGICAL ENGINEERS
(INCORPORATED)

PRINTED IN THE UNITED STATES OF AMERICA

FOREWORD

The Mining Branch of the American Institute of Mining and Metallurgical Engineers presents in this volume a collection of eighty-two technical papers and discussions prepared under the auspices of the Coal Division, the Industrial Minerals Division, the Minerals Beneficiation Division, and the Mining, Geology, and Geophysics Division, which together comprise the Mining Branch of the Institute. Included also is a paper classified for the Mineral Education Division.

The papers deal with subjects pertinent to these professional fields, and it is obvious from the Table of Contents that those engaged in the arts and sciences combining to give to humanity the all-important metal and mineral products represent a widely diverse and complex collection of separate skills and interests. But these people are nevertheless closely knit together by their unity of purpose, and there is much interrelation and overlapping of interests. The subject matter of some of the papers of this volume is, accordingly, of equal interest to several of the separate professional groups represented by the Divisions of the Mining Branch, and such papers have been listed in the Table of Contents under more than one of the divisional headings.

For the convenience of those readers who are interested also in the related subjects of Extractive Metallurgy, a list is appended to the Table of Contents giving the titles of papers published in the contemporary Transactions, Vol. 194, of the Metals Division.

To the authors of the papers we give our thanks for taking the time and effort to put on paper their ideas and the fruits of their experience, work, and researches, so that we may learn and profit therefrom. Thanks are likewise due the Chairmen of each of the various Divisions, the Chairmen of the Auxiliary Papers and Publications Committees, and members of the many technical committees of the Divisions, all of whom have labored hard and unselfishly to collect and process these papers.

The thoughtful reader will surely be benefited in good measure from this work, and it is hoped that he may in return contribute of his knowledge and skill to future Transactions for the benefit of others.

Raymond E. Byler, *Chairman*
Mining Branch Council

CONTENTS

Mining Engineering was paged consecutively throughout 1952. Thus, in this volume of the Mining Transactions there are 11 interruptions in the pagination. The missing pages appeared in Mining Engineering. This volume consists of all the Mining Transactions for 1952.

Metal Mining

Illinois Operations of the Eagle Picher Mining and Smelting Co. By C. O. Dale and W. J. Rundle 72
Diamond Orientation in Drill Bits. By E. P. Pfleider 177
Underground Mining Trends in the Great Swedish Export Iron Ore Mines. By Borje Hjortzberg-Nordlund 187
Pipeline Transportation of Phosphate. By I. S. Tillotson, R. B. Burt, and James A. Barr 273
Discussion 1066
Primary Blasting Practice at Chuquicamata. By Glenn S. Wyman 300
Mining Operations at the Teniente Mine of the Braden Copper Company, Rancagua, Chile. By F. E. Turton 573
Prospecting the Piceance Creek Basin for Oil Shale. By Tell Ertl 601
Deep Hole Prospect Drilling at Miami, Tiger, and San Manuel, Arizona. By E. F. Reed 682
Ore Control Methods at Inspiration Consolidated Copper Company. By J. L. Carne 685
The Development of a Mining Operation from Diamond Drill Data. By George C. Lipsey 784
The Mobile Drill Unit in Use at the Utah Copper Pit. By L. F. Pett and L. E. Snow 799
Cementing in Deep Diamond Drill Holes. By Adrian E. Ross 1061

Minerals Beneficiation

Control of Conveyor Belt Acceleration. By J. W. Snavely 49
Manganese Extraction by Carbamate Solutions and the Chemistry of New Manganese-Ammonia Complexes. By Reginald S. Dean 55
Super High Intensity Magnetic Equipment for Protecting Conveyors. By R. L. Manegold 61
Adsorption on Quartz, From an Aqueous Solution, of Barium and Laurate Ions. By A. M. Gaudin and C. S. Chang 193
Contact Angles and Surface Coverage. By W. Philippoff, S. R. B. Cooke, and Donald E. Cadwell 283
Solid Surface Energy and Calorimetric Determinations of Surface-Energy Relationships for Some Common Minerals. By A. Kenneth Schellinger 369
Radiotracer Studies of the Action of Dithiophosphate in the Selective Flotation of Galena and Sphalerite Using $CuSO_4$ and NaCN. By C. M. Judson, A. A. Lerew, R. B. Booth, J. S. Kennedy, and G. L. Simard 375
Some Dynamic Phenomena in Flotation. By W. Philippoff 386
The Third Theory of Comminution. By Fred C. Bond 484
Discussion 1071
Deleading Zinc Concentrate at the Parral and Santa Barbara Mills. By C. L. Boeke and G. G. Gunther 495
Discussion 1067
Screened Ore Used for Fine Grinding at Lake Shore Mines. By Bunting S. Crocker 499
Discussion 1069
Adsorption of Sodium Ion on Quartz. By A. M. Gaudin, H. R. Spedden, and P. A. Laxen 693
The Effect of Certain Starches on Quartz and Hematite Suspensions. By Strathmore R. B. Cooke, Norman F. Schulz, and Emert W. Lindroos 697
Measurement and Evaluation of the Rate of Flotation as A Function of Particle Size. By T. M. Morris 794
Photoelectric Sorting of Optical Fluorspar. By W. T. Turrall and D. Porter 803
Glass and Chemical Sand Manufacture in the Edwards Paddle Scrubber. By Will Mitchell, Jr., T. G. Kirkland, and R. C. Edwards 875
Factors in the Economics of Heat-Treated Taconites. By Will Mitchell, Jr., C. L. Sollenberger, and Ford F. Miskell 962
Microstructures in Iron Ore Pellets. By Strathmore R. B. Cooke and Thomas E. Ban 1053
Magnetic Roasting of Lean Ores. By Fred D. DeVaney ....
The Effect of Heat Treatment and Certain Additives on the Strength of Fired Magnetic Pellets. By Strathmore R. B. Cooke and William F. Stowasser, Jr. ....
Effects of Alkalinity on the Flotation of Lead Minerals. By Marston G. Fleming ....

Coal

Frothing Characteristics of Pine Oils in Flotation. By Shiou-Chuan Sun 65
Supplement 1082
Recent Coal Geology Research. By Aureal T. Cross 202
Development of the Disco Process of Low Temperature Carbonization. By C. E. Lesher 287
Chemicals from Coal Hydrogenation. By E. E. Donath 381
Thermal Metamorphism and Ground Water Alteration of Coking Coal Near Paonia, Colorado. By Vard H. Johnson 391
Power Facilities at a Modern Anthracite Open-Pit Mine. By Frederick C. Pearson, Albert Brown, and Emil R. Ermert 578
Experiments with an Underground Auger. By J. P. Newell and R. W. Storey 677
High-Efficiency Desliming by Use of Hydraulic Water Additions to the Liquid-Solid Cyclone. By D. A. Dahlstrom 788
Drilling and Blasting Methods in Anthracite Open-Pit Mines. By R. L. Ash, R. D. Boddorff, C. T. Butler, and W. W. Kay 884
Drainage Behavior and Water Retention Properties of Fine Coal. By D. W. Gillmore and C. C. Wright 886
Comparative Effectiveness of Coal Cleaning Equipment by Orville R. Lyons 895
Discussion 1080
Application of Coarse Coal Magnetite Separators in an Existing Circuit. By V. D. Hanson, W. K. Heinlein, and J. M. Vonfeld 983
The Preparation of Low-Ash Coal. By Adam L. Wesner and A. C. Richardson 1059
Theory, Scale-Up, and Operating Variables of the Peterson Top Feed Reservoir. By R. J. Piros, R. A. Brusenback, and D. A. Dahlstrom .....

Industrial Minerals

Dimension Stone in Minnesota. By G. M. Schwartz and G. A. Thiel 77
Pipeline Transportation of Phosphate. By I. S. Tillotson, R. B. Burt, and J. A. Barr 273
Discussion 1066
Saskatchewan's Industrial Minerals. By A. J. Williams 396
Development and Operation of Sulphur Deposits in the Louisiana Marshes. By Z. W. Bartlett, C. O. Lee, and R. H. Feierabend 775
Glass and Chemical Sand Manufacture in the Edwards Paddle Scrubber. By Will Mitchell, Jr., T. G. Kirkland, and R. C. Edwards 875
Solids Fluidization Applied to Lime Burning. By F. S. White and E. L. Kinsella 903
Economic Aspects of Sulphuric Acid Manufacture. By William P. Jones 957
The Cement Industry of Mexico. By Luis Elek 960
Titanium Dioxide Analysis of MacIntyre Ore by Specific Gravity. By Alan Stanley 971
Periclase Refractories in Rotary Kilns. By Leslie W. Austen 980
Features Incorporated in the Design of Lone Star's Two New Dry Process Cement Plants. By Claiborne C. Van Zandt .....

Geology

Geology of the Hayden Creek Lead Mine. By Ernest L. Ohle 477
Geology of the Silver-Lead-Zinc Deposits of the Avalos-Providencia District of Mexico. By W. H. Triplett 583
Discussion 1083
The Surface Expression of Veins in the Pachuca Silver District of Mexico. By C. L. Thornburg 594
Deep Hole Prospect Drilling at Miami, Tiger, and San Manuel, Arizona. By E. F. Reed 682
Geologic Setting of the Copper-Nickel Prospect in the Duluth Gabbro Near Ely, Minnesota. By G. M. Schwartz and D. M. Davidson 699

Mineral Industry Education

The Training of a Geophysical Engineer. By J. B. Macelwane, S.J. 969

Geophysics

Determination of the Temperature and Pressure of Formation of Minerals by the Decrepitometric Method. By F. Gordon Smith 703
Variation of Thermo-Electric Properties of Pyrite in Association with Gold Ore. By A. D. Mutch 880
The Training of a Geophysical Engineer. By J. B. Macelwane, S.J. 969
Gravity Investigations in the Iron River-Crystal Falls Mining District of Michigan. By L. O. Bacon and D. O. Wyble 973

Technical Note
Coal

The Tromp Heavy Media Process. By John Griffen 967

Discussion of Papers Published Prior to 1952

Jaw Crusher Capacities, Blake and Single-Toggle or Overhead Eccentric Types. Author's Supplement. By D. H. Gieskieng. (1951) **190**, p. 971 1069
Flotation Rates and Flotation Efficiency. By Nathaniel Arbiter. (1951) **190**, p. 791 1074
The Formation of Acid Mine Drainage. By K. L. Temple and Arthur R. Colmer. (1951) **190**, p. 1090 1075
Filter Cake Size-Consist and Moisture Relationships. By O. R. Lyons. (1951) **190**, p. 868 1078
Using Electric Furnaces and Heaters to Determine the Free Swelling Index of Coal. By E. Swartzman and G. C. Behnke. (1951) **190**, p. 871 1081

Extractive Metallurgy

As many members of the Mining Branch are interested in the papers of the Extractive Metallurgy Division, the titles of the papers published for that Division in 1952 are listed below. These papers, and discussion, appear in Transactions (1952) **194**, Metals Branch.

Heats of Formation of Sodium-Tin Alloys Determined with a New High Temperature Calorimeter. By RALEIGH L. McKISSON and LEROY A. BROMLEY.
Volatility and Stability of Metallic Sulphides. By C. M. HSIAO and A. W. SCHLECTEN. With discussion.
Mechanism of the Reduction of Oxides and Sulphides to Metals. By CARL WAGNER. With discussion.
Optical Temperature Scale and Emissivities of Liquid Iron-Copper-Nickel Alloys. By DAVID B. SMITH and JOHN CHIPMAN.
Thermodynamics of Iron-Silicate Slags: Slags Saturated with Solid Silica. By E. J. MICHAL and R. SCHUHMANN, JR.
Deleading Zinc Concentrate at the Parral and Santa Barbara Mills. By C. L. BOEKE and G. G. GUNTHER. With discussion.
Chlorination of Zirconium Oxide. By W. W. STEPHENS and H. L. GILBERT.
Observations on the Preparation of Iodide Titanium. By O. J. C. RUNNALLS and L. M. PIDGEON. With discussion.
Scaling of Lead in Air. By ELMER WEBER and W. M. BALDWIN, JR.
Heats of Solution of the Group IB Metals in Liquid Tin. By L. B. TICKNOR and M. B. BEVER.
Electrolytic Zinc Plant at Monsanto, Illinois. By T. I. MOORE and L. A. PAINTER.
Production of Spiegeleisen from Open-Hearth Slag in an Experimental Blast Furnace. By R. C. BUEHL and M. B. ROYER.
Production of High Manganese Slags by Selective Oxidation of Spiegeleisen. By M. B. ROYER and R. C. BUEHL.
Lead Blast Furnace Gas Handling and Dust Collection. By R. BAINBRIDGE.

Control of Conveyor Belt Acceleration

by J. W. Snavely

A practical mathematical treatment is presented for the determination and control of conveyor belt acceleration, particularly for conditions of starting where vertical curves are involved. A typical sample problem is analyzed, with required calculations, to clarify the procedure.

THE part that acceleration plays in starting a belt conveyor and its effect on belt conveyor design are well understood in a general way. Its practical importance is easily overlooked, however, and under some conditions, it is absolutely necessary to give the problem of acceleration detailed study.

Most handbooks on conveyor belting design adequately present basic data for the determination of acceleration values. This paper will only attempt to present practical thinking and a convenient method of treatment of acceleration in belt conveyor design.

Mathematical Analysis

In working out the various problems of conveyor belt acceleration, the starting point, as presented by the handbooks, is the familiar formula of "force of acceleration is equal to the mass times acceleration." By expressing these fundamental quantities in terms of belt conveyor design, it is possible to arrive at the unsuspected conclusion that the acceleration time for horizontal belt conveyors is independent of the load, and instead, dependent upon the belt speed, the type of drive arrangement and drive pulley, and the idler coefficient of friction.

The mathematics leading to this conclusion are shown in Table I, which has been prepared to show this derivation. While at first the conclusion just given may not seem to be reasonable, further reflection indicates that obviously the type of drive pulley and the type of drive do affect materially the tension in the conveyor belt, and thus, as clearly shown, the time of acceleration is dependent upon the factors mentioned.

Inasmuch as all of the factors except time are predetermined by the belt conveyor design, it becomes relatively easy to establish the accelerating time and to reduce further this time determination to a simple graph from which the time in seconds can be read directly. Such a graph is given in Fig. 1.

The table appearing on Fig. 1 should be explained further. For a given belt speed, the time of acceleration can be expressed as a percentage of the belt speed. The time of acceleration is also dependent on the drive arrangement, and changes in the drive arrangement consequently change the time of acceleration. It further follows that for a given belt speed, the time expressed as a percentage of that belt speed also changes with the type of drive.

Obviously then, it becomes possible to graph the percentage of speed for each type of drive against the belt speed and accelerating time, after which, for a given belt speed and type of drive, the time can be read directly in seconds.

Two constants were established for Fig. 1, the first one being the limiting of the maximum acceleration tension to 35 pct of the full load operating tension in the belt. The purpose of this is to limit the total tension imposed upon the belt during the acceleration period to 135 pct of the full load operating tension, which is the amount required to start or breakaway the fully loaded belt conveyor from rest.

The other constant is the friction factor used for the idler equipment, which has been established as 0.022. For installations where it is necessary to establish the values of acceleration, invariably high grade idler equipment is used, and it has been established from field experience that 0.022 for the idler friction factor is amply conservative. The use of this friction factor for idlers must be tempered with judgment, of course, for occasions will arise where more power than indicated is required to start, even with the very best of equipment, such as low temperature operations that tend to congeal the grease in the bearings and thus produce additional friction drag.

An inspection of the table in Fig. 1 affords a convenient rule of thumb method for determining the acceleration time, which conveniently can be 5 pct of the belt speed in seconds. The 5 pct of belt speed figure is close to the average for most types of drives.

In using Fig. 1 it must be emphasized that it applies accurately to horizontal belt conveyors only.

J. W. SNAVELY, Member AIME, is Manager of Engineering, Conveyor and Process Equipment Div., Chain Belt Co., Milwaukee.

Discussion on this paper, TP 3163B, may be sent to AIME before Feb. 28, 1952. Manuscript, Feb. 22, 1951. St. Louis Meeting, February 1951.

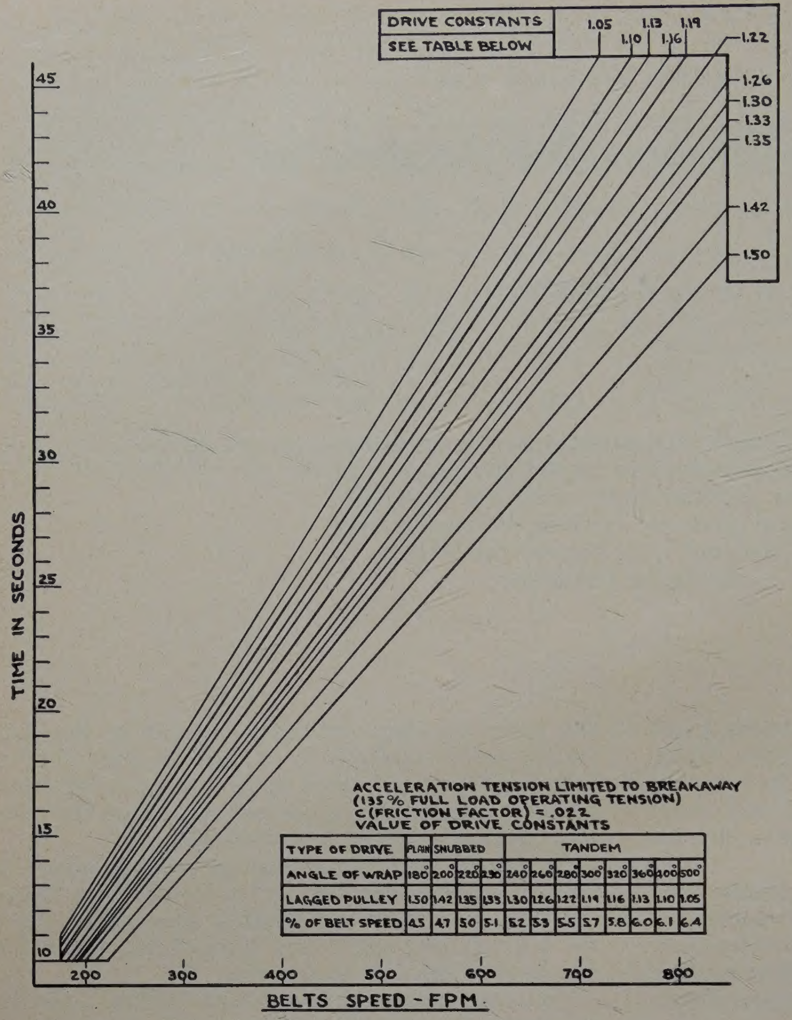

ACCELERATION TENSION LIMITED TO BREAKAWAY
(135 % FULL LOAD OPERATING TENSION)
C (FRICTION FACTOR) = .022
VALUE OF DRIVE CONSTANTS

TYPE OF DRIVE	PLAIN	SNUBBED			TANDEM							
ANGLE OF WRAP	180°	200°	220°	230°	240°	260°	280°	300°	320°	360°	400°	500°
LAGGED PULLEY	1.50	1.42	1.35	1.33	1.30	1.26	1.22	1.19	1.16	1.13	1.10	1.05
% OF BELT SPEED	4.5	4.7	5.0	5.1	5.2	5.3	5.5	5.7	5.8	6.0	6.1	6.4

Fig. 1—Minimum acceleration time for horizontal and inclined conveyors.

Inclined and declined conveyors introduce the effect of the power required or generated in lifting or dropping, which changes the accelerating time accordingly.

Somewhat unexpected is the conclusion that the accelerating time for an inclined conveyor is less than for an equally stressed horizontal belt conveyor. At first thought this would not seem to be consistent or logical, but it can be explained.

For any given maximum conveyor belt stressing, the possible inclined centers will be much less than the possible horizontal centers because obviously much of the tension capacity for the inclined conveyor will be required for lifting. The shorter centers of the inclined conveyor consequently mean much less of a load on the belt itself, less belt and fewer idlers. Therefore, for the same maximum stressing, the inclined belt has less mass to be accelerated, and it is reasonable that the accelerating time be less.

Because the inclined belt conveyor requires less time for accelerating, it becomes convenient to use the chart prepared for horizontal belts, as doing so merely introduces a comfortable factor of safety.

The declined belt conveyor presents a more complicated problem. With horizontal or inclined belts, the maximum running tension and the maximum acceleration tension come at the same point in the system. With declined belts (downhill belts requiring restraint) the running tension peak does not come at the same point as the peak accelerating tension. That is, when starting, the accelerating tension is the maximum just ahead of the drive, but the normal running tension is at its maximum just following the drive. When analyzing the forces involved in a declined belt conveyor, the accelerating tension plus the operating tension at the point of maximum accelerating tension should not exceed 135 pct of the maximum operating tension at any point in the system.

It must be further observed that all of the formulas used and the curves presented are based on the assumption that the entire mass of the conveyor belt with its load is accelerated uniformly. Of course, this actually never happens, and in starting, as the surge of power is applied to the belt, a corresponding surge of elastic stretch travels the length of the belt, which has the effect of starting the load progressively and consequently results in a shorter time of acceleration. It therefore follows that in using the methods given there is a factor of safety, which undoubtedly accounts for the relative freedom of acceleration difficulties in the belt conveyor design that has been done.

Where steel cord conveyor belts are used, at least two of the manufacturers recommend that the results of the calculations for vertical curves be multiplied by 1.5 or 2.0 because of the different characteristics of steel cords as compared with cotton cords or cotton fabrics. The question is raised whether this is being unnecessarily conservative. The formulas used in the derivation of the acceleration values assume that the entire mass is accelerated simultaneously. It has been pointed out that this does not take place with cotton constructions of conveyor belting, but because of the high modulus of elasticity of the steel cord, acceleration of the entire mass simultaneously does essentially take place with a steel cord belt. Sound engineering does dictate the use of a factor of safety, but it is suggested that it should be adequate to treat the actual calculated values as 75 pct of the design values actually used.

While primarily we are concerned with acceleration, mention must also be made of deceleration. It is seldom that deceleration presents a serious problem. From an operating standpoint, it is customary good practice to empty completely the belt conveyor before stopping it. Consequently the necessity of decelerating the load is not present. Further, the flywheel energy of the drive train also softens the stop, and finally, where a brake is used, the relatively gradual application of the friction of the brake provides a gradual stop. Where such braking to a stop is used, the deceleration tensions imposed are seldom serious. The problem of decelerating an inclined belt conveyor is parallel to the condition in accelerating a declined conveyor in that the points of maximum deceleration tension and maximum running tension then do not coincide.

The single exception to the general statement that the deceleration of a belt conveyor is not serious, is the deceleration of a declined conveyor, which becomes a parallel condition to accelerating an inclined conveyor. Again, however, the problem of this deceleration is less serious than acceleration of an inclined conveyor, because the friction stop which is always necessary with a declined unit is automatically a soft stop. The problems of a declined belt conveyor must always be given careful and complete study, and in all such cases, both the belting and the equipment supplier should be consulted.

Starting Time Control

After the minimum accelerating time in seconds has been accurately determined, the problem arises as to how this exact starting time can be introduced into the drive. Generally this can be accomplished readily through the use of a wound rotor motor and an external bank of resistance, with stepped starting. Such step controls are manufactured as standard equipment.

In selecting the control equipment, at least five points of starting should be used, which is standard procedure. The first two points will generally provide the building up of torque within the motor, and breakaway from rest will occur on the third point. Subsequent points add the final blocks of torque at the proper time intervals. While the time intervals for acceleration control usually will provide it automatically, sufficient length of contact at each point must be maintained to achieve stability at each point.

It is possible to achieve similar graduated starting control using dc motors. It is seldom however that dc motors are available, or their use economical, but mention of this type of motor must be included.

A third type of control, reduced voltage starting for squirrel cage motors, also can be used in some cases, and since its application most frequently will be in connection with the treatment of acceleration for conveyors with vertical curves, discussion of this type of control will follow subsequently.

Takeups: Because in part the determination of the

Table I. Formulas for Minimum Acceleration Time for Horizontal and Inclined Belt Conveyors

F = Accelerating force, lb
W = Weight of mass, lb
g = Gravity constant, 32.2
a = Acceleration, ft per sec per sec
$M = \frac{W}{g}$
t = Time, sec
v = Final velocity, fps
v_o = Initial velocity, fps
S = Belt speed, fpm
Q = Weight of moving parts, lb per ft
L = Horizontal centers, ft
L_o = Centers correction constant, 200 ft
T = Capacity, tons per hr
TT_1 = Total tension, horizontal conveyor
TT_2 = Total tension, inclined conveyor
p = Pct of TT
k = Drive constant
C = Idler friction factor
H = Vertical lift, ft

1. $$F = Ma = \frac{W}{g}a$$

2. $$a = \frac{v - v_o}{t}$$

3. $$F = \frac{W\ (v - v_o)}{gt}$$

$$v_o = O;\ v = \frac{S}{60}$$

4. $$F = \frac{W\ S}{1932\ t}$$

5. $$W = Q\ (L + L_o) + \frac{T\ (L + L_o)\ 100}{3S}$$

$$= (L + L_o)\left(Q + \frac{100T}{3S}\right)$$

6. $$F = \frac{S\ (L + L_o)\left(Q + \frac{100T}{3S}\right)}{1932t}$$

For Horizontal Conveyors

7. $$TT_1 = k\ C\ (L + L_o)\left(Q + \frac{100T}{3S}\right)$$

Limiting accelerating force to a pct of TT_1 or p

8. $$\frac{F}{TT_1} = p$$

$$p = \frac{S\ (L + L_o)\left(Q + \frac{100T}{3S}\right)}{1932\ t\ k\ C\ (L + L_o)\left(Q + \frac{100T}{3S}\right)}$$

9. $$p = \frac{S}{1932\ t\ k\ C}$$

10. $$t = \frac{S}{1932\ p\ C\ k}$$

$$p = 0.35;\ C = 0.022$$

11. $$t = \frac{S}{14.88\ k} \text{ or } \frac{WS}{676.2\ TT_1}$$

For Inclined Conveyors

12. $$TT_2 = k\left[C\ (L + L_o)\left(Q + \frac{100T}{3S}\right) + \frac{100TH}{3S}\right]$$

13. $$p = \frac{S\ (L + L_o)\left(Q + \frac{100T}{3S}\right)}{1932t\ k\left[C\ (L + L_o)\left(Q \frac{100T}{3S}\right) + \frac{100TH}{3S}\right]}$$

14. $$t = \frac{W\ S}{1932p\ TT_2}$$

$$p = 0.35$$

15. $$t = \frac{W\ S}{676.2\ TT_2}$$

Vertical Curve Determinations

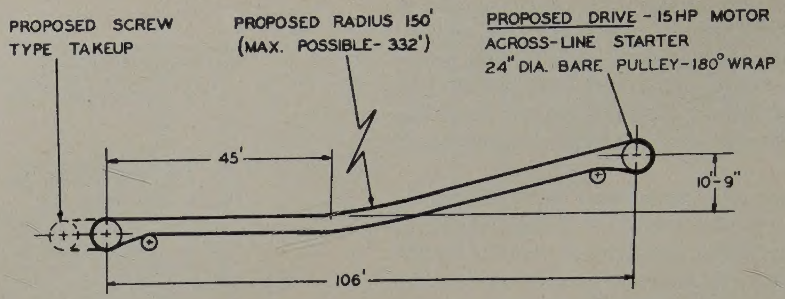
PROPOSED SCREW TYPE TAKEUP
PROPOSED RADIUS 150' (MAX. POSSIBLE- 332')
PROPOSED DRIVE - 15HP MOTOR
ACROSS-LINE STARTER
24" DIA. BARE PULLEY-180° WRAP
45'
10'-9"
106'

Fig. 2—Conveyor design.

Design Data

Material, cold cement clinker at 80 to 95 lb per cu ft
Capacity, 550 bbl per hr or 100 tons per hr
Belt, 24 in. width, 4 ply, 32 oz, 3/16 x 1/16 covers

Belt speed, 200 fpm
Belt wt, 5 lb per ft of length
Load wt, 16.7 lb per ft of length

Tensions Determination

Empty belt $= C\ (L + L_o)\ (Q) = (0.022)\ (106 + 200)\ (25) = 168$ lb
Carrying load horizontal $= C\ (L + L_o)\ (W) = (0.022)\ (106 + 200)\ (16.7) = 112$ lb
Lifting load $= W H = (16.7)\ (10.75) = 180$ lb
$et = 460$ lb

$TT = et \times k = 460 \times 1.84 = 850$ lb
$sst = et \times (k\text{-}1) = 460 \times 0.84 = 390$ lb

Table of Symbols

et = effective tension, lb
sst = slack side tension, lb
TT = total tension, lb
C = idler friction factor
L = projected horizontal length, ft
L_o = centers correction factor, ft
Q = wt of moving parts, lb per ft
W = wt of load, lb per ft
H = vertical lift, ft
S = speed of belt, fpm
k = drive constant — drive factor
T_o = empty belt, plus horizontal loaded section, plus slack side tensions, lb
R = minimum vertical curve radius, ft
U = wt of belt per ft of length
EHP = horsepower required at drive pulley rim

Fig. 3—Minimum radius, running conditions.

T_o = empty belt tension plus horizontal loaded tension plus slack side tension.

$$= 168 + \left(\frac{45 + 200}{106 + 200}\right) 112 + 390 = 648 \text{ lb}$$

$$R = \frac{1.2\ T_o}{U} = \frac{1.2 \times 648}{5} = 156 \text{ ft which is greater than proposed 150 ft}$$

But 1.2 factor is for maximum incline of 25° and correct factor for 15° is 1.038. Therefore

$$R = \frac{1.038 \times 648}{5} = 134 \text{ ft or safely less than proposed 150 ft}$$

accelerating values are predicated upon a definite slack side tension value, the selection of the takeup equipment becomes very important. The only type of takeup to use with vertical curve conveyors is the gravity type of takeup, either vertical or horizontal. It is only with this type of takeup that the tension imposed can be precisely determined and automatically maintained. Where a screw type of takeup is used, an indeterminate amount of tension is introduced, which may seriously upset all of the acceleration calculations.

Fluid Couplings: Recently the use of fluid couplings to provide a soft start for a conveyor has been recommended. Some caution should be used in the application of fluid couplings, however, for while it is true that through the control of slip in the coupling, a soft start can be imparted to the conveyor, the other characteristics of a fluid coupling must also be considered. In applying a fluid coupling to a conveyor drive, aside from the loss of power through slip, at least two other factors must be considered.

With a fluid coupling, a brake on the extended motor shaft becomes impossible. Normally this is not serious, for instead, a solenoid brake can be located on the extended high speed shaft of the speed reducer, but it is serious when a reducer is not used. A more serious consideration is the fact that with a fluid coupling, the overload capacity of the motor cannot be used to pull out when momentary serious overloads are placed upon the conveyor. If for any reason the conveyor should be overloaded beyond the design of the coupling, the conveyor simply cannot be made to start until that overload has been manually removed. This is a condition which actually has occurred.

Belt Fastening: No particular comment is required concerning the type of belt fastening employed, as the tension rating capacity of a given belt is dependent upon the type of fastening used. Where control of accelerating conditions is a part of the belt conveyor design, it is strongly recommended that only the vulcanized type of splice be used. The efficiency of any kind of mechanical splice decreases with age, and consequently where acceleration is a problem, future difficulty is apt to ensue if mechanical splices are used. Unusually liberal factors of safety are apt to require belt and equipment selection that is more expensive than the cost of a vulcanized splice.

Vertical Curves: Thus far the discussion has con-

Fig. 4—Minimum radius, accelerating condition across-line starting.

HP and Torque Requirements

$$EHP = \frac{et \times S}{33000} = \frac{460 \times 200}{33000} = 2.79$$

Motor hp = 2.79 $(1.05)^2$ = 3.0 hp

Max motor torque = Full load torque x pct for locked rotor torque

Actual 3 hp = 9.15 x 250 pct = 22.9 ft lb   Proposed 15 hp = 45.1 x 165 pct = 74.5 ft lb

Max torque at headshaft = Max motor torque x speed reduction x drive efficiency.

3 hp = 22.9 x 55 x 0.95 = 1197 ft lb   15 hp = 74.5 x 55 x 0.95 = 3893 ft lb

Max starting *et* — Max torque at headshaft divided by drive pulley radius

$$3\text{ hp} = \frac{1197}{1} = 1197\text{ lb} \qquad 15\text{ hp} = \frac{3893}{1} = 3893\text{ lb}$$

Minimum Radius Determinations

T_o also = horizontal component of tension in the catenary:

Therefore

$$\text{for 3 hp} \quad R = \frac{1.038\ (1197 \times \cos 15^\circ + 390)}{5} = 320\text{ ft} \qquad \text{for 15 hp} \quad R = \frac{1.038\ (3893 \times \cos 15^\circ + 390)}{5} = 860\text{ ft}$$

If proposed 15-hp drive is used, minimum radius required is 860 ft, which is physically impossible.

If actual 3-hp drive is used, minimum radius required is 320 ft, greatly in excess of prepared 150-ft radius.

Fig. 5—Minimum radius, accelerating condition, reduced voltage starting.

Break-Away Starting Torque Requirement

Breakaway tension for belt = approx. 135 pct full load effective tension.
With belt loaded to the curve

$$\text{Breakaway et} = 168 + \left[\left(\frac{45 + 200}{106 + 200}\right) 112\right] 1.35 = 348\text{ lb}$$

Minimum breakaway expressed as percentage of maximum

$$\text{Actual 3 hp } \frac{348}{1197} \text{ or 29.1 pct} \qquad \text{Proposed 15 hp} = \frac{348}{3893} \text{ or 8.9 pct}$$

Torque varies as square at input voltage; therefore for
3 hp, 29.1 pct torque requires 54 pct voltage;
15 hp, 8.9 pct torque requires 30 pct voltage

Minimum Radius Determination

Actual 3 hp

$$R\text{, empty, 54 pct voltage} = \frac{1.038\ (348 \times \cos 15^\circ + 390)}{5} = 150\text{ ft}$$

$$R\text{, loaded, full voltage} = \frac{1.038\ (1197 \times \cos 15^\circ + 390)}{5 + 16.7} = 74\text{ ft}$$

Therefore a 3-hp drive, with reduced voltage starting at 54 pct will not lift belt from curve when starting empty or partially loaded to the curve or when starting fully loaded.

Proposed 15 hp

$$R\text{, empty, 30 pct voltage} = \frac{1.038\ (348 \times \cos 15^\circ + 390)}{5} = 150\text{ ft}$$

$$R\text{, loaded, full voltage} = \frac{1.038\ (3893 \times \cos 15^\circ + 390)}{5 + 16.7} = 198\text{ ft}$$

Therefore with the proposed 15-hp drive with reduced voltage starting at 30 pct, satisfying the starting empty or partially loaded to the curve, the radius nevertheless must be increased to 198 ft, to satisfy the starting fully loaded condition.

cerned the effect of acceleration forces upon the conveyor belt. The vertical curve in a belt conveyor presents a new aspect in which the conveyor operation becomes involved.

A vertical curve in a belt conveyor becomes necessary when a transition from horizontal to incline is made. A large radius must be provided to keep the belt from lifting off the idlers at the vertical curve, and the handbooks are all explicit in the determination of the minimum radius for such a vertical curve for running conditions.

However, in addition to the running condition, the effect of acceleration when starting must also be checked, as it is easily possible to have a condition in which no difficulty may be encountered with a loaded or partially loaded belt when running, but in which the starting of the empty belt may cause momentary lifting and a sharp slapping back of the belt at the curve, which is obviously an intolerable operating condition.

The effect of starting acceleration is accentuated by the use of across-the-line starting, and further by the surge of tension that is thrown into the belt, which passes the entire length as a wave. A further complicating factor is that larger motors than required are frequently used, either by the plant operator's preference or occasioned by the fact that nothing smaller close to the actual requirement is available.

With the problem of vertical curves, it is generally not the high tension belts which need to be discussed, in which the starting is controlled because of tension requirements, but rather the common variety of plant belts in the low horsepower ranges, where the use of wound rotor motors scarcely ever is considered. The problem is best illustrated by a recent case of a belt conveyor requirement for a cement mill, and to illustrate completely the problem in question, Figs. 2-5 have been prepared.

Fig. 2 presents the overall conveyor belt design problem, which presents nothing unusual. The only item worthy of comment is that the plant arbitrarily intended to use a 15-hp motor for the drive.

Fig. 3 gives the first check and the usual one. It should be noted that the 1.2 factor has been corrected to 1.038. The 1.2 factor in the formula applies to a 25° inclination, which is a maximum, and is used in the formulas as a convenience. For degrees of incline less than 25, a factor of safety is introduced, which at times may become unnecessarily large.

The first check of the effect of acceleration appears in Fig. 4, and in this case, the condition is presented in which across-the-line starting equipment is employed. In following through the determinations which are given, it immediately is apparent that trouble will be encountered when starting up the empty belt or when loaded horizontally to the beginning of the curve. If the 15-hp motor that a plant might want to use is employed, then the radius will need to be 860 ft, which is a physical impossibility. If a 3-hp motor is used, the actual requirement, a radius of 320 ft, is needed, which is greatly in excess of the 150-ft proposed radius.

A second check of the effect of the accelerating condition on the vertical curve, this one using reduced voltage starting equipment, is presented in Fig. 5. Basically what has been done is to determine at what reduced voltage the empty belt can be started from rest, and then to check further the effect of a full voltage start on the fully loaded belt.

Following through the determination in Fig. 5, first the breakaway tension for the belt loaded horizontally to the beginning of the curve, which presents the worst lifting condition, has been determined, and then this breakaway tension has been expressed as a percentage of the maximum tension thrown into the belt when the starting contact has been made. As shown with a 3-hp motor, a starting voltage of 54 pct of the full voltage will start the empty and/or belt loaded horizontally to the curve, from rest; and with the 15-hp motor, only 30 pct of the full voltage is required for similar starting.

As is shown, with the 3-hp drive requirement, with a 54 pct voltage start, the minimum vertical curve radius 150 ft, or just at the proposed design figure of 150 ft. With this same drive, starting the belt fully loaded, with a full voltage start, the minimum radius drops to 74 ft, so that using a 3-hp drive with reduced voltage starting at 54 pct, no condition is encountered during starting either empty and/or partially loaded to the curve, or fully loaded, during which the belt will lift away from the curve.

Using the proposed 15-hp motor, the minimum vertical curve radius when starting empty and/or loaded to the curve, with a 30 pct reduced voltage, results in a radius of 150 ft, or equal to the proposed design radius. However, when a full voltage start is made on a fully loaded belt with a 15-hp motor, the minimum radius rises to 198 ft. Consequently, if the 15-hp motor is to be used, it must be used with a reduced voltage starter at 30 pct for starting the empty and/or loaded belt to the curve, which holds the belt on the curve during that starting condition, and the minimum radius must be increased to 198 ft, to hold the belt on the curve during starting of a fully loaded belt with full voltage applied to the motor.

Reduced voltage starters are standard control equipment, and are normally supplied with taps at 50, 65, and 80 pct of full voltage. However, any desired percentage of the full voltage can be supplied readily, and a 10-sec holding time should be used at the reduced voltage tap to reach a stable condition at that point.

The operation of the reduced voltage starter to the belt conveyor would be approximately as follows:

When the starting button is depressed, the reduced voltage starter allows the specified percentage of the voltage for a period of 10 sec. If the belt is empty, or loaded up to the curve, it will start moving and increase its speed during these 10 sec without lifting from the idlers. If the belt is fully loaded, it will not start until full voltage has been supplied to the motor after the 10-sec delay. It is also possible for the partially loaded belt to slow down after starting, if the load being placed on the belt could exceed momentarily the reduced torque of the motor. In either case, however, the curve of the belt will be loaded, and the design has been such that the belt will not lift from the curve under that condition.

One further possible operating condition has not been covered by the foregoing charts, and that is the case where the belt tensions in a vertical curve application approach maximum stressing. Then reduced voltage is no longer adequate. Using the rule of thumb for determining starting time, 5 pct of the belt speed therefore would mean that a 10-sec holding time at the reduced voltage tap would be good for only about 200 fpm of belt speed or less. Where vertical curves occur in highly stressed belts, that is where the stressing is 80 pct or more of the maximum permissible, in addition to the steps in the foregoing charts, the starting time in seconds must also be determined, and a wound rotor motor with step control starting be used. The belting selection should be rechecked, as frequently it may be more economical to add to ply or increase the weight of the duck rather than provide the type of motor and electrical controls necessary for the precise control of the acceleration.

The complete vertical curve determination can therefore be summarized as follows:

1—Determine the minimum vertical curve radius for the running condition.

2—Determine the minimum vertical curve radius for the starting condition, using the locked rotor torque of the motor, and check for:

> a—Crossline starting with the belt empty and/or partially loaded to the curve.
>
> b—Reduced voltage starting with the belt empty and/or partially loaded to the curve.
>
> c—Full voltage starting, belt fully loaded.

3—Use the largest of the minimum vertical curve radii determined from 1 and 2 above.

4—Whenever the belt is stressed to 80 pct or more of maximum tension rating, determine starting time in seconds (conveniently from Fig. 1), and use wound rotor motor with step starting controls.

Conclusions

It is clear from the foregoing that the effect of acceleration forces must be considered in belt conveyor design when 1—The conveyor belt is stressed to 80 pct or more of its maximum permissible tension rating, and 2—whenever vertical curves are involved. It is hoped that a convenient method of treating and practical methods of control have been presented for both conditions.

Acknowledgment

Credit for the mathematical derivations is hereby given to R. A. Zettel and J. J. Breitzman of Chain Belt Co.

Manganese Extraction by Carbamate Solutions And the Chemistry Of New Manganese-Ammonia Complexes

by Reginald S. Dean

Manganous oxide is readily soluble in concentrated ammonia solutions containing ammonium salts. Lixiviants of ammonia and ammonium carbamate permit ready extraction of manganese from reduced ores and the manganese in such solutions may be precipitated by heating to transform the carbamate to carbonate.

THE widespread occurrence of manganese in low grade oxide and carbonate ores not amenable to mechanical concentration has led to extensive investigations of hydrometallurgical methods for producing a pure manganese compound suitable for further treatment. Manganese carbonate is the preferable compound. This product when fully crystalline and of not too fine crystal size is easily filtrable and stable in air. It can be converted to other compounds such as the oxides by heating in air or can be reacted with acids for producing salts.

A useful hydrometallurgical process must produce relatively concentrated solutions that can be purified easily, reagents must be cyclically used, and heat requirements must be small.

Neither the ammonium sulphate nor sulphur dioxide leaching processes that have been tested extensively fulfill these requirements. Other heretofore proposed processes have obvious limitations and have not been tried on a large scale.

The present process is based on the discovery by the writer of a new group of aqueous manganese-ammonia complex solutions highly concentrated in ammonia, which permit rapid solution of manganous oxide to concentrations of 80 to 100 g Mn per liter and from which a fully crystalline, easily filtrable manganese carbonate is precipitated by the addition of carbon dioxide and partial ammonia removal.

Although the process may be carried out with many ammonium salts, commercial advantages dictate the use of ammonium carbamate, which is obtained when CO_2 is passed into concentrated aqueous solutions of ammonia. If the carbamate is used, the only reagents, ammonia and CO_2, are volatile and may therefore be recovered from solutions and residues by heating, thus eliminating washing and extensive evaporation.

Impurities are controlled easily as most metal oxides are either insoluble in the lixiviant or fail to precipitate with the manganese carbonate. Others are controlled by sulphide addition.

The process has been tested extensively on a small scale on a wide variety of ores, including Three Kids, Artillery Peak, Cuyuna, and Chamberlain, as repre-

---

R. S. DEAN, Member AIME, is Metallurgical Engineer and Consultant, Washington, D. C.

Discussion on this paper, TP 3226B, may be sent to AIME before April 1, 1952. Manuscript, July 6, 1951. Revision, Oct. 17, 1951. New York Meeting, February 1952.

Processes based on the disclosures in this article have been made the subject of patent applications in the United States and other countries.

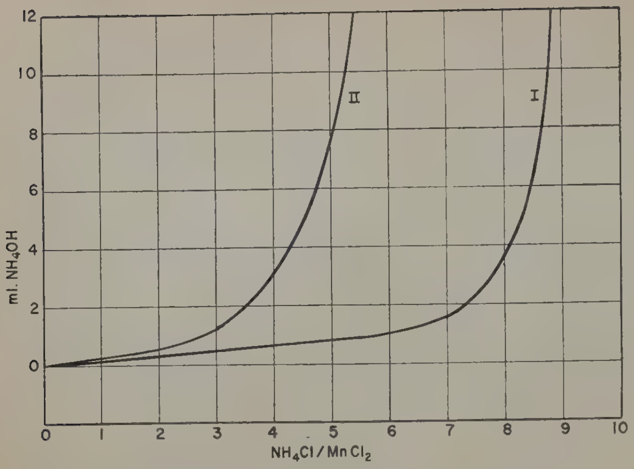

Fig. 1—Precipitation of manganese from manganese-ammonium salt solution with and without hydroxylamine salts. Total concentration, 100 g/liter.

I—Without hydroxylamine salts.
II—With hydroxylamine salts.

senting major domestic sources. Many foreign ores, including African and Cuban, have been tested. Good extractions and recovery can be obtained on all these ores. The lower limit of manganese content for practical treatment is a question of chemical engineering. It would appear that 18 to 20 pct manganese ores would be ideal for the process and that ores down to 7 to 8 pct manganese could be treated if the unit cost of the ore were correspondingly lower.

A commercial plant using this process for the production of manganese carbonate from Cuyuna ores is now being built at Crosby, Minn., by the Manganese Chemicals Co. At the outset, the manganese carbonate produced will be used for the production of battery oxide and manganese chemicals. A large capacity will be required for the eventual production of metallurgical grade manganese oxide at a cost to compete with foreign high grade ores.

Manganese Ammonia Complexes

There are many data in the literature on the reactions between ammonia and aqueous solutions of manganese salts. Some of these data are apparently contradictory because of the failure to state the proportions of all constituents and the solid phase, if any, precipitated.

It may be considered as well established, however, that when ammonia is added to manganous salt solutions, cationic complexes of manganese and ammonia are formed of the type $Mn(NH_3)_n^{++}$.[1-4] According to Firth,[5] who has made the most complete investigation of the system, the equilibrium conditions for the reaction between MnO and ammonium salt solutions can be approximated on the assumption that four cationic complexes are formed, $Mn(NH_3)^{++}$, $Mn(NH_3)_2^{++}$, $Mn(NH_3)_3^{++}$ and $Mn(NH_3)_4^{++}$.

Table I. Fractions Separated on Boiling Complex Solution

Fraction	Total Weight, Pct	Cumulative Weight	pH of Solution	Cl in Separated Solid, Pct
1	12.5	12.5	8.6	2.8
2	35.2	47.7	8.2	11.4
3	11.5	59.2	7.8	10.5
4	11.5	76.7	7.3	19.0
5	9.8	80.5	7.3	—
Residual Solution	19.5	100.0	7.3	—

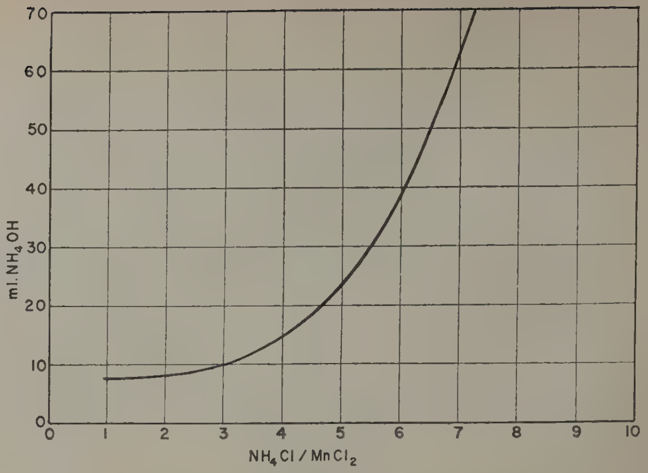

Fig. 2—Precipitation of manganese from manganese-ammonium salt solution in the presence of hydroxylamine salts.

No direct data are given by Firth concerning the complexity of his manganese-ammonia solutions. The precipitation of the solutions by a freshly prepared saturated solution of ammonium carbonate, however, shows that the manganese ion concentration is greater than that corresponding to the solubility of manganous carbonate.

There is much confusion in the literature concerning precipitation of manganese salts from aqueous solutions by ammonia.

Pure manganous hydroxide is not always precipitated when ammonia is added to manganous salt solutions. Frequently a basic salt is formed. The simplest way to keep this situation straight is to plot the data as a ternary system of $Mn(OH)_2$, NH_4OH, and the acid concerned. Even in this case, however, it must be remembered that equilibrium is not always reached and the nature of the precipitate obtained may depend on the rate or order of addition of the reagents. For example, Nasanen[6] has found that when alkali hydroxide is titrated with $MnCl_2$, basic chloride is formed; when additions are made in reverse order, however, the end point corresponds with the theoretical one for $Mn(OH)_2$ precipitation.

The oxidation by air of manganous hydroxide and basic salts often gives the impression that manganous hydroxide is an equilibrium solid phase when in reality no equilibrium solid phase is present. This is particularly true because much of the manganese content of even slightly oxidized manganous hydroxide is not as soluble in aqueous solutions containing ammonia and ammonium salts as it is in acid. As a result, even slight oxidation of a transient precipitate results in irreversibility of the reaction.

In the complete absence of oxidation, ammonium salts in moderate concentrations increase the amount of ammonia that must be added to precipitate manganous hydroxide. When air is present, the apparent amount of ammonia required for precipitation of a solid phase in the presence of a given concentration of ammonium salts is decreased. This may be caused by the impossibility of preventing local ammonia concentrations and the immediate oxidation of manganous hydroxide precipitated by these local concentrations to bring about an effective irreversibility of such precipitation.

In Fig. 1 there is plotted the milliliters of concentrated NH_4OH to produce the first visible precipitate in 50 ml of a solution containing manganese and ammonium chlorides to a total of 100 g per l. Curve I is for the solutions shaken in air as the NH_4OH was added. Curve II is for solutions containing a trace of hydroxylamine acid sulphate, which has been found to have a remarkable stabilizing effect on alkaline manganese solutions.[7] This precipitation phenomenon has been studied further in the range of 5 to 6 g NH_4Cl, and with a dilution to 10 g of total constituents, $Mn(OH)_2$, NH_4OH and HCl, per liter of the solution. Such solutions give irregular results in the presence of air. However, in the presence of hydroxylamine salts, consistent results are obtained. These results are plotted in Fig. 2 and show that in the absence of air, unexpectedly high concentrations of manganese and ammonia may be obtained in solution without precipitation of a solid phase.

Following this lead, it was found that soluble manganese salts such as chloride and sulphate could be dissolved to clear solutions in concentrated NH_4OH provided air was eliminated.

This led to the idea that at high ammonia concentrations, a new type of manganese ammonia complex was formed having manganese in the anion. Such a compound might have the formula

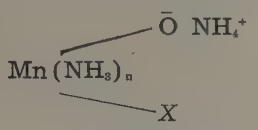

$$Mn(NH_3)_n \begin{cases} \bar{O}\ NH_4^+ \\ X \end{cases}$$

Where X is a monovalent anion.

As a typical example of a system exhibiting the presence of the new manganese-ammonia complex in solution, the manganous hydroxide, ammonium hydroxide, hydrochloric acid system will be considered first.

The phase fields of this system have been approximately determined and are plotted in Fig. 3 as a ternary system with a total concentration of the three components of 500 g per liter. This diagram represents practical equilibrium, that is, the state reached in a period of a few hours. The compositions have, where possible, been prepared in a number of ways, e.g., dissolving powdered electrolytic manganese in a solution of the other constituents, and adding the other constituents to aqueous ammonia. The areas of the phase fields for the several solid phases are approximate.

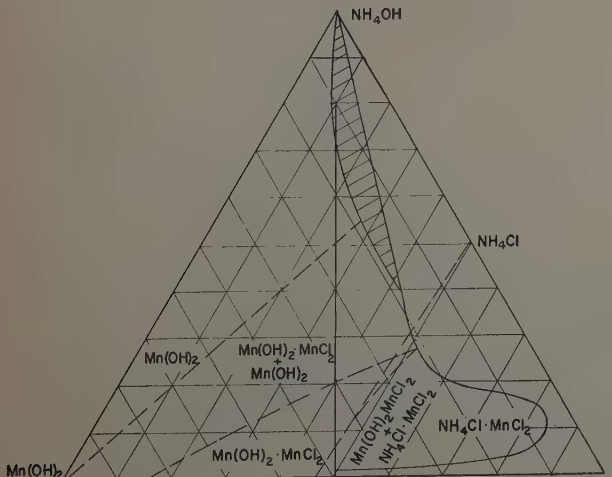

Fig. 3—The system $Mn(OH)_2$ - NH_4OH - HCL.

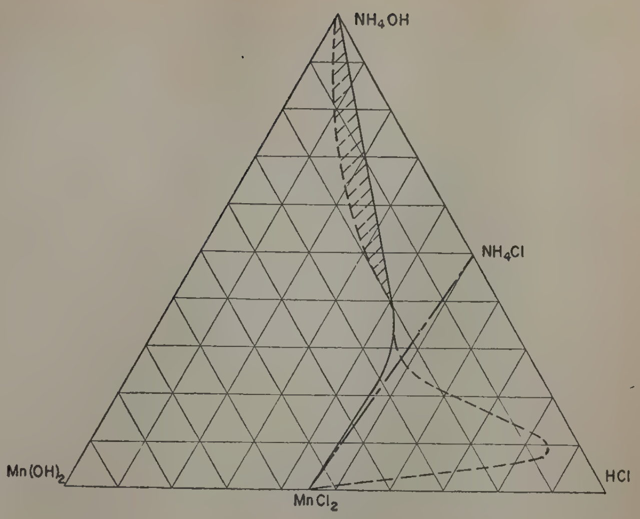

Fig. 4—The system $Mn(OH)_2$ - NH_4OH - HCL.
Total concentration 10 g/liter, dotted line.
Total concentration 500 g/liter, full line.

A consideration of the results previously reported for the precipitation of $Mn(OH)_2$ from dilute solutions containing ammonium chloride, see Fig. 2, in comparison to those in Fig. 3, shows that increasing total concentration has greatly changed the phase field boundaries.

In Fig. 4, these earlier results from Fig. 2 have been plotted on a ternary diagram and the boundaries from Fig. 3 have been added. It is evident that simple solid-phase fields boundary found for low concentrations must be modified for high concentrations by adding the phase field for double and basic salts and an extension of the liquid phase field toward the $Mn(OH)_2$ corner above 40 pct NH_4OH. If the anionic complex exists, it undoubtedly will be found in the composition range represented by this concavity.

The low concentration of manganese ion in these solutions is established by the fact that on adding freshly prepared saturated solution of ammonium carbonate no precipitation of manganese carbonate occurs.

The postulated anionic character of the new manganese-ammonia complex is confirmed by electrolytic transport experiments.

Preparation of $Mn(OH)_2$: It is obvious that if ammonia is removed from the anionic complex by boiling, the products precipitated will be indicated by the path of a line drawn from the ammonia corner of the ternary diagram through the composition of the complex solution. For example, consider the chloride system, starting with a solution in the proportions 1 $Mn(OH)_2$:1 HCl, the line indicated in Fig. 3 may be drawn. The actual fractions separated by boiling such a solution are shown in Table I.

It will be seen that only the first 12.5 pct of the manganese is precipitated as $Mn(OH)_2$ relatively free from chlorine. As a practical means of making $Mn(OH)_2$, the manganese is substantially all precipitated and then leached with 20 pct NH_4OH in sufficient amount to bring the total composition into the field in which pure $Mn(OH)_2$ is the solid phase. No manganese but all chlorine is removed from the solid phase in this way.

Obviously such a process can be made cyclic as indicated in the flowsheet, Fig. 5.

Of the ternary systems studied, the chloride system is best suited to the preparation of hydroxide

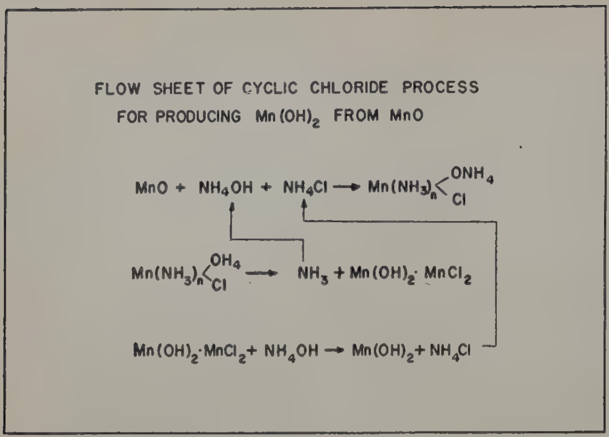
FLOW SHEET OF CYCLIC CHLORIDE PROCESS
FOR PRODUCING Mn(OH)₂ FROM MnO
MnO + NH₄OH + NH₄Cl → Mn(NH₃)ₙ<ONH₄ Cl
Mn(NH₃)ₙ<OH₄ Cl → NH₃ + Mn(OH)₂·MnCl₂
Mn(OH)₂·MnCl₂ + NH₄OH → Mn(OH)₂ + NH₄Cl

Fig. 5—Flowsheet of cyclic chloride process.

although the sulphate and nitrate systems can be used. An examination of the diagram of the acetate system shows that hydroxide can be separated only in a very small area and removing additional ammonia brings about re-solution. Such re-solution will, of course, take place in removing the ammonia from any system where the resulting composition is in the liquid phase field.

For example, in the sulphate system, the Bradley process depends on the reaction:

$$Mn(OH)_2 + (NH_4)_2SO_4 \rightarrow Mn(NH_3)_n\,SO_4 + NH_3\uparrow$$

Precipitation in the Bradley process is accomplished not by reversing this reaction in a field where direct precipitation of a solid phase would take place because this solid phase would be a basic sulphate, but by precipitation of an oxidized product, which takes place in the presence of much higher concentrations of ammonium salts than does the precipitation of pure $Mn(OH)_2$.

$Mn(OH)_2 - NH_4OH - H_2CO_3$ System: This system is of great theoretical and practical interest. The statement is sometimes loosely made that manganese carbonate is not precipitated from manganous salt solutions in the presence of ammonium salts. This is not true, as has been shown by many investigators, including Firth quoted earlier in this paper. Further, manganese carbonate, precipitated or natural, is not soluble in any solution of ammonia and ammonium carbonate. However, a new complex solution is obtained by dissolving either Mn or MnO in a concentrated solution of ammonia containing carbon dioxide. In this way a surprising amount of manganese can be obtained in solution, as will be seen from the ternary diagram, Fig. 6.

This diagram is consistent with the type diagram developed for the previously discussed chloride system, the difference arising from the greater insolubility of manganese carbonate than of manganese hydroxide. It should be pointed out, however, that in the complex system, the solid phase is manganese hydroxide when the carbonate concentration is low.

This system differs from the others discussed in its tendency toward irreversibility. If manganese carbonate is precipitated to a small extent by dilution of the concentrated solution, this precipitation may be reversed by immediate restoration of proper solution concentrations. If the complex solution is boiled to remove ammonia, the whole of the manganese precipitates as carbonate, the precipitation being irreversible.

These observations are consistent with the assumption that this system is in reality a carbamate system in which the carbonate ion never reaches a very high concentration. The classical work of Divers[8] showed that in a strong ammonia solution the carbonate-carbamate equilibrium was displaced very far toward the carbamate. McLeod and Haskins[9] and also H. T. H. Fenton[10] showed that low temperatures and high concentrations favor the formation of carbamate.

Therefore, it appears highly probable that a manganese-ammonia complex is formed with the carbamate ion and that carbonate ion is present in relatively small amounts. The equilibrium is shifted toward carbonate by heating, or dilution, so that in this way, the carbonate ion reaches a concentration where manganese carbonate is precipitated from the complex, resulting in a further shift of equilibrium and eventual complete precipitation of manganese carbonate without substantial removal of ammonia. The freshly formed precipitate redissolves, but the crystalline precipitate formed by boiling is not redissolved in any solution of ammonia and carbon dioxide. This is probably caused by the decrease in solubility on crystallization.

The carbonate precipitate is shown by X-ray spectrometry to be the anhydrous rhodocrosite form, although about one half molecule of water is held in some way.

Other Ternary Systems: The ternary systems presented are typical of the great majority of systems of $Mn(OH)_2$, NH_4OH, and an acid. The following systems behave similarly to the chloride system already discussed: sulphate, acetate, nitrate, sulfamate, thiocyanate, dithionate, alkyl sulphonate, fluoborate, fluosilicate, and fluoride.

The borate system behaves like the carbonate in showing an irreversible deposition of manganese borate $MnB_4O_7 8H_2O$.

The phosphate and arsenate systems are exceptions because they form insoluble manganese-ammonium salts.

Several organic acids forming insoluble manganese compounds behave like the carbonate and borate. This permits their preparation from MnO by solution in ammonia and the ammonium salt of the acid and boiling to precipitate the manganese compound. Salicylic and benzoic acid behave in this way. Manganese metal and MnO are readily soluble in am-

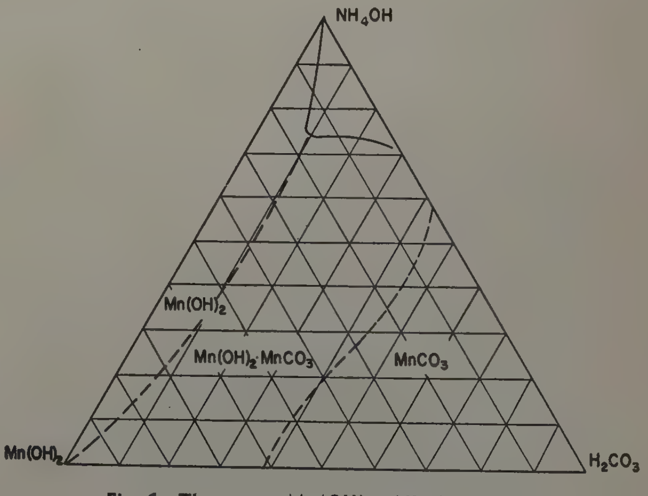

Fig. 6—The system $Mn(OH)_2 - NH_4OH - H_2CO_3$.
Total concentration 500 g/liter.

monium salicylate and benzoate. The similar behavior of naphthenic acids is of possible practical importance in preparing manganese napthenate.

Manganese Recovery

The reactions of the process may be written:

Leaching

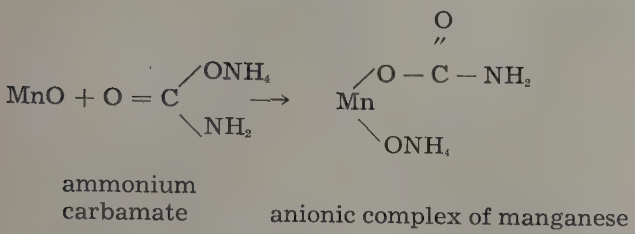

$$MnO + O = C\begin{matrix}\diagup ONH_4\\ \diagdown NH_2\end{matrix} \longrightarrow Mn\begin{matrix}\diagup O - \overset{O}{\overset{/\!/}{C}} - NH_2\\ \diagdown ONH_4\end{matrix}$$

Precipitation

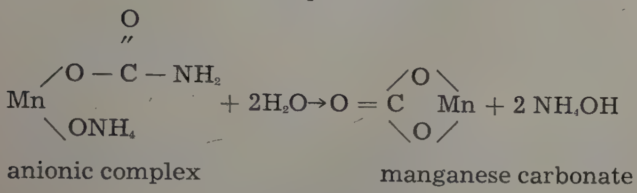

$$Mn\begin{matrix}\diagup O - \overset{O}{\overset{/\!/}{C}} - NH_2\\ \diagdown ONH_4\end{matrix} + 2H_2O \rightarrow O = C\begin{matrix}\diagup O \diagdown\\ \diagdown O \diagup\end{matrix} Mn + 2\,NH_4OH$$

Regeneration

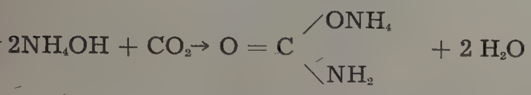

$$2NH_4OH + CO_2 \rightarrow O = C\begin{matrix}\diagup ONH_4\\ \diagdown NH_2\end{matrix} + 2\,H_2O$$

The reaction rate and extraction of pure MnO leaves little to be desired. All manganese ores, however, contain more or less iron. It has been found that the adverse effect of iron found in many manganese ores on the rate and extent of solution may be offset by small amounts of several accelerating agents. The most effective of such reagents are hydroxylamine salts and soluble sulphides. The mechanism of action of these reagents is not fully understood. Their effectiveness, however, is very great, and without their help the process would not be practical on many ores.

As an example of the great effect of these accelerators, the following results are given for a well reduced, high grade manganese ore containing about 5 pct iron.

The effect of accelerators is not only to increase extraction but to increase rate of extraction. With 1200 mg of ammonium sulphide per liter, the maximum extraction on a typical ore was reached in 10 min. Without accelerator, the extraction under similar conditions was 15 min, 39.3 pct; 30 min, 45.8 pct; 45 min, 48.7 pct.

The sulphur added as accelerator goes almost entirely into the residue from the extraction. In tests in which 15 cycles of extraction were made with regenerated leach liquor and ammonium sulphide added in each cycle, there was no cumulative build-up of the sulphur content of the manganese carbonate and this content was only 0.02 pct to 0.03 pct.

Table II. Effect of Accelerators on Well Reduced, High Grade Manganese Ore, Extraction Time, 30 Min

Addition Agent			
Hydroxylamine Acid Sulphate		Ammonium Sulphide	
Mg per Liter	Extraction, Pct	Mg per Liter	Extraction, Pct
0	45.8	0	45.8
100	63.7	600	72.0
250	84.3	1200	92.0
500	91.8	2400	89.0
		4800	85.0

Table III. Relation of Ammonia Concentration to Manganese Remaining in Solution

NH_3 Mols per Liter	Mn g per Liter
16.0	52.0
14.2	50.4
13.0	27.0
12.0	6.3
11.9	1.8

When the iron in the ore is increased substantially, it is necessary to give consideration to the reducing roast so as to obtain as much of the iron as possible as the relatively inert Fe_3O_4. The conditions for obtaining iron as Fe_3O_4 have been studied extensively in connection with the Bradley process and more recently in connection with the ammoniacal extraction of nickel from nickel-iron ores.

With optimum roasting conditions, which must be determined for each ore, the extraction procedure for the process is the same for high iron ores as for low iron ores.

The amount and composition of sulphide accelerator is fairly critical both as to maximum extraction and as to rate of settling of the residue. With the optimum amount for extraction, settling of the residue from most ores is rapid.

The amount of manganese which can be built up in the pregnant solution is increased by ammonia and CO_2 concentration of the solution, minimum concentrations of 14 mols per liter NH_3 and 2.5 mols per liter CO_2 are necessary, but little advantage is obtained by increasing ammonia above about 15 mols per liter and CO_2 above 3.00. There is no disadvantage, however, in carrying NH_3 to saturation (17 to 18 mols per liter) and CO_2 to 4.0 mols per liter. With these concentrations of lixiviant and a high grade manganese ore, pregnant solutions containing at least 80 g per liter can be obtained with 10 to 15 min leaching together with better than 90 pct extraction.

With low grade ores, the pulp density determines the concentration of manganese that can be obtained in a single leach. With 15 to 20 pct manganese, a single leach with 40 g Mn per liter and good extrac-

Table IV. Application of Process to Cuyuna Range Ores, 65 Mesh. All Analyses Reported as Dried Analyses

	Assay, Pct				
	Iron	Phosphorus	Silica	Manganese	Aluminum
Fine grained, hard masses of goethite and manganese with fine chert and some limonite.	37.63	0.347	7.73	14.97	4.07
Soft fine-grained cherty banded limonite and manganese	40.83	0.217	11.80	9.54	4.29
Manganese material and hematite with granular chert	28.32	0.068	17.83	19.38	2.23
Manganese material and hard hematite with soft, granular cherty manganese	23.93	0.101	30.66	16.98	1.86
Massive, hard granular, ferruginous chert with some soft pitted manganiferous chert and some quartz grains	29.77	0.074	40.35	7.80	2.10
Cherty limonite with soft, brown manganese layers. Lenses of hard, fine chert	32.78	0.124	32.32	7.49	3.75
Magnetic material, hard and soft cherty hematite and some limonite	30.86	0.141	32.29	9.61	3.45

Table V. Results of Tests Giving Best Extraction

Ore No.	Ore Analysis, Pct		Extraction, Pct	Analysis, Pct				Distribution, Pct				Recovery, Pct
				Magnetic Conc.		Nonmagnetic Conc.		Magnetic Conc.		Nonmagnetic Conc.		
	Mn	Fe	Mn	Mn	Fe	Mn	Fe	Mn	Fe	Mn	Fe	Mn
1	14.97	37.63	88.0	3.9	56.0	3.6	11.0	9.1	93.0	2.9	7.0	97.1
2	9.54	40.8	83.0	2.4	52.8	2.5	37.4	11.5	88.2	5.2	11.8	94.8
3	19.3	28.3	88.0	2.9	58.5	7.6	10.2	5.3	92.5	6.7	7.5	93.3
4	17.0	23.9	87.0	4.0	51.2	4.6	10.5	6.9	93.2	6.1	16.8	93.9
5	7.8	29.7	93.0	2.39	49.7	1.84	10.6	4.4	86.0	2.6	14.0	97.4
6	7.5	32.8	83.0	1.84	42.0	2.58	17.2	6.5	67.0	10.5	33.0	89.5
7	9.6	30.8	86.0	2.9	48.7	4.4	22.4	5.6	65.0	8.4	35.0	91.6

tion is possible. With lower manganese content of the ore, the problem of building up manganese in the pregnant liquor must be considered on the basis of pulp densities and settling rates for each particular ore.

The Precipitation Step: The manganese from the solution containing the complex manganese carbamate can be quantitatively precipitated by heating under pressure. This regenerates the leaching solution. As a practical matter, however, the precipitation is carried out by simultaneous heating and ammonia evolution. If the ammonia is removed by heating at atmospheric pressure, the manganese will be reduced to less than 2 g per liter by lowering the ammonia concentration to about 11 mols per liter.

The relationship of ammonia concentration to the manganese remaining in solution is given in Table III.

The manganese carbonate precipitated by boiling off the ammonia at atmospheric pressure settles and filters with great facility. It is stable when dried in air or at 110°C. The only impurity found in the carbonate is 0.01 pct to 0.02 pct iron, 0.01 pct to 0.02 pct sulphur, and 0.03 pct alkalis. Phosphorus is absent even when the ore treated is relatively high in phosphorus.

Laboratory Tests on Cuyuna Ores: The application of the process to ores of the Cuyuna range is given in Table IV.

The general procedures for tests were as follows: 1—Roasting, After a number of tests with solid fuel reduction and with dry hydrogen, a reducing roast was used for the tests which consisted in heating the ores at several temperatures varying from 420° to 500°C in hydrogen bubbled through water at 70° to 90°C. The time of roasting was from 1 to 2 hr. 2—Leaching, The leach was carried out using 25 g of ore and 100 ml of leach solution. The material was shaken for 30 min and analyzed. The leach solution contained 17.5 mols of NH_3 and 3.5 mols of CO_2. In most cases $(NH_4)_2S$ was used as the accelerator. 3—Magnetic Separation, The residues from the leach were dried and weighed, then separated on a Davis tube.

The results of tests giving the best extraction on each of the ores are shown in Table V. The final column showing manganese recovery is the total of manganese in the solution and the magnetic concentrate.

These results indicate that it is possible to obtain extractions varying from 83 pct to 93 pct using simple roasting and leaching procedures.

Phosphorus is not extracted from the ores by the process.

Laboratory Tests on a South African Ore: This ore is typical of a group in which iron and manganese are so intimately associated that manganese ferrite $MnO \cdot Fe_2O_3$ is formed under reducing conditions that on Cuyuna ores yield MnO and magnetite FeO Fe_2O_3. Manganese ferrite yields its manganese to acid but not to the high ammonia leach. To get good extraction with an ore of this kind, drastic reduction must be used, which gives MnO together with FeO and Fe. Under these conditions much iron is leached along with the manganese. This is illustrated in Table VI.

Table VI. Effect of Reducing Conditions on Extraction of South African Ore[a]

Temperature of Reduction, Deg C	Atm	Extraction, Pct Mn	Mn/Fe
550	H_2 (dry)	78.2	5.05
550	H_2 saturated with water at 80°C	62.2	24.3
650	H_2 (dry)	97.4	3.20

[a] Analysis of reduced ore: 43.2 pct Mn, 18.8 pct Fe.

The iron in solution can be removed by oxidation conveniently with manganese dioxide so that any desired manganese-iron ratio may be obtained.

Acknowledgment

The assistance of A. L. Fox in carrying out much of the laboratory work reported herein is gratefully acknowledged, as is that of K. M. Leute who sponsored the project and who has undertaken its commercial application.

References

[1] J. W. Mellor: A Comprehensive Treatise on Inorganic and Theoretical Chemistry. **12**.

[2] Brett: *Philosophical Magazine* No. 3 (1836) **10**, p. 95.

[3] Z. A. Yankelvich: Some Physico Chemical Properties of the System $MnSO_4$-$(NH_4)_2SO_4$-H_2O. *Journal of General Chemistry, U.S.S.R.* (1945) **15**, No. 11-12, pp. 884-894.

[4] Agladze: The Complex Ion of Mixed Solutions of Manganese and Ammonium Salts. *Journal of General Chemistry, U.S.S.R.* (1940) **10**, pp. 340-346.

[5] C. V. Firth: Ferro Grade Manganese Ore from the Cuyuna Range, Minnesota; Report No. 2, The Chemistry and Application of the Ammonium Sulphate Process; Mines Experiment Station, Univ. of Minnesota. Nov. 14, 1941.

[6] Reino Nasanen: Potentiometric Determination of the Solubility Product of $Mn(OH)_2$. *Ztsch. Physik Chem.* (1942) **191A**, pp. 54-64.

[7] R. S. Dean: U. S. Patent No. 2,316,937, April 30, 1943.

[8] E. Divers: *Journal* Chem. Soc. (1870) **23**, p. 171.

[9] J. J. McLeod and H. D. Haskins: *J. Biol. Chem.* (1906) **1**, p. 319.

[10] H. T. H. Fenton: *Proc.* Roy. Soc. (1896) **39**, p. 386.

Super High Intensity Magnetic Equipment for Protecting Conveyors

by R. L. Manegold

This paper outlines the reasons for and the application of suspended magnets above belt conveyors for the purpose of removing tramp iron to protect equipment. The design of a magnet strong enough to extract iron through a distance of 24 in. is described along with the proper method of application in the field. Advantages of the suspended magnet in contrast to the conventional magnetic pulley are also discussed.

IN RECENT years there has been a decided trend toward bringing ores and coal out of open-pit and underground mines by long, sloping single-stage belt conveyors.

Because the high investment cost of haulage conveyors dictates maximum speed and full loading for economy, conveyor belts are running faster than ever before, with a greater burden on the belts. In addition, larger blocks of ore are being mined and conveyed. Rougher use of large mining equipment generates more tramp iron; mechanical loading rejects nothing. Therefore the extraction of tramp iron and other deleterious materials for the protection of haulage conveyors at transfer points, chutes, and idlers is becoming an increasingly difficult job.

In our experience, the best method of protecting long haulage conveyor belts is to extract the tramp iron, at least the large tramp iron, ahead of the main haulage conveyor or series of conveyors. It is most practical to collect the tramp iron at the earliest source possible, usually directly after the primary car unloading dump or after the primary crushers, which are ordinarily not affected by tramp iron, see Fig. 1.

The coal or ore from its primary source is fed by chutes or feeders onto a buffer or shock belt conveyor, a short, ruggedly built conveyor system that can be considered somewhat expendable. Its primary function is to bring the ore up to speed for transmission to the haulage conveyor. There is no assured method of protecting this conveyor from tramp iron damage at its feed end. Likewise, there is a possibility, although remote if the magnet applied to this belt is installed correctly, that the tramp iron extraction process will damage the shock belt, which is, however, short and comparatively inexpensive.

Magnetic head pulleys with their maximum effective range of about 8 or 10 in. cannot be considered for large installations, even though they are desirable because of the continuous and automatic tramp iron removal feature. Further, the most dangerous form of tramp iron with respect to potential damage to a haulage conveyor is the long rod, roof bolt, or rail segment, which is not extracted satisfactorily because of the limited tangential contact of such an iron shape with the magnet.

Magnetic head pulleys are also undesirable because the dribble or fines from the head pulley discharge at the same point as the tramp iron. Screens must be used to separate the fines from the magnetics, resulting in additional expense and loss of head room.

Magnetic detectors have been used with success, but they only indicate the presence of iron, and the conveyor belt must be stopped for its manual removal. The stoppage of any conveyor means that all preceding equipment must be stopped or a cascade of material on the idle conveyor will result.

Occasionally combinations of detectors and magnetic head pulleys are used. The detector precedes the magnetic head pulley and detects only large pieces of tramp iron, while the magnetic pulley subsequently takes out the smaller ferrous metals. Suspended magnets overcome the disadvantages of magnetic head pulleys, detectors or a combination of both. There are several magnetic extraction problems involved in applying a suspended magnet at this

---

R. L. MANEGOLD, Member AIME, is President, Dings Magnetic Separator Co., Milwaukee, Wis.

Discussion on this paper, TP 3242B, may be sent to AIME before April 1, 1952. Manuscript, July 23, 1951. New York Meeting, February 1952.

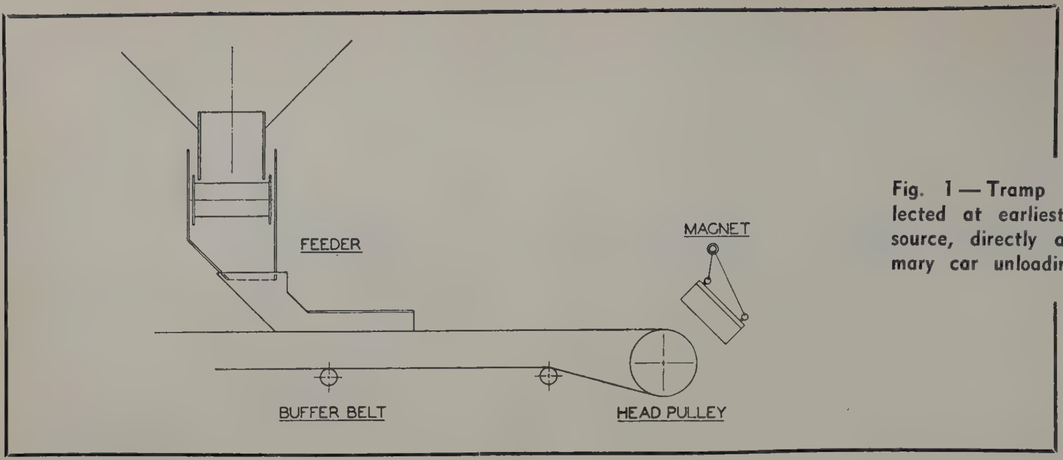

Fig. 1 — Tramp iron collected at earliest possible source, directly after primary car unloading dump.

primary point. First, and most serious of all, lumps of ore or coal from 8 in. and upwards may be on this shock conveyor. It generally is required that the magnet be suspended at a height that more than clears the largest dimensions of the largest lump. In accordance with the inverse square rule of magnetism, a magnet with an effective range of 20 in. must be four times as strong as one with a 10-in. range and a magnet with 30 in. of effective range must have nine times the strength of the 10-in. range unit.

Second, it takes time to induce magnetism into a piece of steel or iron. Some large magnet assemblies take 10 to 15 sec to become energized completely. Also, it takes time to pull tramp iron through a burden of material frictionally holding the tramp iron. Therefore, the suspended magnet must have a long enough magnetic field in the direction of travel of the tramp iron to pull the iron out of the burden.

Third, as previously indicated, long bars are most dangerous to the haulage conveyor and must be removed effectively. Since a bar passing under a magnet has its lead end pulled up to the magnet first, the trailing edge can dig into the shock conveyor and possibly cause considerable damage. There are several solutions to this potential danger which will be discussed later.

There are several problems in designing a suspended magnet with an effective range equal to at least the distance the magnet will be suspended above a conveyor. This distance can be anywhere from 4 in. to 30 in. or more dependent on the burden depth and maximum lump size.

It has been determined with fair accuracy that to extract tramp iron against gravitational forces and through a normal burden, a minimum of approximately 400-gauss magnetic field intensity is required, no matter how far above the conveyor the magnet is suspended. A gauss is the measurement of the number of lines of magnetic force per square centimeter of cross-section of the magnetic field. The 400-gauss figure can be substantiated further by a study of the permeability curves of normal tramp metals.

To design a magnet with a minimum of 400 gauss at X inches away from the magnet face requires the proper balancing of amperes and turns of copper wire (the magnet's magnetomotive force) with the proper cross-section and length of steel to convey the magnetic lines of force where they will be most effective.

The peculiar thing about magnetism is that it is a potential force only. The electrical energy (watts) put into a magnet does no magnetic work at all. (Therefore, there can be such a thing as a permanent magnet.) Thus, speaking of energy consumption only, the amperes of electrical current put into a suspended magnet produce heat only. A large magnet consuming 10 or 15 kw of electrical energy is the equivalent of 10 or 15 toasters hooked up to the line, but because the dielectric materials available to electrically insulate coil windings can withstand only temperatures a little over the boiling point of water, the problem of designing a large magnet consists partially at least of dissipating the heat of the coils.

Therefore, the design of these large magnets includes the largest possible radiation surface, and retains as much of the coil as possible close to the thin radiating walls. We have evolved from the circular-shaped magnet because a heavy steel casting surrounding the magnet coils interferes with heat dissipation.

As stated previously, it takes time to induce and therefore attract steel to a magnet. Coincidentally, in the design of the magnet, when it is required that the lines of force be extended from the face of the magnet, it is also necessary for the distance between the magnet poles to be increased. Thus, the length and penetration of the magnetic field both are increased. We find that our super strength magnets always have a sufficient length of field in the direction of material flow to pull adequately tramp iron to the magnet at belt speeds up to about 600 fpm. Some special applications such as grain conveyors traveling at high speed and with low burden depths must incorporate suspended magnets designed primarily for length of field and not depth or range.

The other factor, time of extraction, that of pulling the tramp iron through the burden of ore against the

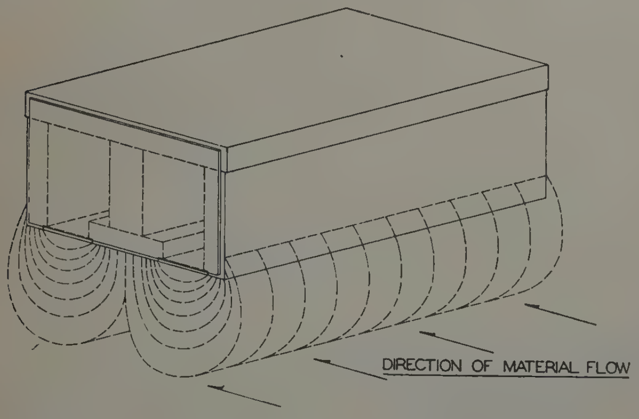

Fig. 2—Parallel magnetic field of the rectangular magnet.

frictional effects of the burden, is resolved by designing the suspended magnet so that its magnetic field is parallel at all points on the magnet to the direction of flow of the material. This compares to a circular magnet that has a field configuration through 360°. Therefore, toward the outside edges of a circular magnet, some of the tramp iron must be pulled through about 1.4 times (square root of 2) the burden of ore as compared to the rectangular design.

The parallel magnetic field of the rectangular magnet is best exemplified by Fig. 2. Fig. 3 shows a field chart of a typical magnet with effective range of about 28 in.

The third problem pertains to the proper installation of a suspended magnet to prevent long rods from pulling up to the magnet on the leading edge and permitting the trailing end to gouge and cut the conveyor belt.

On very fast conveyors where long rods do not occur, it is desirable to install the suspended magnet back of the drive pulley and parallel to the conveyor belt below it. This type of installation permits tramp iron to be within the magnetic field for the longest period of time. Thus, conveyor belts can be run faster, the burden depth for a given tonnage will be less, and the effective range of the magnet need not be as great unless miscellaneous chunks of ore are present.

Since parallel to belt types of installation do not protect the conveyor from long rods, either the conveyor must be considered expendable, as in the case of a shock conveyor, or a self-cleaning cross belt must be applied to the magnet. Such a unit is shown in Fig. 4.

This magnet has wide application where the tramp iron to be extracted is of relatively small size. A large piece of tramp iron is held to a magnet with tremendous force amounting to tons of pressure sufficient to stop the self-cleaning cross belt. Therefore, for heavy mining applications where large chunks of tramp iron can be expected, none of our standard self-cleaning cross belt units have been installed. One or two extremely special installations have been designed, but perhaps because of their high initial cost, they have not been purchased up to this time.

Where rods and heavy tramp iron are to be expected, it is best to install the rectangular suspended magnet at the brow of the shock conveyor head pulley; the magnet at about a 30° to 45° angle. This positioning of the magnet minimizes damage to the shock belt from long rods. It has the further advantage of permitting the magnet to operate on a looser and thinner burden, thus easing the task of pulling tramp iron through the load.

Figs. 5 and 6 show the parallel to belt and brow of head pulley installations. There is an interesting secondary magnetic effect encountered when installing a very large magnet at the head end of a belt conveyor.

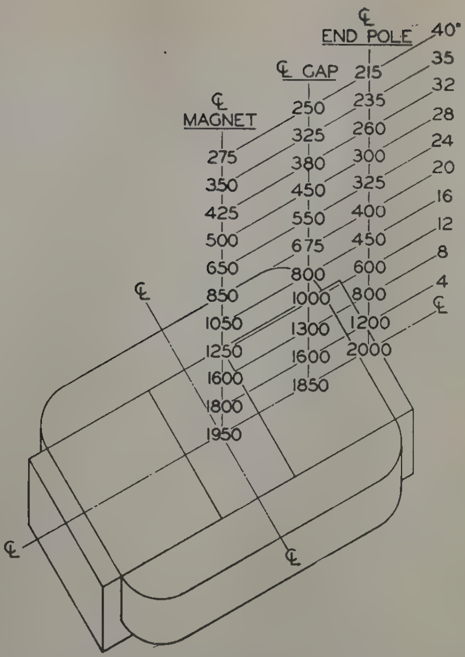

Fig. 3—Field chart of typical magnet with effective range of about 28 in.

There is an intense Dings magnetic separator used for concentrating weakly susceptible magnetic ores, known either as Type EBK cross belt machine or as the Wetherill type of separator. This concentrating device operates on the principle of magnetic lines of force concentrating themselves at sharp edges, which is the same principle as a lightning rod attracting electricity.

Installing a large and long rectangular magnet tangentially to a steel head pulley induces magnetic lines of force into the head pulley. If the diameter of the head pulley is less than the length of magnetic field of the suspended magnet, the pulley in effect concentrates lines of magnetic force at its surface nearest the magnet. These lines of force can be concentrated to such a degree that tramp iron, within a range of 3 or 4 in. of the pulley, actually will be attracted to the pulley and not to the magnet suspended over the pulley. From our experience, this reaction, need be considered only where the length of the suspended magnet is greater than the diameter of the head pulley. However, on magnets exceeding 12 in. of effective range, this relationship is likely, and the only solution is to use a head pulley made of some nonmagnetic material such as stainless steel or manganese steel.

Fig. 4 — Self-cleaning cross belt applied to magnet.

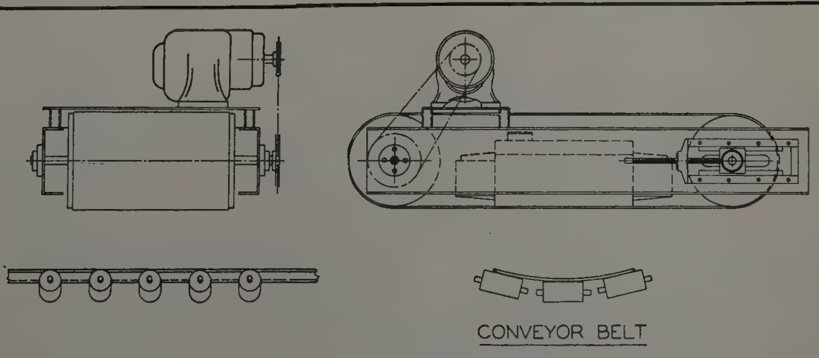

Other secondary considerations in properly applying a suspended magnet for the protection of conveyors are of importance.

The initial cost of large suspended magnets is not low. Some of these units have over 15,000 lb of copper in the coils. The cost of the magnet increases nearly in a squared ratio with the increase in magnetic range.

In many installations the occasional large chunk of ore or coal determines how far above the belt the magnet must be suspended. It would be entirely possible to install a photoelectric cell ahead of a suspended magnet to indicate the approach of a large ore chunk, but to our knowledge, an installation of this type has not been made. The electronic device could be connected to stop the conveyor and preceding feeding equipment, and the large chunk could then be removed manually from the conveyor belt. In this way, a lesser range magnet could be used with consequent lower initial cost, but operating costs would be higher.

Disposal of the accumulated tramp iron on the face of the magnet should also be studied thoroughly. First of all, use a liberal figure for the tonnage of tramp iron that will be collected and provide convenient means for its disposal. There are many installations where the tramp iron and salvagable tools caught by the magnet easily pay for all operating costs of the magnet. In some cases, the value of this scrap also pays for the initial installation in 4 or 5 years.

The most convenient magnet installations are those where the magnet is suspended from a trolley fastened to an I-beam, which permits movement of the magnet for unloading the accumulated iron without stopping the conveyor.

The standard suspended magnet has one failing that should be mentioned, which is not inherent with either a magnetic pulley, a self-cleaning rectangular magnet or a detector installation. In the event of a direct current failure, the standard suspended magnet will drop its accumulated load of tramp iron on the conveyor below. This accumulated load can be more dangerous to following equipment than the same tonnage of tramp iron going through the system piece by piece.

One way to correct this disadvantage is to suspend the magnet from a sloping I-beam, the trolley being held in a normal position by a solenoid catch. Power for the magnet must be supplied by a special motor generator set with a large flywheel between the electric motor and generator. Because of the flywheel, failure of the dc power supply will be gradual, while the solenoid can be set closely so that a slight drop in the dc voltage will trip the solenoid and allow the magnet to slide away from above the conveyor before losing its tramp iron.

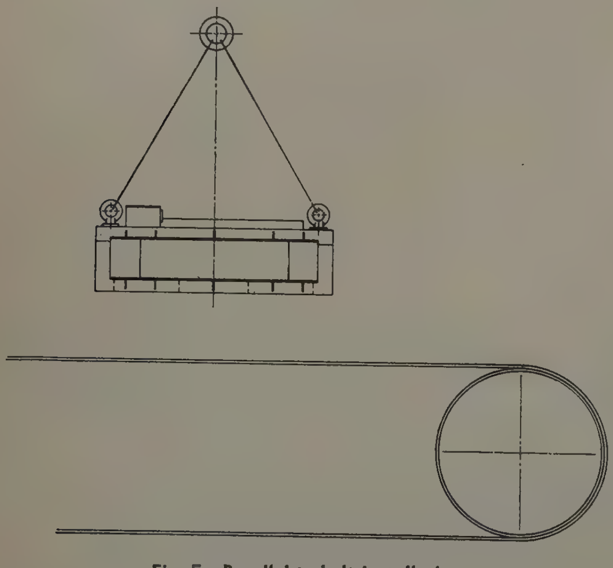

Fig. 5—Parallel to belt installation.

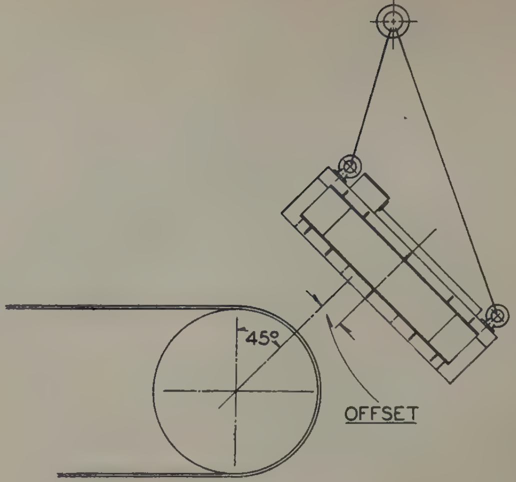

Fig. 6—Brow of head pulley installation.

The disadvantage of this type of installation is that the same inclined I-beam is used to carry the magnet away from the conveyor belt when tramp iron is to be disposed of intentionally. Pulling a heavy magnet back up an inclined slope is a difficult job requiring a winching device of some type.

Another safety measure is to provide the magnet with a compound winding. Of the total power, 80 pct is supplied from a normal power source such as an M-G set or rectifier while the remaining 20 pct of the electrical current is supplied from a rectifier or M-G set connected through batteries to the magnet. In the event of either ac or dc failure, the batteries take over and supply enough current to the magnet to hold all accumulated iron. A signal horn sounds if the power fails, and the operator can investigate the trouble.

Still another precaution, applicable to any type of tramp iron installation, is to have the conveyor drive motor interlocked with the magnet. This arrangement precludes the possibility of carrying ore under, through, or over the magnet without the magnet being energized.

A conscientiously designed magnet installation cannot insure 100 pct tramp iron removal. A properly installed magnetic separator installation will give close to 100 pct tramp iron extraction but not 100 pct. For instance, it is impossible to expect a magnet of any shape or type to pull a piece of tramp iron through a 2-ft slab or a densely packed burden of ore or to pull out a piece of tramp iron imbedded in a large mass of frozen ore, but a properly engineered installation will give nearly perfect results. Any compromise with the optimum should be made with the full knowledge of both the customer and supplier of the magnet and only after all conditions of the installation have been studied thoroughly.

Frothing Characteristics Of Pine Oils in Flotation

by Shiou-Chuan Sun

THIS paper presents the design and operation of a frothmeter capable of measuring the frothing characteristics of pine oils and other frothing reagents. The experimental data show that the frothability of pine oil is governed by: 1—rate of aeration, 2—time of aeration, 3—height of liquid column, 4—chemical composition of pine oil, 5—pH value of solution, 6—temperature of solution, and 7—concentration of pine oil in solution. The effect of mineral particles on the behavior of froth also was studied, and the results can be found in a separate paper.[1]

The results also show that the relative frothabilities of pine oils in the frothmeter generally correlate with those in actual flotation, provided that other factors are kept constant. In addition to pine oils, the other well-established flotation frothers were tested, and the results are included.

In this paper, compressed air frothing is the frothing process performed by means of purified compressed air, whereas sucked air frothing is the frothing process accomplished by purified air sucked into the glass cylinder by a vacuum system. The term vacuum frothing denotes that froth was formed by degassing of the air-saturated liquid under a closed vacuum system.

Apparatus

The frothmeter, shown in Fig. 1, is capable of reproducibly measuring the volume and persistence of froth as well as the volume of air bubbles entrapped in the liquid and is capable of being used for compressed air frothing, sucked air frothing, and vacuum frothing.

Fig. 1a shows that for compressed air frothing, the apparatus consists of an airflow regulating system, 1-3; a purifying and drying system, 4-8; a standardized flowmeter to measure the rate of airflow from zero to 500 cc per sec, 9; and a graduated glass cylinder, 13; equipped with an air regulating stopcock, 10; an air chamber, 11; and a fritted glass disk to produce froth, 12. The fritted glass disk, 5 cm in diam and 0.3 cm thick, has an average pore diameter of 85 to 145 microns. The pyrex glass cylinder has a uniform ID of 5.588 cm and an effective height of 63 cm. The inside cross-sectional area of the glass cylinder was calculated to be 24.53 sq cm, or 3.8 sq in.

For sucked air frothing, Fig. 1b shows that the apparatus for compressed air frothing is used again, with the following modifications: 1—compressed air and its regulating system, 1-3, are eliminated; and 2—a vacuum system, 16, equipped with a vapor trap, 15, and a vacuum manometer, 17, is added. The vacuum system can be either a water aspirator or a laboratory vacuum pump. Any desired rate of airflow can be drawn into the glass cylinder, 13, by adjusting the opening of the air regulating stopcock, 10. The sucked air stream is cleaned by the purifying and drying system, 4-8, before entering the glass cylinder, 13. When this setup is used for vacuum frothing, the air regulating stopcock is closed.

The frothmeter has been used for almost 3 years and has proved to give reproducible results, as illustrated in Table I. With a magnifying glass and suitable illumination, the frothmeter also can be used to study the attachment of air bubbles to coarse mineral particles.[2]

Experimental Procedures

Except where otherwise stated, the data presented were established by means of the compressed air method. The volume and persistence of froth were recorded respectively at the end of 4 and 6 min of aeration at a constant rate of airflow of 29.3 cc per sec, which is equivalent to 71.6 cc per sq cm per min, or 462.6 cc per sq in. per min. The aqueous solution for each test, containing 1000 cc of distilled water and 19.2 ± 0.5 mg frothing reagent, was adjusted to a pH of 6.9 ± 0.2. The volume of froth is expressed as cubic centimeter per square centimeter and is equivalent to the height of the froth column (the distance between the bottom and the meniscus of the froth). The volume of froth was obtained by multiplying the height of froth by the cross-sectional area of the glass cylinder, 24.53 sq cm.

Before each test, the glass cylinder, 13, was cleaned thoroughly with jets of tap water, ethyl alcohol, tap water, cleaning solution, tap water, and finally distilled water. The cylinder with stopcock,

---

SHIOU-CHUAN SUN, Member AIME, is Assistant Professor, Mineral Preparation Div., Pennsylvania State College, State College, Pa.

Discussion on this paper, TP 3190F, may be sent to AIME before Feb. 28, 1952. Manuscript, May 24, 1950. Revision, May 18, 1951. Cleveland Meeting, October 1950.

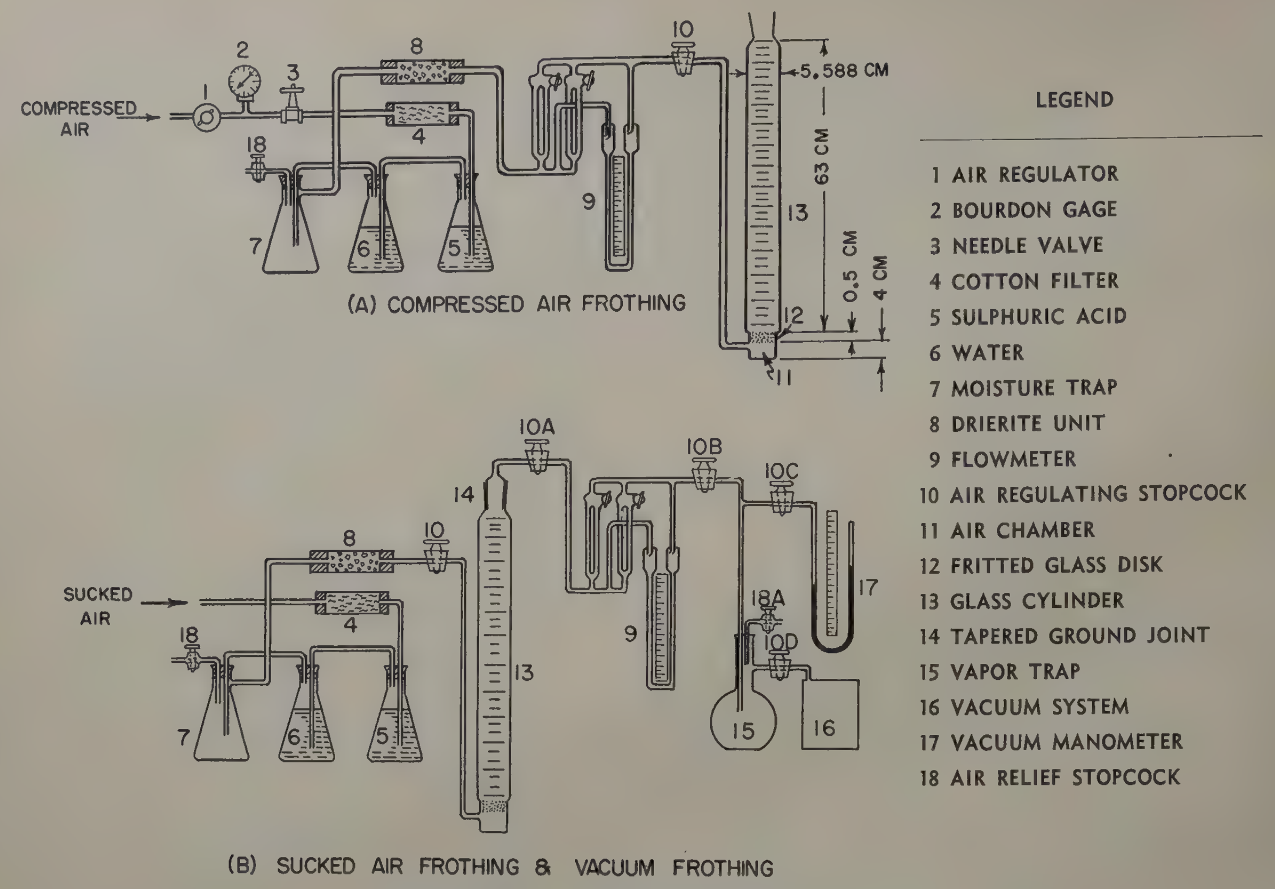

Fig. 1—Schematic diagram of a frothmeter.

10, closed was connected to the flowmeter by rubber tubing. The cylinder was filled first with 1000 cc of distilled water, and a predetermined amount of frothing reagent was added. The pH of the distilled water was adjusted previously in a glass beaker with solutions of sodium hydroxide and hydrochloric acid of cp grade. All pH values were determined by a Beckman pH meter. The upper level of the solution was marked on the cylinder with a crayon pencil. Approximately 30 sec after the stream of compressed air was admitted into the purifying and drying system and the flowmeter, a moderate amount of air pressure was built up to prevent water from dripping through the fritted glass disk, 12. The stopcock, 10, of the cylinder then was opened. A predetermined rate of aeration was obtained by adjusting the needle valve, 3. A stop watch was started simultaneously with the opening of the air regulating stopcock, 10, to record the time of aeration. The volume of air bubbles entrapped in the liquid was indicated by the height of increased liquid portion above the upper level of the solution at rest, and the height of froth column was measured by the graduated scale of the cylinder and further checked with a small ruler. The first measurement was taken 30 sec after the air regulating stopcock was opened, and subsequent measurements were taken after each 30-sec interval. The persistence or stability of the froth was determined by shutting off the air to the glass cylinder and recording the time elapsed before the froth disappeared completely. To protect the flowmeter, the compressed air current had to be shut off in the following order: air regulating stopcock was closed, then the air relief stopcock was opened, and finally the needle valve was closed.

Table I. Frothability of Pure n-hexyl Alcohol at Various Concentrations Showing the Reproducibility of the Frothmeter

Test	Concentration of N-hexyl Alcohol, Mg/L	Volume of Froth Measured at Various Time Periods of Aeration, Cc/Cm²								Stability of Froth at End of 6-Min Aeration, Sec
		30 Sec	60 Sec	90 Sec	120 Sec	180 Sec	240 Sec	300 Sec	360 Sec	
1	9.63	0.9	1.05	1.1	1.1	1.1	1.1	1.1	1.1	5.9
1a	9.63	0.9	1.0	1.0	1.1	1.1	1.1	1.1	1.1	6.0
2	19.26	1.0	1.2	1.3	1.3	1.3	1.3	1.3	1.3	7.6
2a	19.26	1.1	1.15	1.2	1.3	1.3	1.3	1.3	1.3	7.5
3	28.89	1.4	1.6	1.6	1.7	1.7	1.7	1.7	1.7	9.9
3a	28.89	1.5	1.6	1.6	1.6	1.7	1.7	1.7	1.7	9.8
4	48.15	1.5	1.8	1.9	2.0	2.1	2.1	2.1	2.1	10.3
5	77.04	1.4	2.3	2.8	2.9	3.0	3.0	3.0	3.0	11.1
5a	77.04	1.5	2.4	2.8	2.9	3.0	3.0	3.0	3.0	11.0
6	105.93	1.1	1.3	1.4	3.1	3.7	3.8	3.8	3.8	14.0
7	144.45	0.8	1.1	1.5	1.7	5.6	5.7	5.8	5.8	16.4
7a	144.45	0.9	1.2	1.5	1.7	5.7	5.8	5.8	5.8	16.5
8	288.90	1.1	1.4	1.6	2.3	5.7	6.4	6.7	6.7	18.0
8a	288.90	1.2	1.3	1.6	2.4	5.8	6.5	6.7	6.7	18.0

For sucked air frothing, shown in Fig. 1b, the cleaned glass cylinder, 13, with stopcock, 10, closed was filled with 1000 cc of aqueous solution of predetermined pine oil content and pre-adjusted pH. Approximately 15 sec after the vacuum system was turned on with stopcock, 18A, closed, the air regulating stopcock was adjusted to obtain the desired rate of flow of the purified air stream drawn into the glass cylinder. The height of the increased liquid portion and the height of froth were measured in the same way as the height of compressed air frothing. The persistence of froth was determined by closing simultaneously stopcocks 10 and 10A and recording the time elapsed before the froth disappeared. After stopcocks 10B, 10C, and 10D were turned off, stopcock 18A was opened to admit air into vapor trap. Then the vacuum system was turned off. Finally, the apparatus was refilled with air by careful adjustment of the stopcocks, 10 and 10A-10C.

Vacuum frothing was tested in a way similar to sucked air frothing except that the distilled water was saturated with purified compressed air before the addition of the chemical pH regulators and the frother, and the stopcock, 10, was kept closed during the entire testing period.

Frothability Index

The frothabilities of pine oils and other frothers are expressed in terms of *froth volume* and *frothability index* as shown in Tables II and III. The froth volume method is self-explanatory and has been used extensively in the field of froth flotation as well as foam industry. The frothability index method is proposed for the benefit of canceling the idiosyncrasies of the frothmeter employed. For example, Fig. 2a shows that to a certain limit the froth volume or froth height of pine oil increased rapidly with the increase of the rate of aeration. The same data calculated and plotted as frothability indices, shown in Fig. 2b, are roughly constant and independent of the rate of aeration, between 30 and 80 cc per sq cm per min. Therefore another investigator can build a similar frothmeter with a fritted glass disk of somewhat different aerating characteristics without seriously affecting his results. The same is also true for the time of aeration within the range of 3 and 7 min, see Fig. 3b, for the height of liquid column at 30 cm and higher, see Fig. 4b, for the concentration of pine oil between 3 and 23 mg per liter, see Fig. 7, and for the pH value of the solution within the range of 5 to 8 (not presented).

The indices of the frothers were based on a standard frothing substance, pure n-hexyl alcohol. By testing a frother and the standard under the same conditions and considering both the volume and persistence of the standard froth as 100, the indices of the frother were calculated from the following equations:

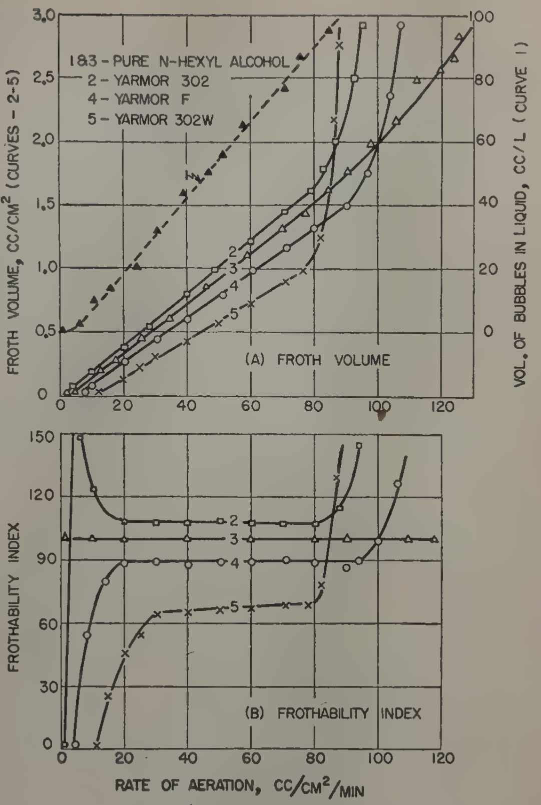

Fig. 2—Effect of rate of aeration on frothabilities of pine oils and pure n-hexyl alcohol.

$$FI = 100 \left(\frac{f_1}{f} \right) \qquad [1]$$

$$SI = 100 \left(\frac{s_1}{s} \right) \qquad [2]$$

Table II. The Frothabilities of Various Flotation Frothers, Tested at 7.0 pH Value with 19.2 ± 0.5 Mg Per Liter Concentration and 71.6 Cc Per Sq Cm Per Min Aeration

			Frothability		Stability	
Test	Frother	Source	Volume of Froth, Cc/Cm²	Index, Using Pure N-hexyl Alcohol as Standard	Persistence of Froth, Sec	Index, Using Pure N-hexyl Alcohol as Standard
1	Pure n-hexyl alcohol	Eastman Kodak	1.3	100.0	7.5	100.0
2	*Tergitol* wetting agent 7	Carbide & Carbon	>15	>1153	90	1200.0
3	*Tergitol* penetrant 4	Carbide & Carbon	3.4	262	23.2	309.5
4	Ethyl silicate, tetra-ethyl orthosilicate	Carbide & Carbon	2.2	169	7.0	95.9
5	Methyl amyl acetate, 4-methyl-pentyl acetate—2	Carbide & Carbon	1.8	138.4	6.1	83.6
6	Methyl amyl alcohol	Carbide & Carbon	1.6	123.0	7.1	97.3
7	Pine oil 302	Hercules	1.4	107.7	7.7	101.2
8	Cresylic acid 1B	Koppers	1.4	107.7	4.0	53.3
9	Cresylic acid No. 1	Reilly	1.3	100.0	3.8	50.7
10	Pine oil F	Hercules	1.2	92.4	6.2	82.7
11	Cresylic acid D2A	Barrett	1.2	92.4	2.9	38.7
12	DuPont frother B23	American Cyanamid	1.2	92.4	5.8	77.3
13	*Tergitol* penetrant 08	Carbide & Carbon	1.2	92.4	8.7	115.9
14	Butyl *Carbitol* solvent, diethyl glycol monobutyl ether	Carbide & Carbon	1.2	92.4	5.0	68.5
15	Cresylic acid, English	American Cyanamid	1.1	84.6	4.5	60.0
16	Pure n-octyl alcohol	Eastman Kodak	1.1	84.6	5.8	77.3
17	Frother 60	American Cyanamid	1.0	76.9	8.3	110.6
18	Pine oil GNS. No. 5	American Cyanamid	1.0	76.9	4.5	60.0
19	Cresylic acid EE	Oronite	0.95	73.1	4.2	56.0
20	Cresylic acid 4020	American Cyanamid	0.9	69.2	7.4	98.6
21	Pine oil 302W	Hercules	0.9	69.2	4.4	58.7
22	Frother H.T.T.	American Cyanamid	0.8	61.5	4.0	53.3

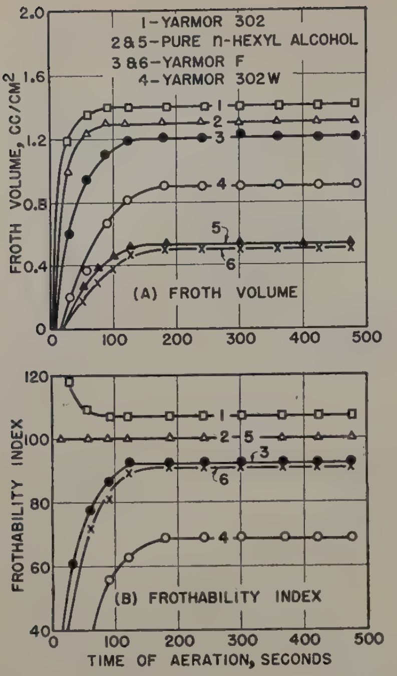

Fig. 3—Effect of time of aeration on frothabilities of pine oils and pure n-hexyl alcohol.

Curves 1-4: 71.6 cc/cm²/min rate of aeration.
Curves 5-6: 25.5 cc/cm²/min rate of aeration.

in which *FI* and *SI* are respectively the frothability and stability index of the tested frother, *f* in cc per sq cm, and *s* in seconds are respectively the volume and persistence of the standard froth, and f_1 and s_1 are respectively the volume and persistence of froth produced by the test frother. The pure n-hexyl alcohol was purified from a practical grade by distilling it four times in a vigreaux distillation column, the final distillation fraction being collected at 165 to 157°C corrected to 760 mm mercury. The purified product was identified further by its refractive index of 1.416 at 25°C.

Aeration

Fig. 2a shows that an increase in the rate of airflow produces an increase of froth and of air bubbles entrapped in liquid. This may be explained by the fact that a high rate of aeration results in 1—better mixing between reagent and liquid, 2—enough air to form more bubbles, and 3—continual replacement of the collapsed bubbles by new ones. Since air bubbles collapse only in air but not in liquid, the increase of air bubbles in liquid is larger than that of froth. From the flotation point of view, the rate of aeration must be sufficient to form enough bubbles for particle-bubble attachment, and the optimum rate of aeration[2] depends on the size and density of the mineral particles. When the rate of aeration is high, as in this case over 95 cc per sq cm per min, all the liquid in the flotation cell can be transformed into air bubbles.

Fig. 3a shows that the time of aeration required for the froth to reach its maximum height is dependent upon the grade of pine oil, see curves 1, 3, and 4, and also upon the rate of aeration, see curves 3 and 6 and also 2 and 5. These can be explained by the fact that high grade pine oil, Yarmor-302, takes less time to reorient itself in the air-water interface than low grade pine oil, Yarmor-302W, and the time of orientation is shortened by the mixing effect of aeration. Fig. 3b shows that the frothability indices of pine oils are practically independent of the aeration time between 3 and 7 min.

Liquid Column Height

Curves 2 to 4 of Fig. 4a show that to a certain extent the shorter the liquid column, the more the froth is produced, other factors being constant. This may be because more air is entrapped in a higher water column, as shown in curve 1 of Fig. 4a. The test data may be useful for the design of flotation machines.

Figure 4b shows that the frothability indices of

Table III. Relation Between Chemical Properties and Frothabilities of Pine Oils and Their Principal Constituents, Tested Under Various pH Values with 19.2 ± 0.5 Mg Per Liter Concentration and 71.6 Cc Per Sq Cm Per Minute Aeration

1	2	3	4	5	6	7	8							9		10	11
Principal Consituents of Pine Oil	Empirical Formula	Polar Group	No. of Double Bonds of Nonpolar Group	Solubility Gm/Liter[a]	Classification	Specific Gravity	Volume of Froth, Cc/Cm², at Various pH Values							Stability of Froth, Sec		Frothability Index at pH 7.0[b]	Stability Index at pH 7.0[d]
							3.4	5.0	7.0	9.8	11.0	11.8	7.0[c]	7.0	7.0[c]		
Beta-terpineol	$C_{10}H_{18}O$	C-OH	1	$2.2^{20°}$	unsat. tertiary alcohol	$0.919^{20°}$	1.3	1.2	1.3	2.1	2.9	3.1	1.6	5.0	5.3	100.0	66.7
Alpha-terpineol	$C_{10}H_{18}O$	C-OH	1	$1.98^{20°}$	unsat. tertiary alcohol	$0.935^{20°}$	1.2	1.0	1.1	1.6	3.1	3.4	1.2	4.8	4.8	84.6	64.0
Fenchyl-alcohol	$C_{10}H_{18}O$	C-OH	None	sl.	secd. alcohol	$0.942^{20°}$	1.3	1.2	1.3	1.5	1.8	1.6	1.8	4.6	5.2	100.0	61.3
Borneol	$C_{10}H_{18}O$	C-OH	None	$0.64^{20°}$	secd. alcohol	1.010	1.2	1.1	1.1	1.3	1.8	1.6	1.8	3.8	3.2	84.6	50.7
Camphor	$C_{10}H_{16}O$	C=O	None	1.6	ketonic	$1.000^{0°}$	1.2	1.0	1.1	1.3	1.7	1.4	1.3	3.7	5.0	84.6	49.4
Dihydro-terpineol	$C_{10}H_{20}O$	C-OH	None		satd. tertiary alcohol	Cis. $0.9124^{20°}$ Trans. $0.901^{20°}$	0.5	0.6	0.7	1.0	1.7	2.6	1.8	3.2	5.8	53.7	42.7
Fenchone	$C_{10}H_{16}O$	C=O	None	i	ketonic	$0.948^{18°}$	0.3	0.3	0.4	0.6	1.7	1.8	1.5	2.9	5.1	30.8	38.6
Anethole	$C_{10}H_{12}O$	C-O-C	4	v.sl.	etheric	$0.985^{25°}$	0.3	0.25	0.3	0.5	0.8	1.1	1.1	2.5	3.7	23.3	33.4
Methyl-chavicol, Estragol	$C_{10}H_{12}O$	C-O-C	4	i	etheric	$0.979^{11°}$	0.2	0.2	0.2	0.4	0.8	1.2	0.9	2.0	3.9	15.4	26.7
Terpinolene	$C_{10}H_{16}$	None	2	i	hydrocarbon	$0.862^{20°}$	trace	trace	trace	0.3	0.6	0.8	0.8	1.8	2.6	trace	24.0
Dipentene	$C_{10}H_{16}$	None	2	i	hydrocarbon	$0.8245^{20°}$	trace	trace	trace	0.2	0.5	0.7	0.6	1.7	2.5	trace	22.6
Camphene	$C_{10}H_{16}$	None	1	i	hydrocarbon	$0.822^{78°}$	0	trace	trace	0.15	0.4	0.6	0.9	1.6	2.6	trace	21.4
Beta-pinene	$C_{10}H_{16}$	None	1	i	hydrocarbon	$0.8675^{22°}$	0	0	0	trace	0.3	0.5	0.8	1.0	2.5	0	13.3
Yarmor-302				$(1.60^{25°})$	high grade		1.3	1.3	1.4	2.4	3.3	3.5	1.2	7.7	4.8	107.7	101.2
Yarmor-F				$(1.24^{25°})$	medium grade	$0.9358^{15.6°}$	1.1	1.1	1.2	1.3	1.8	2.7	1.1	6.2	4.7	92.4	82.7
Yarmor-302W				$(1.08^{25°})$	low grade	$0.9204^{15.6°}$	0.8	0.8	0.9	1.0	1.3	3.1	0.9	4.4	4.3	69.2	58.7
Distilled water	H_2O		None			1.0	trace	trace	0.2	0.5	0.6	1.1		1.0		15.4	1.3

[a] Solubility: Data taken from ref.[12]; i, insoluble; v. sl., very slightly soluble; sl., slightly soluble; data in parentheses are approximate solubilities determined by the author.
[b] Froth: Tr., an incomplete layer of bubbles. [c] Reagent first dissolved in equal volume of absolute ethyl alcohol.
[d] Stability: Data measured at end of 6-min aeration.

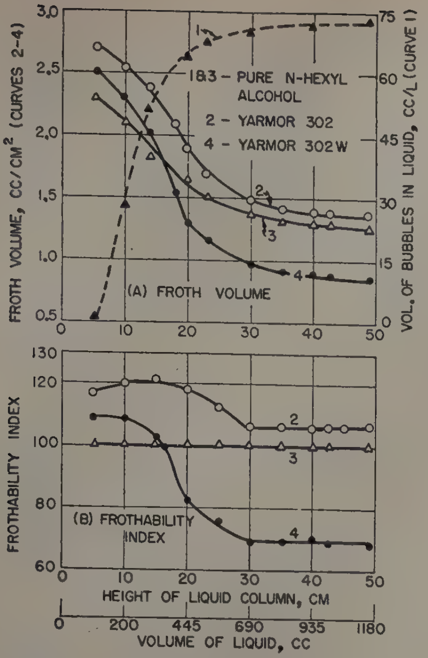

Fig. 4—Effect of height of liquid column on frothabilities of pine oils and pure n-hexyl alcohol.

pine oils are roughly constant and independent of the height of liquid column between 30 and 50 cm.

Chemical Composition of Pine Oil

Pine oil is a complex mixture of terpene derivatives.[3-5] The chemical properties and frothabilities of the principal constituents of pine oil are given in Table III. It can be seen from this table that the frothing power of the constituents in neutral and acid solutions generally decreases in the following order: tertiary alcohols, secondary alcohols, ketones, ethers, and finally hydrocarbons. Since the chemical structure and the number of carbon atoms of the nonpolar groups of these constituents are somewhat similar, the difference of frothability is caused chiefly by the variation of the polar group and solubility. The double bond of the nonpolar group does not influence the frothability significantly.

In regard to the polar group, the hydrophilic property of the hydroxyl group, C-OH, connected to one carbon by a single bond may be slightly larger than that of the oxygen of the carbonyl group, C = O, connecting to one carbon by a double bond. The oxygen of ether group, C-O-C, enclosed by two carbon atoms should have the least affinity for water. Judging from the fact that all the nonpolar groups of the constituents containing more than eight carbons are very water repellent,[6] the polar group must have a strong affinity for water to pull the organic molecule into the air-water interface.[7] In this case the frothing power of these polar groups is OH> CO>COC.

Similarly, the frothabilities of the constituents are increased to a certain extent with the increase of their solubilities. According to Gaudin,[8] the desirable range of solubility for frothers is from 0.2 to 5 gm per liter. Cols. 5 and 8 of Table III bring out two significant points. First, the frothing powers of the less soluble components are increased greatly with the resulting increase of solubility by dissolving them in an equal volume of absolute ethyl alcohol before they are introduced into an aqueous solution. Second, when two chemical compounds have a similar structure, the one with the larger solubility is usually more frothable than the other. This is illustrated by the fact that betaterpineol and camphor, respectively, are more frothable than alpha-terpineol and fenchone.

Table IV. Approximate Chemical Composition of the Different Grades of Pine Oil

Components	Percentage of Components in		
	Yarmor-302	Yarmor-F	Yarmor-302W
Tertiary alcohol, chiefly alpha-terpineol, and a small amount of beta-terpineol, terpinen-4-ol, and dihydro-terpineol	76-80	55-65	58-63
Secondary alcohols, borneols and fenchyl alcohol	8-12	10-20	9-10
Ketones, fenchone and camphor	6-8	5-10	2-4
Ethers, anethole and estragol	4-6	5-10	2-3
Hydrocarbons, monocyclic terpenes as terpinolene, dipentene, camphene, and pinene		10-20	20-30
Moisture		0.4	0.2
Total alcohols	86	75	70

Compared with the important part played by the polar group and solubility, the influence on frothability of the double bond of the nonpolar group is insignificant. For example, camphor, a good frother, has no double bond. The low frothability of dihydro-terpineol was formerly attributed to the lack of a double bond.[3] However, this may be caused by the low solubility instead, since it is found that the frothability of dihydro-terpineol is improved greatly by the increase of solubility with ethyl alcohol. The frothability of ethyl alcohol itself was found to be insignificant.

The frothabilities of Yarmor-302, Yarmor-F, and Yarmor 302W pine oil, as shown in Table III decrease in the same order. Based on the above discussion, this is considered to be caused by the difference of chemical composition of the various grades of pine oil. The frothability of the one with more frothable components, tertiary and/or secondary alcohols, should be higher than the other with more nonfrothable components, hydrocarbons. This is substantiated by the analytical data of Table IV. The data indicate that Yarmor-302 is characterized by its high content of tertiary alcohols and low percentage of hydrocarbons. Compared with Yarmor-302, Yarmor-302W contains less tertiary alcohols and more hydrocarbons; whereas Yarmor-F is intermediate in composition. This explanation is justified further by the experimental evidence, not shown, that the frothability of Yarmor 302W pine oil was increased

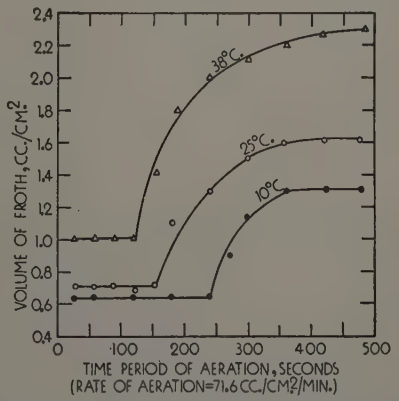

Fig. 5—Effect of temperature of solution on the frothability of Yarmor-F pine oil at 94.15 mg/liter concentration.

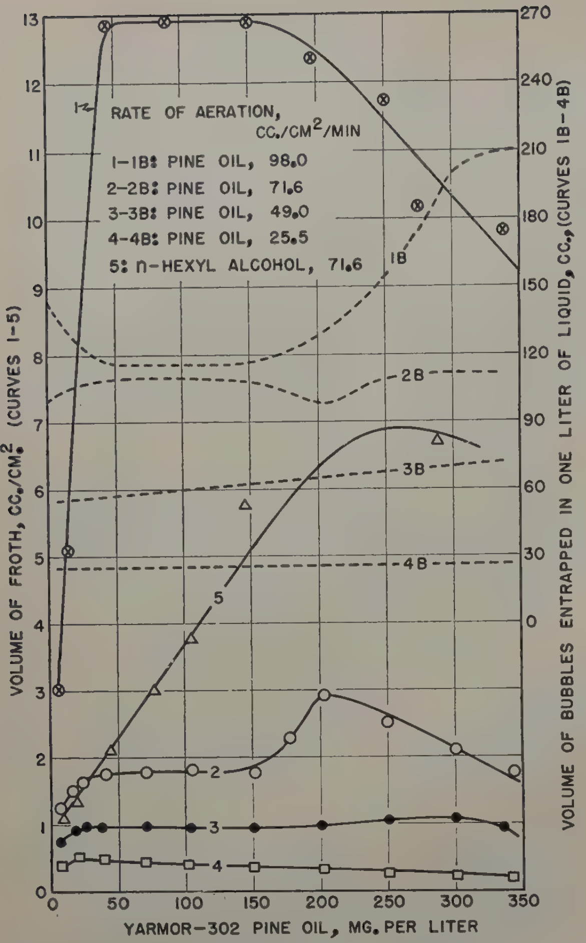

Fig. 6—Effect of concentration on the frothability of Yarmor-302 pine oil at various rates of aeration.

by blending it with alphaterpineol and decreased with the addition of beta-pinene.

pH Values

The effect of pH on the frothability of the different grades of pine oil and its principal constituents, as listed in col 8 of Table III, is very significant when the aqueous solutions are alkaline. Generally, the frothabilities of pine oils and their constituents are affected only slightly by changes of pH values from 3.4 to 8 and start to increase at pH 8.5 until reaching their maxima at pH 11 or higher. This is considered to be caused chiefly by the increase of solubility and the increase of frothing power of distilled water itself at higher pH values.

Table V shows that the solubilities of pine oil Yarmor-302, camphor (ketonic compound) and borneol (secondary alcohol) increase with the increase of pH value. According to the work of Williams[9] and Dickinson,[10] the surfaces of the inert hydrocarbons, alphatic esters, and alphatic halides in solutions of high pH value absorb hydroxyl ions and thus increase their affinity for water. This ought to be true also for pine oils and their components. As explained in the section on chemical composition, with pine oils and their components, particularly the less and nonsoluble ones, the frothability increases with the increase of the solubility. The increase of froth owing to the increase of solubility is reinforced further by the increase of frothability of water itself at high pH value, as shown in the last line of Table III.

Table V. The Effect of pH on the Approximate Solubilities of Pine Oil, Camphor and Borneol at Room Temperature, in Gm per Liter

	Solubilities at Different pH Values			
Chemical Compounds	3.3	7.0	11.0	12.0
Pine oil, Yarmor-302	1.390	1.602	1.602	1.747
Camphor	1.532	1.577	1.673	1.631
Borneol	0.651	0.704	0.876	0.857

Solution Temperature

It is well known to the flotation mill operator that more frothing reagent is required in winter than in summer. The data of Fig. 5 indicate that, to a certain extent, the volume of froth produced by a given amount of pine oil increases with the temperature of the liquid; whereas the time of aeration, required to start a marked increase of froth, decreases with the temperature. Low temperature results in 1—high viscosity and high surface tension of pine oil and liquid and 2—low solubility of pine oil. Therefore, the dispersion and orientation of pine oil in the air-liquid interface, and the sharp decrease of surface tension[11] of the solution are retarded. These deleterious effects can be remedied by a longer period of agitation, aeration or both, in conjunction with the use of more pine oil.

Frother Concentration in Solution

Curves 1 to 4 of Fig. 6 show that the volume of froth increases with the addition of certain amounts of pine oil and that further additions of pine oil decrease the frothing action. Curve 5 indicates that the same thing is also true for n-hexyl alcohol. An explanation of this phenomena can be found in the published literature.[11] The amount of pine oil employed in actual flotation, as currently practiced, is far below the critical concentration that will depress the frothing action. For example, 17 mg per liter pine oil corresponds roughly to 0.14 lb per ton ore in a pulp containing 18 pct solids. Fig. 6 shows also that at high rates of aeration, curves 1B and 2B, the volume of bubbles entrapped in liquid is somewhat inversely proportional to the volume of froth. At the moderate rate of aeration, curve 3B, the volume of bubbles in liquid is somewhat increased with the concentration of pine oil; whereas, at the low rate of aeration, curve 4B, the volume of bubbles is practically independent of pine oil concentration.

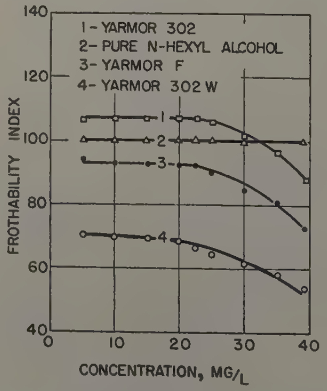

Fig. 7—Effect of concentration on the frothability indices of pine oils at an aeration rate of 71.6 cc/cm²/min.

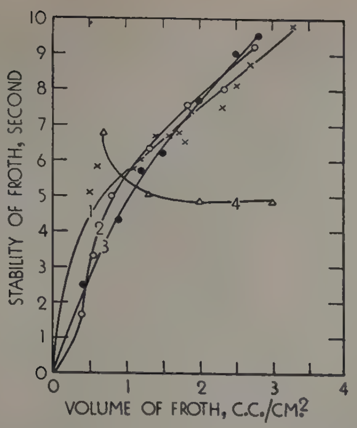

Fig. 8—Relation between stability and volume of froth.

Curve 1: Yarmor-F pine oil at different concentrations.
Curve 2: Beta-terpineol (27.8 mg/liter) at different rates of aeration.
Curve 3: Yarmor-302 pine oil at different pH values.
Curve 4: Yarmor-F pine oil at different heights of liquid column.

Fig. 7 shows that the frothability indices of pine oils are roughly independent of the concentration between 3 and 23 mg per liter. For the purpose of comparing the frothabilities of different frothers, it is desirable to stay in this range of concentration, and this practice was followed in Table II.

Curves 1, 2, and 3 of Fig. 8 show that for a given height of liquid column the stability of froth is generally proportional to the volume of froth, provided that the frothers used are of the same type. The collapse of bubbles proceeds gradually from the top to the bottom of the froth layer, and consequently, the time required for a total collapse is proportional to the thickness of the froth. This relationship does not hold for curve 4, which embodies data from tests with different heights of liquid column as partially shown in Fig. 4a. This is attributed to the fact that immediately after the air was shut off, the entrapped bubbles in the liquid rose to the surface to increase the thickness of the froth layer. Consequently, the stability of froth of a high liquid column containing less froth but more entrapped bubbles will be similar to or even higher than that of a low liquid column containing more froth but less bubbles in the liquid.

Flotation

To find how the relative frothabilities determined by the frothmeter will correlate with that in actual flotation, a Pittsburgh bituminous coal slurry was tested with different pine oils in a laboratory Fagergren machine. The results, given in Table VI, show that the coal recovery decreases in the order of Yarmor-302, Yarmor-F, and Yarmor-302W pine oil. These are in agreement with the data of frothability listed in Table III.

Table VI. Flotation of Pittsburgh Coal Slurry with 0.2 Lb per Ton Pine Oil, at 7.2 pH, 7.7 Dilution, and 4-Min Flotation

Test	Pine Oil	Coal Recovery, Weight, Pct
1	Yarmor-302	68
2	Yarmor-F	60
3	Yarmor-302W	51

Sucked Air and Vacuum Frothing

After a series of tests, under the same environments, the results of sucked air frothing were practically the same as that of compressed air frothing. Sucked air frothing can substitute for compressed air frothing whenever compressed air is not available.

The test data of vacuum frothing, not presented here, indicate that the effect of concentration and grade of pine oils on their frothabilities also can be detected by vacuum frothing. Vacuum frothing differs from both compressed air frothing and sucked air frothing in that the amount of air stored in the air-saturated liquid and in the empty space of glass cylinder is limited. After a short period of continuous frothing of small bubbles, the air is practically used up, and the remanent air is scant and capable only of providing intermittent large bubbles. The rate of degassing is directly proportional to the magnitude of the vacuum system. A high vacuum capable of quick degassing induces an earlier but shorter period of continuous frothing, as compared with a low vacuum.

Acknowledgment

The writer wishes to express his appreciation to Leslie U. Anderson for his kind assistance in the testing work. Thanks are due to W. T. Bishop of the Hercules Powder Co., Wilmington, Del., for his courtesy in supplying the necessary pine oils and their components, and to R. D. Hinkel for his kind assistance in the construction of the frothmeter. Thanks are also due to D. R. Mitchell and R. E. Zimmerman for their heartening encouragement and active interest in the prosecution of this work.

References

[1] Shiou-Chuan Sun: The Frothing Characteristics of Cresylic Acids. Paper presented at the AIME Annual Meeting, St. Louis, Mo., February 1951.

[2] Shiou-Chuan Sun and R. E. Zimmerman: The Mechanism of Coarse Coal and Mineral Froth Flotation. *Trans.* AIME (1950) **187**, p. 616; MINING ENGINEERING (May 1950) TP 2843F.

[3] W. T. Bishop: The Properties of Pine Oil Related to Flotation. *Trans.* AIME (1946) **169**, p. 379; MINING TECHNOLOGY (March 1946) TP 2011.

[4] R. C. Palmer: Developments in Terpine Chemicals. *Industrial and Engineering Chemistry* (September 1942) **34**, p. 1028.

[5] O. A. Pickett and J. M. Schantz: New Uses of Naval Stores Products. *Industrial and Engineering Chemistry* (July 1934) **26**, p. 707.

[6] A. F. Taggart, T. C. Taylor, and C. R. Ince: Experiments with Flotation Reagents. *Trans.* AIME (1930) **87**, p. 285.

[7] R. S. Dean and A. B. Hersberger: New Flotation Reagents. *Trans.* AIME (1939) **134**, p. 81.

[8] A. M. Gaudin: *Flotation.* P. 62 (1932) New York, McGraw-Hill Book Co.

[9] G. C. Williams: The Electrophoresis of Certain Hydrocarbons and Alphatic Esters as a Function of pH. *Trans.* Faraday Society (1940) **36**, p. 1042.

[10] W. Dickinson: The Effect of pH Upon the Electrophoretic Mobility of Emulsions of Certain Hydrocarbons and Alphatic Halides. *Trans.* Faraday Society (1941) **37**, p. 140.

[11] A. F. Taggart and A. M. Gaudin: Surface Tension and Adsorption Phenomena in Flotation. *Trans.* AIME (1923) **68**, p. 479.

[12] A. Seidell: Solubilities of Organic Compounds. (1941) New York, D. Van Nostrand Co.

Illinois Operations Of The Eagle Picher Mining and Smelting Co.

by C. O. Dale and W. J. Rundle

THE upper Mississippi Valley zinc-lead area was the first major lead-producing section in the United States. The lead ore, found near the surface in crevices, was relatively pure galena that could be smelted directly into lead, at first in log hearth furnaces and later in more efficient blast type furnaces.

French Canadian fur traders encouraged the Indians to mine the lead ore and showed them how to smelt it into lead that had a high value for bullets.[1] Nicholas Perrot found lead ore on the Mississippi River bluffs near the junction of Wisconsin and Illinois and in 1690 established a trading post on the Wisconsin side of the river opposite the present site of Dubuque, Iowa.[2]

Shortly after 1720 discovery of Mine La Mott in Missouri diverted considerable attention from the Upper Mississippi area. Mining continued on a desultory basis with operations concentrated in the Galena, Illinois-Dubuque, area. In 1740 at least 20 miners were at work in the Fever River area around Galena and are reported to have shipped 2500 70-lb pigs of lead to Kaskaskia in 1741.[3]

Julien Dubuque established a mining and smelting operation in 1790 near the city that bears his name and was granted sole right to exploit the mining operations on the lands of the Sauk and the Fox Indians. He is reported to have produced 30,000 70-lb pigs of lead in 1805. Following the death of Dubuque in 1810 the Indians refused to let the white miners enter their lands, and little was done on the Iowa side of the river until the Indians were removed by treaty with the United States government in 1832.[4]

Early mining was entirely for lead but as the crevices were followed down, increasing percentages of zinc sulphide and zinc carbonate were encountered and at first discarded. Later a market became available for the zinc ores, and hand jigging devices were made to separate the lead, the zinc, and the rock or waste materials. The first record of zinc production from the area is for 1860. Production of zinc passed that of lead before 1900, reached a peak of 64,000 short tons in 1917, fell off rapidly and continually to about 2000 short tons in 1938, and since 1940 has ranged from 11,000 to 19,000 short tons. Lead has been of considerably less importance since 1900, and at present only about 10 pct as much lead as zinc is produced. Practically all of the zinc ore has come from orebodies that are rather flat and wide with considerable length as compared to width. Most of the early lead came from the crevice type deposit, but present production is from the predominately flat zinc orebodies. The Graham-Snyder orebody, scene of Eagle Picher operations, is practically all zinc with little or no lead being recovered. Marcasite, present in varying amounts, makes production of finished concentrates by gravity separation impractical. Satisfactory lead and zinc concentrates have been produced since flotation was introduced in the area in 1927. An acid recovery plant was operated for about 20 years after World War I, but it has been dismantled, and no recovery of the iron sulphides in the ores of the district is being made at the present time.

In June 1950 there were three companies operating mines and mills, Tri-State Zinc Co., Calumet & Hecla Consolidated Copper Co., and Eagle Picher Mining and Smelting Co. The Vinegar Hill Zinc Co. had completed a shaft at a new orebody and had started to develop the mine which will supply the Cuba City mill. The Cuba Mining Co. was holding the Andrews Mine inactive. The Dodgeville Mining Co. was not operating but was exploring for additional reserves. Several small mines were selling ore to the Eagle Picher mill. A general area map is given in Fig. 1.

The Eagle Picher Mining and Smelting Co. entered the area in 1946 with an active exploration campaign. Leases on a block basis were secured for the area south from the Wisconsin-Illinois line near

C. O. DALE, Member AIME, is Chief Engineer with the Eagle Picher Mining & Smelting Co., Galena, Ill. W. J. RUNDLE, Member AIME, is Assistant Professor, Department of Mining, University of Wisconsin, Madison, Wis.

Discussion on this paper, TP 3224A, may be sent to AIME before Feb. 28, 1952. Manuscript, Nov. 14, 1950. St. Louis Meeting, February 1951.

Hazel Green, Wis. From this work the Graham-Snyder orebody was located and developed into the present state of production.

Shaft sinking was started in November 1947; underground development began as soon as the shaft was bottomed in June 1948. The mill and surface plant were completed and production started in April 1949. In the first twelve months, 198,135 tons of ore were hoisted and milled.

Prospecting

Leases were secured to an area large enough to permit area drilling so as to build up a structural pattern for the area. After an intensive study of the geology of the area, old drill records and mining records, a drilling pattern was established and information correlated to permit interpretation of drill results.

Figs. 2 and 3 show typical sections in ore zones. It is believed that flexures in the underlying Trenton limestone caused zones of weakness in the overlying glass rock, oil rock, and blue and grey limestone. Solutions entering these zones of weakness took some of the limestone into solution and caused slumping and fracturing in these beds. These fractures and crevices gave access for formation of ore from mineralized solutions. The ore is found generally in places where the top of the Trenton is raised as compared to adjacent areas, and the glass rock and oil rock are thinner in these mineralized areas than elsewhere.

Holes are spaced on a square grid at intervals of 660 ft. Drill cuttings are logged in 5-ft intervals above the Grayrock and in 2½-ft intervals in the Grayrock and below into the top of the Trenton where the holes are stopped. Intervals of 2½ ft are used wherever mineralization is noted in the cuttings. Samples are taken for analysis from each interval that shows any mineralization.

Where mineralization is found, additional holes are drilled as needed to outline and sample the mineralized area. Tonnage and grade estimates are made from these sections that usually are about 100 ft apart.

All drilling is done with a churn or well drill with the drill cuttings serving as the record for the hole. Cuttings are bailed out and dumped into a series of piles representing sample intervals. The piles are sampled by taking a channel sample through the pile. Contract price for drilling is $1.40 per ft of 5¼-in. hole. A section of pipe which protects livestock from the open hole is set in the top of each ore hole and rises about 3 ft above the ground. The sleeve keeps the hole open so that it can be used for ventilation when mining operations reach it.

Diamond drilling did not prove satisfactory due mainly to difficulty in getting a good core.

Development

Shaft sinking was started in November 1947, after ore reserve calculations for the Graham-Snyder orebody indicated sufficient tonnage to warrant development. The Graham shaft, which serves as the main hoisting shaft, is 5½x16 ft inside and is 266 ft from the collar to the level below. A concrete collar extends down about 30 ft below the surface, and no support is used below the collar except the spreader timbers, which hold the skip guides. The Graham-Snyder mine is shown in Fig. 4.

A Red Giant hoist set directly over the shaft on a 30-ft derrick served during sinking operations. Muck was hoisted in a can 32 in. in diam by 32 in. high. The cans were watched by the hoistman who dumped them by upsetting them into a hopper by means of a cable that he hooked onto the bottom of the can when it reached the dumping position in the derrick. A sloping door in the derrick served to prevent spillage down the shaft while dumping. This arrangement has been standard in this area and in the Tri-State district for some time.

The standard shaft round was a *V* center cut with eight 7-ft holes drilled together at the bottom of the *V*. The *V* cut holes were backed up by three rows of 6-ft holes at both ends of the shaft. A total of 32 holes requiring about 200 lb of powder were used for each round which averaged about 5 ft. When water was encountered it was found advisable to shoot the *V* cut first and to muck it out before firing the remainder of the round. This reduced the possibility of a misfire spoiling the entire round. Blasting was done with electric caps after a protective cushion of 15 to 25 ft of water had been allowed to cover the tops of the holes.

A quantity of water was encountered in the shaft at 85 ft. A churn drillhole had been drilled 4 ft off the south end of the shaft and a 4-in. Pomona pump installed in the hole. Four-inch jackhammer holes were drilled in the end wall of the shaft into the churn drillhole to drain the water away but the 4-in. pump was not able to handle the inflow of water. A second churn drillhole was drilled and reamed to 16 in. at a point 60 ft north of the shaft, where it was planned the permanent mine sump would be. A 14-in. Pomona pump, belt-connected to a 200-hp L-type Cummins diesel engine added 2500 gpm of capacity. This kept the water down for a few feet farther, but more pumping capacity was soon needed. Because of the inability of the local power company to furnish sufficient power, a 350-kw diesel generator set was ordered.

Pending delivery of the generator unit, work on the Snyder shaft, 750 ft north of the Graham shaft, was started. A sinking derrick was erected and the shaft sunk to a depth of 83 ft where water was encountered. Because of bad ground conditions, the collar of the Snyder shaft was concreted to a depth of 50 ft. Sinking of the Snyder shaft then was held up until the Graham sinking had been completed.

While waiting for the diesel generator set to be installed, a 10-in. Pomona pump was installed in the reamed-out hole that had held the 4-in. Pomona. Another hole was drilled at the north end of the Graham shaft and a 12-in. Pomona pump installed in it. As soon as the generator unit was installed, these pumps were started and sinking resumed. It was soon evident that more pumping capacity was needed so a Byron Jackson 12-in. sinker pump was hung in the shaft. The shaft was completed to a depth of 267 ft in June 1948, with the following pumping equipment in operation: 14-in. diesel driven Pomona, 2500 gpm; 12-in. electric driven Pomona, 1200 gpm; 10-in. electric driven Pomona, 700 gpm; 12-in. electric driven Byron Jackson sinker, avg 1000 gpm; total, 5400 gpm.

Station cutting was started immediately, and a drift north to the Snyder shaft got under way as soon as possible. Water in the shaft had abated enough to permit removal of the Byron Jackson sinker which was then installed in the Snyder shaft.

Sinking was resumed in the Snyder shaft on July 5, 1948, but the pumping capacity was not enough

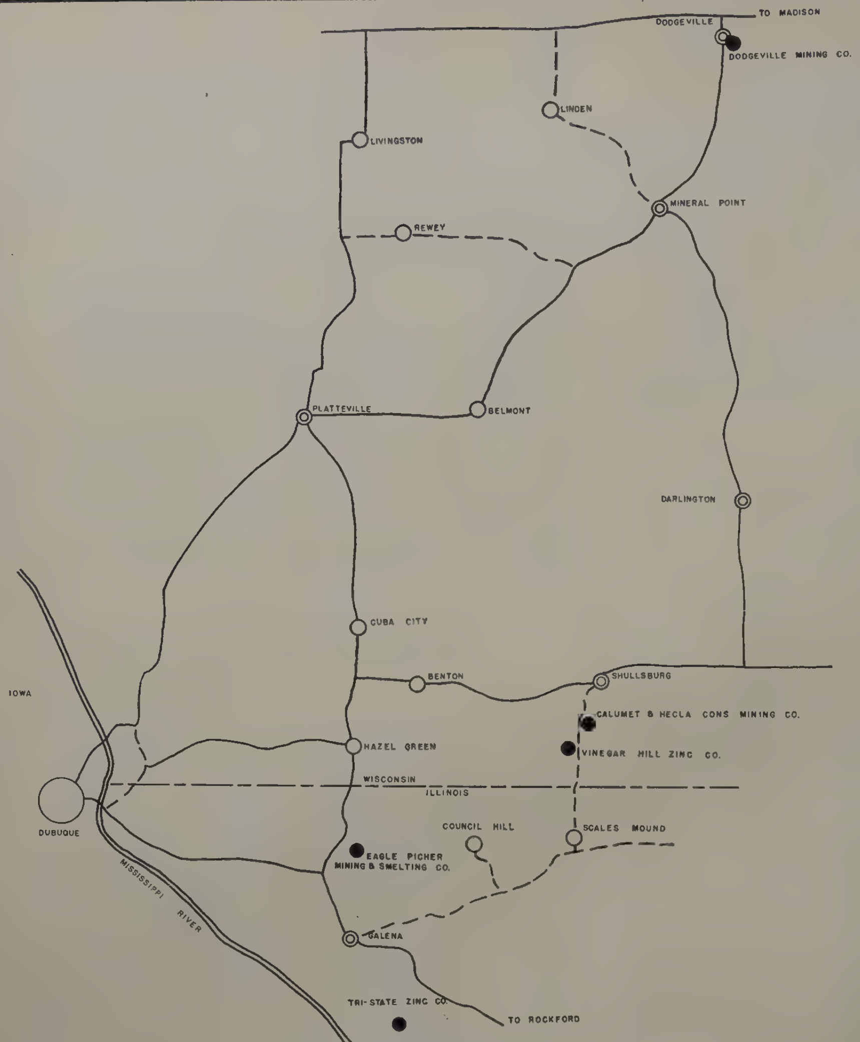

Fig. 1—Map of general area.

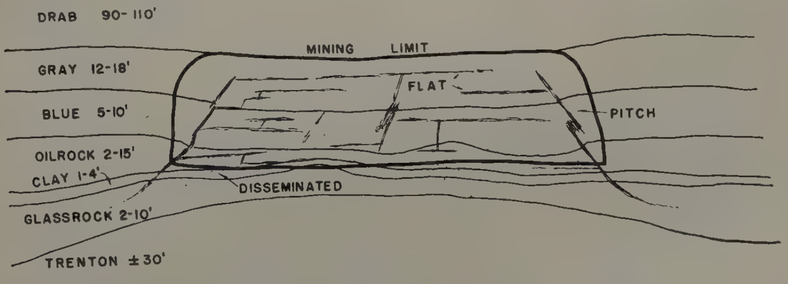

Fig. 2—Typical section through Graham orebody Eagle Picher Mining and Smelting Co., Galena, Ill.

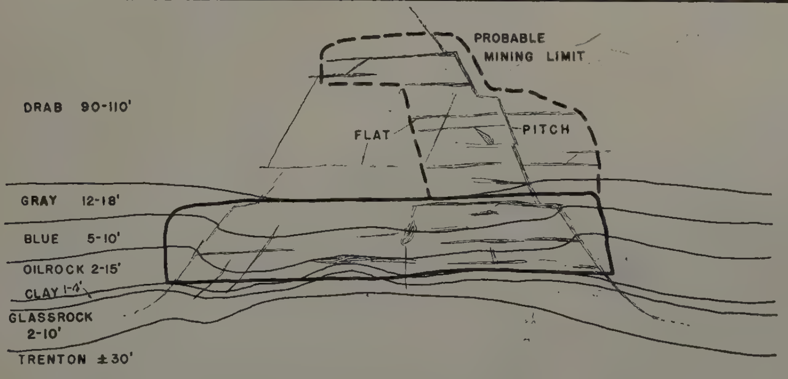

Fig. 3—Typical section through Snyder orebody, Eagle Picher Mining and Smelting Co.

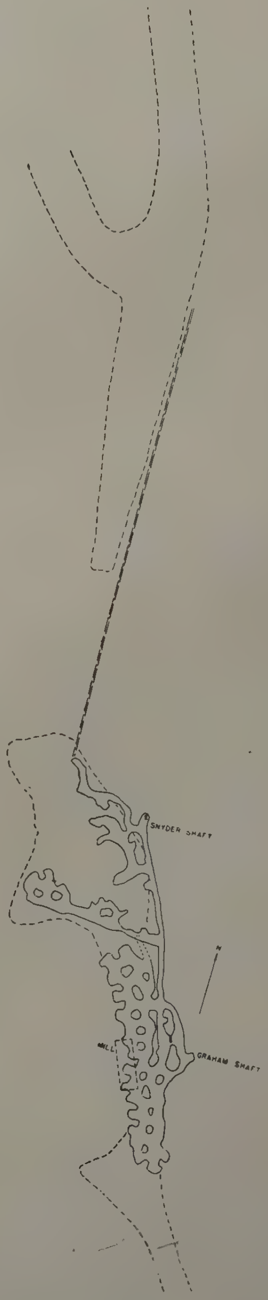

Fig. 4—Graham-Snyder mine, Eagle-Picher Mining and Smelting Co., February 1950.

Scale: ½ in. is approximately 300 miles.

to keep the water out. Since the generator set was taxed to capacity, it was necessary to halt sinking operations until additional power became available. The two 1000-kw diesel generators were available early in October. With this additional power two 12-in. Pomona pumps were installed in holes at each end of the Snyder shaft, and the shaft was bottomed at 242 ft near the end of October. A drift to connect with the Graham drift was started immediately.

At this time it was deemed advisable to attempt to lower the water level in the orebody as quickly as possible. A drillhole in the orebody near the Snyder shaft was reamed to 16 in. and a 3000-gpm, 200-hp Pomona pump installed. From the middle of December 1948 until the middle of April 1949 the total pumping load was slightly over 10,000 gpm. At the end of this period the water began to slack off slightly, and pumps were taken out of service as permitted until at the present time there is a pumping load of about 4000 gpm.

Drifting between the two shafts was done with post-mounted DA 35 drills and Model 12B, 6 cu ft, Eimco air mucking machines. Cans set on small rail-mounted trucks transported the muck from face to shaft. A ropeline was used to tram the cars underground. The drift has a cross-section of 12x14 ft so that it was not necessary to enlarge it when the rail transportation was replaced by diesel trucks. This drift followed the east side of the orebody and served as an attack point when mining started. Ore mined in this drift was stockpiled on surface until the mill was completed. After the connection between the shafts was finished and enough space opened up to permit diesel operation underground, an Eimco Rockershovel mounted on a D4 Caterpillar tractor was used for loading. This unit loaded into temporary hoppers which in turn loaded cans for tramming and hoisting. This arrangement served for about 3 months at which time trucks and skips replaced the hoppers and cans.

In April 1949 the Graham shaft was deepened 55 ft in preparation for skip hoisting. Compartments were formed by the installation of four 8x8 in. spreaders hitched into the shaft walls on 6 ft, 8 in. centers to give two skip compartments each 5x5½ ft and a 3x5½ ft manway compartment. Twenty-foot lengths of 6x6 in. fir guide timbers were fastened to the spreaders by 9-in. lag screws. This work was done with the sinking hoist handling men and materials except that a small hoist was used to lower the timbers. Work started at the bottom and progressed upward with each set serving as a platform for the men to work on while installing the next set above.

A 115-ft A-type steel headframe was erected over the shaft, and a Kimberly type steel dumping structure was erected on top of the two concrete mine ore bins, which are each 24x20x30 ft. Ore can be sent to either bin by control of an electrically operated flapper gate.

Maximum speed is 600 fpm with 4-ton capacity skips. This single drum, counterbalance installation has worked very satisfactorily; however, one of the cables has to be cut off about 2 ft every 3 or 4 months because of rope stretch. This keeps one skip in dumping and the other in loading positions.

A temporary timber skip pocket was constructed on the opposite side of the shaft from the permanent pocket future location. The first skipload of ore was hoisted on July 1, 1949. At this time rail tramming and can hoisting was stopped, and two 5-ton Dart diesel trucks were introduced for tramming from the Rockershovel to the skip pocket. The Snyder shaft now serves as a ventilation entrance and for lowering large pieces of equipment. The skips can handle easily 150 tons per hr whereas can hoisting was never able to produce more than 50 to 60 tons per hr.

In July 1949 work was started on the permanent skip pocket while the temporary pocket was being used for ore hoisting. Excavation for the 80-ton skip pocket was done with extreme caution to eliminate overbreak and to protect the shaft timbers and temporary pocket. It was excavated and concreted in stages to cut down on the amount of open ground and to spread the handling of the muck over the entire excavation period. This decreased interruption to ore hoisting from the temporary pocket. Ready-mixed concrete was chuted down a 6-in. pipe in the shaft into a remixer at the station, which had spouts reaching to the various parts of the permanent pocket.

Power for the operation comes from two 1000-kw

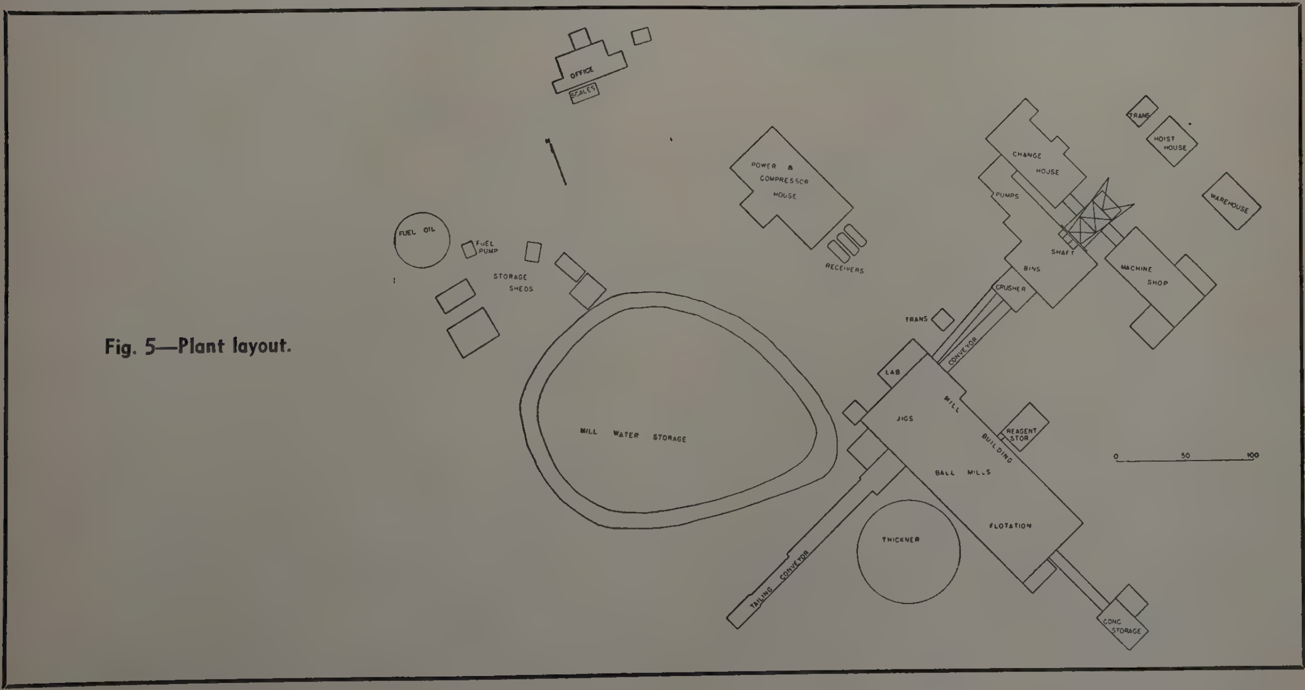

Fig. 5—Plant layout.

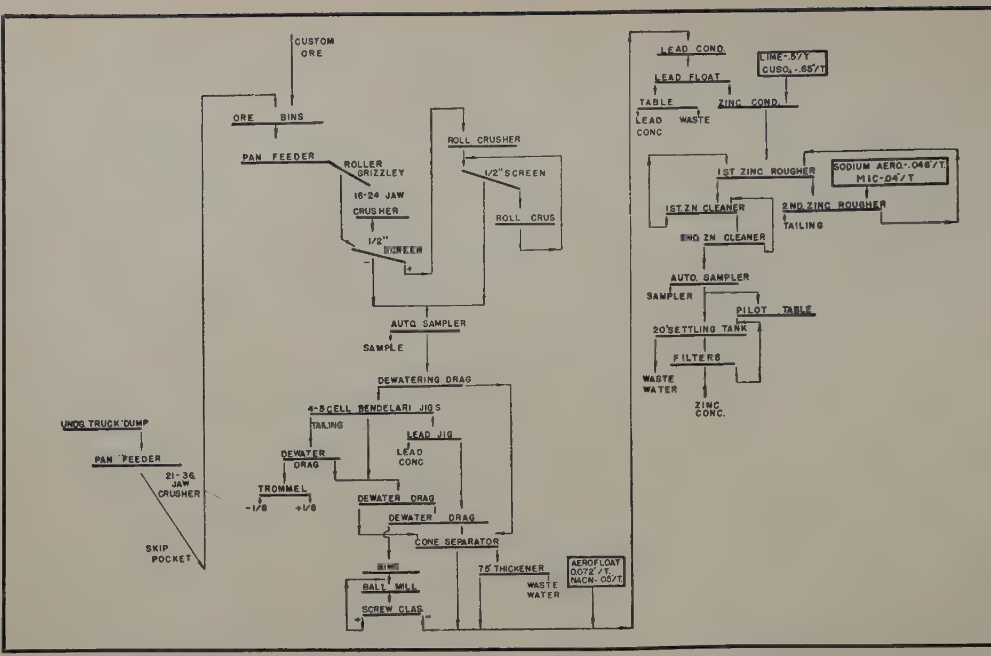

Fig. 6—Mill flowsheet.

generators directly connected to 16-278 General Motors diesel engines and one 300-kw generator directly connected to an 8-268A General Motors diesel engine. The units are controlled automatically and balanced to share the load. The small unit is kept in readiness as a standby unit, and in case of a breakdown of either of the large units, it can be used with the other large unit to supply enough power to keep the plant going. Power is generated at 2300 v, three-phase, 60 cycles. Fuel oil is metered to the engines from a 200,000-gal storage tank. The average cost for power has been about 1½¢ per kw-hr. An emergency standby connection is maintained with the local power company to permit operation of plant lights, shaft signals, and a few small motors. Electrically driven compressors of 1190 cfm and 880 cfm are located in the diesel power house. An additional 600 cfm machine, which was used for shaft sinking and which is powered by a 150-hp diesel engine, is held as a standby unit in a building adjacent to the machine shop.

The machine shop is located near the shaft collar and is equipped to forge drill rods and to repair and maintain all of the equipment used in the operation as well as to build special items. The plant layout is shown in Fig. 5.

Mining

Air-operated, crawler-mounted jumbos mounting two DA-35 drifters on 10-ft sashes and with a 10-ft boom are used for most of the drilling in the orebody. Two miners are assigned to each unit and average 190 ft of hole per shift or about 160 tons per shift. Ten-foot slabbing holes are drilled. Blasting is by electric cap using 40 pct gelatin dynamite. The jumbos can drill holes in a face up to 15 ft high and can be run up onto a muck pile to drill higher holes. In the Graham, or South section, of the mine where the ore is from 12 to 20 ft high the jumbos are used exclusively. Part of the Snyder section of the orebody is over 100 ft high and is drilled with jackleg and post-mounted machines at the top, with jacklegs or tripod-mounted drifters on the benches and with the jumbos for the lower holes. A jumbo with an 80-ft boom is under consideration for the Snyder section.

Three Model 104, 1¼ cu yd, tractor-mounted Eimco Rockershovels are available for loading three 5-ton Dart diesel trucks and one 7-yd Koehring Dumptor diesel haulage unit. One Rockershovel, if supplied with empty trucks, ordinarily loads about 400 tons per 8-hr shift, with a maximum of 698 tons being loaded in one shift with one Rockershovel.

Trucks dump onto a 20x32-in. rail grizzley mounted over a 15-ton hopper. Ore in the hopper is fed into the Rogers 21x36-in. jaw crusher by a 3x10-ft pan feeder. The crushed ore drops into the skip pocket and is loaded into the skips through air-operated guillotine gates and chutes. The skips then hoist the ore to the surface where they are dumped through the Kimberley dump into the mine ore bins, which are adjacent to the shaft.

Arrangements were provided for custom ore by including two bins immediately adjacent to the mine ore bins with truck ramps leading up to either side of these bins. Any of the four bins can be emptied by a pan feeder running underneath them, which dumps into a roll grizzly. The grizzly oversize dumps into a secondary crusher and the ore goes from there to the mill circuit.

Fig. 6 shows the mill flowsheet that is a standard flowsheet for ores in this district. It includes primary and secondary rolls, sample, cutter, Bendelari jigs, ball mill circuit, and flotation circuit. Approximately 50 pct of the waster is rejected on the jigs. The zinc recovery runs from 85 to 90 pct.

The warehouse is stocked with the minimum amount of repair items consistent with economical practice, however, this runs into a sizable amount because of the variety of necessary items and the frequent repairs.

Acknowledgment

The authors are indebted to the Eagle Picher Mining and Smelting Co. for permission to prepare this report.

References

[1] R. G. Thwaites: Notes on Early Lead Mining in the Fever River Region. Wisconsin Historical Collection.

[2] H. Foster Bain: Zinc and Lead Deposits of the Upper Mississippi Valley. Reprinted 1907 by the Wisconsin Geological and Natural History Survey.

[3] T. A. Ricard: A History of American Mining. (1932) AIME Series, New York, McGraw-Hill Book Co.

[4] W. J. Rundle: Mining Operations In The Upper Mississippi Valley Zinc-Lead Area. 1950. An unpublished thesis report. University of Minnesota Library.

Dimension Stone in Minnesota

by G. M. Schwartz and G. A. Thiel

Dimension stone was first quarried in Minnesota in 1820 and a very active industry has grown up over the years. The main basis of the present industry is a wide variety of igneous rocks sold under the general trade name of "granite." Also of considerable importance is the Ordovician dolomite sold under the locality names, Mankato, Kasota and Winona.

THE first record of the quarrying of dimension stone in Minnesota dates back to 1820 when limestone was quarried locally for part of old Fort Snelling. Limestone quarries were operated at Stillwater, Mankato, and Winona as early as 1854. Granite was quarried first at St. Cloud in 1868, and within a few years thousands of tons were shipped to widespread points. Rough dimension stone for large buildings furnished the first important market, but beginning in 1886 paving blocks were in demand. The largest shipment was in 1888, when 1925 cars were shipped from the St. Cloud area. Quartzite was quarried first at New Ulm in 1859 and somewhat later at Pipestone and elsewhere in southwestern Minnesota. The productive dolomite quarries at Kasota were opened first in 1868 and have continued as large producers of a variety of stone to the present time.

At present, the industry is controlled by relatively few operators, and for that reason detailed figures on dimension stone are not released for publication. A general idea may be obtained from the data in the *Minerals Yearbook* for 1948. The figures for total stone produced in Minnesota are 1,804,000 tons valued at $5,090,652. Probably the largest item in the latter figure is received from dimension stone. A better idea of the situation in relation to the country as a whole may be gained by using the data for 1930 when more companies were operating in Minnesota, and complete figures were published. In that year Minnesota produced granite valued at $2,668,119 and ranked third among the states in value. Minnesota's production of granite was almost exclusively for dimension stone. In the same year Minnesota produced 300,000 tons of limestone (dolomite) valued at $840,860, and this likewise was mainly dimension stone. In finished limestone Minnesota ranked second among the states in 1930.

Sandstone and minor amounts of quartzite are the only other dimension stones that have been produced in Minnesota, but the quarries are now inactive.

The commercial stones of Minnesota have been described in two reports by Bowles[1] and by Thiel and Dutton.[2] The early history of quarrying in Minnesota and extensive notes on the various rocks are given by N. H. Winchell.[3]

Small limestone and dolomite quarries were numerous throughout the area of Paleozoic rocks in southeastern Minnesota. Early production was largely dimension stone. With the increased use of Portland cement, most of these ceased production, and today only those at Kasota and Winona remain in operation. In recent years many quarries have reopened and new ones started, but these are devoted to the production of crushed rock and agricultural lime.

As the application of modern quarrying and finishing methods increased, small companies in the granite business have dropped out, and the remaining companies have modernized their plants, purchased old quarries, and opened up new ones, thus furnishing a wide variety of granites suitable for most of the customary uses.

It is the purpose of this review to present notes on the geology and operations of each of the quarries now operating within the state.

Granites and Related Igneous Rocks

The term granite as used in this report includes granites, gneisses, diorites, gabbros, and other igneous rocks. The granites of greatest economic importance are found in three widely separated regions, see Fig. 1. 1—Central Minnesota in the region of the city of St. Cloud, 2—the upper Minnesota River valley region, 3—the northeastern portion of the state, commonly referred to as the Arrowhead region.

The St. Cloud Region: The rocks of the St. Cloud region are mainly granites and related rock types such as monzonites and quartz diorites. The stones may be grouped into three major types, namely, pink granite, red granite and gray granite.

Most of the pink granite occurs in the area to the southwest of St. Cloud. The rock is best described as stone with large pink crystals set in a finer grained black and white background. The minerals of the matrix occur in remarkably uniform sizes, and the pink crystals are sufficiently uniform in their dis-

---

G. M. SCHWARTZ, Member AIME, is Director Minnesota Geological Survey, Minneapolis, and G. A. THIEL is Professor, Dept. of Geology, University of Minnesota, Minneapolis.

Discussion on this paper, TP 3229H, may be sent to AIME before Feb. 28, 1952. Manuscript, Feb. 20, 1951. St. Louis Meeting, February 1951.

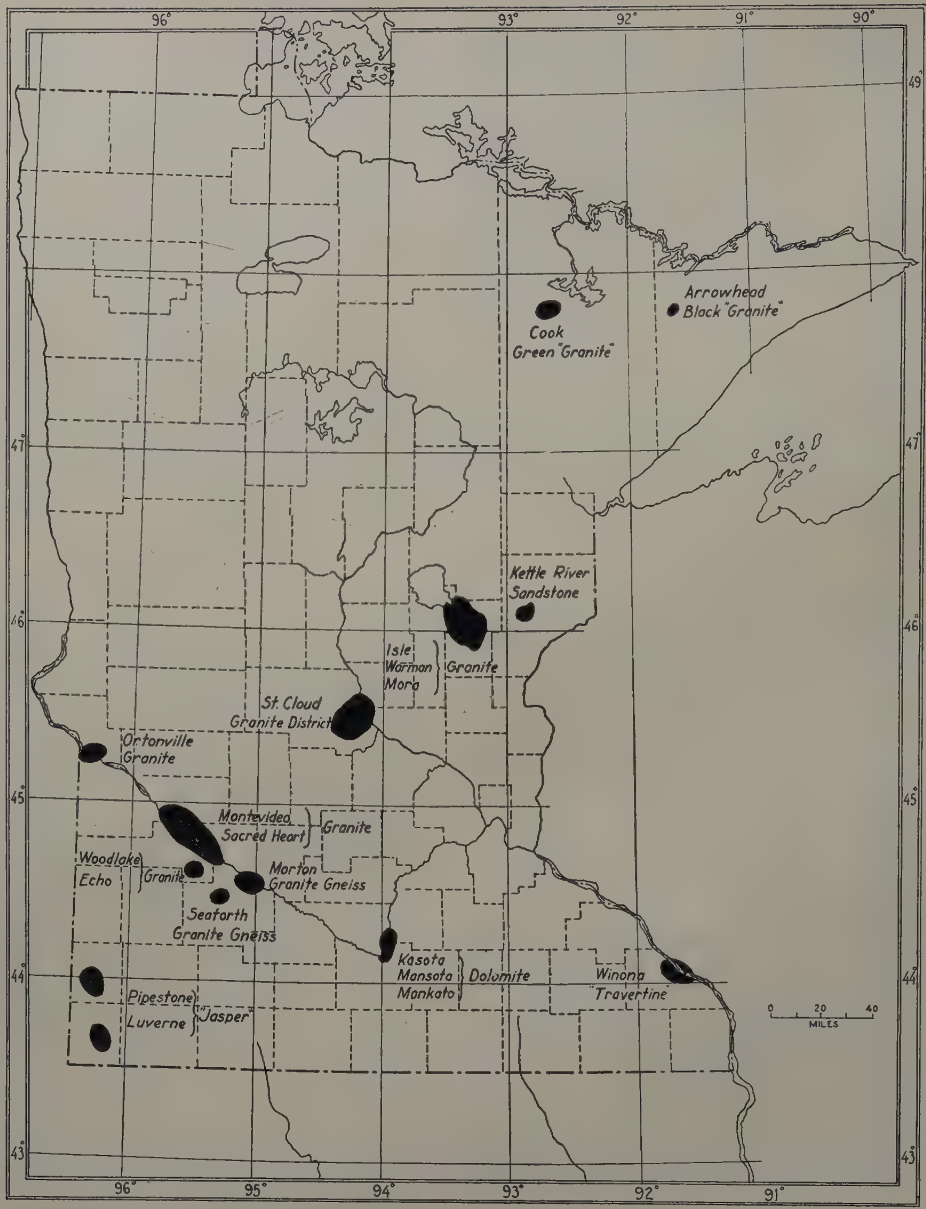

Fig. 1—Most active Minnesota stone-producing areas. After Thiel and Dutton.

tribution to give the stone a very attractive appearance. It is marketed under such trade names as Rockville Pink, Cold Spring Pearl Pink, Original Minnesota Pink, etc. Rockville Pink is exceptionally coarse grained, the angular feldspar crystals being ½ to ¾ in. long. The granite consists of pale pink feldspar, quartz and black mica, the combined effect of which on a hammered surface is pinkish gray.

The red granite of the St. Cloud region is a medium to coarse grained rock, the feldspar grains averaging about ¼ in. in diam. The chief minerals are feldspar and quartz with minor amounts of black hornblende and biotite. Red or pink feldspar constitutes about 75 pct of the rock and gives it its red color. The quartz occurs as coarse, glassy grains. The finished product is marketed under various trade names such as Indian Red, Rose Red, Melrose Red, Ruby Red, Mahogany Red, etc. Many of the quarries that were once prominent are now inactive. Most of the rock was used for monumental purposes, but some architectural stone was fabricated also.

The gray granite of the St. Cloud region occurs in the same general region as the red, and the two are more or less intimately associated. The gray stone is finer grained than the red. The feldspar averages about ⅛ to 3/16 in. long. The minerals that may be recognized in the hand specimen are gray feldspars, black hornblende or mica, and colorless quartz. In some regions quartz is more abundant than hornblende, but it is never very prominent. The stone owes its dark gray color to the gray feldspar and associated black minerals. In some localities part of the feldspar is pale pink. Both orthoclase and plagioclase are present in approximately equal amounts so the rock is a monzonite rather than a true granite.

The gray granite is marketed under such trade names as Minnesota Dark Gray, Pioneer Dark Gray, Reformatory Gray, etc. The term Reformatory Gray is used because the great stone wall of the State Reformatory at St. Cloud is built of this stone and several large quarries were formerly active within the reformatory wall. The term crystal gray is applied to a rock that has exceptionally large phenocrysts in a dark gray matrix. It differs from the coarse grained Rockville pink in that the rock has a greenish gray color, and many of the feldspar grains are larger than those of the pink granite of the Rockville region. Some of the rock contains large blue quartz grains, which add to its dark gray color. It is estimated that about 60,000 cu ft of granite was quarried in the St. Cloud region in 1949.

Dimension stone from the St. Cloud region has been used in many prominent buildings, including the following: Federal Court House Building, New York; Tribune Tower, Chicago; Cathedral, St. Paul, Minn.; Fisher Body Co. Building, Detroit; U. S. Post Office, Milwaukee; Cadillac Building, Boston; Ford Museum Building, Dearborn, Mich.; Merchandise Mart, Chicago; Bell Telephone Building, Dallas; and the First National Bank Building, San Jose, Calif.

Upper Minnesota River Valley Region: Various types of granite crop out on the floor of the valley of the Minnesota River for a distance of 75 miles. Most of the outcrops were exposed by the erosive action of the glacial River Warren that once drained glacial Lake Agassiz during the waning stages of the glacial period.

In the Morton-Redwood Falls region several mounds or domed-shaped outcrops of granite gneiss stand from 75 to 100 ft above the level of the present Minnesota River. A number of quarries have been opened on these outcrops. The rock is a pink and black biotite granite gneiss with contoured laminations or bands. The details of its structure and texture are presented in a paper by Dr. Ernest Lund.[4]

Another area in the Minnesota Valley, where quarries are active at the present time, is in the region of Montevideo and Sacred Heart. The stone quarried near Montevideo is red with some black bands of biotite that give it a gneissic structure. However, the banding is not as irregular and contorted as in the Morton granite. Black knots of biotite, quartz, and aplite veins and irregular pegmatite areas characterize much of the rock. However, some stone of uniform structure and grade is available.

The Sacred Heart quarries are located about 7 miles south of this city in the Minnesota valley. The rock that is quarried at present is a pink granite of medium grained texture. Some stone that is pinkish gray occurs in the same general region, but it is not being quarried at present. Locally the jointing is too closely spaced for large blocks of dimension stone. However, successful quarry operations are carried on by discarding the smaller quarried blocks. Most of the stone from this region is sold under the trade name Sacred Heart Pink Granite.

The Ortonville-Odessa region has seen quarrying operations for a great many years. Ortonville is located at the upper end of the Minnesota Valley where the Minnesota River drains Big Stone Lake. Recently extensive quarrying has been initiated in the area around Bellingham to the south and east of Ortonville. The rock in this area is a red biotite granite that is somewhat gneissic, but the gneissic texture is not so pronounced as at Montevideo and at Morton. It consists of orthoclase, microcline, quartz, and biotite. Microscopic examination shows that the feldspars are intergrown as in microperthite. The quartz is abundant, and the mica occurs as scattered flakes. As seen in the quarry, the rock contains black mica knots, pegmatite masses, and locally it is closely jointed. All of these defects can be avoided by careful quarry operations. About 120,000 cu ft of dimension stone was quarried in the Minnesota valley in 1949.

Dimension stone from the Upper Minnesota River Valley Region has been used in many prominent buildings, including the following: Adler Planetarium, Chicago; Dougherty City Service Building, New York; Cincinnati Telephone Building, Cincinnati; and the Watts Building, Birmingham.

Mille Lacs Lake Region: This area of granite rock is located in a zone that extends northeastward from St. Cloud across Benton and Mille Lacs counties. Most of the rock is buried deeply under glacial drift, but locally low domed-shaped masses crop out at the surface. A quarry operated by the Cold Spring Granite Co. is located 5 miles south of Isle in Section 2, T. 41 N., R. 25 W. At this quarry the joints and sheeting planes are at such distances that blocks as much as 11 ft on a side are cut by drifters. The rock is a comparatively light gray granite composed of large white feldspar crystals embedded in a matrix of colorless quartz and biotite. The larger of the feldspar grains range from ¼ to ½ in. in length. The quartz grains average no more than 1/16 in. in diam, and the biotite occurs in small flakes scattered between the other two minerals. This granite is similar in texture to the stone quarried at Rockville but differs in the color of the feldspar crystals. Cut finishes such as sawed, axed, or hammered, leave the stone nearly white. Because of its uniform color and distance spacing of fractures, many types of structural material are fabricated. The stone is marketed under such terms as Isle Gray, Cold Spring Pearl White, and Diamond Gray.

Table I. Minnesota Dimension Stone

Trade Names of Rock	Location
Granite and Related Rocks	
Arrowhead Green	2 miles west of Cook, St. Louis Co.
Bellingham	Bellingham, Lac qui Parle Co.
Rainbow Granite	Morton
Agate	Ortonville
Minnesota Black	Southeast of Ely
Crystal Gray	St. Cloud
Pearl Pink, Diamond Pink, Minnesota Pink	5 miles southwest of St. Cloud
Diamond Gray, Cold Spring Pearl White	Isle
Warman Gray	Warman
Rockville	Rockville
Opalescent	Cold Spring
Variegated Agate and Odessa	1 mile west of Odessa Lac qui Parle Co.
Pearl Mahogany, Rose Damask	5 miles southeast of Odessa
Mesaba Pink, Mesaba Red	2½ miles north of Mountain Iron
St. Cloud Red, St. Cloud Gray	St. Cloud
Medelian	2 miles southeast of Odessa
Original Minnesota Pink	Southwest of St. Cloud
	4 miles southeast of Odessa
Oriental	Morton
Genuine Bellingham Granite Gneissic Bellingham	Near Bellingham, Lac qui Parle Co.
St. Cloud Red, St. Cloud Gray	St. Cloud
Dolomite	
Kasota Pink, Yellow Interior Pink Veine, Interior Pink Fleuri	Kasota
Mankato Cream, Coarse Yellow	Mankato
Gray, Silver Gray, Gray Buff, Gray Pink, Pink, Pink Buff, Red	
Winona Travertine	Winona

Another quarry in gray granite is located in the northwestern corner of Kanabec County near Warman Creek. The Warman rock is a medium to fine grained light gray or mottled black and white granodiorite that in general appearance resembles the granite of Barre, Vt. It is composed mainly of quartz, white feldspar, and mica. The feldspars are both plagioclase and orthoclase, the latter being somewhat more abundant. All the minerals are fairly uniform in size and distribution. However, a few black knots and inclusions of biotite schists are present. The rock tends to be slightly lighter gray near the surface than at the bottom of the quarry. Near the surface, jointing is quite closely spaced and intercepts at acute angles. Exploratory drilling has indicated, however, that the rock is of more uniform grade at depth. It is sold under the trade names of Warman Granite or Warman Gray.

Dimension stone from the Mille Lacs Lake region has been used in many prominent buildings, including the following: Price Building, Kansas City; Louisiana State Capital, Baton Rouge; Aviation Building, Fort Worth, Texas; and the Capitol Club Office Building, Raleigh, N. C.

Northeastern Minnesota: Black granite is quarried in two widely separated regions in northeastern Minnesota. One quarry is located approximately 20 miles southeast of Ely in the Superior National Forest. The stone is a coarse grained gabbro in which the predominant mineral is plagioclase with small amounts of augite and some yellowish green grains of olivine. The normal surface has a gray color with brilliant reflections from the feldspar cleavage facies. When polished the rock is dark gray with silvery areas caused by the refraction of the light in the feldspars. Formerly this stone had a wide market as an architectural stone for the facing of the lower courses of large buildings. At the present time, practically all of the quarried rock is used for monumental purposes.

Another area that produces Black Granite occurs on the upland slope of the Little Fork River about 2 miles west of the village of Cook. The quarry is in an outcrop of gabbro that is of medium grained texture and possesses a greenish tint caused by the faint color of the plagioclase. On broken surfaces the black and dark gray minerals appear more abundant than the greenish feldspar, but when polished the green color is intensified and so characterizes the rock. Some of it is a mottled green and black. This rock is sold under such trade names as Emerald-Tone Green, Green Granite, etc.

Limestones and Dolomites

The limestones and dolomites that are of economic value belong to the Ordovician and Devonian systems of rocks and crop out in the eastern and southeastern counties of the state. Over most of the area, a heavy covering of glacial drift prevents the opening of quarries. However, along the Mississippi River and its tributaries numerous ledges crop out along the bluffs. Nearly all of the rocks are more or less dolomitic, and many are nearly pure dolomite. Those of the Lower Ordovician strata are somewhat recrystallized and contain bands that are sufficiently crystalline to take a good polish.

The Mankato-Kasota District: In this district the Cambrian and Ordovician sedimentary rocks are exposed in the walls of the valley of the Minnesota River and its major tributaries. The rock formations are nearly horizontal, dipping at a low angle toward the east. Numerous quarries have opened along the east wall of the Minnesota Valley from Mankato northward to beyond Kasota, see Fig. 1.

The individual ledges in the quarries vary from 2 to 5 ft in thickness. Most of the stone is a fine-grained dolomitic limestone, yellow and yellowish pink in color. Certain ledges of yellow stone have large solution cavities that give it a texture similar to that of travertine. When sawed across the bedding plane it is called Veine and when cut parallel to the bands, its design is called Fleuri. The yellow is extensively used for decorative details because of its rich color with markings a trifle darker in shade. Such shadings are also characteristic of some of the pink varieties. When freshly quarried, some of the rock is blue gray in color, but on exposure it changes to a buff. The stone of this district is sold under such trade names as: Mankato: Cream, Yellow, Coarse Yellow, Gray, Silver Gray, Gray Buff, Gray Pink, Pink, Pink Buff, and Red; Kasota: Yellow, Pink, Pink Veine, and Pink Fleuri; and Mansota: Cream, and Pink Buff. It is estimated that about 150,000 cu ft per year has been shipped from this area in recent years.

Winona Region: In the region of Winona the Lower Ordovician dolomite caps the bluffs along the Mississippi River and forms the prominent walls of the tributary valleys leading away from the river. The rock has been quarried in a number of places and furnishes a good grade of architectural stone. The quarry rock reaches from 15 to 60 ft in thickness, and its ledges are from 1 to 6 ft thick. Joints are in general at right angles and are spaced from 3 to 20 ft apart. Much of the stone is sold under the trade name Winona Travertine. It is so called because solution cavities give it a texture that approaches that of spring deposited limestone. The rock is exceptionally hard when quarried and remains hard when exposed to extreme climatic conditions. A number of different color and texture varieties are fabricated. Cream, buff, and gray are the common colors.

Dimension stone from the dolomites of Minnesota has been used in many prominent buildings, including the following: Art Museum, Philadelphia; Bell Telephone Building, Minneapolis; Minnesota State Capitol (interior), St. Paul; Cathedral, Springfield, Ill.

A list of dimension stones that are produced at present is given in Table I. Dozens of other quarries have operated over the years but have been abandoned for various reasons. Some of these may resume production as has happened in other cases.

References

[1] O. Bowles: The Structural and Ornamental Stone of Minnesota. U. S. Geol. Surv. *Bull.* 663 (1918), out of print.

[2] G. A. Thiel and C. E. Dutton: The Architectural, Structural and Monumental Stones of Minnesota: Minn. Geol. Surv. *Bull.* 25 (1935), out of print.

[3] N. H. Winchell: Final Report, Geology of Minnesota. Geol. and Nat. History Survey of Minnesota (1884) **1**, pp. 142-203.

[4] E. H. Lund: Morton Granite Gneiss. Presented at AIME St. Louis Meeting, February 1951.

Diamond Orientation In Drill Bits

by E. P. Pfleider

DIAMOND drill research work was initiated at the School of Mines, University of Minnesota, in late 1949. The Drilling Symposium held in Duluth that spring highlighted the problem of high cost and core recovery and the need for controlled testing. An advisory committee made up of informed representatives of both mining companies and drilling companies was formed to suggest and advise on a program of drill research.

A Hy-Mac hydraulic drill unit, see Fig. 1, especially designed for experimental testing, was obtained for this work by the School of Mines through the courtesy of the Carboloy Co. It is an extremely flexible unit, capable of exerting a forward thrust of about 1750 lb and turning at speeds from 650 to 2200 rpm. The feed arrangement is so designed that the advance can be set either at a constant rate or permitted to vary at a fixed pressure, see Fig. 2. The

---

E. P. PFLEIDER, Member AIME, is Head, Mining Dept., School of Mines, University of Minnesota, Minneapolis, Minn.

Discussion on this paper, TP 3228A, may be sent to AIME before March 31, 1952. Manuscript, July 9, 1951.

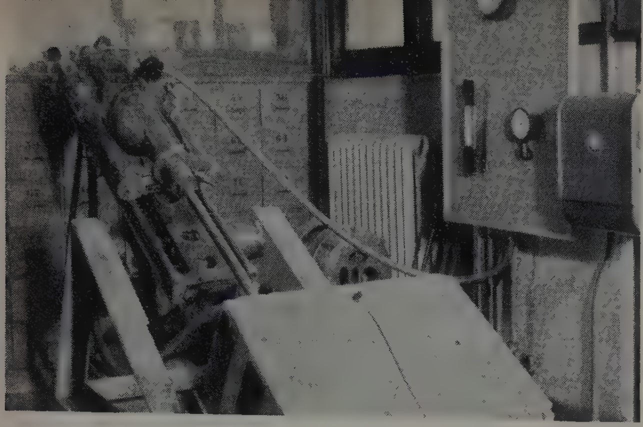

Fig. 1 — Hy-Mac hydraulic diamond drill unit with complete controls for experimental testing.

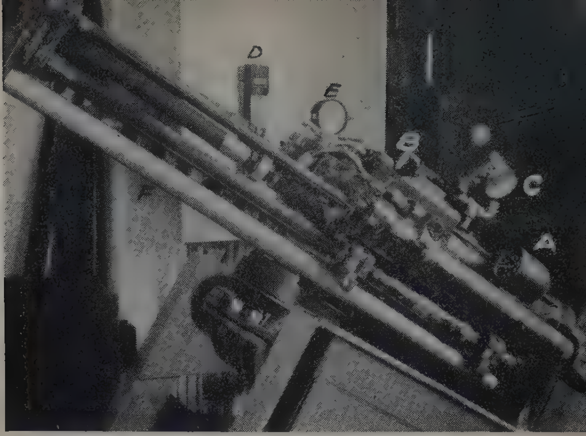

Fig. 2 — Hy-Mac diamond drill setup with (A) tachometer, (B) forward and reverse pressure gages, (C) water pressure gage, (D) flowmeter, (E) hydraulic pump pressure gage, and (F) strip for recording rate of advance.

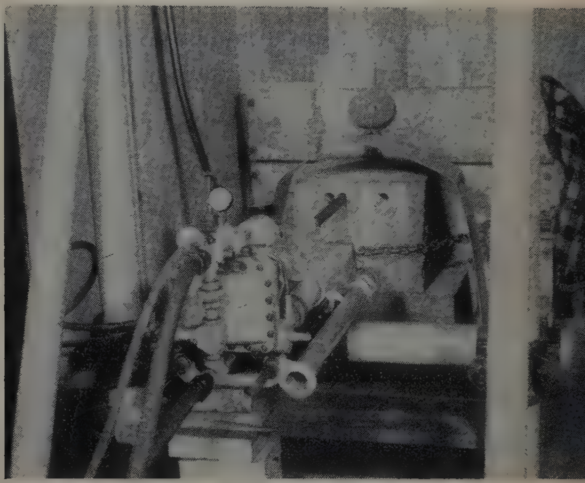

Fig. 3 — Longyear Rotobore hydraulic research drill unit, instrumented same as Hy-Mac.

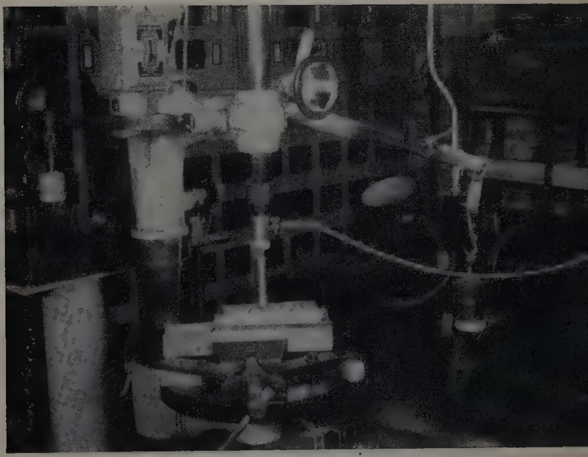

Fig. 4 — Laboratory drill using 1-in. OD core bit, drill press, and controlled pressure loading on bit.

This page of Mining Transactions follows p. 80. The intervening non-Transactions pages appeared in Mining Engineering.

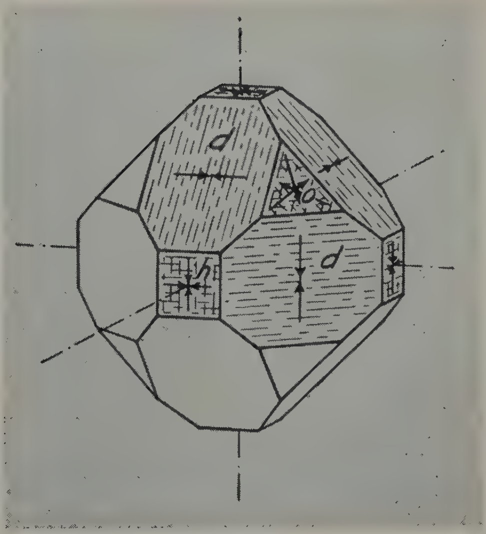

Fig. 5—Combination octahedron cube-dodecahedron crystal habits of the diamond.
After Kraus and Slawson.[1]

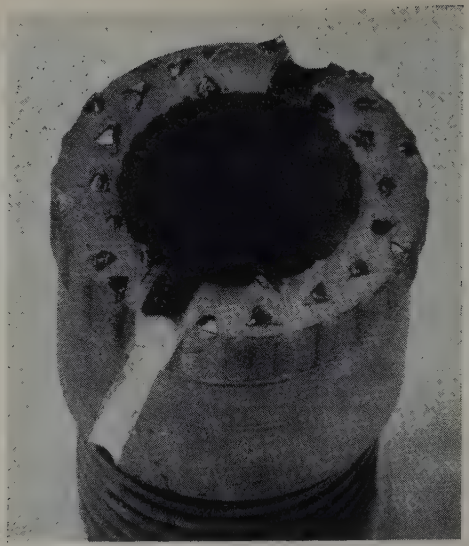

Fig. 7—Experimental drill bit No. M-4 having spiral pattern of diamond placement and negative rake (drag) orientation. Apparent rotation, counterclockwise.

drill is completely instrumented with a tachometer, A; forward and reverse pressure gages, B; water pressure gage, C; flowmeter, D; hydraulic pump pressure gage, E; and strip for recording rate of advance, F.

A second unit, a Longyear Rotobore hydraulic drill, see Fig. 3, was a gift to the school by the Oliver Iron Mining Co. This was overhauled completely through the kindness of the E. J. Longyear Co. and is now set up in a similar manner to the Hy-Mac. It is being used for research work in the problem of the cutting action of the diamond bit on various types of rocks. This project is sponsored by the U. S. Bureau of Mines through a graduate fellowship.

A small laboratory-size drill, see Fig. 4, cutting a ¾-in. core and powered by a drill press, also is used in conjunction with this fundamental study.

Most of the test work done to date has been in a coarse-grained, pink St. Cloud granite, from Cold Springs, Minn., donated by the Cold Springs Granite Co.

The committee decided that work should be of a fundamental nature, and the suggestion of determining the effect of the crystallographic orientation of the diamond in the bit was adopted as the first project. This paper is a progress report on the accomplishments to date.

The gem polisher and the wheel truer have known for many years that there is a great variation in hardness between the different crystal faces of the diamond. This characteristic has been used to good advantage in their work. Kraus and Slawson[1] have related the vector property of the crystal structure to the accepted cutting directions in the gem. Quantitative tests of a polishing operation in the watch industry have shown a ratio of 11,500 parts polished, using the hardest direction on the tris-octahedral face, to 200 parts using the softest direction on the cube or dodecahedral face.

Since there was a wealth of data on the characteristics of the individual diamond, it was decided to test immediately the effect of the orientation of a group of diamonds set in a bit. Messrs. Wing Agnew and Albert Long[7] of the Mount Weather Testing Station of the U. S. Bureau of Mines had initiated some previous work on orientation and assisted greatly in laying out the test procedures. The plan was to use a minimum number of stones in an EXT bit.

The writer visited the plant of the J. K. Smit Co. to observe the techniques in the manufacture of bits.

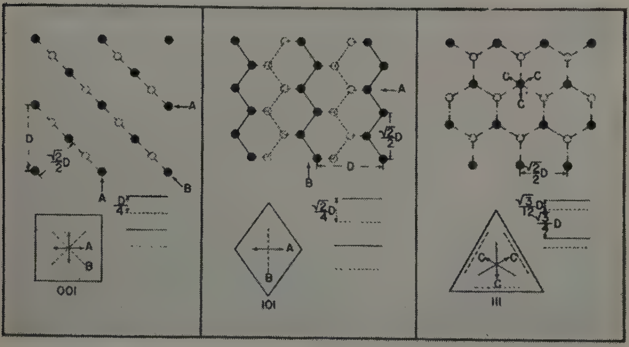

a . b c

Fig. 6a—Diagrams showing (1) distribution of atoms in cube planes, (2) spacing of successive parallel planes, (3) optimum directions for polishing and sawing A, and (4) directions of greatest resistance, B.
b—Same for rhombic dodecahedron planes.
c—Same for octahedron planes. The three optimum polishing directions are indicated by C.
After Kraus and Slawson.[1]

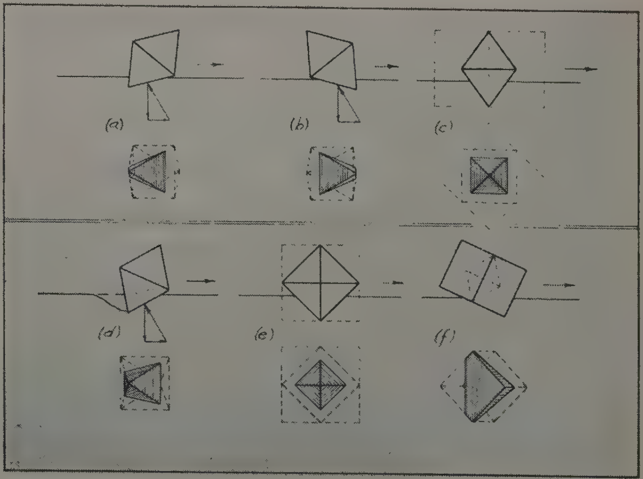

Fig. 8—Various crystallographic orientations of the octahedron diamond crystal tested in EXT core bits.

That company offered to furnish the molds and to manufacture the bits, without charge, as well as to sell the diamonds at cost.

Nine bits have been tested so far, and the results indicate a correlation between the fundamental knowledge of the crystallography of the diamond and the performance of the diamond in the drill bit. Much work remains to be done on different crystal forms and orientations.

Crystallography

The diamond crystallizes in a face-centered cubic lattice. The most common habit is the octahedron, eight faces. The diamond is found also in cubes, six faces, or rhombic dodecahedra, 12 faces, or in combination habits up to 48 faces. The model in Fig. 5 shows all of these planes. The diamond cutter refers to these planes as follows:

Plane	Crystallographic Name	Diamond Cutter	Directions For
100	cube	4-point	sawing-grinding
110	dodecahedron	2-point	sawing-grinding
111	octahedron	3-point	cleaving

The lines show the so-called *grain* and the arrows show the best cutting directions, the last mentioned being always parallel to an axis and perpendicular to the grain.

Cleavage is perfect on the octahedron face and somewhat less perfect on the dodecahedron face. Cleavage, while perfect, does not take place readily.

Kraus and Slawson[1] have made an intensive investigation of the crystallography of the diamond and have offered a theoretical explanation for the hardness variation and cleavage pattern based on the atomic structure. Fig. 6 shows the distribution of the atoms, the spacing of successive parallel planes, the optimum directions for polishing and sawing, and the directions of greatest resistance for the three planes under discussion.

A study of these diagrams reveals the following:

1—The atoms are most widely separated in the plane of the cube face; especially in the direction paralleling the crystallographic axes.

2—In the plane of the dodecahedral face the atoms are spaced more widely in the direction of the short diagonal than in the long diagonal.

3—The atoms are most closely packed in the plane of the octahedral face.

4—The computed number of effective valence bonds per atom between planes, considering two bonds lying in a plane to be equivalent to one additional effective bond, gives the following relationship:

cube $4 = 1$
rhombic dodecahedron $4\sqrt{2} = 1.414$
octahedron (close spacing) $4\sqrt{3} = 1.732$

5—The crystallographic axes intersect valence bonds at larger angles than do any other directions through the structure. Accordingly, those directions in which the atoms are most widely spaced, which have the smallest number of valence bonds, and which intersect those bonds at the greatest angles, can be expected to give the least resistance to cutting, polish, or wear. The full lines marked A on the cube face in Fig. 6a most closely fit these conditions; whereas the dashed lines shown on the octahedral face in Fig. 6c are the most remote. These facts would indicate that the experience of the diamond cutter and theory are well in agreement, namely, that the hardness should be greatest on the octahedral face, least on the cube, and intermediate on the rhombic dodecahedral.

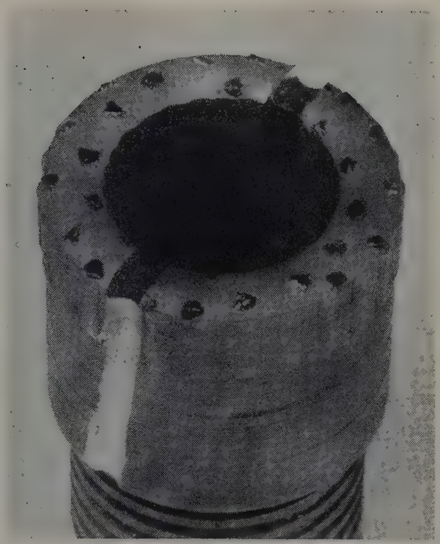
Fig. 9—Bit M-5 having positive rake (gouge) orientation of diamonds.

Cleavage is perfect on the octahedral face, 111, and somewhat less perfect on the dodecahedral face. Again, the crystal structure provides an explanation. The atomic planes parallel to the octahedral face are not uniformly bonded. Alternate layers have weak and strong valence bonds. The cube planes are uniformly and strongly bonded. The layers in the dodecahedral plane are uniform, but intermediate in strength. The calculated relative number of bonds per atom for a unit area, D^2, in the various types of planes are:

	Bonds	*Ratio*
octahedral (wide spacing)	$4/3\sqrt{3}$	$= 1.00$
rhombic dodecahedral	$2\sqrt{2}$	$= 1.22$
cube	4	$= 1.73$
octahedral (close spacing)	$4\sqrt{3}$	$= 3.00$

Hardness Variation: Relative hardness of the various faces, based on an investigation by M. Tolkowsky, were reported by Drane[3] as follows:

Face	Easy Polishing Directions	Relative Max. Polishing Rates
Cubic face	2 and their reverses	0.82
Dodecahedral face	1 and its reverse	1.74
Octahedral face	3, polishing in reversed direction	0.14

Quantitative research work done by Winchell[4] for the Hamilton Watch Co. using the unidirectional rubbing of a flat diamond surface against stainless steel watch parts indicated a probable ratio of 100 to 1 for the hardness of the hardest direction on the hardest surface to the softest direction on the softest surface. The production obtained from the softest directions was less than 200 units, but the same tool, made with equivalent quality of diamond but so oriented to present the hardest direction and surface, consistently produced 20,000 units.

Slawson and Kahn[5] made an intensive study of the rate of polishing by lapping the stones in many directions. They found that, for practical purposes, the only surface directions that are impossible to

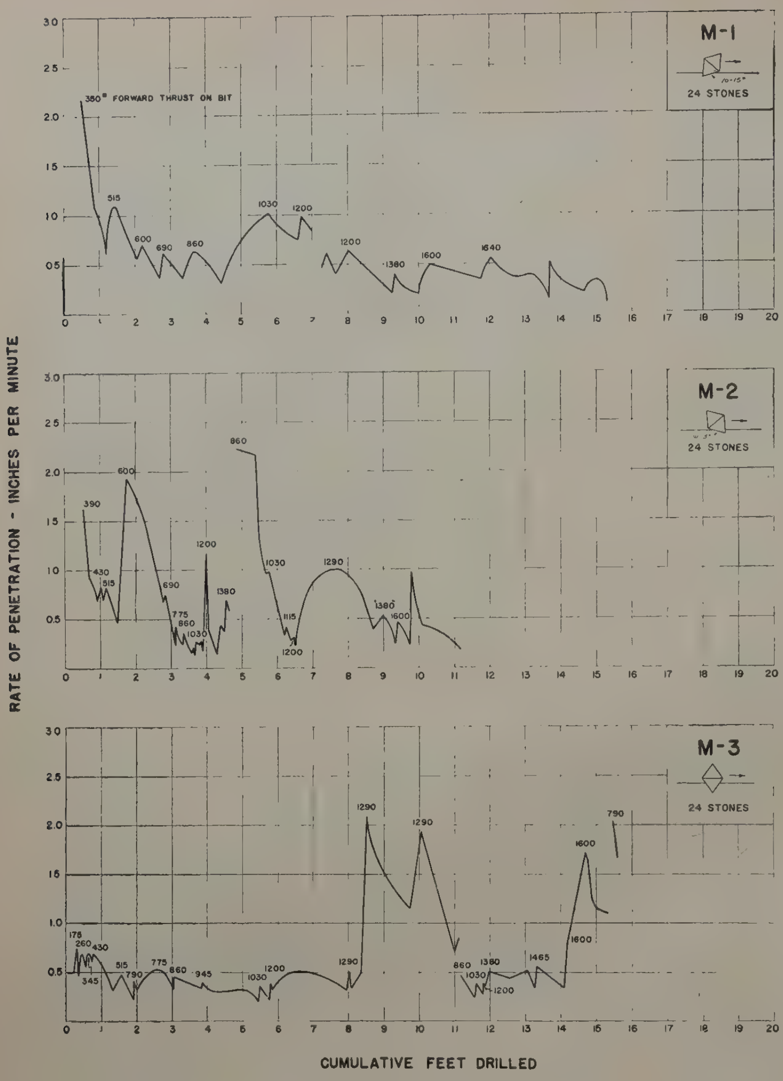

Fig. 10—Test history of EXT diamond drill bits M-1, M-2, and M-3. Constants: rpm of drill, 1000; gpm of water, 1.5. Variables: forward thrust of bit; rate of penetration.

polish are 1—any directions on a surface parallel to the octahedral face, 2—the dodecahedron parallel to the diagonal, and 3—the cube parallel to the diagonal.

The above work is not truly representative of conditions encountered in wheel truing[8] or diamond drilling, where vibration, shock, and tendency to cause fracture would mask the sole factor of hardness. It does, however, emphasize the importance of the relationship between hardness and orientation when independent of other conditions.

Orientation in the Bit

With the above-mentioned background of information from the investigators in other fields employing the industrial diamond, it was decided to proceed directly with the testing of diamond orientation in the bit. The smallest bit size, EXT, and a minimum number of diamonds, 20 in the crown and four *kicker* stones,* were chosen for the first set of three bits, with the thought that these conditions would reduce bit variables to a minimum and give the most accurate testing of the effect of diamond orientation. A diamond size of ten stones per carat was selected because of ease of discerning the crystal faces on this relatively large diamond. Admittedly, these stones are far too large for optimum results in granite. The diamonds were Best Grade Congos, all selected octahedrons and combination octahedron-dodecahedrons.

The blank molds for the bits were furnished by the J. K. Smit Co. After making the depressions in the blank mold to permit the necessary diamond exposure, the diamond was held in the mold at desired orientation by using a lacquer. The mold then was shipped back to the Smit Co. for bit manufacture. Powdered tungsten, or powdered iron, with a bonding alloy was used as the matrix material. A finished bit is shown in Fig. 7 in which the spiral pattern of diamond placement is evident. This pattern was used to insure full coverage of the crown. The bits had two waterways. Three different orientations were tested:

1—A *negative* rake off the octahedral face; i.e., where the apex or point of the octahedron trails the octahedral face along the lines of cutting action. This gives the effect of *dragging* the diamond to produce cutting action. See Figs. 8a and 8d. Bit M-4, having this type orientation, is shown in Fig. 7.

2—A positive rake off the octahedral face; i.e., where the apex or point of the octahedron is leading. This gives the effect of *plowing* or *gouging* with the diamond to produce cutting action, see Fig. 8b. Bit M-5, in Fig. 9, has this form of orientation.

3—*On point* of octahedron, with either the octa-

---

* *Kicker* stone is the trade term for those stones located on the inside and outside of the bit and employed to hold gage by reason of their reaming action.

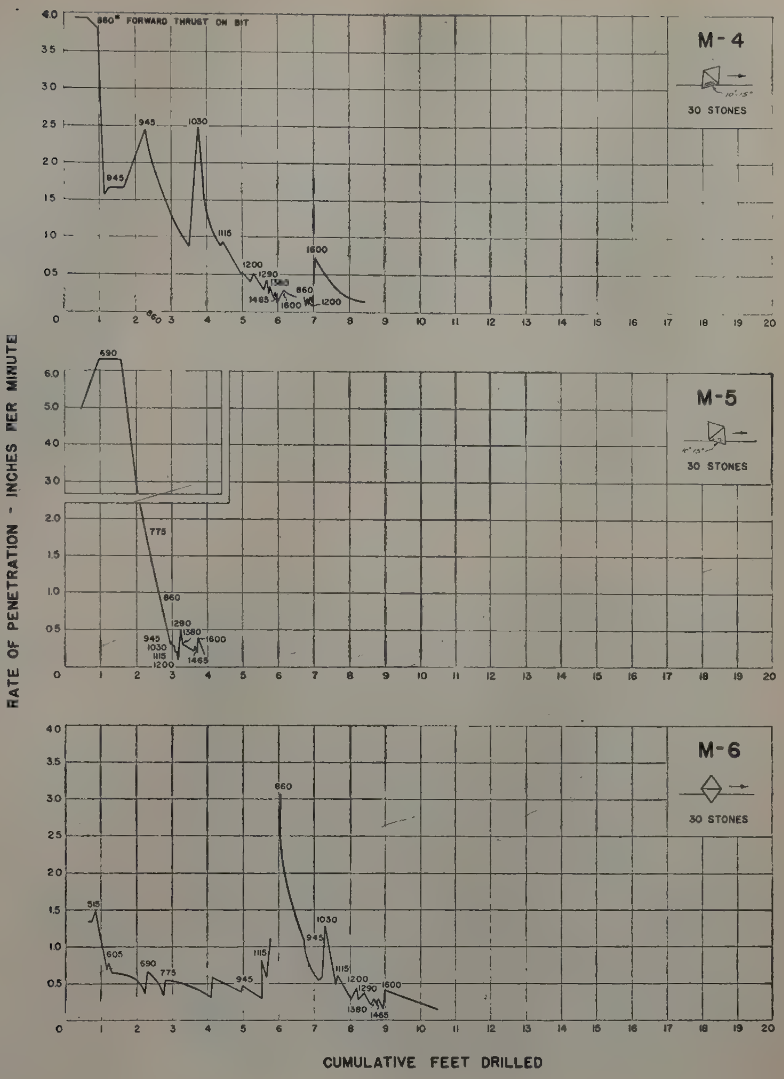

Fig. 11—Test history of EXT diamond drill. Bits M-4, M-5, and M-6. Constants: rpm of drill, 1000; gpm of water, 1.5. Variables: forward thrust of bit; rate of penetration.

hedral face or the dodecahedral face leading. Contact then is on a plane parallel to the cube face, either along the harder direction diagonal to the axes, or along the softest direction parallel to the crystallographic axes, see Figs. 8c and 8e.

Test Procedures

To obtain comparable data in testing the various bits, an attempt was made, insofar as possible, to hold the following conditions constant.

1—bit, except for diamond orientation; 2—rock type, St. Cloud *Pink* granite; 3—drill speed, 1000 rpm; 4—water, 1½ gpm, pressure varied as necessary to produce this flow; 5—force on bit, increased in increments of 10 psi (equivalent to approximately 90 lb thrust) whenever rate of penetration decreased to 50 pct the original rate obtained after applying the increment; and 6—terminal point of test, when penetration fell to 0.2 in. per min or, as in some cases, when gage was lost.

The comparable variables, then, for the various diamond orientations were the rate of penetration (in. per min) and the cumulative feet drilled.

After each run, averaging about 1½ ft, the diamonds were examined under a microscope to study the wear characteristics. Interesting conditions were photographed. It is felt that the correct interpretation of these microscopic observations is as important to the study as the comparison of actual footages drilled by the test drills.

The test results for the first two groups of experimental bits, consisting of three bits in each group, are presented in graph form in Figs. 10 and 11. Bits M-1 and M-4 have the negative rake orientation, 15° off the octahedral face, or otherwise expressed as a 15° drag angle. Bits M-2 and M-5 have a positive rake, approximately 15° off the octahedral face or a 15° gouge angle. Bits M-3 and M-6 are *on point* orientations, with the octahedral face leading.

Bit M-1 gave a very even performance, but continuous microscopic study of the individual diamonds throughout the life of the bit showed an early tendency toward polish. Diamond wear was extremely low. It is believed that these characteristics are typical of a low angle negative rake, since a large area of diamond is exposed to contact at an early stage. Furthermore, the orientation is structurally sound, since the pressure is somewhat normal to the cleavage plane, or the plane of weakness.

Bit M-4 was tested, after a short break in period, with an initial thrust of 860 lb, as contrasted with a starting force of 350 lb for Bit M-1. This increase was made with the dual purpose of determining the ability of the diamond in this orientation to withstand heavy starting loads, and whether large initial pressures would eliminate, or reduce, the tendency to polish. Results were disappointing in both respects.

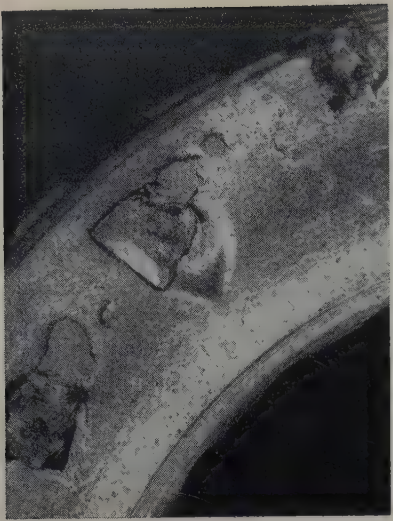

Fig. 12—Bit M-1 (X8) with negative rake diamond orientation (15° drag angle), showing tendency of diamonds to polish after 2.8 ft drilling in granite. Rotation counterclockwise.

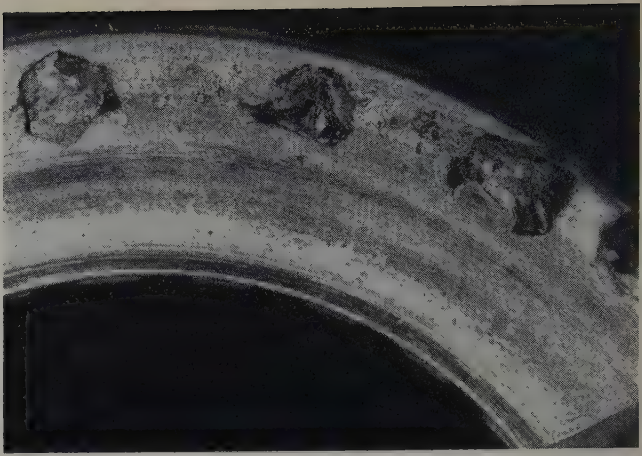

Fig. 14—Bit M-2 (X6) with positive rake diamond orientation (15° gouge angle) showing rough and fractured surfaces after 4.6 ft of drilling in granite.

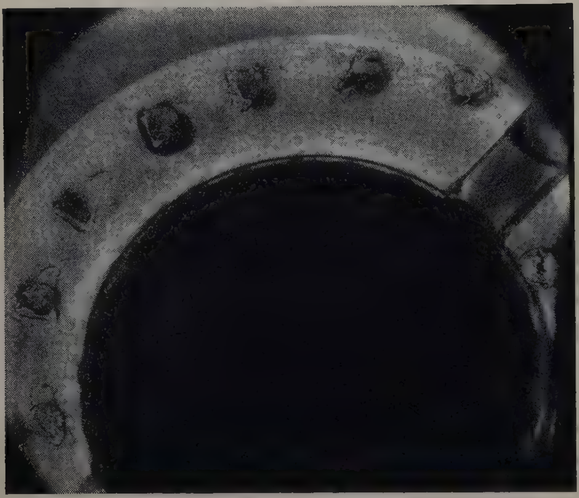

Fig. 13—Bit M-1 (X3) showing polished flats after 13.6 ft of drilling in granite.

Bit M-2 proved to be a very erratic performer. The diamond with a positive rake can give abnormally high penetration rates but cannot withstand the shock loads. The diamonds break up early, probably along cleavage planes. The fragments remain in the bottom of the hole and accentuate the disintegration of the remaining stones. Diamond loss is high, as would be expected with a structurally weak orientation.

Bit M-5 has a positive rake and, similar to M-4, was tested at high starting pressures; although in this case the thrust was lowered to 690 lb in view of the experience with M-4. The initial rate of penetration was above 6 in. per min, but this fell off markedly. Large pieces of diamond were cleaved off, and these in turn accentuated the breakage of remaining stones to a point where advance was practically nil after but 4 ft of drilling.

Bit M-3 had the *on point* orientation with octahedral face leading, equivalent to cutting with the hardest direction of the cube face. Performance was poor for the first 8 ft, during which time the points were wearing down to form flat surfaces. After 8 ft the rate of penetration increased immediately from 0.5 to 2.2 in. per min. There are two possible explanations for this: 1—that the critical force necessary to cause penetration of the diamonds into the rock was reached, or 2—that the points of the few diamonds used in the crown of the bit did not completely sweep the surface to be drilled until they had worn considerably. In any event, results thereafter were erratic, and the bit failed to advance after drilling 15.6 ft because of binding in the hole caused by lack of gage. As previously mentioned, the diamond points wear down rapidly and then form large square polished surfaces, which require high pressures to effect their impression into the rock surface.

Bit M-6 was set with *random* orientation by a person knowing nothing of crystallography. Examination of the bit after manufacture showed that 16 out of the 26 crown diamonds had on point orientation. Apparently, this is the natural and easy method of setting. The bit reacted much like M-3, which it resembles.

Figs. 12 through 16 are micrographs showing some of the diamond wear characteristics described in the test results of Bits M-1 to M-6. When studying these photographs, it is important to bear in mind that the direction of rotation of the bit, when drilling, would be counterclockwise. Fig. 12 is of Bit M-1 (negative rake), and the tendency to polish is seen after but 2.8 ft of advance. Fig. 13 shows the condition accentuated after 13.6 ft drilled. Parts of Bit M-2, after 4.6 ft, and Bit M-5, after 3.96 ft total, both having positive rake orientation, are shown in Figs. 14 and 15. It can be seen that the diamond surfaces are rough, resulting in fast initial penetration. However, the diamonds have parted along cleavage planes, ruining other stones and even gouging into matrix, as evident in the photograph of M-5. Fig. 16 shows Bit M-3, on point orientation, after 9.7 ft drilled. The flat square surfaces resisting penetration are evident.

The cumulative results of Bits M-1 to M-6, including their diamond loss data, are presented in Figs. 17 and 18. Generally the bits with negative orientation gave the best results after considering that M-4 had an excessive starting pressure on the bit. Bit M-1 had an abnormally low diamond loss of 0.0124 carats per ft, which was 40 pct of that for M-3, the next lowest. Positive rake bits are characterized by high initial penetration rates, low total footages, and large diamond loss. Bits with on point and random, 60 pct on point, orientations gave low

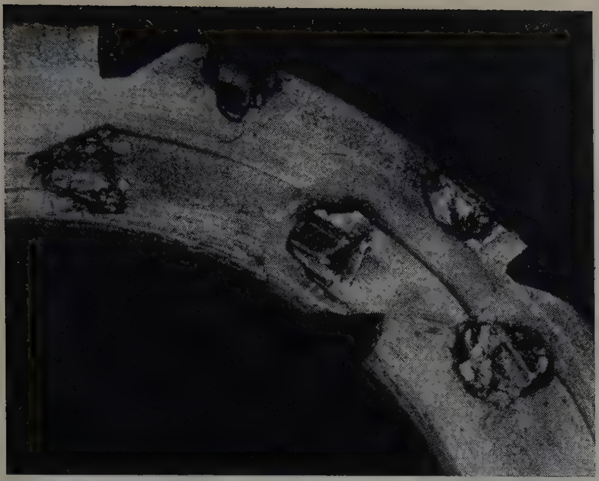

Fig. 15—Bit M-5 (X5) with positive rake (15° gouge angle), showing fractured diamonds and gouged matrix after 3.9 ft of drilling in granite.

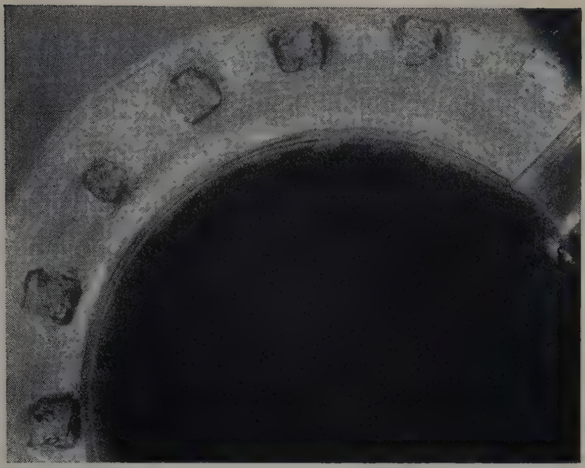

Fig. 16—Bit M-3 (X4) with on point orientation of diamond, showing flat square surfaces resisting penetration after 9.7 ft of drilling in granite.

EXT Bits	M-1		M-2		M-3	
Diamond Type	Congo - Octahedron and Combination Octahedron-Dodecahedron					
Diamond Size	10 per Carat					
Diamond Number	24 Stones (20 Crown; 4 "Kicker")					
Matrix	Powdered Tungsten — Bonding Alloy					
Diamond Orientation and Exposure	Negative Rake-15° Oct. Face		Positive Rake-15° Oct. Face		Cube Face on Oct. Point	
Ft drilled	15.32		11.16		15.61	
Diamond weights	Carats					
Original	2.75	2.75	2.79	2.79	2.79	2.79
Final	2.56		2.32		2.33	
Salvage (reusable)		2.56		2.17		2.33
Diamond loss	Carats					
Net from wear	0.19		0.47		0.46	
Total—after salvage		0.19		0.62		0.46
	Carats per Ft					
Net from wear	0.0124		0.0422		0.0294	
Total—after salvage		0.0124		0.0558		0.0294

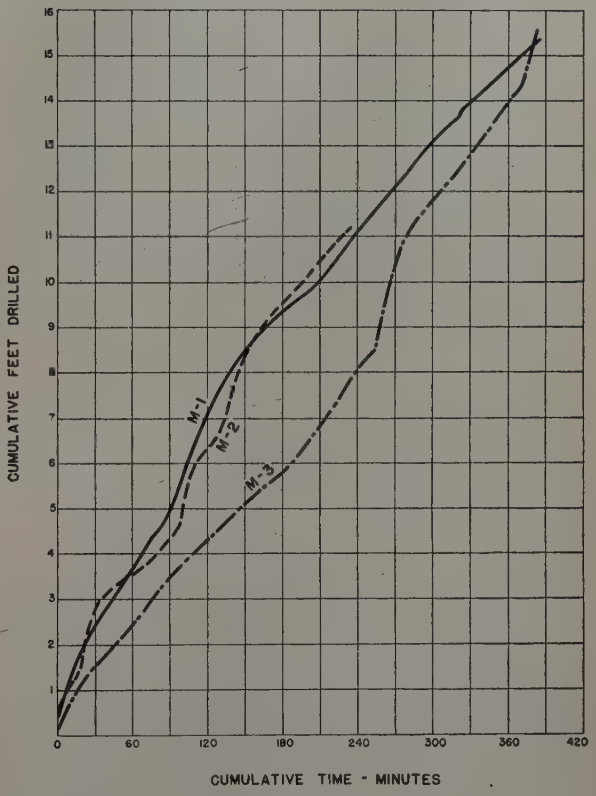

Fig. 17—Cumulative test data, bits M-1, M-2, and M-3.

starting rates, with short lived highs in midlife, and intermediate footages and diamond loss.

The effect of high initial starting pressures on the bit, as used for Bits M-4, M-5 and M-6, is readily evident when comparing the results of these bits with the first three bits. This is particularly true when taking into consideration the fact that the last group had 26 crown stones per bit, whereas the first group had but 20. Total footage for Bits M-1, M-2 and M-3 was 42.1 ft; for Bits M-4, M-5 and M-6, 22.8 ft. A comparison of total diamond wear per foot shows 0.031 carats per ft for the first three bits to 0.081 carats per ft for the last three bits.

Net diamond loss from wear was determined by subtracting the weight of all diamond recovered at the end of the test from the original weight of diamond set in the bit. Total diamond loss was calculated by adding to the wear loss the weight of any recovered diamonds that were rejected for further use because of their small size or fractured condition.

On the basis of experience with the first six bits, it was decided to compare further the negative rake as against the on point setting. It was felt that the early tendency to polish on the negative rake could be diminished by a compromise with diamond loss. Hence, the drag angle was increased to 30° for Bit M-7. It was desired also to test one bit having on point setting with the dodecahedron face leading, to see if this change would make any appreciable difference over that of the on point setting with the octahedral face leading.

The test results of Bit M-7, see Fig. 19, tend to prove the correctness of the reasoning in increasing the rake to 30°. The individual diamonds held up well, and the polishing effect was reduced greatly

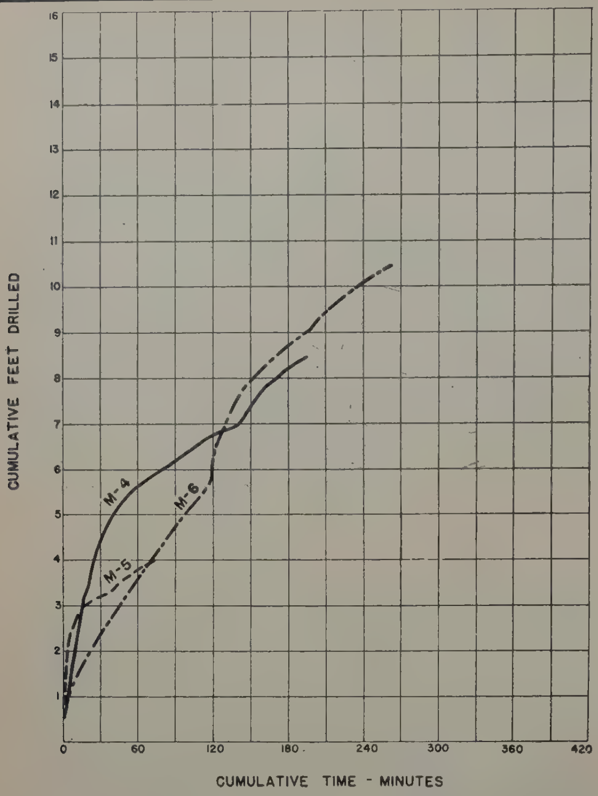

EXT Bits		M-4		M-5		M-6	
Diamond	Type	Congo - Octahedron and Combination Octahedron-Dodecahedron					
	Size	10 per Carat					
	Number	30 Stones (26 Crown; 4 "Kicker")					
Matrix		Powdered Tungsten — Bonding Alloy					
Diamond Orientation and Exposure		Negative Rake-15° Oct. Face		Positive Rake-15° Oct. Face		Random-65 Pct of Stones on Oct. Point	
Ft drilled		8.45		3.96		10.47	
Diamond weights		Carats					
Original		3.30	3.30	3.25	3.25	3.34	3.34
Final		2.65		2.91		2.38	
Salvage (reusable)			2.57		2.85		2.63
Diamond loss		Carats					
Net from wear		0.65		0.34		0.66	
Total—after salvage			0.73		0.40		0.71
		Carats per Ft					
Net from wear		0.0769		0.0858		0.0630	
Total—after salvage			0.0864		0.1010		0.0678

Fig. 18—Cumulative test data, bits M-4, M-5, and M-6.

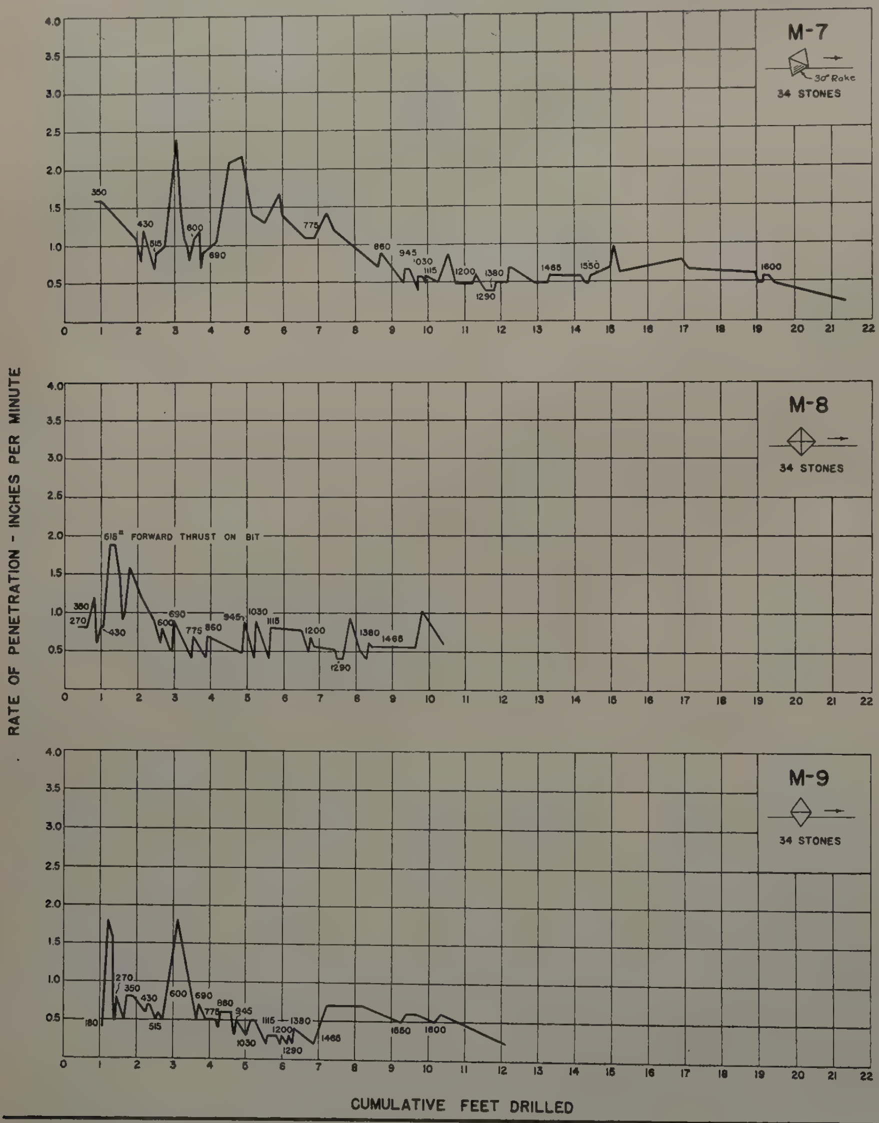

Fig. 19—Test history of EXT diamond drill bits M-7, M-8, and M-9. Constants: rpm of drill, 1000; gpm of water, 1.5. Variables: forward thrust of bit; rate of penetration.

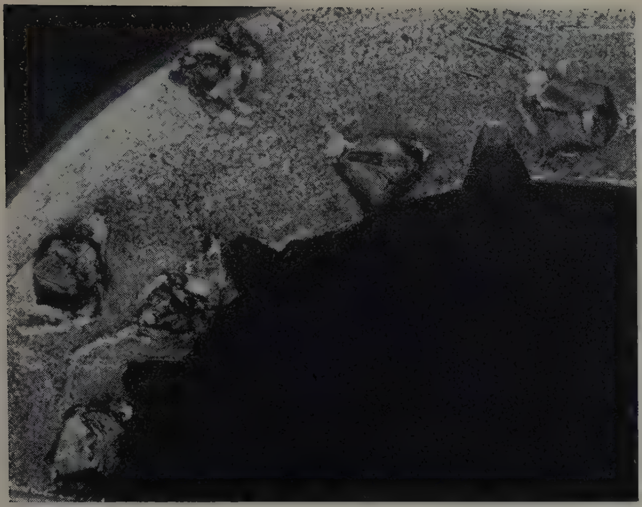

Fig. 20 (above)—Bit M-7 (X5) with negative rake diamond orientation (30° drag angle), showing tendency of trailing edge of octahedron to break away and leave rough surface on diamonds after 9.9 ft of drilling in granite.

Fig. 21 (below)—Bit M-8 (X4) with on point diamond orientation, dodecahedral face leading, showing polished flats and star-shaped fracture patterns after 6.2 ft of drilling in granite.

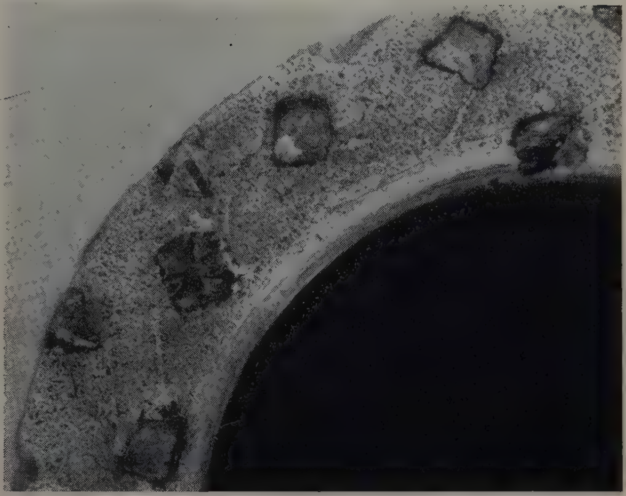

EXT Bits		M-7		M-8		M-9	
Diamond	Type	Congo - Octahedron and Combination Octahedron-Dodecahedron					
	Size	10 per Carat					
	Number	34 Stones (26 Crown; 8 "Kicker")					
Matrix		Iron Powder — Eutectic Bonding					
Diamond Orientation and Exposure		Negative Rake-30° Oct. Face 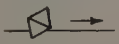		Cube Face on Oct. Point 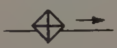		Cube Face on Oct. Point 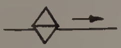	
Ft drilled		21.53		10.38		12.03	
Diamond weights		Carats					
Original		3.70	3.70	3.95	3.95	3.57	3.57
Final		3.15		3.46		2.78	
Salvage (reusable)			3.05		3.41		2.64
Diamond loss		Carats					
Net from wear		0.55		0.49		0.79	
Total—after salvage			0.65		0.54		0.93
		Carats per Ft					
Net from wear		0.0256		0.0472		0.0657	
Total—after salvage			0.0302		0.0544		0.0773

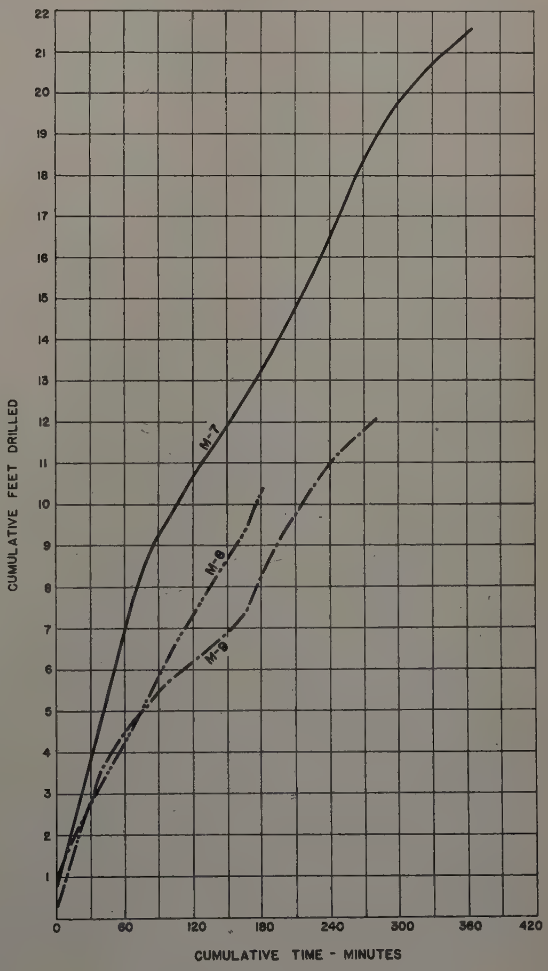

Fig. 22—Cumulative test data, bits M-7, M-8, and M-9.

since the exposed face would fracture just enough to produce a rough surface. This effect gave a 50 pct increase in footage drilled and a 100 pct improvement in average rate of penetration over Bit M-1.

Bits M-8 and M-9 reacted much the same as the other on point orientations after taking into consideration that these bits had ten more diamonds than M-3 and four more than M-6. There was little noticeable difference in the performance of M-8, having the dodecahedral face leading, as compared to M-9, with the octahedral face leading. Both bits reacted remarkably the same.

Fig. 20 shows Bit M-7, 30° negative rake, after drilling 9.9 ft. The stones are still rough, apparently due to the breaking away of the trailing edge. Some consideration has been given to supporting this *trailing* edge with matrix material to decrease breakage and diamond loss. However, this practice might accentuate the polishing effect.

Fig. 21 is of Bit M-8, on point orientation, dodecahedral face leading, after 6.2 ft of advance. The stones are beginning to form polished flats. Several of the diamonds exhibited peculiar star-shaped fracture patterns, possibly caused by breakage along the four cleavage planes paralleling the octahedral face. This is indicated clearly in the third and fourth stones from the left.

The cumulative results of Bits M-7, M-8 and M-9 are presented in Fig. 22. It is evident that M-7 gave much the best performance of all nine bits. A comparison of Bit M-7 to Bits M-8 and M-9 shows double the total advance, double the drilling speed, and half the diamond loss.

Summary

Five different orientations of the octahedron, or combination octahedron-dodecahedron, diamond crystals have been tested to date in EXT diamond core bits. These are illustrated by Figs. 8a through 8e. The results and evaluation for each of these five orientations might be summarized as follows:

1—The low-angle negative rake is a structurally strong orientation, since the resultant reaction is approximately normal to the octahedral plane and cleavage direction. The diamond loss is exceptionally low; the direction of wear being toward the apex and highly resistant. However, the rate of penetration is retarded by the tendency to polish and the lack of a sharp point projection to aid rock penetration and breakage.

2—The positive rake is structurally weak. Furthermore, the wear across the octahedral face is in the softest direction. These two factors cause early stone failure and high diamond loss. The orientation cannot be recommended under usual conditions.

3—On point setting with octahedral face leading is a fair orientation. The movement is along the hardest direction of the cube face; i.e. diagonal. Tendency to polish is less than on the octahedral face. However, the point wears down rapidly to present a flat square surface, difficult of penetration. The bit must be broken in more carefully than when using a negative rake because the orientation is not so strong structurally.

4—A high negative rake of 30° is a compromise orientation sacrificing some diamond wear for increased rate of penetration. The setting is very strong structurally, and the trailing edge fractures just enough to give a rough cutting surface. If desired, more diamonds can be set in a given area than using the on point position. Some consideration might be given to supporting the trailing point by backing it with matrix. However, this backing might again increase the tendency to polish by resisting diamond fracture and by exposing a greater contact surface.

5—On point orientation, in a direction paralleling a crystallographic axis, apparently has the same merits and faults of setting 3. Performance is almost identical. If anything, diamond wear should be higher although fracture characteristics offset this somewhat.

Of course further test work is required to confirm the above results. This should be done now by operational testing in the field, as well as in the laboratory. It is recommended that the bit manufacturers consider orienting those octahedron crystals having discernible faces with a 30° negative rake. Meanwhile, it is hoped that research may be initiated to determine an easy production line technique of orienting diamonds crystallographically.

Future Research

Plans for further research on diamond orientation embrace the following aspects:

1—Testing three additional bits with the 30° negative rake settings, of which one or more bits will have the diamond points backed with matrix for support, as indicated in Fig. 8d.

2—Testing several bits set with cube diamonds. The first orientation of the cubes is as shown in Fig. 8f, approximating a 30° negative rake off the octahedral face.

3—Test procedures will be changed later, whereby drilling will be started, after break-in period, at a predetermined constant rate of penetration. This rate will be held as long as possible within the thrust limitations of the drill, and then allowed to taper down to a set minimum. This technique approximates more closely field practice with a feed screw unit.

4—Research on developing a simple method of obtaining crystallographic directions for diamonds lacking discernible faces.

5—Testing of West African diamonds of size 10 per carat with similar orientations to those used with Congo diamonds to obtain comparative performance data.

References

[1] Edward H. Kraus and Chester B. Slawson: Variations in Hardness in the Diamond. *American Mineralogist,* (November 1939) **24**, pp. 661-676.

[2] Harry Whittaker and Chester B. Slawson: Vector Hardness in Diamond Tools. *American Mineralogist* (1946) **31**, pp. 143-149.

[3] H. D. H. Drane: *Research* (1948) **1**, p. 157, based on M. Tolkowsky, D.Sc. Thesis, London 1920. As reported in article The Physical, Mechanical and Chemical Properties of the Diamond. *Industrial Diamond Review* (August 1944) **4**, pp. 167-168, 178 and 179.

[4] Horace Winchell: Observations on Orientation and Hardness Variation. *American Mineralogist* (1946) **31**, pp. 149-152.

[5] Chester B. Slawson and J. A. Kahn: Maximum Hardness Vectors in the Diamond. *Industrial Diamond Review* (June 1950) **10**, pp. 168-172.

[6] Harry Whittaker: Report on Substitution of Lower Quality Industrial Diamonds in Diamond Dresser Tools. For War Metallurgy Committee of National Academy of Sciences, National Research Council. Nov. 6, 1943 and Oct. 16, 1944.

[7] Albert E. Long: Diamond Orientation in Diamond Bits. U. S. Bur. Mines *R. I.* 4800 (June 1951).

Underground Mining Trends In The Great Swedish Export Iron Ore Mines

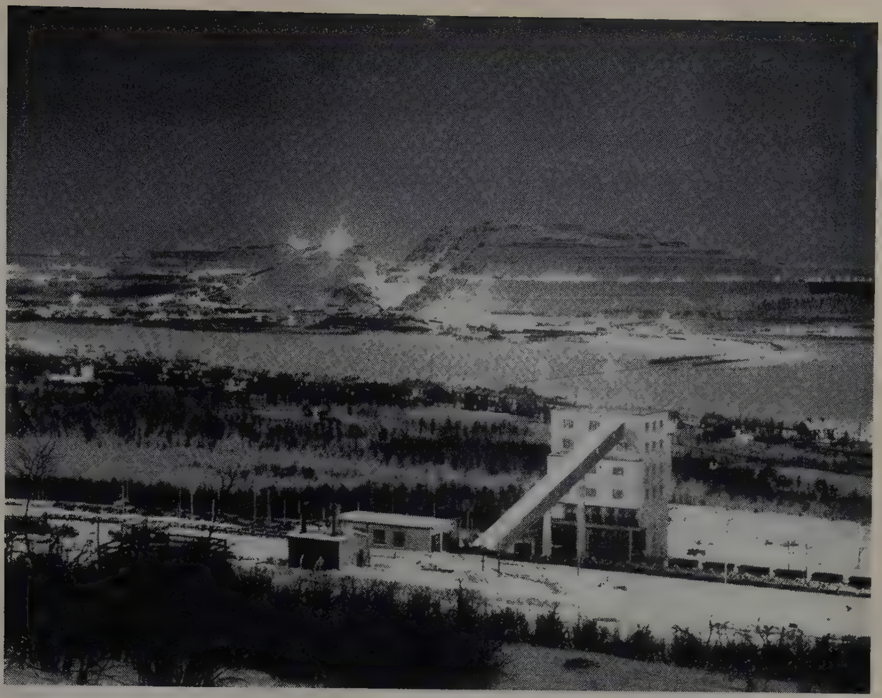

Fig. 1—The Kiruna ore mountain. The cleft shows the dip of the orebody.

by Borje Hjortzberg-Nordlund

THE great Swedish export iron ore mines are Kiruna and Malmberget in the north above the Arctic circle and Grängesberg in Central Sweden, see Figs. 1 to 3. These mines exported in 1951 about 13 million metric tons of high grade iron ore and concentrates.

The origin of these three ore fields seems to be the same. They are of pre-Cambrian age and are regarded as typical instances of primary eruptive ore that has thrust up as glowing masses of lava flow between two somewhat older beds of porphyry. Apparently the ore and the porphyry became segregated from common parent magmas by a process of differentiation.

Despite the fact that the Kiruna orebody belongs to the earliest pre-Cambrian formation, it has been influenced to an unusually small extent by later metamorphosisms, apart from its having been set on edge through folding and wrenching off by a number of later faults. The Kiruna ore occurs along a stretch of more than 4 miles as a series of slabs or lenses sloping steeply toward the east and sandwiched between two beds of porphyry. The main orebody has a length of about 3 miles and an average width of 300 ft with a maximum of 600 ft. The dip varies from 65° to 45° toward the east and the known depth is 3000 ft, although magnetic surveys indicate it may be at least 6000 ft.

Malmberget has undergone a more thorough transformation, having been pressed and crumpled into a meandering band of disconnected layers and lenses. The largest of the more connected bodies of ore, the Great Ore Layer, outcrops on a low mountain ridge and has a total length of about 4 miles and a maximum width of about 300 ft. The dip varies from 30° to 70° towards the north.

The main orebody in Grängesberg, the so-called

BORJE HJORTZBERG-NORDLUND is with Trafikaktiebolaget Grangesberg-Oxelosund, Stockholm, Sweden.

Discussion on this paper, TP 3262A, may be sent to AIME before April 1, 1952. Manuscript, Nov. 9, 1951. New York Meeting, February 1952.

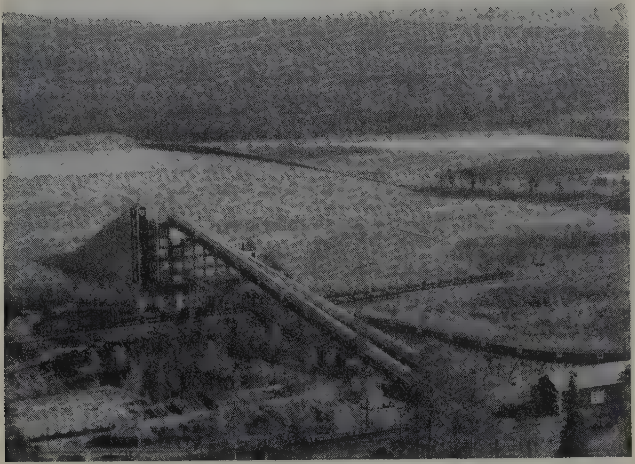

Fig. 2—Formerly four dry-magnetic sorting plants of this type served each adit of the Malmberget mines. Today a centralized plant is being built to handle all the ore.

Export-Field, consists of a great lenticular slab tilted towards the east at 65° to 70°. It is about 300 ft wide and 1 mile long. A number of smaller orebodies occur in the footwall, and all of them are typical apatite ores; consequently they carry a high phosphorus content. Here as well as at Kiruna and Malmberget the ores are sharply defined against the surrounding rock and the intermixture of gangue is small.

The Grängesberg mine is owned by the Trafik AB (Traffic Co.) Grängesberg-Oxelösund (TGO), and Kiruna and Malmberget by a subsidiary company, Luossavaara-Kiirunavaara AB, (LKAB). In the latter company the Swedish Government as ground owner holds half the shares but has only a minority influence on the managing of the mines.

The three mines offer different problems. The trends will be analyzed but details discussed only when necessary.

Mining Methods

Hitherto Kiruna has been mined by the conventional open-pit method. Within the next few years, however, the mining will have to go underground. Then two mining methods will be considered. When possible, shrinkage stoping will be adopted with the stopes placed across the orebody. The distance between the haulage levels will be about 150 ft. If the hanging wall is not reliable, the dip too flat, or various grades of ore occur within the same area, shrinkage stoping is out of the question, and a kind of highly mechanized sublevel caving will be used. Each level will be divided into blocks 600 ft long, and as the orebody averages a width of about 300 ft, the blocks will contain between 4 and 5 million tons of ore. Distances between sublevels will be about 20 ft. As many ore winzes as are needed for the different ore qualities will be driven. The sublevel crosscuts will be 12 x 16 ft. When driving crosscuts, drilling probably will be done by the help of air-leg equipment. Advance should be 15 ft a shift, which would give about 400 tons of ore. When mining proper is started, automatically operated drill rigs will be used, and the daily capacity in each stope will be about 2000 tons, working two shifts. Loading and transportation will be trackless on sublevels but with tracks and trolley locomotives on haulage levels.

In Malmberget the same mining methods are used, but here conditions are often favorable for long-hole blasting. Both horizontal drilling from raises and vertical drilling from drifts have been tried successfully, and also long holes in combination with shrinkage stoping.

The Grängesberg orebody is frequently traversed by younger granite and pegmatite dykes, which make the ore roofs of the shrinkage stopes unreliable. Therefore, sublevel caving methods are used most often, and the ore at the stopes is loaded by Eimco-type loaders. Long-hole drilling in combination with caving has been tried rather successfully.

Since about 1930, time studies, referred to in these mines as work studies, have been a guiding factor. Today all kinds of work are studied carefully to find better methods and more suitable equipment. The results have been very satisfactory and have led to new developments in a number of different phases of underground mining.

However, studies of a small part of a large job may lead to absurdities if the whole is not properly considered. Therefore, when the work studies have been started, they should not be stopped until all jobs in underground mining are covered.

Drilling

The first job tackled was drilling. In choosing among different types of drilling machinery, the choice often was founded on personal likes and dislikes, with no objective basis for selection available. By thorough work and time studies there was designed, in collaboration with Atlas-Diesel Co., the well-known air-leg or jack-leg in combination with a number of rather small drills, which made a lighter type of drilling fast and easy. A complicated, more or less automatic, drilling equipment was obtained, which could be applied when conditions justified heavy machinery, see Fig. 4. This drill is typified by the Bux drill used in Kiruna. In both cases time losses were brought down to a minimum.

During the first studies of drilling operations, the question of drill steel proved of greatest importance. At about the same time the alloy steel was introduced, and it soon replaced the plain carbon drill steel. But the miners had to carry too heavy burdens of drill steel, which required much time in the stopes as well as in the transportation. Several kinds of detachable bits were tried, but the drilling results did not correspond to the costs. Then tungsten carbide bits were tested. From the beginning good results were obtained, but the high costs made excellent results imperative. An almost immense footage per bit was needed, and the average minimum considered in Malmberget was 1000 ft in ore and 500 ft in rock, comparable to bare granite. After 5 to 6 years of experiments and research, the Sandvik coromant bit reached that average, and about 1945 that steel was adopted for all kinds of drilling, and today it is used exclusively. A number of other tungsten carbide bits have also given good results, for example, the Fagersta Seco bit.

An interesting development occurred in Grängesberg. The mining method, sublevel caving with rather narrow crosscuts, made it necessary, when changing the longest drill steel, to bend the steel to get the depth of hole that gave optimum blasting results. This cannot be done with alloy steel, and the use of carbide bits with common carbon steel is not favorable, as the expensive bit outlives the steel. Then it was decided to solder the bit to a hollow flat spring steel rod of good quality, which could be bent when inserting, see Figs. 5 and 6. The durability of the steel is most satisfactory, and no decrease in the drilling speed is noticeable.

As mentioned before, blasthole drilling has been widely—and almost always successfully—applied to different mining methods. Diamond drilling as well as drilling with hammer drills and carbide bits has been tried. The latter seems to be much less expensive but is not yet quite reliable, as it proved difficult to force enough water through the jointed drill steel. This problem, however, is being studied, and there is hope that soon diamond drilling will be necessary only when longer holes than 75 to 90 ft are required and that carbide bits will be used for shorter holes.

Blasting

For a long time the underground blasting practice followed conventional lines. During World War II as well as afterwards there has been a shortage of glycerine, and to maintain the same rate of detonation with the least possible consumption of glycerine, a number of aluminum explosives with a considerably lower content of nitroglycerine were developed, some of which have proved satisfactory and are now in common use in the mines. No increase of dangerous gases has been noticed.

When charging long holes, 5-ft long cardboard cylinders filled with the explosive at the plant are used. The charging requires about one third of the time needed for charging with cartridges of ordinary size. It is interesting that these cylinders, which have a 1.18-in. ID, contain 0.67 lb of dynamite per ft, while a diamond drill hole of 1¼ in. charged by hand takes only about 0.56 lb per ft.

After the last war, short delay blasting has been studied intensely in Sweden. In open-pit mining valuable results have been achieved. Underground long-hole blasting with short delays apparently results in better fragmentation and also in stronger roofs or walls, but it has been difficult to bring these facts out clearly, as in different mines and parts of mines conditions vary so rapidly that approximate statistics must be relied on, and to get even these requires a rather long time.

An effort is being made to increase the depth of the round when tunneling by blasting the burn cut in two short-delay blasts. On an average the depth of a round is 8 ft. There would be a gain in drilling as well as loading capacity if this depth could be increased to say 15 ft. First, the bottom 7 ft are charged and short-delay detonators applied, then a space of about 8 in. is filled with sand or gravel, and finally the outer part of the hole is charged. The short-delay detonators are so placed that the inner parts of the holes are ignited some milliseconds later than the outsides, just enough to remove the burden before the inner parts explode.

Loading

Formerly, loading and transportation normally represented about 40 pct of all underground shifts. Therefore, these operations were among the first to be penetrated carefully.

Hand mucking was one of the heaviest jobs in underground mining. When the time came that the young men did not want underground jobs and management had to try to make mining a more attractive profession, the first consideration was to eliminate hand mucking. A good mucker was able to load 25 tons of rock or 30 to 35 tons of ore a shift, but a man could stand this only 10 or 15 years. Thanks to American inventors and producers, operators now have a number of good loading machines, from scrapers and scraper hoists to shoveling machines of many different types and principles. Mucking is no longer a problem, but to maintain a flowing operation is difficult. Mechanized equipment is expensive and must be kept working as nearly continuously as possible, and here is a crucial point.

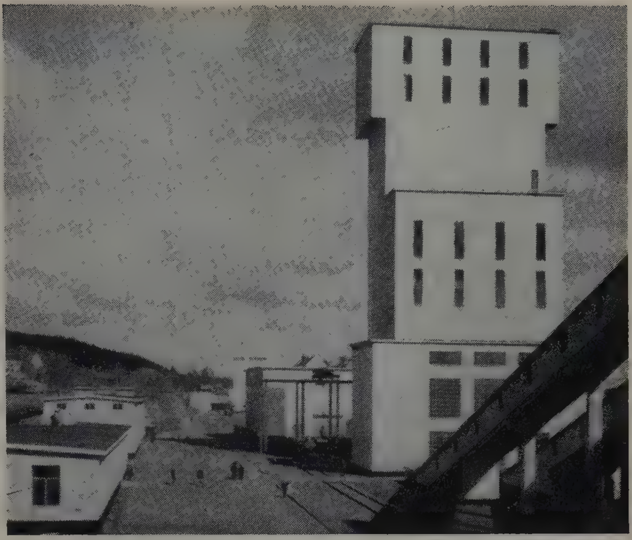

Fig. 3—Grangesberg—head frames, change houses, and dining hall.

In the narrow drifts of a mine, the rapid changing of cars has always caused debate. Cherry pickers, movable switches, passing tracks etc. are used, but are hardly ideal. When changing over to large cars, the problem is more difficult, even if a large car will keep the loader running a longer time for each car. It is believed that the best thing would be to have the loader working into a movable storage car with a discharging arrangement whereby the mine cars could go underneath and be filled quickly. This probably could be done easiest if the storage car is equipped with scraper chain conveyors for loading and unloading. The Joy loader type combined with shuttle cars solves the problem efficiently in places where trackless mining can be applied, which often is the case in Kiruna and probably also in Grängesberg and Malmberget. But in narrow development tunnels and drifts, where distances are long and no winzes are at hand, operators are still looking for the perfect design.

Generally speaking, however, loading from chutes is a better practice than scraping or machine loading. It seems more logical to let the ore run by gravity into the cars if possible. To avoid finger raises and grizzlies, there has been experimentation with large chute openings. When these are wider than 3 ft, they have been found hard to operate by hand, and consequently quite a large number of different types of air-operated chutes have been constructed. Some of these have 10x4-ft openings, see Fig. 7. When such a chute is running smoothly, a car of 20 to 25-ton capacity is loaded in 10 to 15 sec. Work studies of this type of chute have proved that one locomotive driver, one loader, and one man for secondary blasting may draw 1500 to 2000 tons a shift. Then, of course, conditions were not unfavorable, but there is doubt that this could be done by any

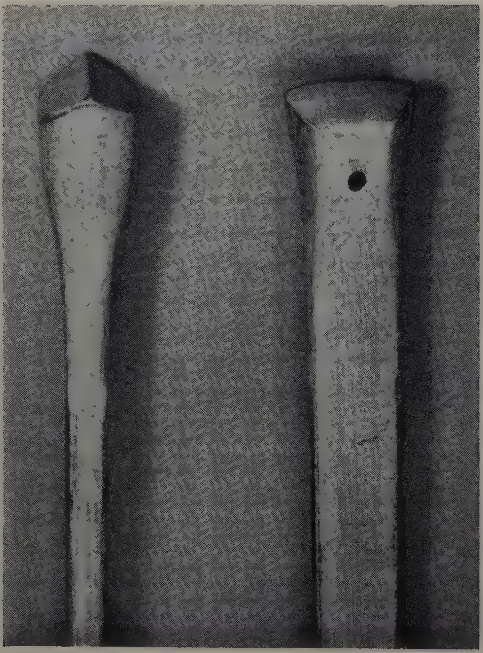

other kind of mechanical loading device in such a constricted space.

Through these chutes very large chunks of ore will be loaded in the cars. The question arose as to the proper size of these mine cars, from the haulage point of view, as large as possible. This meant that, in any case, they would be too heavy to be handled by manpower. If locomotives have to be used even at the loading points, the wheel load will be the size limiting factor. It was decided that 4 tons should not be exceeded, rail weights and tie costs also being considered. A four-wheeled car may then have a gross weight, load included, of 16 tons and a doubletruck car of 32 tons.

Long tests determined that doubletruck cars of 240-cu ft capacity should be used. As long as the older parts of the mines are worked, smaller cars, probably 100 to 130-cu ft Granby type four-wheeled cars must be used. Rotary dumping and also the use of Granby type cars is not favored, as in certain places the ore has a tendency to be sticky, and it is necessary to have men detailed to clean the cars. In Sweden today, the capitalized value of one man is at least 125,000 crowns or about $25,000, and obviously even for that reason it is important to avoid using more men than the absolute minimum. A bottom dumped mine car has been built, see Figs. 8 and 9. At one of the ends the bottom of the car is hinged to the body, and when the car is dumped it is placed on a hinged, counterbalanced dumping bridge. Then a catch is removed, and the bridge and the bottom dumps down to a sufficient angle while the body is resting on a steel frame. The car is emptied in a few seconds, and the counterweight brings the bridge up to horizontal position again. The speed is regulated by two double oil cataracts that perform this complicated task very efficiently. The bumpers of the cars are mounted on the body frame, and automatic couplings of Ohio Brass Co. manufacture will be used. The feeding of the cars on the bridge and the dumping will be mechanized and push bottom operated by the man in charge of the crushing station below the haulage level. A few of these cars have been running on trial in Malmberget, and costs of repairs have been suprisingly low.

For various reasons the intention is to crush the ore before hoisting. Too large lumps cannot be transported on conveyor belts. The filling of the skips and the hoisting should be automatic as far as possible. One of the engineers has designed a hydraulically balanced measuring pocket that will be filled and emptied automatically and seems to meet all requirements. But the ore must be of a size that will run easily. Generally, the purchasers want ore crushed below 4 in., and to facilitate this, as a rule, an underground plant will have to be designed to produce ore of that size, which, obviously, also conforms with plant requirements.

The primary crusher will be a single-toggle type with a receiving opening of 60x70 in. and discharge opening of 16 in. Secondary crushing will be facili-

Fig. 4—The Bux drills are rather heavy and are operated by one man and a helper.

Fig. 5—Carbide bits are soldered to a hollow, flat, spring-steel rod.

Fig. 6—Drill rods of hollow, flat, spring steel bend when inserted into the drillhole.

tated by either a Blake type or a gyratory crusher. Each crushing plant will be built for an average capacity of 1000 tons per hr.

There are different methods for transporting the ore from underground to the surface. The Grängesberg mine is equipped with two drumhoists for ore hoisting and two Koepe-type hoists for men and materials—all more or less of conventional design.

The Kiruna central hoisting plant, now under construction, see Fig. 10, is planned for a maximum capacity of 4000 tons per hr. It consists of eight ore shafts and one man shaft. Each ore shaft is equipped with one Koepe-type hoist with a bottom dumping skip and counterweight, all designed by the Swedish firm ASEA. The skip weight is 15 tons and the useful load 20 tons. Four ropes of about 1.65 in. diam will be used. The diameter of the pulley is about 10 ft. Maximum hoisting speed will be 36 fps. Two shafts will serve one underground crushing plant. The hoists will be push-button operated but, naturally, there are provisions made for simple switching over to manual operation of each hoist. The speed control is effected by means of amplidyne generators according to a system similar to that employed by the General Electric Co.

There are several reasons for this arrangement. The rock is of such structure that rather narrow shafts will stand without any concrete linings while larger shafts have to be entirely concreted. The ore from the mine must be treated in a dry magnetic plant where one section will handle 250 tons. Two sections may be reached from one shaft without any mechanical transportation. The width of the sections gives a distance between shaft centers of about 45 ft. Ore will be hoisted from several levels alternatingly, and then either drum hoists or single-skip, Koepe-type hoists must be used. One rope for a load of 35 tons would be unwieldy, and the pulley or drum necessarily would be large. This is avoided by using several ropes, which is scarcely applicable to anything but the Koepe hoist.

In Malmberget it is intended to have conveyor belt transportation of the ore from the two or three first underground levels. The distance between levels is about 160 ft, which corresponds to 25 to 30 million tons of ore. The conveyor belt installation is of a rather new type, and a more detailed description follows.

For many years the Sandvik steel plant in Sweden has manufactured conveyor belts of cold-rolled, hardened and tempered steel. The material is of high grade charcoal quality, cold rolled to the following physical properties: tensile strength, 170,000 psi; proportional elastic limit, 136,000 psi; hardness (Vickers), 340 to 350; and endurance limit, 78,000 psi.

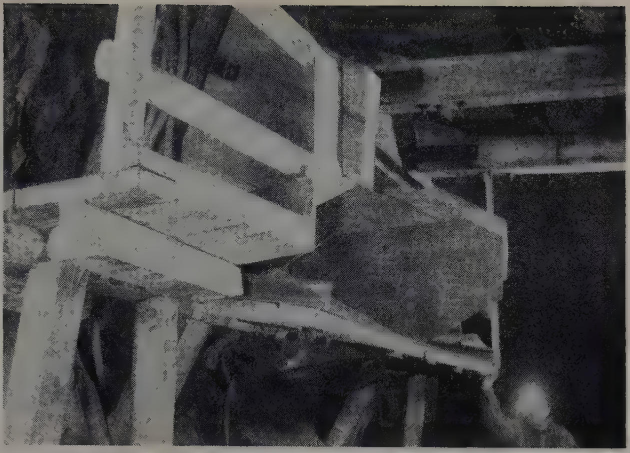

Fig. 7—An air-operated chute, 10x4 ft, permits a 20-ton or 25-ton capacity mine car to be loaded in 10 to 15 sec.

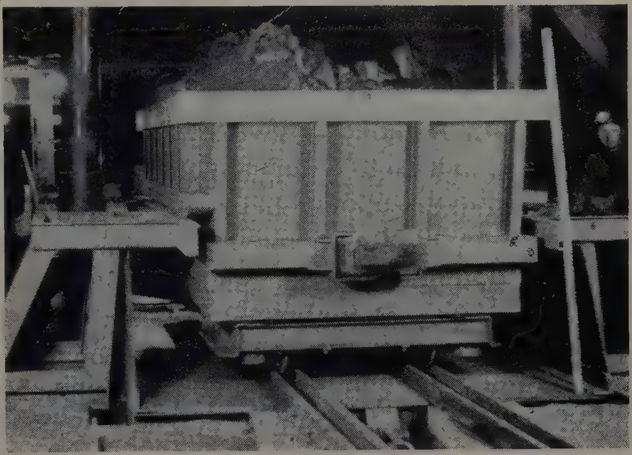

Fig. 8—The bottom of this double-truck car of 240 cu ft capacity is hinged to the body. When the car is dumped, it is placed on a hinged, counterbalanced dumping bridge.

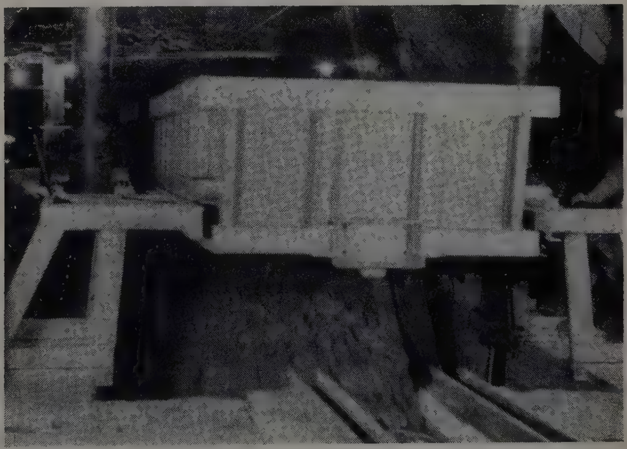

Fig. 9—The body of the dump car rests on a steel frame while the two oil cataracts on each side of the car regulate the speed of the counterbalanced dumping bridge.

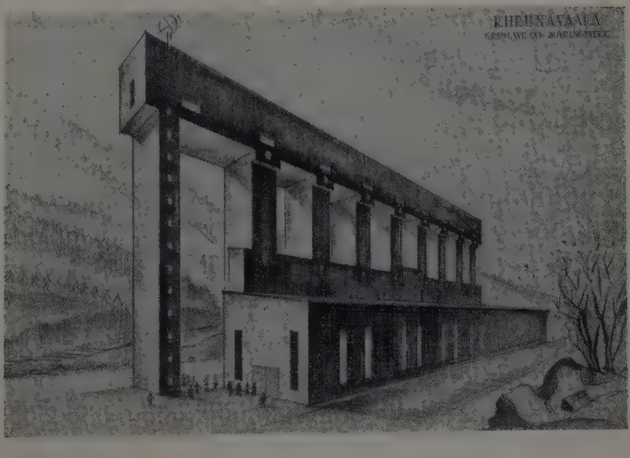

Fig. 10—Head frame and sorting plant as planned for Kiruna. The machinery for man hoists (left) and eight ore shafts (right) is placed in the machine hall 140 ft above ground level.

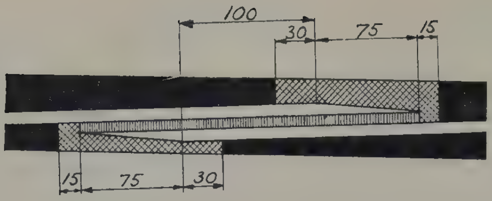

Fig. 11 (above)—Rubber covered steel conveyor belts are used in ore handling. A joint is shown here. The strength of the adhesive used in joining the rubber to the steel provides a bond greater in strength than the shear strength of rubber.

Fig. 12 (right)—When rubber on the belting wears away, there remains a thin layer of rubber that temporarily protects the steel until a patch is put on. In Malmberget, two belts of 700 tons per hr capacity will be required.

For years these belts in different widths and thicknesses have been used for conveying purposes when sticky and nonabrasive materials are being handled. For materials, such as iron ore, they have, however, their limitations. Therefore, to improve their surface to obtain better resistance against wearing, experiments have been conducted for a few years. The result is a rubber-covered steel conveyor belt. This implies that the steel belt is covered completely with rubber and fastened to the steel by a special method, see Fig. 11. The thickness of the rubber covers on the top and bottom of the belt is determined according to the same rules as have been adopted when specifying the cover plates on canvas rubber belts. The strength of adhesion between the steel and the rubber is even greater than the shearing strength of the rubber itself. If for some reason the rubber should be torn away from the steel, there would always remain a thin layer of rubber on the steel which, at least temporarily, protects the steel from corrosion until a new patch can be put on.

The belts are made endless by an overlapping joint. The two belt ends are glued together with a thin sheet of rubber between them and then vulcanized. By making a sufficiently large overlap, the joint can be made stronger than the belt itself, see Fig. 12. As a comparison it can be mentioned that with a shearing strength limit of 128,000 psi, an overlap of approximately 10 in. will withstand the same tension as a 1.66 mm thick, steel conveyor belt. The belt ends are tapered, and this is done to even the stresses in a joint when it passes over the terminal drums.

Fatigue tests indicate that belts and joints should stand combined tension and bending stresses up to 49,000 psi at 10 million bendings. From this it can be seen readily that rubber-coated steel belts possess favorable characteristics as regards the tensile strength, and this makes it possible to install long conveyors with high lifts.

In Malmberget two belts with a capacity of 700 tons per hr each will be needed. The total length is 1700 ft, the lift 490 ft, the belt width 27.5 in. and the thickness of the steel 1/16 in. A calculation shows that at a belt speed of 10 fps, there will be a total stress in the belt of 47,500 psi. Of these, 26,000 psi are required for the bending stresses when a 71 in. diam has been selected for the driving terminal drum, while the pull in the belt is 21,500 psi.

The mechanical accessories are principally of the same design as those used for canvas rubber belts. Some deviations are, however, to be noted, e.g., the total width of the idler sets is somewhat narrower than the width of the belt, and the idler rollers are fastened on springs, which makes the idler sets flexible and enables the idler rollers to adapt themselves to the natural troughing of the belt. If the right choice of springs has been made, the individual idler rollers will always be in contact with the belt, regardless of whether the belt is loaded or unloaded. This ensures a minimum of wear and keeps the transversal bending stresses in the belt due to the troughing within the allowed limits.

An effort has been made to give a short description of the trends in underground mining. Of necessity, this has been a brief account, and there are numerous other problems which have been penetrated to get the best possible total results. The Swedish Ironmasters Association (Jernkontoret) has organized the Mining Research Committee which has aided greatly the mining industry. Today a number of these research groups are studying different problems, among which are: magnetic surveying, rock bursts, explosives and blasting, tungsten-carbide bit drilling, air leakage, track resistances, etc. The research comprises fundamental scientific research and empirical field work. The results are either published or distributed only to the sponsors of the Research Committee.

However, in a few years today's trends should be actual practice. It is hoped that at that time mine production will increase, not only in the interests of Swedish companies, but because there is a serious world shortage of high class iron ore.

Adsorption on Quartz, From An Aqueous Solution, Of Barium and Laurate Ions

by A. M. Gaudin and C. S. Chang

Adsorption was measured for barium ion and laurate radical, using radioactively marked agents, over wide range of concentrations. Laurate adsorbed in absence of barium fails to float. With barium, flotation-effective laurate coating needs not exceed 5 pct of monolayer. Barium adsorption then is several fold larger. No barium laurate coating is obtained.

IN general, fatty acids or their alkali salts do not cause clean quartz to float. However, the presence of multivalent ions, such as the alkaline-earth metal ions and heavy-metal ions, can activate quartz and thus make it respond to soap flotation.

The mechanism of activation and soap flotation of quartz has been studied.[1-4] The problem was attacked by making flotation tests rather than by careful adsorption measurements on suspensions of ground quartz in solutions containing the activator and the collector. Attempts have been made to determine the adsorption of barium ion and calcium ion on quartz. The results have only qualitative value as the analytical methods were not adequately precise.

Artificial radioactivity and progress in radioactivity detection have introduced a new analytical tool, which can have a sensitivity several orders of magnitude greater than that of other methods.[5-6] In the experimental work described in this paper the radioactive tracers, barium 140 and carbon 14, were employed. Lauric acid was synthesized, having a radioactive carbon atom and was used with Ba^{140} to study the adsorption of barium and laurate ions from aqueous solution on ground quartz. Flotation tests, using the vacuum flotation technique,[4] were run in conjunction with the adsorption experiments. The object of this investigation was to understand better the reaction mechanism of barium activation and soap flotation of quartz.

Methods and Materials

Quartz Sample Preparation: Lumps of hand-picked quartz, washed free of stains, were reduced in size to −20 mesh in laboratory crushers. The product was boiled in concentrated hydrochloric acid to remove the abraded iron. The cleaned product then was ground dry in a laboratory porcelain mill, using siliceous pebbles, to pass through a 200 mesh screen.

The ground product was deslimed by sedimentation at 37 microns. This −200 mesh +400 mesh material was subjected again to boiling with concentrated hydrochloric acid, followed by washing with distilled water and further desliming. The cycle was repeated until no trace of iron could be detected in the wash liquor. During the final washing, the pH of the wash water was checked to insure the complete removal of the acid from the mineral. The quartz then was rinsed with conductivity water. The resulting product was dried in a drying oven and stored in mason jars.

The impurities (spectrographic) were as follows: Al, 0.01 to 0.001 pct; Li, Mg, Mn, Na, each less than 0.001 pct; Fe and Cu not detected.

The specific surface of the quartz sample was determined by the krypton gas adsorption method.[7] The average of two measurements was 881 sq cm per g. The calculated specific surface for 37/74-micron quartz particles, using a surface factor of 1.96,[8] is 900 sq cm per g. This is in good agreement with the measured value of 881 sq cm per g.

Beta-Counting Method: The radioactive isotope of barium used in the experimental work was barium 140. It has a sufficiently long half-life, 12.8 days, emits high-energy beta particles (up to 1.0

A. M. GAUDIN, Member AIME, and C. S. CHANG, Junior Member AIME, are Professor of Mineral Engineering and Armour Flotation Research Fellow, respectively, Massachusetts Institute of Technology, Cambridge.

Discussion on this paper, TP 3244B, may be sent to AIME before April 1, 1952. Manuscript, Oct. 25, 1951. New York Meeting, February 1952.

Abstracted from the thesis for the Doctorate in Mineral Engineering by Chen-Siang Chang, May 1951.

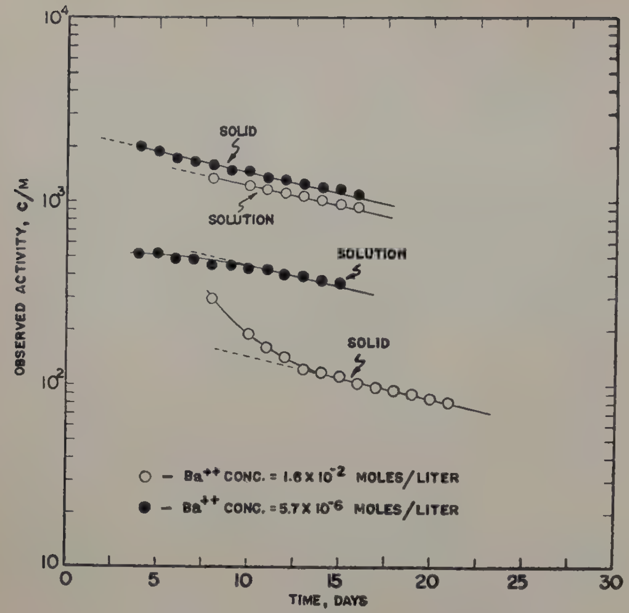

Fig. 1—Gross decay curves of Ba^{140}-La^{140} in samples.

Mev[9]) and is obtainable in high specific activity. The decay scheme is as follows:

$$\mathrm{Ba}^{140} \xrightarrow[12.8d]{\beta.\gamma} \mathrm{La}^{140} \xrightarrow[40h]{\beta.\gamma} \mathrm{Ce}^{140}$$

The fact that Ba^{140} decays to a radioactive daughter La^{140} of 40-hr half-life complicates the counting procedure. But the presence of La^{140} which emits hard beta (70 pct 1.4 Mev, 20 pct 0.90 Mev and 10 pct 2.12 Mev)[9] increases the ease of detection.

Chemically the coexistence of La^{140} when using Ba^{140} as a tracer for barium in an adsorption test will not affect materially the result. Calculation shows that even in the most adverse case there are not less than 25 million times as many stable barium atoms as of radioactive La^{140} atoms. The *chemical* effect of the lanthanum therefore can be neglected.

In radioactive measurements, however, the effect of these La^{140} atoms cannot be ignored. The partition of La^{140} in an adsorption test between quartz and solution may not be the same as that of Ba^{140}. For this reason, attainment of radioactive equilibrium (between La^{140} initially present, La^{140} growing from Ba^{140} and Ba^{140} present) after the mineral-solution separation becomes a necessary prerequisite for all activity measurements. An aging period must be allowed between the time an adsorption test is completed and the subsequent radioanalyses of the test products.

The decay curves of the solid and solution samples from two barium adsorption tests at barium concentrations of 0.0057 and 16 millimol per liter are shown in Fig. 1. At the low concentration the tracers on the mineral reach equilibrium ahead of those in the liquor (11 days). The reverse was true in the case of the test at high concentration. In that test it took 14 days for radioactive equilibrium on the mineral. Therefore, the aging period necessary varies. Inasmuch as all the tests were conducted within the range of concentration shown in Fig. 1, an aging period of 14 days was adopted for all the samples. Radiochemical calculation indicates that aging for 2 weeks would give complete equilibration for samples initially overrich in barium 140, and for any samples overrich in lanthanum 140, provided the lanthanum excess is not more than tenfold. If a

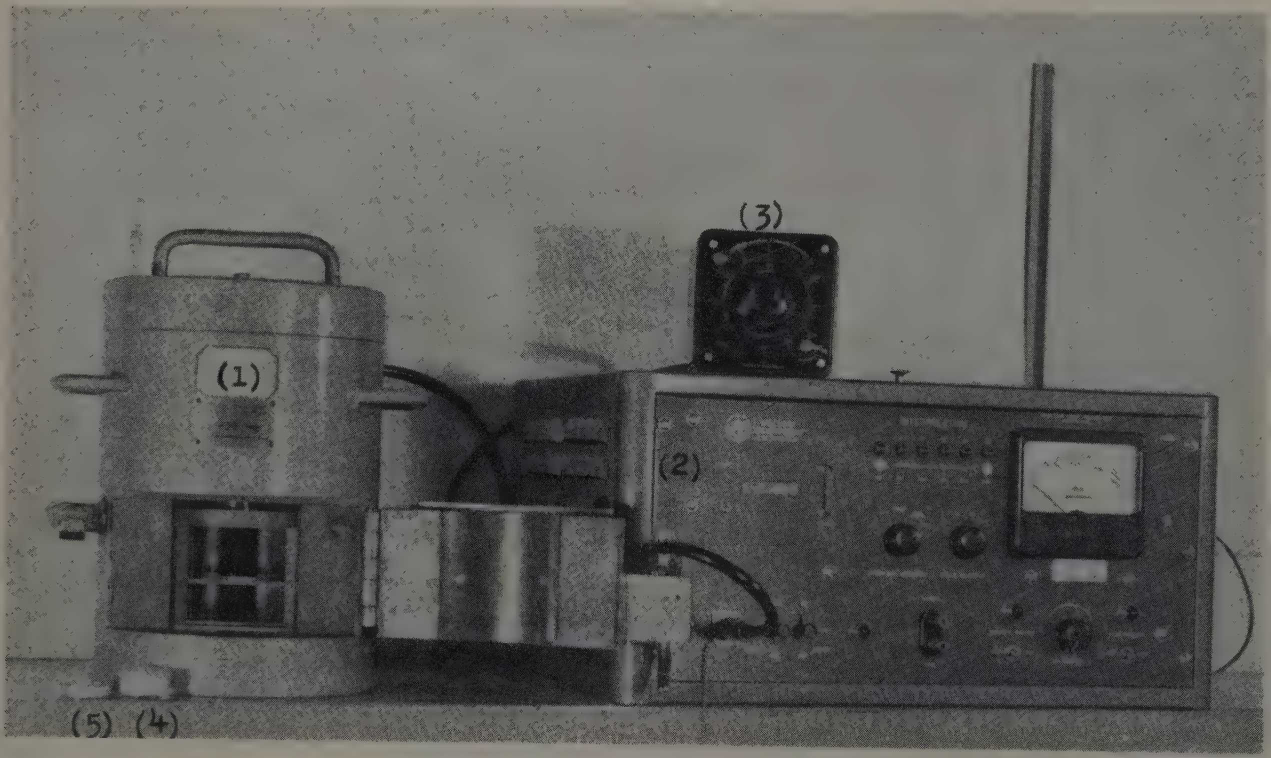

Fig. 2—Counting equipment for radiobarium.

1—Lead housing with end-window inside
2—Model L-163 scaler
3—TI timer
4—Lucite counting container for solid sample
5—Aluminum counting cup for solution sample

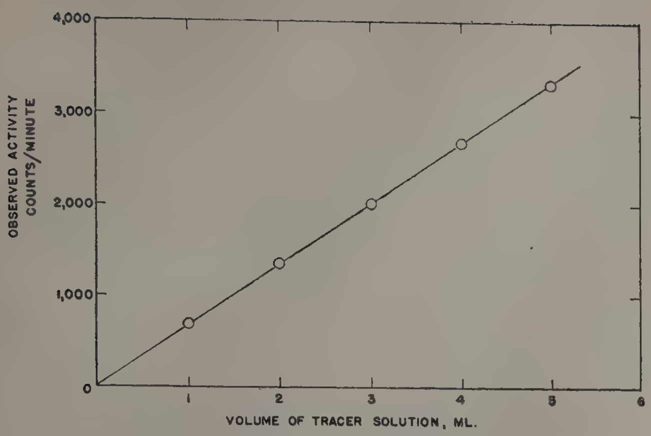

Fig. 3—Proportionality of amount tracer and observed activity in solution counting.

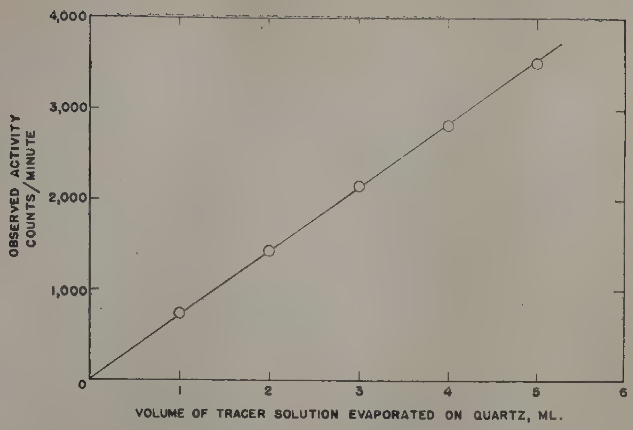

Fig. 4—Proportionality of amount tracer and observed activity in solid counting.

more extreme excess of lanthanum is to occur, still longer than 14 days should be allowed. Incidentally, Fig. 1 suggests that lanthanum is adsorbed on quartz, under the experimental conditions tested, to a greater extent than barium.

The instrument used for radiobarium measurement is shown in Fig. 2. It consists of a mica end-window counter housed in a lead chamber provided with a carefully machined lucite holder with five different geometry shelves, a Model L-163 scaler and a Tl timer manufactured by the Nuclear Instrument & Chemical Corp. of Chicago.

For measurement of radiobarium in solution, the sample was prepared by evaporating a certain volume of the solution in an aluminum counting cup. The linear relationship of the counting rate to amount of tracer is shown in Fig. 3.

To have the same geometry for counting solid samples, in this case, quartz with adsorbed barium, it was necessary that a constant weight of sample be used for each measurement. In all the adsorption experiments 15 g of quartz were used. Therefore, all solid countings were made with 15-g samples. This is more than twice the quantity of quartz needed to provide infinite thickness[10] for the (2.12 Mev.) maximum energy beta-ray of Ba^{140}.

The proportionality between the observed activity and the amount of barium coating on quartz was checked by determining the counting rates of five 15-g samples of quartz on which different quantities of tracer solution had been evaporated, as illustrated in Fig. 4.

To correlate the data from solid and solution countings, the ratio of observed counting rates per unit quantity of tracer in the two methods of counting was determined.

When running a series of barium adsorption tests, the initial tracer concentration was kept constant by adding the same quantity of tracer in each test. For comparison, a standard was prepared by evaporating a certain volume of solution having the same initial tracer concentration as that in each of the adsorption tests. The adsorbed barium and barium in solution were obtained by comparison of the observed activities of the samples from the adsorption experiment to that of the standard.

Radioanalysis Technique: The radioanalysis of labeled lauric acid required conversion of the organic compound into carbon dioxide. This was accomplished by boiling it in the van Slyke-Folch combustion mixture.[11] The carbon dioxide formed was separated from the other gaseous products of combustion by fractional distillation. The activity of the gas was measured by the internal gas counting method originally developed by Miller and Brown.[12, 13] Details have been given previously.[5, 14]

All samples, quartz and solution, from adsorption tests in which lauric acid was used were dried slowly at room temperature by natural evaporation. After evaporation, the samples were placed in the combustion chamber of a wet combustion train for further processing.

Double Tracing Procedure: The fact that C^{14} has a weak maximum beta emission energy (0.154 Mev)[9]

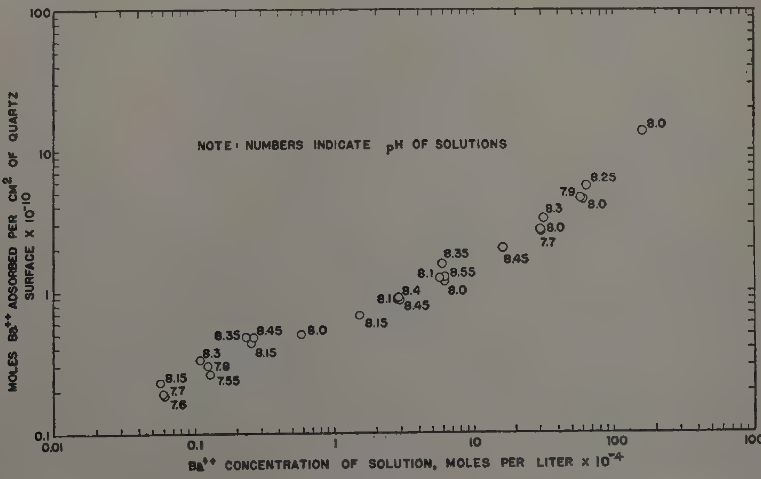

Fig. 5—Adsorption of barium on quartz, effect of barium-ion concentration.

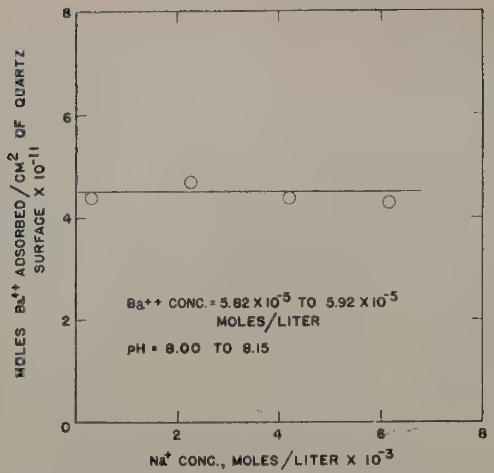

Fig. 6—Adsorption of barium on quartz, effect of Na^+.

and that barium does not form a gaseous compound when subjected to a wet combustion process played an important role in making possible the use of the two tracers in one experiment.

The activity of C^{14} can be shielded completely by the use of an absorber having a thickness of approximately 30 mg per sq cm.[10] In these tests, the radiobarium, in spite of the presence of C^{14}, was measured in the usual manner except that an aluminum absorber, 35.8 mg per sq cm, was placed between the mica end-window counter and the sample. There was no change in the method of analysis for the C^{14} marked lauric acid.

For a sample of quartz coated with both barium and laurate, the radiomeasurement of barium preceded that of the C^{14}.

Adsorption Test Procedure: A weighed 15-g sample of clean ground quartz was agitated in a stoppered 100-ml glass cylinder for 1 hr in an agitation machine with 60 ml of solution containing reagents such as tracer barium, barium nitrate, marked and unmarked lauric acid, sodium hydroxide, sodium nitrate, and hydrochloric acid, depending on the nature of the test. The mineral and the solution then were separated by filtering through a Buechner fritted disk funnel.

To insure the attainment of equilibrium conditions, the filtrate was percolated slowly through the mineral bed five times. The mineral bed was kept covered with solution at all times. At the end of the filtration the fritted disk funnel containing the solution-covered mineral bed was placed in a lusteroid centrifuge tube provided with a rubber cushion and stopper. Further removal of solution from the quartz was accomplished by centrifuging at approximately 2700 rpm for 3 min. The final moisture content ranged from 1.5 pct to 4.5 pct depending on the conditions of the test.

The quartz cake was transferred to a beaker by gentle tapping and applying a slight air pressure to the stem of the fritted disk funnel. The beaker then was given a glass cover and weighed. The cake later was allowed to dry in the beaker and reweighed to determine its moisture content. In the radioanalysis of adsorbed reagents, a correction was provided for the retention of moisture by the quartz. Another small correction was made for handling losses incurred in the quantity of mineral.

The pH of the filtrate was measured with a Beckman Model G pH meter. For the radiobarium in solution, a sample was prepared by evaporating 5 ml of the filtrate in an aluminum counting cup of approximately 3.3-cm diam and 0.7 cm high. For laurate in solution, 1 to 10 ml of the filtrate, depending on the amount of C^{14} activity added, was evaporated in a 10-ml glass beaker, and this beaker was introduced bodily in the wet-combustion flask.

The mode of evaporation of the moisture in the samples, solid and liquid, was governed by the presence or absence of lauric acid in the test. When laurate ion was to be measured, the samples were dried only by exposure to the air at room temperature.

In addition, duplicate standard samples were prepared by evaporating in an aluminum counting cup 5 ml of solution having the same initial barium tracer concentration.

All adsorption tests were run at room temperature, 25 ±3°C.

Vacuum Flotation Test:[4] A sample of approximately 0.5-g clean ground quartz was conditioned with 60 ml of solution in a stoppered 100-ml glass cylinder for ½ hr by agitation. The glass stopper then was removed, and a vacuum line was connected to the glass cylinder. The floatability of the quartz under the existing condition then was observed.

Reagents: For the preparation of solutions, conductivity water only was used. Tracer barium: barium 140 in equilibrium with lanthanum 140, obtained by purification of fission products, was purchased from the National Laboratory at Oak Ridge, Tenn. The tracer came in the form of acidified $Ba(NO_3)_2$ or $BaCl_2$ solutions.

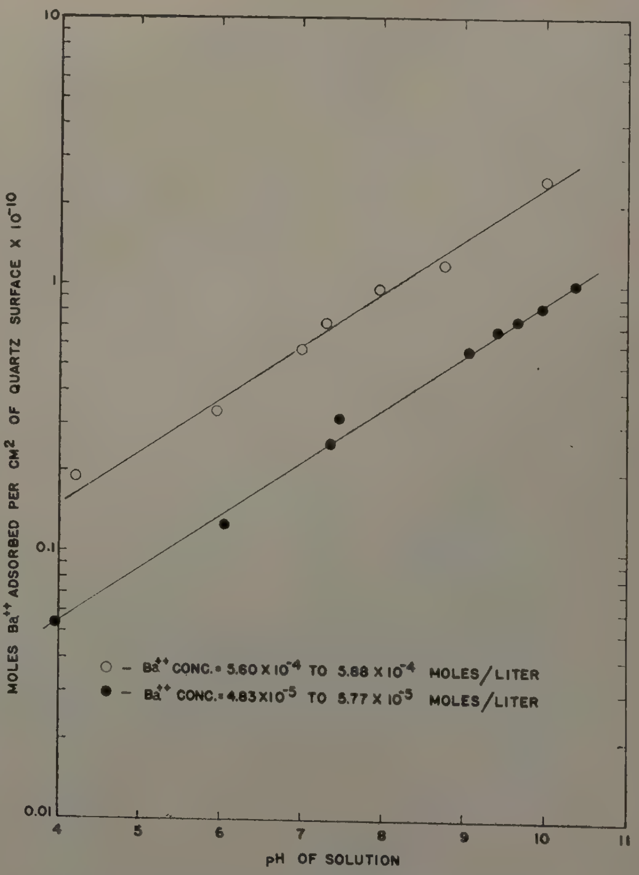

Fig. 7—Adsorption of barium on quartz, effect of pH.

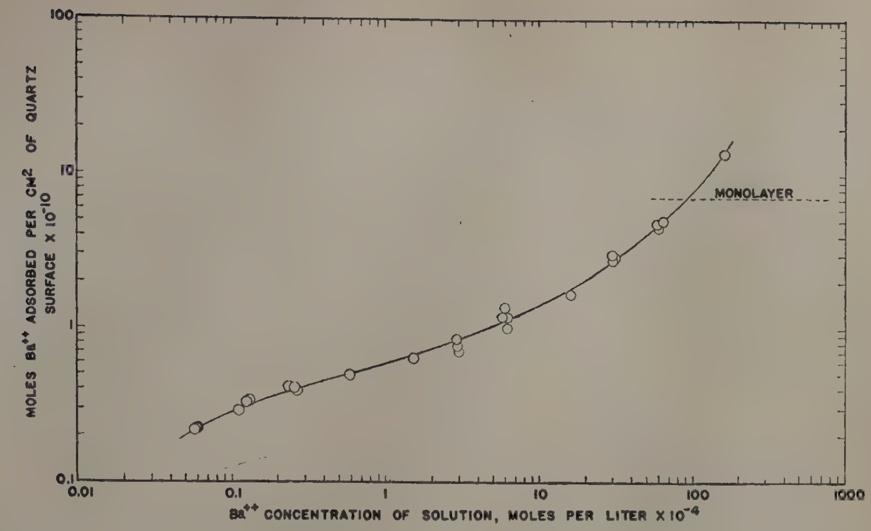

Fig. 8 — Adsorption of barium on quartz, effect of barium-ion concentration at pH 8.

Lauric acid: Harwood and Ralston[15] of Armour and Co. synthesized the radiomarked 12-carbon normal alkyl acid used in these experiments. Part of the carbon in the carboxyl group was replaced with carbon 14. The strength of the radioactive lauric acid was approximately 0.03 millicurie per g. Harwood and Ralston also prepared unmarked lauric acid of high purity.

Because of its low solubility in water, the lauric acid was dissolved by digestion in sodium hydroxide solution. It was in this form that the laurate radical was introduced in the adsorption tests.

Sodium hydroxide solution: Purified sodium hydroxide solution was made as follows: A concentrated aqueous solution (approximately 1 : 1) was prepared, centrifuged to remove the carbonate and other insoluble materials,[4] and diluted to approximately 0.3 N strength. This was then standardized against a standard solution of hydrochloric acid. Solutions of 0.05, 0.01 and 0.0031 N strength were prepared by further dilution of the purified and standardized sodium hydroxide solution.

Other chemicals: Other chemicals such as unmarked barium nitrate, sodium nitrate, and hydrochloric acid, used in the experiment, were of analytical reagent grade.

Experimental

Adsorption of Barium on Quartz: Effects of Ba^{++} concentration: The quantity of barium ion adsorbed on quartz was measured over a 5000-fold range in barium-ion concentration (from 0.0057 to 16 millimol per liter). The pH, in spite of the attempt to maintain it at about 8, varied from 7.55 to 8.45. The reagent used to regulate the pH was sodium hydroxide. Sodium ion, equivalent to 0.26 millimol per liter, was present in each test.

The data, which are shown in Fig. 5, confirm the finding of Gaudin and Rizo-Patrón[1] that quartz adsorbs barium ion. The amount adsorbed, however, depends on the barium concentration of the solution.

Effect of Na$^+$: To evaluate the effect of sodium ion on barium adsorption, the concentration of sodium ion was varied from 0.28 to 6.2 millimol per liter. Aside from the sodium ion provided by sodium hydroxide, the remainder was introduced in the form of sodium nitrate. Both barium ion and pH of the solution were kept constant with the former at approximately 0.059 millimol per liter and the latter at 8.15.

It can be seen in Fig. 6, a graphical representation of the data, that sodium at concentrations up to 6.2 millimol per liter does not affect materially the adsorption of barium by quartz.

Effect of pH: Two series of tests were run to evaluate the effect of pH. The barium concentration was maintained at approximately 0.052 and at 0.57 millimol per liter, respectively. The pH was varied from 4 to 10. Dilute hydrochloric acid was added to make the circuit acid whereas sodium hydroxide provided alkalinity.

Fig. 7 shows that the amount of barium adsorbed increases as the solution becomes increasingly alkaline. The change is not sharp since there is only approximately a 58 pct increase in adsorbed barium for every tenfold increase of hydroxyl-ion concentration.

On the basis of the variation of barium adsorption with pH, it is possible to adjust the barium adsorption data of Fig. 5 to a uniform pH, say 8.0, by the use of the effect shown in Fig. 7. The results are presented in Fig. 8. Only a portion of the data, at barium concentrations ranging from 0.015 to 0.3 millimol per liter, follows the Freundlich adsorption equation, $y = kC^n$. In this equation, y is the amount adsorbed, C the concentration of the adsorbate, and k and n are empirical constants. The slope of the line, n, in this case is approximately equal to 0.3. Beyond 0.3 millimol per liter, the slope increases with increasing barium concentration. It is interesting to note that the barium adsorption of quartz can extend beyond the monolayer. A surface concentration of 7.1×10^{-10} mol per sq cm is considered to represent a monolayer calculated on the assumption that the area for each adsorption site of quartz is equal to 23.4 A^2.[1]

Adsorption of Laurate on Quartz: Effect of laurate-ion concentration: The amount of laurate adsorbed at laurate concentrations ranging from 0.02 to 6 millimol per liter was determined. The pH of the solution was held at about 10. Since sodium hydroxide was used to digest the fatty acid, and also to maintain the high alkalinity, the sodium-ion concentration was not constant (1 to 7 millimol per liter).

The results, plotted in Fig. 9, show that quartz adsorbs laurate from solution containing sodium-hydroxide-digested lauric acid. The quantity adsorbed depends on the laurate-ion concentration and

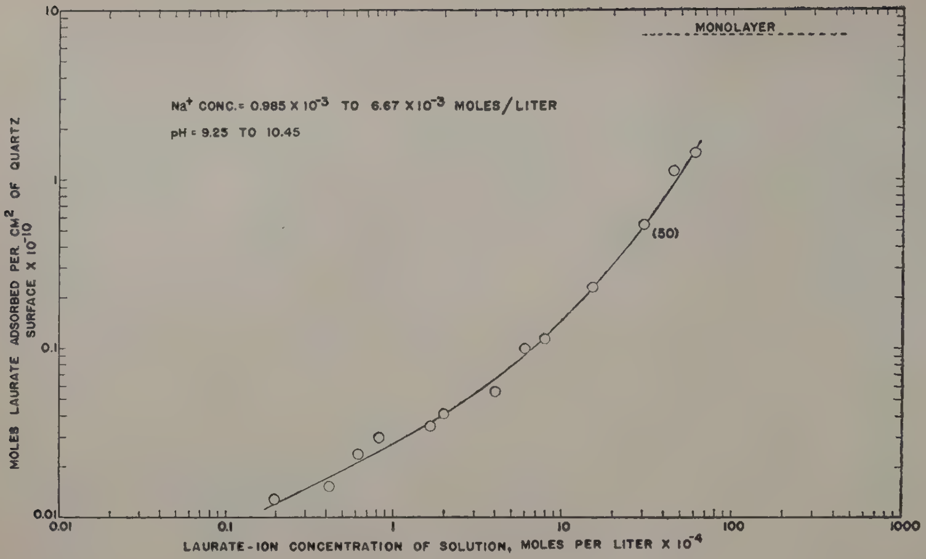

Fig. 9—Adsorption of laurate on quartz, effect of laurate-ion concentration.

is approximately one order of magnitude lower than the amount of barium adsorbed at the same concentration.

In batch vacuum flotation tests, no evidence of flotation was observed under the conditions shown in Fig. 9.

Effect of Na^+ and pH: All the tests, numbering 12, in this series were run at constant laurate concentration, namely, 0.17 millimol per liter. In four of the tests the pH of the solution was maintained at about 9.6 while the sodium concentration was varied from 0.83 to 6.7 millimol per liter. Sodium nitrate supplied the sodium ion in excess of the 0.83 millimol per liter provided by sodium hydroxide. In the remainder of the tests only sodium hydroxide was used to vary both the pH from 8.8 to 11.4 and sodium-ion concentration from 0.5 to 5.5 millimol per liter.

The results, shown in Fig. 10, indicate that increase of sodium-ion concentration increases laurate adsorption by the quartz. Varying pH from 8.8 to 11.4 does not seem to have any effect at all.

Coadsorption of Barium and Laurate on Quartz: Since under the test procedure adopted for the adsorption studies it was impossible to separate the ground mineral from whatever chemical precipitate might be formed, it was necessary to conduct all the tests at conditions under which barium laurate would not precipitate. For this reason the solubility product constant of barium laurate was determined.

The Tyndall-cone method[16,17] was chosen since it did not require an elaborate experimental setup and yielded reproducible results. The average of two experimental determinations gave $4.3x10^{-12}$ as the solubility product constant of barium laurate at 25°C. Therefore, the concentrations of barium and laurate in the tests were fixed in such a way that the product of barium concentration multiplied by the square of laurate concentration was less than $4.3x10^{-12}$.

Effect of Barium on Laurate Adsorption: A series of six tests was run in this experiment. The laurate and sodium concentrations were controlled at approximately 0.17 and 1.7 millimol per liter, respectively. The pH of the solution was held close to 10.15. The barium concentration was varied from 0 to 0.12 millimol per liter.

The data, plotted in Fig. 11, show a definite increase of laurate adsorption with increase of barium activation.

Examination of Figs. 10 and 11 show that laurate adsorption is greater in the presence of activating barium ion than in the presence of nonactivating sodium ion. Increase in barium concentration also causes a much more rapid increase of laurate adsorption than does increase of sodium concentration. Even at the highest Ba^{++} concentration tested the adsorption of laurate falls short by a factor of ten from being stoichiometrically in accord with formation of BaL_2. (*L* indicating the laurate ion).

No flotation of quartz was observed in tests run under the conditions of Fig. 11.

Laurate Effect on Barium Activation: This experiment included three series of tests.

1—The first series consisted of eight tests. The barium concentration of the solution was maintained at about 0.017 millimol per liter and the pH at approximately 10. The laurate concentration was varied from 0.075 to 0.6 millimol per liter. No attempt was made to control the sodium-ion concentration, which ranged from 1.6 to 2.5 millimol per liter.

2—In the second series, consisting of ten tests, the barium concentration was held at about 0.057 millimol per liter and the pH in the neighborhood of 10. The laurate concentration was varied from 0.04 to 0.27 millimol per liter. The sodium concentrations ranged from 1 to 2 millimol per liter.

In one instance, to test the reversibility of the adsorption reaction, the sequence of reagent addition in three duplicate tests, points A in Fig. 12, was varied. The activator and the collector were added simultaneously in the first experiment. In the second, the activator was added first, followed by the collector. This sequence was reversed for the last test.

3—The barium concentration in the third series (six tests) was kept essentially the same as that of the second series, namely, near 0.057 millimol per liter. The pH, however, was increased to approximately 11.1 instead of 10. The laurate concentration in the tests covered a range from 0.042 to 0.25 millimol per liter. The sodium concentration ranged from 4.3 to 5.2 millimol per liter.

The data of the three series of tests are shown in Fig. 12. Included in Fig. 12 is a portion of the data of laurate adsorption on unactivated quartz previously shown in Fig. 9.

Vacuum flotation tests of the quartz indicated that flotation took place only under the conditions of Tests No. 91 and 92, see Fig. 12. From the results shown in Fig. 12, it appears that:

1—The adsorption of activator, barium, is independent of the concentration of the collector, laurate, see upper part of Fig. 12.

2—The adsorption of barium and laurate on quartz is independent of the sequence of reagent addition, points A.

3—The adsorption of laurate increases considerably with increase in barium concentration, that is, increase in barium adsorption. In other words, adsorption of collector is dependent on the degree of activation, see lower part of Fig. 12.

4—Laurate adsorption on barium-activated quartz increases more rapidly with increase of laurate concentration than does laurate adsorption on unactivated quartz, see lower part of Fig. 12.

5—The quantity of adsorbed barium on a mol basis is always greater than that of adsorbed laurate and usually much greater even at a collector concentration 30 times greater than that of activator, see B.

6—Laurate flotation of barium-activated quartz is possible at reagent concentrations well under those required to precipitate barium laurate.

7—The conditions for quartz flotation, as indicated by the results of Test No. 91, are surface concentrations of 1.85x10^{-10} mol of barium per sq cm and 3.23x10^{-11} mol of laurate per sq cm.

In terms of surface coverage, those conditions for flotation represent roughly 26 pct of a complete activator coating and 4.5 pct of a complete collector coating.

Discussion of Results

The experiments described in this paper accord with the adsorption theory of flotation,[18, 19] but they do not substantiate the theory of Taggart, Taylor, and Knoll.[20] For that theory to hold, barium laurate must be precipitated on the quartz surface. And, if that were the case, the following would also be true:

1—The amount of barium at the mineral surface would be dependent on the concentration in solution of laurate.

2—Two laurate ions for each barium ion would report on the mineral surface.

3—Flotation would take place only at concentrations of barium and laurate such that the solubility product constant of barium laurate is exceeded.

The experimental findings do not satisfy the above requirements.

Schuhmann and Prakash[4] proposed the following equation to represent the barium activation reaction at the locus of a ruptured bond on the quartz surface,

$$\boxed{SiO_2}^{-H} + Ba^{++} + 2OH^{-} \rightleftarrows \boxed{SiO_2}^{-Ba-OH} + H_2O \qquad [1]$$

If N_{BaOH} and N_H are the surface concentrations, in mol of adsorbate per unit area, of $(BaOH)^+$ and H^+ respectively, application of the Langmuirian concept of adsorption and the law of mass action give the expression

$$K_1 = \frac{(N_{BaOH})}{(N_H)(Ba^{++})(OH^-)_2} \qquad [2]$$

In this equation (Ba^{++}) and (OH^-) are the concentrations of barium and hydroxyl in the solution and do not represent conditions of saturation of barium hydroxide.

Assuming that all the adsorption sites are occupied by either $(BaOH)^+$ or H^+, N_H is therefore equal to $(N_s - N_{BaOH})$ where N_s is the surface concentration of adsorbate at surface saturation. A surface concentration of N_s = 7.1x10^{-10} mol of adsorbate per sq cm of quartz would make up a complete monolayer. If N_s is large compared to N_{BaOH}, N_H is essentially constant. Even at 25 pct coating with Ba as $(BaOH^+)$ no large error is caused by assuming N_H constant. By keeping the barium-ion concentration constant, eq 2 can be simplified further to give the following approximation:

$$\log (N_{BaOH}) = \log K + 2(\text{pH}) \qquad [3]$$

A plot of log (N_{BaOH}) vs. pH would give a straight line with a slope of two. This, however, does not seem to be the case as can be seen in Fig. 12. The slope is approximately 1/5 instead of 2. It certainly would be more enlightening if the surface concentrations of ions other than barium were known.

The fact that the adsorption of barium is independent of the presence of laurate suggests that the reagents are not adsorbed from solution as $(BaL)^+$ but as individual barium and laurate ions. Since barium adsorption is greater than laurate adsorption, it is also justifiable to assume that each adsorbed barium can hold not more than one laurate. This is in accordance with the views held by Gaudin and Rizo-Patrón.[1] From the study of the mechanism of barium activation and oleate flotation of quartz, they postulated the sequential adsorption of barium and oleate, and that only one oleate can attach to one adsorbed barium.

It is interesting to speculate on the exact position of the adsorbed cation and anion. The filtration-followed-by-centrifuging procedure that was used to separate the loaded mineral from the liquor did not part the solid from the solution at the solid boundary but within the liquor. Actually the film of liquid surrounding the quartz is estimated to have been about 1700 A thick, in those cases where the least liquid was retained in the pores of the centrifuged cake. This suggests that at least a part

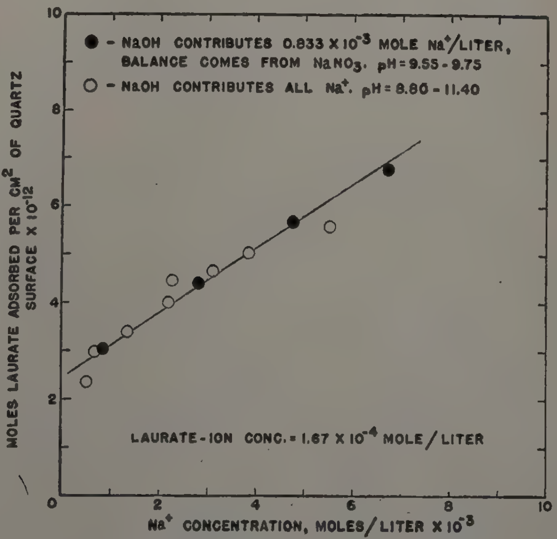

Fig. 10—Adsorption of laurate on quartz, effects of Na^+ and pH.

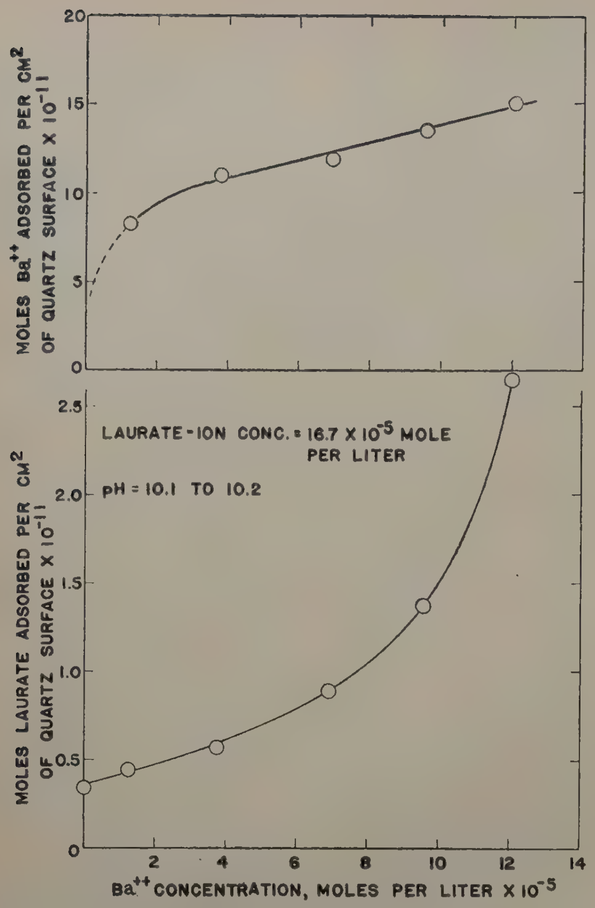

Fig. 11—Coadsorption, effect of barium on laurate adsorption.

and probably most of the so-called diffused double layer known to colloid chemists has been included in the centrifuged cake along with the anchored part of the double layer. It must be noted that it is impossible to part the mineral from the solution within the diffuse layer without causing a rearrangement of the adsorbed ions. Further, it is inevitable that the mineral-solution separation be effected so as to include the diffused double layer present on the particles at the time the separation is made.

The thickness of the diffused double layer, δ in centimeters, has been identified as the reciprocal of the Debye-Hückel function, κ.[21]

$$\delta = \frac{1}{\kappa} = \sqrt{\frac{1000\,DRT}{8\pi e^2 N^2}} \cdot \sqrt{\frac{1}{c}} \qquad [4]$$

In this equation, D is the dielectric constant (about 80 for water at 25°C), R is the gas constant, 8.314×10^7, T is the absolute temperature (298 at 25°C), e is the charge of the electron, 4.77×10^{-10} electrostatic units, N is the Avogadro number, 6.02×10^{23}, and c is the ionic concentration of the solution in gram-ions per liter or moles per liter.

Thus for water at 25°C,

$$\delta = 3.05 \times 10^{-8} \sqrt{\frac{1}{c}}\ \text{cm} \qquad [5]$$

Table I. Surface Conditions of the Quartz and Its Floatability

	Barium Adsorption		Laurate Adsorption		
Test No.	Mol/cm²	Coverage, Pct	Mol/cm²	Coverage, Pct	Vacuum Flotation Test
50	0	0	5.22×10^{-11}	7.4	negative
86	1.38×10^{-10}	19.6	4.18×10^{-11}	5.9	negative
91	1.85×10^{-10}	26.0	3.23×10^{-11}	4.5	positive
92	1.88×10^{-10}	26.5	4.25×10^{-11}	6.0	positive

The lowest concentration of either barium or laurate in experiments described in this paper is 5.7×10^{-6} mol per liter, see Fig. 5. The thickness of the diffused double layer at this ionic concentration is roughly 1300A. The quartz sample in the adsorption tests retained a minimum of 1.5 pct moisture at the end of mineral-solution separation. Since the quartz sample has a specific surface of 881 sq cm/g, each quartz particle has, therefore, a liquid layer approximately 1700A thick all around it. This extends to include the diffused double layer. In spite of the fact that a correction has been provided for the reagents in the retained moisture, the measurements of adsorbed reagents prescribed by the methods described in this paper represent not only those adsorbed on the mineral surface, inner layer, but also those adsorbed within the diffuse layer. This is in agreement with the fact that quartz can adsorb barium in a quantity more than that necessary to form a monolayer, see Fig. 8.

With the incorporation of the concept of diffused double layer, it is interesting to compare the results of Tests No. 50 (see Fig. 9) 86, 91, and 92 (see Fig. 12). The surface conditions of the quartz and its floatability are given in Table I.

Although laurate adsorption is roughly the same in each test, flotation of quartz was not obtained unless a certain minimum barium adsorption was effected. The degree of barium activation seems to be the determining factor. This substantiates the view that as long as there is sufficient concentration of collector present, quartz flotation is activator-controlled rather than collector-controlled.

Based on the foregoing evidence, the following hypotheses are proposed:

1—Only the reagents adsorbed in the inner layer are responsible for flotation.

2—In the absence of an activator in a flotation system necessitating the use of an activator as well as collector, very few collector ions are adsorbed on the mineral surface. But there may be a considerable concentration of collector ion in the diffuse layer, a short distance away.

3—The presence of an activator tends to encourage the migration of the collector ions onto the mineral surface.

Summary and Conclusions

Radioactive barium and radioactive-carbon-labeled lauric acid were used to study the adsorption of barium and laurate at equilibrium on a sample of ground quartz. In this paper *adsorption* is used to mean the amount measured to have been abstracted without reference to the position the abstracted material holds in the double layer surrounding the adsorbent.

From the results of the experimental work the following conclusions are reached:

Regarding barium adsorption: 1—Quartz adsorbs barium from solution. This adsorption is a function of barium concentration and pH. 2—The presence of sodium, up to 6 millimol per liter does not materially affect barium adsorption at barium concentration of 0.06 millimol per liter.

Regarding laurate adsorption: 1—Quartz adsorbs laurate from solution. This adsorption is also a function of laurate concentration but is independent of pH within the range 8.8 to 11.4. 2—An increase of sodium concentration causes a slight increase of laurate adsorption. 3—Laurate adsorption increases with great rapidity with barium concentration. 4—Laurate adsorption increases more rapidly with laurate concentration on barium-activated quartz than it does on unactivated quartz.

Regarding coadsorption of barium and laurate: 1—In barium activation and laurate flotation of quartz, the adsorption of activator is independent of the presence of collector. The reverse is not true. 2—Adsorption of barium and laurate on quartz is independent of the sequence of reagent addition. 3—The two-dimensional concentration of adsorbed barium is always greater than that of adsorbed laurate even at a laurate concentration in solution 30 times greater than the barium concentration.

Regarding flotation of quartz: 1—Flotation of quartz occurs at reagent concentrations such that the solubility product of barium laurate is not reached. 2—Flotation of quartz was observed with surface coverages of roughly 26 pct of a complete barium monolayer and 4.5 pct of a complete laurate monolayer.

Acknowledgment

This research work was made possible through the generosity of Armour and Co. in setting up the Armour Flotation Research Fund in the Dept. of Metallurgy, Massachusetts Institute of Technology. The authors wish to express their appreciation to H. M. Corley, Manager of New Products Department, J. D. Porsche, Director of Research and Development, and J. A. Barr, Jr., Manager of Chemical Derivatives Department, Armour and Co., and V. L. Parsegian, Director of Division of Technical Advisers, U. S. Atomic Energy Commission, for their invaluable encouragement. Acknowledgment and thanks are also extended to H. J. Harwood, Assistant Director of Research of Armour and Co., for his work in preparing the lauric acids, and to H. R. Spedden, R. Schuhmann, Jr., P. L. deBruyn, C. D. Coryell and J. W. Irvine, Jr., for their valued suggestions and criticism.

References

[1] A. E. Alexander and P. Johnson: *Colloid Science*, **1**, p. 297, (1949) Clarendon Press, Oxford.

[2] S. R. B. Cooke and Marcus Digre: Studies on the Activation of Quartz with Calcium Ion. *Trans.* AIME (1949) **184**, p. 299; Mining Engineering (August 1949) TP 2606B.

[3] S. R. B. Cooke: The Flotation of Quartz Using Calcium Ion as Activator. *Trans.* AIME (1949) **184**, p. 306; Mining Engineering (August 1951) TP 2607B.

[4] R. Schuhmann, Jr., and Brahm Prakash: Effect of $BaCl_2$ and Other Activators on Soap Flotation of Quartz. *Trans.* AIME (1950) **187**, p. 591; Mining Engineering (May 1950) TP 2826B.

[5] A. M. Gaudin, P. L. deBruyn, F. W. Bloecher and C. S. Chang: Radioactive Tracers in Flotation. *Mining and Metallurgy* (August 1948) **29**, p. 432.

[6] A. M. Gaudin and P. L. deBruyn: Radioactive Tracers in Mineral Engineering Problems and Particularly in Flotation. Can. Min. & Met. *Bull.*, **42**, p. 331 (July 1949).

[7] F. W. Bloecher, Jr.: A New Surface Measurement Tool for Mineral Engineers. *Trans.* AIME (1951) **190**, p. 255; Mining Engineering (March 1951) TP 3013B.

[8] A. M. Gaudin and R. T. Hukki: Principles of Comminution. *Trans.* AIME (1944) **169**, p. 67.

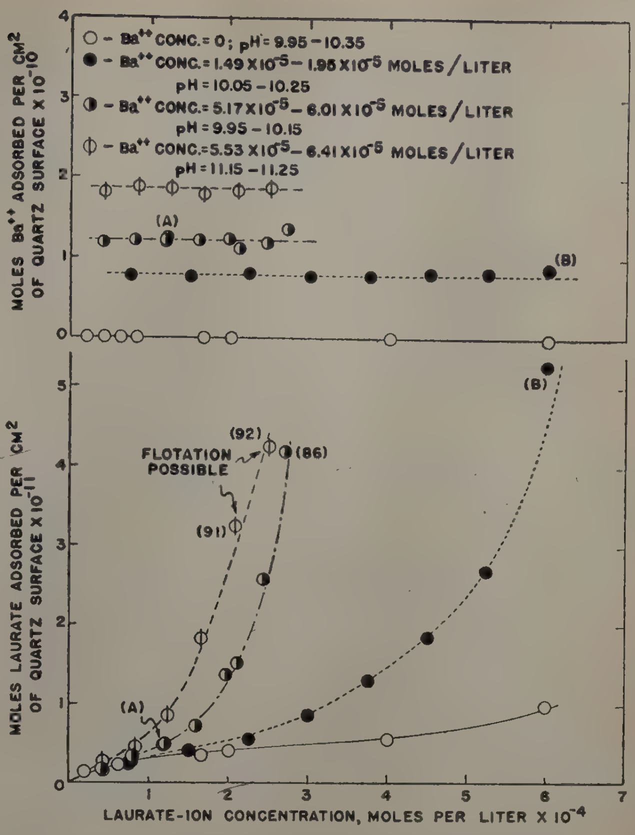

Fig. 12—Coadsorption, effect of laurate on barium activation and effect of laurate concentration on laurate adsorption of barium-activated quartz.

[9] G. T. Seaborg and I. Perlman: Table of Isotopes. *Reviews of Modern Physics* (1948) **20**, No. 4, p. 585.

[10] G. Friedlander and J. W. Kennedy: *Introduction to Radiochemistry*, pp. 164-165 (1949) John Wiley & Sons, Inc., New York.

[11] D. D. van Slyke and J. Folch: Manometric Carbon Determination. *Journal Biological Chemistry* (1940) **136**, p. 509.

[12] W. W. Miller: High-Efficiency Counting of Long-Lived Radioactive Carbon as CO_2. *Science* (1947) **105**, No. 2718, p. 123.

[13] S. C. Brown and W. W. Miller: Carbon Dioxide Filled Geiger-Müller Counters. *Review of Scientific Instruments* (1947) **18**, No. 7, p. 496.

[14] F. W. Bloecher, Jr.: The Adsorption of Dodecylamine on Quartz. Master's Thesis, Mass. Inst. of Tech. (May 1949).

[15] H. J. Harwood and A. W. Ralston: The Synthesis of Lauric Acid and Dodecylamine Containing Carbon Fourteen. *Journal Organic Chemistry* (1947) **12**, p. 740.

[16] S. Popoff and E. W. Neuman: Solubility of Inorganic Precipitates in Various Aqueous Solvents and Its Relation to Modern Theories of Solution. I. Silver Chloride. *Journal of Physical Chemistry* (1930) **34**, p. 1853.

[17] E. W. Neuman: Solubility Relations of Silver Chloride in Aqueous Solutions of Strong Electrolytes. *Journal* Amer. Chem. Soc. (1932) **54**, p. 2195.

[18] A. M. Gaudin: *Principles of Mineral Dressing* (1939) McGraw-Hill Book Co., Inc., New York.

[19] A. F. Taggart, T. C. Taylor, and A. F. Knoll: Chemical Reactions in Flotation. *Trans.* AIME (1930) **87**, p. 217.

[20] A. M. Gaudin and Alfonso Rizo-Patrón: The Mechanism of Activation in Flotation. *Trans.* AIME (1942) **153**, p. 462.

[21] I. W. Wark: Principles of Flotation. Australasian Inst. Min. Met., Australia (1938).

Recent Coal Geology Research

by Aureal T. Cross

THIS paper is a review of the published literature on research in coal geology, principally exclusive of resource studies, which appeared or became available during 1950 and the latter part of 1949. This report is not to be construed as being complete. The papers referred to in the bibliography are those among many more, which were read either in full or in abstract.

Undoubtedly other papers were published which either escaped the author's notice or were not available to him. Those which were seen in abstract only (about one fourth of those listed) were not available in time for the inclusion of more than a notice.

An outline of all papers listed in the bibliography has been arranged by subjects and reasonable subdivisions with some papers cited under more than one subject. Most papers are indexed according to the principal subject of discussion or research only as to an unusual or noteworthy section of the entire report. There will likely be some disagreement as to the quality or merit of some of the papers selected and the specialist may be supercritical of the outline or organization of papers in his field. It may be that attention has occasionally been drawn to papers reporting old information or conclusions of questionable value.

Conferences and Meetings

One of the best indications of the growing interest in coal geology problems in the United States is the increasing number of times this field has been the focus of attention at conferences and meetings. Notable among these are the joint meeting of the Society of Economic Geologists and the Geological Society of America at El Paso, November 1949, at which the principal thesis was concerned with low rank carbonaceous fuel deposits, especially of western United States. Among the papers given which are already available were those presented by Barghoorn,[16] Parry,[139] Roe,[153] and Parks.[162]

At the annual meeting of the Botanical Society of America in New York, December 1949, a joint meeting of the Paleobotanical and Microbiological Sections was held for which a symposium on Microbiology in Relation to the Geologic Accumulation of Organic Complexes was organized. Publication of the six papers presented by Ralph G. H. Siu, Elso S. Barghoorn, Irving Breger, Claude E. ZoBell, James M. Schopf, and A. C. Thayson is anticipated. At the regular meetings of the Paleobotanical Section at the same time, several other papers of interest reported on coal ball studies, partial coalification of petrified wood, and floras.

In Chicago, April 1950, a symposium on Applied Paleobotany was held by the Society of Economic Paleontologists and Mineralogists in conjunction with the American Association of Petroleum Geologists. The five papers presented at this meeting dealt with the use of Paleozoic plant microfossils for stratigraphic work, J. M. Schopf, Devonian-Mississippian fossils of the black shales, Aureal T. Cross, Mesozoic plants of stratigraphic value, Th. Just, plant microfossils of the Tertiary, L. R. Wilson, and studies of the Brandon lignite, Elso S. Barghoorn. Early publication of these in the *Journal of Paleontology* is expected.

The Nova Scotia Research Foundation and the Nova Scotia Dept. of Mines sponsored an excellent 3-day conference in June 1950, which dealt with several aspects of coal geology. Papers on coal classification, P. A. Hacquenbard, structure and sedimentation problems in Nova Scotia, T. B. Haites, new techniques of thermal analysis, W. L. Whitehead, geochemical investigations of Nova Scotia coals, Irving Breger, the role of fossil plant spores in coal correlation and the stratigraphy of the coal-bearing strata of the Appalachian Region, Aureal T. Cross, were given. Some discussions of these papers by those in attendance were recorded, and the entire proceedings is being prepared for publication.

In September 1950, an unusual 3-day field conference was held by the Ohio and West Virginia Geological Surveys under the sponsorship of the Coal Geology Committee.[89] This study of the stratigraphy, sedimentation, and nomenclature of the Upper Pennsylvanian and Permian coal-bearing strata of southeastern Ohio, southwestern Pennsylvania, and northern West Virginia was augmented by two discussions on associated rocks (clays and shales) and stratigraphic nomenclature at Wheeling and Morgantown, West Va. An extensive guidebook was prepared, and transcriptions of the Morgantown meeting were made.

As a follow-up of the September field conference, a round-table discussion was held on this general topic at a special open meeting of the Coal Research Committee in conjunction with the November meeting of the Geological Society in Washington. Short prepared statements to invite discussion were given on each of several topics by L. M. Cline, Carl O.

AUREAL T. CROSS is Coal Geologist and Paleobotanist with the West Virginia Geological Survey, and Assistant Professor of Geology, West Virginia University, Morgantown, West Va.

Discussion on this paper, TP 3247F, may be sent to AIME before March 31, 1952. Manuscript, Feb. 22, 1951. Joint session of Coal Division, AIME, and the Society of Economic Geologists. St. Louis Meeting, February 1951.

Dunbar, Harold R. Wanless, Wm. C. Krumbein, and Aureal T. Cross. The discussion leader, Monroe G. Cheney, encouraged free participation from the floor and about 15 persons entered into the discussion of problems of nomenclature, sedimentation, tectonics, and stratigraphy of Pennsylvanian and Permian strata of the Appalachian and midcontinent regions. The entire transcription has now been prepared and distributed to those who attended.

At the 1950 annual meeting of the Paleobotanical Section of the Botanical Society at Columbus in September, several papers were given on plant microfossils, coal balls, and general flora studies of coal-measures rocks. Of special interest were two studies on roof shale floras by Maxine Abbott on an Allegheny coal and A. J. Miklausen.[117] Three papers on plant microfossils and related modern forms were given by Mart P. Schemel (Missouri coals), John C. Ferm (Pennsylvania coal), and Clyde Reed (spore types). A special field trip for collecting typical floras from several Pottsville and Allegheny coals was conducted by Maxine Abbott.

Four foreign conferences were noted. The British Association for the Advancement of Science sponsored a meeting Aug. 30 to Sept. 6, 1950, at Birmingham University to deal with the concealed coalfields in the Midlands. A number of geologists participated in the discussion which considered coalfield extensions in faulted areas under as much as 3000 ft of cover.

A second conference on oil shale and cannel coal, July 3-7, 1950, at Glasgow, was sponsored by the Institute of Petroleum. The section on geology and mineralogy heard papers on difficulties of classification, R. A. Mott, Australian torbanite, J. A. Dulhunty, and a new Swedish venture in extracting oil shales *in situ* by electrical heating.

An international conference on classification of coal was held in Paris in February 1949, sponsored by the Coal Committee of the United Nations, at which an attempt was made to formulate an international classification of coals and standardized tests for coals.[88]

A conference was called in Geneva under the auspices of the Economic and Social Council of the United States.[91] Austria, Belgium, Czechoslovakia, France, Germany (western zone), Holland, Poland, Sweden, United Kingdom, and United States were represented. A classification was studied which would be based on two properties of coals, the content of volatile matter and swelling properties.

The Fourth World Power Conference, which was held in London in July 1950, dealt with preparation and production aspects of fuel and power, but several of the 180 papers given dealt with energy resources and microscopic studies and physical properties of coal.

New Research Laboratories

Several new laboratories with facilities and/or plans to conduct research in various phases of geological sciences allied with coal studies were instituted or formally opened during 1949 and 1950. Of the three of these important to Americans, the first is the Coal Geology laboratory established by the Fuels Division of the U. S. Geological Survey at Ohio State University, Columbus. James M. Schopf, who planned this fine, modern laboratory, is in charge. The second, which began operation in January 1949 in spacious quarters at Sydney, Nova Scotia, is sponsored by the Coal Division of the Geological Survey of Canada and the Nova Scotia Research Foundation. P. A. Hacquebard and T. B. Haites are in charge. The laboratory is well equipped to handle most problems except those in coal geochemistry. A third research center is the U. S. Bureau of Mines Lignite Research Laboratory, which was opened at the University of North Dakota at Grand Forks.

Three new foreign laboratories have been established in France, Spain, and India. An extensive laboratory at Verneul-sur-Oise, France, was to open in 1950.[148] It is planned to conduct extensive research and coordinate technical information in mining. The National Institute for Fuel in Spain has a new laboratory in connection with its headquarters at the University of Zoragoza.[6] A new laboratory, the Central Fuel Research Institute at Digwadhi in Bihar, India, was opened April 22, 1950. Extensive plans have been laid to conduct research in modern, well-equipped laboratories on colloids, chromatography, phyto-chemistry, electric and magnetic properties of coal, coal petrography, spectroscopy, X-ray, coal constitution, etc. This laboratory was opened just a year following the Birbal Sahni Institute of Paleobotany at Lucknow, a unique paleobotanical laboratory designed to bring together various paleobotanists of India for concerted studies, both economic and academic.

Numerous laboratories of various state agencies in United States were opened or considerably expanded their coal geology programs.

Acknowledgment

The assistance of Mart P. Schemel, West Virginia Geological Survey, in preparing some of the abstracts in numerous translations and in preparation of the manuscript is gratefully acknowledged.

Bibliography by Subjects

Origin of coal.
- Botanical components: 153, 16, 15, 14, 149.
- Mineral components: 23, 173.
- Types and origin of deposits: 74, 88, 198, 159, 200, 154, 191.

Coal constitution and analysis.
- General: 163, 79, 55, 171, 11.
- Botanical constituents.
  - Microscopic analysis: 52, 56.
  - Electron microscopy: 18, 140, 201, 116, 89, 25.
- Chemistry (geochemistry).
  - Chemical constitution: 118, 48, 49, 195, 120, 196, 119, 70, 162, 80, 22, 172, 191, 64.
  - Chemical analysis (methods):
    - Chemical: 206, 205, 122.
    - Spectroscope: 82, 125, 126, 124, 208.
    - X-ray: 20, 104.
- Physical properties.
  - Porosity, density, hardness: 204, 166, 12, 49, 24, 99, 63, 203, 2.
  - Reflectivity: 41, 10.
  - Electrical and thermal: 35, 1.
- Applied petrography: 167, 21, 73, 87, 138, 131, 195.

Coal development and classification.
- Development and alteration: 136, 50, 142, 31, 195, 66, 67, 104, 86, 194, 193, 53, 51, 202, 150, 199, 181, 114, 173.
- Classification: 165, 139, 157, 91, 33, 208.

Coal stratigraphy, sedimentation and tectonics.
- Paleontology.
  - Paleobotany.
    - Flora (megascopic): 7, 117, 37, 69, 113, 112, 179, 19, 27.
    - Flora (microfossils): 158, 59, 75, 8, 94, 95, 156, 44, 62, 93, 111, 96, 97, 146, 188, 186, 187, 65.

- Paleozoology: 176, 128, 17, 160, 177.
- Sedimentation: 42, 101, 102, 100, 143, 192, 103, 71.
- Stratigraphy: 36, 121, 144, 58, 180, 43, 178.
- Tectonics: 26, 102, 105-108, 127, 129, 130, 202, 77, 78.

Coal exploitation.

- Exploration.
  - Resource studies: 139, 28, 168, 189, 161.
  - Techniques: 13, 45, 46, 54, 57, 76, 115, 145, 175, 182, 197.
- Coal mining engineering.
  - General and underground mining: 151, 170, 132, 137, 92, 152, 164, 207, 9, 83.
  - Underground extraction: 60, 34.
  - Roof-rock control.
    - Stress studies: 169, 72, 105, 123, 133, 134, 5.
    - Support: 40, 147, 30, 29, 169, 185, 84, 174, 61, 183, 184, 141, 109.
    - Sealing: 4, 85.
  - Strip mining: 137, 192, 110, 155, 3.
- Coal utilization.
  - Carbonization: 98, 90.
  - Hydrogenation, liquefaction, etc.: 190, 135, 38, 68, 81.

Bibliography

1. A. A. Agroskin and I. G. Petrenko: Electrical Resistance of Coals and Shales When Heated. *Izvestiya Akademii Nauk* Soyusa Sovetskikh Solsialistichiskikh Respublik, *Otdelenie Technische Nauk* (*Bull.* Akad. Sci. U. S. S. R., Sect. Tech. Sci.), (1950) No. 1, pp. 89-100. (Abst. in *Fuel Abstracts*, New Series, (1950), **6**, No. 5738).

2. W. Anderson: A New Method of Coal Sampling at Face. *Mining Journal,* (April 1950), **234**, pp. 338-339.

3. Anonymous: Better Auger Mining. *Coal Age,* (June 1950), **55**, No. 6, pp. 72-77.

4. Anonymous: Red Jacket Tries Liquid Plastic to Prevent Roof Spalling. *Coal Age,* (June 1950), **55**, No. 6, p. 102.

5. Anonymous: Beam Action in Mine Roof. *Coal Age,* (November 1950), **55**, No. 11, pp. 102-104.

6. V. Gomez Aranda: Fuel Research Projects in Spain. *Ion,* (January 1950), pp. 29-34. (Abst. in *Fuel,* (1950), **29**, No. 7, p. 166).

7. C. A. Arnold: Fossil Flora of the Michigan Coal Basin. *Contributions Museum of Paleontology,* (December 1949), **7**, No. 9, pp. 131-269, Ann Arbor, Michigan, Univ. of Michigan Press.

8. C. A. Arnold: Megaspores from the Michigan Coal Basin, ibid, (June 1950) **8**, No. 5, pp. 59-111.

9. S. H. Ash, H. D. Kynor, R. W. Fatzinger, B. S. Davies, and J. C. Gilbert: Inundated Anthracite Reserves: Eastern Middle Field, Pennsylvania. *Bull.* U. S. Bur. Mines, (1950) **491**, pp. 1-28.

10. K. Balyi and F. Papp: Light-reflecting Capacity of Some Hungarian Black and Brown Coals. Földtani Közlöny, (1945-1946) **75-76**, pp. 42-44. (Abst. in *Fuel Abstracts*, New Series, (April 1950), **7**, No. 2825).

11. D. H. Bangham, Editor: *Progress in Coal Science.* (1950), London, Interscience Publisher. (Book Review in *British Coal Utilization Research Association,* (1950), **14**, No. 7, p. 266).

12. D. H. Bangham, R. E. Franklin, W. Hirst, and F. A. P. Maggs: A Structural Model For Coal Substance. *Fuel,* (October 1949), **28**, No. 10, pp. 231-237.

13. J. E. Banks: Particle-type Well Logging. *Bull.* Amer. Assoc. Petroleum Geologists, (1950), **34**, No. 8, pp. 1729-1736.

14. Elso S. Barghoorn: Boylston Fishweir II. Paleobotanical Studies of the Fishweir and Associated Deposits. *Papers by the Peabody Foundation for Archeology,* (1949), **6**, pp. 49-83.

15. Elso S. Barghoorn: Degradation of Plant Remains in Organic Sediments. *Botanical Museum Leaflets,* Harvard University, (1949), **14**, pp. 1-20.

16. Elso S. Barghoorn and William Spackman: Geological and Botanical Study of the Brandon Lignite and Its Significance in Coal Petrology. *Economic Geology,* (1950), **45**, No. 4, pp. 344-357.

17. Helmut Bartenstein: Micropaleontological Research in European Upper Carboniferous Stratigraphy. *Geological Magazine,* (July-August 1950), **87**, No. 6, pp. 253-260.

18. Thomas F. Bates: The Electrical Microscope Applied to Geological Research. *Trans.* New York Academy Science, (February 1949), Series 2, **11**, No. 4, pp. 100-107.

19. W. A. Bell: Uppermost Cretaceous and Paleocene Floras of Western Alberta. *Bull.* Geological Survey, Canada Dept. of Mines, (1949), **13**, 229 pp.

20. P. Belugou and P. Conjeaud: The Determination of the Ash Content of Coals by Means of X-rays. *Colliery Guardian,* (1950), **181**, No. 4683, pp. 408-409. (Abst. of paper presented to International Congress on Coal Preparation in Paris, June 1950).

21. N. Berkowitz: The Distribution of Coking Properties in British Commonwealth Coals. *Fuel,* (June 1950), **29**, No. 6, p. 138.

22. J. Berteloot: Presence of Native Sulphur in Coal. Variations in Sulphur Content from Top to Bottom of Vein. *Annales* Société Géologique du Nord. (Lille-France), (1947), **67**, pp. 195-206. (Abst. in *Fuel Abstracts,* New Series, (May 1950), **7**, No. 3788).

23. D. Bertrand: (transl. by Vera Lee), Survey of Contemporary Knowledge of Biogeochemistry. 2. Biogeochemistry of Vanadium. *Bull.* Amer. Museum Natural History, (1950) **94**, pp. 407-455.

24. R. L. Bond, M. Griffith, and F. A. P. Maggs: Water in Coal. *Fuel,* (April 1950), **29**, No. 4, pp. 83-93.

25. B. von Borries: *Ultramicroscopie.* 416 pp., (1949), Aulendorf/Württemberg, Edition Cantor.

26. J Harlen Bretz: Origin of the Filled Sink-structures and Circle Deposits of Missouri. *Bull.* Geol. Soc. Amer., (August 1950) **61**, No. 8, pp. 789-834.

27. Roland W. Brown: Cretaceous Plants from Southwestern Colorado. U. S. Geol. Survey *Professional Paper,* (1950), No. 221-D, 22 pp.

28. A. F. Buckham and B. A. Latour: The Groundhog Coalfield, British Columbia. *Bull.* Canada Geol. Survey, (1950), **16**, 82 pp.

29. Philip B. Bucky: Theory and Principles of Roof Bolting (Abst.), *Mining Congress Journal* (June 1950), **26**, No. 6, p. 65.

30. Philip B. Bucky: Theory of Roof Bolting. *Coal Mining Modernization 1950 Yearbook,* (1950), pp. 13-18, Washington, D. C.

31. G. H. Cady: Review, Die Metamorphose der Kohle und ihr Einfluss auf die sichtbaren Bestandteile derselben by W. Petrascheck. (*Sitzungsberichten der Osterreich* Akademie der Wissenschaften in Wien, mathematische-naturwissen-schaftliche Klasse, (1947) Abteilung I, **156**, Nos. 7-8, pp. 375-444). (Review in *Journal of Geology,* (September 1949), **57**, No. 5, pp. 551-554).

32. G. H. Cady: Research in Coal Geology. *Trans.* AIME, (1950) **187**, p. 275-278, *Mining Engineering,* (February 1950), TP 2774F.

33. H. Cassan and R. Martin: International Classification of Coals. *Chaleur et Industr.,* (January 1950), **31**, pp. 3-10.

34. Thomas C. Cheasley: Electrocarbonization of Coal. *Mining Congress Journal,* (January 1950) **36**, No. 1, pp. 18-19.

35. J. D. Clendenin, K. M. Barclay, H. J. Donald, D. W. Gillmore, and C. C. Wright: Thermal and Electrical Properties of Anthracite and Bituminous Coals. *Trans.* Seventh Annual Anthracite Conference, Lehigh University, (May 1949), pp. 12-67. (Reprinted as Pennsylvania State College, Mineral Industries Experiment Station; *Tech. Paper* No. 160, (1949), pp. 11-67.

36. L. M. Cline and Frank C. Greene: A Stratigraphic Study of the Upper Marmaton and Lowermost Pleasanton Groups, Pennsylvanian, of Missouri. *R.I.,* No. 12, Missouri Geol. Survey and Water Resources, (1950), pp. 3-75.

37. P. Corsin: Age of Coal Measures of Blanzy Basin (Saône-et-Loire), *Comptes Rendu* Academie Science Paris, (1948), **227**, pp. 858-860.

38. W. L. Crentz, J. D. Doherty, and E. E. Donath: Coal Preparation for Synthetic Liquid Fuels. *Trans.* AIME, (1950), **187**, MINING ENGINEERING, (April 1950), pp. 507-510, TP 2832F.

39. Aureal T. Cross: Pennsylvanian-Permian Field Conference. *Science,* (November 1950), **112**, No. 2915, p. 573.

40. Aureal T. Cross, and Paul H. Price: Overhead Roof Support: An Appraisal of Progress in Scientific Application of Roof Bolting. *Mining Congress Journal,* (February 1951), **37**, No. 2, pp. 90-92.

41. A. Dahme and M. T. Mackowsky: Physico-chemical and Petrographical Investigation of Coals, Cokes, and Graphites. Pt. IV. New Method of Measurement Based on Reflectivity of Coals. *Brennstoff-Chemie,* (May 1950), **31**, pp. 129-138. (Abst. in *Fuel,* (October 1950), **29**, No. 10, p. 243).

42. E. C. Dapples: Sedimentation: An Appropriate Field of Research in Natural History of Coal Beds. *Economic Geology,* (November 1949), **44**, No. 7, pp. 598-605.

43. T. W. Edgeworth David (Edited and Supplemented by W. R. Browne): *Geology of the Commonwealth of Australia.* 372 pp., (1950), New York, Longmans, Green and Co.

44. N. J. de Jersey: Principal Microspore Types in Ipswich Coals. *Papers,* Dept. Geology, University of Queensland, (October 1949), **3**, No. 9, pp. 1-8.

45. L. U. de Sitter: Eindverslag van het Geophysiche Onderzoek in zo-Nederland door de geophysische dienst der Staatsmignen. *Mededeelingen* van de Geologische Stichting, (1949), Serie C-I-**3**-No. 1.

46. George Dott: Prospecting for Coal. *Colliery Engineering,* (July 1950), **27**, No. 317, pp. 280-282, 292.

47. Eva M. Dresel and Margery Griffith: The Significance of the Heat of Wetting of Coal Powders Ground to Various Degrees of Fineness. *Fuel,* (September 1949), **28**, No. 9, pp. 193-199.

48. I. G. C. Dryden: Behaviour of Bituminous Coals Toward Solvents. I. *Fuel,* (September 1950), **29**, No. 9, pp. 197-207.

49. I. G. C. Dryden: Behaviour of Bituminous Coals Toward Solvents. II. *Fuel,* (October 1950), **29**, No. 10, pp. 221-228.

50. J. A. Dulhunty: Some Effects of Compression on Physical Properties of Low Rank Coals. *Journal and Proceedings,* Royal Society New South Wales, (February 1950), **82**, pp. 265-271. (Abst. in *Fuel Abstracts,* New Series, (July 1950), **8**, No. 104).

51. J. A. Dulhunty: Relations of Rank to Inherent Moisture of Vitrain and Permanent Moisture Reduction by Drying. idem, (February 1950), pp. 286-293. (Abst. in *Fuel Abstracts,* New Series, (July 1950), **8**, No. 108).

52. A. Duparque: The Use of Polarized Light in the Microscopic Examination of Polished Surfaces of Anthracite and the Determination of These Fuels in Ligneous Tissues. *Comptes Rendu* Academie Science Paris, (1949), **228**, p. 1143.

53. A. B. Edwards: Rank and Type of Some Australian Coals. *Fuel,* (June 1950), **29**, pp. 125-133.

54. M. M. Elinson: Possibility of Sampling Coal Deposits by Means of Gas from Boreholes. *Izvestiya Akademii Nauk* Soyusa Sovetskikh Solsialistichiskikh Respublik, *Otdelenie Technische Nauk* (*Bull.* Akad. Sci. U. S. S. R., Sect. Tech. Sci), (1949), No. 7, pp. 1002-1009. (Abst. in *Fuel Abstracts,* (June 1950), **7**, No. 5344).

55. C. Ellis: Recent Research on Coal. (Abst.), *Colliery Guardian,* (March 1950), **180**, pp. 330-332.

56. D. Ellwood: Note on Method of Microscopic Examination of Victorian Brown Coals. *Proceedings* Australian Institute Mining and Metallurgy, New Series, (1947), **146-147**, pp. 71-74. (Abst. in *Fuel Abstracts,* New Series, (September 1950), **8**, No. 1682).

57. W. D. Evans: Photogrammetry and Coal Field Surveying. *Proceedings* South Wales Institute Engineers, (October 1949), **65**, pp. 25-42.

58. V. A. Eyles, et al.: Geology of Central Ayrshire. *Memoir* Geological Survey Scotland, 2nd Ed., (1949), 160 pp., Edinburgh.

59. Knut Faegri and Johs Iversen: *Textbook of Modern Pollen Analysis.* 168 pp., (1950), Copenhagen, Ejnar Munksgaard, publ.

60. Milton H. Fies: Progress Report on Second Experiment in Underground Gasification (Gorgas, Alabama). *Power Engineering,* (May 1950), **54**, pp. 101-102, 122, 124.

61. Milton H. Fies: Greater Coal Production at Gorgas Mine by Roof Bolting and Continuous Miner. *Trans.* AIME, (1950), **187**, pp. 1238-1243; *Mining Engineering* (December 1950).

62. Rudolf Florin: Upper Carboniferous and Lower Permian Conifers. *Botanical Review,* (May 1950), **16**, No. 5, pp. 258-282.

63. R. E. Franklin: Study of the Fine Structure of Carbonaceous Solids by Measurements of True and Apparent Densities. I. Coals. *Trans.* Faraday Society, (1949), **45**, pp. 274. (Abst. in *Fuel,* (1949), **28**, No. 12, p. 288).

64. A. W. Gauger: Nature of Coal. *Selecta Chimie,* (1949), No. 8, pp. 17-68. (Abst. in *Chemical Abstracts,* (1950), **44**, No. 3235).

65. A. K. Gosh and J. Sen: Study of Microfossils and Correlation of Some Productive Coal Seams of Raniganj Coal Field, Bengal, India. *Trans.* Mining Geology Institute India, (July 1948), **43**, pp. 67-95.

66. A. Gillet: Coal Carbonization Is a Short Cut to Geologic Evolution. *Revue Universelle des Mines,* (1946), **2**, No. 2. (Abst. in *Fuel Abstracts,* New Series, (August 1950), **8**, No. 921).

67. A. Gillet: Parallel Between Carbonization of Wood and Its Transformation to Oil in the Course of Geologic Time. idem., (1950), **9**, pp. 18-22.

68. R. A. Glenn, A. N. Basu, J. S. Wolfarth, and M. Katz: Coal Hydrogenation Progress Studies. I. On the Role of Coal Sulphur in the Hydrogenation of Coal. *Fuel,* (July 1950), **29**, No. 7, pp. 18-22.

69. Walther Gothan: Die Unterkarbon-flora der Dolbrilugker Tiefbohrungen. *Abhandlungen* Geologischen Landesanstalt Berlin, Neue Folge (1949), No. 217, 32 pp.

70. Walther Gothan and H. P. Mojen: Classification of Bitumen. idem., (1948), No. 215. (Abst. in *Fuel,* (1949), **23**, No. 7, p. 165).

71. L. C. Gottschalk, et al.: *Annotated Bibliography on Sedimentation.* Sedimentation Bull. No. 2, Soil Conservation Service, U. S. Dept. of Agriculture, Washington, D. C., (February 1950), pp. 1-351.

72. G. J. A. Grond: Disturbance of Coal Measures Strata Due to Mining Activities. *Iron and Coal Trade Review,* (June 1950), **160**, pp. 1323-1325, 1377-1382, 1445-1449; (July-August 1950), **161**, pp. 37-40, 85-88, 135-137, 197-200, 249-251, 295-297, 353-356, 360, 394-397.

73. J. Gyorki: Factors Determining Cokability of Coals. *Bányaszanties Kohászati Lapok,* (1948), **81**, pp. 322-327. (Abst. in *Fuel Abstracts,* New Series, (April 1950), **7**, No. 2827).

74. T. C. F. Hall: Coal of Gondwanaland. *Mining Magazine,* (April 1950), **82**, pp. 201-210.

75. Henry P. Hansen: Pollen Content of Moss Polsters in Relation to Forest Competition. *American Midland Naturalist,* (1949), **42**, No. 2, pp. 473-479.

76. George L. Hess: Aerial Mapping. *Coal Age,* (October 1950), **55**, No. 10, pp. 74-77.

77. H. G. A. Hickling: Undersea Coalfield Extension. *Colliery Guardian,* (March 1950), **180**, pp. 261-271.

78. H. G. A. Hickling: Undersea Coalfield Extension. (a discussion of above paper), idem., (July 1950), **181**, pp. 101-103.

79. L. Horton: The Constitution of Coal. *Journal* Institute of Fuel, (March 1950), **23**, pp. 91-95.

80. L. Horton and K. V. Aubrey: Minor Elements in Coal. *Fuel*, (March 1950), **29**, No. 3, p. 72. (abstract of paper to Coal Research Club.)

81. Bela Hubbard: Coal as a Possible Petroleum Source Rock. *Bull.* Amer. Assoc. Petroleum Geologists, (1950), **34**, No. 12, pp. 2347-2351.

82. Richard G. Hunter and A. J. W. Headlee: Spectrographic Analysis of Coal and Coal Ash. *Analytical Chemistry*, (March 1950), **22**, pp. 441-445.

83. F. Illingworth: Coal Mining in Spitzbergen. *Mine Quarry Engineering*, (June 1950), **16**, pp. 179-182.

84. D. E. Ingersoll: Application of Roof Bolting to Steeply Pitching Measures. *Coal Mine Modernization 1950 Year Book*, (1950), Washington. pp. 25-30. (Abstr. in *Mining Congress Journal*, (June 1950), **36**, No. 6, p. 65).

85. D. C. Jones: Roof Sealed with Paint Protects Against Falls. *Mechanization*, (January 1950), **14**, No. 1, p. 81.

86. O. T. Jones: Distribution of Coal Volatiles in South Wales Coal Field and Its Probable Significance. *Proceedings* Geological Society London (abst.), (July 1950), p. 122.

87. E. S. Kardoss: Formation of Coke from Viewpoint of Coal Petrography. *Bányaszanties Kohászati Lapok*, (1949), **82**, pp. 173-178. (Abst. in *Fuel Abstracts*, (June 1950), **7**, No. 4614).

88. E. I. Kazakov: Investigation of Process of Low Temperature Disintegration of Components of Peat. *Izvestiya Akademii* Soyusa Sovetskikh Solsialistichiskikh Respublik, *Otdelenie Technische Nauk* (*Bull.* Akad. Sci. U. S. S. R., Sect. Tech. Sci.), (1949), No. 8, p. 1187.

89. E. Kellenberger: Particles: Mounting for Electron Microscopy. *Experientia*, (1949), **5**, pp. 253-254. (Abst. in *Fuel Abstracts*, (June 1950), **7**, No. 5392).

90. J. J. Kipling: Retention of Sulphur by Cokes and Activated Charcoals. *Fuel*, (March 1950), **29**, No. 3, pp. 62-63.

91. W. A. Kirkby: International Coal Classification. *Fuel*, (August 1950), **29**, No. 8, pp. 193-194.

92. F. Kimbauer: Summary of Literature on Rock Pressure in Mining and Tunnelling. Pt. I. 1900-1930. *Berg.-Bohr. a. Erd.*, (March 1950), **66**, Suppl. 1-4.

93. E. M. Knox: The Spores of *Lycopodium*, *Phylloglossum*, *Selaginella*, and *Isoetes* and Their Value in the Study of Microfossils of Paleozoic Age. *Trans.* Botanical Society Edinburgh, (1950), **35**, pt. 3, pp. 209-357.

94. Robert M. Kosanke: Pennsylvanian Spores of Illinois and Their Use in Correlation. *Bull.* Illinois Geological Survey, (1950), No. 74, 128 pp.

95. Gerhard Kremp: Pollenanalytische Untersuchung des miozänen Braunkohlen-lagers von Konin an der Warthe. *Paleontographica*, (1949), **90**, pp. 53-93.

96. Gerhard Kremp: Pollenanalytische Braunkohlenuntersuchungen im sudlichen Teil Niedersachsen, inbesondere im Solling. *Geologischen Jahrbuch* 1943-1948, (1950), **64**, pp. 489-517.

97. Gerhard Kremp: Pollenanalytische Untersuchung des Braunkohlenflozes von Beuern bei Gieszen. *Notizblatt* d. Hessische Landesamtes Bodenforsch. Iv. F. (1950), **6**, No. 1, pp. 269-271.

98. D. J. W. Kreulen: Concerning the B. S. Swelling Number of Coal. *Fuel*, (May 1950), **29**, No. 5, pp. 112-117.

99. F. G. Kreulen-van Selms: Water in Coal. *Fuel*, (August 1950), **29**, No. 8, p. 196.

100. W. C. Krumbein and L. L. Sloss: *Stratigraphy and Sedimentation.* 497 pp. (1951), San Francisco, W. H. Freeman and Co.

101. W. C. Krumbein, L. L. Sloss, and E. C. Dapples: Sedimentary Tectonics and Sedimentary Environments. *Bull.* Amer. Assoc. Petroleum Geologists, (November 1949), **33**, No. 11, pp. 1859-1891.

102. Ph. H. Kuenen: Slumping in the Carboniferous Rocks of Pembrockshire. *Quarterly Journal* Geological Society London, (1949), **104**, No. 3, pp. 365-386.

103. Ph. H. Kuenen: *Marine Geology.* 568 pp., (1950), New York, John Wiley & Sons, Inc.

104. A. S. Kumpan: Changes of the Inner Structures of Coals by Metamorphism. *Zapiski Vsesoyuz Mineral.* Obschestva, (1938), **77**, pp. 285-303. (Abst. in *BCURA*, (September 1950), **14**, No. 8637).

105. H. Labasse: Soil Pressure in Coal Mines I. *Revue Universelle des Mines* (Liege), 9th Series, (1949), **5**, pp. 5-13.

106. H. Labasse: Soil Pressure in Coal Mines II. ibid., (1949), **5**, pp. 78-88.

107. H. Labasse: Horizontal Cross Galleries. ibid., (1950), **6**, pp. 3-18.

108. H. Labasse: Rock Pressures Round Drift in Seams. ibid., (1950), **6**, pp. 41-44.

109. Sterling S. Lanier, Jr.: Pinning Roof With Wood. *Coal Age*, (June 1950), **55**, No. 6, pp. 79-80.

110. L. Don Leet: Vibrations from Heavy Overburden Blasting. *Mining Congress Journal*, (June 1950), **36**, No. 6, pp. 56-59.

111. Britta Lundblad: De Geologiska Resultaten Fran Borrningarna vid Höllviken. Del. 3. Microbotanical Studies of Cores from Höllviken, Scania., *Sveriges Geologiska Undersökning*, Series C, No. 506, (1949), Arsbok **43**, No. 4, pp. 1-17.

112. Britta Lundblad: De Geologiska Resultaten Fran Borrningarna vid Höllviken. Del. 4. On the Presence of *Lepidopteris* in Cores from "Höllviken II". ibid., No. 507, (1949), Arsbok **43**, No. 5, pp. 3-11.

113. Reinhard Maack: *Lycopodiopsis Derbyi* Renault, documento da idade Paleozóica das camadas Terezina do Brasil meridional. Paraná Instituto Biologia e Pesquisas Tecnologicas *Arquivos de Biologie e Tecnologia*, (1948), **2**, part 81, pp. 155-208.

114. A. K. Matveev: Original Boundaries of Genesis of Coal Fields. *Doklady Akademii Nauk* Soyusa Sovetskikh Solsialistichiskikh Respublik, (Rep. Acad. Sci. U. S. S. R.), (1950), **70**, pp. 687-689. (Abst. from *Fuel Abstracts*, (June 1950), **7**, No. 4606).

115. R. McAdam and W. R. Burnett: Magnetic and Electrical Aids to Coalfield Development. *Colliery Guardian*, (1950), **181**, No. 4686, pp. 483-491.

116. J. T. McCartney: Electron Microscopy of Coal. *Economic Geology*, (November 1949), **44**, No. 7, pp. 617-620.

117. Anthony J. Miklausen: A Contribution to the Fossil Flora of the Roof Shales of the Pittsburgh Coal Bed of Southwestern Pennsylvania. Univ. of Pittsburgh *Bull.*, (June 1950), **46**, No. 10, pp. 1-6. Preprint.

118. Horace P. Miller: The Problems of Coal Geochemistry. *Economic Geology*, (December 1949), **44**, No. 8, pp. 649-662.

119. Ahmed Mofizud-Din and C. R. Kinney: Pyrolysis of Humic Acids Prepared from Oxidized Bituminous Coal. *Journal* American Chemical Society, (January 1950), **72**, pp. 556-559.

120. A. C. Monkhouse: Minor Constituents of Coal (Abst.). *Iron and Coal Trades Review*, (February 1950), **160**, p. 318.

121. Raymond C. Moore: Divisions of the Pennsylvanian System in Kansas. *Bull.* Kansas Geol. Survey, (1949), **83**, 203 pp.

122. R. A. Mott: Rapid Determination of the Forms of Sulphur in Coal. *Fuel*, (March 1950), **29**, No. 3, pp. 53-61.

123. Louis Moyd: Determination of the Coefficient of Linear Thermal Expansion of Rock Specimens by Means of Resistance Wire (SR-4) Strain Gauges. *Trans.* AIME, (1950), **187**, pp. 683-684. *Mining Engineering*, (June 1950), TP 2861H.

124. B. Mukherjee: A Note on the Constituents of the Ashes of Indian Coals Determined Spectroscopically. *Fuel*, (August 1950), **29**, No. 8, pp. 190-192.

125. B. Mukherjee: Detection of Rare Earths in the Ashes of Indian Coals. *Fuel*, (November 1950), **29**, No. 11, pp. 264-266.

126. B. Mukherjee and R. Dutta: Spectrographic Analysis of Indian Coal Ash. *Science and Culture*,

(1948), **14**, pp. 212-213. (Abst. in *Chemical Abstracts,* (1950), **44**, No. 2202).

127. A. Nelson: Some Complex Coal-measure Disturbances. *Colliery Engineering,* (October 1949), **26**, No. 308, pp. 347-349, 368.

128. A. Nelson: Coal Measure Correlation. *Iron and Coal Trades Review,* (February 1950), **160**, pp. 381-383.

129. A. Nelson: Folding Movements During Carboniferous Times. *Colliery Engineering,* (May 1950), **27**, No. 315, pp. 180-182.

130. A. Nelson: The Flowage of Coal Seams. ibid., (December 1950), **27**, No. 322, pp. 491-494.

131. W. Neubauer: Examination of Petrography of Lunzer Coals. *Berg-und Huttenmannisches Monatshefte,* (1949), **94**, pp. 355-360.

132. Oskar Niemczyk: *Bergschadenkunde* (The Science of Damage Caused by Mining). 288 pp., (1949), Essen, Glückauf, . . . (Book review in *Colliery Engineering,* June 1950).

133. Leonard Obert and Wilbur I. Duvall: A Gage and Recording Equipment for Measuring Dynamic Strain in Rock. U. S. Bur. of Mines *R. I.* No. 4581 (December 1949), pp. 1-12.

134. Leonard Obert and Wilbur I. Duvall: Generation and Propagation of Strain Waves in Rock. Part I. ibid., (May 1950), No. 4683.

135. W. H. Ode and W. A. Selvig: Extractable Waxes from American Lignites. *Journal Industrial Engineering Chemistry,* (1950), **42**, pp. 131-135.

136. W. Oversohl: Contribution to the Knowledge of Bituminous Coals. *Brennstoff-Chemie,* (April 1950), **31**, pp. 103-111. (in German) (Abstract in *BCURA,* (June 1950), **14**, No. 8243).

137. Sydney Paige, Chairman: *Application of Geology to Engineering Practice.* 327 pp., (1950), Geological Society of America, Berkey Volume.

138. Bryan C. Parks: Petrographic Analysis of Coal by the Particle Count Method. Illinois Geological Survey, *R. I.* (1949), No. 143, 48 pp. (Reprinted from *Economic Geology,* **44**, No. 5, pp. 376-424).

139. V. F. Parry: Production, Classification and Utilization of Western United States Coals. *Economic Geology* (September-October 1950), **45**, No. 6, pp. 515-532.

140. J. Peltier and A. Leauté: Preliminary Studies of Electron Microscopy at Laboratorie des Ponts et Chaussées. *Revue Generale Routes,* (1949), **19**, No. 205, p. 47. (Abst. in *Fuel Abstracts,* (June 1950), **7**, No. 5393).

141. John Peperakis: Roof-bolting at Sunnyside. *Coal Age,* (October 1950), **55**, No. 10, pp. 67-69.

142. Walther E. Petrascheck: Ein Versuch zur quantitative Bestimmung der Faltungskraft. *Geologische Rundschau,* (1950), **38**, No. 2, pp. 134-138. (Abstract from G. H. Cady, personal communication).

143. F. J. Pettijohn: *Sedimentary Rocks.* 576 pp., (1949), New York, Harper and Brothers.

144. F. B. Plummer: The Carboniferous Rocks of the Llano Region of Central Texas. Univ. of Texas, Bur. of Econ. Geol. *Bull.* 4329, (February 1950), 170 pp.

145. Edward Jan Polak: Rotary Mud Flush Boreholes. *Colliery Guardian,* (August 1950), **181**, No. 4673, pp. 111-117.

146. Robert Potonié: Zum Stand der micropaleobotanischen Tertiärstratigraphie. *Geologische Rundschau,* (1949), **37**.

147. Paul H. Price and A. T. Cross: Geologic Considerations of Roof Support. *Mining Congress Journal,* (December 1949), **35**, No. 12, pp. 45-48.

148. Y. Prax: Research Institute of French Coalmining Industry. *Chemistry and Industry,* (October 1949), p. 743.

149. S. R. Narayana Rao: Occurrence of Fossil Resins in the Oil Shales of the Punjab Saline Series. *Nature,* (April 1950), **165**, No. 4199, pp. 654-655.

150. J. Roberts: Thermodynamics of Hilt's "law". *Colliery Guardian* (March 1950), **180**, pp. 325-329.

151. T. Robertson: Practical Use of Geology in Coal Mining. *Trans.* Institute Mining Survey, (1949), **29**, pp. 129-163.

152. T. Robertson: Mining Subsidence—Geological Aspects and Their Relationship to Town Planning in County Durham. (Abst.). *Colliery Guardian,* (November 1949), **179**, pp. 575-578.

153. Walter B. Roe: Geologic Features of North Dakota Lignites. *Economic Geology,* (August 1950), **45**, No. 5, pp. 434-440.

154. Maretti Salmi: Physical and Chemical Peat Investigations on the Pinomäensuo Bog. *Bull.* La Commission Géologique de Finlande, (1950), No. 145, 31 pp.

155. C. N. Savage: Earth Flow Associated with Strip Mining. *Mining Engineering,* (March 1950), pp. 337-339.

156. Mart P. Schemel: Carboniferous Plant Spores from Daggett County, Utah. *Journal Paleontology,* (March 1950), **24**, No. 2, pp. 232-244.

157. James M. Schopf: Cannel, Boghead, Torbanite and Oil Shale. *Economic Geology,* (January-February 1949), **44**, No. 6, pp. 68-71.

158. James M. Schopf: Research in Coal Paleobotany Since 1943. *Economic Geology,* (September-October 1949), **44**, No. 6, pp. 492-513.

159. M. Schwarzbach: Duration of Deposition of Thick Lignite Seams. *Braunkohle,* (1950), **1**, pp. 57-59. (Abst. in *Fuel Abstracts,* New Series, (May 1950), **7**, No. 3781).

160. M. Schwarzbach: Marine and Non-marine Strata in German Maritime Coal Basin. *Glückauf,* (1949), **85**, No. 23/24, pp. 417-420.

161. Walter V. Searight: The Status of Coal Resource Studies. *Economic Geology,* (June 1950), **45**, No. 4, pp. 324-330.

162. W. A. Selvig, W. H. Ode, B. C. Parks and H. J. O'Donnell: American Lignites: Geologic Occurrence, Petrographic Composition, and Extractable Waxes. U. S. Bur. of Mines, *Bull.* No. 482, (1950).

163. C. A. Seyler: Coal Systematics and Petrology. (Abst.). *Fuel,* (July 1950), **29**, No. 7, p. 166.

164. R. Shepherd: Physical Properties and Drillability of Mine Rocks. *Colliery Engineering* (December 1950), **27**, No. 322, pp. 468-470.

165. E. Sherlock: A Classification of Alberta Coals. *Fuel,* (December 1949), **28**, No. 12, pp. 276-280.

166. E. Sherlock: Studies on Some Properties of Alberta Coals I. Density. *Fuel,* (November 1950), **29**, No. 11, pp. 245-252.

167. Reynold Q. Shotts: An Oxidation Method for Investigating the Petrographic Composition of Some Coals. *Trans.* AIME, (1950), **187**, MINING ENGINEERING, (August 1950), pp. 889-897, TP 2867H.

168. Raymond Siever: Structures of Herrin (No. 6) Coal Bed in Marion and Fayette Counties and Adjacent Parts of Bond, Clinton, Montgomery, Clay, Effingham, Washington, Jefferson, and Wayne Counties. Illinois Geological Survey *Circular* No. 164, (1950), 100 pp.

169. E. M. Sipprelle and H. L. Teichman: Roof Studies and Mine Structure Stress Analysis. Bureau of Mines Oil Shale Mine, Rifle, Colorado. *Trans.* AIME, (1950), **187**, pp. 1031-1036, MINING ENGINEERING, (October 1950), TP 2942A.

170. J. Spalding: *Deep Mining.* 402 pp., (1950), London, Mining Publ. Ltd. (Book Review in *Colliery Engineering,* (February 1950), **27**, No. 43).

171. Erich Stach: *Lehrbuch der Kohlenmicroskopie.* **I**. 285 pp., (1949), Kettwig, Verlag Glückauf.

172. Erich Stach: Occurrence of Metals in Anthracite. *Mikroskopie,* (1949), **4**, pp. 321-329. (Abst. in *Chemical Abstracts,* (1950), **44**, No. 3412).

173. Erich Stach: Volcanic Ash Rain over Bituminous Coal Moors. *Glückauf,* (January 1950), **86**, pp. 41-50. (Abst. in *Fuel Abstracts,* New Series, (July 1950), **7**, No. 103).

174. E. H. Stevens: Successful Practice in Alabama (Roof Bolting). *Mining Congress Journal,* (June 1950), **36**, No. 6, p. 65.

175. T. H. Stonhouse: Boring for Minerals. *Iron and Coal Trades Review,* (June 1950), **160**, pp. 1269-1275.

176. T. H. Stonhouse: Proving of Concealed Extensions. *Colliery Guardian,* (1950), **181**, No. 4683, pp. 383-388.

177. C. J. Stubblefield and W. Edwards: Marine Bands in the Coal Measures of Britain and Germany. *Geological Magazine,* (July-August 1950), **87**, No. 4, pp. 253-260.

178. E. K. Sturmfels: Geology and Coal Resources of Oaklands-Courabin Coalfield, New South Wales. Bur. of Min. Resources, Geology and Geophysics, Ministry of Nat. Devel., Commonwealth of Australia, Maribyrnong, W. 3, (1950), *Rept.* No. 3.

179. H. C. Sze: Die Mesozoische Flora aus der Hsiangchi Kohlen Serie in Westhupeh. *Paleontologie Sinica,* New Series, (1949), No. 2, 71 pp.

180. Curt Teichert: Some Recent Additions to Stratigraphy of Western Australia. Amer. Assoc. Petroleum Geologists *Bull.,* (September 1950), **34**, No. 9, pp. 1787-1794.

181. Rolf Teichmüller and M. Teichmüller: Problems in Coalification in Ruhr. *Zeitschrift* Deutsche Geologische Gesellschaft, (1947), **99**, pp. 40-75. (Abst. in *Fuel Abstracts,* (September 1950), **8**, No. 1634).

182. Rolf Teichmüller and R. Weber: Physical and Geological Investigations of Boreholes in Bituminous Coal. *Glückauf,* (1950), **86**, No. 11/12, pp. 193-204. Abst. in *Colliery Engineering,* (August 1950).

183. Edward M. Thomas: More from Roof-bolting. *Coal Age,* (April 1950), **55**, No. 4, pp. 71-75.

184. Edward M. Thomas: Roof Bolting in the United States. U. S. Bur. of Mines, *Inf. Circ.* No. 7583, (September 1950), pp. 1-8.

185. Edward M. Thomas, A. S. Barry, and Arthur Metcalfe: Suspension Roof Supports. Part I. *Mining Congress Journal,* (August 1949), **35**, No. 8, pp. 18-22. Part II, ibid., (September 1949), **35**, No. 9, pp. 50-53, 57. Reprinted U. S. Bur. of Mines, *Inf. Circ.* No. 7533, (September 1949), pp. 1-13.

186. P. W. Thomson: Beitrag zur Mikropälaontologie und Waldeschichte des Neogens (Jungtertiärs) von Niedersachsen und Schleswig-Holstein. *Neues Jahrbuch für Mineralogie, Monatshefte,* Jahrgang 1945-1948, (1949), Abteilung B, *Nos.* 9-12, pp. 364-371.

187. P. W. Thomson: Origin of Coal Seams Based on Micropaleontological Investigations of Main Seam of Rhine Brown Coal. *Braunkohle,* (February 1950), **2**, pp. 39-43.

188. P. W. Thomson: Grundsätzliches zur tertiären Pollen-und Sporenmikrostratigraphie auf Grund einer Untersuchung des Hauptflözes der Rheinischen Braunkohle in Liblar, Neurath, Fortuna und Brühl. *Geologische Jahrbuch,* (May 1950), **65**, pp. 113-126.

189. H. M. Thorne and A. J. Kraemer: Oil Shale in Spain. U. S. Bur. of Mines, *R. I.* No. 4736, (October 1950).

190. N. G. Titov, N. P. Federovskaya, and I. N. Tautsyrev: Sapropele Coals of the Moscow Basin and Effect of Their Petrographic Character on Yield and Composition of Light Tar Distillate. *Izvestiya Akademii Nauk* Soyusa Sovetskikh Solsialistichiskikh Respublik, *Otdelenie Technische Nauk* (*Bull.* Akad. Sci. U. S. S. R., Sect. Tech. Sci.), (1947), pp. 835-842. (Abst. from *Fuel Abstracts,* New Series, (February 1950), **7**, No. 925).

191. N. G. Titov, A. V. Zharkova, and L. A. Borozdina: Genetic Classification Parameters of Brown Coals and Lignites. idem., (1948), pp. 359-366. (Abst. from *Fuel Abstracts,* New Series, (August 1950), **8**, No. 868).

192. Parker D. Trask, Editor: *Applied Sedimentation,* 707 pp., (1950), New York, John Wiley and Sons, Inc.

193. F. M. Trotter: The Devolatilization of Coal Seams in South Wales. *Quarterly Journal* Geological Society London, (1949), **104**, No. 3, pp. 387-419. Discussions by Hickling, Himus, Roberts, Gee, Seyler, Jones, Rees, Shackleton, George, Fearnsides, Marshall, and Owen, ibid., pp. 419-437.

194. F. M. Trotter: Devolatilization Equation for South Wales. *Geological Magazine,* (May-June 1950), **87**, pp. 196-208.

195. Max Ussar: Über die Bitumina und harze Österreichischen Braunkohlen. *Berg. und Hüttenmanische Monatschafte,* (Jahrgang 1949), **94**, Nos. 1/2. (Abst. by G. H. Cady, *Economic Geology,* (1950), **45**, No. 2, pp. 181-184).

196. Y. Uzumasa: Minor Inorganic Constituents of Coal. *Chemical Research.* (Japan), 1949, *Inorganic and Analytical Chemistry* (1949), pp. 1-17. (Abst. in *Fuel Abstracts,* New Series, (April 1950), **7**, No. 2841).

197. J. Vallet: Natural Electrical Currents of Carboniferous Region of Salins-Chandoline-Bramois near Sion (Valais). *Archive Science* (1949), **2**, No. 1, pp. 22-56. (Abst. in *Fuel Abstracts,* New Series, (January 1950), **7**, No. 7).

198. S. Van der Heide: Influence of Compaction on Development of Coal Seams. *Mededeelingen* van de Geologische Stichting, New Series, (1948-1949), **3**, pp. 37-40. (Abst. in *Fuel Abstracts,* New Series, (August 1950), **8**, No. 871).

199. D. W. Van Krevelen: Graphical-statistical Methods for the Study of Structure and Reaction Processes of Coal. *Fuel,* (December 1950), **29**, No. 12, pp. 269-284).

200. W. W. Varossieau: Opgegraven en Aangetast Hout uit Biologisch Oogpunt Bezien (Ancient Buried Wood Seen from a Biological Point of View). In W. Boerhave Beekman: *Hout in Alle Tijden,* (December 1949), Deel **I**, hoofdstuk 5, pp. 331-387.

201. W. W. Varossieau: On the Use of the Electron Microscope in Wood Anatomy. *Proceedings* Conference on Electron Microscopy, Delft, July 4-8, 1949, Delft, (1950), pp. 107-110.

202. W. H. Wellman: Geology of the Pike River Coalfield, Northwestland. *New Zealand Journal of Science and Technology,* (1948), **30** (B), pp. 84-95. (Abst. in *Journal of Geology,* (November 1950), **58**, No. 6, pp. 670-671).

203. J. W. Whitaker: Densities of Indian Coals. *Fuel,* (February 1950), **29**, No. 2, pp. 33-41.

204. S. L. Windes: Physical Properties of Mine Rock. Part II. U. S. Bur. of Mines, *R. I.* 4727, (September 1950).

205. Y. Yamamoto: Pseudo-photographic Effect of Coal on Photographic Plates. *Memoirs of College of Science,* Kyoto Imperial University (1944), No. 24A, pp. 73-78. (Abst. in *Chemical Abstracts,* (1950), **44**, pp. 963-964).

206. G. R. Yohe: Coal Oxidation: Active Oxygen and the Russell Effect. *Fuel,* (July 1950), **29**, No. 7, pp. 163-165.

207. David Zegeer: Core Drilling for Air. *Coal Age,* (February 1950), **55**, No. 2, pp. 92-96.

208. V. V. Zinovev: Possible Use of Spectral Method for Identification of Coal Deposits, *Izvestiya Akademii Nauk* Soyusa Sovetskikh Solsialistichiskikh Respublik, Serie Fiz. (*Bull.* Akad. Sci. U. S. S. R., Phys. Ser.), (1948), **12**, pp. 475-476. (Abst. in *Fuel Abstracts,* New Series, (August 1950), **8**, No. 869).

Correction

In the December 1951 issue, p. 1068, TP 3194B, *Basic Laboratory Studies in the Unit Operation of Crushing* by J. W. Axelson, J. T. Adams, Jr., J. F. Johnson, J. N. S. Kwong, and E. L. Piret: The next to the last sentence in the last paragraph should read as follows: Rittinger's law is probably too simple a concept to encompass a complicated phenomenon and may very well not be a particularly desirable base or starting point for the development of a full understanding of crushing.

Pipeline Transportation of Phosphate

by I. S. Tillotson, R. B. Burt, and James A. Barr

THE pumping of solids in water suspension is an important part of many metallurgical and mining operations. In most cases, it is still in the rule of thumb category for which no universal formula has been developed, and much research is needed.

Because of the limited and incomplete data available, this article may be classed as an experience paper, which is presented with the hope that some contribution will be made toward the development of the so-called universal formula. This formula, if and when developed, may be evolved from several factors, many of which are not now available for general application.

The designing engineer is interested in obtaining accurate forecasts on: 1—the minimum velocities needed to prevent choke-ups in the pipeline, which in turn dictates pipe sizes, 2—power required for pumping, 3—pump selection. The basic factors for a given problem will include: 1—weight per unit of time of solids to be handled, 2—specific gravity of solids, for calculation of volume, friction and power, 3—screen analysis of solids with the colloidal acting, i.e., the slime fraction, a very important factor, 4—shape of particle or some means of determining a friction constant, 5—effects of percentage of solids, 6—development of a viscosity factor to be used in the overall calculations, 7—calculation of the lower limits of pipeline velocities permissible, 8—calculation of total head, pump horsepower, and 9—setting up of pump specifications.

In certain limited cases horsepower and total heads and minimum velocities may be computed and a suitable pump selected from basic data, but in many cases, as in mining of Florida pebble phosphate, experience rather than a hydraulic formula still should be used as a basis of selection.

Pumping Florida Pebble Matrix

Pumping at the Noralyn mine of International Minerals and Chemical Corp. will be used as an example. Other areas will vary as to the characteristics of the matrix, especially the slime content.

A typical screen analysis of this matrix is: +14 mesh, pebble size,* 2.1 pct; −14 +35 mesh, 11.4 pct; −35 +150 mesh, 60.5 pct; −150 mesh, 25.0; total, 100 pct; moisture in bank, 20.0 pct; weight per cu ft in bank, 120 lb.

The −150 mesh fraction may increase to as much as 35 pct in adjacent areas.

When thoroughly elutriated, the matrix has a relatively slow settling rate, which is an important factor in permitting lower pipeline velocities without choke-ups. Exact data is not available to evaluate settling rates. For a factor of 100 a suspension of clean building sand in water is suggested. When pumping long distances, a quick settling matrix allows the coarser solids to settle out along the bottom of the pipeline, causing drag, turbulence, and increased friction. With a slow settling matrix as at Noralyn, turbulence acts to keep the solids in suspension at a lower friction head, regardless of the pumping distance.

When the *pebble* content of the matrix, i.e., the +14 mesh fraction, is in excess of 10 pct of the total solids, trouble may be expected from settling out even in normal pumping distances. To prevent choke-ups and maintain tonnage, an additional pump must be added in the long runs, where one pump would otherwise be satisfactory.

A typical pulp handled is: total volume, 7800 gpm; water, 4500; solids pumped per hr, 4200 lb; sp gr pulp, 1.4; percent solids in pulp, 46.; pipe size, 16-in. ID; pulp velocity, 12.85 fps; probable critical velocity, 10 fps, as below this minimum velocity choke-ups would be numerous.

In calculating friction heads the Armco handbook is used where a roughness factor based on 15-year-old pipe is set up.

Because the pipe used in pumping matrix is smooth and polished because of the scouring action of the phosphate and its silica content, the head losses in the Armco table for water are practically the same as in pumping the Noralyn matrix through smooth pipe, plus the fact that conditions vary widely over short periods, making accurate determinations difficult to obtain.

New pumps and pump changes are being tested continuously and a wealth of data built up. This has resulted in a substantial improvement and lower relative costs in pumping matrix. The Florida phosphate industry is constantly seeking to offset higher wage and material costs with improved technique.

Until a few years ago a 12-in. discharge pump was commonly used, with heads as low as 80 ft. Sizes have gradually increased and heads more than doubled.

For example, the following pump was placed under test at the Noralyn mine: make, Georgia Iron Works; size, suction 16 in., discharge 14 in.; impeller, 39-in. diam; motor, 600 hp, slip ring; full load speed, 514 rpm.

The results were increased head, higher capacity than the older design, with fewer pumps in the line from mine to washer.

I. S. TILLOTSON, Member AIME, is Mining Superintendent, International Minerals and Chemical Corp., Mulberry, Fla. **R. B. BURT** is Chief, Plant Chemical Control Section, Tennessee Valley Authority, Wilson Dam, Ala. **JAMES A. BARR**, Member AIME, formerly Consulting Engineer, Mt. Pleasant, Tenn., is now with the Defense Minerals Administration.

Discussion on this paper, TP 3248AH, may be sent to AIME before March 31, 1952. Manuscript, Feb. 20, 1951. St. Louis Meeting, February 1951.

---

* *Pebble* is a commercial designation for the coarser fraction of finished phosphate from a washer, usually +14 mesh.

This page of Mining Transactions AIME follows p. 208. The intervening non-Transactions pages appeared in Mining Engineering.

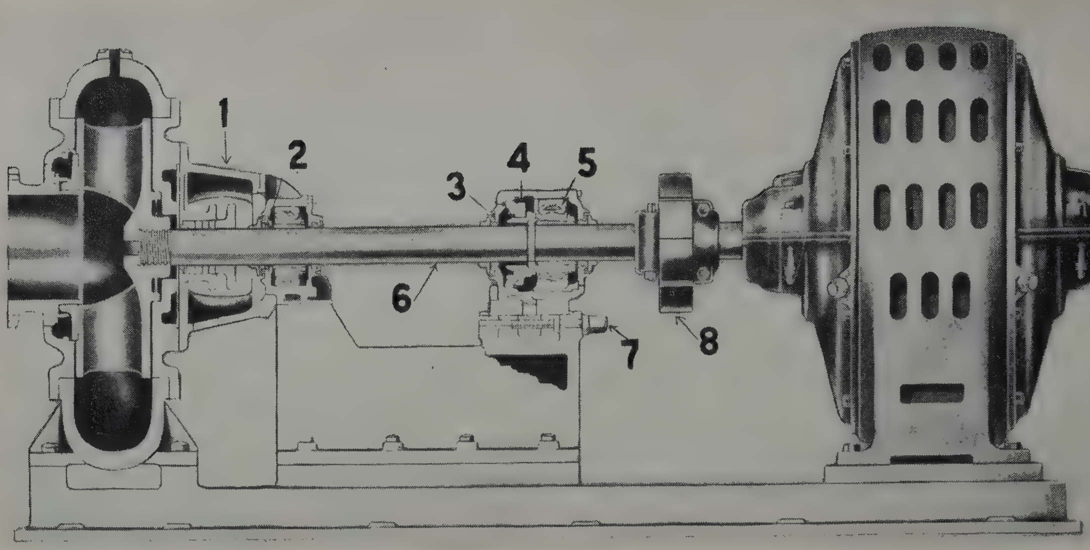

Fig. 1—General design of the discharge pump.

1—Rigid construction to support pump shell and maintain alignment.
2—Double Klozure on forward end with flinger retains oil and prevents entrance of water.
3—Labyrinth seals in combination with flinger effectively retains oil and guards against contamination.
4—Steep angle SKF spherical roller thrust bearing.
5—Radial SKF spherical roller bearing arranged to carry all radial load without thrust and self aligning with thrust bearing.
6—Heavy alloy steel shaft.
7—Precision adjustment for impeller clearance 2-in. screw with 12 threads per in.
8—Heavy duty flexible coupling built by G.I.W. especially for severe service.

The next pump tried was: size, suction 16 in., discharge, 14 in.; impeller, 43¾-in. diam. A typical test indicated: pulp capacity, 7100 gpm; solids, 625 cu yd bank measurement per hr; head, 160 ft (water equivalent); water added, 4580 gpm; brake hp, 490; pump efficiency, 78 pct. Level pumping distance, one pump with 16-in. pipe 7000 ft as against 3000 ft with the 12-in. pump formerly used.

The general design of the pump is shown in Fig. 1 and the operating characteristics of the 16-in. size are shown by the curves, see Fig. 2.

The latest pump tested is: size, suction and discharge 16 in.; impeller diameter, 49 in.; and designed for: efficiency, 65 pct; capacity, 6700 gpm; head, 188 ft; brake hp pump, at 505 rpm, 650.

The former pump did not fully load the motor because the efficiency of the pump was greater than design calculations indicated.

Pumping distances, head, volume, and tonnages vary according to plant demands and operating conditions; pump speeds must be varied frequently, often below peak efficiencies. So far, the slip ring motor has been the only practical drive found, but consideration is being given to other types of ac motors, hydraulic or magnetic couplings, and dc motors served by rectifiers.

Formerly 600-rpm motor drives were used, but for the existing conditions it was found that 500 rpm gave smoother operation at higher efficiency.

In the course of test work, one formula has evolved which has been found suitable for calculating runner diameters, i.e., $D = \dfrac{1837 \cdot \sqrt{H(0.93)}}{\text{rpm}}$, where D is in inches, and H = water equivalent of head, in feet.

At the Georgia Iron Works, M. R. Creasy, Chief Engineer, equipped a trailer for field test work, as shown in Figs. 3 and 4, for obtaining the necessary test data. Velocity of flow is determined by the electric titration method at 20-min intervals.

Table I. Data and Results, Achan Mine, International Minerals and Chemical Corp., G.I.W.,[a] 39¼x12 In., 16-In. Suction, 38-In. Diam

Matrix Line Velocity, Ft per Sec	Gpm	Suction Head Equiv. Ft Water	Discharge Head, Equiv. Ft Water	Total Dynamic Head, Equiv. Ft Water	Water Hp	Kw	Rpm	Brake Hp	Efficiency, Pct
12.69	6104	12.00	187.11	199.11	306.90	360	580	439.14	69.80
13.33	6412	12.46	187.11	199.57	323.14	372	580	453.80	71.20
11.59	5575	12.00	187.11	199.11	280.31	360	580	439.14	63.80
12.31	5922	10.20	187.11	197.31	295	360	580	439.14	67.10
13.56	6523	11.90	187.11	199.01	327.81	390	580	475.7	68.90
13.56	6523	16.54	184.80	201.34	331.65	390	580	475.7	69.70
11.59	5575	9.06	189.42	198.48	279.43	360	580	439.14	63.60
13.11	6306	17.00	191.73	208.73	332.39	372	580	453.80	73.20
13.33	6412	11.33	189.42	200.75	325.05	372	580	453.80	71.60
11.94	5744	15.86	182.49	198.35	287.71	360	580	439.14	65.60
Avg 12.70	6109	12.84	187.34	200.18	308.93	369.60	580	450.85	68.44

[a] Georgia Iron Works.

A tabulation of the test of a 39¼x16x12-in. pump is given in Table I. Data on matrix handled was gathered by the Engineering Department of International. Some of the previous records are of value in making comparisons; these are shown in Tables II and III. The effects of partial speeds and worn pumps apply to old as well as the later design pumps.

Fig. 5 shows the general exterior design of an Allen-Sherman Hoff G frame Hydroseal pump, now used in the Florida phosphate field. The clear water characteristics are given in Table IV.[1]

Pumping Tennessee Matrix†

The Tennessee Valley Authority built and operated a 3-mile pipeline between the Akin mine and the Godwin beneficiation plant, in Maury County, after a thorough study of various forms of transportation. Because of the terrain and operating requirements, pipeline transportation has proved the most economical and has furnished valuable hydraulic data.

The matrix, consisting of a conglomerate mass of clay, silica, and phosphate particles, is mined from open pits by draglines at the rate of 70 to 90 tons per hr.

The matrix next is crushed in a hammer mill, to —1½-in. size, slurried with water, pumped to a blunging-classifying system for desliming at a —10 micron split, which overflows the final thickener into tailing ponds. The solids thus wasted consist principally of clay.

Table II. Data on Pumping from Parker Property to No. 92 Washer, Operated from March 26 to 30, 1938

	"F" Frame ASH[a] Lift Pump, 39-In. Runner and "E" Frame ASH Pit Pump 32-In. Runner
Time operated, hr	53.5
Matrix pumped, cu yd	13,203
Matrix per hr, cu yd	248.7
Rock mined, tons	3,312
Rock per hr, tons	61.9
Matrix per ton rock, cu yd	3.98
Water pumped, gpm	4,400
Solids pumped, pct	25.32
Distance from lift pump to washer, ft	3,080
Distance from lift pump to pit pump, ft	1,220
Total pumping distance, ft	4,300
Size of pipeline, in.	14
Static head on lift pump, ft	−5.5
Total static head, ft	36.02
Suction head on pit pump, ft	22.6
Discharge pressure on pit pump, lb	52
Suction pressure on lift pump, lb	+4
Discharge pressure on lift pump, lb	92
Total head on pit pump, ft	142.7
Total head on lift pump, ft	203.3
Total dynamic head, ft	346.0
Friction head per 100-ft pipe	7.21
Kwh used	34,880
Kwh per hr	651.9
Kwh per cu yd matrix	2.642
Water hp	514.8
Electrical hp	873.8
Motor efficiency, pct	90
Overall pumping efficiency, pct	65.46
Saving in favor of ASH[a] pumps, pct	10.6

[a] Allen-Sherman Hoff.

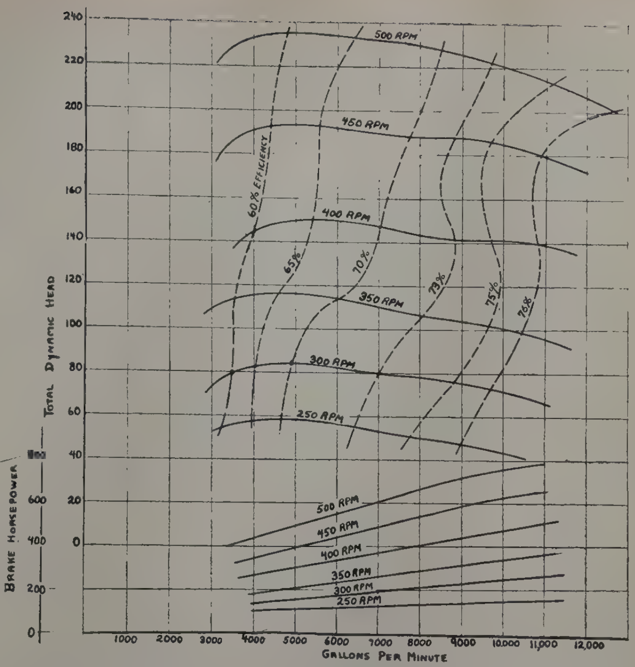

Fig. 2—Operating characteristics 16x52-in. dredge pump, 51 in. diam impeller, 16 in. diam suction.

The 1½ to 65 mesh and the 65 mesh —10 micron splits called concentrate are mixed in a surge tank, which is brought to the proper pumping density with water for pumping through the pipeline.

There is little reserve storage, and the pumping is continuous to the Godwin plant where the —10 micron size left from the first desliming or formed by abrasion in the pipeline is separated again and sent to tailing ponds.

The deslimed sands, often called washed sands, are drained in wet storage piles and shipped to the TVA electric furnace phosphorus plant about 80 miles away at Wilson Dam, Ala.

Because of the engineering value the following section is presented in its entirety.

Hydraulic Transportation System

In general the design problem presented by the requirements of the flowsheet of the beneficiation

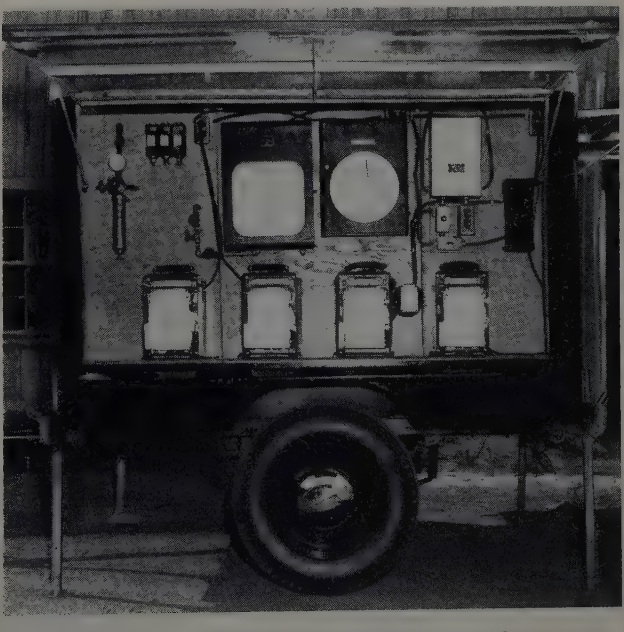

Fig. 3—Trailer equipped for field test work.

---

† Abstracted from "TVA's Experience with Hydraulic Transportation of Phosphate Concentrates," by R. B. Burt.

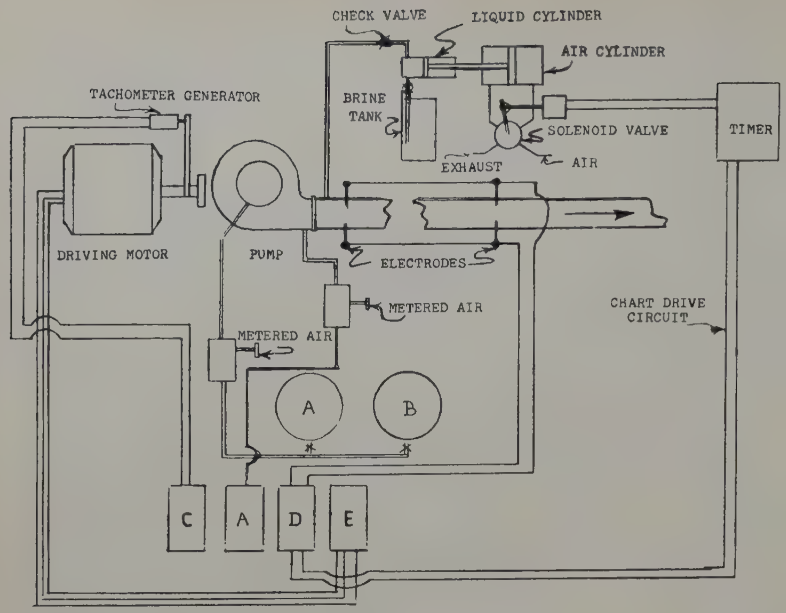

Fig. 4 — Schematic diagram for testing phosphate pulp line pumps with Georgia Iron Works Co. testing unit.

A—Recording pressure gage.
B—Recording vacuum gage.
C—Tachometer.
D—Conductivity recorder.
E—Recording kw meter.

plant was to provide a hydraulic transportation system consisting of pumping equipment and accessories and a pipeline approximately 16,000 ft long for transporting up to 90 tons per hr of concentrate, as a water slurry or pulp, from the Akin plant to the Godwin plant.

Since the preceding operations of mining, scrubbing, and concentrating were to be successive and continuous, provision was made to insure uninterrupted operation of the concentrate line. Other factors which influenced the selection and location of pumping equipment and the determination of pipe diameter were: 1—the water requirement of the classification equipment at Godwin, 2—the pumping pressures required, and 3—the lowest velocity at which the required tonnage of sand and water could be delivered without deposition of solids in the pipelines.

Since the water used to transport the solids was also to serve as dilution water in the classifiers at Godwin, it was desirable that the quantity be held within limits necessary for proper classification with the addition of a minimum of makeup water at the Godwin plant. This resulted in a flow requirement of from 1200 to 1500 gpm.

Safe operating pressure on pumps suitable for the system imposed a further limitation on design. In selecting pumping equipment, a choice was made between the use of five low-head pumps, or three comparatively high-head pumps. It was necessary that the pumping layout require no pumping pressures in excess of 150 psi. It was anticipated that with a high-head installation, pump maintenance costs would be greater and more frequent renewal of pump parts would be necessary than with a low-head installation. However, based on estimates of installation, operating, and maintenance costs, the high-head installation appeared to be more economical.

Theoretical Considerations

Previous investigators have reported that two types of flow exist for slurries or pulps similar to the laminar and turbulent states of flow which are characteristic of true liquids.[2-4] Also, it has been found that Poiseulles' equation for viscosity does not apply to laminar flow of slurries as it does for true liquids, although it does apply to both type fluids in the turbulent flow range, and in this range the viscosity of the slurry is the same as that of the liquid in which the solids are suspended.[3] It has been found that with slurries, laminar flow changes to turbulent flow at a rather clearly defined velocity, referred to as the critical velocity, and that this velocity depends on the solids content of the slurry and the particle size distribution of the solids.[3, 5] Work of other investigators indicated that in pumping sludges, pulps, and muds, the Fanning friction factor, *f* is proportional to the Reynolds number; that the friction factor varies with velocity to about the same extent in slurries as in true liquids within the turbulent flow range, and the factors for slurries are only slightly higher than those for true liquids. The latter difference also depends on the solids content of the slurry and the particle size distribution of the solids.[3, 5]

Although the mechanism of transporting slurries in pipelines had been investigated considerably in small scale tests, with limited verification by data on dredging operations, most of the information reported involved material dissimilar to phosphate

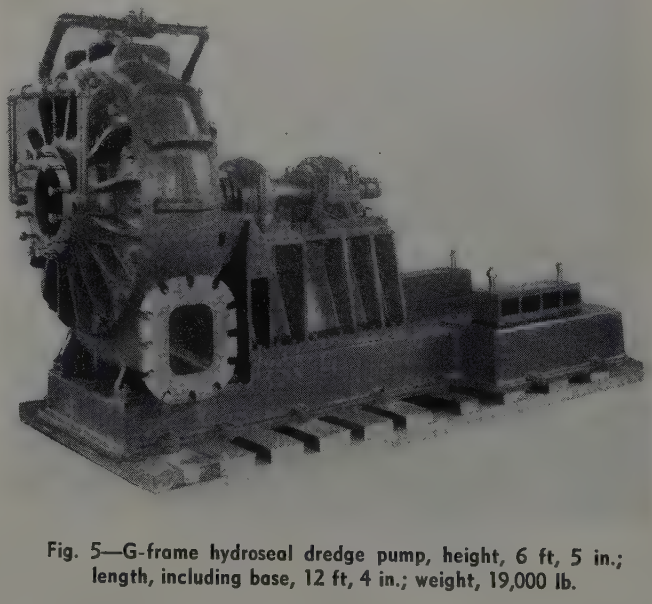

Fig. 5—G-frame hydroseal dredge pump, height, 6 ft, 5 in.; length, including base, 12 ft, 4 in.; weight, 19,000 lb.

Table III. Pump Tests, July 28, 1941. Type 711 Pump Tested, 12-In. G.I.W., HD 39¼-In. Matrix Pump, Mine No. 122[a]

4½-In. Calibrated Nozzle								
Controller position	Switch	2	4	6	8	10	12	Open
Rpm	400	416	428	458	520	538	565	592
Vacuum, in.	7½	7½	8	8	9	9½	10	10
Nozzle pressure, lb	29½	31	33	38	48	52	56½	63
Total dynamic head, ft	76.6	80.1	85.3	96.8	121.1	130.9	141.8	156.9
Gpm	2960	3030	3130	3350	3770	3920	4090	4320
Water hp	57.3	61.4	67.5	81.9	115.2	129.5	146.5	171.0
Motor load, kw	123.2	128.0	134.0	152.0	194.0	206.0	226.0	252.0
Electrical hp	165.0	171.5	179.4	203.5	260.0	276.0	303.0	338.0
Overall efficiency	34.7	35.8	37.6	40.2	44.3	47.0	48.4	50.7
Pump efficiency[b]								56.3
5½-In. Calibrated Nozzle								
Controller position	Switch	2	4	6	8	10	12	Open
Rpm	400	412	422	440	500	535	552	590
Vacuum, in.	8½	9	9	9½	11	11½	12½	14
Nozzle pressure, lb	23½	25	26½	31	42	46	51	57½
Total dynamic head, ft	63.9	67.9	71.4	82.4	109.5	119.3	132.0	148.7
Gpm	3930	4060	4180	4520	5200	5500	5780	6150
Water hp	63.5	69.5	75.5	94.0	143.5	165.7	192.7	230.5
Motor load, kw	134.8	141.2	146.0	173.2	228.0	246.0	270.8	306.0
Electrical hp	180.5	189.0	195.5	232.0	305.0	330.0	363.0	410.0
Overall efficiency	35.2	36.8	38.6	40.5	41.0	50.2	53.2	56.3
Pump efficiency[b]								62.5

[a] Service prior to test: pump runner, 1053½ hr; pump shell, 1053½ hr.
[b] Assuming motor is 90 pct efficient at full speed.

concentrates, and it was not believed that these data were adequate for the design of TVA's transportation pipeline.[4–6] Therefore, to study more thoroughly the effect of slurry properties on transporting characteristics and to provide data for design purposes, an experimental program was carried out on pumping phosphate slurries containing from 2 to 35 pct solids through 400 ft of 2 and 4-in. diam iron pipe at velocities of from 7 to 11 fps. These velocities were found to be above the critical velocity for this system; below a velocity of about 7 fps the solids tended to settle out and resulted in stoppage of the pipelines.

In this work it was observed that the pumping of the phosphate concentrates through the pipe polished its walls to such an extent that the head loss due to friction was lower than has been reported as normal for steel pipe. Specifically, the surface smoothness constant, C, used in the following Williams and Hazen formula was 160, whereas, this factor is normally 140 to 150 for steel pipe.[7] On the basis of this, friction factors in the lower range were used in determining the requirements for the plant pipeline.

$$Hw = \frac{(V)}{(1.318\ CRO.63)}\ 1.85$$

Where: Hw = friction loss, in feet of water per foot of pipe length; V = velocity, in feet per second; C = constant, varying with the kind of pipe and the conditions of the wall; and R = the hydraulic radius.

In transporting slurries or pulps through a pipeline of given diameter the effect of variation in the solids content of the pulp on the head loss while pumping at a given velocity, relative to the head loss resulting when water alone is pumped at the same velocity can be represented by the formula:

$$\frac{\Delta Hp}{\Delta Hw} = Y$$

Where, the particle size distribution of the solids is constant Hp = head loss in feet of pulp per foot of pipe length and Hw = head loss in feet of water per foot of pipe length.

It has been found that at values above the critical velocity the friction factor for slurries increases with a decrease in velocity and increases with an increase in pulp density (solids concentration).[5] Since head loss is directly related to the friction in pipelines, the ratio $\frac{\Delta Hp}{\Delta Hw}$ may be considered to increase with a decrease in velocity or an increase in pulp density

Table IV. Clear Water Performance of "G" Frame, Hydroseal Dredge Pump, 14-In. Suction, 12-In. or 14-In. Discharge

	435 Rpm						500 Rpm						585 Rpm						
U.S. Gpm	36-In. Imp.		37-In. Imp.		38¾-In. Imp.		36-In. Imp.		37-In. Imp.		38¾-In. Imp.		36-In. Imp.		37-In. Imp.		38¾-In. Imp.		Imperial Gpm
	TDH[a]	Hp	TDH[a]	Hp	TDH[a]	Hp	TDH[a]	Hp	TDH[a]	Hp	TDH[a]	Hp	TDH[a]	Hp	TDH[a]	Hp	TDH[a]	Hp	
4000	91	150	97	162	107	180	123	210	130	226	142	254	170	323	180	348	196	382	3330
4500	90	161	96	173	106	191	121	225	129	242	141	269	169	342	179	367	195	403	3750
5000	89	171	94	183	104	202	120	240	127	257	140	284	168	360	178	386	194	423	4160
5500	87	182	93	194	102	214	118	254	125	272	138	298	166	378	176	404	193	443	4580
6000	85	193	91	205	100	226	116	268	123	287	136	312	164	395	175	421	191	463	5000
6500	83	202	89	217	98	238	115	281	121	301	134	327	162	412	173	438	189	483	5410
7000	82	211	87	228	96	250	113	294	120	315	132	342	160	429	170	455	187	503	5830
7500	80	222	85	239	94	261	110	307	117	329	130	357	158	445	168	474	185	523	6250
8000	78	232	83	249	91	271	108	319	115	343	127	372	156	461	166	492	182	543	6660
8500	75	241	80	258	88	281	106	331	113	356	125	387	153	478	164	510	180	562	7080
9000	73	250	78	266	86	291	103	343	110	369	122	401	151	495	161	529	177	580	7490
9500	70	258	76	275	83	301	101	355	108	381	119	415	148	512	158	547	174	599	7910
10000	68	266	73	284	80	310	98	367	105	393	116	428	146	528	156	565	171	617	8330
10500	65	274	71	292	78	320	95	379	102	404	112	441	143	545	153	583	167	636	8740
11000	63	281	68	300	74	329	93	390	100	415	109	453	140	561	150	600	164	654	9160
11500	60	288	65	309	70	337	90	400	97	427	106	466	137	578	147	618	160	673	9580
12000	57	295	62	317	67	344	86	410	93	439	102	478	133	594	143	635	156	693	9990

[a] Total dynamic head.

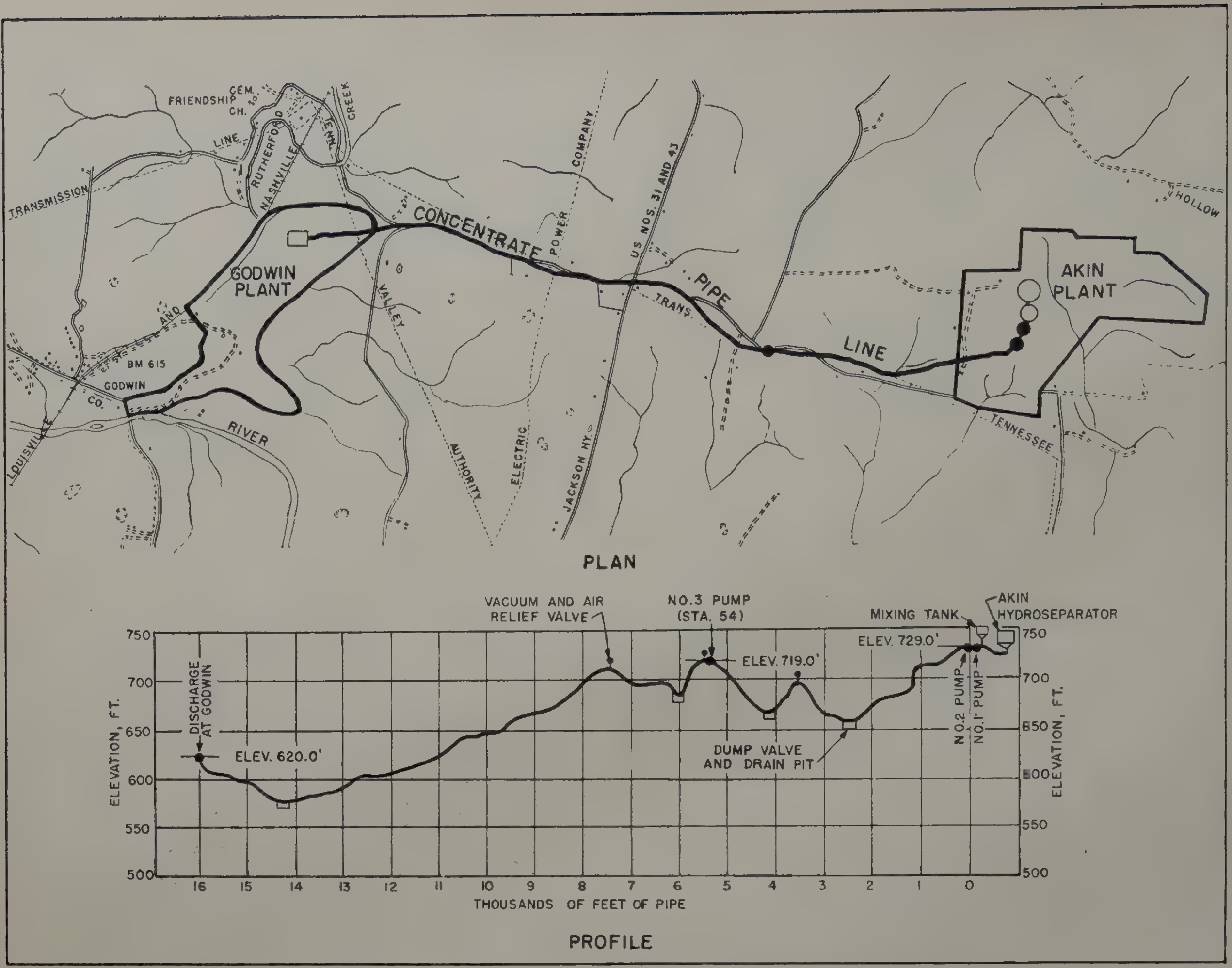

Fig. 6—Phosphate concentrate pipeline from Akin plant to Godwin plant.

and approaches a value of one at high velocities or very low pulp densities.

The ratio of $\frac{\Delta Hp}{\Delta Hw}$ calculated from experimental data averaged 1.5 at velocities of 7 to 13 fps when the slurry contained 25 pct solids. On this basis the desired transporting capacity of the pipeline, the total head loss, and pump requirements for pipelines of several different diameters were calculated. It was decided that with a minimum velocity of 8 fps (considered safely above the critical velocity), an 8-in. diam pipe would provide the necessary capacity with a maximum pulp concentration of 25 pct solids and would have pumping requirements within the range of standard pumping equipment.

Pipeline Location

After the size of the pipe diameter had been determined, it was necessary to make a detailed study of the location of the line and to determine the total head, select and locate the pumping equipment in the system, provide facilities to insure continuous operation, and incorporate certain features considered necessary for safe operation of the line.

From study of several preliminary locations, the final location shown in Fig. 6 was selected because it appeared to be the most practical route between the Akin and Godwin plants when consideration was given to distance, topography, and construction costs.

The line as originally installed was an 8-in., wire-wound, wood-stave pipe. Several test sections of cast-iron pipe lined with wood staves and sections of abrasion-resistant, spiral-welded, steel pipe were included in the line. After several months' operation, examination of the line revealed that the unlined steel pipe was withstanding the abrasive action of the phosphate sands better than the wood pipe, and experience has shown that maintenance of the wood pipe was high because of a leakage which required frequent detailed examination of the line. Therefore plans were made for conversion to an all-steel line as replacements became necessary. Subsequent experience has indicated that wear of the steel pipe amounts to only about 0.02 in. per year.

The 8-in. spiral-welded, abrasion-resistant, steel pipeline is laid in 40-ft lengths connected by flanges and Style 38 Dresser couplings. The couplings are used every third length to provide for expansion and contraction, and the play in the couplings, together with the flexibility of the pipe itself, permits long curves, which facilitate laying the line in the rolling topography of the area. The line is laid on uniform grades conforming closely to the surface of the ground. Small cuts and fills in both earth and rock were made where necessary to obtain uniform grades and vertical curves. At points where fill would have been excessive, and at points where the line crossed natural drainage channels, the pipe is laid on wooden trestles built on concrete foundations. At road crossings the line is buried. At about station 85 + 00 the line passes underneath U. S. Highway No. 31, the main highway from Columbia to Nashville, Tenn. At this point a 36-in. diam corrugated steel pipe was jacked through the base of the highway fill and the concentrate line laid through this pipe. At station 141 + 50, the line crosses Rutherford Creek, a stream 85 ft wide. To support the line over this stream, a suspension bridge was built with a central span between towers of 120 ft and with 60-ft side spans between each tower and the anchorage. The main cables and the floor system girders are on 5-ft 8-in. centers that provide ample space for maintenance and a walkway for inspection.

Pumping Equipment

Three pumps are used, see Fig. 6. Pumps Nos. 1 and 2 are located at the Akin plant near the hydroseparator, and pump No. 3 is located on the line at station 54 + 00. All three pumps are 6-in., centrifugal, closed impeller sand pumps, and at a speed of 1200 rpm develop 265 ft of head of a pulp of 1.20 sp gr. No. 1 pump is directly connected to a 250-hp, 1200-rpm, 2300-v synchronous motor running at a constant speed under a fairly constant load for power factor correction. Pump No. 2 is driven by a 250-hp, 2300-v, slip ring motor with speed variations from 640 to 1170 rpm and develops heads from 80 to 250 ft. No. 3 pump is also driven by a 250-hp, 2300-v, slip ring motor having speed variations from 760 to 1170 rpm and develops heads from 110 to 250 ft. The piping is arranged so that any combination of pumps can be used to transport the concentrate. The sand pumps are provided with water seals to prevent the passage of sand from the pumps into the bearings. A supply of clean, high-pressure, water is provided for the seals by small low-capacity, centrifugal pumps.

It was anticipated that the combinations normally used would be pumps Nos. 1 and 3 or with pumps Nos. 2 and 3, and calculations indicated that these combinations would result in a velocity in the line of from 8 to 9 fps, a flow of from about 1285 to 1450 gpm, pump pressures from 140 to 170 psi, and delivery rates of 95 to 110 tons of solids per hr when the pulp contained 25 pct of solids. The three-pump installation provides considerable flexibility in the total head that can be placed on the line. The No. 2 pump is considered a standby for the No. 1 pump; it also can be thrown on the line when No. 3 pump is down, and in cases of emergency due to surges or a too heavily loaded line, when it is necessary to use all three pumps. It has been found that with close control the use of three pumps is not frequently necessary.

When transporting 80 tons of concentrate per hr at velocities of from 8 to 9 fps, 40 to 45 tons of solids are in the line. In case of power failure, or if for any other reason all pumps are down and the problem of accelerating the mass in the line when starting up again is encountered, there is danger of the line becoming completely plugged. As a safety measure, and to provide means for getting the line back into operation without excessive loss of time, dump valves and vacuum and air relief valves are located at four points in the line as shown in Fig. 6. A drain pit with sufficient capacity to hold the pulp contained in the line between the two high points is provided under each drain valve. The pits are constructed with drains near the bottom that permit the water to drain out of the sand, which then may be reclaimed from the pits with trucks. The dump valves were designed originally for automatic operation, being held closed by an energized solenoid so that in case of power failure the solenoids would become deenergized and the holding mechanism released, allowing the valves to dump. In actual practice, however, the automatic operation of the valves was not entirely successful so they are now manually operated, although dumping is not frequently necessary.

To insure continuous operation, the pumps are provided with a dual power supply consisting of two substations feeding from a single 12-kv, three-phase transmission line. The two substations, one at the Akin plant and the other at station 54 + 00 on the concentrate line, have 2300-v secondaries. The pumps can be fed from either substation or from both substations operating in parallel. When the substations are operating in parallel, the transformers at each station are protected by directional overcurrent relays. In the case of a transformer failure at either station, the entire transformer bank at that station is automatically cut out of the circuit, which allows the concentrate pumps to continue feeding from the remaining transformer bank.

The flow rate in the line is determined by means of a velocity meter at the discharge end of the line, which consists of a 6-in. diameter nozzle and a scale calibrated to read in gallons per minute. The flow rate is determined by noting the intersection of the trajectory of the stream on the calibrated scale located at a fixed distance below the center line of the nozzle.

The discharge end of the line, the pump at station 54 + 00, and the two pumps at the Akin plant are connected by an automatic magneto monophone system for interplant communication. When the flow deviates too greatly from the desired rate, the pump operators are notified by telephone, and the pump speeds are adjusted accordingly.

Hydraulic Transportation System

After the wood pipe had been replaced with steel pipe, a test was made of the hydraulic transportation system, while operating under normal conditions during which only pumps Nos. 1 and 2 were used. Pressure gages were installed at all the principal points in the line, recording wattmeters were connected to each of the concentrate pump motors, and the speed settings of the rheostats on the variable-speed motors were calibrated. The pulp was sampled at the discharge end of the pipeline to determine the solids content and the particle size distribution of the solids. The data collected at 30-min intervals were averaged for periods of approximately 8 hr during which there was little variation in the operation. Data were also collected for two short periods on part of the line, station 54 + 00 to Godwin, while pumping water only, to provide a comparison with the data on slurries. The results of these tests are given in Table V. These data show that the load on the No. 1 pump motor was practically constant, and the additional pumping load required was taken up by pump No. 2 as was anticipated. The speed-head-power relationships of pumps Nos. 2 and 3 are shown in Figs. 7 and 8. Normal operation during the test period involved the use of pumps Nos. 1 and 2 only, but it is believed that the consumption of energy for pumps Nos. 1 and 3 would be about the same as that for pumps Nos. 1 and 2. Increasing the solids content of the pulp from 11.1 to 17.4 pct resulted in a decrease in the energy consumption from about 4.6 to 3.0 kw-hr per tons of dry solids transported, see Fig. 9. It may be also noted from Fig. 9 that the power consumed per ton of dry solids pumped decreases with an increase in the solids transportation rate. About 76 pct of the energy consumed in pumping was used by pump No. 1. During one 8-hr period, period No. 8, pump No. 2 was used alone, and the power consumption was fairly low, as is shown in Table V. It will be noted that the percentage solids and the pumping rate were both low during this period, thereby resulting in a lower than normal solids transportation rate and correspondingly low-head losses, which permitted operation under these conditions. The velocity of 8.2 fps was only slightly above the safe operating velocity, and it is believed that a significant increase in the solids content of the pulp while using only one pump would have resulted in a lower velocity and stoppage of the pipeline.

The pumping efficiency

$$\left(\frac{\text{theoretical, hp-hr}}{\text{actual, hp-hr}} \times 100\right)$$

varied from 41 to 54 pct according to the load on the pumps, and was lowest when the solids concentration of the pulp was lowest. All of the data obtained during the test were taken with velocities above the critical point, that is, within the turbulent flow region, so that the principal variables affecting the friction losses in the pipeline were solids content, velocity, and particle size distribution of the solids. From the data collected, the values for the Reynolds number were calculated for the various tests; these values are given in Table V. The Fanning's friction factor f was calculated from the actual head losses obtained from gage readings taken during the tests corrected for the change in elevation, see Fig. 6. The friction factors f were calculated from the equation,

$$H = 2f \frac{L}{D} \frac{V^2}{g}$$

Where: H = head loss in feet of fluid flowing (pulp); L = feet of pipe, D = pipe diameter in feet, V = pulp velocity in feet per second, and g = acceleration due to gravity in feet per second.

The Reynolds numbers are equal to

$$\frac{DVP}{w}$$

Where: D = pipe diameter in feet, V = pulp velocity in feet per second, P = pulp density in pounds per cubic foot, and w = viscosity of water at 70°F in pounds per second-ft ($w = 6.6 \times 10^{-4}$ lb per second-ft). The diameter of the pipe was 2/3 ft, and the length of the pipe was 16,000 ft. All of the calculations were based on the flow from the No. 2

Table V. Observed and Calculated Data From Test Operation of Hydraulic Transportation System for Tennessee Brown Phosphates

	Pulp Data					No. 1 Pump Press.			Head at Akin					
Period	Flow Rate, Gpm	Solids Content, Wt, Pct	Sp Gr[a]	Solids Rate, Tph	Pulp Rate, Tph	Inlet (Gage), Psi	Disch. (Gage), Psi	Devel. Head, Psi	Disch. Press. No. 2 Pump, Psi	Equiv. Ft Pulp	Total Head, Ft of Pulp	Pulp Velocity, Fps	Head Loss for Pulp, ΔHp, Ft/100 Ft	Fanning Friction Factor,[b] f
1	1344	12.7	1.092	47	368	4	103	99	148	316	420	8.6	2.62	0.0038
2	1372	16.3	1.120	63	384	4	106	102	172	369	476	8.8	2.98	0.0041
3	1421	11.1	1.080	42	384	4	103	99	142	304	411	9.1	2.57	0.0033
4	1383	14.0	1.102	53	382	4	126	122	148	310	417	8.8	2.60	0.0036
5	1423	13.3	1.096	52	390	4	108	104	152	321	428	9.1	2.68	0.0035
6	1357	16.8	1.125	64	382	4	112	108	167	344	451	8.6	2.82	0.0041
7	1317	11.9	1.084	42	356	4	105	101	139	296	403	8.4	2.52	0.0038
8	1286	10.7	1.075	37	346	4			109	234	341	8.2	2.13	0.0034
9	1344	16.6	1.123	62	377	4	102	98	164	337	444	8.6	2.77	0.0040
10	1322	17.2	1.128	64	372	4	127	123	161	330	437	8.4	2.73	0.0042
11	1481	17.4	1.129	73	418	4	128	124	181	371	478	9.4	2.99	0.0036
12	1359	14.4	1.105	54	376	4	124	120	162	339	446	8.7	2.79	0.0040
13	1447	15.8	1.116	67	424	4	123	119	181	375	482	9.1	3.01	0.0039
14	1282	17.3	1.128	62	361	4	120	116	191	392	499	8.2	3.12	0.0050
15	1388	14.9	1.109	57	385	4	117	113	189	395	502	8.8	3.14	0.0043
16	1342	0[d]	1.000	0					20[e]	46	150	8.6	1.41	0.0021
17	1460	0[d]	1.000	0					54[e]	125	229	9.3	2.16	0.0027

Table V. (continued)

Reynolds Number $\frac{DVP}{w} \times 10^{-3}$	No. 1 Pump		No. 2 Pump		Total Energy Input		Pumping Efficiency, Pct	Head Loss for Water, Ft/100 Ft, Hw	$\frac{Hp}{Hw}$[c]	Particle Size Distribution, Wt Pct of Solids			
	Oper. Time, Hr	Energy Input, Hp-Hr	Oper. Time, Hr	Energy Input, Hp-Hr	Hp-Hr Ton Solids	Kw-Hr Ton Solids				+6 Mesh	−6 Mesh +35 Mesh	−35 Mesh +200 Mesh	−200 Mesh
594	8.00	1672	4.30	885	5.5	4.1	45	1.96	1.34	5.1	6.8	57.6	30.5
622	8.00	1672	7.92	751	4.8	3.6	48	2.03	1.47	5.1	6.8	57.6	30.5
620	7.37	1720	4.49	349	6.2	4.6	46	2.17	1.18	3.3	10.8	54.0	31.9
612	8.00	1632	3.22	269	4.5	3.4	50	2.06	1.26	3.5	8.6	48.8	39.1
628	8.00	1592	4.32	350	4.7	3.5	52	2.18	1.23	4.9	12.9	50.8	31.4
611	8.00	1592	5.17	418	3.9	2.9	53	1.99	1.42	4.9	12.9	50.8	31.4
575	8.00	1672	4.77	387	6.1	4.6	41	1.89	1.33	9.2	9.2	48.4	33.2
556	0	0	8.00	1353	4.6	3.4	48	1.80	1.18	7.4	13.6	54.9	24.1
610	8.00	1672	4.40	478	4.3	3.2	48	1.96	1.41	8.5	12.0	54.6	24.9
598	8.00	1672	5.62	457	4.2	3.1	47	1.90	1.44	8.5	12.0	54.6	24.9
670	8.00	1672	7.25	646	4.0	3.0	54	2.34	1.28	4.3	12.6	57.2	25.9
606	8.00	1632	4.80	479	4.9	3.7	49	2.00	1.40	8.0	7.7	60.6	23.7
640	8.00	1672	7.79	816	4.6	3.4	52	2.24	1.34	10.2	10.2	52.0	72.4
582	8.00	1632	8.00	794	4.5	3.4	47	1.79	1.74	7.4	13.6	54.9	24.1
615	8.00	1632	7.01	781	5.3	4.0	51	2.08	1.51	8.0	7.7	60.6	23.7
541													
585													

[a] Based on true density of solids of 2.85.
[b] Calculated using Williams and Hazen formula with C = 168.
[c] Ratio of head loss with pulp to calculate head loss with water.
[d] Testing with water only.
[e] Data taken from No. 3 pump to Godwin.

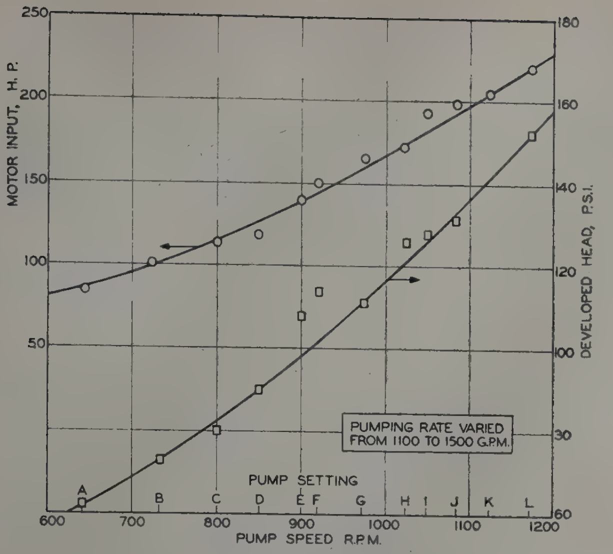

Fig. 7—Characteristic curves for No. 2 concentrate pump.

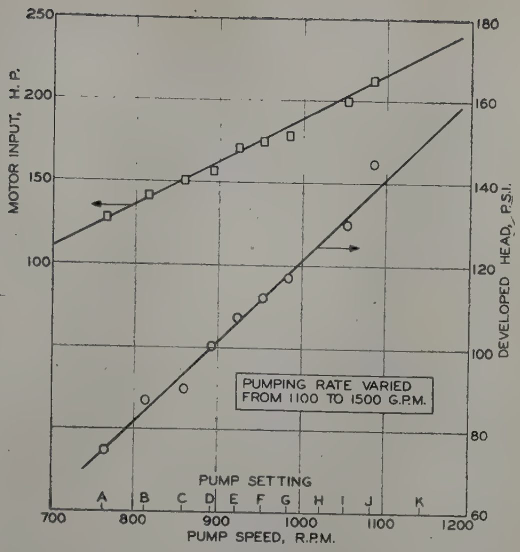

Fig. 8—Characteristic curves for No. 3 concentrate pump.

pump discharge to the pipeline discharge at Godwin. It may be seen in Fig. 10 that the friction factors obtained for conditions while pumping water were only slightly lower than those for the pulp normally handled in this system. Additional data are given in Fig. 10 to show the relation between the Reynolds number and the Fanning friction factor for water, as presented by other investigators.[3] It may be seen that most of the test data agree closely with the published data presented for steel pipe. The variations in the factors calculated from test data were attributed to variations in the concentration and particle size distribution of the solids in the pulp. Since pulps should show higher friction factors than water, it is presumed that the concentrate line was smoother, as a result of the polishing action of the solids, than the clean steel pipe used in the investigation reported by Caldwell and Babbitt. Calculation of the smoothness factor in the Hazen-Williams formula showed that when pumping water the factor C was equal to approximately 168. This value is considerably higher than the value of 140 reported as a normal smoothness factor for smooth steel pipe.[7]

Using a smoothness factor of 168, the head loss was calculated for conditions in which only water was pumped; the same flow rates were used as those observed during each of the test conditions in which concentrate pulp was pumped. This head loss for water at each rate, and its ratio to the corresponding head loss for pulp, $\frac{\Delta Hp}{\Delta Hw} = Y$, is shown in Table V. The ratios are also plotted in Fig. 11 with a curve representing data obtained in the experimental work with the 2 and 4-in. diam pipeline. Variations due to changes in velocity within the range studied and the particle size distribution of the solids are not correlated in this presentation, and these variations account for the scattering of the datum points. For example, the wide difference in the ratios shown for pulp containing solids within the range of 17.2 to 17.4 pct is attributed to the variation in velocity during three periods (periods Nos. 11, 10, and 14) which had velocities of 9.4, 8.4, and 8.2 and ratios of $\frac{\Delta Hp}{\Delta Hw}$ of 1.28, 1.44, and 1.74, respectively.

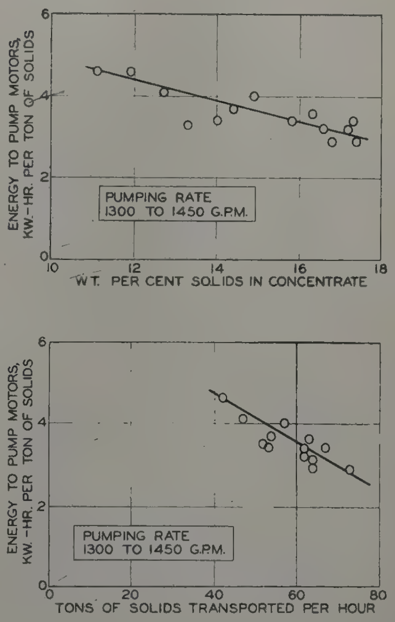

Fig. 9—Energy consumed in pumping phosphate concentrate from Akin to Godwin.

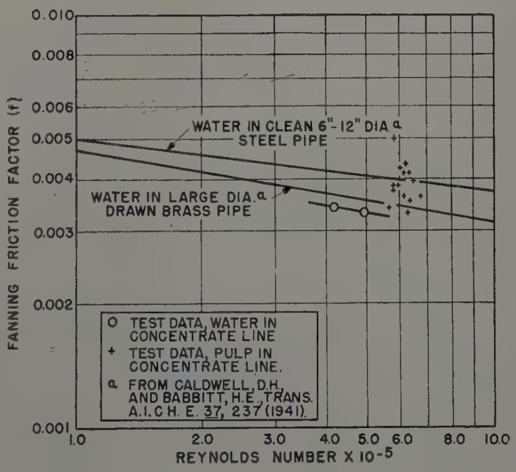

Fig. 10—Fanning friction factors vs. Reynolds numbers for concentrate pipeline.

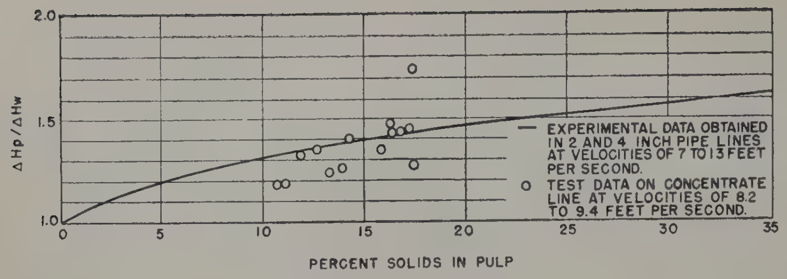

Fig. 11—Effect of solids content of pulps on ratio of head loss in pipelines when pumping pulp to head loss when pumping water.

The experience of the Tennessee Valley Authority with the hydraulic transportation of phosphatic concentrates has demonstrated the feasibility of using this method to transport phosphates under the conditions existing in its phosphate beneficiation plant. Transportation costs have compared favorably with the costs of more conventional methods, and operation of the system is not limited by factors, such as bad weather and poor roads, which characteristically interfere with other methods, such as trucking. Although this system for hydraulic transportation lacks some of the flexibility of other transportation methods in that its operation must be integrated with the concentrating and classifying operations, this has not been a disadvantage in the TVA operations. In other words, the pipeline is not operated unless the processing units at Akin and Godwin are operated, and similarly, the processing units cannot be operated unless the pipeline is operable. This, of course, prevents the accumulation and storage of surplus material at points beyond the washer to provide for emergency operation of subsequent units, a disadvantage not encountered with other methods of transportation. Thus, it is apparent that with any hydraulic transportation system, the process steps immediately preceding and following the pipeline are important factors in its design.

Operating data on the TVA pipeline show that it is not normally operated at its maximum practical capacity. Although the solids content of the pulp is usually in the range of 12 to 17 pct, concentrations of 20 to 25 pct may be handled readily. Reaching the higher concentration in the TVA system while keeping the flow rate in the pipeline above the critical velocity would entail operating the related process steps at higher rates; this has not been considered expedient. Of course, a pipeline of smaller diameter, and consequently lower cost, could be used satisfactorily with pulp solids concentrations in the upper range. However, since a pulp containing 12 to 17 pct solids also contains about the required amount of water for the operation of the classifying equipment at Godwin, and since the problem of obtaining an adequate water supply is greater at Godwin than at Akin, it has been found desirable to pump the necessary water for proper operation of the classifiers from Akin along with the phosphate concentrate.

After replacing the original wood-stave piping with abrasion-resistant steel pipe, maintenance of the pipeline became a minor problem. Since wear of the pipe walls is greatest on the bottom of the pipe, the sections of pipe are turned periodically to equalize the wear on all sides. This results in maximum life from the pipe and reduces replacements to a minimum. Turning of the pipeline is a regular maintenance job and is carried out, a few sections at a time, on a prearranged schedule coordinated with scheduled shutdowns of other parts of the plant. Wear has also been noted to be greater at curves or bends, as might be expected. When leaks occur in the pipe, they are repaired in the field by means of clamps which encircle the pipe, holding a rubber gasket over the leak. Wear on the pump housings is not serious but replacement of pump impellers is a regular maintenance item. Wear and replacement of the pump bearings is also a significant factor. The frequency of replacement depends upon the adequacy of the seal-water supply and upon keeping the seal-water pressure above the internal pump pressure to prevent passage of sand into the bearings. Although this was a major source of difficulty in early operations because of an inadequate seal-water supply, improvement of the seal-water supply system to correct this deficiency has greatly alleviated the bearing problem.

In normal operation of the pipeline, two pump operators are required, and the nominal pumping rate is 40 to 50 dry tons of concentrate per hr. During 1949 and 1950, when pumping concentrate was at the rate of about 350,000 dry tons annually, the cost of operating the hydraulic transportation system was about $0.24 per dry ton of material handled. Approximately 50 pct of the cost was for direct labor, 8 pct was for power, 34 pct was for maintenance, and 8 pct was for depreciation. This amounts to about $0.08 per dry ton mile for transporting the approximately 3-mile distance between the Akin and Godwin plants. However, in comparing this cost with costs for other methods of transportation, it should be kept in mind that the TVA system eliminates certain handling operations that would exist at both locations if other methods of transportation were used. Thus, it is only fair to credit the above transportation cost with the savings involved in the elimination of these handling costs.

References

[1] W. B. Stephenson: Practical Aspects of Pumping Sands, Slurries, and Slimes. *Trans.* AIME (1946) **169**, p. 665; MINING TECHNOLOGY (May 1946), TP 2013.

[2] R. H. Wilhelm, D. M. Wroughton, and W. L. Loeffel: Flow of Suspensions Through Pipes. *Industrial and Engineering Chemistry* (1939) **31**, p. 622.

[3] D. H. Caldwell and H. E. Babbitt: The Flow of Muds, Sludges, and Suspensions in Circular Pipe. *Trans.* Amer. Inst. Chem. (1941) **37**, p. 237.

[4] M. P. O'Brien and R. G. Folsom: The Transportation of Sand in Pipelines. University of California Publications in Engineering (1937) **3**, No. 7.

[5] G. W. Howard: Transportation of Sand and Gravel in a Four-Inch Pipe. *Proc.* Am. Soc. Chem. Engrs. (1938) **64**, p. 1377.

[6] Fred R. Brown, Joseph E. Montgomery, Elliott J. Dent, and David L. Neuman: Transportation of Sand and Gravel in a Four-Inch Pipe. Discussion. *Proc.* Am. Soc. Chem. Engrs. (1938) **64**, p. 2080.

[7] G. V. Shaw and A. W. Loomis: *Cameron Hydraulic Data.*

Contact Angles and Surface Coverage

by W. Philippoff, S. R. B. Cooke, and Donald E. Cadwell

THE importance of contact angles in flotation has long been recognized, but little has been done to get quantitative relationships between the surface coverage of the mineral by the reagent, the length of the hydrocarbon chain, and the contact angle. It is well known that for a complete monolayer on the surface of a mineral the contact angle θ is determined only by the reagent[1] and principally by the chain length of the hydrocarbon radical. Although for flotation the monolayer usually is regarded as being complete, early experiments of Wark and Cox[2] showed that at very small concentrations of potassium ethyl xanthate the contact angle on galena changed in a continuous way from 0° to the equilibrium value of 60°. Further, Gaudin and Vincent[3] showed a similar continuity using heptylic acid and sphalerite. This shows that with probably incomplete monolayers, θ varies with the degree of surface coverage. At the time these experiments were made it was impossible to measure the actual amount of surface coverage, especially since the decrease of the collector concentration in the liquor could be influenced by chemical side reactions. Through the use of the radioactive tracer method for the measurement of the amount of collector adsorbed on the surface of the mineral, Gaudin and Bloecher[4] were able to determine accurately the actual surface coverage of dodecylamine acetate on quartz, but they did not measure any contact angles. It is believed that the relationship between the surface coverage and the contact angle is extremely important in flotation, especially as Gaudin and Bloecher showed that a 95 pct recovery is possible with a coverage of only 5 pct.

Theoretical Considerations

The work of adhesion W is the energy bound (in ergs per sq cm) when an interface is formed. It is determined by the difference of the free surface energies (surface tensions) of the respective phases γ_1 and γ_2 before contact and the interfacial free surface energy γ_{12} after contact. The definition of the contact angle permits the elimination of the unknown surface energy of the solid and hence the calculation[5] of W from the surface tension of the liquid γ and the contact angle θ:

$$W = \gamma\,(1 + \cos\theta) \qquad [1]$$

Consider a surface consisting of two components, identified as 2 and 3, 1 being the liquid. The amount of 2 in the composite surface is x, where $0 < x < 1$. The respective contact angles with 1 and air are θ_2 and θ_3. The total work of adhesion of such a surface is the sum of the values of the components multiplied by their respective areas. A formal relation can be written:

$$W_m = x \cdot W_2 + (1 - x) \cdot W_3 \qquad [2]$$

in which W_m is the work of adhesion of the composite surface. Eq 1 can be introduced into W_2 and W_3, but in the case of W_m some discussion is needed. If the two components are segregated, each component forming an integral part of the composite surface there is *no* physical meaning for a contact angle θ_m calculated from W_m by using eq 1. If, on the other hand, the area of each *patch* of the components is small in comparison with, say, the diameter of the bubble used in measuring, it could be expected that θ_m would have a physical significance, because of the action of the surface tension of the liquid-gas interface tending to smooth out sharp corners. How small these patches would have to be is difficult to predict, but by using composite surfaces with microscopically

---

W. PHILIPPOFF, formerly Research Associate, Mines Experiment Station and School of Mines and Metallurgy, University of Minnesota, Minneapolis is now with the Franklin Institute, Philadelphia. **S. R. B. COOKE**, Member AIME, is Professor of Metallurgy and Mineral Dressing, School of Mines and Metallurgy, University of Minnesota, and **D. E. CADWELL**, formerly Research Assistant, Mines Experiment Station, School of Mines and Metallurgy, University of Minnesota, is with Consolidated Mining and Smelting Co., Kimberley, B. C.

Discussion on this paper, TP 3266B, may be sent to AIME before April 1, 1952. Manuscript, Feb. 20, 1951. Revision August 14, 1951. New York Meeting, February 1952.

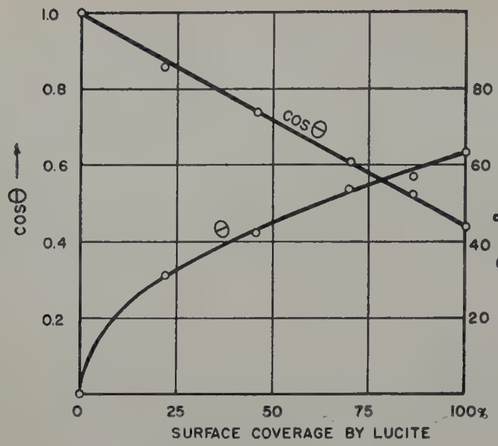

Fig. 1—Results of experiments on the composite surfaces of glass and lucite. Each value on the curve is a mean of five measurements at different places on the composite surface.

measurable patches a direct experimental approach is feasible.

Using this restriction, eq 1 can be introduced into eq 2 and, after rearrangement, gives:

$$\cos\theta_3 - \cos\theta_m = x\,(\cos\theta_3 - \cos\theta_2) \qquad [3]$$

For the practically important case of a hydrophobic film of material 2, having a contact angle θ_2 at 100 pct coverage and a hydrophilic substrate 3, for which $\cos\theta_3 = +1$, the very general eq 3 can be simplified as follows:

$$1 - \cos\theta_m = x\,(1 - \cos\theta_2) \qquad [4]$$

The meaning of this equation is that if $\cos\theta_m$ is plotted against x, the graph is a straight line descending, with increasing values of x, from 1 at $x = 0$, the limit being $\cos\theta_2$ at 100 pct coverage.

It is now possible to visualize what happens to the hydrophilic surface when the equilibrium concentration of the collector is increased gradually. At first it is natural that only very few collector molecules are adsorbed. This is equivalent to a gaseous film at the interface in which the molecules are independent of each other, and the gas law $p \cdot v = RT$ is valid. In the case of surface films: (surface pressure in dynes per cm) × (area per molecule in sq A) $= kT \cong 400$ at room temperature. All the evidence as summarized by Adam[6] indicates that even with the longest hydrocarbon chains used (22 carbon atoms in the chain) the molecules lie flat on the surface of water.

The complete monolayer is considered to be formed by molecules standing up, their cross-section independent of the chain length being 20.5 sq A. Logically, it might be expected that there would be a transition between the gaseous and the closely packed film, in which the originally horizontal molecules assume a perpendicular position.

On the basis of eq 4 it is possible to calculate the conditions to be expected if a hydrophilic surface is covered with hydrocarbon molecules, the cross-sectional area of each molecule being F_m. A value of from 104° to 109° for the contact angle of paraffin (θ_2) can be assumed. The amount of collector necessary to form a complete monolayer is given by the following calculation:[4]

The area of 1 molecule is F_m sq A

The area of 1 mol is $F_m \cdot N$, where N is the Avogadro constant

The area of 1 g of collector is $F_m \cdot N/M$, where M is the molecular weight of the collector

The area of 1 g of mineral is S, the specific surface, here in sq A per g

Then for complete coverage:

Grams of collector/grams of mineral $= S \cdot M/N \cdot F_m$

The surface coverage is given by the ratio of the amount actually adsorbed to the calculated value for the complete monolayer: this means that eq 4 can be written as:

$$1 - \cos\theta_m = N \cdot F_m/S \cdot M\,(1 - \cos\theta_2) \cdot \frac{\text{grams of collector}}{\text{grams of mineral}} \qquad [5]$$

Using the values of Gaudin and Bloecher, eq 5 can be evaluated. $F_m = 23.4$ sq A, the area of an active site of quartz, as calculated by Gaudin; $M = 245$, the molecular weight of the dodecylamine acetate; $S = 2340 \times 10^{16}$ sq A per g, the specific surface of the quartz powder; $\theta_2 = 106°$, the contact angle of paraffin. This gives in convenient units:

$$1 - \cos\theta_m = 1.28 \cdot \frac{\text{micrograms of amine/gram quartz}}{401}$$

$$1 - \cos\theta_m = 0.00319 \text{ (micrograms of amine/gram quartz)} \qquad [6]$$

$$1 - \cos\theta_m = 1.28 \cdot x \qquad [7]$$

Eq 6 would mean that a contact angle less than that of paraffin is determined only by the percent coverage of the surface by hydrocarbon (paraffin). As an example, an angle of 20° as calculated by the present authors, from measurements of Coghill and Anderson[7] on a highly cleaned and dried polished glass specimen, is determined by a coverage of only 5 pct. If the contamination were paraffin, this means that only 5 pct of the surface would be covered. This infinitesimal amount of matter, of the magnitude of 10^{-9} g per sq cm, would make the known sensitivity of dry hydrophilic surfaces to impurities easily understood. On the other hand, the contact angle on built-up layers of Ba-stearate, as investigated by Bikerman,[8] was 90°, corresponding to about 78 pct coverage by paraffin. For crystals of long-chain acids and alcohols, θ is 100°,[9] corresponding to a coverage of 92 pct by paraffin. These results mean that a complete monolayer of a collector on a hydrophilic surface does not ensure a hydrophobicity in the sense of a paraffin coating.

A distinction between paraffin coverage and collector coverage must therefore be made. It is known that θ depends, even at very high collector concentrations, on the length of the hydrocarbon part of the collector molecule.[1] For instance a monolayer of potassium ethyl xanthate gives an angle $\theta_2 = 60°$. corresponding to $x = 39$ pct, meaning that this layer is only as active as a coverage by paraffin of that magnitude should be. In this case the polar part of the collector molecule causes the monolayer to behave as if 61 pct of the surface were hydrophilic. The longer the hydrocarbon chain, the more nearly the value for a paraffin coverage is attained. Short chain collectors apparently cannot inhibit completely the attraction of the water molecules to the mineral surface.

Using an appropriate experimental value for θ_2 (for complete coverage) the relative coverage x and θ_m can each be calculated, knowing the other one, by using eq 4.

It has often been stated that the absorbed layer on a hydrophilic surface is in equilibrium with the collector in solution. The partition coefficient between the surface and the solution seems to depend on the pH. Kellogg and Vasquez-Rosas[10] have shown that at a constant collector concentration the contact angle of dodecylamine chloride on quartz can range from nearly 0° to about 80°. At pH 6.5 their value was 10°, corresponding to a coverage by paraffin of 1.3 pct; at a pH of 10, θ was 80°, or $x = 64$ pct. This change of the quantity of *adsorbed* collector at a constant collector concentration at different pH values, which follows from the theory evolved here to explain the change in θ at different pH, has not yet been investigated experimentally.

The adsorption of an amount of collector equivalent to a complete monolayer does not necessarily mean that a uniform coating is present, for it is equally possible that a patchy polymolecular adsorption occurs. The measurements of θ permit the calculation of the equivalent actual coverage by paraffin, independent of whether the adsorbed layer is mono or polymolecular, complete or incomplete.

Experimental Approach

To check eq 4, some experiments were made on composite surfaces of glass and lucite. Fine glass fibers were packed, similarly to the bristles of a paint brush, in a hole drilled in a piece of brass, then mounted in lucite by polymerizing the monomer around the fibers. Sections of different surface coverages x, determined by the ratio of the lucite to the total surface were made by cutting across the fibers at different distances from the brass. These sections were moulded in lucite in a press and polished on a lead lap with alumina on a Graton-Vanderwilt machine. After cleaning with carbon tetrachloride, then lightly buffing on a cloth lap with —3 micron quartz in distilled water, they were tested with an air bubble in the same bubble machine used for the quartz specimens.

The only case where the amount of coverage probably is known exactly is that of quartz and dodecylamine acetate, investigated by Gaudin and Bloecher. The writers relied on their determinations of the amounts of collector adsorbed and measured θ for different collector concentrations. A bubble machine was used, the contact angles being measured by means of a position-angle ocular. The precision of each experiment is estimated at ±0.5°. Samples of crystalline quartz, mounted in lucite, were polished on a cloth lap with distilled water and fine quartz to eliminate any possibility of contamination, and were tested under water for absence of a contact angle. They were conditioned for periods of some hours in about 200 cc of the amine solution, making sure that equilibrium of the contact angle was obtained. To attain this, tapping the holder and long observation times, sometimes more than 24 hr, were needed, thus making the investigation time consuming. The change in collector concentration due to adsorption on the approximately 1 sq cm of quartz surface was disregarded. For the range of amine acetate concentrations used in the present paper, 1 to 300 mg per liter, Gaudin and Bloecher's work covered the pH range of 5.83 to 6.33. In the present investigation the pH was maintained at 6.5 ± 0.2.

The following procedure was used to obtain the surface coverages x from the measurements of Gaudin and Bloecher. In the range through which their square root relationship is valid, up to 200 mg per liter, the proportionality constant between the square root of the concentration in mg per liter and the quantity of amine adsorbed in micrograms per gram of quartz (having a specific surface $S = 2340$ cm^2 per g) was calculated for each of their experimental points. The mean of these constants, 6.95, was used to calculate the adsorbed quantities at the concentrations taken for the contact angle measurements. The surface coverage x is the ratio of the calculated adsorbed quantity and 401 mg per g, the value for the complete monolayer, as given by eq 7.

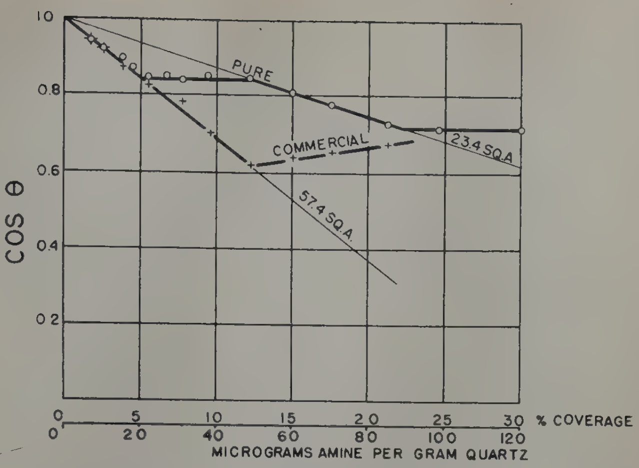

Fig. 2—Results on the quartz specimens. The curves for both the pure and commercial sample are given.

Results

The results of the experiments on the composite surfaces of glass and lucite are shown in Fig. 1. The angle θ_2 for lucite of that polish was determined experimentally as 63½°. Each value on the curve is a mean of five measurements at different places on the composite surface. No time dependence was noticeable.

The results on the quartz specimens are summarized in Fig. 2, the curves for both the pure and the commercial sample being given. In the range up to 5 pct coverage, calculated on the assumption that the molecules are perpendicular to the surface, both curves practically coincide. In the range from 5 to 12 pct coverage, corresponding, to an equilibrium concentration of from 8.3 to 50 mg/liter for the pure amine, θ remains constant at 32° within ±1°. Then θ increases (cos θ decreases) to about 22 pct coverage (150 mg/liter), to remain apparently constant with an angle of 44° to 45°. The commercial sample apparently shows the first transition beginning at 50 mg/liter. Its curve then merges with the curve for the pure sample, θ decreasing with increasing concentration. This has yet to be confirmed exactly. Experimental difficulties in more concentrated solutions arose from the lack of enough pure material and from the crystallization at concentrations above 200 mg/liter of some impurity in the solutions of the commercial sample. In any case the range of concentrations occurring in practice was fully covered.

Discussion

The experiments on the composite surfaces, where there is no doubt regarding the degree of surface coverage, have confirmed eq 4. Equally the linear relation between cos θ and the calculated surface

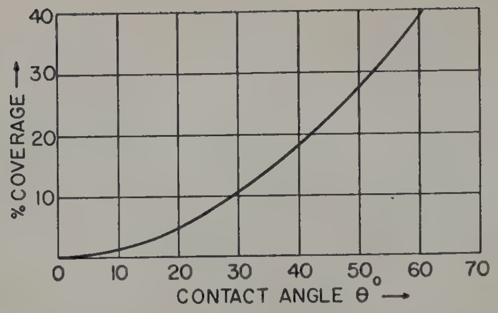

Fig. 3—Equation 6 used to compute surface coverages by paraffin from measured contact angles.

coverage x for the quartz experiments is valid through a large range, especially for the solutions of the commercial amine. In the case of quartz however, the angle for complete coverage by paraffin, 106°, was not attained.

These results form a basis to discuss contact angle phenomena using eq 7, connecting the surface coverage by paraffin to the contact angle of the composite surface.

The experimental slope of the graph between 50 and 150 mg/liter of the pure amine checks exactly with that calculated from eq 7. This means that in this region the molecules conform to the concept of being perpendicular to the surface. By evaluating F_m from the initial slope, 57.4 sq A is obtained instead of 23.4, the area of the active site. As the molecules lie flat in the gaseous film, the ratio of $57.4/20.5 = 2.80$ represents the relation between the cross-sectional area and the axial section, 20.5 sq A, of the amine molecule. Taking an estimated breadth of the hydrocarbon chain of 4.4 A, a chain length of 13A is obtained. Eleven C-C bonds would give 14A, so that the value of 13A seems very probable. This check would seem to prove that this gaseous film, which is 2.45 $(= 57.4/23.4)$ times as active on the surface as the layer of perpendicular molecules, is the one actually used in flotation with good results. Gaudin's recovery of 95 pct corresponds to the end of the gaseous film region.

The area where a constant θ is reached corresponds to 5 pct coverage, giving 472 sq A per molecule, equivalent to a surface pressure of only 0.85 dynes per cm, assuming the gas laws to be valid. It should be noted that Harkins et al[11] found such first order transitions in investigating the adsorption of heptane on iron oxide, silver, and graphite from the gaseous phase. The beginning of these transitions occurred at 400 to 600 sq A per molecule, comparable to our value of 472.

This check, together with the general discussion previously made, indicates that the molecules are adsorbed lying in the surface up to about 470 sq A per molecule, then begin to stand up perpendicularly to the surface. The surface coverage with hydrocarbon chains remains approximately constant until an area of $472/2.45$ sq A $= 193$ per molecule is reached. The amount of adsorbed collector increases in this region, but the coverage by paraffin chains remains essentially constant. The behavior of the layer then follows closely the theory of molecules perpendicular to the surface to a point of saturation beyond which the coverage, according to this theory does not increase any more. In fact, only about 22 pct of all possible sites then are occupied by the dodecylamine molecules.

The accordance permits the assumption that eq 6, which gives a quantitative relationship between any contact angle and the surface coverage x by paraffin, has a physical meaning and can be used to compute surface coverages by paraffin from measured contact angles, as shown in Fig. 3. This also permits the possibility of evaluating the efficiency of collectors when the total amount added and the amount active on the surface from the measurements of θ are known.

There are further aspects of the activity of compounds of different chain lengths. In the range of the validity of the theory for the perpendicular molecules, at concentrations of 50 to 150 mg/liter, the curve is probably independent of the chain length. The curve or its continuation should form a limit at some as yet unknown concentrations for amines of different chain lengths. Longer chain amines, such as hexadecylamine, have a greater ratio of length to width than dodecylamine. For the same surface coverage, as calculated on the assumption of perpendicular molecules, the values of θ should be greater than those for the dodecylamine at low concentrations of the collector. Logically, the shorter amines (octyl and decyl) should not show as much of a difference between the slopes of the two lines as the dodecylamine. This is easily tested experimentally.

Practically, this investigation has proved that *any* contact angle between 0° and 45° can be realized in a predetermined way for the system dodecylamine acetate-quartz. This opens the way for the experimental determination of θ necessary for the flotation of certain particle sizes.

From the results of Gaudin and Bloecher, it is calculated that a recovery of 95 pct for their particular size corresponding to $S = 4340$ sq cm per g, was obtained at an actual surface coverage by paraffin of 12 pct and an angle of 32°. A recovery of 10 pct was achieved at 1.3 pct coverage with an angle of 10°. This gives an approximate range of the contact angles necessary to float quartz of that fineness.

References

[1] E. E. Wark and I. W. Wark: *Journal Physical Chemistry* (1933) **37**, p. 805.

[2] I. W. Wark and A. B. Cox: *Trans.* AIME (1934) **112**, p. 189.

[3] A. M. Gaudin and K. C. Vincent: MINING TECHNOLOGY (November 1942) TP 1242.

[4] A. M. Gaudin and F. W. Bloecher: *Trans.* AIME (1950) **187**, p. 499; MINING ENGINEERING (February 1950) TP 2813.

[5] N. K. Adams: *The Physics and Chemistry of Surfaces.* Third Ed., p. 179 (1941) London.

[6] N. K. Adam: ibid. pp. 40 and 56; N. K. Adam: *Proc.* Royal Society London (1930) **126A**, p. 533.

[7] N. K. Adam: ibid. p. 186.

[8] J. J. Bikerman: *Trans.* Faraday Society (1940) **36**, p. 412.

[9] N. K. Adam and C. Jessop: *Journal* Chemical Society (1925) **127**, p. 1863.

[10] H. H. Kellogg and H. Vasquez-Rosas: *Trans.* AIME (1945) **169**, p. 476.

[11] G. Jura, E. H. Loeser, P. R. Basford and W. D. Harkins: *Journal Chemical Physics* (1945) **13**, p. 535, and (1946) **14**, p. 117; G. Jura, W. D. Harkins, and E. H. Loeser: *Journal Chemical Physics* (1946) **14**, p. 344.

Development of The Disco Process Of Low Temperature Carbonization

by C. E. Lesher

THE Disco* process for the production of low temperature coke and its immediate predecessor, the Wisner or Carbocite process have been described in the voluminous literature of low temperature carbonization.[1-4]

This paper will describe the development of the process from the first attempt at commercial operation by the American Gas and Electric Co. at Philo, Ohio,[5] in the 1920's to the successful operation in 1949 by the Disco Co., a division of the Pittsburgh Consolidation Coal Co., of the 1000-ton per day Disco plant near Pittsburgh, see Figs. 1-2.

In the 1924 coal industry depression following the hectic post World War I expansion, the northern Appalachian, unionized bituminous coal fields were affected first and foremost, and Western Pennsylvania as hard as any. Competitive market pressure was heaviest on the lower grades of steam coals, notably those from the Panhandle district where ash and sulphur are inherently higher than in the same Pittsburgh coal bed to the east along the rivers. The firm structure of Panhandle coal while favoring the prepared sizes, depressed the usefulness and value of the finer sizes. Panhandle slack and nut slack were marketed with difficulty at consistent, and at times considerable, loss.

Many solutions were suggested, and the Pittsburgh Coal Co. investigated all. Lower delivered prices through lower mine costs and more advantageous freight rates were obvious goals, but equally obvious were the difficulties of self attainment of either in any substantial measure. Selling Btu's in pipes was abandoned as an idea after a thorough study of the economics of distribution of what was then, and is even now, the only developed continuous process of complete gasification of bituminous coal-producer gas.

Although the coal company purchased huge blocks of electric power, it sold not a car of coal to the central power stations. Public utilities controlled the markets for electric current, and it was found that no matter at how low a cost current might be put on the bus bars by the coal company, distribution to its widely scattered coal mines made such an enterprise practically impossible.

Consolidation of underground operations and a huge modernization program of mining operations in the 1920's were but preparation for the introduction of mechanical cleaning of the coal for market, particularly the smaller sizes of steam, gas, and by-

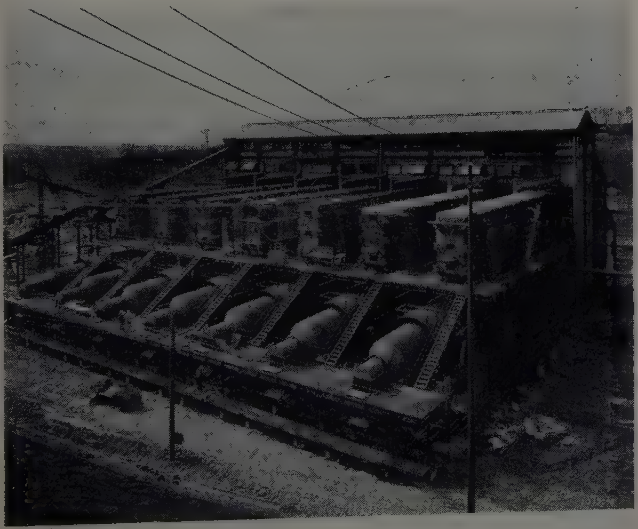

Fig. 1 (top)—Plus 2-in. Disco from the new plant, with the largest pieces about 8 in. This view was taken at the base of a 10,000-ton stockpile.

Fig. 2 (bottom)—The 1200-ton per day Disco plant under construction. The rectangular structures above each retort are roaster-storage units in which the coal and recycle is preheated before charging into the carbonizers.

---

* Disco is the registered trade name of a solid fuel made by the Disco process of low temperature carbonization of coal.

C. E. LESHER, Member AIME, is a Consulting Metallurgical Engineer, Pittsburgh.

Discussion on this paper, TP 3264F, may be sent to AIME before April 1, 1952. Manuscript, Sept. 24, 1951. New York Meeting, February 1952.

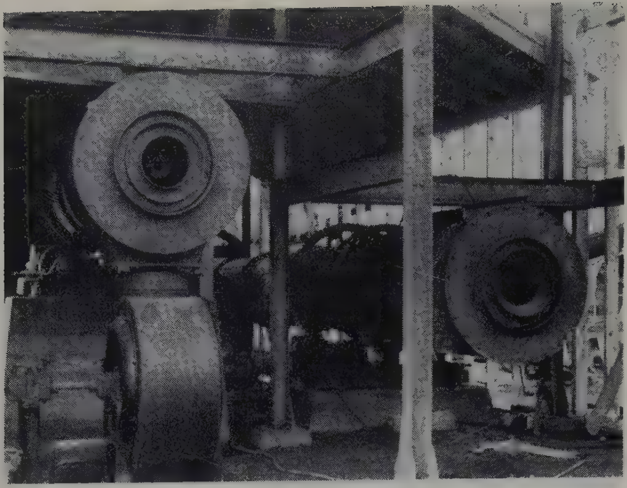

Fig. 3—Thermodizer, at left, and carbonizer, each 3 ft diam by 50 ft long, in the Wisner pilot plant under construction in 1932.

product coals. Mechanical cleaning was a necessary step in anticipation of mechanical loading at the face. Upgraded Panhandle slack, however, continued to be a difficult product to sell. In the meantime mechanical stokers, large and small, were coming to the fore and by splitting the 1¼ in. slack at about ⅜ in., a double screened stoker size was made available on a large scale and at substantially better market realization than for slack. But this left the — ⅜ in. size to compete with more easily grindable coals with lower ash and sulphur from other fields. The problem was narrowed down to the economic disposal of this fine Panhandle slack. If the — ⅜ in. coal could be sold in some form and return no more than total, overall cost of mining and cleaning, the cleaned, carefully screened, and prepared larger size of this firm structure coal would carry the load and there would be an overall profit for the enterprise. This was, and still is, the economic incentive for processing this coal.

Low Temperature Carbonization

The Pittsburgh Coal Co. produced and sold solid fuel. Carbonization was the obvious route to explore for converting this fine coal to larger sizes suitable for hand firing. Full oven tests of several sizes of steam slack were made in Koppers ovens at Chicago and at Philadelphia. The coke was fingery and small sized. Yields were not encouraging; the initial investment was high; and selling the surplus gas and other byproducts was alien to the coal company. Furthermore, high temperature coke, although an accepted smokeless hand-fired domestic fuel in other sections of the country, would, it was believed, meet serious sales resistance in the markets where the coal company sold its lump and preferred sizes of high volatile bituminous coal because of differences in ignition and burning characteristics.

It was not difficult to write the specifications for the desired fuel that was to be made from this smaller size. It must be dense, firm, clean, smokeless, easily ignitable, and able to stand stockpiling. Above all, the cost of making it must be such that it could be sold competitively with other smokeless solid fuels. With compromises here and there along the line, those objectives have been met with Disco.

Low temperature carbonization of coal had just about passed the zenith of public acclaim and common stock financing when in 1928 the Pittsburgh Coal Co. first seriously considered it. There was little to encourage a venture into the field, for the record was a succession of failures. However, there seemed to be a firm foundation for a start, and with the backing of its Board of Directors and support of A. W. Mellon, management of the Pittsburgh Coal Co. authorized a beginning in 1929.

Two early decisions narrowed the field and simplified the economics: no process was to be given serious consideration if it gave a solid product requiring briquetting, and the sole byproduct to be valued would be tar, and that only at its fuel value. Three processes were selected for study: the Plassmann in Germany, the Illingworth in Wales, and the Wisner in the United States. For each there was already a sizable pilot plant in operation and at each, in 1929 and 1930, substantial quantities of coal were processed and the products given consumer trials. Not one of the three pilot plant tests was encouraging, but the Illingworth, a vertical cast-iron retort, made a good coke. Rights for this process were secured, detailed engineering estimates were made for a large installation, and in 1931 a pilot plant with about 3 tons per day capacity was built and operated for nearly a year. Low capacity, high cost and intricate construction finally ruled out this as well as the Plassmann process.

The Wisner *coal ball* process was adopted for development. This paper is concerned primarily with the problems encountered in building the first commercial, low temperature coking plant in this country and so far as known, the only continuous, economic operation anywhere. Starting with a pilot plant in 1933 which grew to a three-unit semicommercial operation in 1936, and in 1940 processed 100,000 tons of highly coking coal, the project then stalled until, under the farsighted and able management of the Pittsburgh Consolidation Coal Co., a full-scale plant was authorized in 1947, see Fig. 2. This plant, costing over 3 million dollars, was in full operation by the end of 1949, and has been since then processing its design quota of over 1000 tons of coking coal a day and to this extent relieving the market of a fine coal product from the Champion Preparation Plant of the coal company and upgrading it to a premium, smokeless household fuel. There has never been a time since the first plant was started that 1000 tons of coal to the Disco plant did not give the mines an extra 4000 tons of operating time.

The Disco plant is a part of an integrated coal company operation covering mining, preparation, and sale of solid fuel. Of the three elements in the economics of this operation, conversion cost alone is the concern of the coke plant management, for the price charged in the books of account for coal and the realization for products are determined by markets and overall company policy. Of conversion cost, that which is direct is controllable from day to day—labor, supplies, power, and maintenance. Property and payroll taxes, insurance, reasonable amortization, and share of top company overhead are more or less fixed. From the receipt of 4 pct moisture coal to the loading of Disco into railroad cars and dehydrated tar into tank trucks, the cost of hourly labor is 1 man-hour for 2.5 tons of coal processed. This includes maintenance labor but not supervision. For 1 ton of coal processed, there is purchased approximately 20 kw-hr of power, a relatively small quantity of water and of natural gas for pilot lights.

Operating and maintenance supply costs are between 5 and 6 pct of plant investment.

Wisner Pilot Plant

A Wisner pilot plant for from 10 to 12 tons of coal per day was built and operated on the same site and simultaneously with the Illingworth, see Fig. 3. C. B. Wisner, inventor and Walter Keenan, chief engineer of Foster Wheeler Corp., who was representing the owners of Wisner's patents at that time, designed the retorts and flowsheet according to Wisner's specifications, which followed the design of the Philo plant. Until his death in November 1932, Mr. Wisner assisted in starting the pilot plant. Two 3x50-ft retorts, each with an annular heating space between inner and outer rotating steel shells, were thermodizer and carbonizer respectively. Heating was indirect through the inner steel shell from hot flue gases traveling in a closed circuit through the annular spaces, circulating fans and gas fired heating furnace. In all essentials this process heating system has been used in subsequent installations.

Feed coal entered the high end of the thermodizer, where it was dried and conditioned for carbonizing by heating in air to 600°F. From the low end of the thermodizer, the coal was carried in a screw conveyor to the high end of the carbonizer, where it was distilled at 800°F and was discharged as coal balls. Tar was collected and stored; gas was wasted. The unit was heated with natural gas. The charge material was — 10 mesh coal, containing oil flotation concentrates from the Champion Preparation Plant of the company.

The experience gained in processing 500 tons of ⅜ x0 coal at Philo, Ohio, in 1929 provided a starting point for the work in the new pilot plant. At Philo there had been short periods during which coal balls were produced, but there were longer periods when the retorts were plugged with masses of coke or the machinery failed. As work progressed at the pilot plant, it became obvious that the trouble was lack of control at every step, but more important, too little was known of what should be controlled.

Certain problems were considered fundamental. Feed coal to the rotating preheater would not flow down the retort according to schedule. It packed and built up in the shell; it did not discharge regularly either as to quantity, temperature, or moisture content. A surge bin for intermediate storage between the thermodizer and carbonizer to equalize the feed to the latter was ineffective because the hot coal ignited, coked, and would not flow or feed.

Once in the carbonizer the preheated and preoxidized coal became unpredictable. At times the coked product was in small balls or just fines, again in masses too great to pass the exit throat of the carbonizer, see Figs. 4 and 5. That is, this pilot plant carbonizing coal in a revolving retort was behaving like all others before it.

In England several attempts had been made to make low temperature coke in revolving kilns and in every case final resort had been to devices in the drums to break up the scale and crust that always formed. None were known to have succeeded. The K.S.G. retorts when brought to this country from Germany by the International Combustion Corp., failed because the plastic coal plugged the retort. The first few months' operation of the Wisner pilot plant at Champion confirmed the experience of others with rotary retorts, but it was found that, as Wisner claimed, the proper, and just the proper, amount of preliminary oxidation would prevent excessive encrustation on the retort walls.

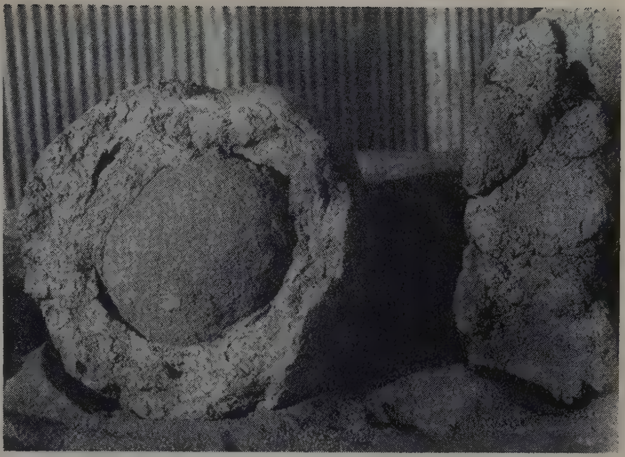

Fig. 4—Strange shaped coke made in the first retort before it was learned how to control the operation.

In fact, it was found that the precision in roasting required to maintain steady carbonizer operation and production was beyond practical limits. Laboratory tests were developed to show and permit control of the amount of oxidation of the coal prior to feeding it to the carbonizer, but it was found that it required 2 hr in the laboratory for a determination that the carbonizer itself would give in 50 pct that time. It was apparent that some immediate and effective control of the feed to the carbonizer was essential if there was to be smooth operation and a product of good quality, and that preoxidation alone was not a dependable way to accomplish that end.

It will be recalled that Wisner had placed reliance on preoxidation and declared[6] that "coal blending is not a satisfactory answer" to the "rolling up of softened coal into balls too big to get out of the gastight container"—the rotary retort. On the contrary, Roberts,[7] Wheeler, and others advocated blending of noncoking coal, anthracite, and coke fines with coking coal to control the plastic property of the mixture in rotary retorts. Reduction to practice of the theory of blending however, appears to have been confined to the Davidson retort in Great Britain, where, according to Roberts, by proper temperature

Fig. 5—Another sample of large irregular masses made in the first retort.

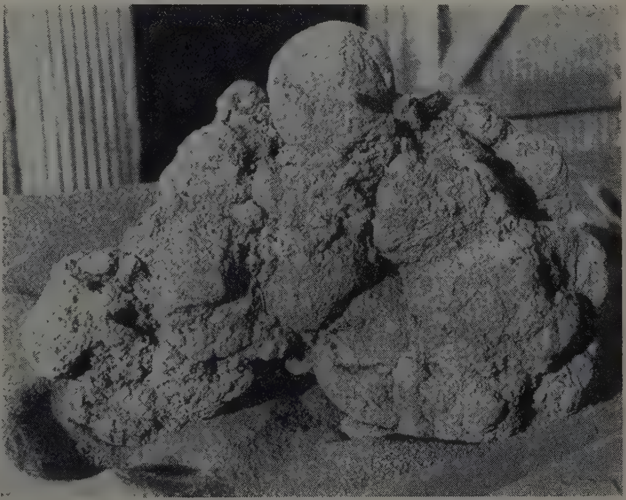

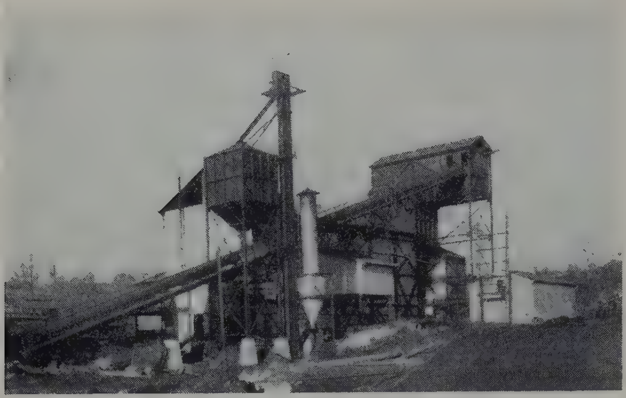

Fig. 6—The first commercial Disco plant. Built in 1933 on the site of the pilot plants, the carbonizer was 6 ft in diam and 90 ft long, and produced 60 tons of Disco per day for 15 years.

control it was possible with the aid of scrapers to keep the shell quite free from carbon crusts.

Wisner Process Departures

As the first departure from the Wisner process, experiments were made of blending. The theory on which extensive tests were made at the pilot plant in the winter of 1932-1933 was that the ball size of product could be controlled by the addition of breeze to reduce, or of fresh coal to increase, the size. Auxiliary bins with individually controlled feeders were installed, one containing pulverized low temperature coke, the other fresh coal. Neither was preheated. Small amounts of one or the other were added to the main stream of preheated and partially oxidized coal as it entered the 3 ft carbonizer. The results were highly satisfactory. For the first time the operators were able to control the product of the carbonizing retort. This method has in principal become a part of the Disco process, except that the control has been confined to varying the percentage of recycle breeze, with this breeze preheated.

The second departure from the Wisner flowsheet was the introduction into the circuit between the thermodizer and carbonizer of a storage or surge bin. Early experience demonstrated the necessity of a means of regulating the irregular flow from the preheating retort to a steady flow into the carbonizer. The simple solution of a surge bin was a failure because the hot, fine coal either caked or took fire. The solution was found in a loaded conveyor, which was in effect a surge bin in which the hot coal was kept in motion and from which the desired quantity was withdrawn under controlled conditions and fed into the carbonizer. In this storage the hot carbonizer feed was mixed, heated uniformly throughout, and from it a reliable feed, both as to rate and quality, was possible.[8]

The third important departure from the original design was the development of the rabble hearth for preheating and oxidation of the coal. The rotary kiln for drying and preheating was unsatisfactory. Heat transfer was limited; the coal packed and caked on the walls; the temperature and moisture content was exceedingly irregular. A small, four-deck, rabbled preheater built and operated as the last important step in the operation of the pilot plant solved this problem. In May 1933 the pilot plant was torn down to make way for the installation of the first commercial sized retort.

The pilot plant development had demonstrated that with adequate controls, the rotating retort would make a satisfactory low temperature coke and that adequate controls were possible with the rabbled hearth, the intermediate storage, and recycle of breeze.

Commercial Plants

Three commercial sized units were built in the period 1933 to 1936 and operated continuously until dismantled in 1949 when the present plant went into production. These units have been described in detail[9-12] and reference will be made here only to the steps in the development from pilot plant to this first commercial operation and then to the design of the present plant.

The first unit, started in November 1933, see Fig. 6, had a four-deck, rabble-hearth roaster and a two-deck storage in which buckets carried coal around the circuit, and from which a constant amount was withdrawn for carbonizer feed, and of which a part was recirculated to the roaster. This piece of equipment had a remarkable record. Except for a few wrecks caused by drive shaft failures, this roaster-storage combination was almost trouble free. The original heavy rivetless chain (with pin renewals, of course) lasted the life of the unit; high carbon steel track installed in 1934, original buckets and rabbles, the casing, top, bottom and sides, hearth plates, and heating gas ducts, were all intact and in perfect condition when dismantled in 1949.

However, results with the No. 1 carbonizer were different. It was designed, as were the Philo unit and the 3-ft pilot plant, with integral concentric revolving shells, insulated outside with slag wool mattresses. No way was ever found to hold this insulation for more than a year. The tires and drive sprocket were positioned in from the ends, which necessitated hot gas hoods each with two heating gas seals. Maintenance was high, but the unit continued to produce good Disco to the end.

A radical change was made in the design of the second unit. Tires and drive were mounted on the ends of the retort, which eliminated two heating gas seals. The outer shell was stationary, the inner alone rotating. Both original cost and maintenance were reduced materially. For the second and third units the roasters were the Wedge-type, all steel, circular, with nine decks, each deck above a heating gas duct. The rabbles were on radial arms attached to a vertical shaft. Although these machines gave satisfactory service, their high initial cost ruled them out for future installations. The same is true of the revolving double shell retort designed for the storage conveyors for these units.

There were many things learned in the operation of the first plant in which, in the years from 1939 to 1948, few alterations in plant or process were made. By the end of 1939 those who managed and operated the Disco plant were satisfied that the development had reached the stage where expansion was desirable, either by addition of more units or by a new installation. During World War II such construction did not appear to be feasible. The economic incentive remained however, and after the war the Pittsburgh Consolidation Coal Co. authorized construction of the seven-unit plant. This was completed in 1949, and the old plant was dismantled and sold for scrap in 1950.

Starting with one unit and production of 816 tons of Disco in 1933, this plant processed a total of 1,155,400 tons of coal in the years 1934 to 1948; produced and sold 829,400 tons of Disco and 15,834,000 gal of tar. The last month it was in full operation, December 1948, this plant had its record output of 8172 tons of Disco.

Open Ends, Dams, and Lifters

Important as were the control methods developed at the pilot plant, two discoveries made in the early operation of the three-unit plant were of great importance; both contributing to the final success of the process. One discovery was that by leaving the discharge end of the carbonizing retorts open to the atmosphere and controlling the suction at the other end, solid product quality was improved greatly and operation steadied. The other improvement was the introduction of simple dams and lifters in the retort to control the flow and retain material in process.[18]

The Wisner process as practiced at Philo and as engineered into the Champion pilot plant had a large rotary, star-shaped seal through which the solid product was discharged. The purpose was to prevent air from entering that end of the retort. This was a large cast-iron device moved from Philo to Champion. In the course of time it became worn and battered and was no longer even the semblance of a gas seal. However, the more the seal leaked, the better the operation of the carbonizer. This fundamental was not appreciated fully or accepted however, until the three large units comprising the first Disco plant had been built and operated for some time. Leaving the discharge end of the carbonizer open and by suction on the upper closed end, pulling the product gases together with air into the open end, solved some difficult problems of continuous carbonizing in a revolving retort. There was no necessity for a seal to withhold air and yet pass large pieces of solid product. The combustion of the oxygen developed heat where it was most needed, supplementing that which was transferred from heating gas through shell. Without the supplemental heat from combustion by open-end air, the solid product was soft and smoky. Open-end operation presumably burns tar, for the tar yield is much lower than with the closed-end operation. However, the discovery of the open-end made it possible to produce Disco with a marketable structure.

Control of the flow of material through the carbonizer by dams and lifters was another important development in the ball-making process that came from the operation of the three large units. Some aspects of open-end operation and dams and lifters are covered later in this paper, but for more detailed discussion of these factors and the theory of ball making, the reader is referred to the earlier paper on the Disco process.[2]

Seven Unit Plant

The Pittsburgh Consolidation Coal Co. in March 1947 authorized the construction of a new Disco plant to carbonize 1000 tons of coal per day. The first unit was in production in April 1949 and the plant in full operation in December. The coal, which contained 13 pct moisture, was to be delivered by belt from the Champion preparation plant of the Pittsburgh Coal Co. to a storage pile from which it would be withdrawn currently, heat dried to 3 to 4 pct moisture and processed to Disco, tar, and gas. Seven process units were specified, each to take 150 tons of coal in 24 hr. The new plant site adjoined the original three-unit plant.

The record of more than 2 years' performance of the process units has been particularly gratifying. Unit input in the first year of full operation was 148 tons of dry coal per day, with a yield of over 75 pct commercial Disco and between 16 and 17 gal of tar per ton of dry coal. In 1951 the throughput was increased about 10 pct to 165 tons of coal per day. The yield has been maintained at 75 pct. At this rate of input the daily production of Disco is 860 tons as compared with the design figure of 770 tons.

Carbonizer

The carbonizing retort, its length, diameter, slope, speed of rotation, and its capacity, was the first consideration in design and layout of the new plant. The carbonizer in this process has the primary function of rolling plastic coal into balls. The retort is not an efficient heat transfer machine, and its capacity cannot be calculated from the theory of heat transfer. Given properly prepared feed, and adequate heat input to complete the carbonizing reactions, the capacity of the Disco retort is determined by volumetric considerations. The limiting factor is bed depth in the plastic zone.

Three stages are represented in the progress of material down the length of the carbonizer. The first is heating the coal and recycle breeze from about 600°F to its softening temperature. The second begins when the material softens into a plastic mass. The third begins when the plastic material has solidified sufficiently for individual pieces to retain their identity. In other words, a dry, a wet, and a dry stage. The size of the individual pieces, the balls, is entirely fortuitous in any given bed condition, with the largest balls resulting where the depth of plastic material is greatest.† The diameter of the retort also has its effect on ball size. Along any foot of horizontal length, the larger the radius of retort, the more volume at any given maximum depth, hence the more likely that large pieces will result when the postplastic stage is reached. This is evidenced by the larger proportion of maximum sized balls from the largest sized retorts. It had been found by experience with the 8-ft retorts that a 6-in. bed of coal and breeze was the deepest practical depth. This was controlled by the height of internal dams, 6 in. high, at intervals along the shell.

Experience gained in the operation of 3, 6, and 8-ft diam continuous retorts and 3, 8, 10, and 12-ft diam batch retorts had supplied the essential data for the design of the new retorts. A 10-ft batch carbonizer, originally 12-ft, is shown in Fig. 7. Slopes of ¼, 1/3, ⅜ and ½ in. to the foot had been tried on different retorts. Experimenting with the effect of varying speeds of rotation had demonstrated that a peripheral speed of 75 to 100 fpm was a good compromise between power consumption and effective

---

† In the earlier report on the Disco process, it was categorically stated that the size of the balls is determined by the agglutinating property of the coal when it has become plastic; and that structure is determined by the inerts as well as by time-temperature treatment. This is not inconsistent with the present assertion that depth of bed in the carbonizer is the controlling factor. One factor supplements the other. Other factors being equal, bed depth controls, but in any given depth of bed, the coal that has the greater agglutinating property will stick together in larger masses before solidifying than another less strongly coking coal. This has been demonstrated experimentally in the batch retort where the bed depth can be predetermined and other process conditions be controlled with the coal quality as the only variable.

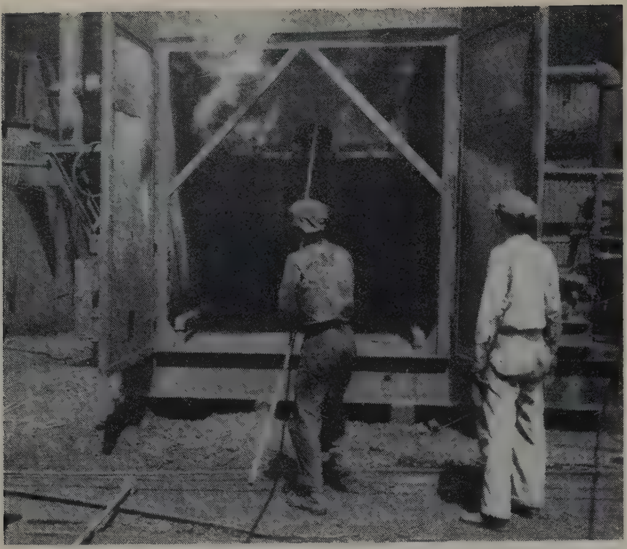

Fig. 7—Ten-foot batch carbonizer used for study of the effect of retort diameter on Disco ball formation.

mixing and conveying of the charge. The new retorts have a peripheral speed of 75 fpm and a slope of ⅜ in. to the foot.

The hot gas seal at the upper end of a 9-ft carbonizer is shown in Fig. 8. Two steel rings forming the seal are indicated by the arrows. The ring at the left revolves with the retort. The ring at the right is anchored from revolving, but moves in and out on the axis of the retort. It is held in contact with the revolving ring by counterweights. To the left of the tire is the packed gland which is the seal for the byproduct gas. Both seals are under pressure of a few millimeters. The steel wear strips on the hot gas seals are lubricated by graphite plugs in the metal and frequent applications of flake graphite.

The gas offtake end of the carbonizer is shown in Fig. 9. The large elbow duct in the center leads from the upper cone end of the retort into the cast-iron dust box in lower center. Tar vapor and gas pass down onto a water seal in this box, depositing the greater part of their dust burden, then to the right and up through the water scrubber at extreme right. The conveyor in lower left removes dust from water in the center box. In the upper left is the carbonizer feed screw leading into the retort through the side of the gas elbow. The charge enters the screw through a vertical chute from the roaster-storage feeder on the floor above. The next adjacent carbonizer shows in left background.

It is customary to relate the capacity of the Disco retort to the tons of coal processed in 24 hr. This is misleading, however, because the total heat load and processing requirement is the coal plus the recycle breeze. In the first plant the ratio of coal to breeze had varied, by units, from 25 to 30 pct breeze, with a general average of 30 pct for the larger units. That is, for 70 parts of coal charged, there were 30 parts of breeze. Tests had been made in which the ratio of coal to breeze was 60 to 40, and with improved conditions as to preheat temperatures, it was decided that it was practical to design the new plant for such a ratio. It was decided further to preheat breeze and coal together in the roaster storage system, instead of separately.

To process 1000 tons of coal per day and recycle 670 tons of breeze would require eight of the 8-ft retorts, or seven, of 9-ft diam. The 9-ft retorts were specified, each rated at 150 tons of dry coal and 100 tons of recycle breeze, a total load of 250 tons per day, or more than 10 tons per hr.

The length of the new carbonizers was specified as identical with original No. 3, 129 ft, cold. With center lines of heating gas hoods 92 ft 9¾ in. apart, the effective heating area was 3016 sq ft. The original unit, with 6-ft diam was 76 ft between centers of heating gas hoods, the second was 8 ft in diam but with the same length. The third had the same diameter as the second but was 20 ft longer. Operating experience over a period of years with substantially the same heating gas temperatures and the same feed conditions showed that an increase in diameter had more effect on capacity than an increase in length. Thus with the two retorts of the same length, the 8 ft, with an increase in heating area of 25 pct, had 37.5 pct greater capacity than the 6 ft. Comparing the two 8-ft retorts, the longer, with an increase of 29 pct in heating area, gained but 18 pct in capacity. The new units, 9 ft in diam, have 13 pct more heating area than old No. 3, and were designed to carbonize 15 pct more coal. As will be explained subsequently, the new units are handling 23 to 25 pct more coal than the largest older 8-ft unit.

The minimum necessary length of the carbonizing retort is that required for heating the preheated coal to and through the plastic range. After the charge has hardened sufficiently to assume the final shape and size of product, longer retention in the revolving retorts serves only to devolatilize it further and to grind it as in a ball mill. One result is desirable; the other is not. Experimental evidence of the reactions in the continuous carbonizer is confined to observations of the elapsed time for predetermined changes in feed to be noted in product discharge and to inspections of the cold interiors of retorts after a shutdown. The time of transit through the retort is approximately 1 hr. Additional and highly informative data are available from studies in batch carbonizers in which temperatures were controlled and measurable, and in the operation of which a test was terminated at any desired stage of heating or carbonization and the products examined and analyzed.

From consideration of all the data thus available, it is estimated that charge entering the 126-ft continuous carbonizer at 600°F travels about 45 to 50 ft in 25 to 30 min before it becomes plastic. In this time it has been heated to nearly 800°F at an average rate of 8°F per min. In the next 15 min the coal has passed through the plastic range and with the recycle breeze has become consolidated into irregular-shaped masses not yet hardened. In the next 10 min the material has traveled another 25 ft, has increased in temperature to about 875°F, and has become hard and firm.

There is on the discharge end of the retort what is termed the cold extension, extending about 20 ft beyond the tire and the heating furnace. In this extension the balls are retained for about 10 min for further devolatilizing and cooling before being discharged at about 800°F.

The conditions described above were set by experimental work on the three retorts in which, in the first few years of operation, dams and lifters were raised repeatedly, lowered, and moved to affect the flow and heating of charge to attain the maximum desired effects. Retention time in the shorter retorts was maintained substantially the same as in the longer one by slower feed rates, not by deeper beds.

It has been noted previously that the new 9-ft retorts handle a much greater tonnage than the old 8-ft, No. 3 of the same length. The input tonnage, coal and recycle breeze, to the 8 ft was from 185 to 200 tons in 24 hr. The seven new units each take over 300 tons in 24 hr. The overall increase in capacity—in excess of that due to greater heating area—arises from better design of heating gas seals, more effective insulation, both conserving heat and in large part to the higher preheat of charge. In the old plant the average temperature of coal to carbonizer was 540°F and of recycle breeze, heated independently, 435°F. In the new plant the coal and the major portion of recycle breeze are heated together and delivered to the carbonizer feed screw at from 580°F to 610°F, with the remainder of the breeze charged simultaneously at 700°F or higher.

Roaster-Storage System

Three fourths of the heat required to make Disco is that necessary to dry and raise the charge material to 600°F for delivery to the carbonizing retort. This is done in the roaster-storage system by indirect heating.

Design data for the new roasters were derived from a study of the performance records of the two types used in the old plant, supplemented by analysis of heat balance data. No practical design of circular multiple hearth roaster gave the required capacity for the new units. The straight line rectangular hearth, originally developed for the first unit in 1933, was extended and widened for the new plant. The design called for 2100 sq ft of roaster hearth per unit, on four hearths 6 ft wide and 90 ft long, with rabbles every 3 ft, travelling at 30 ft per min. The bucket conveyor on the lower two decks, the storage, carries around; that is, material not taken from its discharge by the carbonizer vane feeder is lifted to the upper deck and makes another trip around. Because the carry-around capacity is limited, fine adjustment is required between feed rate to roaster and storage discharge rate. Charge material is in the four decks of roaster about 40 min, and in storage conveyor from 10 to 30 min depending upon the load.

The normal rate of temperature increase in process is from 150°F as charged to 435° to 475°F off the second roaster deck; 540°F to 560°F off the fourth deck and 580° to 610° at the final discharge from the storage into the carbonizer. Air for oxidation of coal need be admitted only to the lowest or storage decks. It is of greatest importance to maintain the coal in this preheating equipment below the softening point, and of course to avoid fires on the decks. Experience has shown that a top temperature of 600°F of the roaster-storage discharge is safe; that if it strays above 640° trouble will result, for this hot material is highly reactive and will *take off*, coke or fire, or both. Temperatures at ten points in the system are recorded currently and constantly watched by the control room operators, as are the power loads on all heavy equipment.

The four roaster decks and the top storage deck rest on ducts through which flue gas returns from the upper end of the carbonizer to the recirculating fan and furnace without contacting the coal. Temperature of the heating gas drops from about 900°F

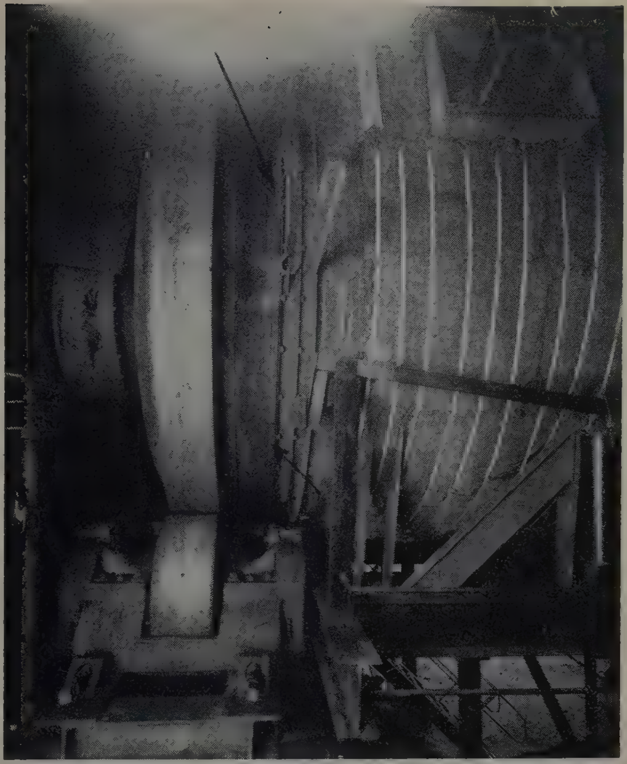

Fig. 8—The hot gas seal at the upper end of a 9-ft carbonizer. Two steel rings forming the seal are indicated by arrows.

Fig. 9—The gas offtake end of the carbonizer. The elbow duct in the center leads from the retort into the dust box.

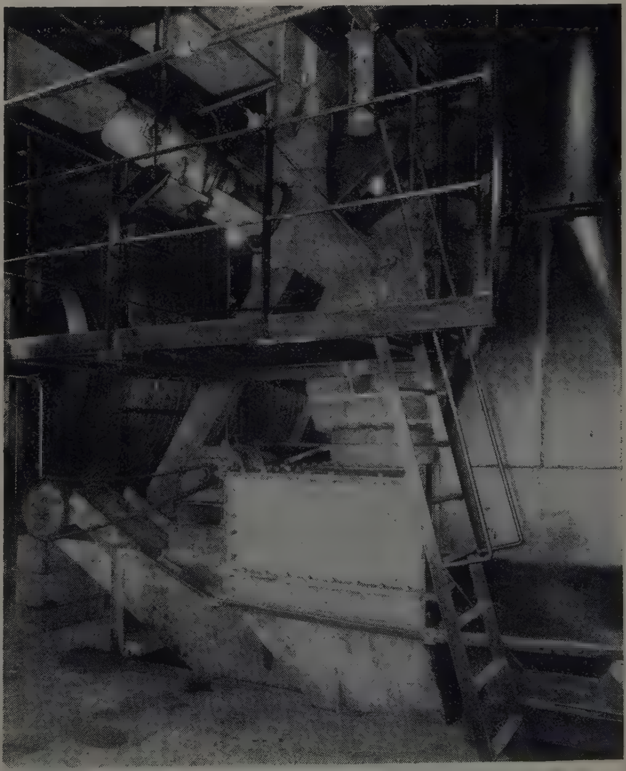

to 600°F in its passage through the roaster-storage duct system. Dampers in the inlet to each deck permit close control of temperatures. As designed, excess flue gas may be vented from a point between the fan and furnace to the second deck of the roaster, and in turn vented from the top deck to atmosphere through unit cyclone dust collectors. This hot, 600°F, sweep gas over the first two decks not only assists in initial heating but keeps the effluent gases above the dew point, below which serious corrosion of steel would result.

Serving the seven units is a distributing conveyor containing the desired proportions of coal and recycle breeze. From this common conveyor through a 1-hr supply bunker, a measured quantity is taken to the top deck of each roaster and after heating is delivered to the carbonizer feed screw. Each unit, roaster and carbonizer, is an individual process machine for which it is necessary to maintain uniform conditions of temperature and material flow. Changes in feed rate and temperature through the system are gradual; no quick reactions can be expected, but rather slow upward or downward trends. Effective and positive results, however, follow changes in the coal-breeze ratio to the carbonizer. The operator, who, by frequent visual inspections of the solid product from each unit, finds it necessary to alter the product, because either too small or too large in average size, has the means of correction at hand in the rate of flow of supplemental hot breeze directly to the carbonizer feed. The breeze for this circuit is that screened out through ½-in. round perforations in the nozzle at the discharge end of each retort. It is collected and elevated to a higher level in insulated conveyors for distribution at about 750°F. By remote control the operator manipulates the feeder and the flow of this hot breeze to each carbonizing retort. Approximately 25 pct of the total recycle breeze flows in this circuit, giving a marked improvement over previous design in heat utilization as well as in product control.

Operation

This is a continuous operation, designed with comparatively little leeway. From the stockpile, coal moves continuously to and through the heat drier, a single surge bin holding a 1-hr supply, a weightometer, and finally to individual bins above each roaster. From the stockpile, through the heat drier and roaster, and out the carbonizer as Disco, adds up to less than 4 hr in process. The heat drier, surge bin, and roaster feed bins normally afford 1 hr or more of time to recover from failure in this line of supply, and complete stoppage here would not introduce any hazard or serious operating problem.

However, from the carbonizer discharge to the cooling wharf, the line of flow is vulnerable because the material is hot and will take fire at any stoppage. No machine is infallible, particularly those handling hot, combustible material, hence every effort has been made to provide alternate routes around possible points of breakdown. The many provisions in the original design have been supplemented as experience indicated the necessity. The ability and resourcefulness of the experienced key operating personnel, both supervisory and hourly, has surmounted one problem after another until now the major deficiencies in the original design have been largely overcome.

It is fortunate for the economics of the Disco process that recirculation of fines is necessary for marketable product. Since the process requires all the fines incidental to the operation, there is no problem of breeze disposal. It has been noted that the old Disco plant charged 70 parts coal to 30 parts recycle breeze. Under normal conditions this worked out in balance when the breeze was all solid product through 1¼-in. screen.

The new plant was designed for 60:40 coal to breeze ratio, and as has been stated, is operating on approximately a 50:50 ratio. The difference between the two plants is in the amount of oxidation, which in the new plant is much less than in the old. There are two sources of breeze, normal degradation in the retorts and in the handling that follows through cooling to final screening, and degradation from rehandling from a stockpile, see Figs. 10 and 11. In the operation of the present plant, it has been found that when reclaiming a tonnage equal to production, sufficient breeze for recycle is available to allow the loading of +1½ to 1¼ in. Disco. When going into stock with current production, as in the summer months, it is necessary to crush everything below 2 in. to get sufficient breeze.

Retort Maintenance

Deposits on the inner walls of retorts plague every user of the rotary kiln in which material is heated until it becomes soft or plastic. If the end product is to be a liquid, or clinker or coke, the problem is the same. Charged dry, to emerge in any of these forms, the material must pass through a soft or sticky stage, and in the transformation, fused material clings to what it contacts, whether steel or refractory.

Distilling or carbonizing coking coal in a kiln or revolving retort by either direct or indirect heating has always been a troublesome operation by reason of build-up of carbonaceous accumulations on the walls. Innumerable attempts to remove such accretions as they formed by devices rolling around in the retort, cutting or chopping scale from the shell, have proved futile. The reduction of this problem by a combination of roasting the coal and admixture of inerts, as developed in the Disco process, has already been described.

However, there are in the Disco retort accretions that do not affect operations over long periods. Carbon from cracking of the tar vapor makes a hard, dense, slick coating that clings tightly to the steel. It is evenly deposited and shows every minute irregularity of the surface on which it is deposited, such as welds. Such a surface is shown in Fig. 12. This type of deposit is particularly noticeable in the upper part of the retort, above the region where coal becomes plastic. After months of operation this type of deposit will vary in thickness from less than ¼ in. at the feed end to ½ in. half way down the length of retort. This deposit does not greatly interfere with heat transfer through the shell, nor does its accumulation interfere with the orderly process of carbonization.

From the location where the coal becomes soft and sticky to the discharge end, the deposit over a period of months becomes much thicker than that nearer the feed end. It has a rough pitted surface, differing from the glassy surface of the first type described, and is very hard. After several months of continuous operation this hard deposit in the lower one half or two thirds of the retort becomes thick enough to affect heat transfer and thus quality of product unless removed. Normal practice is to clean each retort twice a year. A unit is off the line for 7 days for cleaning with air-chipping tools.

In the immediate area where the coal softens, a porous deposit, often 2 or 3 in. thick, collects on the harder scale. This porous material breaks off intermittently and is discharged in small amounts with the Disco balls. The operators recognize the pieces as flats. For the most part, such pieces, when they fall off, are ground up by the balls before discharge.

A third type of deposit, the ring or doughnut was of regular occurrence in the three-retort plant. Concentric rings of a mixture of pitch, coke, and coal accumulated on the steel at the upper end of the retort. These rings, which grew to such heights as to obstruct the flow of incoming feed, were caused by condensation of pitch on the cooler charge as it flowed from the feed screw. No such ring accumulations have been found in the new units after more than 2 years of operation. The explanation of this improvement is that the charge, coal and breeze, is not only more carefully and intimately mixed, but that the charge as well as the steel retort itself are hotter in the new design and more uniform in temperature, hour by hour than in the old. The story of deposits in the carbonizers can be summarized by noting that although initially an outstanding problem in the development of the Disco retort, there is now no difficulty on this score.

Physical Structure of Disco

The current measure of quality of Disco for commercial shipment is its shatter index. Usual testing procedure is daily determination of the shatter index, ASTM standard, on +2-in. sq hole screen. Normal operation gives a product off the cooling wharf ranging between 65 and 70 shatter index. The strength of the ball as measured by its shatter index is directly related to the rate at which it was cooled. Balls collected as they were discharged from the retort and tested while hot, have shown shatter tests of over 80 pct on 2 in. The same balls cooled suddenly, as by immersion in water, will be very fragile. Slow cooling in the air has been developed as the way to preserve the strength of the Disco ball.

There is another factor affecting the structure of the larger pieces. The larger balls are the result of soft masses having been rolled and kneaded in the retort. A mass of plastic material that is to become a ball is folded and rounded as it becomes solidified. The surfaces folded together are weak joints that may extend deep into the final pieces. This is illustrated in Figs. 13 and 14. The 10-lb ball of 800°F coke shows how this folding takes place. Smaller balls, 6 to 8 in. or less are initially more substantial than the largest balls.

These Disco balls were made in a batch retort in which 60 lb of 35 pct volatile matter coal and 40 lb of recycle breeze were charged for each test. Fig. 13 is a large ball taken from the retort when the charge temperature reached 800°F. The ball in Fig. 14 was taken from the retort when the charge temperature reached 900°F. The 800° ball was soft, plastic, and emitted tar vapor when taken from retort. If this ball had been retained in the revolving retort at increasing temperature, the crevices and cracks would have disappeared, and its appearance would have been that of the 900° ball. Moisture and ash free

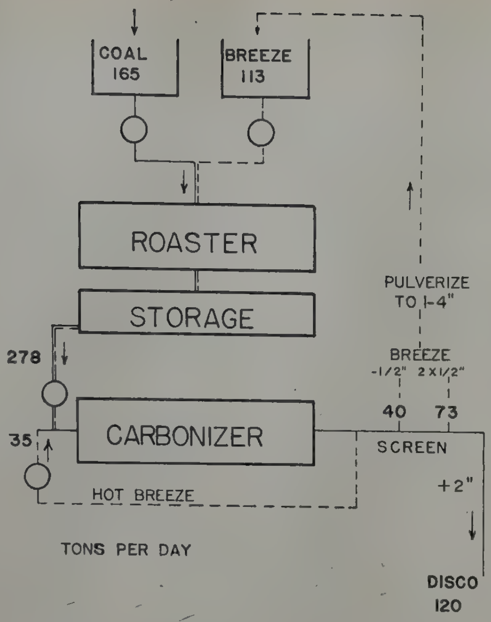

Fig. 10—Flow diagram of solids in one 9-ft Disco carbonizer unit, in tons per day, 165 tons of dry coal making 120 tons of +2-in. commercial product.

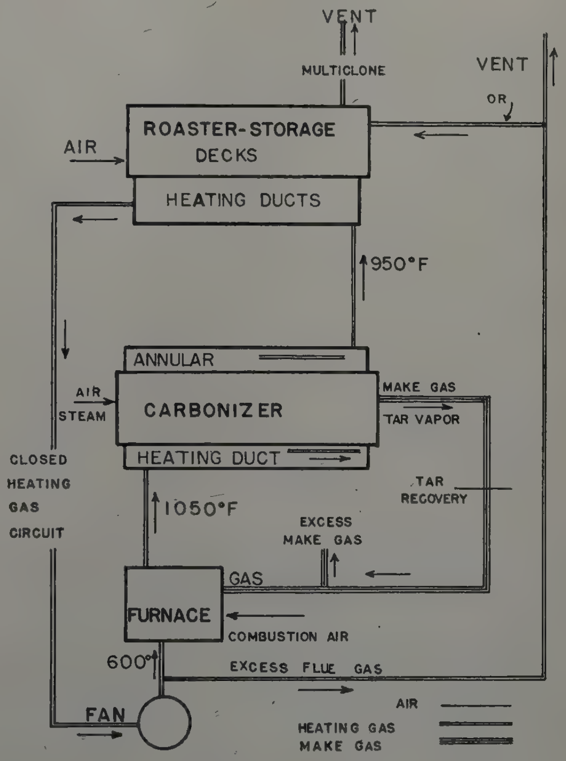

Fig. 11—Flow diagram of heating gas and of product gas and tar vapor in a unit of the Disco process. Heating gas does not contact the coal in process except in the open-end carbonizer.

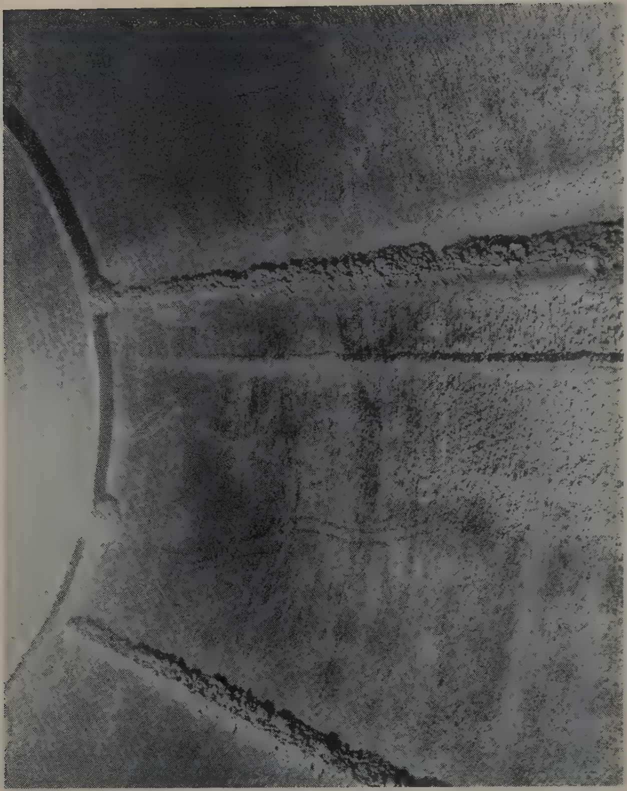

Fig. 12—Interior wall of carbonizer showing accumulation of hard, pitch-like crust on every irregularity of the steel.

volatile content of the 800° ball was 22.0 pct and of the 900° ball, 18.4 pct.

Volatile Matter in Disco

The analysis of any coke will depend upon the coal from which it is made insofar as ash and sulphur are concerned. The volatile matter content will vary with the process, depending largely upon the temperature of carbonization. Volatile content of Disco is limited within a fairly definite range by two factors. One limitation is that imposed by the process which follows from the fact that once the plastic material has become the Disco ball, there is little subsequent change in analysis. The other factor is that the temperature of carbonization is limited by the safe working temperature of the metal in the retort. Disco carbonizing retorts have all been constructed of low carbon steel of flange quality for which the safe limit of working temperature has been considered to be 1112°F (600°C). Normal operation is with maximum heating gas temperatures of 1050°F and, of course, something less for the steel. The steel in the three original retorts, when dismantled and scrapped in 1950, after 12 to 15 years' operation under these conditions, exhibited no signs of deterioration or failure due to heat.

Solid product as it is discharged from the continuous retort ranges in size from large egg-shaped balls, 10 to 20 in. in length, to fine dust, the result of grinding. There are measurable differences in volatile content of different sizes. Because low temperature coke is a very poor heat conductor, the larger pieces are devolatilized but little after having been formed; the smaller sizes, and particularly the fine, −¼-in. material, is devolatilized further as it contacts the hottest metal of the retort. Test data have shown an average of 0.6 pct lower volatile matter in the 1x2-in. size as compared with the large +2-in. balls, and a further drop of 0.5 pct from the 1x2-in. to the −⅜-in. breeze; a total difference of 1.1 pct.

Table I. Volatile Matter, Disco Compared with Fischer Retort

Temperature of Carbonization, °F	Fischer Retort Dry	Fischer Retort MAF[a]	Disco Batch Retort Dry	Disco Batch Retort MAF[a]
700	31.7	35.3		
750	24.8	27.9		
800	19.4	22.1	20.0	22.0
850	16.7	19.1	17.4	19.4
900	13.9	15.9	16.3	18.4
950	13.1	15.1	15.9	17.7
1000	10.3	11.9		

[a] Moisture and ash free.

Available evidence indicates that the balls are formed by the time the plastic material has reached 800°F. At that point the volatile content is about 20 pct, dry basis. The larger pieces lose volatile matter from that point on until finally cooled. From the data available, it is believed that the conditioning of the solid product in the continuous retort, that is, the retention in the retort after balls are formed, results in a reduction in volatile matter of 1 to 1½ pct, and that there is a further devolatilization of the large balls after discharge of a fraction of 1 pct, perhaps as much as 0.5 pct. The net result is that the larger pieces from the new 9-ft retorts, when cooled, analyze about 18 pct volatile matter. This strongly suggests that the actual temperature of carbonization in these retorts is between 825° and 850°F. Measurements of the temperatures at centers of medium sized balls as discharged give a consistent record of 800° to 810°F.

Significant correlations of the effect of time and temperature on the production of Disco balls are offered by test results in the 3-ft laboratory batch carbonizer. In this retort, weighed quantities of coal and recycle breeze were carbonized at predetermined rates of heating and to measured temperatures of the material in process. Table I gives the volatile matter analyses of a series of such tests compared with analyses of the carbonized products obtained in the Fischer retort. The charge to the Fischer retort was a few grams of coal alone; to the batch retort the charge was 60 lb of coal and 40 lb

Table II. Analysis of Byproduct Gas, a Composite of Gas from Seven Units as Fed to Burners

Component		Pct
Carbon dioxide		5.3
Hydrogen sulphide		0.9
Oxygen		0.1
Carbon monoxide		9.4
Hydrogen		3.4
Methane		10.9
Higher paraffins, as ethane, C_2H_6		8.9
Ethylene, C_2H_4		2.6
Propylene, C_3H_6		1.2
Butylene, C_4H_8		1.0
Nitrogen		56.3
		100.0
Calculated heating value	Gross	412.6 Btu/SCF[a]
	Net	380.2 Btu/SCF[a]
Calculated specific gravity		0.95
Quantity per ton of dry coal		3700 SCF[a]

[a] Standard cubic feet.

Table III. Typical Analysis of Disco Tar

Moisture, pct by volume	3.5
Specific gravity at 25°C, dry	1.15
Distillate to 270°C, wt pct	23.4
Ash, wt pct	1.7
Dry tar acids in tar, volume pct	12.5
Specific gravity of tar acids	1.03
Cresol, volume pct	8.0
Creosote oil in dry tar, volume pct	31.0
Phenol in dry tar acids, volume pct	10.0
Phenol in dry tar, volume pct less than	1.0

of recycle breeze. The analyses in this table are of balls about 9 lb each.

Byproduct Gas

Byproduct gas produced is more than sufficient for process heating. During the first few years of operation of the three-unit plant there was a surplus, but in later years insulation became impaired and the original unit, No. 1, with its four hot gas seals, was difficult to maintain, with the result that after 10 years' service, the plant had a deficit in available heat from make gas. As a further indication of inefficient use of gas in the old plant, it is noted that flue gas from No. 1 unit had 4 to 5 pct CO_2; from No. 2, 7 pct; but No. 3 was between 11 and 12 pct, as are the units in the new plant. Corresponding static pressures over the heating gas circuits were respectively 2.8 in., 2.2 in. and 1.8 in. for units 1, 2, and 3. Static pressures across the circulating hot gas fans are 2.2 in. of H_2O in the new plant. An analysis of byproduct gas is given in Table II.

The deficiencies were overcome in the design of the new plant by the best possible insulation, effective seals and gas tight expansion joints, with particular attention to pressures on the plus side of the rubbing seals. A considerable part of the unaccounted for heat loss, as shown in heat balance, is unavoidable leakage through the two rotating heating gas seals on each carbonizer.

Tar

Tar is the only byproduct presently available from the Disco operation and as such is important in the economics of the process. When the project of making low temperature coke was initiated, it was recognized that whereas the market for the solid product was obvious, that for tar was unknown and uncertain. It is true that many ambitious schemes for thus processing coal had been advanced on the basis of exceptional values from the tar and oil byproducts, but none had then, nor have they since, materialized. The steps in the development of the manufacture of a smokeless lump fuel have been described, and it has been indicated that the effort was directed toward improving the solid product with little or no reference to the tar. However, the time came when it was necessary to find outlets for a tar that was a new and different material and for which there was no recognized market.

Table IV. Material Balance, Basis 1 Ton Coal, 4.2 Pct Moisture (For the Seven-Unit Plant)

Input	Lb Per Ton Coal
Dry coal	1916
Moisture in coal	84
Natural gas (pilot flames)	1
Air for combustion, dry	1069
Air to roasters, dry	740
Air to open ends of carbonizers, dry	189
Moisture in air	10
Steam entering open end of carbonizer	26
	4035
Output	
Disco	1502
Tar, dry	155
Gas, excess, dry	69
Moisture in tar and gas	6
Vent gas with entrained dust and moisture	2136
Liquor and losses	167
	4035

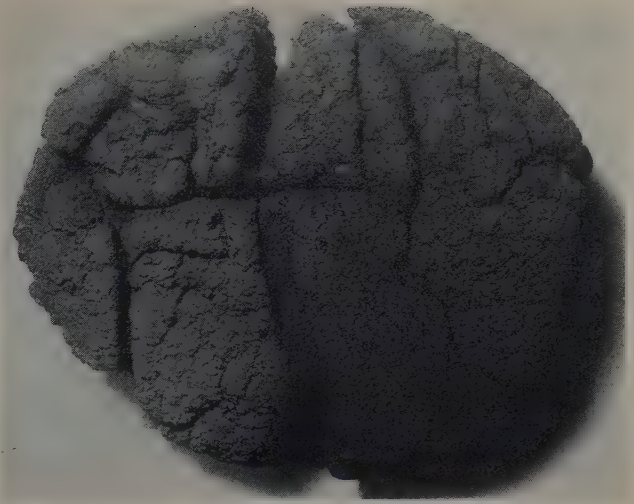

Fig. 13—Large ball taken from retort when the charge temperature reached 800°.

The problem of the tar thus was one of finding a market, and as this paper is concerned primarily with the process of making Disco by low temperature carbonization, the story of tar will be but briefly covered. From 1933 when the first tar was produced until the end of 1948 when the old plant was abandoned, nearly 16 million gal of Disco tar were produced and marketed in one form or another.

It is interesting to note that over 17 years of operation tar sales represented 24 pct of gross revenue and Disco 76 pct.

One ton of the 35 pct volatile coal from the Pittsburgh bed will yield 25 or more gal of tar when carbonized at 850°F to 900°F in a closed retort. The same coal carbonized in the open-end continuous Disco retort yields 15 to 17 gal of tar of essentially the same analysis. Table III is a typical analysis of Disco tar.

Marketing this tar met with many difficulties. None of the established high temperature coke oven

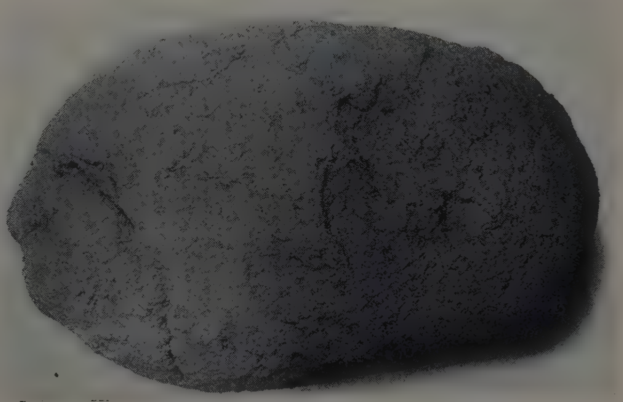

Fig. 14—Ball taken from retort when the charge temperature reached 900°.

Table V. Heat Balance on Disco Plant, Thousands of Btu

	Three-Unit Plant 1947		Seven-Unit Plant 1950	
	Btu/Ton Coal	Pct	Btu/Ton Coal	Pct
Input				
Gross heating of underfiring				
Byproduct gas	1577.9	68.0	1122.0	72.7
Natural gas	278.0	11.8	56.0	3.6
Open-end combustion	260.2	11.0	225.0	14.5
Roaster air combustion	72.9	3.0	65.0	4.2
Sub total	2189.0	93.8	1468.0	95.0
Sensible heat in coal	20.0	0.8	32.4	2.2
Sensible heat in steam	96.5	4.0	28.9	1.8
Sensible heat, water vapor in air	33.6	1.4	15.8	1.0
Sub total	150.1	6.2	77.1	5.0
Total	2339.1	100.0	1545.1	100.0
Output				
Sensible heat in solid product	525.0	22.5	606.4	39.3
Sensible and latent heat in tar	49.2	2.1	62.3	4.0
Sensible heat in dry byproduct gas	68.7	2.8	67.8	4.4
Sensible and latent heat in water, in gas, liquor and tar	280.0	12.0	214.0	13.8
Sensible heat in wash box refuse	0.5	0.2	1.7	0.1
Sensible and latent heat in moisture in stack gas	247.0	10.5	224.0	14.5
Sensible heat in dry stack gas	277.4	11.9	150.0	9.7
Radiation and convection	704.0	30.0	150.8	9.8
Not accounted for	187.3	8.0	68.1	4.4
Total	2339.1	100.0	1545.1	100.0

tar refiners wanted it. It was barred from road surfacing by specifications in many localities. In a region where steam coal was abundant and cheap, it could not be sold for fuel. The first sizeable outlet was as road tar, where by adjusting viscosity and by blending with purchased high temperature tar, a satisfactory road material was made and sold in quantity. Theoretically, however, the principal value should be in the low boiling, high tar acid content fraction; hence the next step was to refine the tar acid oil for sale as disinfectant oil. Wood preserving oils were then produced. During World War II the tar was refined into tar acid oil, creosote oil, fuel pitch and coke, all of which were marketed without difficulty. Subsequently, further refining was added and pure cresols were prepared for resin manufacture.

Fig. 15 shows the changes in Disco tar refining and market development over a period of years. During all this period the Disco organization designed and built the tar refining equipment, sold the products, and simultaneously did continuing research[14] on low temperature tar products. There remains much to be learned about such products, as for instance the high boiling tar acids, or the reduction of heavy pitches to high grade carbon.

Material Balance

The simplified material balance that follows, Table IV, and Figs. 10 and 11, recognizes coal and air as the materials in, and Disco, tar and make gas as the products. Recycle breeze does not appear in this record because the quantity used is equal to that made. Air into the system is not measured and the figures given are calculated, mainly from gas analyses. In Table IV the air to roaster is an approximation based on studies at the three-unit plant. The air admitted to roaster decks is appreciably less in the new plant than it was in the old plant. For neither, however, have reliable quantitative measurements of the air passing over the hot coal been possible; that is, of the quantity that could be expected to oxidize coal in the short interval of time it is exposed at temperatures above, for example, 300°F.

Heat Balance

There are three sources of heat in the Disco process: 1—Combustion of byproduct gas in the unit furnaces, 2—low grade oxidation of coal in the roaster, and 3—direct oxidation of solids and vapors in the carbonizer. A fourth source, of uncertain and undetermined magnitude is exothermic heat of carbonization in the carbonizer. Whether there is, or is not, exothermic heating during carbonization is a debatable point. Such possible heat has not been taken into any calculations of heat balance in this study. The three named sources of heat are, within limits, controllable; the fourth is not.

In the discussion that follows of heat developed and utilized in the Disco process, reference will be made to the three-unit plant and the seven-unit plant. It is important to note that the former comprised three units differing greatly in utilization of heat and that the data given are a weighted composite of the whole operation taken in 1947 after 12 to 15 years of use. The original No. 1 carbonizer was wasteful of heat, which explains the excessive use of supplemental heat from natural gas shown in Table V. No. 3 carbonizer gave the best record of the three as to tonnage and heat efficiency, and operating data from this unit were used in designs for the new plant.

In Table V are shown the input and output of heat for the new, compared with the old plant. Gross heat of underfiring, the heat from combustion of gas in the furnace, needs no explanation. The figures are for a given test period and are believed to be representative and accurate to within less than 10 pct. Data for the heat developed in the roaster decks by low grade oxidation and in the carbonizers by combustion are necessarily derived from studies of gas analyses, together with measurements of combustion air and gas involved.

It was estimated that 36 Btu per lb of coal resulted from oxidation in the roasters of the old plant,

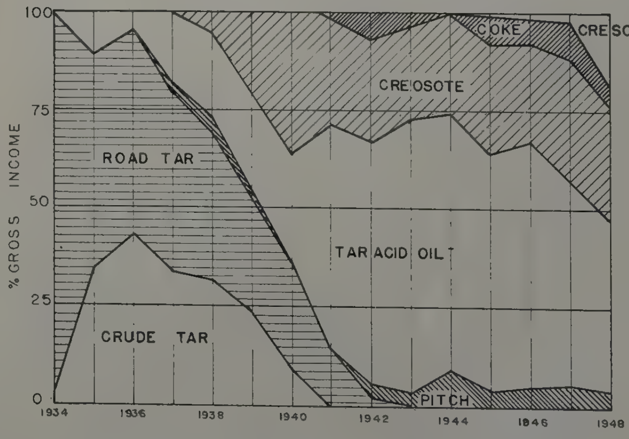

Fig. 15—Progress in development of refining and marketing of low temperature tar from the Disco process. Percentage of gross income from tar products from 1934 to 1948 of the operation of the original three-unit plant.

and a smaller quantity in the new plant where there is less dependence than in the earlier operation on reduction of coking property or more particularly on boosting coal temperatures in the roasting step.

Heat developed in the carbonizer by combustion of air pulled in the open end is a very important item in making Disco. Here again, the quantity of heat released is calculated from considerations of quantity and analysis of byproduct gas. Composition of the gas varies with the suction on the retort, operating temperatures, and the rate of coal feed. The composition and quantity of byproduct gas may be quite variable, and because proper working of the process depends upon uniformity of conditions, the control of suction in each retort is a matter for constant attention by the operators.

Stack losses of less than 25 pct are shown in Table V. All vented gases pass through the roaster dust collectors; flue gas from the furnaces over the top decks; roaster air direct; and open-end air into the byproduct gas, thence to furnaces and into flue gases. Waste gas is vented at temperatures ranging from 170° to 250°F; an average of 210°F was used in these calculations.

Heat was conserved in the new plant by better insulation and improved gas seals. In the newer plant there are, with minor exceptions, no packed stationary gas seals. Bellows-type metal connections replaced seals at points where it was necessary to take care of expansion. The rubbing seals at each end of the rotating carbonizers were redesigned for greater accessibility. A material saving in heat was realized by returning recycle breeze at high temperatures, as has been described.

From Table VI, which shows gross heat balance for the seven-unit plant, it can be calculated that the operation has a cold thermal efficiency of 85.5 pct; which compares with 74.6 pct for the three-unit plant. This figure is the ratio of heating value of products recovered, Disco, tar and surplus gas, 21,623,000 Btu, to heating value of coal and natural gas input, 25,256,600 Btu. Greater yields of Disco, tar, and gas contribute to this improvement.

Table VI. Gross Heat Balance, Seven-Unit Disco Plant, Basis 1 Ton of 4½ Pct Moisture Coal

	Thousands of Btu
Input	
Heating value of coal	25,200.0
Heating value of natural gas in pilots	56.5
Heat content of coal, and of process air and steam	77.1
	25,333.6
Output	
Heating value Disco	18,680.0
Heating value tar	2,570.0
Heating value excess gas	373.0
Heating value recovered dust	160.5
Heating value wasted dust	864.0
Radiation and convection	199.3
Heat content of products	1,269.8
Not accounted for	1,217.0
	25,333.6

Acknowledgments

Many contributed to the development of the Disco process as it has been described. It is not possible here to name all those whose unremitting efforts and intelligent research contributed to the success of the project, but special credit is due J. B. Goode, who has been in charge of operation from the beginning, A. A. Archer, Chief Engineer, R. A. Zimmerman and L. A. Winter, for conducting the research, and Caleb Davies, Jr., to whom, with C. C. Clark, is given credit for the development of the refining and the uses of the low temperature tar. Heat balance calculations were by David Kindler and Frank Crowe, Jr.

References

[1] C. E. Lesher and R. E. Zimmerman: 325 Tons Daily Treated at Disco Plant of Pittsburgh Coal Carbonization Co. *Coal Age* (March 1939).

[2] C. E. Lesher: Production of Low-temperature Coke by the Disco Process. *Trans.* AIME (1940) **139**, p. 328.

[3] C. E. Lesher: Review of Low Temperature Carbonization with Special Reference to the Disco Process. Presented at the Symposium on Low Temperature Carbonization, Division of Gas and Fuel Chemistry, Amer. Chem. Soc., St. Louis. (Sept. 6, 1948).

[4] H. H. Lowry, Ed.: Chemistry of Coal Utilization. National Research Council (1945), pp. 814, 916.

[5] W. H. Allen, Jr.: Low Temperature Distillation of Coal by the Carbocite Process. *Proc.* International Coal Conference, Pittsburgh (1928), pp. 403-412.

[6] C. B. Wisner: The Missing Link in Coal Carbonization. *Proc.* International Coal Conference, Pittsburgh (1926), pp. 800-806.

[7] J. S. Roberts: Blending: With Special Reference to the Davidson Rotary Retort. *Proc.* Third International Coal Conference, Pittsburgh (1931), **1**, pp. 339-351.

[8] U.S. Patent No. 2,080,946.

[9] M. Lelyn Branin: Low Temperature Carbonization Becomes an Economic Reality. *Utilization* (May 1949).

[10] R. S. McBride: Low Temperature Coking Plant. *Chemical Engineering* (June 1950), pp. 112-114.

[11] Philip J. Wilson, Jr. and Joseph H. Wells: *Coal, Coke, and Coal Chemicals.* (1950) McGraw-Hill Co., pp. 423-427.

[12] Andrew W. Pitney: New Disco Plant and Process. *Mines Magazine,* (September 1947), pp. 12-26.

[13] U.S. Patent No. 2,287,437.

[14] Caleb Davies, Jr.: Tar and Byproducts from the Disco Process. *Industrial Engineering Chemistry.* (July 1941), **33**, p. 860.

Primary Blasting Practice at Chuquicamata

by Glenn S. Wyman

CHUQUICAMATA, located in northern Chile in the Province of Antofagasta, is on the western slope of the Andes at an elevation of 9500 ft. Because of its position on the eastern edge of the Atacama Desert, the climate is extremely arid with practically no precipitation, either rain or snow.

All primary blasting in the open-pit mine at Chuquicamata is done by the churn drill, blasthole method. Since 1915, when the first tonnages of importance were removed from the open pit, there have been many changes in the blasting practice, but no clear-cut rules of method and procedure have been devised for application to the mine as a whole. One general fact stands out: both the ore and waste rock at Chuquicamata are difficult to break satisfactorily for the most efficient operation of power shovels. Numerous experiments have been made in an effort to improve the breakage and thereby increase the shovel efficiency. Holes of different diameter have been drilled, the length of toe and spacing of holes have been varied, and several types of explosives have been used.

Early blasting was done by the tunnel method. The banks were high, generally 30 m, requiring the use of large charges of black powder, detonated by electric blasting caps. Large tonnages were broken at comparatively low cost, but the method left such a large proportion of oversize material for secondary blasting that satisfactory shovel operation was practically impossible. Railroad-type steam and electric shovels then in service proved unequal to the task of efficiently handling the large proportion of oversize material produced. The clean-up of high banks proved to be dangerous and expensive as large quantities of explosive were consumed in dressing these banks, and from time to time the shovels were damaged by rock slides. As early as 1923 the high benches were divided, and a standard height of 12 m was selected for the development of new benches.

The recently acquired Bucyrus-Erie 550-B shovel, with its greater radius of operation compared to the Bucyrus-Erie 320-B formerly used for bench development, allowed the bench height to be increased to 16 m.

Churn drill, blasthole shooting proved to be successful, and tunnel blasts were limited to certain locations where development existed or natural ground conditions made the method more attractive than the use of churn drill holes.

Liquid oxygen explosive and black powder were used along with dynamite of various grades in blasthole loading up to early 1937. Liquid oxygen and black powder were discontinued because they were more difficult to handle due to their sensitivity to fire or sparks in the extremely dry climate. At present ammonium nitrate dynamite is favored because of its superior handling qualities and its adaptability to the dry condition found in 90 pct of the mine. In wet holes, which are found only in the lowest bench of the pit and account for the remaining 10 pct of the ground to be broken, Nitramon in 8x24-in. cans, or ammonium nitrate dynamite packed in 8x24-in. paper cartridges, is being used. This latter explosive, which is protected by a special antiwetting agent that makes the cartridges resistant to water for about 24 hr, currently is considered the best available for the work and is preferred over Nitramon.

Early churn drill hole shots detonated by electric blasting caps, one in each hole, gave trouble because of misfires caused by the improper balance of resistance in the electrical circuits. Primarily, it was of vital importance to effect an absolute balance of resistance in these circuits, the undertaking and completion of which invariably caused delays in the shooting schedule. Misfires resulting from the improper balance of electrical circuits, or from any other cause, were extremely hazardous, since holes had to be unloaded or fired by the insertion of another detonator. The advent of cordeau, later followed by primacord, corrected this particular difficulty and therefore reduced the possibility of missed holes.

After much experimentation, the blasting practice evolved into single row, multihole shots, with the holes spaced 4.5 to 5 m center to center in a row 7.5 to 8 m back from the toe. Such shots were fired from either end by electric blasting caps attached to the main trunk lines of cordeau or primacord. The detonating speed of cordeau or primacord gave the practical effect of firing all holes instantaneously.

Double row and multirow blasts, fired instantaneously with cordeau or primacord, proved to be unsatisfactory in the type of rock found at Chuquica-

---

G. S. WYMAN, Member AIME, is with the Chile Exploration Co., Chuquicamata, Chile.

Discussion on this paper, TP 3261A, may be sent to AIME before April 1, 1952. Manuscript, Oct. 2, 1951. New York Meeting, February 1952.

mata. The relatively high powder factor required to give anything like suitable breakage caused excessive back break, which in turn made drilling for subsequent shots difficult and in some cases made a satisfactory length of toe impossible to obtain on the next shot drilled. In cases where holes were drilled with an excessive toe, hard bottom invariably developed. Toe holes shot with the main blast were an expensive expedient used to correct the condition. Double row as well as multirow shots generally produced a large proportion of oversize material, which in turn caused excessive secondary blasting and poor shovel efficiency.

Loading sheets for all blasts were made up in the engineering office. These generally called for a large bottom charge extending from the bottom of the hole (1 m below grade) to a short distance above grade. One or more deck charges of smaller size were placed in the barrel of the hole. Hole size varied greatly, but in general it can be said that the comparatively small 6-in. diam holes used in earlier blasting were replaced by larger holes to eliminate insofar as possible the need for springing pockets at the bottom of holes.

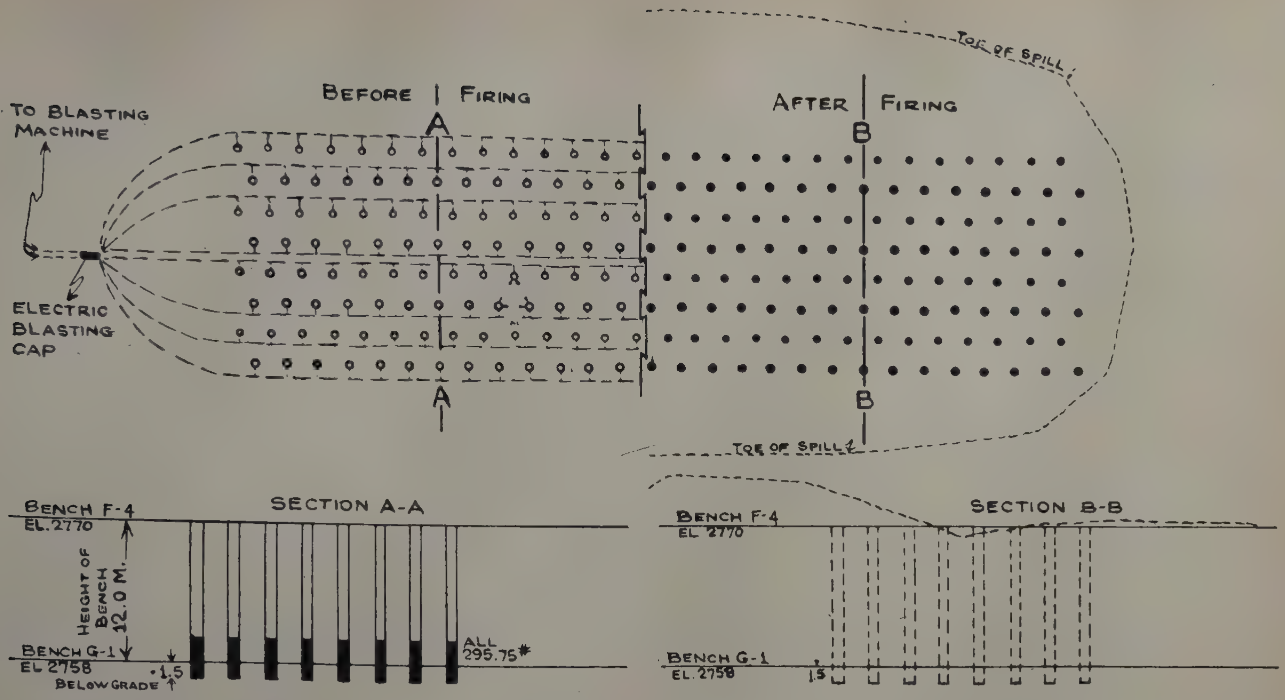

Shot No. 23 G-1 (Eight rows)

No. of holes	224	Between rows, m	3.12
Length of shot, m	99x21.9	Drilled below grade, m	1.5
Diam of holes, in.	9½	Tons broken	111,747
Toe, m	none	Tons broken per ft drilled	11.44
Spacing, m	3.6 m equilateral	Tons broken per lb explosive	1.69

Fig. 1—Eight rows of churn drill holes all fired instantaneously, using primacord throughout.

New benches were developed by thoro-cut shots, also known as box-cut shots, 100 m long by 21.8 m wide. The blastholes were spaced 3.6 m center to center in rows 3.12 m apart, and the holes were staggered in the rows, thus giving an equilateral triangle pattern of 3.6 m a side. A shot of these dimensions required approximately 210 churn drill holes, all of which were fired instantaneously, using primacord throughout, see Fig. 1. These large shots were detonated from two points at either end of the center row trunk lines. The quality of breakage in thoro-cut shots was generally less than could be desired for the best shovel operating conditions, and back break, along with swell over the top rim, caused extra track work because a shovel cut was required around the entire area to allow for drilling the subsequent side shots. The first side shots were drilled before the broken material was loaded to obtain reasonable toe length, but this generally did not allow for drilling at short enough toe distance to give good breakage in these shots so that both thoro-cut and first side shot tonnage had to be loaded under poor conditions.

During 1949 considerable revision of shot layout was made because of the adaptation of the *short toe wide space between holes* pattern of drilling and the use of electric shot timers. A great improvement in fragmentation, as well as less back break resulted from this change. For example, it has been found that rock, which in the past would have been drilled to an 8-m toe with 5-m space between holes, can be broken to better advantage using a 7-m toe and 9-m space between holes with an increase in tonnage broken per foot of churn drilling and at no increase in explosive factor.

In recent years manufacturers of electric blasting caps have developed millisecond delay caps. The use of these caps permits a close rotation, or sequence, in firing. To avoid the necessity of carrying many different interval caps in stock, and also to decrease any probable differences in the time interval inherent in the caps as manufactured, a machine, or timer has been developed that permits blasting with millisecond interval delays when using the ordinary electric blasting caps.

Timers make multirow shots possible with no sacrifice in quality or breakage and with no increase in explosive factor, and at the same time they have the advantageous effect of limiting throw. By the use of timers it has been possible to lay down double row shots in the same bench area formerly required for single row blasts. This gives an advantage to the power shovel because the height of cut during

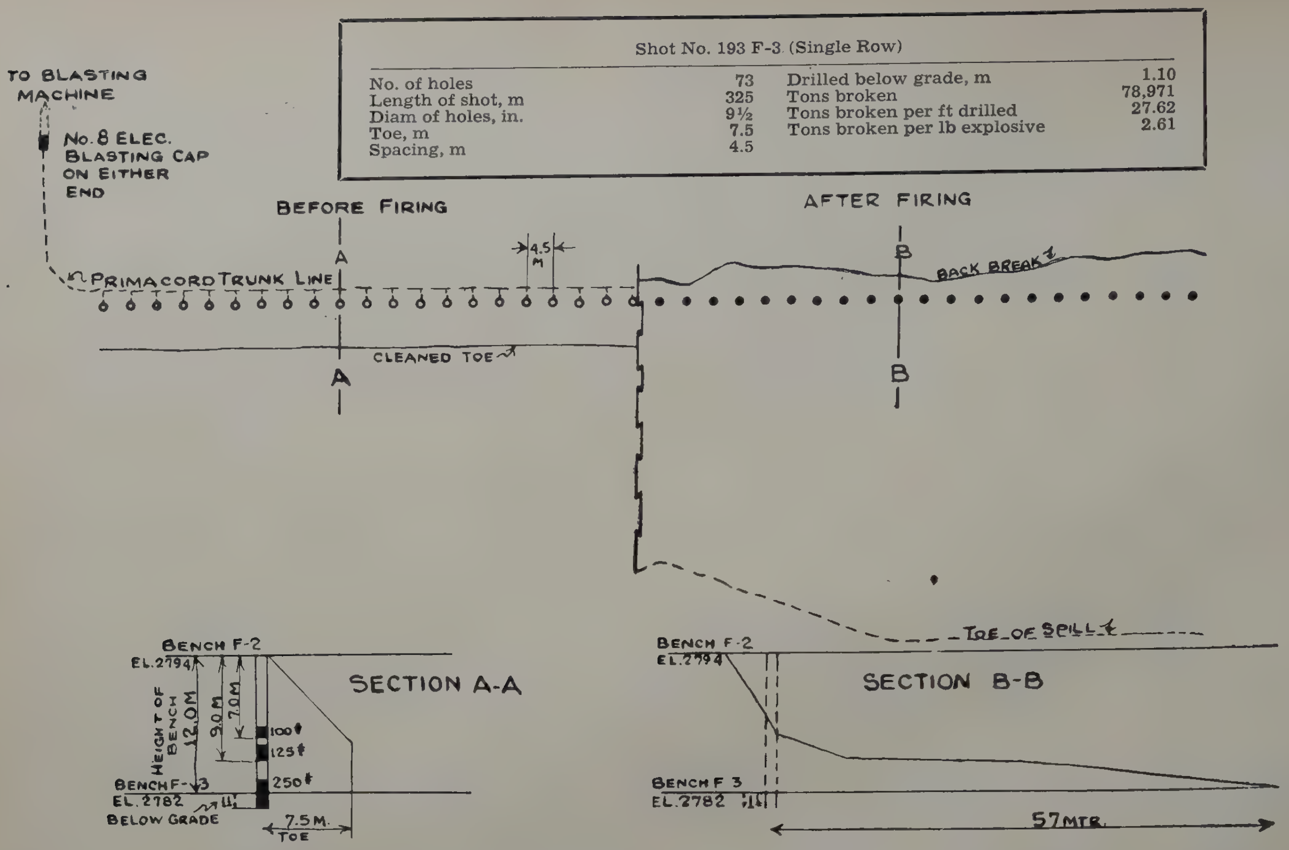

Shot No. 193 F-3 (Single Row)

No. of holes	73	Drilled below grade, m	1.10
Length of shot, m	325	Tons broken	78,971
Diam of holes, in.	9½	Tons broken per ft drilled	27.62
Toe, m	7.5	Tons broken per lb explosive	2.61
Spacing, m	4.5		

Fig. 2—Single row shot, which breaks about 28 tons per ft of hole drilled.

the first pass is greater. The tons loaded for each position of the loading track are increased.

The double row shots fired using four timed circuits have numerous advantages over the single row closely spaced type of shots fired instantaneously. There is a saving in churn drill footage since the single row shot, shown in Fig. 2, breaks about 28 tons per ft of hole drilled while the double row shot, due to wider spacing of the holes, breaks about 47 tons per ft of hole. It will be seen from a comparison between Sections BB of Figs. 2 and 3 that the throw of the single row shot is about the same as the throw of the double row shot measured from the back row, and it is obvious that shovel loading conditions will be superior in the higher cut obtained by the double row shot provided that fragmentation in the two types of shot is equal.

The dynamite factor used in the particular shots shown in Figs. 2 and 3 is actually more favorable in the case of the double row shot, being 2.61 tons broken per lb for the single row compared to 3.16 tons broken per lb for the double row. In general, it has been possible to improve the explosive factor through the use of the short-toe, wide-space, timed circuit type of blasting. Without doubt, some of the possible gain in cost per ton broken has not been exploited to the fullest degree because an attempt is being made to improve overall breakage and thereby improve overall efficiencies of shovel operations. The point at which savings in first cost of breaking ground become real gains through savings in the amount of explosive used is a delicate one. Apparent savings can be dissipated easily in indirect costs brought about by the inferior quality of the broken ground. Such indirect costs are increased secondary blasting, repairs to shovels, and preparation for subsequent blasts in areas where high bottom must be removed before a succeeding shot can be fired. Experiments with explosive factors must be made in locations where changes in the quality of breakage will not have a direct effect on shovel production and at times when total mine tonnages are not of paramount importance.

A single failure in an ore area may have a direct effect on copper production and this loss, coupled with the cost of extra labor and material expended in handling poorly broken ground with power shovels, can overbalance savings made through reduced explosive cost.

To insure against misfires due to broken or cut primacord trunk lines, good practice has dictated the use of electric blasting caps at both ends of each line. In adhering to this procedure while using a single timer, certain difficulties were encountered. For example, in firing a double row shot, alternate holes of each of the two rows were connected to separate circuits by employing four primacord trunk lines. The average double row blast is 350 m long, consequently the use of duplex electric leading wire the full length of the shot for each circuit, plus damage caused to these leading wires by flying rock, proved both costly and time consuming. The complicated electrical connections invited errors because it was difficult to check circuits between the ends of long shots.

Current practice at Chuquicamata calls for the use of two synchronized timers, one placed at either end of the shot to be fired. Power for both timers is supplied simultaneously from a common source through one duplex leading wire running the entire length of the shot. The circuits from the holes to the synchronized timers thus are shortened and consequently are easier to check. This makes for less chance of error when connecting up and thereby decreases the possibility of misfires. To insure perfect results when using more than one timer in the

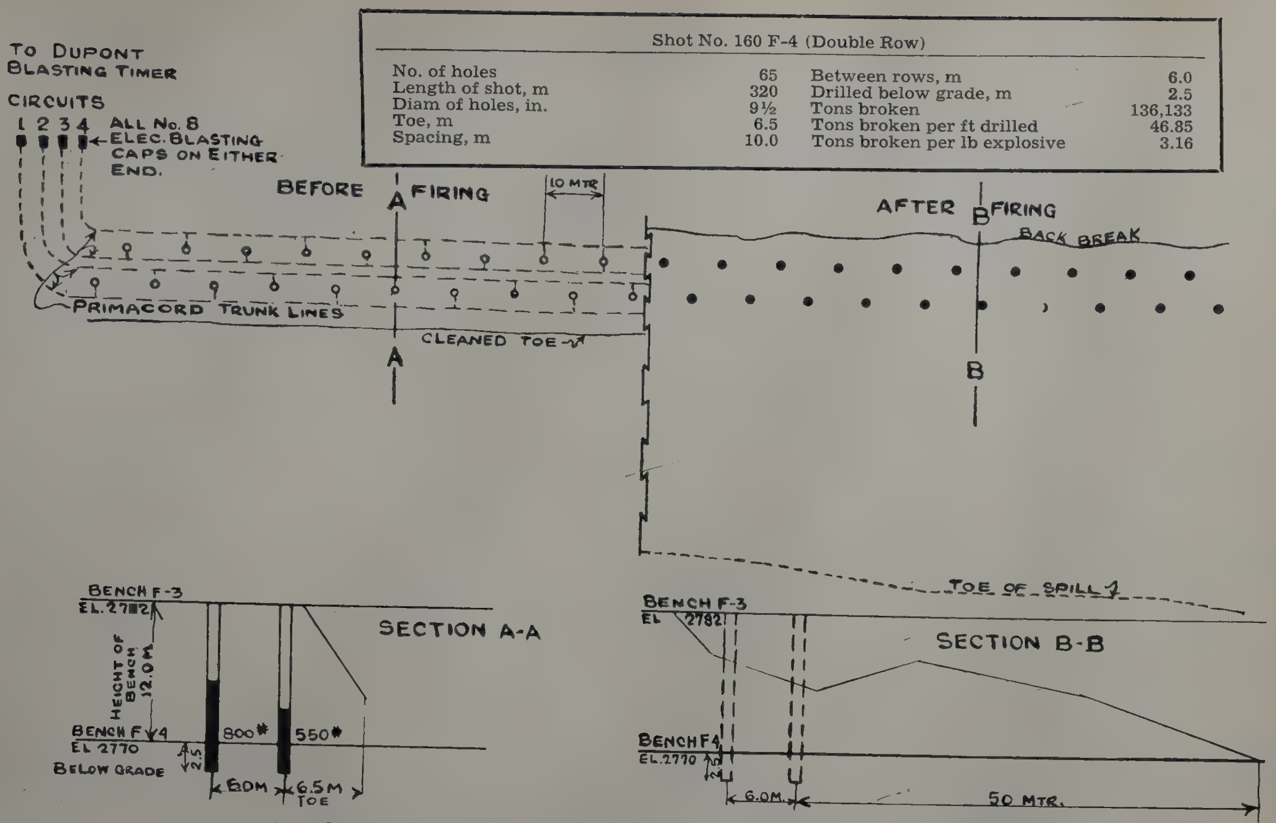

Shot No. 160 F-4 (Double Row)

No. of holes	65	Between rows, m	6.0
Length of shot, m	320	Drilled below grade, m	2.5
Diam of holes, in.	9½	Tons broken	136,133
Toe, m	6.5	Tons broken per ft drilled	46.85
Spacing, m	10.0	Tons broken per lb explosive	3.16

Fig. 3—Double row shot, which breaks about 47 tons per ft of hole drilled.

same shot, it is necessary to check the synchronization of the timers so that there will be no possibility of any time lag between the two units.

A great advantage is gained by shooting multirow shots, three and four rows, in areas that are to be worked by motor truck haulage, because sufficient floor space for turning the large 30-ton units is achieved with the first shot on the bench. On benches where the operations have been such that floor space had to be sacrificed or reduced to a minimum and subsequently must be regained, multirow shooting reduces the amount of overcasting to be done by the shovels in providing space for laying the railroad track.

Thoro-cut shots are made in the solid floor of the bottom of the pit to develop new benches. After the first 150-m block is broken by shots drilled to a pattern similar to that described above, the cut is advanced by smaller shots consisting of four rows of holes in which the holes are spaced 7 m center to center and the rows are 7 m apart. These shots are fired in conjunction with side shots in which the holes are drilled 10 m center to center and 9 m back from the toe, see Fig. 4. This has been made possible by the timers and has resulted in better broken ground with a consequent reduction in cost due to a greater number of tons broken per foot of hole and a greater number of tons broken per pound of explosive.

The advance of a thoro-cut by means of the old system where the holes were spaced close together required considerable preparation before drilling could be started, since each shot had a tendency to swell and spill over on the sides, as well as at the ends. This spillage had to be cleaned off before side shots could be drilled and before loading tracks could be put in position.

With the new type of blasting, four rows at a time, there is a limited back break and a minimum amount of work is required to permit drilling the side shots and placing the loading track in position. Fragmentation is improved greatly, thus increasing the shovel loading rate and decreasing the amount of secondary blasting required. Figs. 1 and 4 show the two types of shot and also indicate the order in which the circuits are connected to the timers.

Fig. 2 shows a representative single row blast fired instantaneously, in which the holes are drilled 4.5 m center to center in a row 7.5 m back from the toe. All holes are drilled 1.1 m below grade.

Fig. 3 shows a double row blast fired by the use of four timed circuits. In this case the holes are drilled 10 m center to center, in a row 6.5 m back from the toe. The second row is drilled 6 m back of the first, and all holes extend 2.5 m below grade. From a comparison of Section AA on Figs. 2 and 3, it will be noted that deck charges used in the single row shot are eliminated in the double row shot. This is because the charge per hole, due to the greater burden, is large enough to rise well up into the hole and thus take the place of the deck charges. This feature simplifies the loading operation in the field and reduces labor on the shot.

At present, preparations are being made to allow for drilling a large percentage of the total footage in 12-in. diam holes, rather than 9½-in. diam, which is the size now generally in use. As ground in different sections of the mine varies in breaking characteristics, experiments with even wider spacings than the 10 m shown on Fig. 3 are being made. A shot on Bench B-1 is being drilled to an 8.5-m toe with 12-m space between holes and 8 m between rows. The 12-in. diam holes will take the comparatively large charges required by this wide spacing without excessive rise of the explosive in the column of the holes. From previous blasting experience in this area good breakage can be expected. The breakage per foot of churn drill hole will be raised from 47 tons for a double row shot as shown on Fig. 3 to 61 tons at this increased spacing. As

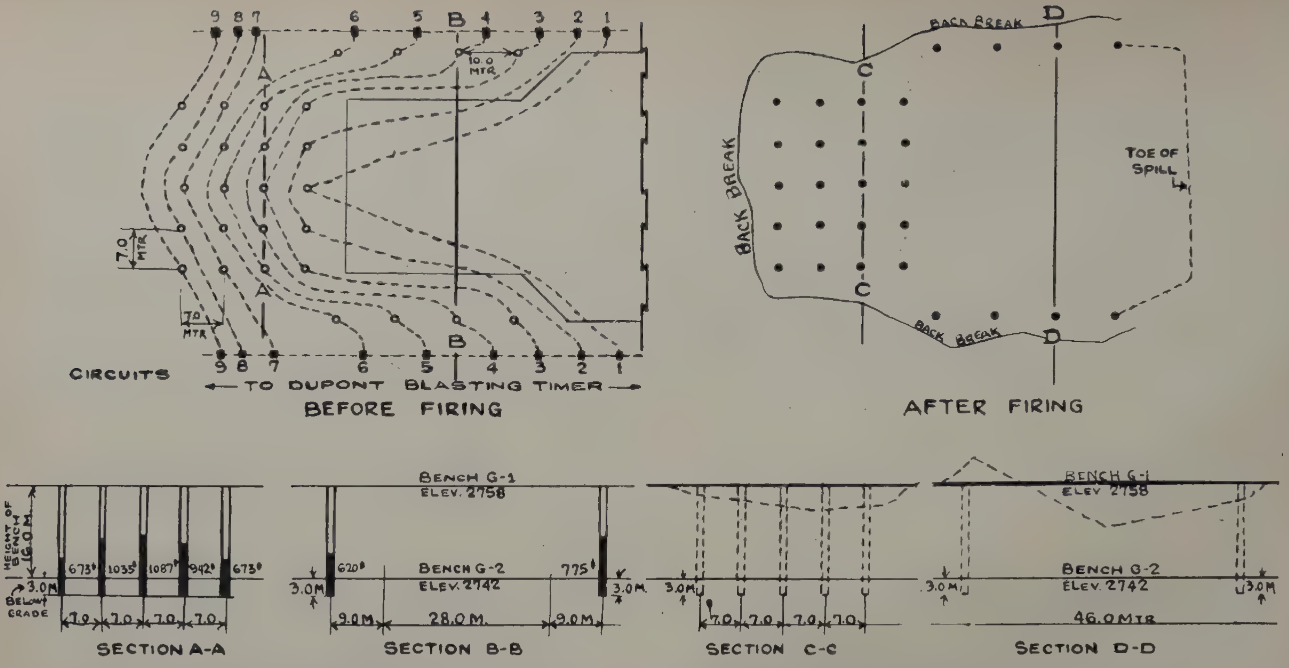

Shot No. 20 G-2 (Four Rows)	20G-2"A"	24G-2"A"	Shot No. 24 G-2 (One Row)	20G-2"A"	24G-2"A"
No. of holes	20	8	Between rows, m	7.0	—
Length of shot, m	28x28	80	Drilled below grade, m	3.0	3.0
Diam of holes, in.	9½	9½	Tons broken	39,034	25,737
Toe, m	7.0	9.0	Tons broken per ft drilled	33.70	51.98
Spacing, m	7.0	10.0	Tons broken per lb explosive	2.33	3.62

Fig. 4—Four row shot fired in conjunction with side shots.

spacing is widened, the charge for a given churn drill hole becomes greater so that larger diameter holes are required to give suitable concentration at the bottom of the hole and to keep the column of explosive within reasonable height limits.

Experience tends to show that changes in length of toe produce a direct effect on the fragmentation, tendency to leave hard bottom, and general quality of breakage, a great deal quicker than changes in width of spacing. In other words, an increase of ½ m in the length of toe, see Figs. 1-4, shows detrimental effects from several viewpoints such as high bottom, excessive back break and general blockiness of the material broken while a change in spacing between holes of as much as 1 m in any given type of rock has shown no detrimental effect. The indication seems to be that there is a possibility of using even wider spacing between holes without sacrificing the quality of breakage and thus further increasing the tons broken per foot of churn drill hole. In hard and medium hard sections of the mine the size of the explosive charge that could be loaded in a 9½-in. churn drill hole limited the width to which spacings could be extended. Drilling with 12-in. tools will allow continued experimentation with hole spacings.

The successful substitution of paper casing for steel casing in the collars of the holes has resulted in a considerable saving. Experiments with quick-setting cement around the starter pipe indicate that there may be great possibilities in the use of this material and may result in holes being protected at even lower cost than is now done with paper casing. In certain sections of the mine raveling ground will require the use of some casing, but there is a possibility of lower costs by reducing casing consumption.

There is a question as to the most suitable delay period between circuits for the different shot layouts. The large majority of blasts fired at Chuquicamata with the electric timers have been with delays of 0.018 sec between circuits. Several also have been shot at 0.024-sec delay. The higher delays are probably more desirable as an aid in starting the holes of the first circuit in motion, thus furnishing relief for the holes of the next circuit. In formations free from cracking there seems to be little doubt that the higher delay periods will give the best results. The danger of cutoff holes becomes great in cracked or bedded formations, and while practically no missed holes have been encountered when using 0.018-sec delay period, there have been some holes cut off in shots where 0.024-sec delay periods were used. The electric timers are powered by 60-cycle motors and designed to give 0.010, 0.015, 0.020 and 0.025-sec delay intervals. Power in use in Chuquicamata is 50 cycle, and therefore the intervals mentioned above are changed accordingly.

The use of the timed circuit type of blasting becomes a separate study for each type of rock to be broken. There is little or no chance of cutoff holes in areas of little bedding or with few slips in the formation at any of the delay periods possible with the timing machine. In certain areas of the pit the rock is more difficult to break than in others, and in these areas slips and bedding are usually more pronounced. Therefore, the higher delay intervals are not considered practical, and while the higher delay intervals would no doubt produce better broken ground, they are not used because of the possibility of cutoffs and consequent misfires.

In conclusion, it can be stated that great advantage has resulted from the use of the short-toe, wide-space, churn drill hole pattern of shot layout in double or multirow blasts that are made practical by the millisecond delay intervals available with the electric motor-driven millisecond timing machines. There is still room for continued experimentation with the promise of improved quality of breakage and lower costs in Chuquicamata.

Solid Surface Energy and Calorimetric Determinations Of Surface-Energy Relationships for Some Common Minerals

by A. Kenneth Schellinger

THE terms *surface tension* and *surface energy* are well known when applied to liquids and are generally described by referring to the excess energy of the air: liquid interface as a result of unsaturated molecular forces surrounding the surface molecules of the liquid due to the presence of the air phase on one side. Such unbalanced forces produce the familiar water droplet of spherical form and are generally summed up as a surface tension measured in dynes per centimeter which can be shown mathematically to be equal numerically to a corresponding surface energy expressed in ergs per square centimeter. A specific surface energy, however, is best thought of as the energy necessary to produce one unit of new surface on a substance. Hence, in producing a bubble in a flotation cell the impeller must supply surface energy corresponding to the air: liquid interfacial area on the interior of the bubble. Inasmuch as it is relatively easy to extend or contract the surface of a liquid, there are a number of successful methods for liquid surface tension, or energy, measurement based upon surface deformation. This happy state of affairs does not, however, extend to solids, which are considered to possess surface energies for the same reasons as do liquids, i.e. because of unsaturated ionic bonds at the solid: gas interface.

As in the case of the flotation cell producing surface on liquids as new bubbles, it takes energy to produce new surface on solids as new particles. As every mill man knows, this surface is produced on mineral solids in a grinding mill by the action of a tumbling mass of iron balls. But here so much energy usually is wasted by the inefficient action of these balls that a large amount of heat is generated, and the surface energy production may be easily confused with the energy necessary to produce this ineffective heat. The tumbling balls and fracturing minerals ultimately take their energy from a rather large electric motor. It has been variously estimated that from 10 to 20 pct[1-3] only of this energy from the motor does not appear as heat and may be presumed to appear as surface energy on the minerals present. Such a production of new surface on the mineral phases is accompanied, of course, by a size reduction that is inevitable as more and more mineral interior molecules become surface molecules by the fracture exposure. This size reduction of mineral particles, although the most obvious feature and perhaps the sole object of the milling operation, is from this energy viewpoint the outward manifestation of the production of surface energy only.

Measurement of the characteristic surface energies of pure minerals and their various mixtures in ores would be a step towards understanding of the energetics of the commercial grinding operation. In addition, the characteristic surface energy of a mineral is probably a physical property specific for that mineral, and therefore, from a scientific standpoint, should be measured. It is interesting to note that, in contrast to the large body of work on the surface tensions of liquid systems and biological systems, the field of solid surface energies has been neglected. Prior to 1920 it is difficult to find more than one or two references to work on solid surface energies in *Chemical Abstracts*. Since 1920 such references number somewhat less than 100, while those on liquid systems are numbered in the thousands.

Much of this apparent neglect of the field of solid surface energies (the term is intended to be somewhat inclusive at this point and refers both to the solid: gas, and the solid: liquid interface) is because of the lack of a reliable method of measurement rather than any lack of scientific curiosity. It was, and still is, difficult to produce new surface on a solid without the simultaneous production of interior changes in the same solid which may consume part of the energy used. The extension in the surface area can be measured, but the interior crystal-

---

A. K. SCHELLINGER, Member AIME, is Metallurgist with the U. S. Bureau of Mines, College Park, Md.

Discussion on this paper, TP 3223B, may be sent (2 copies) to AIME before May 30, 1952. Manuscript, Feb. 8, 1951. Revision, Oct. 1, 1951. St. Louis Meeting, February 1951.

This page of Mining Transactions AIME follows p. 304. The intervening non-Transactions pages appeared in Mining Engineering.

Fig. 1—Components of the grinding calorimeter.

lographic changes are more subtle and not so susceptible to measurement. Experimental methods that have been used to determine the surface energies on solids include:

1—The production[4] of a balancing effect between a weight and the surface tension of a vertical fiber of the amorphous solid used to suspend it in space. Surface tensions of pitch and glass were thus found to be in the neighborhood of the measured value for water, about 72 dynes per cm.

2—A method based on the use of the Gibbs-Thomson[5] derivation:

$$RT\ln X_s/X = 2MY/rd$$

where, X_s is the enhanced vapor pressure of very small ($<1u$) particles. X is the vapor pressure of a flat surface of the same solid. M, Y, r, and d are molecular weight, surface tension, radius and particle density respectively. Measurements[6] of vapor pressures and particle radii were made for some oxide and carbonate salts, which yielded calculated values for their surface tensions of 100,000 to 750,000 dynes per cm. These values have been looked upon as high by other workers in the field but check in order of magnitude those values found through grinding experiments.

3—A method based upon measurement of the heat[7, 8] of solution of a soluble salt such as NaCl. Measurements made by this method range from about 400 ergs per cm² for NaCl to more than 8000 for $Mg(OH)_2$.

4—A solubility method based on a derivation from the Gibbs-Thomson equation given under 2. It was found that the very small particles of a soluble solid have a higher solubility than the larger due to the increased surface energy of the former. Dundon[9] used this method to obtain the surface energy of $BaSO_4$-1250 ergs per cm² and that of CaF_2-2400 ergs per cm².

In addition to such direct attempts at measuring solid surface energies, some physicists have made calculations of surface energies of solids based on ionic field theory. Alkali halides, which have space lattices made up of two kinds of ions alternately arranged, lend themselves particularly to this type of calculation. Madelung, Born, Stern, Biemuller[10] and others have found values ranging from 100 ergs per cm² for NaI to 417 ergs per cm² for NaF by considering the lattice as an array of point charges in space interacting directly and indirectly as dipoles, quadrupoles, etc. Such calculated values for solids were found on comparison to the measured molten values for the same salts extrapolated to the same temperature to be only slightly higher.

Edser[11] used known physical constants of solids (compressibility, thermal expansion, and density) to estimate surface energies for quartz and pyrite, obtaining values of 920 and 1175 ergs per cm², respectively. These values in addition to being lower are reversed in magnitude from the finding of investigators in the field of comminution.

Interest in the surface tensions of metals has led to a number of calculations and measurements on these ductile solids. Tammann and Bohme measured the surface tensions of gold strips and thus assigned pure gold a value of about 1600 dynes per cm at room temperature. Recently, Udin, Shaler, and Wulff[12] used a somewhat similar method to determine the surface tension of solid copper and so obtained a value of about 1800 dynes per cm at room temperature. Fricke[13] developed an equation for calculating the specific surface energies exposed on certain planes of atoms in solid metals. His calculated value for the (111) plane of solid copper was 2535 ergs per cm² at absolute zero. This value is not unreasonable when compared with the measured value of 1800 at room temperature, inasmuch as the temperature coefficient would lower Fricke's value somewhat. Incidentally Fricke also calculated a value of 3696 ergs per cm² for the (001) plane of Ni, and one of 3980 ergs per cm² for the same plane of atoms in alpha Fe.

Such values for ductile, soft metals such as copper and gold are seen to be higher than those estimated for hard substances such as quartz and pyrite. This situation is not only contrary to experience but is not very likely to be valid. In any case no direct measurement of the surface energy of quartz, a common ore mineral, has been reported as such, although Edser's value[11] is not the only estimate that has been made. Sutherland,[14] in a recent review of the topic of solid surface energies, sums up the situation by saying "the lack of precise data on the surface tension, or total surface energy, of a solid is a real hindrance in the study of processes such as catalysis, adsorption and cohesion, and it leads to even greater difficulties in dealing with still more complex problems such as crushing and grinding."

The Grinding Calorimeter

A grinding calorimeter shown in Figs. 1 and 2, described in a previous paper,[2] was designed to give an accurate measure of all of the heat energy output from a small tumbling mill using cast-iron shot as the grinding medium. The kinetic energy input was obtained from a special recording torquemeter that indicated the net torque exerted continuously by the tumbling mass. Suitable calibrations and precautions, such as the use of an air thermostat container, gave an instrument capable of a balance of unloaded energy input against heat energy output within a fraction of a percentage. Here, with only the cast-iron shot in the tumbling chamber, the kinetic energy input was changed completely to

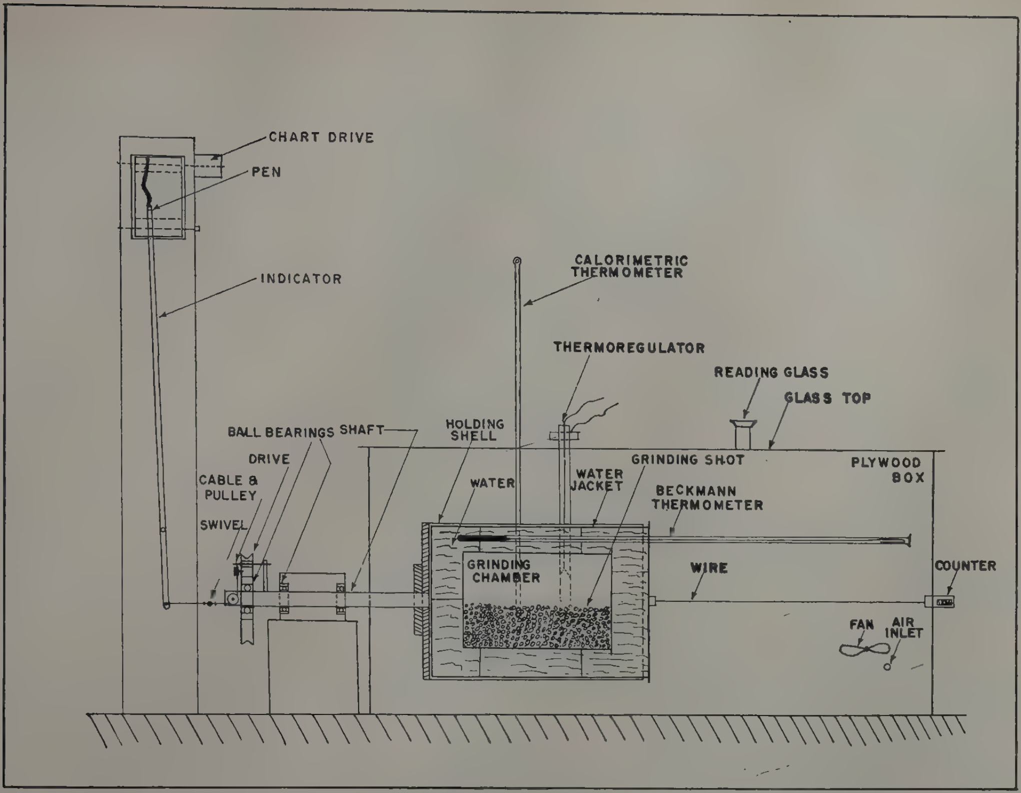

Fig. 2—Assembled grinding calorimeter.

heat energy by collision and by frictional rubbing. The resultant heat energy passed into the water jacket surrounding the tumbling chamber and caused a temperature rise on a Beckmann thermometer immersed therein.

Introduction of several hundred grams of a brittle material, such as quartz sand, into the tumbling chamber upset this energy balance to the extent of some 10 to 20 pct. That is, the output heat energy was less than the input kinetic energy by this percentage of the input. It seemed reasonable to postulate that this disappearance of energy was caused by the creation of surface energy within the tumbling chamber—an energy absorption from the tumbling system. This quantity of energy was then taken as the total created mineral surface energy in calories. To translate this total into a specific energy figure for the mineral, it was necessary to measure the extent of the surface created during the absorption of a given amount of energy. This was done by the use of the BET method of gas adsorption isotherms, a method which has found wide application in recent years.

Surface Area Measurement

The surface, or air: mineral interfacial area, produced on the mineral while grinding in the calorimeter tumbling chamber was similar to that on any ground mineral. That is, it probably consisted of cleavage planes, incipient cracks, re-entrant angles, peaks, and valleys, and corners, all on a submicroscopic scale. Methods for estimating the area of this surface are numerous, but generally are of low accuracy. Many of them are based upon a plotted sizing analysis of the ground mineral from which a mathematical expression giving the size distribution is derived. An assumption as to regular geometric shape followed by a suitable correction factor, designed to allow for irregularities, produces a calculated figure for the surface area which may or may not be within 100 pct of the true value. Such methods obviously must fail where the material is porous or of a very irregular shape. More direct methods depend upon the particles interfering with transmitted light, or upon the surface film of fluid which forms on all solid: fluid interfaces resisting the passage of the main body of fluid through a mass of the particles. This latter method, or permeability method, is capable of yielding rapid results after proper calibration, but pores and cracks in particles are not taken into account during the surface measurement, especially if present on atomic dimensions. A tedious method for homogeneous material based on Wenzel's law, which says that initial solution rate is proportional to total surface exposed, is capable of giving accurate results if proper calibrations are made and a suitable solvent is found for the material.

The discovery of monolayer and multilayer adsorption of gas molecules at low temperatures on solid surfaces in contact with the gas phase led to newer methods of estimating the area of such solid surfaces. The most successful of these methods, known as the BET, was developed by Emmett,[25] Brunauer, and Teller some 15 years ago and was later applied to minerals by Gaudin and coworkers.[16] This method was based upon a firm theoretical derivation which yielded an equation that checked experimental work in a satisfactory manner.

The BET theory and derived equation make it possible to calculate the volume of gas going to make up the monolayer by plotting functions of pressures and volumes as parameters to obtain a straight line whose slope is proportional to the volume condensing as the monolayer, see Fig. 3. Such a straight line is widely regarded as verification of the multilayer adsorption mechanism. Furthermore, it can be obtained rather easily with a large num-

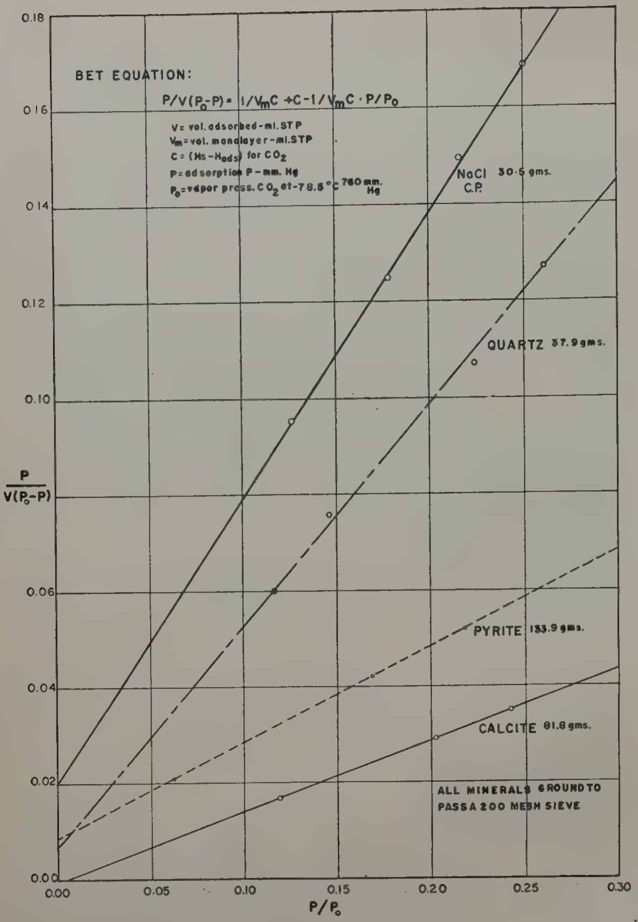

Fig. 3—BET plots of CO_2 adsorption runs on various mineral powders.

ber of solids and gases, provided a suitable measurement apparatus is used, see Fig. 4. Although objections can be found to this method of surface measurement on fine particles, time has confirmed the validity of the method by a large body of comparison data which seems consistent. As it is generally accepted as giving the closest approximation to the true interfacial area of fine irregular mineral powder obtainable at present, it was used in this experimental work on mineral surface energies.

Nitrogen gas, adsorbed at liquid nitrogen temperatures, is generally used as the measuring gas, or adsorbate, for measurement of the surface on mineral powders. Emmett, in his original work on the BET method, reported adsorption isotherms obtained with a number of gases on several different substances such as oxide catalysts and carbon blacks. All of these isotherms were of the S-type and conformed to the BET theory and equation. One of the gases used was carbon dioxide at the sublimation temperature of dry ice (—78.5°C). Dry ice, in contrast to liquid nitrogen, is readily available, comparatively inexpensive, and easy to handle. For this reason medical CO_2 was chosen as the adsorbate, or measuring gas, in this work on mineral surface energies. Good isotherms, and BET plots, were obtained on all minerals investigated. Fig. 3 illustrated BET plots for CO_2 adsorbed on quartz, salt, pyrite, and calcite. As far as the author knows, this is the first use of CO_2 as a measuring gas for surface areas in mineral work; no special advantages other than those mentioned above are claimed for this gas, although it seems to give just as satisfactory results as nitrogen.

Calibration of the method was attempted by several procedures, although the BET method theoretically needs no calibration. Gaudin and Bowdish[16] found that they could check the calculated surface on carefully prepared glass beads by their nitrogen gas method if solid-type packing of the adsorbed molecules was assumed. Other investigators had found also that solid-packing molecular areas seemed to check more closely with areas deduced by other methods than did liquid-packing molecular areas. The calculated solid-type molecular area of one CO_2 molecule is 14.1 sq Å and was used as the basic area unit in the present experimental work.

The present BET adsorption measurements with CO_2 gas at —78.5°C were compared with surface area measurements made by the air permeability method, by the HF dissolution method of Gross and Zimmerly, and by a sizing analysis made with a Roller air analyzer. A standard Portland cement powder, No. 114f, of the Bureau of Standards was used first. The BET method with CO_2 gave a surface area of 3770 sq cm per g as compared with the 3230 reported by the Bureau as obtained by the Blaine air-permeability method. Sized quartz sand between 65 and 100 mesh and also —200 mesh was run by the dissolution method of Gross and Zimmerly[17] with hydrofluoric acid as the solvent. Their calibration factor of 170 was used to convert initial dissolution rate (IR) to specific surface area. This factor had been worked out by means of a silver plating technique on a large regular shape of quartz. Areas obtained by the dissolution method and the corresponding areas obtained by the BET adsorption technique were as follows:

	Dissolution	BET CO_2	BET Ethane (18)
—200 mesh quartz	2460 cm^2/g	1890 cm^2/g	
—65 + 100 quartz mesh	374 cm^2/g	310 cm^2/g	286 cm^2/g

Experimental Procedure

Combination of the calorimetric energy determination technique[2] and the BET surface area measurement technique promised to give further experimental data on surface-energy relationships in the comminution of common minerals. Techniques[17, 19] for obtaining such data on a number of minerals had been published somewhat earlier. However, these earlier methods had employed drop-weight crushers for energy measurements. Plots of new surface produced versus the energy input held responsible for that surface had resulted in straight lines passing through the origin of such plots. Each straight line represented a different mineral and had a unique slope. This characteristic slope, termed the Rittinger coefficient of the mineral, can also be thought of as the surface energy of the mineral if one accepts the premise that substantially all of the absorbed energy goes to new surface rather than to heat production and to the production of internal lattice rearrangements in the mineral. Such plots, originally presented by Gross and Zimmerly[17] were also adopted by the author to derive the surface-energy relationships for quartz glass sand, crystalline NaCl, specimen-grade pyrite, and specimen-grade calcite.

In general, the same experimental procedure was used for each mineral. The coarse mineral was ground in a pebble mill, which was lined with por-

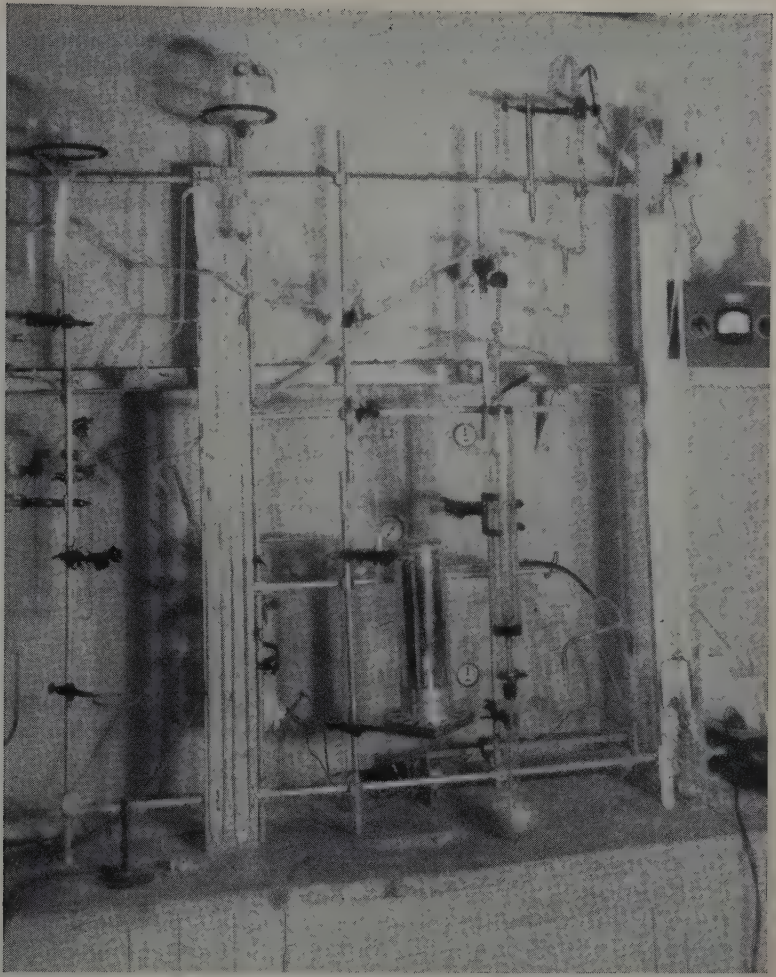

Fig. 4 — Adsorption apparatus for surface area measurement with CO_2 gas.

celain and charged with Danish flint pebbles, until it passed a 200-mesh sieve. After mixing the sieved mineral thoroughly on a mixing cloth a large sample was taken at random and enclosed in the adsorption tube, see Fig. 4, for a surface area determination. This sample ranged from 50 to 150 g of the powdered mineral, dependent on the specific gravity and size. The total surface on the mineral charge was determined by use of the BET method with CO_2 as the adsorbate. Reproducible area determinations were easily made on mineral samples that had been passed through the 200 mesh sieve. A standard 300-g charge of the mineral was placed in the grinding chamber of the calorimeter with about 3000 g of chilled cast-iron shot. A calorimetric run was then made on the material, and the energy absorption due to the creation of surface energy was calculated. This procedure has been described in an earlier paper.[2] The net quantity of energy absorbed as surface energy could be varied by changing the time of the run. Each calorimetric run, then, corresponded to one point on the surface-energy plot.

The ground charge was removed from the calorimeter chamber and screened from the shot, mixed thoroughly, and a large sample used for another surface determination in the BET apparatus. The net surface produced in the calorimeter then was obtained by subtracting the total surface charged to the chamber from the total surface discharged from the grinding chamber. This net figure was used as the surface parameter on the surface-energy plot.

The experimental points resulting from the foregoing procedure are plotted as Fig. 5. Energy was converted to ergs as this is the commonly used unit for surface energies, although it is inconveniently small in the case of solids. Surface area is, of course, in square centimeters. The figure presents the points for each mineral averaged as a straight line. The slope of each of these lines is the surface-energy relationship, or the surface energy within the assumptions outlined, of the mineral concerned. These relationships then can be summed up numerically, as follows:

Mineral	Ergs per Cm^2	Moh's Hardness No.
Quartz	107,000	7
Pyrite	60,000	6
Calcite	32,400	3
Halite (C.P. NaC1)	26,100	2.5

The order of arrangement and magnitudes are seen to be in substantial agreement with the hardness of the minerals on the well-known Moh's scale with the exception of quartz. Moh's scale, devised at least a century ago, assigns a maximum value of 10 to diamond as the hardest known substance and has been criticized as nonlinear on the grounds that diamond should be assigned a much higher value, in conformity with its actual hardness.

The method of averaging the points on the surface energy plot is thought to give a more accurate figure for the final surface energy relationship shown by each mineral than could be obtained by adding separate determinations and dividing by the total number. The origin of the plot is thought to be a significant point in the determination. With a brittle

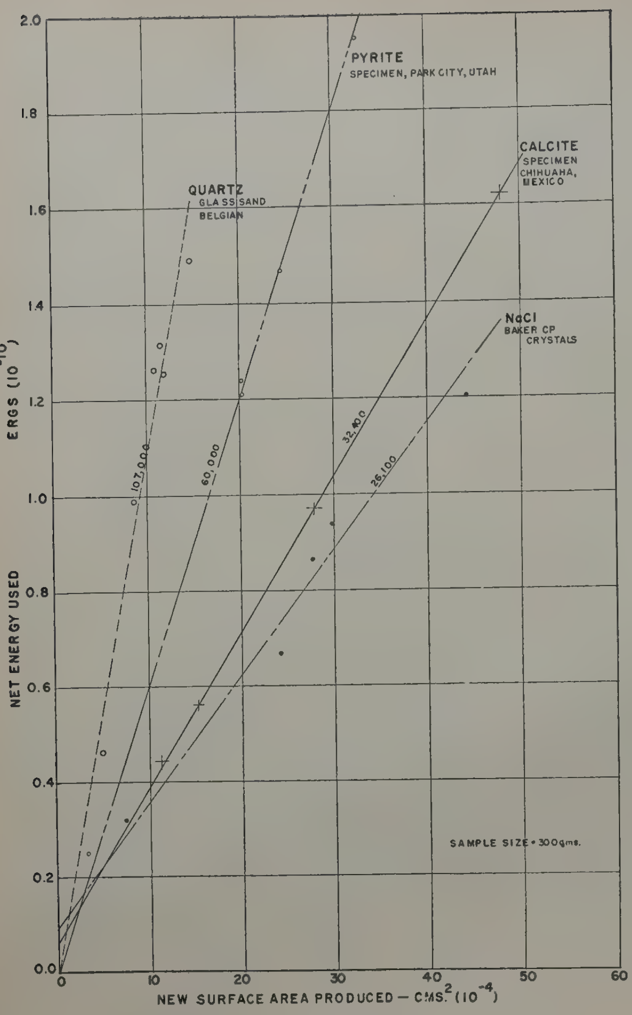

Fig. 5—Surface energy plots for quartz, pyrite, calcite, and NaCl.

mineral, such as quartz, unless the scales used for both the energy units and surface units are quite detailed, the surface energy line should normally pass through the origin or quite close to it. This would not be true if the mineral were ductile, that is, absorbed considerable energy by the internal processes of twinning and gliding for this energy then obviously would not show up as new surface. The surface energy line would be expected to intercept the energy axis somewhat above the origin, as indeed the lines do in the cases of NaCl and calcite, two minerals which have been found to exhibit ductile behavior in other investigations. The intersection shown in Fig. 5 for NaCl is about 10^9 ergs or, on the basis of a constant 300 g of sample, about 3.3x10^6 ergs per g. Such a figure would represent the maximum energy stored during work hardening of the NaCl crystals during grinding. It is interesting to note that copper and brass, ductile metals, store approximately ten times this amount (about 3x10^7 ergs per g) as cold work prior to fracture. Therefore the energies of lattice dislocation stored by calcite and halite as shown by the present calorimeter investigations are at least in qualitative agreement with previous experience. Quartz and pyrite were much too brittle to show other than a direct passage of the surface energy line through the origin of the plot in each case.

As was mentioned earlier, experimental data on the surface energies of solids in general and of mineral solids in particular are not numerous in the literature. Much of the work on minerals has been derived by the use of the drop-weight crusher for energy measurements and a variety of methods of estimating the resultant surface production. Most mineral workers do not claim to have measured surface energies directly and yet, for the sake of argument, if the drop-weight crusher is considered to be 100 pct efficient, then the data can be calculated to surface energies, as shown in Table I.

Table I. Surface Energies in Ergs Per Cm^2

Mineral	Present Work	Gross and Zimmerly[17]	Piret, et al[19]	Theoretical
Quartz	107,000	56,000	174,000[a] 89,000[b]	920 (Edser) 520 (Martin)
Pyrite	60,000	43,400	None	None
Calcite	32,400	13,000	92,000[a]	None
Halite	26,100	None	89,000[b]	152 (Biemuller)

[a] Surface measurement by permeability method.
[b] Surface measurement by gas adsorption method.

The divergences shown by the experimental and theoretical data are impressive. No reliable clue has yet been discovered as to why such differences should exist. Certainly it is safe to say that much more work is needed in this interesting field to clear up the existing anomalies. The order-of-magnitude agreement found by mineral workers is a promising start in the direction of clarification of the vital question of the surface energies of mineral solids.

References

[1] A. W. Fahrenwald, G. W. Hammar, H. E. Lee, and W. W. Staley: *Trans.* AIME (1931) , pp. .

[2] A. Kenneth Schellinger: *Trans.* AIME (1951) **190**, p. 522; MINING ENGINEERING (June 1951) TP 3071B.

[3] A. Kenneth Schellinger and Rustam D. Lalkaka: *Trans.* AIME (1951) **190**, p. 523; MINING ENGINEERING (June 1951) TN 78B.

[4] B. Berggren: *Annalen der Physik* (1914) **44**, No. 4, p. 61.

[5] J. W. Gibbs: Collected Works. **1**, pp. 314-328.

[6] J. Krustinson and M. Centnerszwer: *Ztsch. Physik. Chem.* (1927) **130**, pp. 187-192.

[7] O. Maas, S. G. Lipsett, and F. M. Johnson: *Journal* Amer. Chem. Soc. (1927) **49**, pp. 1940-1949.

[8] R. Fricke, Schnable, and Z. Becke: *Elektrochem.* (1932) **42**, pp. 881-926.

[9] M. H. Dundon: *Journal* Amer. Chem. Soc. (1933) **45**, pp. 2658-2666.

[10] J. Biemuller: *Ztsch. Physik* (1926) **38**, pp. 759-771.

[11] E. Edser: Brit. Assoc. Adv. Sci. (1922) 4th Rept. Coll. Chem., pp. 40-114.

[12] H. Udin, A. J. Shaler, and J. Wulff: *Trans.* AIME (1949) **185**, p. 186; JOURNAL OF METALS (February 1949) TP 2530.

[13] R. Fricke: *Naturwissenschaften* (1941) **29**, p. 365.

[14] K. L. Sutherland: Austr. Chem. Inst. *Journal* and *Proc.* (July, 1947) **14**.

[15] P. H. Emmett and S. Brunauer: *Journal* Amer. Chem. Soc., **59**, p. 311.

[16] A. M. Gaudin and F. W. Bowdish: *Trans.* AIME (1946) **169**; MINING TECHNOLOGY (May 1944) TP 1666.

[17] J. Gross and S. R. Zimmerly: U. S. Bur. Mines *RI* 2880 (July 1928).

[18] A. M. Gaudin and R. T. Hukki: *Trans.* AIME (1946) **169**, p. 67; MINING TECHNOLOGY (November 1944) TP 1779.

[19] J. N. S. Kwong, J. T. Adams, J. F. Johnson, and E. L. Piret: *Chemical Engineering Progress* (1949) **45**, pp. 508, 655, 708.

Radiotracer Studies of the Action of Dithiophosphate In the Selective Flotation of Galena and Sphalerite Using $CuSO_4$ and NaCN

by C. M. Judson, A. A. Lerew, R. B. Booth,
J. S. Kennedy, and G. L. Simard

DITHIOPHOSPHATE collectors are commonly used in the flotation of sulphide minerals. Studies of the interaction of a typical dithiophosphate collector with galena surfaces have been previously reported from these laboratories.[1,2] These fundamental studies were carried out by employing phosphorus labeled radioactive dithiophosphate. Radioactivity determinations then could be used to measure readily and accurately the small concentrations of dithiophosphate that are present under conditions of flotation processes. Measurements were made on ground mineral, determining the amount sorbed indirectly from the concentrations in solution; and studies were also made with single crystals, determining the amount sorbed directly by counting the crystal surface. The rates, isotherms and reversibility characteristics of dithiophosphate sorption, the competition between phosphate and dithiophosphate for the mineral surface, and the exchange of sorbed dithiophosphate with dissolved dithiophosphate were studied.

These studies have now been extended by sorption measurements in flotations with a Fagergren machine. For this work, the selective flotation of galena and sphalerite from quartz was chosen, using ammonium di-(sec-butyl) dithiophosphate as the collector, sodium cyanide as depressant for sphalerite, and copper sulphate as an activator for sphalerite. While the selective flotation of galena and sphalerite using a single dithiophosphate collector is not typical of flotation practice (two different collectors are generally used), it was found that a reasonably good separation could be obtained by using zinc sulphate with the sodium cyanide in the galena flotation and by cleaning the sphalerite concentrate or by carrying out the sphalerite flotation in an alkaline medium.

Data of practical importance on the distribution of collector between the concentrates, tailings, and solutions were obtained, particularly with regard to the effect of copper sulphate and sodium cyanide. In addition to the selective flotation of galena and sphalerite from quartz, single flotations of galena-quartz and sphalerite-quartz mixtures were carried out, along with blank flotations on quartz alone. The present paper describes the results of these experiments. As in previous papers, the term sorption is used to designate uptake of collector by the mineral, without implication as to the nature of the processes involved.

Experimental

Materials: The mineral system was a ground synthetic mixture of galena, sphalerite, and quartz. The galena was from Galena, Kans., and contained 75 pct lead (theoretical 85.6 pct Pb for PbS); the sphalerite, from Ottowa County, Okla., contained 63 pct zinc (theoretical 67.2 pct Zn for ZnS); and the quartz from Klondike, Mo., analyzed as 99.97 pct SiO_2.

Sulphur labeled radioactive di-(sec-butyl) dithiophosphate was prepared from S^{35} supplied by the Oak Ridge National Laboratory on allocation from the U. S. Atomic Energy Commission. The synthesis consisted of precipitating barium sulphate, reducing the barium sulphate to barium sulphide, acidifying to form hydrogen sulphide, and oxidizing the hydrogen sulphide with iodine to elemental sulphur.

C. M. JUDSON, A. A. LEREW, G. L. SIMARD, Research Division, J. S. KENNEDY, Member AIME, and R. B. BOOTH, Mineral Dressing Division, are with the Stamford Research Laboratories, American Cyanamid Co., Stamford, Conn.

Discussion on this paper, TP 3306B, may be sent to AIME before May 30, 1952. Manuscript, Oct. 16, 1951. New York Meeting, February 1952.

The elemental sulphur then was combined with phosphorus to form phosphorus pentasulphide, and the ammonium dibutyl dithiophosphate prepared therefrom by the method previously described for the synthesis of the phosphorus labeled compound.[1]

Details of the synthesis were as follows: Carrier sodium sulphate was added to a solution containing 26 g of neutron irradiated potassium chloride in which the chlorine had been transmuted to sulphur. After digesting with hydrogen peroxide, barium sulphate was precipitated in 98 pct yield (534 mg). One half of this barium sulphate was mixed with an equal amount of charcoal (Darco-S-51) and covered with another 100 mg of charcoal, and the mixture was heated to 1100°C under nitrogen for 4 hr. The barium sulphide obtained was heated on a steam bath for 1 hr in a closed system with 30 ml of 3 M hydrochloric acid. The hydrogen sulphide evolved was carried in a stream of nitrogen into two successive traps containing 0.12 M potassium iodide, 0.009 M potassium iodate, and 2.5 M hydrochloric acid. The solution was then boiled for a few minutes to complete the removal of hydrogen sulphide. The excess iodine in the traps was removed by adding a freshly prepared clear solution of 0.1 M stannous chloride and digesting on the steam bath for 1 hr. The elemental sulphur was separated by centrifuging and was digested with a small amount of water to complete the removal of iodine. It was centrifuged again and then dried in a vacuum desiccator. The yield based on barium sulphate was 77 pct (28 mg).

Table I. Size Distribution in Ground Minerals

Taylor Screen Size	Galena-Quartz Wt, Pct	Sphalerite-Quartz Wt, Pct
+65	4.0	5.0
−65 +100	32.0	32.5
−100 +150	22.0	23.0
−150 +200	10.5	11.0
−200	31.5	28.5

The labeled sulphur was thoroughly mixed with 124 mg of nonradioactive carrier sulphur (USP flowers of sulphur), 66 mg of amorphous red phosphorus and 198 mg of carrier phosphorus pentasulphide, reagent grade, purified by extraction with carbon disulphide. The mixture was heated slowly under dry nitrogen to 270°C and kept at 270° to 300°C for 4 hr. The labeled phosphorus pentasulphide obtained was allowed to react with sec-butyl alcohol at 80° to 85°C. The crude dibutyl dithiophosphoric acid obtained was dissolved in heptane and filtered and the ammonium salt formed by reaction with anhydrous ammonia. On cooling, the ammonium dibutyl dithiophosphate separated as a crystalline product. The yield of air-dried product based on the total sulphur taken was 48 pct (453 mg).

Table II. Time for Conditioning and Flotation, Min

	Single Flotations		Selective Flotation
	Galena	Sphalerite	
NaCN, if added	5	5	5
$CuSO_4$, if added	5	5	—
Dithiophosphate	5	5	1
Pine oil frother	1	1	—
Flotation of galena	2	—	2
$CuSO_4$	—	—	5
Pine oil frother	—	—	1
Flotation of sphalerite	—	2	2

Two samples of nonradioactive ammonium di-(sec-butyl) dithiophosphate were used. One of these samples was prepared from Baker's phosphorus sulphide by a procedure similar to that used for the radioactive dithiophosphate. The second sample was a commercial product manufactured by the American Cyanamid Co.

The pine oil frother was Newport Industries, Inc., G.N.S. No. 5. The other chemicals used in the flotation tests were reagent grade chemicals.

Flotations: The flotations were carried out with 200 g of mineral in a Fagergren flotation machine having a 250-g cell. The galena, sphalerite, and quartz were crushed separately to pass a 10 mesh sieve, using a gyratory crusher for the quartz and a porcelain mortar and pestle for the galena and sphalerite. Synthetic mineral mixtures were made up with quartz to contain about 4.4 pct lead as galena or about 4.7 pct zinc as sphalerite, or to contain these amounts of galena and sphalerite together. The mineral mixtures were wet ground in a porcelain ball mill for 20 min with Danish pebbles at 30 pct solids, then immediately diluted to 20 pct solids, conditioned with the reagents required, and floated. The size distribution of the mineral is shown in Table I for two typical experiments.

The time and order of reagent additions for conditioning and the time for flotation are shown in Table II. In the selective flotation, a shorter time was allowed for conditioning with dithiophosphate, and the use of pine oil frother for the galena separation was omitted. A better separation was obtained in the selective flotation by making these changes in procedure. Except in one group of experiments in which a very large amount of quartz was obtained in the rougher concentrate, the rougher concentrate was not cleaned.

The concentrate and tailing samples obtained from the flotation experiments were immediately filtered in a Buchner funnel to separate the mineral from the solution for counting. In the single flotations with radioactive dithiophosphate, the amount of wash water used in transferring the mineral to the filter was kept at a minimum, and in the selective flotations with radioactive dithiophosphate, the wash water was omitted and the filtrate was used to wash the mineral onto the funnel. Although dithiophosphate can be desorbed quite readily by washing with water, it does not appear that there were any significant differences caused by the failure to use the filtrate for washing in all of the experiments.

Each flotation experiment was carried out separately with radioactive dithiophosphate and with nonradioactive dithiophosphate. The experiments with radioactive dithiophosphate were used to measure the sorption of dithiophosphate on the minerals and the concentration of dithiophosphate remaining in solution. The experiments with nonradioactive dithiophosphate were used to determine the lead and zinc content of the flotation products by chemical analysis. Separate experiments with nonradioactive dithiophosphate were carried out to avoid carrying out chemical analyses on the radioactive minerals. The dry weight of the filtered mineral samples was determined in all of the experiments. In the single flotations, the nonradioactive dithiophosphate was a special sample prepared by the same method as the radioactive dithiophosphate. In the selective flotations, the nonradioactive dithiophosphate was a sample of the commercial product.

Table III. Single Flotations Without Copper Sulphate Activation, 0.12 Lb Per Ton of Ammonium Di-(sec-butyl) Dithiophosphate (DTP) and 0.08 Lb Per Ton of Frother

Ore	NaCN, Lb/Ton	Concentrate		Sorption of DTP, Mg/G		DTP in Filtrate		
						Concentration, Mg/Liter		Amt., Pct of Total
		Wt, G	Pct of Total PbS or ZnS	Conc	Tail.	Conc	Tail.	
$PbS-SiO_2$	—	13.4	99.6[a]	—	—	—	—	—
	—	14.7		0.15	0.002	8	5	73
	—	12.8		0.03	0.002	11	7	81
	—	12.3		0.10	0.002	8	8	74
	0.10	13.8	98.6[a]					
	0.10	13.6		0.06	0.003	6	9	89
$ZnS-SiO_2$	—	11.4	47[a]					
	—	8.5		0.08	0.003	6	6	88
	—	7.3		0.03	0.002	8	10	95
	—	8.3		0.09	0.002	7	9	84
	0.10	2.2	7[a]					
	0.10	3.4	[a]					
	0.10	3.8	[a]					
	0.10	6.5		0.03	0.002	10	9	93
	0.10	5.0		0.05	0.003	7	10	90
	0.20	3.1		0.04	0.002	8	10	93
SiO_2	—	—		—	0.007	7	8	—
	—	5.7		0.15	0.008	8	7	72
	0.10	1.2		0.06	0.003	9	10	94

[a] Nonradioactive experiments.

Radioactivity Determinations: Radioactivity determinations for the mineral samples and filtrates were used to calculate the amount of dithiophosphate present, assuming that all of the radioactive sulphur was present as dithiophosphate.

These measurements were made with a mica-window Geiger counter. Solutions were analyzed by counting dried 0.1 ml aliquots under the mica-window tube. The total radioactivity present in each experiment was determined by dissolving the tagged dithiophosphate in 10.0 ml of water and counting an aliquot of a suitable dilution to which was added an equivalent amount of sodium hydroxide. The remainder of the 10 ml of solution was used for the flotation experiment. Filtrates were analyzed by adding to 100-ml portions a small amount of sodium hydroxide, which was equivalent to the amount of dithiophosphate that would have been present if no sorption had occurred, and by counting a suitable aliquot. More reproducible measurements were obtained when sodium hydroxide was added, presumably because loss by volatility in the drying process was less for the sodium salt than for the ammonium salt.

The sorption on the minerals was measured by counting thick mineral samples directly. A glass dish 5 cm in diam and 1.7 cm in height was used for low levels of radioactivity, and a cupped planchet 0.5 cm in height and 1.7 cm in diam was used for high levels. These were filled to a constant height with mineral. For samples of constant density, the count observed can be assumed proportional to the count per unit weight under some standard conditions at infinitesimal thickness. Since the thickness of the samples used was considerably larger than the range of the beta particles emitted by radioactive sulphur, the proportionality constant was to an approximation independent of the density and the thickness of the sample, although not of the distance from the top of the sample to the counter. The proportionality constant was determined empirically by two techniques. In one technique, a quantity of dry mineral was treated with a small measured amount of solution containing radioactive dithiophosphate, and after having been thoroughly mixed in a mortar and pestle, the mineral was counted. In the second technique, the mineral was suspended in solution and treated successively with dithiophosphate and with copper sulphate solution. The mineral was then filtered off and counted, with corrections allowed for the amount of dithiophosphate remaining in solution. With either technique a mineral sample was obtained with a known count per gram of mineral for standard conditions and infinitesimal thickness. The standard conditions were arbitrarily defined as those used for counting 0.1 ml aliquots of solution. The requirement of infinitesimal thickness was adequately met in counting 0.1 ml aliquots, since the total weight of salts in 0.1 ml was of the order of 1 to 10 mg.

The proportionality constant used in measurements of mineral concentrates was an average value obtained from four experiments with galena and sphalerite concentrates by the two methods described. The proportionality constant used in measurements of mineral tailings was a value obtained from experiments with a quartz tailing by the first method.

Results

Single Flotations without Copper Sulphate Activation: The data obtained in the single flotation of galena from quartz, of sphalerite from quartz, and of quartz alone are shown in Table III for all of the experiments in which no copper sulphate was added.

Flotation: The effectiveness of the separations accomplished was essentially as expected. The separation of galena from quartz under the conditions used was good (99.6 pct of the galena in the concentrate), while the separation of sphalerite from quartz was poor (47 pct of the sphalerite in the concentrate). Quartz was found in the concentrates from the galena-quartz and sphalerite-quartz flotations, and some quartz was also floated in the blank with quartz alone, but the amounts were not excessive in any of these experiments.

The addition of cyanide depressed the flotation of sphalerite from quartz, from 47 pct to 7 pct of the sphalerite in the concentrate, and the flotation of quartz in the blank, but the flotation of galena from quartz was not affected significantly. The weight of quartz floated along with the sphalerite and galena was not changed appreciably. The weight of quartz in the concentrate is calculated from the total weight of concentrate less the weight of galena or sphalerite based on a total of 11.5 g of galena or 14.9 g of sphalerite taken for flotation.

Although the weight of the concentrate using radioactive and nonradioactive dithiophosphate agreed satisfactorily for the galena-quartz system, it did not agree very closely for the sphalerite-quartz. In flotations without cyanide, the sphalerite concentrate obtained with radioactive dithiophosphate weighed appreciably less than the concentrate obtained with nonradioactive dithiophosphate. With cyanide, the concentrate obtained with radioactive dithiophosphate weighed appreciably more than the concentrate obtained with nonradioactive dithiophosphate. It appears that even though the procedures for the preparation of radioactive and nonradioactive materials were similar, there may have been some slight differences in the products. Because of this disagreement, the analyses of galena and sphalerite obtained with nonradioactive dithiophosphate may differ somewhat from those which would have been obtained in flotations with radioactive dithiophosphate.

Sorption: A major part, 72 to 95 pct, of the dithiophosphate present remained in solution in all of the experiments. The concentration in the solutions from the concentrate was in fair agreement with the concentration in the solutions from the tailing. The differences observed were not consistent.

The dithiophosphate sorption on the concentrate varied considerably between experiments. Values of 0.03, 0.10, and 0.15 mg per g were obtained in the flotation of galena without cyanide, and the values observed in the remaining experiments were all within the same limits. Except for the quartz flotation without cyanide, the dithiophosphate sorption on the tailing was relatively more consistent, 0.002 to 0.003 mg per g, and was lower than the sorption on the concentrate by a factor of at least ten.

There was no significant difference between the amount of dithiophosphate sorbed on concentrates of galena, sphalerite, or quartz. On the average, cyanide appeared to cause a slight depression of the amount of dithiophosphate sorbed on the concentrate: from 0.09 to 0.06 mg per g for galena flotation, from 0.07 to 0.04 mg per g for sphalerite flotation, and from 0.15 to 0.06 mg per g for the blank flotation of quartz). However, this depression of the dithiophosphate sorption on the concentrates was relatively small compared to the variations in replicate experiments. Because of the preponderance of quartz in the tailing, it was not possible to determine from the data whether there was any depression of the dithiophosphate sorption on the sphalerite in the tailing.

Single Flotations with Copper Sulphate Activation: The data obtained in the single flotations with copper sulphate activation are shown in Table IV. Galena can be separated readily from quartz without copper sulphate and therefore its activation was not studied.

Flotation: The effectiveness of the separations was again essentially as expected. With copper sulphate used as an activator, the separation of sphalerite from quartz was almost complete (99 pct of the sphalerite in the concentrate compared to 47 pct without copper sulphate). The depressant effect of cyanide on the flotation of sphalerite was overcome completely. The weight of quartz floated with the sphalerite and the weight of quartz floated in the blank with quartz alone were not increased significantly. Agreement in the weight of concentrate between experiments using radioactive and nonradioactive dithiophosphate was good.

Sorption: The amount of dithiophosphate remaining in solution was reduced from 72 to 95 pct of the total in experiments without copper sulphate to 2 to 4 pct with copper sulphate. Corresponding to this reduction in the concentration of dithiophosphate in solution there was an increase in the amount of dithiophosphate sorbed on the mineral (from 0.03-0.15 to 0.2-1.4 mg per g in the concentrate and from 0.002-0.003 to 0.01-0.04 mg per g in the tailing). The tailing here was essentially pure quartz.

Selective Flotations: The data obtained in the selective flotations are shown in Table V. Each selective flotation experiment consists of two parts: part G, the flotation of galena in the presence of cyanide, and part S, the flotation of sphalerite from the tailing of part G using copper sulphate to activate the sphalerite.

Flotation: Reasonably good separation of galena was obtained by using cyanide and zinc sulphate to depress the sphalerite flotation. One flotation made without zinc sulphate had a considerable sphalerite contamination in the galena, the separation appearing to be of such poor quality that no assays were made.

A reasonably satisfactory separation of sphalerite was obtained, not more than 5 pct of the sphalerite remaining in the tailing. When the sphalerite activation was accomplished with copper sulphate alone, that is, without calcium hydroxide, there was a large amount of quartz in the sphalerite concentrate, experiments 1S and 2S. This amount of quartz was reduced considerably by cleaning, but the amount remaining was still somewhat large, 30 g of total concentrate compared to 20 g obtained in the single flotations of sphalerite using copper sulphate. When calcium hydroxide was used with the copper sulphate, only a normal amount of quartz was floated.

Agreement in the weight of concentrate between experiments using radioactive and nonradioactive dithiophosphate was satisfactory.

Sorption: Radioactivity measurements could not be made for the galena tailing, since the tailing had to be used for the sphalerite flotation. A separate galena flotation therefore was carried out, experiment 5G, under similar flotation conditions to get radioactivity measurements for the galena tailing.

The results obtained in the selective flotations for the sorption of dithiophosphate and the concentration of dithiophosphate remaining in solution were in general agreement with the results obtained in single flotations. In the galena flotation without copper sulphate, the major part of the dithiophosphate remained in solution, and the sorption in the concentrate and tailing was typical of that found in the single flotations. In the sphalerite flotation using copper sulphate activation, only a relatively small amount of dithiophosphate remained in solution and considerably higher sorption values were obtained, again typical of that found in single flotations with copper sulphate activation. The single exception to

Table IV. Single Flotations with Copper Sulphate Activation, 0.12 Lb Per Ton of Di-(sec-butyl) Dithiophosphate (DTP), 0.5 Lb Per Ton of Copper Sulphate and 0.08 or 0.16 Lb Per Ton of Frother

							DTP in Filtrate		
	Reagents, Lb/Ton		Concentrate		Sorption of DTP, Mg/G		Concentration, Mg/Liter		
Ore	NaCN	Froth.	Wt, G	Pct of Total PbS or ZnS	Conc	Tail.	Conc	Tail.	Amt., Pct of Total
$ZnS-SiO_2$	—	0.08	16.6	98.6[a]					
	—	0.08	17.0		0.22	0.044	0.5	0.1	3.1
	—	0.08	17.3		0.24	0.031	0.6	0.2	2.5
	—	0.16	20.3		0.39	0.021	0.5	0.2	2.8
	0.10	0.16	19.2	99.6[a]					
	0.10	0.16	18.0		0.45	0.010	0.4	0.4	3.6
	0.10	0.16	18.9		0.82	0.006	0.5	0.3	3.9
SiO_2	—	0.08	—		—	0.022	0.3	0.1	—
	—	0.08	3.1		1.4	0.029	0.4	0.1	2.1
	0.10	0.08	3.2		0.80	0.031	0.8	0.3	4.0

[a] Nonradioactive experiments.

the general agreement was the result obtained in the sphalerite flotation at high alkalinity with the addition of calcium hydroxide, experiment 4S. A much larger part of the dithiophosphate remained in solution, 64 pct as compared to 13 pct when calcium hydroxide was not added.

It would have been of considerable interest to measure directly the sorption of dithiophosphate on quartz, galena, and sphalerite separately in the rougher concentrates. Attempts to separate the quartz from the galena or sphalerite were unsuccessful. Separation by flotation could not be used because dithiophosphate would desorb. A separation was achieved by gravity in acetylene tetrabromide, but it was found that dithiophosphate also desorbed in this medium. An attempted magnetic separation was likewise unsuccessful. However, an estimate of the sorptions on the separate minerals in the concentrate can be made. The sorption observed in experiments without copper sulphate on concentrates from the flotation of galena-quartz or sphalerite-quartz mixtures was in general agreement with the sorption on concentrates from the blank flotation with quartz alone. This indicates that the sorption per gram of mineral floated was about the same on all three minerals and is of some interest, since good separation was obtained with galena and poor separation with sphalerite. The sorption on the part of the sphalerite that does not float may be considerably lower. That is, flotation may take place whenever there is sufficient sorption of dithiophosphate, and only a part of the sphalerite may have sufficient sorption when no copper sulphate is present. An estimate could not be made of the separate sorptions on sphalerite and quartz in the tailings. It was calculated that, even if the sorption on the sphalerite in the tailing were as high as on the sphalerite in the concentrate, because of the preponderance of quartz there would have been no measurable increase in the overall sorption in the tailing.

It is of practical interest that only a small quantity of dithiophosphate is sorbed on the mineral surface in flotation, with a major part of the dithiophosphate remaining in solution. However, it should be noted that a relatively high concentration of dithiophosphate in solution may be required to get this small amount sorbed on the mineral.

The measured surface areas of a typical galena concentrate and a typical sphalerite concentrate were 4500 cm^2 per g as measured with a Fisher subsieve sizer. The calculated sorption of dithiophosphate on the concentrates was then 0.3 to 1.3 x 10^{-10} mol per cm^2 for both galena concentrates and sphalerite concentrates. The sorption was definitely lower than that calculated for a monolayer, 2.5 x 10^{-10} mol per cm^2 from Fischer-Hirschfelder models, showing that only part of the mineral surface needs to be covered for flotation in agreement with previous investigations.[1, 3]

The difference by a factor of ten or more in the observed sorption between the concentrate and tailings is believed sufficient to account for the difference in flotation. For example, it was previously found[2] in the flotation of galena alone (without quartz) with dithiophosphate that 10 pct of the galena was floated at 0.1 x 10^{-8} mol per g and nearly 100 pct floated at 1.0 x 10^{-8} mol per g.

Cyanide was shown to cause only a relatively small decrease in the sorption of dithiophosphate on the concentrates. The sorption on the sphalerite in the tailing could not be measured. It seems likely that the sorption on the sphalerite that does not float

Table V. Selective Flotations. Part G: Flotation of Galena, 1.0 Lb Per Ton $ZnSO_4$ and 0.1 Lb Per Ton NaCN with Reagents Listed. Part S: Flotation of Sphalerite, 0.5 Lb Per Ton $CuSO_4$ and 0.08 Lb Per Ton Frother with Reagents Listed

								DTP in Filtrate		
	Reagents, Lb/Ton		Concentrate			Sorption of DTP, Mg/G		Concentration, Mg/Liter		Amt., Pct of Total
				Pct of Total						
Exp. No.	DTP	$Ca(OH)_2$	Wt, G	PbS	ZnS	Conc	Tail.	Conc	Tail.	
1G	0.09		18.6	97.8[a]	20.6					
1S	0.12		91.2[b]	1.9[a]	79.4					
2G	0.09		20.2			0.10	—	8.1	—	
2S	0.12		48.4[b]			0.27	0.035	1.2	0.7	13.1
3G	0.09		14.8	93.0[a]	13.7					
3S	0.12	1.0	18.2	06.0[a]	82.0					
4G	0.09		17.3			0.13	—	9.7	—	
4S	0.12	1.0	15.5			0.29	0.010	13.0	7.8	64.1
5G	0.09		16.2			0.19	0.004	7.8	4.7	62.4

[a] Nonradioactive experiments.
[b] Weight of cleaner concentrate was about 30 g.

is considerably lower, but the experiments do not provide any way of proving this point.

Since copper dithiophosphate is a compound of low solubility, it appeared likely that the low dithiophosphate concentrations in solution when copper sulphate was present resulted from bulk precipitation of copper dithiophosphate. Dithiophosphate was added to a solution of copper sulphate using the same concentrations as in the flotation experiments but without the minerals and other reagents. A visible precipitate formed. Filtering through a sintered glass filter a few hours after precipitation left only 14 pct of the dithiophosphate in solution, some of which may have been unfiltered solids. This strongly indicates that copper dithiophosphate was precipitated in the flotation experiments. The marked increase in the measured sorption of dithiophosphate was probably caused in large measure by the inclusion of precipitated copper dithiophosphate by the minerals. However, an actual sorption of some copper and dithiophosphate must also have occurred on the surface of the mineral. Recent work by Gaudin et al[4] has shown that, in the absence of a collector, copper is sorbed by sphalerite to a limiting amount of approximately 1 monolayer. Any mineral-dithiophosphate interaction in the presence of copper sulphate would have been masked, in the present work, by the precipitation of copper dithiophosphate.

The selective flotations at high alkalinity using lime with the copper sulphate did not appear to involve the bulk precipitation of copper dithiophosphate. This is seen most obviously by comparing the solution concentrations of experiment 4S (pH 10.8) with experiment 2S (pH 6.8). In experiment 4S, a considerable portion of the dithiophosphate remained in solution. One might assume that in the alkaline solution copper was precipitated as a basic salt, leaving the dithiophosphate unprecipitated, as has been suggested by Wark.[5]

It may be suggested that the quartz which sorbed dithiophosphate and floated was activated by metal ions present, as, for example, in the flotation of quartz with a fatty acid collector studied by Schuhmann and Prakash.[6] The reason was not established for the unusually large amount of quartz floated with the sphalerite in the selective flotation without lime as compared with the smaller amount floated in the single flotation of sphalerite alone from quartz. The differences in the experimental conditions in the two flotations were that in the selective flotation zinc sulphate was present, dithiophosphate was present before the copper sulphate activation as well as after, and a shorter period of conditioning with dithiophosphate was used. In practice, the sphalerite flotation is generally carried out under alkaline conditions so that the quartz flotation will be depressed.

Summary

Previous radiotracer studies[1,2] of the interaction of a dithiophosphate collector with galena have been extended by a study of the distribution of dithiophosphate during the selective flotation of galena and sphalerite from quartz in a Fagergren machine using sodium cyanide to depress and copper sulphate to reactivate the sphalerite. By tagging dithiophosphate with radiosulphur, the amount of dithiophosphate taken up by the mineral concentrates and tailings and the amount remaining in solution could be easily determined. The single flotations of galena from quartz and sphalerite from quartz were studied in addition to the selective flotation of the three minerals.

When no copper sulphate was added, only a small part of the dithiophosphate was taken up by the mineral, about 80 pct of the added dithiophosphate remaining in solution. There was at least ten times more dithiophosphate sorbed on the concentrates than on the tailings. The amounts sorbed on the galena, sphalerite and quartz in the concentrates appeared to be approximately equal, and to correspond to less than a monolayer on the mineral surfaces.

When copper sulphate was added, the measured amounts of dithiophosphate in the concentrate and tailing increased by about tenfold. However, since there is evidence that copper dithiophosphate precipitated, these values are not believed representative of the amounts active in flotation. Using copper sulphate in a highly alkaline medium, a much larger amount of dithiophosphate remained in solution, apparently because dithiophosphate was not precipitated.

The addition of cyanide, which does not depress the flotation of galena, caused at most a small decrease in the sorption of dithiophosphate on the galena concentrate. In floating sphalerite, where the flotation is strongly depressed by cyanide, it was not possible to determine experimentally the sorption on the portion of the sphalerite which did not float, because of the preponderance of quartz in the tailing. On the small amount which did float, there appeared to have been a slight decrease in sorption, comparable to that observed for the galena concentrate.

These results were obtained under conditions more closely approximating conditions of actual practice than heretofore. The results support former beliefs that a relatively small amount of collector need be sorbed on the mineral for its flotation. The use of a considerably larger quantity of collector in solution may nevertheless be necessary to get this small amount onto the mineral surface.

Acknowledgment

The authors wish to express their appreciation for encouragement and support from S. J. Swainson, J. K. Dixon, and D. J. Salley, and for technical assistance from various other members of these Laboratories during this investigation.

References

[1] G. L. Simard, J. Chupak and D. J. Salley: Radiotracer Studies on the Interaction of Dithiophosphate with Galena. *Trans.* AIME (1950) **187**, pp. 359-364; MINING ENGINEERING (March 1950), TP 2815B.

[2] G. L. Simard, M. Burke and D. J. Salley: Radiotracer Studies on the Interaction of Dithiophosphate with Galena; The Depressant Action of Phosphate. *Trans.* AIME (1951) **190**, pp. 39-44; MINING ENGINEERING (January 1951), TP 2968B.

[3] A. M. Gaudin and F. W. Bloecher, Jr.: Concerning the Adsorption of Dodecylamine on Quartz. *Trans.* AIME (1950) **187**, pp. 499-505; MINING ENGINEERING (April 1950), TP 2813B.

[4] A. M. Gaudin, H. R. Spedden and M. P. Corriveau: Adsorption of Silver Ion by Sphalerite. *Trans.* AIME (1951) **190**, pp. 780-784; MINING ENGINEERING (September 1951), TP 3142B.

[5] I. W. Wark: Principles of Flotation. Australasian Institute of Mining and Metallurgy (1938), p. 191.

[6] R. Shuhmann, Jr. and B. Prakash: Effect of $BaCl_2$ and Other Activators on Soap Flotation of Quartz. *Trans.* AIME (1950) **187**, pp. 591-600; MINING ENGINEERING (May 1950), TP 2826B.

Chemicals From Coal Hydrogenation

by E. E. Donath

Application of the coal hydrogenation process for the production of chemicals is described. It has been estimated that a plant to produce 31,090 bbl per day of chemicals and fuels would cost $326,000,000. These products would consist of 6.1 pct by weight tar acids, 50.8 pct aromatics, 16.4 pct LPG, and 26.7 pct gasoline.

THE coal hydrogenation process is well known as a means for the production of liquid fuels from coal. In this paper the possibilities of the coal hydrogenation process as a source of chemical raw materials will be discussed. The recovery of chemicals from coal hydrogenation products necessitates some modifications and additions to the equipment used for the production of fuels. The conversion of coal into liquid fuels such as gasoline requires two steps: liquid phase and vapor phase hydrogenation. Intermediate oils obtained in the liquid phase contain oxygen and nitrogen compounds, especially aromatic compounds, since the coal itself is composed mainly of cyclic compounds. These oils are the raw material for the separation of high molecular weight aromatics and of tar acids and tar bases. The relative amounts of heavy and middle oil—boiling above and below, e.g., 325°C—can be influenced by temperature, residence time, and catalyst of the liquid phase hydrogenation. In the vapor phase hydrogenation a solid bed catalyst is used to convert the intermediate oil from the liquid phase operation into hydrocarbons of the gasoline boiling range. Essentially pure hydrocarbons with a low content of sulphur, oxygen, nitrogen, and olefines are obtained. Depending mainly on the catalyst, the high ring compound content of the liquid phase oil can be preserved and gasoline rich in aromatics obtained. However, with other catalysts, these ring compounds can be split into gasoline with a high content of isoparaffins.[1] Again, depending on the operating conditions, products of varying boiling range can be obtained. Selection of catalyst and operating conditions therefore makes possible the production of different grades of motor fuel and also variations in the relative amounts of benzene, toluene, and xylene when aromatic hydrocarbons are produced.

The schematic flowsheet, Fig. 1, shows the main steps of the coal hydrogenation process, and the product streams used for the recovery of chemicals are indicated. In the liquid phase hydrogenation stage, coal is made into a paste with recycle heavy oil. The coal paste is mixed with hydrogen and preheated at a pressure of 300 to 700 atm in heat exchangers and preheaters. The coal paste and hydrogen enter high pressure converters where the liquefaction of coal, conversion of the high boiling liquid materials initially obtained, into intermediate oils is performed at a temperature around 470°C. The reaction products enter the hot catchpot in which lower boiling oil vapors are separated from the residue containing unreacted coal, ash, and heavy oil. This residue, usually called H.O.L.D. (heavy oil let down), is processed to separate solid and liquid material. By thermal treatment of the residue, e.g., a coking process, distillate oil is obtained, which can be recycled as part of the pasting oil. This stream is rich in polynuclear aromatics and can be, and has been, used for the recovery of such material.

The oil vapors and hydrogen from the hot catchpot are cooled in heat exchangers and a cooler, and the condensed oil is separated from the recycle hy-

---

E. E. DONATH is with the Research Dept., Koppers Co., Inc., Pittsburgh, Pa.

Discussion on this paper, TP 3263F, may be sent to AIME before May 30, 1952. Manuscript, Oct. 22, 1951. New York Meeting, February 1952.

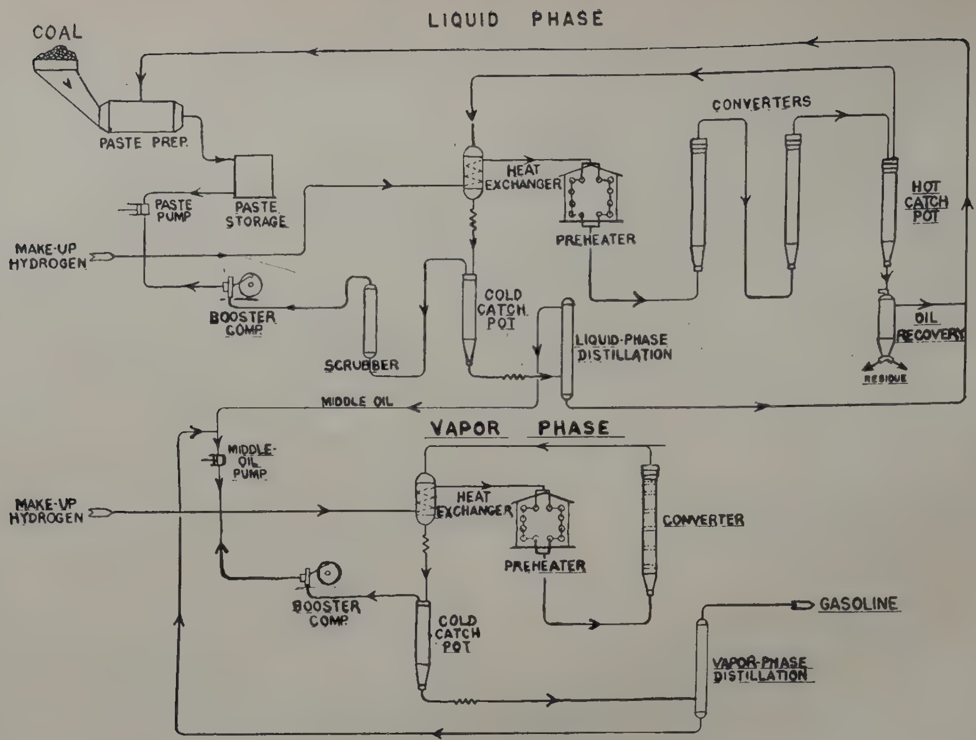

Fig. 1—Coal hydrogenation.

drogen. The oil condensed in the cold catchpot is depressured and separated from dissolved gases. It passes to the liquid phase distillation facilities and is separated into an overhead stream, usually boiling below 325°C, and bottom oils, which are recycled as pasting oil. The overhead stream, or middle oil, is the fresh feed to the vapor phase hydrogenation stage where it is converted into gasoline. Because of its content of tar acids and tar bases, this middle oil is the main source of these compounds.

After the separation of tar acids, this middle oil is converted in the vapor phase, with a fuller's earth-molybdenum catalyst, into gasoline with a high content of ring compounds. The gasoline is the raw material for the production of aromatic hydrocarbons. Benzene, toluene, xylene, and higher aromatics can be separated from this gasoline by extraction with selective solvents or by extractive distillation. Additional aromatics can be obtained from the naphthenes by dehydrogenation using Hydroforming, Platforming, or similar processes.

During coal hydrogenation the nitrogen and sulphur contained in the coal react with hydrogen. The nitrogen and sulphur content of the coal is recovered as ammonia and hydrogen sulphide from offgases and aqueous effluents. Hydrogen sulphide is converted by conventional processes into sulphur or sulphuric acid. Both sulphur and ammonia at present are in short supply.

Table I. Atomic Composition of Coal and Coal Hydrogenation Products

	Molecular wt, Avg	Carbon-Atoms per Molecule, Avg	Atoms per Atom Carbon			
			H	O	N	S
Coal	(800)	(60)	0.75	0.1	0.02	0.01
Residual heavy oil	400	30	0.9	0.01	0.01	0.00
Coker distillate	300	23	0.8	0.02	0.01	0.00
Distillate heavy oil	300	23	1.1	0.01	0.01	0.00
Middle oil	200	15	1.3	0.03	0.01	0.00
Gasoline	100	7	1.8	0.00	0.00	0.00

Coal and coal hydrogenation products are compounds of carbon and hydrogen with minor proportions of oxygen, nitrogen, and sulphur. The reactions that occur during the coal hydrogenation process are indicated to some extent by the average molecular weight of the products obtained and the ultimate composition expressed in atoms of hydrogen, oxygen, nitrogen, and sulphur per atom of carbon, Table I.

The general trend, as the molecular weight decreases, is an increase in hydrogen and a decrease in oxygen, nitrogen, and sulphur content. One exception is the coker distillate which, because of the thermal treatment without hydrogen, shows a decrease in hydrogen content in comparison with the residual heavy oil from which it is obtained. This coker distillate, therefore, contains polynuclear aromatics. Another exception is the middle oil with a higher oxygen content indicating the presence of tar acids.

The position of coal and coal hydrogenation products in comparison to hydrocarbons of known com-

Table II. Liquid Phase Middle Oil from Wyoming Bituminous Coal, Pct

Total tar acids	17	
Tar bases	4	
Separated tar acids:		
Phenol		1.66
o-Cresol		0.50
m-p-Cresol		2.44
Xylenols		1.93
C_{6-8} tar acids		6.53
Sulphur content of C_{6-8} tar acids		0.03-0.05

position can be seen in Fig. 2 in a diagram according to Van Krevelen.[2] In this diagram the atomic hydrogen to carbon ratio is plotted against the number of carbon atoms per hydrocarbon molecule for different hydrocarbon series. The hydrogen content of coal and heavy oils indicates that they are mainly aromatic compounds. The hydrogen content of middle oil and of gasoline indicates that they contain saturated hydrocarbons in addition to aromatics.

The general nature of the coal hydrogenation products as indicated by the ultimate analysis is borne out by the individual compounds which have been identified or separated. As in other mixtures, e.g., coal tar or petroleum, especially in the high boiling fractions, only part of the compounds can be identified. Condensed aromatic rings were identified in the heavy oil fractions. From coker distillate compounds have been separated in pure form.[3] Aromatics from coker oil are as follows: carbazole, 1 pct; pyrene, 8 to 10 pct; pyrene homologues, 1 to 2 pct; benzperylene, 0.1 pct; and coronene, 0.5 to 1 pct.

The normal method for the separation of these compounds is combined distillation and crystallization. Besides carbazole, other high molecular weight nitrogen bases and tar acids have been recovered from heavy oil, although individual compounds have not been identified.

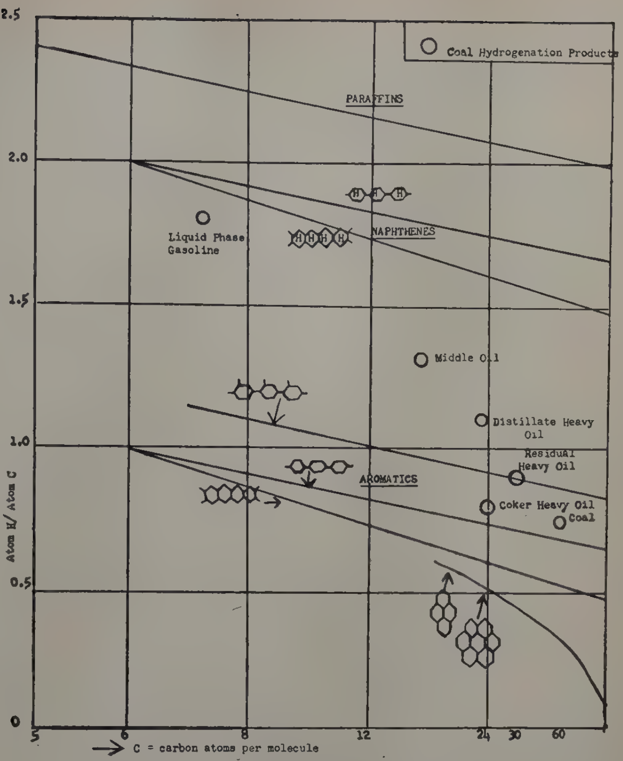

Fig. 2—H/C ratio of hydrocarbons and coal hydrogenation products.

Table III. Gasoline Composition

	Naphthenes, Pct	Aromatics, Pct	Total Ring Compounds
Coal hydrogenation gasolines			
Liquid phase	32	37	69
Vapor phase, fuller's earth catalyst	38	40	78
Vapor phase, tungsten sulphide catalyst	50	5	55
Straight run gasolines			
Midcontinent crude oil	35	2	37
Gulf coast crude oil	52	2	54

The liquid phase middle oil is the raw material for the recovery of tar acids. An investigation of the tar acids contained in coal hydrogenation oil from Pittsburgh bed coal has been made at the Bureau of Mines Station in Bruceton[4] and 16 individual phenols have been identified. The tar acid content of coal hydrogenation middle oils boiling below 325°C is 15 to 25 pct. The middle oil fraction boiling from 160 to 225°C contains about 30 pct commercially useful tar acids from phenol to xylenol. Tar acids* separated from liquid phase middle oil from hydrogenation of Rock Springs Wyoming coal in the U. S. Bureau of Mines demonstration plant at Louisiana, Mo., are shown in Table II. This middle oil had a total tar acid content of 17 pct and also contained 4 pct tar bases. The phenol, cresol, and xylenol, the commercially important tar acids, amount to 6.53 pct of the middle oil. The sulphur content of these tar acids from coal hydrogenation is about 0.03 to 0.05 pct, which is similar to the sulphur content of tar acids from coke oven tar.

Gasolines from coal hydrogenation as indicated by the hydrocarbon ratio are rich in ring compounds. This is confirmed by actual hydrocarbon group analyses shown in Table III. Liquid phase gasoline contains about 69 pct total ring compounds and vapor phase gasoline obtained with fuller's earth catalyst about 78 pct. The ring compound content of a gasoline obtained with tungsten sulphide catalyst is only 55 pct. For the production of low boiling aromatic hydrocarbons such fuller's earth catalysts would be used. In comparison, straight run gasolines from midcontinent crude oil contain only 37 pct and from Gulf coast crude oil 54 pct ring compounds, and the aromatic content is small. Since naphthene rings can be converted readily into aromatics, the coal hydrogenation gasolines because of their high content of aromatics and total ring compounds give a higher yield of benzene, toluene, xylene, and other aromatics than straight run gasolines obtained from petroleum, which at present are used for the production of aromatics. The ratio of the individual aromatics can be changed within wide limits in the boiling range of gasoline. By using lower throughput, higher temperature or higher recycle ratio in the vapor phase hydrogenation, the percentage of benzene, e.g., can be increased at the cost of higher boiling aromatics. The aromatics are pure, sulphur-free compounds; benzene and toluene are of nitration grade. The xylene fraction obtained from German bituminous coal contained about 30 pct ortho-, 25 pct meta-, 15 pct para-xylene and 30 pct ethylbenzene.

A more detailed analysis of some of the cyclic compounds that were identified in the 50 to 150°C fraction of vapor phase gasoline from Wyoming coal[5] with an activated fuller's earth catalyst is given in Table IV. The gasoline fraction in addition to 5.9 pct benzene present as such contains 12.2 pct methylcyclopentane and cyclohexane, which can be converted into benzene. It might be mentioned that with other catalysts different amounts of aromatics

---

* According to analyses by R. S. Detrick, J. Beaumont, P. M. Salinger and W. M. Lee, Mellon Institute and Koppers Co., Inc., Pittsburgh, Pa., under terms of the cooperative agreement between U.S. Bureau of Mines, Demonstration Branch, Louisiana, Missouri and Koppers Co., Inc., Pittsburgh, Pa.

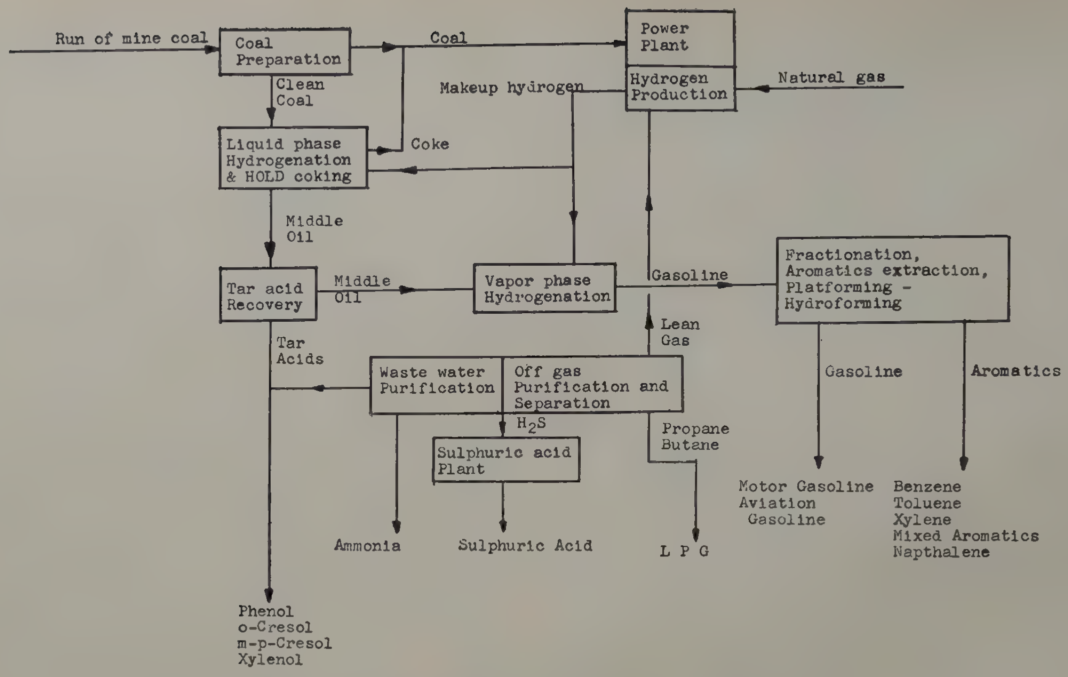
Run of mine coal
Coal Preparation
Coal
Power Plant
Clean Coal
Makeup hydrogen
Hydrogen Production
Natural gas
Liquid phase Hydrogenation & HOLD coking
Coke
Middle Oil
Tar acid Recovery
Middle Oil
Vapor phase Hydrogenation
Gasoline
Fractionation, Aromatics extraction, Platforming - Hydroforming
Lean Gas
Tar Acids
Waste water Purification
Off gas Purification and Separation
H_2S
Sulphuric acid Plant
Propane Butane
Gasoline
Aromatics
Ammonia
Sulphuric Acid
L P G
Motor Gasoline Aviation Gasoline
Benzene Toluene Xylene Mixed Aromatics Napthalene
Phenol o-Cresol m-p-Cresol Xylenol

Fig. 3—Coal hydrogenation plant for production of chemicals and fuels.

can be obtained as well as a different distribution between five and six number ring naphthenes.

In the preceding paragraphs the general types of chemicals that can be obtained by coal hydrogenation have been described. It has been shown that coal hydrogenation products are a very suitable raw material, especially for chemicals of the aromatic series. These chemicals are not only in short supply today, but a rapidly increasing demand is anticipated in the future. Data for an integrated plant for the production of chemicals will now be given.

A plant for the production of about 30,000 bbl per day of products has been assumed. Economic studies have indicated that a plant of this size shows marked decrease in plant and operating cost per unit over plants of 10 to 15,000 bbl per day capacity. Such a plant, in addition to facilities for the manufacture of hydrogen and the power plant and auxiliary facilities, would contain the main processing units shown in the block diagram, Fig. 3. Use of Illinois coal from No. 6 bed has been assumed. In the coal preparation plant, run-of-mine coal is separated in a heavy media cleaning plant into clean coal for the hydrogenation plant, middlings for the power plant, and refuse. The clean coal is dried, ground, and after addition of iron catalyst, is made into a paste with recycle heavy oil for injection into the liquid phase unit. Liquid phase hydrogenation at 700 atm pressure and 480°C combined with H.O.L.D. coking convert the coal into middle oil and separate the recycle pasting oil from solid residue. Tar acids, phenol, cresols, and xylenols are obtained from the middle oil by fractionation and extraction. The remaining middle oil is converted into gasoline in the vapor phase hydrogenation unit using an activated fuller's earth catalyst at 700 atm pressure and 500°C. From the gasoline, hydrocarbons with less than six carbon atoms are separated as light ends, and from the higher fractions, the aromatics are separated by a combined treatment with extraction, Platforming and Hydroforming processes. Benzene, toluene, xylenes, mixed aromatics, and naphthalene are obtained. The nonaromatic fractions and some of the aromatics are blended into motor and aviation gasoline.

Hydrogen sulphide is removed with ethanolamine from off-gases from liquid and vapor phase, coking, and hydroforming units. The off-gas is separated further into lean gas, containing mainly hydrogen, methane and ethane used for hydrogen production and LPG, containing propane and butane. From the aqueous effluent tar acids are extracted and ammonia and hydrogen sulphide separated. Hydrogen sulphide from waste water and off-gas is converted into sulphuric acid.

Table IV. Vapor Phase Gasoline from Wyoming Coal, Fraction 50 to 150°C

	Weight Pct	
Naphthenes:		
Methylcyclopentane	8.6	12.2
Cyclohexane	3.6	
Dimethylcyclopentane	8.0	17.1
Ethylcyclopentane	2.9	
Methylcyclohexane	6.2	
C_8-naphthenes	13.3	
	42.6	
Aromatics:		
Benzene	5.9	
Toluene	11.2	
C_8-Aromatics	10.4	
	27.5	

Table V. Plant Cost—30,000 Bbl Per Day Coal Hydrogenation Plant

	Million $
Coal handling and preparation	9.3
Liquid phase hydrogenation and coking unit	67.0
Tar acid recovery and purification	5.0
Vapor phase hydrogenation	32.5
Aromatics production and separation	21.5
Off-gas and waste water purification and disposal and LPG recovery	14.3
Sulphuric acid and ammonium sulphate plant	4.5
Hydrogen production	66.0
Power plant	54.5
General facilities and utilities and tankage	51.4
Total plant cost	326.0

The hydrogen required is produced by steam splitting of lean gas and natural gas because of low plant and operating costs. If natural gas should not be available, hydrogen would be produced from off-gas and coal.

The main raw materials for the production of 30,000 bbl per day chemicals and liquid fuels are 16,000 tons per day of run-of-mine coal of 11,000 Btu per lb heating value for process and power plant coal, and 83 million cu ft per day of natural gas for hydrogen production. Plant costs of $326 million, corresponding to $10,500 per daily barrel of products, have been estimated as indicated in Table V. These costs do not include cost of the plant site, mine development, interest during erection, starting up expense, and operating capital.

Products obtainable are listed in Table VI. The tar acids amount to 6.1 pct by weight, the aromatics to 50.8 pct of total products. The ammonium sulphate and sulphuric acid production is shown separately. LPG which can be used as fuel, as well as chemical raw material, is 16.4 pct of the total. Motor and aviation gasoline, 15.6 and 11.1 pct respectively, amount to 26.7 pct of the total products. The value of these products per year, at present market prices, is $135 million, about 40 pct of the aforementioned plant cost.

Gasoline, LPG, ammonia, and sulphuric acid from such a plant amount to only 0.2 to 2 pct of the present production of the United States. The contribution of the aromatics and tar acids produced to United States production of these materials, however, would be substantial, as indicated by Table VII. The tar acids produced in such a plant are equivalent to 50 pct of the 1950 production, while the aromatics are equivalent to 54 pct. Benzene and phenol are the two chemicals in this group that are produced in greatest quantity in the United States. The contribution of a 30,000 bbl per day plant would be equivalent to 18 pct of the present benzene and 17 pct of the present phenol production. The 1950 production data for toluene and xylene are only for that portion of these chemicals that is produced in pure form. Considerable additional amounts are used in the form of solvents and motor fuel. At present these materials tend to be in short supply, and large quantities of tar acids and benzene are imported in addition to the production recorded in Table VII. The demand for tar acids and aromatics in the plastic, synthetic fiber and other industries is increasing rapidly, and, therefore, no overproduction is anticipated. If erection of such a plant were started now, operation could not begin in less than 3 years. It should be mentioned that the proportions of the various chemicals produced can be influenced by the selection of operating conditions.

It has been shown that the products from such a coal hydrogenation plant would mean a substantial contribution to the production of chemicals now in short supply and for which the demand is rapidly increasing. In addition, such a plant would make available know-how and experience for the erection and operation of coal hydrogenation plants for the production of synthetic liquid fuels when they are needed in the future to supplement petroleum production.

Table VI. Chemicals and Fuels Production, 30,000 Bbl Per Day Coal Hydrogenation Plant

	Lb per Day	Bbl per Day	Tons per Day	Wt Pct of Total Product
Tar Acids				
Phenol	157,400	428		1.9
o-Cresol	17,600	48		0.2
m-p-Cresol	192,000	530		2.4
Xylenols	136,000	374		1.6
	503,000	1,380		6.1
Aromatics				
Benzene		2,210		8.2
Toluene		3,770		13.9
Xylenes		4,190		15.4
Mixed aromatics		1,780		6.8
Ethylbenzene		750		2.8
Naphthalene	316,000	790		3.7
		13,490		50.8
LPG		7,300		16.4
Gasoline				
Motor gasoline		5,260		15.6
Aviation gasoline		3,660		11.1
		8,920		26.7
Total		31,090		100.0
Ammonium sulphate			450	
Sulphuric acid			89	

Table VII. Chemicals from 30,000 Bbl Per Day Coal Hydrogenation Plant in Comparison to 1950 U. S. Production

	1950 Production, Million Lb	1950 Production, Million Gal	Products from 30,000 Bbl/Day Plant as Pct of 1950 Production
Tar Acids			
Phenol	312		18
Cresols	19		400
Xylenols, cresylic acid	37		135
	368		50
Aromatics			
Benzene		200	17
Toluene		84	69
Xylene		72	89
Mixed aromatics			
Ethylbenzene		(80 estimated)	14
Naphthalene, 290 million lb		(30)	40
Aromatics		386	54

Acknowledgment

The writer wishes to acknowledge contributions and helpful suggestions by W. E. Simmat, Koppers Co., Inc., Pittsburgh, Pa.

References

[1] M. Pier: Hydrogenation Gasolines. *Ztsch.* Ang. Chem. (1938) **51**, p. 603-608.

[2] Van Krevelen: Graphical-Statistical Method for the Study of Structure and Reaction Processes of Coal. *Fuel* (1950) **29**, pp. 269-283.

[3] Boente: TOM Reel 163, Frames 288-289; recently pyrene and coronene have been identified in H.O.L.D. (heavy oil let down) oil obtained from Wyoming coal at the Bureau of Mines, Louisiana, Mo., by R. A. Glenn and C. W. Donald. Paper presented at the Amer. Chem. Soc. meeting in New York, Sept. 3 to 7, 1951.

[4] E. O. Woolfolk, C. Golumbic, R. A. Friedel, M. Orchin, and H. H. Storch: Characterization of Tar Acids from Coal Hydrogenation Oil. U.S. Bur. of Mines *Bull.* 487 (1950).

[5] T. Feldman, R. A. Friedel, and M. Orchin: Composition of Gasoline from Hydrogenation of Coal. Presented at the 12th International Congress of Pure and Applied Chemistry, New York, N. Y., Sept. 10 to 13, 1951.

Some Dynamic Phenomena in Flotation

by W. Philippoff

ALTHOUGH Gaudin[1] and more recently Sutherland[2] have calculated the probability of collision of a falling mineral particle with a rising bubble, there is no published information concerning the details of the mechanism of attachment of a collector-coated particle to a bubble. During the past year the writer has developed a theory for the mechanism of attachment, which has been substantiated experimentally. Funds for the investigation and for some of the equipment used have been supplied by the Mines Experiment Station of the University of Minnesota.

Motion picture studies of the phenomena involved in the collision between mineral particles and bubbles, such as those of Spedden and Hannan,[3] show that the contact can be completed within 0.3 millisec. Formulas developed for rigid bodies have hitherto been used[4] for the calculation of the motion of bubble and particle, but it is obvious that a bubble cannot be regarded as a rigid body. On the contrary, Spedden and Hannan's pictures show a great degree of deformation during the collision. The time of attachment was calculated as the time the particle drifted past the bubble.

Time of Collision

The theory presented in this paper enables calculation of the time of collision, using the concept that the bubble, or more generally, a liquid-air interface, acts as an elastic body. The elasticity, defined as the restoring force on a mechanical deformation, is caused by the surface tension and is the result of the principle of the minimum of free surface energy. It is well known that an elasticity together with a mass determines a frequency of vibration. The vibrations of jets and drops caused by the elasticity of the interface are known to comply exactly with the classical theory of capillarity.[5] However, the vibrations of isolated bubbles, as distinct from foams, have not been investigated previously. The following equation, presented elsewhere,[6] has been deduced for these frequencies:

$$f_B = 9.20\cdot\sqrt[3]{V}\cdot\sqrt{n\cdot(n-1)\cdot(n+2)/8} \qquad [1]$$

in which f_B is the frequency of a harmonic of the bubble in cycles per second, V the volume of the bubble in cc, n a number determining the order of the harmonic, and $n = 2$ the basic vibration. The first (basic) harmonic describes a change of the spherical bubble to an ellipsoidal bubble. The higher harmonics are more complicated, for the circumference of the bubble is divided approximately into as many parts as the order of the harmonic. As an example, Spedden and Hannan's published motion picture of a vibrating bubble corresponds to the sixth harmonic. Eq 1 shows that only the first and third harmonics are simple multiples (1 and 3), all the others being irrational fractions of the basic frequency. This means that the shape of the vibration can change with time and is in general unsymmetric in respect to the time axis. Such conditions prevail when there is a distributed elasticity or mass, as in the case of vibrating membranes or rods. The constant 9.20 is valid for water at room temperature, but a general solution involving the physical constants of the liquid has not been found.

The case of the floating particle is much easier to treat than that of the bubble. It can be assumed that the elasticity is caused exclusively by the interface and that the mass is concentrated in the particle together with some adhering water. The following expression for the frequency of a system of one degree of freedom can be applied:

$$f_P = \frac{1}{2\pi}\sqrt{E/m} \qquad [2]$$

Here f_P is the frequency of the particle vibration in cycles per second, E the elasticity in dynes per cm, and m the mass in grams. The classical theory of impact phenomena gives the time of collision during the striking of a spring (in this case the surface of the bubble) by a mass, as:

$$t_c = 2/f = \pi\sqrt{m/E} \qquad [3]$$

It is now possible to develop an expression for the elasticity of a floating cylindrical particle. The force equilibrium of a cylinder floating end on at the air-liquid interface is given by the well-known equation (Poisson[7] 1831)

$$P = \frac{\pi}{4}D^2\cdot\rho_L\cdot g\cdot h + \pi D\cdot\gamma\sin\alpha \qquad [4]$$

which accounts for the buoyancy *and* the action of the surface tension where P is the force acting on the particle in dynes (weight-buoyancy), D the diameter of the cylinder in cm, ρ_L the density of the liquid in grams per cc, g the acceleration of gravity = 981 cm per sec^2, h the depression of the cylinder below the surface of the liquid in cm, γ the surface tension in dynes per cm and α the supporting angle[8] or the one required to insure equilibrium, α being smaller than the contact angle θ.

Although demonstrated by Poisson, it has not

W. PHILIPPOFF is Senior Staff Engineer at the Franklin Institute Laboratories for Research and Development, Philadelphia. The work outlined in this paper was done while the author was Research Associate, Mines Experiment Station, University of Minnesota, Minneapolis.

Discussion on this paper, TP 3265B, may be sent to AIME before April 1, 1952. Manuscript, Feb. 19, 1951. New York Meeting, February 1952.

been pointed out since that h and α are interrelated. Introducing the Laplace constant a:

$$a = \sqrt{2\gamma/g\cdot\rho_L} = 3.85 \text{ mm for water} \qquad [5]$$

the relation for particles the diameter of which is small compared with a is:

$$h = (D\cdot\sin\alpha)/2[\ln(a/D) + 0.46251] \qquad [6]$$

Inserting this relation into eq 4, simplifying, and as the elasticity $E = P/h$, the following expression is obtained for E, see Fig. 1:

$$E = 2\pi\gamma\,[D^2/4a^2 + 1/\{\ln(a/D) + 0.46251\}] \qquad [7]$$

or for the sake of simplicity:

$$E = 2\pi\gamma\cdot\phi^2 \qquad [8]$$

where ϕ^2 is the expression in brackets, depending only on the ratio D/a. In Table I this function is tabulated for the range of particle sizes important in flotation. Having now calculated E, eq 8 is introduced in eq 3, and the following expression for the time of contact (t_c) is obtained:

$$t_c = \sqrt{\frac{2\pi}{\gamma}}\cdot\sqrt{m}/\phi = 4.67\sqrt{m}/\phi \qquad [9]$$

In the simplified expression t_c is in milliseconds and m in milligrams, convenient units for the particle size-range investigated, the value being calculated for water ($\gamma = 72$ dynes/cm).

It must be stated that a direct contact of the surfaces of the cylinder and the bubble is not needed to cause a deformation of the bubble, i.e., the elasticity is present also with a layer of water between them. This layer of water is being pressed out during contact, as will be seen.

Eq 9 can be evaluated by using arbitrarily a particle of a height equal to its diameter, somewhat like a cube, with a density of 7.5. The results are given in Table I. Under the assumed geometric conditions the time of contact t_c is proportional to $D^{3/2}/\phi$. The calculated times are little dependent on the shape of the particle, for the function ϕ as seen from Table I varies only about 1 to 3 in a range of particle sizes of 1 to 20000. Of course, as has been mentioned, the actual mass is somewhat larger than that of the particle. The calculated times are comparable to the time of 0.3 millisec, measured by Spedden and Hannan. Wolkowa[4] calculated t_c approximately as (diameter of the bubble)/(velocity of the bubble) to 5 and 10 millisec independent of the diameter of the particle.

These considerations show clearly that the attachment of a mineral particle to a bubble is necessarily extremely fast, otherwise the particle will tend to jump off the surface of the bubble after t_c has elapsed. This has actually been observed by Spedden and Hannan. The high-speed phenomenon of attachment requires special equipment hitherto not used to analyze it and would make any long-time phenomena such as the *induction time* of Sven-Nilsson[9] questionable as to their influence on the mechanism of attachment.

Table I. Times of Contact (t_c) and the Required Velocities of Film Recedence (v_F)

Diam of Particle, (D), Microns	Function, ϕ	Time (t_c), Millisec	Velocity (v_F) Cm per Sec
1000	0.741	15.3	3.27
500	0.635	6.33	3.95
200	0.541	1.88	5.32
100	0.4925	0.74	6.75
50	0.4560	0.28	8.90
20	0.4185	0.077	13.00
10	0.3955	0.029	17.3
5	0.3750	0.0117	21.4
2	0.3522	0.0029	34.5
1	0.3390	0.0011	45.4

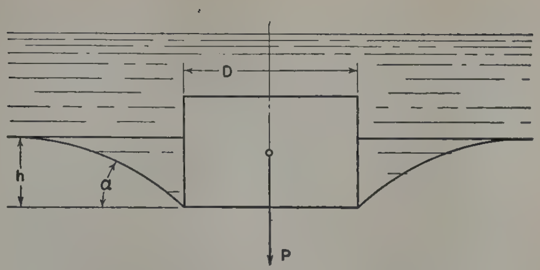

Fig. 1—Equilibrium at the bubble surface.

Film-Recedence Velocity

Assuming a radial recedence, an approximation of the velocity with which a liquid film should recede after being punctured in the center to form a mineral-air interface during the time t_c is simply:

$$v_F = D/2t_c \qquad [10]$$

The calculated velocities are listed in Table I.

The next step is the calculation of the velocity of the film-recedence, which should at least equal v_F. This necessitates the calculation of the thickness of the liquid film δ between the flat face of the cylindrical particle and the assumed flat bubble surface.

Stefan's equation[10] gives the dependence of the time t and the force P for the case of two circular planes moving towards each other:

$$t = (3\pi\eta\, D^4/64P)\cdot(1/H_1^2 - 1/H_2^2) \qquad [11]$$

in which η is the viscosity of the liquid in poises and H_1 and H_2 the final and initial film thicknesses in cm. Assuming a particle coming from infinity: $1/H_2 = O$ and $H_1 = \delta$, where δ is the required film thickness. This gives:

$$P\cdot t = (3\pi/64)\ \eta\ D^4/\delta^2 \qquad [12]$$

Applying the law of impulse:

$$P\cdot t = \epsilon m\cdot v$$

where ϵ is the change of the velocity of the particle before and after the impact. Assuming a large bubble hitting a small particle, it is necessary to consider only the mass of the particle. Likewise the Stokes' velocity of the particle can be disregarded compared with the rising velocity of the bubble v_B. It is not difficult to obtain a closer approximation. The final expression is:

$$\delta = D^2/8\sqrt{3\pi\eta/\epsilon\cdot v_B\cdot M} \qquad [14]$$

This mode of calculation has been used by Eirich and Tabor[11] for a hammer striking an anvil under a liquid. The film thicknesses δ, evaluated according to eq 14, are listed in Table II.

The case of a fluid receding under the influence of surface tension on a hydrophobic surface has never been visualized and therefore not treated. If a thin film of liquid on a solid, the system having a finite contact angle θ, is pierced centrally, the film will recede radially, the decrease in free surface energy being converted into kinetic energy of the receding

Table II. Minimum Film Thicknesses During Collision

Diam of Particle, D, Microns	Film Thickness, δ, Microns	δ/D
1000	9.8	0.010
500	6.9	0.014
200	4.4	0.022
100	3.1	0.031
50	2.2	0.044
20	1.4	0.070
10	1.0	0.10
5	0.7	0.14
2	0.44	0.22
1	0.31	0.31
0.5	0.22	0.44
0.2	0.14	0.70
0.1	0.10	1.00

film. This concept has been used by Boys[12] to calculate the bursting velocity of a bubble. The diameter of the initial central break has to be larger than the one determined by eq 6 when α equals θ. This is the criterion for the film stability. The driving force is obviously the surface tension, which acts at the angle α to the surface, whereas the equilibrium value is θ. This velocity, which is independent of the radius, is computed according to:

$$v = D/2t = \sin\theta/2 \sqrt{\frac{4\gamma}{\delta\rho_L}} = 17\cdot\sin\theta/2\cdot 1/\sqrt{\delta} \quad [15]$$

The second expression is for water with $\gamma = 72$ dynes/cm.

Contact Angle

Having now established the basic relations, it is possible to calculate the contact angle θ that would, under the assumed somewhat idealized conditions, be necessary to enable a contact to be established during the time t_c. For this purpose the velocity v_F from eqs 9 and 10 is made equal to the velocity from eq 15 using eq 14, and the following expression for the minimum necessary contact angle is obtained:

$$\sin\theta/2 = \phi/8\pi \sqrt[4]{\frac{3\eta\rho_L{}^2}{\epsilon V_B\cdot\rho_P{}^3}}\,(D/L)^3\, 1/\sqrt[4]{D} \qquad [16]$$

Putting the viscosity of water $\eta = 0.01$ poises, the velocity of the rising bubble $v_B = 30$ cm per sec, $\epsilon = 1$, the particle density $\rho_P = 7.5$, the water density $\rho_L = 1$ and $D/L = 1$ the final expression is obtained in which D is in microns:

$$\sin\theta/2 = 1/(22.7\sqrt[4]{D}) \qquad [17]$$

The evaluation of eq 17 is given in Table III, together with the minimum equilibrium contact angles computed from eq 4. Both values are of the same order of magnitude for the larger particles, but the equilibrium values fall off with D^2, whereas the dynamic values calculated from eq 17 tend to assume higher values for smaller particles. This relation is important in regard to the possible connection of the phenomena considered with the known difficulty of flotation of fine particles or slimes. Both values of θ however are far smaller than those usually accepted as necessary for flotation, especially if one considers that $(1\text{-}\cos\theta)$ falls off exceedingly fast at small angles. It is improbable that an air-mineral interface could be destroyed after contact is established as then not the small contact angle, α, calculated but the maximum possible one has to be overcome. Of course these calculations must be supplemented by the deductions of Gaudin and of Sutherland to give the actual decrease in flotability of fine particles due to the decreased probability of collision.

Table III. Minimum Necessary Contact Angles

Diam of Particle, D, Microns	Sin $\theta/2$ Dynamic	θ Dynamic, Deg	θ Static, Deg
1000	0.00583	0.675	12.0
500	0.00590	0.675	3.10
200	0.00634	0.726	0.50
100	0.00687	0.787	0.13
50	0.00755	0.865	0.032
20	0.00874	1.000	0.0050
10	0.00978	1.121	0.0013
5	0.01100	1.265	0.00032
2	0.01309	1.500	0.000050
1	0.01495	1.715	0.000013

If account is to be taken of the centrifugal force in the flotation cell, the equilibrium values should be multiplied by the assumed number of g's increasing them accordingly. The dynamic values will also be diminished, especially the relative velocity v_B of bubble and particle. But this does not affect the general picture. An increase in acceleration increases ρ_P and v_B. The time of contact t_c in eq 3 is independent of the acceleration.

The values for the dynamic θ also vary only little with a change in particle size, accounting for an approximately equal floatability in a large range of particle sizes, as is sometimes the case in flotation. Equilibrium considerations require enhanced floatability of smaller particles, but generally speaking this is not the case. On the other hand larger particles probably do not float because their equilibrium θ is too large and because of the acceleration phenomena investigated by Gaudin. Thus dynamic considerations provide a reason for the nonfloatability of very small particles analogous to the known limits for large particles.

Energy Considerations

It is interesting to compare the kinetic energies of particles hitting rising bubbles at an assumed constant velocity of 30 cm per sec with the amount of energy released by the formation on the air-mineral interface. These computations are shown in Table IV, the decrease in free surface energy being calculated as (area of the interface) x $(1 - \cos\theta)$; θ was taken as 60°. Up to 100 microns, the kinetic energy is larger than the loss in free surface energy, but with particles of 1 micron the decrease in free surface energy is nearly 100 times larger than the kinetic energy. Even for 10 microns the ratio is 1 to 12. This clearly shows that the particle cannot pierce the bubble surface by its kinetic energy alone. This can only trigger the film-recedence, which is governed by forces of much greater magnitude in this range of particle sizes.

Experiments

To check these deductions, experiments were made, using particles within the range of sizes used in flotation, but large enough to give easily measurable times t_c. Regular cylinders were filed from short lengths of steel wire. They were allowed to fall on a captive bubble blown in a cavity bored in a paraffin block. The cylinders were made *hydrophilic* to insure that they did not stick to the bubble but bounced off. This was done by treating them with chromic acid immediately before the experiment.

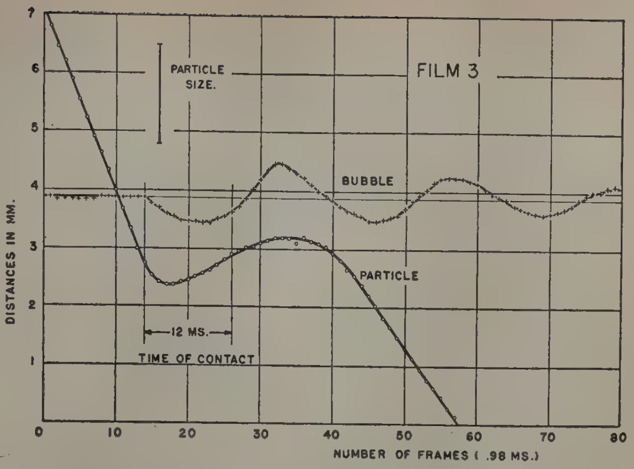

Fig. 2—Evaluation of a collision experiment from the film.

They were suspended by an electromagnet directly over the captive bubble. When the current was switched off, the general area of the top of the bubble was photographed at suitable illumination with a high-frequency camera operating at about 1000 frames per sec. The film velocity was timed by using a spark discharge of 120 sparks per sec simultaneously photographed on the bubble image. Knowing the diameter of the particle, the magnification could be determined exactly. The evaluation of the film in terms of time-displacement curves was done with a Gaertner spectrum-comparator. The positions of the perforations varied by only a few microns and could be chosen as reference points for the displacements.

The results of the evaluation of one experiment as time-displacement curves are shown in Fig. 2. From these curves the time of contact t_c was determined as shown, the point of departure of the particle from the bubble surface being taken as the point of nearest approach of the curves of the bubble and of the particle. The particle generally did not strike the bubble exactly at the apex, but somewhat in front or behind, so that the instant at which the particle left the bubble was not directly observable. Some particles such as the one in film 6 jumped several times on the surface of the bubble before it finally fell off. In film 3 the velocity of rebound could be measured accurately; it amounted to 56 pct of the initial velocity, corresponding to $\epsilon = 0.44$ in eq 13. In all the cases investigated the vibration of the bubble is not harmonic, and the shape of the curve changes with the number of periods elapsed, as would be expected from the theory. The relative magnitude of the harmonics depends on their relative exitation, i.e. on the exact spot the bubble is hit by the particle. The different particles have widely different energies of impact, controlled by the height of fall h and the mass m of the particle according to the law that energy $= mgh$. The larger the energy, the larger are the induced bubble vibrations and the larger the eventual rebound of the particles. At very high energies the particle pierces the bubble surface.

Table V summarizes the results of the measurements. The size of the particles, the energy of impact, and the calculated and measured times of impact are shown. In the four valid experiments the measured time was about 15 pct longer than the calculated, doubtless due to the influence of the adhering water. This could not be accounted for in the calculations. Such a check is as close as could be expected. These experiments with particles purposely chosen so as to make the time of contact measurable definitely show that the attachment of a particle to a bubble is a high-speed phenomenon and that the times calculated in Table I are a good approximation to those encountered in practice.

The second relation to be investigated was the measurement of the velocity of film recedence with different contact angles and different film thicknesses. This was done by placing a circular polished piece of metal or mineral of about 4 cm in diam on a leveled glass slab in a dish with water or a solution of a collector. By siphoning, the water level could be lowered to give any required film thickness, which remained practically constant during the recedence, as the dish was much larger than the specimen. The thickness was measured by a previously calibrated eyepiece micrometer in a low-power microscope. Through an optical phenomenon the double film thickness could be measured with suitable illumination. When the required film thickness was attained, a bubble was blown in the center of the specimen by means of a hypodermic syringe reaching into a small central depression bored in the specimen. The time necessary for the water to recede from the center to the circumference of the specimen was determined by means of a stopwatch. The radius, divided by this time gave the velocity of the receding film. Numerous experiments with this arrangement were not quite conclusive. There was a definite increase of the velocity with thinner films, as expected from eq 15. Any other assumed mechanism for film recedence, notably one taking into account the viscous flow, would have given the reverse effect. But the measured velocities, ranging from 0.1 to 20 cm per sec were still about 10 pct of the calculated values, using the magnitude of the contact angle as measured at equilibrium in the bubble machine. It was strange that copper conditioned in a ½ pct solution of sodium Aerofloat gave consistently higher velocities than paraffin or vaseline-coated glass. These experiments must be continued to ascertain the origin of the velocity of the film-recedence. However, it is certain that velocities of the order of 20 cm per sec, as calculated in Table I, are possible. This is true even at film thicknesses of 0.6 mm, probably much thicker than those encountered in flotation. The reader is referred to Table II.

Apparently the discrepancy is due mainly to the value of the contact angle θ used in the calculations. It is well known that an induction time is necessary for equilibrium to develop in the bubble machine. In experiments concerned with high-speed film recedence this induction time cannot possibly be con-

Table IV. Comparison of the Kinetic Energy of Colliding Particles with the Free Surface Energy

Particle, Diam of D, Microns	Kinetic Energy, E, Ergs		Change in Free Surface Energy, Ergs	
1000	2.3		0.28	
500	0.30		0.07	
200	0.018		0.011	
100	0.0023		0.0028	
50	0.30	$\times 10^{-3}$	0.70	$\times 10^{-3}$
20	0.018		0.11	
10	0.0023		0.028	
5	0.30	$\times 10^{-6}$	7.0	$\times 10^{-6}$
2	0.018		1.1	
1	0.0023		0.28	

Table V. Results of Impact Experiments

Film No.	Particle No.	Particle Diam, Mm	Particle Length, Mm	Particle Mass, Mg	Particle Velocity, Cm/Sec	Energy of Impact, Erg	Time of Impact, Millisec Calcd.(t_c)	Exper.
I	1	0.740	0.930	3.055			11.9	
II	2	0.405	0.560	0.320	9.1	0.013	4.35	~ 6
III	4	0.740	0.770	2.490	17.8	0.40	10.7	12.0
IV	6	0.890	1.040	5.000	24.2	1.46	14.5	~17.3
V	2	0.405	0.560	0.320			4.35	
VI	5	0.508	0.620	1.035	15.0	0.12	7.50	8.5

sidered. How large the contact angle could be under these conditions is as yet unknown. It may be definite fraction of the equilibrium contact angle, but this seems doubtful as seen from the copper-Aerofloat experiments described. It could be that this dynamic receding contact angle, active in the velocity of the film recedence, is only of the magnitude of a few degrees compared to the 30° to 60° equilibrium values. These investigations have yet to be made, but the low values do not seem improbable.

Table II further shows that the minimum film thicknesses for small particles are appreciable fractions of their diameters, so that for particles of only 0.1 micron size the nearest approach is approximately equal to the diameter. It seems unlikely that the initial break of the bubble surface could occur because of surface irregularities of the particle. For particles of 10 microns the film thickness is 10 pct of the diameter and that seems to be the approximate limit to a probable initial break of the bubble surface due to surface irregularities.

The velocities of film-recedence, of the order of 25 cm per sec, are comparable to those measured for the spreading of liquids on water to form surface films. In fact no higher velocities have been found.[13] This would limit the range of flotation to about 5 micron particles under the geometric conditions chosen. On the other hand calculations and measurements of the velocity of bursting bubbles,[12] which were used as a starting point in these calculations, give values up to 3,000 to 10,000 cm per sec. Detailed investigations of these conditions have yet to be made.

The theory developed leads, as has been seen, to a dependence of the contact angle necessary for flotation dependent on the reciprocal fourth root of the particular diameter, whereas statical considerations lead to a dependence on the *square* of the particular diameter. However, should an acceleration of, say, 50 gs be included in the calculations, this would only displace this relationship to higher contact angles not changing its dependence on the diameter. Both relationships can be tested experimentally by making precise measurements of the recovery of a monomineral suspension with exactly known contact angles. Of course, it is very possible that the calculated contact angles of 0.7° to 1.7° are only a small fraction of the necessary ones due to the fact that only idealized conditions can be calculated, and the difference of the static and dynamic contact angles has also to be accounted for. Experiments should not be too difficult to perform.

Summary

A possible mechanism for the attachment of a conditioned mineral particle to a rising bubble has been developed. The time during which the phenomenon occurs is determined by the time of impact, which can be calculated and was substantiated by experiments. During this time the film of liquid between the particle and the bubble must recede, creating the particle-air interface. This velocity of film-recedence has been both calculated and measured and found to be dependent on the "dynamic receding contact angle," which is much smaller than the equilibrium contact angle measured in the bubble machine. This mechanism, as distinct from the static equilibrium, accounts for the more difficult flotation of fines and slimes, and supplements the probability calculations of Gaudin and of Sutherland.

Acknowledgments

The author wishes to express his thanks to Prof. John D. Akerman, Dept. of Aeronautical Engineering, University of Minnesota, for permission to use the high-speed motion picture apparatus, and to Dr. W. G. Luyten, Chairman of the Department of Astronomy at the same Institution for the use of the spectrum-comparator in measuring the films; and to Dean T. L. Joseph for his continued interest in the prosecution of the work.

References

[1] A. M. Gaudin: *The Principles of Mineral Dressing.* p. 354 (1939) New York.

[2] K. L. Sutherland: *Journal Phys. Chem.* (1948) **52**, p. 394.

[3] O. S. Bogdanov and M. S. Filanowski: *Journal Phys. Chem.* (Russ.) (1940) **14**, p. 244.

H. R. Spedden and W. S. Hannan: *Trans.* AIME (1949) **183**, p. 208; *Mining Technology* TP 2354 (March 1948).

[4] Z. Wolkowa: *Acta Physicochim.* URSS. (1945) **20**, p. 469.

[5] W. Thomson: *Philosophical Mag.* No. 4 (1871) **42**, p. 375.

Lord Rayleigh: *Proc.* Royal Society (1879) **29A**, p. 71.

Ph. Lenard: *Ann. Physik* No. 3 (1887) **30**, p. 209.

N. Bohr: *Philosophical Trans.* Royal Society (1909) **209A**, p. 316.

H. Stocker: *Ztsch. Physik. Chem.* (1920) **44**, p. 149.

R. C. Brown: *Proc.* Physical Society (1936) **48**, p. 312.

[6] W. Philippoff: Paper presented in the Colloid Division at the Meeting of the American Chemical Society in Chicago, Ill. in Sept. 1950.

[7] S. D. Poisson: Nouvelle Theorie de l'action capillaire. Paris (1831) pp. 236-240.

[8] H. H. Kellogg: Discussion, *Trans.* AIME (1950) **187**, p. 1154; MINING ENGINEERING (November 1950).

[9] J. Sven-Nilsson: Kolloid-Z (1934) **69**, p. 230.

Proc. Swedish Inst. Engineering Reserve (1935) **133**.

[10] J. Stefan: Sitzber. Akad. Wiss. Wien II (1874) **69**, p. 713.

O. Reynolds: *Philosophical Trans.* Royal Society (1886) **177A**, p. 157.

[11] F. R. Eirich and D. Tabor: *Proc.* Cambridge Philosophical Society (1948) **44**, p. 566.

[12] C. V. Boys: Soap Bubbles. 2nd Edit. p. 110. (1916), London.

[13] R. Brinkmann and A. V. Szent-Gyorygi: Biochem. *Ztsch.* (1923) **139**, p. 261.

R. S. Burdon *Proc.* Physical Society (1926) **38**, p. 148.

Thermal Metamorphism and Ground Water Alteration Of Coking Coal Near Paonia, Colorado

by Vard H. Johnson

IN 1943 the U. S. Bureau of Mines undertook drilling in an effort to develop new reserves of coking coal in an area near Paonia, Colo., as a part of an attempt to alleviate the shortage of *known* coking coal of good quality in the western United States. Geologic mapping of the area was undertaken by the U. S. Geological Survey with the purpose of first furnishing guidance in location of drillholes and later aiding in interpreting the results of the drilling.

The drilling program was under the general supervision of A. L. Toenges of the U. S. Bureau of Mines. J. J. Dowd and R. G. Travis were in charge of the work in the field. Geologic mapping was started by D. A. Andrews of the Geological Survey in the summer of 1943 and was continued from the spring of 1944 to 1949 by the writer.

The first few holes drilled failed to locate coking coal, but in the summer of 1944 coking coal was discovered by drilling 6 miles east of Somerset, Colo., the site of present mining. In the succeeding years, 1945 to 1948, 100 to 150 million tons of coal suitable for coking were blocked out by drilling.

The ensuing discussion of the geologic controls on the distribution of coking coal in the area is based on the geologic mapping as well as the drilling done in the Paonia area, more complete descriptions of which have appeared or are in process of publication.[1-5] In order that the possible geologic controls affecting the present distribution of coking coal may be considered, it is necessary to discuss briefly the indicators of coking quality coals.

Coking Coal

Coal that cokes has the property of softening to form a pastelike mass at high temperatures under reducing conditions in the coke oven. This softening is accompanied by the release of the volatile constituents as bubbles of gas. After release of the contained gases and upon cooling, a hard gray coherent but spongelike mass remains that is referred to as coke. This substance varies greatly in physical properties and, to be suitable for industrial use, must be sufficiently dense and strong to withstand the crushing pressure of heavy furnace loads.

Western coals have a generally high volatile content and therefore form a satisfactory coke only when they attain a rather high fluidity during the process of heating and distillation in the coke oven. When this high degree of fluidity is developed, the volatile constituents escape and leave a finely porous coke. On the other hand, when the degree of fluidity is low the product is an excessively porous and therefore physically weak mass that is called char.[6]

Small quantities of oxygen present in coal are believed to decrease the fluidity of the material during the coking process and to favor the development of char rather than coke. In consequence, coal chemists have for some time considered the possibility of developing an index to coking qualities by inspection of chemical analyses of coals.[7]

A formula has now been developed that does permit a rough preliminary estimate of the cokability of coal on the basis of the analysis on an ash and moisture-free basis. Coals may be eliminated as possible coking fuels if the oxygen content is greater than 11 pct. Similarly the ratio of hydrogen to oxygen must be greater than 0.5 and the ratio of fixed carbon to volatile constituents must be greater than 1.3. If the coal, on the basis of these limiting factors, appears to have possible coking qualities, the following formula permits determination of the coking index:

$$\text{Coking index} = \frac{a+b+c+d}{5}$$

a equals 22/oxygen content on ash and moisture-free basis,

b equals two times the hydrogen content divided by oxygen content on moisture and ash-free basis,

c equals fixed carbon/1.3 x volatile matter, and

d equals the heating value on moist, ash-free basis/13,600.

Coking indices higher than 1.0 suggest that the coal will coke, and indices above 1.1 indicate good coking tendencies. Although generally usable, this formula is not completely satisfactory because the percentage of oxygen shown in ultimate analyses is derived only by difference; i.e., by subtracting the sum of the percentages of the constituents determined analytically from 100 pct.[8,9]

Although the coking index indicates the coking tendencies of coal, it is necessary to make physical tests of coke before its industrial value can be determined. The U. S. Bureau of Mines has developed a standard procedure for determining the approximate strength of coke that would be formed from a given coal. In this test one part of ground coal, mixed with 15 parts of carborundum, is baked to form a standard briquette. The weight, in kilograms, necessary to crush the briquette is termed the *agglutinating index*. This test determines the relative fluidity attained in the coking process by measuring the cementing strength of the coal in the briquette. A

V. H. JOHNSON, Member AIME, is with the U. S. Geological Survey, Salt Lake City.

Discussion on this paper, TP 3267FI, may be sent to AIME before May 30, 1952. Manuscript, May 15, 1951. Revision, Nov. 19, 1951. New York Meeting, February 1952.

Paper published by permission of the Director, U. S. Geological Survey.

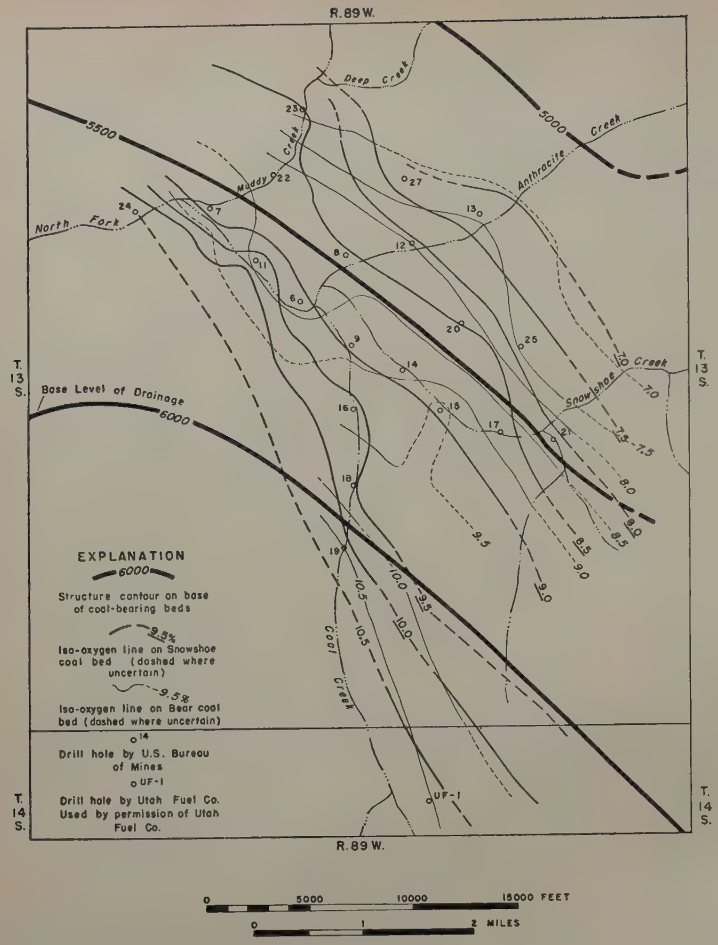
R.89W.
Deep Creek
Anthracite Creek
Muddy Creek
North Fork
Snowshoe Creek
Coal Creek
5500
5000
6000
Base Level of Drainage
T. 13 S.
T. 14 S.
R.89 W.
EXPLANATION
Structure contour on base of coal-bearing beds
Iso-oxygen line on Snowshoe coal bed (dashed where uncertain)
Iso-oxygen line on Bear coal bed (dashed where uncertain)
Drill hole by U.S. Bureau of Mines
UF-1
Drill hole by Utah Fuel Co. Used by permission of Utah Fuel Co.
0 5000 10000 15000 FEET
0 1 2 MILES

Fig. 1 — Coking coal area, T.13S., R.89W., Mt. Gunnison quadrangle, Colo., showing drill-holes, iso-oxygen lines and structure contours.

coal having an agglutinating index greater than 2.5 will make coke. Higher indices indicate better coke.

Thermal Metamorphism of Coal

The halos of high-rank coal occur, under some circumstances, adjacent to intrusive bodies of igneous rock. This relationship has been observed frequently in western coal mining districts. The factors that control such local increases in rank are understood in only a general way but appear to be:

1—Regional rank of coal prior to emplacement of the intrusive body. 2—Temperature and composition of the magma. 3—Size and form of the intrusive body. 4—Amount and character of the overburden at the time of igneous emplacement (closed or open system as used in physical chemistry). 5—Distance of coal from intrusive.

In the Paonia and adjacent districts Tertiary intrusive bodies are numerous and several are of large size. These are chiefly quartz monzonite porphyry and kindred types, which locally intrude the coal-bearing Mesaverde formation of Upper Cretaceous age. Small halos of high-rank coal occur adjacent to these intrusions.

An example of such thermal metamorphism may be observed at the Richardson mine on Carbon Creek, 15 miles north of Gunnison and about 25 miles from the Paonia district.[10,11] A laccolithic intrusive body of quartz monzonite porphyry lies immediately north of the mine and cuts the coal-bearing formation at a low angle. The leading edge extends southward, and at the mine the floor of the main mass lies about 100 ft above the coal bed. This relation is clearly exposed on the west bank of Carbon Creek north of the mine.

Chemical analyses as well as field inspection reveals that in a distance of 2000 ft beyond the flank of the intrusive body the coal varies in rank from semianthracite to high-volatile bituminous. The former evidently is the highest rank that has been reached as a result of the thermal metamorphism, whereas the latter approaches the regional rank of the coals in the Mesaverde formation. Between the two extremes there is an irregular belt of medium to low-volatile bituminous coal that has coking qualities. It is interesting to note that the coal of semianthracite rank is coextensive with the intrusive body where it lies but a short distance above the coal.

In the vicinity of Placita, Pitkin County, Colo., which is approximately 20 miles northeast of Coal Creek, additional evidence of thermal metamorphism has been observed. Coking coal locally occurs in the vicinity of an intrusive body in an area where the regional rank is high-volatile bituminous.

It is rather apparent that local advances in rank, of the types cited, are results of natural distillation of volatile substances, including oxygen, during emplacement of magma masses. In the two cases cited, bodies of higher rank coal thus formed have not been sufficiently altered, by secondary additions of oxygen, to destroy their coking tendencies, in spite of the fact that they lie above the water table. It may be inferred from the above that higher rank coals have less tendency than low-rank coals to absorb oxygen from ground water.

At the Crested Butte mine, 6 miles north of the Richardson mine, the mildly coking medium to high-volatile A bituminous coal lies in a shallow southwest-plunging synclinal trough between semianthracite and noncoking high-volatile coal in the same bed. Semianthracite coal has been produced at several mines northwest of Crested Butte, and noncoking, high-volatile bituminous coal from the old Bulckley mine about 2 miles to the southeast.[12]

In the cases cited above, thermal metamorphism has apparently had a beneficial effect on the coking characteristics of the coal. Contrariwise, the agglutinating index values of the higher rank coal, see cols. 2 and 3 in Table I, from drillhole UF-1 are 0.01 and 0.5, despite the low oxygen content. This coal is from a bed, known as the Oliver bed, that pinches out south of drillholes 18 and 21. Most of the coking coal is in the Snowshoe bed which is about 400 ft lower in the Mesaverde beds. Coal in the Snowshoe bed at drillhole UF-1 contains only 52.8 pct fixed carbon but has 10.2 pct of oxygen and an agglutinating index of only 2.0, see Figs. 1 and 2.

Thick sequences of metamorphosed shale in the northern half of the Anthracite and Crested Butte quadrangles (east of Mount Gunnison quadrangle) indicate the deep source area of the magma which gave rise to the orthomagmatic monzonite intrusions in the West Elk mountains. These latter extend across the southern ends of the quadrangles mentioned and produced little, if any, contact metamorphism of the sedimentary rocks. The higher rank coals at location N, see Fig. 3, in section 20, T. 12 S., R. 88 W. are on the western fringe of the metamorphosed area. The samples represent weathered coal from a stream channel and only proximate analyses were made.

Ground Water Effect on Coals

The present coexistence and relative distribution of coking and noncoking coal within single beds in the Mount Gunnison quadrangle cannot be explained on the basis of thermal metamorphism, dynamic metamorphism, or depth of burial. The difference between coking and noncoking coal in this area is not related to rank. A brief study of the fixed carbon volatile ratios, Fig. 5, shows that there is no well-defined trend in the very minor variations in rank. Further, the rank of the coal in the Snowshoe bed is essentially average for coal in the West Elk Mountain and Grand Mesa fields. Oxygen is the principal variant and the one most closely related to the coking characteristics of coal in this area. This is in accord with Parry's coking index formula which gives oxygen a triple weighting.

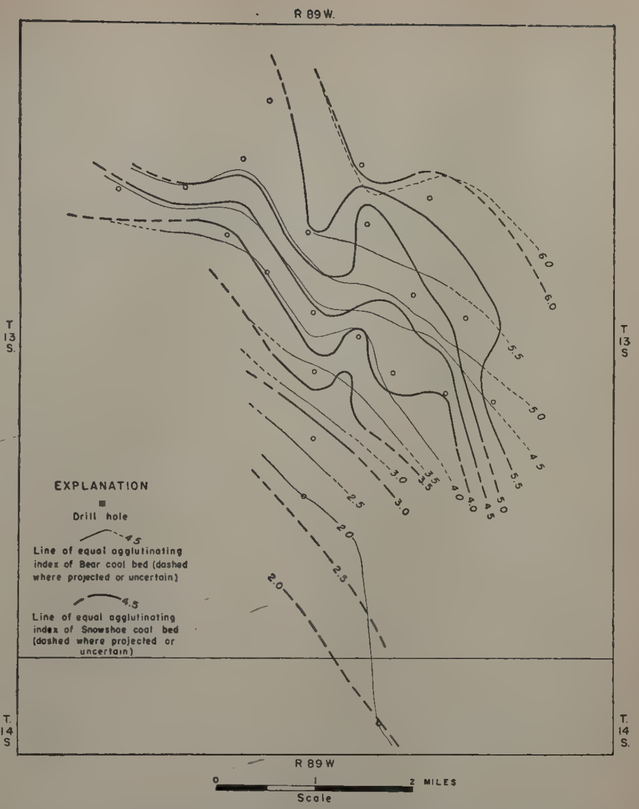
R 89 W.
T 13 S.
T 13 S
T. 14 S
T. 14 S.
R 89 W
6.0
6.0
5.5
5.0
4.5
5.5
5.0
4.5
4.0
4.0
3.5
3.5
3.0
3.0
2.5
2.0
2.5
2.0
EXPLANATION
■
Drill hole
4.5
Line of equal agglutinating index of Bear coal bed (dashed where projected or uncertain)
4.5
Line of equal agglutinating index of Snowshoe coal bed (dashed where projected or uncertain)
0
1
2 MILES
Scale

Fig. 2—T.13S., R.89W., Mt. Gunnison quadrangle, Colo., showing trend lines of equal agglutinating index in Snowshoe and Bear coal beds.

To find the reason for the present distribution of

Table I. Coal Analyses Showing Thermal Metamorphism Due to Intrusions, Moisture-free Basis[a]

Example and Map Symbol	UF-1 (Drill Core)			A		B		C	D	E	N	Regional Avg
	1[b]	2[c]	3[d]	4[e]	4[e]	5[f]	5[f]	6[g]	7[h]	8[i]		9[j]
Distance, ft from nearest contact	0	7+	10	50	400	300±	500±	10±	200±	<1 mile	2000±	
Distance, ft from outcrop	400	450	450	0	0	5	20	40	?	2600	0	
Thickness of intrusive body, ft	16	16	16	2000+	2000+	2000+	2000+	40	1000+	1000+	5000±	
Proximate analysis, pct												
Fixed carbon	83.1	71.7	57.2	75.4	62.2	71.4	56.3	80.5	63.2	61.1	86.4	52
Volatile matter	8.3	21.7	36.2	20.6	33.3	24.2	39.2	14.2	30.7	35.3	7.4	42
Ash	8.6	6.7	6.6	4.0	4.5	4.6	4.5	5.3	6.3	3.6	6.2	6
Sulphur	0.71	0.7	0.8	1.0	0.6	0.65	1.09	0.72	0.44	0.4	0.7	0.8
Ultimate analysis, pct												
Hydrogen		4.9	5.8	4.4	4.9					5.6		
Carbon		87.4	82.5	85.8	78.7					83.3		
Nitrogen		2.1	1.9	2.2	1.9					1.7		
Oxygen		5.9	9.0	6.6	13.9					8.9		12

[a] Other examples may be found in the U. S. Geol. Survey *Bull.* 510. Localities Nos. 79, 120, 121, 127, Floresta, and at Phillip mine. Several analyses of thermally metamorphosed coal are included in the report on Mt. Gunnison Quadrangle and Paonia Coal Fields, being prepared for publication by the author.

[b] Four-in. coal seam at top of 16-ft sill.

[c] Top half of 6-ft coal bed below the sill.

[d] Bottom half of same bed.

[e] Two outcrop samples of same bed.

[f] Second bed is 200 ft above first (U.S. Geol. Survey *Bull.* 510, p. 205).

[g] Coal bed underneath 40-ft sill (U.S. Geol. Survey *Bull.* 510, p. 206).

[h] Location of Richardson mine (U.S. Geol. Survey *Bull.* 510, p. 208).

[i] Crested Butte mine, also in bed between semianthracite and noncoking coal, (U.S. Geol. Survey *Bull.* 510, p. 181).

[j] Regional average for Grand Mesa coal fields.

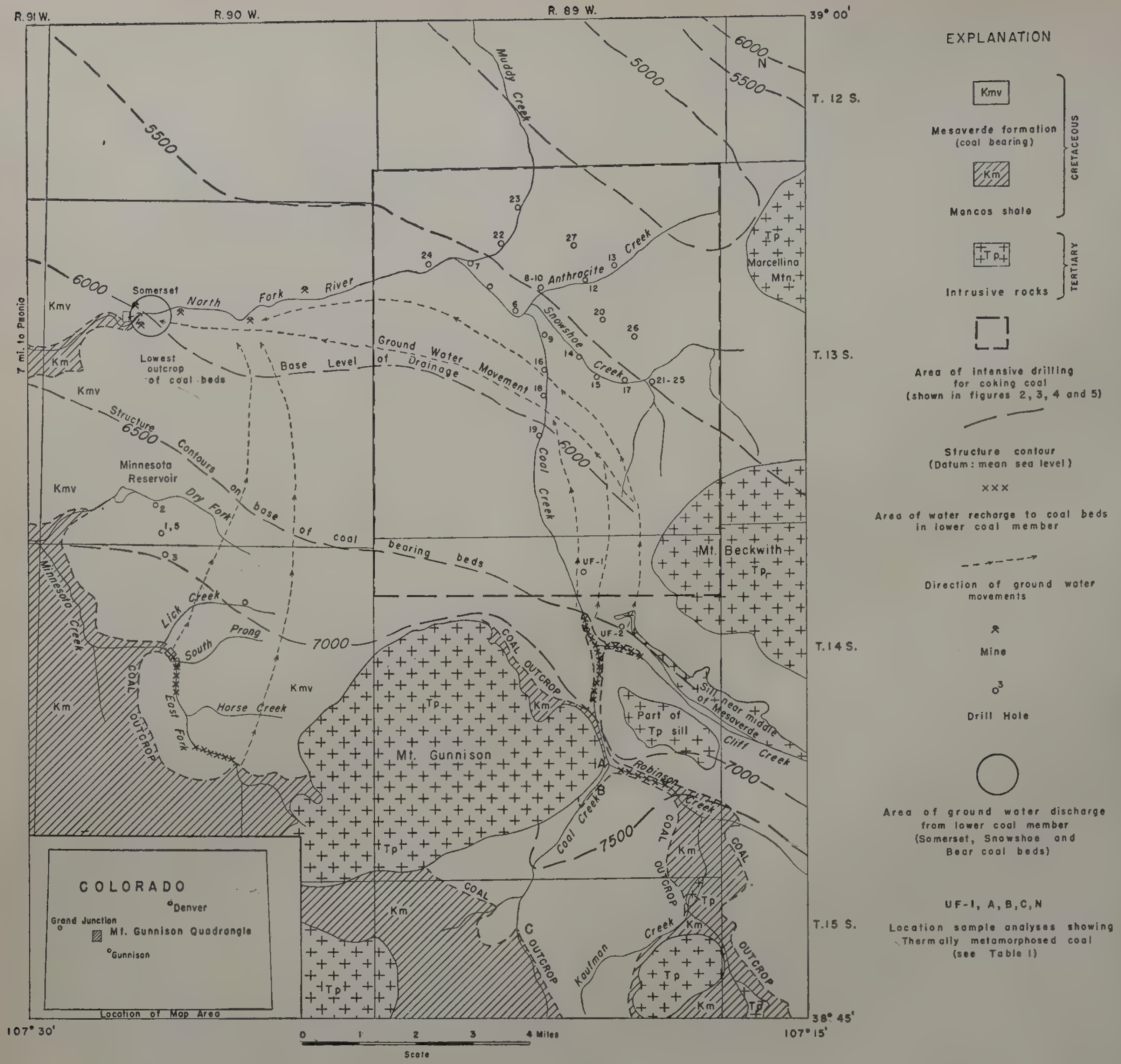

Fig. 3—Mt. Gunnison quadrangle, Colo., showing relations of coal-bearing cretaceous strata to tertiary intrusive bodies and general pattern of ground water circulation at the base of the coal-bearing beds.

coking and noncoking coal, it is necessary to explain the present distribution of oxygen in the coal beds. Analyses of coal from areas above the 6000-ft structure contour, see Fig. 3, show oxygen contents ranging from 10 to 14 pct with a median between 11 and 12 pct (moisture and ash-free basis). In the drill core samples from the area shown in Figs. 1, 2, 4, and 5, the average oxygen content in 44 analyses is 8.87 pct (moisture and ash-free basis) with one analysis showing only 6.8 pct. The reader will note, in Fig. 1, that trends of the iso-oxygen lines representing 9 pct, or less, are approximately parallel to the structure contours. The 10 pct lines rise more steeply toward the east, as might be expected if oxidation were due to ground-water circulation. Lines of equal value for the other variables in the coking index follow similar patterns, see Figs. 2-5.

In the areas where permanent streams and wet gravel lie on the upturned edges of alternating shale, coal, and sandstone beds, the bulk of the ground water enters and percolates through the coal and sandstone beds. The water follows these aquifer beds to the water table and thence along the water table toward the lowest point of outcrop. This point establishes the base level of drainage for those beds, or the level to which the water table would ultimately drop if influent seepage ceased. The gradient of the water table between areas of influent and effluent seepage establishes a hydraulic head, which forces lateral circulation toward the effluent area. Some of this circulation will extend below the base level of drainage, especially near the effluent area. Fig. 3 shows the general structure and pattern of groundwater movement in the Mount Gunnison quadrangle.

It has been shown that the cokability of coal is inversely related, within certain limits, to the quantity of oxygen present in the coal. The proportion of oxygen in coal may be increased by the circulation of meteoric waters. In the zones of downward and lateral movement, such waters are generally aerated and therefore, in percolating through coal beds, provide sources of oxygen that may be absorbed or adsorbed by the coal. This process of alteration may, in fact, increase the oxygen content

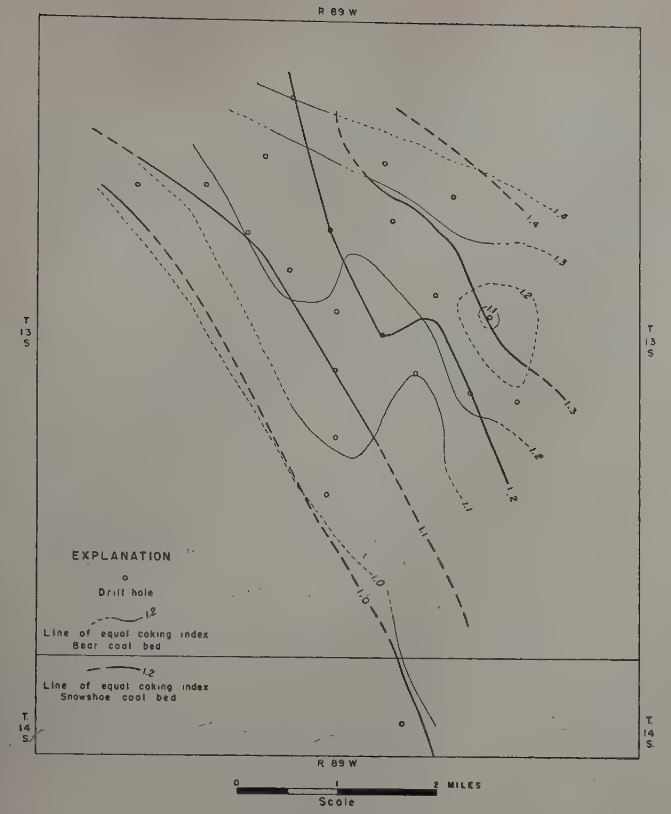
R 89 W
T 13 S
T 14 S
1.4
1.3
1.2
1.1
1.0
EXPLANATION
Drill hole
1.2
Line of equal coking index Bear coal bed
1.2
Line of equal coking index Snowshoe coal bed
0 1 2 MILES
Scale

Fig. 4—T.13S., R.89W., Mt. Gunnison quadrangle, Colo., showing trends of lines of equal coking index of coal in the Bear and Snowshoe beds.

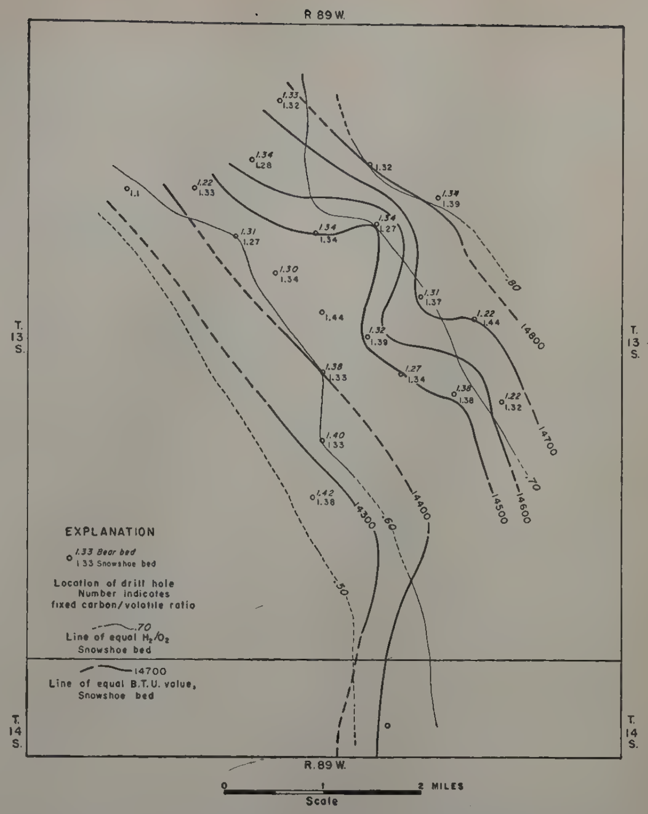

Fig. 5—T.13S., R.89W., Mt. Gunnison quadrangle, Colo., showing values of fixed carbon/volatile ratio for Snowshoe and Bear beds and trends of H_2/O_2 ratio and heat values of coal in Snowshoe bed.

to such an extent that the coal will no longer coke even though it was cokable when the regional water table stood at a higher level and it was below the zone of active ground-water circulation, i.e., an area of stagnant ground water. The addition of oxygen to coal may be expected particularly in the zone of downward percolation of water under climatic conditions characterized by alternate wet and dry seasons. In this zone, where seasonal wetting and drying occurs, oxygen is provided not only by downward-moving ground water but also by air that moves into the space vacated by water moving to lower levels during the dry season. This air is in turn moved downward by the wave of saturation that starts down the coal bed and associated joints and channels during the succeeding wet season. The coking properties of high-volatile western coals may be destroyed for a distance of several miles from the outcrop, if large volumes of water move through the coal bed.

Conclusions

Many factors may, and do, influence the coking characteristics of coal, especially high-volatile coal. The writer has cited several examples of coking and noncoking coal occurring in adjacent areas of the same coal beds. In the cases cited, two geologic processes, thermal metamorphism and oxidation, are believed to be mostly responsible for the present relative distribution of coking and noncoking coal. Thermally metamorphosed coal, of intermediate rank, has better coking qualities than the unmetamorphosed coal adjacent to it and apparently has less tendency to oxidize. Oxygen absorbed, or adsorbed, from actively circulating ground water has apparently reduced or destroyed the coking characteristics of much of the coal in this area.

References

[1] A. L. Toenges, et al: Investigations of Coal Deposits in the Coal Creek District, Gunnison County, Colorado. U. S. Bur. Mines *R. I.* 4104 (1947).

[2] A. L. Toenges, et al: Reserves, Petrographic and Chemical Characteristics, and Carbonizing Properties of Coal Occurring South of Dry Fork of Minnesota Creek, Gunnison County, near Paonia, Colorado, and the Geology of the Area. U. S. Bur. Mines Tech. Paper 721 (1949).

[3] W. T. Lee: Coal Fields of Grand Mesa and West Elk Mountains. U. S. Geol. Survey *Bull.* 510 (1912) p. 203.

[4] V. H. Johnson: Paonia Coal Field, Delta and Gunnison Counties, Colorado. U. S. Geol. Survey Prelim. Coal Map (1948).

[5] V. H. Johnson: Mount Gunnison Quadrangle and the Paonia Coal Field, Delta and Gunnison Counties, Colorado. U. S. Geol. Survey *Bull.* (in preparation).

[6] J. L. Gibson, et al: Low-temperature Carbonization of Utah Coals. Utah Conservation and Research Foundation (1939) pp. 187-220.

[7] V. F. Parry: Trends in the Use of Energy in the Western States with Particular Reference to Coal. U. S. Bur. Mines *R. I.* 3680 (1943) p. 31.

[8] H. H. Lowry: *Chemistry of Coal Utilization.* National Research Council, pp. 662, 666, 668 (1942) New York, John Wiley and Sons.

[9] A. C. Fieldner and W. A. Selvig: Notes on Sampling and Analysis of Coal. U. S. Bur. Mines Tech. Paper 586 (1938) p. 26.

[10] U. S. Bur. Mines: Reports of Coal Analysis (individual analyses).

[11] G. E. Dollard: Oral communication (August 1944).

[12] W. T. Lee: Coal Fields of Grand Mesa and the West Elk Mountains, Colo. U. S. Geol. Survey *Bull.* 510 (1912) pp. 168-173, 181-187, 207-208.

Saskatchewan's Industrial Minerals

by A. J. Williams

THE province of Saskatchewan, situated in the center of the Great Plains region of Canada, has, like most prairie areas, an essentially agricultural economy. Most of its population of about 860,000 is located in the southern half of the province in the farming and ranching areas. To the north of the prairie is a broad forested belt supporting a considerable timbering industry, and the northern one third of the province is glaciated pre-Cambrian rock formation. This latter area is relatively barren of vegetation, but the presence within it of a considerable variety of radioactive, noble and base metals, and industrial minerals has been shown by prospecting in recent years.[1]

Glacial Geology

The Keewatin ice sheet, considered to have accumulated in the country to the west of Hudson Bay in Pleistocene time, covered at its maximum advancement almost all of Saskatchewan and extended south of the international boundary. Only in the Cypress Hills in the southwest and around Wood Mountain in the south central portion of the province did the preglacial formations escape the action for this glacial period. The bedrock of the plains and forest areas therefore is overlain by moraines and modified glacial drift, which vary in thickness from a few feet to 400 or 500 ft.[2] Glacial action in the pre-Cambrian area of the province was largely erosional, most of the more recent formations and some of the pre-Cambrian rock being transported out of the area to the south and west. It has been estimated that about 13 pct of this area is composed of lakes and rivers not too adaptable to rail or water transportation, so that until the use of aviation for exploration purposes became general, development of the area was slow. To the south, the heavy mantle of glacial drift has to some extent deterred the discovery of industrial minerals in the bedrock underlying the forest and prairie regions.[3] At the same time, this drift contains numerous deposits of those most elementary and necessary industrial minerals, sand and gravel.

Sedimentary Basin

The major feature of the sedimentary deposits underlying the plains regions is the basinal structure known as the Moose Jaw syncline, which runs from the southeast corner of the province in a northwesterly direction. To the west of this syncline the formations curve upward, then have been faulted and further upthrust to appear at the surface in the foothills of the Rockies in Alberta; to the east and north they curve upward into Manitoba and northern Saskatchewan, but the surface contacts are covered mostly with glacial drift.[2,3] The axis of the syncline dips to the southeast, so that there is also an upward trend of the formations along the axis to the northwest. In illustration of the regional structure underlying the province, the pre-Cambrian *basement* has been logged in drillholes at the following depths in several locations: Ogema (south central), 9390 ft; Gronlid (northeast), 2599 ft; Vera (northwest), 4422 ft; Big River (north northwest), 2348 ft.

Fig. 1 indicates the general surface geology of the province, ignoring such glacial overburden as may overlie many of the bedrock formations. Also indicated is the approximate location of the axis of the Moose Jaw syncline.[4]

Industrial Minerals

Clays: The province is fortunate in possessing a widespread distribution of clays of ceramic value, ranging from those used for heavy structural products to the high grade pottery and china clays. Shales suitable for brick and tile production are found in the Upper Cretaceous and Tertiary formations across the south of the province where the glacial drift is thin or nonexistent. Many deposits of glacial lake clays suitable for such wares are found scattered over the rest of the province south of the pre-Cambrian area.

The Whitemud formation of the Upper Cretaceous is a narrow sedimentary band of secondary clays found intermittently at points across the south of the province where glacial action did not disturb or remove them.[8]

In the southwest corner of the province, around Eastend in the Frenchman River valley, the refractory clays of this formation are contaminated somewhat with iron compounds or other alteration products of basaltic rocks. This eliminates the use of those clays in true whitewares, as they fire to creamy buff shades at the lower temperatures and to a blue-specked grey at cone 8 to 12, (2280°F to 2390°F), the range commonly used in firing whiteware. However, for use in the production of colored artware, caneware, stoneware or crockery, and sewerpipe, this type of clay makes an excellent body that requires little or no addition of flint, feldspar, or other fluxing materials such as are required in the higher class of ware.[9] It is not a grade of clay that can be shipped great distances to the manufacturing centers, but a market for considerable tonnages has developed at nearby Medicine Hat, where cheap natural gas is available for the firing of the ware.

Farther east in the south central portion of the province, the clays of the Whitemud formation are generally more refractory and white burning. The formation is divided into three zones, consisting of white clays, brown shale, and white sandy clays.

A. J. WILLIAMS is Director of Resources Utilization, Province of Saskatchewan, Regina, Sask., Canada.

Discussion on this paper, TP 3286H, may be sent to AIME before May 30, 1952. Manuscript, Feb. 16, 1951. Revision, Nov. 13, 1951. St. Louis Meeting, February 1951.

Paper published by permission of the Minister, Saskatchewan Dept. of Natural Resources.

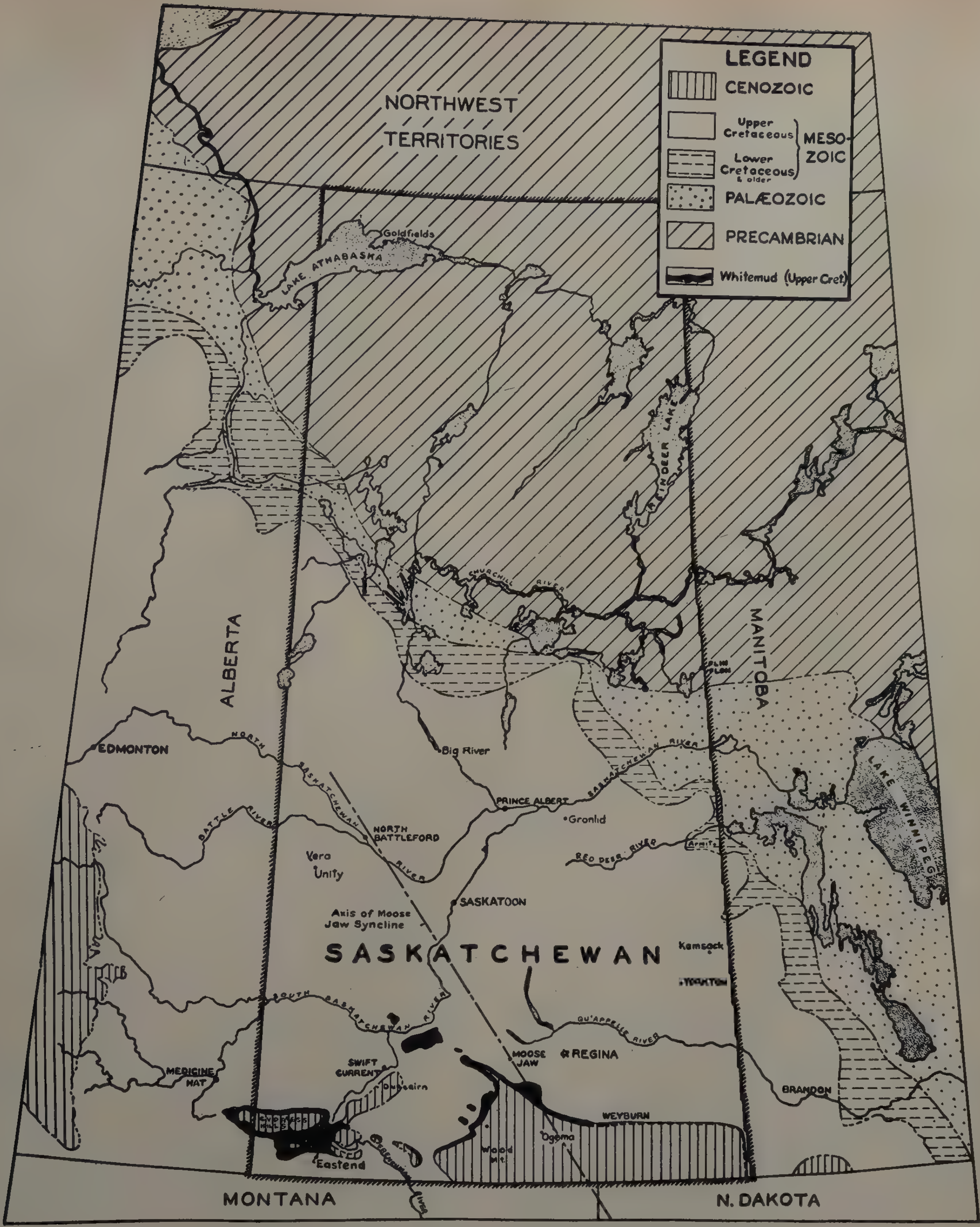

Fig. 1—Geology of Saskatchewan and its environs.

The upper strata of the white sandy zone consists of a weathered breakdown of feldspathic rocks, resulting in an intimate mixture of kaolin or china clay and quartz grains, with some mica and other impurities. This is as a whole a highly refractory clay and has been used to some extent in the production of firebrick. China clays suitable for ceramic use and as fillers in the manufacture of rubber, paper, and other commodities can be separated from this material, but the long freight hauls to the major markets have deterred such development to date. Some test work aimed at bleaching the china clay to a whiteness suitable for coating papers currently is being carried out by the Resources Utilization Branch; if this work is successful, the outlook for production of refined china clay in the province will be improved considerably.

The brown shale above the sandy white zone is moderately refractory but does not burn to a good white color, so is used largely as a component of sewerpipe or firebrick mixtures.

The white clay zone is probably the most important of the three, since it contains valuable white-burning ball clays of exceptional raw strength. A ball clay is a plastic refractory material used in whitewares as a bonding agent for the other nonplastic components such as kaolin, flint, and feldspar. Though it does form a definite part of the refractory body, its chief value lies in the way it improves the workability of the body mixture and reduces breakage of ware in the handling prior to its being fired. Most Saskatchewan ball clays have greater raw unfired strength than any of the English and American ball clays, and it therefore appears feasible to ship them to the eastern Canadian and American ceramic production centers. To support such development, the Saskatchewan Dept. of Natural Resources has carried out a lengthy program of exploration and testing of all of these refractory clays.

This program has now outlined large commercial tonnages of ball clays, fireclays, and stoneware clays, and the next step, that of carrying forward test work with various ceramic firms to fit the clays to the needs of industry, is going forward at the present time. Reports on the exploration and testing of the more promising clays are available at Regina.[5, 6]

Bentonites: In line with the clay research program, the Department has been investigating reserves of bentonites. These can be used for a great variety of purposes, the foremost being as bleaching agents, as bonding material for foundry sands, and as circulating mud for rotary drilling exploration. While no industry has been based on production of this mineral in the province to date, reserves of over 100,000 tons of high grade montmorillonite bentonites have been proved up and may shortly be providing at least part of the needs of the drilling crews in the present oil and gas exploration boom in Saskatchewan. Work is also being done on some of the nonswelling bentonites for use as bleaching agents. Again, these reserves are found in the relatively unglaciated areas of the south central portion of the province or at more northerly points where river valleys have cut through a thin layer of drift.

Sodium Sulphate: One of the most important surface minerals being exploited in the province today is sodium sulphate, commonly known as salt cake and used in large tonnage by the kraft paper industry.

More than 200 alkali deposits and lakes containing a reserve in excess of 60 million tons of anhydrous sodium sulphate have been located in the province. Their origin is attributed to seepages of water containing calcium and magnesium sulphate through bentonitic clay beds, where an exchange of calcium for sodium ions takes place. The deposits occur in undrained basins, where evaporation over long periods of years has developed the concentration of the alkali salt. In some deposits the salt is present as a strong brine, and in others as a brine overlying permanent beds of solid crystal mixed with varying amounts of clay impurities.

The process of mining and refining the salt cake is relatively simple; the main problem of the industry is maintenance of equipment and buildings because of the corrosive action of the alkali brine, crystal, and dust being handled. In some deposits clean permanent beds of Glauber's salt are quarried and the crystal subjected to a very minor countercurrent washing to remove included silt or clay. To meet the demand for high purity salt, several plants have installed crystallizing ponds. Alkali brine from lake deposits is pumped into these ponds in late summer, when at its highest concentration, and impounded until cold fall weather precipitates the bulk of the Glauber's salt. The supernatant brine then is drained back into the lake, and the clean salt is harvested from the reservoirs with heavy earth-moving equipment.

The balance of the salt cake operation consists of removal of the water of crystallization of Glauber's salt, which amounts to 55.9 pct of the raw material. This is carried out in oil or coal-fired rotary kilns, sometimes preceded by melters and evaporators to obtain greater fuel economy.

Saskatchewan production in the past decade has varied between 100,000 and 150,000 tons of anhydrous salt cake annually.

Magnesium Compounds: Associated with some of the major sodium sulphate deposits is another potentially important mineral substance, a mixture of magnesium chloride and sulphate. Though there has been no development of this resource to date, it could form the basis for an industry producing either the natural magnesium salts or magnesium metal and magnesia refractories, using processes similar to those now extracting magnesium materials from seawater. The magnesium content of the larger lakes is from three to five times that of seawater, while in some smaller lakes up to 4.5 pct magnesium equivalent may be found. A preliminary estimate from a survey of six such lakes in 1950 indicates reserves of over 13 million tons equivalent of magnesium oxide.

Volcanic Ash: Several large deposits of volcanic ash are located in south central and southwestern Saskatchewan. This fine-grained abrasive material has been used to some extent for production of kitchen cleansers; at the present the Saskatchewan Research Council is investigating its usefulness as an additive to concrete for waterproofing purposes. The Department is also trying to develop a cheap process to expand it with heat for use as an insulating material or as a lightweight aggregate.

Analysis of ash[10] from one of the better deposits (Duncairn) is as follows: SiO_2, 68.64 pct; Al_2O_3 and Fe_2O_3, 13.05 pct; CaO, 2.11 pct; MgO, 0.40 pct; Na_2O, 0.91 pct; K_2O, 7.40 pct; H_2O (+105°C), 7.28; and total, 99.79 pct.

Silica Sand, Marl, and Quartzite Pebbles: Among the other quarriable minerals of the province of lesser importance can be included silica sand, marl, and quartzite pebbles. Silica sand from at least one deposit has been tested and proved satisfactory for use as a glass sand and for foundry work, but the market for this material in western Canada has not yet warranted its development.

Chemical and screen analysis of silica sand as mined from the Armit deposit and of a sample subjected to simple Wilfley table washing (85 pct product recovery) have been reported by the Dominion Mines Branch[11] as shown in Table I.

Table I. Analysis of Silica Sand as Mined from the Armit Deposit

Raw Sample					
Screen Analysis					
Mesh	Retained, Pct	Chemical Analysis, Pct		Washed Product, Chemical Analysis, Pct	
20	nil	SiO_2	97.4	SiO_2	99.65
28	15.3	Al_2O_3	0.93	Fe_2O_3	0.027
35	19.2	Fe_2O_3	0.073	TiO_2	0.027
48	21.7	TiO_2	0.056		
65	26.2	CaO	0.043		
100	12.3	MgO	0.086		
150	3.3				
200	0.8				
—200	1.2				

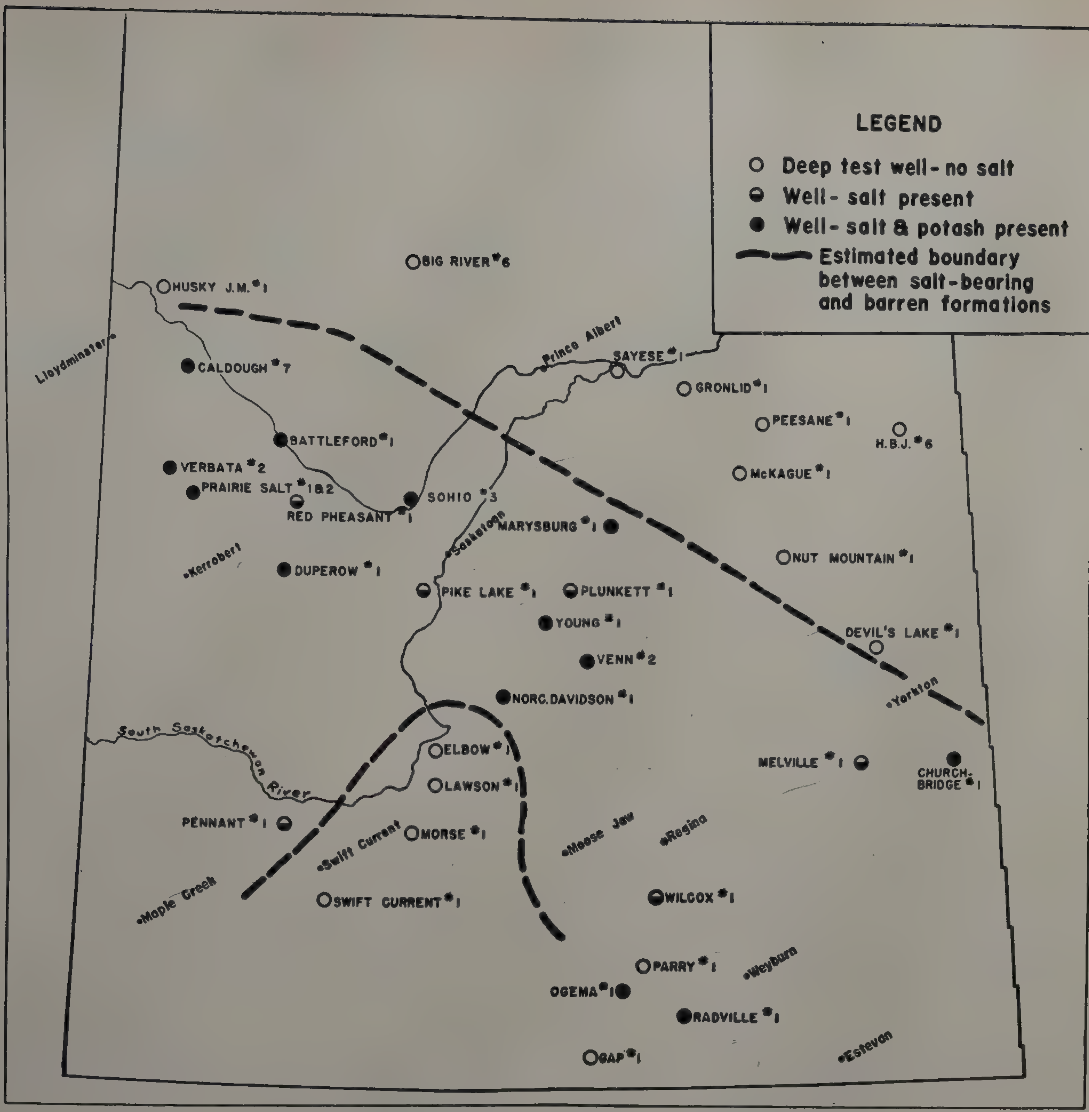

Fig. 2—Saskatchewan salt and potash occurrences.

Several marl deposits have been noted at various points such as Kamsack, Swift Current, and Sturgeon Lake, but have not been investigated to any extent.

The retreating glaciers left numerous eskers of washed and sorted rocks, sand, and gravel in their wake.[1] Among these are several in the southwest portion of the province, which are composed almost entirely of clean, uncemented quartzite pebbles, sometimes used in industry for ballmilling of iron-free materials.

Subsurface Sedimentary Minerals

Salt: From test holes drilled in the search for oil and gas, it has become apparent that a vast salt deposit underlies most of the plains region of the province. Geologists have not yet definitely settled on its age, but it apparently occurs close to the contact between the Devonian and Silurian deposits of the Palaeozoic era.

In the south of the province, at Radville and Ogema, salt beds 250 to 300 ft thick were encountered at a depth of about 7000 ft. More or less following the axis of the syncline, at Davidson two beds totalling about 800 ft in thickness were found at around 5000 ft, and near Unity, further to the northwest, a thickness of 435 ft was encountered at a depth of 3700 ft. A rough estimate of the area underlain by salt is shown on the salt-potash map, see Fig. 2.

To date, one salt plant has been established in Saskatchewan to extract salt from this basin. This plant was built at Unity, where natural gas is also available, in 1947. It is a conventional brine well and triple effect evaporation plant, with a rated capacity of 125 tons per day.

Potash: Associated with the aforementioned salt beds, several occurrences of potash in the form of sylvite (KCl), and carnallite ($KCl \cdot MgCl_2 \cdot 6H_2O$) have been noted. At the present time there is no production of potash salts in Canada, and the total annual Canadian consumption, valued at about 4 million dollars, has been imported from the United States and Europe.

While Saskatchewan has the only commercially interesting potash discovered in Canada to date, the depth at which it occurs poses a major mining problem. Potash deposits relative to position in the province are shown in Table II.

Until late in 1950, the occurrence at Vera was the only one which seemed to have commercial significance, and even it was located at nearly 3500-ft depth, compared with the strata being mined at 800 to 1200-ft depths elsewhere in the world. The discovery at Churchbridge in the fall of 1950 has opened up entirely new and perhaps better possibilities. Though at only 500 or 600 ft shallower depth than the Vera potash, it indicates a deposit which may easily extend up the dip of the formations to depths more comparable with conditions in Carlsbad, New Mex.

It is hoped that further drilling in the province will locate potash at shallower levels. The occurrences noted to date are of considerable importance to Saskatchewan and Canada as a whole. Several firms already have expressed interest in the obtaining of exploration permits and production leases on potash areas in the province. It is therefore quite possible that this mineral will be produced, for at least the Canadian market, from these deposits within the next 4 or 5 years.

Surface and Subsurface Pre-Cambrian

The industrial mineral discoveries in the northern pre-Cambrian area have been relatively recent. The search for uranium ores, the provincial government's geological survey, and a Prospector's Assistance Plan have all contributed to a better knowledge of the mineral wealth of this territory. The bulk of discoveries to date have been precious and base metals such as are mined and smelted by the Hudson Bay Mining and Smelting Co., at Flin Flon. This mine takes about 25 million dollars worth of copper, zinc, silver, gold, cadmium, selenium, and tellurium annually from its Saskatchewan orebodies. The complex sulphide ores being smelted at Flin Flon also represent an important potential source of sulphur or sulphuric acid. It is understood that the possibility of recovering such products from the mill and smelter wastes is being given serious consideration at the present time. However, the lack of large-scale nearby markets is an adverse economic factor that may deter such development for some considerable time.

Feldspar: A discovery of high grade feldspar suitable for the ceramic or glass industries was made in the summer of 1950 near Lac La Ronge at the south central fringe of the pre-Cambrian. The discovery is a flat-lying dyke about 4 ft thick, with an estimated 5000 tons exposed at the outcrop. A Dominion Bureau of Mines analysis of a sample from the outcrop indicates that it is a potash feldspar, as follows: SiO_2, 65.14 pct; Al_2O_3, 19.55 pct; MgO, 0.13 pct; Fe_2O_3, 0.04 pct; CaO, 0.20 pct; K_2O, 11.38 pct; Na_2O, 3.52 pct; TiO_2, 0.026; and loss on ignition, 1.11 pct. This is essentially the same type of feldspar produced in vast quantities from the South Dakota quarries.

Asbestos: There have been no asbestos discoveries of commercial significance in Saskatchewan to date, but recent prospecting has uncovered some promising leads. Narrow veinlets of cross-fiber chrysotile asbestos ranging up to ¾ in. in thickness have been found at Ruth Lake near the Flin Flon mine and farther north near Reindeer Lake. The present demand and rapidly expanding market for this mineral has created considerable interest in new finds, and there is little doubt that the Saskatchewan indications will be prospected thoroughly. At present little is known about the extent or importance of these asbestos occurrences.

Limestone: One of the major industrial minerals, high calcium limestone, is missing from the list of Saskatchewan's resources. Dolomitic limestone suitable for building stone and other purposes is plentifully scattered along a broad zone north of the Saskatchewan River, near the fringe of the pre-Cambrian. Much of the boulder deposition over the southern half of the province is the same dolomitic material, so that it appears unlikely that relatively pure limestone will be found in the northern reaches. Limestone beds containing up to 98.7 pct $CaCO_3$ have been noted in cores taken in deep test oil well drilling, particularly in the Devonian formations. It is doubtful if these would be of commercial interest unless mined as a coproduct from a shaft sunk for potash or other minerals.

Table II. Potash Deposits in Saskatchewan

	Depth, Top of Potash Zone, Ft	Bed Thickness, Ft	K_2O Content, Pct
Radville	7653	10½	16.4
Ogema	7420	2½	20.0
	7440	4½	18.6
Davidson	4358	10	10.8
Vera	3466	11	21.64
Churchbridge	About 2900	10	12.7

Conclusion

To summarize the situation, Saskatchewan is blessed with a good variety of important industrial minerals, several of them unique as far as Canada is concerned. Development of some has been retarded because of lack of local markets and complementary industries, others have been discovered too recently to have reached the production stage as yet, and still others have formed the backbone of the province's nonagricultural industry to date. The impetus given to the northern mining industry by recent uranium development, the industrial follow-up to the discoveries of natural gas and crude oil in Western Canada, the availability of vast tonnages of cheap lignite fuel, and the generally expanding usefulness of industrial minerals in the world today are all factors which should shortly bring Saskatchewan's industrial minerals to a proper position of importance in the economy of the continent.

References

[1] The Natural Resources of Saskatchewan, Departmental Staff Report, 1947.

[2] F. H. Edmunds: Soil Survey Report No. 12 of Southern Saskatchewan, Section of Geology.

[3] E. W. Shaw and G. C. Wells: Principal Types of Oil and Gas Occurrences in Western Canada. *The Precambrian* **24**, No. 8.

[4] J. C. Sproule: Report on Geological Survey of the Saskatchewan Portion of the Williston Basin—1941.

[5] Taken in most part from Map 820 A, Geological Map of the Dominion of Canada, Dept. of Mines and Resources of Canada.

[6] G. S. Crawford: Recent Clay Exploration in Saskatchewan.

[7] D. I. Peterson and R. V. Tomkins: Light Burning Saskatchewan Clays of High Strength.

[8] Fraser, McLean et al.: Geology of Southern Saskatchewan. Canadian Geological Survey, Memoir 176.

[9] W. G. Worcester: Clay Resources of Saskatchewan. Technical and Economic Series, Report No. 2, Resources Utilization Branch, Sask. Dept. Natural Resources (1950).

[10] V. L. Eardley-Wilmot: Abrasives, Part I, Siliceous Abrasives, Dept of Mines, Ottawa Mines Branch No. 673.

[11] Preliminary Report on the Beneficiation of a Siliceous Sand from the Red Deer River, Saskatchewan Report, June 2, 1947, Canadian Bur. of Mines.

[12] L. Heber Cole: Potash Discoveries in Western Canada (1948).

Geology of The Hayden Creek Lead Mine, Southeast Missouri

by Ernest L. Ohle

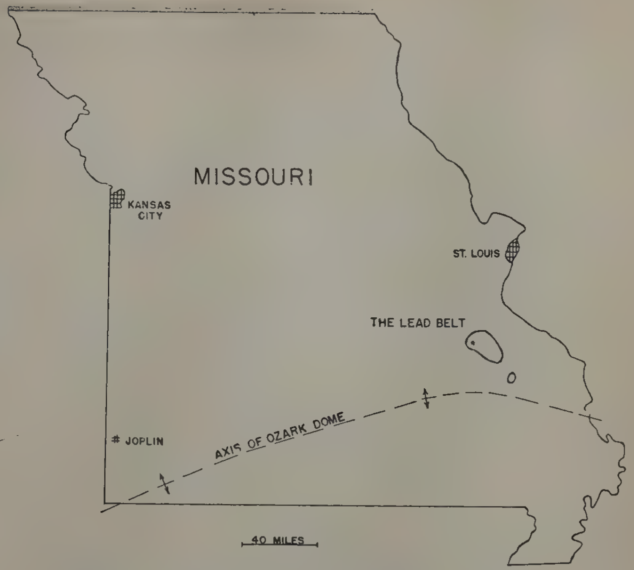

Fig. 1—Index map of Missouri showing the location of the two producing areas in the Southeast Missouri Lead Belt and the position of the Hayden Creek Mine (asterisk).

The newly opened Hayden Creek lead mine represents a variation from the usual Southeast Missouri type. Galena mineralization occurs in sandy dolomite cementing a conglomerate of granite boulders and in cracks in the boulders. The conglomerate occurs at the base of the Bonneterre formation on the slopes of two buried pre-Cambrian knobs.

IN 1943 diamond drilling from the surface in an area 2 miles southwest of Leadwood, Mo., discovered a lead deposit of a markedly different character from the usual southeast Missouri type. Subsequent drilling of about 500 holes indicated several million tons of ore, and in 1950 a 701-ft vertical shaft was sunk into the orebody. This paper describes the geology of this interesting occurrence insofar as it is known from the drilling and the small underground exposure at the bottom of the shaft.

Geology

The location of the Southeast Missouri Lead Belt and of the Hayden Creek property are shown in Fig. 1. As shown here, there are two separate producing areas, one from which the larger tonnage has come, located near Bonne Terre, Flat River, Desloge, and Leadwood, and the other to the south around Fredericktown and including famous old Mine LaMotte.

The best published description of Lead Belt geology is by Tarr.* In pre-Cambrian time in this area, an assemblage of granites and rhyolitic flow rocks was eroded to a mature topography. Sedimentation, beginning in the Upper Cambrian, filled in the valleys and gradually covered even the highest hills. The first formation deposited was the Lamotte sandstone; it is successively overlain by the Bonneterre dolomite, the principal lead-producing formation, then the Davis shale, the Derby-Doerun limestone, and a succession of Cambro-Ordovician cherty dolomites. Several of these formations may be found in direct contact with the pre-Cambrian as their deposition progressively overlapped the older rocks on the flanks of the igneous knobs and ridges.

Immediately overlying the pre-Cambrian there is, not uncommonly, a thin basal conglomerate of granite or porphyry boulders, which is incorporated into the overlying sediments. Deposition of the lower part of the rock section was fairly continuous, and the Lamotte sometimes grades almost imperceptibly into the lower sandy Bonneterre. Since the sediments were deposited on an uneven floor, they tend to reflect the irregularities in that floor. Most of the steep dips found in the district, that is, dips in excess of 10°, are original dips and not caused by deformation. Such domelike structures in the sedimentary rocks around the igneous knobs have localized a considerable number of the orebodies in the district and particularly those in the Fredericktown area. Many of the larger orebodies, however, have no close relation to the pre-Cambrian topography. Most of the lead production has come from the lower 150 ft of the Bonneterre formation, where disseminated ore spreads laterally parallel to the bedding for great distances. Average stoping height is about 20 ft, but in a few places there are stopes over 175 ft high.

---

* W. A. Tarr: Origin of the Southeastern Missouri Lead Deposits. Economic Geology (1936) 31, Nos. 7 and 8, pp. 712-754, 832-866.

E. L. OHLE, Member AIME, is Geologist with the St. Joseph Lead Co., Bonne Terre, Mo.

Discussion on this paper, TP 3227I, may be sent to AIME before June 30, 1952. Manuscript, June 29, 1951. St. Louis Meeting, February 1951.

This page of Mining Transactions AIME follows p. 400. The intervening non-Transactions pages appeared in Mining Engineering.

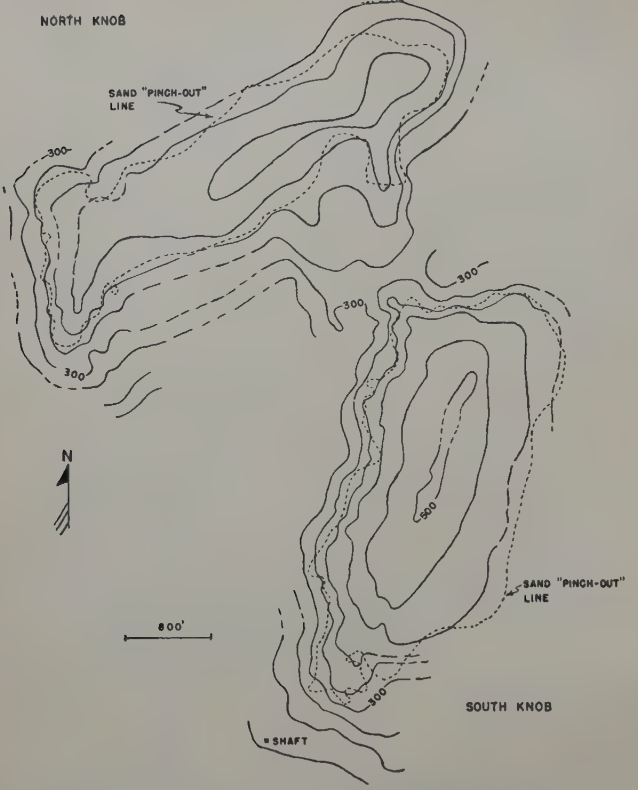

Fig. 2—Configuration of the pre-Cambrian granite surface in the Hayden Creek area. The dotted line indicates the position of the sand pinch-out.

Fairly strong faulting has occurred in southeast Missouri and the main Lead Belt area is surrounded by three faults with displacements ranging from 100 to 600 ft. The 600-ft down drop of the north side of the Simms Mountain fault has resulted in a reversal of the regional dip and the rocks in the Flat River area now dip 1° to 2° southwest.

Hayden Creek Mine

The orebodies of the Hayden Creek area are related to highs in the pre-Cambrian surface. Fig. 2 shows the configuration of the top of the granite as known from drillholes. As shown here, there are two elongated pre-Cambrian hills in the area that gave rise to domal structures in the overlying sediments. These may be designated as the South Knob and the North Knob.

These two prominences are separated by a deep saddle that joins the north end of the South Knob and a point midway along the south side of the North Knob. Lamotte sand is present in this saddle. The line along which the sandstone feathers out up the granite slopes, locally called the "sand pinch-out line," is indicated in Fig. 2. It will be noted that the sandstone rises 50 to 100 ft higher on the northeast slopes than on the southwest slopes of both knobs. This is believed to indicate a prevailing direction of current movement from southwest to northeast during Lamotte time. Other knobs in the Lead Belt show a similar relationship.

Granite is not exposed here at the surface, but the dome structures are reflected in the Davis and Derby-Doerun formations outcropping in the area. The knobs extend up into the lower Bonneterre, but upper Bonneterre beds are present over the highest points. Drillholes show that the area had over 400 ft of relief in pre-Cambrian time.

The South Knob is roughly 4000 ft long by 2000 ft wide, with the long axis trending slightly east of north. The ridge line is sharply defined and the sides have a fairly constant angle of slope from the crest line to the lowest known points where the granite is covered by Lamotte sandstone. The west flank is slightly steeper than the east flank and has an average slope of 20 pct. The largest known body of ore lies on the southwest end of this knob.

The North Knob trends about N 60° E and has approximately the same lateral dimensions as the South Knob. However, it is not as high. Consequently the slopes are more gentle and the crest is not as sharp. Here again, the western slopes are the steepest. The known orebodies associated with this knob are along this western slope.

The interesting thing about the Hayden Creek orebodies is that the ore, instead of being in dolomite, is in a conglomerate of granite pebbles and boulders. Ore in boulders has been mined or is known to exist at several other places in the district, both in the main Lead Belt and in the Fredericktown area. In these bodies, however, the tonnages have been small, ranging from a few hundred to a few tens of thousands of tons and, further, their geological history has been relatively simple. The unusual character of the host rock and a unique stratigraphic setting make the Hayden Creek orebodies of more than passing interest.

Hayden Creek Conglomerate

Part of the conglomerate at Hayden Creek is the common 2 to 20 ft thick basal boulder layer that directly overlies the solid granite hill and was covered by deposition of the Lamotte and Bonneterre formations, a relationship that can be found in many places in the central Ozark region. However, the largest bodies of conglomerate and the ones containing most of the ore had a more complex history. These bodies lie not beneath the Lamotte in the

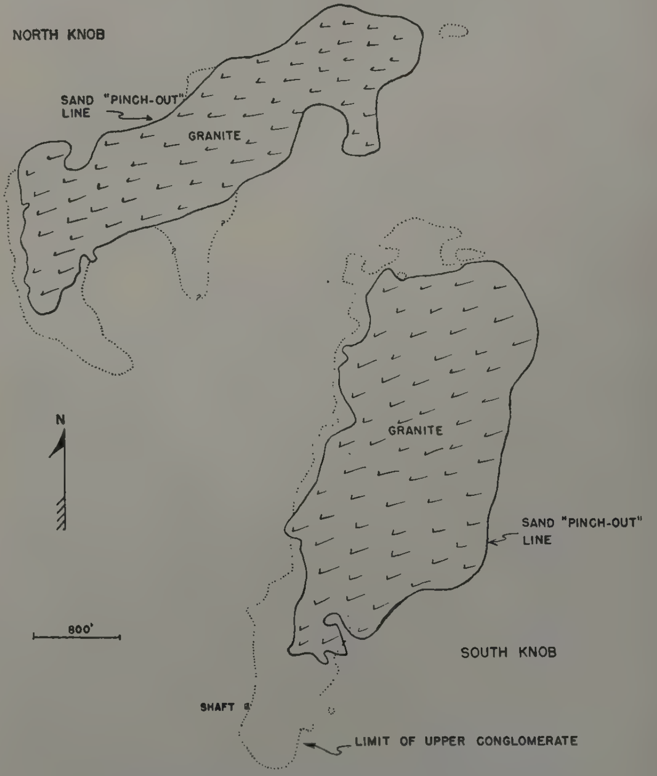

Fig. 3—Location of the bodies of upper conglomerate around the North and South knobs.

normal basal conglomerate position but on top of it and separating it from the overlying carbonate rocks of the Bonneterre. Thus, in selected places, drillholes penetrate two boulder zones, one on top of the Lamotte and the other beneath it. This situation has not been recognized outside of the Hayden Creek area.

Fig. 3 shows the location of the bodies of upper conglomerate around the North and South Knobs, the outline of the knobs being indicated by the sand "pinch-out" lines. It is at once apparent that the largest concentrations of boulders are on the west sides of the two knobs and that both knobs have elongated tongues or tails of boulders that extend southward out over the top of the Lamotte for hundreds of feet. In the case of the South Knob, the boulder tongue is 1200 ft long. It is this boulder mass which contains the bulk of the ore in the Hayden Creek area and in which No. 22 mine is located.

Fig. 4 shows the conglomerate associated with the South Knob in greater detail and also indicates the position of the two cross-sections reproduced in Figs. 5 and 6. These two cross-sections indicate the interrelations of the boulder beds, the Lamotte sand, and the underlying granite hill. Where the sand wedges out up the slope, the upper and lower conglomerate beds cannot be distinguished, and there is a continuous boulder layer from the base of the sand-free Bonneterre dolomite to the top of the granite, except for thin beds or pockets of sandy dolomite that are found locally in the conglomerate. In many places there is no sandy dolomite in the lower Bonneterre, other than as cement between boulders, and the conglomerate occupies all of the position where the sandy transition beds normally would be found.

It will be noted in Figs. 5 and 6 that the angle of slope of the Lamotte surface flattens to the westward where the Lamotte has filled in the pre-Cambrian valley. Section BB′ particularly shows that near the toe of the conglomerate the slope actually reverses itself. This reversal must have opposed the tendency of the main boulder mass to migrate further westward. The front of the conglomerate is quite steep and in one place the thickness decreases from 110 ft to zero between two holes 100 ft apart.

Fig. 7 shows the main South Knob boulder pile in greater detail. By contours on the top of the Lamotte, that is, the base of the upper boulder bed where it is present, it shows the westward and southwestward slope under most of the conglomerate. The reversal in slope indicated before in section BB′ is shown to be an embayment in the contours so that the boulders seem to have been trapped in a small pocket on the sand floor.

Fig. 8 shows the third dimension of this boulder body by thickness contours. Several drillholes cut over 100 ft of boulders. The contours indicate a slightly asymmetric distribution of the boulders with the greater concentration, and hence the steeper marginal slope, occurring on the southeast side of the mass. The edge shows a sharp drop-off everywhere; only two holes were so located near the edge that they cut less than 10 ft of boulders and only five holes cut less than 20 ft. The thickness of the average intersection was 60 ft. In general the axis of this boulder body is parallel to the axis of the South Knob.

The main boulder mass associated with the North Knob is a tongue extending out over the Lamotte for 900 ft in a S 45° E direction. Thus it is elongated nearly at right angles to the long axis of the knob. The average thickness of boulders in this body as shown by the drillholes is only 20 ft and the total volume of boulders is less than one eighth of the volume of the big mass near No. 22 shaft. The maximum thickness cut was 40 ft. From observation of the drill cores, it is believed that the average size of the boulders here is smaller than in the main South Knob orebody.

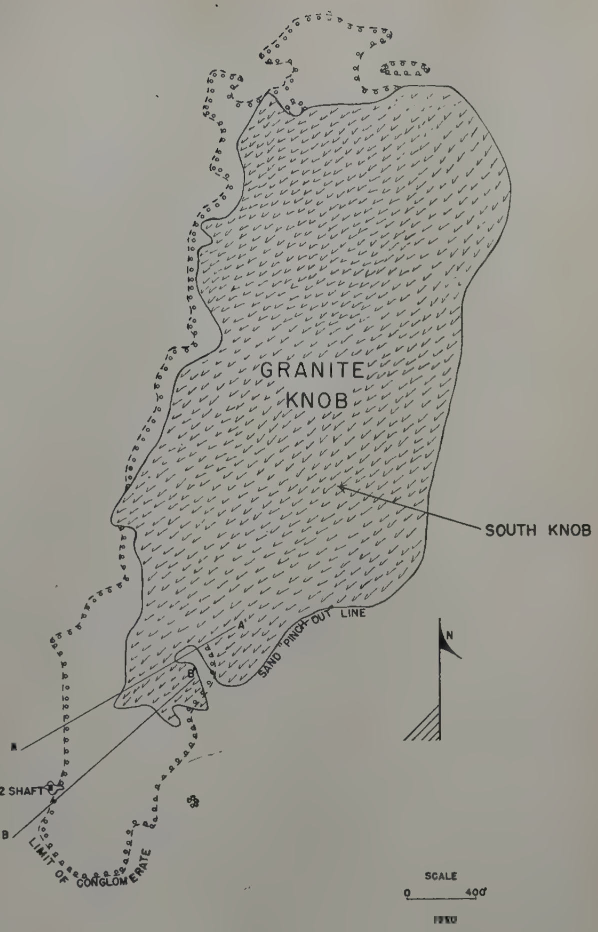

Fig. 4—Plan of the upper conglomerate associated with the South knob.

The granite boulders and fragments of the Hayden Creek area range in size from about a millimeter to several feet. The larger ones, 6 in. and over, are almost all well rounded; the smaller fragments are markedly angular and apparently are the result of sharp impacts of the big boulders against one another at the time the boulder mass moved. Many of the big boulders are cracked and shattered, see Fig. 9. This is especially true of those that are well weathered. The fractures are contained entirely within individual boulders and do not pass from boulder to boulder or into the dolomitic cement. Some of them may represent joint planes that were present in the original granite mass; others, and these include most of the galena-filled cracks, seem more likely to have resulted from boulder impact or crushing.

The cement between the boulders is dense, fine-grained dolomite ranging in color from light gray green to dark gray. Much of it is sandy, especially near the Lamotte contact, and the dark gray parts are usually argillaceous.

Many of the large boulders are standing on end or in other odd positions such as the one shown in

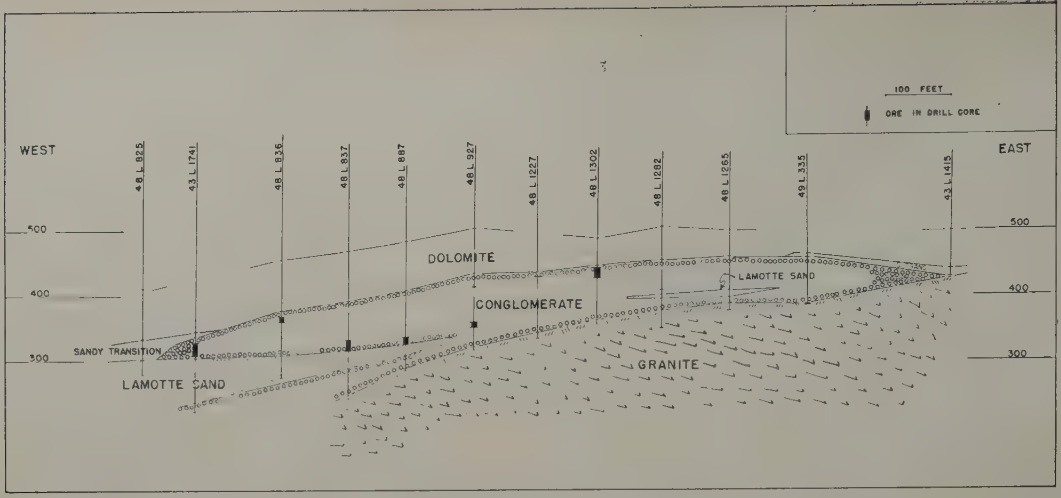

Fig. 5—Cross-section along line A-A′. See Fig. 4.

Fig. 10. Most of them are resting on other boulders or on top of the Lamotte sandstone. There is no sorting; large and small fragments occur scattered at random as individuals or in nests. Many of the small angular broken pieces are scattered through the dolomite and do not touch each other. Some of these are shown in Fig. 11. These fragments seem to have fallen into a calcareous ooze and been buried. The heavier large boulders would tend to sink until they encountered a more substantial base; hence they are not found in the suspended position of the small fragments.

A sandy ooze, which would have become the sandy transition beds in the Bonneterre, apparently overlay the Lamotte at the time (or times) that the boulders shifted. This ooze was disturbed until it lost any semblance of bedding. Some of it was stiff enough to support small granite fragments while letting the big boulders sink in; undoubtedly much of it was stirred up by the grinding force of the rock slide (or roll) only to settle back around the clastic fragments, cementing them together. The filling in process was very complete, and unfilled open spaces are almost nonexistent.

The degree of alteration of the fragments varies widely. Many pieces, small and large, are fresh red granite, while some of the boulders over 1 ft in diam are completely bleached to a dull gray. Quite a fair percentage have fresh interiors and an outer margin of alteration. Significantly the angular fragments, which have been ascribed to impact shattering, exhibit no zoning, being either entirely unaltered or else uniformly altered throughout. It is believed that the greatest share if not all of the alteration in the granite is caused by weathering, much of it probably ante-dating the movement of the boulders to their present location. Whether there is any ore solution alteration such as sericitization is yet to be determined.

Ore Occurrence

In the mine face the galena distribution is erratic and pockety, but the overall grade of the orebody is fairly uniform. The greatest share of the galena occurs in disseminated grains in the cementing dolomite. Crystals up to ½ in. in size may be found, but most of them are smaller. A lesser but still important share of the lead occupies the cracks within the boulders, see Fig. 12. These veinlets range up to ½ in. in width, but thin galena films less than 1 mm wide are more common. The cracks are tensional in character with sharp angular offsets and parallel walls. Quite frequently several parallel cracks lie close to each other as in Fig. 9. The crack-filling veinlets are found in altered boulders but do not occur in fresh red granite.

As shown in the cross-sections, Figs. 5 and 6, the largest continuous ore zone lies just above the top of the Lamotte in the lower part of the upper boulder bed and west of the "sand pinch-out." In some places the underlying top few feet of the Lamotte also contains pay ore. Other smaller, less continuous ore zones are found higher in the upper boulder bed, and some holes have shown considerable thicknesses of low grade mineralization between pay runs. The lower basal conglomerate occasionally is of minable grade. The overlying middle and upper Bonneterre beds above the boulder ore contain only traces of lead.

Galena is the only ore mineral, although traces of sphalerite have been noted. Marcasite and calcite constitute the bulk of the gangue mineralization.

Conglomerate Origin

No theory as to the method of accumulation of these huge masses of large rounded boulders can be supported with complete assurance until more has been seen underground, but some of the data now available have an important bearing on the problem. Two theories have been suggested, both of which explain certain features of the occurrence. One is that the boulder piles are simply talus accumulations on the upper slopes of the knobs which were caused to slide or roll down hill in early Bonneterre time. The original impulse that caused the piles to shift could have been faulting or wave action in the sea, which was rising in level at this time. In any event the theory proposes that the piles gravitated down the granite slopes and out onto the top of the Lamotte, stirring up the sandy Bonneterre ooze which, upon settling, filled in between the boulders and eventually cemented them into a solid mass. It seems likely that such movement would be concentrated in a few more or less violent actions.

There is evidence that faulting has occurred in the Hayden Creek area, which could have started the downhill shift of boulder accumulations on the upper slopes of the knobs, but the exact age of the fault movement is not known. Quite possibly it was recurrent. Fig. 7 shows an abnormally steep slope

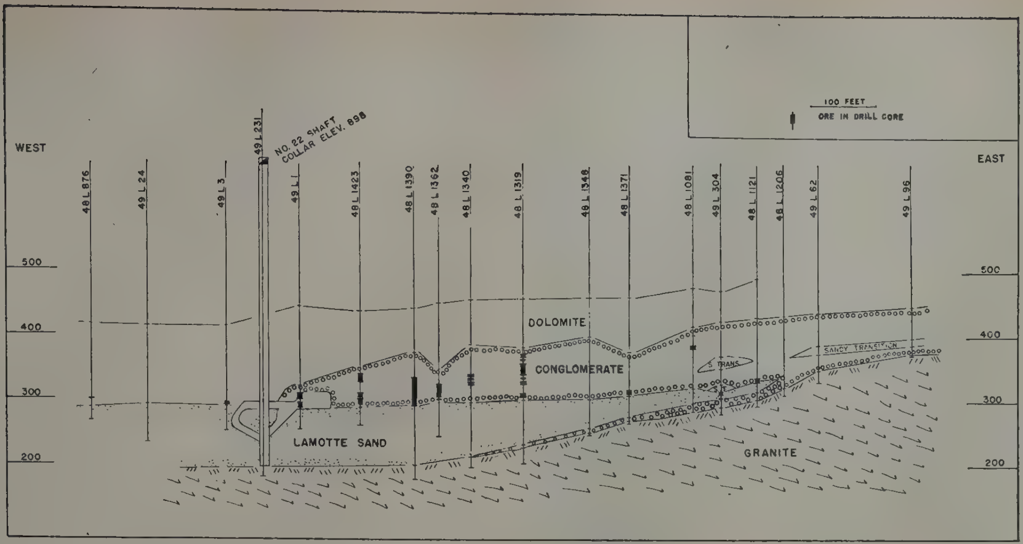

Fig. 6—Cross-section along line B-B'. See Fig. 4.

Fig. 7—Detail of the main South knob conglomerate body showing its relationship to the surface of the underlying Lamotte sand.

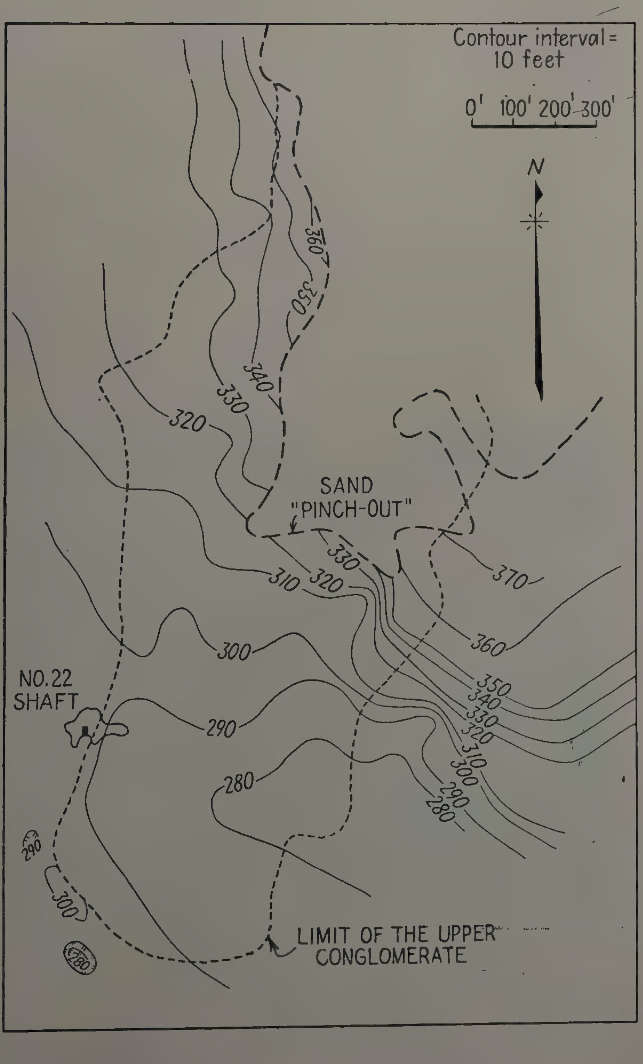

Fig. 8—Thickness contour map of the main South knob conglomerate mass.

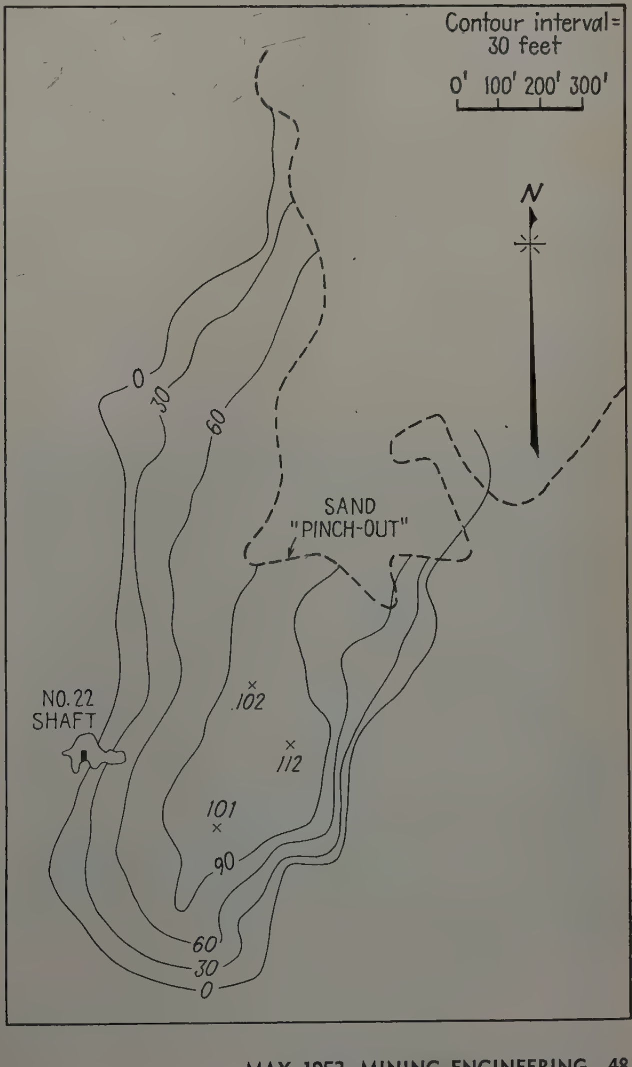

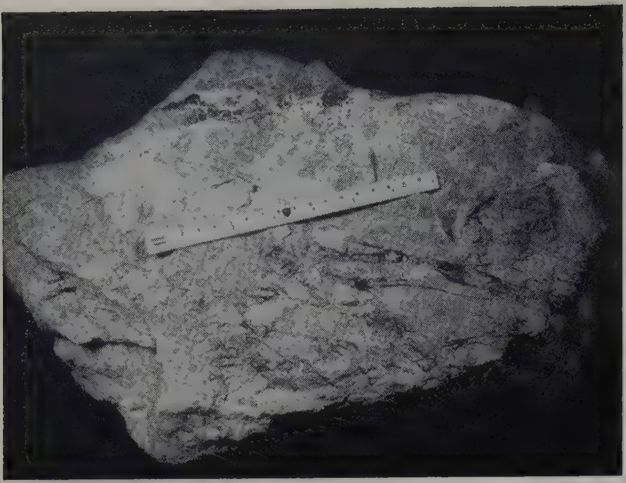

Fig. 9—Shattered granite boulder with galena filling the cracks.

on top of the Lamotte about 1000 ft east of No. 22 shaft. Part of this sharp drop in sand elevation to the southwest is the result of a zone of step faulting with northwest strike. If movement occurred along this fault zone at the critical time when a mass of boulders was in delicate equilibrium on the hillside, the mass might well have been set in motion to the southwest. Similarly, some minor early adjustment along the great Simms Mountain fault zone lying about ½ mile to the south might have triggered the action. The main Simms Mountain faulting, however, occurred long after the conglomerate was buried by younger sediments.

The talus theory explains very well the lack of size sorting and the impact shattering of the boulders. It is confronted with the serious problem, however, of why a talus pile should move southwest as it has from the South Knob when more direct downhill slopes were available to the west and southeast. Fig. 2, which shows the topography of the granite knobs at the time the boulders were formed, shows that there was only a rather small potential source area on the South Knob for boulders likely to move southwest. In the case of the North Knob, the main boulder tongue, being of much smaller volume than the South Knob tongue, is in better proportion to the size of the potential source area for its boulders. But, even here, the location of the main concentration is not a likely looking spot for gravity alone to have caused such a concentration of boulders. The talus theory offers no good explanation for the absence of similar boulder accumulations elsewhere around the knobs.

The smooth rounded exteriors of the large boulders might suggest that they had been rolled and abraded more than would be likely in talus migration downhill. It must be noted in this connection, however, that the outcropping granites in the Ozark region commonly round themselves quite remarkably by exfoliation, and it is probable that practically all of the rounding of the Hayden Creek boulders is the result of exfoliation and not a product of abrasion. This is true no matter what origin is advocated for the conglomerate.

What would seem to be a strong argument against the talus theory obtains from the calculation of the volume of boulders in the upper boulder bed and comparison with the potential source areas up the granite slopes. In the main boulder body on the South Knob, taking the boulders lying west and south of the sand "pinch-out line," there are 56 million cu ft. This does not include the considerable volume of upper boulders which cannot be positively identified as such because of the absence of Lamotte sand higher up the slopes but which surely is present as indicated by boulder thicknesses in excess of 100 ft just east of the "pinch-out." A layer of boulders 20 ft thick over an area 1680 ft square is equivalent to 56 million cu ft. Reference to Fig. 2 would seem to indicate that it would be most unlikely that the southwest slope of the South Knob could produce this volume of boulders at one time. Even if all of the solid granite available to erosion in this area were reduced to boulders and if all of the boulders formed moved in the right direction, i.e., southwest, it would be necessary for 15 to 20 ft of granite to be broken down to provide the boulders that are piled up in the No. 22 mine area. The time available for the accumulation in their present position is that period between the end of Lamotte time and the deposition of the non-sandy middle Bonneterre. Since this interval is quite short, there is serious question whether adequate time was available for weathering to produce from this small area

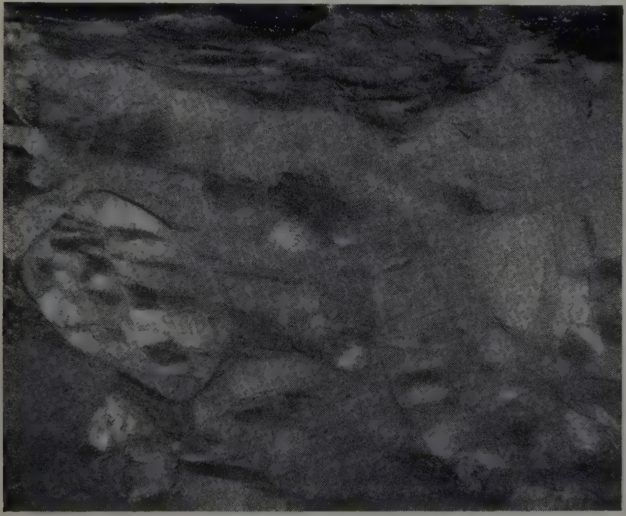

Fig. 10—Underground view showing the random orientation of large and small boulders.

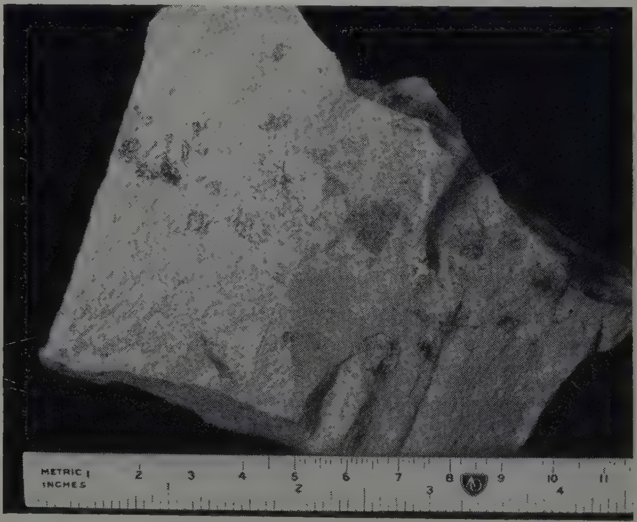

Fig. 11—Isolated angular granite fragments (dark gray) scattered through a matrix of dense sandy dolomite.

the boulders found in this one large conglomerate body.

The drillhole intersections of several feet of sandy dolomite within the conglomerate deserve some mention in this discussion of the history of the boulder mass. In Fig. 6, these intersections are interpreted as beds of sandy dolomite because they were logged as such when the holes were drilled. These holes did cut sandy dolomite at such depths that, on the section, it appears that there is a layer of this material in the midst of the upper boulder bed. If this is correct, it has significance because it indicates that there were at least two periods of boulder accumulation separated by an interval when more normal Bonneterre sedimentation occurred. Furthermore, it is shown that the deposition of the uppermost conglomerate was not so violent as to disturb a limey layer less than 10 ft thick and hence there probably could not have been talus migration with its attendant grinding.

Before any final conclusion is drawn based on this evidence, however, consideration should be given to another possible interpretation of these sandy dolomite core intersections. This conglomerate body consists of boulders up to 8 or 10 ft in diam cemented by sandy dolomite. The boulders are not tightly packed together, and in the mine, pockets of dolomitic cement of considerable size may be seen. Whether a drillhole cuts a granite boulder or the cementing dolomite at a given elevation depends on its location a few feet one way or the other. A drillhole passing between large boulders might show a section several feet long of sandy dolomite that entirely resembled normal basal Bonneterre rock and would be logged as such. Interpretation of the intersection as representing a bed of dolomite would be in error. Additional mine exposures will be necessary to ascertain whether the conglomerate is divisible into units separated by dolomite beds or whether it is entirely the product of one period of boulder deposition.

The other theory of conglomerate formation is that the tonguelike masses are the result of ocean current action, that is, boulder spits piled up at the ends of islands in the sea. The motivating force would be long-shore currents that rolled the boulders southward until they slid into deeper water at the ends of the knobs and came to rest. Such accumulation would probably have been more gradual than that advocated in the talus theory.

The location of the two main boulder piles strongly favors the ocean current hypothesis. Currents moving southward along the shores of the granite islands might be expected to carry along the rounded boulders and to build up a leeward accumulation. The huge size of some of the boulders and the fact that many of them are by no means spherical, though rounded, indicate that a strong current would be required.

If such a concentrated current was responsible for these boulder spits, it seems strange that it should have deposited its load without regard to size. The lack of sorting is very striking. The frontal slope of the piles is very steep and sharply defined and there is no trailing off of finer sized material. This is perhaps the strongest argument against the ocean current hypothesis, for even if the long shore current were related to a short, violent storm, some size sorting would be expected.

The proposal of a southward moving current is contrary to independent evidence in the Lead Belt that the major currents of the area at this time were moving northeastward. The distribution of the sandy dolomite in the lower Bonneterre in long northeast-trending bars or ridges and their relations to the pre-Cambrian knobs are strong evidence for this belief.† The presence of Lamotte sand at higher elevations on the northeast sides of the knobs here and elsewhere in the Lead Belt is evidence that northeastward-moving currents also prevailed in Lamotte time. Thus the postulated southward current in the Hayden Creek area at this same time would have been purely local in scope.

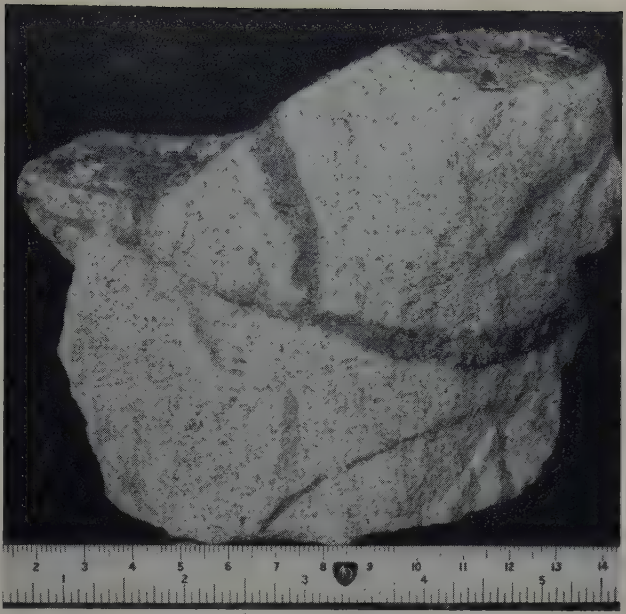

Fig. 12—Galena occupying tensional shatter-cracks through a granite boulder.

The shattering observed in many of the weathered boulders is evidence of violent emplacement, and there is good reason to believe that once most of these boulders fell into their present positions and were shattered by impact they did not move again. Had they been shifted further, they would have fallen to pieces. Some of them did fall apart and gave rise to the smaller angular fragments, but most of them apparently did not. These observations support the belief that the piles were emplaced by short violent movement rather than gradual long-continued growth. The erratic, on-end positions of some of the large, rudely tabular boulders also suggests a lack of opportunity for shifting about and settling into the most stable position.

Summary

Prospecting in southeast Missouri in recent years has discovered several million tons of lead ore in an environment quite different from the usual southeast Missouri situation. The host rocks are masses of granite boulders which, in large part, overlie the Lamotte sandstone around buried pre-Cambrian granite knobs. Galena replaces the dolomitic cement and fills cracks in shattered boulders. The conglomerate bodies may represent talus accumulations or may have been caused by shore current action when the knobs were islands in the Cambrian Sea.

Acknowledgment

The author is indebted to the St. Joseph Lead Co. for permission to publish this report.

---

† Geological Staff, St. Joseph Lead Co. Unpublished Guidebook, AIME Annual Meeting Field Trip, February, 1951.

The Third Theory Of Comminution

by Fred C. Bond

MOST investigators are aware of the present unsatisfactory state of information concerning the fundamentals of crushing and grinding. Considerable scattered empirical data exist, which are useful for predicting machine performance and give acceptable accuracy when the installations and materials compared are quite similar. However, there is no widely accepted unifying principle or theory that can explain satisfactorily the actual energy input necessary in commercial installations, or can greatly extend the range of empirical comparisons.

Two mutually contradictory theories have long existed in the literature, the Rittinger and Kick. They were derived from different viewpoints and logically lead to different results.

The Rittinger theory is the older and more widely accepted.[1] In its first form, as stated by P. R. Rittinger, it postulates that the useful work done in crushing and grinding is directly proportional to the new surface area produced and hence inversely proportional to the product diameter. In its second form it has been amplified and enlarged to include the concept of surface energy; in this form it was precisely stated by A. M. Gaudin[2] as follows: "The efficiency of a comminution operation is the ratio of the surface energy produced to the kinetic energy expended." According to the theory in its second form, measurements of the surface areas of the feed and product and determinations of the surface energy per unit of new surface area produced give the useful work accomplished. Computations using the best values of surface energy obtainable indicate that perhaps 99 pct of the work input in crushing and grinding is wasted. However, no method of comminution has yet been devised which results in a reasonably high mechanical efficiency under this definition. Laboratory tests have been reported[3] that support the theory in its first form by indicating that the new surface produced in different grinds is proportional to the work input. However, most of these tests employ an unnatural feed consisting either of screened particles of one sieve size or a scalped feed which has had the fines removed. In these cases the proportion of work done on the finer product particles is greatly increased and distorted beyond that to be expected with a normal feed containing the natural fines. Tests on pure crystallized quartz are likely to be misleading, since it does not follow the regular breakage pattern of most materials but is relatively harder to grind at the finer sizes, as will be shown later. This theory appears to be indefensible mathematically, since work is the product of force multiplied by distance, and the distance factor (particle deformation before breakage) is ignored.

The Kick theory[4] is based primarily upon the stress-strain diagram of cubes under compression, or the deformation factor. It states that the work required is proportional to the reduction in volume of the particles concerned. Where F represents the diameter of the feed particles and P is the diameter of the product particles, the reduction ratio Rr is F/P, and according to Kick the work input required for reduction to different sizes is proportional to log Rr/log 2.[5] The Kick theory is mathematically more tenable than the Rittinger when cubes under compression are considered, but it obviously fails to assign a sufficient proportion of the total work in reduction to the production of fine particles.

According to the Rittinger theory as demonstrated by the theoretical breakage of cubes the new surface produced, and consequently the useful work input, is proportional to $Rr-1$.[5] If a given reduction takes place in two or more stages, the overall reduction ratio is the product of the Rr values for each stage, and the sum of the work accomplished in all stages is proportional to the sum of each $Rr-1$ value multiplied by the relative surface area before each reduction stage.

It appears that neither the Rittinger theory, which is concerned only with surface, nor the Kick theory, which is concerned only with volume, can be completely correct. Crushing and grinding are concerned both with surface and volume; the absorption of evenly applied stresses is proportional to the volume concerned, but breakage starts with a crack tip, usually on the surface, and the concentration of stresses on the surface motivates the formation of the crack tips.

The evaluation of grinding results in terms of surface tons per kw-hr, based upon screen analysis, involves an assumption of the surface area of the subsieve product, which may cause important errors. The evaluation in terms of kw-hr per net ton of —200 mesh produced often leads to erroneous results when grinds of appreciably different fineness are compared, since the amount of —200 mesh material produced varies with the size distribution characteristics of the feed.

This paper is concerned primarily with the development, proof, and application of a new Third Theory, which should eliminate the objections to the two old theories and serve as a practical unifying principle for comminution in all size ranges. Both of the old theories have been remarkably barren of practical results when applied to actual crushing and grinding installations. The need for a new satisfactory theory is more acute than those not directly concerned with crushing and grinding calculations can realize.

In developing a new theory it is first necessary to re-examine critically the assumptions underlying

---

F. C. BOND is Engineer in Charge, Technical Research, Processing Machinery Dept., Allis-Chalmers Mfg. Co., Milwaukee.

Discussion on this paper, TP 3308B, may be sent (2 copies) to AIME before June 30, 1952. Manuscript, Sept. 14, 1951. Revision, March 5, 1952. Mexico City Meeting, October 1951.

the old theories, which may have been accepted previously without due consideration.

The first of these assumptions to be questioned is concerned with the neglect of the work previously done on the feed particles. Any subdivided material represents work input, and the total work input to a material should be the primary consideration, not the work input increment below a certain feed size.

The second assumption which should be questioned is the derivation of both theories from the consideration of cubes under compression. Compressive stress applied evenly to parallel plane surfaces of cubes constitutes an almost nonexistent case in actual crushing and grinding, and applications of the theory derived from the theoretical breakage of the cubes into a certain number of smaller cubes are usually misleading. In actual operation the stresses are applied at protruding points of irregularly shaped bodies, these points crumbling until sufficient area is developed to break the particles under nonuniform stress. Theoretical consideration of the breakage of spheres under compression should be more applicable than that relating to cubes.

The strain energy theory[5] also employs the first and second assumptions and to this extent is open to the same objections as the Rittinger and Kick theories.

The third assumption is that useful work input is equivalent to energy content, or that the energy of a material after breakage is increased by the amount of useful work applied during breakage, even though this energy increment is not recoverable by any known means. This assumption is inherent in the second form of the Rittinger theory and underlies much of the current thinking on comminution. It postulates that the bulk of the energy input required in all known methods of breakage, which is released as heat, represents wasted work input.

These three assumptions were avoided in the derivation of the new Third Theory to be presented here. However, assumptions cannot be completely eliminated from the development of any theory.

The requirements of a successful theory should be considered:

1—It should give consistent results when applied to all comminution operations over all size reduction ranges, for all materials, in all types of machines. The different breakage characteristics of different materials over different size ranges, in different machines with varying efficiencies in each size range, should be properly evaluated by the new theory. After sufficient study under the correct theory, it should be possible to develop factors for the correction of each of the above differences and unerringly select the operation with the highest mechanical efficiency.

2—It should be supported by a large mass of operating data on a wide variety of materials correlated with laboratory tests on the same materials.

3—The correlation should be made by a work index, representing the total work input to a definite product size, which should be obtainable from any laboratory or commercial operation when the energy input and size analyses of feed and product are known.

4—It should be possible to calculate the useful energy input required for any size reduction from the work index or from any similar reduction in a different size range, when allowance is made for possible different breakage characteristics and machine efficiencies at different sizes.

Nomenclature

C = Impact crushing strength in foot-pounds per inch.[10]
D = Diameter of cubes or spheres.
F = Feed size = 80 pct of feed passes in inches or microns.
Fc = Cutoff size of scalped feed.
Fe = Equivalent feed size of scalped feed.
Fp = Percentage of feed passing product size P.
G_{b_p} = Ball mill grindability at product size.[10]
G_{r_p} = Rod mill grindability at product size.[10]
L = Effective crack length in centimeters per short ton.
m = Slope of percentage passing line on log-log plot. For normal material $m = 1/\sqrt{2}$.
P = Product size = size 80 pct of product passes inches or microns.
P_1 = Grindability test sieve opening in microns.
Rr = Reduction ratio = F/P.
S = Specific gravity.
W = Work input in kw-hr per short ton to any comminution operation.
Wi = Work index = Wt for P = 100 microns.
Wp = Total work input in kw-hr per ton represented by a product size P.
Wu = Useful work input.
Wu/W = Mechanical efficiency.
Y = Percentage passing any diam X.
Yc = Percentage passing cutoff size Fc of normal feed with 80 pct—size F.

5—It should have a theoretical basis confirmed by previously determined empirical relationships.

6—The absolute mechanical efficiency should be obtainable.

Definition of Terms

Work input, *W*, is the work or energy input in kw-hr per short ton to a machine reducing material from a definite feed size to a definite product size.

Total work input, *Wt*, represents the total work or energy input in kw-hr per ton applied to obtain a size reduction from a feed of theoretically infinite particle size to a definite product size. The total work input is the sum of the work input in reduction of the feed to the product and all work previously put into the feed.

Useful work input, *Wu*, represents that portion of the work input which causes breakage and eliminates that portion of the work input consumed in machine friction, wear of machine parts, contacts not including materials to be reduced, and contacts resulting in stresses below the critical breaking stress. It represents the theoretical minimum work input necessary at 100 pct efficiency. Its theoretical value has not been derived in the present paper. Mechanical efficiency is the ratio of useful work to work input, or *Wu/W*; it does not necessarily correspond to the thermodynamic efficiency, since comminution is not necessarily reducible to an adiabatic process, although it may have an adiabatic component.

The feed size, *F*, is the diameter in microns or inches of the square hole that will pass 80 pct of the feed and is found from the plotted screen analysis.

The product size, *P*, is the size 80 pct of the product passes and is found from the plotted screen analysis.

The reduction ratio, Rr, equals F/P.

The work index, Wi, is the calculated kw-hr per ton applied in reducing material of infinite particle size to 80 pct passing 100 microns, equivalent to approximately 65 pct passing 200 mesh. It establishes the relative reduction resistance of a material in the size range tested and the relative mechanical efficiencies of different machines and different processes. It can be found from any commercial or laboratory operation where the work input and size distribution of the feed and product are known.

The following definition of the comminution process is proposed in agreement with the concepts of the Third Theory.

The comminution process is a procedure in which mechanical kinetic energy is transformed into heat through internal and external friction, under conditions such that critical strains are exceeded and material is broken.

The mechanical efficiency is the ratio of the amount of breakage to the amount of energy transformed, or to the total energy input.

Derivation of the Third Theory

Experience has shown that the average slope, m, of the size distribution percent passing line of crushed and ground products, on a log-log plot of the percent passing against the sieve opening, is very close to $1/\sqrt{2}$, or 0.7071. The slopes vary somewhat with the nature and history of the material, but the average indicates that the normal slope of a homogeneous material that has been reduced by a nonselective comminution action is $1/\sqrt{2}$.

The normal size distribution line follows this equation:[5, 6]

$$Y = 80\left(\frac{X}{P}\right)^{1/\sqrt{2}} \qquad [1]$$

where Y is the percent weight passing any diam X, and P is the diameter 80 pct passes. The percent passing varies as the particle size X to the power m, which equals $1/\sqrt{2}$.

The surface areas of a unit volume of material in particles of similar shape of diam X vary as $1/X$. With normal materials the percent weight in each size fraction in the $\sqrt{2}$ sieve scale series varies as $1/\sqrt{2}$. Therefore, the surface area of each fraction varies as

$$X^{1/\sqrt{2}}/X \text{ or as } 1/X^{0.2929}$$

If the slope m were unity, the surface area of each size fraction would be the same or would vary as $1/X^0$, while if the slope were ½, the surface areas would vary as

$$1/X^{1/2}$$

According to Rittinger the energy input required to break a cube of diam D varies as D^2, while according to Kick it varies as D^3. The strain energy absorbed by a cube under compression varies as its volume, or as D^3. However, with the formation of the first crack tip the strain energy effectively flows to the surface, which varies as D^2. When irregularly shaped pieces are broken, the strain energy is not evenly distributed throughout the rock, and the first crack tip forms and starts the energy flow, which develops a breakage pattern, when the proportionate energy absorbed is intermediate between D^2 and D^3. The average value is $D^{5/2}$.

The theoretical energy required to break spheres of similar material of diam D appears to be proportional to $D^{5/2}$.

Both surface and volume factors affect the breakage of stone, and when these effects are equal the energy to break should be proportional to $D^{5/2}$, which is midway between the Rittinger and the Kick assumptions.

The number of particles of similar shape in a unit volume varies as $1/D^3$, so that the energy input required to break a unit volume or unit weight should be proportional to $D^{5/2}/D^3$, or $1/\sqrt{D}$. This is the basis of the Third Theory.

Statement of the Third Theory

The Third Theory can be stated concisely as follows:

The total work useful in breakage which has been applied to a stated weight of homogeneous broken material is inversely proportional to the square root of the diameter of the product particles.

Where K represents a proportionality constant and P is the product diameter

$$Wt = K/\sqrt{P} \qquad [2]$$

Eq 2 is the fundamental statement of the Third Theory.

According to the Third Theory the work input W in breakage from a feed size F of one unit to a product size P of ¼ unit with a reduction ratio Rr of 4:1 equals the previous work input to the feed, or $Wt = 2W$.

For any values of F and P, where W is the kw-hr per ton required to break from F microns to P microns, the total work input, Wt, is proportional to $1/\sqrt{P}$, and W is proportional to $1/\sqrt{P} - 1/\sqrt{F}$.

$$\frac{Wt}{1/\sqrt{P}} = \frac{W}{1/\sqrt{P} - 1/\sqrt{F}} = \frac{W}{\dfrac{\sqrt{F} - \sqrt{P}}{\sqrt{F}\ \sqrt{P}}}$$

$$Wt = W\left(\frac{\sqrt{F}}{\sqrt{F}-\sqrt{P}}\right) \qquad [3]$$

and

$$W = Wt\left(\frac{\sqrt{F}-\sqrt{P}}{\sqrt{F}}\right) \qquad [4]$$

The term $\sqrt{F}/(\sqrt{F}-\sqrt{P})$ equals $\sqrt{Rr}/(\sqrt{Rr}-1)$.

The work index Wi is the kw-hr per ton required to break from infinite size to P = 100 microns, and

$$Wi = W\left(\frac{\sqrt{F}}{\sqrt{F}-\sqrt{P}}\right)\sqrt{\frac{P}{100}} \qquad [5]$$

Eq 5 is not empirical but is derived directly from the previous statement of the Third Theory.

When the work index is known, the energy input W required to break at the same efficiency from any feed size F to any product size P, in microns, is found from

$$W = Wi\left(\frac{\sqrt{F}-\sqrt{P}}{\sqrt{F}}\right)\sqrt{\frac{100}{P}} \qquad [6]$$

When F and P are in inches the number 100 in eqs 5 and 6 should be replaced with 0.003937, and $\sqrt{0.003937} = 0.0627$.

The ratio of the work inputs required for any two reductions, W_1 and W_2, is

$$W_1/W_2 = \frac{\sqrt{F_1} - \sqrt{P_1}}{\sqrt{F_1P_1}} \Big/ \frac{\sqrt{F_2} - \sqrt{P_2}}{\sqrt{F_2P_2}} \qquad [7]$$

If breakage characteristics of a material remain constant over all size ranges, and the mechanical efficiency of all machines employed is the same, then the values of the work index calculated under all different conditions should be constant. The work index expresses primarily the resistance of a material to breakage. The variations reveal differences in the breakage characteristics at different sizes and differences in the efficiencies of varying machines and operations.

If a typical normal material requires 3 kw-hr per ton for reduction from a feed size F of 1600 microns to a product size P of 400 microns, then according to the Third Theory the previous energy input to the feed was 3 kw-hr per ton, and the work index Wi is 12.

The practical test of the correctness of the Third Theory, as well as the value of the work index, lies in the comparison of a large number of plant and laboratory results. If these show that the work index under a wide range of sizes and operations remains substantially constant or varies in a predictable and explainable manner, then the Third Theory must constitute the fundamental law of comminution. No such correspondence has ever been demonstrated for the other two theories.

Confirmation by Crushing Quartz

Quartz crystals were broken under slow compression and the new surface area produced was measured by gas adsorption.[7] When the reported average energy concentration at fracture was plotted by the present author on log-log paper against the new surface area produced per unit of energy input, the points obtained were somewhat scattered, but were bisected by straight line with a slope of $1/\sqrt{2}$. The equation for this line is

$$sq\ cm/kg\text{-}cm = 172/(kg\ cm/g)^{1/\sqrt{2}}$$

or

$$\text{joules/sq m} = 59\ (\text{kw-hr/ton})^{1/\sqrt{2}} \qquad [8]$$

According to eq 8, at an energy input of 10 kw-hr per ton the input surface work of the quartz is 300 joules per sq m, while at 20 kw-hr per ton it is 492 joules per sq m. Tests have shown that about 300 joules per sq m are required on silicious ores,[8] but eq 8 shows that the input surface energy is not constant but increases as the $1/\sqrt{2}$ power of the energy input. This contradicts both forms of the Rittinger theory.

According to the Third Theory the input surface work should remain constant only when the slope m of the log-log plot of the percent passing size distribution line is 1/2. Since the normal slope is $1/\sqrt{2}$, the input surface work at this slope should vary as the energy input to the $\sqrt{2}/2$ or $1/\sqrt{2}$ power, showing that the Piret tests[7] confirm the Third Theory if it is assumed that the effective size distribution of the broken quartz follows the normal slope. The effective size distribution is affected by the use of large single crystals of feed and the abnormal breakage characteristics of pure crystallized quartz.

Confirmation by Breaking Spheres

A number of glass marbles of different diameters were broken by slow compression between parallel plane surfaces in the Allis-Chalmers Laboratory, the deformations measured, and the energy input values calculated.

The results were scattered, but the averages showed that the energy input required to break was approximately proportional to the diameter to the 5/2 power. The deformation at constant applied load appeared to be proportional to $1/D^{1/3}$.

Little information was found in technical literature on the energy required to break spheres, and the need for additional tests is very obvious. The data available at the present time tend to indicate the validity of the Third Theory as applied to spheres. However, the Third Theory may still apply to the reduction of broken rock even if it does not apply to the breakage of spheres.

Crack Length and Surface Area

The Third Theory has established that the total useful work done in crushing and grinding a stated weight of homogeneous material is inversely proportional to the square root of the diameter D of the product particles. It also postulates that the bulk of the necessary work input is utilized in deformation of the particles and released as heat through internal friction. Local deformation beyond the critical strain results in the formation of a crack tip, normally on the particle surface.[9] The formation of this crack tip is the immediate object of the work input. Once the crack tip is formed, the surrounding energy in the stressed rock immediately flows to the crack tip, which rapidly extends throughout the particle, splitting it and resulting in a break. The energy flow and stressed condition of the rock create additional crack tips, resulting in a breakage pattern. Little or no additional external energy need be applied to brittle materials to cause the break after the first crack tip is formed. The surface energy of the new surface formed may represent the useful work applied in splitting after the crack tip is formed, and may be supplied by the strain energy present in the deformed particle. The useful work input is essentially consumed in the formation of the crack tips and is directly proportional to the length of the crack tips formed.

When a single particle of diam D is broken, the average strain energy concentration per unit volume is proportional to the particle volume, or to D^3, while the surface area on which the crack tips form is proportional to D^2. The work necessary for breakage is proportional to the square root of $D^3 x D^2$, or to $D^{5/2}$.

The work necessary to break a unit weight or unit volume of rock is proportional to

$$D^{5/2}/D^3, \text{ or to } 1/\sqrt{D}$$

Since the length of the crack tips is directly proportional to the useful work input, it is necessary to define the crack length. It seems convenient to consider the crack length as that length which subtends an equal length of normal extension of the crack tips in each particle, since the particles concerned in crushing and grinding approach equal dimensions in the two normal breaking directions. If a break across a square cross-section, D units on a side, is considered, the crack length equals D, since the transverse length of the crack equals the distance of propagation of the crack. If a break across a cylindrical cross-section of diam D is considered, the crack length is $\sqrt{\pi D^2/4}$ or 0.886D.

The quantity L equals the total crack length formed in the reduction of a short ton of material.

Under this definition of L the new surface area formed by any reduction of a short ton equals $2L^2$.

Effective cracks are considered here to be crack tips that extend through the particle and split it without the external application of additional energy other than that already present in the stressed particle. Partial cracks, which do not completely split the less brittle materials, are not complete cracks under this definition, but they decrease the energy required for complete breakage in a subsequent reduction stage.

Since the total surface area formed in breaking a stated weight of rock to particles of diam D is inversely proportional to D, and the Third Theory useful work input is inversely proportional to $\sqrt{D}$, the useful work input is directly proportional to the square root of the surface area formed. The useful work input is directly proportional to $1/\sqrt{D}$ and also to the total crack length L, which equals the square root of one half the surface area formed by extension of the crack tips.

The total crack length, L, in the reduction of a short ton of rock, multiplied by the net energy input required to form a crack of unit length, gives the theoretical net energy input required, Wu, and this divided by the actual energy input required, W, gives the mechanical efficiency of any reduction process.

New techniques are required for laboratory measurements of the net energy input necessary to form a crack of unit length. The effective crack length equals the square root of one half the surface area formed; however, the measured surface area may include surface which did not result directly from the extension of the crack tips. The crack length is also related to the product diam D by a function which varies with the particle shape.

The unit cracking energy required in the commercial reduction of stone can be estimated as being in the order of 5 to 10 joules per cm. If an efficient grinding operation requires 300 joules per sq m of new surface area produced,[8] it requires 6 joules per cm of crack tips produced. Application of 10 kw-hr per ton, or 3.6×10^7 joules per ton, will result in the formation of a crack length L of 6×10^6 cm, or 60 km.

Variations in the slope m of the product size distribution line from the normal value of $1/\sqrt{2}$ greatly affect the new surface area produced, but have only the square root of this effect upon the energy input required.

The Rittinger theory is concerned with the measurement of surface areas, the Kick theory with the volumes of the product particles, and the Third Theory with the crack length formed. The Rittinger theory can be designated as the surface area theory, the Kick theory as the particle volume theory, and the Third Theory as the crack length theory.

Appreciation of the fact that the immediate objective of all crushing and grinding operations is the formation of crack tips will initiate a new stage of development in the theory of comminution, which will require years of study and controversy to complete. However, it promises to supply the actual explanation of the process which has hitherto eluded the Rittinger and Kick advocates.

Effect of Scalping Feed

Perhaps the most troublesome feature in the application of the Third Theory is the correction necessary for unnatural feeds which have had the fines removed by scalping. When the crusher feed has had part or all of the material passing the product size removed by screening, the energy input required per ton of feed is increased above that required for normal feed.

The necessary correction for a scalped feed when the work index is being calculated can be made as follows:

Let Fe represent the effective feed size, or the feed size of a normal feed, which would be equivalent in total work input per ton to the feed size F, which 80 pct of the scalped feed passes; Fe is larger than F. Let Fc represent the scalping cutoff size below which the fines in the feed have been effectively removed; Fc is known or estimated from the screen analysis of the scalped feed. Let Yc represent the percent passing the cutoff size Fc of a normal feed with 80 pct passing size F.

When the value of Fe has been found, the work index Wi for the scalped feed is calculated by substituting Fe in place of F in eq 5.

Solution Using Eq 1: In eq 1 Fc is substituted for X, F for P, and Yc for Y, and the equation is solved for Yc. Then in eq 1 $80 - Yc/2$ is substituted for Y, F for X, and Fe for P, and the equation is transposed and solved for Fe. The transposed equation is

$$Fe = F \Bigg/ \left(\frac{80 - Yc/2}{80}\right)^{\sqrt{2}}$$

and the combined equation for calculating Fe from Fc and F is

$$Fe = F \Bigg/ \left(\frac{2 - (Fc/F)^{1/\sqrt{2}}}{2}\right)^{\sqrt{2}} \qquad [10]$$

Graphical Solution: On a log-log plot of the percent passing versus particle diameter a line with the normal slope $1/\sqrt{2}$ is drawn through the diam F, which 80 pct of the scalped feed passes to its intersection with the scalping cutoff size Fc, which determines Yc. A parallel line is drawn through the point F, $(80 - Yc/2)$; its intersection with the 80 pct passing line gives the value of Fe.

Specimen Calculations: 1—If the feed is normal and $F = 1600$, $P = 400$, and $W = 3$ kw-hr per ton, from eq 5 the work index $Wi = 12.00$.

However, if the feed is scalped at the product size, all particles smaller than 400 microns are removed, and F, P, and W have the above values, then $Fc = 400$, $Yc = 30.0$, $Fe = 2145$, and $Wi = 10.55$.

2—If the feed is all -10 $+14$ mesh, or all -1680 $+1190$ microns, $P = 400$, and $W = 3$, then $F = 1680 - \frac{(1680\text{-}1190)}{5} = 1582$, and $Fc = 1190$.

By substitution in eq 10 $Fe = 3330$, and from eq 5 $Wi = 9.18$.

Work Index Calculations

Some of the published data by which the Third Theory was checked against actual operations are contained in a former AIME publication.[10] The testing methods are described and test results listed on a large variety of ores and other materials. Empirical formulas have previously been computed by the author from actual plant operations by which these test results can be translated into kw-hr per ton required for size reduction at the average operating efficiency of the plants used for comparison. In these formulas the particle size is the size which 80 pct of the materials pass as found by graphs of the screen analyses. The grindability at the product

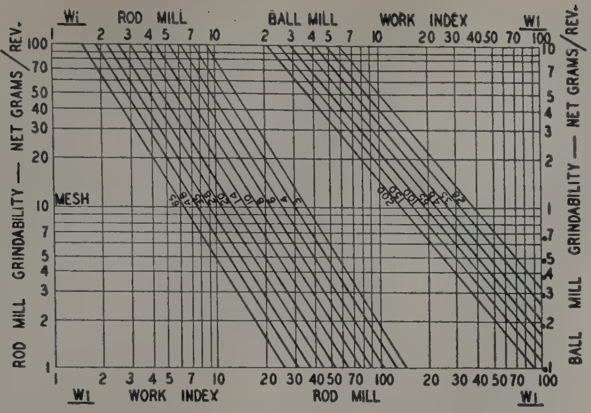

Fig. 1—Work indexes computed from rod and ball mill grindabilities.

size P is found by plotting the grindability for the various mesh sizes tested. If the grindability is available at only one size near the product size, a line is drawn through the plotted grindability parallel to the plotted percent passing size distribution line, to its intersection with the product size.

Impact Crushing Tests: It has been determined empirically from impact crushing tests,[10] and plant and pilot mill tests on the same materials, that the hp-hr per ton required to crush a scalped feed of specific gravity S and impact strength of C foot-pounds per inch of thickness, at a reduction ratio of 5:1, where P is the size in inches, which 80 pct of the product passes, equals $0.219C/SP^{0.293}$.

At a reduction ratio of 5:1 a normal feed has 25 pct passing the product size P, or $F_p = 25$.

If a feed with normal slope is used instead of a scalped feed, the exponent of P should increase from $1-1/\sqrt{2}$ to 1/2, according to the Third Theory, and the energy required to crush at any reduction ratio is

$$\frac{\text{hp-hr}}{\text{ton}} = \left(\frac{0.219C}{S\sqrt{P}}\right)\left(\frac{\sqrt{F}-\sqrt{P}}{\sqrt{F}}\right)\left(\frac{\sqrt{5}}{\sqrt{5}-\sqrt{1}}\right)$$

$$\left(\frac{80\text{-}25}{100}\right) = \left(\frac{0.218C}{S\sqrt{P}}\right)\left(\frac{\sqrt{F}-\sqrt{P}}{\sqrt{F}}\right) \qquad [11]$$

From eq 3 the total input energy required in kw-hr per ton is

$$Wt = \frac{0.1626C}{S\sqrt{P}}$$

and since 100 microns equals 0.003937 in., the work index from eq 5 is

$$Wi = 2.59C/S \qquad [12]$$

Eq 12 is used to calculate the work index from impact crushing tests. The work required to crush a normal feed from a given feed size to a given product size is calculated from the work index and eq 6, using 0.003937 in place of 100 when F and P are in inches.

Rod and Ball Mill Tests: Where G_{r_p} is the rod mill grindability, and G_{b_p} is the ball mill grindability[10] at the product size P, the kw-hr per net ton of material passing the product size (Wp) is found from the following empirical equations, which represent the average of a number of installations. The ball mill equation applies to a wet grinding overflow ball mill 7½ ft in diam inside the shell, operating in closed circuit with a classifier. The rod mill equation applies to a wet grinding overflow rod mill 6 ft in diam inside the shell, operating in open circuit.

$$Wp = 23/G_{r_p}^{0.625} \qquad [13]$$

$$Wp = 20/G_{b_p}^{0.820} \qquad [14]$$

The kw-hr per ton of new feed to both types of mills is found from the equation

$$W = 0.80\,Wp\left(\frac{\sqrt{F}-\sqrt{P}}{\sqrt{F}}\right) \qquad [15]$$

The total work input Wt at any size P is found by multiplying eq 15 by

$$\frac{\sqrt{F}}{\sqrt{F}-\sqrt{P}}$$

and the work index is found by multiplying Wt by $\sqrt{P_1/100}$. Then

$$Wi = 0.80\,Wp\left(\frac{\sqrt{F}-\sqrt{P}}{\sqrt{F}}\right)\left(\frac{\sqrt{F}}{\sqrt{F}-\sqrt{P}}\right)\sqrt{\frac{P_1}{100}}$$

$$= 0.80\,Wp\sqrt{P_1/100} \qquad [16]$$

The values of $0.80\sqrt{P_1/100}$ were calculated for each mesh size at which tests have been made, where P_1 is the sieve opening in microns, and this factor multiplied by the Wp value obtained from the grindability tests by eqs 13 and 14 gives the work index for the test at that mesh.

The values of the work index factor, $0.80\sqrt{P_1/100}$, for each mesh size in both rod and ball mill tests are as follows:

Mesh	Wi Factor	Mesh	Wi Factor
3	6.54	28	1.942
4	5.52	35	1.639
6	4.637	48	1.378
8	3.902	65	1.159
10	3.280	100	0.9785
14	2.760	150	0.8190
20	2.318	200	0.6883

Work indexes can be found directly from rod and ball mill grindabilities by Fig. 1 or an enlargement thereof.

Proof of Third Theory

From Laboratory Tests: Since consistent data covering a wide variety of materials, size ranges, and machines are necessary to prove the correctness of a comminution theory, the work index has been calculated for reported materials on which more than one test has been made.[10] Comparison of these Wi values for different rod and ball mill grinds and for crushing tests shows the correspondence obtained; differences at different size ranges in these results, which are greater than the experimental error of about 5 pct in sampling and testing, are caused principally by differences in the ease of breaking at different sizes.

The general consistency of the work index values obtained for a large number of different materials and conditions by the Third Theory and by empirical equations, which fairly represent actual plant operating results, is regarded as conclusive proof of the correctness of the theory. Nothing approaching such consistency has ever been shown in support of the Rittinger or Kick theories, neither of which has been particularly helpful in actual crushing and grinding operations.

These tests are listed alphabetically in Table I; they include 559 tests on 144 different materials. The

Table I. Work Indexes Calculated from Allis-Chalmers Laboratory Tests, Work Index = Kw-Hr Per Ton from Infinite Feed Size to 80 Pct Passing 100 Microns, or About 65 Pct Passing 200 Mesh.

Key: BM Mesh - Work Index = Ball Mill Mesh - Work Index
RM Mesh - Work Index = Rod Mill Mesh - Work Index
IC S - Work Index = Impact Crushing Sp. Gr. - Work Index

Name	Test	Mill	Mesh—Wire Index	Mesh—Wire Index	Mesh—Wire Index
Ajo-New Cornelia	684	BM	28-18.27	35-16.40	48-14.95
	2081	BM	65-14.05	100-13.47	200-14.45
		IC	2.69-21.36		
Alan Wood Steel	931	BM	35-8.34	48-8.20	65-9.76
Alcoa-Pet. Coke	700	BM	35-105.7	48-73.3	100-76.4
Al-Ke-Me Fertilizer	252	BM		48-13.33	100-15.10
Alum. Co. of Canada	1080	BM		48-6.62	65-7.06
	2149	RM		48-8.21	65-7.80
		IC	2.87-11.49		
Alum. Ore Co.	1858	RM	10-10.74	14-9.52	
Anaconda 1	910	BM	28-11.46	35-11.90	48-12.08
	1226		65-11.05	100-11.73	150-12.36
			200-14.00		
Anaconda 2	1477	BM	28-12.65	35-12.20	48-10.97
			65-10.80	100-11.81	150-12.88
			200-12.04		
Bagdad, Ariz.	2623	BM	48-11.72	65-11.12	200-12.45
Basic Refractories	1033	BM	48-6.82	65-7.02	
	2643	BM	100-6.07	200-8.93	
Benguet Cons.	550	BM	28-15.00	35-16.06	48-14.39
			65-14.50		
Bernheim-Rand	477	BM	28-31.9	48-30.8	100-33.6
			200-22.0		
	2016	IC	2.93-23.40		
Black River Falls	1023	BM	100-8.58	150-9.61	
Bingham		BM	48-6.38	100-7.82	200-8.28
Bolidens Gruv.	2324	BM	200-8.89		
		RM	10-14.10	14-13.70	
		IC	3.81-9.32		
Bowring	288	BM	35-13.13	35-13.40	65-13.48
Broken Hill—Lead	2422	BM	100-11.25	150-11.87	
		RM	14-6.27		
Broken Hill—Zinc	2422	BM	100-12.33	150-13.90	
		RM	14-7.26		
Buffalo Ankerite	1639	BM	200-17.02		
		RM	14-21.90		
Bunge Corp.	1555	RM	14-17.89	48-16.55	
Butte Highlands	861	BM	100-7.64	200-8.38	
Can. Nephelene-	663	BM	28-9.52		
Syenite		RM	28-11.95		
Carlota	660	BM	100-14.03	200-13.26	
C&H Tailings 1	771	BM	35-27.4	100-22.6	200-20.1
2	2411	BM	100-16.84	200-17.21	
		IC	2.82-15.86		
Castle Dome—Miami	1042	BM	28-13.42	35-13.23	48-12.88
			65-13.02	100-12.12	150-12.45
			200-13.37		
Chino-Nevada Cons.	1060	BM	28-8.40	35-10.24	48-9.45
			65-10.28	100-10.34	150-10.81
			200-11.42		
Cleveland Cliffs	2123	RM	10-18.77	14-15.73	
		IC	3.3-13.42		
Climax Moly.	1560	BM	100-9.47		
		IC	2.62-13.95		
	2596	IC	2.67-12.24	2.65-10.25	
Cline Lake	745	BM	65-11.66	100-11.38	200-11.67
CMS—Golden Rose	864	BM	48-9.22	100-9-10	150-9.17
			200-10.30		
CMS—Kimberley 1	1692	RM	10-17.08	14-15.38	
2	2150	RM	10-13.07	14-11.14	
		IC	2.97-14.39		
Cobrecite	830	BM	35-6.56	65-4.79	
Cohart Refract. 1	809	RM	4-49.80	10-41.00	20-38.80
2			20-29.45		
Cons. Copper, Nev. 1	188	BM	48-6.98	65-8.51	
2	276	BM	48-11.24	65-12.57	
Cons. Feldspar	1103	BM	35-8.04		
		BM	28-12.81	35.10.66	
Cyprus Mines	432	BM	65-12.47	100-12.10	200-11.21
East Malartic	779	BM	28-9.73	48-9.36	65-9.04
			100-9.24	150-8.60	200-9.28
East Sullivan	1923	BM	100-7.44	200-8.81	
Massive		RM	14-11.85		
East Sullivan	1923	BM	100-13.90	200-14.10	
Normal		RM	14-18.50		
Elect. Met. Chrom.	1008	BM	65-60.3	100.60.1	
		RM	28-30.0		
Emsco Refractories	1178	BM	48-7.55	65-9.70	
Exolon-SiC	1052	RM	8-9.49	20-20.08	20-19.07
			20-15.20	20-13.79	
Federal Chem.	814	RM	8-8.70	28-9.56	
	533	RM	35-12.45		
Ford Motor	1035	BM	100-15.67	200-19.20	
Fresnillo	2675	BM	100-16.40		
		RM	14-17.65		
Getchell Mines	1241	BM	35-10.63	65-11.50	100-11.59
			200-11.50		
Golding-Keene	784	BM	200-11.37		
	1553	RM	14-11.84	20-10.65	
Granby Cons.	1566	BM	200-21.13		
Graphite Conc.	860	RM	14-21.60		
		BM	150-42.6	200-45.8	
Grootvlei—					
Banket	2054	BM	48-13.30	100-14.30	200-16.50
BM Feed	2054	BM	48-13.00	100-14.60	200-14.90
Shale	2054	BM	48-13.00	100-14.00	200-12.60
Quartzite	2054	BM	48-13.00	100-15.60	200-16.60
Hanna—Taconite	1397	BM	28-11.17		
	1022	RM	20-11.23	28-11.17	35-9.40
	2240	IC	4.24-9.57		
Homestake	1965	BM	28-12.68	48-11.30	65-10.74
			100-11.18	200-11.33	
		RM	10-15.40	28-11.76	
		IC	3.15-9.45		

Name	Test	Mill	Mesh—Wire Index	Mesh—Wire Index	Mesh—Wire Index
Industrial Silica	1204	RM	10-11.94	20-15.05	
Inland Steel	837	BM	48-6.27	100-8.58	150-8.73
	1023		150-9.61		
Int. Nickel	2128	BM	200-14.60		
		RM	14-20.65		
		IC	2.92-19.00		
Ipanema	352	BM	65-11.94	100-14.15	
H. J. Kaiser 1	877	BM	65-9.08	200-11.39	
2		BM	65-7.05	200-9.38	
Kerr Addison 1	799	BM	28-20.24	35-17.30	150-13.00
			200-12.21		
		RM	14-16.29		
2	1765	BM	28-14.30	35-13.45	150-11.37
			200-12.02		
Kelowna Exp.	881	BM	48-21.20	65-19.22	100-19.41
			150-18.35	200-17.55	
Kinetic Chem.	763	RM	14-14.06	48-11.02	
Lake Shore	1831	BM	200-16.73	200-16.55	
	1644	RM	6-21.40	8-19.92	10-18.80
			14-20.70	14-18.25	
LaLuz	932	BM	28-18.50	35-17.73	48-16.54
			65-16.11	100-15.62	
Lawrence Cement	972	BM	150-9.76	200-8.95	
Limestone Prods.	1700	RM	14-11.19	35-9.34	
Little Long Lac	570	BM	28-17.00	35-16.25	48-16.90
			65-16.80	100-17.40	150-15.34
			200-14.90		
Madsen Red Lake	626	BM	65-14.73	100-13.90	
Magma-San Manuel 1	2419	BM	48-13.63	65-13.10	100-13.21
			200-11.33		
		RM	14-14.23		
2	2563	BM	65-13.31	100-14.15	200-12.66
		IC	2.58-6.24	2.63-6.60	2.53-7.87
			2.59-10.72		
Malartic	586	BM	28-15.35	35-16.40	48-13.98
			65-13.05	100-12.69	150-12.88
			200-13.44		
	1592	RM	10-18.38		
	1853				
	1952	IC	2.71-22.00		
Maine Dev.	1679	BM	100-13.22		
		RM	20.15.20		
Marievale, S.Af.	2050	BM	48-14.30		
		RM	14-16.27		
McIntyre Porcupine	2036	BM	65-12.98	200-13.18	
		RM	6-17.96	14-14.78	
Miami Copper	1042	BM	28-14.35	48-12.46	100-11.94
			200-12.37		
Mines Dominiales	726	BM	65-10.24		
	1716	RM	35-8.93		
		IC	2.15-3.42		
Mines de Bor	249	BM	150-12.27	200-7.99	
Mineral Mining	782	BM	35-6.07		
		RM	35-11.14		
Minn. Mines	637	BM	65-11.20	150-12.63	
Moose Mountain	756	BM	65-11.50	150-10.65	200-11.62
		RM	6-29.44		
Montecatini	469	BM	48-12.15	65-11.36	
Morenci	913	BM	28-8.53	35-9.60	48-10.20
	1937		65-10.85	100-11.54	150-12.45
			200-12.80		
		RM	20-9.98	28-9.52	35-11.78
			48-11.70		
		IC	2.66-13.85		
Mozan	914	BM	65-7.20		
		RM	20-21.85		
Nat. Lead-Tahawus	1017	BM	35-9.02	48-10.46	65-9.92
	1757		100-11.92	150-13.70	200-16.32
	1800	RM	14-13.38	20-11.60	28-11.28
	1941		65-13.96		
		IC	4.46-14.10		
Nevada Cons. McGill	188	BM	48-11.24	65-12.57	
	278				
New Jersey Zinc	1951	BM	48-15.53		
		RM	14-24.42		
N.W. Magnesite	1031	BM	65-8.61	100-9.46	
	1911	IC	3.00-9.15		
Noranda		BM	48-19.95	100-18.25	200-16.00
Oglebay Norton Taconite	1167	BM	28-10.24	35-10.58	48.10.00
			65-10.57	100-10.64	150-11.57
			200-12.06		
Ozark Ore Co.	1889	RM	8-21.60	10-19.70	14-18.36
	1979				
	2355	IC	3.40-17.62	2.88-18.50	
Pacific Coast Aggregates	324	BM	28-26.8	35-26.5	
Parcoy	567	BM	65-11.30	150-11.78	
Picacho	880	BM	48-11.18	65-11.86	65-13.70
	517	RM	8-9.65		
Pickands-Mather Taconite	1803	RM	10-24.62	14-21.13	20-19.71
		IC	2.92-26.93		
Pitts. Coal Co.	1861	RM	14-9.83	29-8.34	
Pitts. Met. FeSi	839	RM	28-6.72	35-7.38	
	1612	IC	6.53-9.95		
Pitts. Plate Glass 1	1018	BM	100-10.07	150-10.72	
2		BM	100-9.67	150-10.16	
Portland Gold		BM	28-22.20	48-18.30	100-16.14
			200-13.38		
Powell-Rouyn	949	BM	150-13.66	200-14.20	
Preston East Dome	604	BM	150-9.26	200-8.88	
Quartz-Crystallized		BM	28-11.16	48-12.05	100-13.72
			200-15.29		
Queenstown-Gold	2082	BM	65-15.21		
		RM	6-23.00		
Quincy	1036	BM	28-15.00	35-17.20	48-15.83
			65-15.91		
Rand-Springs Mines	504	BM	28-14.77	35-15.80	48-15.65
			65-14.85	100-15.44	150-15.05
			200-15.50		
Real del Monte	730	BM	28-16.14	35-15.48	48-14.74
		BM	100-14.65	200-18.58	

Name	Test	Mill	Mesh—Wire Index	Mesh—Wire Index	Mesh—Wire Index
Rep. Steel					
Chateaugay	868	BM	28-8.70	35-9.18	
Harmony	868	BM	28-8.70	35-9.18	
	822	RM	20-8.58	35-9.29	
	1377	IC	3.29-5.18	3.30-4.46	
Old Bed	868	BM	28-8.70	35-9.18	
	822	RM	20-6.99	35-9.50	
	1377	IC	3.29-5.18	3.30-4.46	
New Bed	822	RM	20-6.66	35-9.67	
Reserve Taconite (Different samples)	1748	RM	14-16.28	14-25.70	
	2476	RM	14-18.80	14-13.80	
	2475	RM	14-18.50	14-21.42	14-17.75
	2159	IC	3.50-11.10		
	1877	IC	3.76-14.86	3.75-15.00	3.73-19.28
	1748	IC	3.07-15.88		
	1456	IC	3.16-16.29		
	39R	IC	3.48-12.07		
Rochester-Plymouth	518	BM	100-11.66	200-12.36	
St. Joe, Lead (Different samples)	847	BM	48-6.76	65-13.47	200-12.37
	2632	BM	65-11.59	100-11.25	200-9.55
	1657	RM	14-15.49	14-9.17	
	2632	IC	2.90-15.04		
San Luis	730	BM	28-16.14	35-15.48	48-14.74
			100-14.65	200-18.58	
Santa Maria del Oro	574	BM	65-11.60	100-13.42	
Sherritt-Gordon	206	BM	48-11.27	65-12.14	100-12.98
	1970		200-11.15		
Silver Bell	1050	BM	48-9.30	65-9.92	200-12.23
South Am. Dev.	752	BM	48-8.67	65-9.29	100-9.38
			200-10.86		
Sullivan Mines	740	BM	28-4.31	35-5.72	
Sutton Steele & Steele	530	RM	20-10.67	35-11.59	
Sydvaranger	1921	RM	20-19.95		
		IC	3.36-20.72		
Tenn. Copper Co.					
Isabella	2287	BM	48-7.65	65-8.72	100-9.00
	1750	RM	14-10.90	14-10.45	
	2613	IC	2.74-8.80		
London	2287	BM	48-6.27	100-8.50	
	1750	RM	14-7.45	35-7.50	
	26.3	IC	2.81-5.92		
Tri-State Flint	440	BM	48-30.3	100-29.0	200-24.5
TVA-Fontana	1055	BM	48-9.43	100-9.29	
	1372	RM	14-10.10		
	1750	IC	2.65-9.42	2.60-15.84	
Union Potash					
Langbeinite	842	RM	14-6.35	35-8.35	48-10.60
Sylvanite	842	RM	35-8.35	48-11.00	
Utah Copper	1763	BM	28-12.64	35-10.67	48-10.44
			65-10.41	100-10.35	150-10.97
			200-11.49		
	938	RM	14-13.45	20-12.80	28-12.25
			35-11.45	48-11.00	
		IC	2.57-12.64		
Volunteer-Cement Clinker	828	RM	3-18.47	4-16.56	10-15.20
Waite-Amulet	1761	RM	14-19.14		
		IC	3.35-10.72		
Western Minerals	883	BM	48-3.55		
Tripoli		RM	48-9.51		
Western Mining Australia	2193	BM	100-10.20		
		RM	14-17.65		
		IC	2.91-20.10		
Weston Brooker	1864	RM	4-19.61	6-17.94	
	1719	IC	2.65-21.85		
White Pine (Copper Range)					
Shale	1000	BM	28-15.57	35-14.76	48-13.92
	2078		65-13.48	100-13.57	150-12.25
			200-13.14		
Sandstone 1	1000	BM	28-11.50	35-10.35	48-11.16
			100-13.40	150-13.59	200-13.36
2	2028	BM	28-6.52	35-9.59	48-10.71
			100-16.14	65-15.44	200-15.76
		RM	48-13.82		
Amygdaloid	1000	BM	28-24.4	35-23.0	48-21.2
			65-20.26	100-19.64	150-18.45
			200-17.70		
		BM		48-20.68	
Wright-Hargreaves 1	406	BM	28-30.5	48-23.0	100-19.95
			200-16.94		
2			48-17.09	100-17.40	200-16.89

Table II. Work Indexes Calculated from Plant Data in Taggart[11]

Machine Plant		Ref. Taggart, Sect., Page	KW-Hr/Ton, W	Feed, F	Product, P	Work Index		Fe
						Plant	Test	
Gyratory crusher								
Utah copper		4-28	0.0932	206,000	152,400	12.0	11.49	315,000
Chino		4-27	0.0643	(76,200)	76,200	7.5	10.13	130,000
Ajo	1	4-28	0.1400	183,000	152,400	20.0	21.36	290,000
(New Cornelia)	2	4-28	0.1316	206,000	177,800	20.9	21.36	330,000
Cone crusher								
Utah copper		4-50	0.166	26,700	18,000	6.8	11.49	40,000
Chino		4-50	0.219	26,700	22,100	11.8	10.13	42,000
Crushing rolls								
Utah copper		4-64	2.240	27,920	795	7.6	11.49	29,000
Ajo (New Cornelia)		4-67	0.910	11,690	2,540	8.0	21.36	14,000
McIntyre Porc.		4-65	0.530	97,500	34,000	20.3	17.96	126,000
McIntyre Porc.		4-67	0.633	12,800	7,300	14.9	17.96	18,000
C & Hecla		4-61	2.175	16,000	3,000	20.2	20.00	18,000

Table II (continued). Work Indexes Calculated from Plant Data in Taggart[11]

Machine Plant	Ref. Taggart, Sect., Page	KW-Hr/Ton, W	Feed, F	Product, P	Work Index Test	Work Index Plant	Fe
Rod mill							
Chino (Old)	5-43	1.850	1,590	577	11.18	10.13	
Tenn. Cop—London	5-42	2.91	13,400	365	6.65	7.45	
Fresnillo	5-43	7.41	19,800	670	23.35	17.65	
Morenci 1	5-42	1.416	2,600	665	7.40	9.98	
Morenci 2	5-42	0.917	2,850	1,150	8.50	9.98	
Ball mill, overflow							
Utah copper	5-57	1.67	1,510	650	12.36	11.49	
Chino	5-57	7.24	770	129	13.91	10.13	
Ajo (New Cornelia)	5-56	7.37	5,400	150	10.83	13.47	
White Pine (C.R.)	5-57	7.94	3,750	265	17.63	20.66	
Ball mill, grate							
Chino	5-82	3.88	1,150	290	13.26	10.13	
Wright-Hargreaves	5-84	8.60	5,300	295	19.31	20.25	
Ball mill, conical							
McIntyre Porc.	5-64	4.81	23,000	600	14.05	13.08	
Wright-Hargreaves	5-65	10.33	4,800	300	23.85	20.25	
Miami	5-64	1.787	15,000	1,710	11.15	12.78	
Miami—Sec.	5-66	9.55	2,190	140	15.12	12.78	
Miami—Sec.	5-66	4.66	2,300	340	13.94	12.78	
Buffalo Ankerite	5-64	5.06	8,300	700	18.85	19.46	
Sherritt-Gordon	5-67	2.985	4,200	750	14.15	11.89	
Anaconda	5-68	4.38	30,000	805	14.87	12.00	
Tube mill							
McIntyre Porc.	5-91	5.84	1,580	230	14.31	13.08	
Kelowna	5-91	16.00	1,700	67	16.38	17.55	
Kelowna	5-91	10.76	151	51	18.33	17.55	

Work Index	Utah	Chino	Ajo	McIntire Porcupine	Wright-Hargreaves
Gyratory	12.0	7.5	20.0 (20.9)		
Cone	6.8	11.8			
Rolls	7.6		8.0	14.9 (20.3)	
Rod mill		11.18			
BM—overflow	12.36	13.91	10.83		
Grate		13.26			19.31
Conical				14.05	23.85
Tube mill				14.31	
Test IC	12.64		21.36	(17.96)	
BM	11.49	10.13	13.47	13.08	20.25

work input required for any feed and product size of any material listed is found from the work index nearest that product size and eq 6.

It is noted that the work index of pure crystallized quartz increases regularly from 28 mesh to 200 mesh, with a slope of —0.15 on a log-log plot against the product size, indicating that a general theory of comminution should not be based on the behavior of this material unless corrections are applied.

From Direct Plant Data: Work indexes were calculated from published plant operating data for comparison with each other and with those calculated from laboratory test results and are listed in Table II. All the published operating data are from Taggart's *Handbook of Mineral Dressing,*[11] with references to section and page. The examples were chosen largely at random, for the purpose of enabling those interested to become familiar with the calculation method, and have no particular significance in themselves other than to demonstrate the utility of the Third Theory in comparing relative efficiencies over the complete comminution size range. No such consistent comparison is possible under the Rittinger or Kick theories.

Much of the published data on crushing is not sufficiently complete for the calculation in Table II. To obtain uniformity in the crusher calculations, the cutoff size *Yc* was assumed to equal one half the product size *P*, which was taken as the open side crusher setting. The feed size *F* was considered equal to 15 pct of the crusher gape. These arbitrary approximations were necessary in the absence of exact size analyses, and the work indexes calculated therefrom are of value chiefly in illustrating the correction methods for scalped feeds.

The work indexes were calculated by eq 5 from the kw-hr per ton, feed size, and product size derived from the published data. In cases where the feed is marked *Fe* the equation is modified, as previously described. Similar corrections for closed circuit grinding installations are usually small and were not made because of incomplete data. Comparisons of the relative efficiencies of different plants can be made by dividing the plant work index by the laboratory work index. Additional comparisons can be readily made by anyone interested in a particular ore.

Work Index Use

The work index *Wi* can be calculated from laboratory tests by the methods shown and can be calculated for any plant operation by eq 5 from the feed and product sizes and the work input in kw-hr per ton. The kw-hr per ton required for any size reduction can be calculated from the work index by eq 6. The correction described should be applied when the feed is scalped.

When laboratory or plant results show an appreciable and consistent difference in the work index at different product sizes, indicating a difference in the breakage characteristics, the work index at the proper size should be used. Higher work indexes for scalped feeds may indicate concentration of a hard fraction in the scalped feed, which can be confirmed by additional laboratory tests made upon it.

Judgment must be used in each case regarding the effects on the relative efficiency of such variables as: different breakage characteristics at varying sizes and natural grain sizes, segregation of harder fractions, different machines, oversize feed, ball and rod sizes, circuit change, and differences in circulating loads. After the work indexes are obtained for a variety of conditions, correction factors for each variable can be developed, and the range of the judgment factor required at present will be decreased still further.

The relative efficiencies at different plants can be compared by dividing their work indexes by those obtained from standard laboratory tests on their ores, and the most efficient operation can then be selected. The work index of a material is the most valuable single item of information regarding its crushing and grinding that can be obtained at the present time.

The comparisons made to date show much less variation in the relative mechanical efficiencies of various crushing and grinding installations than had been expected. This agreement in relative efficiencies between different machines and circuits indicates that the absolute mechanical efficiency of existing machines, as yet undetermined, is comparatively high and is certainly far above the 1 pct or so postulated by the second form of the Rittinger theory. The determination of the absolute mechanical efficiency of existing machines is important in evaluating the possible savings to be made by new machines and methods.

Summary and Conclusions

A completely new theory of comminution has been derived by the author, stating that the total work required for crushing and grinding varies inversely as the square root of the product size. When the work input, feed size, and product size of one reduction are known, the theory permits rapid calculation of the work required for any size reduction and permits direct comparisons of efficiency. The relative efficiencies of different operations and circuits involving different feed and product sizes can be compared directly, and after laboratory tests have been made the relative efficiencies of plants reducing various materials can be compared.

The Rittinger and Kick theories are not correct and cannot be applied in a practical manner to ordinary crushing and grinding over a large size range.

Crushing and grinding do not follow the laws of the theoretical breakage of cubes.

This new Third Theory states that the total work useful in breakage that has been applied to a stated weight of homogeneous broken materials is inversely proportional to the square root of the diameter of the product particles, directly proportional to the length of the crack tips formed, and directly proportional to the square root of the surface area formed.

The immediate objective of crushing and grinding is the formation of cracks, which are then propagated through the deformed particles by the flow of resident energy to the crack tips. The essential work input is that necessary to deform the particles beyond their critical strain and thus to form crack tips. The total useful work input per ton of material reduced from theoretically infinite particle size is directly proportional to the effective length of the crack tips formed, which is directly proportional to the square root of the surface area formed and inversely proportional to the square root of the diameter of the product particles.

When F is the diameter that 80 pct of the feed passes, P is the diameter that 80 pct of the product passes and W is the work input in kw-hr per ton; then Wt, the work input required to reduce from an infinite feed size, is

$$Wt = W\left(\frac{\sqrt{F}}{\sqrt{F}-\sqrt{P}}\right)$$

When F and P are in microns and Wi is the work index, or total kw-hr per ton required to reduce from infinite size to 80 pct passing 100 microns, or to approximately 65 pct passing 200 mesh,

$$Wi = W\left(\frac{\sqrt{F}}{\sqrt{F}-\sqrt{P}}\right)\sqrt{\frac{P}{100}}$$

If F and P are in inches the number 100 should be replaced by 0.003937.

If the feed has been scalped, the equivalent feed size of a normal feed should be used.

The work index Wi can be calculated from laboratory tests, or from any plant operation where W, F, and P are known, by the above equation. When the work index is known, the work input required for any size reduction can be calculated by transposing the equation.

The work index should be constant within the experimental error over all size ranges for a homogeneous material reduced at the same relative mechanical efficiency. The work index is the key figure in any crushing or grinding problem.

The work index has been calculated and compared for a large number of laboratory impact crushing, ball mill grinding, and rod mill grinding tests and from published data for large plant installations. The values are consistent and reasonable over all size ranges. They permit comparisons of relative efficiencies.

Judgment must be used in applying the work index to specific problems to allow for variables such as: different breakage characteristics at different size ranges, concentration of harder fractions when part of the plant feed has been removed, circulating loads, machine speeds and sizes, oversize in feed, and pulp dilution. After work indexes for the different variables have been obtained correction factors may be determined.

The Third Theory and its work index permit closer predictions and more accurate comparisons of all crushing and grinding installations than have heretofore been possible and should result in more efficient operations.

References

[1] P. Ritter von Rittinger: *Lehrbuch der Aufbereitungskunde.* Berlin, 1867.

[2] A. M. Gaudin: *Principles of Mineral Dressing,* Chap. VI. McGraw-Hill Publishing Co., New York, 1939.

[3] John Gross and S. R. Zimmerley: Crushing and Grinding, I—Surface Measurement of Quartz Particles. *Trans.* AIME (1928) **30**, p. 7.

[4] Friedrich Kick: *Das Gesetz der proportionalem Widerstand und Seine Anwendung.* Leipzig, 1885.

[5] Fred C. Bond and Jen-Tung Wang: A New Theory of Comminution. *Trans.* AIME (1950) **187**, p. 871; MINING ENGINEERING (August 1951) TP 2902B.

[6] R. Schuhmann, Jr.: Principles of Comminution—Size Distribution and Surface Calculations. AIME *Mining Tech.* (July 1940) TP 1189.

[7] Axelson and Piret: Crushing of Single Particles of Crystalline Quartz. *Industrial and Engineering Chemistry* (April 1950) **42-44**, p. 665. Also: Basic Laboratory Studies in the Unit Operation of Crushing. *Trans.* AIME (1951) **190**, p. 1061; MINING ENGINEERING (December 1951) TP 3194B.

[8] Fred C. Bond and Walter L. Maxson: Grindability and Grinding Characteristics of Ores. *Trans.* AIME (1939) **134**, p. 296.

[9] Eugene F. Poncelet: Fracture and Comminution of Brittle Solids. *Trans.* AIME (1946) **169**, p. 37.

[10] Fred C. Bond: Standard Grindability Tests Tabulated. *Trans.* AIME (1949) **183**, p. 313; MINING ENGINEERING (August 1949) TP 2180.

[11] Arthur F. Taggart: *Handbook of Mineral Dressing.* John Wiley & Sons, New York, 1945.

Deleading Zinc Concentrate

At the

Parral and Santa Barbara Mills

by C. L. Boeke and G. G. Gunther

THE zinc deleading processes at the Parral and Santa Barbara mills are described separately to provide a basis for comparison. Although the two procedures are fundamentally alike, there are some differences in application to meet specific conditions.

The Asarco mill at Parral in the State of Chihuahua is a flotation plant treating 1450 metric tons per day of complex sulphide copper-lead-zinc ores. In general, the procedure used for selective separation of the minerals into a copper, a lead, and a zinc concentrate follows the usual practice.

First, a bulk copper-lead concentrate is floated and then separated into a final copper and a final lead concentrate by the sulphurous acid process. A small tonnage of high grade gravity lead concentrate is tabled from the bulk copper-lead cleaner tailing before it is reground so as to avoid undesirable overgrinding and sliming of this portion of the lead mineral. Next, a zinc concentrate is floated from the lead rougher tailing and, as described later, is separated into a final lead product and a final zinc concentrate. Finally, the zinc rougher tailing receives a strong scavenger float to remove all recoverable middling values for regrinding and return to the flotation circuits. The slime is separated from the scavenger flotation product, and only the sand portion goes to the regrind section. The minerals in the separated slime are extremely resistant to all methods of selective separation and pose one of the major problems awaiting solution. Nevertheless, the slime shows a profit when mixed with either the lead or the zinc concentrate, except when metal prices are very low, so it is accepted as a final product for lack of a more profitable method of handling it. In contrast, the minerals in the reground sands of the

C. L. BOEKE, Member AIME, is Mill Superintendent, Cia. Minera Asarco, S. A., Parral, Chihuahua, Mex., and G. G. GUNTHER is Mill Superintendent, Cia. Minera Ascaro, S. A., Santa Barbara, Chihuahua, Mex.

Discussion on this paper, TP 3287BD, may be sent to AIME before June 30, 1952. Manuscript, August 27, 1951. Mexico City Meeting, October 1951.

Table I. Parral Mill Products—Second Quarter of 1951

Product	Assays							Recoveries Crude Ore Content, Pct					
	Grams		Pct										
	Au	Ag	Pb	Cu	Zn	Fe	Insol	Au	Ag	Pb	Cu	Zn	Fe
a-b—Bulk copper-lead float	7.01	1954	46.7	12.0	5.5	11.2	1.0	45.3	66.0	68.9	74.3	4.6	16.6
a—Separated copper concentrate, final	2.94	673	8.1	30.3	2.9	26.2	1.0	5.3	6.3	3.3	52.2	0.7	10.8
b—Separated lead concentrate, final	8.57	2447	61.55	4.9	6.4	5.4	1.0	40.0	59.7	65.6	22.1	3.9	5.8
c—Gravity lead concentrate, final	17.43	2296	71.4	1.5	3.9	4.2	0.7	2.9	2.0	2.7	0.2	0.1	0.2
d—Lead from zinc concentrate, final	7.35	1805	42.8	5.2	16.3	8.0	2.0	6.1	7.8	8.1	4.1	1.7	1.5
b-c-d—Total lead concentrate	8.65	2349	59.08	4.9	7.8	5.8	1.0	49.0	69.5	76.4	26.4	5.7	7.5
e—Scavenger slime product, final	2.80	435	7.0	1.1	19.0	18.6	12.0	4.1	3.3	2.3	1.6	3.6	6.3
b-c-d-e—Combined lead concentrate and scavenger slime[a]	7.45	1956	48.4	4.1	10.1	8.4	3.3	53.1	72.8	78.7	28.0	9.3	13.8
d-f—Zinc concentrate before deleading	1.67	274	4.5	1.2	52.6	5.5	3.4	19.7	16.9	12.1	13.6	79.9	14.9
f—Zinc concentrate after deleading, final	1.24	158	1.6	0.9	55.3	5.3	3.5	13.6	9.1	4.0	9.5	78.2	13.4
g—Tailing, final	0.26	21	0.57	0.1	0.85	2.5		28.0	11.8	14.0	10.3	11.8	62.0
								100	100	100	100	100	100

[a] Final lead products b-c-d-e are combined in a thickener to form a single concentrate before filtering.

scavenger product are highly amenable to separation and recovery.

The assays and recoveries for the products removed in various stages from the Parral mill circuits are listed in Table I.

One deviation from ordinary procedure is the retreatment of the final zinc concentrate for the recovery of lead. This is accomplished by depressing the zinc minerals with cyanide and zinc sulphate and then refloating to remove a lead concentrate.

Certain characteristics of the minerals in the Parral mill feed make such a deleading process necessary and advantageous. The ore supply comes from various veins that contain minerals covering a wide range of floatability. In addition, the veins that supply the major part of the tonnage have been cut by a fault which created an extensive shattered zone in which the minerals are in various stages of alteration. As a consequence, the lead minerals in the mill feed include a large proportion of easily floated clean galena, mixed with more refractory and partially altered minerals, which do not float readily. The separation of lead from zinc is complicated further by the ever-present problem of the slimed minerals, which do not respond satisfactorily to the procedure that is best suited for selective recovery of the granular portion.

It is evident then that part of the lead mineral is readily floatable and can be separated easily and cleanly from the zinc, another part has the same degree of floatability as the zinc and requires special treatment for selective separation, while the remaining and most refractory part is less floatable than the zinc and can be recovered only by a strong scavenger flotation of the zinc circuit tailing.

Such conditions preclude a reasonable recovery of the lead in a single flotation operation without floating an excessive amount of zinc. This led to experiments with a zinc concentrate deleading circuit in 1945, with such beneficial results that the procedure has been continued without interruption since that time. The advantages of the deleading process are as follows:

1—It simplifies the operation of the lead flotation circuit by making unnecessary any attempt to float the more refractory portion of the lead mineral at the expense of floating an excessive amount of zinc. Instead, a high grade lead concentrate low in zinc is floated, thereby dropping more of the zinc mineral into the lead circuit tailing for recovery in a zinc concentrate.

2—The lead mineral that floats in the zinc circuit has the same degree of floatability as the zinc mineral, and the segregation and treatment of minerals in the same restricted range of floatability favors a more effective separation. Even a slight deactivation of the zinc makes it less floatable than all of the lead mineral within this limited range. Such favorable conditions for separation cannot be established in the lead rougher circuit where the most refractory portion of the lead mineral is still present.

3—A high concentration of cyanide is used on the relatively small tonnage of zinc concentrate for maximum deactivation of the zinc, and it would not be economically permissible to use the same concentration of cyanide for the large tonnage in the lead rougher circuit to deactivate the zinc to the same degree. For example, 3.5 lb of cyanide and 2.0 lb of zinc sulphate per ton of zinc concentrate are used in the zinc deleading circuit at Parral, equal to 0.3 lb of cyanide and 0.2 lb of zinc sulphate per ton of crude ore mill feed. The high concentration of cyanide in the deleading circuit requires only one twelfth of the quantity that would be needed to establish the same concentration in the lead rougher circuit, and the cyanicides in that circuit make the cyanide less effective than when it is used on the clean zinc concentrate.

Cyanide and zinc sulphate are the only reagents used in the deleading circuit. The residual reagents in the feed to the circuit provide all the activation and froth needed to float the lead, but on occasions a small amount of alcohol frother is used to help carry the lead through the cleaner cells. Thickening and long conditioning were found to be detrimental to the separation, although some benefit is derived from a brief contact with cyanide and zinc sulphate

Table II. Deleading of Zinc Concentrate at Parral Mill

Product	Zinc Conc., Pct	ASSAYS					
		Grams		Pct			
		An	Ag	Pb	Cu	Zn	Fe
Zinc conc.	100.00	1.67	274	4.5	1.2	52.6	5.5
Lead from zinc conc.	7.04	7.35	1805	42.8	5.2	16.3	8.0
Deleaded zinc conc.	92.96	1.24	158	1.6	0.9	55.3	5.3

	RECOVERIES BASED ON ZINC CONCENTRATE, PCT				
	Au	Ag	Pb	Cu	Zn
Zinc conc.	100.0	100.0	100.0	100.0	100.0
Lead from zinc conc.	31.0	46.4	67.0	30.5	2.2
Deleaded zinc conc.	69.0	53.6	33.0	69.5	97.8

to permit their complete diffusion throughout the pulp before flotation. The feed has a slight natural alkalinity of pH 7.8, and experimental additions of lime have had no noticeable effect on the separation.

As shown in Table II, the deleading procedure recovers 67.0 pct of the lead content of the zinc concentrate with a loss of only 2.2 pct of the zinc content, and based on the crude ore mill feed, see Table I, this is equivalent to a recovery of 8.1 pct of the lead with a loss of only 1.7 pct of the zinc. The percentage of gold, silver, and copper removed with the lead makes the procedure still more desirable when the zinc concentrate is sold on a schedule that pays for the zinc content only.

Table III shows the percentage of crude ore lead content in the zinc concentrate before and after the zinc deleading circuit was placed in operation. During 1942, 1943, and 1944, when lead was recovered in a single step in the lead flotation circuit only, from 6.5 pct to 7 pct of the crude ore lead content remained in the zinc concentrate, and it could be kept at that point solely by floating from 12 pct to 13 pct of the crude ore zinc content with the lead concentrate. After the introduction of zinc deleading in 1945, the lead in the zinc concentrate gradually decreased to less than 4 pct of the crude ore content, with at the present time the inclusion of less than 10 pct of the crude ore zinc content in the combined lead products, see Table I. This represents a 2.5 pct increase in lead recovery in conjunction with a 2.5 pct decrease in zinc recovery in the lead concentrate, and at the same time, the zinc dropped from the lead concentrate improved the recovery in the zinc concentrate by an equal amount.

Table III. Crude Ore Lead Content in Zinc Concentrate After Zinc Deleading Circuit

Procedure	Year	Crude Ore Lead Content Remaining in Zinc Conc., Pct
Zinc conc. not deleaded	1942	6.5
	1943	7.0
	1944	6.7
Deleading started July 30th	1945	4.8
Zinc conc. deleading circuit in continuous operation	1946	4.3
	1947	4.1
	1948	4.3
	1949	3.9
	1950	3.6

The concentrating plant of the Asarco's Santa Barbara unit is located near the village of Santa Barbara, which lies in the foothills of the Santa Barbara mountain range in the southcentral part of the State of Chihuahua at an elevation of 6300 ft. The prevailing rock in the district is shale which has been intruded by rhyolite and basalt dikes. This shale is cut by numerous veins that have been mined since early colonial times. The work of the Spaniards was limited to the oxide portion of the veins, which extends several hundred feet below the outcrops except in those areas where erosion has been excessive. At the present time, mining is confined to the deeper sulphide areas of the veins. Ores from five different mines make up the mill feed, and the principal minerals are lead, mainly occurring as galena, copper in the form of chalcopyrite and to some extent as chalcocite, and zinc as a marmatitic sphalerite, all associated with pyrite and some gold and silver in a siliceous gangue.

For a number of years, and till the middle of 1949, the flowsheet of the mill followed the conventional lines of most plants practicing selective flotation of lead and zinc. As additional features, this flowsheet included—and still includes—gravity concentration of the lead liberated in the primary grinding circuit, a lead-copper separation process by means of sulphurous acid, and a scavenger circuit following the zinc float.

In view of the fact that most of the Santa Barbara ores presently treated show varying degrees of alteration and oxidation of the mineral surfaces and, with few exceptions, cannot be classed as clean ores as regards selectivity and floatability of the lead and zinc constituents, they require strong flotation conditions in the lead circuit for optimum lead-copper recoveries and the subsequent production of a zinc concentrate of acceptable grade. It is obvious that this procedure tends to float a good deal of zinc into the lead concentrate, especially when the ore is very refractory. In the past, these zinc losses, and the resulting comparatively low grade lead concentrates, were tolerated as long as the value of the refractory lead recovered was greater than the value of the zinc that had to be taken into the lead concentrate and thus was lost as a pay product.

Early in 1949, however, the amounts of refractory material in the various ores delivered to the mill increased to such an extent that it became more and more difficult to produce marketable lead and zinc concentrates and maintain recoveries. In spite of the customary strong flotation conditions in the lead circuit, a good deal of the lead and also copper dropped into the zinc section and floated there under the activating influence of the copper sulphate but to the detriment of the grade of the zinc concentrate produced. Attempts to retard this lead in the zinc circuit with potassium bichromate and to float it in the scavenger circuit were not successful. Therefore it was decided to try a deleading retreatment of the final zinc concentrate along the lines developed in the Parral mill. When it was possible to show that the lead could be floated away successfully from the zinc after the latter had been depressed with cyanide and zinc sulphate, this deleading operation became part of the regular flowsheet in July 1949. The immediate result of this procedure was a noticeable improvement in the zinc concentrate grade through the removal of considerable amounts of lead, copper, and iron minerals from the original zinc concentrate with relatively low losses of zinc in the refloat lead concentrate. In turn, the lead and copper values thus recovered and added to the original lead-copper concentrate correspondingly increased the recoveries in the lead and copper circuits.

As soon as the deleading operation had been firmly established, it became possible to change the conditions in the original lead float. Instead of attempting to recover as much lead as possible in the lead circuit, the operators were instructed to disregard the lead section tailings, to produce a high grade lead concentrate of minimum zinc content and to allow the refractory lead minerals to pass into the zinc circuit for their subsequent recovery in the refloat circuit.

The overall effect of the refloat operation and typical results obtained are shown in Table IV.

Table IV brings out the fact that the refloat operation not only produces a relatively high grade final zinc concentrate and a lead-copper concentrate of acceptable grade, but also recovers 8.4 pct of the total lead in the mill feed with a loss of only 2.1 pct of the total zinc. The value and effectiveness of the refloat circuit are thus clearly emphasized. At the same time assays of the zinc concentrate before the deleading reflect the operation of the original lead circuit and indicate the amounts of lead and copper that were allowed to drop into the zinc section. It is obvious that, without a deleading circuit, a zinc concentrate assaying 5.4 pct lead, 1.6 pct copper, and only 50.2 pct zinc would not be produced for financial reasons, even if such a concentrate were acceptable to the smelter, and that the lead circuit would be operated so as to produce a greater recovery of the lead and copper values, which naturally means a lower grade concentrate and a higher loss of zinc.

It is to be understood that the figures in Table IV represent average results only. It will be readily seen that the overall value of the entire refloat operation increases as the refractoriness of the ore treated increases, whereas with cleaner ores the results are less spectacular.

In the zinc deleading operation as practiced at Santa Barbara the primary zinc is double-cleaned in a ten-cell No. 24 Denver Sub-A machine, and then is pumped to an eight-cell No. 24 Denver Sub-A machine. A rougher lead concentrate is taken from cells No. 3, 4, 5, and 6 to be cleaned in No. 2 cell and recleaned in No. 1 cell. The rougher concentrate from the last two cells of the machine is returned to No. 4 cell. The double-cleaned lead concentrate joins the original lead-copper concentrate for further treatment in the lead-copper separation section, the tails of the machine constituting the final zinc concentrate.

Principal reagents added ahead of the pump are cyanide, zinc sulphate, and lime. Minor amounts of xanthate, cresylic acid, and of an alcohol frother are added at the machine as needed. Approximate reagent requirements per ton of primary zinc concentrate feed to the refloat section are: 2.3 lb cyanide, 4.4 lb zinc sulphate, 3.2 lb lime, 0.03 lb xanthate, and 0.01 lb each cresylic acid and Du Pont frother B-22.

Cost of operating the section, including reagents, power, and maintenance, amounts to approximately 8¢ to 10¢ per ton of crude ore milled.

Both cresylic acid in the rougher and alcohol frothers in the cleaner section have been found necessary and, if judiciously used, helpful. Obviously, overfrothing is to be avoided not only in the refloat circuit but also in the primary zinc rougher and cleaner section. The importance of the latter factor was demonstrated in the plant some time ago when Aerofloat No. 242 was tried in the zinc rougher float as a substitute for the standard xanthate collector. It was found that the frothing properties of this reagent, even if used in less than the necessary amounts, were so pronounced as to make the refloat circuit uncontrollable in a very short time.

Table IV. Overall Effect of Refloat Operation and Typical Results

	ASSAYS					
	Grams		Pct			
	Au	Ag	Pb	Cu	Zn	Fe
Zinc Conc.						
Before deleading	1.2	294	5.4	1.6	50.2	7.5
After deleading	0.8	171	1.1	1.1	54.5	7.2
Refloat lead conc.	4.6	1364	42.6	6.0	12.9	10.2
	RECOVERIES IN REFLOAT LEAD CONC., PCT					
	Au	Ag	Pb	Cu	Zn	Fe
Based on crude ore mill feed	2.9	6.8	8.4	8.7	2.1	2.4
Based on deleading section feed	39.6	47.9	81.4	38.7	2.6	14.0

Table V. Comparison of Parral and Santa Barbara Deleading Results

	ASSAYS					
	Grams		Pct			
	Au	Ag	Pb	Cu	Zn	Fe
Zinc conc. before deleading						
Parral	1.7	274	4.5	1.2	52.6	5.5
Santa Barbara	1.2	294	5.4	1.6	50.2	7.5
Zinc conc. after deleading						
Parral	1.2	158	1.6	0.9	55.3	5.3
Santa Barbara	0.8	171	1.1	1.1	54.5	7.2
Lead conc. from zinc conc.						
Parral	7.4	1805	42.8	5.2	16.3	8.0
Santa Barbara	4.6	1364	42.6	6.0	12.9	10.2
	RECOVERIES IN REFLOAT LEAD CONC., PCT					
	Au	Ag	Pb	Cu	Zn	Fe
Based on deleading section feed						
Parral	31.0	46.4	67.0	30.5	2.2	10.3
Santa Barbara	39.6	47.9	81.4	38.7	2.6	14.0
Based on mill feed						
Parral	6.1	7.8	8.1	4.1	1.7	1.5
Santa Barbara	2.9	6.8	8.4	8.7	2.1	2.4

pH Control

For reasons as yet unknown, the great amount of laboratory work done to study the effect of lime has, so far, failed to furnish the necessary data on which definite conclusions may be based, and a good deal more work will be required to answer the fundamental question as to whether lime should be used or not. Results obtained in the plant show that, without lime, the operation of the refloat section becomes rather unstable and erratic, a fact also borne out in some of the laboratory series where the absence of lime led to poor lead-copper recoveries because of a pronounced lack of selectivity. On the other hand, quite a few test series showed a normal float and an acceptable lead-zinc separation when no lime was used. Notwithstanding this erratic and as yet unexplained behavior of the different mill pulps tested, certain general trends resulting from the use of lime may be summarized as follows. Up to a pH value of 9 or 9.5, recoveries of lead and copper are better than those obtained at a pH value of 8 which is the natural pH of the primary circuit in the plant. As the pH value of the refloat is raised above 9.5, the floatability of the lead and copper begins to decrease, and in the case of the copper, sometimes so rapidly as to lead to a definite rejection. Zinc rejection improves as the pH value of the float increases. From the few data presented it is obvious that the use of lime in the refloat circuit is, if anything, critical, and requires a careful study and balancing of all the factors involved in each individual case.

A comparison of the Parral and Santa Barbara deleading results is shown in Table V.

The results obtained at Parral and Santa Barbara indicate that a zinc concentrate deleading process may be a valuable means of improving concentrate grades and recoveries wherever a poor lead-zinc selectivity poses a major metallurgical problem.

Screened Ore Used for Fine Grinding at Lake Shore Mines

by Bunting S. Crocker

PEBBLE grinding at Lake Shore is not a temporary wartime substitute. The tube milling plant, with a 1000 ton per day capacity, grinds a hard siliceous ore to 90 pct —325 mesh. The plant, prior to using pebbles, was consuming 4.3 lb of 1¼-in. grinding balls per ton of ore, which amounted to 785 tons of balls per year. At September 1951 prices, $132.60 per ton, this steel cost amounted to $104,400 per year, or $0.285 per ton milled. By the Lake Shore method of substituting screened rock for this steel, all of this cost is saved. This is one of the major economies in Lake Shore mill practice. Regardless of the ultimate price of grinding balls, a change back to steel balls is not considered. The present pebble plant is more flexible than a steel ball plant and equally efficient. For example, if it is desired to change the size of grinding media, the pebble charge in any mill can be changed completely in 4 to 5 days, as against 76 days to change completely a 1¼-in. steel ball charge.

To change pebble size it is necessary only to change two sets of screens and clean out the rock feed storage bin. This will take 8 to 10 days as against 3 to 4 months to clean out the customary supply of grinding balls kept on hand. Also it has not always been possible to purchase all desired sizes of balls at any price.

In an analysis of savings effected by the use of the pebble mills, the flexibility of the Lake Shore grinding plant should be discussed, as it has a direct bearing on these savings. The plant has always used several units to handle tonnage rather than sending all the tonnage through a single unit. This principle may result in using small diameter mills, but no objection to that is seen. At no time has any advantage been found in cost per ton ground in large diameter mills. Both the capacity and the power of any mill varies as the diameter raised to the 2.6th power. Consequently large or small mills are equally efficient, and a plant should be designed to use as many units or combination of units as is consistent with reasonable operating practice. Mills under 5 ft diam are harder to reline, etc.

To define the case at Lake Shore, 2600 tons per day formerly were milled in seven 7x6-ft ball mills and twelve 5x16-ft (and two 6x16-ft) tube mills.* This gave an excellent test plant and an extremely efficient one. In this plant the ratio of ball mills to tube mills was 1:2. When the much cheaper pebble mills were substituted for the tube mills, this ratio was changed to one ball mill to four pebble mills to take the greatest possible advantage of the cheaper operating mill, i.e., the pebble mill.

This flexibility without loss in efficiency has been an important item in the cost savings.

It is interesting to note that the use of pebbles for fine grinding was proved first in the laboratory in a 12-in. ball mill. In fact, since 1934 all testing on —8 mesh material has been done in this 12-in. mill.

Scope of the Tests

A paper on fine grinding at Lake Shore Mines was published in July 1940.[1] This paper covered 7 years of intensive research on fine grinding as well as sizing methods and equipment, plant scale grinding tests on 5x16-ft tube mills with and without grate discharges both with 1¼-in. and ¾-in. balls, the use of laboratory mills to evaluate plant changes, and several reports on classifiers and classification. In the following July the addendum report[2] was added in which the idea of series-circuit grinding was introduced, and the results of running five stages of tube mills and bowl classifiers were shown.

Since 1940, the ball milling end of the plant has been altered extensively as a result of tests on the use of 3½-in. rods in 7x6-ft mills and the use of the Tyler repulping screen with from 7 to 14 mesh screens. These tests are lengthy and may be covered in a separate report later.

The scope of this report is confined to ore ground by rod milling and ball milling until it passed through an 8 mesh Tyler Ty-rod screen. The —8 mesh screen undersize then was pumped to a primary bowl classifier in open circuit and the sands from the bowl sent to the primary pebble mills, see Fig. 1. In the pebble mill circuit the ore is ground to 90 pct —325 mesh (24 pct + 28 microns). In studying the flowsheet, attention should be paid to the efficiency of the classification equipment used. The Tyler repulping screen is an efficient machine on the 8 to 10 mesh separation, and the bowl classifier is equally efficient at the 325 mesh separation. Efficient classification is a necessity for series-circuit stage grinding.

The ore is hard siliceous porphyry, 60 pct SiO_2, 80 pct insoluble. Its grindability at different meshes has been shown near the top of the list in F. C. Bond's grindability tests.[3] Lake Shore is not shown, but an adjacent mine with identical ore, Wright-Hargreaves, is.

Reasons for the Changeover

Since 1936 grinding balls have been rising steadily in price with no sign of stopping. For a mill that used 4.5 to 5.2 lb of grinding balls for every ton of ore ground this rise represented an alarming increase in grinding costs. In many cases the quality of the grinding balls fell off as the scrap steel became more difficult to obtain. The ratio of tube mills to ball mills increased with the use of the Tyler repulping screen in the ball mill circuit. Originally only 3.0 lb of balls per ton were used in the tube mills, and this

---

* Throughout this paper, the term *tube mill* is used in referring to a mill filled with *small* steel balls and, incidentally, a mill in which the length *is at least* two times the diameter.

B. S. CROCKER, Member AIME, is Mill Superintendent, Lake Shore Mines, Ltd., Kirkland Lake, Ontario, Canada.

Discussion on this paper, TP 3303B, may be sent to AIME before June 30, 1952. Manuscript, July 30, 1951. Mexico City Meeting, October 1951.

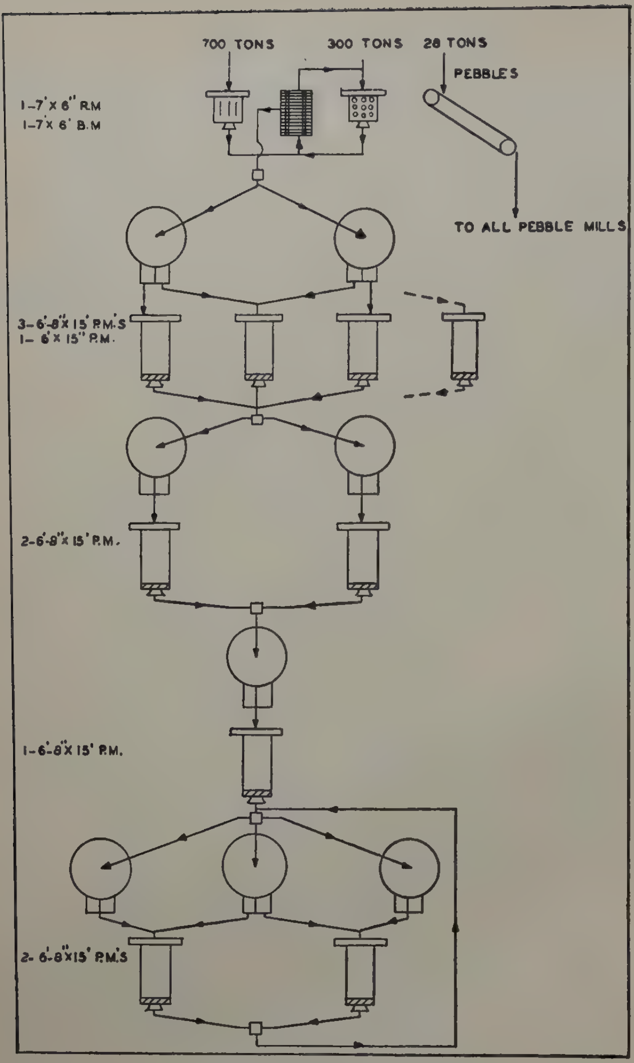

Fig. 1—Grinding flowsheet.

figure had risen 43 pct to 4.3 lb per ton by 1949 because of above-mentioned factors, see Fig. 2.

Inability to obtain ¾-in. grinding balls in the summer of 1948 was one of the final factors in the decision to convert. Lake Shore had pioneered the use of this small ball and had made a saving of 23½ pct more capacity at 7 pct more cost. Not only did the manufacturers refuse to supply the small ball, but they indicated that when the scrap metal situation eased up they would put the ball back on the market at a price of $150 to $160 per ton. At this price differential, the economic use of small balls is prohibited. United States manufacturers of grinding balls have always maintained a much greater price differential for various sizes of grinding balls than Canadian manufacturers, and as a result the use of small balls has been discouraged.

Fig. 2—Price of 1¼ x ¾ in. grinding balls in Canada by years.

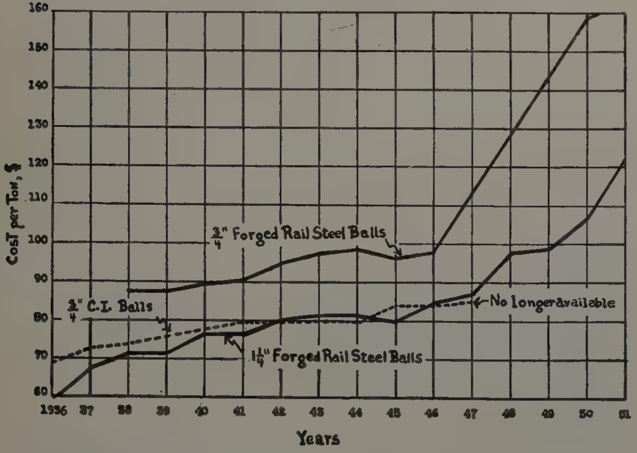

Table I. 10-G Slugs Vs 10-G Balls

Mesh	Feed No. 9 Secondary Class Sands	15-Min Grind with		18-Min Grind with	
		Slugs	Balls	Slugs	Balls
8	0.1	0.2	0.3	0.2	0.2
10	0.6	0.5	0.7	0.5	0.6
20	2.0	1.8	1.5	1.4	1.4
35	4.5	1.6	1.0	1.5	2.4
65	18.3	9.0	9.9	10.0	9.4
150	26.3	21.1	20.7	20.4	16.1
+325	38.6	38.5	39.2	35.0	39.9
−325	9.6	27.3	26.7	31.0	30.0
	100.0	100.0	100.0	100.0	100.0

It should be mentioned that Lake Shore laboratory tests had always shown, for the final stage of the grinding plant, 5 to 10 pct — 65 mesh feed to final mills, that ½-in. grinding balls were 22 pct more efficient than ¾-in. balls. However, Lake Shore has been unable to interest anyone in manufacturing them.

It has also been found that ¼-in. grinding balls were not so satisfactory as ½-in., and ⅛-in. balls failed entirely on all but — 250 mesh material.[4] Laboratory and plant tests proved conclusively that the same size of ball could be used with the same efficiency in mills between 1-ft and 6 ft 8-in. diam.

The loss of the small ball also spoiled the application of the theory behind the multistage grinding plant. If the size of grinding media could not be controlled in successive stages, part of the efficiency of stage grinding would be lost.

The above-mentioned points were important in themselves and more important as a whole in their effect on the company's attitude toward research that sought a permanent solution.

It is necessary that the reason for the use of ore as a grinding media be explained. The basic idea of pebble grinding is very old. Danish pebbles and pebbles from local quarries have been used from time to time, but usually to keep the circuit free from iron or for special grinding, seldom to cut costs, as they were generally more expensive to use in this country. They have, however, been used extensively in West Australia.

Many prominent metallurgists from South Africa who visited the plant told the company that the pebbles from the Rand Conglomerate were an excellent material for grinding. However, the necessity for cheap native labor both to hand pick the pebbles and to cull the loads from time to time and remove unsuitable fine material would make such a process impossible in Canada, even if the ore itself should prove to contain rock suitable as pebbles. The timely visit of Dr. Jackson in 1948 helped to dispel some of this feeling of pessimism. He reported that many mills had stopped the practice of culling the loads and generally encouraged the idea of trying ore as a grinding media.

Test on Ball Shape in Fine Grinding

Before Dr. Jackson's visit, when it was realized that the ¾-in. ball would no longer be available, a cheap steel substitute was sought. One early idea was

Table II. Tungsten Carbide Balls Vs Steel Balls on Fine Feeds

Mesh	Feed	Tungsten Carbide 1¼ In. Load 400 Rev.[a]	Steel 1¼ In. Load 667 Rev.
3			
6	0.1		
10	5.7	0.2	0.2
20	21.6	0.2	0.2
35	25.6	0.5	0.5
65	20.9	11.0	10.7
150	13.5	31.2	30.2
270	6.9	19.9	19.9
−270	5.7	37.0	38.3
	100.0	100.0	100.0
Cum + 10	5.8	0.2	0.2
Cum + 35	53.0	0.9	0.9
Cum +150	87.4	43.1	41.8

[a] Mill speed 60 rpm.

to use ¾-in. and ½-in. rods cut into cylinders, and another idea was to use the punchings from holes on the ends of rails. It was reasoned that grinding media of this type might be inefficient but because of its low cost might prove economical. However, when these odd shapes were tested for fine grinding it was found that they ground as efficiently as a ball of the same weight. Old Erickson bits had been tested previously as a substitute for 1¼-in. balls, and although the test was not as long as desired, the mills kept grinding through the run with no marked loss of efficiency.

A test was made in the 12-in. Haultain mill using a charge consisting of 10-g punchings from the Algoma Steel Co. These punchings were approximately ⅝-in. diam, by ¼-in. thick. Balls of equal weight, slightly over ½-in., were taken from a 1¼-in. ball load and were all reasonably spherical. Since both grinding media were made of steel, equal weight and equal mean size would be the same. The results of the tests on odd shapes are shown in Table I.

On these fine sands, the odd-shaped flat slug ground as well as a spherical ball. Both grinding media had the same weight and therefore the same mean size and performed the same work. Both media failed to grind the 10 and 20 mesh material, and larger slugs would be necessary for plant grinding. Feed up to 10 mesh was chosen deliberately to determine the effect of shape on the top meshes.

The fact that in grinding −8 mesh sand the grinding media need not be too spherical helped greatly to eliminate some of the worries about Lake Shore ore. Characteristically this ore breaks with one long dimension, particularly the product from the Symons cone crusher. Broken ore at Lake Shore did not appear to be suitable grinding media.

However, it should be remembered that every conceivable shape of grinding ball, i.e., concave balls and even cubes, has been patented. It is thought that much of the confusion in the industry regarding the shape of the grinding ball probably came from the failure of operators to use the right correction factor for liner wear when testing various media in small diameter mills.

Tests on Tungsten Carbide Balls

A test was run in the Lake Shore Mines experimental laboratory on the use of various sizes of tungsten carbide grinding balls. These tests were made possible through the courtesy of D. Weston of Aerofalls Mills Ltd., who loaned the ball charges. The tungsten carbide ball tests showed clearly that balls will grind in capacity according to their specific

Table III. Tungsten Carbide Balls Vs Steel Balls on Coarse Feeds

Mesh	Feed	Tungsten Carbide 1¼ In. Load 1000 Rev.	Steel 1¼ In. Load 1680 Rev.
3	17.8	9.2	9.4
6	36.3	14.9	14.4
10	16.3	1.1	1.2
20	10.8	0.4	0.4
35	5.7	0.4	0.4
65	3.4	0.7	0.6
150	2.2	3.4	1.8
−150	7.5	69.9	71.8
	100.0	100.0	100.0
Cum + 10	70.4	25.2	25.0
Cum + 35	86.9	26.0	25.8
Cum +150	92.5	30.1	28.2

Table IV. Effect of Surface Hardness in Grinding

Mesh	Grind Head	1¼ In. Steel, 667 Rev.	1¼ In. Tungsten Carbide, 400 Rev.	1¼ In. Stellite, 600 Rev.
+ 8	1.1	trace	trace	trace
+ 10	11.2	0.3	0.2	0.3
+ 20	42.1	0.4	0.4	0.5
+ 35	23.2	1.2	1.8	1.2
+ 65	10.9	23.5	25.2	22.9
+150	6.0	23.4	23.4	23.3
+325	4.6	21.1	20.7	21.3
−325	0.9	30.1	28.3	30.5
	100.0	100.0	100.0	100.0

Table V. Size of Ball or Pebble Required for Fine Grinding

Mesh	Classifier No. 4and 5 Primary Sands	Classifier No. 7 and 8 Secondary Sands	Classifier No. 12 Tertiary Sands
+ 6	0.4		
+ 10	7.0	0.5	0.2
+ 20	28.4	2.3	0.5
+ 35	23.4	5.8	0.7
+ 65	16.3	16.7	5.5
+150	11.8	31.7	31.7
+270	6.2	24.3	39.1
−270	6.5	18.7	22.3
	100.0	100.0	100.0
Cum + 10	7.4	0.5	0.2
Cum + 35	59.2	8.6	1.4
Cum +150	87.3	57.0	38.6

Table VI. First Laboratory Pebble Test

	Head Primary Sands	1¼ In. Steel Load, 500 Rev	1¼ In. Pebbles, 1500 Rev	Pebble Analysis[a]		
				Size	No. Pieces	Pct Wt
Capacity rating, pct		100	33	+1½	12	15.8
+ 6 mesh	0.4			+1	76	57.2
+ 10 mesh	1.3	0.3	0.2	+¾	85	23.8
+ 20 mesh	1.8	0.2	0.2	+½	8	0.9
+ 35 mesh	3.6	0.2	0.3	−½		2.3
+ 65 mesh	17.5	5.3	4.9			100.0
+150 mesh	36.8	31.7	29.0			
+325 mesh	32.6	37.4	36.6			
−325 mesh	6.0	24.9	28.8			
	100.0	100.0	100.0			
Pct new −325 produced		18.9	22.8			
Capacity rating, pct		100	120			

[a] Average weight per piece is 48 g, equivalent to a pebble sphere 1.28 in. in diam or equivalent to a steel sphere 0.9 in. in diam.

Table VII. Diam of Balls of Different Material Having the Same Weight

Weight, G	Diam of Steel Ball, In. (7.8 Sp Gr)	Diam of Ore (2.66 Sp Gr)	Diam of Tungsten Carbide (13.1 Sp Gr)
3.52	0.375	0.53	0.32
8.37	0.50	0.72	0.42
16.3	0.625	0.89	0.53
28.2	0.75	1.07	0.63
43.4	0.875	1.24	0.73
66.9	1.00	1.42	0.84
131.	1.25	1.77	1.05
226.	1.50	2.14	1.26
347.	1.75	2.48	1.46
535.	2.00	2.86	1.68
1807.	3.00	4.27	2.52
4282.	4.00	5.72	3.36
8364.	5.00	7.17	4.20

gravity, see Tables II and III. A tungsten carbide ball of the correct size will handle 68 pct more tonnage than a steel ball of the same weight. The correct size of ball must be determined first with regard to the size of material being ground. This means that the Lake Shore pebble would be expected to handle only 34 pct of the tonnage of steel balls. This realization was an important factor in the ultimate success of pebble testing at Lake Shore. Early scouting tests on grinding with a rock grinding media had never shown any promise and had been abandoned. They had been tested at too high a feed tonnage and naturally showed little grinding under these conditions. The main value of the tungsten carbide test was that the balls themselves proved too expensive for general use, although the ⅜-in. tungsten carbide balls showed great efficiency and might be used in special applications.

The fact that the pebble mills would have less capacity than steel mills was no handicap in itself, as the mill formerly handled 2600 tons and was now milling 1000 to 1200 tons, and there were several idle 5x16-ft mills and one 6x16-ft mill that could be pressed quickly into service.

Tests were made in the 12-in. Haultain grinding mill with loads of 1¼, 1, and ¾-in. balls according to the Prentice formula. The same volume of balls was used in each case. Thus the tungsten carbide load was 1.68 times as heavy as the steel load with 13.1:7.8 to 1.68:1. sp gr.

Several grinds were run with different lengths of time, i.e., varying revolutions of the mill with the speed of the mill constant, 80 pct critical. It was established finally that the two loads would do identical grinding when the steel load was run 68 pct longer than the tungsten carbide load. Thus the tungsten carbide load has 68 pct more capacity than the steel load, see Table II. Another test on coarse feed was run to see if the heavier ball would handle coarser material. When the tungsten carbide mill is handling 68 pct more feed than the steel mill, both mills have equal ability to handle the top meshes, see Table III.

In this test, balls of equal size were used rather than of equal weight, and at a capacity differential of 68 pct the lighter steel ball is slightly more efficient. A steel ball of equal weight, 1½-in., probably would have shown the same capacity as the tungsten carbide under the above conditions. This is a delicate problem and one which must be investigated carefully when testing balls of different specific gravity.

Some interesting test work also was done with ⅜-in. tungsten carbide balls as compared to ⅜-in. and ¾-in. steel balls. With steel balls running at proper gravities for good grinding, the ½-in. grinding ball is the lower limit. The ⅜-in. ball is slightly off and the ¼-in. ball a definite failure. The tungsten carbide ball, which is 68 pct heavier, retains the advantage of its extra surface and showed 80 pct more capacity than ⅜-in. steel and 96 pct more capacity than ¾-in. steel.

Surface Hardness in Grinding

Tungsten carbide grinding balls have a surface hardness much greater than rail steel balls. To check if this superior hardness had anything to do with the increased grinding capacity, a test was made using steel balls, tungsten carbide balls, and stellite balls. The stellite is 11 pct heavier than steel but has a much harder surface, comparable to that of the tungsten carbide. The time of grind, and thus the capacity, in each test was varied inversely as the specific gravity of the grinding media so that the final grinds would all be the same, if capacity varies according to specific gravity and surface hardness has no effect.

The results of this test, given in Table IV, show that surface hardness has no effect. The tungsten carbide ball is slightly off its capacity rating since the same size ball was used instead of the same weight. A 1.05 in. tungsten carbide ball is the equivalent in weight of a 1¼-in. steel ball. This fact was not appreciated at the time the test was made. It became more apparent with greater difference in specific gravity between the grinding media. The 11 pct difference between steel and stellite would not have any appreciable effect.

The sand analyses given in Table V shows the type of feed being handled by each stage of milling.

Tests at Lake Shore show that the most efficient

Table VIII. The Effect of Pebble Size on the Grind, July 1948

	Mesh	1 Final Class Sands	2 ¾ In. Pebbles with 11 Pct −¼ In. in Load, 1250 Revs	3 Same Load with −¼ In. Removed, 1250 Revs	4 50 Pct −1 In. + ¾ In. 50 Pct −¾ In. + ½ In., 1250 Revs	5 All −1 In. + ¾ In., 1250 Revs	6 −¾ In. Steel Load 500 Revs
	+ 10	0.1	—	—	—	—	—
	+ 20	0.7	0.5	0.5	0.1	trace	0.1
	+ 35	1.6	2.2	1.5	1.0	0.5	0.1
	+ 65	8.6	11.0	8.8	7.8	6.6	3.0
	+150	19.0	15.4	13.5	15.2	15.8	13.7
	+325	54.0	42.7	42.0	43.6	44.5	47.5
	−325	16.0	28.2	33.7	32.3	32.6	35.6
		100.0	100.0	100.0	100.0	100.0	100.0
Cum.	+ 35	2.4	2.7	2.0	1.1	0.5	0.2
Cum.	+150	30.0	29.1	24.3	24.1	22.9	16.9
Cum.	+325	84.0	71.8	66.3	67.7	67.4	64.4

ball for primary sands is 1-in. to 1¼-in.; for secondary sands, ¾ to ⅞-in.; for tertiary sands, ½-in. balls.

Early Laboratory Tests

Most of the laboratory tests with the 12-in. mill are *tonnage tests*. At least four varying times of grind are made, each at the correct pulp density, with each different variable being tested. The variable may be 1—coarse or fine sand feeds, 2—different size of grinding media, or 3—different types of grinding media. The time of grind has been tested against the operating plant, and time of grind can be related to tonnage per day through a 6 ft 8-in. x 15-ft pebble mill or a 5-ft x 16-in. tube mill. The log of this tonnage then is plotted against the log of the percentage reduced[†] of any reliable mesh in the screen analysis. The resulting plot has been found to be a straight line with the laboratory mill and with plant pebble mills, tube mills, ball mills, and rod mills. This relationship holds with normal variations in feed analysis so that tests done at different times can be compared. This relationship has proved of tremendous help in checking laboratory work and in designing alternate layouts or new plants. It has been used successfully for the past 10 years. To describe the method fully is a report[5] in itself, and it is simply mentioned here that such a method is used. Some illustrative tests are quoted in this report, but plant design is based on the more detailed methods mentioned above.

Capacity and Size of Pebbles

After Dr. Jackson's visit and with the capacity ratings from the tungsten carbide tests available, encouraging grinds on the first half dozen laboratory tests using ore as a grinding media were obtained, see Tables VI and VII.

This first pebble load produced a finer grind than the 1¼-in. steel load, which was encouraging at the time. Reviewing the test now, it is found that 1—The pebble load chosen was of approximately equal size rather than of equal weight. A 0.9-in. steel load is known from the 1940 report to be 14 pct stronger on this type of sand feed than 1¼-in. balls. The size distribution of this load indicates that it is slightly superior to a 0.9-steel load. 2—The test was run at 1500 rev instead of 1470 rev for 34 pct capacity. Thus when all corrections are made, the pebble load at a rated capacity of 34 pct is at least as good as the 1¼-in. steel balls.

These tests indicated that a large pebble of the same weight as a 1¼-in. ball would grind satisfactorily. The next question was whether the work of the ¾-in. grinding ball with fine pebbles could be duplicated. The tests in Table VIII were run to check this point.

These tests showed that if the pebble size is kept above ¼ in. to ⅜ in. a good grind can be obtained (compare cols. 2 and 3). The −¾-in. steel load was run at 500 rev instead of 417 rev for its proper capacity rating. When corrected graphically for its extra time of grind, it checks the pebble of the same weight almost exactly, i.e., all −1 in. +¾ in.

Within a month of the start of the laboratory testing, the conclusion was reached that ore could be used as a grinding media if a cheap method could be found.

When the idea of grinding with rough screened rock was discussed first, it was felt that the broken rock would tend to chip, producing tremendous quantities of 3, 4, and 6 mesh material which would be too large for the pebbles to handle and would thus build up in the mill load and also might tend to block the grate discharge. Several tests were run which demonstrated that this would not happen. Rock loads ground for 24 hr showed smooth pebbles and fine slimes with a noticeable absence of intermediate sizes.

It was noted that the heaviest pebble consumption occurs during the first 2 hr, but the original pieces are not chipped into large intermediate size pieces. After 2 hr the pebbles were observed to be well rounded. During the next 24 hr the pebble consumption per 2 hr period was almost constant and only about 20 pct of the consumption during the first 2-hr period. These tests have been confirmed by over 2 years' operations in 6 ft 8-in. diam mills. There is no problem of this nature on Lake Shore ore on 5 ft, 6 ft, and 6 ft 8-in. grate discharge pebble mills.

Early Tube Mill Tests

High Discharge Pebble Mills: The first plant scale tests were made in No. 14 tube mill on Oct. 8, 1948. The 18 tons of mixed 1¼-in. and ¾-in. steel grinding balls were dumped out and 6.0 tons of approximately −2½ in. +¾-in. screened rock were put in. (The lighter rock resulted in the mill speed increasing slightly from 30 rpm to 31 rpm.) This mill was run as a high discharge pebble mill for several months with a wide variety of results. The following conclusions were reached.

1—Pebble mills require some sort of lifter bars to obtain correct pebble action. The mill was run at high speed 34 rpm (96.6 pct critical) but did not approach the effectiveness of lifter bars. Four lifter bars seemed as effective as seven, but it was considered good practice to have some lift on at least every second liner.

2—For best grinding, the mill had to be run with

Table IX. Summary of Preliminary Testing with Pebbles in 5x16 Ft High and Low Discharge Mills

Period	1948	Avg Hp	Hp Minus No Load[a]	Capacity[b] Rating	Hp Per Capacity	Speed	No. of Lifter Bars	Discharge Level
5′x16′	Steel ball mill	182	162	100	1.62	30	0	high
1st	Oct. 7-15	59.0	39.0	24.5	1.59	31	0	high
2nd	Oct. 16-28	57.6	37.6	21.9	1.71	31	0	high
3rd	Oct. 29-Nov. 4	60.6	40.6	25.3	1.61	34	0	high
4th	Nov. 5-14	73.5	53.5	31.4	1.70	34	4	high
5th	Nov. 15-24	80.0	60.0	33.3	1.80	34	7	high
6th	Nov. 26-28	78.0	58.0	33.0	1.75	31	7	high
7th	Nov. 30-Dec. 15	98.5	78.5	47.8	1.64	31	7	low
9th	Feb. 8-15	97.6	77.6	47.5	1.63	31	0	low

[a] No load — shell only 20.
[b] As determined by tonnage tests in the plant.

[†] Percentage reduced =

$$\frac{\text{cum pct + any reliable mesh in the feed} - \text{cum pct + same mesh in the discharge}}{\text{cum pct + same mesh in the feed}}$$

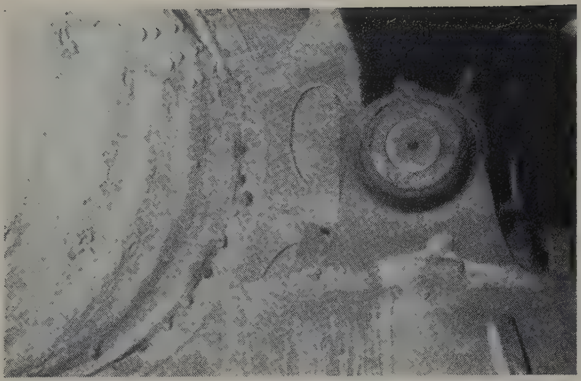

Fig. 3—Pinion drive of original 5x16 Allis-Chalmers tube mill.

more dilution than the steel mills, with 1.550 to 1.650 sp. gr. (56 to 65 pct solids) found best on fine feeds as opposed to 1.650 to 1.750 (65 to 70 pct solids) for steel mills.

3—High discharge pebble mills were a nuisance to operate. Changes in gravity would put the fine pebbles through the discharge trunnion and into pumps, launders, etc.

4—The capacity of the mill was spotty, varying from 22 pct to a maximum of 33 pct of the capacity of a steel mill. It took careful operating to maintain 33 pct capacity at all times.

5—The horsepower of the mill went up and down with the capacity. At all times the amount of finished material produced per horsepower was the same as with the high discharge steel mill, i.e., the total horsepower minus the power to drive the empty shell, etc. The *no-load* power is such a high percentage of the total in a test of this kind that it is necessary to make this correction to arrive at a fair power comparison between steel and pebble mills, see Table IX. Later on the 6 ft 8-in. mills the motors are properly loaded, and no correction is necessary.

All in all, high discharge pebble mills did not seem an attractive proposition, and Lake Shore Mines hesitated to try to run such a plant.

Low Discharge Pebble Mills: The pebble load was transferred from No. 14 mill to No. 13 mill on Nov. 30, 1948. No. 13 mill had been a regular low discharge primary tube mill using 1¼-in. balls and had a grid and scoop discharge.[6] The grid had 3/16-in. openings. This mill then was run as a low discharge pebble mill for 2 years and is still in operation.

Low discharge pebble mills draw 40 pct more power and have 40 pct more capacity than high discharge (or trunnion discharge) pebble mills. They are also much easier to operate, maintaining a steady power reading and capacity provided, of course, that the pebble load is kept at or near the center line of the mill.

This tremendous difference between high and low discharge pebble mills is in sharp contrast to the capacity change for steel mills, which is 27 pct at Lake Shore on these same mills. Apparently the 2.7 sp. gr. pebble has difficulty in grinding in high discharge mills where the pulp gravity is 1.650. This same capacity differential was found at the Rand in South Africa 20 years ago, according to C. W. Dowsett, who gave the writer the figure before the tests were run at Lake Shore. This would explain why all the South African fine grinding pebble mills are provided with grates and low discharges.

Grates with ⅜-in. openings were tried during the tests and found to be slightly too large for the size of the pebble in use at that time. The original steel grate opening of 3/16 in. was satisfactory. Later ¼-in. slots were used.

Pebble Consumption

On a rock feed with an average weight of 120 g per piece and with a screen analysis of 17 pct + 2 in., 68 pct + 1½ in., 15 pct + 1 in., the following pebble consumption figures were obtained: Without lifter bars on a 5x16 ft high discharge pebble mill, the daily consumption was 927 lb per day. Without lifters the load could be observed through the discharge trunnion to be riding only part way up one side. This resulted in the pebbles wearing into exaggerated flat shapes. When lifter bars were put in, the pebble consumption rose to 1500 lb per day, 30.9 rpm, and 1650 lb on higher speeds, 34 rpm. When the load was changed over to a low discharge mill and raised from 0.45 load to 0.50 load, the consumption rose to 2400 lb per day at 30.9 rpm.

Pebble consumption varies with the size of rock feed; the larger the rock the greater the consumption. There is apparently some breakage of large pieces, and the resulting load is not proportionately larger on the top meshes.

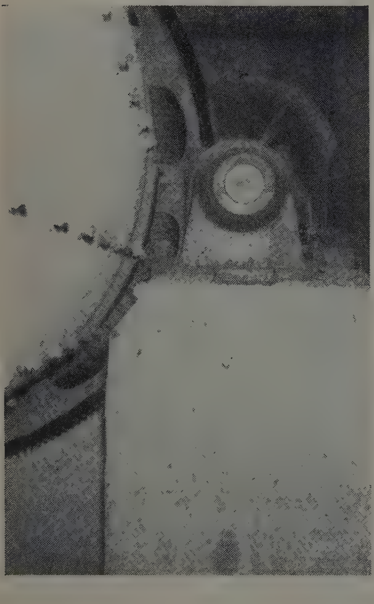

Fig. 4—Pinion drive of new 6 ft 8 in. x 16 in. pebble mill. Note the shell clearance and corner cut off foundation to allow liner bolts to clear.

Conversion Plans

Mechanical Problems: The laboratory and the plant low discharge tests both indicated that satisfactory grinding could be done with pebbles, but the problem of converting the whole plant to pebble mills still remained. The problems were:

1—If the 5x16-ft mills were used, 20 would be required for a 1000-ton plant. All the motors would be running low power factor under the condition of half load. The Ontario Hydro Power Commission was already imposing restrictions on power.

2—Building new and larger mills would involve new motors, which were difficult to obtain, and an acute steel shortage meant that complete new mills were not available.

The problem was solved at little capital cost and with little difficulty in conversion by expanding the diameter of the shell of the mills until the new mill with pebbles would draw the same horsepower as a 5x16-ft high discharge steel mill, i.e., the normal capacity of the motors 180 to 185 hp. The original mills had large spur gears and would allow for the required 10-in. expansion, only necessitating the chipping of the corner of the cement foundation under the pinion gear, see Figs. 3 and 4.

The expanded mills had to be slowed down in speed, requiring a 17-tooth pinion in place of the original 19 and 21-tooth pinions. A ⅝-in. welded steel shell was made to fit over the existing ends of the 5x16-ft mills, expanding them to 6 ft 8 in. in diam. See Figs. 3 and 5.

Allis-Chalmers engineers, particularly Mr. Hollefriend, together with Mr. Purdie, Lake Shore Mechanical Superintendent, helped to work out the final details of this relatively simple conversion plan. The ultimate cost of the conversion job was:

New 6 ft, 8-in. shell	$4,450.00
New pinion	400.00
Removing old shell, installing new shell, and changing pinion	200.00
Total cost per mill changed	$5,050.00

This mill could then be relined with a Ni-hard liner shell and feed end for $2,800, plus $400 for discharge grates.

In calculating the required diameter of a low discharge pebble mill to equal a high discharge 5x16 ft steel mill: 1—The capacity of 5x16 ft high discharge mill, 182 hp, is taken as 1.00. 2—The tests showed that a 5x16 ft high discharge pebble mill with lifter liners had a capacity of 0.34. 3—A 5x16 ft grate discharge pebble mill with lifter bars had a capacity 40 pct greater, or 1.4x0.34 = 0.475.

Then, let X = diameter of a grate discharge pebble mill with a capacity equal to a 5x16 ft high discharge mill = 1.0, and knowing that the capacities of mills vary as $d^{2.6}$[1]

$$\text{Then } 0.475\,X^{2.6} = 5^{2.6} = \frac{65.6}{0.475} = 138.1.$$

Solving for X = 6 ft 7¾ in., use 6 ft 8 in.

Since in all tests with pebbles the horsepower per ton ground was directly proportioned to the capacity of the mill, the assumption was made that the 6 ft 8-in. would draw the same horsepower as the 5x16 ft high discharge mill, 182 hp. In the previous grinding report it had also been found that the capacity, power, and steel consumption varied as the 2.6 power of the diameter. This assumption proved to be correct.

Rock Feeding

The problem of handling 35 to 40 tons of rock per day (3½ to 4 tons per day to each of ten mills) without excessive labor charges was still to be solved. The original 5x16-ft mill was kept in pebbles by building a small hopper of 2½-ton capacity and filling it each day with the mill fork lift truck with a scoop shovel attachment. The pebble consumption is great enough that a pebble mill should be fed at least every 12 hr and preferably every 8 hr or even every 6 hr. Since this is a grate discharge mill, the load must be kept within 1 in. ± of the center line to get maximum capacity from the mill.[7]

The original 5x16-ft mills all had drum feeders. These would not handle 3-in. screened rock at a greater rate than 200 lb per min. Many of them were worn out, so it was decided to replace them with hopper feeders. The original trunnion liners were 7½-in. outside to 11 in. on the inside of the liner and would not take the elbow from an 8-in. pipe. It had been established previously that 3-in. rock required at least 8-in. pipe to carry it. These old trunnion liners were removed, and the ends of the mill were lined with ½-in. Linatex. These were built up to give a slope of 1 3/16 in. in 22 in. with an outside opening of 10 in. and an inside opening of 12⅜ in. This gave an opening big enough to allow a hopper with an 8 in. elbow at the bottom, see Fig. 6.

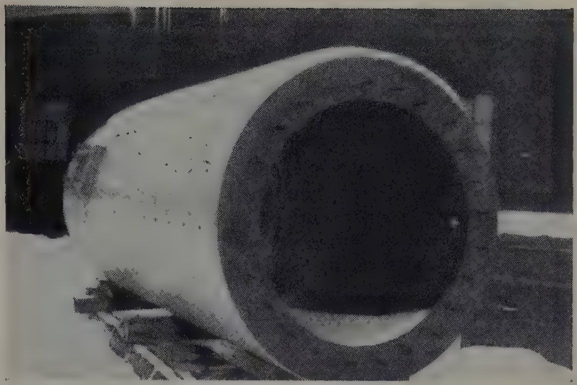

Fig. 5—New welded plate shells for 6 ft 8 in. x 16 in. pebble mills. The studs on the end fit over the original 5 ft tube mill ends.

These hoppers work well and allow the pebbles to be fed from an overhead conveyor running the length of the pebble mill floor with angle ploughs scraping the rock into the desired mill.

The Linatex lined trunnions have another operating advantage. It is not possible for grinding material to get behind the trunnion liner and wear out the trunnion itself without being noticed. The rubber is glued directly to the mill trunnion and wear must come from the outside where it can be seen.

There is also a power saving through using hopper feeders over the old drum type feeders. Our tests show that the drum feeders formerly used on the mills required about 5 hp to operate the feeder.

No. 8 Mill:	Maximum hp before removing drum feeder	190
	Maximum hp after removing drum feeder	185
	Saving	5
No. 7 Mill:	Hp immediately before removing drum feeder	155½
	Hp immediately after installing new hopper feeder and on the same pebble load (which was 4 in. low)	150
	Saving	5½

The problem of holding the pebble load within 1 in. of the center line was a difficult one. Two alternatives were considered:

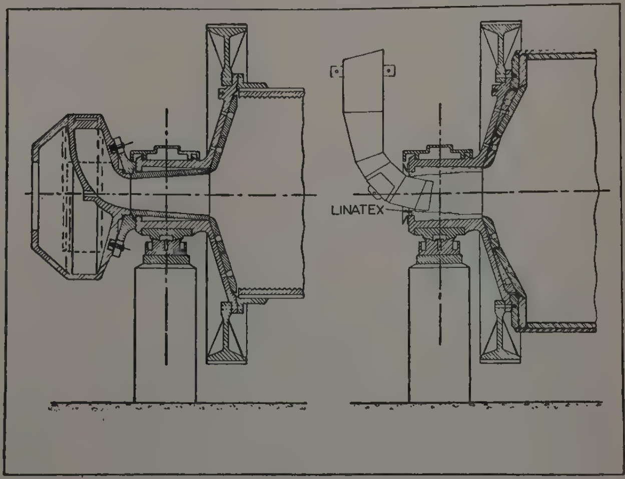

Fig. 6—Old arrangement, left, of 5x16-ft tube mill with drum feeder. New arrangement, right, of 6 ft 8 in. x 16 ft pebble mill with hopper feeder.

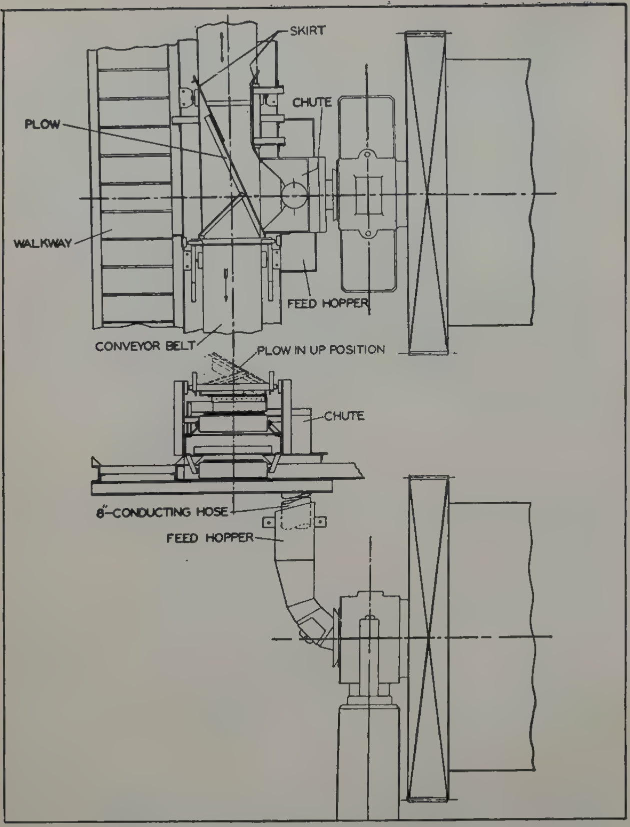

Fig. 7—Pebble feed system to pebble mill.

Fig. 8—Batch-weighing hopper.

1—To put sensitive kilowatt meters on each mill so that the mill would be held at maximum power at all times and loaded each shift until the power reached its peak, since it has been established that the mill will draw maximum power when the load is exactly at the center line. The difficulty with this operation is that the power falls off when the load is both over and under the center point. Therefore it would be necessary to have a recording chart on each mill to obtain enough evidence to state definitely that a low horsepower meant that the load was low rather than too high. All types of recording kilowatt meters were investigated, and it was found that for ten mills the cost of any suitable installation of recording meters would be prohibitively high.

2—The other alternative was accurately to weigh the pebbles into the mill each shift according to their liner age, liner design, and type of grind (i.e., primary, secondary or tertiary) and to assume that the ore hardness would be consistent enough to maintain our load requirements. It has been found that Lake Shore ore, because of the sequence mining system employed underground to control rock bursting, was very consistent in hardness; also, 10 years' experience in having one man weigh steel into the mill had proved that accurate weighing methods were the most satisfactory.[8] These weighings would be backed up by kilowatt meter readings, of course, but on a relatively cheap meter such as a kilowatt demand meter. The Lincoln maximum demand meter type WD3 made by Sangamo has been found to be very suitable. The operators are warned not to read them within 20 min of a shutdown or power failure.

This second alternative was the one finally decided upon, and it has proved most satisfactory.

Rock Screening and Handling

Preliminary screening tests indicated that Lake Shore ore screened through a 3x3-in. opening and retained on a 2x2-in. opening gave a pebble load in the mills with 51 pct of the pebbles −1½ in. and +¾ in. Tests showed that this load ground with about the same efficiency as a 1¼-in. ball load.

By varying the screens, pebbles of different sizes can be obtained easily.

Since the primary crushers are usually set at 1 in., this meant screening the ore as it comes up the shaft from the underground crushers (−6 in.).

This involved alterations to the crushing plant. It was decided to send all −¾-in. material in the hoisted ore (amounting to 30 to 35 pct) directly to

Table X. Shell Liner Costs

Type	Grinding Media	Type Liner	Material	Thickness Liner, In.	Total Weight Shell Liner, lb	Cost per lb. Nihard, c	Total Cost, $	Life, Days	Cost per Day, $	Cost[a] per Ton, $
5x16 ft H. D.	1¼ in. balls	M. Black Groove	Nihard	2-1/16	20,000	11.8	2360.00	600	3.93	0.032
6 ft 8 in. x 16 ft L. D.	1¾ in. pebbles	Hendry Wave	Nihard	1-11/16	20,000	11.8	2360.00	700	3.37	0.027

[a] Based on one rod mill, one ball mill and eight pebble or tube mills for 1000 tons per day.

Table XI. Comparison of the Initial Cost of Buying New Tube Mills and New Pebble Mills of Equal Grinding Capacity and Power

High Discharge Tube Mill	Equivalent Grate Discharge Pebble Mill	Ball Load, Tons	Rock Load, Tons	Cost of Initial Load Balls at $122.80[a] Per Ton, $	Rock	Complete Cost of New Mill Plus Nihard Liners Less Motor, $[b]		Tube Mill Plus Initial Load, $
						Tube Mill	Pebble Mill	
5x16 ft	6 ft 8 in. x 16 ft	18.0	14.0	2,210	—	17,300	19,770	19,510
6x16 ft	8 ft 0 in. x 16 ft	25.8	20.1	3,170	—	21,225	24,652	24,395
7x16 ft	9 ft 4 in. x 16 ft	36.2	27.4	4,450	—	30,150	33,995	34,600
8x16 ft	10 ft 8 in. x 16 ft	46.1	35.7	5,660	—	38,500	43,900	44,160

[a] January 1951 price.
[b] These figures are supplied by Canadian Allis-Chalmers Co.

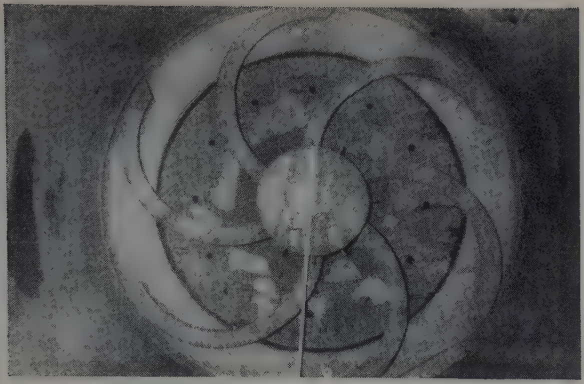
Fig. 9—Low discharge lifter scoops used on all pebble mills. The grate sections are placed directly at the front of these scoops resting on the short lugs shown in the center and flush with the center plate.

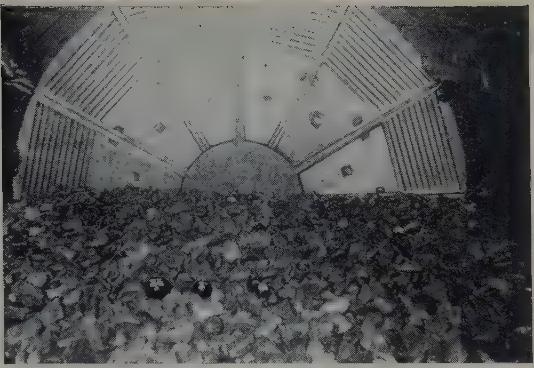
Fig. 10—Pebble load at discharge end. Note pebble load at center line and 5/16-in. slats in Nihard grate sections.

the rod mills. The +¾-in. material then was crushed in two open circuit Symons cones with a screen between them. This replaced a three cone and closed circuit screening plant. The removal of the −¾-in. material from the hoisted ore required a triple decked screen, the upper decks to protect and screen out the coarser material. Therefore, these decks were used, when necessary, to produce the correct size of rock feed for the pebble milling. Two triple decked 5x10-ft Ty-Rock positive circle throw screens were installed.

The rock that passes the top deck, 3x3 in., and is retained on the second deck, 2x2 in., then is conveyed to a single deck 3x6-ft screen on the top of the rock feed* storage bin of 300-ton capacity in the mill. This screen splits the rock feed into coarse and fine fractions, which are stored in separate halves of the main bin. Separate Jeffrey feeders draw either coarse or fine rock feed or a mixture for the pebble mills. These feeders discharge into the weighing hopper of the Toledo scales system. A batch of a definite weight up to 1000 lb can be withdrawn as needed, usually 200-lb batches at a time. These weighed batches are elevated with a bucket conveyor that discharges onto the conveyor belt running the length of the pebble mill floor and is located directly over the feed hoppers of the pebble mills. Ploughs have been installed opposite each mill and the rock feed directed to the desired mill through an 8-in. rubber hose. Classifier sands help to wash the pebbles through the linatex lined trunnion into the mill. See Figs. 6 to 11.

On the 6 ft 8-in. mills, the primaries are fed 7900 lb per day of coarse rock feed, with the average theoretical mean diam 1.87 in. The final stages are fed 5300 lb per day of fine rock feed, with the average theoretical mean diam 1.44 in. The wattmeters are read every 2 hr and used to check the pebble load in the mill.

Pebble Mill Costs

Among the factors involved in pebble mill costs are the following:

1—The saving effected by using screened ore in place of 1¼-in. grinding balls has already been discussed. This saving amounted to $0.285 per ton milled at September 1951 steel prices.

2—To mill 1000 tons per day, one rod mill, one ball mill, and eight pebble mills were required. Each mill uses approximately 3½ tons of rock per day, 840 tons per month. This rock is taken from the underground ore before crushing. To crush and grind this rock to the fineness at which it leaves the pebble mills would cost $0.50 per ton. On 2.8 pct of the tonnage this amounts to $0.014 per ton milled. This saving should pay for running the extra conveyors and pebble feeding equipment.

3—The horsepower per ton milled is the same for pebble mills as for steel mills.

4—Liner costs are slightly cheaper in pebble mills. This saving, however, is only $0.005 per ton milled. Shell liner costs are given in Table X.

The 6 ft 8-in. pebble mills are easier to reline than 5-ft steel mills. By cutting the pebble feed for 1 day the load drops 7 to 8 in., and the mill can be relined easily without dumping the remaining pebble load. The worn liners are not so rigidly wedged together as they are with steel. The 5-ft steel mills were always relined by dumping the 18-ton ball load on the floor and then replacing it.

5—Operating labor is the same.

---

* The screened rock used to make pebbles is referred to as *Rock Feed*. The term *pebble* is not used until the rock feed has been in the mill long enough to become rounded.

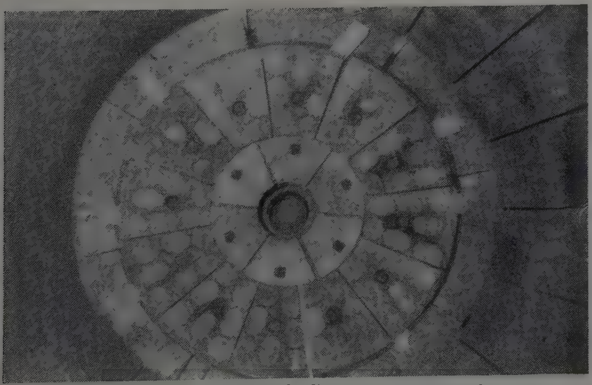
Fig. 11—Feed and liner arrangement. The eight outside 9-in. segments are not bolted.

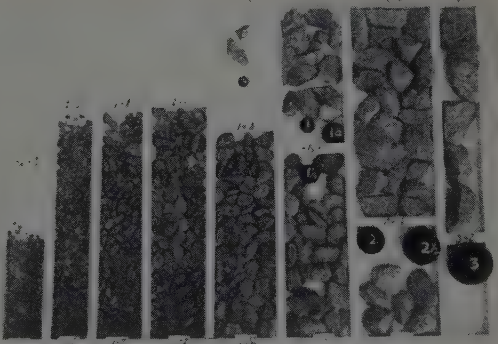

Fig. 12—Rock feed and pebble load tray.

Table XII. Sizing of Rock Feed and Resultant Pebble Load

Size, In.	Wt, g	Rock Feed March 11-17-20, 1950 Avg Wt per Piece = 117 G Pct Wt	Resulting Pebble Load March 1950 Pct Wt
−2½ + 2	−356 + 184	29	14
−2 + 1½	−184 + 78	55	28
−1½ + 1	− 78 + 23	15	23
−1 + ¾	− 23 + 9.7	1	17
−¾ + ½	− 9.7 + 2.9		11
−½ + ⅜	− 2.9 + 1.2		5
−⅜ + ¼			2
−¼ + 3/16			
		100	100

6—Maintenance is slightly higher since all the mills have grate discharges.

7—To feed the pebbles takes 9 man hr per day at the moment as against 6 man hr per day for feeding steel. It is anticipated that this will be reduced to 6 hr as the plant is tuned up.

A comparison of the initial cost of buying new tube mills and new pebble mills of equal grinding capacity and power is given in Table XI.

It will be noted that although the large diameter pebble mill costs more than the tube mill to purchase, by the time the tube mill is loaded with balls at $122.80 per ton, the cost of the two installations are nearly equal.

Rock Feed and Pebble Load

A typical analysis of the primary rock feed and pebble load first used at Lake Shore is given in Table XII.

The rock feed was screened on a 3x5-ft Dillon screen (a temporary setup) through 2½ in. and +2 in. The pebble load was sampled by driving a 10-in. pipe down through the load at intervals.

The sizing of these odd shaped particles presented a problem, as ordinary screening on Tyler screens was unsatisfactory. It was found necessary to size by first roughly screening or sorting and then actually weighing each piece of rock between upper and lower limits to determine its proper size.

A rock feed of 5000 g and pebbles of 5000 g were sized by screening and weighing and are shown in Fig. 12. Steel balls marked with their sizes are shown for comparison.

The best guide for proper pebble size is to start by using a pebble of the same weight as the correct size of steel ball. Later, if the tonnage being handled is not too high (i.e., the time of contact in the grinding mill is relatively long) the pebble size may be gradually reduced to approach, but never quite reach, the same diameter as the steel ball. The smaller the grinding media, the greater the production of finished material, provided the top sizes are not allowed to build up.

Summary and Conclusions

1—Shape of grinding media is not important for −8 mesh grinding.

2—The capacity of the grinding media is directly proportioned to its specific gravity; thus siliceous ore pebbles, steel balls, and tungsten carbide balls are in the ratio of 0.34, 1.00, and 1.68.

3—A method of using a 12-in. grinding mill to evaluate plant fine grinding practice is explained.

4—High discharge pebble mills are erratic in performance.

5—Low discharge pebble mills use 40 pct more power and have 40 pct more capacity than high discharge pebble mills. Under identical conditions steel mills show only 27 pct difference.

6—A cheap and practical method of converting existing steel mills to pebble mills is outlined. A 5x16-ft mill is converted for $5050. Low discharge pebble mills have 47.5 pct of the capacity of the same mill filled with steel balls and equipped with standard trunnion discharge. Thus, to use the same motor and get the same capacity out of pebble mills, the capacity of the mill has to be increased 2.1 times. This can be done by 1—increasing the diameter on $d^{2.6}$ basis or 2—by lengthening the mill 2.1 times. The following table shows the expansion necessary on standard diameter mills for pebbles at 2.6 sp. gr.

H.D. Steel Mill Diam, Ft	Equivalent L.D. Pebble Mill Diam
5	6 ft 8 in.
6	8 ft 0 in.
7	9 ft 4 in.
8	10 ft 8 in.

The initial cost of each of these two mills, when loaded, is nearly the same.

7—The horsepower per ton milled is the same for pebble mills as for steel mills.

8—A method of feeding rock to the mills and of controlling the pebble load is described.

9—Liners with some lift—at least 1 in. in every second row—are required for pebble mills. Operating speeds are normal, 83 pct critical; but high speeds are more attractive than they are with steel balls.

10—Slightly more dilute pulps (7 pct less solids) are recommended.

11—For 1¾-in. and 1¼-in. pebbles, grates with slots up to 1/4 in. are best and 5/16 in. is maximum.

12—On Lake Shore ore the pebble consumption per 6 ft 8-in. mill varied from 5300 lb per day for 1¼-in. pebbles to 7900 for 1¾-in. pebbles.

13—Practice has been to start by using a pebble of the same weight as the steel ball being replaced.

14—The annual savings due to the installation of pebble milling amount to 785 tons of steel, or over $104,400.00. The saving amounts to $0.285 per ton milled.

Acknowledgment

The author would like to acknowledge the invaluable assistance of the following men who contributed to the success of this project: J. E. Williamson, formerly chief of the Lake Shore Research Staff, now with Union Corp. of South Africa, conducted the original experimental work. He was assisted in this by G. H. McCrank and Austin Murphy, C. Whitman, Mill Foreman, and the mill crew who helped to develop the operating end. J. G. W. Purdie, Mechanical Superintendent, G. Honer, Chief Electrician, and E. H. Bronson, Consultant, helped with the design and installation of the plant. J. C. Adamson, Mine Superintendent, and A. L. Blomfield, President, gave valuable advice and encouragement.

References

[1] Fine Grinding at Lake Shore. The Staff, Canadian Institute of Mining and Metallurgy. *Trans.* (1940) **43**, pp. 299-434.

[2] Addendum: Fine Grinding at Lake Shore. The Staff, Canadian Institute of Mining and Metallurgy. *Trans.* (1941) **44**, pp. 379-395.

[3] F. C. Bond: Standard Grindability Tests Tabulated. *Trans.* AIME (1949) **183**, p. 313; *Mining Technology* (July 1947), p. 2180.

[4] P. 409 ref. 1.

[5] B. S. Crocker discussion on paper by E. J. Roberts: The Probability Theory of Wet Ball Mining and Its Application. *Trans.* AIME (1951) **190**, p. 988; MINING ENGINEERING (November 1951).

[6] P. 387 ref. 1.

[7] P. 383 ref. 1.

[8] P. 396 ref. 1.

Mining Operations at The Teniente Mine of The Braden Copper Company, Rancagua, Chile

by F. E. Turton

THE town of Rancagua, at the junction of the state and Braden Copper Co. railroads, is located 82 km south of Santiago, the capital of Chile. From Rancagua 70 km to the east, situated in the Andes at an elevation of 7000 ft, is the town of Sewell, the location of a millsite. Two and one half km east of Sewell by underground railroad at an elevation of 7500 to 10,000 ft is the Teniente orebody.

The history of *El Teniente* dates from the eighteenth century, when according to legend a Spanish lieutenant, or *teniente*, a fugitive from justice, escaped to the Andes and camped at what afterwards became known as the *Mineral El Teniente*. This man reputedly discovered a vein of high grade copper ore. The first official records date from 1819, when some exploitation was begun, and continue until 1870. The orebody was large and of relatively low grade and was beyond the capabilities of the small groups attempting to operate it. No effort was made to erect a concentrator until William Braden became interested in the property.

In 1901 Mr. Braden promoted the necessary capital for the first practical exploitation of the orebody. Barton Sewell and E. W. Nash, both of the

---

F. E. TURTON, Member AIME, is Vice President of the Braden Copper Co., a subsidiary of the Kennecott Copper Corp.

Discussion on this paper, TP 3314A, may be sent (2 copies) to AIME before July 31, 1952. Manuscript, Aug. 28, 1951. Mexico City Meeting, October 1951.

This page of Mining Transactions AIME follows p. 508. The intervening non-Transactions pages appeared in Mining Engineering.

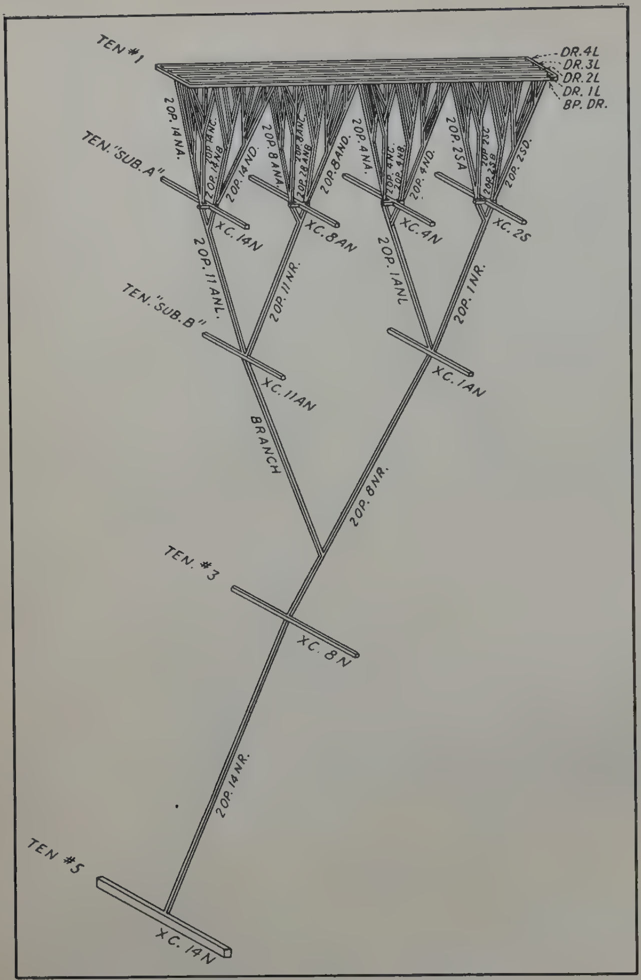

Fig. 1—Typical Braden ore pass system.

American Smelting and Refining Company, financed the original installation of a 250-ton concentrator, a 100-hp hydroelectric power unit, the necessary campsite, and the underground development of the Fortuna orebody. Actual production started in 1906, and from that time until 1920 the capacity of installations was gradually increased, with a resulting yearly production of 1,600,000 tons of ore.

The existence of a larger lowgrade ore deposit, the Teniente, was established by prospecting beginning in 1903 and terminating in 1911. At this time, with the end of ore reserves in the Fortuna mine in sight, full scale development of the Teniente orebody started. This program resulted in initial production in 1915 of 60,000 tons yearly and was increased to the present yearly tonnage of 9,000,000 tons. The property now is serviced by a 45,000-kw hydroelectric power system and a 30-in. gauge railroad consisting of 72 km of trackage carrying 1,800,000 ton-km of freight yearly. Both steam and diesel locomotives are in service, with a program in effect for complete conversion to diesel type on the main line.

There are 1600 men on the mine payroll. This includes all phases of underground operation: mechanical, electrical, tonnage control, contract and time card accounting, and engineering departments. The Braden Copper Co., a subsidiary of the Kennecott Copper Corp., has built and maintained a number of townsites for operations and is directly responsible for the welfare of the 16,900 persons inhabiting the various localities. It also claims the distinction of having treated over 200 million tons of ore, and it is one of the few billion-dollar mining camps in existence.

The orebody extends around the periphery of an extinct explosive vent in crescent-shaped masses, which are limited on the inside by the tuff contact where they are of higher grade. The upper limit is formed by the bottom of the oxidized zone which is from 50 to 100 m below the surface. At one time the lower limit was believed to be the contact with the primary zone, but in recent years more efficient mining methods and a somewhat higher than expected grade of the primary ore make it likely that it will be of commercial value.

The explosive eruption that formed the Braden vent fractured the andesite porphyry surrounding its periphery to a width of 100 to 600 m. After the crater was refilled, the mineralizing solutions deposited copper minerals in the fractures, and these again were the channels which aided the secondary enrichment. The main primary mineral is chalcopyrite, while the principal secondary mineral is chalcocite.

Mining Methods

Access to the mine is through the haulage adit 2.6 km in length, at which point are located two 500-m shafts. There are additional haulage drifts to the various ore chutes, all haulage drifts and adits being lined with concrete sets. The two 3-compartment shafts service production and sublevels. For men and materials there is also one auxiliary shaft servicing the production levels. Three inclines are in active operation, two for servicing the control sublevels and the third for removing contaminated air in connection with the mine ventilation.

Mining methods have changed greatly through the years, the first being the sorting and shipping of high grade ore, probably cuprite. This type of mining was practiced by the Spaniards. In the Fortuna mine, the original method was mining by shrinkage stopes and later a combination of shrinkage stopes followed by the caving of the intermediate pillars. When the present Teniente mine was put into production the method employed was the same as in the Fortuna mine. Subsequent mining

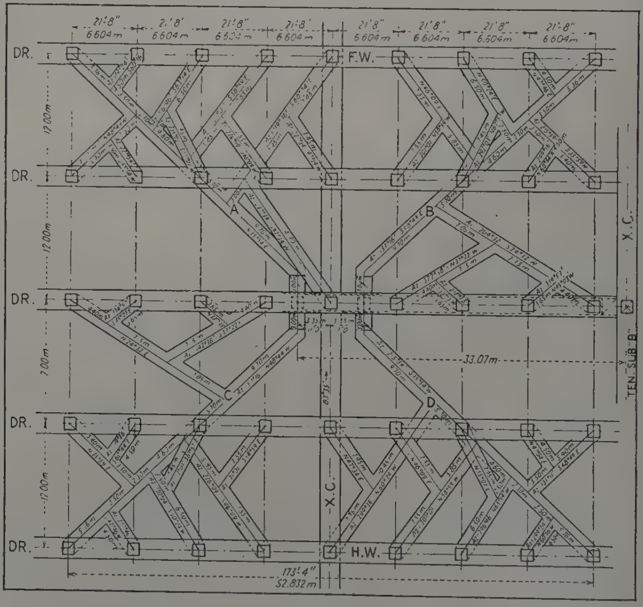

Fig. 2—Standard 45 Buitras ore pass system with ore passes independent, Braden Copper Co., Rancagua, Chile.

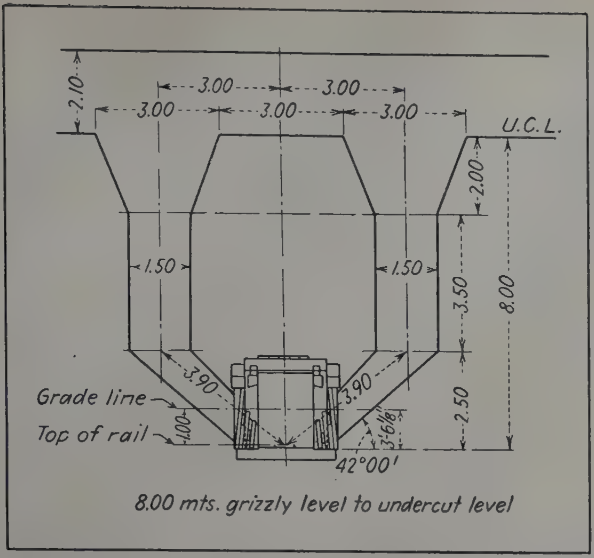

Fig. 3—Cross-section of finger raises in mining method used by Braden Copper Co., Rancagua, Chile.

practice developed the progressive block caving method in conjunction with shrinkage stope-pillar caving areas and eventually resulted in the progressive caving method directly on the drift timber.

At the present, progressive caving on an 8 or 9-m pillar is employed. The topography of the area is advantageous in that no hoisting of ore or pumping of water is required. Men and materials are transported on the haulage level and hoisted to the various sub and production levels. Ore is passed by gravity through a series of connected gathering raises to the haulage level, as illustrated in Fig. 1. Fragmentation of the ore in transfer to the haulage level by gravity is equivalent to a primary crushing operation.

Production Levels: At the present time four production levels are maintained to assure flexibility of operation. The drifts are driven center to center at 12 m with Ingersoll-Rand J-50 jackhammers mounted on a 3-in. col. and crossarm. Mucking is accomplished by Gardner-Denver 9 or Eimco 12-B mechanical shovels. The drifts are driven 6x7½ ft, and 10 to 12 holes are required, depending on the hardness of the ground. Miners are given two headings and drill and blast both headings in an 8-hr shift. They work on contract, and break about 3½ m per shift between the two headings. Since production levels are kept well in advance of caving operations, only one blast per day is required in each heading, which has proved to be a very economical procedure.

Before undercutting operations are started, drifts are timbered and grizzlies installed. Grizzlies are spaced 6.60 m center to center north and south along the production level drifts and 12 m center to center east and west. The gathering systems driven from the level 60 m below are stopped 2½ m under the production level floor, see Fig. 2. Each grizzly corresponds to the location of the branches of the gathering system beneath. A winze is sunk to connect with the gathering system. Experience has proved that if raises are driven from below and directly connected to the production level drift an unusually large opening results, and this is prevented by sinking the winze. All drifts are timbered with native lumber. Between draw points 8x8-in. sets are used, while 12x12-in. sets are placed at all draw points.

Undercutting: Undercutting blocks are laid out over an area, usually 60 m by 60 m, with a vertical lift of approximately 110 m. This is equivalent to about one million short tons of caved ore. The supporting undercut pillar is 8 m in thickness and is honeycombed by drawpoint chimneys on the undercut level floor, as shown in Fig. 3. Pillars on the undercut horizon are blocked out by drifts and crosscuts. Pillar drilling, see Fig. 4, is done with CF-89 Gardner-Denver drifters using 1¼-in. round steel with 4-ft changes up to 12 ft, and 5-L Liddicoat bits. Blasting is done with Gelamite No. 2, 40 pct powder, and Atlas Manasite No. 6 detonators and fuse. Undercut crews consist of six miners and three helpers and blast 162 sq m of undercut area daily.

In most sections of the Braden mine actual caving of the undercut rock does not begin until 36 m of width over the length of the block have been undercut. Rapid undercutting is therefore of utmost importance. Before caving is induced, the weight of the unsupported ground is transmitted to the areas adjoining the undercut area. If this weight is allowed to remain, the supporting pillar between the undercut floor and the production level will be crushed and destroyed and the weight supported by the production level timber, with subsequent high maintenance cost during operation. It has been found that two crews, each taking a slice 18 m in length on opposite sides of the entrance drift, can work safely and reduce by half the time needed for undercutting the first 36 m of width. This has now become the standard undercutting practice. When two undercutting crews are employed, an area of 60 m by 36 m can be undercut in 7 days and an initial cave obtained.

The moment caving has started, chutepullers begin the extraction of ore, drawing all undercut chutes with the exception of those in proximity of the undercutting crews. These chutes must remain closed to insure the safety of the men in the undercut. As the work progresses more draw points are opened for draw and every effort is made to induce a rapid cave. This eliminates the excess weight caused by arching and prevents damage to the pillar between the undercut and production levels.

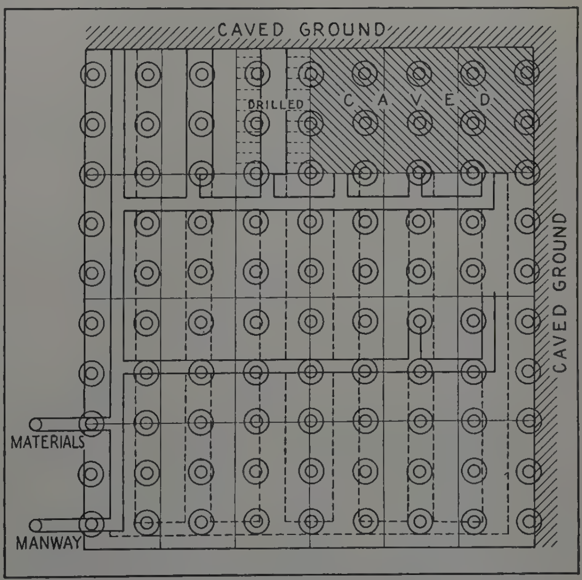

Fig. 4—Modified Braden mining method showing progress of development in widening and caving. Scale 1: 200.

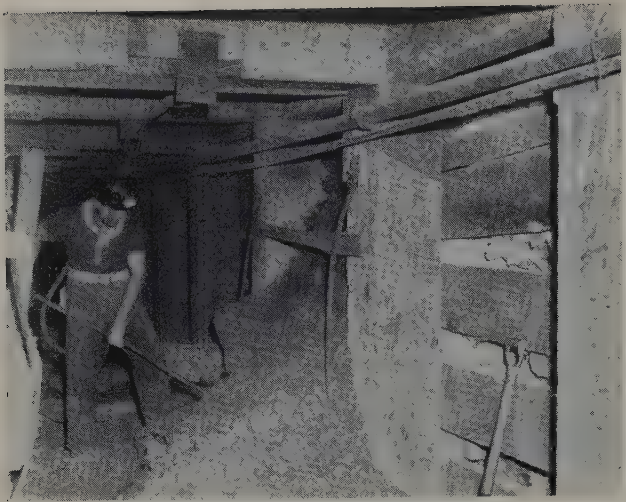

Fig. 5—Drawing of ore on production level.

Draw Control: The drawing of ore as shown in Fig. 5 begins when the undercutting over the production level has progressed to the point when caving starts. Drawing is done by chutepullers who are required to do any necessary secondary drilling and blasting. They also place charges when large boulders that hang up in the chimneys cannot be reached by 12-ft drill steel. These men work on contract and are paid an established price per ton of ore drawn.

Depending on the nature of the rock, the tonnages per chutepuller during an 8-hr shift may vary from 60 to 100 tons during the first 10 pct extraction. This figure increases to 400 tons at 35 pct extraction and goes as high as 2000 tons at 80 pct plus extraction, with an average of 700 tons per manshift for the life of the block.

The consumption of dynamite per ton of ore in secondary blasting decreases with increasing extraction. At 70 to 80 pct extraction it is normal practice to produce 13,000 to 15,000 tons per production level using only 10 to 15 lb of dynamite. Under these conditions a crew of four chutepullers per shift for each production level is required.

Draw control is of the utmost importance in block caving, and at Braden every care is taken in this direction. Draw charts (visual bar-graphs) for every drift are brought up to date twice weekly by the Tonnage Control Office. In addition to this, the mine foreman controls his daily extraction for the block. These two factors enable him to control the draw, bringing the block down evenly, and preventing the possibility of dilution.

All blocks are pulled so the side next to virgin ground reaches 35 pct extraction before the side next to the waste area. The first pair of chutes next to virgin ground side are closed at 35 pct extraction, the second pair closed at 47 pct, and the third pair at 60 pct. This procedure creates a barrier of 18 m in width, which prevents waste from being drawn in when the next block is undercut. These barriers are always maintained next to the virgin ground whether there are one or more sides.

Each gathering system collects the ore from an area 60x60 m. Within this area there are 45 grizzlies with two draw chimneys each, making a total of 90 draw points per gathering system. All main legs and branches in the gathering system are calibrated for volume on a tonnage basis. These systems are filled from the draw points on the production level by the chutepullers, under the direction of the mine foreman. The systems are then emptied, and this procedure is repeated until the desired tonnage is obtained.

Once the entire block is under draw, every effort is made to draw at a fast rate, about 3 tons per sq m of undercut area each 24 hr. One gathering system will produce about 10,000 tons per 24 hr.

It has been found that a fast undercut and a fast draw up to 35 pct extraction are the two factors which prevent arching and consequent pillar failure and give satisfactory fragmentation during the life of the block. Failure to do this not only results in increased timber maintenance, pulling in of waste suckers, and loss of copper extraction, but also lowers the overall tons per chutepuller shift. In the event of pillar failure and resultant timber failure on the grizzly level, a heavy draw is placed on the affected area to reduce the weight. Stulling, crossbracing, lining the sets, and placing intermediate false sets will usually keep draw points open for draw until it is desirable to replace the timber. Timber consumption is less than three-tenths of a board-ft per ton of ore drawn.

During the four winter months milling is somewhat curtailed by a shortage of water and power, but during a favorable year the total tonnage may exceed 10 million wet tons. Ore passes and gathering systems have a reserve capacity to supply the mill for 24 hr.

Ore Delivery: The electric haulage system consists of 4½ km of 30-in. gage underground trackage, see Figs. 6 and 7. Four ore trains are used in tandem, each train consisting of one 30-ton locomotive and twelve 25-ton ore cars. Enclosed passenger trains convey the shifts to and from Sewell, transporting 52,000 passengers per month, see Fig. 8. The railroad has a haulage capacity of 950,000 tons per month and has hauled as much as 36,000 tons during a 24-hr period.

Ore trains are loaded at the ore passes by manually operated arc gates. Under normal conditions a train of twelve 25-ton cars can be loaded in 3 min. All train movement is controlled by a dispatcher. A round trip from loading chute to mill ore bins requires about 45 min.

Safety

Intensive safety training of all personnel at Braden Copper Co. has been carried on through the years and has yielded excellent results. It is im-

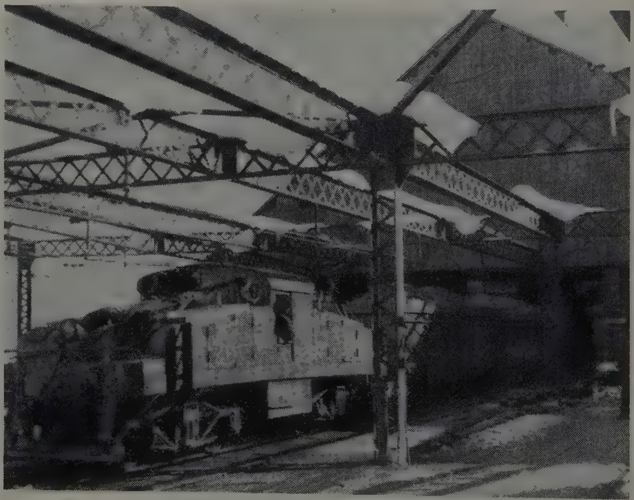

Fig. 6—Ore train entering mill ore bins.

possible to compare accident rates between mining operations unless the type of mining involved is considered. Table I illustrates the rates for different types of mining.

Table I. Accident Rates in the United States in 1947 and at Braden Copper Co., Chile, 1945 to 1947

Method of Mining	Rate Per Million Man-Hr Worked	
	Killed	Injured
Top slicing	0.45	20
Sublevel caving	0.63	25
Square set	1.28	133
Open stopes	1.36	80
Cut and fill	1.63	103
Shrinkage stopes	2.25	122
Block caving	2.73	143
Braden block caving for years 1945 to 1947	0.35	53.4

While Chileans are excellent workers, a large majority of the personnel has had little or no previous mining experience. Consequently the low accident rates indicate a successful accident prevention campaign. The mine department operated consecutively 27 months with 11,423,021 man-hr of exposure and a production of 17,421,600 tons of ore without a fatality. During four consecutive years, 1947-1950, Braden Copper Company has been awarded the Inter-American Safety Plaque for attaining the lowest frequency of accidents in its group classification in Latin American countries.

Mine Rescue Training: Twelve crews of selected men holding medical certificates of physical and mental fitness are trained at monthly intervals in the use of oxygen-breathing apparatus and other equipment, and approximately 150 men from all sections of the mine are trained annually in first aid.

Ventilation: For the purpose of maintaining dust counts within permissible limits, seven fans with capacities ranging from 175,000 to 50,000 cfm have been installed. In so far as possible the ventilation of each level is operated independently. A split system permits fresh-air supply to each of the major production areas. Each drift in the production levels is also provided with an independent and regulated fresh-air supply. A total of 86 ventilation control points has been established throughout the mine, where monthly surveys furnish a check of the ventilation system.

Dust Control: The mine is comparatively dry; consequently the tonnages dropped by gravity and the drilling and blasting of approximately 4000 shots per day present dust problems that are extremely difficult to combat. The results obtained at Braden in the suppression of dust can be attributed to the following measures: 1—Adequate ventilation for the removal of dust and gas from the various levels. 2—The installation of water foggers in all development headings and undercutting operations. 3—Wet drilling. 4—Blasting of undercuts and development work regulated to the end of the shift. 5—Wetting down before and during mucking operations and sprinkling down of all drifts where dust is present. 6—Provision of approved respirators to all men employed in dusty operations.

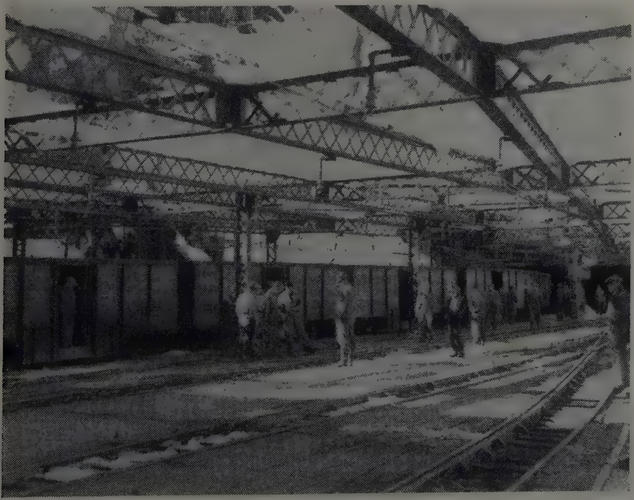
Fig. 7—Haulage level showing loaded ore train.

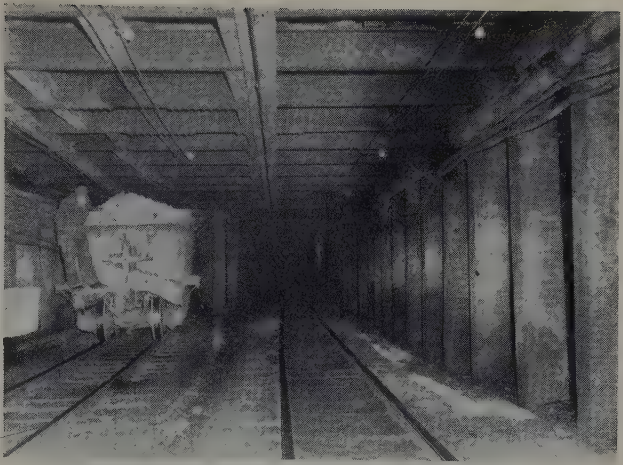
Fig. 8—Passenger train at portal of haulage level.

Fire Protection: In order to minimize the hazard of underground mine fires, the following precautions have been taken: 1—Complete fireproofing of all underground offices and shops. 2—Adequate fire-control equipment, such as water hydrants and portable fire extinguishers. 3—Metal containers with self-closing lids for the disposal of combustible material. 4—Underground oil storages and electrical distribution stations set in concrete vaults of raw-rock sections and isolated by means of steel doors set in concrete frames. 5—The use of Pyranol oil in all underground electrical transformers. 6—Provision for rapid isolation of the three shafts of the mine by means of fire doors on the various levels, provided with sprinkling systems that can be set in operation by the hoisting engineers.

In the event of an underground fire, a powerful siren installed at the portal of the mine warns all persons who may be off shift, as well as officials of various departments. A dual alarm system warns personnel within the mine: 1—Light flashing consists of an automatic device for flashing lights on all levels of the mine, giving first the international fire signal, which is followed by long flashes indicating the level where the fire has been reported. 2—The stench system introduces a stench fluid, ethyl mercaptan, into the discharge air line leading to the mine, equivalent to about 6 cu cm per 1000 cu ft of air in circulation.

Fire drills are held at regular intervals, two or three times yearly, using the three standard methods for notifying underground personnel, telephone, light-flashing and stench, these drills being carried out with complete evacuation of mine personnel. All escapeways leading from the mine are marked with directional signs, and fire-procedure plans have been prepared so that orderly evacuation drills are conducted in a routine manner.

Power Facilities at a Modern Anthracite Open-Pit Mine

by Frederick C. Pearson, Albert Brown, and Emil R. Ermert

EARLY in 1946 the Shen-Penn Production Co., a subsidiary of the Philadelphia and Reading Coal and Iron Co., was organized to operate the Shenandoah Stripping, one of the largest open-pit anthracite mines in the world. This mine is located in the Western Middle Field near Shenandoah, Schuylkill County, Pa., and involves the removal of approximately 60,400,000 cu yd of overburden to permit the recovery of 9,200,000 gross tons of rough cleaned coal from an area 8000 ft long and 2700 ft wide, with a maximum depth of 400 ft. Operations began in August 1946, and within the next few years 31,811,000 cu yd of overburden and 2,994,000 gross tons of rough cleaned coal had been removed.

During the early days of open-pit mining operations, steam was the primary motive power. However, as the size of the equipment increased, so did the problems of fuel, water, labor, and maintenance. Because of its efficiency and convenience, electric power rapidly replaced steam. Later the modern diesel engine was developed, and today practically all stripping equipment is either electric, diesel-electric, or diesel-powered.

In locations where electric power is not readily available or where operations are scattered over a large area, diesel power is favored. At Shenandoah operations are highly concentrated in a relatively small area, and this fact, coupled with the availability of ample electric energy, indicated the selection of electric-powered equipment.

Since this was a new company, it was necessary to purchase every item, from the smallest tools to stripping shovels. Although the organization period was hampered by the postwar scarcity of materials, an excellent opportunity was afforded to set up a thoroughly modern plant. This paper will describe the power facilities, with particular emphasis on the more unusual features.

The substation is a major item in a power distribution system, and a simple arrangement utilizing high quality equipment is an excellent investment. With this in mind, a 3000-kva unit type substation was selected and installed. This unit is made up of three sections, which are assembled simply by bolting together the various sections and connecting the power leads, see Fig. 1.

The transformer proper, rated at 3000 kva, is oil-filled and nitrogen-sealed, having a 66,000-v Delta primary and 4160-v Wye secondary with a grounded neutral and 46-ohm ground resistor. The function of this resistor will be described later.

Electrical energy is purchased from a public utility and is delivered to the main substation at 66,000 v over one or the other of two incoming lines. These lines terminate on a high voltage switching section on which high voltage fuses and Thyrite lightning arresters are installed.

The outgoing feeder switching unit is made up of the following:

1—An auxiliary compartment consisting of potential and current transformers with necessary terminal blocks for connecting to power company metering equipment.

2—Another auxiliary compartment containing a control transformer, battery, and battery charger for the furnishing of power for tripping and reclosing of power circuit breakers. The assemblies in these auxiliary compartments are mounted on carriages that can be rolled in and out with ease. Potential transformers are readily accessible for inspection and fuse replacement. When withdrawn from the operating position they are completely de-energized and grounded.

3—Two feeder breaker compartments, each with a 1200-amp, 5000-v, solenoid-operated magneblast air circuit breaker, voltmeter, ammeter, overcurrent relays, and a ground relay. These power circuit breakers can be quickly and safely withdrawn or repaired. A built-in isolating mechanism is used for lowering the breaker to a transfer truck for repair or inspection or as a means of disconnecting the breaker from the source of power as an added precaution when working on power lines. Thus inspec-

---

F. C. PEARSON, Member AIME, Electrical Superintendent, and E. R. ERMERT, Member AIME, Chief Engineer, are with Shen-Penn Production Co., Shenandoah, Pa. ALBERT BROWN, who died April 8, 1952, was Electrical Engineer, Philadelphia and Reading Coal and Iron Co., Philadelphia.

Discussion on this paper, TP 3268F, may be sent (2 copies) to AIME before July 31, 1952. Manuscript, Nov. 26, 1951. New York Meeting, February 1952.

tion and maintenance on this type of equipment are greatly simplified.

There are two methods of supplying electric power to stripping equipment, one being the use of portable cable from the primary substation to the driven machine and the other, of course, a combination of overhead line from substation to a central point and portable cable beyond. Each method has its advantages and disadvantages.

The cost of a pole line is approximately 50 pct that of a portable cable of the same length and capacity, but unless the pole line can be placed originally in a position from which the work may be completed either without disturbing the line or by retreating the line as the work advances, it will be necessary to provide sufficient material to construct a second line while the first is still in use. Otherwise a shutdown will be necessary while the line is being relocated, and under these circumstances the cost advantage will be heavily in favor of the cable. The relative security of an overhead line from mechanical damage must be considered as well as its vulnerability to storm damage, particularly ice and wind.

Formerly the use of portable cable was curtailed because of the difficulty encountered in locating faults. However, with the advent of modern cable fault-detecting apparatus this disadvantage has been virtually eliminated.

At the project under discussion it was decided after careful planning to use the combination power transmission system. Power is transmitted from the main substation to various strategically located points about the operation through two overhead pole lines. The line serving the eastern pit consists of one 4160-v circuit 2500 ft long, while the line serving the western pit is 4100 ft long and consists of a two-circuit line of 1540 ft and a one-circuit line of 2560 ft.

Class 4, 35-ft, treated Southern yellow pine poles were used, occasionally as long as 60 ft where necessary to provide clearance for railroads, highways, and shovel crossings. A spacing of 100 ft between poles was decided upon to facilitate work during periods of ice loading and windstorms. Despite exceptionally severe storms in the past 2 years, there have been no shutdowns due to power failure on the lines.

Crossarms, made of fir, are 5 ft 7 in. long except where two circuits are carried on one pole, in which event the crossarms are 8 ft long. All crossarms, insulators, guy wires, and hardware were installed while the poles were on the ground, in most cases making it necessary for a lineman to climb the poles only twice, once when the wires were installed and again when they were sagged in.

All conductors are of seven-strand, 4-0 hard-drawn, bare copper wire, three for phase wires in each circuit and one grounded neutral for the ground protective system.

Bulldozers were used to clear the right of way for the pole lines so that all materials could be trucked to the place of installation. Wherever possible, pole holes were drilled by a 9-in. churn drill. In one shift of 7 hr a crew of two men on such a machine can drill from fifteen to twenty 5-ft holes.

It was planned that both these pole lines would serve for the greater part of the life of the operation and as they conflicted with the work in the final stages would be retreated toward the substation. At various points along the lines disconnecting switches were mounted on the poles to provide convenient taps for shovel switch houses and drill transformer stations.

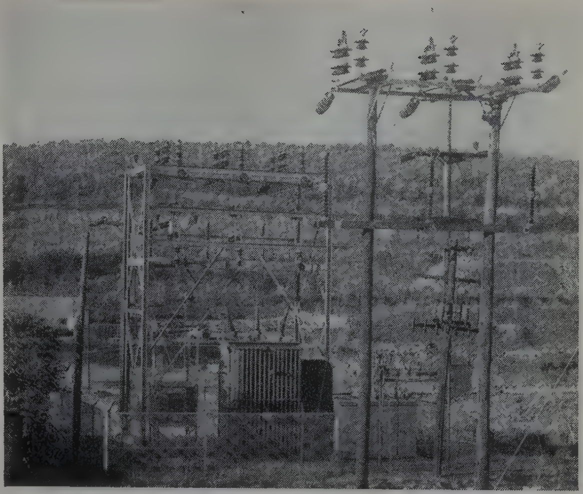

Fig. 1—A 3000-kva 66,000-4160-v unit type main substation.

Although several types of flexible cable are used to transmit electric power, the one considered best from all viewpoints is the SHD, three-conductor, 5000-v cable. No. 4 is standard for all shovels, while No. 4-0 is used for trunk transmission lines. Cable is laid in convenient places throughout the operation and behind each shovel is carried from the edge to the center of the cut on standards to permit the customary two-side loading of trucks. Each standard consists of an L-beam base supporting a socket made of a section of 8-in. steel pipe. Into this socket is inserted the butt of a 30-ft pole carrying a block for rope attached to cable hanger. Smaller all-metal standards are used to carry cables over roadways in areas being drilled.

The basic cable construction consists of three rubber-insulated power wires, with a wrapped or braided sheath of tinned copper wires around the insulation of each power wire. The ground wires are laid in the valleys between the triangularly spaced power wires. A heavy reinforced outer jacket of neoprene completes the assembly. The purpose of the sheathing over the insulation of the phase conductors is to reduce the voltage stresses in the cable, to give protection to workmen should a fault occur while the cable is being handled, and to eliminate

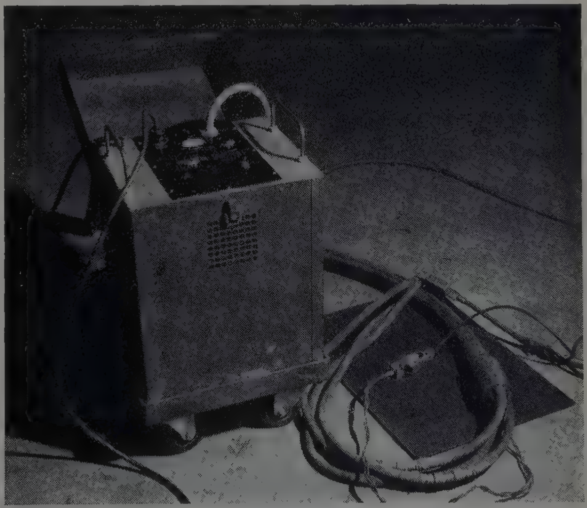

Fig. 2—Cable fault locator in operation.

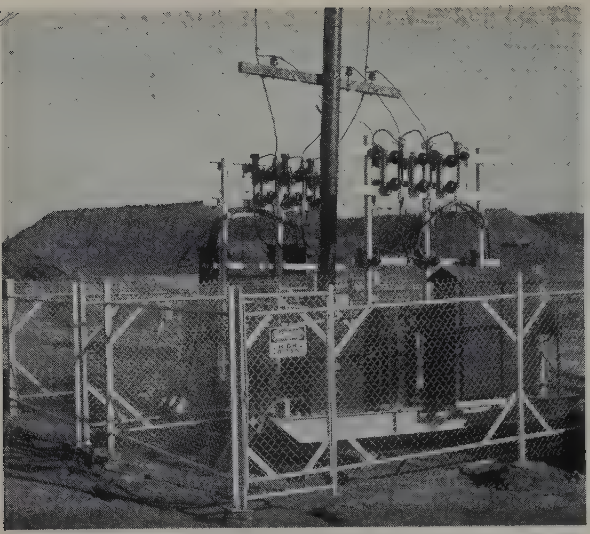

Fig. 3—Installation of two 150-kva 4160-480-v drill substations.

corona and the accompanying formation of ozone, which is injurious to rubber.

The ground wire in contact with the sheath has a total cross-sectional area equivalent to that of the power wires. Potheads, from which phase and ground wires extend about 30 in., are vulcanized on each end of the cable. Originally it was the practice to place stress cones on each conductor and to braid ground wires and sheaths together inside the potheads, but corona cutting of conductors operating the ground protective system resulted in delays, and later it was found necessary to extend the stress cones and sheaths outside the potheads.

On the drills type G 600-v cable is used, No. 4 size on single machines fed to a central point by a 2-0 cable. This cable is of construction similar to type SHD, but without sheathing.

Inasmuch as ground fault currents are limited by the ground fault resistor, ground faults frequently do not become visibly evident, and since a cable lying on the ground is subjected to a variety of hazards during a highly mechanized stripping operation, it is vitally necessary to test cables regularly so that the incipient faults can be located and corrected before probable shutdowns.

Soon after the commencement of work at this operation, information was received concerning a 10,000-v testing machine recently developed, and following consultation with the manufacturer a 15,000-v unit was designed for the work in progress. This proved very successful, and later two additional models were purchased. The cable tester locates faults in the insulation of electrical conductors and determines its condition by subjecting it to instantaneous high dc voltage. It is an impulse or surge device producing at intervals of 1 to 3 sec a loud cracking noise, much like a pistol shot, at the location of the fault. The basic component of this fault locator is a capacitor bank consisting of two 15-kv, 1-mfd capacitors. They are charged by means of a plate transformer and a rectifier tube. Two resistors are used to control the rate of charge to the capacitor bank, one allowing it to charge from 0 to 12 kv in 3 sec and the other from 0 to 7 kv in 30 sec. A 15-kv meter is included to indicate the voltage charge in the capacitor bank, see Fig. 2.

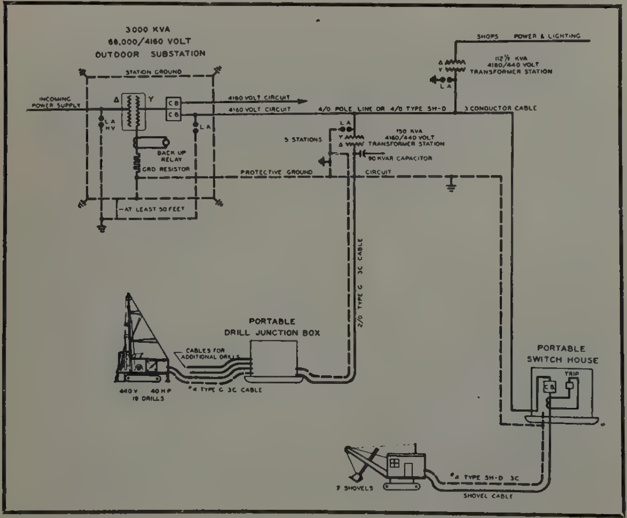

Fig. 4—Line diagram of power distribution system.

The output of the capacitor bank is connected to a fixed sphere, adjacent to which is a movable sphere that can be spaced from 0 to ¼ in. A third sphere is connected to ground and sheath at the output cable. The output cable is connected by Mueller clips to the cable to be tested. The sphere gap is adjusted so that the capacitor bank will discharge at about 2-sec intervals unless conditions dictate faster or slower firing time. If during the location of the fault the sound is not loud enough to be readily heard, opening the sphere gap will increase the intensity. This will also decrease the firing time interval. A thin blue spark at the sphere gap at intervals of several seconds indicates a good cable. To locate the fault in a defective cable, it is necessary only to locate the noise, no other instruments or calculations of any kind being required.

The 9-in. blasthole drills are usually operated in groups of from four to six machines, which are furnished with power at 480 v from a bank of 3-50-kva, 2300-v Wye-Delta connected transformers. These transformers are mounted on steel skids designed and built in the company shop. Included are two sets of disconnecting switches for power takeoffs for shovels, lightning arrestors, and cutouts for transformer protection. A bank of 90-kvar capacitors and a type AK1-15, 600-v, 225-amp, 15-kva interrupting capacity air circuit breaker are mounted in weatherproof steel enclosures.

Each station is enclosed by a steel mesh fence made up of six interchangeable sections each 10 ft long and 6 ft high, one section including a gate. The fence is bolted together by 36½-in. bolts and can be taken down or assembled in about 1 hr, see Fig. 3.

The subject of grounding has been receiving more and more attention. Electric shovels and machines of a similar nature are not located on permanent foundations and are usually supplied with electric energy at 2200 v or more, delivered to the machinery by a flexible trailing cable. When electric power first came into use for movable equipment, the portable cables developed had only three conductors. No provisions for ground connections were made since it was presumed that the machine would be well grounded because of the large area of contact of its tread on the ground. The fallacy of this assumption soon became apparent. Indeed, where the machine is resting on a rocky surface, the ground resistance may be so high as to practically insulate the machine from the ground. It is obvious that the occurrence of ground faults either on equipment or cables represents a serious threat to the safety of personnel unless suitable protection is provided. An electric current as small as 1/6 amp flowing for 1 sec can cause fatal injury, and an even smaller amount can cause loss of muscular control. These low currents can flow through the body at voltages as low as 100 if the skin is moist. Provisions must be made so that upon the occurrence of a ground, the ground fault current will be limited to a safe value and the faulty piece of equipment disconnected from the line as quickly as possible.

With ungrounded circuits, a ground fault on one-phase wire places the faulted conductor at ground potential. There is no interruption in the service, and the system may operate indefinitely with the existence of a single ground fault undiscovered. A second ground fault on another phase wire produces a short circuit, and a heavy fault current will flow, the amount depending upon the overall impedance of the circuit. If at the time of these faults a man standing on the ground should touch any part of a machine on the line, he would receive a severe or fatal shock.

The Impedance Grounded System is used by this company and is believed to be the most practical and positive system yet devised for protection against such hazards. Connections of the lowest practical impedance are provided between machine frame and ground, limiting the ground fault current to such a value that the voltage rise of the machine frame above ground potential will not exceed a voltage ordinarily considered safe for workers. Thus the fault circuit is disconnected as quickly as possible, see Fig. 4.

The frames of all shovels, switch houses, junction boxes, and portable transformer stations are connected by a ground wire to the substation and to driven grounds at intervals along the lines. All ground conductors have the same current carrying capacity as the phase conductors. This ground circuit resistance comes well within the 2-ohm limit considered a reliable value and assures adequate safety even if the ground resistance of these other paths is high.

A 50-amp, 46-ohm resistor and a current transformer are connected between the transformer neutral and the substation ground. The ground resistor limits the fault current to a safe value. The current transformer is connected to a relay arranged to trip the main feeder breaker with a short time delay. This is known as a back-up relay and operates only in the event that the relays in the portable switch houses to which each shovel is connected fail to operate. For example, disregarding reactance, if a fault should occur at the distant end of 3000 ft of 4-0 overhead line with a resistance of 0.0499 ohms per 1000 ft and 2000 ft of No. 4 cable with a resistance of 0.310 ohms per 1000 ft, giving a total resistance of 1.54 ohms, the voltage of the shovel frame above ground would be 77 v, a value well below the voltage considered dangerous.

In a small operation where only one shovel is supplied from the main substation, protective equipment at the substation is generally sufficient. However, on a multishovel operation, protection against dangerous voltages at shovel frames is lost if a second ground fault occurs at another machine before the first fault is cleared.

As ordinarily used, shovel cables are subject to rough use and so are liable to mechanical damage and insulation failure. Therefore the logical place to install protective devices capable of interrupting short circuits is at the point where the cables are connected to the relatively permanent feeder line.

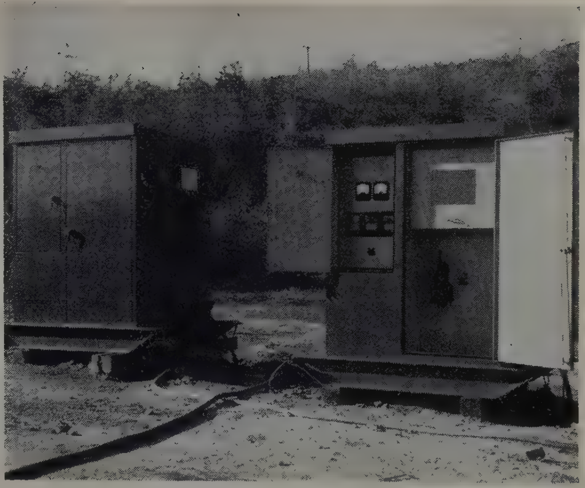

Fig. 5—Skid-mounted shovel switch houses.

Switch gear and protective equipment for this purpose are carried in skid-mounted portable switch houses. The switch house is completely waterproof and is fitted with doors for access to the various compartments. The high voltage compartments are secured against entry by unauthorized persons. Inside are grouped disconnects, oil circuit breaker, ammeter, voltmeter, and necessary overcurrent and ground protective relays, see Fig. 5.

The protective scheme of the switch house differs somewhat from that used at the main substation. Should two lines to ground faults exist simultaneously on different phases at different locations, current of line to line short circuit magnitude will flow in the protective ground circuit between the two fault locations. This current is not limited by the neutral ground resistors and could produce unsafe voltages on the ground circuit. To avoid this possibility, it is necessary to depend on metering the unbalanced current in the three phases caused by the ground fault. This insures that in case of trouble on a given feeder, the actual feeder breaker involved will be tripped rather than some other feeder, as would be the case if there were a current transformer on the ground wire itself at the various switch houses. It is probable that the safety grounding of the secondary 480-v circuits will come into general practice in the future and will be accomplished in the same manner as that described above for the 4160-v circuits.

In the case of the 480-v circuits it is almost invariably necessary to deal with transformers that are delta-connected on the secondary, so that a zigzag grounding transformer must be used to establish the neutral point. In addition, since no high voltages are involved and voltages need not be limited to ground to such a low percentage of the line voltage, a smaller maximum ground current may be used. Instead of the 50 amp usually used as the limit for ground current on the 2300 and 4160-v circuits, only 5 or 10 amp are used. This reduces the size of the grounding transformer and the grounding resistor while still insuring reliable tripping and sufficient protection.

Plans are now being prepared for placing all the 9-in. churn drills, operating in groups of four to six machines, under this ground protective system. To insure efficiency, all equipment and cables are inspected regularly. The insulation of all cables and the continuity of ground conductors are tested once every 2 months. The resistance of substation grounds is tested annually by the public utility, while the overcurrent and ground protective relays are tested semiannually. It is important that the ground protective equipment for each shovel be checked by applying intentional grounds at the time the cables are tested. Too much emphasis cannot be placed on this testing.

When cables are tested and found defective, they are repaired and vulcanized in the field. It usually requires 2½ hr to make a splice and about the same time for vulcanizing. If the damage occurs during working time, a temporary repair may be made to the conductors and the cable enclosed in a steel junction box 8 in. wide x 8 in. high x 36 in. long, skid-mounted. The cable is anchored by clamps and grounds are properly connected. This usually requires about ½ hr from the time the defective spot is found. If several repairs are to be made, the vulcanizing may safely be done later with the power in the cable.

When the shifting of shovels permits cables to be removed, they are taken to the repair shop to be inspected for cuts and bruises. The 5000-v cables are subjected to a 15,000-v test and the 600-v cables to a 5000-v test. Upon completion of any necessary repairs, the cables are placed on reels ready for use. Needless to say, with this systematic repair and maintenance program, shutdown time due to cable failure has been negligible.

Two cable vulcanizers are used, one being a small direct heat type that takes cords and cables up to ¾ in. in diam and the other a steam type that accommodates cables up to 4 in. in diam. Both are electrically heated, with automatic temperature controls, and are simple to operate.

Two types of compounds are in use for vulcanizing cables. One is the insulating compound in rolls both vulcanized and unvulcanized, while the other is the black outside jacket compound, which assumes the mould form when vulcanized.

The large 5 kw 440-v vulcanizer, which weighs about 365 lb, is mounted on a steel stand equipped with casters so that it may be readily moved about the shop. Underneath is mounted a 5 kw 110-220-v gas engine driven power plant and a 5 kw 440-110-220-v transformer. When used in the shop, the unit is connected directly to the 440-v building circuit and when used in the field is entirely self-contained. Auxiliary outlets are provided for connecting soldering irons, buffers, and heat lamps, see Figs. 6 and 7.

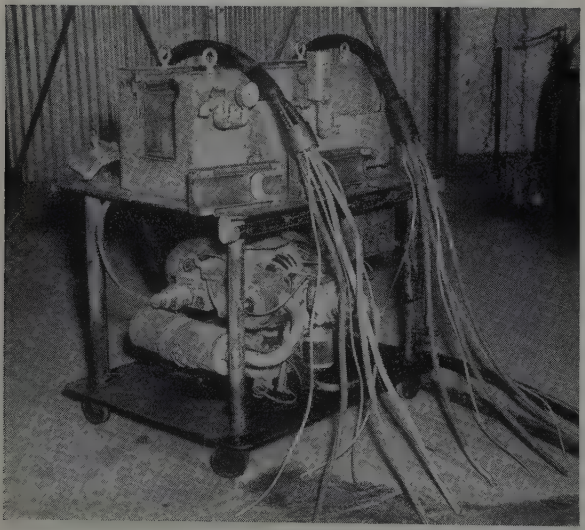
Fig. 6—A 5 KW 440-v cable vulcanizer. Type G cable at left prepared for pothead with a completed pothead at right. Self-contained power supply mounted beneath.

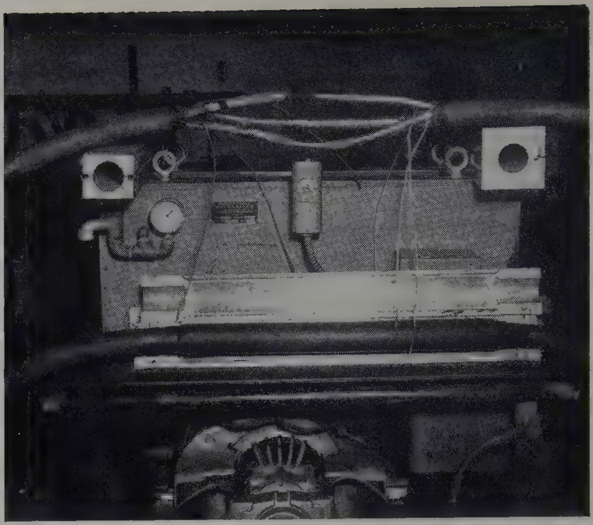
Fig. 7—Upper cable, type SHD: Lower conductor spliced with sleeve, upper conductor with insulation, center conductor complete with sheathing. Lower cable: Completed splice with moulds.

Fittings are arranged so that the entire unit may be attached to one of the pole line trucks for rapid and easy transportation to the scene of any trouble. Telescoping brackets are also mounted on the truck, over which a canvas covering is fastened for cable repairs in stormy weather.

Accurate logs are maintained covering electric motors, generators, and other major electrical apparatus on all the equipment. Reference to these logs gives an indication of the internal condition of the apparatus so that upon the occurrence of idle time through breakdown or other causes an excellent opportunity is afforded to examine and possibly overhaul items which may soon give trouble. This policy has often uncovered developing faults which can be economically and quickly repaired if detected at an early stage.

All the electrical work is carried on from a modern electric shop. This is an insulated, 32x56-ft steel building with a concrete floor. Ample facilities and equipment are included to handle all types of electrical repair work, and storage space is alloted for pole line trucks.

The total connected load at Shenandoah Stripping is 3629 hp. The average 15-min demand at the main substation is at present 1640 kw at 80 pct power factor. Since none of the equipment in operation is synchronous motor driven, power factor conditions were not of the best. The churn drills, driven by 40-hp induction motors, are normally about 50 pct loaded when drilling, and to compensate for the effect of this type of load on the power factor, 90-kvar, 440-v, outdoor-enclosed, three-phase capacitors were installed on each of the five 150-kva, 4160-480-v transformer banks supplying the power to the drills operating from four to six per bank. This improved the power factor from 67 pct to the present 80 pct. Further improvement is contemplated for the immediate future by the installation of 2400-v capacitors on the overhead lines supplying power to the shovels.

Geology of the Silver-Lead-Zinc Deposits of The Avalos-Providencia District of Mexico

by W. H. Triplett

Silver-lead-zinc replacement deposits occur in limestones of the anticlinal Caja range at Providencia, near Avalos, Zacatecas, Mexico. The description deals with intrusives, outcrops, preferred horizons, changes from bedding to fracture, control in depth, and variations in abundance and ratios of minerals throughout a vertical range of 500 m.

THE purpose of this paper is to record a few field observations and accumulated office data concerning outcrops, relation of ore occurrences to intrusive and host rock, and mineral zoning. Reasons for some of the phenomena are not clear to the author so the facts are given with the hope that other investigators may be able to furnish the explanations.

The Avalos unit of the Compania Minera de Penoles, S. A., operates the Alicanté, Bonanza, Providencia, Albarradon, San Eligio, Nazareno, Leona, Salaverna, and Santiago mines situated between Avalos railroad station and Concepcion del Oro on the Coahuila and Zacatecas railroad in the State of Zacatecas, Mexico. Some of these mines are within Penoles property while others are on mining claims leased from the Compania Nazareno y Catasillas, S. A., Mazapil Copper Co., and the American Smelting and Refining Co. The main office and camp are at Providencia, about 170 km southwest of Monterrey, N. L., so the silver-lead-zinc mines of the district are usually referred to as the Providencia mines.

The Aranzazu, Catarroyo, and Cabrestante copper-gold mines are situated a few kilometers to the southeast on the same mountain range near Concepcion del Oro, the name by which the camp is known. It is operated by the Mazapil Copper Co.

The main theme in the following pages is a description of the silver-lead-zinc ore occurrences of the district.

Rock Formations

Sedimentary Rocks: Many competent geologists have contributed generously to an ample fund of information concerning the sedimentary columns of northern Mexico. Among them are Carlos Burckhardt, E. Böse, L. B. Kellum, and R. W. Imlay. Carlos Burckhardt, who covered a number of extensive areas in many parts of the Mexican Republic, devoted years to mapping the geology of the Caja, Zuloaga, and Santa Rosa mountain ranges around Mazapil, Concepcion del Oro, and San Pedro de Ocampo, Zacatecas. He did most of the original mapping which has been used as a basis and amplified by others. C. E. Burbridge and, more recently, John

---

W. H. TRIPLETT, Member AIME, is with the Compania Minera de Penoles, S. A., Monterrey, Mex.

Discussion on this paper, TP 3304B, may be sent (2 copies) to AIME before July 31, 1952. Manuscript, Oct. 3, 1951. Mexico City Meeting, Oct. 29, 1951.

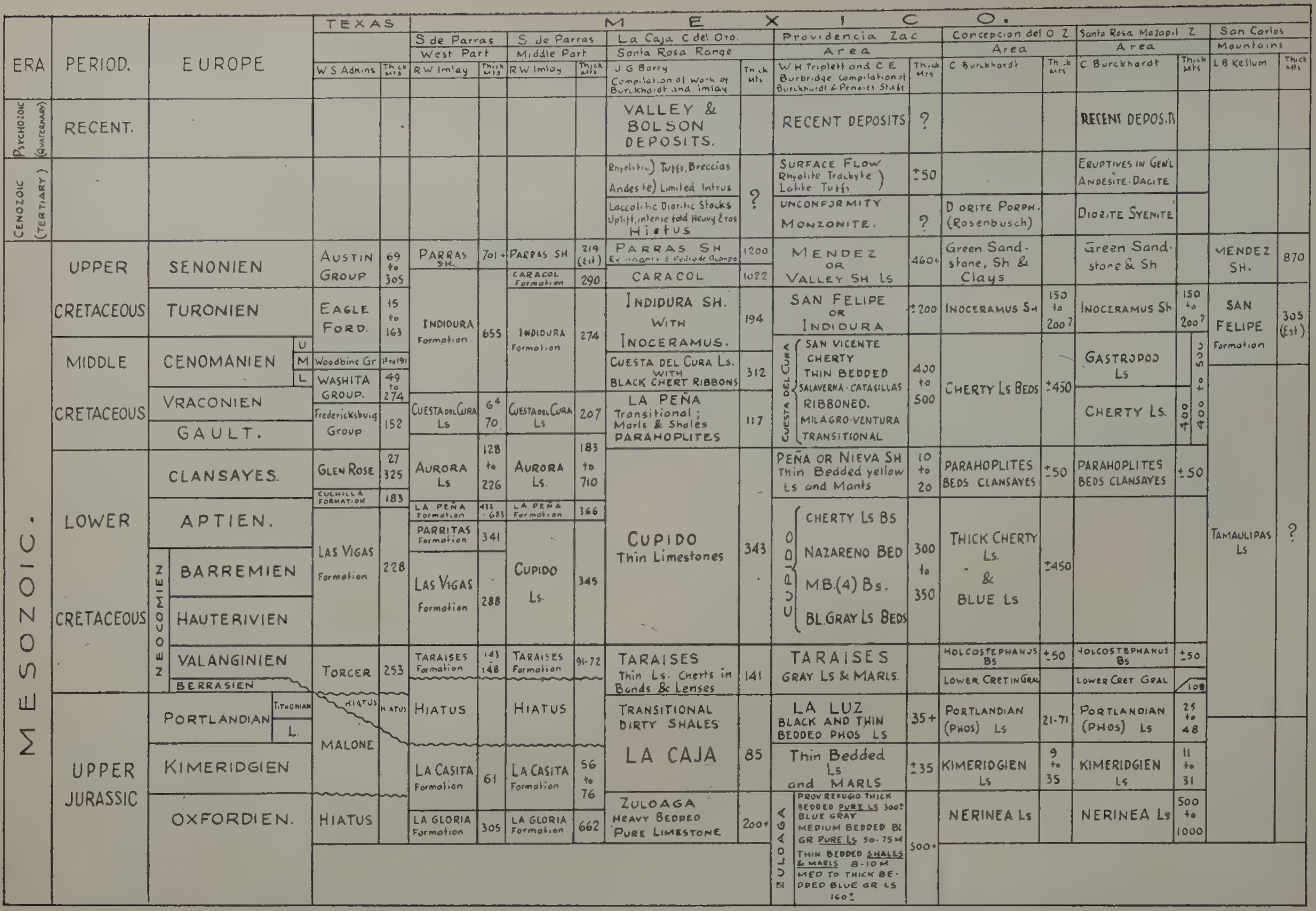
M E X I C O.
ERA
PERIOD.
EUROPE
TEXAS
W S Adkins
Thick Mts
S de Parras
West Part
R W Imlay
Thick Mts
S de Parras
Middle Part
R W Imlay
Thick Mts
La Caja C del Oro.
Santa Rosa Range
J G Barry
Compilation of Work of Burckhardt and Imlay
Thick Mts
Providencia Zac
Area
W H Triplett and C E Burbridge compilation of Burckhardt & Penoles Staff
Thick Mts
Concepcion del O Z
Area
C Burckhardt
Thick Mts
Santa Rosa Mazapil Z
Area
C Burckhardt
Thick Mts
San Carlos
Mountains
L B Kellum
Thick Mts
PSYCHOZOIC (QUATERNARY)
RECENT.
VALLEY & BOLSON DEPOSITS.
RECENT DEPOSITS
?
RECENT DEPOSITS
CENOZOIC (TERTIARY)
Rhyolitic) Tuffs, Breccias
Andesite) Limited Intrus
Laccolithic Dioritic Stocks
Uplift, intense fold Heavy Eros
Hiatus
?
SURFACE FLOW
Rhyolite Trachyte
Latite Tuffs
±50
UNCONFORMITY
MONZONITE.
?
DIORITE PORPH.
(Rosenbusch)
ERUPTIVES IN GEN'L
ANDESITE-DACITE
DIORITE SYENITE
MESOZOIC.
UPPER
CRETACEOUS
SENONIEN
AUSTIN GROUP
69 to 305
PARRAS SH.
701+
PARRAS SH
219 (Est)
PARRAS SH
Remnants S Pedro de Ocampo
1200
MENDEZ OR VALLEY SH LS
460+
Green Sandstone, Sh & Clays
Green Sandstone & Sh
MENDEZ SH.
870
CARACOL Formation
290
CARACOL
1022
TURONIEN
EAGLE FORD.
15 to 163
INDIDURA Formation
655
INDIDURA Formation
274
INDIDURA SH. WITH INOCERAMUS.
194
SAN FELIPE OR INDIDURA
±200
INOCERAMUS SH
150 to 200?
INOCERAMUS SH
150 to 200?
SAN FELIPE Formation
305 (Est)
MIDDLE
CRETACEOUS
CENOMANIEN
U
M
L
Woodbine Gr
13 to 191
WASHITA GROUP.
49 to 274
CUESTA DEL CURA LS. WITH BLACK CHERT RIBBONS
312
CUESTA DEL CURA
SAN VICENTE
CHERTY
THIN BEDDED
SALAVERNA-CATASILLAS
RIBBONED.
MILAGRO-VENTURA
TRANSITIONAL
400 to 500
CHERTY LS BEDS
±450
GASTROPOD LS
CHERTY LS.
400
400 to 500
VRACONIEN
GAULT.
Fredericksburg Group
152
CUESTA DEL CURA LS
64 70
CUESTA DEL CURA LS
207
LA PEÑA Transitional; Marls & Shales PARAHOPLITES
117
LOWER
CRETACEOUS
CLANSAYES.
GLEN ROSE
27 325
AURORA LS
128 to 226
AURORA LS.
183 to 710
PEÑA OR NIEVA SH Thin Bedded yellow Ls and Marls
10 to 20
PARAHOPLITES BEDS CLANSAYES
±50
PARAHOPLITES BEDS CLANSAYES
±50
CUCHILLA FORMATION
183
LA PEÑA Formation
433-683
LA PEÑA Formation
366
APTIEN.
LAS VIGAS Formation
228
PARRITAS Formation
341
CUPIDO Thin Limestones
343
CUPIDO
CHERTY LS BS
NAZARENO BED
M.B.(4) Bs.
BL. GRAY LS BEDS
300 to 350
THICK CHERTY LS. & BLUE LS
±450
TAMAULIPAS LS
?
NEOCOMIEN
BARREMIEN
HAUTERIVIEN
LAS VIGAS Formation
288
CUPIDO LS.
345
VALANGINIEN
BERRASIEN
TORCER
253
TARAISES Formation
143 148
TARAISES Formation
91-72
TARAISES Thin Ls. Cherts in Bands & Lenses
141
TARAISES GRAY LS & MARLS.
HOLCOSTEPHANUS Bs
±50
HOLCOSTEPHANUS Bs
±50
LOWER CRET IN GRAL
LOWER CRET GRAL
108
UPPER
JURASSIC
PORTLANDIAN
TITHONIAN
L.
HIATUS
HIATUS
MALONE
HIATUS
HIATUS
TRANSITIONAL DIRTY SHALES
LA CAJA
85
LA LUZ BLACK AND THIN BEDDED PHOS LS
35+
PORTLANDIAN (PHOS) LS
21-71
PORTLANDIAN (PHOS) LS
25 to 48
KIMERIDGIEN
LA CASITA Formation
61
LA CASITA Formation
56 to 76
Thin Bedded Ls and MARLS
±35
KIMERIDGIEN LS
9 to 35
KIMERIDGIEN LS
11 to 31
OXFORDIEN.
HIATUS
LA GLORIA Formation
305
LA GLORIA Formation
662
ZULOAGA HEAVY BEDDED PURE LIMESTONE
200+
ZULOAGA
PROV REFUGIO THICK BEDDED PURE LS 300±
BLUE GRAY MEDIUM BEDDED BL GR PURE LS 50-75 M
THIN BEDDED SHALES & MARLS 8-10 M
MED TO THICK BEDDED BLUE GR LS 160±
500+
NERINEA LS
NERINEA LS
500 to 1000

Fig. 1—Correlation of sedimentary formations of the Providencia, Concepcion del Oro, Santa Rosa, Mazapil, Aranzazu, and San Eligio Areas, Zacatecas, Mexico, with those of other Texan and Mexican areas.

G. Barry, compiled the data in the accompanying correlations of sedimentary strata, see Fig. 1.

Jurassic: Ore deposits of this district have occurred more abundantly in the Nerinea limestone of the Upper Jurassic than in any other formation. It is a moot question whether this abundance of mineral is due to the inherent physical and chemical qualities of the limestone or to its nearly uniform confined position between a large intrusive stock and overlying hornstones. The Nerinea limestone is very nearly pure calcium carbonate, light blue-gray in color, medium-bedded (0.5 to 1.0 m) and usually crystalline white near the intrusive. Here the bedding can be recognized only by stylolites. The thin-bedded overlying Kimeridgean hornstone, originally shaly limestone, and the dark-colored Portlandian limy phosphatic shale formation, each of which is 30 to 40 m thick, constitute a tight hanging wall for nearly all the San Eligio, Albarradon, and Providencia orebodies, see Figs. 2 and 3. There is almost no ore at all in the Kimeridgean and Portlandian even close to the channels of mineralization, in contrast with the abundance in the Nerinean limestone. Whether the marls and shales were less amenable to replacements than the pure limestone or acted as a retarding barrier to the circulation of mineralizers, or whether the selective action was due to both, or to some other influence, is a matter of opinion.

Lower Cretaceous: The Taraises limestone is yellowish gray to gray in color, stratified in beds usually 15 to 50 cm in thickness. It contains some impurities such as a little clay and occasional cherts. The San Marcos ore chimneys occur in this formation. The overlying Cupido limestone, blue-gray in color, is a purer limestone, with the exception of occasional beds of chert. The beds are usually 20 to 60 cm in thickness. The large Animas ore chimneys follow the steeply inclined bedding near the middle of this formation. Some smaller orebodies occur near the top of the Cupido under the Pena limy shales. The total thickness of the Taraises and the Cupido is about 450 m. These constitute the second and third important ore horizons.

The fourth important ore horizon is the upper part of the middle Cretaceous, the thin-bedded Cuesta del Cura or Cenomanian limestone. The strata are bluish gray to yellowish in color, 10 to 30 cm thick, consistently wavy with abundant black cherts. The Santiago, Salaverna, and San Vicente orebodies all occur near the top of these wavy limestones, just beneath the Indidura (Turonian) limy shales.

Upper Cretaceous: The Indidura or San Felipe formation, the lowest member of the Upper Cretaceous, consists of alternating thin beds of limestone, marl, and shale that break up into smooth flagstones in contrast to the wavy Cuesta del Cura cherty

Table I. Typical Specimen of Quartz Monzonite Taken Away from Limestone Contact on Level 5

Essential Minerals, Pct		Accessory, Pct		Alteration Products	Introduced Minerals
Plag.-Andesine Orthoclose Quartz Pale Hornblende	40 30 15 5	Biotite Magnetite Apatite	4	Chlorite Sericite Epidote Leucoxene Titanite and Rutile	Pyrite

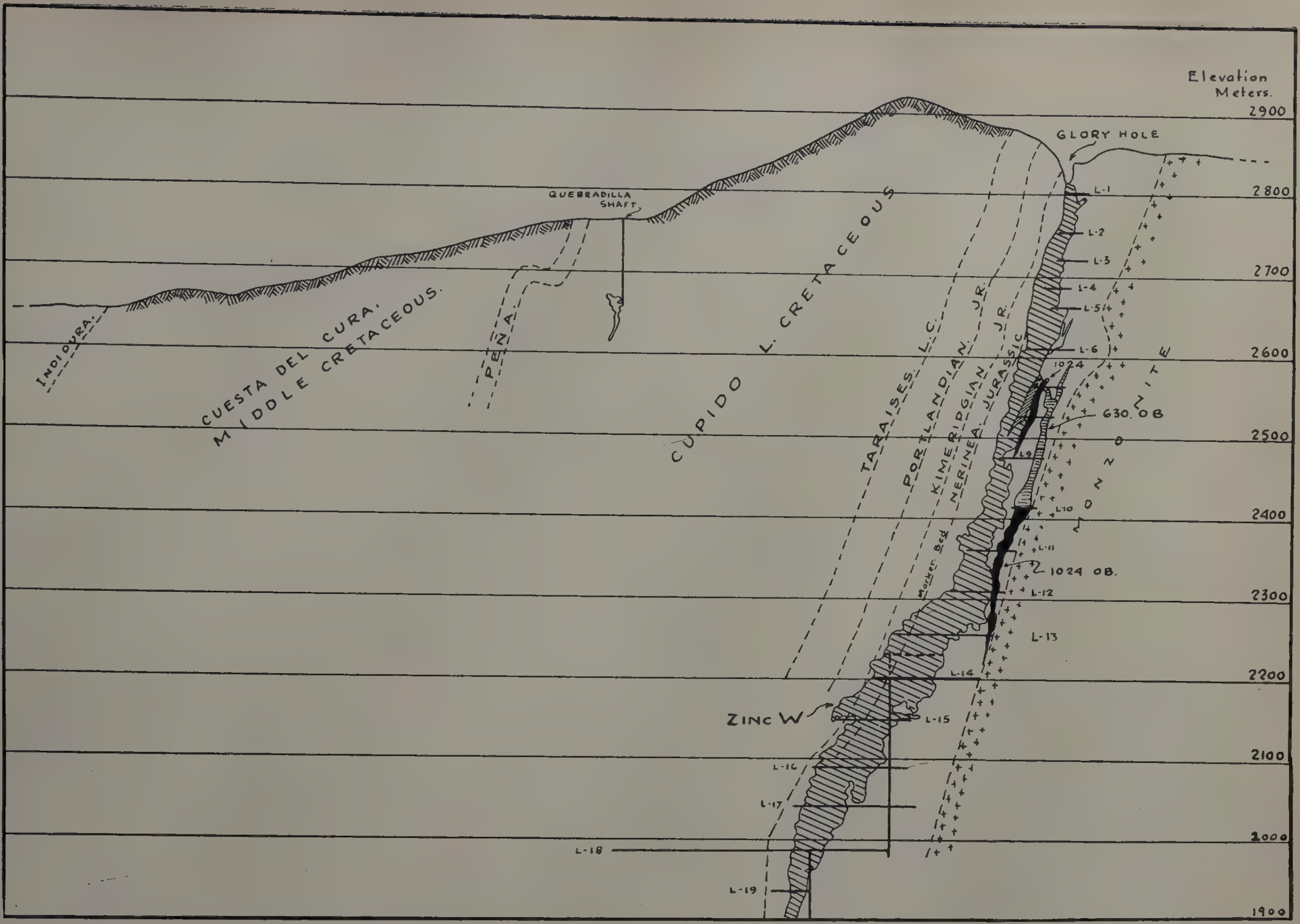

Fig. 2—N. 30° E. projection looking N. 60° W. at the Zinc West, 1024, and 630 orebodies in the Jurassic limestones. The overlying middle and lower Cretaceous are also shown. Mines of the Cia. Minera de Penoles, S. A., and Cia Minera Nazareno y Catasillas. Providencia, Avalos, Zacatecas. Scale 1:5000.

limestones. It can be identified by numerous inocerami. Its lowest shaly beds constitute the hanging wall of some of the Santiago orebodies and apparently guide them to the outcrops, see Fig. 3. One small but high grade silver-lead-zinc orebody, the San Gregorio, occurs in the Indidura formation where the sulphides replace the limy members.

Practically all of the important limestone replacement ore deposits of Mexico occur in the lower Jurassic, lower Cretaceous, and middle Cretaceous formations described above. A few of the smaller replacement deposits are found in the Indidura or San Felipe limy shales. The silver-lead deposits in the San Carlos Mountains of Tamaulipas, described by L. B. Kellum, are examples. Overlying the Indidura formation there is a very thick series of shales known by various names, Senonien, Parras, and Mendez. They are widespread over northeastern, eastern, and central Mexico, but so far as is known no important replacement ore deposits have been found in them.

Intrusive Rocks: A number of intrusive masses crop out in the Caja Range, but only two of these are closely associated with the largest ore deposits, see Fig. 4. These are the diorite stock at Concepcion del Oro and the quartz monzonite stock forming Temeroso peak near Providencia. These are very much alike petrographically and are probably connected underground, forming one continuous mass. Frank F. Grout's report on a typical specimen of the quartz monzonite taken away from the limestone contact on level 5 is given in Table I.

The diorite stock around which are clustered the Cabrestante, Catarroyo, and Aranzazu deposits is the high temperature end of the district. Here the intrusive is enclosed in an envelope of epidote and garnet many meters in thickness, and the baking and alteration of the sedimentary rocks extend far back into the walls. Contact metamorphism around the Providencia quartz-monzonite intrusive is much less intense. The envelope of epidote and garnet is only 1 or 2 m thick. The limestone near the contact is recrystallized but still pure limestone. The limy shale beds, which roughly parallel the contact at 120 to 200 m distance, have been converted to a very hard, tight, overlying wall of thin-bedded hornstone and slates.

In the Salaverna area there are several dikes and sills, which vary in character from monzonite to quartz porphyry. Northwest of the Providencia-Refugio-Rusio area, near Mascaron peak, there is a rhyolite plug. Monzonites outcrop along a great normal fault, which runs along the northeast side of the Caja range, but they have not yet all been plotted on Fig. 4.

Extrusive Rocks: The above sedimentaries and intrusives, which were uplifted to form the Caja mountain range, were eroded down to such an extent that both the lowest Jurassic limestones and the intrusive rocks were exposed on an eroded surface before the extrusives were laid down, see Fig. 4. The latter consists of rhyolite tuffs with variations toward latite. The extrusives are premineral as far as one minor

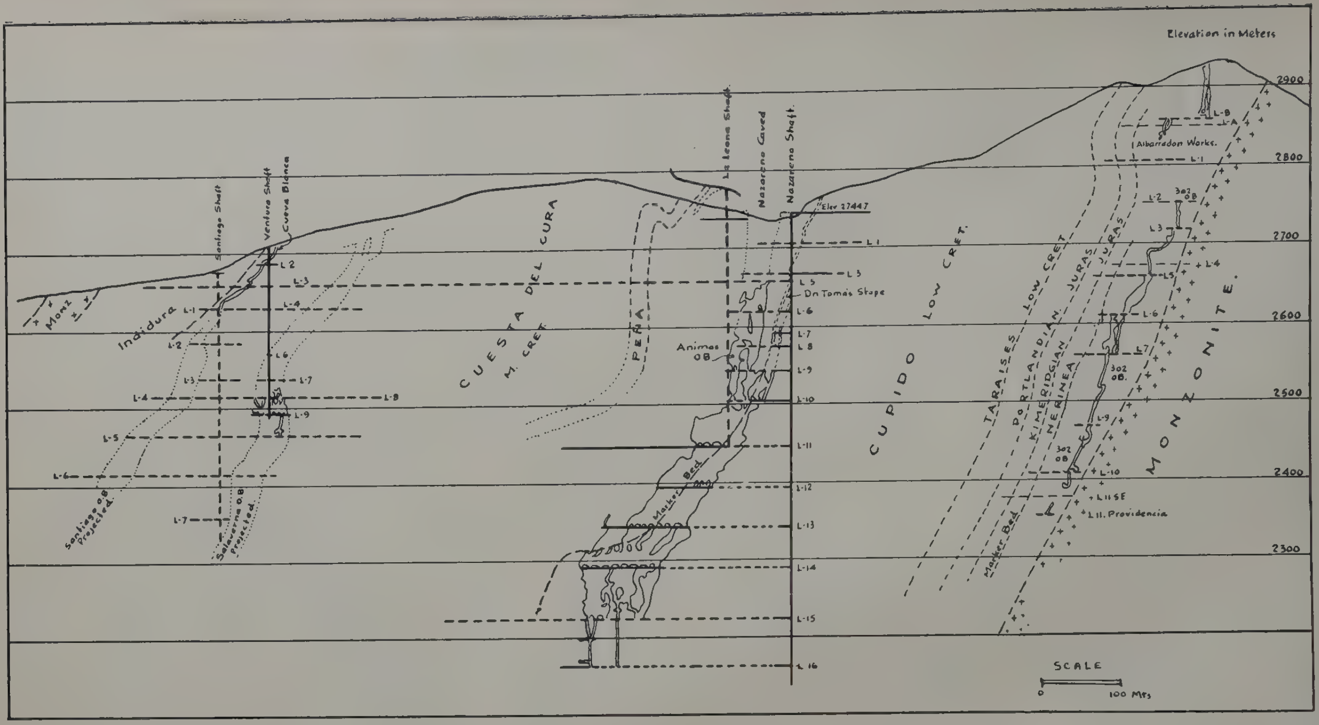

Fig. 3—N. 33° W. projection looking N. 57° W. at Albarradon, Las Animas, Salaverna, Santiago, and Cueva Blanca orebodies. Mines of the Cia. Minera de Penoles, S. A., Cia. Minera Nazareno y Catasillas, S. A., and Mazapil Copper Co., Providencia, Avalos, Zacatecas.

ore shoot is concerned, but it is not known whether or not they predate all of the orebodies. Before erosion they covered and possibly sealed the narrow, steeply dipping corridor between the monzonite foot wall and the hornstone hanging wall, where the San Elias, Albarradon, Providencia, Bonanza, Alicante, and other chimneys are located, see Figs. 2 and 3. Most of the extrusives have been eroded, but there still remain a few isolated remnants capping some of the higher peaks along the southwest side of the Caja Range.

Regional Structure

The Bonanza-Providencia-San Elias-Animas-Salaverna and smaller groups of silver-lead-zinc deposits, the Concepcion del Oro copper-gold and the Santa Rosa lead-gold deposits all occur at a pronounced bend in the mountain chains where they change strike from northwest to west. The axis of this bend strikes northeast from this district through the Diente mine near Monterrey. All of the mountain chains between these two districts bend concentrically around the region herein described. The ranges are successive anticlines and synclines, many of which are slightly overturned toward the northeast, see Fig. 5.

In the Mazapil district the Concepcion del Oro diorites, the Providencia monzonites, and the Santa Rosa rhyolites have welled up within the anticlinal folds but are confined in most parts of the district under the Jurassic limestones, see Fig. 4. In the Caja Range there are discontinuous outcrops of intrusives from Concepcion del Oro through Providencia to the Noche Buena and San Francisco del Alto mine, a distance of about 28 km. Faulting is of minor importance as compared to the intense folding. There are a few faults in the southeastern end of the range at Concepcion del Oro and also from Milanesa peak westward to San Francisco del Alto, but almost no faulting from the Aranzazu mine to Milanesa peak. Between these two points, the sedimentaries have been uplifted so evenly in a N. 55° W. line almost parallel to the intrusive contact that the marker beds can be followed with relative ease. It is in this least disturbed belt that mineralization has been most intense, particularly the silver-lead-zinc mineralization, see Fig. 6.

Local Structure

Jurassic Limestone Belt: The Aranzazu copper mine and the San Eligio, Albarradon, Providencia, Bonanza, Alicante, and Rusio silver-lead-zinc mines all occur in the narrow band of Nerinean (Jurassic) limestone along the southwest side of the diorite and monzonite intrusives. The narrow band, which dips 60° to 70° to the southwest, is confined between the intrusives and the overlying Kimeridgian hornstone. This is the most productive belt of the two camps. Fig. 2 shows a vertical N. 30° E. projection of the formation and the Providencia orebodies including the Zinc West stope.

The Cretaceous limestones overlying to the southwest are productive but to a lesser degree, as described under Rock Formations. The northeast limb of the anticlinal fold on the other side of the intrusives is almost vertical or slightly overturned. Very little mineralization and no mines have been found on the northeast limb, except at Noche Buena and San Francisco del Alto, 28 km to the northwest of Concepcion del Oro.

There are myriads of small to tiny fractures, mostly N. 10 W. to N. 80 E., running outward from the intrusive. The N. 30 E. fractures, which are normal to the igneous contact and to the strata, and the N. 70° to 80° E. fractures are the only ones that have been definitely proved to be mineralized in depth. Shrink-

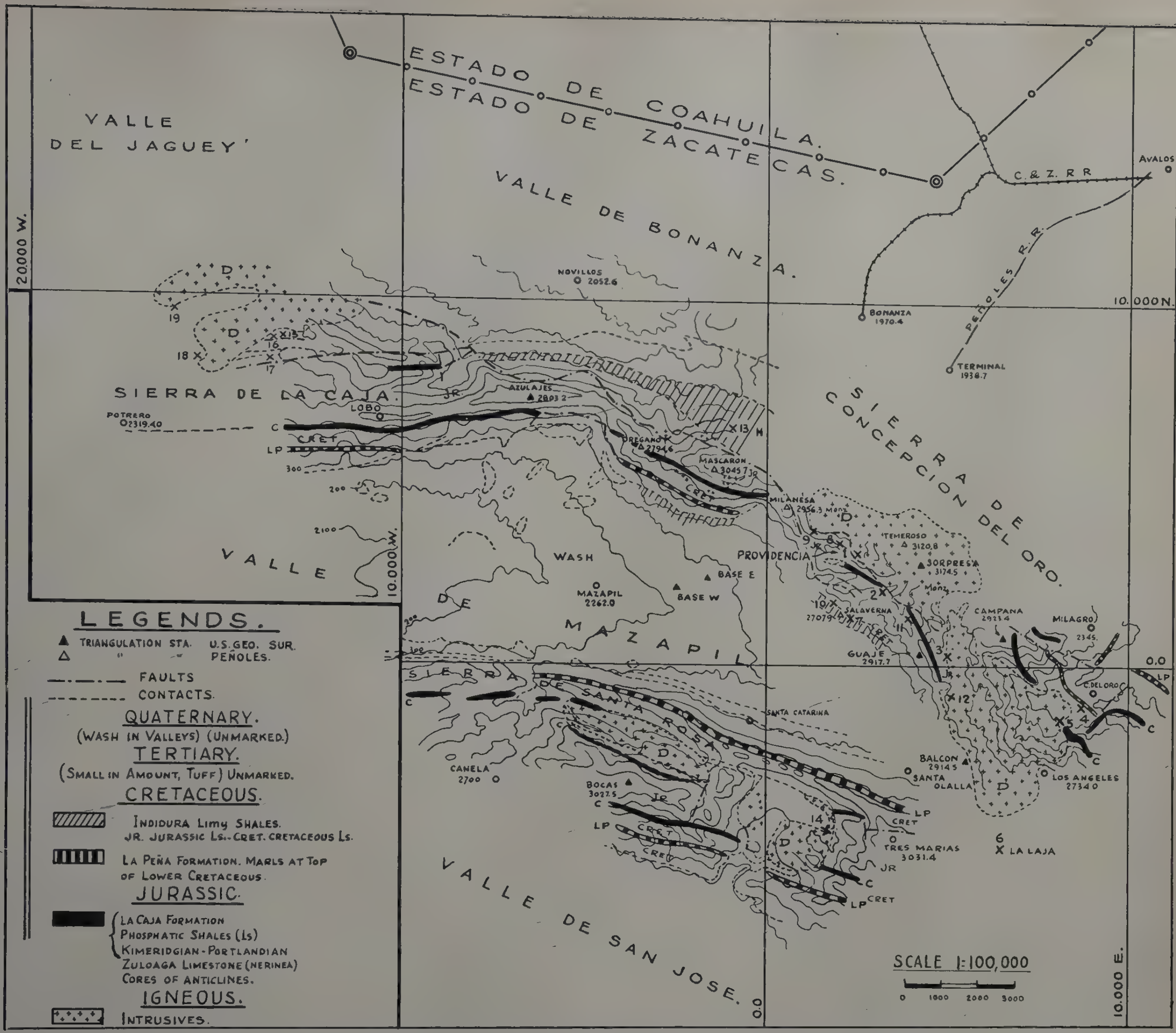

Fig. 4—Sketch of the Caja and Santa Rosa mountain ranges in the Mazapil region, showing important mine openings.$^{1-7}$

1—Providencia Tunnel (Penoles).
2—San Eligio Shaft (Mazapil).
3—General Adit, Aranzazu (Mazapil).
4—Cabrestante Shaft (Mazapil).
5—Cata Arroyo Shaft (Mazapil).
6—La Laja Mine.
7—Santiago Shaft (Nazareno).
8—Refugio Tunnel (American Smelting and Refining Company).
9—Rucio Mine (Mazapil).
10—San Vincente Shaft (Mazapil).
11—San Marcos Mine.
12—San Antonio Adit, Aranzazu (Mazapil).
13—Siempre Adelante Mine.
14—Santa Rosa Shaft.
15—Noche Buena Adit.
16—Chivo Entrance (Noche Buena).
17—Manganeso Prospect (Noche Buena).
18—San Francisco del Alto Mine (Nazareno).
19—Portrero Adit (Mazapil).

age of the intrusives has opened up the N. 55 W. bedding planes of the steeply inclined limestones on the upper levels but not on the Providencia levels below level 11, which is about 550 m below the outcrops. They become increasingly tight on each succeeding deeper level.

A series of level maps of the Zinc West area, see Fig. 7, shows the channels that carried mineralization from level 20 upward. These channels are along N. 25° to 30° E. fractures on the lower levels, but when the mineralization reached the vicinity of level 12, the opening and loosening bedding planes apparently became the channels of least resistance, and the mineral carriers changed over to N. 55° W. beds in preference to the N. 30° E. fissures. On the upper levels some of the orebodies are either tabular replacement bodies conforming in strike and dip with the Nerinean limestone or are steeply inclined chimneys, which are lenticular in horizontal section.

The Alicante-Refugio-Albarradon and San Eligio orebodies, all of which are in the narrow band of Jurassic limestone between the intrusive and the Kimmeridgian hornstone, are similar in structural characteristics to the Providencia bodies, but the predominant mineralized cross fissures strike N. 70° to 80° E.

Nazareno-Leona Area: The Animas silver-lead-zinc body is an oval-shaped cluster of pipes with a combined horizontal ore cross-section of 700 to 800 sq m, see Fig. 3. The pipes have been followed steeply downward to a depth of about 600 m and have stayed with the same beds most of the way. At one place near the 14th level, where the beds flatten out in a minor monoclinal bend, the ore chimneys go down almost vertically through the flat beds until the beds regain their normal steep dip. At this point the best root rakes off along a series of beds flatly to the northwest. There are numerous insignificant cross fractures, but the ore does not take shape on any of them. The only fissure on which ore occurs is a strike fissure on the upper levels. The bedding served as a guide on the upper levels but no reliable guide has

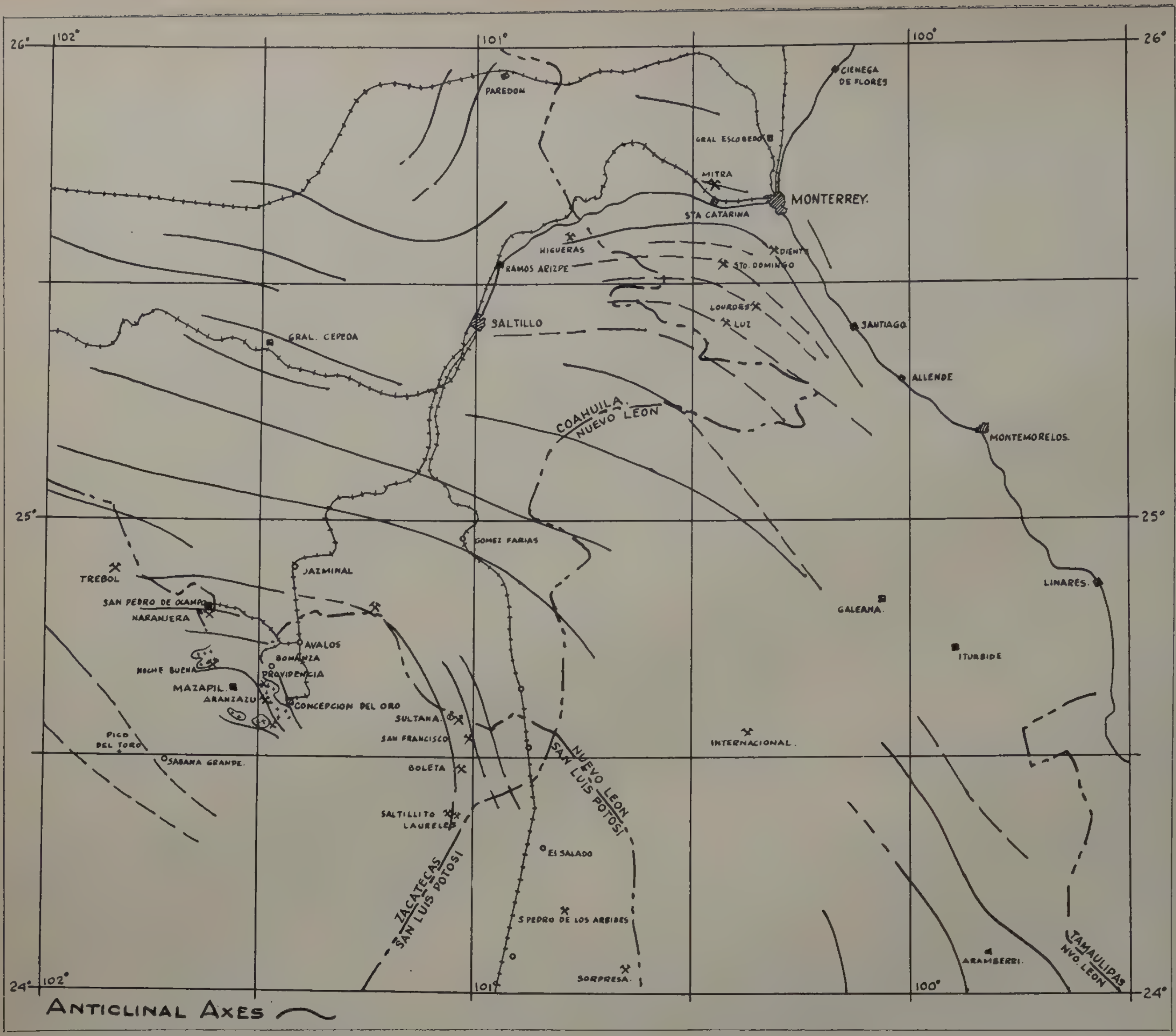

Fig. 5—Approximate locations of mining camps in the bends of the mountain ranges between Providencia, Concepcion del Oro, and Monterrey, Mexico.[8] Scale 1:1.000.000.

been found on the lower levels. The staff is still wrestling with the vagaries of the occurrence and wondering where the ore came from.

Salaverna-Santiago Group: There are four branches of the Santiago Zn-Ag-Pb orebody which crop out along the contact between the Cuesta del Cura cherty limestone and the Indidura shaly limestones, see Fig. 3. The sedimentaries are intensely folded and irregular, but the branches were followed downward approximately along the contact until they came together into one larger body. They are now being worked downward, but they go down a little more steeply than the bedding. The Salaverna is a single irregular body in the intensely folded Cuesta del Cura limestone. Though steeper than the dip of the strata, the latter is the main guide in following the ore in depth.

These examples are characteristic of nearly all the silver-lead-zinc orebodies of the region. Except for a few cross fissures normal to the intrusive contact at great depth, the beds of limestone, silicified limy shales, and shales seem to have exerted the greatest control over mineralization and have proved the best guides in following ores. There are occasional minor bends or folds in the limestone that have caused local enlargements of some of the ore chimneys.

Silver-Lead-Zinc Ores

The greatest production of the district, by far, has come from the many steeply inclined chimneys in the Zuloaga (Nerinea) limestone corridor between the quartz-monzonite intrusive and the metamorphosed Kimeridgian limy shales. These hornstones form an extremely hard impermeable hanging wall dipping 60° to 70° to the southwest, see Figs. 2, 3, and 6.

It is not known whether the large main ore shoots are of post lava capping age or not, but there is one small ore shoot in the Luz mine which outcrops in the capping rock, so the other larger shoots may also have had an overlying felsite roof. Even though the larger bodies may have gone through the capping, this roof may also have had a retarding influence which tended to increase replacement in the underlying limestones.

On the upper levels, each ore shoot replacing a certain steeply inclined limestone bed or series of beds tended to stay with the same bedding as it was developed downward, but occasionally it stepped across into the foot wall to an underlying bed. Some of the smaller shoots, occasionally dipping more steeply than the strata, reached the intrusive contact in the oxidized zone. At this point they consisted of masses of very low grade iron oxides.

Other chimneys, like the 1024 orebody of the Providencia mine, reached downward to the contact in the sulphide zone, where they terminated in masses of pyrite. There are no high temperature minerals in this body of pyrite, sphalerite, and galena, except the thin envelope of garnet, 1 to 2 m in thickness, which covers the whole intrusive. In the opinion of Frank Grout and G. M. Schwartz, specimens submitted to them are mesothermal to epithermal ores occurring during one general replacement period. In all specimens the pyrite was followed by sphalerite-chalcopyrite and finally galena. Rhodochrosite, calcite, and quartz followed the sulphides.

Some of the larger bodies were worked down the bedding to a greater depth, but below level 10 they were found to have been controlled more by N. 30° E. and N. 70° to 80° E. cross fractures than by N. 55° W. striking beds, see Fig. 7. On the bottom levels the only remaining influence of the bedding seems to be the limiting effect of the tight overlying hornstones. On the 20th level of the Providencia mine, about 1000 m below the outcrop, the Zinc West orebody lies along a N. 30° E. fracture under a hornstone hanging wall, and its minerals consist almost entirely of pyrite, with only a little sphalerite and very little galena. The sill floor of this still undeveloped pyritic mass is about 130 to 175 m projected distance from the intrusive contact.

Referring only to the orebodies in the narrow corridor between the intrusive and the hornstone hanging wall, the ore shoots are most numerous near the intrusive. They terminate with their roots at the igneous contact and contain more iron than those farther away. Many Alicante and Refugio and a few Providencia bodies are examples of this habit. The bodies farther away from the intrusive reach greater depths before becoming very pyritic and terminate only when the proportion of pyrite and unreplaced limestone renders them noncommercial.

The ore chimneys in the Cretaceous limestone farther away from the intrusive are still less numerous, but some of them are large, see Figs. 3 and 6. The Animas cluster of three shoots, which joined and separated repeatedly, was developed downward on steeply inclined bedding. A marker bed, see Fig. 3, shows definitely how closely the ore stayed in one group of limestone beds from the 14th level to the surface, but climbing across individual beds on the upper levels, to shorten its channel toward the surface. On the 14th level, there is a minor monoclinal bend through which the chimney rose vertically. Below the 15th level two of the shoots are being worked vertically downward while a third, apparently influenced by the monoclinal bend, is being

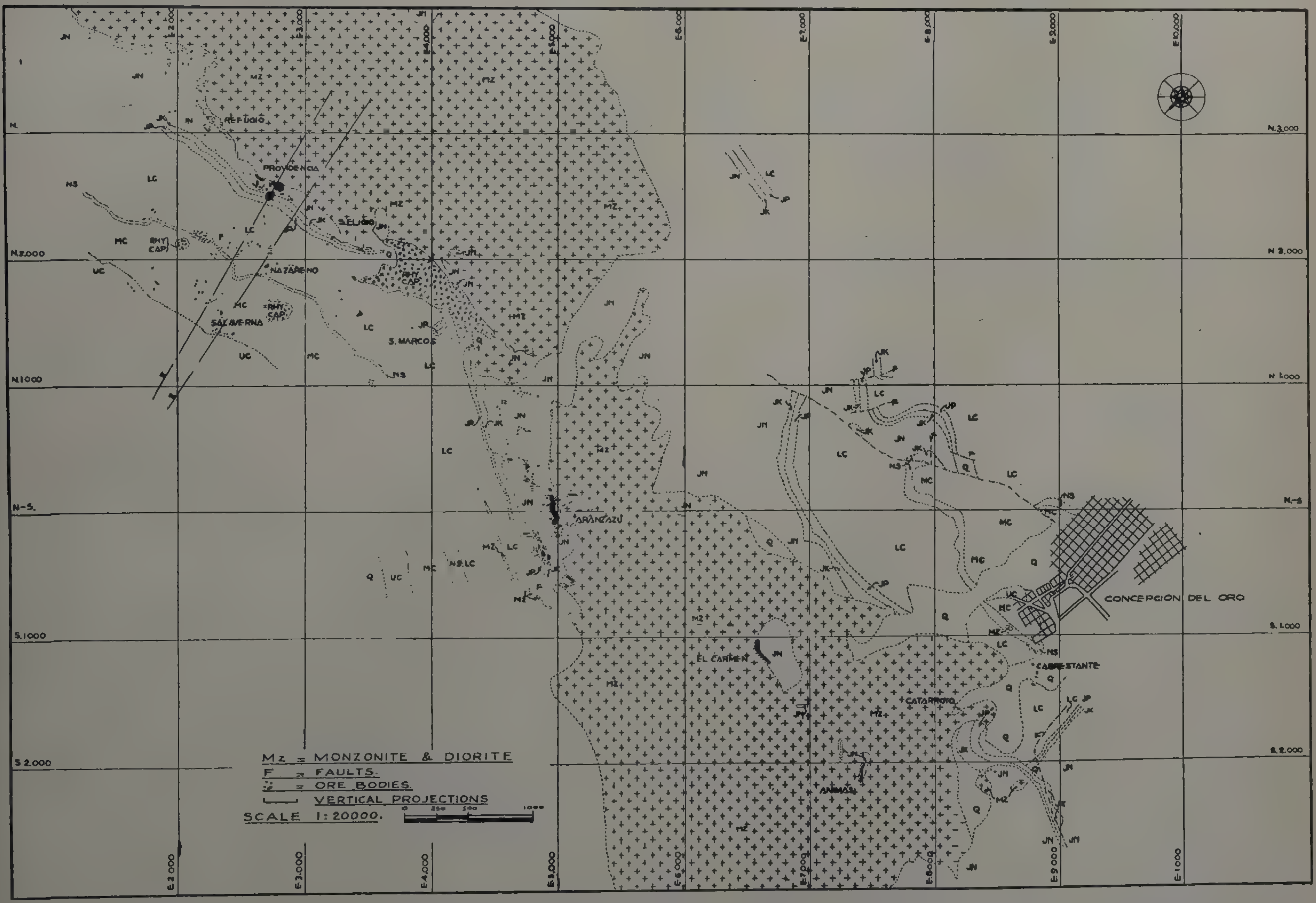

Fig. 6—Geological setting of Refugio, Providencia, San Eligio, Salaverna, San Marcos, Aranzazu, and Concepcion del Oro mining camps.

Q	Quarternary.
RHY	Rhyolite and Latite Capping.
UC	Upper Cretaceous. Mendez Shales. Indidura Limy Shales.
NS	Lower Cretaceous: Pena or Transitional Nieva Shale.
MC	Middle Cretaceous: Cuesta del Cura Cherty Limestone.
LC	Lower Cretaceous. Cupido Limestone, Cherty Taraises Limestone.
UP	Upper Jurassic: Portlandian, Phosphatic Shales.
JK	Upper Jurassic: Kimeridgian, Limy Shales.
JN	Upper Jurassic; Nerinea, Zuloaga, and Providencia Limestone.

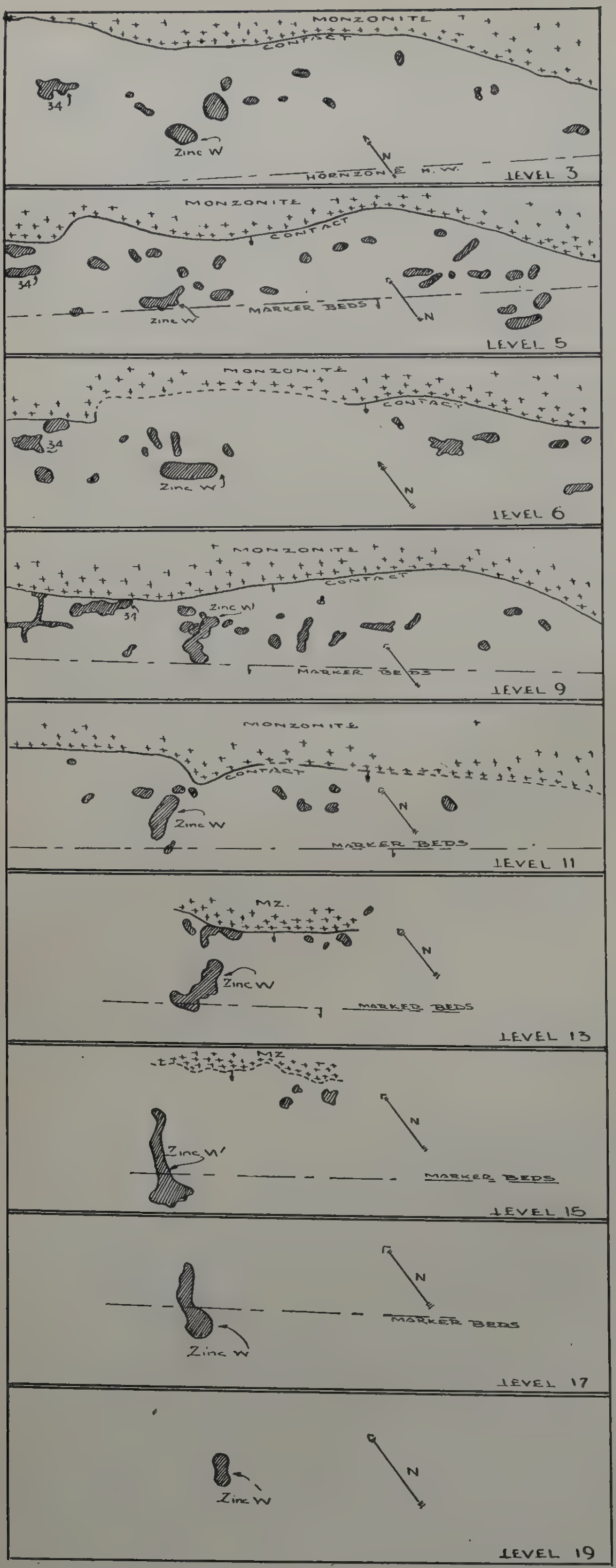

Fig. 7—Horizontal cross sections of Providencia and Albarradon ore chimneys. Cia. Minera Penoles, S. A. Scale 1:4000.

mined down its flatly inclined axis toward the northwest. On level 16 it is now 200 m away from the other two shoots near some cross fractures where the fold plays out. Especially interesting is the fact that recent diamond drilling has shown that the orebody again turns steeply downward at this change in structure. Up to the present stage of devlopment, the limestone bedding appears to have been the dominant control in channeling the mineralizers of the Animas group and several smaller bodies consistently close to a horizon identified by the marker beds.

Still farther southwest, about a kilometer away from the intrusive, there is another horizon of ore pipes near the top of the middle Cretaceous limestone, under a hanging wall of the Indidura limy shales. The Cuesta del Cura cherty limestone in which they occur together with the Indidura are intensely folded. The Santiago ore shoot lies close to the shaly hanging wall from the surface to level 4, but below that level the chimney dips more steeply than the average dip of the bedding. The Salaverna body outcrops in the Cuesta del Cura limestone further back from the Santiago. It sticks fairly close to its horizon but tends to dip more steeply than the average dip of the contorted limestones.

The San Gregorio orebody, from the outcrop to level 4, is in the Indidura limy shales, some of its impure limestone members having been replaced by pyrite, sphalerite, and galena. If past experience serves as a guide in this instance, it will be found stepping down across steeply inclined beds toward the Cuesta del Cura cherty limestone. This is the only known example of a commercial body of this camp outcropping in the Indidura limy shales, and if it does step down into the more favorable formation, the shoot may have a larger cross-section.

Outcrops

After years of scantily rewarded search for promising outcrops, one cannot help envying the Spanish colonists who began working the silver-lead mines about 400 years ago. According to bits of history that have come down to us, Indians guided Francisco Urdinola to the Bonanza and Providencia outcrops. Many of them were wide and continuous, some elongated in the direction of the steeply dipping strata. Iron oxides with an abundance of box work were found at the surface for some of the material can still be observed clinging to the walls of the open cuts. Diggings in the old dumps close to the surface workings yield yellow, orange, brown, maroon, and black iron oxides, both of the migrated type and the residual type with box work. Malachite and azurite stain and crystals are rather common, although the primary ores contain only a few tenths of one percent copper. Yellow jarosite, canary yellow to yellow-green mimetite, and pyromorphite are usually present. Occasional crystals of orange-colored wulfenite and white to yellow calamine can be observed. Silica is present as crystallized quartz and chalcedony, in iron-stained jasperiod, in zinc silicate abundant on the upper levels, and jaboncillo, a hydrous alumina silicate with considerable zinc and other elements of secondary origin also found in the oxidation zone. Calcite is abundant and gypsum rare. Cerussite is usually obscured by iron oxides. Fluorite is rare.

Some of the outcrops that have not responded to exploration contain abundant calcite and barite, but only small quantities of iron oxide, arsenates, cerussite, calamine, antimony oxides, sulphide, galena, and sphalerite. Occasionally there are a few specks of cinnabar. Quartz is often abundant. The conspicuous difference between the productive and unproductive outcrops is the relative abundance of iron oxides.

There are exceptions to this generalization, but not many. One that is hoped will turn out to be an exception is a mineral showing with very little iron, found by trenching through soil and caliche. All that appeared at first was a faint barely noticeable gray streak an inch or two wide. As this streak was followed downward it took on a tabular form of recognizable minerals and widened gradually to 2 ft at 3 or 4 m depth. The mineral is mostly cerussite and anglesite, with a very few crystals of mimetite or pyromorphite, calamine, wulfenite, and galena. At the start a 10 cm width along the gray streak assayed:

Width, Cm	Au, G	Ag, G	Pb, Pct	Zn, Pct
10	1.3	2500	51.0	7.0

Trenching revealed three other similar prospects under covers of caliche. Samples from these assayed:

Width, Cm	Au, G	Ag, G	Pb, Pct	Zn, Pct
25	4.0	40	19.5	1.8
13	0.25	40	36.0	3.0
15	0.15	320	22.4	4.3

A meter or so below the surface the calichelike material takes another form, that of semidecomposed and leached thin-bedded silicious limestone with the normal dip to the southwest. The development of these four high grade stringers may yield some interesting information because the orebodies of this area, whose outcrops were reported to have been high grade in the shallow surface workings, assay only about 125 g silver, 3 to 4 pct lead, and about 15 pct zinc on the 5th and 6th levels. If these eventually go down into low grade sulphides with an abundance of pyrite and zinc, they will be fresh examples of shrinkage, collapse, and enrichment by secondary processes, which also altered the wall rocks and concealed the outcrop beneath the products of decay. They may, of course, lead to an entirely different type of ore shoot.

Trenching by hand is slow and costs $1.50 a lineal meter or $0.15 a sq meter of prospected surface area. A new method is now being tried out. Pits from ½ to 1 m deep are dug at 5-m intervals across a favorable limestone horizon. All samples have contained traces to a few tenths pct lead and from a few tenths to over 2 pct zinc. It is too soon to expect results from this new adventure.

Another type of outcrop, or rather a hole in the ground where there was probably once a mineral outcrop, is the empty limestone pit. There are in this camp as well as in other Mexican mining camps holes of various shapes and sizes, usually oval or elongated, sometimes with little iron and zinc oxide patches on the walls and sometimes with clean limestone. These steeply inclined chimneys are usually nearly or entirely filled with debris, but deep under the debris, at 100 m more or less, there is often a shoot of oxidized ore. The steeply inclined debris-filled hole represents shrinkage due to oxidation and leaching. There are several examples of this type of shrinkage in the Dulces Nombres camp of Nuevo Leon.

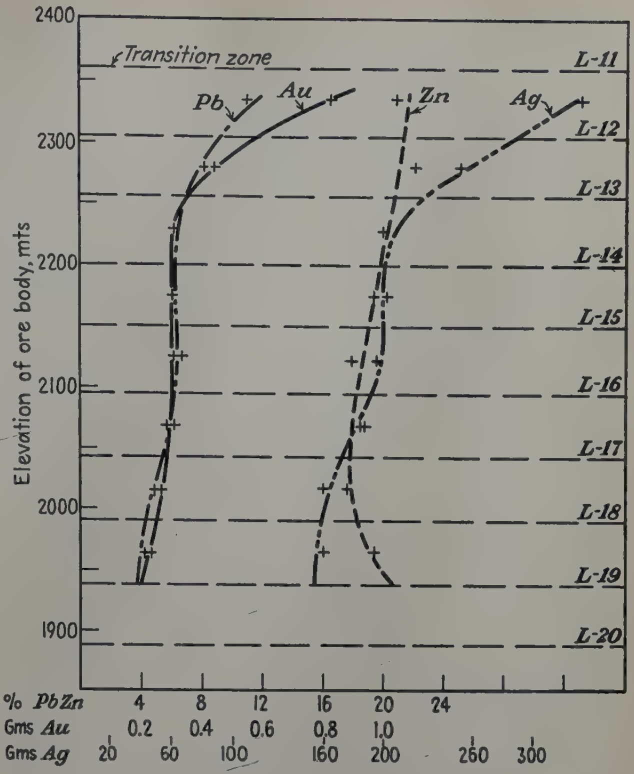

Fig. 8—Avalos unit of zinc west orebody, sulphide assays vs. depth. Cia. Minera Penoles, S. A.

Zoning

Copper and iron deposits occur in and around the diorite plug at Concepcion del Oro where the garnetization is most intense. The copper ores contain a little gold. Farther back from the intrusive contact there are a few small gold-silver-lead-zinc bodies, the largest of which are La Perla, La Laja, and Balcon, and also a few narrow gold bearing stringers. Still farther back from the contact a few meager showings of mercury have been observed. The main silver-lead-zinc deposits occurring in the narrow band of Jurassic limestone between a silicious hanging wall and the Providencia monzonite intrusive extend northwestward from the Aranzazu copper shoots for a distance of 5½ km. The alteration to garnet and epidote on the Providencia monzonite contact is not nearly as intense as it is on the Aranzazu diorite contact near the copper deposits.

For several kilometers still farther northwestward along the same sedimentary structure there are occa-

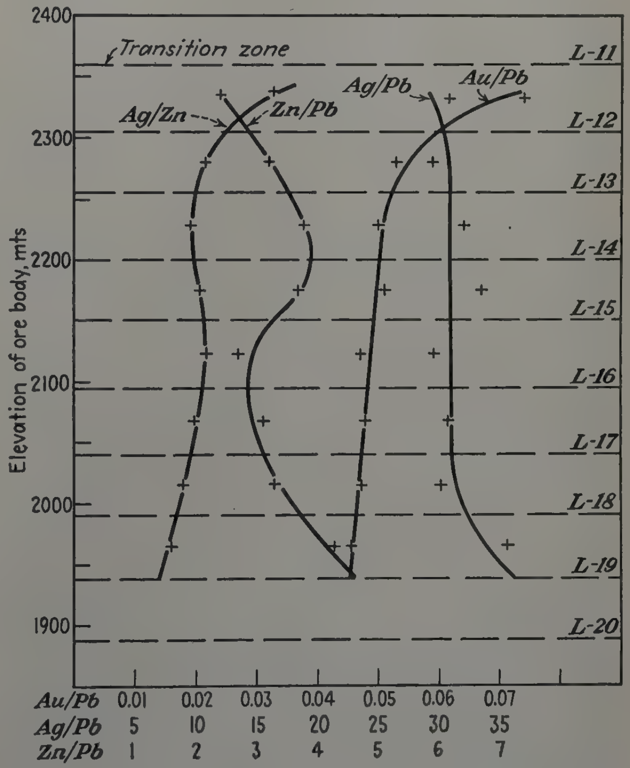

Fig. 9—Avalos unit of zinc west orebody, metal ratios vs. depth. Cia. Minera Penoles, S. A.

sional small showings of silver-lead-zinc antimony-mercury minerals accompanied by an abundance of barite. Some of these have been prospected without commercial success.

No investigations have been undertaken to identify different periods of mineralization, but many observers* have noticed that the oxidized iron in the N. 70° to 80° E. fractures of the Alicante and Refugio mines carry several grams of gold where they cross the base metal ore shoots. The highest assays are found associated with mimetite.

Zoning in depth is an interesting and more practical study, for it differs much from that in some other limestone camps and has a bearing on ore estimation. The transition from oxides to sulphides of the Zinc West body occurs about 500 m below the outcrop at an altitude of approximately 2400 m while that of the Animas bodies is more or less at 175 m below the surface or about 2600 m above sea level.

Immediately below the transition zone, both of these chimneys were almost solid galena, sphalerite, and pyrite. As they were worked downward, patches of limestone showed up in the ore although the total horizontal areas of the chimneys remained almost constant, see Fig. 7. On each succeeding deeper level the proportion of sulphides to limestone diminished. This gradual change is more evident in the Zinc West orebody, for it has been worked 300 m deeper than the Animas bodies. Ore estimates were made by cutting channels across the backs of stopes 1 m apart. Each channel was divided into samples of 1 m lengths. The pay ore showed up in patches, the areas of which were measured with a planimeter, and the proportion of pay ore to limestone was estimated. On the lowest levels the ore amounts to 40 to 50 pct of the total cross-section.

Replacement was not as complete on the lower levels as the upper ones, and the result is that an ore shoot resembles the trunk of a limbless tree with a lot of tenuous rootlets. At Ojuela, Durango, the gradual pinching out of the orebodies is distinctly different. Each chimney or manto has only a single root, which diminishes in size on each succeeding lower level. There, a chimney is like a tree with two or three or more branches and a single tap root, which is more slender on each lower level. For instance, the main Ojuela chimney, which has a horizontal cross-section of 1000 sq m in the oxide zone 500 m below the surface, has only 175 sq m in the sulphide zone at 750 m depth, 85 sq m at 800 m, 40 sq m at 850 m, and 15 sq m at 865 m depth. The ore consisted of almost solid lead, zinc, and iron sulphides all the way to the bottom. There are no data available concerning changes in the grade of Ojuela ore with depth, but no important variations were noted, nor any noticeable increase in the pyrite-galena ratio as at Providencia. Intrusive alaskite that is believed to account for the mineralization was found in diamond drill holes nearly 200 m below the bottom stope, or about 1050 m below the collar of Tiro Norte at Ojuela.

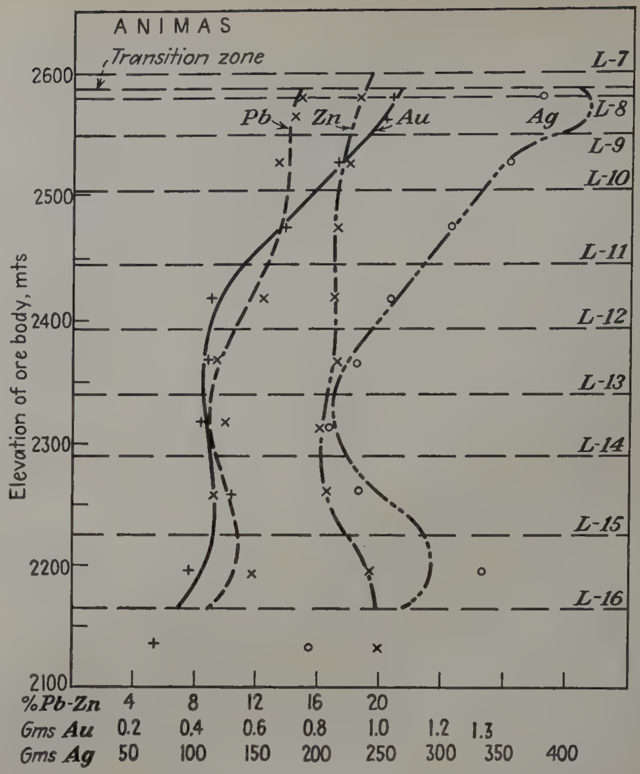

Fig. 10—Avalos unit of Leona and Nazareno orebody, sulphide assays vs. depth. Cia. Minera Penoles, S. A.

At Providencia, the transition zone consisted of semistratified layers of mud, sand, pieces of limestone, chunks of carbonate ore, and some leached silicious irony material in place overlying semi-oxidized sulphides, which were low in grade. Only a part of the muddy sandy material was minable. There are also evidences of higher transition zones at levels where the water level apparently stood for long periods of time.

Just below the transition zone, the Zinc West sulphides ran comparatively high in precious metals, very likely due to secondary enrichment. Gold, silver, and lead values fall off rapidly in the first 100 m depth. From level 14 downward the decrease is fairly

---

* John Barry recognized a number of stages but up to this date he has not published his observations.

Table II. Providencia and Demasias Del Paraiso Mines Zinc West Orebody Assays and Metal Ratios, 1936 to November 1951

		ASSAYS				METAL RATIOS			
Level	Tons	Au, G	Ag, G	Pb, Pct	Zn, Pct	Au per Pb	Ag per Pb	Ag per Zn	Zn per Pb
11-12	10,493	0.82	339	11.0	20.8	0.074	30.8	16.3	1.90
12-13	60,496	0.44	240	8.2	22.1	0.053	29.5	10.8	2.69
13-14	91,431	0.31	199	6.2	20.7	0.050	32.0	9.6	3.33
14-15	88,422	0.31	201.5	6.0	19.4	0.051	33.5	10.3	3.23
15-16	80,343	0.31	195.5	6.6	17.9	0.047	29.6	10.9	2.71
16-17	71,993	0.29	185	6.0	18.6	0.048	30.8	9.9	3.10
17-18	41,522	0.25	160	5.3	17.6	0.047	30.1	9.0	3.32
18-19	28,157	0.21	160.1	4.5	19.4	0.046	35.6	8.2	4.31
19-20	3,355	0.23	115	2.3	13.7	0.100	50.0	8.3	5.95
	476,212	0.32	198.8	6.4	19.5				

Table III. Leona and Nazareno Mines Animas Orebodies Assays and Metal Ratios, 1936 to November 1951

		ASSAYS				METAL RATIOS			
Level	Metric Tons	Au, G	Ag, G	Pb, Pct	Zn, Pct	Au per Pb	Ag per Pb	Ag per Zn	Zn per Pb
7-8	9,905	1.33	381.1	14.7	18.5	0.090	25.9	20.6	1.26
8-9	39,855	1.11	454.6	14.3	19.5	0.077	31.8	23.3	1.36
9-10	84,080	0.86	355.6	13.3	17.9	0.064	26.7	19.8	1.34
10-11	144,125	0.69	310.5	13.7	17.1	0.050	22.6	18.1	1.24
11-12	109,781	0.45	265.8	12.4	16.9	0.036	21.4	15.7	1.36
12-13	96,744	0.44	210.1	9.4	16.9	0.046	22.3	12.4	1.79
13-14	110,544	0.42	216.3	9.9	16.1	0.042	21.8	13.4	1.62
14-15	152,110	0.52	241.1	9.2	16.5	0.056	26.2	14.6	1.79
15-16	131,430	0.38	339.0	11.8	19.3	0.032	28.7	17.5	1.64
16-17	5,927	0.27	184.3	4.6	19.9	0.058	40.0	9.2	4.32
Totals	884,501	0.56	285.2	11.5	17.4				

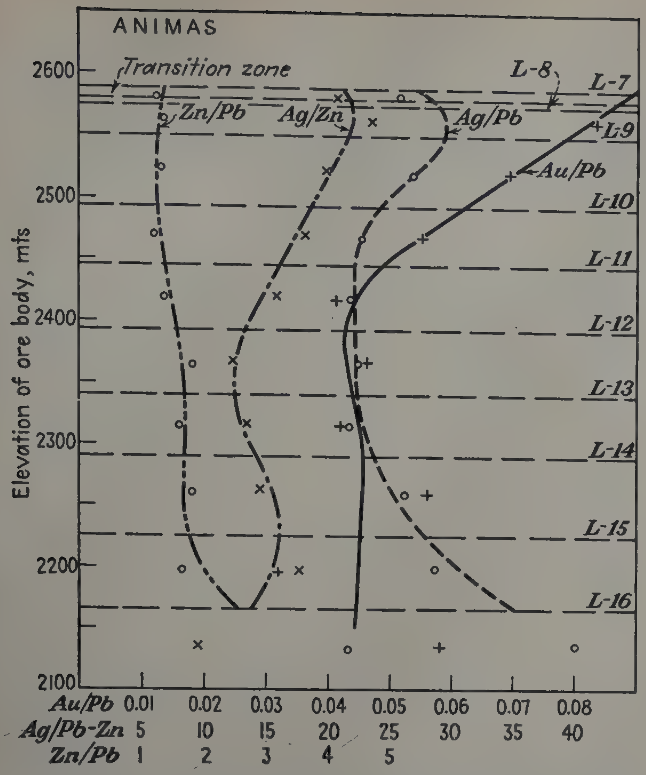

Fig. 11—Avalos unit of Leona and Nazareno orebody, metal ratios vs. depth. Cia. Minera Penoles, S. A.

uniform, see Fig. 8. Zinc assays, although somewhat erratic, fall off gradually throughout the entire vertical range down to level 18 where they take an unexplained turn for the better. Diamond drill holes and uncompleted development on level 20 indicate a sharp decrease in all metals except iron, as shown in Table II. Unfortunately, there are no iron assays available. If there were, observations indicate that the lower levels would show an increase in iron assays and a decided increase in the ratio of iron to the other metals.

Table II and Fig. 9 show the ratios of gold and silver to the base metals, and zinc to lead, plotted against depth. It is interesting to note that the silver-lead ratio increases on the lowest levels as well as the zinc-lead ratio, and the silver-zinc ratio remains nearly constant. A polished surface of sulphide ore from the 14th level of the Providencia mine examined by G. M. Schwartz showed abundant minute inclusions of chalcocite in dark brown sphalerite, but no silver minerals were observed. Supergene chalcocite and covellite were also found. The sulphide ores contain 0.2 to 0.4 pct copper, and possibly some silver may be associated with the copper. No study has been made of this phenomenon, which may possibly account for the behavior of the silver.

In the Leona and Nazareno mines the Animas ore chimneys, which are not oxidized as deeply as the Zinc West, were also comparatively rich in precious metals immediately below the transition zone. This was probably due to secondary enrichment. The gold and silver grades fall off all the way from the transition zone to level 13, a vertical range of 250 m, see Table III and Figs. 10 and 11. Lead behaves in a similar way down to level 12, but the grade drops sharply below level 12 and rises again below the 15th level. The level 12 drop in lead values is more severe than the gradual change in the Zinc West body and no explanation is in sight. The increase in silver and lead below level 15 is accompanied by an abrupt change in the direction of one member of the cluster of steeply inclined chimneys to a flatly inclined manto, which takes off toward the northwest along the axis of a monoclinal fold behind the chimneys shown in Fig. 3. The vertical chimney in the section is low in lead but fair in zinc and high in pyrite, behaving in a way similar to the Zinc West body.

A couple of hundred meters northwest of the main chimney the flatly inclined ore shoot steepens and goes vertically downward in the vicinity of a series of cross fissures as indicated by recent diamond drill holes on level 19. Here the ore is much lower in lead but still high in zinc. Apparently the successive changes in metal ratios from transition zone downward are similar to those in the Zinc West and many other orebodies of this district, although there are variations due to other local influences.

These data, based on substantial tonnages, are included as a matter of record for those interested in the depth changes of replacement mineralization who wish to estimate the depth to which an orebody of commercial grade may extend.

Acknowledgments

The author thanks Charles H. Behre, Jr., and Marden W. Hayward, both of whom are familiar with the Providencia-Concepcion del Oro mining district, for having reviewed and discussed the observations described herein. Edward A. Manderfield, Manager of the Avalos Unit, Paul Pyburn, and Carl Millikan all cooperated in gathering and assembling data. Charles Y. Manderfield, who found new prospects by trenching through caliche, described his newest method of surface prospecting. David B. Dill contributed the general structure of the mountain ranges and made many valuable suggestions. John G. Barry, who has been active in consultation work for the Mazapil Copper Co. and the Cia. Minera Noche Buena, contributed many helpful ideas. Frank F. Grout's and George M. Schwartz' descriptions of the wall rocks and ore minerals were invaluable in interpreting and confirming field data.

The author especially thanks M. C. Haas, General Manager of the Compania Minera de Penoles, S. A., in Monterrey, for his encouragement in writing the paper and his authorization to publish it.

References

[1] C. Burckhardt: Excursion du Nord. Tenth Congrés Geólogique International, Mexico, 1906.

[2] C. Burckhardt: Etude Synthetique sur le Mezozoique Mexican. *Memoires de la Société Paleontologique Suisse,* 49-50, p. 126. Emile Birkhauser et Cie, Basle, 1930.

[3] Ralph W. Imlay: Studies of the Mexican Geosyncline. Geol. Soc. Amer. *Bull.* **49**, p. 1656.

[4] E. H. Sellards, W. S. Adkins, and F. B. Plummer: *The Geology of Texas Stratigraphy,* Bur. Econ. Geol., Univ. Texas (1933) **1**, pp. 270-271.

[5] Lewis B. Kellum: *The Geology and Biology of the San Carlos Mountains, Tamaulipas, Northern Mexico.* Univ. Mich. Press, 1937.

[6] John G. Barry: Unpublished compilation of the work of C. Bruckhardt and R. W. Imlay in relation to sedimentary columns of the Sierra de la Caja and Santa Rosa, Mazapil District, Zacatecas.

[7] Local data compiled by the staff of the Cia. Minera de Penoles, S. A.

[8] D. B. Dill: Compilation from the World Aeronautical Chart 522 and Philip B. King's Geological Map of the Northern Part of Mexico, Plate 1, Cartas Geologicas y Mineras de la República Mexicana (October 1947) No. 3, translation U. S. Geol. Survey publication.

The Surface Expression of Veins in The Pachuca Silver District of Mexico

by C. L. Thornburg

FLANKING the Valley of Mexico on the northeast is a mountain range known as the Sierra de Pachuca. This northwesterly-trending range is about 30 miles long and 5 miles wide, its summit attaining an elevation of more than 10,000 feet above sea level, or 2000 feet above the valley floor. Pachuca, a town of 50,000 inhabitants, lies nestled at the southwest base of the range, 60 miles northeast of Mexico City. Three miles to the east, just over the summit and on the northeasterly slope, is the mountain town of Real del Monte with a population of about 20,000. These are the two principal towns in a 40-sq mile area whose yield has brought the district to its high rank among the world's silver producers. Total production probably exceeds 1.25 billion ounces of silver and 4.5 million ounces of gold.

Exploitation by the Spanish was under way by 1530. As the mines were deepened operations became handicapped by the inadequate method of handling water with horse whims and bull skins. To offset this disadvantage a two-mile drainage tunnel was started in 1749 and completed ten years later. John Taylor of London acquired the mines from the third Count of Regla in 1824 and formed the Compania de Real del Monte y Pachuca. Two years later Cornish pumps were brought from England. A Mexican company purchased the British interest in 1848 and within a few years resumed an old project of driving a second, lower three-mile drainage tunnel, completing it in 1857. After American interests acquired control of the property in 1906 operations expanded to an unprecedented scale, despite periods of political strife, unstable prices, labor problems, and a growing burden of taxation. An idea of the scale of operations may be gained from records of the last two decades prior to 1947, the last year for which production information is at hand, during which time production ranged from 1.4 million to 1.1 million tons per year, and the combined development and exploration, exclusive of diamond drilling, amounted to about 18 miles annually.

Pachuca differs from Zacatecas and some other Mexican silver vein districts that flourished and declined in earlier centuries in that a substantial part of its total production was made after 1900. While the district's accelerated activity in this century was largely due to the successful application of the cyanide process to the treatment of the ores, improved pumping methods, and new mechanical equipment, it was at the same time stimulated by the opening up of important new orebodies as a result of active and extensive exploration of the vein system. Some of these orebodies were found on veins which terminate upward far below the surface, and though these particular veins do not crop out, they show relationship with a type of alteration which may be their surface expression.

The district has been studied by many able geologists, and a large store of information has been accumulated, much of which is recorded in published as well as private papers.

Wall Rocks

Extrusive Rocks: The Sierra de Pachuca is a thick accumulation of Tertiary eruptive rocks consisting mainly of flows, breccias, and tuffs. Numerous recognizable volcanic vents within the range itself manifest that the range was built up by material ejected from these vents. The maximum thickness of the volcanic pile is not known, but from deep exploration and from relationship with Mesozoic sediments to the north and east it is inferred that the average thickness in the main part of the district may be at least 6000 ft. The extrusive rocks comprise four general types, which in ascending order of age are: andesite, rhyolite, dacite, and basalt.

The veins are confined largely to the andesite, the dominant rock of the region. Characteristically this rock is augite andesite, but it includes comparatively acidic as well as basic layers, the acidic strata being

---

C. L. THORNBURG, Member AIME, was formerly Chief Geologist, Cia. de Real del Monte y Pachuca, and is now Mines Geologist, U. S. Smelting, Refining and Mining Co., Salt Lake City.

Discussion on this paper, TP 3315I, may be sent (2 copies) to AIME before July 31, 1952. Manuscript, Aug. 8, 1951. St. Louis Meeting, February 1951.

classified as interbedded dacites. The andesite is locally overlain by rhyolite, while the still younger dacite occupies a vast area along the crest of the range. Although strong mineralization is confined to the andesite, the rhyolite and at least the lower part of the dacite are of pre-ore age. The basalt is definitely post-ore and is confined to isolated areas, some of which are in lower outlying parts of the range.

Intrusive Rocks: The intrusive rocks consist of dikes and irregular stocklike masses, the various types of which range from rhyolitic to dacitic. With few exceptions the dikes have a northwesterly trend, the direction of early fracturing. In those cases where dikes form one of the vein walls the relationship is structural, the dike contacts being planes of premineral fractures.

Mineralization in Veins: Approximately 70 veins in the main part of the district are characterized by similar outstanding features. The vein pattern consists of three dominant trends: northwest to east-west, north-south, and northeast. In all three systems quartz is the dominant gangue mineral. Calcite, though common, is only locally abundant. Rhodonite, which is typical of the north-south veins, is rare in veins of the other systems, although there are a few exceptions to this rule. A more detailed list would include various additional gangue minerals that are less common. The veins are ordinarily 3 to 5 ft wide; however, stoping is typically 8 to 10 ft wide because of precious metal value in the immediately adjoining wall rock and in parallel stringers. In some veins base metals and silver sulphide are visible in narrow, threadlike, wavy seams conformable to vein attitude, although well-defined vein banding is not the rule. Commonly veins are composed of wall rock breccia in which the fragments are cemented by quartz and silicified and cut by quartz stringers, the degree of replacement by quartz and other gangue minerals varying with intensity of mineralization. Sulphides are typically in subordinate quantity, in blebs, disseminations, and tiny stringers without uniform orientation. Galena, sphalerite, and pyrite are locally prominent, and in some veins base metals are sufficiently abundant to be produced as by-products. The ratio of gold to silver in the ores is about 1 to 200 for most veins.

Oxidation: As a rule complete oxidation does not extend more than 100 ft or so below the surface, except in certain extensively oxidized veins which lie below valley alluvium.

Wall Rock and Surface Alteration in the Productive Area

Chloritization of the andesite is the most widespread type of alteration. It is too general to show definite relationship with individual veins but is a characteristic of productive areas. In a very general way it becomes weaker and more irregular beyond the outer reaches of silver deposition. Although this statement is made with some reservations, it has sufficient basis to explain a tendency to regard areas of unchloritized rock as unfavorable ground for prospecting. Sericitization, kaolinization, and pyritization are much more local than chloritization and are more definitely associated with productive veins. Strong silicification is usually closely limited to the vein zone; as a rule it does not extend more than 5 or 10 ft into the walls. The relationship between silicification and ore is variable because the phases of quartz deposition extended over a wider range spatially and lasted longer than metallization.

A striking feature of much of the surface rock is the extent to which the grayish-green color of the andesite gives way to a buff color caused by weathering of hydrothermally altered andesite. This effect gives the impression of widespread iron stain; in fact, it is due in part to oxidation of more or less pyritized andesite. Whitish to pale buff to yellowish-brown tints all indicate some degree of hydrothermal alteration; and bleached areas, especially where strewn with quartz float, may indicate relationship to ore mineralization. Local areas of such discolored rock in some cases appear to be the only surface expression of veins whose uppermost limits lie far below the surface. Although this surface feature is a characteristic of much of the productive area, its relationship to ore mineralization is uncertain mainly because the range of hydrothermal alteration is vastly more extensive than that of ore deposition. Obviously the weathering of rock to reddish or brownish shades is not necessarily always related to hydrothermal alteration; for example, some darker types of andesite weather to a reddish-brown color apparently caused by oxidation of original rock constituents.

The effect of weathering on hydrothermally altered andesite varies with the extent of erosion. In areas of less rugged terrain where erosion is delayed the altered andesite is marked by weathering that produces an extensive uniformly buff-colored porous shell; whereas in areas of rapid erosion the buff coloring is limited to irregular patches separated by areas of relatively fresh grayish-green andesite.

The common type of pyritization consists of sparsely disseminated minute grains of pyrite in a matrix of greenish andesite. Its range is far greater than that of ore deposition, vertically as well as horizontally. Though of widely varying intensity it is not normally strong for more than a few yards outward from the veins. In some exceptional localities, as in one described later, strong to moderate pyritization extends hundreds of yards outward and upward from the veins.

Expression of Veins at the Surface

In order to provide a general picture of Pachuca veins showing relationship to outcrops, definite surface expression, and less definitely related surface alteration, veins are classified in groups and their locations shown in Fig. 1 by Roman numerals.

Veins Below Valley Alluvium: In Locality I are the Alamo, El Lobo No. 2 and other veins in the vicinity of Pachuca and miscellaneous veins farther east in the Dos Carlos area that lie beneath valley sediments. In Fig. 2 they are shown in section. Prior to their burial beneath wash these veins must have shown strong outcrops.

Veins Below Post-ore Basalt: The Paricutin vein, unique in several respects, is shown in Locality II, Fig. 1, and in section in Fig. 2. In the ores of this gold-bearing vein the approximate ratio of gold to silver is about 1 to 40. Situated in Cubitos Hill at the extreme southern limit of the known district, it lies mainly beneath a blanket of post-ore basalt. The basalt shows no alteration whatsoever. At one isolated spot between the edge of the basalt and the valley alluvium, a small exposure of andesite shows minor barren quartz stringers and weak alteration. While this might conceivably be related to the vein, it can be said that there is nothing anywhere at the surface to indicate an ore-bearing structure. Underground exploration penetrated this locality mainly in accordance with a policy of searching well beyond

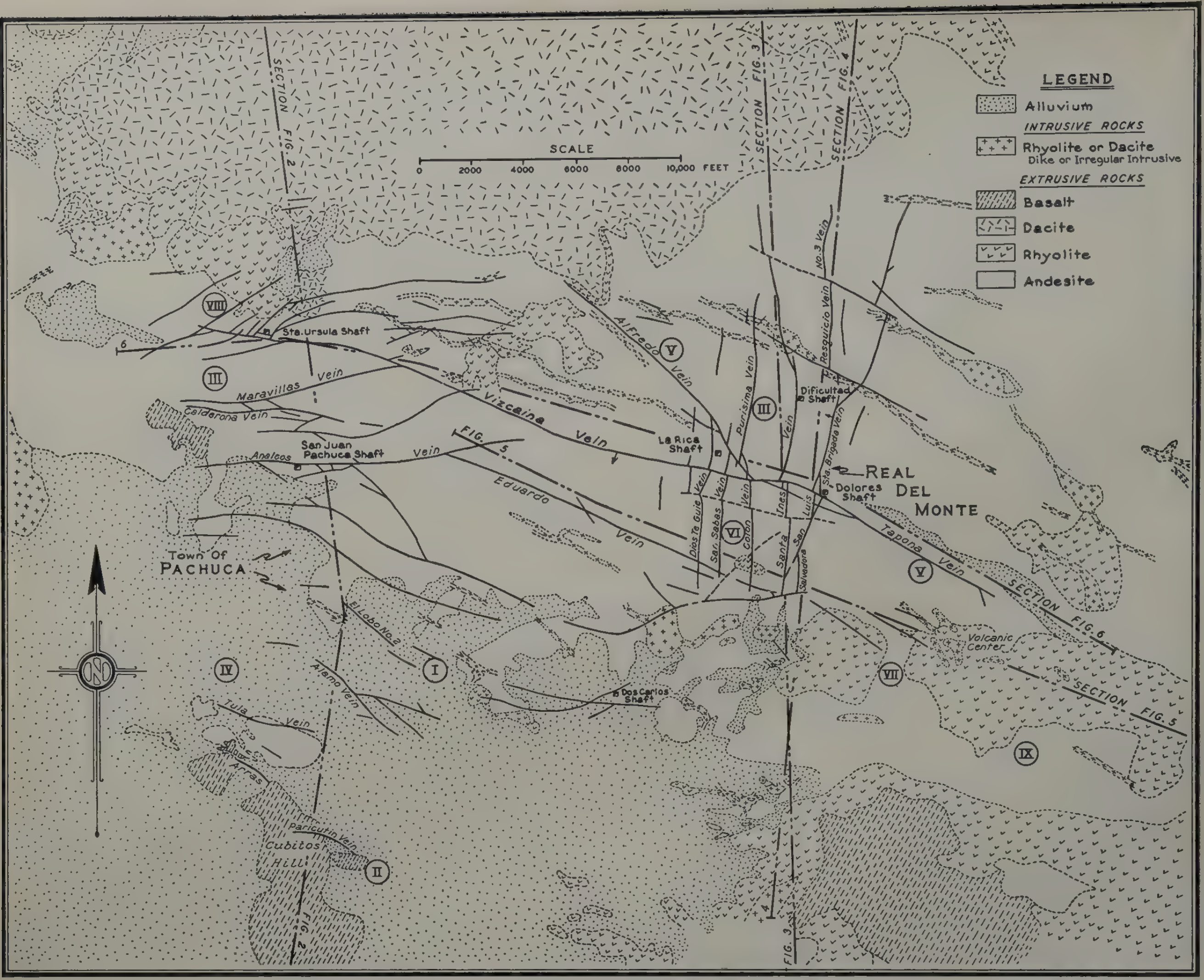

Fig. 1—Generalized geologic plan of main Pachuca district.

the limits of known mineralization. The Paricutin vein is still undergoing development. The productive dimensions as last reported are 1000 ft or so along strike, a width of about 15 ft, and vertical range of 600 ft.

Although this case contributes nothing to the subject of surface expression, it provides useful data pertinent to the study of wall rock alteration. The vein was discovered by a long hole that had to be drilled from an underground base where working conditions were extremely difficult because of excessive heat. As in all venturesome and costly enterprises, the project was attended by periods of discouragement, and after the hole passed from chloritized andesite into rock which showed no alteration, hundreds of feet short of the point where the vein was intersected, a question arose as to the advisability of continuing the drilling. Carefully recorded geological detail showed the unchloritized rock to be a familiar dacitic type which did not show much alteration even in the proximity of a vein; therefore it was not to be considered a discouraging feature which would justify stopping the diamond drill hole. The distinction between these rock types is also alluded to below in description of the Tula vein.

Outcropping Veins Bearing Ore Near the Surface: In the area adjoining the town of Pachuca on the northwest are the Maravillas, Calderona, and Analcos veins shown in Locality III, Fig. 1, and in section in Fig. 2. They are south of the Vizcaina vein in a block of ground which is elevated in relation to the block to the north because of faulting along the Vizcaina, see Locality VIII. Intense erosion of the elevated block has removed the upper extremities of the veins and has left bold outcrops of quartz, gossan, and local ore. Hydrothermal alteration has been moderate and except for rather general chloritization and irregular pyritization does not extend for more than a few yards into the vein walls. North of the Vizcaina there are a number of veins whose upper limits of ore lie hundreds of feet below the surface. There, however, the surface rock is rhyolite, a rock which does not prominently exhibit effects of hydrothermal alteration as does the andesite, and in that vicinity there is practically no surface expression of the underlying veins.

In the Real del Monte area the above structural condition is reversed. Here faulting along the Vizcaina has dropped the south block with respect to the north one, although this faulting does not account for the fact that the tops of the quartz veins in the south block lie so far below the surface, see Figs. 3 and 4. In the north block are numerous vein outcrops, and locally the ore shoots reach the sur-

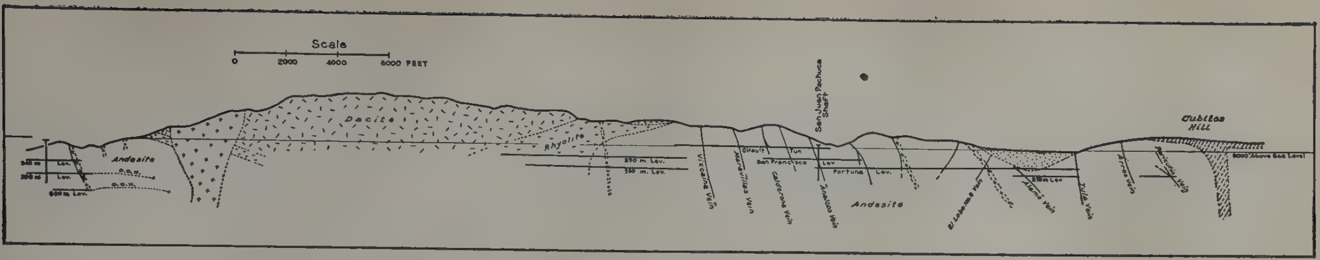

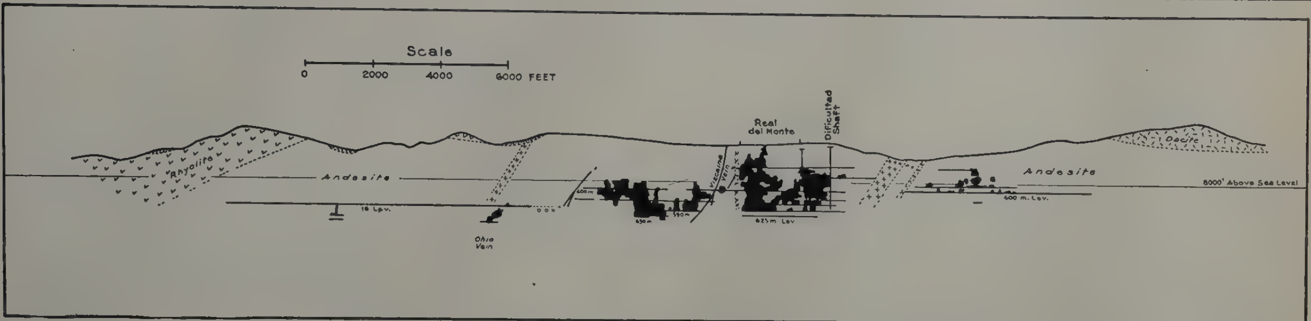

Fig. 2 (Above)—Santa Rosa-Cubitos section, looking east.

Fig. 3 (Below)—Santa Ines section, looking west.

face. Vein outcrops consist of quartz bands ranging in width from a few inches up to several feet, being invariably between hydrothermally altered walls marked by light iron stain. Since their ore shoots are exposed at the surface, these veins were exploited in early times. Drainage of the northeastern slope has eroded this area into strong relief, and the rugged country is dotted with shafts and surface workings along the veins. The zones of hydrothermal alteration are marked in a rough way by large irregular patches of weathered iron-stained andesite. Intervening exposures of less altered rock consist of andesite which is moderately chloritized but otherwise relatively fresh. The adjacent block to the south, as shown in Locality VI, presents some striking contrasts and is described below under *Veins Below Moderate Surface Alteration.*

Outcropping Veins with Ore Shoots Not Reaching the Surface: Some examples of these veins are found in the northern part of Cubitos Hill, north of the blanket of post-ore basalt, see Locality IV in Fig. 1 and the section in Fig. 2. The Tula vein, which is about 7 ft wide, consists of a 3 or 4-ft dominant band of white porous crushed quartz, separated from narrower quartz bands by silicified, partially replaced andesite or dacite. Metallic minerals are not prominent but sparse specks of pyrite, silver sulphide, and native silver may be detected with the hand lens. Locally the wall rock is bleached and pyritized for several feet outward from the vein but is not otherwise notably altered. The proximity of valley alluvium to the projected position of the vein at the surface leaves some doubt as to whether the main structure is really exposed at the surface, but the strip which may represent at least part of the vein consists of a 30-ft band of quartz stringers which vary in width from ¼ in. to 6 in. Minor specks of pyrite are present and limonitic stain is prevalent. Silicification is locally intense, although it does not extend more than a yard or two laterally into surface rock. The only general primary alteration of the wall rock appears to be characteristic chloritization of the andesite; however, within the vertical range of ore a considerable part of the wall rock is a reddish-brown dacitic member of the andesite series that shows little or no chloritic alteration. The top of ore is several hundred feet below the surface and the vertical range of ore is approximately 700 ft. There is no evidence of appreciable removal of silver by leaching, and the top of ore, as in practically all other cases, represents the upper limit of silver deposition in commercial quantities.

Veins Below Strong Surface Alteration: Above the rich and highly productive Tapona vein there is strong surface alteration, shown in Locality V, Fig. 1, and in section in Fig. 6. In this particular locality the characteristic common type of alteration and weathering is outstanding. There is no outcrop of quartz or other normal vein filling, but in a strip of bleached and iron-stained surface some 200 ft long and 50 ft wide there is an unusual accumulation of quartz float, presumably residual, from thin, sparse quartz stringers. Bed rock exposures are too limited to indicate accurately the extent of the band of alteration. A tight northwesterly-striking fracture is discernible in discontinuous exposures. Surface samples of tiny stringers in this obscure fracture zone have assayed as high as 0.5 oz Ag.

Below this area of accumulated quartz fragments the main productive section of the Tapona vein has been mined up to within 300 ft of the surface, and the top of the continuous quartz vein may reach to within 200 ft of the surface. The main productive section extends approximately 1500 ft on strike and 1000 ft vertically. Beyond the main section ore reoccurs far to the southeast in shoots of less extensive vertical range whose tops lie much farther below the surface than the upper limit of ore in the main part of the vein. Above these ore shoots to the southeast surface alteration is comparatively moderate. Here the more intensely altered surface corresponds, therefore, to the section of heaviest ore deposition.

In the range between its upper and lower extremities the Tapona vein typically consists of a 5 or 6-ft zone of quartz bands and ribbons in silicified and otherwise mineralized andesite, the adjoining wall rock being chloritized and locally sericitized. Base sulphides are prominent in the lower productive part of the vein. The upper and middle sections of the vein were locally the source of rich specimens of silver sulphide and wire silver, which could be

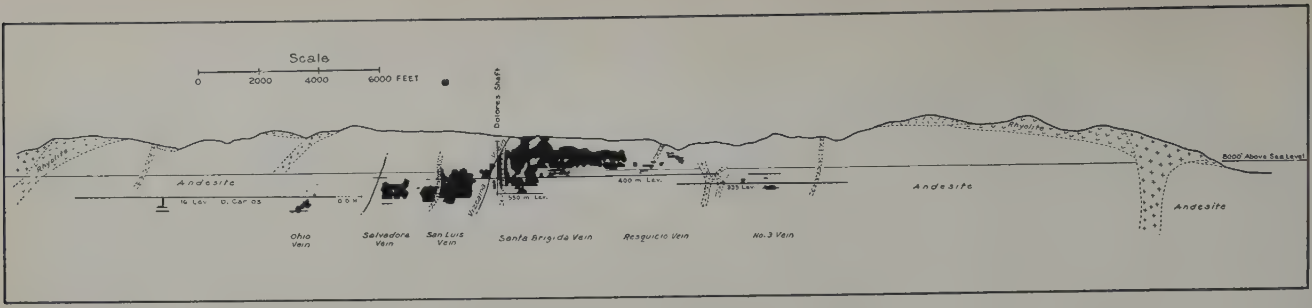

Fig. 4—Section along North-South veins, looking west.

seen in the ore of normal grain only with the aid of a hand lens. The width of ore was highly variable. Normally the stoping width was about 12 ft, but in some places the wall rock was so impregnated with silver that stoping widths reached 100 ft, the orebody consisted of partially-sericitized, chloritized andesite cut by numerous quartz stringers. In these wide sections much of the ore looked like ordinary unmineralized greenish andesite, and stoping limits had to be determined by close assay control.

Quartz gangue increases in width to 8 or 10 ft in the lower productive part of the vein, and still deeper, where a diamond drill hole cut the vein 100 ft or so below the general bottom of ore, the width of vein quartz and highly silicified andesite is about 25 ft. Thus from a maximum known depth below commercial values quartz diminishes upward and fails to reach the surface except in the minor degree of tiny discontinuous stringers. It is supposed that below the diamond drill hole intercept the quartz decreases downward as it is known to do in other deeply explored veins.

The Alfredo vein, one of the rich discoveries of more recent times, is a good example of strong surface alteration far above the top of ore. Ore shoots within the productive strike length are spaced along a stretch of 2000 ft. The vertical range of ore is about 1800 ft, the top being about 700 ft below the surface. A quartz-rhodonite gangue is most abundant from the middle to the lower vertical range of ore. The upper limit of the vein consists of minor quartz stringers in a seam of soft, bleached, clay-like substance. Kaolinization is locally intense in the walls of the upper part of the vein. The surface shows a 200-ft zone of iron-stained weathered andesite elongated along the northwesterly course of the vein, though the total extent of surface alteration along strike is indefinite because of accumulations of soil. At the surface the color of this elongated area is a rather uniform buff shade which stands out prominently against less discolored adjacent areas. Within the zone of more pronounced iron stain there are patches of bleached andesite and marked concentrations of quartz float. The only visible quartz outcrop is a lens about 10 ft long and 8 in. wide enclosed in residual hydrothermally altered and weathered andesite. Curiously, this isolated and possibly erratic stringer does not show the northwesterly strike of the vein but has a northerly trend. As in other zones of alteration which overlie veins, it is difficult to find either quartz or altered rock which shows even low silver assays. One familiar with the significance in the Pachuca district of these surface features would probably consider such an area favorable, but he would see little, if anything, on the surface to indicate the position or attitude of the ore-bearing structure. If a prospect shaft were sunk in this area, it would not show iron-stained andesite for more than a few feet below the surface, below which the rock would be moderately kaolinized and chloritized and locally pyritized and sericitized. If a prospector sank on the small quartz lens previously mentioned, he would probably find it too elusive to follow. It would present a discouraging aspect for hundreds of feet below the surface. As a matter of fact, some time before the turn of the century, a prospect shaft was sunk at the west end of the altered zone in the hanging wall of the vein, and at about 300 ft below the surface the shaft cut the vein. At this point the vein consists of 6 or 8 in. of quartz in soft, bleached andesite and shows low silver assays. After a little drifting the work was abandoned at an elevation of some 400 ft above the top of ore. It was not until later that exploration at greater depth reached this part of the district and the Alfredo vein was developed.

Veins Below Moderate Surface Alteration: The foregoing representative cases illustrate that surface alteration is especially conspicuous in areas where the top of the vein is roughly several hundred feet below the surface. It may be added that the closer the top of the vein to the surface, the greater the indication of a mineralized fracture. However, it does not follow that surface alteration is always most prominent in the areas of vein outcrops.

An example of moderate surface alteration above veins is the area immediately south of the town of Real del Monte and south of the Vizcaina vein. It is indicated in Fig. 1 by Locality VI. Some of the veins are shown in section in Figs. 3 and 4. This area has undergone less intensive erosion than that to the north and the terrain is rolling rather than rugged. The remarkable feature of this general locality is that though it is a block of ground of enormous aggregate production from a number of strong veins there are no vein outcrops or exposures of mineralized fractures which might be vein structures. This is the area of the Dios Te Guie, Colon, San Luis, and other notable north-south veins. These north-south veins have quartz-rhodonite gangues with fine metallic bands of silver and associated sulphides. Minute crystals of base sulphides are usually present. As a rule it is only in and near the lower zone of ore deposition that base sulphides become relatively abundant in erratic shoots and segregated masses. Only in the extreme upper zone, very near the top of ore, do the gangue minerals diminish until the veins become one or more narrow quartz stringers usually ½ in. or less in width. These veins show practically no gouge due to movement. Claylike material along the fracture above the ore zone is mainly attributable to the action on wall rock of hydrothermal agencies and the subsequent action of surface waters. Here also are several strong veins of northwesterly strike whose upper limits of ore are far below the surface. In their upper zones these

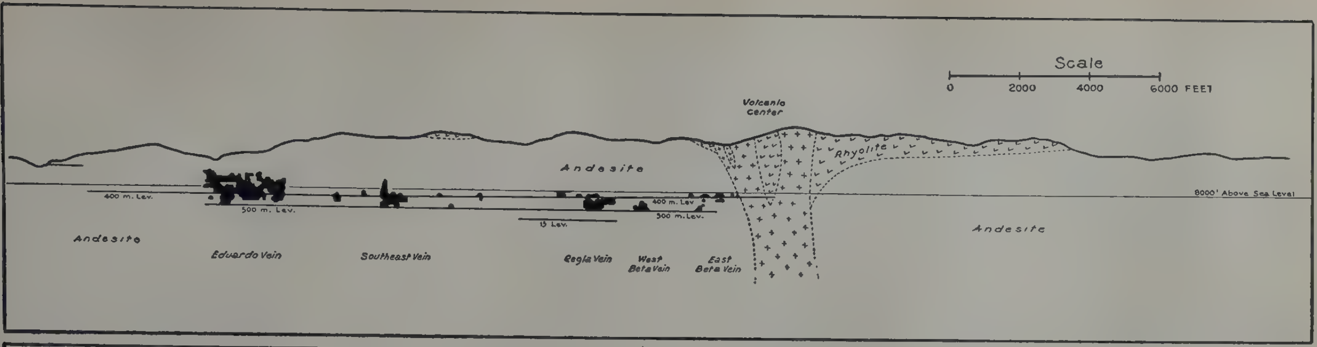

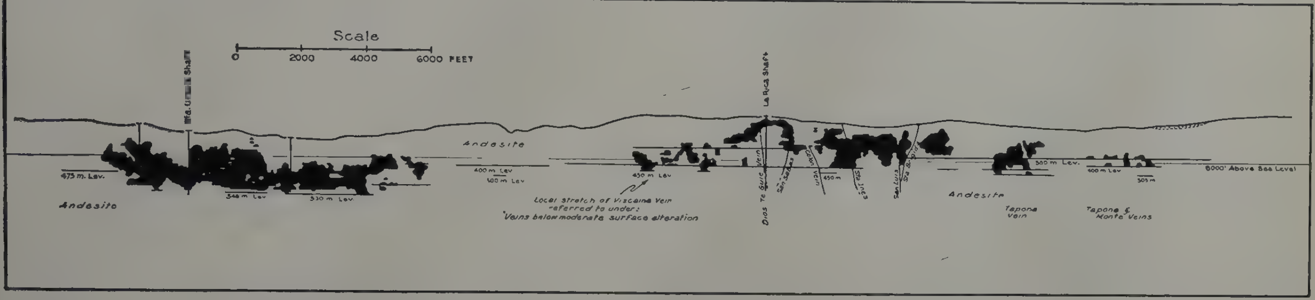

Fig. 5 (Above)—Section along Eduardo vein and veins to southeast, looking northerly.

Fig. 6 (Below)—Vizcaina-Tapona section, looking northerly.

show a more marked predominance of claylike material over quartz than do the north-south veins. The northwesterly-striking veins are marked by more or less post-ore faulting.

The entire area shows lightly iron-stained, slightly bleached andesite, the alteration being so extensive that it can hardly be associated with vein mineralization except in a general way, and yet it is undoubtedly coincident with the extensive, highly productive veins which exist at relatively great depth. Subsurface alteration consists of extensive chloritization and local pyritization. The distance between the top of ore and the surface ranges from 1100 to 1600 ft. Here and there on the surface are patches of small pieces of quartz float, which locally are numerous enough to suggest the presence of one or more quartz stringers. Traceable fractures are nonexistent, although there are some poorly-defined trends of quartz float and belts of relatively strong bleaching which might possibly be the more specific surface expressions of certain deep-seated veins. Prior to development it would have been impossible to make a fair appraisal of such a block of ground. Early property seekers could surmise the prospective value because of its proximity to neighboring productive ground, because of possible extension of known veins into this ground, and finally, perhaps, by comparison of the surface alteration with that above neighboring productive ground to the north. The last would be of doubtful value because of the tendency of this type of alteration to extend well beyond known veins.

The Eduardo vein and a certain productive stretch of the Vizcaina are included in Locality VI and shown in section in Figs. 5 and 6. Neither vein shows an outcrop in this locality, although in neighboring areas the Vizcaina is marked by an easily traceable mineralized structure. Surface alteration is locally strong but in this general area is moderate and widespread, and while it is apparently the result of hydrothermal activity indefinitely associated with ore, there is no specific surface feature to indicate the position of ore-bearing fractures. The alteration is characterized by extensive but irregular bleaching and iron-staining in the andesite, resulting in prominent discoloration with various shades of tan and yellow.

Exploration of the Vizcaina vein in this locality was a matter of driving on it westerly from Real del Monte workings at a convenient elevation well within the vertical range of ore on numerous other veins, this being the 400-m level, which is about 1500 ft below the surface. Ore shoots were found within the interval of strongest surface alteration, a stretch which consists of prominently bleached, iron-stained andesite. Earlier work in a long stretch of this vein farther to the northwest, where the surface shows similar but less intense and less extensive surface alteration, showed only weak metallization.

The Eduardo vein was found as a result of general exploratory cross-cutting combined with diamond drilling. The dimensions of the productive portion of this vein are roughly as follows: The width, as in most veins, is normally 8 to 10 ft. The vein is 2300 ft along strike and 1000 ft in vertical range, and the top of the ore is 400 ft or more below the surface. Quartz deposition was strongest in the middle and lower elevations of ore deposition. Quartz bands and stringers with an aggregate width of several feet persist to hundreds of feet below the bottom of the ore, but this chief gangue mineral eventually diminishes with depth. In the uppermost workings above the top of ore quartz pinches out and the vein diminishes to a thin gouge seam measurable in inches. The andesite wall rock is moderately and uniformly chloritized, and in the upper extremities of the vein it shows some kaolinization. At the buff-colored surface there is an inconspicuous fracture which shows locally minute quartz stringers up to ¼-in. wide. This may represent the vein at the surface, but correlation is doubtful.

Veins Below Weak Surface Alteration: In Locality VII are several comparatively small isolated areas of alteration similar to the large ones described above, though weaker and less extensive, see *Veins* in section in Fig. 5. In a general way these areas might be correlated as surface expressions of the Regla, Beta, Delta, and Monte veins, whose tops and upper limits of ore are 1000 ft or so below the surface. The altered areas span hundreds of feet, but their irregularity of exposure does not permit description of shape and alignment. The veins of this locality are mainly of northwesterly strike. They do not have the length and vertical range of the great north-south veins of Locality VI, but as a group they have contributed appreciably to the Real del Monte production. Quartz predominates as the gangue only in the lower sections. It gradually decreases from the middle to the upper portion of the productive zone, and there is a corresponding increase upward of soft hydrous minerals including sericite and kaolinite. When production from the middle and upper portions of these veins began to supplant that from the more quartzose north-south veins, the large amounts of these claylike gangue minerals caused a new and permanent settling problem in the cyanide mill. The characteristic wall rock alteration is uniform though moderate sericitization, just as chloritization is common to the wall rock of contiguous productive areas to the north and west. Pyritization is widespread but less extensive than sericitization. These alteration products are the work of agencies which permeated the wall rock for hundreds of yards outward from the veins, and upward beyond the limits of ore deposition.

At its upper productive extremity a typical vein of this area consists of a soft, claylike seam confined to a fracture zone one foot or so in width. It is doubtful that specific surface fractures can be correlated with these veins; however, in the areas of surface alteration there are zones of quartz float which lie close enough to the upward projections of certain veins to suggest relationship. These areas were trenched and sampled for the purpose of obtaining data which might be useful in future exploration. Only discontinuous quartz stringers were found and assays rarely showed more than traces of silver.

Veins Not Below Surface Alteration: Prior comment refers to Locality VIII north of the Vizcaina where veins lie below a large area of rhyolite. This exposure of rhyolite shows no sign nor alteration which suggests that the upper limit of one of the strongest veins of the district is but a few hundred feet below the surface.

Altered Areas Below Which No Veins Were Found: As the foregoing descriptions suggest, surface alteration may be a definite indication of underlying veins in certain cases, while in other cases it may be only a broad and general indication. Reliance on this indefinite guide alone involves the difficulties of determining the location and trend of the ore-bearing fracture. Where alteration is comparatively weak there is the additional problem of ascertaining the extent to which regional alteration outreaches silver deposition. Locality IX is an outlying part of the district where there are a number of isolated areas of altered andesite similar in type but less extensive than those already described under *Veins Below Weak Surface Alteration.* In the search for new veins this locality was explored within an assumed favorable vertical range. Strong fractures were found showing locally abundant pyrite, sericite, and calcite, but with only minor quartz and no silver. That neither silver nor appreciable amounts of quartz were shown indicates the locality to be beyond the limit of metallization, though still within the range of agencies of hydrothermal alteration.

Summary

Of those Pachuca veins whose upper limits lie below the surface, there are some which are obviously associated with strong surface alteration; others, which lie far below large areas of altered surface rock, are not definitely indicated by any discernible surface feature. Where the surface shows intensely altered andesite and conspicuous quartz float several hundred feet above the upper limit of a vein, it may be inferred that this is a definite surface expression; but where surface alteration is moderate and widespread, its relationship with underlying veins is less definitely indicated. The alteration results in a certain amount of bleaching as well as moderate to light iron staining. The areas of alteration may extend hundreds of yards beyond the immediate locality of a productive section of a vein, especially along strike, the lateral extent into wall rock being somewhat less; consequently these altered areas may not give more than an approximate indication of the position of an underlying vein. Moreover, because hydrothermal alteration outreaches district metallization it cannot be assumed that every isolated altered area is underlain at some depth by an economically important vein. But in spite of the uncertainty as to the interpretation of all altered areas, a common relationship between extensively altered surface rock and underlying veins is manifested in some cases.

The study of alteration above the upper limits of ore in the Pachuca district, as in others, is viewed as a progressive one. More detailed work on the identification and associations of significant minerals might provide important contributions to the present knowledge of this subject. A study of representative specimens of altered rock forwarded by A. R. Geyne, geologist for the Cia. de Real del Monte y Pachuca, has corroborated the conclusions of former investigators as to the presence of sericite and kaolinite mentioned in the foregoing descriptions. These specimens also showed montmorillonite and other clay minerals not mentioned in this paper because of the relatively few check samples involved.

Acknowledgment

The writer wishes to acknowledge helpful suggestions and comments by Mr. R. N. Hunt and Mr. C. B. E. Douglas of the U. S. Smelting, Refining and Mining Co., and Dr. P. J. Shenon of the University of Utah. He is obligated also to Mr. A. R. Geyne of the Pachuca staff for constructive suggestions and contribution of miscellaneous data.

References

Ezequiel Ordoñez: The Mining District of Pachuca, Mexico. *Trans.* AIME (1902) **32**, pp. 224-241.

Horace V. Winchell: Geology of Pachuca and El Oro, Mexico. *Trans.* AIME (1921) **66**, pp. 27-41.

Carlton D. Hulin: Geology and Mineralization at Pachuca, Mexico. Abstract in Geol. Soc. Amer. *Bull.* **40** (1929).

Edward Wisser: Formation of the North-South Fractures of the Real del Monte Area. *Trans.* AIME (1937) **126**, pp. 442-486.

E. S. Bastin: Mineral Relationships in the Ores of Pachuca and Real del Monte, Mexico. *Econ. Geol.* (1948) **43**, No. 1, pp. 53-65.

C. L. Thornburg: Some Applications of Structural Geology to Mining in the Pachuca-Real del Monte Area, Pachuca Silver District, Mexico. *Econ. Geol.* (1945) **40**, No. 4, pp. 283-297.

Prospecting the Piceance Creek Basin For Oil Shale

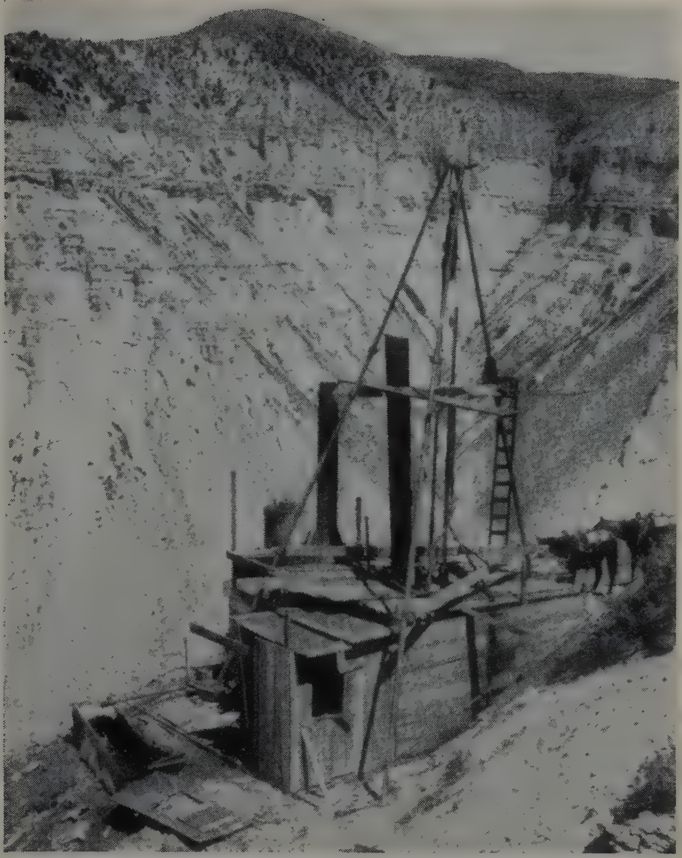
Fig. 1—Oil shale drilling near DeBeque, Colorado, shortly after World War I.

by Tell Ertl

THE Piceance Creek Basin in northwestern Colorado is believed to contain the richest large deposit of oil shale in North America. The major portion, about 1650 sq miles, is bounded by the White River on the north, the Grand Hogback, which runs from Meeker to Rifle, on the east, the Colorado River to the south, and the drainage basin of Salt and Douglas Creeks on the west. The Basin is a plateau 7000 to 9000 ft high, composed of 3000 ft of the Green River series of Eocene age and surrounded by a steep escarpment of 1000 to 3000 ft. From the escarpment the beds dip gently toward the center.

Although oil shale is found in all members of the Green River series, the rich thick beds are found chiefly in the Parachute Creek member. This is normally capped by 100 to 200 ft of the Evacuation Creek, the youngest member of the Green River series.

Actually the Piceance Creek Basin oil shale is not a shale, nor does it contain oil. It is magnesium marlstone holding solid organic matter capable of being broken down by heat into gases, some of which can be condensed into oil. The marlstone is resilient nonporous rock, difficult to sample by pick or hammer and moil.

Many companies and individuals prospected the Colorado oil shale shortly after the first World War,[1] see Fig. 1, but because of the discovery of large quantities of petroleum in the late 1920's in California, Oklahoma, and East Texas, interest in oil shale development waned and did not revive until World War II. In 1944 the writer, employed by the Bureau of Mines, prospected the high grade oil shale in numerous places along the southern outcrop of the Piceance Creek Basin. Several channel samples about 100 ft in length were cut, see Fig. 2. An eight-man crew needed a week to cut a satisfactory channel 80 ft long in the cliff face. The Phillips Petroleum Co., the Union Oil Co. of California and others also prospected the oil shale outcrop. In 1945 the Bureau of Mines initiated a core drilling program for the purpose of obtaining accurate samples from the Piceance Creek Basin. The U. S. Geological Survey set up a program for the geological study of the Basin that is still going on.[2]

Until the end of 1951 a total of 31 holes was drilled for core with diamond drills, and, in addition, cuttings through the oil shale have been obtained from 4 gas wells drilled by standard rotary oil well rigs. The Bureau of Mines drilled 12 of the holes, the Union Oil Company of California 8, the Standard Oil Company of California 6, the Sun Oil Company 3,

---

TELL ERTL, Chairman, Dept. of Mining and Petroleum Engineering, Ohio State University, is Chairman, Papers and Program Committee, Mining Subdivision, AIME.

Discussion on this paper, TP 3316A, may be sent (2 copies) to AIME before July 31, 1952. Manuscript, Nov. 5, 1951. New York Meeting, February 1952.

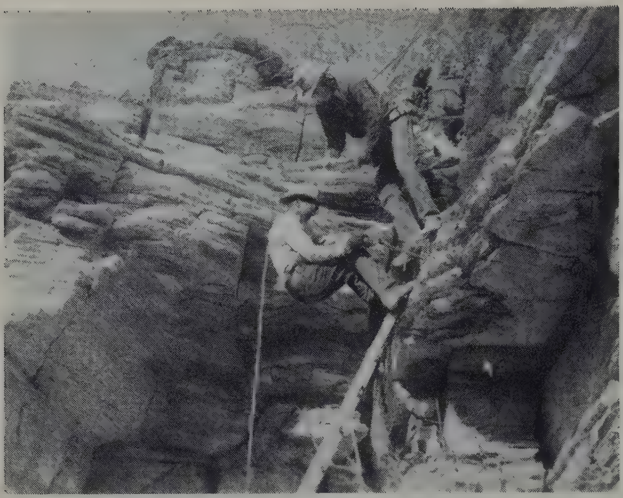

Fig. 2—Channel sampling the oil shale cliff.

and the Pure Oil Company and the Cities Service Company 1 each. Assays of the cores and cuttings delineate an area of 1000 sq miles that can yield 125 billion bbl of shale oil from plus 25-gal-a-ton oil shale, called the mahogany ledge, or 500 billion bbl from the plus 15-gal-a-ton oil shale.[8] The present United States petroleum reserves are estimated to be about 30 billion bbl or about one-quarter the amount that can be obtained from the mahogany ledge of the Piceance Creek Basin.

Core Drilling

The oil shale beds throughout the greater portion of the Piceance Creek Basin dip less than 3°. They are exceptionally uniform in character and thickness. The best method of obtaining samples of the oil shale beds has been found to be by drilling vertical holes for core from the plateau through the rich oil shale. This has been done exclusively by diamond drilling. The first recent oil shale core drilling was done for the Bureau of Mines by the E. J. Longyear Co., which pioneered the techniques used by the other contractors. Among the companies that have drilled for core on the plateau are the Continental Drilling Co., Boyles Brothers, and John Latham.

Because of the semi-arid nature of the Plateau, core holes have been positioned close to the widely-separated streams or springs rather than at locations more desirable for sampling. Nevertheless, a good pattern exists among the holes drilled, although it has been necessary to haul or pipe water long distances to at least six of the holes. At several locations a dam thrown across a dry stream caught enough water for drilling from local thunderstorms that occur in the region during summer afternoons. Snow remains on the plateau until June; therefore access to the sites and drilling cannot start until the beginning of summer. It is foolhardy to attempt to work on the plateau past the latter part of October. Mornings after the middle of September are so cold that water freezes in pipelines and hoses.

At present the following procedure is used in drilling holes on the plateau. A truck trail is built to the site by dozer. The dozer levels off a drillsite and in the more rugged areas, a campsite. The dozer also is used to throw a dam across the local drainage.

Holes 300 to 1100 ft deep are necessary to penetrate through the objective bed, or mahogany ledge, and several have been drilled deeper to explore lower lying oil shale beds. The equipment most often used is comparable to the gasoline engine driven, skid-mounted Longyear UG Straitline or the Joy 22-HD, though lighter machines have been used for some of the shorter holes, see Fig. 3. No portable rigs have been used. Most holes have been drilled 3 in. in diam to yield the 2⅛-in. diam NX core. This large core is desirable because each foot of core provides an adequate sample for assay and permits joint and bedding plane observations. In many holes it has been necessary to case and continue with a smaller hole to yield BX core. In general no additional drilling speed was gained, though core recovery was nearly as satisfactory with BX as with NX. Core recovery through the Parachute Creek formation, which is the chief oil shale member, has been from 95 to 100 pct of the drilled distance when a double tube core barrel was used.

Two holes for dead-men are dug adjacent to the collar site, and logs from local timber are buried about 6 ft deep. To the logs are attached anchor cables to hold the drill firmly in position during the drilling operation. A tripod derrick is erected consisting of built-up timbers, power poles, or locally cut Engelmann Spruce logs. Each leg is 32 ft long and connected on top by a king pin, from which hangs a stationary sheave. A minimum of bracing is used. A ladder or cleats nailed to the main leg is used as a ladderway to the derrick floor, constructed about 16 ft above ground level.

A level base of timber is constructed above the dead-men, and the skid-mounted drill is set on the base and tied down. A hole to firm subsoil or rock is dug and a short, light pipe is placed as a ground casing pipe. A large hole is drilled through the casing pipe and a conductor casing of 3-in. pipe large enough to pass the NX bit is set. This casing is seldom longer than 20 ft and is not cemented. At one site, drilling with the NX bit started on the surface, which was smooth, firm rock.

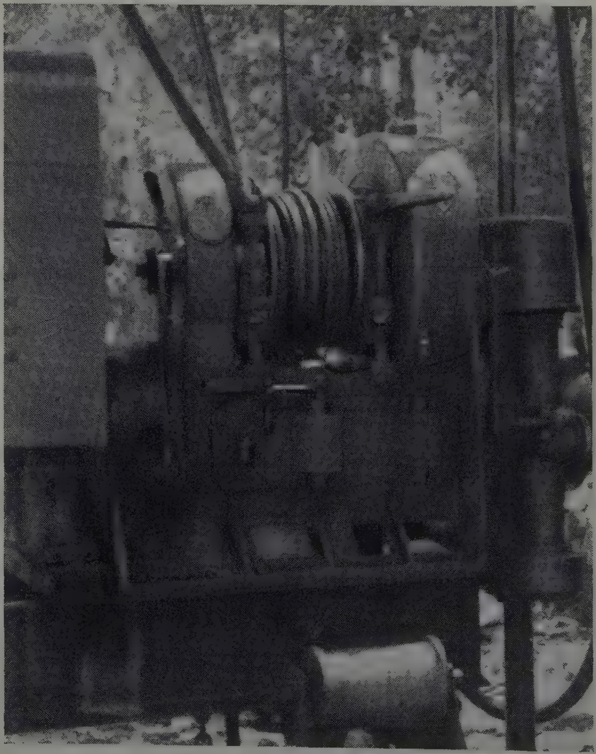

Fig. 3—Class of drill used in diamond drilling for oil shale.

A stock tank or other type of tank with a capacity of 300 to 1000 gal is used adjacent to the rig as a supply tank. A pump draws water from the tank and pumps it at pressures in excess of 100 psi through the swivel head into the hole. Another pump is set near the reservoir to pump the water to the supply tank. If water is hauled it is dumped directly into the supply tank.

Though oil shale is nonporous it contains intercalated layers of volcanic ash and beds from which gypsum, anhydrite, nahcolite, and perhaps other salts have been leached. These intercalated beds are porous and carry away drill water rapidly. As a consequence few holes have been drilled into the oil shale from which water return has been obtained.

The first recent hole was drilled in 1945, see Fig. 4. Because oil shale recovery conditions were unknown, the drilling contract called for core and sludge recovery. The contractor valiantly tried to obtain water return and sludge recovery and spent a great deal of money cementing the hole and using aquagel, oakum, rope, manure, oatmeal, and other specifics successful in sealing drill holes in other instances. As drilling progressed core recovery increased, and it was agreed with the contractor that if he maintained 95 pct core recovery no sludge would be required. That the contractor kept his part of the bargain is shown by Fig. 5. Cores were so good that the contractors now are permitted to pull 10-ft cores rather than 5-ft cores, and many complete 10-ft cores have been recovered.

Because no water return is obtained no provision is made for it, and larger quantities of water than usual are required for drilling. A rough estimate of water consumption is about 100 gal per ft of drilling. Since drilling rates are about 3 in. per min, water consumption is about 25 gpm of actual drilling.

Constant vigilance must be observed during drilling operations because of the cavities and porous zones that are penetrated. Cavities up to 2 ft in vertical height have been intersected, generally without any difficulty except water loss. However, the rapid water loss has resulted in the burning in and consequent sticking of the bit. The bit and core barrel sometimes become stuck because of the caving of beds above the core barrel. Often when these cavings settle above the core barrel they can not be washed away because water is lost below the top of the barrel. When bits and core barrels become stuck, the use of a 400-lb hammer on the hoist line sometimes sets them free. However, several core barrels have been abandoned in the bottom of holes in the Piceance Creek Basin.

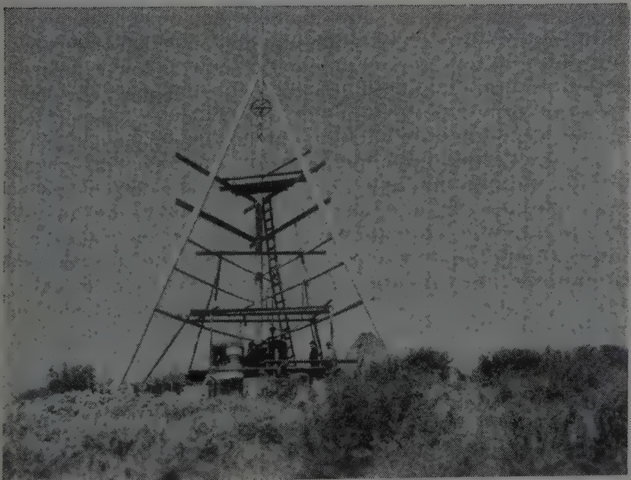

Fig. 4—Outfit used for core drilling oil shale.

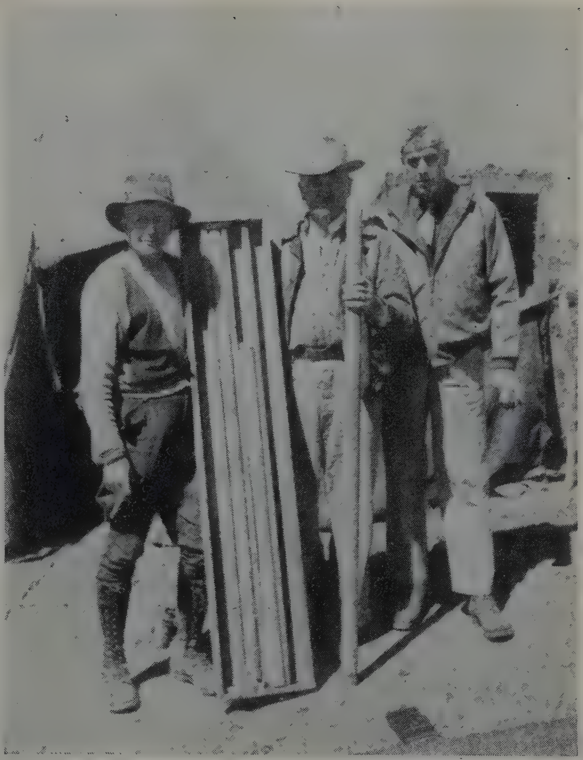

Fig. 5—Typical oil shale cores.

An extra large load is imposed upon the tripod when the rods are lowered into or raised out of the hole because no water is in the hole to help support the weight of the rods. A tripod has been known to fail and a string of rods to part because of the load.

Standard core lifter springs are used to catch and hold the core when it is being pulled loose. The core cut from the fine-grained oil shale is so smooth that often the core lifter does not hold the core tightly enough to break it loose. An experienced driller can feel when the core is broken loose, but even the best drillers have had to fish for it after pulling out an empty core barrel. Most often the core remains standing in the hole and the core barrel is easily passed over it for another try at breaking the core free.

In some holes inclined joints are found which cause the cores to wedge in the bit or barrel, and this in turn prevents further penetration of the drill. Oil shale is so strong that no advance can be made by grinding core. An alert driller can feel the core wedge and stop his machine to make a pull. Poor core is recovered when a driller tries to put 10 ft 1 in. of core in a 10 ft barrel. This practice forces the core against the top of the barrel and the pressure shears the entire core in a spiral pattern.

Despite these difficulties contractors seem to want to renew contracts at $6 per ft for drilling. The cost of road and dam construction and hauling water is in addition to the contractor's price.

Logging, Sampling and Assaying

The drilling contractor delivers the recovered core into a trough or core box at the drill site. A representative of the contractee, usually a geologist, stays with the drill crew to oversee the work and to log the drill cores. Because the holes have been drilled far apart and generally far from the outcrop, careful logging has been necessary to find the objective horizon, the mahogany ledge. The mahogany ledge is that series of oil shale beds that cumulatively assay 25 gal per ton or higher. A persistent 6-in. thick bed of analcitized tuff known as the mahogany marker is found 20 ft below the top of the ledge and 40 to 100 ft above the bottom. This marker is found throughout the Piceance Creek Basin and also in the Uinta Basin in Utah, 100 or more miles from the Piceance Creek Basin. It is a volcanic ash fall, part of which has been altered to well-formed dodecahedral analcite crystals of the size of sand grains. Because of its appearance earlier field geologists called the mahogany marker the sandstone marker or the oolitic limestone bed.[4]

The core from a typical hole is as follows. The hole is collared in the Evacuation Creek member in brown or yellow oxidized sand or siltstone. When the unoxidized Evacuation Creek member is reached it is found to be gray sand and siltstone, in many places containing broken pieces of carbonized vegetable matter. Some marlstone and low grade oil shale beds are found in the member. Marcasite bands are common throughout the section and joint cracks and bedding planes may contain solid bituminous material. The first thick marlstone or oil shale bed is considered to be the top of the Parachute Creek member. This marlstone is gray or olive in color and contains many irregular bands up to 6 in. thick from which gypsum and anhydrite has been leached to leave porous zones of small connected crystal casts. The overall leached zone may be 15 to 20 ft thick. From the leached zone to the bottom of the mahogany ledge the core consists chiefly of oil shale, interbedded with minor amounts of marlstone and shaly marlstone and containing several zones that can be logged over a wide area. A high grade oil shale bed between 4 and 10 ft in thickness frequently is logged 40 to 60 ft below the top of the leached zone. About 100 to 120 ft below the leached zone is found a 10 to 20 ft section of oil shale and marlstone banded with many layers of volcanic ash up to 1 in. in thickness. Partly analcitized volcanic ash bands up to 6 in. in thickness are found in a thin zone about 170 to 200 ft below the leached zone. Another 80 ft down in the hole is found a band of tuff 1 to 4 ft in thickness. The mahogany marker is expected about 100 ft below this thick tuff. The dull white, marcasite-layered marlstone 10 to 12 ft thick that lies directly above the mahogany ledge is a good diagnostic bed. From 10 to 20 ft below the mahogany marker is found the extremely high grade zone of oil shale averaging over 50 gal per ton and recognizable by its appearance and low specific gravity. Below the high grade the tenor of the oil shale gradually decreases, and when low grade oil shale is encountered the hole usually is considered to have reached total depth. Many other less persistent leached zones and volcanic ash zones are found throughout the section.

The cores after they are logged are placed in wooden core boxes made up of four compartments each 2⅛x2⅛x62 in. in size. Each box holds core from at least 20 ft of hole. When full the wooden cover is nailed onto the box. A full box is a good load for one man. The wooden boxes are used chiefly to protect the core throughout the rough truck trip from the drill site to Rifle where the core is split or sawed for sample.

The first cores taken were split in the conventional manner. It was found that oil shale does not split readily into equal halves, and to get accurate samples for assay it was decided to cut the samples longitudinally with a diamond saw. Not only were accurate samples obtained, but the cost of halving the cores was reduced. Furthermore the sawed cores fit neatly into corrugated paper core boxes and can be stored in tall stacks. The half of the core that is not stored is shipped for assay. Sample intervals have coincided with the macroscopic determination of geologic intervals. However, because the change of tenor of the oil shale is gradual, it has been found desirable to take the sample at regular intervals. Most often the sample interval has been 1 ft through the high grade zone, though sample lengths of 2, 4, 5, 10, and 50 ft also have been used. Samples are referred to their distance above or below the top of the mahogany marker.

Samples have been assayed by the Bureau of Mines and the various oil companies. Since 1946, when the Bureau of Mines developed a method of assaying by a modified Fischer retort,[5] all assays have been run in an identical manner. Oil shale assays are indicative only because pilot-plant sized retorts have been operated that yielded as much as 115 pct of Fischer assay.

Assay results of all the drill holes have been made available to the Bureau of Mines and through them to the public. The results have been graphed and compared and a remarkable similarity noted. The U. S. Geological Survey has had access to all the cores and has logged them independently as part of a broad study of the geology of the entire basin.

The present estimates of oil yield from the Piceance Creek Basin, 125 billion bbl from the mahogany ledge and 500 billion bbl from the plus 15-gal-a-ton oil shale, are a result of the prospecting of the Basin done up to the present time. But a sampling of 31 cores from 1000 sq miles of oil shale conveys only a general picture of the reserve. Before any commercial exploitation of the oil shale can begin, each mining area will have to be prospected thoroughly to ascertain the grade and thickness of the oil shale to be mined, the strike and dip of the beds in the immediate mining area, the physical properties of the roof and pillar rocks, and the bedding planes and leached zones which may affect mining practice.

References

[1] R. Burnham: The Oil Shales of Colorado. *California Oil World* (February 1922) **14**, pp. 3, 6, 75.

[2] D. C. Duncan and N. M. Denson: Geology of Naval Oil Shale Reserves 1 and 3, Garfield County, Colorado. U. S. Geol. Survey *Oil and Gas Investigations* (1949) Preliminary Map 94.

[3] Carl Belser: Green River Oil-Shale Reserves of Northwestern Colorado. U. S. Bur. Mines *R. I.* 4769 (February 1951).

[4] Martin J. Garvin and John S. Desmond: Construction and Operation of the Bureau of Mines Experimental Oil-Shale Plant 1925-1927. U. S. Bur. Mines *Bull.* 315, p. 31.

[5] K. E. Stanfield and I. C. Frost: Method of Assaying Oil Shale by a Modified Fischer Retort. U. S. Bur. Mines *R. I.* 4477 (June 1949) revision of *R. I.* 3977.

[6] E. G. Woodruff and D. T. Day: Oil Shales of Northwestern Colorado and Northwestern Utah. U. S. Geol. Survey *Bull.* 581 (1914) pp. 1-21.

[7] Dean E. Winchester: Oil Shale of the Rock Mountain Region. U. S. Geol. Survey *Bull.* 729 (1923) pp. 1-204.

Experiments With an Underground Auger

by J. P. Newell and R. W. Storey

This paper deals with a trial operation in underground auger mining with a machine especially developed for this purpose. The experiment was carried out in a thin coal seam with bad roof conditions. Total elapsed time of the operation was about 10 months, ending in August, 1951.

AUGER mining is a form of continuous mining in that it completely replaces with a one-cycle operation the older conventional cut, drill, shoot, and load method of mining. Relatively new, having been utilized only within the last few years, it is even more continuous in its production of coal than some other forms of continuous mining being practiced in this country today.

There are at present coal recovery augers in operation working along strip-mined highwalls from the outside. This paper will deal with underground mining, specifically with an experiment which was carried out with a machine developed for this purpose.

The location of this experiment was in Pike County in eastern Kentucky in the upper split of the No. 3 Elkhorn seam. Coal height was 32 in. and roof conditions were very bad, with 10 in. of soft draw slate coming down with every cut in conventional mining. The coal is high-grade bituminous, excellent for metallurgical coking.

Underground auger mining fills a need for a method of recovering coal in thin seams, under bad roof conditions or in split seams. In many cases it might save money by eliminating the handling of excessive quantities of rock. In fact, if the coal can be recovered, as in the case of this experiment, without mixing with any impurities outside the seam, it may be possible to load or ship a satisfactory product with little or no preparation or cleaning expense. The need for some economical method for recovering coal from thin seams is becoming more pressing as the more profitably mined seams are exhausted.

Basic Principles of Auger Mining

The principles of the auger, or screw conveyor, have long been used in drilling small diameter holes for blasting and other purposes. These same fundamentals apply to large diameter drilling. However, considerably more attention was given to designing a cutting head that would not pulverize the coal and consequently would require a minimum of power to drive it.

The head, as designed for this job, consists of a cylinder 25 in. in diam with steel bits set in 3 positions spaced around the forward rim. A conventional coal drill bit, at the head of a bursting cone in the center of the cylinder, trails the forward rim slightly, see Fig. 1. The bursting cone and auger connections are anchored to the cutter barrel by 3 arms spaced at 120°. This head design proved to be very satis-

---

J. P. NEWELL and R. W. STOREY are with Consolidation Coal Co. (Ky.), Jenkins, Ky.

Discussion on this paper, TP 3334F, may be sent (2 copies) to AIME before Aug. 31, 1952. Manuscript, July 27, 1951. New York Meeting, February 1952.

This page of Mining Transactions AIME follows p. 604. The intervening non-Transactions pages appeared in Mining Engineering.

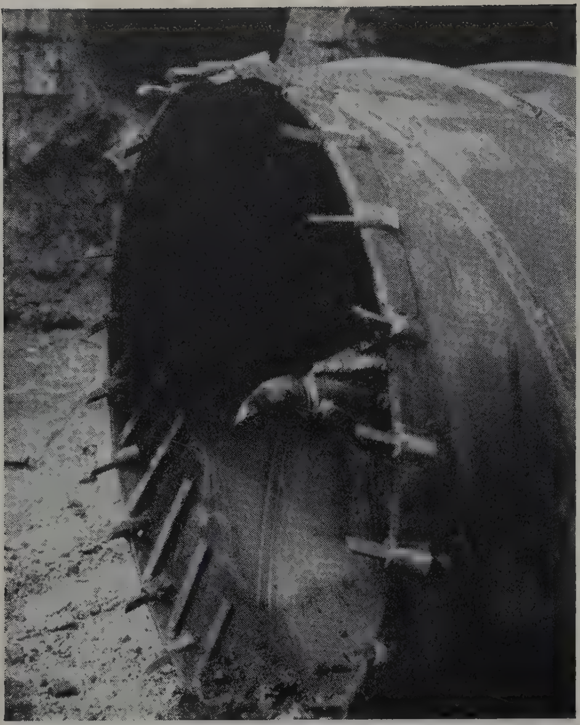

Fig. 1—The drilling head.

factory in producing lump coal as shown by the following screen analysis:

Screen Hole Diam, In.	Pct
8 x 5	13
5 x 3	11
3 x 1	22
1 x ¾	4
¾ x ⅜	12
⅜ x 3/16	14
3/16 x 0	24
	100

Results such as this were found to be obtainable only when cutting at full speed. If a slower drilling rate is used because of weak pressure or dull bits, there is a heavy transfer from the 3x3/16-in. size range to 3/16x0-in. range. The +3-in. size is affected only slightly.

In drilling, the head has a tendency to drift to the right because of clockwise rotation. However, this was not serious since the drift was substantially the same in every hole and the holes remained parallel. Another characteristic of the head as it was originally designed did give considerable trouble: a dip or downward curve in the path of the head was so steep that even with the maximum upward angle short, or penetrating the roof, the holes hit bottom within 40 to 50 ft. Once the head was started into the hole no means was found to influence its direction, either by fast or slow drilling or by changing the angle or elevation of the machine.

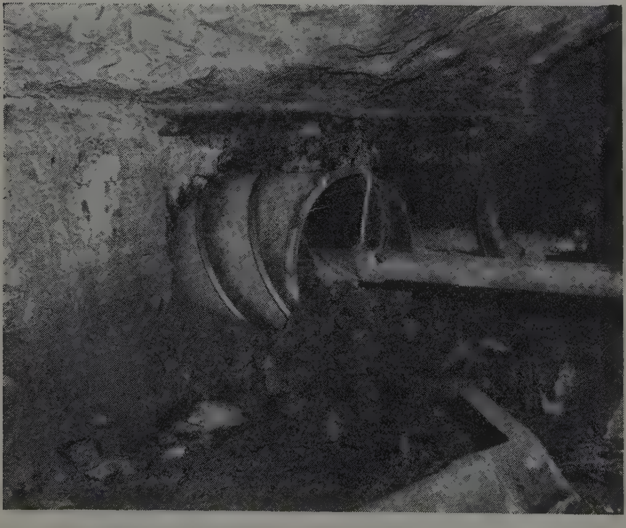

Fig. 3—Drilling head starting into coal. Note lugs around rear edge of head, designed to relieve any downward pressure from the cutting teeth.

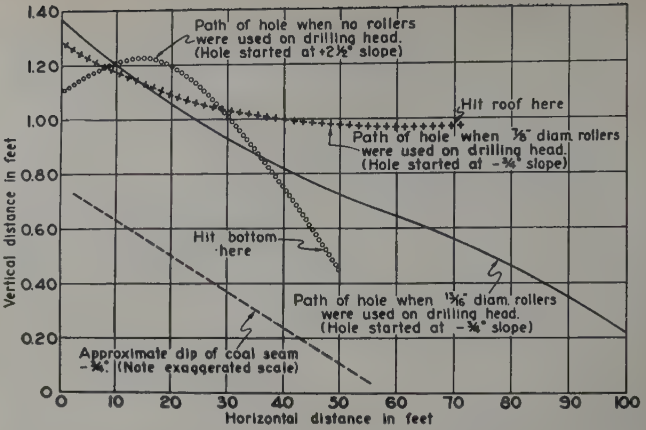

Fig. 2—Typical curves of holes using various methods of controlling vertical movement of head.

Levels were run on the top of each hole (to discount the effect of abrasion on the bottom) and results plotted on a graph, see Fig. 2. The curves of all holes drilled with the same head were similar in shape. This similarity gave some hope that a very uniform performance might be expected after a solution to the dropping curve could be found.

It was thought that if some means were found to remove any downward pressure from the forward end of the cutting head, especially the weight of the head itself, the curved path of the hole could be flattened. This was accomplished by welding a series of lugs around the outside of the cylinder approximately 2 ft back from the cutting edge, as illustrated in Fig. 3. This would give a fulcrum, so to speak, upon which the cutting edge could be cantilevered upward, thus raising the teeth up from the bottom of the hole. It was found that varying the size of these lugs not only flattened the curve but also caused it to curve upward; the larger the lugs the more upward the curve. These lugs seriously reduced drilling speed so that later they were changed to the solid steel rollers shown in Fig. 4. These are similar to spherical roller bearings and are 13/16 in. in diam and 1½ in. long.

Experimentation with the rollers to get them set in the right position proved that holes of 90 to 115 ft could be drilled without cutting into top or bottom.

Construction and Operation of the Drilling Machine

The machine used in this experiment was a Cardox-Hardsocg underground coal recovery drill demonstrated in Fig. 5. It is 24 in. high, 10½ ft long in direction of drilling, and 6 ft 4 in. wide, weighing 8000 lb. It is powered by a 25-hp permissible, 250-v D. C. motor driving through a fluid coupling, see Fig. 6. A clutch, a forward and reverse gear box, a chain drive, and a square bar deliver the power to the drive chuck transmission, which travels 6½ ft along the square bar as the head is pushed

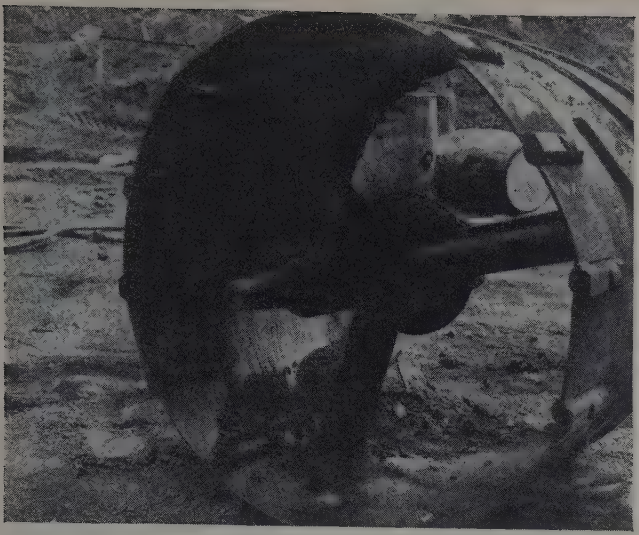

Fig. 4—Rear view of cutting head showing rollers used to support weight of head.

into the coal, giving a rotation speed of 45 rpm, Fig. 7. There is a drive chuck on either side of the transmission, so that by reversing the rotation and using a second set of augers with reverse scrolls to deliver coal on the outby side the operator can drill on both sides of the entry without turning the machine around.

The 25-hp motor also drives a hydraulic pump which furnishes an 18,000-lb thrust, or pull, on the drive chuck, engages and disengages the clutch, operates the gear shift, and raises and lowers the four floor and three roof jacks. The former are necessary to place the head the proper distance from the top and bottom of the seam and at the correct angle, while the latter hold the machine rigidly in position so it cannot shift out of line while drilling. Needle valves lock the jacks once the machine has been set. The frame of the machine is of all-welded steel pipe construction serving also as a reservoir for the hydraulic oil and a housing for the roof and floor jacks, thrust jacks, and cables.

For moving long distances the machine is equipped with detachable rubber-tired wheels on which it can readily be pulled. For short moves from hole to hole there are two pairs of small double-flanged rollers on the bottom of the frame. Thus while the machine is raised on the floor jacks, two sections of light rail may be placed under these rollers. After the jacks are withdrawn the machine can be rolled to the next drilling position; by slightly raising the inby end of the rails one man can accomplish this moving easily. There is also a roller-bearing turntable under the machine which is used to correct any misalignment or to turn the machine 90° or more if necessary.

A puller bar, see Fig. 8, extending from the machine approximately the distance of the hole centers is bolted to the drive chuck transmission. This may be detached during long moves of the drilling machine, see Fig. 9. A hook and chain allow coupling to the string of augers in the completed hole, and by using a second drill head the operator may recover the string a section at a time and use it in the new hole as it is being drilled. This feature prevents cluttering up the operating entry with auger sections and saves time in getting ready to move to the next drilling position when a hole is completed. In other words, there is very little lost motion or nonproductive time once drilling has begun on a certain length of rib line.

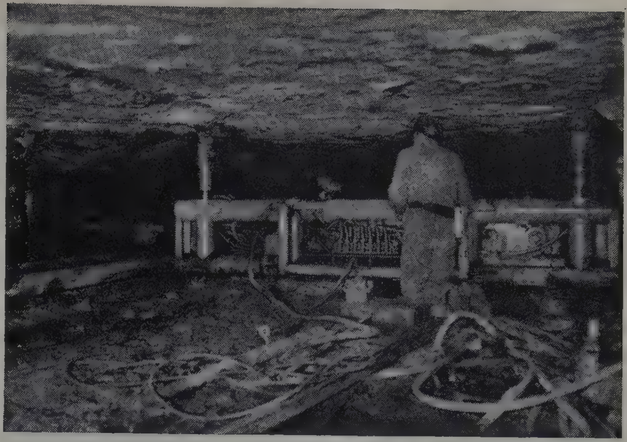

Fig. 5—The drilling machine.

Since the auger delivers its coal at the mouth of the hole on the side opposite the direction of rotation, it may be a problem to pick up the coal and get it to another means of transportation. In this case, where no bottom was taken, a shaker conveyor was used for the purpose, see Fig. 10. A flat pan about 3 ft wide attached to the end of the shaker was placed immediately under the auger string and against the rib. This removed the coal from the scrolls before it travelled more than a foot or two.

Since drilling was done on one side of the entry only, in this case the shaker was very satisfactory. However, this arrangement would present some serious problems if drilling on both sides were contemplated. Possibly some conveyor arrangement could be devised that would not be too cumbersome and would pick coal up from the augers on each side of the entry. This is a much needed feature of the machine that to date has not been satisfactorily achieved for all conditions.

Possibilities and Limitations of Projected Methods

For any system of mining it is generally more economical to get a maximum amount of coal with a minimum amount of development or dead work. This is true in the case of auger mining. For this

Fig. 6—The drilling machine showing string of augers coupled to the drive chuck transmission.

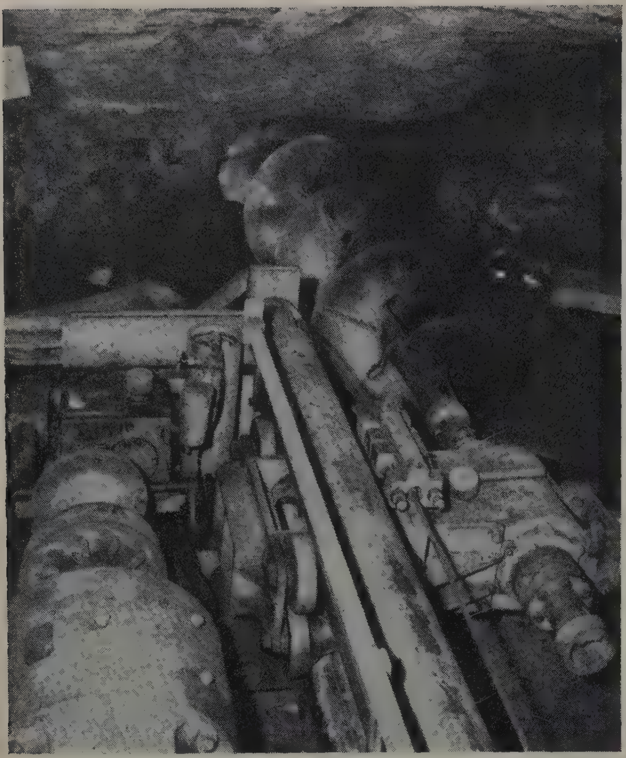

Fig. 7—The drive chuck transmission. Note chucks for drilling in both directions.

reason it is desirable to get maximum length or depth of holes, to be able to drill holes alternately or at the same time on both sides of an entry, and to get a maximum percentage of recovery from the territory developed.

This experiment has proved that under uniform seam conditions of slope and height, holes of at least 100 ft may be anticipated. Rolling or other adverse seam conditions could materially reduce this figure. Also, available power in the drilling machine would limit the depth to which holes could be drilled, although no accurate data on power required were derived from this experiment.

It has been explained previously that the machine used in this instance could drill holes alternately on both sides of an entry. It is entirely feasible that a machine could be developed that would drill on both sides at the same time. This feature in itself brings up the problem of how to develop a territory leaving 100-ft wide pillars for drilling on both sides of the entries and still remain within allowable limitations of ventilation. This may be accomplished by driving entries 200 ft apart and drilling auger holes for air as the entries are advanced, as will be seen in some tentative projections.

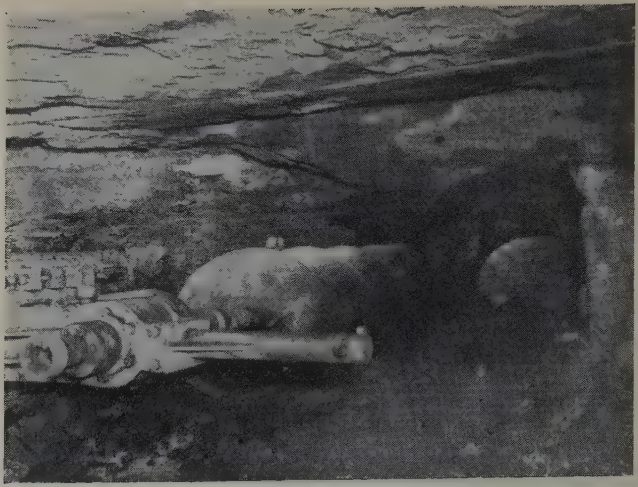

Fig. 8—Puller bar fastened to drive chuck transmission.

The highest practicable recovery will vary from 45 to 55 pct according to seam height and other conditions, owing to the fact that an auger some 6 in. less in diam than the seam height must be selected and pillars of 4 to 8 in. must be left between holes for roof support. A recovery of 50 pct is probably average.

Fig. 11 shows a system of auger mining wherein entries are driven two or three at a time in the conventional manner, with blocks 100x200 ft, one on each side of a single entry, being left for drilling. This system requires a considerable amount of development but may be economical if seam conditions are more favorable toward conventional methods of mining. An advantage is that a considerable territory could be developed ahead of the actual auger mining. Also, ventilation could be kept up by the usual methods, and no auger would be kept in the entry during development.

Fig. 12 shows a system that should be more readily adaptable to thin seam or bad top conditions, since it lends itself to a relatively high production from a concentrated area and requires much less development per ton of auger-mined coal recovered.

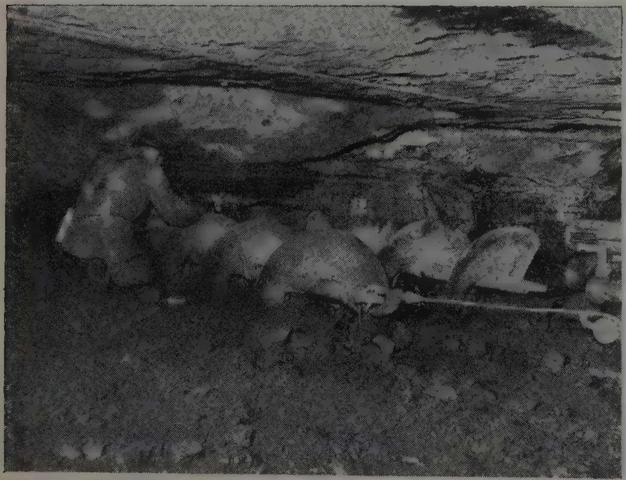

Fig. 9—Pulling a section of auger from the completed hole.

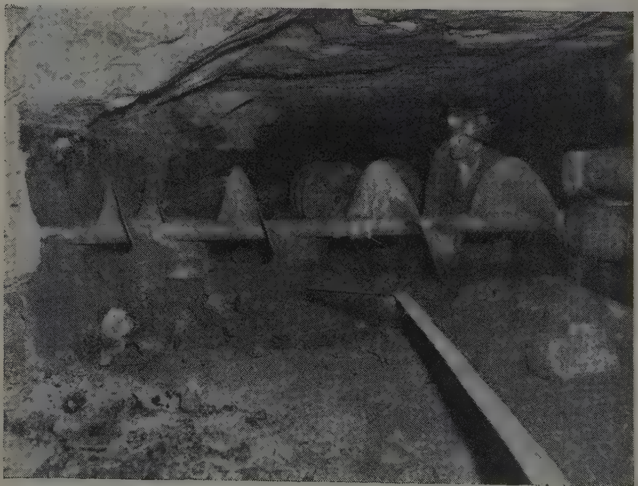

Fig. 10—Shaker conveyor used for transportation of coal from the augers.

Table I. Evaluation of Time Factors in Auger Mining

	Min per Hole
Moving of drill from previous hole, once every 2 holes	7
Leveling and locking drill	5
Starting hole and removing Kelly bar	7
Drilling 100 ft at 0.41 min per ft	41
Retrieving and inserting 16 auger sections	18
Minor delays, 10 pct added	8
Total time per 100-ft hole	86

However, it demands that a machine be available continually for drilling ventilation crosscuts as the entries advance. This projection is far from complete and some serious problems of ventilation have not as yet been solved.

While no details have been shown in either of these systems it is entirely possible that some of the development could be done by auger mining equipment. This might be accomplished by drilling several parallel holes straight ahead and then using some means of removing the pillars between holes to make an entry of whatever width is required. It remains to be seen whether or not this method of entry driving would be practical.

There are, no doubt, other systems of auger mining that will be devised. For instance, it might be adapted very readily to a seam where parting is too thick to allow profitable mining by conventional methods. Such conditions could justify an entirely different approach to the subject of projections, development, and various other factors.

Economics of Underground Auger Mining

For the purposes of this experiment an entry 700 ft long was prepared, with solid coal on one side, and while several difficulties were encountered that impeded the project, a complete time study was made on the drilling of 54 holes. This used up about 150 ft of the entry. The remaining distance was drilled without keeping exact time study records, but the first 54 holes provided sufficient data to make reliable production estimates. Evaluation of the time study data showed that certain results could be expected, see Table I.

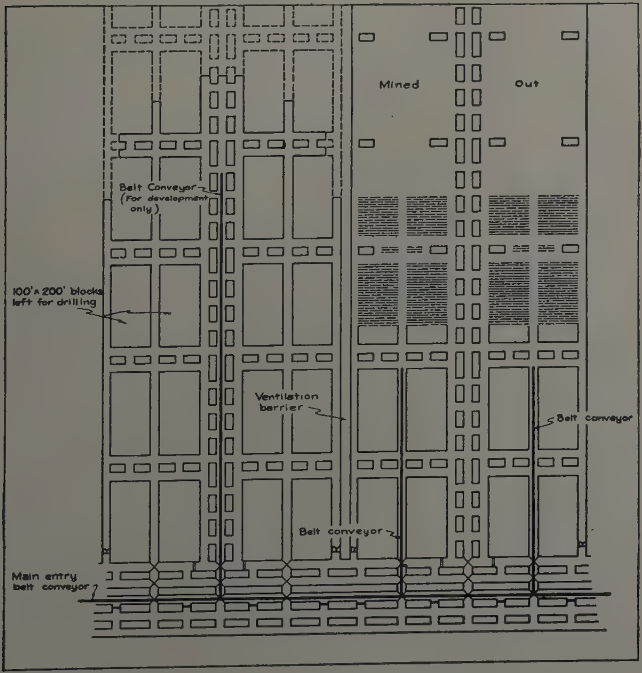

Fig. 11—Projection for a system of auger mining wherein entry development is by conventional mining methods.

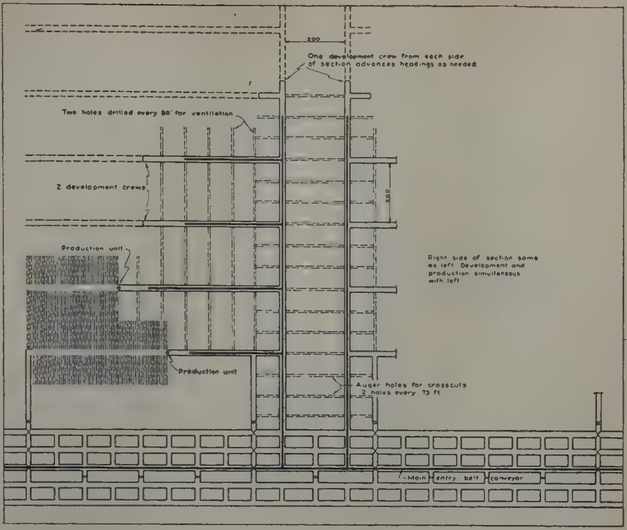
200
One development crew from each side of section advances headings as needed
Two holes drilled every 80' for ventilation
2 development crews
200
Production unit
Production unit
Right side of section same as left. Development and production simultaneous with left
Auger holes for crosscuts 2 holes every 75 ft
Main entry belt conveyor

Fig. 12—Projection for a system of auger mining incorporating a very low ratio of development to production.

With 420 min of work time per shift this would allow 4.9 holes per unit per shift to be drilled. On this basis, using a 25-in. diam cutting head, a production of 13.6 tons per hole or 66.6 tons per unit shift would be realized.

Probably the best way to show what production and economy could be expected from underground auger mining would be to assume a complete section, such as that shown in Fig. 12. This theoretical section would employ eight coal recovery augers and four development units. Actually only four of these augers would be on full production of coal at any given time, the other four being kept on hand by development crews for drilling ventilation crosscuts. If a 25-in. diam cutting head is used, assuming a coal height of 30 to 32 in., production is estimated as shown in Table II. The figures would resolve into 967 tons daily, at 12.3 tons per man-shift on the section. At 80 pct performance the production would be 774 tons.

If seam height were such that larger diameter holes could be drilled the production per unit would increase greatly. For instance, if drilling 37 in. diam holes were feasible, using four machines on three shifts, coal production could reasonably be estimated at a total of 1980 tons per day, with full production at 1750 tons and development recovery at 230 tons. An 80-pct performance would give 1584 tons and on the basis of an assumed 21-man section would mean a production of 25.1 tons per man-shift.

The preceding figures show some very interesting possibilities. Just where the practical limit of hole diameters would be is a matter that will probably be established in the future as the underground mining of coal by auger methods becomes further advanced.

Table II. Estimated Personnel and Production Rates Per Section for a System of Auger Mining

Required Crew	Men per Shift	Daily Production, Four Units on Three Shifts	
Drill operators and helpers	8	Full production	800
Development operators and helpers	8	Development tonnage recovered from entries and crosscuts	167
Cleaners and utility men	2		
Repair man	1		
Misc. (pumper, electrician, etc.)	1	Total	967
Section foreman	1		
Total personnel	21		

Deep Hole Prospect Drilling At Miami, Tiger, and San Manuel, Arizona

by E. F. Reed

CONSIDERABLE deep hole prospect drilling has been done in the last few years in the Globe-Miami mining district about 70 miles east of Phoenix, Arizona, and in the San Manuel-Tiger area about 50 miles south of the Globe-Miami region. More than 205,000 ft of churn drilling have been completed by the San Manuel Copper Corp. at their property in the Old Hat Mining District in southern Pinal County. The deepest hole on this property is 2850 ft; there are 49 holes deeper than 2000 ft. At the adjoining Houghton property of the Anaconda Copper Mining Co., where only one hole reached 2000-ft depth, there were 27,472 ft of churn drilling and 3436 ft of diamond drilling. Three churn drill holes were deepened by diamond drilling methods. Near Miami in the Globe-Miami district the Amico Mining Corp. drilled four holes by combined churn and rotary drilling methods, the total amounting to 13,879 ft, of which 2256 ft were drilled with a portable rotary rig. In the same district, besides doing a large amount of shallow prospect drilling, the Miami Copper Co. drilled two holes of 2560 and 3787 ft, respectively, which were completed by churn drilling methods.

The rocks encountered in drilling at San Manuel and Tiger are described by Steele and Rubly in their paper on the San Manuel Prospect[1] and by Chapman in a report on the San Manuel Copper Deposit.[2] The rocks are well-consolidated Gila conglomerate, quartz monzonite, and monzonite porphyry. In some places these formations stand very well while being drilled, and three holes were drilled without casing, the deepest of which was 2200 ft. In other holes faulted and fractured ground made drilling difficult.

In the Globe-Miami district the deep drilling was done in the down-faulted block of Gila conglomerate east of the Miami fault and in the underlying Pinal schist. The geology of this area is described by Ransome.[3] In the Amico holes the conglomerate varied from material consisting entirely of granite boulders and fragments to a rock made up of schist fragments in a sandy matrix; in the Miami Copper Co. holes there were more granite boulders and the material was poorly consolidated. Drilling was much more difficult and expensive in the Miami area than in the San Manuel district, mainly because of the depth of the holes and the formations drilled.

All the deep hole prospecting described in this paper was done with portable rigs. The churn drill rigs were of several types, of which the Bucyrus-Erie were the most popular. Bucyrus-Erie 28L, 29W, and 36L rigs were used on some of the deeper holes on the San Manuel property. A few Fort Worth spudder types were tried, and the deepest hole at San Manuel was drilled with a Fort Worth Jumbo H. The spudder type is considerably larger than most other rigs used on this work and required a larger location site. The spudders were belt-driven machines with separate power units, and time required for setting up and moving was much longer than with the more portable drills.

All the churn drilling was done by contractors or with machinery leased from them. A few of the contractors had complete equipment, including most of the necessary fishing tools. Unusual and special fishing tools were obtainable from the supply companies in the oil fields of New Mexico or in the Los Angeles area. Most of the contractors used equipment with standard API tool joints, so that much of it was interchangeable.

Failure of tool joints is one of the principal causes of fishing jobs. It can be minimized if the joints are kept to the API specifications and the proper sized joints are used in the various holes. The minimum sizes that should be used with various bits are as follows: 12-in. and larger bits, 4x5-in. tool joints; 10-in. bits, 3¼x4¼-in. tool joints; 8-in. bits, 2¾x3¾-in. tool joints; 6-in. bits, 2¼x3¼-in. tool joints; 4-in. bits, 1⅝x2⅝-in. tool joints.

Two rotary drill rigs were tried at San Manuel on the same hole, and a portable rotary drill rig was used on the Amico drilling for test coring the formation and for drilling in holes 3 and 4. Rotary drilling differs from churn drilling or cable tool drilling in that the bit is revolved by a string of drill pipe and the cuttings are removed from the hole by a thin solution of mud pumped through the drill pipe. The principal parts of a rotary rig are the power unit, a rotating table to revolve the drill pipe, hoists to raise and lower the pipe and to handle casing, and a pumping system to circulate the drilling liquid. The rig used on the Amico property at Miami was mounted on a truck. The larger rig used on the San Manuel property was hauled by several trucks and had separate turntable and pumping units.

Diamond drill coring equipment was used successfully with the rotary rig in the holes on the Amico property. To allow for 2⅜-in. drill pipe with tool joints, 3½-in. core barrels and bits were used. With the standard 3½-in. core barrel there was considerable difficulty in maintaining circulation with mud, so a barrel was designed with a smaller inner tube and a broad-faced bit. This allowed coarser material to circulate between the barrels. Rock bits of 5⅝ to 3⅞ in. were used with the rotary rig for drilling between core runs.

Diamond drill equipment is much lighter than churn drill tools, so that fishing tools can usually be obtained from supply houses by air express when needed. Three churn drill holes on the Houghton property at Tiger were deepened by diamond drilling with Longyear UG Straitline gasoline-driven machines. The open churn drill hole was cased with 2½-in. black pipe.

In deep hole churn drilling, casing is one of the most important items, especially in drilling in unconsolidated material like the formations drilled by

---

E. F. REED, Member AIME, is a geologist with Anaconda Copper Mining Co., Inspiration, Ariz.

Discussion on this paper, TP 3337AI, may be sent (2 copies) to AIME before Aug. 31, 1952. Manuscript, Dec. 3, 1951. New York Meeting, February 1952.

the Miami Copper Co. and the Amico Mining Corp. At Miami it was furnished by companies. At San Manuel it was furnished by contractors and the company paid for casing which could not be recovered from the holes.

When available, casing for deep wells should be seamless, with API long collar joints and 8 round threads to the inch. Pipe lengths as long as the rig will handle should be obtained. Miami Copper holes were started with 24-in., double-ply 8-gage casing, as the first part of the holes was drilled through tailings. This was followed by 20-in. water well casing. Some 16-in. water well or slip joint casing was used in Amico hole No. 4.

The strings used by Miami Copper Co. allow drilling the deep part of the holes with larger tools and make it possible, when necessary, to complete a hole by running a 4¾-in. liner, see Table I. The 6⅝-in. and 4¾-in. strings used by Amico give more clearance. If the hole is advanced much beyond the larger sized casing the 6⅝ and 4¾-in. strings will follow better.

Casing is recovered from a completed hole by driving it up from the bottom with a casing spear while it is being pulled at the top by elevators. When it is too tight in the hole to be recovered it frequently can be loosened if part of the string is cut off. Collar busters and casing rippers will usually cut a string at the required point. Casing can also be parted by blasting, but this often bells out the break and causes further difficulty in recovery.

After the collars and threads were cut off some of the casing used in the first Amico holes it was used again as a butt-welded string in holes 3 and 4. This is at least as strong as thread and collar casing, but if it becomes stuck it is very difficult to recover without rotary casing-cutting equipment. About 85 pct was recovered in the drilling at Miami.

Churn drilling at San Manuel has been described by Steele and Rubly[1] and by Chapman.[2] Four of the deepest holes on that property were drilled with different types of churn drills, with the results shown in Table II.

Table I. Thread and Collar Casing Used at Miami

Miami Copper Co.		Amico Mining Corp.	
Size, In.	Weight, Lb.	Size, In.	Weight, Lb.
16	70		
13⅜	48	13⅜	54.5
10¾	40.5	10¾	45.5
8⅝	28	8⅝	36
7	23	6⅝	26
5½	15.5	4¾	16

These figures indicate that in the holes where the longest runs were made the greatest speed of advance was obtained. It is likely that if properly handled the various rigs would have equivalent drilling speeds in the same rock. The Jumbo H takes more time to set up or move than the other rigs but would probably drill just as fast. In recent work at San Manuel a new type of Bucyrus-Erie 36L has been used with a stronger power unit, allowing the handling of heavier strings of casing.

The Bucyrus-Erie 36L type of rig was used on both the Amico drilling and on the two deep holes drilled by Miami Copper Co. Two drill rigs were used simultaneously on both projects, and drilling speed depended on the ground encountered and not on the drill crews. In much of the drilling at Miami it was necessary to lower and underream casing to be sure to reach the depth required. This work was found to entail approximately the same time and cost per foot as the original drilling of the hole. Amico holes 3 and 4 were not underreamed, but neither hole could have been completed by churn drilling to the depth finally reached by rotary drilling methods without considerable underreaming and carrying of casings. In this ground the underreaming method would probably have been less expensive than rotary drilling.

Table III shows the churn drilling performance on the four Amico holes. In No. 1 hole, 1210 hr

Table II. Drilling Results in Four Deep Holes

Hole number	76	86	90	105
Type of rig	B-E 29W	Jumbo H	B-E 36L	B-E 28L
Date started	Sept. 14, 1946	Dec. 19, 1946	Jan. 4, 1947	Dec. 29, 1947
Date completed	Dec. 6, 1947	May 3, 1947	March 3, 1947	Feb. 17, 1948
Shifts worked	206	309	223	142
Total depth	2725	2850	2750	2635
Ft per shift	13.2	9.2	12.3	18.6
Ft per hr	1.65	1.15	1.54	2.32
Drilled with 12-in. bit	1135	1285	1305	920
10-in. bit	525	765	425	955
8-in. bit	425	165	375	685
6-in. bit	640	635	237	75
5-in. bit			408	
Ft drilled, total	2725	2850	2750	2635

Table III. Drilling Results, Amico Mining Corp.

	No. 1 Hole		No. 2 Hole		No. 3 Hole		No. 4 Hole	
	Hr	Total, Pct	Hr	Total, Pct	Hr	Total, Pct	Hr	Total, Pct
Setting up	22	0.3	42	0.6	65	1.6	58	1.3
Drilling	3955	60.2	3326	50.9	3367	81.0	3007	68.2
Not working	551	8.4	736	11.3	336	8.1	518	11.7
Reaming	1093	16.6	1597	24.4	—	—	192	4.4
Preparing tools	96	1.5	126	1.9	65	1.6	129	2.9
Fishing	337	5.1	110	1.7	8	0.2	216	4.9
Repairs	57	0.9	96	1.5	111	2.7	80	1.8
Casing	271	4.2	411	6.3	142	3.4	210	4.8
Miscellaneous	183	2.8	92	1.4	62	1.4	—	
Total	6565		6536		4,156		4410	
Depth drilled, ft	2872		2915		2,769		3067	
Ft per hr, pct	0.44		0.45		0.67		0.70	
Ft per hr (drilling only), pct	0.73		0.87		0.82		1.02	

Table IV. Drilling Results, Miami Copper Co.

	No. 1 Hole		No. 2 Hole	
	Hr	Total, Pct	Hr	Total, Pct
Setting up	194	2.5	34	0.4
Drilling	3563	46.5	5387	63.1
Reaming	701	9.2	1310	15.3
Casing	938	12.2	840	9.8
Fishing	499	6.5	84	1.0
Repairing	100	1.3	129	1.5
Miscellaneous	315	4.1	236	2.8
Not working	1348	17.7	524	6.1
Total	7658		8544	
Depth drilled	2560		3787	
Ft per hr, pct	0.33		0.44	
Ft per hr (drilling only), pct	0.72		0.70	

Table V. Diamond Core Drilling from Churn Drill Holes

	Depth, Ft		
	Hole 5	Hole 6	Hole 8
Diamond drilling, depth started	1218	1005	1530
BX, depth drilled	1610	1305	1710
BX, no. of ft drilled	392	300	180
Core recovery, pct	29.3	23.2	19.3
Rate of drilling, ft per day	8	9	9
AX, depth drilled	1724	1405	1855
AX, no. of ft drilled	114	100	145
Core recovery, pct	7.2	9.0	13.7
Rate of drilling, ft per day	13	33	24

were lost drilling past a length of 8-in. casing which parted and remained in the hole. The two Miami Copper Co. holes were drilled simultaneously. Drilling performance is shown in Table IV.

Different types of bits and various methods of sharpening them were tried on the Amico work without any definite change in drilling speed, which was faster in holes where fewest hard boulders were found in the conglomerate. A number of crew members who had worked with Amico also drilled the Miami Copper Co. holes, using similar equipment, so that relative drilling speeds were influenced chiefly by the formations encountered.

The conglomerate drilled on the San Manuel property was better consolidated and had fewer boulders than the conglomerate at Miami, and the porphyry formations at San Manuel drilled much faster than the Miami schist. Both formations at San Manuel appeared to stand better. The average advance of each size bit in the four holes shown in Table II was 645 ft, while the average depth of open hole drilled by Miami Copper Co. after landing a string of casing was only 118 ft.

The San Manuel Copper Corp. did not allow the use of drilling mud to seal off the water from the walls and help prevent caving, but it was used in all the holes at Miami. The Miami Copper Co. devised a method of mixing a known amount of barite with the drilling mud so that the samples could be analyzed for barium and the amount of mud dilution of the samples determined. Standard methods of churn drill sampling were used in all the drilling.

Two rotary rigs of the portable type sometimes used in drilling oil wells were tried on hole No. 59 on the San Manuel property to obtain some core for metallurgical tests and geological information. The first proved too small, and only one attempt was made to core in the 945 ft drilled with that rig. The second rig drilled to 1000 ft and cored from 1000 to 1608 ft. The core from a hole of 9⅝ in. was 3½ in. in diam. In all, 108 ft of core were recovered, or 17.76 pct of the depth drilled. Drilling and coring took 12 days, so that the rate of advance was about 50 ft a day. This is considerably faster than churn drill advance, but rock bit costs were excessive.

On the Amico property it was found that the deeper part of the conglomerate formation consisted entirely of schist fragments, so that it became impossible to tell by means of churn drill cuttings whether the holes were in conglomerate or solid schist. When hole No. 1 had been drilled to 2870 ft and hole No. 2 drilled to 2915 ft, it was decided to recover core for proof of solid formation. Diamond drill contractors were unwilling to attempt coring at that depth with equipment available, so a portable rotary rig was obtained. Cores were cut from the bottom of both holes, using 3½-in. diamond drill core barrels and 2⅜-in. drill pipe. The rotary rig was equipped with special weight indicators and pressure gages to adapt it to diamond drill work. Excellent and conclusive results were obtained, but the work was expensive for the amount of drilling done.

For similar reasons, coring methods with the same equipment were used in Amico holes 3 and 4. These holes were found to be still in conglomerate, and so were drilled between core runs with rotary drill rock bits. The formation was very abrasive and rock bit costs were high, but the holes were completed by this method with satisfactory results. In drilling with rock bits a large proportion of the cuttings were removed from the drilling liquid with a shaker screen; the fines were removed in settling tanks. These materials were used as rough samples of the formations drilled, but all clay material remained in the drilling stream. Core samples were the only satisfactory indication of the values encountered.

A rock bit core barrel was tried in the conglomerate but did not prove satisfactory, as only 15 pct of the core cut was recovered. Core recovery with the diamond drill equipment averaged more than 50 pct and was better in the schist than in the conglomerate.

At the Houghton property near Tiger, three churn drill holes were deepened by diamond drill methods and equipment. The results of this drilling are shown in Table V. The Longyear U. G. Straitline rigs used were capable of drilling in BX and AX sizes at the depths required, so the holes were started by placing 2½-in. standard black pipe in the churn drill holes. This pipe was cemented in at the bottom and stretched at the top to cut down vibration.

Sludge and core samples were weighed and assayed separately, and satisfactory average values were calculated. In work when high core recovery is necessary, this method could be used with heavier equipment and larger diameter core barrels.

Acknowledgments

Acknowledgment is due the officials of the Anaconda Copper Mining Co., the Miami Copper Co., the San Manuel Copper Corp., and the Inspiration Consolidated Copper Co. for permission to publish this information.

References

[1] H. J. Steele and G. R. Rubly: San Manuel Prospect. *Trans.* AIME (1948) **178**, p. 181; MINING TECHNOLOGY (September 1947).

[2] Thomas L. Chapman: San Manuel Copper Deposit, Pinal County, Arizona. U. S. Bur. Mines *R. I.* 4108.

[3] F. L. Ransome: The Copper Deposits of Ray and Miami, Arizona. U. S. Geol. Survey Professional Paper 115.

Ore Control Methods at Inspiration Consolidated Copper Company

by J. L. Carne

ORE control is a matter of planning and supervision based on a foreknowledge of the content and distribution of ore. The Inspiration orebody is predominately a copper-sulphide blanket, overlain by an oxidized zone of copper silicates, copper carbonates, and barren capping. Most of the ore is treated by leaching, and the optimum requirement of this method is the goal toward which the mining schedule is aimed. Both open-pit operations and underground mining are used. The problems of ore control at Inspiration are: 1—maintenance of metallurgical balance, 2—conservation of oxide ore, and 3—mining out of the orebody at an average grade which parallels that of the reserve figure.

Prior to the fall of 1926 all of the Inspiration division ores were treated by flotation, but the mixed ores of the Live Oak—Keystone section carried too large a proportion of copper in the form of chrysocolla for satisfactory flotation. For this type of mixed ore the leaching process now in use had been worked out, and the plant was put into operation in the fall of 1926.

The process is known as the ferric sulphate leach, and the leaching solvents contain both ferric sulphate and free sulphuric acid. Sulphide copper in the form of chalcocite is leached by the ferric sulphate, and the oxidized copper minerals are dissolved by the sulphuric acid.

From the beginning of operations to the present time the plant has treated some 67 thousand tons of ore having an average copper content of 1.142 pct, of which 0.605 pct has been in the form of oxidized copper minerals. The plant is currently being operated at the rate of 11,500 tons per day, 7 days per week. However, this tonnage is produced in 6 days of mine operation. The average current grade is approximately 1 pct copper, of which about 50 pct is present as oxidized or acid-soluble copper.

Close control of metallurgical procedures is a vital factor in operation of the plant and is in turn dependent upon careful regulation of feed. An excess of sulphide copper requires the presence of more ferric sulphate in the leaching solvents. On the other hand, an excess of ferric sulphate in the presence of a low sulphide feed seriously reduces the efficiency of electrolytic precipitation in tank house operations. This condition must be avoided at all costs.

An additional factor must be considered. It is known that the sulphide content is predominant in the ore which remains in the reserve. To maintain the necessary sulphide-oxide proportion, so that the entire reserve will mine out at both a grade and a sulphide-oxide ratio that will be permissible throughout the remaining life of the property, it is obvious that the oxide reserve must be currently preserved to as great an extent as possible.

Fortunately much of the oxide reserve is found in the open-pit operation. This happy circumstance adds flexibility to the procedure and makes it possible to maintain the close regulation necessary to insure best overall results, both mining and metallurgical.

The two ore streams from the pit and underground operations join at the coarse-crushing plant, and proper control must be exercised before the ore reaches this point. The open pit is currently providing about 55 pct of the ore and underground operations the balance of production. Both operations are under a single superintendent so that the closely interrelated problems may be more readily controlled.

The least flexible of the two producing units is the underground mine, where the mining method is block caving. Although a block of ground may be undercut and developed, characteristics of the material determine its caving action. The ore in the chutes must be drawn.

The area currently mined from underground is in a zone predominately sulphide and is generally

---

J. L. CARNE, Member AIME, is Assistant Chief Mine Engineer, Inspiration Consolidated Copper Co., Inspiration, Ariz.

Discussion on this paper, TP 3347A, may be sent (2 copies) to AIME before Aug. 31, 1952. Manuscript, Dec. 12, 1951. New York Meeting, February 1952.

overlain with a varying column of carbonates and silicates of lower grade. Under the circumstances, these constitute excellent diluting material. They are in turn covered with a column of leached schist or granite porphyry varying from 200 to 500 ft. The Live Oak 800 level, producing about 4000 tons daily, is typical.

In the mining of the Live Oak 800 level, which has produced several million tons, about 30 pct of the copper has been found to be acid-soluble. This information is not available from the original churn drill logs, and it was only after several years of mining that sludges from subsequent sampling were assayed for oxide and sulphide copper. This was a tremendous forward step in classifying the ore. However, where complete churn drilling data are not available past mining records are the only source of information concerning this important classification. As mining records indicate, 30 pct of the copper that comes from the Live Oak 800 level is oxidized in the ore. An attempt is made to get this proportion daily and not as an average of highs and lows. In drawing the blocks it has been found that the first 20 pct of the column will be a very high sulphide, 10 pct or less as oxide; the next 20 pct approximately 20 pct oxide; the following 20 pct about 30 pct oxide, and the final draw assays about 40 pct oxide. With a planned development schedule it is possible to keep one block in the early stages of draw, where drawing is kept at a curtailed rate to get good caving action; two blocks will be in the middle stages of draw, and as good caving action should have taken place by this time, these two blocks will furnish the major portion of production. The fourth block is then in the final stages of life with considerable dilution showing in a majority of the draw points, necessarily limiting the amount of tonnage available. Keeping these producing areas in the above stages of draw prevents the occurrence of slugs of high sulphide from this area. The result is a more uniform character of feed to the leaching plant with better control of the overall oxide-sulphide ratio, which meets the desired condition.

To recapitulate, the basic factors in controlling mined grade from underground sources and maintaining the desired oxide ratio on a day to day average are: 1—a well planned long range development program, with sequence of mining the individual blocks determined by good mining practices, as well as a constant source of production at the overall level grade, and 2—maintenance of the even and planned draw required in the various stages of extraction in any given block.

A careful check is kept on daily underground production by the sampling of the individual train loads from the various blocks, a grab sample being taken from each car before it is dumped. These returns are available to the supervisory staff the morning following sampling. Grab samples are also taken from the stope draw points as needed. This applies particularly when blocks are approaching exhaustion or when dilution has appeared. Quick results are obtainable from the Mine Assay Office, and no draw point need remain idle very long waiting for assay returns. With the information obtained from underground sampling, any necessary change may be made within the level limits to vary the grade, provided that good mining practices are not violated.

At present the open pit produces a higher percentage of acid-soluble copper than the underground operation. The productive area includes the eastern portion of Live Oak orebody and the entire Keystone orebody. The column in this area has a relatively low back of leached waste, and the greater part of the ore is in the oxidized zone with a lesser column of sulphides on the bottom. In the open pit mining the grade can be mined in place, as no dilution problems exist, but in turn it has been necessary to mine down through the oxidized strata to uncover sulphides. The physical characteristics of this pit currently require mining more oxides than desired in the process of exposing the sulphides. Long range planning requires the uncovering of large tonnages of sulphides in the next few years to take up the loss in production from underground sources, but at the same time the oxide reserve must be nursed.

Within the limits of the ore that is exposed in the pit a very close, day to day control of grade can be imposed. The assaying of the blast hole sludges renders the problem a simple one by avoiding the long interpolations common with the normal grid. The following procedure gives the operating staff a detailed knowledge of the material available for mining. Benches are carried at 50-ft intervals and blast holes drilled 5 to 6 ft below grade with sludge from the first 50 ft going into a sample. Normally, one sample is taken for the entire 50 ft, the sludge first being cut by a modified Jones Riffle sampler, mounted on the deck of the drill, retaining one part in 100. The sample is cut by a small hand riffle sampler into a 1-gal bucket, retaining one part in two. The assay values of the sludges are then recorded on the bench assay plans. These are blocked out by blasts averaging 35,000 tons, and the total copper and acid-soluble copper are calculated by averaging numerically the value of the holes in the blast. A broken reserve of 200,000 tons of ore is about normal. The approximate grade of material that will be taken from the mine, coupled with the accurate information of the broken ore on the benches, indicates the digging area on the bench or benches.

For the first ten months of mining in 1951 the grade has averaged 1.022 pct in total copper, of which 0.471 pct is acid-soluble, to be compared with a planned grade at 1.00 pct total copper with 0.40 pct acid-soluble. In total copper this is an extremely close control, considering the variable ground that has to be mined. The acid-soluble copper is higher than desired, but the current schedule in pit mining will give a more flexible control of this phase during the coming year.

The major reserves of sulphide in the open pit lie in the Inspiration division, or eastern section of the orebody. For the past year stripping of this area has been pushed, so by early 1952 the sulphides necessary to hold the overall oxide content to the required minimum can be furnished from the pit. As long as the underground production is limited, and exposed reserves in the open pit contain extremely high oxides, the difficulty in control is keeping the oxide ratio down to the minimum requirements until such time as the sulphides are available in the open pit.

It is safe to say that Inspiration has a unique problem in ore control. For successful and most efficient extraction of the entire remaining ore reserve, great care must be exercised concerning both grade and oxide-sulphide content of the ore as mined.

Some Effects of Sewickley Seam Mining on Later Pittsburgh Seam Mining

by F. R. Zachar

Unmined blocks in the Sewickley seam, surrounded by worked out areas, have been found to transmit overburden loads through the interval strata to the Pittsburgh seam workings 90 ft below. Operating experiences under these conditions are described in this paper.

IT has always been understood, in northern West Virginia where both the Pittsburgh and Sewickley seams are mined, that pillaring or splitting in the lower Pittsburgh seam could break the interval strata and make mining in the overlying Sewickley difficult or impossible. In some instances, however, mining methods practiced in the overlying Sewickley have reversed the problem, resulting in a shifting of the intermediate layer and destroying valuable acreages of the Pittsburgh seam below.

The Pittsburgh seam in this area is, on the average, 102 in. thick. About 18 in. of low-quality head coal are left for roof protection as it is mined. Immediately over the coal are two draw slates, two rider seams, and a good hard black shale, locally called black rock, which serves as a permanent roof where draw slates and riders are taken down on certain main haulroads. In most areas mined in this seam in the past the bottom has been satisfactory but soft. However, in areas now being mined by the Christopher Coal Co. in Monongalia County the bottom is very hard and unyielding.

The Sewickley seam, lying 85 ft above the Pittsburgh, will average nearly 70 in. in thickness and is overlain by massive shales and sandstones. Much of the seam is mined only down to the "sheep skin," a hard band about 4 in. above the bottom, which is composed of relatively hard shale. Fig. 1. shows a typical cross-section through the Pittsburgh and Sewickley seams in the area being discussed. The thin Redstone seam is not deep-mined but is stripped in some locations where it outcrops.

Most of the Sewickley seam in the Morgantown areas has been mined out from 10 to 30 years. There are at present only two large mines and five or six others of small production operating in that seam. Mining systems in the past were generally of the room and pillar type with some full pillar extraction. This seam in the Scott's Run area was operated by as many as thirty or forty different companies at one time, during an era beset with strikes, market failures, and depressions. Most of the barrier pillars along the many main haulroads were abandoned, and blocks of Sewickley coal that would be fully recovered with today's machinery were left unmined when conditions became anything less than favorable. Consequently the mined-out Sewickley is spotted throughout with solid blocks varying in size from 100x100 ft to 200x400 ft and larger. It is these unmined Sewickley blocks surrounded by worked-out portions that have caused transmissions of roof stresses to underlying Pittsburgh mining areas, see Fig. 2, resulting in untold difficulty.

As the Christopher Coal Co. operates both the Pittsburgh and Sewickley seams, accurate maps of workings in both seams are readily available and are regularly consulted. The first Pittsburgh squeeze attributed to overlying Sewickley blocks occurred in the Arkwright mine, where a shuttle car crew was developing a section consisting of seven panel headings. These entries were being driven in solid coal 3400 ft from the nearest worked-out Pittsburgh area. As mining advanced it was noticed that certain ribs began to slough and certain areas to show signs

---

F. R. ZACHAR, Member AIME, is General Superintendent with the Christopher Coal Co., Pursglove, W. Va.

Discussion on this paper, TP 3335F, may be sent (2 copies) to AIME before Aug. 31, 1952. Manuscript, Feb. 15, 1952. New York Meeting, February 1952.

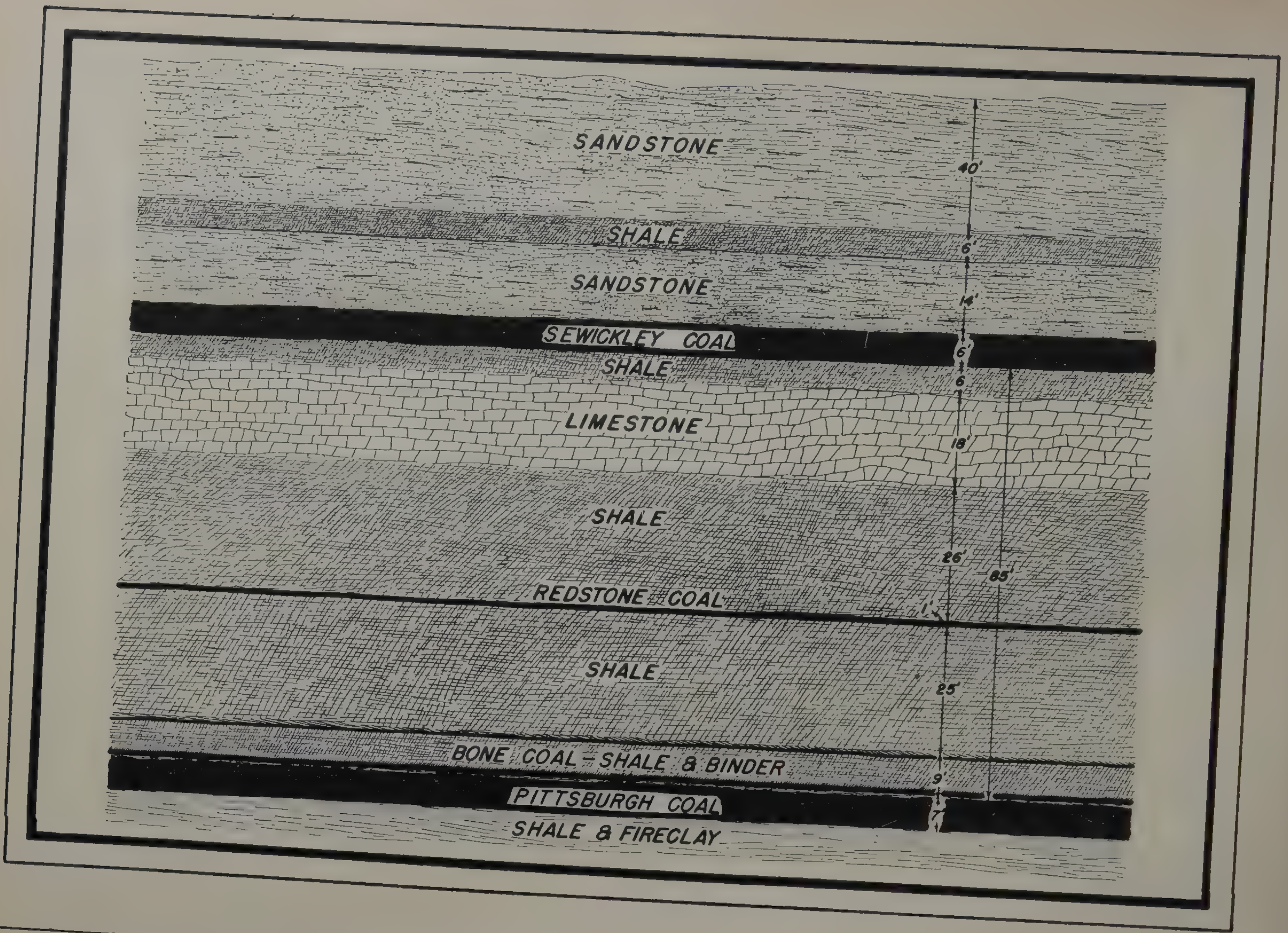

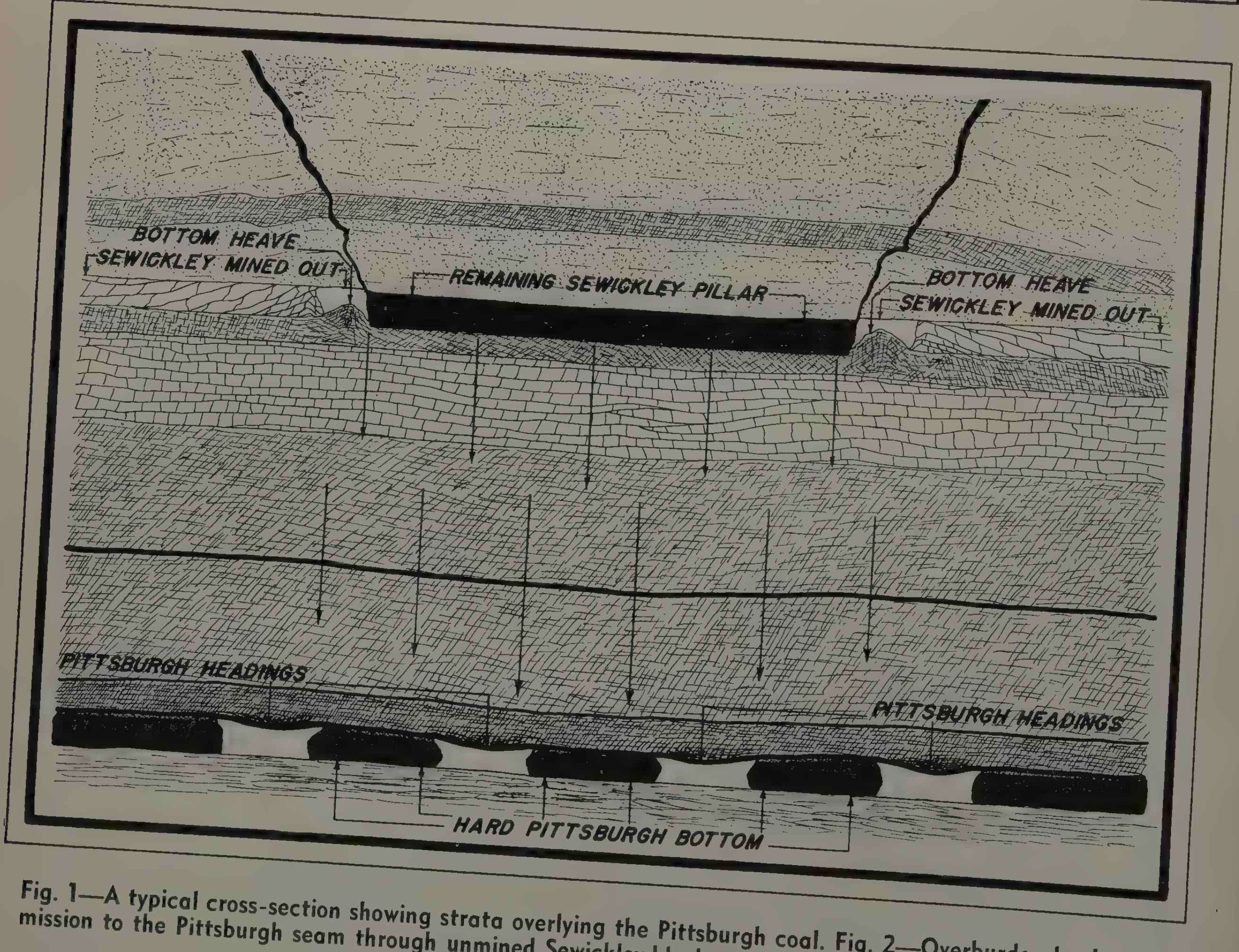

Fig. 1—A typical cross-section showing strata overlying the Pittsburgh coal. Fig. 2—Overburden load transmission to the Pittsburgh seam through unmined Sewickley blocks.

of roof breaks along the ribs. Finally, when the section had been developed to the extent shown in Fig. 3, it was necessarily abandoned and all material and equipment removed because the return air courses could not be kept open. Examination of an overlay map showing both Pittsburgh and Sewickley seams illustrated with remarkable clarity that the squeeze areas in the Pittsburgh were directly under large blocks left unmined in the Sewickley. This is revealed in Fig. 3, where crosshatched lines show squeezed ribs and dotted lines indicate the blocks remaining in the Sewickley seam.

The sketch in Fig. 2 shows what the writer and others believe was the cause of the squeeze. It is their contention that the overburden load pushes the Sewickley block down into its soft bottom. This soft bottom heaves; consequently the ribs of the block do not crush. The load is transmitted through the interval strata to the Pittsburgh below. The Pittsburgh bottom in this area is extremely hard, and inasmuch as it does not crack and heave, the ribs crush and break and the roof breaks over them, as shown in Fig. 2. It is thought that the extremely hard Pittsburgh bottom is altogether responsible for the rib and roof failures in that seam where workings pass under unmined blocks in the Sewickley.

Depth of Sewickley overburden plays an important part in these squeezes. Where the Sewickley cover varied from 50 to 200 ft little difficulty has been encountered in the Pittsburgh seam under the remaining Sewickley blocks. Where Sewickley cover is in excess of 200 ft, however, squeezes can be expected, and where the cover exceeds 300 ft difficulties are almost certain in the Pittsburgh seam under the blocks described.

Another group of headings in the Arkwright mine reacted to the overlying Sewickley blocks in much the same way as those described above. These headings were very difficult to mine where they passed under the blocks, but when they were turned to go between rows of overlying blocks they became normal and profitable to develop and retreat. In Fig. 4 these headings may be seen, together with overlying Sewickley blocks. Here again the crosshatched lines represent the squeeze areas. It was not possible to split the blocks back beyond those shown. Roof failure caused by squeezed ribs is illustrated by Fig. 5 and the manner in which the ribs crush by Fig. 6, a photograph of a corner in the Pittsburgh headings that lie directly under a large Sewickley block. These two photographs were taken in the now abandoned headings in solid coal shown in Fig. 3.

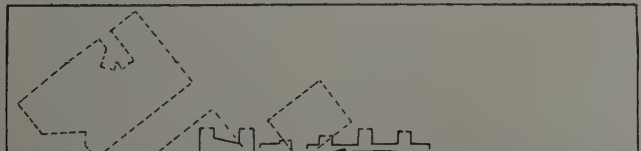

Fig. 3—Squeezed Pittsburgh headings under Sewickley blocks.

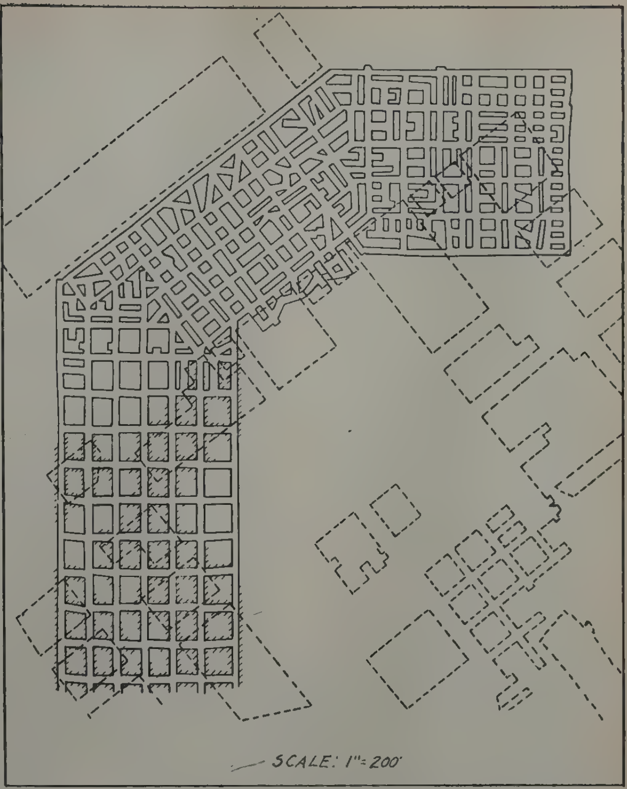

Fig. 4—Squeezed Pittsburgh headings under Sewickley blocks.

Difficulties in keeping haulways open where they pass under these overlying solid blocks can best be shown by the cribbing, see Fig. 7, necessary to maintain the haulway of the section, shown in Fig. 4, developing solid acreage 3000 ft from the nearest worked-out Pittsburgh area. The entry was driven 16 ft wide and all crosscut intersections were roof-bolted with conventional timbers on 4-ft centers between crosscuts. Rib spalling became so severe that in places the entry widened itself to nearly 24 ft. The cribbing shown was necessary to sustain the ribs and to provide cross timber supports. Note how the 6-in. steel H beams are bowed and the wooden beams broken. The steel beams were placed when it became apparent that the squeeze was threatening the entry.

Roof bolting has proved helpful in postponing final caving of headings under these conditions but has stopped neither the final cave nor the squeeze. The entries shown in Fig. 3 were completely roof-bolted with six bolts anchored securely in the black rock to the cut. As the rib failures increased the places widened, and after widening to around 22 ft the black rock sheared at the ribs, causing the entire place to fall and bringing the roof bolts down

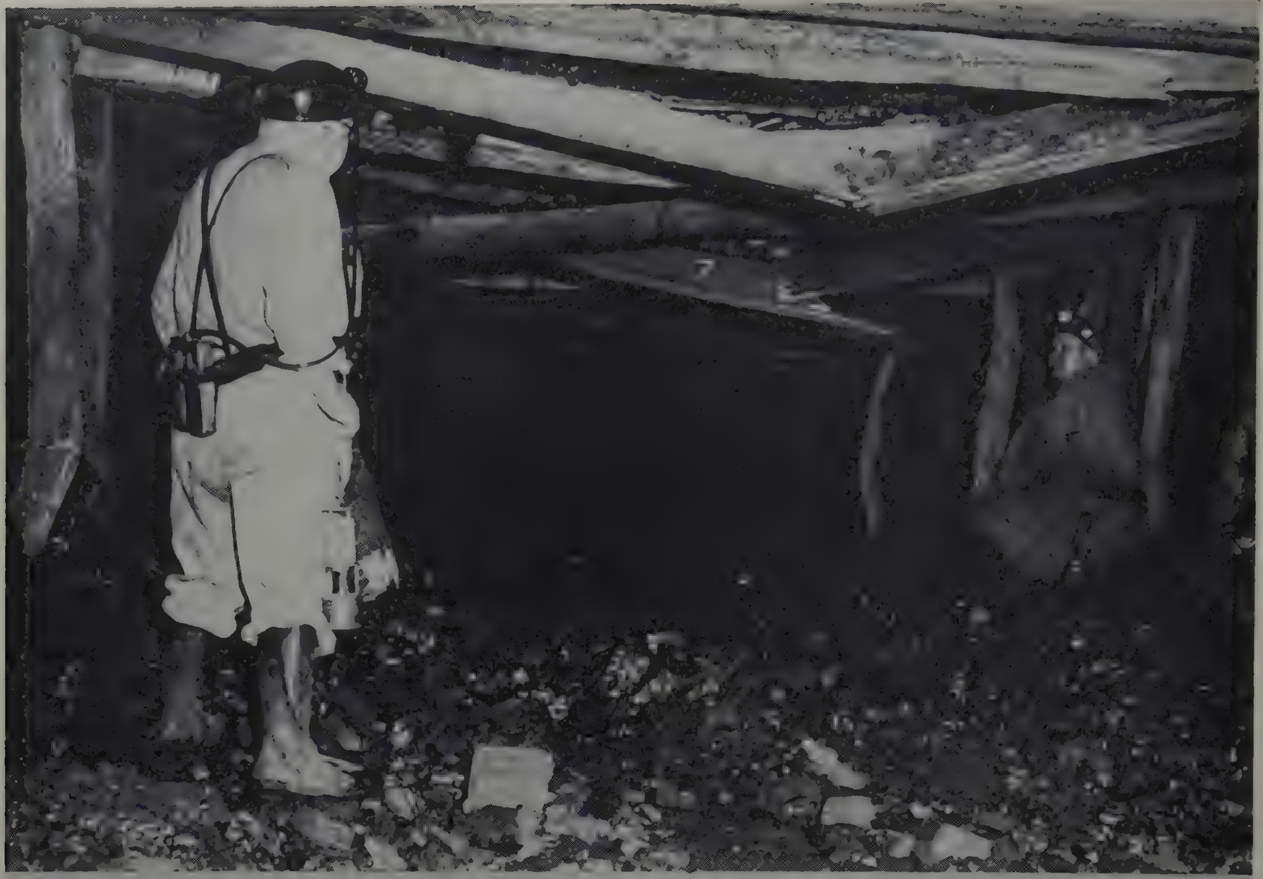

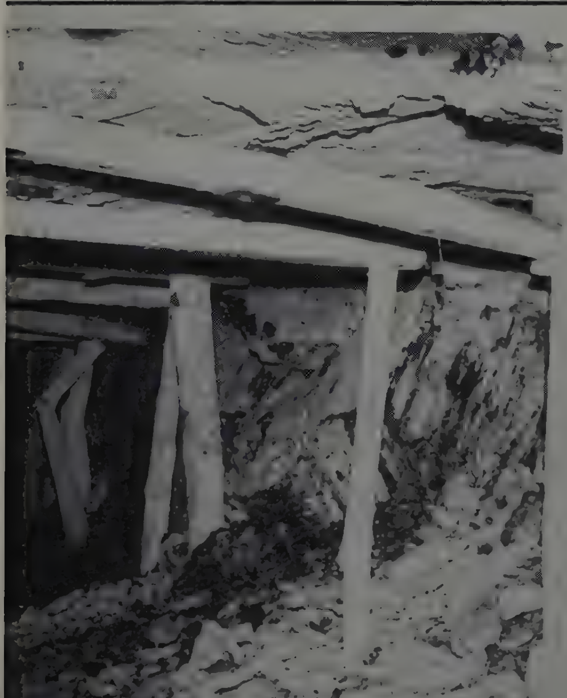

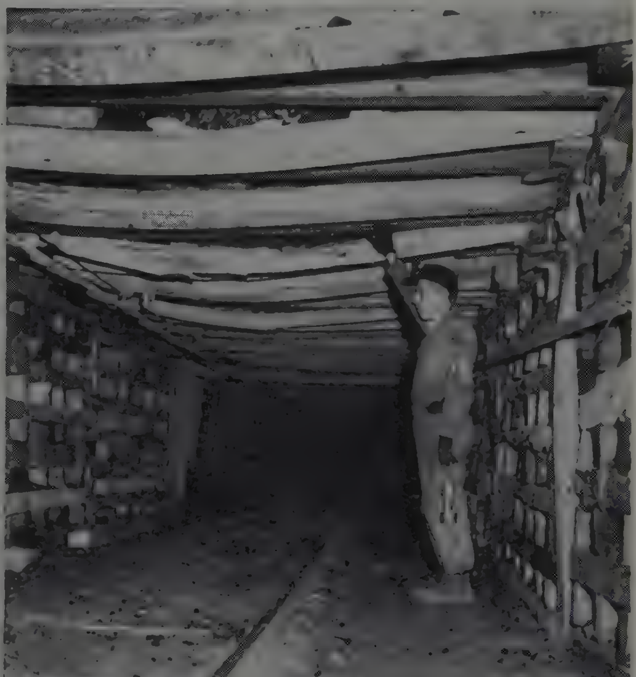

Fig. 5 (Above)—Rib failure on a corner of the Arkwright mine. Fig. 6 (Lower left)—An example of roof failure in the Arkwright mine. Fig. 7 (Lower right)—Cribbing installed in the Arkwright mine to protect the West haulway.

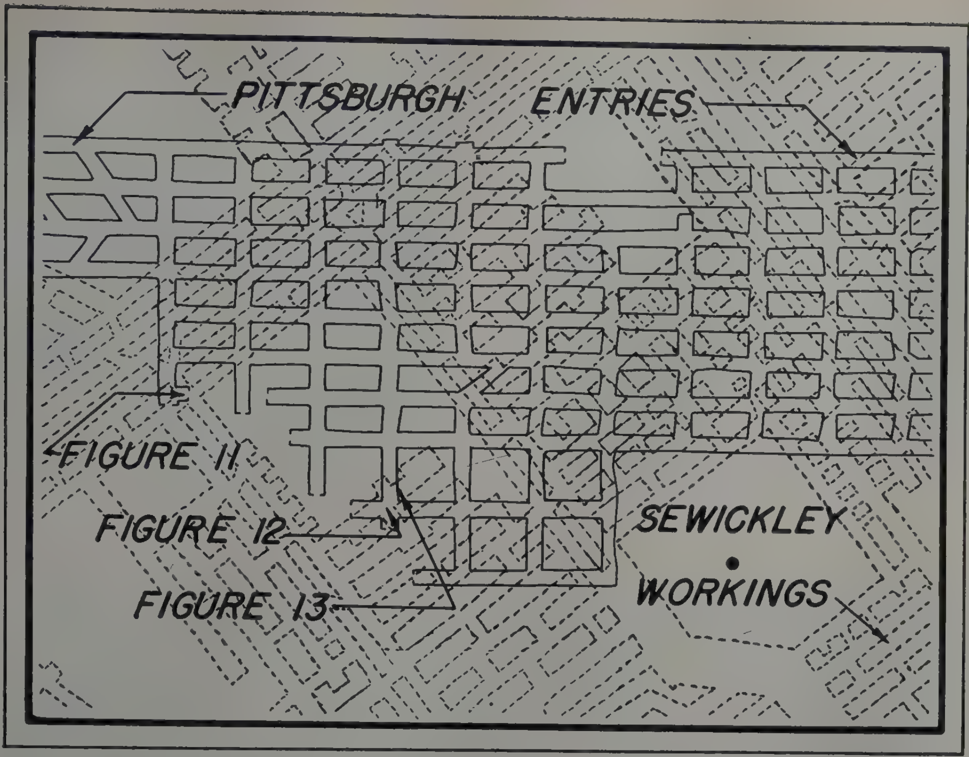

Fig. 8—Squeeze area in Osage mine with overlying Sewickley.

at the same time. Roof bolting does have the advantage, however, of giving mine management more time ~~to~~ install cribs or steel beams, whereas ordinary wood crossbars take the weight so rapidly that they sag and it is difficult or impossible to work under them.

The Osage mine of the Christopher Coal Co. is adjacent to the Arkwright mine, and its development sections are in the same general area. Until recently it has been worked successfully under old Sewickley mines. The past Osage workings were in areas where the Pittsburgh seam bottom was soft and where loads transmitted from the Sewickley above merely caused bottom heave and hence no crushing of the ribs. However, Osage is now developing an area under the old Brock mine workings where the Pittsburgh bottom is extremely hard. In an attempt to develop the main headings of the mine Osage was forced to abandon four headings and to change from off-track to track-mounted equipment to get these entries advanced to a desired point.

Fig. 8 shows the Osage Main West headings and two large overlying blocks of Sewickley coal. The entries under the larger of the two blocks finally had to be stopped, as the squeeze condition became too difficult to work. It will be seen that owing to the same difficulty the outside air course under the smaller block was never driven.

Fig. 9 shows the first stages of rib failure in this area of the Osage mine. This section was entirely roof-bolted but had to be cross-timbered to reinforce the bolts and finally center-posted as shown. Fig. 10 shows later stages of rib failure with beginnings of roof failure on this same entry. Note how deeply the crushing has penetrated the rib and how the roof is breaking away from the bolts in the background. This entry later fell in completely and had to be abandoned.

Further examination of the cause of these squeezes, carried out in the Sewickley seam old works in the Brock mine, revealed at first hand conditions of the entries adjacent to large remaining blocks causing Pittsburgh seam troubles. A study

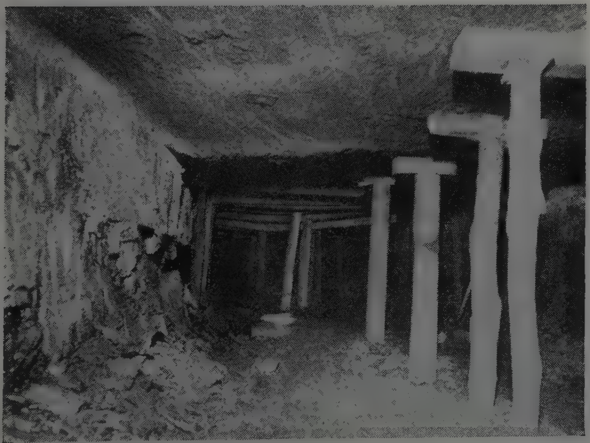

Fig. 9—Early stage of rib failure in the Osage mine.

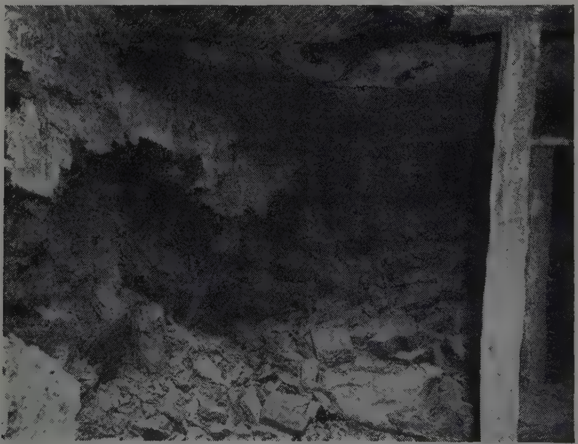

Fig. 10—Later stage of rib and roof failure in the Osage mine.

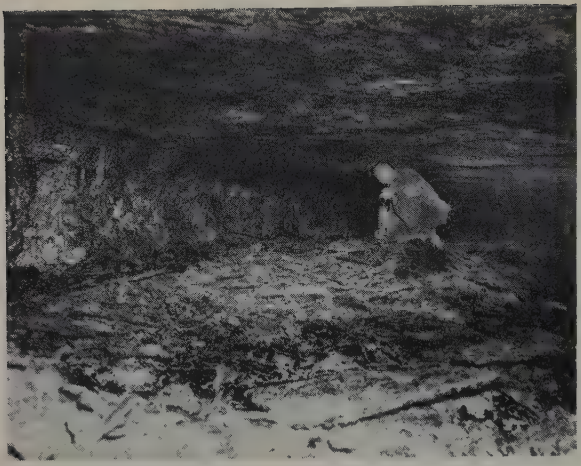

Fig. 11—Bottom heave adjacent to unmined block in the Brock mine, Sewickley seam.

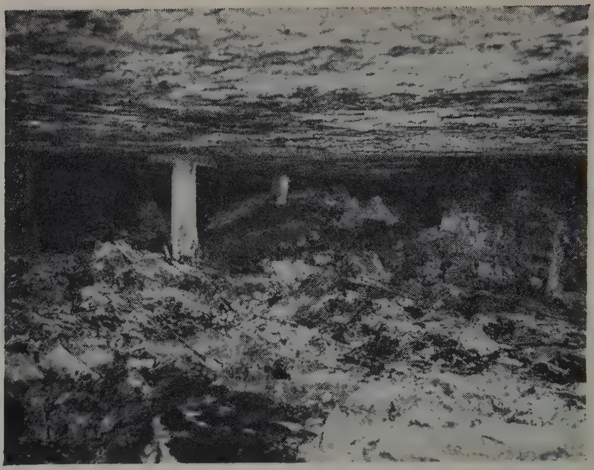

Fig. 12—Extreme bottom heave in the Sewickley seam adjacent to unmined block in the Brock mine.

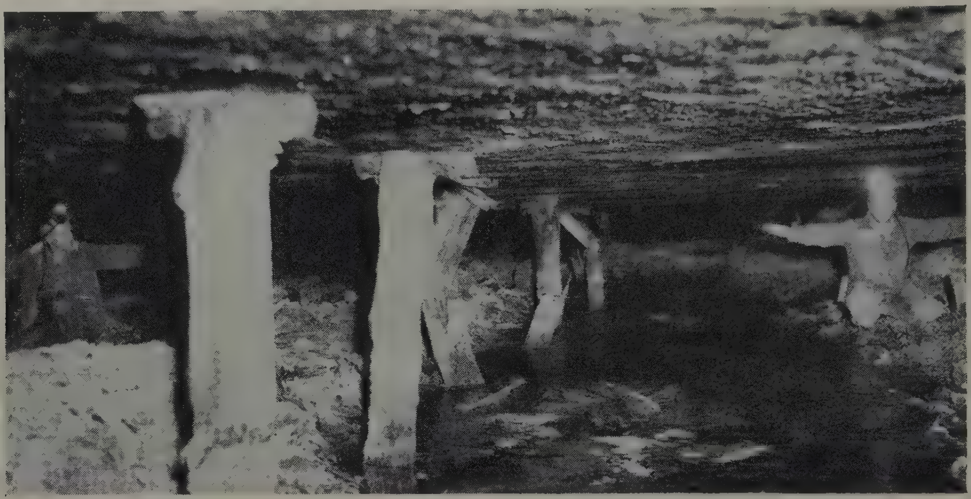

Fig. 13—Bottom heave in a 38-ft wide room adjacent to unmined block in the Brock mine.

of Figs. 11-13 will prove that all disturbance due to overburden load has been in the soft bottom, leaving ribs and roof in sound repair. The first of these three photographs shows the entry at location 11 on the map in Fig. 8. Note that the bottom has heaved to within 24 in. of the top of a 72-in. seam; observe also the absence of rib spalling and the excellent condition of the roof.

Inasmuch as the squeeze in the Osage mine directly under this general area was the worst of its type encountered, conditions in the overlying Sewickley were thoroughly investigated, with the resulting photographs: Fig. 12, corresponding to location 12 in Fig. 8, shows extreme bottom heave to within 10 in. of the roof and Fig. 13 a bottom heave to within 18 in. of the roof near the ribs. Here again it will be seen that no rib spalling is apparent and the roof shows no evidence of load. A similar examination was made in the Sewickley entries adjacent to the large standing blocks and in the area overlying the squeezes shown in the Arkwright mine, Fig. 4. The same conditions were found throughout. This further bears out the theory that overburden is transmitted through the Sewickley block and interval strata to the Pittsburgh; the Pittsburgh roof and ribs fail because the hard bottom will not break, whereas the Sewickley bottom heave takes the load off the coal and roof. This was shown earlier in Fig. 2.

Not all Pittsburgh difficulties occur in advance mining under old Sewickley workings with standing blocks. One costly experience occurred at Booth No. 6 mine where another company was retreat-mining the Sewickley directly over the Booth main haulway. The Pittsburgh entries were driven on the face and the Sewickley was retreating a panel on the butts. At the point where the retreat crossed over the Pittsburgh, there was a Booth power and water discharge borehole on No. 1 heading and an active gas well 100 ft to the right of No. 5 heading and 600 ft inby the borehole. In retreating, the Sewickley mine left large protection areas around both the borehole and the gas well; when the retreat mining had passed beyond the gas well the Pittsburgh headings below squeezed badly with rib and roof failures requiring extensive steel timbering and cribbing. No information is available as to what damage was done to the gas well, as it had been abandoned for several years. The borehole, however, was destroyed between the seams, and of course at its bottom in the Pittsburgh. Since 100 ft of solid coal surround the gas well where it passes through the Pittsburgh seam, it probably has not been damaged. Undoubtedly several other factors were involved, but it is felt that this is another instance in which Sewickley seam mining affected the underlying Pittsburgh seam.

Adsorption of Sodium Ion on Quartz

by A. M. Gaudin, H. R. Spedden, and P. A. Laxen

WHEN a mineral particle is fractured, bonds between the atoms are broken. The unsatisfied forces that appear at the newly formed surface[1] are considered to be responsible for the adsorption of ions at the mineral surface. A knowledge of the mechanism and extent of ion sorption from solution onto a mineral surface is of interest in the development of the theory of flotation.[2,3]

Study of the adsorption of sodium from an aqueous solution on quartz offers a simple approach to this complicated problem. The availability of a radioisotope as a tracer element meant that accurate data could be obtained.[4,5]

Three main factors which appeared likely to affect the adsorption of sodium are: 1—concentration of sodium in the solution, 2—concentration of other cations in the solution, and 3—anions present in the solution.

Hydrogen and hydroxyl ions are always present in an aqueous solution. By controlling the pH, the concentration of these two ions was kept constant. The variation in the amount of sodium adsorbed with variation in sodium concentration was then determined under conditions standardized in regard to hydrogen ion. The effect of concentration of hydrogen ions and of other cations was also measured. A few experiments were made to get a preliminary idea on the effect of anions.

The active isotope of sodium was available as sodium nitrate. Standard sodium nitrate solutions were used throughout these experiments except when the effects of other anions were studied.

It was found that sodium adsorption increased with sodium-ion concentration, but less rapidly than in proportion to it. Increasing hydrogen-ion concentration, or conversely decreasing hydroxyl-ion, brings about a comparatively slight decrease in sodium-ion adsorption. Increasing the concentration of cations other than hydrogen or sodium decreases somewhat the adsorption of sodium ion. It would appear as if the kind of anion is a secondary factor in guiding the amount of sodium ion that is adsorbed.

Materials and Methods

Quartz

The quartz was prepared as in previous work in the Robert H. Richards Mineral Engineering Laboratory[4] except for the refinement of using de-ionized distilled water for the final washing of the sized quartz, prior to drying.[5] To minimize the laborious preparation of quartz, experiments were made to determine whether the sodium-covered quartz could be washed free of sodium and re-used. The experiments were successful as indicated by lack of Na^{22} activity on the repurified material and by its characteristic sodium adsorption.

Table I gives the spectrographic analyses of the quartz used. The quartz ranged from 16 to 40 microns in size, averaging about 23 microns (microscope measurement), and had a surface of 1850 sq cm per g (lot I), 2210 (lot II) and 2000 (lot III) as determined by the Bloecher method.[6]

Radioactive Sodium

Method of Beta Counting for Adsorbed Sodium: Na^{22}, the radioisotope of sodium, possesses convenient properties.[7] It has a half-life of 3 years, thus requiring no allowance for decay during an experiment. On decay it emits a 0.575 mev β^+ radiation and a 1.30 mev γ radiation. The decay scheme is illustrated in the following equation:

$$Na^{22} \xrightarrow[\text{3 years}]{\beta^+,\gamma} Ne^{22}$$

The β radiation is sufficiently strong to penetrate an end-window type of Geiger-Mueller counting tube. This, in turn, makes it possible to use external counting, a great advantage in technique. Furthermore, it permits the assaying of solids arranged in infinite thickness, while assaying evaporated liquors on standardized planchets.

The equipment used was standard and similar to that employed by Chang.[8]

The original active material was 1 ml of solution containing 1 millicurie of Na^{22} as nitrate. This active solution was diluted to 1000 ml. Five milliliters of this diluted active solution was found to give a quartz sample a sufficiently high activity for accurate evaluation of the sodium partition in the adsorption measurements. Also, 1 ml of final solution gave a sufficiently high count for precision on the liquor analyses.

The sodium concentration of the diluted active solution was 1.2 mg per liter, so that 6 mg of sodium for 60 ml of test solution and 12 g of quartz was the minimum amount used. The active solution was stored in a Saftepak bottle.

Procedure for Adsorption Tests: The method consisted of agitating 12 g of quartz with 60 ml of solution of known sodium concentration for enough time to establish equilibrium between the solution and the quartz surface. The quartz was separated as completely as possible from the solution by filtering and centrifuging. The activity on the quartz and in the equilibrium solution was measured and the partition of the sodium was calculated from the resulting data.

The detailed procedure for the adsorption test is set forth in a thesis by Laxen.[5] In brief, it included the following steps:

1—Ascertainment of linearity between concentration of Na^{22} and activity measured.

2—Evaluation of factor to translate activity on solid of infinite thickness in terms of activity on an evaporated active film of minute thickness, on the various shelves of the counter shield.

3—Taking precautions to avoid evaporation of water during centrifuging.

A. M. GAUDIN and H. R. SPEDDEN, Members AIME, are Professor and Assistant Professor of Mineral Engineering, respectively, Massachusetts Institute of Technology, Cambridge, Mass. P. A. LAXEN, Student Associate AIME, is now in Transvaal, South Africa.

Discussion on this paper, TP 3276B, may be sent (2 copies) to AIME before Aug. 31, 1952. Manuscript, Nov. 2, 1951. New York Meeting, February 1952.

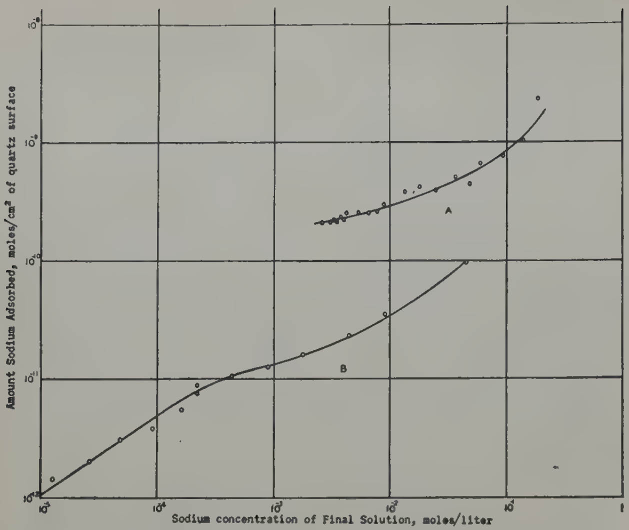

Fig. 1—Adsorption of sodium on quartz. Curve A shows effect of Na^+ concentration at pH 10. Curve B shows effect of Na^+ concentration at pH 6.

4—Weighing accurately the moisture retained in the pores of the filter cake and deducting the activity due to this retained solution as well as the background activity from the gross activity observed, so as to obtain the net activity of the coated mineral.

Experimental Results

Attainment of Equilibrium: Three adsorption tests were conducted in which the only variable was the time of agitation. The tests were run for 1, 2, and 3 hr. The results obtained are summarized in Table II. This table shows that the amount adsorbed (col. 4) does not differ from test to test significantly more than the pH (col. 2). As is shown below, the amount abstracted varies as the pH. If the data of col. 4 are corrected to the same pH (9.70) as explained further, these data support the conclusion that agitation for 1 hr is sufficient for equilibrium.

Effect of Na^+ Concentration: Two series of tests were conducted in which the sodium-ion concentration was varied. In one it was aimed to keep the pH at 10 and in the other at 6. Actually, the pH values of the solutions from the first series varied between 9.4 and 10.2, while those in the second series varied between 5.5 and 6.1.

The sodium concentration was varied between 1.95 and 182 millimols per liter in the first series and between 0.00848 and 45.3 millimols per liter in the second series. Lower sodium-ion concentrations in the first series could not be used, as some NaOH was required for pH-control purposes.

Fig. 1 presents the data in condensed fashion. The scales in this figure are both logarithmic. Curve A covers a range of Na^+ concentration of about 100-fold and curve B about 10,000-fold. The overall range in adsorption of Na^+ on quartz is from 10^{-12} to 10^{-9} mol per sq cm, or over 1000-fold. Fig. 1 shows that the adsorption increases as the sodium-ion concentration, but much more slowly. In fact, in most ranges the sodium-ion adsorption varies about as the square root of the sodium-ion concentration in the liquor, or even less rapidly.

Table I. Spectrographic Analyses of Quartz Samples

Element	Abundance, Pct Lot I	 Lot II	 Lot III[a]
Al	0.1 to 0.01	0.1 to 0.01	
Na	Less than 0.001	0.01 to 0.001	Less than 0.001
Mg	0.1 to 0.001	0.01 to 0.001	Less than 0.001
Cu	Less than 0.001	Less than 0.001	Less than 0.001
Fe	Less than 0.001	0.01 to 0.001	Less than 0.001
Ti	Less than 0.001	Less than 0.001	Less than 0.001

[a] Repurified after earlier use with Na^{22}.

Table II. Attainment of Equilibrium

Time of Agitation, Hr	Final pH	Na^+ Concentration, Mols x 10^{-3} Per Liter	Amount Na^+ Adsorbed Mols x 10^{-10} Per Sq Cm Observed	 Corrected to pH 9.70
1	9.6	2.40	1.89	1.98
2	9.7	2.40	1.99	1.99
3	9.8	2.40	1.99	1.90

Effect of pH: One series of tests was conducted in which the sodium concentration was kept constant while the pH was varied with dilute nitric acid. The results obtained are given in Fig. 2. The amount of sodium adsorbed decreases with increase of hydrogen-ion concentration.

Two additional series of tests were carried out to substantiate the results of Fig. 2. Qualitative support was obtained, although the scatter in these later tests was greater than in the earlier set. At present it seems as if a straight line relationship may exist between the logarithm of the amount of sodium adsorbed and the pH of the solutions. A linear relationship had also been shown to hold between the amount of barium adsorbed onto a quartz surface and the pH of test solutions.[8]

Fig. 2 shows that for a tenfold increase in hydroxyl-ion concentration the sodium ion adsorbed is increased by a factor of 1.5 only, or 50 pct. This correction was applied for the data in order to pre-

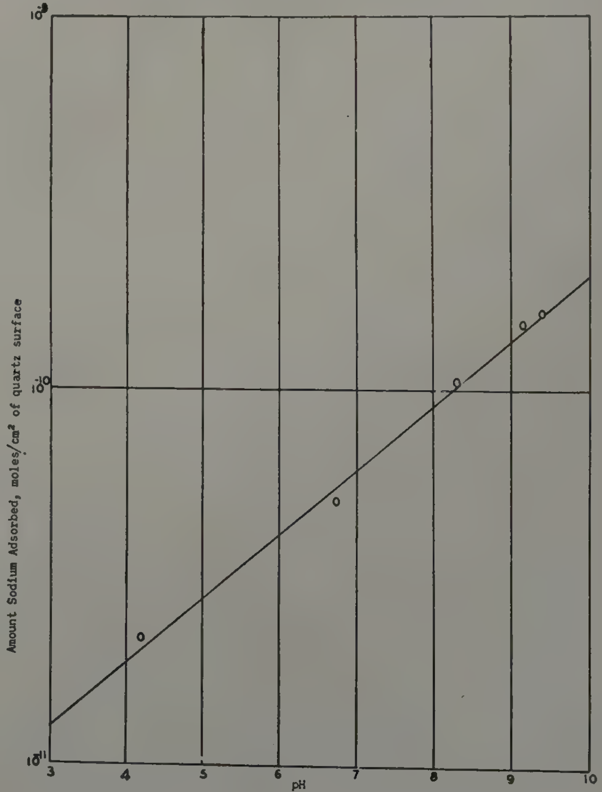

Fig. 2—Effect of pH on adsorption of sodium on quartz.

Table III. Effect of Cation Additions on Adsorption of Sodium on Quartz

Cation Present, Millimols Per Liter	Final pH	Na^+ Concentration, Millimols Per Liter	Amount Na^+ Adsorbed		
			Mg per g of Quartz	Mols x 10^{-10} Per Sq Cm	
				Observed	Corrected to pH 10
	9.8	2.62	0.00761	1.98	2.13
0.242Li^+	9.6	2.64	0.00705	1.39	1.67
1.21 Li^+	9.5	2.64	0.00622	1.23	1.54
0.257 Cs^+	9.5	2.64	0.00652	1.28	1.60
1.33 Cs^+	9.5	2.66	0.00464	0.913	1.12

pare curves A and B of Fig. 1 using pH 10 and pH 6 respectively as the norms.

Effect of the Presence of other Cations: Four tests were run in which varying concentrations of cesium or lithium nitrate were added to the test solutions. The test results are summarized in Table III. This shows that cesium and lithium displace sodium from the surface of quartz and that cesium is more effective than lithium.

Effect of Variation of the Predominant Anion Present: Six tests were conducted in which standard sodium solutions other than sodium nitrate were added. Solutions of sodium chloride, sodium fluoride, and sodium sulphate were added and the adsorption of sodium determined.

The results obtained, which are summarized in Table IV, indicate that the anion present has some effect. More work is needed to evaluate it more than qualitatively.

Reversibility of Adsorption: Three tests were run to verify the exchange between active and inactive sodium at the surface of quartz.

In each test 1 liter of sodium solution was allowed to percolate slowly through a bed containing 12 g of quartz. The time allowed for percolation was approximately 3 hr. The solutions used in the tests were all of the same sodium concentration, but some were made active and others not.

In the first test 1 liter of active solution was percolated through the quartz bed and the activity on the quartz determined. In the second test 1 liter of active solution was followed by 1 liter of inactive solution and the activity remaining on the quartz again determined. In the final test 1 liter of inactive solution, then 1 liter of active solution were passed through the bed and the activity on the quartz determined.

The results obtained from the tests are summarized in Table V. These results indicate that almost complete exchange takes place on passage of 1 liter of solution through a 12-g bed in 3 hr. With sufficient time of contact complete reversibility of adsorption of active and inactive sodium appears certain.

Table IV. Effect of Anion Present on Adsorption of Sodium on Quartz[a]

Sodium Salt	Actual Final pH	Actual (Na^+) Millimols Per Liter	Actual Na^+ Adsorbed	
			Microgram Per g Quartz	Molsx10^{-10} Per Sq Cm, Corrected to pH 6
NaCl	6.0	0.453	0.371	0.0806
Blank ($NaNO_3$)		0.453		0.114
NaCl	5.8	4.54	0.529	0.124
Blank ($NaNO_3$)		4.54		0.248
NaF	6.0	0.106	0.266	0.0577
Blank ($NaNO_3$)		0.106		0.052
NaF	5.6	0.0137	0.069	0.0176
Blank ($NaNO_3$)		0.0137		0.013
Na_2SO_4	5.6	0.106	0.212	0.055
Blank ($NaNO_3$)		0.106		0.052
Na_2SO_4	5.8	0.0138	0.065	0.0152
Blank ($NaNO_3$)		0.0138		0.013

[a] Values read from graph of Fig. 1.

Table V. Reversibility of Adsorption

Solutions Added		Wt of Moisture, g, Retained by 12 g of Quartz	Activity on 12 g of Quartz, cpm[a]	Pct of Activity Compared to Standard Test on Quartz Sample
Solution 1	Solution 2			
Active	None	0.3877	393	100
Active	Inactive	0.4054	7.2	1.83
Inactive	Active	0.3856	355	90.4

[a] Counts per min.

Discussion of Results

The present-day concept of adsorption at a solid-liquid interface visualizes the existence of a so-called double layer of ions at the interface.[9] This double layer is thought to be made up of an inner part attached to the surface and an outer diffuse part.[10] For a quartz-solution interface the ζ potential is negative (—44 mv according to Freundlich). Likewise, for a fused-silica interface recent accurate measurements by Wood[11] give the still higher negative potential of —177 mv. Therefore the double layer may be considered to consist of an inner layer of anions and an outer layer of cations. The cations are loosely held and therefore wander off into the solution imparting a net negative potential to the surface. The diffuse part extends into the solution and is also made up of both cations and anions.

When a quartz particle is placed in pure water, hydroxyl and hydrogen ions are adsorbed onto the surface and into the diffuse layer.[12] A dynamic equilibrium is established between the ions in the solution and those on the surface. The presence of other ions would alter this equilibrium, the new equilibrium depending upon the nature and concentration of the ions in the solution.

The thickness and concentration of ions in the diffuse part varies with the concentration of the solution. The thickness is equal to the reciprocal of the Debye-Hückel function, *K*, and can be calculated from the following equation:

$$\delta = 1/K = \sqrt{\frac{1000\,D\,R\,T}{8\,e^2\,N^2}}\sqrt{1/c}\ .$$

In this equation δ is the thickness of the diffuse layer in centimeters; *D* is the dielectric constant, about 80 for water at 25°C; *R* is the gas constant, 8.314x10^7; *T* is the absolute temperature in degrees Kelvin; *e* is the charge of the electron, 4.77x10^{-10} electrostatic units; *N* is the Avogadro number, 6.02x10^{23}; and *c* is the ionic concentration of the solution in gram ions per liter or mols per liter.

The thickness δ does not represent a distance beyond which there is no diffuse layer. Rather, it represents a theoretical thickness which would give exactly the same electrical effect at the interface as actually occurs, if all the ions in the outer layer were maintained at the distance δ from the ions in the inner layer. It would be necessary to select a double layer about 4δ in thickness in order to include in it about 98 pct of all the ions in the diffuse layer.

In the experimental results presented here in condensed form and found in detail in the thesis by Laxen,[5] it is shown that the filtered and centrifuged solids contain in general about 3 pct moisture by weight. Since the specific surface of the quartz used in this work is about 2000 sq cm per g and since 3 pct moisture may be accepted as an average value of the liquor content of the filter cake, it may be shown that the thickness of liquor film around each mineral particle averages 1600Å. From the equation giving δ, the thickness of the diffuse layer at the lowest concentration of sodium, $8.48 x 10^{-6}$ mols per liter, would be approximately 1000Å. For more concentrated solutions the diffuse layer would be thinner, and for the most concentrated solution it would be about 13Å. In each test, therefore, the diffuse layer has been part of the solution retained to a greater or lesser extent by the quartz bed. The adsorbed sodium as measured in our experimental work has, therefore, been that due to the sodium absorbed at the surface of the quartz plus most of the excess sodium in the diffuse layer.

When the suspension of quartz and solution are filtered and centrifuged, it is quite probable that the equilibrium distribution of ions between the solution and the solid surface are disturbed somewhat. This is one phase of the experimental procedure which might well be studied further.

For each 23.4Å^2 of quartz surface, there exists an anionic and a cationic adsorption site.[13] If one sodium ion is assumed to be adsorbed at each cationic site (or one sodium ion is assumed to be adsorbable in the diffuse layer in apposition to each anionic site on the quartz), a monolayer would require $\frac{1}{23.4x10^{-16}}$ ions per sq cm or

$$\frac{1}{6.02x10^{23} + 23.4x10^{-16}} = 7.1x10^{-10}$$

g-ions per sq cm. Inspection of Fig. 1 shows that adsorption equal to such a monolayer is obtained only at sodium-ion concentrations over 0.07 M and at a high pH.

If it be assumed that sodium ions in water are hydrated so that the overall diameter of a sodium ion equals the diameter of two water molecules plus that of one anhydrous sodium ion, or about 7.5Å, it is clear that a monolayer adsorbed at the quartz will contain fewer ions than $7.1x10^{-10}$ g-ions per sq cm, since the ion size is too large to be accommodated at each site.

On the value for the diameter of the hydrated sodium ion obtained by Remy[14] and used recently by Nachod and Wood,[15] that is 16Å, each sodium ion would occupy approximately eight adsorption sites on the quartz surface. A surface concentration of $7.9x10^{-11}$ g-ions of sodium per sq cm corresponds to a completed monolayer of sodium ions on the basis of the above diameter for the hydrated sodium ion. Even on the basis of Remy's liberal evaluation of the size of the hydrated sodium ion, it is clear that a monolayer would be obtained only under the circumstances of high pH or high concentration.

Neither the Freundlich[13] nor the Langmuir[16] adsorption isotherm can be applied to fit the adsorption isotherms in Fig. 1 over the entire range. A Freundlich equation can, however, be applied to the straight line portion of curve A giving the adsorption from solutions at very low sodium concentrations.

The results obtained on the addition of other cations such as cesium and lithium to sodium solutions confirm those obtained by previous investigators on the relative magnitude of adsorption of ions onto clays and other materials.[1, 17, 18] Cesium displaced more sodium from the quartz than an equivalent concentration of lithium, agreeing with their positions in the so-called *Lyotropic Series* for alkali metals, $Cs^+ > Rb^+ > K^+ > Na^+ > Li^+$. This series has been used to represent the order of magnitude of adsorption of the alkali metals. The adsorption affinity increases with decreasing hydrated ionic radius.

The amount of sodium adsorbed was shown to be also dependent on the anion present. With the four anions tested, the most sodium was adsorbed in the presence of fluoride ions and the order of decreasing sodium adsorption was as follows:

$$F' > SO_4'' > NO_3' > Cl'.$$

The authors hope that this contribution to the accumulation of data regarding the adsorption of ions onto minerals will result in a better understanding of the nature of solid-liquid interfaces so essential in the development of flotation theory and practice.

The generous support of the Atomic Energy Commission through its Research Division is gratefully acknowledged.

References

[1] E. A. Hauser: Modern Colloidal Concepts of the Phenomenon of Coagulation, *Journal of Physical and Colloidal Chemistry* (April 1951) **55**, No. 4.

[2] A. M. Gaudin: *Principles of Mineral Dressing.* McGraw-Hill Book Co., New York, 1939.

[3] I. W. Wark: Principles of Flotation. Australasian Inst. Min. and Met., Australia (1938).

[4] A. M. Gaudin and F. W. Bloecher, Jr.: Concerning the Adsorption of Dodecylamine on Quartz. *Trans.* AIME (1950) **187**, pp. 499-505; MINING ENGINEERING (April 1950).

[5] P. A. Laxen: Concerning the Adsorption of Sodium onto Quartz. Master's Thesis, Massachusetts Institute of Technology (September 1951).

[6] F. W. Bloecher, Jr.: A New Surface Measurement Tool for Mineral Engineers. *Trans.* AIME (1951) **190**, p. 255; MINING ENGINEERING (March 1952).

[7] G. T. Seaborg and I. Perlman: Table of Isotopes. *Reviews of Modern Physics.* (1948) **20**, No. 4, p. 589.

[8] C. S. Chang: Adsorption of Barium and Laurate Ions on Quartz. Doctor's Thesis, Massachusetts Institute of Technology (May 1951).

[9] A. E. Alexander and P. Johnson: *Colloid Science.* **1**, p. 297. Oxford, Clarendon Press, 1949.

[10] E. K. Rideal: The Electrical Double Layer. General Introduction. *Trans.* Faraday Soc. (1940) **36**, p. 1.

[11] Lloyd A. Wood: The Measurement of the Potential of the Interface Between Vitreous Silica and Pure Water Fused Silica. *Journal* Amer. Chem. Soc. (1946) **68**, pp. 437-441.

[12] A. M. Gaudin and A. Rizo-Patron: The Mechanism of Activation in Flotation. *Trans.* AIME (1943), **153**, pp. 462-472.

[13] H. Freundlich: *Kapillarchemie.* **1**, pp. 154 and ff. (1930) Leipzig Akademische Verlagogesellschaft M.B.H.

[14] H. Remy: Beitrage zum Hydratproblem. *Ztsch. Physik Chem.* (1915) **89**, p. 467.

[15] F. C. Nachod and W. J. Wood: The Reaction Velocity of Ion Exchange. *Journal* Amer. Chem. Soc. (1945) **67**, p. 629.

[16] I. Langmuir: The Adsorption of Gases on Plane Surfaces of Glass, Mica and Platinum. *Journal* Amer. Chem. Soc. (1918) **40**, p. 1361.

[17] G. E. Boyd, J. Schubert, and A. W. Adamson: Ion Exchange Equilibria. *Journal* Amer. Chem Soc. (1947) **69**, p. 2818.

[18] Hans Jenny: Studies on the Mechanism of Ionic Exchange in Colloidal Aluminum Silicates. *Journal of Physical Chemistry* (1932) **36**, p. 2217.

The Effect of Certain Starches on Quartz and Hematite Suspensions

by Strathmore R. B. Cooke, Norman F. Schulz,
and Emert W. Lindroos

DURING the course of an investigation of the effects of various starch products on hematite and quartz in regard to their separation by flotation, it was found that whereas most starches flocculated suspensions of hematite in water, they did not flocculate similar suspensions of quartz. However, a derivative of whole corn starch containing approximately one tenth aminoethyl group ($-CH_2CH_2NH_2$) per glucose unit proved to be an exception. This aminoethyl starch was a very good flocculant for both hematite and quartz, and also possessed the property of depressing both minerals in cationic flotation tests. In view of the widespread use of starch as a flocculating agent of solids in tailing water, pulps, and for coal slimes, ore and various other purposes in sulphide and nonsulphide flotation, attention is called to the effective surface activity of aminoethyl starch in flocculating suspensions of the two minerals investigated.

Test Materials

The starch products employed included Globe Pearl starch No. 144 and fresh aminoethyl starch, both supplied by the Corn Products Refining Co. Dr. A. L. Elder[a] has kindly furnished a description of the preparation of the aminoethyl starch: "Three hundred and sixty grams of powdered unmodified corn starch was slurried in 3 liters of water and stirred during gelatinization. Eighty-six grams of ethylenimine was added slowly during reflux which was continued for 4 hr. The yellow solution set to a gel upon cooling. This was broken up and neutralized with HCl. The thick paste was dried on hot rolls. Adsorbed polyethylenimine and salts were removed from the yellowish products by washing first with acidified aqueous '60 per cent' alcohol. The white product contained nitrogen corresponding to about one aminoethoxy group per ten glucose residues." Only laboratory samples of this starch derivative have been prepared.

The starch reagents for use in flocculation, flotation, and adsorption tests were made up by dispersing the appropriate quantities of air-dry starch in cold water, adding boiling water, and heating for 30 min at 120°C under pressure. When used in adsorption tests, the starch solutions first were cleared of insoluble matter by centrifugation.

The minerals used in the various tests are listed in Table I. Their specific surfaces were determined by the air permeability method, which gave results reproducible to within plus or minus 3 pct. Surface areas obtained by krypton adsorption were greater than the air permeability values by a factor of 2.0 for quartz and 62.4 for hematite.

Starch Adsorption on Mineral Surfaces

Starch adsorption data were obtained by agitating for 1 hr measured volumes of neutral starch solutions of known concentrations with weighed quantities of finely divided mineral of measured specific surface. The mineral then was separated from the pulp liquor by centrifugation and the residual starch content determined by chemical analysis. The analytical procedure consisted of oxidizing the starch with an excess of dichromate in acid medium at elevated temperature and titrating the excess dichromate by the ferrous ammonium sulphate—potassium permanganate method. Analytical results were reproducible to within less than 1 pct.

Adsorption data obtained in unbuffered solutions near the neutral point are plotted in Fig. 1. The adsorption on either mineral was far greater for the aminoethyl starch than for the Pearl starch.

Flocculation

The degree of flocculation was determined for a given pulp by measuring the time required for the supernatant liquid to reach a certain degree of clarity. This was accomplished by passing a standard light beam through the pulp, contained in a glass settling tube, and measuring the time required after agitation ceased for the intensity of the transmitted beam to reach a predetermined value. Starch reagent was added to each pulp in small uniform increments, and the settling time was determined after each such addition. Increase in pulp liquor volume due to the added starch reagent was ignored in these tests. Pulps were maintained at or near neutrality.

---

[a] Director of Research, Corn Products Refining Co., Argo, Ill.

S. R. B. COOKE, Member AIME, Professor of Metallurgy and Mineral Dressing, School of Mines; N. F. SCHULZ, Corn Products Refining Co. Research Fellow, School of Mines; and E. W. LINDROOS, Graduate Student, are with the University of Minnesota, Minneapolis.

Discussion on this paper, TP 3289B, may be sent (2 copies) to AIME before Aug. 31, 1952. Manuscript, Oct. 29, 1951. New York Meeting, February 1952.

Plots of the settling time against starch content, see Fig. 2, show that the two starch products produced similar results in the flocculation of hematite ore. Quartz suspensions were not flocculated by the Pearl starch but were well flocculated by the aminoethyl starch derivative.

Optimum flocculation effects were observed at starch concentrations producing considerably less than a saturated adsorption coating on hematite ore.

Table I. Characteristics of the Minerals Tested

Mineral	Density, G per Cc	Screen Mesh	Analysis, Pct	Specific Surface Cm^2 per G	Composition, Pct
Quartz: Ottawa sand, leached in hot HCl, ground in Abbe pebble mill.	2.65	65/200 —200	12.0 88.0	2800	SiO_2
Hematite Ore: Hand-picked, high grade ore, ground in sample pulverizer.	4.5	65/200 —200	34.7 65.3	2060	62.4 Fe
Wash Ore Tails: From W. Mesabi Range, Minn., ground and deslimed.		+65	0.5		27.5 Fe
		65/100	3.7		
		100/150	9.8		
		150/200	17.9		
		200/270	16.8		
		270/13.5 micron	42.6		
		Slimes: —13.5 micron	8.7		(36.5 Fe)

The flocculation effect of aminoethyl starch on quartz continued to increase as more starch reagent was added, up to the volumetric limit on the apparatus used.

Flotation

Flotation tests were made on samples of iron wash-ore tails that were prepared by a brief grinding and a thorough desliming operation, using 0.33 lb of quebracho per ton of ore, which removed the particles smaller than 13.5 microns. The sands were scrubbed as a pulp containing 50 pct solids with 2.24 lb of sulphuric acid per ton, prior to flotation. A 250-g Minerals Separation type of flotation cell with an open type impeller was used.[1] A cationic collector, normal dodecylamine acetate (Armac 12D) and an aliphatic alcohol frother (B-24), were used to float the quartz from the ore at a pH of from 10.8 to 11.0, sodium hydroxide being used for pH adjustment.

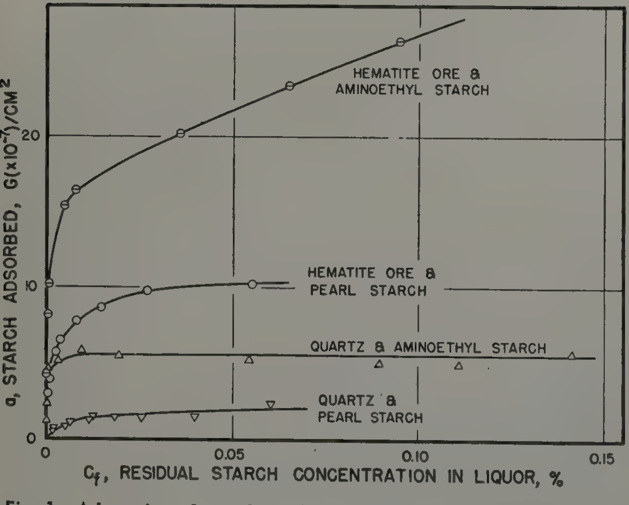

Fig. 1—Adsorption of starch products on quartz and hematite ore.

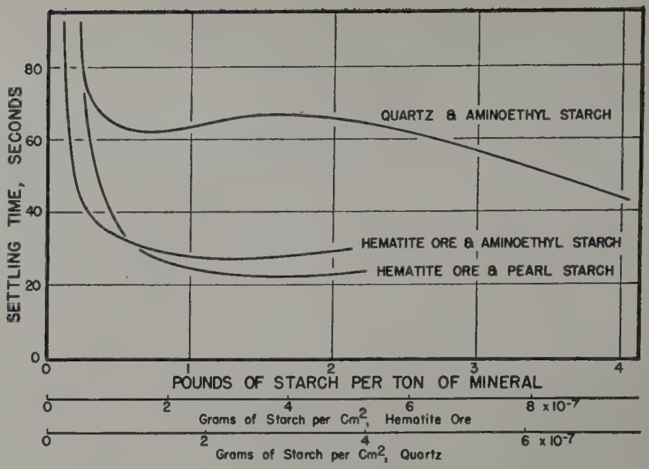

Fig. 2—Flocculation of mineral pulps with starch products.

Pearl starch markedly improved the iron recovery of the flotation process, when used in quantities up to 1 lb per short ton, by selectively depressing the hematite. With no starch, the iron recovery was 64.1 pct, with 1 lb of starch per ton, 80.6 pct, increasing slowly to 83.5 pct with 10 lb per ton. Grade of concentrate was but little affected, averaging about 53.5 pct Fe for starch additions of from 0 to 10 lb per ton.

Aminoethyl starch, at 2 lb per short ton of ore, almost completely inhibited flotation of all the minerals present, the froth was scant, and even the addition of excess collector failed to improve the flotation. However, a good grade of concentrate (59.6 pct Fe) with fair recovery (74.0 pct) was obtained when a starvation quantity of only ½ lb of aminoethyl starch was used per ton of ore.

These contrasting effects of Pearl and aminoethyl starches on the flotation of quartz from hematite ore were apparently a direct result of the differences between their adsorption characteristics.

Summary

An aminoethyl derivative of whole corn starch, unlike unaltered corn starch, was found to be an effective flocculant for water suspensions of finely ground quartz and hematite, although ordinary starches are not good flocculants for quartz. This phenomenon was traced to the fact that the presence of the aminoethyl group enabled the starch to be more readily adsorbed on quartz surfaces. The aminoethyl starch depressed both hematite and quartz in cationic flotation, presumably because of the closure of the surfaces of both minerals to the collector.

Acknowledgments

The starch products and funds for the experimental work thereon were furnished by Corn Products Refining Co., New York, through a fellowship grant to the University of Minnesota. The work was also partially supported by funds furnished by the Graduate School of the University of Minnesota.

Reference

[1] J. Bruce Clemmer and B. H. Clemmons: An Improved Flotation Test Cell, *Engineering and Mining Journal* (1943) **144**, p. 72.

Geologic Setting of the Copper-Nickel Prospect In the Duluth Gabbro Near Ely, Minnesota

by G. M. Schwartz and D. M. Davidson

THE Duluth gabbro outcrops containing sulphides of copper, nickel, and iron are located on both sides of State Highway No. 1 an airline distance of 8.5 miles southeast of Ely in northeastern Minnesota. The region of known sulphide occurrences includes parts of sections 5, T. 61 N., R. 11 W., and parts of sections 25, 26, 32, 33, and 34, T. 62 N., R. 11 W. These sections, given in Fig. 1, are all in Lake County, Minnesota. Part of the area, which lies entirely within the Superior National Forest, is shown on the topographic map of the Ely quadrangle.

The original discovery was made in 1948 when a small pit was opened in weathered gabbro rubble for use on a forest access road. A shear zone had caused unusual decomposition in this glaciated area, and the resulting copper stain was noted by Fred S. Childers, Sr., an Ely prospector, who began searching the outcrops along the base of the intrusive. He was joined in further exploration by Roger V. Whiteside of Duluth. In the summer of 1951 a small diamond drill was moved into the area and a hole 188 ft deep was drilled, passing through 11 ft of glacial drift into sulphide-bearing gabbro. This paper is a preliminary report on the geology of the newly discovered ore.

The Duluth gabbro is one of the largest known basic intrusives and may be defined as a lopolith.[1] It extends northeastward from the city of Duluth as a great crescent-shaped mass that intersects the shore of Lake Superior again near Hovland, 130 miles to the northeast, see Fig. 2. The distance around the outside of the crescent is nearly 170 miles. The form of the intrusive is simple at Duluth where it ends abruptly north of the St. Louis River; at the east end, however, the gabbro splits into two elongated, sill-like masses separated mainly by lava flows and characterized by minor irregularities. The outcrop reaches a maximum width in the central part where it is about 30 miles across, and a maximum thickness of about 50,000 ft. It may be significant that the sulphides occur at the base of the thickest part.

The lopolith has segregated into rock types ranging from peridotite to granite. The most abundant types are olivine gabbro, gabbro, troctolite, anorthosite, and granite. Of lesser importance quantitatively are peridotite, norite, pyroxenite, magnetite gabbro, and titaniferous magnetite. Grout estimates that two-thirds of the gabbro at Duluth is olivine gabbro. Variations in the percentages of plagioclase, augite, olivine, and magnetite-ilmenite constitute the only essential differences found among the basic rock types. The predominant mineral is plagioclase, mainly labradorite. Plagioclase and olivine seem to have crystallized early, and the olivine rich rocks, usually troctolite, are found in the lower part. Segregations of titaniferous magnetite are abundant near the base of the gabbro along the eastern part and also occur far above the base. These have recently been described in detail by Grout.[2] Near the top, segregation has produced a gradation to granite, or "red rock," as it is known locally. This consists of quartz, red feldspar, and hornblende. The red rock forms a zone with a maximum width of nearly 5 miles but is quantitatively unimportant from Duluth northward for 35 miles. In Cook county, where the gabbro splits, each of the two sill-like masses has a red rock top somewhat thicker in proportion to the gabbro below than in the main central mass.

The intrusive ranges from coarse to medium in grain size and from granitoid to diabasic in texture. Throughout much of the Duluth gabbro in Minnesota banding and foliation are well developed, as Grout has emphasized.[3] The bands are mainly a result of variation in the percentage of minerals, as in troctolite with alternating bands high in olivine and in plagioclase. A few bands may consist largely of one mineral, as is true of some segregations of magnetite. Many of the banded rocks show a clearly developed parallelism of platy plagioclase crystals, and both banding and foliation are believed to conform to the floor of the lopolith.

Throughout its extent in Minnesota the Duluth gabbro dips east and south toward Lake Superior. It is generally believed to extend beneath Lake Superior and is found as a smaller mass exposed along the north side of the Gogebic district in Wisconsin and Michigan. The dip at and near the base ranges along most of its length from 20 to 40°, but at places the internal banding dips even more steeply. The dip of the upper part is much less, and if it is assumed that the flows along the north shore of Lake Superior are a dependable indication, it does not exceed 15°.

The formations shown in Table I which are intruded by the gabbro range from Keewatin to Middle Keweenawan in age. They present a significant picture. At the top, the gabbro and its accompanying

---

G. M. SCHWARTZ, Member AIME, is Professor of Geology and Director, Minnesota Geological Survey, University of Minnesota, and D. M. DAVIDSON, Member AIME, is Vice President and Chief Geologist, E. J. Longyear Co., Minneapolis.

Discussion on this paper, TP 3346I, may be sent (2 copies) to AIME before Aug. 31, 1952. Manuscript, Feb. 25, 1952. Revised May 19, 1952. New York Meeting, February 1952.

red rock facies intrude Keweenawan lava flows and possibly some diabase sills throughout its length. It appears to be only moderately discordant. The base of the lopolith, however, is very different, as gabbro is in contact with formations ranging from Keewatin to Middle Keweenawan in age. A significant point is that the base at both ends lies at about the same horizon near the base of the Keweenawan flows. Grout[1] suggests that the magma must have spread for the most part along an unconformity at the base of the Lower Keweenawan formation, which is of Puckwunge sandstone.

The rocks at the contact with gabbro are recrystallized to hornfels almost regardless of the mineralogical character of the original rocks.[4-6] The contact rock and also numerous inclusions in the gabbro have a sugary texture with grains averaging about 5 mm in diam. Where the intruded rock is basic in character the hornfels may closely resemble the gabbro except that they are always coarser-grained.

As might be expected for such a large area, the amount of gabbro exposed varies greatly from place to place. At and near Duluth the exposures are abundant and are well shown on maps included in a recent report.[7] North of Duluth, where the lopolith trends away from Lake Superior, glacial deposits are thicker, and therefore outcrops become scant and are altogether lacking over a large area south of the Mesabi range. From the Mesabi range eastward, outcrops are common and sometimes abundant near the base, but to the south glacial moraines cover large areas. Eastward in Cook County outcrops are fairly general. Considerable detail will be shown on maps to accompany a report on that county being prepared by Dr. Frank F. Grout.

The Copper-Nickel Rocks

As previously noted, the sulphide-bearing gabbro has been found in scattered outcrops over a length of 5 miles. This, however, is not the first discovery of sulphides in the Duluth gabbro. Sporadic occurrences have been noted in the past by many geologists, and a few have been described,[8,9] but none of these were extensive enough to receive serious consideration as possible economic deposits.

Although much geological work has been done on the Duluth gabbro, the outcrops have never been completely mapped because large areas occur in heavily brush-covered wildland. No detailed work has been done in the vicinity of the sulphide prospects; available information is shown on Fig. 1.

Petrography: The sulphide-bearing rock ranges from medium to very coarse-grained gabbro. Specimens from different outcrops over a length of 5 miles show considerable variation in grain size and in mineral composition. The fine to medium-grained gabbro is a medium dark grey, and the coarser-grained varieties are a medium gray color. The coarsest-grained rock is practically an anorthosite and contains plagioclase grains up to an inch in length. Previous studies of the gabbro where it is well exposed have shown that the different varieties usually make up bands of varying thickness. The bands extend some distance along the strike of the gabbro mass, although some are lenticular and cannot be traced far.

Examination of thin sections and polished surfaces of the gabbro indicates that it contains the following minerals in decreasing order of abundance: labradorite, olivine, augite and hypersthene, magnetite-ilmenite, biotite, chalcopyrite, cubanite, pyrrhotite, pentlandite, apatite, and bornite.

Thin sections of most known sulphide-bearing outcrops as well as samples from the diamond drill hole at a depth of 47 and 87 ft have been examined. The writers are indebted to Dr. Frank F. Grout for checking the interpretations. The thin sections represent different facies of the gabbro, no two resembling each other very closely. The range is from feldspathic gabbro to troctolite; the approximate percentages of the essential minerals are shown in the following tabulation of thin sections.

Plagioclase	75	75	65	65	65	65	55	50
Pyroxene	5	10	—	25	15	20	5	25
Olivine	15	2	30	5	15	10	35	15

None of the sulphide-bearing rocks had sufficient orthorhombic pyroxene to warrant use of the term "norite," but elsewhere norite has been observed, particularly by Nebel.[8]

The sulphides occur in all of the silicates but are most abundant in plagioclase. A characteristic texture is disseminated sulphide in plagioclase adjacent to larger areas of sulphide. Many inclusions are somewhat elongated and arranged parallel to the twinning bands of the feldspar, see Fig. 3. There is no alteration of the feldspar associated with the inclusions, so that the nearly simultaneous formation of feldspar and sulphide is indicated. The areas of sulphides are commonly interstitial to the silicates, especially feldspar. The dominant pyroxene is augite, but enstatite is almost equally abundant in one section, and diopside and hypersthene were noted in a complex intergrowth. A small amount of biotite characteristically occurs at or near sulphide areas but rarely elsewhere, see Fig. 4. The biotite

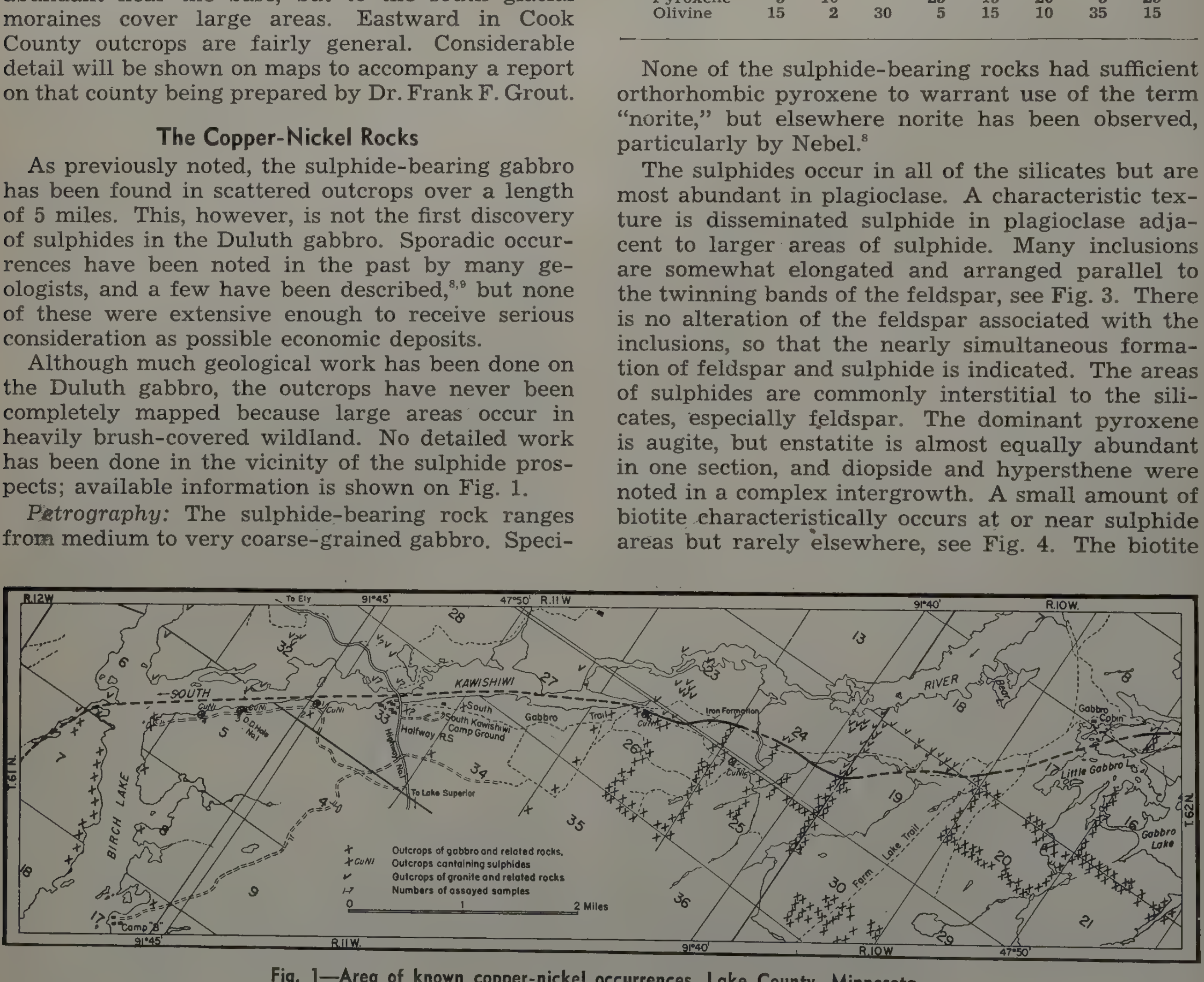

Fig. 1—Area of known copper-nickel occurrences, Lake County, Minnesota.

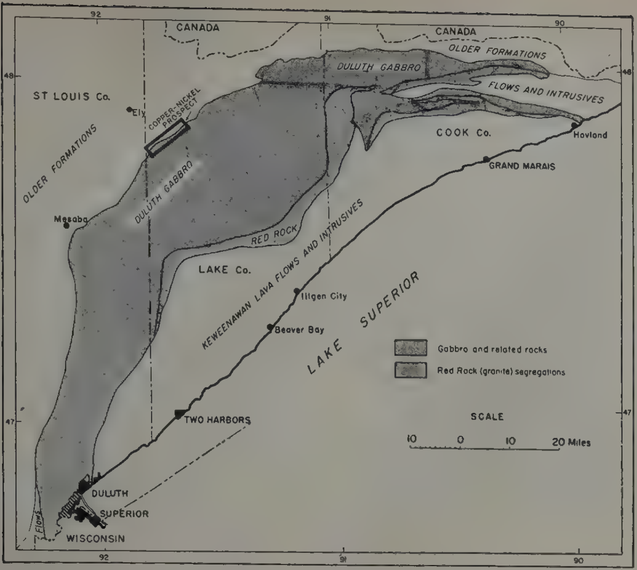

Fig. 2—Map showing the outline of the Duluth gabbro and its relation to other formations.

replaces other silicates and is possibly deuteric. Some sulphide may also be classified as deuteric. Most grains of olivine are not altered, but some show attack at the edges by complex veinlets consisting of antigorite, chrysotile, and iddingsite, either separate or intermixed. Some olivine is cut by irregular stringers of magnetite with narrow borders of serpentine. There is a small amount of alteration of pyroxene to chlorite and in a few places to carbonate. One thin section shows graphic intergrowths of sulphides in augite, see Fig. 5. The augite in the intergrowth is conspicuously finer-grained than surrounding grains of pyroxene, some of which are in contact with the intergrowth. The texture suggests simultaneous crystallization of pyroxene and sulphide.

Chalcopyrite is the most abundant sulphide in most specimens, but cubanite may predominate in some aggregates. Where the two minerals are together they form the familiar lath-like crystallographic intergrowths that result from exsolution. Pentlandite and pyrrhotite occur as irregular grains interlocked with chalcopyrite and cubanite. A very small amount of bornite occurs with the other sulphides in some polished sections. The small bornite areas almost invariably contain excellent exsolution intergrowths of chalcopyrite. More common is bornite along the pseudo-tetrahedral, or tetragonal bisphenoidal, planes of chalcopyrite.

Table I. Formations Intruded by the Duluth Gabbro Range

Age	Formation	Rocks
Pleistocene	Glacial drift	Moraines, glacial lake deposits, and outwash
Keweenawan	Fond du Lac beds	Sandstone and shale
	Duluth gabbro, Beaver Bay complex, Logan sills	Gabbro, granite, diabase
	Keweenaw Point volcanics	Basic and acidic lava flows, interbedded arkose, sandstone and tuffs
	Puckwunge formation	Sandstone, conglomerate
Algoman	Giant's Range and other masses	Granite
Knife Lake time	Knife Lake group	Slate, graywacke, conglomerate and agglomerate
Laurentian	Saganaga mass	Granite
Keewatin	Soudan iron-bearing formation Ely greenstone	Jasper and hematite Metamorphosed volcanics and intrusives

Some polished sections reveal a few tiny veinlets of sulphide that are later in origin than the silicates. These, however, do not contradict the fact that sulphide is intergrown with plagioclase without any evidence of having been introduced after crystallization of the plagioclase. It seems probable that these veinlets, like the sulphide with biotite, are deuteric.

Magnetite-ilmenite is abundant in some specimens. The two minerals can be distinguished when a very high polish is obtained. Ilmenite occurs as an intergrowth in magnetite and also in the form of grains.

Copper-nickel content: Results of systematic sampling are available only from the vertical diamond drill hole drilled by Messrs. Fred S. Childers, Sr., and Roger V. Whiteside, who have generously given permission for the results to be quoted. Bedrock was reached at 11 ft, core was split, and one-half was crushed for assay samples of 5-ft lengths down to 115 ft. For a core length of 104 ft the average assay is 0.36 pct copper and 0.13 pct nickel. The highest grade 5-ft section from 21 to 26 ft assayed 1.02 pct copper and 0.21 pct nickel. The sludge from 115 to 124 ft, where core recovery was poor, assayed 0.21 pct copper and 0.10 pct nickel. Below 124 ft the sulphide content diminished rapidly and no more was found to the bottom of the hole at 188 ft. The rock from 124 to 188 ft is rather uniform, dark gray, coarse-grained feldspathic gabbro. An unnumbered hole was originally started about 50 ft south of No. 1 hole but yielded little sulphide and was discontinued at 20 ft.

Various samples from outcrops of the sulphide-bearing rock have been assayed and the results made available by the Minnesota Geological Survey, U. S. Bureau of Mines, E. J. Longyear Co., and Messrs. Childers and Whiteside. These show about the same range in copper and nickel content as the diamond drill hole noted above. Results of samples collected by the Minnesota Geological Survey at the seven locations shown on Fig. 1 are given in Table II. A sample collected at Location No. 1 by E. P. Chapman of the U. S. Bureau of Mines and assayed independently revealed 1.06 pct copper and 0.38 pct

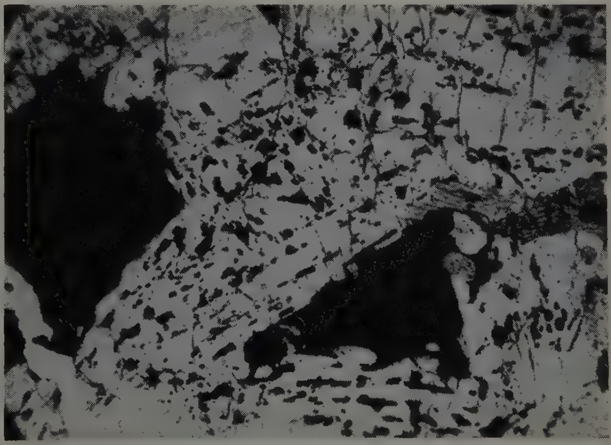

Fig. 3—Copper-nickel sulphides (black) in gabbro. The silicate is mainly plagioclase and the disseminated sulphide is oriented parallel to the twin bands. Thin section, plain light. X50.

Table II. Surface Sampling of Cu-Ni Content in the Duluth Gabbro

Location	Cu Pct	Ni Pct
1	1.12	0.28
2	0.36	0.10
3	0.70	0.14
4	0.72	0.14
5	0.37	0.09
6	0.39	0.07
7	0.32	0.10

nickel. Inasmuch as the samples were collected after several blasts in the outcrop, this is satisfactory confirmation. A second sample collected by Mr. Chapman about 3 miles to the northeast, near the east end of the known sulphide-bearing outcrops, contained 1.16 pct copper and 0.21 pct nickel.

A total of 29 grab and chip samples from about 12 outcrops averaged 0.59 pct copper and 0.17 pct nickel. Although these were not systematic and were taken by several different men, they may be accepted as indicating the copper and nickel content in outcrops along the known belt of sulphide occurrences.

Summary

The significant features of the occurrence of copper and nickel sulphides near the base of the gabbro may be briefly listed as follows:

1—The sulphides are well disseminated throughout over 100 ft of rock and appear to be primary constituents.

2—Widely scattered outcrops extend to a length of more than 5 miles not far from the base of the Duluth gabbro and approximately parallel to it.

3—The Duluth lopolith is known to be well banded or layered throughout much of its extent, and it is a reasonable inference that the distribution of the sulphides is related to this layering near the base of the widest part of the intrusive.

4—The sulphide minerals are those characteristic of copper-nickel deposits elsewhere.

5—The known extent of rock that will average 1 pct or more of combined copper and nickel is strictly limited, and the outcrops are too far apart to be considered with certainty as being connected by sulphide-bearing rock. The structure of the intrusive, however, indicates a possibility that the sulphides are continuous.

6—The location of the prospect is favorable. It is crossed by a paved highway and is about 8 miles from a railroad. As indicated by scattered outcrops, the glacial drift is probably thin over much of the area.

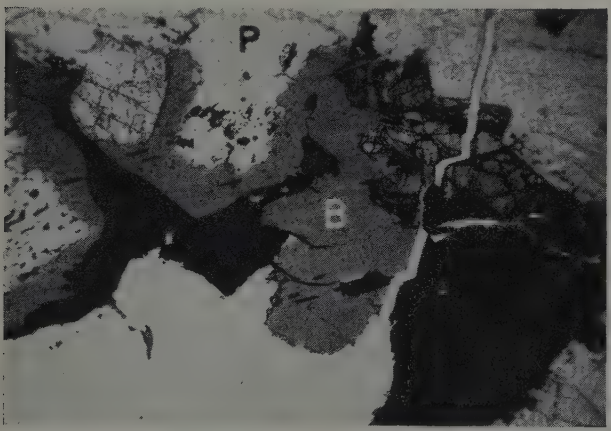

Fig. 4—Sulphides (black) associated with biotite (B) which is probably a deuteric replacement of olivine and plagioclase (P). The white at lower left is balsam. Thin section, plain light. X30.

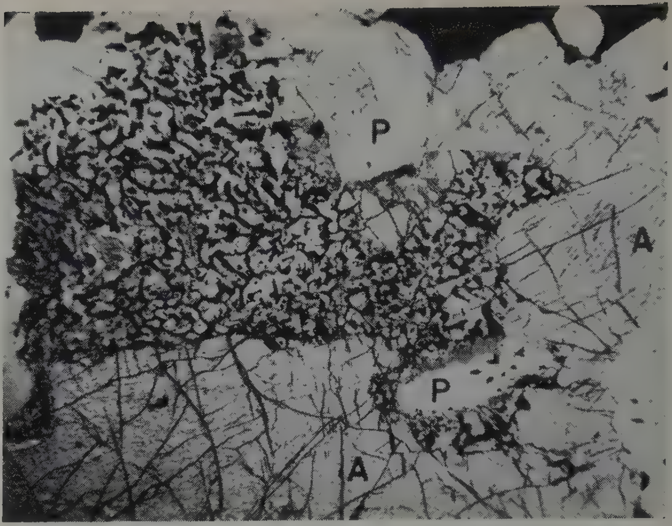

Fig. 5—Sulphides (black) intergrown in augite (A) and plagioclase (P). Thin section, plain light. X25.

7—At present there are no dependable indications of the presence or absence of massive sulphides such as exist in the Sudbury district, but exploration seems warranted because of the structure of the Duluth gabbro, its immense size and large degree of segregation. Strong evidence of the syngentic origin of the sulphides and the considerable length over which they occur also indicate that there is an excellent geological probability of finding a commercial deposit.

These facts, when compared with general knowledge of intrusives of the Duluth gabbro type, suggest that the place to search for extensions of the deposit or for similar deposits is near the base of the gabbro. It is possible that the base near the thickest part of the intrusive is more favorable than the thinner ends near Duluth and in eastern Cook County. In any event there are areas 25 or 30 miles long on each side of the deposit that should be given careful examination. Over much of this length there are scattered and sometimes abundant outcrops of gabbro. South of the Mesabi range, however, there is a distance of over 30 miles where not a single outcrop is known near the base of the Duluth gabbro.

References

[1] F. F. Grout: The Lopolith, an Igneous Form Exemplified by the Duluth Gabbro. *American Journal of Science* (1918) **46**, pp. 516-522.

[2] F. F. Grout: The Titaniferous Magnetites of Minnesota. State of Minnesota Commissioner of the Iron Range Resources and Rehabilitation, St. Paul, 1950.

[3] F. F. Grout: Internal Structure of Igneous Rocks: Their Significance and Origin, with Special References to the Duluth Gabbro. *Journal of Geology* (1918) **26**, pp. 439-458.

[4] G. M. Schwartz: The Contrast in the Effect of Granite and Gabbro Intrusions on the Ely Greenstone. *Journal of Geology* (1924) **32**, pp. 89-138.

[5] F. F. Grout: Contact Metamorphism of the Slates of Minnesota by Granite and by Gabbro Magmas. Geol. Soc. Amer. *Bull.* 44 (1913) pp. 889-1040.

[6] G. M. Schwartz: Metamorphism of Extrusives by Basic Intrusives in the Keweenawan of Minnesota. Geol. Soc. Amer. *Bull.* 54 (1943) pp. 1211-1226.

[7] G. M. Schwartz: The Geology of the Duluth Metropolitan Area. Minn. Geol. Survey *Bull.* 33 (1949).

[8] M. L. Nebel: The Basal Phases of the Duluth Gabbro Near Gabemichigami Lake, Minnesota. *Economic Geology* (1919) **14**, pp. 367-402.

[9] G. M. Schwartz: The Relations of Magnetite and Ilmenite in the Magnetite Deposits of the Duluth Gabbro. *Amer. Mineralogist* (1930) **15**, pp. 243-252.

Determination of the Temperature and Pressure of Formation of Minerals by the Decrepitometric Method

by F. Gordon Smith

ALTHOUGH several geological indicators of the critical type are known, including quartz inversions and decomposition of hydrous minerals such as serpentine, there are very few of the general type. Solid solutions are excepted, but the limitations of use are very restricted and interpretations are sometimes ambiguous. General methods for determining temperature and pressure conditions during the crystallization of minerals would have considerable scientific and economic value.

It is not the purpose of this paper to discuss the various methods of geological thermometry and barometry, but to present one general method, applicable to all minerals, and to describe what progress has been made in the methods of measurement. The general method, in brief, is a study of the stress conditions in and around various types of foreign inclusions which are trapped in minerals during growth.

The method depends upon the fact that any homogeneous gas, liquid, or solid will in general have coefficients of thermal expansion and volume compressibility different from those of any given mineral. Therefore stress must develop in and around all types of inclusions in minerals if the temperature or the pressure, or both, are changed from the conditions which prevailed during the growth of the mineral. The methods of measurement consist of determinations of the temperature-pressure conditions of fit of the inclusions in the host mineral.

The types of inclusions in minerals are: 1—gas, or liquid plus vapor, when observed at room temperature, due to crystallization under pneumatolytic conditions; 2—liquid, or liquid plus vapor when observed at room temperature, due to crystallization under hydrothermal conditions; 3—glassy solid, or devitrified glass, due to crystallization under magmatic or high temperature metamorphic conditions, in a siliceous liquid; and 4—crystals, due to overgrowth of other minerals crystallizing simultaneously or of other minerals which crystallized previously.

A survey of the literature shows that much valuable earlier work on inclusions, especially that carried out in England in the last century, has dropped out of current knowledge. The following is a brief summary of the significant contributions to the problem up to the present day.

Davy in 1822 asserted that fluid inclusions in minerals consist of an aqueous solution of salts and a gas bubble, the whole being either at lower or higher pressure than atmospheric.[1]

At intervals from 1823 to 1862, Brewster contributed information concerning other types of inclusion consisting of 1—aqueous solution, a much more expansible liquid, and a gas; 2—aqueous solution, salt crystals, and a gas; and 3—the very expansible liquid and a gas. The very expansible liquid fills the gas space between 20° and 30°C. Compression strain effects were seen around inclusions in diamond, topaz, and other minerals.[2-6]

Sorby in 1858 and 1869 further advanced the study begun by Davy, stating that fluid inclusions represent a sample of the mother liquor of crystallization and that the degree of filling of aqueous inclusions at room temperature defines the temperature-pressure relations during formation of the host. The degree of filling may be measured by determining the minimum temperature of filling of the inclusion by the liquid phase. The very expansible liquid in some fluid inclusions is liquid carbon dioxide. The temperature at which salt crystals in fluid inclusions completely dissolve in the fluid is the minimum temperature of formation. Inclusions of glass or devitrified glass indicate crystallization from a melt. Inclusions of crystals in minerals are often centers of strain, which may be seen by optical effects or by radial tension cracks. Sorby realized that an analysis of stress-strain relations about inclusions could be used to provide precise data on the temperature of crystallization, but the matter was never pursued.[7, 8]

Hartley (1876, 1877),[9,10] Hawes (1881),[11] Wright (1881),[12] Johnsen (1920),[13] and Holden (1925)[14]

F. GORDON SMITH is Professor of Geology, University of Toronto. Discussion on this paper, TP 3338L, may be sent to AIME (2 copies) before Aug. 31, 1952. Manuscript, April 9, 1951. St. Louis Meeting, February 1951.

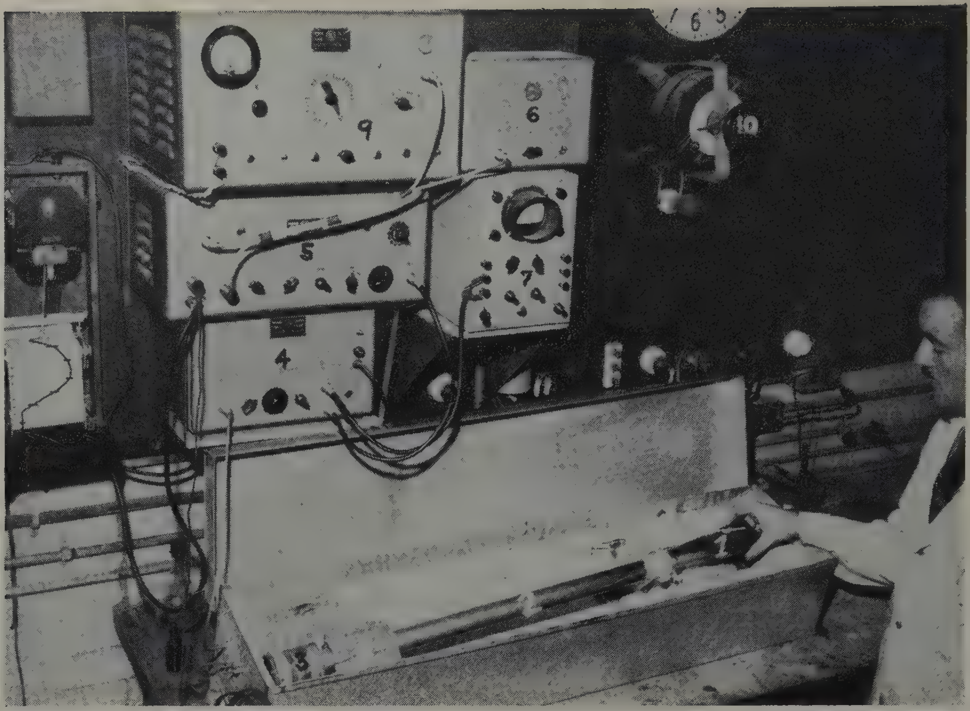

Fig. 1—Decrepitation apparatus. 1. Heating block. 2. Sound conducting tube. 3. Crystal microphone. 4. Two-stage preamplifier. 5. Ratemeter. 6. Neon flash lamp to indicate ratemeter functioning. 7. Oscilloscope. 8. Recording milli-ammeter. 9. Temperature fiducial marker. 10. Variac to control temperature of furnace, which encloses heating block. 11. Cold junction of thermocouple, the hot junction of which is in the heating block.

confirmed the presence of liquid carbon dioxide in many minerals, and in the years between 1901 and 1941 Königsberger,[15] Lindgren and Whitehead,[16] Buerger,[17] Newhouse,[18] and Faber[19] established beyond question the presence of salt concentrations, of the order of 10 to 20 pct, in the liquid of fluid inclusions. Such high salt concentrations eliminate certain theories of ore deposition.

Ingerson in 1947 reviewed the heating stage method of measuring the temperature of filling of fluid inclusions and produced charts showing the deposition temperature and the deposition pressure.[20] These charts were modified in 1950 by Kennedy,[21, 22] who restudied the pressure-volume-temperature relations of water.

In recent years H. S. Scott,[23] F. Gordon Smith,[24-27] and P. A. Peach[28, 29] have found that the temperature of filling of fluid inclusions can be detected by recording the beginning of decrepitation during heating.

Two-Phase Fluid Inclusions

The minimum temperature of filling of two-phase fluid inclusions by the liquid phase is the minimum temperature of deposition of the host, and the vapor pressure at that temperature is the minimum pressure of deposition. Both values are subject to a small correction because of the thermal expansion and compressibility of the host, but Ingerson[20] has shown that this correction can be neglected.

In general, the temperature-pressure relations within fluid inclusions above the temperature of filling are not known, because 1—the composition of the fluid is not known in each case, and 2—no data are available on the solutions which have geological importance in this respect, i.e., aqueous solutions of salts and carbon dioxide. However, it is assumed as a first approximation that the temperature-pressure relations on the liquid side of the vapor pressure curve are the same as for water, these data being known with some exactness. Consequently, the temperature of filling defines the approximate temperature-pressure relations during deposition of the host.

Determinations of temperature of filling may be made by heating while observing under the microscope. The newer method is to heat small fragments and record the temperature at which the rate of decrepitation increases abruptly. This method was developed at the University of Toronto in three main stages. The first technique consisted of heating the powdered mineral while listening with a stethoscope arrangements.[23] A modification of this technique was microphonic detection and amplification before the earphones. The second change was incorporation of an electronic calculator instead of the human brain to determine the discontinuity of rate of decrepitation.[28, 29] Several different types of heating blocks were designed and discarded for various reasons. The present design, consisting of a cylinder of inconel with a flattened termination to hold the sample, is satisfactory. This allows good sound coupling to the microphone, sound insulation from outside, and rapid cooling after each run. At this stage, temperature fiducial marks were made by a recorder watching a temperature indicator. This was replaced by an electronic temperature fiducial marker which puts 20°C pips on the record. In this way the heating rate and the decrepitation rate are recorded simultaneously. The circuit and other details of the apparatus are now being prepared for publication. The apparatus is shown in Fig. 1.

The calibration of the apparatus is based on an empirical method. A mineral which gives a sharply defined beginning of decrepitation is heated at several different rates, and the recorded temperatures of beginning are plotted against the heating rate and projected to zero rate of heating. Some of the same preparation is preheated to a temperature in excess of that at the start of decrepitation and the sequence of runs is repeated with this material. By selection of different specimens, the entire working range of temperature and heating rate is covered, for one grain size of one mineral. This has been determined for quartz, —40+80 mesh, as a standard, see Fig. 2.

As a control over interpretation of decrepigraphs, it is current practice to observe the degree of filling of two-phase inclusions in polished thin sections of transparent minerals and to estimate the approximate temperature of filling. A chart has been prepared to aid in this estimation, see Fig. 3, when it is determined that the liquid phase is aqueous. The estimated temperature of filling and the decrepitation temperature generally agree within 50°C, in the case of both primary and secondary inclusions. Several hundred determinations of this kind, on 16 different mineral species, have shown that the measured decrepitation is due to the filling of the fluid inclusions, and that there is probably no significant overshoot correction.[23, 28]

Three-Phase Fluid Inclusions

Some attempts have been made in the past to use three-phase fluid inclusions as thermometers and barometers (Johnsen, 1920, and Holden, 1925) but there are many uncertainties. The method depends upon finding, in the one mineral, inclusions of liquid carbon dioxide and gas and also of water and gas and then determining the temperature and pressure, by calculation, from the respective degrees of filling. This method has merits if it can be made quantitative.

It appears to be fairly common, in so-called high temperature minerals, that the three-phase inclusions have a variable water-carbon dioxide ratio, as if the two were immiscible at the time of deposition. Therefore, while most of the inclusions are of three phases, some are essentially of the two types of two phases, i.e., water and vapor and carbon dioxide and vapor. The unknown factors are the mutual solubilities of fluid water and carbon dioxide as functions of temperature and pressure. Until this system is studied under geologically important conditions, the method cannot be used, but it is a fertile field for investigation.

Saline Inclusions

Two-phase inclusions frequently contain crystals of various salts. Generally these are isotropic cubes, probably of sodium chloride, but sometimes they are elongated anisotropic crystals, possibly gypsum. In any case, they appear to have been deposited from the trapped fluid during cooling, because the ratio of salt crystal to fluid is visibly constant, independent of size of inclusion. On warming, the cubic crystals dissolve in the fluid, and the minimum temperature of disappearance is the minimum temperature of deposition.

In most cases, the salts dissolve in the liquid phase before it fills the inclusion. Occasionally they remain, and the temperature of disappearance provides new data. The salt disappearance temperature and the bubble disappearance temperature taken together give a minimum pressure of deposition.

This method has not been used very much since it was described by Sorby in 1858.[7] Lindgren and Whitehead used it in one case,[16] but the calculation method was challenged by Bowen some 14 years later.[30]

In general the method is not very useful, since only temperature and pressure minima are determined.

Glass Inclusions

A very interesting type of inclusion described by Sorby[7] could be used as an exact thermometer. The inclusions are of glass and/or devitrified glass in minerals which crystallized from siliceous melts. Such inclusions have a multitude of gas vacuoles within the glass or between the minute crystals. The method of measurement would consist of observing devitrified glass inclusions, and determining the temperature at which they become one phase.

Since glasses in general have a greater coefficient of thermal expansion than the corresponding denser crystals, it will be apparent that if the mineral is heated above the temperature at which the glass inclusion is one phase, the pressure on the glass should abruptly increase, thus causing decrepitation of the mineral.

The effect of pressure at the time of deposition has not been calculated; this requires a knowledge of the thermal expansion and compressibility of the glass as well as the host mineral. However, a first approximation calculation shows that the pressure correction probably is positive. That is, if the glass fits in the space of the inclusion at a determinable temperature at room pressure, it would fit in the space at a somewhat higher temperature at a higher pressure.

Glass and devitrified glass inclusions were seen by Sorby[7] in feldspar and augite in pitchstone and greenstone, and in leucite and augite in basalt.

The study of inclusions offers a method of discriminating between minerals which crystallized from a siliceous melt and those which crystallized from a hydrothermal solution. In the case of certain pegmatites this is now a question for debate, but the types of inclusions may be used in settling the problem.

Crystal Inclusions

During growth, crystals frequently include others which either grew on the growing faces and were covered or were enveloped from the matrix by a growing face. The first type is usually oriented, the second, unoriented. When the temperature and pressure fall to those at the surface of the earth, a misfit of the crystal inclusions develops, and this provides not only a very interesting type of thermometer but also a barometer.

Neglecting the effect of pressure, the temperature, volume, and stress relations in inclusions can be treated very simply, see Fig. 4. Two types of inclusions may be imagined, one type with a thermal expansion greater, and the other less than that of the host. The misfit during cooling to surface conditions develops tension and compression effects, respectively. Brewster[3-6] and Sorby[7, 8] noted effects arising from compression in diamonds and other minerals. Possibly some of the cracking of minerals, even those in vugs, may be due to this effect.

The effect of heating a mineral with the two types of crystal inclusions is to relieve the stress in and around both types, up to the temperature of formation. Above this temperature, both compression and tension effects begin again, in opposite sense, and the compression type may cause decrepitation.

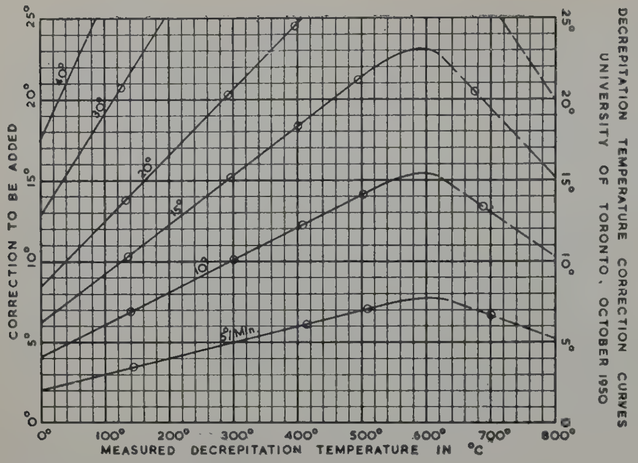

Fig. 2—Heating rate correction curves for decrepitation of quartz. Correction: (— 40 + 80 mesh).

Several tests have been made of this relationship. For example, a number of specimens of garnet metacrysts were heated in the decrepitation apparatus. A stage of decrepitation beginning between 590° and 660°C was found in every case, and those with abundant solid inclusions gave much more vigorous decrepitation than those transparent types with only a few solid inclusions.* Similar results have been obtained using cordierite and kyanite metacrysts. This work is continuing, and the results so far obtained indicate the possibility of general use of the method for the metamorphic minerals.

The effect of pressure during crystallization is not negligible in the case of crystal inclusions, but the data for quantitative calculations are limited. For most mineral pairs, the temperature correction appears to be positive, and of the order of 10° to 20° per 1000 atm. At present all of the data of thermal expansion and compressibility of minerals are being compiled.

Fig. 3—Relations between specific volume and diameter of bubbles and cavities in two-phase fluid inclusions, showing the approximate temperature of filling when the liquid phase is water.

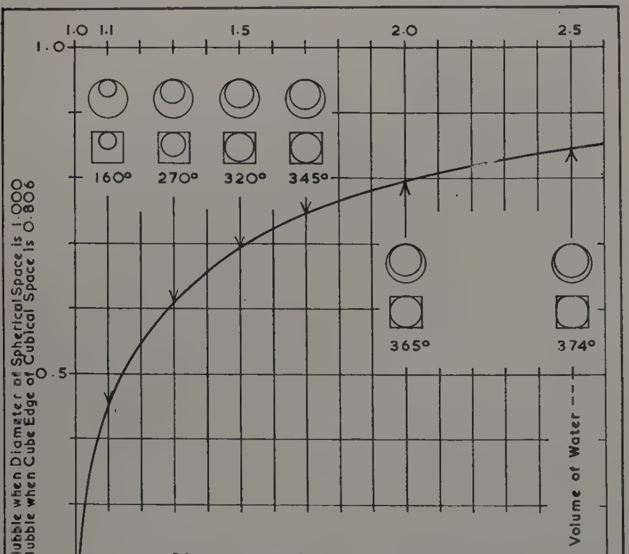

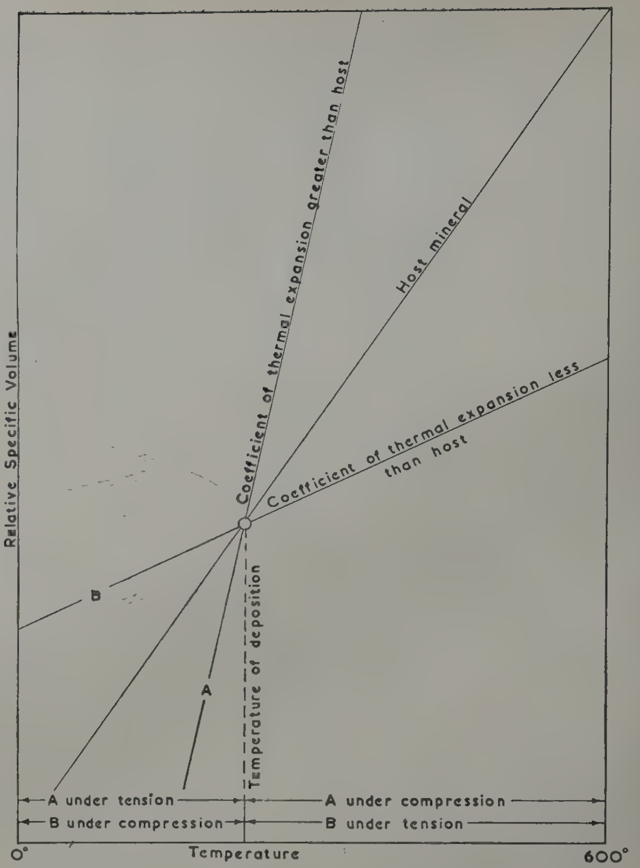

Fig. 4—Schematic diagram showing relations between temperature, volume, and compression and tension of solid inclusions in a mineral.

Another defect in the data is that while there is, for some minerals, information on the volume-temperature relations at one atmosphere, and volume-pressure relations at temperatures below 100°C, there is almost none on the volume-temperature-pressure relations over a geologically important range.

A first approximation may be made by assuming that the ratio of thermal expansion to compressibility remains constant if the volume remains constant, no matter what the temperature and pressure. On this basis, a start has been made in preparing approximate pressure-volume-temperature charts for some of the common minerals.

By superimposing two such charts, one can determine the curve of fit, if the fit can be determined at atmospheric pressure. Very much more work has to be done in this field, and probably the body of existing physical data of minerals will have to be increased.

Even though the quantitative aspects of the problem are not fully developed for use, there is now abundant evidence that most minerals begin to decrepitate at temperatures *above* those at which the fluid inclusions are filled. Characteristically, hydrothermal minerals give two stages of decrepitation, one due to filling of fluid inclusions and one due to an unknown cause. This has been recorded in several hundred cases, and in 28 mineral species.

---

* Since this was written the common varieties of garnet have been studied in more detail, and the results are now in press (*American Mineralogist*).

Other pertinent facts are: 1—If early minerals decrepitate, because of fluid inclusions, at higher temperatures than late minerals in any one deposit, the anomalous decrepitation temperatures also are different, in the same sense, and are of the same magnitude. 2—Minerals with no visible solid inclusions do not give the anomalous decrepitation. 3—Through selection of grain size of a mineral, either the fluid inclusion decrepitation or the anomalous decrepitation may be accentuated at the expense of the other; it is more frequently found that fluid inclusion decrepitation is destroyed first when progressively finer grain sizes are used, but the reverse has been found occasionally.

Calculations Using Decrepitation Data

Ideally, if the temperature of filling of fluid inclusions and the temperature of fit of solid inclusions can be measured, and exact data are available concerning the pressure-volume-temperature relations of the homogeneous fluid, the solid inclusions, and the host mineral, then the temperature and pressure of formation of the mineral can be determined. There appear to be no limits of accuracy of the results other than the experimental.

Of course, it is necessary to be certain that fluids have neither entered nor left the fluid inclusions since the formation of the host, and similarly this applies to solid inclusions. While the body of data on fluid inclusions points to no communication between the inclusions and the boundaries of the host, and this isolation within the crystal structure framework of the host is generally considered to be reasonable, it was postulated by Kennedy in 1950 that fluids may enter and leave inclusions depending on the pressure differential. Until this can be conclusively demonstrated, it will be assumed that, although some fluid inclusions may leak because of cracks caused by deformation, those not so tapped retain the original density and composition. Similarly, unless solid diffusion can be demonstrated to have modified the amount of solid inclusions, these will be assumed not to have been altered in mass.

There is good evidence from fluid inclusions that they do not leak. For example, it is commonly found that primary inclusions in vein quartz contain liquid carbon dioxide as well as water and a gas bubble, but the secondary inclusions contain a salt crystal, water, and a very much smaller gas bubble. If the latter were derived from the former, carbon dioxide must have been removed and salt added. The two types of inclusions may be seen to lie only a few microns apart within the host crystal.

Large variations in degree of filling of fluid inclusions have been discovered in single crystals of fluorite by Twenhofel.[31] This has been confirmed at the University of Toronto in the case of fluorite from Rosiclare. It has been found that there is a substantially lower temperature of decrepitation due to fluid inclusions in the later ruby blende than in the earlier brown sphalerite of the Tri-State region. Also, a sequence of decrepitation temperature over a range of about 50°C is typical of crustiform zinc ore from Wisconsin. Such systematic variations do not suggest that there has been leakage of fluids into or out of inclusions.

To date, most of the temperature-pressure calculations made at the University of Toronto have been based on decrepitation data. These fall into four classes, as follows:

1—The pressure during deposition is assumed to be constant and the variation of temperature of fluid inclusion decrepitation is taken to mean variation of temperature during deposition. The quantitative variation is obtained by the intersection of iso-volume curves and a probable geothermal gradient at the time of deposition. This method may be justified in the case of deposits such as in the Mississippi Valley, which frequently show the sequence of deposition by textures of progressive encrustation.

2—The temperature during one stage of deposition is assumed to be constant and the variation of fluid inclusion decrepitation temperature is taken to mean variation of pressure during deposition. The assumption of temperature constancy has been partially verified using the pyrite geothermometer[24] in a few cases. This method seems to be useful in the gold quartz veins of the Canadian Shield, especially with regard to the latest low temperature stage of mineralization.

3—The temperature of deposition of pyrite as given by the thermo-electric results is combined with pyrite decrepitation results to give the pressure of deposition of the pyrite. This pressure is then assumed to be constant during deposition of the other minerals, which allows conversion of the decrepitation temperatures to deposition temperatures. In 1951 this method was used by Peach in the study of a pegmatite assemblage.

4—The anomalous decrepitation is assumed to give the temperature of deposition. Therefore when fluid inclusion decrepitation temperatures and anomalous temperatures are combined, the pressure during deposition can be calculated. This method is being tested in several ways, one being synthesis of quartz, barite, and other minerals at known temperatures and pressures. The results are not yet conclusive.

Possible Uses of Temperature-Pressure Data

At present, mineral deposits are said to be of high, medium, or low temperature type depending on the occurrence, or absence, of certain minerals. This scheme of classification, developed by Lindgren and others, is not on a factual basis, because it has never been shown that the critical minerals are deposited in nature in restricted temperature ranges, and no reliable thermometric methods were used to establish the limits. In other words, the present scheme is a speculation rather than a reliable theory. As methods of geothermometry are devised and refined, the temperature classification of ore deposits, if such a classification is possible, will be made more factual, but a more important contribution will be a better understanding of the origin of ore deposits.

Temperature-pressure measurements should aid very greatly in determining the controls of ore deposition in veins. For example, it would be useful to know whether a fall of temperature or of pressure is more effective in depositing the various minerals. Some quantitative data on the possible effect of these two variables on the solubility of silica in water were reported by Kennedy.[21] In this system, at high temperature, pressure is the major variable.

Another use of temperature-pressure data will be in determining the zoning of a system of veins, by relating the temperature and pressure changes during deposition of any one mineral, in three dimensions. Such relations will show the direction of flow of the mineralizing solutions, and the structural control over the flow of the solutions. This may ultimately lead to exact predictions of depth of ore in any vein belonging to one system of mineralization.

The details of mineral paragenesis in complex ores could be resolved by exact temperature-pressure data. The order of deposition, degree of overlap, gaps in the sequence, and other factors could be determined without the use of the present subjective methods.

It would be of theoretical interest and perhaps also of some practical value to determine the genetic relations between pegmatites and hydrothermal veins. They are usually considered to be either sequential or parallel expressions of igneous activity. There are some mineralogical data suggesting a parallel history, such as both high and low temperature of filling of fluid inclusions in both pegmatite and vein minerals, but the whole matter must be restudied in detail.

The present controversy over the origin of granite could be settled if enough data on temperature of formation of igneous minerals were available. Probably the decrepitation method would detect the temperature above which misfit of solid inclusions occurs in igneous and metamorphic minerals. The shape of the resultant temperature profiles across granite bodies might discriminate between injection of a magma and metasomatic processes. The quantitative relations in the case of intrusion show that if the profile of maximum temperature in the intruded rock can be determined, then the temperature of the intruded rock and the thickness and temperature of the intrusive can be calculated.

Related to this is the possibility of detecting unexposed cupolas of intrusives in a metamorphic terrain by contouring the temperature of crystallization of one or more minerals.

In conclusion, a quotation from the writings of Sorby would be to the point: "I argue that there is no necessary connection between the size of an object and the value of a fact, and that, though the objects I have described are minute, the conclusions to be derived from the facts are great."[7]

Acknowledgments

The above results are based, in considerable part, on the coordinated research efforts of a number of students at the University of Toronto, notably A. D. Mutch, W. M. Little, P. A. Peach, R. W. Boyle, G. D. Springer, H. S. Scott, and W. M. M. Ogden.

Funds for equipment were supplied by the Advisory Committee on Scientific Research of the University of Toronto and by a number of mining companies of Canada and the United States.

References

[1] H. Davy: On the State of Water and Aeriform Matter in Cavities Found in Certain Crystals. *Philosophical Trans.* Royal Soc. London (1822) pp. 367-376.

[2] D. Brewster: On the Existence of Two New Fluids in the Cavities of Minerals, Which Are Immiscible, and Possess Remarkable Physical Properties, pub. 1823. *Trans.* Royal Soc. Edinburgh (1826) **10**, pp. 1-14.

[3] D. Brewster: Observations Relative to the Structure and Origin of the Diamond. *Trans.* Geol. Soc. London (1835) **3**, pp. 455-459.

[4] D. Brewster: On the Modification of the Doubly Refracting and Physical Structure of Topaz, by Elastic Forces Emanating from Minute Cavities. *Trans.* Royal Soc. Edinburgh (1845) **16**, pp. 7-9.

[5] D. Brewster: On the Optical Phenomena and Crystallization of Tourmaline, Titanium, and Quartz, Within Mica, Amethyst, and Topaz. *Trans.* Royal Soc. Edinburgh (1853) **20**, pp. 547-553.

[6] D. Brewster: On the Pressure Cavities in Topaz, Beryl, and Diamond, and Their Bearing on Geological Theories. *Trans.* Royal Soc. Edinburgh (1862) **23**, pp. 39-44.

[7] H. C. Sorby: On the Microscopic Structure of Crystals, Indicating the Origin of Minerals and Rocks. *Quarterly Journal* Geol. Soc. London (1858) **14**, Pt. I, pp. 453-500.

[8] H. C. Sorby: On the Microscopical Structure of Some Precious Stones. *Monthly Microscopical Journal* (1869) **1**, pp. 220-224.

[9] W. N. Hartley: On Variations in the Critical Point of Carbon Dioxide in Minerals and Deductions from These and Other Facts. *Journal* Chem. Soc. (1876) **30**, pp. 237-250.

[10] W. N. Hartley: Observations on Fluid-Cavities. *Journal* Chem. Soc. (1877) **31**, pp. 241-248.

[11] G. W. Hawes: On Liquid Carbon Dioxide in Smoky Quartz. *American Journal of Science* (1881) **21**, pp. 203-209.

[12] A. W. Wright: The Gaseous Substances Contained in Smoky Quartz from Branchville, Connecticut. *American Journal of Science* (1881) **21**, pp. 209-216.

[13] A. Johnsen: The Paragenesis of Alpha Quartz and Carbon Dioxide. Sitzb. Bayer. Akad. Wiss., *Math.-Phys. Kl.* (1920), pp. 321-328.

[14] E. F. Holden: The Cause of Color in Smoky Quartz and Amethyst. *American Mineralogist* (1925) **10**, pp. 203-252.

[15] J. Königsberger: Die Minerallagerstatten im Biotit-Protogin des Aar Massivs. *Neues Jahrbuch für Mineralogie,* Beil.-Bd. (1901) **14**, pp. 533-547.

[16] W. Lindgren and W. L. Whitehead: A Deposit of Jamesonite Near Zimapan, Mexico. *Economic Geologist* (1914) **9**, pp. 435-462.

[17] M. J. Buerger: The Negative Crystal Cavities of Certain Galena and Their Brine Content. *American Mineralogist* (1932) **17**, pp. 228-233.

[18] W. H. Newhouse: The Composition of Vein Solutions as Shown by Liquid Inclusions in Minerals. *Economic Geology* (1932) **27**, pp. 421-422.

[19] H. Farber: On the Salt-Solutions in Microscopic Cavities in Granites. *Danmarks Geol. Unters* (1941) Ser. 2, No. 67.

[20] E. Ingerson: Liquid Inclusions in Geologic Thermometry. *American Mineralogist* (1947) **32**, pp. 375-388.

[21] G. C. Kennedy: Pressure-Volume-Temperature Relations in Water at Elevated Temperatures and Pressures. *American Journal of Science* (1950) **248**, pp. 540-564.

[22] G. C. Kennedy: "Pneumatolysis" and the Liquid Inclusion Method of Geologic Thermometry. *Economic Geology* (1950) **45**, pp. 533-547.

[23] H. S. Scott: The Decrepitation Method Applied to Minerals with Fluid Inclusions. *Economic Geology* (1948) **43**, pp. 637-654.

[24] F. G. Smith: The Pyrite Geothermometer. *Economic Geology* (1947) **42**, pp. 515-523.

[25] F. G. Smith: The Ore Deposition Temperature and Pressure at the McIntyre Mine, Ontario. *Economic Geology* (1948) **43**, pp. 627-636.

[26] F. G. Smith: A Method for Determining the Direction of Flow of Hydrothermal Solutions. *Economic Geology* (1950) **45**, pp. 62-69.

[27] F. G. Smith and P. A. Peach: Apparatus for Recording of Decrepitation in Minerals. *Economic Geology* (1949) **44**, pp. 449-450.

[28] P. A. Peach: A Decrepitation Geothermometer. *American Mineralogist* (1949) **34**, pp. 413-421.

[29] P. A. Peach: Geothermometry of Some Pegmatite Minerals of Hybla, Ontario. *Journal of Geology* (1951) **59**, pp. 32-38.

[30] N. L. Bowen: Geological Thermometry: *Laboratory Investigation of Ores,* ed. E. E. Fairbanks, McGraw-Hill, 1928, pp. 192-197.

[31] W. S. Twenhofel: The Temperature of Crystallization of a Fluorite Crystal from Luna County, New Mexico. *Economic Geology* (1947) **42**, pp. 78-82.

Development and Operation Of Sulphur Deposits in The Louisiana Marshes

by Z. W. Bartlett, C. O. Lee, and R. H. Feierabend

DESPITE the fact that American brimstone production has increased 2½ times since the prewar period 1935–1939, the demand for sulphur exceeds the supply. To alleviate this situation efforts are being made to increase the production of sulphur and bring the shortage to an end. The most important developments are being undertaken on the Gulf Coast. One new brimstone mine has been put into operation and three others are being developed. These projects are expected to account for a large part of the additional sulphur production now anticipated for the free world.[1,2]

Except for a small amount of byproduct sulphur from sour natural gas and refinery gases, American brimstone is produced by the same process devised by Frasch 60 years ago, consisting essentially of the injection of superheated water at about 325°F into sulphur-bearing formations through wells which are drilled from the surface by standard oilfield methods. Sulphur deposits vary in depth from a few hundred feet to 2500 ft from the surface; in a typical deposit the sulphur occurs as crystalline aggregates in porous limestone and gypsum in concentrations varying from 5 to 40 pct, the thickness of the formation ranging from a few feet to several hundred.[3] The deposits are usually surrounded by formations impermeable to the flow of hot water, the top and sides being enclosed by impermeable sediments and the bottom by dense impermeable anhydrite. As the hot water leaves the well bore, it percolates through the formation and transmits its heat to the rock and sulphur. When the sulphur reaches 240°F it melts, separates from the rock, and flows through the hot channels downward to the bottom of the well. Here it is freed from incoming water and from formation water, which saturates the porous rock, by gravity separation, liquid sulphur being 1.8 times as heavy as water. It then is pumped to the surface in a relatively pure state, 99.5 pct or better. Chief contaminants are organic impurities, such as petroleum residues, which are soluble in sulphur and tend to discolor it.[4]

Sixteen deposits of commercial magnitude have been discovered in the Gulf Coast area. Five of these deposits have been depleted and abandoned with production totalling more than 26,886,000 tons. Eight properties are operating and have produced 65,875,000 tons to Jan. 1, 1952, for a total Frasch-type production of 92,761,000 tons. Three new deposits are under development. Aforementioned deposits are listed in Table I.

Each of these deposits has been found in the caprock overlying shallow intrusive salt plugs or domes and buried in several hundred to as much as 2500 ft of sediments. All salt domes do not contain sulphur; only 16 sulphur deposits have been found in a total of 231 salt domes which are known to exist in the Gulf Coastal states of Texas, Louisiana, Mississippi, and Alabama. Ten of the salt domes lie in the Gulf of Mexico offshore from the Texas and Louisiana coasts. Additional offshore domes may be found, but their value as a sulphur potential is questionable owing to the great hazard and high cost that can be visualized at these exposed locations where depths of water reach 50 ft.

Marsh operations of Freeport Sulphur Co. are in the southeast section of Louisiana. In general, the country is low, flat, relatively uninhabited marshland broken by many shallow lakes and bayous which extend for irregular distances inland. Geologically, the coastal area is of sedimentary origin, having been built up gradually under the sea by deposition of material carried down by large streams to their deltas. Offshore bars were formed enclosing

---

Z. W. BARTLETT, C. O. LEE, and R. H. FEIERABEND, Members AIME, are Assistant General Manager, Technical Assistant to the General Manager, and Production Superintendent, respectively, with Freeport Sulphur Co., New Orleans.

Discussion on this paper, TP 3363H, may be sent (2 copies) to AIME before Sept. 30, 1952. Manuscript, March 18, 1952. New York Meeting, February 1952.

This page of Mining Transactions AIME follows p. 703. The intervening non-Transactions pages appeared in Mining Engineering.

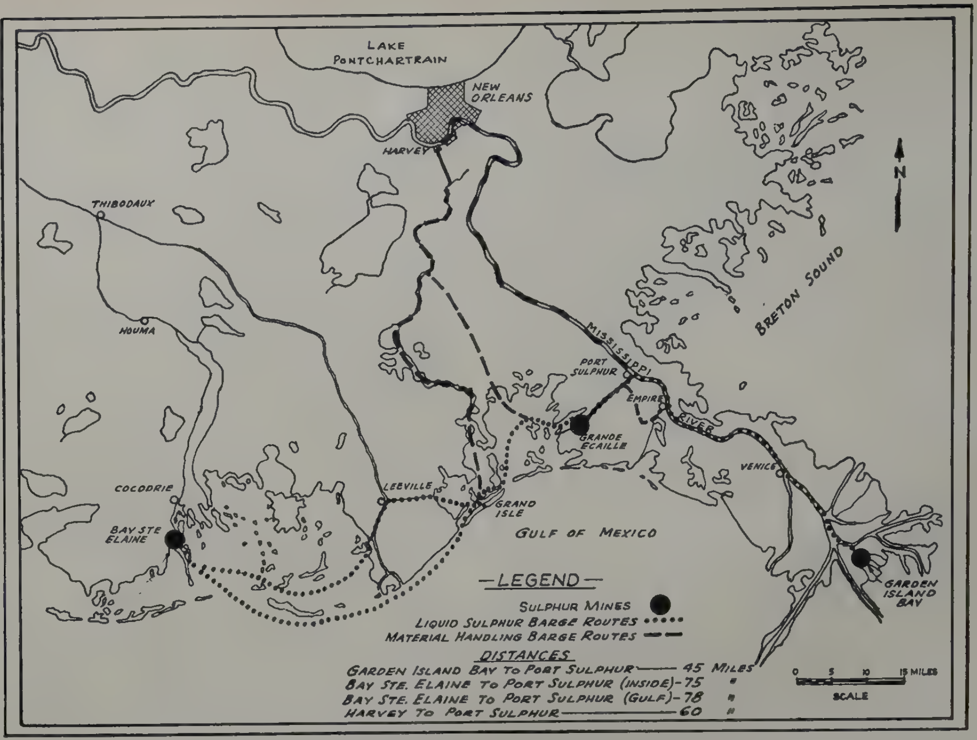

Fig. 1—Sulphur mines in the Louisiana marshes under development and operation by Freeport Sulphur Co.

long narrow lagoons connected to the open sea by tidal inlets.[5] No truly solid sediments exist near the surface, and foundations for all structures of a permanent nature or of substantial size and weight must be supported by piling. In this region mosquitoes, gnats, and deer flies abound. The salt marshes produce muskrat, while fresh water marshes have both alligators and water moccasins.

The first sulphur mining venture in this area, where many vexing problems had to be overcome, was in 1933 when Freeport Sulphur Co. started development of the Grande Ecaille mine. The location of this mine, shown in Fig. 1, is 10 miles southwest of the right descending bank of the Mississippi River approximately 45 miles below the city of New Orleans. Within the last year Freeport has announced plans to build mining facilities at Bay Ste. Elaine dome and Garden Island Bay dome, both of which are even less favorably located. Bay Ste. Elaine is near the open Gulf about 35 miles southeast of Houma, La., and Garden Island Bay is at the extreme southeastern tip of Louisiana near the mouth of the river.

Table I. Sulphur Deposits of Commercial Significance Found in the Gulf Coast Area

Deposit	Producer	Dates of Operation	Approximate Production
Sulphur, La.	Union	1895-1924	9,412,000
Bryanmound, Tex.	Freeport	1913-1935	5,001,000
Gulf, Tex.	Texas Gulf	1919-1936	11,805,000
Hoskins Mound, Tex.	Freeport	1923 to date	10,149,000
Palangana, Tex.	Duval	1928-1935	237,000
Boling Dome, Tex.	Duval	1935-1940	571,000
Boling Dome, Tex.	Texas Gulf	1929 to date	36,327,000
Long Point, Tex.	Texas Gulf	1930-1938	402,000
Long Point, Tex.	Jefferson Lake	1946 to date	990,000
Lake Peigneur, La.	Jefferson Lake	1932-1936	431,000
Grande Ecaille, La.	Freeport	1933 to date	11,970,000
Clemens, Tex.	Jefferson Lake	1937 to date	2,104,000
Orchard, Tex.	Duval	1938 to date	2,611,000
Moss Bluff, Tex.	Texas Gulf	1948 to date	712,000
Starks, La.	Jefferson Lake	1951 to date	39,000
Spindletop, Tex.	Texas Gulf	Start 1952	
Bay Ste. Elaine, La.	Freeport	Start late 1952	
Garden Island, La.	Freeport	Start late 1953	

Prospecting

The growth of geophysical methods of prospecting since 1924 has played an important part in prospecting and locating salt dome structures. The reliability and value of geophysics in the petroleum industry were quickly demonstrated,[3] and the entire Gulf coast area has been surveyed repeatedly. Reflection seismograph and gravity meter surveys first are made of large areas. On indication of a favorable structure, torsion balance surveys, now replaced by gravity meter, are made to secure more detailed information on size, depth, and configuration of the caprock area. The ultimate check is drilling.

The nature of the formations overlying the domes and the variable depth and character of the caprock materials dictate the use of relatively heavy drilling equipment except under ideal conditions. Accordingly, conventional shallow oilfield rotary drilling equipment is used. In the case of marsh operations, drilling machinery and equipment are mounted on barges identical except in size and capacity to units which the oil industry uses for marsh drilling work. Freeport Sulphur Co. recently built two drilling barges, capable of drilling to 3000 ft, at a cost of $250,000 each, see Fig. 2. The cost of prospecting in the marshes is considerably higher than in "hard ground" country. Prospecting two domes in south Louisiana cost approximately $800,000 for 20 holes, or $40,000 per hole. On a footage basis, this is about $17.00 per ft, almost double the rate for drilling similar domes on land.

Until the advent of oilfield-type diamond coring equipment within the past few years, accurate sampling of sulphur formations for reserve estimates

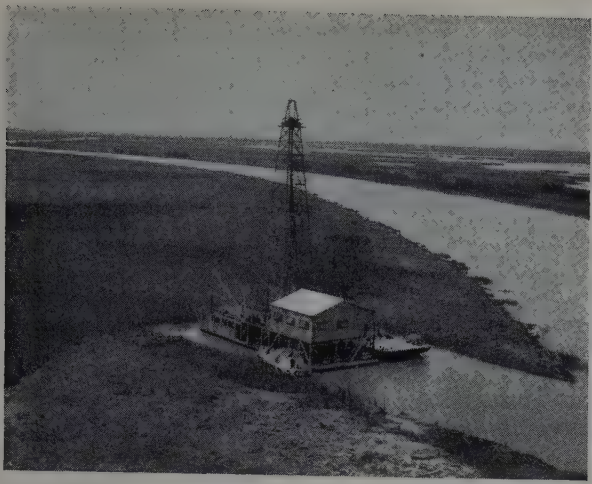

Fig. 2—A Freeport Sulphur Co. floating drilling rig at Garden Island Bay, site of one of the company's new mines in the Louisiana swamplands. These rigs, which cost $250,000 each, can drill to 3000 ft.

was difficult because of loss of fluid returns in porous formations and because of the soft, friable nature of sulphur. Now, with diamond coring equipment, 90 to 100 pct recovery can be expected from cores 3½ in. to 4⅜ in. in diam. The bits cut holes 6⅛ in. and 7⅞ in., respectively, and the cost for bit heads ranges from $1.00 to $1.25 per linear ft of hole.

Terrain and Foundation Conditions

In the vicinity of Grande Ecaille the surface of the marsh consists of salt grass and decayed vegetable matter at elevations of 1 to 2 ft above mean Gulf level. The marsh is underlain by 5 or 6 ft of humus, 40 ft of very soft clay, 20 ft of soft clay, and medium stiff clay thereafter to a depth of 130 ft. Some thin sand streaks and lenses are present, but these have negligible supporting value. Seventy-five foot pine piling will support 8 tons per pile, this value being developed in skin friction alone. Sulphur storage bins, which impose an area load of about 2500 lb per sq ft on 60 to 75-ft wood piling, have subsided 3 to 5 ft because of compression of the medium stiff clay below the pile tips. The power plant, see Fig. 3, supported by 75-ft piling with a semi-rigid foundation has subsided 6 in. under an area load of 1200 lb per sq ft. More than 100,000 piles have been driven at the Grande Ecaille mine.

Marshes in the Garden Island Bay area are more recent than those at Grande Ecaille and are subject to overflow by fresh water from Mississippi River distributaries. Natural banks at the edges of the distributaries are fairly firm and reach elevations of 2 to 4 ft above mean Gulf level for widths of 50 to 100 ft. The intervening marshes consist of very soft clay at elevations ranging from 1 ft above to 3 ft below mean Gulf level, covered with cane, grass, and water hyacinths. The entire area is underlain by very soft clay to a depth of 50 ft and soft clay to a depth of 150 ft. Soil analyses indicate that a 75-ft wood pile will support 7 tons by skin friction and that an area load of 1200 lb per sq ft supported on 75-ft wood piling with a rigid foundation cap will subside approximately 9 in. Further studies have revealed that the present rate of geological subsidence of this area is 1 ft in 20 years and that mean Gulf level is rising 3 in. each 20 years.[6]

Marshes in the Bay Ste. Elaine are similar to those at Grande Ecaille, and soil analyses indicate about the same supporting values.

Water Supply

An adequate supply of suitable water is a fundamental requisite of the Frasch Process. Tide water is available at all marsh domes, but the high salinity of this water makes it objectionable for use in a conventional Frasch Process plant. For the Grande Ecaille mine the only source of fresh water is the Mississippi River 10 miles distant. Normal river water contains 1.6 grains salt per gal, 28 ppm as NaCl, and 6.9 grains total hardness, 118 ppm as $CaCO_3$. During late summer and early fall, however, the flow in the river is reduced to such an extent that sea water invasions occur upstream along the bottom of the river. This phenomenon occurs each year, but its duration and the upstream distance of the invasion depend on the amount and distribution of rainfall within the watersheds of the river and its tributaries. At Port Sulphur, which is 55 miles upstream from the mouth of the river, contaminations by sea water occur each year, and to mitigate the effect of the contamination a 240,000,000-gal earthen reservoir has been provided.

The location of the Garden Island Bay mine, which is only 3 miles above the mouth of one of the distributaries of the river, greatly intensified the water supply problem for a fresh water plant. A study of the river flow and salinities indicated that the period of poor quality would be much longer than at Port Sulphur. These predictions left no alternative but to provide a reservoir for approximately 6 months' storage of fresh water if seasonal crippling interferences to the operation of a fresh water plant were to be avoided. The amount of water for mining purposes plus that lost by evaporation, transpiration, and seepage requires a 600-acre reservoir with an available capacity of 600,000,000 gal. Construction of suitable reservoir levees with the soft material at the site presents a difficult problem in itself. To construct levees 10 ft in height, it is estimated that five lifts of dirt will be required with a period of soil consolidation between each lift. The base of the levee will be about 180 ft in width. Time required for construction will be about 20 months,[6] and levee construction costs alone are estimated to be $250,000.

At the Bay Ste. Elaine mine the only source of

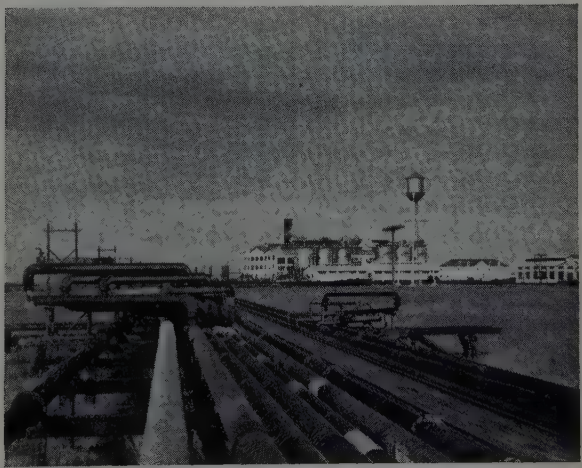

Fig. 3—Freeport Sulphur's power plant at Grand Ecaille, La., mine, which heats 6.5 million gal per day. The plant is constructed on 5000 piles. Both compressed air and hot and cold water go to the field via the pipes in the foreground.

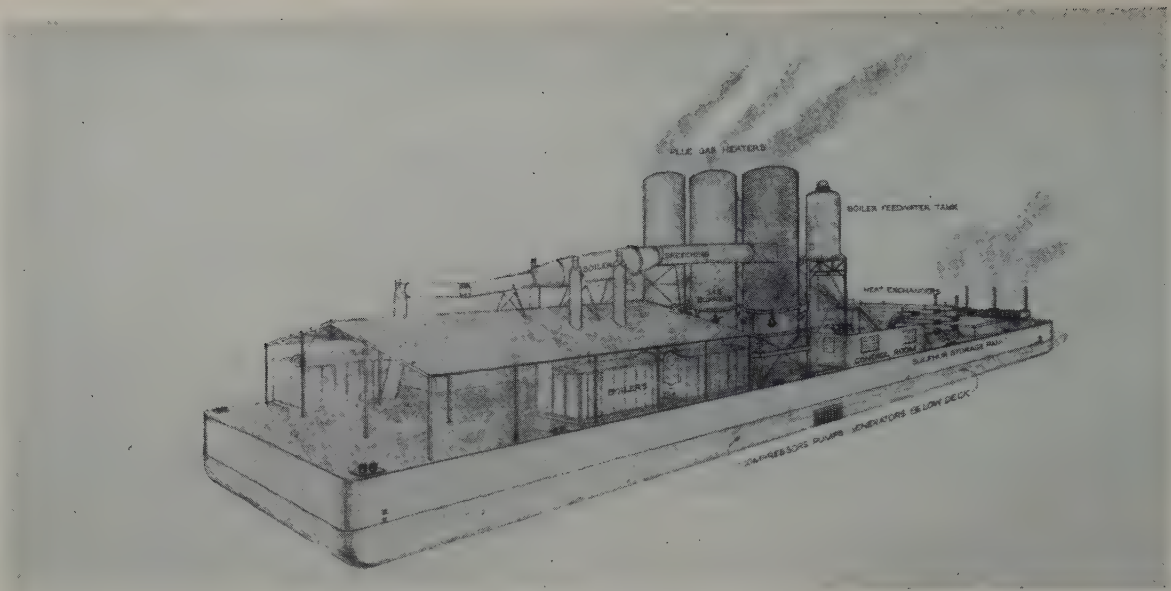

Fig. 4—Mining barge for Bay Ste. Elaine sulphur mine.

fresh water is approximately 35 miles distant. The cost of pipe lines and pumping stations for this distance would be prohibitively high, especially since the deposit is too small to justify a large capital investment. To solve this problem, Freeport Sulphur Co. has developed a process in which brackish water or sea water, which surrounds the property, can be heated to mining temperatures. This process is decribed in the following paragraphs.

Heating Plants

The heating plants used in all existing Gulf Coast sulphur mines are almost identical in their flowsheet and vary chiefly in size. A number of papers have been published which describe these plants; therefore only a brief description is included below.

The Grande Ecaille plant was built in 1933 with a capacity of 2,800,000 gal of hot water per day but has subsequently been expanded[7] so that the output now averages 6,470,000 gal per day of 325°F water. The plant now includes six 50,000 gal per hr hot process water treating units. The boilers are of the four-drum Stirling type. Each of the six has a capacity of 75,000 lb steam (200 psig) per hr, and each of two others has a capacity of 85,000 lb steam (400 psig) per hr. Capacity of power generation amounts to 4250 KW, which is furnished by three 750-kw turbo-generators and one 200-kw unit. Compressed air for pumping sulphur wells is furnished by four 700-cfm (800 psig) air compressors. Four heat reclaimers recover heat from the boiler flue gases and contribute to the high overall plant efficiency, which averages 85 pct. All pumps which handle the cold and hot water in the plant are of the centrifugal type and driven by steam turbines. Foundation for this plant,[5] which was very costly, consists of over 5000 piles 75 ft long driven on 2-ft 8-in. centers. The pilings were cut off at ground level and capped by a concrete mat 2 ft 6 in. thick with extra heavy piers closely spaced to support the heavy plant floor, which was elevated to about 12 ft above mean Gulf level.

The flowsheet of the Garden Island Bay plant is similar to that of Grande Ecaille. The plant, which is now under construction, is designed to deliver an average of 2,700,000 gal of 325°F water per day with an overall plant efficiency approaching 90 pct. The plant will include three 50,000 gal per hr hot process water-treating units, four water-wall Integral Furnace-type boilers each having a capacity of 60,000 lb of steam (425 psig) per hr, two 800-kw turbo-generators, three 500-cfm (800 psig) air compressors, four flue gas heat reclaimers, and turbine-driven centrifugal pumps for handling water. Foundations for this plant will be similar to that of Grande Ecaille but will cost considerably more per ton of supported load, because the supporting power of the subsoil is even less than that at Grande Ecaille.

The Bay Ste. Elaine deposit introduced additional problems over those encountered at Grande Ecaille and Garden Island Bay. One of these problems was the small size of the orebody which would not support a large capital investment. This prompted investigation of a portable type of plant that could be moved to other locations if the venture proved unsuccessful or if the life of the property was short. Consequently, the heating plant is being constructed on a large steel barge which will be floated to the mine site and sunk into position, see Fig. 4.

Another serious problem was the lack of a source of fresh water. Fortunately this problem had been foreseen when it was realized that new brimstone sources would probably be located in tidewater areas, and research extending over the past 8 years has been conducted by Freeport. This work led to the development of a new process[8] in which bay water having a salinity as high as 1640 grains of salt per gal, 28,000 ppm, will be heated to 325°F for mining purposes instead of piping fresh water from a source 35 miles distant.

The heating of sea water for sulphur mining purposes[8] will represent the first time in history that such a process has been attempted, mainly because of the scaling and corrosive problems ordinarily expected. Scale deposited from sea water when it is heated to high temperatures is made up of two different classes: 1—the deposition of calcium and magnesium as carbonates and hydroxides owing to the decomposition of bicarbonates, and 2—the deposition of sulphate scale caused by the lowering of the solubility of calcium sulphate when the water is heated. A normal approach to eliminating scale would be to remove all or part of the calcium and magnesium by chemical treatment. In the case of sea water, however, this would involve a very high cost because of the large amount of these elements present.

Freeport's approach to the problem was not the removal of these elements but the development of a process and equipment for heating the water in such a way that decomposition of bicarbonates is prevented. It is hoped that details of the processes which have been developed by Freeport Sulphur Co. will be the subject of a paper at a future date. Basically, the process to be used at Bay Ste. Elaine consists in heating the sea water under controlled conditions which minimize decomposition of bicarbonate and through proper controls prevent the deposition of calcium sulphate.

The corrosiveness of water having high salinities even in a cold state has been observed for a long time. In a hot state and during heating, corrosion should be excessive. Freeport has developed a process which overcomes excessive corrosion by the use of a unique apparatus. The removal of oxygen from sea water substantially reduces its corrosiveness, especially in a hot state. The removal of oxygen is accomplished in an apparatus consisting of a packed tower in which cold sea water flows downward through packing. In the upper part of the bed the water is contacted with flue gases discharged from the boilers and in the lower part of the bed with the products of combustion of natural gas burned directly into the tower. This apparatus serves several purposes. First, the temperature of the water is raised from about 75°F to 145°F and a large amount of heat reclaimed from the boiler flue gases, thereby maintaining the overall plant efficiency at 85 to 90 pct. Secondly, the water is raised to 190°F by burning fuel in the base of the tower using theoretical combustion air in a premix burner. This eliminates the heat normally supplied by boiler steam in raising the temperature from 145°F to 190°F. Third, the water is effectively de-aerated to less than 1/10 ppm of dissolved oxygen by contacting the water with the inert flue gases in the base of the tower.

Following the heating of the water to 190°F, the water is raised to 325°F by means of steam in indirect heat exchangers. Some soft sludge accumulates inside the tubs of the heat exchangers and a reduction in heat transfer rate occurs. Restoration of the heat transfer rate is accomplished by periodic flushing with steam which effectively removes the sludge from the exchangers. Although the corrosiveness of the water is reduced by de-aeration, corrosive resistant alloys are needed in the heat exchangers and small pipe fittings. In larger fittings and pipelines, cement-lined steel has been found suitable, and in well equipment a protective scale can be deposited by small and controlled injections of chemicals into the water as it enters the well head.

It is not anticipated that the new plant and process will be preferable to the conventional plant where fresh water is available. The initial plant cost is less, but the operating costs are expected to be greater.

The Bay Ste. Elaine plant is designed to deliver an average of 1,750,000 gal of 325°F water per day, 400 cfm of compressed air (500 psig), a power load of 600 kw, and miscellaneous steam for heating sulphur lines and equipment. Five water tube packaged-type boilers will be provided, each having a capacity of 30,000 lb steam, 400 psig, per hr. The sea water while passing through the flue gas heaters is heated from an average of 75°F to 190°F. High pressure centrifugal pumps then force the 190°F water through tubular heat exchangers where the latent heat of evaporation of the steam is transferred through the tube walls and into the water. The condensed steam is then re-cycled back to the boiler. In this manner, where distilled water is continuously used in the boilers, a water treating problem is eliminated and fresh water requirements are reduced to only that which leaks from the system. To make up for this loss of distilled water, an evaporator will be provided to distill either sea water or fresh water barged to the plant site. The pressure of the hot water leaving the exchangers will be sufficient to convey it through surface pipe lines and to inject it into sulphur-bearing formations. Three flue gas heaters will be provided, each being 10 ft in diam by 52 ft in height with two layers of packing. Specially designed shell and tube heat exchangers will be provided, each having three passes with alloy tubes in each pass. The boilers, see Fig. 5, operate at 400 lb psig and the steam will be expanded through prime movers, discharging at various back pressures to the exchangers. The mining barge, which is illustrated in Fig. 4, will be 40 ft wide by 200 ft long and 12 ft deep. When completed it will have a draft of about 5 ft, and after being towed to its location at Bay Ste. Elaine it will be sunk on a prepared bottom so that the final elevation of the deck of the barge will be about 6.5 ft above mean Gulf level.

Producing Operations

It is difficult to make a prediction of the rate of production from a new deposit because the productive capacity of two mines with similar facilities is seldom equal. Production varies from day to day and no area or even individual well will yield identical results. This variation of production is due primarily to the everchanging thermal conditions of the rock structure into which water or heat is injected.[9] Many factors upon which little or no control

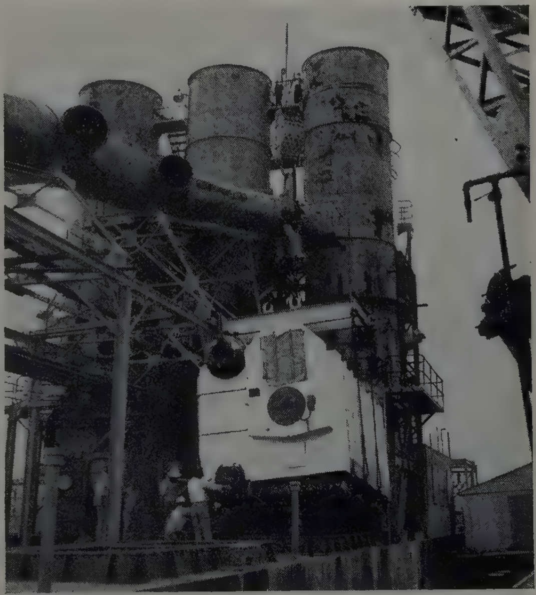

Fig. 5—One of the five boilers which will supply the Freeport Sulphur operation at Bay Ste. Elaine with 1.75 million gal of water daily is installed on a barge presently under construction. When completed it will be towed to the mine site and partially sunk on a prepared bottom.

can be exercised enter into the thermal efficiency of the individual deposits, areas, or wells. The major factors probably are the physical nature of the rock structure, reserves and concentrations of sulphur, and the rapidity of subsidence. Efforts are made to account for each of these factors in the design of surface facilities and operating procedures, but actual performance frequently dictates changes after operations have begun.

The pattern of melting is dependent on the course taken by the mining water from the point of injection. Because in most cases there is complete lack of uniformity of the formations, only generalized heat flow patterns can be predicted. Formation temperatures at the beginning of production are about 100° to 125°F. Both the sulphur and the enclosing rock must be raised above the sulphur fusion temperature. Cold formation water must be displaced and the loss of heat by conduction to overlying sediments must be supplied in order for the process to work. Permeability of the sulphur horizon and the barren caprock is usually so great that the only motivating influence which governs the flow of hot water through the rock structure is gravitational force. This force is obvious when it is realized that the incoming hot water has a density of about 0.9 compared to cold formation water at 1.01.

The consequent upflow of hot water continues until an impervious barrier is reached, or until the density of the mining water equals the density of formation water, and then lateral spreading occurs. As this takes place sulphur is being melted, the permeability and porosity of the rock is changing, and entirely new water channels may develop, sometimes favorable, but frequently detrimental. It is a known fact that extraction of sulphur takes place from the top of the deposit and progresses downward. Lateral extraction is quite limited, as indicated by the close well spacing necessary for depletion. A number of schemes have been attempted to control the extraction patterns or to overcome unfavorable channel conditions. Most successful of these has been the injection of mud[4] to block off cavities or to cause a more uniform permeability. Another method has been the use of a high density mining fluid[10] such as concentrated salt brine. Hot concentrated brine, having a density greater than formation water, initiates a downflow of heat pattern. In practice these two schemes are costly and therefore are used only when absolutely necessary.

The existence of a thick permeable barren zone atop the sulphur horizon is detrimental, as it allows the escape of water away from the melting area. It can be visualized that such a zone must be heated above the melting point of sulphur, actually forming a hot water cap, before substantial progress toward extraction can be accomplished. Experience has shown that domes of this character are high water consumers and generally low rate producers.

The thickness of the sulphur horizon and the concentration of sulphur have marked effects on the yield. Thick but lean zones cannot be expected to produce with the same ease or efficiency as rich zones of lesser thickness, even though the indicated tonnage may be equal in each case.

Subsidence

Subsidence, that is, the collapse of the rock from which sulphur has been removed, is of major importance in Frasch mining. It materially aids ultimate recovery by reducing the voids and preventing rapid escape of hot water from the producing area, and since it manifests itself at the surface in large sink holes, it influences the selection of the original plant location, operating facilities, and methods.

Because of the soft, unstable surface conditions of the marsh and the anticipated large area of surface subsidence, the plant at Grande Ecaille was located about 4000 ft away from the edge of the orebody. As a result plant subsidence has been negligible. The original well control station located near the edge of the orebody has settled almost 6 ft, and although the nearest production is 2000 ft away, this station last year settled 2½ in. Maximum subsidence amounting to 24 ft in depth has taken place over the area of greatest underground extraction. After 18 years of operations, the total volume of surface subsidence has about equaled the volume of sulphur removed from this deposit.

Hydraulic dredges are used to restore the surface to an operating level above sea level. To date over 22,000,000 cu yd of dirt have been pumped from outlying areas to refill the subsided mining area. This amount is in addition to about 8,000,000 cu yd pumped underground to fill cavities which originally existed in the deposit.

Land Mining

Grande Ecaille is a land-type operation. Initially the marshland over the orebody was filled to a height of 4 to 8 ft above sea level by hydraulic dredge. Since then the area has been partitioned by levees into smaller areas so that sections of it could be refilled while production continued on other portions. To refill an area all derricks, ramps, pipe lines, and buildings must be removed, and after refilling, drying, and consolidation requiring two or more years' time derricks, ramps, and pipe lines must be replaced before production can be resumed. This cycle is repeated several times before the area becomes depleted of sulphur, because no area can be depleted before surface subsidence extends below sea level. Several attempts have been made to continue mining with the surface below sea level, but the cost of levee maintenance and surface drainage is excessive.

All operations involving machinery must be on board roads or heavy mats. Currently there are over 5 miles of heavy board roads in service. These roads are designed to carry 30-ton moving loads, cost about $8 per ft, and last about 4 years. Conventional oilfield equipment is used for drilling wells. Material handling has been mechanized by the use of fork lift trucks, straddle trucks, mobile rubber-tired cranes, and winch tractors for skidding derricks and other heavy equipment.

Marine Mining

The small size of the Bay Ste. Elaine deposit, the unusual terrain, and the urgency of the need for increased sulphur production demanded a new type of drilling and producing operations, comparable to land mining as practiced at Grande Ecaille. Land mining, which requires surface filling, is cumbersome. A deposit such as Bay Ste. Elaine, where well life is expected to be short and surface subsidence negligible, adapts itself to a marine form of mining requiring no surface fill. Machinery will be barge-mounted instead of land-based, boats will be used instead of trucks and tractors, canals will replace roads, and all pipe lines will be supported on piling bents.

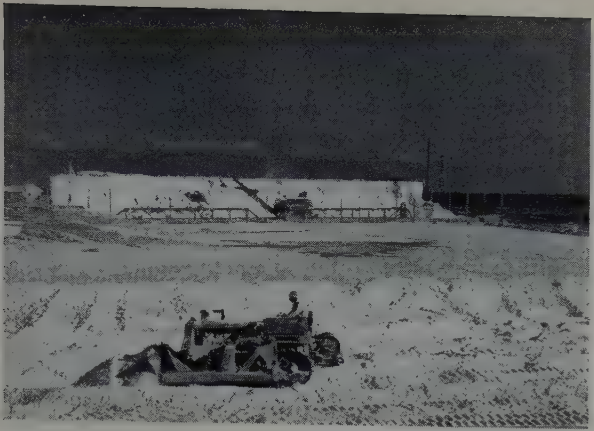

Fig. 6—A bulldozer in the foreground prepares the vat site at Grand Ecaille. A thin layer of molten sulphur is being sprayed in the center.

A similar mining system is planned for Garden Island Bay. At this mine considerable surface subsidence will no doubt occur; but since one of the distributaries of the river crosses the mining area, sedimentation from this distributary may be sufficient to replace the surface elevation lost by subsidence. However, although this and other advantages of the marine system of mining may outweigh the disadvantages, the constant exposure to winds, waves, and tides may present serious problems.

Sulphur Storage and Transportation

Bins for the storage of sulphur at most sulphur mines are built on firm ground and require no expensive foundation. Sulphur mines in marshes are severely handicapped in this respect, since the surface must first be elevated by means of a hydraulic fill because of the low elevation. At Grande Ecaille the storage area was filled to an elevation about 10 ft above mean Gulf level. After the fill became consolidated, 17,000 pilings 60 to 75 ft in length were driven on 4-ft 3-in. centers. These pilings have supported bins of sulphur 20 ft in height, but in 18 years have subsided 5 ft because of compression of the soil below the pile tips. The working storage of the bins, or vats, is about 160,000 long tons, see Fig. 6.

Since the terrain and foundation conditions are somewhat better at Port Sulphur[11] than at Garden Island Bay and Bay Ste. Elaine and since shiploading facilities have already been installed at Port Sulphur, it was decided that this location was the preferable storage and shipping point for all three of these marsh deposits and that sulphur would be barged in liquid form from the outlying deposits. A new storage area at Port Sulphur is now under construction. A hydraulic fill to an elevation of about 8 ft has been placed on an area comprising 80 acres. A study of the soil encountered in shallow bore holes indicated that sulphur bins 30 ft in height could be supported on wood piling 30 to 70 ft in length if driven on 4-ft centers. With this load, ultimate subsidence is expected to be 2 to 4 ft. The driving of 25,000 pilings started in 1950 and is still in progress. These pilings will provide two parallel storage sites each measuring 200 by 1125 ft and when filled to 30-ft height will provide working storage of about 450,000 tons of sulphur. Cost of the hydraulic fill and pile driving is estimated at more than $1,000,000, which is a high penalty over land deposits where no such expenditure is necessary. Pile driving has been completed on a few of the bins, and some are now in use handling a portion of Grande Ecaille's production, which is barged in liquid form to this site.

The liquid sulphur barges as they arrive at Port Sulphur are emptied into tanks on the dock. From these the sulphur is pumped through surface lines to a number of small tanks, elevated about 45 ft, immediately adjacent to the sulphur bins. The elevated tanks hold about 20 tons of sulphur, are filled in 8 min and emptied in 1 min, and when pumped full automatically empty themselves through a siphon into the bin, where the sulphur distributes itself in a thin layer over the entire bin surface. The size of the tanks and the pumping rate are designed so that sufficient time is allowed for this layer of liquid to freeze and solidify before another layer is deposited. This method of freezing avoids the creation of pools or pockets of liquid sulphur within the bin and consequent hazard to operating personnel.

Forms to confine the liquid are composed of aluminum sheets which are periodically raised and reinstalled at a higher elevation as the bin progresses upward and removed when it has been filled to its full height of 30 ft. The bin is then ready for loading into ships, river barges or railroad cars. Loading equipment consists of power shovels, cross conveyors, and a main belt which conveys the sulphur to a tipple tower mounted on the river dock. Electric-driven shovels having 3½ yd dippers and equipped with magnetorque hoist, swing, and crowd mechanisms are used, see Fig. 7. This new type of shovel has proved very satisfactory in the dusty condition that exists when sulphur is being handled. Formerly sulphur bins were blasted before loading, but in recent years it was found that shallow bins can be shoveled without blasting, provided the shovels have sufficient power to withstand the added load. This shovel handles up to 500 tons per hr. The sulphur is received from the shovel by a movable cross conveyor, 185 ft in length with a 36-in. belt, which is equipped with a portable hopper and a specially designed screw feeder.[12] By choke-feeding the screw it serves as a crusher and reduces chunks over 3 ft in size to 10 in. and smaller before they reach the cross-conveyor. The cross-conveyor discharges onto the main belt, which carries the sulphur about 3300 ft to the tipple tower and thence into the holds of ships or river barges.

A sulphur dock 225 ft long with mooring piling which totals 936 ft in length has been provided in

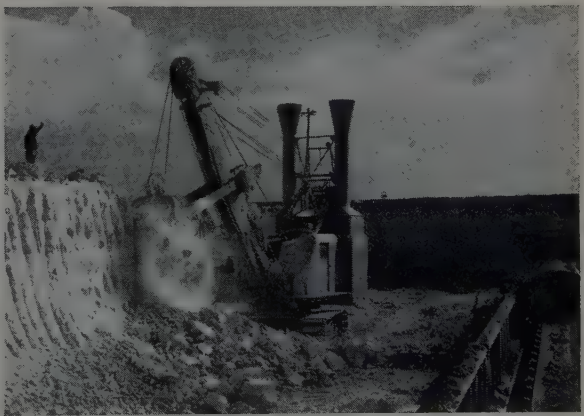

Fig. 7—Three and one half yard electric shovels break down a vat at Freeport Sulphur's Port Sulphur storage site. A conveyor belt carries the sulphur to loading points.

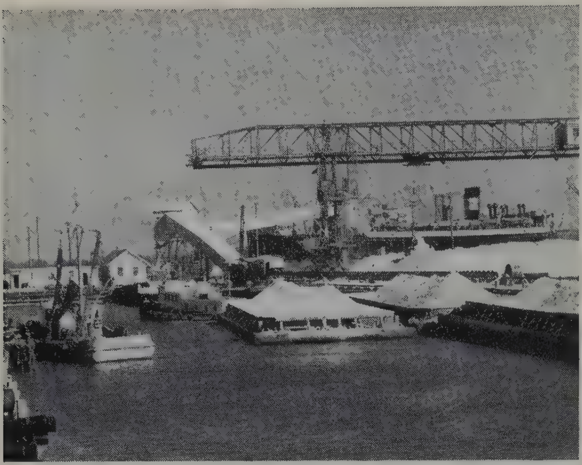

Fig. 8—The Mississippi dock of Freeport Sulphur at Port Sulphur, La., handles the entire output of the Grande Ecaille mine.

the Mississippi River at Port Sulphur, see Fig. 8. Original construction in 1933 required 95-ft piling, but recession in the river bank during the 1945 flood necessitated reconstruction with 12-in. pipe piling 135 ft in length. Recession of the river bank continues and revetment work will soon be necessary if sulphur shipments are to go forward. All types of ships are loaded, but maximum cargo lifted is about 11,000 tons. Maximum rate of loading ships will be about 800 tons per hr. River barges are loaded over the same dock and a transfer tower can divert sulphur from the belt conveyor to gondolas or box cars on a railroad siding located on the land side of the river levee.

Barging of hot liquids in tank cars or barges is not a novel feature, but the transportation of relatively large quantities of a crude, nonmetallic mineral in a liquid form is unusual. From Garden Island Bay to Port Sulphur the distance is 45 miles, and from Bay Ste Elaine 75 miles. The proposed barging routes are shown in Fig. 1. For the Garden Island Bay deposit four barges and three tow boats will be required and for the Bay Ste. Elaine deposit two barges and one tow boat. A liquid sulphur barge, illustrated in Fig. 9, will be 224 ft long, 39 ft across the beam, and 8 ft 5 in. in depth. When loaded with 1000 tons of liquid sulphur it will have a draft of 6½ ft. Although equipped with steam coils to prevent freezing of sulphur, no heat will be applied while en route because insulation will prevent excessive heat losses.

Since some of the barges must travel in the open water of the Gulf of Mexico they all have been designed to meet American Bureau of Shipping specifications for limited coastwise service which are considerably more rigid than those required for inland service. The twin-screw tow boats of all-steel construction will be 80 ft long and 22 ft in beam, will have a 6-ft draft, and will be equipped with two 400-hp Diesel engines. Communication equipment includes shortwave radio, ship to shore telephones, and radar. Cost of a 1000-ton liquid barge is estimated at $140,000 and the cost of each tow boat at $200,000. Total cost of transportation equipment for both Garden Island Bay and Bay Ste. Elaine will approximate $1,700,000.

Fog, wind, and storms will interrupt the scheduled transportation of sulphur from these mines. Some storage will be afforded by ample standby capacity in liquid barges, and this will circumvent the shutdowns of producing wells and the curtailment of production when transportation is interrupted.

Auxiliary Operations

Early in the development of Grande Ecaille, Freeport acquired a strip of marshland along the Mississippi River 10 miles east of the mine site and 45 miles below New Orleans. The surface of this area was elevated by hydraulic fill and the townsite of Port Sulphur was established. This townsite consists of 249 company-owned family dwelling units and dormitories for 194 single employees. Many employees have built homes on property adjoining the townsite. The permanence of Port Sulphur and the complete shop facilities at Grande Ecaille as well as their central location with respect to other new mines belonging to Freeport Sulphur Co. make these facilities ideally suited to central operating, maintenance, and administrative headquarters. At present all offices are located at Grande Ecaille. A new office will be erected soon at Port Sulphur where general supervision of all operations will center. Only operating departments will have offices at the various mines.

Transporting employees from Port Sulphur to Grande Ecaille requires a fleet of eleven 50-passenger, twin-screw Diesel-powered cabin cruisers, see Fig. 10. The remoteness of Bay Ste. Elaine and Garden Island Bay precludes daily crew changes, so that special schedules must be provided. Conditions

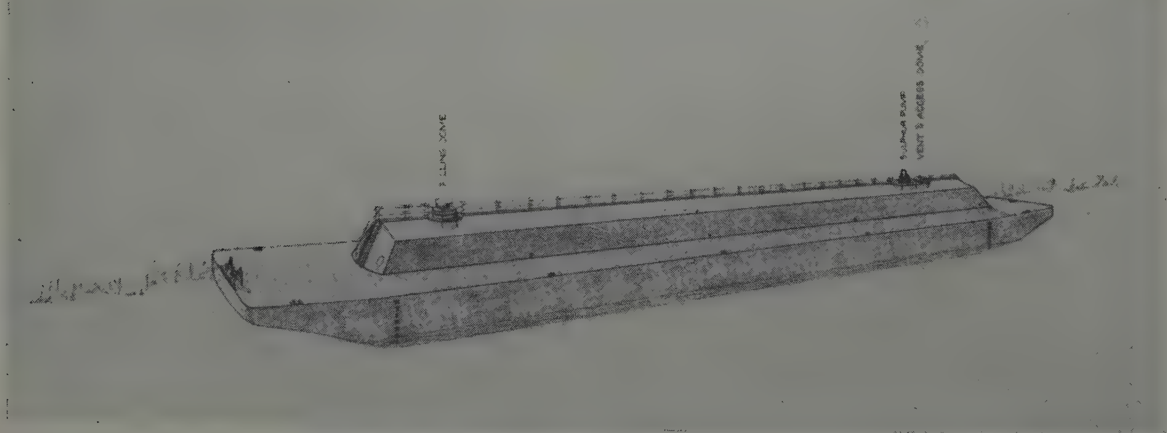

Fig. 9—A liquid sulphur barge. Capacity, 1000 long tons.

Fig. 10—One of the eleven 50-passenger boats which carry Freeport Sulphur employees between Grande Ecaille and Port Sulphur on the company-built canal.

at these mines permit no family dwellings or living with families at the mines, and dormitories with eating facilities must be provided.

Freeport's warehouse terminal at Harvey on the west bank of the Mississippi River across from New Orleans is the central receiving and dispatching station for materials and supplies en route to Grande Ecaille. Converted landing craft[13] used for tanks during the last war transport pipe and supplies to Grande Ecaille semiweekly, and barge trips are made as required for larger materials such as piling. This system is being expanded to include Garden Island Bay and Bay Ste. Elaine. The barge route is shown in Fig. 1.

A plant for centrifugally casting cement linings in steel pipe is operated at Harvey Terminal. Cement-lined pipe is used in all phases of operation involving handling of corrosive fluids. Costs range from $0.25 per ft for 4-in. pipe to $0.40 per ft for 8-in. pipe.

Two 12-in. hydraulic suction dredges are required for surface filling operations at Grande Ecaille. These dredges, one a Diesel-electric and the other an all-electric which uses plant power, each have dredging rates of 10,000 cu yd per day. They are capable of maintaining rates of 8,000 yd per day even though discharging two miles from the dredge cut.

Meteorological and Oceanographic Conditions

Grande Ecaille is located immediately to the west of the Mississippi River estuary and is protected by river levees from the damaging tides of most hurricanes. However, two unusual hurricanes have approached from a southwesterly direction, causing tides of 7 to 9 ft above sea level. These occurred in 1893 and 1915. No serious tidal conditions have been experienced since the plant was put into operation in 1933. The plant is alerted for hurricane precaution on an average of about twice each year, but to date complete evacuation has not been necessary.

Some serious fog conditions have been experienced in canal traffic between Grande Ecaille and Port Sulphur. Line squalls developing winds up to 70 miles per hr have also disrupted canal traffic on several occasions. Normal tides range from minus 2 ft during severe northers to plus 3 ft during southwesterly squalls. Annual mean temperature is about 70°F and annual mean rainfall about 65 in.

A meteorological and oceanographic report[4] prepared on the Garden Island Bay area points out that this exposed location on the southeastern tip of the Mississippi River estuary is more vulnerable to storm conditions than Grande Ecaille. According to this report, hurricane winds can reach a velocity of 135 miles per hr which can cause tides of 12 ft above mean Gulf level and up to a maximum of 17 ft where movement of the tides is obstructed. Hurricanes with winds of lesser velocity, but in excess of 50 miles per hr, can be expected once each 1.78 years. In addition, heavy fog will occur frequently during winter months and wind swells in the Mississippi River will prevent barging on an average of 2 days per month.

The Bay Ste. Elaine area lies some 75 miles west of the Mississippi River estuary and will not receive the protection from hurricane tides that exists at Grande Ecaille. Situated on the west side of a large bay, it is exposed to the maximum storm tides within the bay. Wind, tide, and wave conditions are expected to be approximately the same as those indicated for Garden Island Bay. Transportation from Bay Ste. Elaine to Port Sulphur is routed through the Gulf of Mexico for a distance of 45 miles, and it is anticipated that wave conditions[15] over this section of the Gulf will make barging hazardous during 20 pct of the time, but because of the distance of the Bay Ste. Elaine area from the Mississippi River, fog will probably be negligible.

References

[1] Z. W. Bartlett: The Sulphur Situation. Paper presented American Mining Congress, Los Angeles, California, October 23, 1951.

[2] J. C. Carrington: Current Developments in the Sulphur Situation. Paper presented Industrial Minerals Division, AIME, Morgantown, West Va., Sept. 14, 1951.

[3] W. T. Lundy: Known and Potential Sulphur Resources of the World. *Industrial and Engineering Chemistry* (November 1950) **42**, p. 2199.

[4] W. T. Lundy: Sulphur and Pyrites. *Industrial Minerals and Rocks,* sec. ed., Chap. 47, AIME, New York, 1949.

[5] W. T. Lundy: Development of the Grande Ecaille Sulphur Deposit. *Trans.* AIME (February 1934) **109**.

[6] Eustis Engineering Co.: Private Report of Foundation Investigation, Garden Island Plant Site, for Freeport Sulphur Co., New Orleans, December 1951.

[7] F. B. Blackstone: Power Plant Expansion for Sulphur Mine. *Southern Power and Industry.* (February 1949) p. 76.

[8] Freeport Sulphur Co., General Patent Application Cases: Sea Water Heating, No. 133.038; Sea Water Treatment and Heating, No. 133.041; Sulphur Mining Employing Sea Water Heating Process, No. 133.042.

[9] Williams Haynes: *The Stone That Burns.* D. Van Nostrand Company, Inc., New York, 1942.

[10] Freeport Sulphur Co. Patent License No. 2,493,413 covering use of brine, Jan. 3, 1950.

[11] Eustis Engineering Co.: Report on Sulphur Storage at Port Sulphur, Louisiana, for Freeport Sulphur Co., New Orleans, January 1950.

[12] A. A. Gustafson: Screw Crusher Solves Problem for Freeport. MINING ENGINEERING, AIME (October 1950).

[13] A. A. Gustafson: Thirteen Ways a Sulphur Producer Cut Costs and Improved Handling. *Engineering and Mining Journal* (January 1950) **151**, No. 1.

[14] A. H. Glenn and Associates: Meteorological-Oceanographic Design for the Freeport Sulphur Company Garden Island Bay Plant. Report prepared for Freeport Sulphur Co., New Orleans, December 1951.

[15] A. H. Glenn and Associates: The Frequency and Duration of Hazardous, Marginal, and Excellent Wave Conditions for Offshore Sulphur Barging from Terrebonne Bay to Barataria Pass. Report prepared for Freeport Sulphur Co., New Orleans, September 1951.

The Development of A Mining Operation From Diamond Drill Data

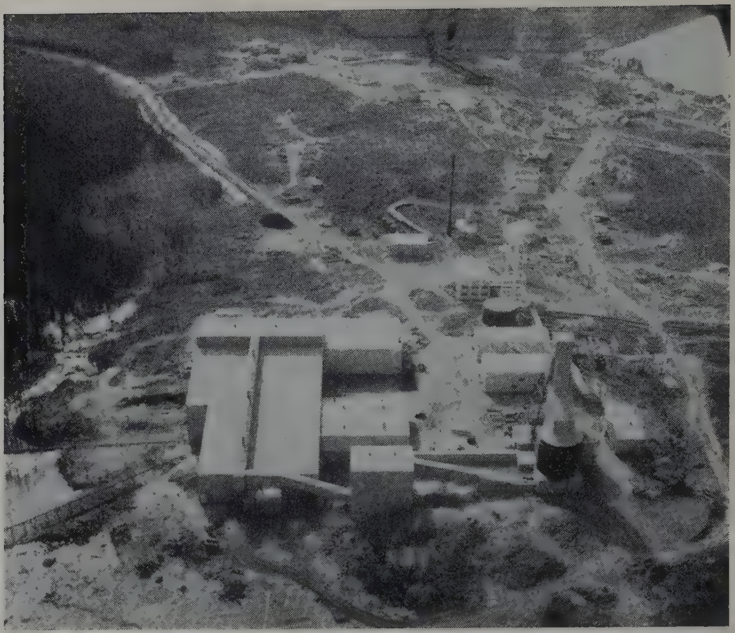

Fig. 1—The surface plant, Howe Sound Exploration Co., Ltd., Snow Lake, Manitoba.

by George C. Lipsey

FOR many years the mining of coal and other minerals occurring in sedimentary formation has been planned according to information obtained by diamond drilling. Placer mines have used churn drills for sampling and estimating deposits, and some metal mines have used the method either wholly or in part. The diamond drill method, therefore, although not entirely new, has come into more prominence in the last few years. Several large-scale developments now being planned or in the production stage have used this method in varying degree. This paper will describe the operations of the Howe Sound Exploration Co., Ltd. at Snow Lake, Manitoba, where a gold mine was developed and equipped for mining and milling wholly on the basis of diamond drilling results. The property has been in operation nearly 3 years, so that results can be compared with the estimates and assumptions made from the diamond drilling.

In developing the subject it is necessary to outline as briefly as possible the normal method of mining, from discovery to production stage. Table I sets forth these various stages, the methods of financing, the percentage of total cost, and the relative time interval required for each section of the work. The plan presented in this table cannot be applied to all mining developments, but it gives a basis on which to work. In Stages 2 and 3 the investment is moderate, and if the property does not respond favorably the options or interests can be terminated. Stage 4 represents a sizeable investment, and it is more difficult to drop the property after this part of the operation is completed. Stages 2, 3, and 4 may be repeated several times by different groups or companies before Stage 5 is reached, but when Stage 5 has been started the total capital investment must be provided and there can be no turning back.

It will be noted that there is a total of 116 units of investment in the overall cost if one company proceeds with Stages 2, 3, 4, and 5 in order. Stage 4, however, consumes time which is important when markets are being considered. Bringing a property into production when metal prices are low is much more difficult than when the prices are high, and if this stage can be set aside production is attained more quickly. When Stage 4 is eliminated the total becomes 86 units of cost for Stages 2, 3, and 5, but an adjustment of 14 units must be added to Stage 5. These 14 units represent the useable value of Stage 4. Thus Stage 4 represents an investment of 30 units if carried on before Stage 5, but 14 units if included with Stage 5. This is accounted for by the fact that development work can be accomplished more cheaply under Stage 5, since everything that is done is planned on a production basis with permanent services. Stage 4 must of necessity be governed by expenditures, and a great many temporary services, including housing and power plants, must be provided. The prospect shaft is a small one, and drifts,

---

G. C. LIPSEY, Member AIME, is Manager, Snow Lake Div., Howe Sound Exploration Co., Ltd., Snow Lake, Manitoba.

Discussion on this paper, TP 3354A, may be sent (2 copies) to AIME before Sept. 30, 1952. Manuscript, Dec. 14, 1951. New York Meeting, February 1952.

crosscuts, and raises are driven as small as possible for the purpose of obtaining the information required at the lowest possible cost. On the assumption, therefore, that Stage 4 can be eliminated, a saving of approximately 16 units can be effected.

The capital required to complete Stages 2 to 6 varies from 107 to 123 units of cost, not taking into consideration the cost of the property. It will be observed that in Stage 6 there is an allowance of 7 units of cost which may be higher in certain operations.

Location, Topography, Vegetation, and Climate of the Snow Lake District

Snow Lake is situated in northern Manitoba at Latitude 54°55′ and Longitude 100°. It is 400 miles northwest of Winnipeg, 80 miles northeast of The Pas, 80 miles east of Flin Flon, and 38 miles from Wekusko, a siding on the Hudson's Bay Railroad which runs from The Pas to the Port of Churchill on Hudson's Bay. It is close to the southern edge of the Precambrian Shield. The topography is typical Precambrian country of low relief with many muskegs, lakes, and rock ridges with clay overburden in the depressions. The vegetation consists of spruce, poplar, birch, jackpine, and tamarack trees with occasional fair stands of merchantable spruce. Heavy moss covers most of the ground except for a few small grassy plots on edges of lakes and rivers. There is a wide variation in temperature between summer and winter. In summer the days are long with 21 hr daylight in June, and temperatures vary from 70° to 95°F. In midwinter there are 8 hr of daylight and temperatures throughout the season vary from −15° to −50°F and occasionally lower. Although the days are short in winter they are generally bright and sunny. The lakes are frozen over from November to May. By mid-April the winter snows on the land are generally gone. Average yearly precipitation amounts to 11½ in. of rain, most of which falls in heavy thunderstorms in June and July, and 40 in. of snow, which rarely lies over 2 ft deep on the ground. Until an all-weather road was constructed to Wekusko all heavy supplies were hauled by tractor and sleigh over the frozen lakes and muskegs from late December to the end of March. From May to October pontoon-equipped planes or canoes and portages provided transportation.

Fig. 2—The Howe Sound Exploration Co. plant at Snow Lake in relation to the townsite.

Stage 1, Discovery: The exact date of the gold discovery at Snow Lake is not known, but it is thought that work was done on the property before the turn of the century. Chris Parres Associates restaked the claims in 1927 and did considerable trenching between this date and 1938, when Nor-Acme Gold Mines Ltd. was incorporated.

Stage 2, Preliminary Examinations: Frank Ebbutt, geologist for the Howe Sound Co., examined the property in the fall of 1940 and sampled the surface outcrops. He returned in the spring of 1941 and drilled 5 shallow holes with an X-ray machine. The results of this drilling were encouraging, as the values averaged better than those of the surface outcrops. An option to lease the property from the Nor-Acme Co. was then entered into.

Table I. Stages of Mining Development from Discovery to Production

Stage No.	Stage of Development	Financing	Units of Cost	Time Interval
1	Discovery	Prospector Grubstake Government assistance Mining company	A few hundred dollars to 1 unit	1 to 20 years
2	Preliminary Examinations	Individual Partnership Syndicate Mining company	A few thousand dollars to 1 unit	A few weeks to several months
3	Preliminary Development Includes surface trenching, diamond drilling, geological mapping, geophysical or geochemical prospecting, and in some cases underground work	Partnership Syndicate Sale of stock in company formed to develop the prospect Funds provided by mining company	Several thousand dollars to 2 units	6 months to 3 years
4	Underground Development To block out positive ore reserves	Sale of company capital stock Funds provided by mining company	30 units	2 to 5 years
5	Installation of a Mining and Treatment Plant Includes the development of the mine for mining, the mining plant, the treatment plant, power and water supply, transportation facilities, and townsite.	Further sale of company capital stock Funds supplied by mining company Bank loans obtained by an established company Sale of bonds	83 units	2 to 3 years
6*	Tune-up period merging into production stage	Working capital which must be provided from the above sources or generally by a bank loan until returns from the operations are made available	7 units	1 to 6 months

* Cost of property must be provided for and may vary from 1 to 20 units.

Stage 3, Preliminary Development: Diamond drilling was started on August 29, 1941, and continued throughout the winter of 1941-1942. From 103 holes, totaling 50,000 ft, there was an EX core recovery of 100 pct. The deep holes were surveyed. The whole core was used for a sample and 8-ft sections were standard. Rejects of all samples were saved for metallurgical test work and check assays. The diamond drilling outlined two orebodies containing roughly 5,000,000 tons of low grade arsenical gold ore. The Dick orebody was drilled to a depth of 1000 ft, roughly 700 ft in length, with an average width of 70 ft. The Toots orebody was drilled to a depth of 400 ft and showed a length of 400 ft and an average width of 16 ft. The 52 claims in the group were surveyed for lease and a geological map of the claims was made in the spring and summer of 1942. Active work at the property ceased during World War II.

Investigations Made Between 1942 and 1945

The rejects from the drill core samples were made up into composite samples for test work and testing was carried on independently at two of the company's operating divisions at Holden, Washington, and Britannia Beach, B. C. A satisfactory flowsheet for the treatment of the ore was worked out.

Estimating of Ore Reserves from Diamond Drill Results: Independent estimates of the orebodies were made by two groups of company engineers both as to grade and tonnage. These estimates were remarkably close. The following points were considered in arriving at the grade of the ore: 1—Core recovery in the ore sections was 100 pct. 2—Original assays were checked independently by another assayer. The assays of the rejects, used for making composite samples for testing, were checked by three independent custom and two Howe Sound assayers. The calculated heads from test work were checked against the assays heads. 3—There were no extremely high assays or extremely low ones within the ore zones. 4—Calculating by the ounce-foot method, the ounce-block method, and an arithmetical average of all ore samples checked closely. 5—The method used to correct for erratics, developed by the Hollinger Gold Mines,[1] was used to make a calculation of the ore grade and to check the other methods employed. 6—The variation in all the estimates of grade was less than 4 pct. 7—The total weight of samples from the drill core in the ore zone was approximately 1.6 tons, the ore sample being 1 part in 3,000,000. If the core had split, as it commonly does, the ore sample would have been 1 part in 6,000,000. It is believed that results would have been the same.

Consideration of Mining Methods from Diamond Drill Records: A study of geological data, diamond drill core, and drill logs brought forth several facts which were of help in developing a mining method. It was found that the wall rock as well as the ore was very competent and that a mine relatively free from costly timbering could therefore be anticipated. The impervious clay overburden was tight to the bed rock, very little porous sand was encountered, there were no large fault zones, and no water appeared in the various formations. It was evident that the ore zone would lend itself to breaking with diamond drill holes or long hole drilling.

A mine model made up from the drill logs revealed further advantages. It was shown that the walls were fairly regular, with no apparent bad rolls, and that the dip of the footwall varied from 45° to 60° with an average of 53°. The length of the Dick ore zone was approximately 700 ft, the width varying from 30 to 100 ft with a 70-ft average. The length of the Toots zone was about 400 ft and the width varied from 10 to 30 ft with a 16-ft average. It was observed that the orebodies had a rake or plunge of 45° to the east. This indicated that the ore could be mined from the top down, level by level, the sill pillars being recovered as the mining progressed and the subsidence of the hanging wall, if any, being delayed until the stopes on the lower levels were mostly under solid ground. Provision for filling could be delayed with reasonable safety for several years. It was apparent that the orebody would lend itself to cheap primary breaking by some method of long hole drilling and that it was large enough to produce 2000 tons a day from one level, indicating a concentrated mining operation. The ore could be drawn through bulldoze chambers or by scrapers.

In 1944 the writer saw the district for the first time, spending the better part of two weeks studying operating conditions in this northern section of Canada on property owned by the Hudson's Bay Mining & Smelting Co. and the Sherritt Gordon Mines Ltd. Much valuable information was gathered at this time.

To plan intelligently during the next winter it was necessary to obtain definite information on access to the property and also to check the location for shaft and mill sites. A small survey party was assembled in July, and between August 1 and October 31 the following work was completed.

Preliminary road survey was made from Snow Lake to Wekusko on the Hudson's Bay railroad a distance of approximately 38 miles; a contour map of the surface area was made on 5-ft intervals with 2-ft intervals on likely areas for the shaft and milling plant. From the preliminary geological map several possible mill and plant sites were selected and these spots were mapped in detail. Where clay overburden covered the bedrock, soundings were made with auger drills to a depth of 10 ft so that the bedrock detail was known as well as the surface detail. When the contours were plotted, sections on the co-ordinate lines were made of the bedrock and surface, with the overburden colored. From this plan estimates could be made of general excavations and foundations. Model buildings could be placed on the plan and the foundation excavation and bedrock for footings could be visualized at a glance by using the contour plan with sections on the co-ordinate lines on the same map.

After the above information was obtained, possible sites for the shaft and plant were soon narrowed to three locations. Each was assessed as to: 1—The relation to known orebodies and possible extensions. 2—Freedom from the effects of subsidence at a later date. 3—Possibilities of placing the mill building so that any natural slope could be used for gravity flow in the milling operation. 4—The best foundation footings for the buildings and machinery. 5—The minimum surface excavation. 6—Possible townsite locations. 7—Water supply.

The location which best suited all requirements was located a few hundred feet east of the surface showings on a relatively high large outcrop. There was a good mill site and yard area and sufficient room for proposed plant buildings and expansion. The only disadvantage was that the general rock excavation was heavy.

Completion of Stage 3: By the end of 1944 Stage 3 was completed and the following facts determined about the property. By diamond drilling a possible 5,000,000 tons of low grade arsenical gold ore above the 1000-ft level had been blocked out. The chances of finding more ore were good. Mineralogically there was no change in the ore for 1000 ft so no sudden changes in depth were to be anticipated. There was no rapid dropoff in grade of ore in the first 1000 ft as the values were remarkably uniform throughout. Although only a few holes penetrated to a depth of 1000 ft there was no indication as to rapid diminishing of the size of the Dick orebody. The orebodies were centrally located in the group of claims allowing considerable scope for further prospecting. It is a miner's faith that orebodies of this type are not orphans and that the development of one orebody generally leads to the finding of others. According to the old adage, "Ore Begets Ore."

According to the rejects from diamond drill core samples two flowsheets had been worked out for treating the ore: 1—flotation, followed by cyanidation of the concentrates, with recoveries estimated at 80 to 83 pct, and 2—flotation, followed by roasting of the concentrates and cyanidation of the calcines, with recoveries estimated at 85 to 90 pct.

The main extraction shaft and mill site had been tentatively located, a proposed mining method had been developed for mining of the ore, and the following items had been investigated: labor and material supply, power, transportation, water supply, townsite, and source of sand and gravel. An estimate of the cost of a complete mining and milling plant of 2000 tons daily capacity had been made, as well as an estimate of the probable cost of operating and the possible financial outcome of the operations.

Up to this time the Howe Sound Exploration Co. investment in the property was nominal. To proceed with Stage 4 would represent a considerable capital outlay. Because of such factors as the isolation of the property and the lack of power and of transportation facilities, a large capital outlay would be required to carry out an adequate underground development program to block out positive ore reserves. The idea was then advanced as to whether Stage 4 could be eliminated and a decision made to go directly to Stage 5 and bring the property into production without waiting for underground investigation.

This idea was a radical departure from accepted mining practice. The advantages of eliminating Stage 4 were that a considerable saving in total capital outlay could be made, and the production stage reached at least 2 years sooner. The disadvantages were that the total capital outlay had to be provided and that there was no turning back once started. If Stage 4 was proceeded with, at least 30 pct of the total estimated capital investment would be spent to bring the property to the production stage. There was a question as to whether the company, after spending this amount of money, would be in any better position to judge the expected grade of the ore, as the same factors which make appraisal of values in drill cores difficult would still continue and possibly the actual true grade would not be determined until "experience factors" based on milling results could be developed. Ground conditions, of course, would be better known.

The careful examination of all factors mentioned previously made it possible for the engineers to recommend to the management that a definite decision be made to bring the property into production without waiting for underground investigation or Stage 4 in the ordinary process of development.

It should be stressed that in making this recommendation the engineers needed considerable courage, but their decision was simple compared to the problem faced by the directors, who had to decide on a very large capital outlay based on the results of diamond drilling with no checking of this information by underground investigation.

In early 1945 it was decided to bring the property into production as soon as possible and to omit Stage 4. As the cost of a roasting plant to treat 100 tons of arsenical concentrates would be high and the storage of arsenious oxide derived from the roasting would be difficult, it was decided to use the straight cyaniding of concentrates flowsheet and store the cyanide residues for future treatment. With the cessation of European hostilities and the impending collapse in the Japanese theater of war a start was made on the development in August, 1945.

Stage 5: The purpose of this paper is not to describe in detail the plant construction or mine development, which will be the subject for a later article. Fig. 1 shows the surface plant and Fig. 2 the plant in relation to the townsite.

Stage 6, Production Stage: The milling plant was started late in March of 1949 and the first bullion poured on April 22. In April and May there was considerable difficulty, which was not overcome until June, with ore hanging up in the raises. June tonnage was 1600 tons per day, increasing to 1800 tons in October and 1900 tons in November. It has continued at a nominal rate of 2000 tons per day since. There were the usual problems of tuning up and starting a mining operation. To date the 320 level has been mined out in the Dick orebody except for the surface pillar. The 580-level stope in the Dick orebody is approaching the 320 sill, and the 780 level is being prepared for mining. A small shrinkage stope is being mined in the Toots orebody above the 320 level. The sinking of the shaft was completed to 1470 ft in September 1951, bringing in two more levels for mining and a third, the 1280 level, for development.

Results After Mining 1,550,000 Tons of Ore

The Checking of the Assumptions as to Mining Methods from Study of Drill Cores and Logs in the Preliminary Stage: 1—Ore and wall rock is very competent. No timber sets have been required to date. Shaft lagging is not required except at stations, since there is no sloughing in empty stopes. 2—The attitude of the walls is not quite so regular as anticipated. 3—The underground water, approximately 50 gal a min, has to be pumped. 4—In primary breaking, flat hole-ring drilling from footwall raises started with diamond drilling AX holes, superseded by tungsten carbide bits, 2 in. and 2⅛ in. in size, with sectional rods, burden 10-ft vertical, spread on a hanging wall approximately 20 ft. The powder factor to date is .272 pounds per ton, including undercuts. 5—On the 320 level the ore was drawn through bulldoze chambers spaced at 35 ft with a grizzly spacing of 30 in. On the 580 level the ore was scraped directly into 100 cu ft Granby-type cars with 60 hp slushers, ¾-in. cables, and 54-in., 60-in. and 66-in. scrapers, both folding and rigid types. The maximum pull was 120 ft. All production is obtained from one level, with slight overlap when a new level is being brought into production. 6—No unnecessary drifting, cross-cutting or raising was done. To date there are probably only 100 ft of drifting not being actually used in the mining operations.

Recoveries have been very close to the estimated and are currently running at 80 pct.

Preliminary Ore Reserve Estimates as Compared to Millheads

After the milling of 1,550,000 tons the grade of ore milled has been 8 pct lower than the original ore estimates, with no allowance for dilution on the original estimates. If a normal 10 pct dilution factor had been used the tons milled to date would have roughly averaged 2 pct higher than the estimated grade. It is estimated that when 2,000,000 tons are drawn the millhead grade will be within 5 pct of the original estimate.

General Facts of Operations in the Mining of the First 1,550,000 Tons

Twelve tons are produced per underground manshift, 6 tons per overall man-shift, including all employees, 55 milled tons per manshift, and 55 to 60 tons per manshift in bulldoze chambers or scrapers. There are 60 tons produced per ft of development driven, and 30 tons per ft of exploration diamond drilling. The average length of development rounds is 7 ft. Tungsten carbide drilling for blast holes amounts to 66 pct of the cost of diamond drilling. The ratio of labor to supplies is about equal.

When a correction is made for increased labor costs of 50 pct and supplies of at least the same percentage, the current costs are below the estimated costs. Capital costs were higher than anticipated because of the large increase in cost of labor and supplies during construction between 1946 and 1949.

To summarize, it is believed that with certain types of orebodies it is possible to calculate ore plants, even at a newly discovered property remote from other mines, wholly on the basis of information obtained from diamond drilling.

Reference

[1] Canadian Institute of Mining and Metallurgy *Bull.* (1943) pp. 209-225.

High-Efficiency Desliming By Use of Hydraulic Water Additions To the Liquid-Solid Cyclone

by D. A. Dahlstrom

THE necessity for slime elimination from valuable mineral and coal products has become increasingly significant within the past 5 years.[1, 2] Most of the mechanized mining and present beneficiation methods have resulted in larger tonnages of extreme fines, silts, and clay, commonly called slimes, processed by the preparation plant. Economics in turn have forced the plant operator constantly to lower the bottom size of effective beneficiation, necessitating an almost complete recovery of valuable solids regardless of particle size. When these important factors are considered, the need for an efficient slime removal method for fine solids becomes self-evident.

Ordinarily slimes have been classified as ranging from 75 microns, or 200 mesh, down to colloidal dimensions of less than one micron. At the same time there is general agreement that the most troublesome slimes are primarily clays, silts and extreme fines, so that the actual top size may be placed at approximately 30 to 40 microns. This immediately restricts any desliming operation to classification, as screening or other methods would be both uneconomical and grossly inefficient at such dimensions.

The liquid-solid cyclone has been recognized as one of the most efficient fine size classifiers available to the mining industry. Applications of cyclones to thickening, high efficiency solid recovery, degritting,

D. A. DAHLSTROM, Member AIME, is Associate Professor, Chemical Engineering Department, Northwestern University.

Discussion on this paper, TP 3353F, may be sent (2 copies) to AIME before Sept. 30, 1952. Manuscript, March 10, 1952. New York Meeting, February 1952.

Table I. Typical Desliming Results with Cyclones

	Cyclone Diam				
	24-In.	24-In.	9-In.	14-In.	9-In.
Solids, Type	Phosphate Rock[10]	Phosphate Rock[10]	Coal	Coal	Sand
Feed					
Pressure—psi	14	14.0	3¾	25	10
Solids, pct	20.4	20.2	15.71	11.72	41.6
−200 mesh, pct	45.8	22.9	43.7	28.5	3.0
Tons per hr solids	49	41.4	3.32	6.14	28.7
Gpm slurry	785	776	79.3	203.4	221
Tons per hr per ft² (solids)	15.6	13.17	7.51	5.75	65.0
Gpm per ft²	250	247	180	191	500
Overflow					
Solids, pct	10.1	5.1	8.60	3.98	1.98
−200 mesh, pct	95.7	91.9	81.4	75.5	98.84
Tons per hr solids	22.0	9.6	1.52	1.75	0.7
Gpm slurry	692	684	67.8	174.8	143
Underflow					
Solids, pct	71.4	76.6	52.6	53.4	78.0
−200 mesh, pct	5.6	2.0	11.8	5.2	0.6
Tons per hr solids	27.3	31.8	1.80	4.39	28.0
Gpm slurry	93	88	11.5	28.6	78.0
Recovery of 100x200 mesh solids in underflow, pct	87.0	72.5	41.1	82.5	100.0
Elimination of −200 mesh, pct in overflow	93.2	93.2	85.4	87.1	80.0
Feed water to cyclone underflow, pct	4.3	6.0	9.1	8.3	19.9
Desliming coefficient	1.58	1.13	1.60	1.55	1.004

and heavy media beneficiation are well known and widely reported in the literature.[3-5] Simultaneously the cyclone has been put to practical use for high-speed slime removal, particularly in the coal, phosphate, and sand industries.[3-8] In all such instances, desliming efficiency must be measured not only by the percent of slime removal but also by the recovery of valuable solids, especially the 100x200 mesh material, in the cyclone underflow. A third index of efficiency if the cyclone is operating with a properly thickened underflow is the desliming coefficient.[7,8] This has been defined as the percent of feed slimes recovered in the cyclone underflow divided by the percent of feed water reporting to that point. Desliming coefficients for any nonhydraulic water classifier can *at best* exhibit a *minimum* desliming coefficient of 1.0. Evaluation of desliming equipment should properly take into consideration these three factors as well as economic and operational qualities.

Table I illustrates typical cyclone desliming operating results on various solids. Capacities range from 180 to 500 gpm per sq ft of cyclone cross section for feed slurries and 5.75 to 65.0 tons per hr of feed solids per sq ft of cross section—the highest capacity of any fine size classifier. Attention should also be focused on the high recovery of 100x200 mesh solids in the cyclone underflow, the 80 to 93.2 pct removal of slimes, and the low desliming coefficients. The cyclone when correctly applied will consistently exhibit desliming coefficients approaching more closely the theoretical minimum of 1.0 for nonhydraulic water units than other types of classifiers.

In cases where feed solid loading is high or pressure available is low, it may be more expedient to utilize a two-stage process.[4,8] In this instance the overflow from the primary cyclones is fed directly or through a pump to secondary units where the remaining desirable solids are deslimed. Typical results from two installations are given in Table II. Data for each stage are comparable with those in Table I, while overall recovery of desirable solids is very high.

In many desliming processes on fine solids, slime removals of 80 to 90 pct are unsatisfactory. Two predominant reasons can be cited for the higher restrictions. 1—In today's market, there is an ever-increasing demand for higher purity in fine solids, necessitating slime removals of higher than 95 pct. 2—Because of water shortages, waste water disposal restrictions, or high clay percentages in the run-of-mine solids, circulating water slime contents must be held at a relatively high level in many preparation plants. Thus it is not uncommon for the slurry fed to a desliming operation to have a slime content in the total solids of greater than 30 or 40 pct.

There are two possible solutions to the above problems if they are to be solved by classification. The first, reported in an earlier paper,[8] consists of repulping the thickened underflow with fresh water

Table II. Typical Two-Stage Desliming Cyclone Results

	Coal[7]		Sand	
	First Stage, 2 to 20-In. Cyclones	Second Stage, 6 to 14-In. Cyclones	First Stage, 2 to 36-In. Cyclones	Second Stage, 2 to 30-In. Cyclones
Cyclone pressure drop—psi	5	26	3⅞	4½
Feed—per cyclone				10.83
Solids, pct	13.12	10.3	45.0	20.8
—200 mesh slimes, pct	29.0	41.5	3.0	18.2
Tons per hr solids	33.75	7.22	151.2	621.0
Gpm slurry	900.0	272.0	962.0	3.7
Tons per hr per ft² (solids)	15.4	6.76	21.4	126.3
Gpm per ft²	410.0	254.0	136.0	
Overflow per cyclone				2.54
Solids, pct	10.3	5.83	10.83	96.3
−200 mesh slimes, pct	41.5	77.9	20.8	3.8
Tons per hr solids	21.65	3.72	18.2	587.0
Gpm	815.0	250.0	621.0	
Underflow per cyclone				78.0
Solids, pct	48.6	54.8	79.2	0.9
−200 mesh slimes, pct	6.8	10.6	0.6	14.4
Tons per hr solids	12.1	3.5	133.0	34
Gpm slurry	85	22	140.0	
Elimination of −200 mesh slimes to overflow, pct	92.25	88.7	82.6	96.5
Desliming coefficient	1.23	2.46	1.0	1.295
Overall +200 mesh recovery	89.5		99.9	
Overall pct −200 mesh slimes in product	8.4		0.62	

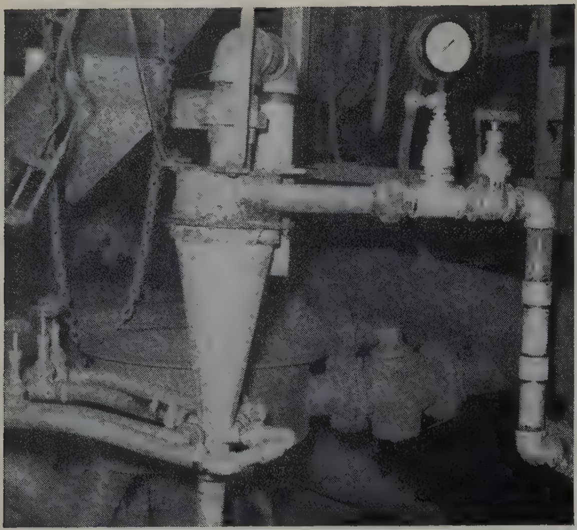

Fig. 1—Experimental hydraulic water cyclone.

and reclassifying so that total slime removal will be at the proper level. This course is entirely feasible, but another stage of classifying units plus the auxiliary equipment of pumps, surge tank, and pipe lines is a drawback. Furthermore, water requirements may be higher than those necessitated by the second solution.

The second solution involves lowering the desliming coefficient of the classifier by addition of hydraulic water so as to force more of the slimes to the overflow.[7] The cyclone appears particularly applicable to this modification. Its classification efficiency is already high, indicating that the amount of hydraulic water will be relatively small. This will be especially true if the water can be introduced at a point where solid concentration is relatively high and thus associated with the least amount of slime-bearing water. Furthermore, definite economy and process simplification would be effected by performing the high slime removal in one unit.

Hydraulic Water Cyclone Theory

Criner in a recent paper made an extensive theoretical analysis of the liquid solid cyclone, discussing in detail the flow pattern within the unit.[9] From experimental evidence and a mathematical study he proposed that radial flow into the cyclone core between overflow and underflow ports is uniform at any radius within the cyclone. Thus radial velocity at a radius r_1 lying between the overflow and underflow nozzles is independent of elevation. Furthermore, he hypothesized that after a fluid particle reached a certain plane near the apex of the cyclone, it could then no longer return in a path towards the overflow but must be discharged in the underflow. The location of this plane is directly proportional to the percent of feed volume reporting to the underflow. Thus if the fluid particle attains a level normal to the cyclone cross-section, whose ratio of distance from the underflow divided by distance between overflow and underflow nozzles is equal to the volume fraction reporting to the underflow, then that fluid must exit from the underflow. As a simple example, suppose that there is a 20 in. distance between overflow and underflow nozzles. If the cyclone operates with a 20 pct volume split to the underflow, when any fluid travels to within $0.2 \times 20 = 4$ in. of the underflow, it must eventually be discharged from that port.

In view of the above facts, it would appear appropriate to inject the hydraulic water at or slightly above the level at which all water reports to the cyclone underflow. Thus it may be possible to replace the slime-bearing water with fresh water, forcing the former to report in larger percentages to the overflow. This replacement would be considerably more efficient than dilution of the slime-bearing waters; accordingly lower slime contents in the cyclone underflow could be expected. If the water is introduced at a level closer to the overflow, larger amounts would be required to do the same job, while introduction at levels nearer the apex might seriously disrupt the cyclone flow pattern at high hydraulic water rates. The latter would be caused by forced movement of undesirable fluid towards the cyclone overflow, resulting in an inefficient centrifugal force field.

In order to maintain the flow pattern within the cyclone, the hydraulic water should be added tangentially in the same direction as the feed nozzle. By this means, further energy will be added to maintain the same centrifugal force pattern and prevent loss of solids above the normal classification point to the overflow.

Experimental Equipment

To test the proposal, a 9-in. cyclone of galvanized sheet metal was constructed with a 2-in. standard pipe feed entry and a 2½-in. I.D. copper tubing overflow. The included angle was 20°, and interchangeable underflow cones were made of different lengths so that any underflow diameter could be obtained. Four standard 1-in. pipes were brazed to the unit at 90° around a circle normal to the cyclone centerline near the apex. Through flexible connections from regulating valves on a 2-in. manifold to the tangential nozzles, hydraulic water could be admitted to the cyclone. Water rate was measured by a calibrated orifice on the 2-in. line. The unit was then installed at the preparation plant of the Truax-Traer Coal Co., Fiatt, Ill., to obtain experimental evidence. Fig. 1 shows the cyclone placed on the circulating water line of the washing tipple.

In performing tests, rate and analyses samples were taken of both overflow and underflow streams as well as feed pressure and hydraulic water rates. From this data it was possible to back-calculate to the feed conditions.

At the Fiatt Plant the —200 mesh fraction could not be considered as containing only slimes. There are small quantities of pyrite, calcite, sand, and high-ash coal which are of near 200 mesh size. Thus to eliminate these by classification would entail severe losses of coal up to 30 or 40 mesh in size. Naturally this cannot be tolerated, and such particles must be removed by other cleaning methods. It should be pointed out that in most cases the quantity of these near mesh solids is relatively small in comparison to the amount of true slimes present. However, because of their size and density, the former will report primarily to the underflow while the true slimes will report chiefly to the overflow. Thus if a distinction is not made between the two classes of solids, a true picture of desliming results will not be obtained in any test work. Furthermore, the near mesh material is not responsible for the lowered capacity and excessive moistures in the mechanical dewatering and thermal drying process steps, and because of its usually low concentration does not contribute as significantly to higher impurity percentages as do the greater quantities of slime.

The Fiatt slimes had a top size of approximately 25 to 30 microns. Accordingly in this study all wet screen analyses were performed with a bottom screen of 200 mesh. The −200 mesh solids were thoroughly agitated and allowed to settle 1 min to permit the +30 micron material to separate. The slime-bearing water was then carefully decanted and the near mesh solids transferred to a beaker. The latter were thoroughly rinsed three times with fresh water and decanted as before. When all slime-bearing waters were combined and filtered, a sufficiently accurate analysis for −30 micron slimes was possible. Several runs were made to test and prove the reproducibility of the results.

Test Results

The unit was first installed on the circulating water line of the plant where cyclone feed pressures up to 15 psi could be obtained by use of a throttling valve. Several preliminary runs were first made to determine the feasibility of the hydraulic water design. Results indicated desliming coefficients could be lowered to less than 0.35 with only about 25 pct of the total feed water, that is, slurry water plus hydraulic water, being fresh water additions. Such operation would permit elimination of 93 pct or better of all slimes fed to a cyclone.

This result apparently substantiated the original hypothesis that the hydraulic water additions were largely replacing rather than diluting the slime-bearing water. To add weight to this conclusion a series of tests were made at constant cyclone nozzle dimensions and a feed pressure of 5 psi with varying amounts of hydraulic water rates. Desliming coefficients were calculated and plotted as a function of pct hydraulic water volume of total feed volume as indicated in Fig. 2. A reasonable smoothed curve of the data exhibited a straight line relationship for hydraulic water percents of total feed volume above 7.5 pct.

To establish the significance of the above results, some important background material must first be discussed. The distance between overflow and underflow nozzles in this series of tests was 24¼ in. with the top of the hydraulic water nozzles located on a plane 7⅜ in. above the underflow. According to the cyclone radial flow theory previously mentioned, (7⅛ ÷ 24¼)100 = 30.4 pct of the *total* feed volume, which is slurry plus hydraulic water, will pass this plane. Theoretically then, the maximum amount of hydraulic water that could be fed to the cyclone at this point of insertion is 30.4 pct of the *total* feed volume minus the volume occupied by the underflow solids. Lesser percentages could be added without any injury to the flow pattern, but greater quantities might force appreciable amounts of coarser solids to the overflow because of excessive radial velocity currents.

While solid concentration in the plant circulating water ranged from 11 to 12 pct by weight, −200 mesh content of the solids averaged 80 pct by weight with only 10-15 pct coarser than 100 mesh. Accordingly volume splits to the underflow ran less than 3 pct of the total feed volume. Approximately 50 pct of the underflow volume was occupied by solids, indicating a theoretical maximum amount of hydraulic water for these tests of 30.4 — 0.5x3 = 28.9 pct of the *total* feed volume. Because of a lack of water pressure, hydraulic water percent of *total* feed volume never exceeded 28.5 pct and the theoretical maximum could not be checked. Even at the highest rate, however, no loss to the overflow of solids above the classification point for nonhydraulic water conditions was experienced.

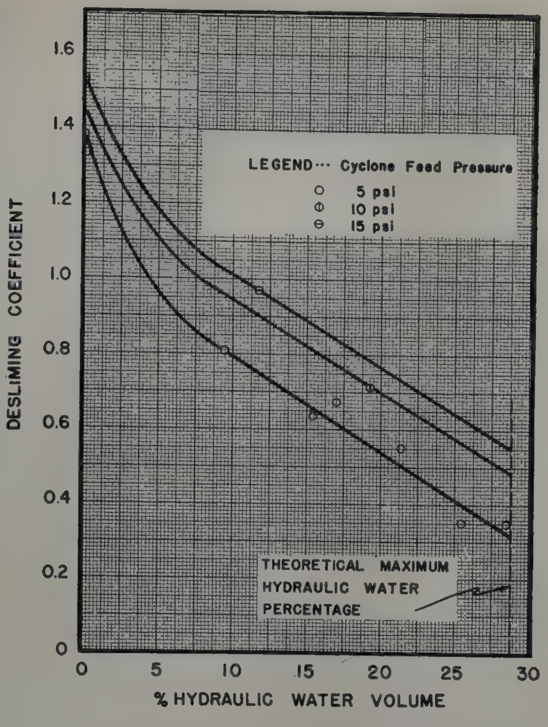

Fig. 2—Desliming coefficient as a function of hydraulic water volume percentage of total cyclone feed volume.

Referring again to Fig. 2, the theoretical average minimum desliming coefficient at the maximum hydraulic water rate would be 0.31. If the hydraulic water additions were entirely a replacement rather than dilution of slime-bearing waters, the desliming coefficient should equal the perfect value of 0.0. However, it will be observed that the desliming coefficient averaged 1.35 for the case in which no hydraulic water was added, indicating that the centrifugal force field utilized in this cyclone was above that required to have no concentrating action on the slimes. In other words, if this latter desliming coefficient had been equal to 1.0, then a perfect value of 0.0 for this same term should be expected at the maximum hydraulic water rate. Naturally, there will be some mixing of slime-bearing and fresh water, but with the above consideration the assumption of a largely displacement action of the hydraulic water seems justified. The original desliming coefficient for no hydraulic water additions was 1.35 — 1.0 = 0.35 points above its theoretical minimum of 1.0, while at maximum hydraulic water additions the desliming coefficient was 0.31 points above its theoretical minimum of 0.0.

Further proof of the influence of centrifugal force on the vertical displacement of the correlation of Fig. 2 was obtained by performing more runs at feed pressures of 10 and 15 psi. At the resultant higher centrifugal force fields the curves were displaced upwards to higher desliming coefficients at the same hydraulic water percentage rates as indicated in the graph. This not only strengthens the displacement theory, but also emphasizes the importance of correct cyclone design and operation to obtain a centrifugal force field that will yield maximum slime elimination. This must be tempered by considerations of desirable fine solids recovery in the cyclone underflow. If maximum slime elimination were the sole criterion, the feed pressure that should be used for any hydraulic water cyclone would be the maximum value that would still yield a desliming coefficient of 1.0 if no hydraulic water is admitted.

The hydraulic water cyclone was next installed on the underflow line from the fine coal settling cone to obtain additional data. Unfortunately the solid concentration in this feed slurry ranged from 22.5 to 28.18 pct by weight, necessitating volume splits in excess of 31 pct to the underflow with no hydraulic water additions to the cyclone. As larger underflow nozzles had to be used to accommodate the greater volume rate at this port, the hydraulic water jets were only 15.6 or 20.6 pct, depending on which of the two possible insert cones were used, of the overflow-underflow distance away from the underflow. According to cyclone flow path theory, hydraulic water introduced closer to the apex than the plane at which all volume will report to the underflow will not be as efficient in displacement of slime-bearing water. The fluid already between the jets and this plane cannot escape passing out in the underflow; therefore this slime-bearing water will not be displaced by the hydraulic water. Accordingly the desliming coefficient will be lowered to a much lesser degree. Furthermore, there will exist a maximum amount of hydraulic water that can be efficiently added under such conditions which will be less than that if the hydraulic jets were located at or slightly above the plane at which all liquid passing must report to the underflow. If this maximum is exceeded, the extra hydraulic water merely reports directly to the underflow without performing any effective action. If the rate is still further increased, it will eventually largely destroy the centrifugal force pattern within the cyclone.

A series of tests were made to prove definitely the above hypothesis. Results are reported in Table III. Investigation of the data reveals the following:

1—Slime recovery in the underflow with no hydraulic water was 42.9 pct. With the addition of fresh water, this figure could only be lowered to a probable minimum of 23 to 25 pct, regardless of the quantity of fresh water added.

2—The underflow solid concentration became considerably diluted as excessive amounts of hydraulic water were added. This indicates the direct short-circuiting of fresh water to the underflow.

3—Slime content could be lowered from 16.6 pct to about 8.5 pct, which represents a definite improvement. However, it is not indicative of the better efficiency that could be obtained if the water had been inserted at the correct level. If all data is recalculated on the basis of 55 pct solids concentration in the underflow and the same desliming coefficients, slime content in the underflow would be reduced from 8.3 pct for nonhydraulic water conditions to 2 to 3 pct for fresh water additions. This still does not represent the potential results, as much of the hydraulic water had been inefficiently used.

4—When greater amounts of hydraulic water than reported in Table III were used, the centrifugal force pattern was definitely destroyed. The amount of underflow became very small with almost all solids forced to the overflow. All of these facts definitely point to the correctness of the proposed theoretical cyclone flow pattern. They also emphasize again the need for correct location of the hydraulic water jets as well as good cyclone design.

The location of the hydraulic water jets can be quickly calculated and best demonstrated by a simple example. Suppose that it is desired to feed a cyclone 100 gpm of feed slurry, 20 gpm of which will issue from the underflow with no hydraulic water additions. The actual volume of water and slimes in this underflow could easily be calculated or measured in the real case, but it will be assumed for simplicity that it is equal to 50 pct of the underflow volume. Thus it would be desirable to add up to 10 gpm of hydraulic water to replace the required amount of slime-bearing water in the underflow to obtain a sufficiently deslimed product. If the same underflow solid concentration is to be maintained, the new volume split to the underflow for 10 gpm of hydraulic water will be $\frac{20}{100 + 10} \times 100 = 18.2$ pct. Thus the hydraulic water jets should be placed at least 18.2 pct of the distance between overflow and underflow away from the latter nozzle. It

Table III. Summary of Results, Hydraulic Water Cyclone Tests

	Run 45	Run 46	Run 47	Run 48	Run 49
Feed pressure, psi	4⅛	4½	4¼	4⅜	4
Feed slurry rate, gpm	116.4	102.1	93.0	107.9	99.2
Hydraulic water rate, gpm	40.3	21.3	0	24.0	16.9
Overflow rate, gpm	66.7	62.4	49.0	66.8	57.1
Underflow rate, gpm	90.0	61.0	44.0	65.1	59.0
Feed solids rate, tons per hr	7.10	6.30	5.80	7.37	7.57
Feed solid concentration, wt pct	22.5	23.08	23.0	25.1	28.18
Overflow solid concentration, wt pct	9.20	8.55	8.71	10.59	9.53
Underflow solid concentration, wt pct	22.8	30.2	38.0	31.2	37.96
Total volume to underflow, pct	57.5	49.4	47.4	49.5	50.9
Total water to underflow, pct	54.0	43.1	39.4	43.5	42.7
Total solids to underflow, pct	77.3	77.8	80.7	74.7	81.3
—200 mesh slimes in feed, pct	26.9	28.8	31.3	26.4	22.9
—200 mesh slimes in overflow, pct	88.4	91.3	92.8	80.6	86.2
—200 mesh slimes in underflow, pct	8.9	11.0	16.6	8.1	8.4
Solid recovery in underflow, pct					
+20 mesh	100.0	100.0	100.0	99.5	100.0
20x40	99.6	99.7	99.8	94.7	99.9
40x60	93.7	98.6	98.4	83.2	98.4
60x100	80.5	93.5	95.4	72.8	88.6
100x140	61.8	76.6	87.8	56.7	74.3
140x200	68.9	70.5	77.5	63.3	68.4
—200 coarse solids	74.7	81.2	78.3	74.0	71.3
—200 slimes	25.5	29.6	42.9	22.8	29.8
Desliming coefficient	0.472	0.685	1.087	0.524	0.697
If underflow withdrawn at 55 pct solids					
Removal of —200 mesh slimes, pct	94.3	90.5	80.5	91.1	84.4
—200 mesh slimes in underflow solids, pct	2.1	3.8	8.3	3.3	4.6
Hydraulic water of total feed volume, pct	25.8	17.2	0	18.2	14.5
Hydraulic water of total feed water, pct	29.2	20.3	0	21.5	18.0
$\frac{\text{Distance from hydraulic jets to underflow}}{\text{Distance from overflow to underflow}} \times 100$	15.6	15.6	15.6	20.6	20.6

would probably be advisable to add 1 or 2 pct to insure against short-circuiting of hydraulic water to the underflow.

Two other points are evident from Table III and observed in the other runs performed. 1—No loss of solids above the top size classification point for no hydraulic water additions was experienced when fresh water was fed to the cyclone. The loss of solids to the overflow below this top size will increase as particle size decreases. However, the loss is relatively small in sizes near the top limit. This is very important, as desirable solid recovery will not be appreciably affected by hydraulic water. 2—Fresh water additions will not lower the amount of feed slurry processed at any cyclone feed pressure. Therefore, cyclone capacity per sq ft of cross-sectional area for slurry handling will remain the same.

Industrial Correlations

A commercial installation of the hydraulic water principle has just been made to deslime a high-quality chemical sand. Contamination must be less than 0.5 pct slimes to meet purity restrictions. A two-stage cyclone process was necessary because of heavy feed solid loading and available pressure drop. Two primary 36-in. diam cyclones were designed to handle 1000 gpm of slurry containing 45 pct solids at 3⅞ lb per sq in. pressure drop. The overflow from these units still contained valuable solids and was accordingly fed to two 30-in. secondary cyclones. Results for the installation are indicated in Table II. It will be observed that practically all sand was recovered by this process, but at an unsatisfactory slime content of 0.62 pct.

Hydraulic water jets were added to the primary cyclones to lower the slime content. Because of fabrication difficulties, the jets could not be added on a plane normal to the cyclone cross-section but rather were placed at calculated points along the slant height of the conical section to achieve a displacement action. A comparison of results before and after is given in Table IV. Slime content in the primary underflow was reduced from 0.6 pct to 0.03 pct, resulting in an increase in slime removal from 82.6 pct to 99.1 pct. The desliming coefficient was lowered to an almost perfect 0.055. When combined with the product from the secondary cones, the resultant slime content was only 0.12 pct.

The results form a striking comparison with the previous gravitational classifying operation employed. Approximately 2000 gpm of fresh water were required to achieve a washed sand that would pass specifications but not equal the hydraulic water results. Furthermore, appreciable quantities of high-value fine sand were lost in the process. With the new method, only a total of 150-200 gpm of fresh water are required to obtain the much-reduced slime content. As indicated in Table IV, 99.1 pct of the sand is also recovered, yielding further economies.

Summary

The feasibility of hydraulic water cyclones has been proved, and desliming coefficients of 0.3 or less are now obtainable. This makes possible the elimination of better than 90 pct of unwanted slimes from the underflow product, and in most cases removal should average above 95 pct. Added advantages are the lesser quantities of fresh water required, when compared with classifiers operating at the same slime removal percentages, and the higher slime content in feed slurries that can be tolerated. This last consideration is particularly important where plants must operate with a closed water circuit or using only a small plant bleed stream. Slime disposal problems will be lessened because of the smaller amount of fluid volume that must be handled.

By the use of hydraulic water additions, the required desliming can be obtained in one piece of equipment without any sacrifice of slurry rate or appreciable loss of desirable solids. Through correct hydraulic water design and application as described in the paper, the operation can be made simple and will require little if any attention.

Table IV. Comparison of Cyclone Desliming Results on Chemical Sand With and Without Hydraulic Water

	Without Hydraulic Water, Per 36-In. Cyclone	With Hydraulic Water, Per 36-In. Cyclone
Feed		
Pressure, psi	3⅞	3⅞
Solids, pct	45.0	45.0
−200 mesh slimes, pct	3.0	3.0
Gpm slurry	962	962
Tons per hr solids	151.2	151.2
Gpm hydraulic water	0	65.0
Overflow		
Solids, pct	10.83	10.50
−200 mesh slimes, pct	20.8	23.8
Tons per hr solids	18.2	18.9
Underflow		
Solids, pct	79.2	77.9
−200 mesh slimes, pct	0.6	0.03
Tons per hr solids	133.0	132.3
Removal of slimes to overflow, pct	82.6	99.1
Desliming coefficient	1.0	0.055
Hydraulic water of total water fed to cyclone, pct	0	7.6

Acknowledgments

The author wishes to express his sincere appreciation to the Truax-Traer Coal Co. for the opportunity of performing the required basic experiments. Particular thanks are due R. L. Sutherland of that company for his constant cooperation, sound advice, and patient understanding.

References

[1] *Coal Preparation*, AIME, 1950.

[2] A. F. Taggert: *Handbook of Mineral Dressing.* John Wiley and Sons, New York, 1945.

[3] R. I. Kingman: Cyclones Prove Satisfactory for Thickening, Desliming Flotation Feed. MINING ENGINEERING (August 1950).

[4] R. L. Sutherland: Recovering and Desliming Fine Coal with Cyclones. Cincinnati Meeting, American Mining Congress (April 1950).

[5] F. T. Weems: Some Metallurgical Applications of the Dorrclone. *Trans.* AIME (1951) **190**, pp. 681-690.

[6] A. Crago: Three New Steps in Treating Florida Phosphate Rock. *Engineering and Mining Journal* (November 1950).

[7] D. A. Dahlstrom: High-Speed Classification and Desliming with the Liquid-Solid Cyclone. *Trans.* AIME (1951) **190**, pp. 153-165.

[8] D. A. Dahlstrom: Low-Cost Industrial Desliming of Fine Solids. Joint Fuels Conference, AIME, ASME, Roanoke, Va. (October 1950).

[9] H. E. Criner: The Vortex Thickener. International Conference on Coal Preparation. Paris, 1950.

[10] A. F. Taggert: *Elements of Ore Dressing.* John Wiley and Sons, New York, 1951.

Measurement and Evaluation of the Rate of Flotation as A Function of Particle Size

by T. M. Morris

THE rate of flotation of solid particles determines the percentage recovery of these particles which can be obtained during a given time interval. It is an established fact that the recovery is greatest in the fine sand size range and falls off on either side of this size range. It is also a fact that the history of the development of concentrating devices has been marked by a desire to recover the small particles: tables were developed to treat material too fine to recover in jigs; flotation recovers material too fine to be recovered on tables. As our ores become more complex and require finer grinding, a greater proportion is in the slow-floating size range. It is therefore of economic importance that the effect of size of particle upon rate of flotation be studied.

Many studies have been made along this line. The present investigation attempts to quantify the rate of flotation by means of a rate equation, and then compares the effect of size upon the rate of flotation. It was found that the flotation rate constant increases with increase in diameter of particle in the size range smaller than the optimum size particle. The flotation rate constant decreases with an increase in diameter of particle in the size range coarser than the optimum size particle. This suggested two different actions taking place, and these are discussed. Suggestions for further work in order to improve the flotation rate of both fine and coarse particles are made.

The usual method of expressing rate is to plot cumulative percent recovery vs time. If we knew the equation of this kind of curve we could replot it as a straight line, and the slope of the line would be an index of the magnitude of the flotation rate. It is easier to compare straight lines than curves.

The basis used for obtaining the equation of the recovery vs time curve is the law of mass action. This law states that the "rate of a chemical reaction is proportional to the 'active masses' of the reacting substances present at any given time." This, of course, implies a constant temperature. We can modify this for our use by using the term *flotation reaction* instead of *chemical reaction* and the term *floatable particle* instead of *active masses*.

$$\text{Thus } -\frac{dC}{dt} = kC \qquad [1]$$

where C denotes concentration of particles, t denotes time, k denotes a proportionality constant.

If the exponent of C is 1, then we have a first order rate reaction. If the exponent of C is 2, then we have a second order rate reaction.

For a first order rate reaction, we obtain, after integration,

$$k = \frac{1}{t} \ln \frac{C_o}{C_t} \qquad [2]$$

where k is again a proportionality constant and has the dimension of the reciprocal of time.

C_o is the original concentration or weight or percentage of floatable particles.

C_t is the concentration or weight or percentage of floatable particles remaining in the flotation cell after time t.

If all particles of the mineral to be floated were capable of floating we could take C_o as *100* and C_t would be *100 - R*, where R is the cumulative percentage recovery of mineral at time t. But it is not usual for all of the particles to be capable of floating, because of surface oxidation, etc. Therefore, we must introduce a factor x which is the percentage of unfloatable mineral. Hence the first order equation is

$$k = \frac{1}{t} \ln \frac{C_o - x}{C_t - x} \qquad [3]$$

It has been proposed by various workers[1-3] that this equation describes the flotation rate.

More recently N. Arbiter[4] states that a second order rate equation fits the recovery vs time curve more closely than does a first order rate equation. Morris[5] has discussed the evidence presented for this statement. It has been concluded that the first

---

T. M. MORRIS, Member AIME, is Associate Professor of Metallurgical Engineering, Dept. of Metallurgy, Missouri School of Mines, Rolla, Mo.

Discussion on this paper, TP 3358B, may be sent (2 copies) to AIME before Sept. 30, 1952. Manuscript, Dec. 10, 1951. New York Meeting, February 1952.

Part of the data used in this paper is taken from a thesis submitted by the author in partial fulfillment of the requirements for the degree of Doctor of Philosophy at the University of Missouri, May 1950.

Table I. Results of Test A

Pan	Time, Sec	Cum. Time, Sec	Weight, G Run 1	Run 2	Run 3	Totals
1	20	20	17.4	17.4	18.8	53.6
2	20	40	9.8	10.8	8.0	28.6
3	20	60	6.6	7.2	6.7	20.5
4	30	90	5.9	7.1	8.2	21.2
5	60	150	8.4	7.3	8.7	24.4
Tails			24.7	23.0	22.4	70.1

order rate equation is the more desirable one to use in evaluating the rate measurements.

Experimental Procedure

Four different kinds of tests were made: A. Laboratory batch tests on cleaned concentrate made from Tennessee Copper Co. ore. This concentrate contained pyrite and pyrrhotite. B. A laboratory batch test using metallic copper particles. C. Laboratory batch tests on plant classifier overflow in the Tennessee Copper Co. concentrator. D. Tests on samples from a 10-cell plant flotation machine floating pyrite. Flotation rates for various size ranges were calculated.

In the laboratory tests the general procedure was to remove froth in consecutive intervals, see Table I. For example, froth was collected in a pan for 20 sec from the time the machine was started and the air turned on. The froth was collected in another pan for the next time interval and so on.

The various concentrates and the final tailing were then washed with acetone or ethyl alcohol, dried and weighed. Then each was screened and elutriated, and the ratio $\ln \frac{C_o - x}{C_t - x}$ was calculated for each concentrate and for each time interval; the values obtained were plotted against time. The slope of the straight line gave the k value or flotation rate constant for each size fraction.

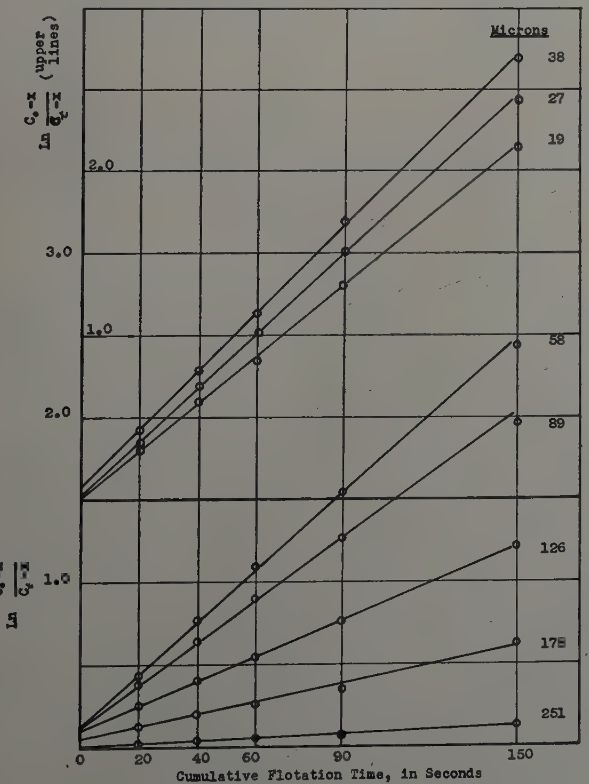

Fig. 1—Variation of flotation rate with average diameter of particle, tests A.

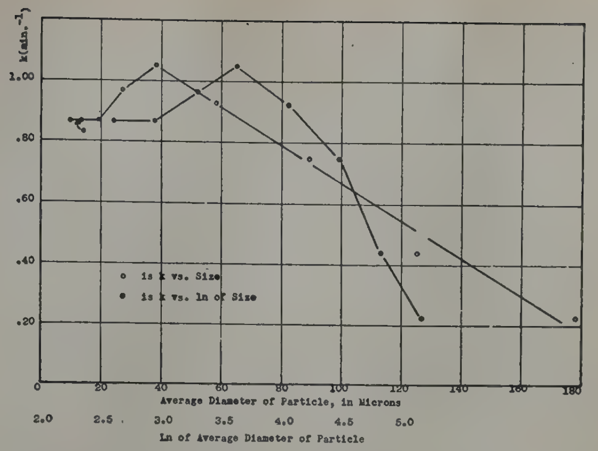

Fig. 2—Variation of k with average diameter of particle and with ln of average diameter of particle, tests A.

In the tests referred to previously under (A), a 250-g mechanical-type cell similar to that described by Dietrich et al.[6] was used. Potassium ethyl xanthate was the collector and terpineol was used as the frother. Sulphuric acid was used to obtain the desired pH of 3.5. Preliminary tests were conducted in which the amount of xanthate used with 75 g of solids was varied. Percentage recovery, of course, increased as xanthate was increased until 37 mg of xanthate were used. Additional xanthate did not significantly increase recovery. It was therefore concluded that when 37 mg of xanthate were used all particles had maximum collector coating.

In the test (B) with metallic copper, the copper was cleaned with nitric acid and washed with distilled water. The particles were very bright and shiny after this treatment. The same cell was used as in the first tests. Sodium aerofloat was the collector, and again the optimum quantity to use was determined by preliminary tests.

The tests (C) on plant classifier overflow were made in the mill laboratory of the Tennessee Copper Co. using a 2000-g Denver machine. The following plant reagents were used: potassium ethyl xanthate, Tennessee Eastman oil as frother, and sulphuric acid for pH control. These tests were made to investigate the effect of the quantity of acid upon the flotation rate of various-sized sulphide particles. In the tests shown the quantity of acid was twice as great in test 2 as in test 1.

In the (D) test on samples of feed, concentrate and tailing were taken from a 10-cell mechanical-type flotation machine. The feed to this machine was a rougher pyrite concentrate. Each product was screened and elutriated and each size fraction was assayed for iron. Recovery was calculated for each size fraction. The calculations for flotation rate constant will be discussed later.

Table II. Size Distribution in Products of Tests A

Mean Diam, Microns	Weight, G Pan 1	Pan 2	Pan 3	Pan 4	Pan 5	Tails	k(min^{-1})
251	0.10	0.06	0.05	0.07	0.25	13.30	
178	1.43	0.73	0.56	0.86	1.94	14.16	0.23
126	4.02	2.03	1.53	1.97	2.97	7.52	0.44
89	6.22	2.97	2.24	2.37	2.98	5.87	0.75
58	23.05	10.84	8.13	7.46	8.00	13.31	0.93
38	7.15	4.25	2.77	2.91	2.34	5.06	1.05
27	4.07	2.69	1.92	1.91	1.76	3.67	0.97
19	3.11	2.27	1.21	1.95	1.81	2.65	0.87
13.5	1.73	1.33	0.98	0.97	0.90	1.90	0.87
9.5	0.51	0.56	0.22	0.23	0.33	0.54	0.87
−7.5	0.45	0.33	0.19	0.23	0.25	0.41	

In tests A, C and D the —200 mesh material was elutriated in a Haultain Infrasizer. In test B a long column water elutriator was used, with gelatin as the dispersing agent.

Experimental Results

Tests A: Three tests were run and the respective products were combined for sizing. Table I lists the results obtained. Fig. 1 shows ln $\frac{C_o-x}{C_t-x}$ plotted vs time for the various sizes. The lines cross the abscissa at minus time, indicating that flotation had started before the air was turned on. This was caused by skin flotation after the xanthate was added and before the air was admitted to the cell.

Table III. Size Distribution in Products of Test B

Mean Diam, Microns	Solids in Froth, G, After				Solids in Tail, G	k(min^{-1})
	20 Sec	15 Sec	30 Sec	60 Sec		
251	0.035	0.110	0.150	0.090	0.135	1.25
178	0.200	0.265	0.265	0.130	0.250	2.52
126	0.720	0.840	0.570	0.180	0.260	4.27
89	1.910	1.975	1.025	0.190	0.380	4.95
61	3.690	4.075	1.530	0.135	0.380	5.37
53	7.580	6.140	2.320	0.130	0.590	4.90
37.5	3.920	2.550	0.860	0.020	0.190	4.65
26.5	2.445	2.115	0.770	0.035	0.190	3.72
18.7	2.690	3.215	1.480	0.090	0.310	2.88
13.2	1.390	2.680	2.210	0.380	0.470	1.80
—10.0	0.580	1.380	2.360	0.940	1.380	

The k values obtained are listed in the last column of Table II. When these values are plotted against the arithmetic mean diameter of the particles in each size range, Fig. 2 results.

The rate lines for the size ranges 19 and 13.5 microns coincided with the rate line for the size range 27 microns. Flocculation of the finer material in this test may have given this result. Fig. 2 also shows how the k values vary with the natural logarithm of the average diameter of particle in each size range.

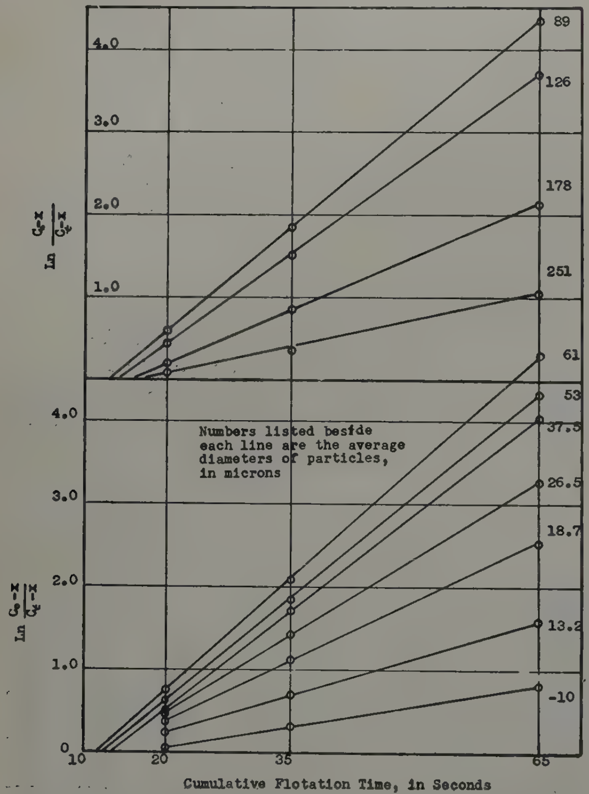

Fig. 3—Variation of flotation rate with average diameter of particle, test B.

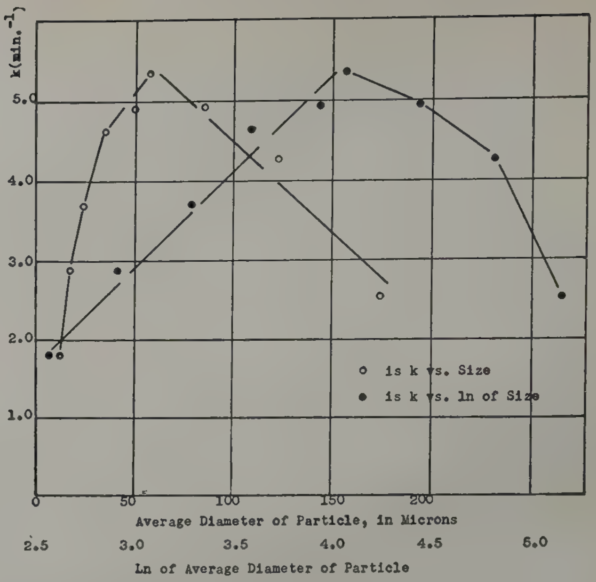

Fig. 4—Variation of k with average diameter and with ln of average diameter of particle, test B.

Test B: Table III shows the sizing results obtained when the concentrates and tails were screened and elutriated. The k values are listed in the last column of this table.

Fig. 3 shows the plot obtained when ln $\frac{C_o-x}{C_t-x}$ is plotted against time for the various size ranges. The lines intercept the time axis at about 12 sec. This was the time lag from zero time until flotation started. The procedure used for marking zero time was different in tests A and B.

Fig. 4 shows the variation of k with average diameter of particle and also variation of k with the natural logarithm of the average diameter of the particle.

Table IV. Recovery, Pct, in Products of Test D

Mean Diam, Microns	Rec. Fe, Pct	k(min^{-1})
251	93.10	.224
178	98.47	.349
126	99.00	.386
89	99.03	.389
58	99.19	.404
38	98.20	.336
27	96.30	.275
19	94.00	.236
13.5	88.10	.179
9.5	79.90	.135
—7.5	72.50	.108

Test C: For the sake of brevity the data obtained are not tabulated, but Fig. 5 shows the variation of k with average diameter of particle for the two different acid additions in the float. Fig. 6 shows the variation of k with average diameter of particle and also variation of k with the natural logarithm of average diameter of particle.

Test D: Table IV shows the calculated percentage recovery of iron in the 10-cell plant flotation machine for each size fraction. The calculated k values are also shown for each size fraction.

The ratio of concentration of this operation was 1.25, as calculated from iron assays of feed, concentrate, and tailing. No middling was made in this machine. The average time of residence of pulp in

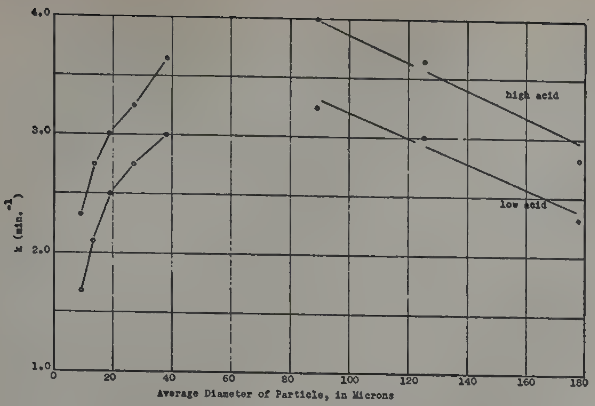

Fig. 5—Variation of k with average diameter of particle, tests C.

the machine was calculated as 12.0 min. This took into account the volume of the machine, and the tons of pulp passing through the machine per unit of time. No great accuracy is claimed for this calculation. In any event an error in retention time would affect all sizes of particles to the same extent; therefore the relative values of k for each size range are valid.

The assumption was made that $x = 0$ since the feed to this cleaner machine consisted of particles which had floated in the preceding rougher operation. This assumption is open to criticism.

The 10-cell machine was regarded as similar to a batch operation in that the concentration of floatable particles in the pulp decreased with time as the pulp passed from the head end toward the tail end of the machine. In a batch operation the concentration of floatable particles in the pulp decreases with time of flotation. In a batch test k can be calculated by using the data obtained in one time interval. By analogy, k can be calculated from the recovery obtained during the retention time of the pulp in the machine, using eq 3, with $x = 0$, $C_o = 100$, $C_t = 100 - R$.

Fig. 7 shows the variation of k with average diameter of particle and also the variation of k with the natural logarithm of average diameter of particle.

Discussion of Results

If eq 3 is applicable to our data a straight line may be drawn through the points obtained when $\ln \frac{C_o-x}{C_t-x}$ is plotted vs time. Fig. 1 illustrates that the first order rate equation may be used to evaluate the rate measurements made in tests A. Additional tests which have been made using the same material used in tests A yield the same results. Fig. 3 contains three points for each line. Although more points are desirable, the metallic copper floated at such a fast rate that it was difficult to obtain three points.

In Figs. 5 and 6 the k value corresponding to the size range of particles obtained in the first cone of the Haultain Infrasizer has been omitted. The k value plots were erratic for this size.

In all of the graphs where k was plotted as a function of particle size the k values for the coarsest fraction and the finest fraction (cone 7 of the Infrasizer) were omitted because it was difficult to assign an average diameter of particle to the coarsest and finest fractions. For the screen sizes the average diameter was taken as the arithmetic mean of the passing and holding screens in each size range. For the elutriated sizes a plot was made of logarithm of cumulative percent passing vs logarithm of size in microns of the sulphide particles in a classifier overflow sample from the Tennessee Copper Co. mill. The equivalent passing screen opening was determined for each cone and the arithmetic mean was taken of the equivalent screen opening of the passing and retaining cone for each size range.

The method used for obtaining the value of x is to use different values of x until the calculated values of $\ln \frac{C_o-x}{C_t-x}$ at the various time intervals lie on a straight line. If the value of x used is too small the later values of $\ln \frac{C_o-x}{C_t-x}$ will lie below a straight line. If the value of x used is too large these later values will lie above a straight line. Small changes in x affect the position of the later values of $\ln \frac{C_o-x}{C_t-x}$ greatly. Therefore x can be determined quite accurately.

It should be emphasized that x is not necessarily the percentage of mineral in the tailing. If the flotation time was prolonged until no more mineral floated, then the tailing assay could be used to determine x. This would assume that no floatable particles were mechanically prevented from being kept in suspension in the pulp. For example, some of the copper particles in test B had deposited on the sloping bottom of the spitzkasten in the cell used and therefore were removed from the zone of bubble-particle contact.

The x value determined in the manner described cannot be greater than the tailing assay obtained after the elapsed flotation time used in the tests; otherwise the method would not agree with actual experimental results.

This method can be checked against the rate plot for the $-100 + 150$ mesh fraction in Fig. 1. The actual cumulative percentage recovery after cumulative flotation time of 90 sec was 47.8 pct. The k value was .44 min^{-1} and the x value used to obtain the straight line was 11. Using eq 3, the calculated cumulative recovery after 90 sec was 48 pct. This is a good check.

Variation of k with Particle Size

The results of all tests show that maximum flotation rate is obtained in an intermediate size range and that the rate decreases on either side of this range. It is difficult to determine whether the flotation rate constant k varies directly with particle size or with the logarithm of particle size on the fine side of the maximum. The results of tests A and C

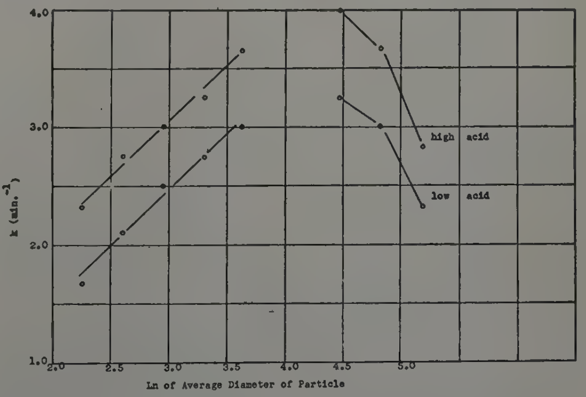

Fig. 6—Variation of k with ln of average diameter of particle, tests C.

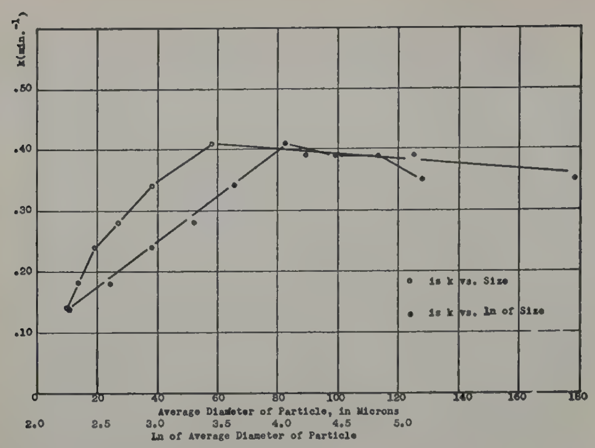

Fig. 7—Variation of *k* with size of particle and with ln of size of particle, test D.

seem to indicate that the variation is logarithmic, but the evidence is not conclusive. However, on the coarse side of the maximum *k* seems to vary directly with the size of particle.

Sutherland[7] made a mathematical analysis of the factors entering into the determination of flotation rate, based on the collision theory of bubble-particle union. He derived an equation which predicted that *k* would vary directly with radius of particle. Thus *k* would increase as the size of the particle increased, and it is implied that this increase would continue up to the maximum size particle that could be floated.

Gaudin, Schuhmann, and Schlechten[8] investigated the influence of particle size upon flotation rate, using the steady state, and found that specific flotation rate varied with size of particle. They used — 40 micron galena and showed that flotation increased as size of particle increased. They deduced that "particles of a size near the maximum that can be floated should have the optimum floatability."

There are two different types of actions taking place in a mechanical-type flotation cell. The first action is concerned with the probability of encounter of bubble and particle. The second action is concerned with the probability of the bubble-particle aggregate reaching the surface of the cell, without disruption taking place between particle and bubble.

Morris[9] measured the forces acting between a bubble and particle under static conditions and found that for any given bubble, the smaller the attached particle, the greater is the probability of the bubble-particle system being able to withstand the disruptive forces present in the flotation cell. Thus the greater is the probability that the particle-bubble aggregate will reach the surface of the cell and be removed.

These two opposing influences of particle size upon flotation rate may be combined as follows to explain the experimental results obtained. The flotation rate increases with size of particle up to the critical size, maximum *k* value. Before this critical size is reached the probability of union between bubble and particle increases as size of particle increases. This is factor 1. However, the opposing factor 2 is also operating, tending to whittle down the advantage of size. Thus the variation of *k* with size on the fine side of the critical size is not a straight line, but tends to bend inward as size increases.

When the critical size is reached, any particle coarser than this is not affected or is very slightly affected by factor 1. In other words, the inertia of a particle of this size or larger is enough to enable the particle to make contact with a bubble without being affected by laminar flow or fluid around the bubble. Factor 2 then is dominant for particles larger than the critical size, and the flotation rate could be expected to decrease as particle size increases beyond the critical size.

Suggestions for Further Work

The use of a rate equation provides a valuable analytical tool in evaluating the effect of changes in reagents, impeller speed, type of impeller, and air volume upon the flotation rate of various sizes of particles. For example, in tests C it was demonstrated that increase in acid added to the pulp changed the flotation rate. But all particles were affected to the same extent, as can be seen by the parallel lines in Figs. 5 and 6 when *k* was plotted vs particle size. The recovery of the fine particles was increased to a much greater extent than was the recovery of the coarse particles, and if recovery alone had been used as a criterion it might have been deduced that increase in acid increased the rate of flotation of fine particles to a much greater extent than the increased rate of flotation for the coarser particles. The reason that the recovery was increased is that the percentage of unfloatable particles was decreased as the acid was increased and the percentage of unfloatable particles was decreased to a greater extent in the fine sizes compared to the coarser sizes.

There is an investigation under way at the Missouri School of Mines pertaining to the effect of impeller speed and volume of air upon the flotation rate of various sizes of particles.

Comparison of different types of flotation machines could be made and evaluated by the use of a rate equation. It appears probable that one kind of machine may yield a higher flotation rate in a given size range than another type. Thus by means of such a study it might be possible to use combinations of different types of machines for the best overall flotation rate. This idea is not new, but study of the possibility could be aided by use of a rate equation.

Acknowledgments

The author is indebted to the following friends and colleagues: Dr. A. W. Schlechten, Chairman, Dept. of Metallurgical Engineering, Missouri School of Mines, for his constructive criticism and encouragement; Mr. J. F. Myers, Superintendent of Concentration, and Mr. E. M. Jones, Superintendent of the Chemical Engineering Dept., Tennessee Copper Co., for permission to use much of the data in this paper and for their constructive criticism; and Mr. William Horst, graduate student at the Missouri School of Mines, for the data used in Tests A.

References

[1] H. Garcia—Zuniga: *Bol. Minero Soc. Nacl. Mineria*, (Chile, 1933) **47**, pp. 83-86.

[2] K. F. Beloglazov: *Tsvetnye Metal* (1939) **70**, No. 9.

[3] W. Grunder and F. Kadur: *Metall u. Erz* (1940) **18**, p. 367.

[4] N. Arbiter: *Trans.* AIME (1951) **190**, p. 791.

[5] T. M. Morris: *Trans.* AIME (1951) **190**, p. 991.

[6] W. F. Dietrich et al.: *RI* 3328, U. S. Bur. Mines (1937).

[7] K. L. Sutherland: *Journal of Physical and Colliod Chemistry* (1948) **52**, p. 394.

[8] A. M. Gaudin, R. Schuhmann, Jr., and A. W. Schlechten: *Journal of Physical Chemistry* (1942) **46**, pp. 902-910.

[9] T. M. Morris: *Trans.* AIME (1950) **187**, pp. 91-96.

The Mobile Drill Unit in Use at the Utah Copper Pit

by L. F. Pett and L. E. Snow

AT the Utah Copper Pit of Kennecott Copper Corp. a versatile mobile drill unit has been developed and tested. Through increased drilling speed and additional available drilling time, an improvement of 233 pct in drill performance has been realized. Operators using drill power can quickly and easily convert the unit from a vertical to a toe hole drill. Drilling is done with the machine in line with the unit or at right angles to it.

Table I covers the 1950 drill record at the mine, showing the types of machines used and the footage obtained.

Table I. Drilling Record for 1950 at the Utah Copper Pit

Type of Hole	Type of Wet Drill Used, In.	Type of Mounting	Total Ft Drilled	Pct	Ft Per Drill Shift	Ft Per Man-Hr
24-ft toe	3½	Tripod	552,411	66	95.7	4.78
28-ft vertical	4	Wagon	250,620	30	127.0	7.94
24-ft bank	3½	Tripod	35,708	4	61.2	2.55
Totals and Averages			838,739		100.7	5.20

Development of the new units was prompted by a desire for solution of the following problems:

1—The ever-expanding operations within the Utah Pit, requiring some 65 miles of transmission pipe lines radiating from a central compressed air plant, have now taxed this compressor plant beyond capacity. While 100 lb per sq in. pressure is maintained at compressors, transmission losses from innumerable small leaks result in low terminal pressure at the drills. Fig. 1 illustrates that while terminal pressure varies according to size of air hose and fittings used, the average drill is operating on air pressures within the 60 to 70-lb range.

The compressor plant is operated primarily for air rock drills. All drilling is done on day shift, but it is necessary to run two of the three 3720 cu ft capacity compressors during night shift in order to prevent drastic loss of pressure through leaks. On day shift all three compressor units are operated at capacity, so that there is no reserve safeguard available for extensive repairs to any compressor. The calculated volume of compressed air required for operation of 25 drills is but 33 pct of three day-shift compressors.

While compressed air is being used to a minor extent for purposes other than drilling, it is felt that satisfactory substitute facilities could be provided in the event that air lines were no longer available.

2—Drill performance has increased beyond the capacity of present 3½-in. drifter machines.

3—The installation, maintenance, and moving of air lines in routine mining is a growing problem. The 2-in. level lines are placed outside electrification towers and must be moved to new location upon completion of each shovel cut. In addition to these moves it is often necessary to dismantle level lines so that excessive shovel spillage, or material covering track following a blast, can be pushed in the clear with bulldozers. Where level room is limited, it is often necessary to remove air lines in giving bulldozers room to prepare grades for wagon drills. In spite of precautions taken, many level lines become buried, twisted, and constricted, with excessive air loss resulting. Excessive back break in blasting often leaves several sections of air line suspended in mid-air. Occasionally air lines come in contact with defective electric transmission towers, so that holes are burned through pipe.

4—Rail-handling of drilling equipment such as wagon drills from one location to another requires considerable locomotive crane crew time. Any new unit developed should travel under its own power.

5—Present practice requires accessory material including hose, water pressure tanks, water barrels, drill steel, and bits to be transported by means of push cars when drill locations are changed on any level.

6—In order to supply numerous drill locations with material, many stock piles of new drill rods, drill bits, and other essentials must be left at strategic points, usually in the vicinity of powder magazines. This practice makes for poor housekeeping and contributes to the loss of supplies.

Planning the Unit

It was felt that a mobile drill unit which would rectify the foregoing problems should meet certain demands:

1—It must furnish compressed air to operate a 4-in. rock drill at a pressure of 90 to 100 lb.

L. F. PETT, Member AIME, is General Mine Superintendent, Utah Copper Co., Bingham Canyon, Utah, and L. E. SNOW, Member AIME, is Research Engineer, Utah Division, Kennecott Copper Corp., Salt Lake City.

Discussion on this paper, TP 3352A, may be sent (2 copies) to AIME before September 30, 1952. Manuscript, Dec. 10, 1951. New York Meeting, February 1952.

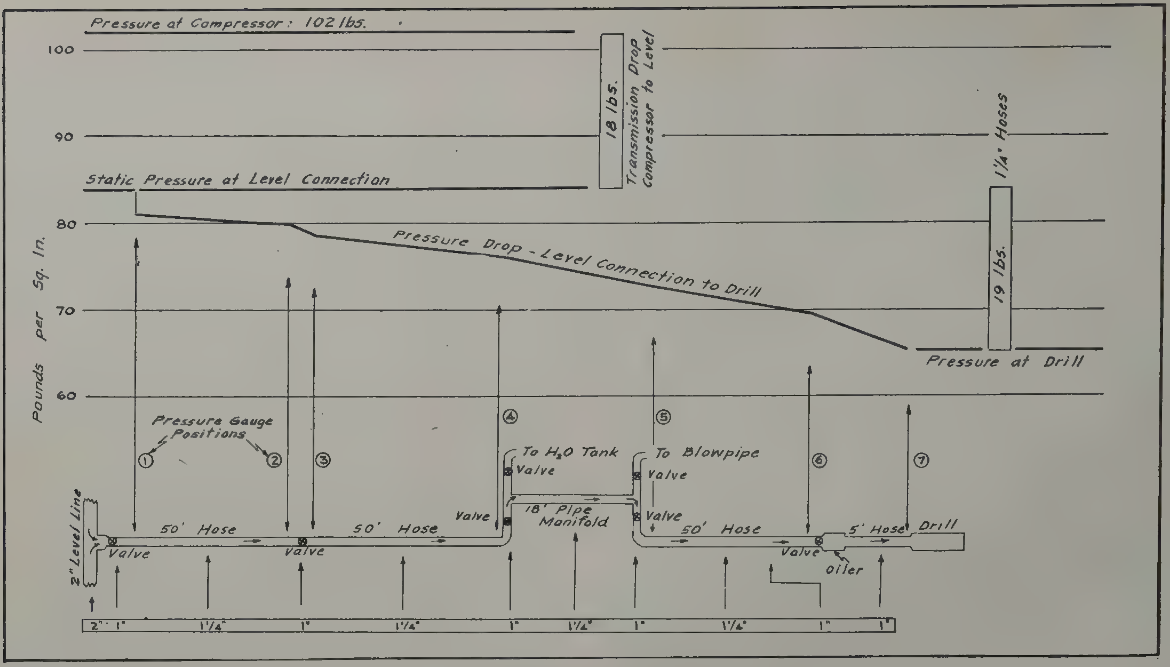

Fig. 1—Air Pressure chart of representative level.

2—It must withstand travel over rough terrain on levels and must negotiate grades on 20 pct bulldozer ramps in moving from level to level. Although ample electric power was available, it was decided that diesel-driven tractors would furnish mobility and be free from interference or dependence upon other mine equipment.

3—The drill mounting must be such that the unit could be quickly converted from a vertical hole machine to a toe hole machine by drill operators and by use of its own power. As a toe hole machine, it must be capable of drilling with the carriage in line with the tractor or, where sufficient clearance is not available for this position, at right angles to the tractor. In this latter position, the tractor is merely moved along the grade between holes, while with the *in line* position, the operator points the tractor in the desired direction of the hole and rides in to a set-up. The in line position would be used in approximately 90 pct of the toe hole drilling, since it places drill and crew farther from falling rocks.

4—The drill must be safer than those used in present operating practice. With either of the toe hole drill positions, operating controls should be placed farther from the collar of the hole than are present machines, to increase the safety of the operating crew. In all cases, the operator must have clearance in getting away from bank caves without climbing around or over drill machinery. The helper on this machine remains away from the collar of the hole, whereas with tripod drilling he was required to spend most of his time near the collar, manipulating the sliding cone and changing drill rods for each 4 ft of hole.

5—The unit should be equipped with a water pressure tank and an ample air receiver and should provide storage for supplies such as extra drill steel, bits, blow pipes, and hose and tool box. A winter cab should be placed on the drill, and heat from the engine and compressor distributed for the convenience of the operator and for the purpose of preventing water in the tank from freezing.

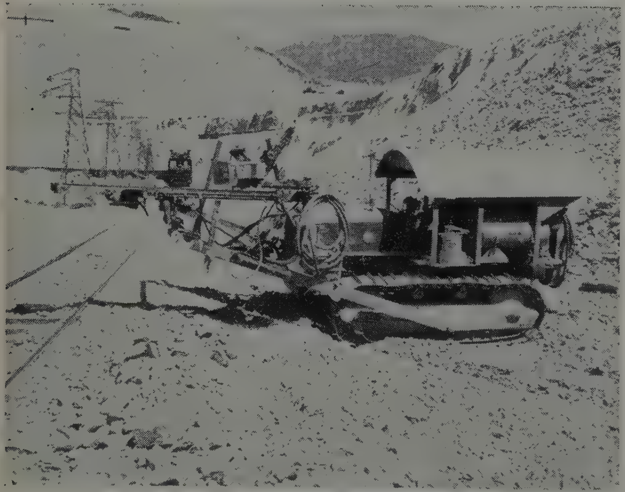

Fig. 2—A D-7 Caterpillar tractor is the primary power unit of the mobile drill rig.

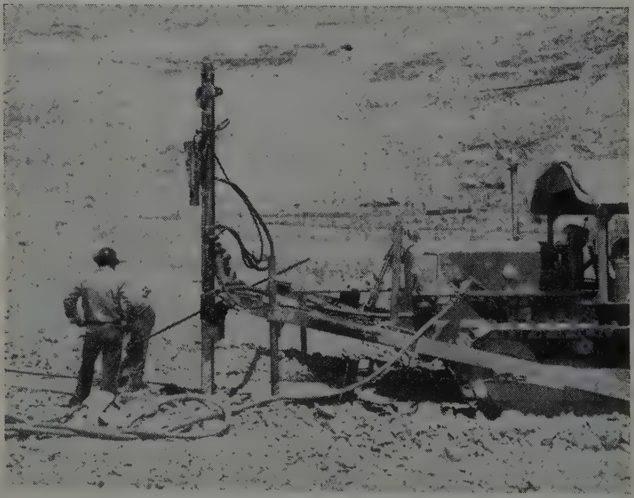

Fig. 3—Mobile drill unit, front end assembly.

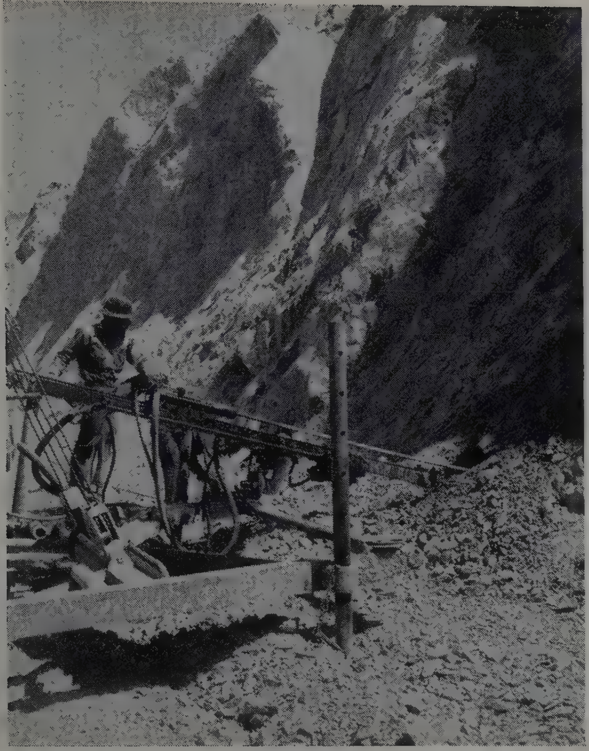

Fig. 4—The mobile drill unit in operation.

6—Advance drill grades must be prepared by regularly assigned bulldozers to reduce hand grading.

7—The unit must be equipped with a long drill carriage so that 12-ft steel changes could be made, ground condition permitting.

8—Drill mounting should be equipped with sufficient centralizers to insure drilling straight holes, since it is necessary to insert a 1½-in. loading pipe in springing and loading toe holes.

Construction of the Unit

With the foregoing requirements in mind, the present test machine, shown in Figs. 2-5, was assembled and put into operation on June 24, 1951, in the busiest part of the mine, the bottom section. The assembly job consisted of fitting standard units—tractor, compressor, air and water tanks, drill mounting, and drill adjustments—into a complete mobile drill unit.

Engine: A D-7 Caterpillar tractor, see Fig. 2, was chosen for the primary power unit. This engine furnishes power for moving the unit over the same terrain and ramps used by other mine tractors. It also provides power through the front end take-off for hoisting and lowering of drill assembly in much the same manner that an angledozer blade is raised and lowered. The rear power take-off is used to drive the compressor.

Compressor: A Worthington M-80 two-stage compressor, see Fig. 5, is mounted vertically over the rear power take-off of the D-7 tractor and is driven by nine V-belts. The intercooler is placed directly behind the operator's cab with the V-belt drive at the extreme rear of the unit and covered by a safety guard. Tests of this unit show that with tractor engine speed of 1000 rpm the compressor speed is 875 rpm while the compressor is delivering approximately 294 cu ft of air per min at a 6500-ft elevation. An auxiliary valve is set to maintain pressure in the 90 to 105-lb range. Additional pressure controls within this range are installed to regulate engine speed with compressor demands. The air pressure, while the drill is operating, has remained close to 93 lb. Changes were made in the forced feed oiling system of the compressor, allowing lubricating oil to be circulated while the compressor was on a 20 pct grade. By the disengaging of the rear power take-off clutch, the compressor remains idle while the machine is traveling. Compressed air is piped through a "U" pipe welded into the water pressure tank and then to the air receiver. The water acts as an after-cooler and is heated by the compressed air. This after-cooler is a desirable feature for both winter and summer operation of the unit. A safety valve to prevent steam from building up excessive pressure inside the water tank is installed. A pop-off safety valve is used on the air receiver. An air injector pump quickly fills the water tank from any source of water. From the air receiver air is piped to the front end of the tractor and through a line oiler to the hose coupling for the drill connection. A spud and valve for connecting the blow pipe is provided so that the previous hole can be blown out while the next hole is being drilled. Use of the blow pipe while drilling causes a temporary drop in air pressure to almost 65 lb, but pressure quickly returns to the normal 93 lb upon completion of blowing.

Front End Assembly: The front end assembly, shown in Figs. 3 and 4, is attached to the side frame of the tractor at the same place and in the same manner as are blade attachments on tractor angledozers. This entire assembly is adjusted with the front single drum cable control from the control in the cab or from the drill operating platform. The front end assembly, once in proper position for drilling, is dropped a few inches to an adjustable supporting leg. Tension is maintained on the hoist cable. At the extreme forward position, a 4-in. slotted bar with a double clamp is attached. This allows the drill to slide along the width of the unit in drilling toe holes at right angles to the tractor. While a Worthington drill carriage capable of making 8-ft steel changes was originally installed, experiments with a drill carriage accommodating 12-ft steel changes has improved drill performance. The carriage is mounted on a 7-in. cone. The air motor

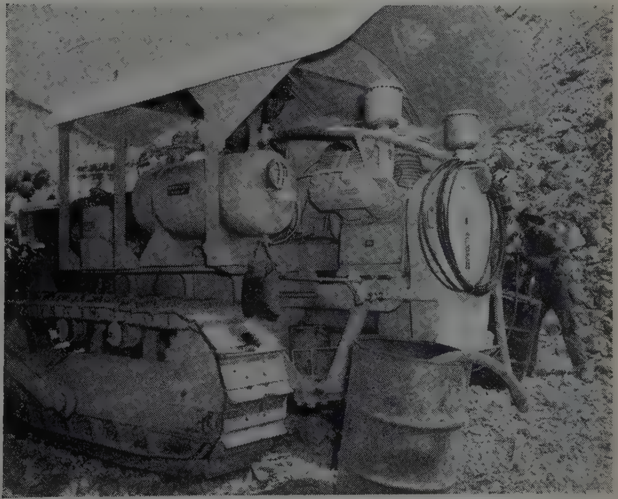

Fig. 5—Rear assembly showing Worthington M-80 two-stage compressor.

Table II. Summary of Operations, Mobile Drill Unit No. 1, June 24 to Nov. 1, 1951

Months, 1951	Man-Hr 2-Man Crew	Man-Hr 3-Man Crew	Man-Hr Total	Ft Drilled 2-Man Crew	Ft Drilled 3-Man Crew	Ft Drilled Total	Total Operating Days	Ft Drilled Per Day	Ft Drilled Per Man-Hr	
June	110		110	2320		2320	7	331.4	21.09	Worthington 4-in. drill, W D 40—2 needles, and 8-ft drill carriage.
July	358	144	502	7448	2326	9774	30	325.8	19.50	
Aug.	163.5	335.25	498.75	2708	4978	7686	25	307.4	15.41	
Sept.	351.25	140	491.25	7569	2390	9959	29	343.4	20.30	IR-505 and 12-in. carriage, Oct. 13th.
Oct.	304	216	520	7154	3960	11114	28	396.9	21.37	
TOTAL	1286.75	835.25	2122.00	27199	13654	40853	119	343.3	19.25	

Average Ft Drilled Per Operating Day 2-Man Crew	Average Ft Drilled Per Operating Day 3-Man Crew*	Average Ft Drilled Per Man-Hr 2-Man Crew	Average Ft Drilled Per Man-Hr 3-Man Crew*
323.8	390.1	21.14	16.35

* The third man is added to the operation only when additional hand work is necessary to prepare the grade for drill.

Additional Data

Average air pressure maintained while drilling with 4-in. drill	93 lbs
Cu ft of free air at 1000 rpm on tractor and 875 rpm compressor	294 cu ft
Average diesel fuel used per 8-hr day	18.2 gals
Average lubricating oil used per 8-hr day	0.14 gals
Cable replacements after 4 months' operation	1 cable
Angledozer time charged for preparing advanced drill grades	1.96 hrs per drill shift
Rock drill repair cost after drilling 33,271 ft	$0.0063 per ft drilled

	12-ft Starter	24-ft Rod	Average
Typical drill speeds in ft drilled per min	2.47	2.07	2.27

can be clamped to the drill carriage at any desired position. Besides the drill centralizer at the end of the carriage, an intermediate centralizer is installed to keep drill rods from whipping. A rear leg is used to give additional support to the carriage. For vertical hole drilling, an 11-ft pipe is inserted in the rear support clamps in place of the shorter pipe support used for toe holes.

Winter Cab: The unit has an enclosed cab placed over the tractor seat, with compressor, air receiver, and water pressure tank. A rack constructed alongside the unit provides storage space for additional drill rods and tools.

Machine Performance

The unit, placed in operation June 24, 1951, has with few exceptions been used daily since that time. All minor repairs, adjustments, oil changes and grease jobs have been done at the drill location during regular operating time. Gages showing first stage and final stage air pressure and lubricating oil pressure are placed alongside Caterpillar engine gages within sight of the operator.

In Table II, performance data of the mobile unit is given for 119 operating days. An operating day is considered any day or part of a day during which the drill is used and includes the time for servicing, minor repairs and adjustments, lubrication, and moving from one location to another.

Tests covering 3½-in. and 4-in. drills, as well as 8-ft and 12-ft steel changes, indicate that a 4-in. drill is preferable to the lighter 3½-in. drill and that a 12-ft feed carriage is preferable to an 8-ft feed carriage. This 12-ft carriage is placed on the unit in the same manner as the 8-ft carriage having a 7-in. cone approximately 5 ft from the end-rod centralizer. The extra length of carriage extends alongside the tractor without increasing the overall length of the unit. The 12-ft carriage requires use of only one 12-ft starter drill rod and one 24-ft finisher rod per standard toe hole of 24 ft and provides for machine withdrawal of the drill rod from the bottom of the hole, eliminating considerable hand labor.

The unit has been used only a limited number of days as a vertical hole machine since 50-ft bench heights prevailing in the sub-pit area require few vertical holes. In drop-cutting for a new level, holes angled at a 45° slope have been used. Performance of the unit for vertical hole drilling is as good as in toe hole drilling. In certain fractured ground it becomes necessary to make frequent blowouts with a blow pipe, and under these conditions the unit is slowed down when air pressure drops, as is the case with wagon drills. It requires approximately 30 min for the crew to make the change from toe hole to vertical hole position.

One of the earlier test conclusions proved that it would not be practical to attempt vertical holes exceeding 28 ft in depth because of the reduction of drill speed as this depth is approached. It may be possible, with the improved drilling pattern obtained, to extend the present depth by use of sectional drill rods. It would be an advantage, in 70 and 80-ft banks, to drill 40-ft vertical holes and eliminate bank holes.

Bit Performance on the Tractor Drill

Tests made on bits used on the tractor drill show that bit performance is improved over results obtained with similar bits on drifter or wagon drills. Table III shows results and comparisons.

Table III. Comparison of Bit Performance on Drills, 1950-1951

	1951 Tractor Drill	1950 Drifter and Wagon Drill Average
Average operating air pressure, lbs	93	60-70
Average drill speed, ft per min	2.27	1.17
Total gage loss for 24-ft hole while drilling only, in 32nds of an in.	4.9	9.1
Average footage per bit per sharp use	18.4	10.83
Average number of regrinds possible	2.08	2.52
Number of uses, new and regrinds	3.08	3.52
Total footage per new and reground bit	56.7	38.12

The retarding effect of depth of hole on drilling speeds is such that larger starter bits have greater rate of penetration than smaller finisher bits.

Sufficient sharp bits are placed on the tractor drill at the beginning of the shift and the helper changes bits as needed. Carrying bits on the unit, both sharp and dull, makes for better housekeeping and reduces appreciably the number lost over previous practice.

Drill Rod Performance on Tractor Drill

While insufficient data has been collected to determine the life of new alloy steel rods, it is estimated that approximately 5 drill rods per week are replaced, indicating an average life of 500 ft per drill rod. Some loss of drill steel is anticipated in utilizing broken pieces on longer drill feeds. This may be minimized by using three steel changes in harder ground sections of the mine. This disadvantage is offset by the fact that with two steel changes used on the mobile drill only 36 ft of drill rod are necessary per hole, whereas for 4-ft changes on present drifters 84 ft of drill rod are needed. Reduction in number of drill units and elimination of present level stock piles will reduce steel rod consumption.

During 119 operating days of the unit, the average of feet drilled per 8-hr shift has been 343.3. Based on the 1950 Report of the Drilling and Blasting Department, which shows 838,739 ft drilled annually, 2300 ft per day, the mobile drill performance represents approximately 1/7 of the total mine drill since it was put in service.

Table IV compares the mobile drill with the 3½-in. drifter and 4-in. wagon drill in the same subpit area of the mine.

Table IV. Comparison of Drill Performances

	Ft Drilled	Ft Per Drill Shift	Ft Per Man-Hr	Cost Per Ft of Hole, $
1950 subpit record, drifter and wagon drill	350,000	111.9	5.78	0.301
Mobile drill average on same footage	350,000	343.3	19.25	0.090
Difference in favor of mobile drill		231.4	13.47	0.209

An estimated annual saving of $73,000.00 in drill labor could be achieved by using three mobile drills to cover the subpit area of the mine.

Photoelectric Sorting of Optical Fluorspar

by W. T. Turrall and D. Porter

The paper describes a machine developed for the purpose of concentrating clear optical grade fluorspar crystal from a feed material containing less than 1 pct impurities. The principle of concentration is based on the fact that in a liquid having an index of refraction equal to that of fluorite (n — 1.434) clear crystals are invisible, whereas crystals containing occluded impurities absorb a part of the light. As the crystals pass through a light beam, undesired crystals give themselves away by creating a shadow on a photoelectric receiver. The shadow is converted by the photoelectric cell into an electric pulse. An electronic circuit amplifies this pulse and commands the operation of a mechanical concentrator.

THE crystal laboratory, Dept. of Physics, Massachusetts Institute of Technology, was confronted with the problem of obtaining a supply of optical grade calcium fluoride (CaF_2) for use in growing synthetic CaF_2 crystals. A search of the known fluorspar deposits did not indicate that any quantity of optical spar could be obtained. Even the best material had to be sorted by hand to remove impurities.

The process for growing CaF_2 crystals developed by Professor D. C. Stockbarger of the Dept. of Physics, M.I.T., necessitates very pure feed materials. Exclusion of impurities is required, even in amounts detectable only spectrographically. The impurities occurred as minute inclusions of SiO_2, $BaSO_4$, $CaCO_3$, FeS_2, water or air. Crystals up to 4 in. in diam and weighing several pounds are made by the Harshaw Chemical Co. in Cleveland. Since the time required to grow a 4-in. crystal is about one week, and since the cost of manufacture is high, removal of impurities by any concentration method appeared practical.

The mineral engineering section of the Dept. of Metallurgy undertook to investigate the possibility of concentrating clear optical fluorspar, —4 mesh +10 mesh, from a feed containing over 99 pct CaF_2. Various innovations of the known methods of concentration were considered, but in each case the minute amount of impurities associated with the crystal produced such extremely small differences

---

W. T. TURRALL, Member AIME, formerly Assistant Professor of Metallurgy, Mineral Engineering Section, Massachusetts Institute of Technology, is now Supervisor and Technologist of Coal Preparation, Lehigh Navigation Coal Co., Lansford, Pa. D. PORTER is a student, Dept. of Physics, Massachusetts Institute of Technology.

Discussion on this paper, TP 3351B, may be sent to AIME (2 copies) before Sept. 30, 1952. Manuscript, March 15, 1951. St. Louis Meeting, February 1951.

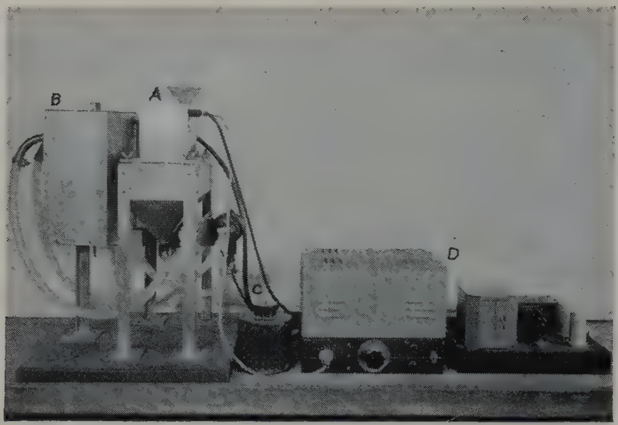

Fig. 1—Photograph of photoelectric concentrator showing: A. Housing for exciter lamp, phototube, sorting column, and gate mechanism; B. Product container; C. Variac and pump for liquor circulation; D. Electronic unit with adjustable sensitivity control and exciter lamp power supply.

in physical properties of the particles as to eliminate the usual methods of mineral concentration.

Since the concentrated product was to be used for its optical properties, it was decided to explore the prospects of developing a photoelectric concentrator, utilizing as the fundamental basis of separation optical differences between those particles which were clear and those which were not.

Principle of Photoelectric Concentration

Photoelectric concentration of fluorite is based on the fact that in a liquid having an index of refraction equal to that of fluorite ($n = 1.434$) clear crystals are invisible, whereas crystals containing occluded impurities absorb or scatter a part of the light. Thus if crystals pass through a horizontal light beam, the undesirable crystals give themselves away by changing the light received by a photoelectric receiver. This change in light flux is converted by the photoelectric cell into an electric pulse. An electronic circuit amplifies this pulse and commands the operation of a mechanical gate. The essential parts of the concentrator are: 1—a sorting tank filled with optical liquor (toluene in ethanol), 2—a beam of light at right angles to the path of the particles, 3—a photocell and an electric amplifier, 4—a gate or flipper to guide the particles into one compartment or another of the sorting tank, and 5—a pumping system to facilitate the collection of particles in their respective product baskets.

The first model, constructed of lucite, was essentially an exploratory machine and as such contained many gadgets, but it served its purpose in developing an electronic circuit, indicating necessary changes, and proving the approach feasible. Figs. 1 and 2 show the completed machine with its electronic control.

A feeder was designed to present sized particles to the horizontal light beam one at a time. The feeder employs vacuum to pick up particles on the end of radial nozzles connected through a control valve to the main vacuum tank. The control valve permits each particle to stick to the nozzle for about ¾ of a turn, and since the driving shaft is horizontal, it allows the feeder to pick particles up from a supply layer and deliver them in regular sequence as bodies falling in a viscous fluid across the beam of light.

The sorting column is ¾ in. wide and square in cross section. Its length is about 5 in. It has been found advisable to use hoppers with discharge openings of several sizes, so that each opening permits the passage of some particular size of particles. In this way the particles can be centered through the sorting column and are sorted when in the same position with respect to the beam of light. To facilitate adjusting and cleaning of the concentrator, the sorting column and all mechanical parts are built into the removable top of the product compartments. The sorting column is centrally located above an adjustable dividing bar between the compartments into which the crystals fall. At the bottom of the column are deflecting gates mechanically operated by a small reversible motor through a train of gears.

On being deflected to their proper compartment, the particles settle to the bottom and discharge through an opening into the pumping system, see Fig. 3. The liquor transports the particles into removable concentrate and reject basket containers, or product baskets. These have bottoms of 14-mesh copper screen and are fitted in the upper compartment of the product container, unit B in Fig. 1.

The product container is divided into an upper and lower compartment so that as the products are collected in the baskets solution height in the system is kept constant by allowing displaced solution to overflow into the lower compartment. The solution can be drained readily and returned to the pumping system after the products have been removed. It is important to maintain a constant solution level in the sorting column; otherwise a change in settling

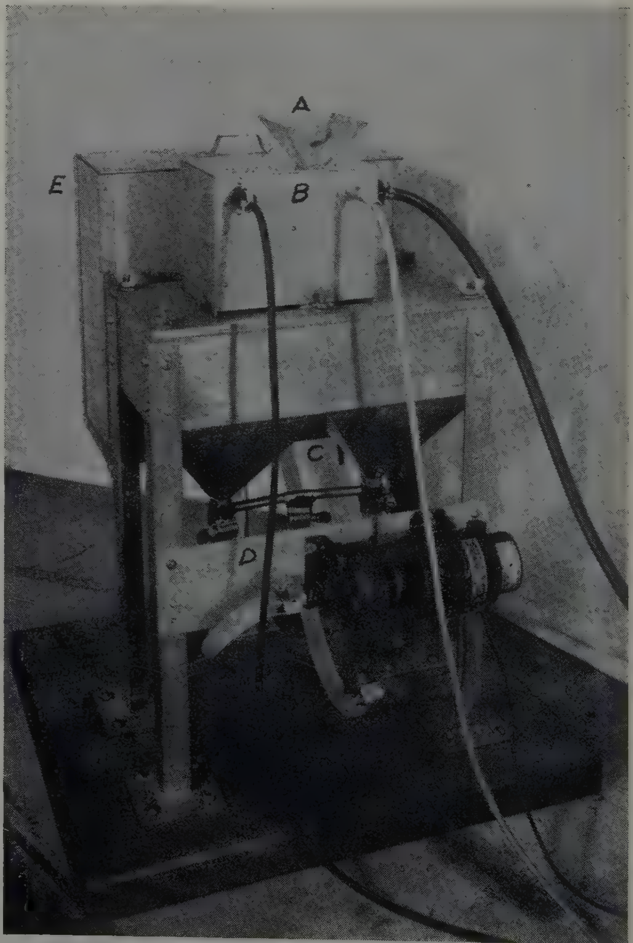

Fig. 2—Photograph of photoelectric concentrator showing: A. Feed hopper; B. Housing for exciter lamp, phototube, sorting column, and gate mechanism; C. Discharge hoppers; D. Pumping system; E. Product container.

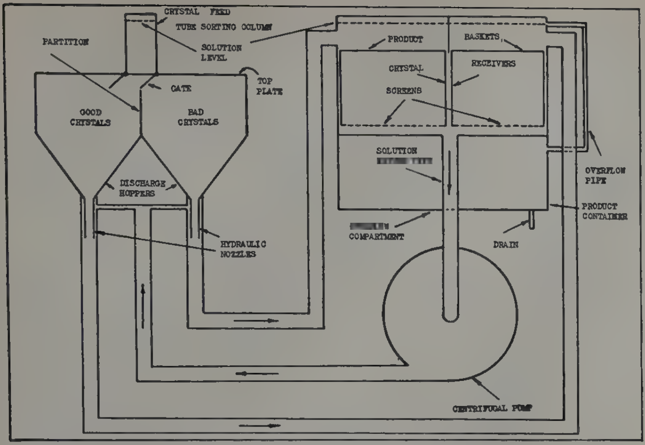

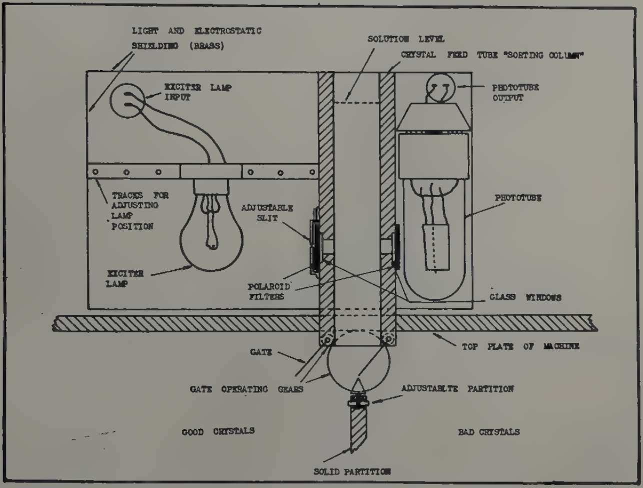

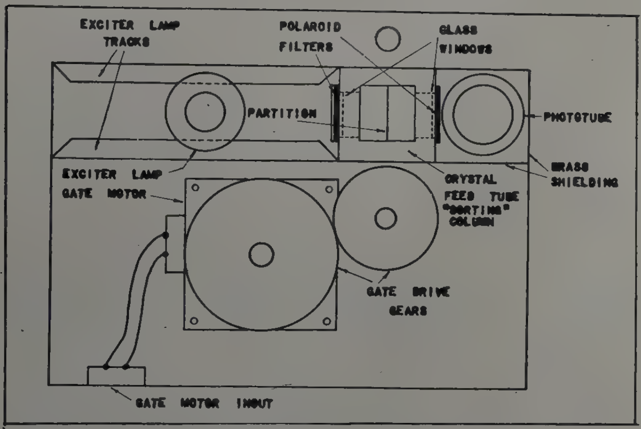

time of particles can be troublesome once the feed rate and the electrical time delay of the gate mechanism have been synchronized.

A small centrifugal pump controlled by a variac, unit C in Fig. 1, is used to circulate the liquor. Particles do not pass through the pump but are impelled by the flow as the solution is forced through nozzles located at the discharge of the product hoppers. As can be seen in Fig. 3, the liquor, carrying the products, passes through the screen in the product baskets and returns to the pump. By utilizing such a flow system, it is possible to obtain constant circulation of liquor for transporting purposes and also to maintain the liquor in the crystal-sorting zone in the state of quiescent pool. This condition eliminates interference with the settling of the crystals. Tygon tubing is used to make connections in the pumping system, the machine proper being of brass construction.

The Optical and Electronic System

The optical system employed in this machine, see Figs. 4 and 5, is relatively simple. It consists of glass windows mounted in opposite sides of the sorting column and backed by two crossed polaroid filters to provide dark-field illumination. An exciter lamp having an input of 6-v direct current is used as the light source. It is mounted on tracks so that its distance from a phototube located directly opposite can be varied. This adjustment permits a variation in the excitation of the phototube.

The amount of light permitted to pass through the optical liquor is controlled by an adjustable slit placed in the optical path. The variation in the light flux evaluated by the phototube depends in part on the size and in part on the opacity of the passing particles. The rate of change of the light flux determines the rise time of the pulse delivered by the phototube.

The purpose in using polaroids in the light path is to provide a system in which virtually no light strikes the photocell when a perfect crystal is interposed, whereas an appreciable light flux reaches the photocell when an imperfect crystal is interposed and depolarizes the light. This gives a very large proportionate increase in light flux when an imperfect crystal passes. If dependence is placed on the use of ordinary light instead of polarized light the variations in flux on a percentage basis are very small.

The electronic system may be referred to as the brain of the concentrator. When it receives a signal

Fig. 3—Diagram showing flow of optical liquor. Fig. 4—Optical system with portion of gate mechanism illustrated. Fig. 5—Plan of optical system, gate motor, and gate driving gears. Fig. 6—Diagram of exciter lamp power supply.

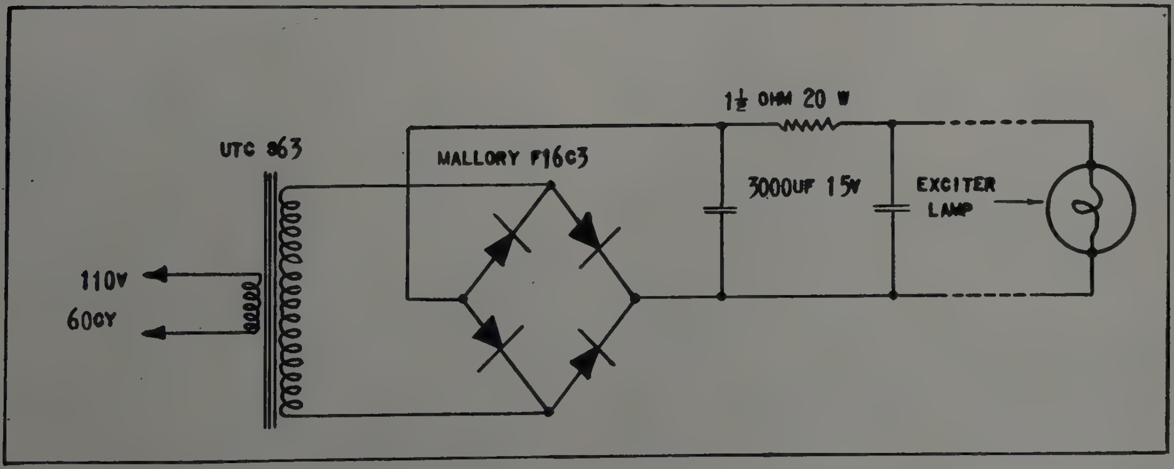

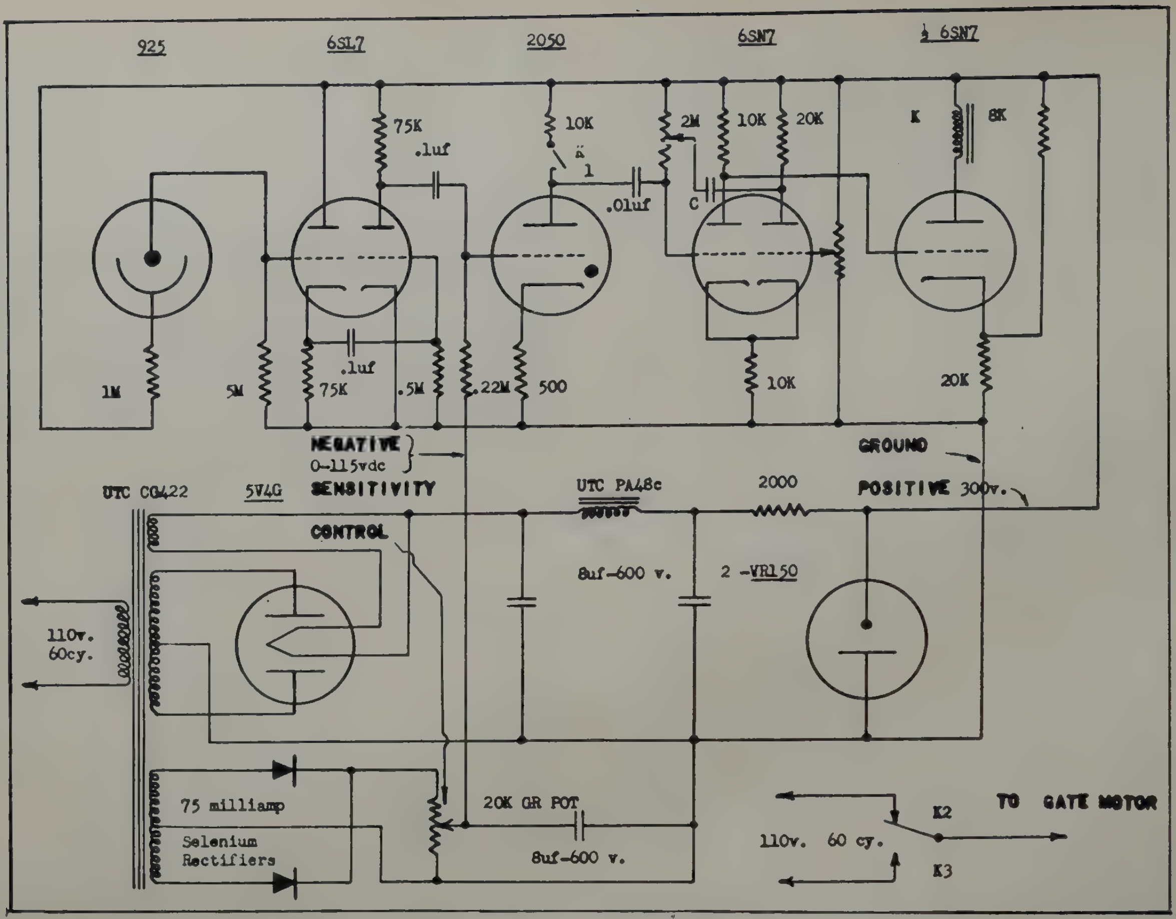

Fig. 7—Diagram of electronic circuit.

from the phototube as an undesirable particle is passing through the sorting column, the signal is amplified to operate a relay which energizes the deflecting gate mechanism for a specified duration of time. The magnitude of light pulse which will cause action is referred to as the *threshold.* This threshold is adjustable by a control known as the *sensitivity control.* In operation, therefore, it is this control which is the regulator for the purity of the concentrate. It should be understood that the gates are normally at rest in the "good" position so that particles which contain no impurities will have passed into the discharge hopper before the next particle is presented to the light beam. The length of time the gates stay closed when an undesirable particle is to be rejected depends on the settling velocity of the crystals through the liquor and the distance between the beam of light and the gates. Because of mechanical inertia of the gate system, the maximum repetition rate for one cycle of operation is about 0.8 sec. To allow for possible discrepancies in settling rate due to shape and size, the particles are fed to the machine at the rate of about one every 1.5 sec.

It is not the purpose of this paper, however, to discuss the electrical circuits in detail. Wiring diagrams of the exciter lamp power supply and electronic system, Figs. 6 and 7, respectively, are included to show the basic requirements.

An attempt was made to determine the efficiency of the machine by quantitative spectrographic analyses of the feed, concentrate, and reject. No significant differences were obtained by this method. This is because there was an extremely small concentration of noxious impurities in all products and also because some of the undesired constituents were anions and did not show up in the spectrographic analyses. The answer was provided by growing small crystals using material representing the feed and material representing the concentrate. The concentrate produced a clear synthetic crystal, whereas the feed did not.

Summary

The photoelectric concentrator provides a method for sorting high quality optical fluorite crystals. Although each crystal has to be examined individually by the apparatus, the process is continuous. The sensitivity of the electronic circuit is such that it rejects those crystals which to visual examination appear to be unsatisfactory. It is realized that such a device will have limited application and will be used only for the solution of problems where tonnage and cost are not critical factors.

Acknowledgments

The writers are greatly indebted to Professor A. M. Gaudin, Mineral Engineering Section, Dept. of Metallurgy, MIT, for his continued encouragement in this interesting and challenging research and for his suggestions in the editing of this paper. The writers also wish to thank Professor H. Rush Spedden of the Mineral Engineering Section, Dept. of Metallurgy, and Professor D. C. Stockbarger, Dept. of Physics, for their constructive criticism during the development of the machine. To H. A. Lundquist, Dept. of Physics, much credit is due for the mechanical success of the machine.

This work was made possible by the support given by the Harshaw Chemical Co. to the crystal laboratory of the Physics Dept. at M.I.T.

Glass and Chemical Sand Manufacture In the Edwards Paddle Scrubber

by Will Mitchell, Jr., T. G. Kirkland, and R. C. Edwards

A scrubber of new design has been invented for the beneficiation of glass and chemical sands. The machine is described and its capacity and metallurgical efficiency compared with the performance of other sand cleaning devices.

THREE years ago, when the Process Research Laboratory at Allis-Chalmers Manufacturing Co. sought a remedy for the increasing cost of disposing of great quantities of spent sands from foundries, R. C. Edwards developed a continuous inclined paddle scrubber which removed a substantial amount of the charred coatings from the grains with a surprisingly small amount of degradation of the sand itself.[1] The satisfactory results obtained on foundry sand, using this piece of equipment in conjunction with classification, suggested that a similar procedure could probably be applied to the cleaning of other sands, such as those required by the glass and chemical industries.

This paper describes the flowsheet and the results of tests performed on impure natural sands. The four materials tested were silica sands obtained from widely separated geographical areas. Three of the sands tested contained various amounts of iron oxide and the fourth an excessive amount of calcareous bonding material. The iron oxide was present predominantly in the form of grain coatings, which were scuffed by the paddle scrubber, and in all cases a product was manufactured which would meet one of the sets of specifications imposed by the glass industry.[2]

The Edwards paddle scrubber used in these tests consists of a rubber-lined steel cylinder 18 in. in diam and 48 in. long, mounted on a frame so that its slope can be varied 5° to 35° from horizontal. This variable slope permits controlled flow of material through the machine. Rubber paddles rotate inside the cylinder and are secured to a center shaft 2 in. square, which extends through the entire length and is turned at both ends so that it can be supported by sleeve bearings centrally fixed in the end plates of the shell. At the upper or feed end it extends through the bearing on the end plate into a sheave, to which the motor drive is connected by means of Texrope transmission.

The four sets of paddles mounted on the shaft, two in each set, are made of rubber belting, ¼ in. thick, 9 in. wide, and 16 in. long. The two paddles in each set are secured on opposite sides of the square shaft, but in the same longitudinal position along the shaft axis. In other words, the two paddles in the set operate 180° apart. Each successive set is mounted 90° from the preceding one. One end of each paddle is bolted to the square shaft and the other weighted by a steel bar, 1x1½x9 in. long, which is attached about ½ in. from the outer tip of the paddle. By centrifugal force at proper shaft speed, these weights force the paddle surface to rub smoothly against the rubber lining of the cylinder. During operation, the sand forces its way between the paddle face and the surface of the cylinder, providing the necessary abrading action as the pulp flows by gravity down the length of the cylinder.

The capacity of the machine is limited by the amount and the hardness of the coating material and by the quality of product desired. The degree of scrubbing is governed by the retention time in the scrubber, which in turn may be changed by varying the feed rate, water content of the feed, and

---

WILL MITCHELL, JR., Member AIME, is with Research Laboratories, Allis-Chalmers Manufacturing Co., Milwaukee. T. G. KIRKLAND, Member AIME, and R. C. EDWARDS are with the Processing Machinery Dept.

Discussion on this paper, TP 3382BH, may be sent (2 copies) to AIME before October 31, 1952. Manuscript, Dec. 10, 1951. Revised June 20, 1952. Los Angeles Meeting, February 1953.

This page of Mining Transactions AIME follows p. 806. The intervening non-Transactions pages appeared in Mining Engineering.

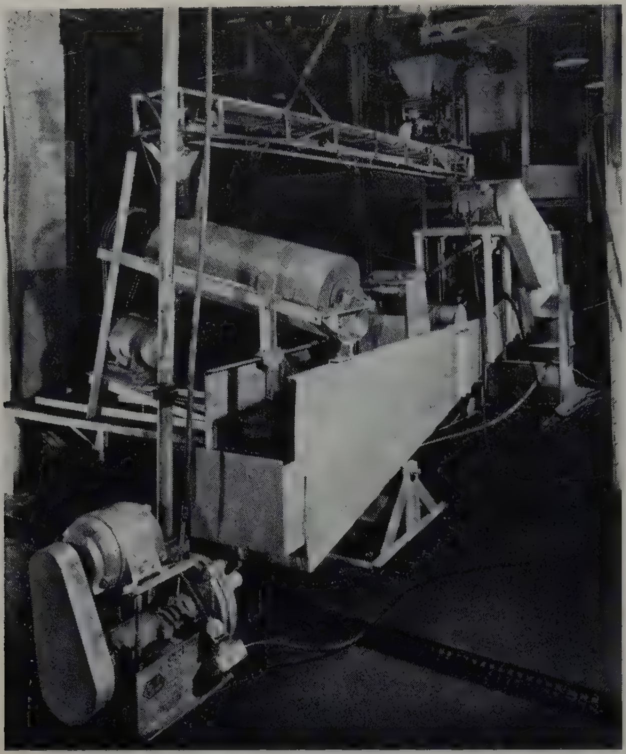

Fig. 1—Feeder, scrubber, and classifier circuit in operation.

slope of the tube, as well as the speed of the paddles. In the tests to be described the shaft was turned at 400 rpm, the slope of the tube was maintained at 13°, and the water content of the feed was kept at 18 to 20 pct.

The wear of the rubber lining of the cylinder is negligible if proper conditions are maintained, that is, regulation of feed rate and slurry so that the bulk of the sand grains scrape against each other rather than against the rubber surfaces. Seventy-five tons of foundry sand have been cleaned in a continuous process without causing measurable wear of the lining. Until recently the paddles had been fashioned from neoprene-covered belting, but because of an excessively high rate of wear they now are being manufactured from abrasion-resistant natural rubber. Data on the life of the new paddles are not yet available.

Table I. Iron Oxide Distribution

	Distribution, Pct	Weight of Total Sample, Pct
Fe_2O_3 in −200 mesh cementing material	25.0	0.06
Fe_2O_3 as stain on quartz grains	45.0	0.11
Fe_2O_3 in quartz grains	15.0	0.04
Fe_2O_3 as partially decomposed magnetite	8.0	0.02
Fe_2O_3, as partially decomposed pyrite	4.0	0.01
Fe_2O_3 as free limonite	3.0	0.007
Total	100.0	0.247

Pilot Plant Tests

The general flowsheet for tests of the paddle scrubber included a coarse grinding device, required only if the particle size was larger than 20 mesh, a vibrating screen, the paddle scrubber, a rake classifier operated to separate at 200 mesh, a thickener, and a filter for dewatering slimes. A rotary drier was used for dewatering the cleaned sands. Fig. 1 shows the feeder, scrubber, and classifier unit in operation. A schematic flowsheet of the process is shown in Fig. 2.

In wet screening, 12 to 18 pct moisture was removed from the sand by means of a rake classifier where the −200 mesh fraction was eliminated. In dry screening, it was necessary to add water by means of a spray at the feed end of the scrubber; the fines were allowed to pass through the scrubber to be removed later in the final classifier.

The four sands used for this series, obtained from Nevada, Michigan, Illinois, and Ohio, possessed two properties in common: the main impurity to be eliminated occurred predominantly as 1—coating on the grain surfaces or, 2—as cementing material binding the grains together. Thus all could be beneficiated by a scuffing action and were treated in general as described in the flowsheet.

The Nevada Silica Sand Test: The raw material for this test came from a deposit near Overton, Nevada, and was treated to determine whether or not the iron content could be lowered sufficiently to make it acceptable as glass sand. It was a light brown, loosely cemented, quartzitic sandstone. Particle size varied from cemented pieces as large as 4 in. in diam to individual grains smaller than 74 microns. Cementing material consisted of siliceous clay minerals, quartz, chalcedony, opal, and iron oxide.

The quartz grains were predominantly equidimensional; however, their surface was not smooth. The grain size of the quartz varied from 74 to 840 microns; the average was 210 microns.

Iron oxide occurred as free limonite, limonite stain or coating on the quartz grains, and limonite and magnetite contained within the quartz grains. The Fe_2O_3 content in the sample as received was 0.247 pct, the average of six analyses. Table I shows the distribution of the iron minerals, the form in which they occurred, and the percentages of each.

The feed rate to the scrubber was 1000 lb per hr, and the power requirement was 13 kw-hr per ton. However, the scrubber was not operated at capacity for this test.

Fig. 2—Flowsheet of cleaning process.

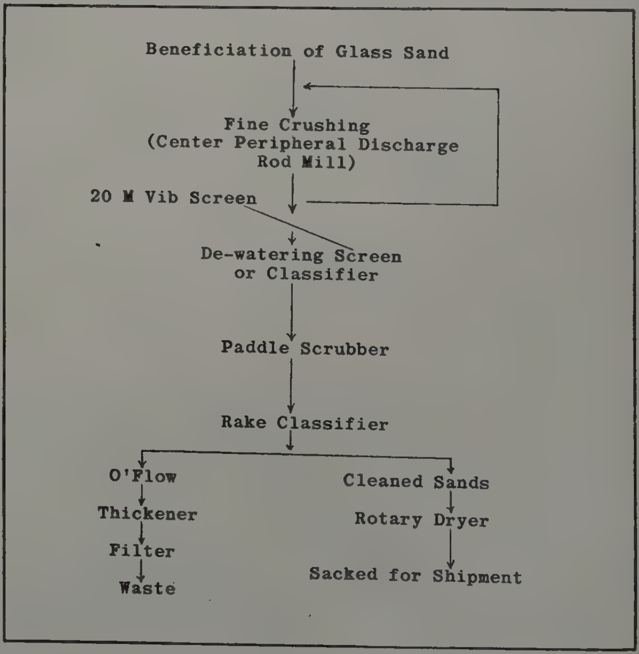

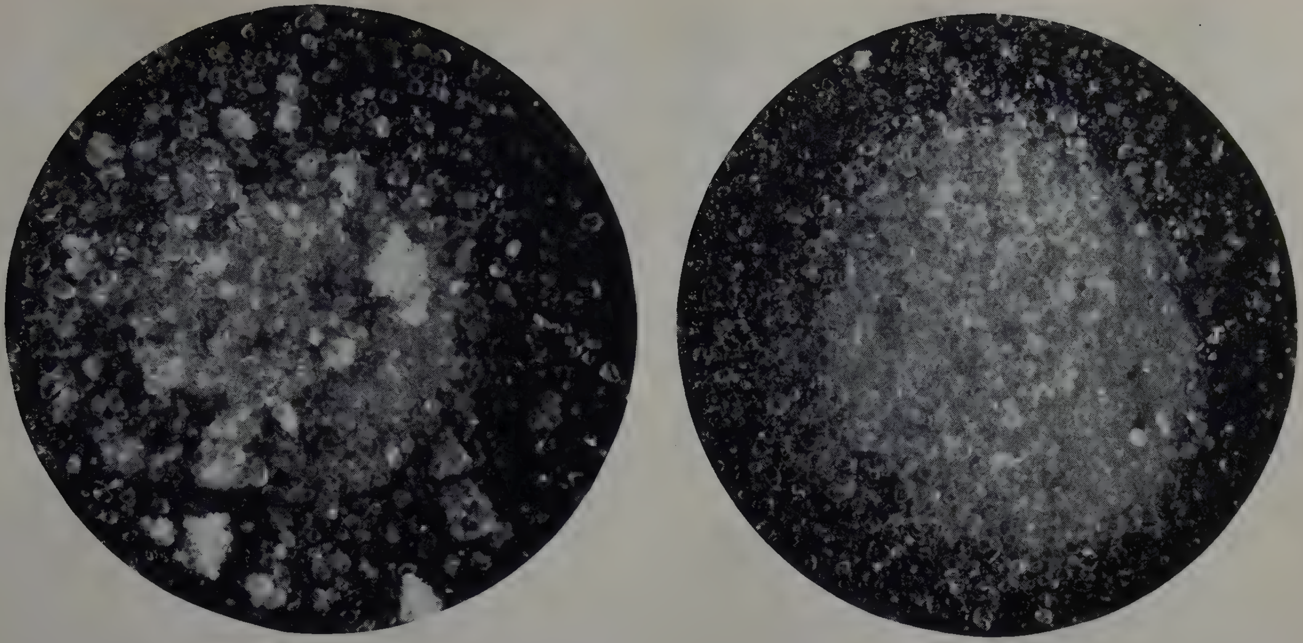

Fig. 3—Photograph of the feed (left) and the classifier sands (right). Note the clusters of cemented quartz crystals in the feed and the absence of these clusters in the classifier sands. X4.

Complete chemical analyses of the feed and the deslimed sand scrubber product are shown in Table II. A metallurgical balance for the classifier products is shown in Table VII. Observation by means of a microscope showed that the iron oxide remaining in the product did not occur in the form of grain coatings, but as inclusions in the grains and as precipitated oxide in the internal cracks. The surfaces were well cleaned. Reduction of impurities in the Nevada sand accomplished by the paddle scrubber and classification without further processing make this sand acceptable as "fifth quality glass sand," used chiefly for sheet glass.

The Michigan Silica Sand Test: The sand for this test, found in Wayne County, Mich., was to be used in the chemical industry. Impurity elimination of lime and magnesia was of prime importance, with iron oxide elimination of secondary importance. The sand as received was almost pure white in color, having the general appearance of beach sand, and was −20 mesh in size. The quartz occurred as clear, well-rounded grains, approximately 1/10 of 1 pct of the grains coated with limonite stain. A very small amount of pyrite was noted in the otherwise clear crystals. Calcite and dolomite, 1 pct each in quantity, were present in two forms, as individual grains and as cementing material bonding together grains of quartz. Small clusters of quartz grains surrounded a grain of calcite, and often the whole cluster was cemented together by calcium carbonate. Small pieces of calcite adhered to some quartz grains, indicating that during the mining and previous milling operation a number of clusters of cemented quartz grains had been broken.

The scrubber tests on the Michigan sand were conducted at three different feed rates, 500 lb per hr, 1000 lb per hr, and 1500 lb per hr. Chemical analyses of the feed and products from the three tests, with the calculated percentage elimination of contaminants, are shown in Table III.

Table II. Chemical Analysis of Feed and Sand Scrubber Product

	SiO_2 Pct	Fe_2O_3 Pct	Al_2O_3 Pct	CaO Pct	MgO Pct	TiO_2 Pct	Loss on Ignition
Feed	95.69	0.247	2.190	1.08	0.202	0.032	0.56
Classified Sand scrubber Product	97.90	0.061	1.27	0.292	0.141	0.016	0.29

Observation of the finished product under the microscope showed that the action in the sand scrubber circuit had broken the clusters of cemented quartz and had dislodged and eliminated the calcite adhering to the quartz grains. Fig. 3 shows the feed and also a classifier sand product. The feed shows clusters of quartz crystals cemented together with calcite. As can be seen in the picture of the product, the clusters are completely broken up and the quartz crystals are clear. Much of the iron stain was removed from the quartz grains, but the included pyrite remained.

The power requirement of the scrubber was as follows: 500 lb per hr feed rate, 20 kw-hr per ton; 1000 lb per hr feed rate, 12 kw-hr per ton; 1500 lb per hr feed rate, 9 kw-hr per ton.

The MgO and CaO content of the Michigan sand

Table III. Chemical Analyses of the Feed and Paddle Scrubber Products, Michigan Sand

	Loss on Ignition	SiO_2	Fe_2O_3	Elimination of Fe_2O_3, Pct	CaO, Pct	Elimination of CaO, Pct	MgO, Pct	Elimination of MgO, Pct	Al_2O_3, Pct	TiO_2, Pct	Elimination of SiO_2, Pct
Feed	1.24	97.27	0.030		0.80		0.56		0.09	0.01	
500 lb per hr	0.66	98.58	0.019	32.25	0.41	29.01	0.26	27.50	0.05	0.02	0.20
1000 lb per hr	0.72	98.36	0.036	8.40	0.48	22.80	0.30	23.40	0.09	0.01	0.15
1500 lb per hr	0.86	98.99	0.020	12.40	0.62	15.00	0.42	14.30	0.07	0.02	0.09

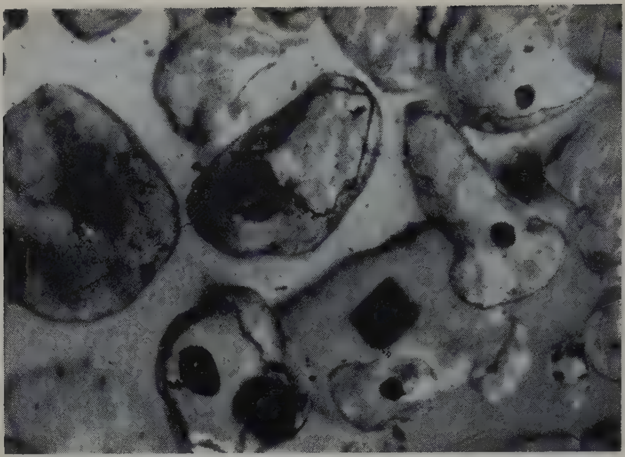

Fig. 4—Photomicrograph of quartz grains showing magnetite inclusions. X57. Area reduced approximately 50 pct for reproduction.

was reduced sufficiently to meet the specifications for chemical sands, and the iron content was reduced to meet the iron specifications for first quality glass sand. However, the MgO plus CaO content was too high to make it acceptable for this purpose.

The Illinois Silica Sand Test: The sand for this test, intended for the glass industry, came from LaSalle County, Ill. Impurity elimination of iron oxide was of prime importance.

Table IV. Chemical Analyses of the Feed and Classified Products Illinois Silica Sand

Test Feed Rate	Loss on Ignition	SiO_2, Pct	Fe_2O_3, Pct	Elimination of Fe_2O_3, Pct	Al_2O_3, Pct	TiO_2, Pct
Feed analysis	0.10	99.77	0.032		0.092	0.10
500 lb per hr	0.11	99.77	0.020	48.20	0.089	0.008
1000 lb per hr	0.12	99.79	0.024	22.20	0.056	0.011
1500 lb per hr	0.11	99.77	0.024	23.90	0.083	0.010

The sand as received was almost pure white and was all —20 mesh in size. The quartz occurred as clear, well-rounded grains, but not smooth. Iron oxide occurred as limonite, 0.04 pct; pyrite, 0.01 pct; and magnetite, 0.04 pct. Ninety-five percent of the limonite occurred as coatings on individual quartz grains. The remainder was in the form of free particles. The ratio of coated quartz particles to clear quartz particles was approximately 1 to 1000. The magnetite was present mainly as inclusions in individual quartz grains. This occurrence was apparently an intergrowth of silica and magnetite, not a deposition of magnetite in cracks in the quartz particles. Noted also were some free magnetite particles. Pyrite occurred mainly as cementing material, but some individual particles were present.

Tests were run at three feed rates, 500 lb per hr, 1000 lb per hr, and 1500 lb per hr. Chemical analyses of the feed and classified products of these tests are shown in Table IV. These analyses showed that the iron oxide content of the sands had been reduced by the sand scrubber. The finished product was observed under the microscope to determine which minerals had been eliminated and to what extent they had been eliminated. It was estimated that about half the coated quartz crystals had been scrubbed clean and the iron oxide eliminated in the classification operation. The pyrite in the form of cementing material had been eliminated, but discrete particles of pyrite and magnetite as well as magnetite in the form of inclusions still remained in the finished product. Fig. 4, a photomicrograph of quartz grains showing magnetite inclusions, readily proves that this form of contaminant could not be removed by a scrubbing operation.

The impurity in the Illinois sand was reduced sufficiently to make the sand acceptable as first quality glass sand.

The power requirement was as follows: 500 lb per hr feed rate, 22 kw-hr per ton; 1000 lb per hr feed rate, 13 kw-hr per ton; 1500 lb per hr feed rate, 10 kw-hr per ton.

Table V. Elimination of Fe_2O_3 Contaminants

Feed Tests	Weight, Pct	Fe_2O_3, Pct	Fe_2O_3 Distribution, Pct
First run		0.45	
Classifier sands	96.5	0.20	38.0
Classifier overflow	3.5	8.90	62.0
Calculated head	100.0	0.51	100.0
Second run		0.20	
Classifier sands	97.3	0.17	77.3
Classifier overflow	2.7	1.9	22.7
Calculated head	100.0	0.22	100.0
Third run		0.17	
Classifier sands	98.5	0.15	93.7
Classifier overflow	1.5	0.67	6.3
Calculated head	100.0	0.16	100.0
200-mesh screening without scrubbing		0.45	
Oversize	93.4	0.35	75.0
Undersize	6.6	1.7	25.0
Calculated head	100.0	0.43	100.0

Ohio Silica Sand: The sand for this test came from near Garrettesville, Ohio, and was an agglomerate containing fine sand, as well as pebbles ranging up to 1 in. in diam. The first three sands described in this paper had a natural grain size below 20 mesh; therefore the procedure worked out for preceding sands had to be altered. The material was first ground in a center peripheral discharge rod mill to —6 mesh. The —6 mesh product was sorted on a screen clothed with 20 mesh stainless steel. The undersize was a mixture of rounded quartz grains

Table VI. Fe_2O_3 Analysis of Feed and Test Products

	As Received	Log Washer	Pebble Mill	Blade Mill	Rod Mill	Paddle Scrubber
Fe_2O_3 in feed, pct	0.247	0.247	0.247	0.247	0.247	0.247
Fe_2O_3 in classified product, pct	0.193	0.176	0.207	0.182	0.137	0.061
Fe_2O_3 in non-magnetic fraction of classified product, pct	0.164	0.138	0.124	0.124	0.107	
Fe_2O_3 in acid leach of non-magnetic fraction, pct	0.123	0.091	0.100	0.107	0.089	0.057
Fe_2O_3 in flotation products, pct						
Classified product as feed		0.107				
Non-magnetic fraction as feed		0.081				
Loss of silica by degradation, pct		3.8	19.0	3.9	3.9	4.7

and angular quartz fragments, brown in color and −20 mesh in size. It was classified in a rake classifier and the sands were fed to the sand scrubber.

The major contaminants were limonite, 0.3 pct, and magnetite, 0.1 pct. More than 50 pct of the quartz grains were coated with limonite, and some occurred as clusters cemented together with limonite. Magnetite was observed as inclusions within the quartz grains and also as individual particles.

It was decided that this material should be run through the scrubber three times, because of its exceptionally high iron content. The material was fed to the scrubber at the rate of 750 lb per hr. The classifier sands from the first run were sampled, then fed back into the scrubber at the same feed rate, and the classifier sands from the re-run were similarly treated. Table V shows metallurgical balances of the test products. A sample of the feed was washed through a 200 mesh screen to give an idea of the cleaning effect of classification alone. The results of this test are also shown in Table V.

Table VII. Metallurgical Balance of Test Products, Nevada Silica Sand

Test	Weight, Pct	Fe_2O_3, Pct	Fe_2O_3 Distribution, Pct	Silica Distribution, Pct
Head		0.247		
Classification				
Classifier sands	96.2	0.193	83.5	96.5
Classifier overflow	3.8	5.355	16.5	3.5
Calculated head*	100.0	0.222	100.0	100.0
Log washer				
Classifier sands	96.0	0.176	68.7	96.2
Classifier overflow	4.0	5.744	31.3	3.8
Calculated head	100.0	0.246	100.0	100.0
Pebble mill				
Classifier sands	81.0	0.207	66.4	81.0
Classifier overflow	19.0	0.447	33.6	19.0
Calculated head	100.0	0.253	100.0	100.0
Blade mill				
Classifier sands	95.9	0.182	76.9	96.1
Classifier overflow	4.1	5.118	23.1	3.9
Calculated head	100.0	0.227	100.0	100.0
Rod mill				
Classifier sands	95.8	0.137	49.5	96.1
Classifier overflow	4.2	5.990	50.5	3.9
Calculated head	100.0	0.265	100.0	100.0
Paddle scrubber				
Classifier sands	95.1	0.061	21.2	95.3
Classifier overflow	4.9	4.383	78.8	4.7
Calculated head	100.0	0.273	100.0	100.0

* Discrepancies in calculated head analysis fall well within limits of experimental error.

After the third treatment, the iron content in this sand was reduced sufficiently to make it acceptable as sixth quality glass sand.

The feed rate to the scrubber was 800 lb per hr for each of the three runs. The power requirement was 15 kw-hr per ton for each run.

Comparison of Several Sand Cleaning Processes

The methods in use today for cleaning sand are mainly washing or classifying operations; however, some include use of gravity shaking tables, blade mills, and blunging. Occasionally ball or pebble mills with light charges of grinding media or rod mills with rubber-coated rods have been used to give a light scuffing action. Further refining has been accomplished by acid leaching, magnetic separation, or froth flotation.

In order to determine the value of the paddle scrubber, the Nevada sand was subjected to various types of cleaning processes. The Nevada sand was selected because a high percentage of its contaminant occurred as a surface coating. The following devices were used as the main beneficiating agent: a log washer, a blade mill, a pebble mill with a light grinding charge, a rod mill with rubber-coated rods, and the paddle scrubber. Products of all of these devices were hydraulically classified with a rake classifier or a constriction plate classifier for slime removal. Some products were refined by acid leach or magnetic separation or by flotation.

Table VIII. Comparative Efficiency of Sand Cleaning Devices

	Sand Scrubber	Log Washer	Pebble Mill	Blade Mill	Rod Mill Rubber Covered Rods	Classifier Only
Feed pct Fe_2O_3	0.247	0.247	0.247	0.247	0.247	0.247
Classified products, pct Fe_2O_3	0.061	0.176	0.207	0.182	0.137	0.193

Iron oxide analyses of the feed and products may be found in Table VI. Both silica distribution and a metallurgical balance for iron oxide in the product are shown in Table VII.

From these tests it was concluded that the paddle scrubber did the most effective job in eliminating surface contamination with minimum degradation; Table VIII shows its superiority over other methods in eliminating iron contamination in Nevada silica sand. Table IX summarizes the performance of the sand scrubber on four sands contaminated by coatings or cementation.

Table IX. Comparative Performance of the Paddle Scrubber on Various Sands

	Contaminant	Contaminant in Feed, Pct	Contaminant in Product, Pct	Elimination of Contaminant, Pct
Nevada sand 1000 lb per hr	Fe_2O_3	0.247	0.061	78.8
Michigan sand 500 lb per hr	CaO	0.80	0.41	29.01
	MgO	0.56	0.26	27.50
	Fe_2O_3	0.030	0.019	32.25
Illinois sand 500 lb per hr	Fe_2O_3	0.032	0.020	48.20
Ohio sand	Fe_2O_3			
800 lb per hr		0.45	0.20	62.0
1st re-run		0.20	0.17	22.7
2nd re-run		0.17	0.15	25.0

The power requirement and capacity of the sand scrubber is governed by the desired product quality. For the tests described here the average power requirement was 14 kw-hr per ton and the capacity ranged as high as 1500 lb per hr. The power requirement for foundry sand reclamation has been found to be as low as 3 kw-hr per ton at a capacity of 5,000 pounds per hr.

These tests prove that the sand scrubber, with accessory equipment, may be used to prepare glass and chemical sands economically from contaminated high silica deposits.

References

[1] U. S. Patent No. 2,578,180 (December 11, 1951).
[2] Industrial Minerals and Rocks, AIME (1949) p. 971.

Variation of Thermo-Electric Properties of Pyrite In Association with Gold Ore

by A. D. Mutch

IT has long been known that there are wide variations in the thermo-electric potential of pyrite. In the last few years a study of this variation and other properties of pyrite was carried out at the University of Toronto by F. G. Smith on specimens of pyrite from many localities.[1-3] As a result of these studies the pyrite geothermometer was developed by Professor Smith.

The calibration of the pyrite geothermometer is based on the assumption that "crystals of any one electronically conducting mineral species deposited at a high temperature have a more positive thermo-electric potential than crystals deposited at a low temperature, and the thermo-electric potential varies continuously between any given limits of the temperature of deposition." The cause of the variation was postulated to be crystal discontinuities, such as lineage boundaries. As yet this postulated relationship has not been established as fact. On theoretical grounds it is indicated that the thermo-electric potential of pyrite or any other partial conductor is dependent upon a number of factors as well as the temperature of formation. For this and other reasons there is ground for doubt as to the validity of the relationship postulated above.

To date a large number of readings have been made with the pyrite geothermometer which have been recorded in terms of the calibration of the instrument in degrees centigrade. So far most of the pyrite tested by this technique has been in association with gold ore. The values for the temperature of formation obtained in these tests appear to be reasonable and, in relation to geological problems, to vary in the right sense. Determinations on some specimens not in association with gold ore have given readings that appear to be much too high, taking into account the probable maximum temperature of the host rock. To sum up, although many determinations made with the pyrite geothermometer appear to give reasonable values for the temperature of formation of the pyrite, there are at the same time other readings which seem anomalous.

On the basis of an examination of available results of work with the pyrite geothermometer, two problems must be considered: 1—the validity of the calibration of the pyrite geothermometer; and 2—the nature of the distribution of the thermo-electric potentials of pyrite in relation to the specific problems that have been examined.

In this paper the academic problem relating to the validity of the calibration of the pyrite geothermometer will not be discussed. Instead, the variations of thermo-electric potential of pyrite in association with gold veins will be discussed with regard to specific examinations.

The first of these two examinations deals with the distribution of thermo-electric potentials of pyrite in association with a gold vein and was carried out in the McIntyre Porcupine Mine, Schumacher, Ont., in the summer of 1949 as part of a study with this technique. The second problem deals with variations of thermo-electric potential of pyrite in gold ore specimens from all over the world. The specimens used in this study were part of the private collection of Frank Ebbutt, geologist for Howe Sound Exploration Co.

Results of Detailed and Reconnaissance Studies

In discussion of the results of determinations made in these two studies the values of thermo-electric potential in millivolts will be used. It will be noted that in some of the diagrams the determinations are recorded in terms of pyrite geothermometer temperatures. Fig. 1 is a calibration chart relating pyrite geothermometer temperatures and thermo-electric potentials.

A full discussion of the technique is given in the original paper by F. G. Smith.[4] Briefly, the determinations are made by placing two stainless steel probes, one hot and the other cold, against the surface of the pyrite crystal being tested. The thermo-electric potential that is developed is read with a null-point potentiometer that is calibrated in what

---

A. D. MUTCH is a mining geologist at Falconbridge Nickel Mine, Ontario, Can.

Discussion on this paper, TP 3355L, may be sent (2 copies) to AIME before Oct. 31, 1952. Manuscript, April 9, 1951. St. Louis Meeting, February 1951.

is believed by Smith to be the temperature of formation of the pyrite. It can be seen that the technique is simple and that the determinations can be made rapidly.

The operational errors of the instrument may be very large. Because of the small potentials that are measured, changes in the surface conditions between the pyrite and the stainless steel probes cause substantial variations in the readings. The prejudices of the operator also may affect the results in two ways: 1—The instrument is calibrated only at every 100°, and it is necessary to estimate to the nearest 10°. The operator therefore tends to avoid certain values and this in turn affects the averaged results. 2—With two or more groups of readings from one specimen many readings of an intermediate value are obtained and there is a tendency for the operator prematurely to discard some of the readings as anomalous. In the work of the two studies discussed below all readings were recorded and considered.

The data recorded below were obtained with the use of two different pyrite geothermometers. The work around a vein at McIntyre Porcupine Mine was done with one instrument and the work on Frank Ebbutt's worldwide collection of specimens was done with another. As part of the study, not discussed in this paper, carried out by the writer at McIntyre Porcupine Mine the distribution of the pyrite values in relation to the Pearl Lake porphyry was examined. This problem had already been treated in a reconnaissance manner by Smith with the second of the two pyrite geothermometers used in the work discussed below.[5] Comparison of the results of these two studies of the same problem with the two different pyrite geothermometers indicates that because of a personal or instrumental error, the instrument used by the writer on the McIntyre problem read slightly higher than the one used in a study of pyrite in specimens in the Ebbutt collection.

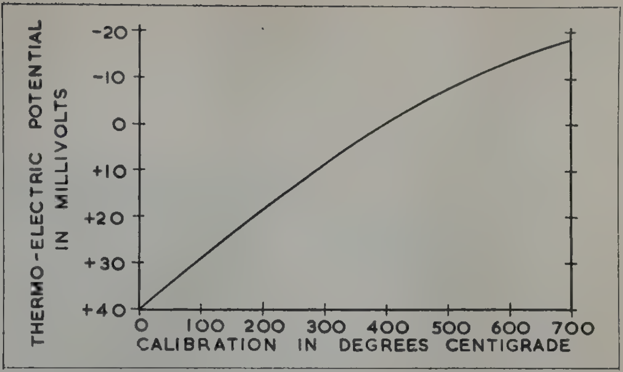

Fig. 1—Calibration curve of the pyrite geothermometer at the University of Toronto.

During the work on both problems, care was taken to reduce the operational errors of the technique to a minimum: 1—all readings were made by the same operator; 2—all readings were taken to the nearest 10°C of the instrument; 3—no results of any phase of the work were plotted until all the determinations were made; and 4—no more than three readings were taken on any one crystal of pyrite.

In the McIntyre work, when enough pyrite was available, up to 20 readings were made on the pyrite in any one specimen. In the work on the Ebbutt collection, a maximum of 10 readings was made on any one specimen.

A detailed description of McIntyre Porcupine Mine is not necessary in understanding this problem. In

Fig. 2—Location of specimens for pyrite geothermometer determinations, No. 25 vein, 3500 level, McIntyre Porcupine mine.

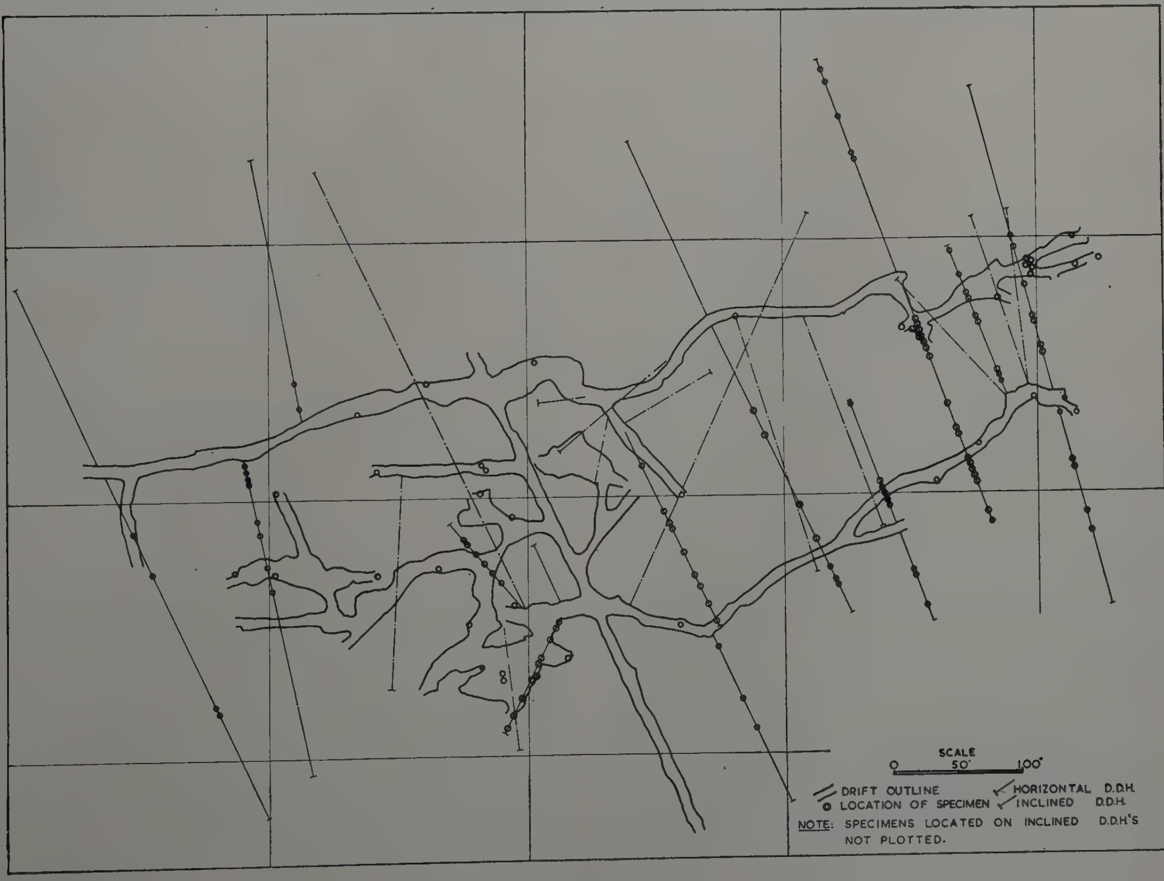

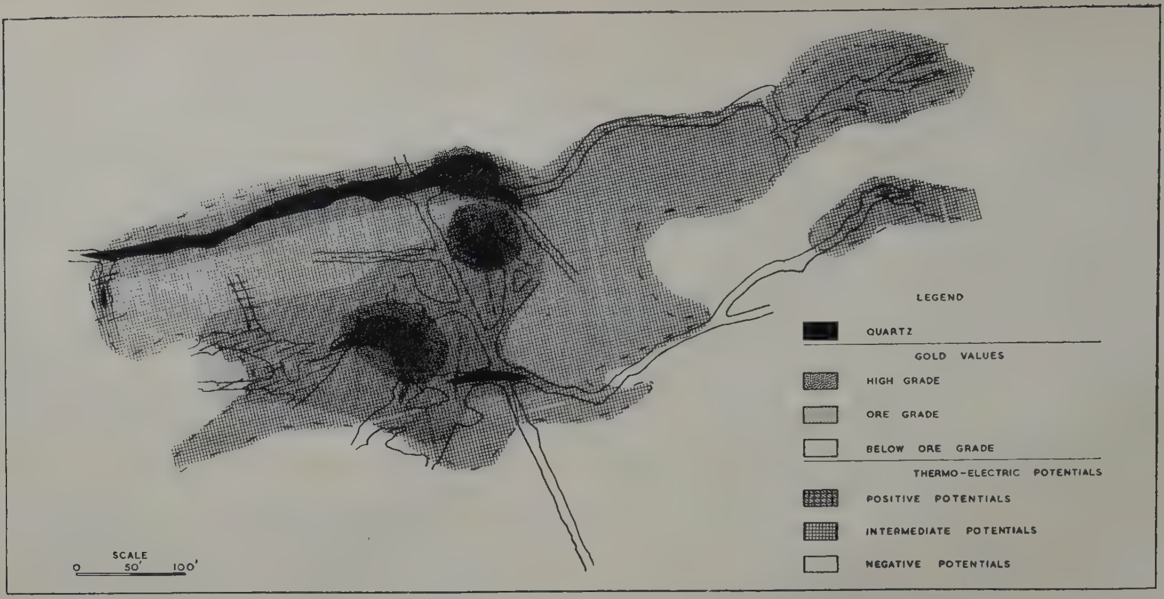

Fig. 3—Variations of the thermo-electric potential of pyrite in association with gold as determined by the pyrite geothermometer, No. 25 vein, 3500 level, McIntyre Porcupine mine.

brief, the mine is a so-called hypothermal gold mine with most of the gold occurring in quartz veins.

For the purpose of examining the detailed variations of thermo-electric properties of pyrite in association with one of these veins, the 3500 level of No. 25 vein was selected. On this level the vein had been well exposed by mining and had been well intersected by diamond drilling. The core from all the drill holes was examined, and where pyrite was found measurements were made with the pyrite geothermometer. A systematic coverage of the drifts was made; specimens were collected and the pyrite in these specimens was tested. As can be seen in Figs. 2 and 3, a good coverage of the vein and the adjoining area was made. Examination of Figs. 2 and 3 indicates a well-defined pattern of distribution of the determinations in relation to the vein areas. Outside the vein area, readings of about −6 mi were obtained, and in the ore shoot, readings of about +22 mi. In the intermediate areas, readings of intermediate and mixed values were obtained.

The Ebbutt collection of gold ore specimens was accumulated by the owner over a period of the last 30 years. In the work discussed below, 462 specimens, of which almost three quarters contained pyrite, were examined and tested with the pyrite geothermometer.

As would be expected, the numerical distribution of the specimens was not truly representative of the distribution of gold mines throughout the world, since 277 of the specimens were from the Canadian Shield, 76 from the province of British Columbia, and the remaining 109 from Nova Scotia, eastern and western United States, Alaska, Mexico, Central and South America, Scandinavia, Europe, Russia, Rhodesia, the Gold Coast, eastern and western Australia, India, the Philippines, and other areas.

Examination of the overall problem indicated that there were enough specimens available from the Canadian Shield to allow an examination of the pattern of distribution of pyrite determinations in relation to the hypothermal type of deposits of this area. It was indicated that there were sufficient specimens from British Columbia so that a similar coverage relative to the Late Mesozoic deposits of this area could be considered. Specimens from the rest of the world were representative of deposits of so many different ages and types that they appeared sufficient to give a confirmatory check if there were any distinct difference between the patterns obtained in the specimens from the Canadian Shield and from British Columbia.

The study of the Ebbutt collection was carried out in two stages. Testing of specimens from the Canadian Shield was done first, followed by work on the specimens from British Columbia. In the testing on the specimens from the Canadian Shield it was found that samples from the mines in the Province of Quebec seldom gave the +22 mi type of reading.

Results of the determinations made in this part of the study were divided into three groups according to the assay of the specimen. Frequency of occurrence curves was plotted with the results of the determinations in these three groups, see Fig. 4. It is noteworthy that in the frequency of occurrence curve for the specimens of low assay, the +22 mi type of reading did not occur.

Results of the second part of the study are shown in Fig. 5 along with the totaled frequency of occurrence curve for the data on the specimens from the Canadian Shield. It will be noted that in these curves there are three peaks, at +22, −6 and −10 mi, that appear to be common to all areas. It is also noteworthy that the −6 mi peak was very high in the curve representing the results of determinations made on specimens from the Canadian Shield and that the +22 mi peak was very high in the curve representing the results of determinations made on the specimens from British Columbia. The relative heights of the peaks on the worldwide curve are intermediate to those on the other two curves.

Critical examination of the results of the determinations combined to make the worldwide curve indicates that the readings obtained on the pyrite from the many types of deposits varied in the same sense as was expected from differences between the frequency of occurrence curves of the Canadian Shield type of deposit and British Columbia types.

Discussion

Disregarding the postulated relationship between the thermo-electric potential of pyrite and the temperature of formation of that mineral, determinations obtained from the pyrite from all types of gold deposits suggest that all pyrites have similar temperatures of formation.

From an economic standpoint, the pattern of the pyrite determinations obtained in relation to the vein area at McIntyre Porcupine Mine is of the most interest. R. W. Boyle has found that corresponding patterns are indicated at Yellowknife, in the north-west territories of Canada.[6]

Critical examination of the distribution of the pyrite geothermometer determinations in relation to No. 25 vein at 3500 level in McIntyre Porcupine Mine shows that the change in type of determinations can be detected a considerable distance from the vein in the greenstone and porphyry wall rock. When this problem was examined further at McIntyre Porcupine Mine it was indicated that the distance at which the pyrite began to give the +22 mi type of reading of the vein was about 50 ft normal to the vein, about 200 ft along the strike of the vein, and probably a great deal more on the dip. Here, then, may be a technique which will give an indication of the distance from an ore shoot.

There is still much work to be done before the reason for the variation of thermo-electric properties of pyrite is known. The fact that interesting patterns of thermo-electric potentials have been obtained in relation to orebodies suggests that work along these lines should be continued. The problem cannot be fully understood until a thorough study has been made of data on semiconductors that has become available in recent years. It may be that there are other naturally occurring semiconductors, in addition pyrite, which may warrant investigation by the use of a similar technique.

Fig. 4—Frequency of occurrence curves of pyrite geothermometer determinations in relation to assays of specimens of gold ore from the Canadian Shield. The heavy line and circles indicate determinations recorded, totaled, and plotted irrespective of the sample in which they were found. The dashed line and crosses indicate the totaled and plotted averages of determinations for each specimen, weighted for the number of determinations.

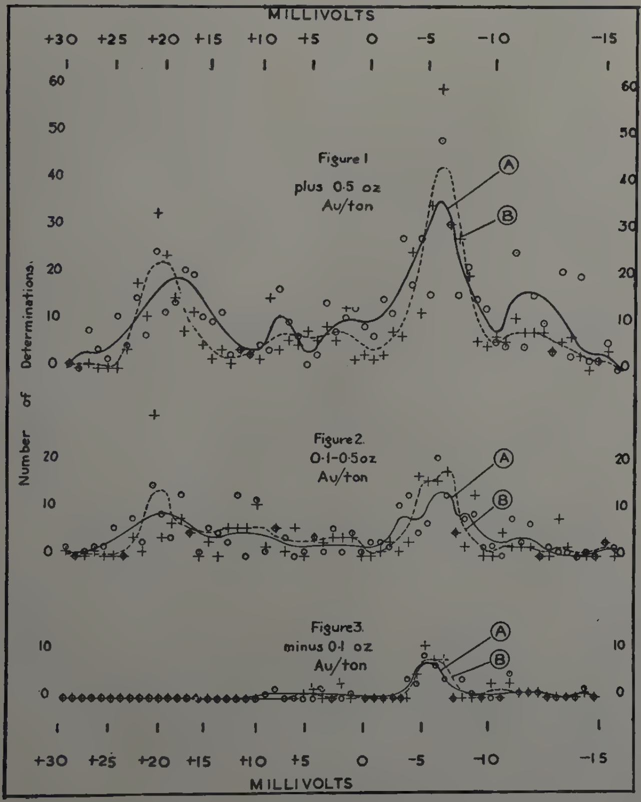

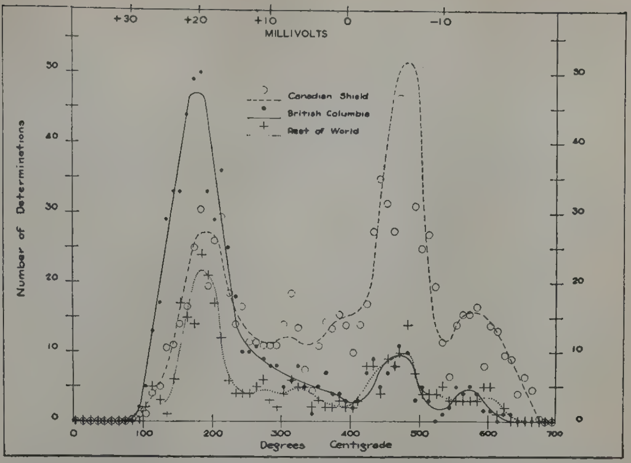

Fig. 5—Frequency of occurrence curves of geothermometer determinations of pyrite in gold ore specimens of the Ebbutt collection.

Summary

1—Further research along several different directions is necessary before the qualitative and quantitative aspects of the calibration of the pyrite geothermometer can be reviewed. 2—The frequency of occurrence curves of thermo-electric potentials of pyrite in association with gold ore, representing hypogene gold deposits of all types and all geological ages, show three peaks at +22, −6 and −10 mi. 3—In the frequency of occurrence curve of thermo-electric potentials of pyrite from so-called hypothermal deposits, the highest peak was −6 mi. 4—In the frequency of occurrence of thermo-electric potentials of pyrite from so-called epithermal and so-called mesothermal deposits, the highest peak was +22 mi. 5—In McIntyre Porcupine Mine, Schumacher, Ont., it was found that the +22 mi readings were confined to the orebearing parts of the vein area and that −6 mi readings were confined to the area outside the orebearing parts of the vein. 6—Since the area of the vein containing this modified pyrite is in excess of the ore section, determinations of thermo-electric potential of pyrite may have an economic application in locating and outlining orebodies.

References

[1] F. Gordon Smith: Variation in the Electrical Conductivity of Pyrite. *University Studies,* Geol. Ser., (1940) **44**, pp. 83-93.

[2] F. Gordon Smith: Variation in the Properties of Pyrite. *American Mineralogist* (1942) **27**, pp. 1-19.

[3] F. Gordon Smith: Lineage Structure and Conditions of Deposition of Pyrite. *Economic Geology* (1942) **37**, pp. 519-523.

[4] F. Gordon Smith: The Pyrite Geothermometer. *Economic Geology* (1947) **42**, pp. 515-523.

[5] F. Gordon Smith: The Ore Deposition Temperature and Pressure at McIntyre Mine, Ontario. *Economic Geology* (1948) **43**, pp. 627-636.

[6] R. W. Boyle: Personal Communication.

Drilling and Blasting Methods in Anthracite Open-Pit Mines

by R. L. Ash, R. D. Boddorff, C. T. Butler, and W. W. Kay

DRILLING and blasting in anthracite open-pit mines is a continuous problem to contractors and explosive engineers because of the diverse conditions caused by the nature of the geological formations, the extensive mining of the portions of coal beds near the surface, and the proximity of many strip pits to populated areas.

Pennsylvania anthracite occurs in four separate long and narrow fields totaling only 480 sq miles. The coal measures are rock strata and coal beds that are considerably folded and faulted. The crests of the anticlines are eroded extensively. The beds outcrop on the mountain sides and dip under the valleys. At first only the upper portions of the synclines could be stripped. Now stripping to increasingly greater depths is economically possible, as is indicated by the fact that the proportion of freshly mined anthracite produced by strip mining has increased from 3.7 pct of the total tonnage in 1930 to 29.6 pct in 1950.

Much of the rock overlying the deeper beds now being stripped is so extensively broken that considerable difficulty is experienced in drilling satisfactory blast holes and in using explosives in such manner as to insure a uniformly broken material easily removed by the excavating machinery. Such breaking of rock strata has occurred because the bed now being stripped has been mined extensively in former years by underground methods, and tops of gangways and chambers have subsequently failed.

Draglines are used to uncover coal where the overburden can be moved with little or no rehandling. These machines range in size from those having a 2 cu yd capacity bucket on a 60-ft boom to those handling a 25 cu yd bucket on a 200-ft boom. Draglines are also used to strip to the bottom of the coal basins if the depth and the distance between the crops are not too great. For this type of operation blast holes are drilled full depth to the bed. These holes are commonly 30 to 90 ft deep; however, in exceptional cases, holes may be as shallow as 12 ft or as deep as 130 ft. Drilling is normally done for blasts of 12,000 to 60,000 cu yd of overburden, 30,000 cu yd being considered an average blast if vibration is not the controlling factor.

Where the stripping of wide basins or the exposure of a moderately pitching vein makes the use of draglines impractical, dipper front shovels equipped with 4 to 6½ cu yd buckets load into trucks. Overburden is removed in benches of 25 to 30 ft with blast holes drilled 4 or 5 ft deeper than the planned floor of the bench. For shovels under 5 cu yd bucket capacity the volume blasted varies from 8000 to 12,000 cu yd, whereas a volume of 30,000 to 50,000 cu yd of overburden is frequently blasted at one time for the larger shovels where vibration is not an important factor.

During the past decade the churn drill, generally the Model 42-T Bucyrus-Erie blast hole drill equipped for drilling 9-in. diam holes, has become the most common blast hole drilling machine. Electricity powers half the churn drills in use and is preferred on the large strippings where electric shovels are operated and the working area is concentrated. On these operations the cost of additional electricity for the drills is less than the cost of fuel to operate diesel units because of the existing large demand load of the excavating equipment. Moreover, electric motors start more easily in cold weather and generally are less expensive to maintain. Diesel driven units are employed where a higher degree of mobility is required.

The average drilling speed is 8 ft per hr, although in softer rocks a rate of 15 ft per hr is attained. Where rock is hard and strata is badly broken, drill speeds may be less than 2 ft per hr. Low drilling production results under these circumstances when loose material falling from the upper portion of the drill holes causes drill stems to be jammed.

Rock formations vary so greatly in the region that a 9-in. diam churn drill bit may become dull after drilling only 2 ft or may drill satisfactorily for 56 ft; however, an average of 35 ft is usual in sandstone of medium hardness. Dull bits are hoisted to flat bed trucks by the sand line of the drill and are usually sharpened in the contractor's bit shop adjacent to the job. Care is generally taken to cover the thread end of the bit with a cap. To facilitate handling of bits around the drill, a heavy thread protector having an eye top is becoming more popular than the flat-top rubber or metal cap furnished with new bits.

The 9-in. diam blast holes for a 25 to 30 ft bench are normally on 18x18 ft to 20x20 ft spacings, depending on the character of the overburden, although in broken ground 15x18 ft centers may be used to obtain better breakage and a more even bottom for the bench. The patterns of holes for shots

---

R. L. ASH, Member AIME, is Mining Engineer, Atlas Powder Co., Wilkes-Barre, Pa.; R. D. BODDORFF, Member AIME, is Explosive Engineer, Hercules Powder Co., Hazleton, Pa.; C. T. BUTLER, Member AIME, is Executive Vice President, Mining Division, Central Pennsylvania Quarry Stripping & Construction Co., Hazleton, Pa.; and W. W. KAY, Member AIME, is Representative, Explosives Sales, E. I. du Pont de Nemours & Co., Wilkes-Barre, Pa.

Discussion on this paper, TP 3356F, may be sent (2 copies) to AIME before Sept. 30, 1952. Manuscript, Feb. 18, 1952. New York Meeting, February 1952.

to the coal vary from 18x18 ft to 24x24 ft centers because of the generally greater depth of the holes.

In the past two years, 12-in. diam bits with correspondingly heavier drill stems have been substituted for the standard 9-in. tools on some of the Model 42-T blast hole drills. For the most part, the larger holes are drilled where hole depths over 60 ft are required and a dragline with a 22 or 25 cu yd bucket capacity is the excavating unit. By increasing the spacing to 30x36 ft on one operation where a cut ranging from 90 to 130 ft deep across the open face is being taken, 3 drills handling 12-in. tools make available the same volume of shot material as 5 drills with the 9-in. bits.

The hardness and pitch of the rock strata severely limit the application of the horizontal-type auger drills. Nevertheless, in the northern portion of the anthracite region, several contractors have used these drills where the pitch of the vein approaches the horizontal. In one application, a Model 103 McCarthy horizontal drill bored 6-in. diam blast holes to a depth of 36 ft at a speed of 10 ft per hr. The tungsten-carbide cutting teeth were changed before starting each hole because of the abrasiveness of the rock. Holes were spaced 15 ft apart to insure breakage of the 32 ft high, solid sandstone face.

Wagon drills are seldom used for primary drilling, since overburden depths are generally greater than 24 ft, and economical production demands greater volume drilling for large excavating machines.

The Ingersoll-Rand Model QD-8 Quarrymaster percussion drill, equipped with 2 International UD24 diesel engines each driving 412 cfm air compressors to provide air at 150 lb per sq in., was introduced to the region early in 1951. With 35-ft stems and a 6-in. diam bit, these drills have averaged 15 ft per hr in conglomerate and hard sandstone, while twice this rate has been attained in shale and soft sandstone. Production drilling is possible to a depth of 75 ft, but holes have been sunk to 105 ft. Depending upon the material being penetrated, the life of the bit varies from 1500 to over 10,000 ft. The dressing of the spare bits is done at the machine by the operator or his assistant while the drilling continues.

The drilling of blast holes by rotary drilling machinery was started in October 1951, using a Joy Model 58B-H Heavyweight Champion drill, equipped with a 50-hp General Motors diesel engine to drive the rotating table and a 125-hp General Motors diesel engine to operate the 544-cfm air compressor. A 30-ft length of stem can be used without being taken apart; however, standard sections are either 10 or 20 ft long and are screwed together to provide the total length needed. Manufactured by the Hughes Tool Company, the Tri-Cone rock bits used are 7⅜ in. in diam. In hard, broken conglomerate an overall average of 10 ft per hr has been attained with an average bit life of 160 ft. In 20 min, 30 ft have been drilled in shale. When the bit has been used in shale and soft sandstone, a life of 2200 ft has been reached. Experience is limited with respect to drilling deep holes; however, holes are now being drilled to a depth of 65 ft in rock of moderate hardness at a rate of 30 ft per hr.

With the exception of churn drills, all the machines described drill dry holes and deposit fine material near the hole that is suitable for stemming, thus eliminating the costs of supplying water and furnishing stemming material. Bits other than those for churn drills are readily handled by one man without the use of machinery and are discarded or easily resharpened. Because of more continuous contact with the rock to be drilled, the rate of penetration is faster with these machines than with churn drills. To offset these advantages, where air is applied to clean the hole, dust control becomes a serious matter.

Although seemingly high drilling speeds are obtained with some types of equipment, the volume made available for explosives in holes equally deep varies as the square of the diameter of the hole. Thus to produce an equivalent volume per unit time as compared with a 9-in. diam hole drill, a drilling speed 13 times as great is required of a drill making 2½-in. diam holes, 2¼ times for the 6-in., 1½ times for the 7⅜-in., and 0.56 times for the 12-in. diam holes.

Bench shooting is made under comparatively uniform conditions. However, in shooting to the coal, drill patterns of vertical blast holes vary considerably because of the abrupt changes in surface topography and variations in geology caused by the rolls and faults in the tightly folded veins. When drilling is done in broken ground, holes cannot always be drilled to the depth required, since some hit openings and others are abandoned because the upper portion of the holes falls in. Consequently, a planned uniform drill pattern is made irregular by field conditions. Varying depths and burdens, together with strata of vastly different degrees of hardness and brittleness, make it necessary to control carefully the loading of each hole. The burden on the front row often is 24 and 35 ft for 6-in. and 9-in. diam holes respectively, and can be 60 ft for the 12-in. holes at the 130 ft depth.

Because anthracite mining was begun many years ago when a man's home had to be within easy walking distance of his work, towns were built close to the mine openings, directly over the coal basins and near coal outcroppings. Present-day stripping is removing overburden to the very edge of these populated areas, necessitating the utmost caution in blasting to avoid injury to persons or property from flying material and to avoid excessive vibration. Blasts seldom exceed 50,000 lb of explosives for shots to coal, while bench shots average from 8000 to 12,000 lb. However, in some instances it is necessary to place mats over holes and shoot as little as 350 lb of explosives at one time. Several years ago, on the other hand, 660,000 lb of explosives were detonated in a single blast in an area sufficiently removed from property that might be damaged. Heavy shooting is generally required because of the hard and often badly broken overburden. Powder factors range from 0.6 to 1.2 lb of explosives per cu yd of material blasted, but a factor of 0.8 to 0.9 is most common.

Probably one of the most distinguishing characteristics of blasting in the anthracite open-pit mines is the predominant use of relatively insensitive ammonia-type powders in the larger diameter vertical holes. Such powders require special primer charges. Semi-gelatin powder is largely replacing the gelatin, its adoption resulting from the necessity for decreased costs. The semi-gelatins are used almost exclusively for secondary blasting, which is negligible, and for most wagon drill projects.

Explosives are generally delivered directly to blast areas and loaded almost immediately into the blast holes each day. This is made economically possible because of the industry's concentration, the closeness of the powder companies' magazines, and the large quantities involved with each delivery. Lowering of the large-size powder cartridges is the usual loading practice because the primacord or electric blasting cap wires used for detonating the charges must be protected and because the walls of the blast holes are often jagged. In some circumstances powder is either poured, or dropped, or both, to obtain a denser concentration of the explosives. Often, before loading, holes must be blocked at a desired depth with timber when openings in the coal veins have been encountered. Charges are placed in decks in holes where multiple veins, mine openings, and rock strata of highly differing characteristics are encountered along the depth of the holes. Frequently, to avoid redrilling, holes must be loaded with powder immediately upon being drilled.

For churn drill holes, the surface material immediately available and the breaker slate sometimes used are generally unsatisfactory for stemming, since these materials do not pack properly and the sharp edges of rock so used are likely to damage the primacord or the insulation covering the leg wires if electric caps are used in the hole. Excessive water in stemming is also undesirable, since it prevents proper confinement and causes stemming to be violently dislodged. One large contractor loads silt into a dump truck equipped with a chute so that each hole can be stemmed directly with minimum of labor.

Control of blast by milli-second electric caps or primacord delay connectors is becoming generally accepted and preferred to instantaneous blasting. This type of delay blasting produces less vibration and reduces concussion.

Other advantages over instantaneous blasting include movement of overburden in definite directions, better fragmentation and displacement of rock, and a reduction in overbreak which permits drilling closer to the last row of holes of a previous blast.

The United States Bureau of Mines determined by actual tests[1] that vibrations which did not cause a displacement in excess of 0.05 in. did not cause damage to buildings. The Department of Mines of the Commonwealth of Pennsylvania has established a maximum allowable ground displacement of 0.03 in. at any building to avoid the possibility of damage or undue disturbance. Portable seismographs are frequently used to determine and record the actual ground movement during blasts. The amplitude of vibration is thereby scientifically established and the size of the blasts carefully regulated so as not to create objectionable disturbances.

Acknowledgments

The assistance, co-operation, and guidance of the many anthracite contractors, mining companies, and drill and explosives manufacturers in the preparation of this paper are gratefully acknowledged.

Reference

[1] U. S. Bur. of Mines *Bull.* 442.

Drainage Behavior and Water Retention Properties of Fine Coal

by D. W. Gillmore and C. C. Wright

DEWATERING is a major problem in the preparation and utilization of fine-sized coals now being recovered in increasing amounts from colliery effluents, refuse banks, and silt ponds. Of the various methods which have been proposed for dewatering fine coal, gravity drainage is probably the oldest and most widely used, and yet little information on this subject has been published. Consequently a laboratory investigation of gravity drainage phenomena was undertaken not only to provide basic data for predicting the drainage behavior of fine coals in cars, bunkers, basins, and silos, but also to obtain some understanding of the moisture retention properties of fine coal.

Because of practical interest in the problem, a reproducible laboratory technique, which simulated plant conditions as closely as possible, was developed for the evaluation of drainage variables. The apparatus selected consisted of vertically-mounted lucite columns, nominally 4 to 8 ft in length and 2, 3 or 6 in. in diam; the bottom of the column was provided with a rubber stopper through which was inserted a ½-in. diam drainage tube; a wad of glass wool was placed on the upper part of this outlet tube to retain the coal and a plug was temporarily located at the lower end to prevent drainage during charging of the column, see Fig. 1.

The most satisfactory testing procedure is as follows: 1—The fine coal, which has been thoroughly

---

D. W. GILLMORE and C. C. WRIGHT, Member AIME, are with the Division of Fuel Technology, Pennsylvania State College, State College, Pa.

Discussion on this paper, TP 3384F, may be sent (2 copies) to AIME before October 31, 1952. Manuscript, December 17, 1951. Revised June 19, 1952. Presented at the Annual Joint Fuels Conference, AIME-ASME, Cleveland, October 1950.

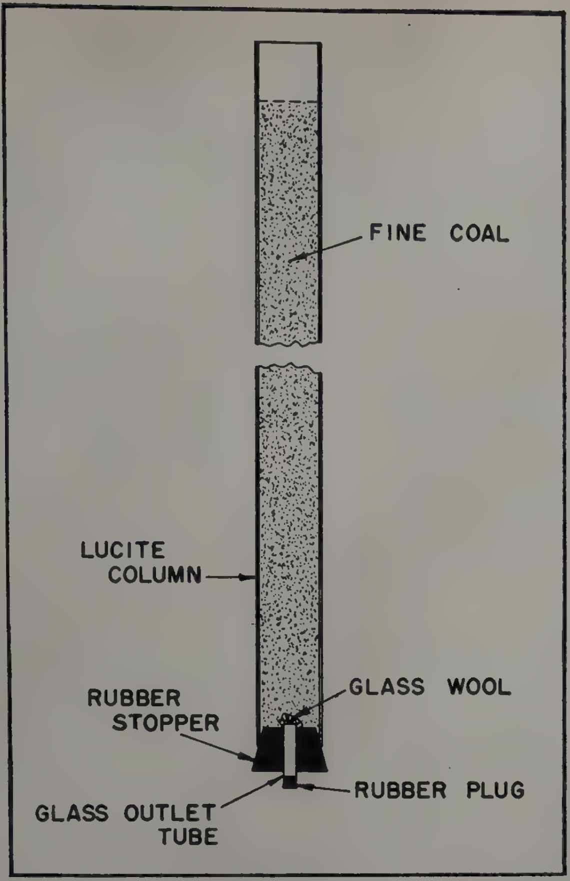

Fig. 1—Drainage column.

wetted by careful mixing and overnight standing, is charged as a slurry of about 50 pct solids in increments of several hundred grams after the glass wool has first been secured with a small amount of moist coal and several inches of water have been added to provide a water pool into which the charge is added. During the charging the column is frequently tapped with a wooden rod or rubber mallet to insure uniform packing and to lessen the occlusion of air. The column is charged to some definite height of coal, e.g., 48 in., and a definite amount of supernatant water is allowed to remain on the coal. 2—Drainage is started by removing the outlet plug and the drainage water is collected in a suitable receiver. When the supernatant water has disappeared, it is advisable to puncture the scum film which forms on top of the draining column and retards drainage. The top of the column should be partially covered during drainage to prevent loss of moisture due to evaporation. 3—The weight of water draining over given times is recorded for the duration of the test so that drainage rates can be computed. 4—At the end of the specified drainage period, usually 24 hr, the column is laid horizontally and, as quickly as possible, small increments of drained coal are cut out successively along the length of the column, starting from the bottom, using a spatula or flat knife. 5—Individual sections are analyzed for total moisture content by determining the percent of weight loss on drying overnight at 100°C. 6—The moisture distribution pattern is obtained by plotting the average height of an increment in the column against the moisture content of that increment.

Equilibrium Moisture Distribution Pattern

A column of drained fine coal normally divides into three zones, a saturation zone at the bottom, a low-moisture zone in the upper section, and a transition zone between these two. In general, the saturation zone is that height of coal in which the moisture content remains at some constant high value substantially equivalent to the saturation value for the particular type of packing. The transition zone is a region of rapidly decreasing moisture content between this saturation zone and a low-moisture zone where the moisture content appears to level out and approach some limiting value. However, for some packings containing a large pore space, such as the anthracite buckwheat sizes, a sharply-defined saturation zone does not exist and the transition zone represents the only section of increased moisture values. Consequently for purpose of discussion throughout this paper the region below the low-moisture zone is frequently referred to as the high-moisture region.

Preliminary drainage tests have shown that for the sizes of coal investigated the moisture distribution pattern is essentially independent of the diameter of the column for diameters of 2, 3 and 6 in. The height of the coal column, for heights up to 8 ft, has no significant effect on the height or moisture content of the saturation or transition zones. Increasing the column height will, of course, decrease the overall moisture content of the column by virtue of lengthening the low-moisture zone.

The rate at which a column of wet coal reaches equilibrium with respect to the formation of the moisture zones has been investigated over a wide range of drainage times. The results for anthracite flotation product* have shown that the pattern of the water-retention equilibrium is established in a few hours and that on further drainage only a small percentage change in the moisture contents or in the heights of the zones is observed. Fig. 2 shows the change in the moisture distribution pattern for drainage times of 3, 12, and 24 hr. The existence of the drainage pattern at shorter times could not be ascertained because of the rapid drainage which occurs during the first 2 hr and the danger of redistributing the water when the column is laid on its side preparatory to sectioning. Additional tests on flotation coal showed that the moisture pattern after 24 days was substantially the same as that obtained

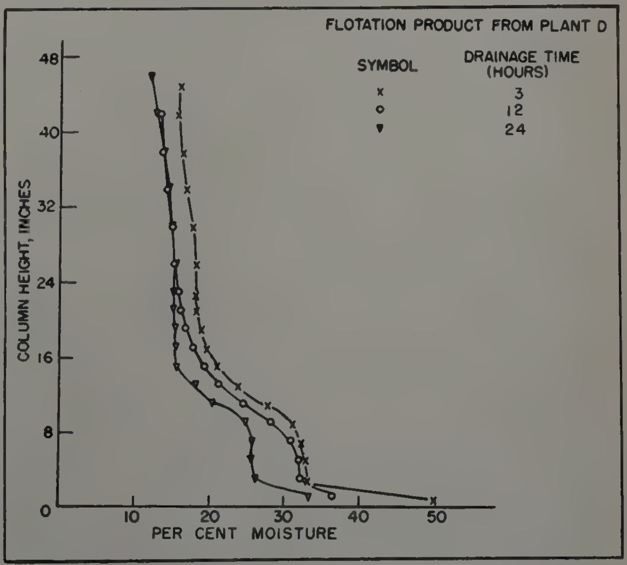

Fig. 2—Effect of drainage time on moisture distribution.

---

* A typical size analysis for each of the fine coals studied in this program is given in Table I, anthracite, and Table II, bituminous.

Table I. Typical Size Analysis of Anthracite Fine Coals Used in Drainage Tests, Ro-Tap Method, 200 G Sample, 10 Min

	Weight, Pct											
	Buck No.1	Buck No. 2, Rice	Buck No. 3, Barley	Buck No. 4	Buck No. 5		Spiral Plant Product	Flotation Products				
					Plant E	Plant D		Plant D	Plant A	Plant B1	Plant B2	Plant E
Screen Size, Round Hole												
+9/16	5.2											
9/16-5/16	74.5	6.8										
5/16-3/16	18.0	80.5	10.4	0.2								
3/16-3/32	2.3*	10.9	67.0	10.5	0.2	0.3						
3/32-3/64		1.3	21.1	74.0	26.2	17.9						
−3/64		0.5	1.5	15.3	73.6	81.8						
Sieve Size, Tyler												
+28				95.1	55.2	47.8	14.7**	16.1	3.3	3.2	2.5	13.3
28x48				4.0	33.5	41.1	56.7**	40.0	43.2	38.9	29.8	37.7
48x100				0.5	8.4	11.1†	21.5	27.5	42.0	37.1	38.3	33.1
100x150				0.1	1.2		2.6	7.7	5.9	9.3	11.4	7.1
150x200				0.1	0.5		1.8	3.8	3.2	6.3	7.4	3.4
−200				0.2	1.2		2.7	4.9	2.4	5.2	10.6	5.4

* −3/16.
† −48 mesh.
** 20 mesh instead of 28 mesh.

in 1 day. It is concluded that the drainage pattern established in 24 hr will not be significantly different even at "infinite" drainage time, and therefore will be considered for purposes of comparison as equilibrium moisture values.

Effect of Particle Size and Size Consist on Drainage Behavior

The drainage characteristics of a column of fine coal appear to be dependent mainly upon the particle size, or mesh size, and the particle size distribution, or size consist, of the material, assuming that the same type of packing is maintained in all the tests. Fig. 3 shows the moisture distribution patterns for a series of closely-sized anthracite fractions, prepared by the multiple screening of dry flotation coal. In general, the height of the high-moisture region and the moisture contents of both the low-moisture and saturation zones increase with decreasing mesh size.

Fig. 4 presents the drainage rates for these selected sizes, plotted as the total moisture content in a 4-ft column of coal at a given time versus the drainage time. The rate and amount of water draining out of a column are shown to increase with increasing particle size. However, in all cases, most of the drainable water is removed during the first few hours and on further drainage a limiting equilibrium moisture content for the entire column is slowly approached. The equilibrium moisture distributions for commercial fine sizes of anthracite are illustrated in Figs. 5 and 6. The drainage rates for some of these sizes are shown in Fig. 7.

In the case of the commercial fine sizes of anthracite the results show that the high-moisture region gradually increases from zero in the case of the coarse product, buckwheat No. 1, to 11 in. for buckwheat No. 5, and to 24 in. or greater for flotation products which contain a substantial percentage of −100 mesh material. The water content of the low-moisture zone appears to increase only slightly with decreasing size either for the more closely sized products, buckwheats No. 1 to No. 4, or for buckwheat No. 5, spiral plant and flotation products, containing a wide distribution of sizes. The high-moisture region increases in moisture content with a decrease in average particle size, but does not show a sharply defined saturation zone until the average size is finer than buckwheat No. 5. The saturation zone for all these smaller sizes generally contains about 35 pct moisture.

Similar drainage tests were performed on various bituminous fines obtained from a central Pennsylvania strip coal. The original sample, prepared to pass a ½-in. screen, was further crushed and screened to give the various size consists shown in Table II.

The results presented in Fig. 8 show the effect of decreasing average mesh size on the moisture distribution pattern in a 4-ft column. In general, the height and moisture content of the saturation zone, as well as the high-moisture region, and the moisture content of the low-moisture zone increase with decreasing mesh size. However, it should be noted

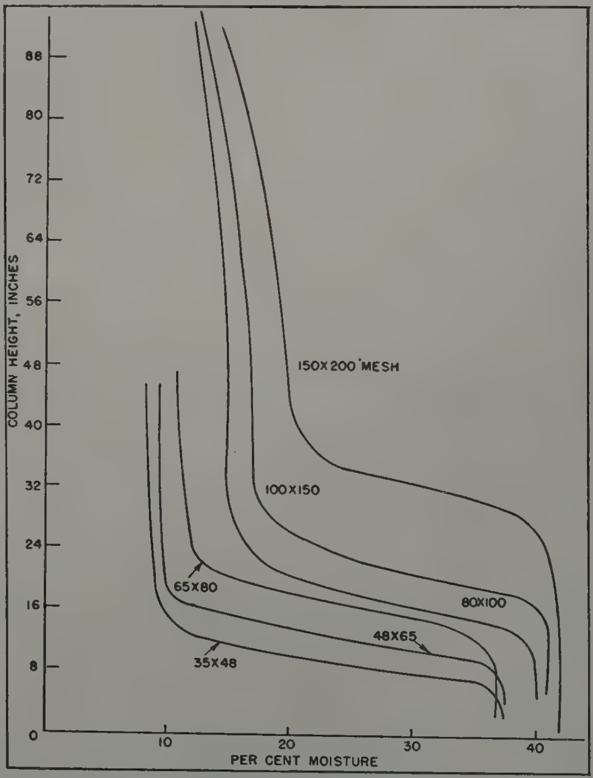

Fig. 3—Moisture distribution for selected sizes of anthracite fine coal, drainage time 24 hr.

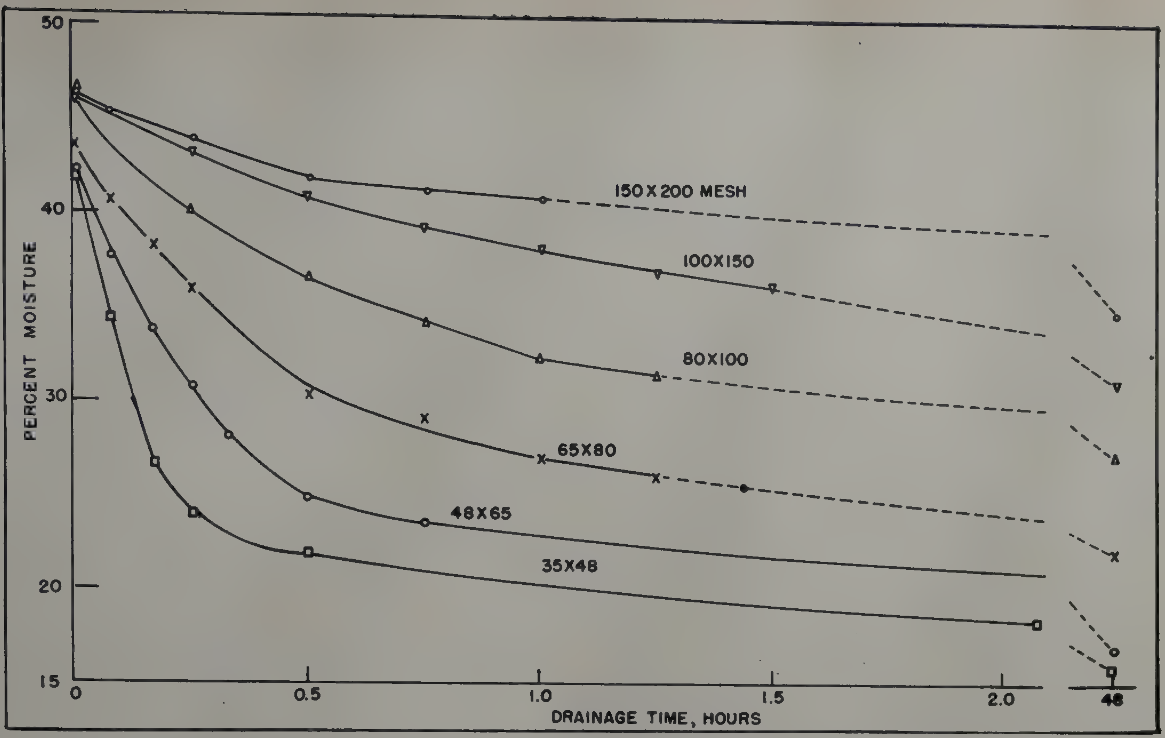

Fig. 4—Change of moisture content with drainage time, selected sizes of anthracite fine coal. Four-foot column.

that with bituminous coal samples, and to a lesser extent with most anthracite sizes, considerable segregation of fines occurred during charging of the coal slurry, causing a sudden increase in the moisture content in the upper few inches of the drained coal. These points have not been plotted in Figs. 8 and 9. It was found that this difficulty could be partly remedied by carefully charging the wet coal into a minimum amount of water in the column. A small water pool is necessary to avoid occlusion of air during charging. Also it was concluded that these drainage tests could be performed more satisfactorily in 8-ft columns to avoid the distracting influence of this "tail" at the top of the column. The slight decrease in moisture values at the lower part of the saturation zone in most tests was due to the admittance of air during drainage and could have been eliminated by the use of a water seal.

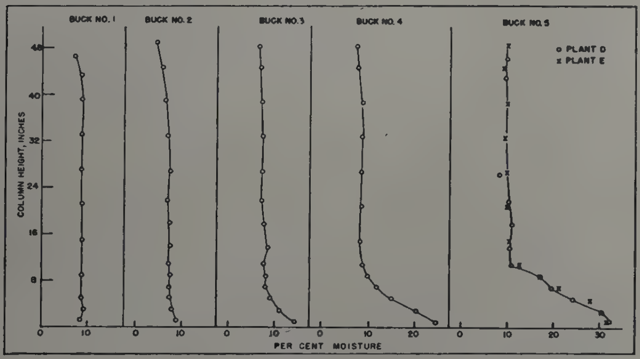

Fig. 5—Moisture distribution for commercial fine sizes of anthracite, drainage time 24 hr.

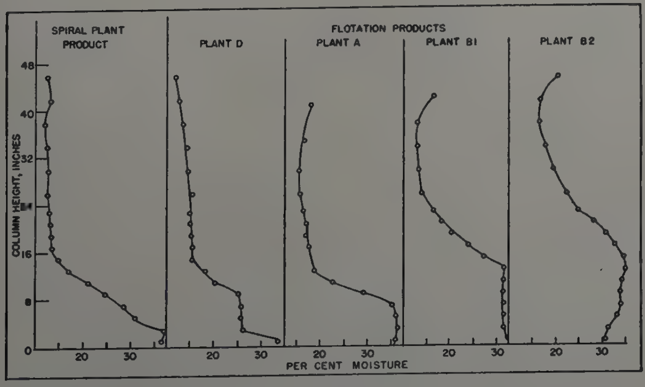

Fig. 6—Moisture distribution for commercial fine sizes of anthracite, drainage time 24 hr. Flotation product, plant A, 48 hr.

Fig. 9 gives the moisture distribution patterns in 8-ft columns for two widely differing size consists, see Table II. The results agree with those described above for 4-ft columns, and with the findings in regard to the effect of size on drainage for anthracite fines. However, bituminous fines exhibit more sharply-defined saturation zones for the coarser sizes; also, these zones increase in moisture content with decreasing average size, possibly because of a wider distribution of sizes in the bituminous fine coals. The results with a wetting agent shown in

Table II. Typical Size Analysis of Bituminous Fines Used in Drainage Tests, Hand-Screened Method, 100 G Sample

Sieve Size, Tyler	FC-96 Original	Weight, Pct				
		FC-96A	FC-96B	FC-96C	FC-96D	FC-96E
+3	22.0					
3x8	34.4	34.1	0.6			
8x14	19.8	25.6	39.6	0.8	29.4	1.7
14x20	6.8	10.9	16.7	1.3	16.6	1.7
20x28	4.8	8.3	11.8	29.4	12.9	15.5
28x48	6.3	11.4	15.5	32.7	19.0	32.7
48x65	1.7	3.2	5.0	11.7	5.9	11.1
65x100	1.6	2.9	3.2	8.6	5.5	11.7
100x150	0.7	1.4	2.0	4.4	3.5	7.4
150x200	0.6	1.0	2.3	3.7	1.7	4.2
—200	1.3	1.2	3.3	7.4	5.5	14.0

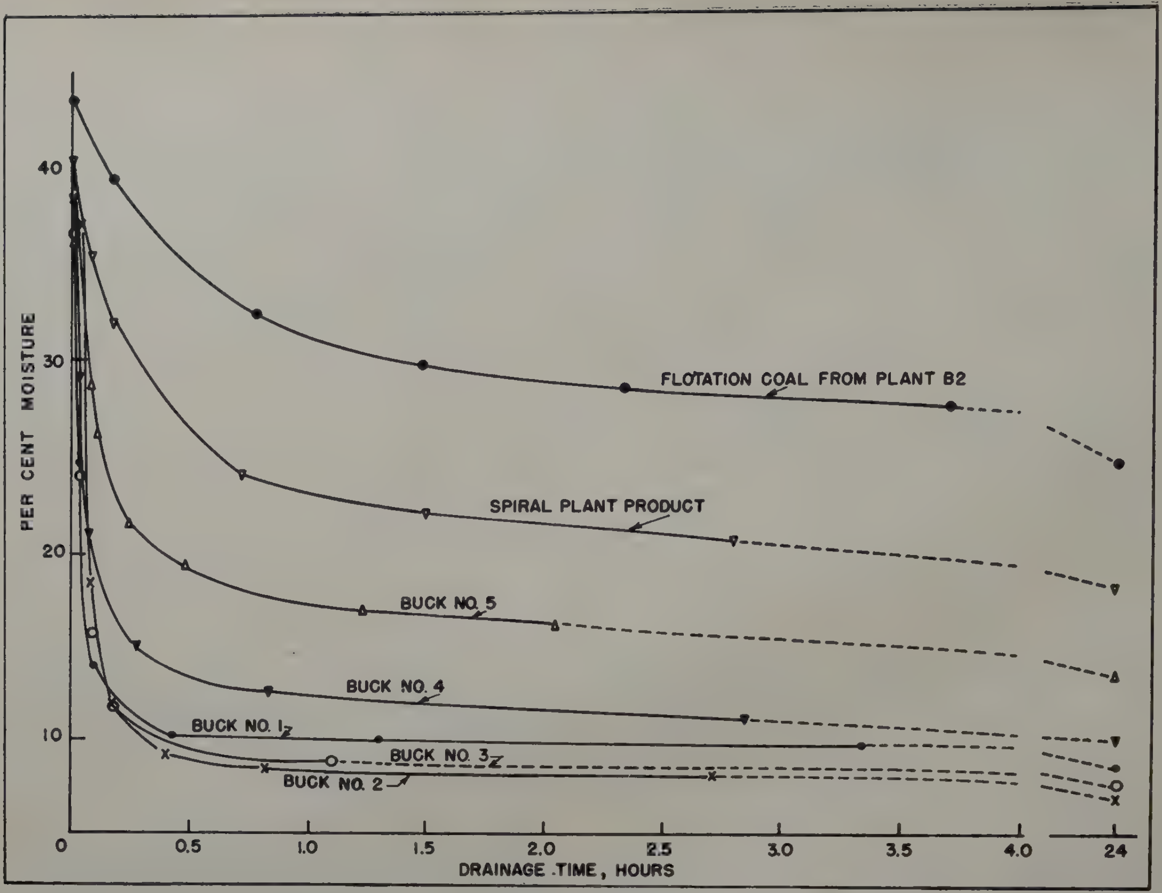

Fig. 7—Change of moisture content with drainage time, commercial fine sizes of anthracite. Four-foot column.

Fig. 9 will be discussed later in the section describing the effect of wetting agents on drainage.

Blending of coarse coal, e.g., 10x16-mesh anthracite equivalent to buckwheat No. 4, with flotation product prior to dewatering results in a decrease in the height of the high-moisture region and a general lowering of the equilibrium moisture values for the entire column, as compared to flotation coal alone, Fig. 10. For example, when a 4-ft column is charged with flotation product, the coal drains to an overall moisture content of 22.4 pct; when 20 pct of the coarse coal is carefully blended with a slurry of fine coal, the overall moisture percentage after drainage drops to 19.0; when 40 pct coarse coal is added, the mixture drains to 16.6 pct overall moisture content.

However, when any appreciable stratification or segregation of the coarse and fine coal occurs through classification or improper mixing, the practice of blending coarse coal with fine coal is of doubtful value in promoting drainage and may actually retard the process. The effect of segregation on the moisture distribution was demonstrated, as shown in Fig. 10, by alternately charging a column with slurries of coarse and fine coal. The drainage results show a pattern of alternating low- and high-moisture layers. Each individual layer represents an independent column of coal in which a drainage pattern is established typical of the size consist of that coal. The overall moisture content of a column charged in this manner was 23.0 pct.

Thus it appears that coarse coal blended with fine coal prior to dewatering effects a lower moisture content in the product, provided that extreme care is taken to avoid segregation of sizes during discharge into the drainage basin, bunker or car.

The removal of undersize, e.g., —200 mesh material, from fine coal also tends to lower the moisture retention. For example, when the percentage of —200 mesh in a flotation coal was reduced from 10.6 to 1.6 by wet screening, the high-moisture region decreased from about 30 to 24 in. and the moisture

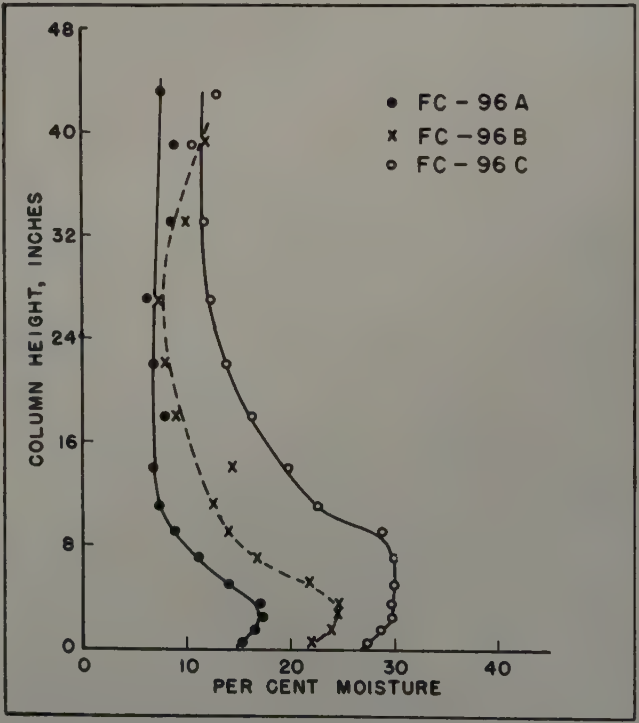

Fig. 8—Moisture distribution for various bituminous fines, drainage time 24 hr. Four-foot column.

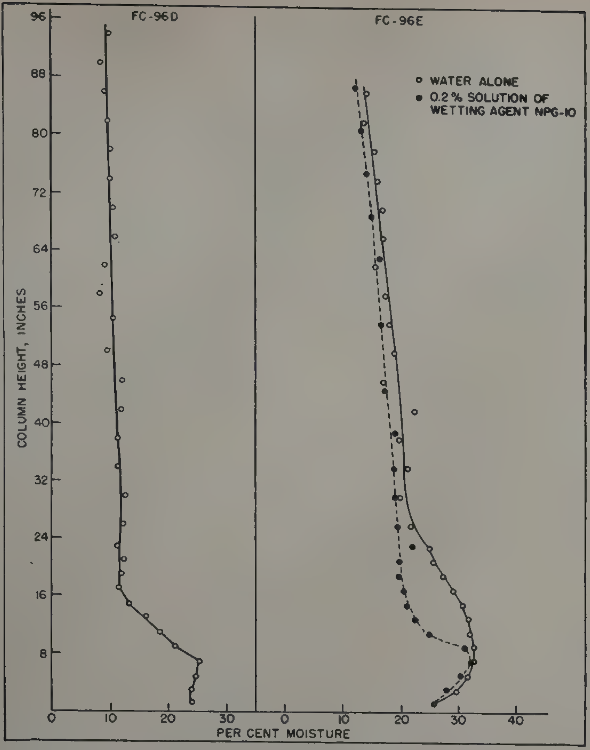

Fig. 9—Moisture distribution for various bituminous fines, drainage time 24 hr. Eight-foot column.

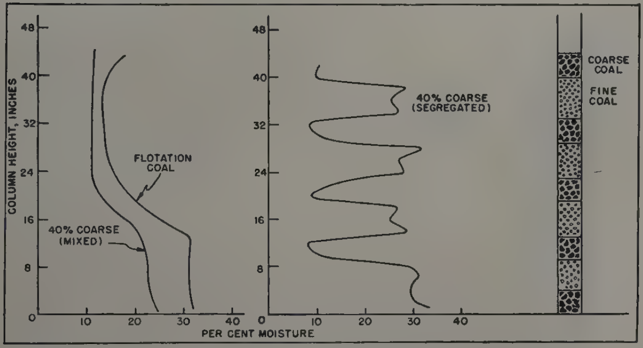

Fig. 10—Effect of blending coarse coal, 10x16 mesh, with the flotation product on moisture distribution, drainage time 24 hr.

content of the low-moisture zone from about 15.0 to 12.5 pct after draining in a 4-ft column for 24 hr; the overall moisture content, however, was lowered only from 24.4 to 22.8 pct.

Experiments Influencing the Design of Bunkers or Basins

Unloading and Recharging Tests: The existence of moisture zones in a column of drained coal immediately suggested the possibility of obtaining a drier product from a drainage bunker, provided that only the coal in the low-moisture zone is removed. Laboratory tests have been made simulating this procedure in an apparatus consisting of a 4-ft, 3-in. ID column, fitted with a flange, to a 2-ft section of the same diameter. The entire column was loaded in the usual manner with flotation product and was allowed to drain for 24 hr. At the end of the drainage period, the 4-ft top section was removed and the coal emptied and analyzed for total moisture content; then the top column was refitted to the undisturbed lower section and was recharged with coal slurry, etc. Twenty-five rechargings were made by this procedure.

Results showed that the moisture content of the replaceable low-moisture section for each of 26 unloadings had essentially the same value, i.e., 18.9 ±1.2 pct. Fig. 11 gives the moisture distribution in the entire column before and after the 25 unloadings and rechargings above the undisturbed high-moisture section. It is of interest to note that the final moisture content for the entire 6-ft column was 23.6 pct, for the low-moisture section, above the flange, 18.5 pct, and for the high-moisture section, below the flange, 32.8 pct.

After the 25 operations, small increments of the high-moisture section were cut out successively along the length of the column and size analyses made on each fraction. The results showed no significant change in size consist in the high-moisture section as compared to either the coal in the low-moisture section or an original sample of the flotation product. Moreover, no plugging or retarding of drainage was observed during the test.

Thus it appears feasible to obtain a drier product from a drainage bunker if the bunker is emptied only above the high-moisture region.

Drainage Leg Experiments: Attempts were made to employ a drainage leg or sump at the bottom of a large column or bunker to learn if such a device would function as an entire high-moisture region, thereby eliminating the high-moisture region above the leg. The results in Fig. 12, for a 4-ft long, 6-in. ID column fitted directly to a 2-ft long, 2-in. ID leg, show a noticeable reduction in the moisture content and in the height of the high-moisture region of the large mass of flotation coal after drainage for either 24 or 48 hr. In a similar experiment, in which the area between the column and the leg was reduced by means of an 8-in. conical section, Fig. 13, no further reduction in the moisture content of the coal in the 6-in. column was observed.

Thus it appears that a leg or sump in the base of a coal column may effectively reduce, but not completely eliminate the high-moisture region in the

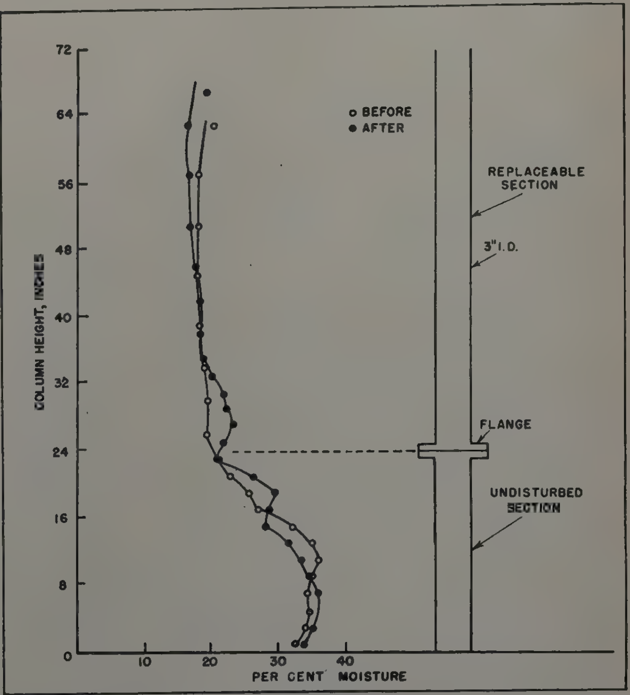

Fig. 11—Moisture distribution before and after 25 unloadings and rechargings above an undisturbed section of flotation coal from plant B2, drainage time 24 hr.

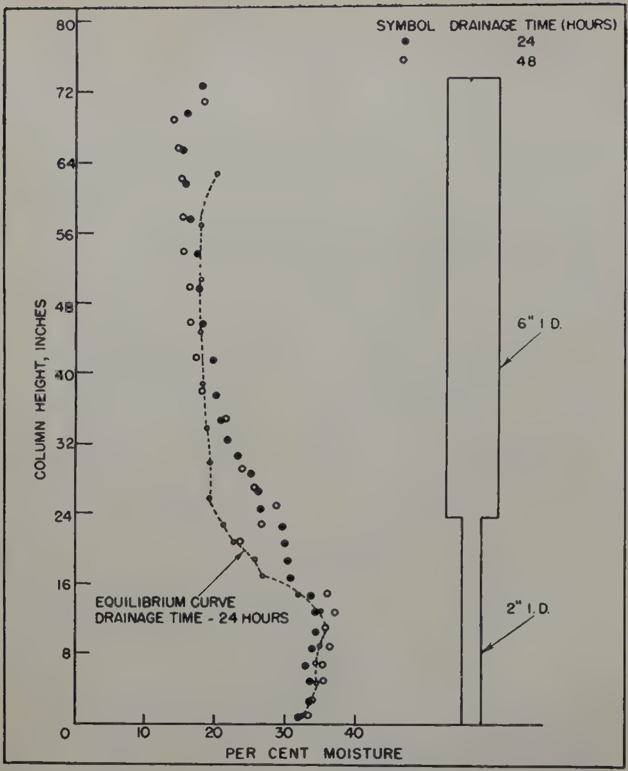

Fig. 12—Effect of drainage leg on moisture distribution of flotation product from plant B2.

main body of the draining coal. It should be noted that the moisture distribution patterns for the columns with a leg were not significantly different from a 6-ft column of a single diameter, see equilibrium curves in Figs. 12 and 13; however, it must be understood that the rate of formation of these patterns and the initial drainage rates were considerably impaired by the nine-fold reduction in cross-sectional area. The effectiveness of any sump or leg arrangement in lowering the moisture percentages also depends on the ability of that device to permit drained water to flow away readily.

Effect of Bedding Material on Drainage: Tests on the effect of bedding material on the drainage of a column of flotation coal indicate that the drainage equilibrium of the fine coal is affected by the nature, particle size, size consist, and thickness of the bed of supporting material. In general, relatively coarse beds do not appear to influence the moisture distribution pattern of the fine coal, but as the size of the supporting material approaches or falls below the size consist of the coal being dewatered, the high-moisture region is greatly reduced and in some cases disappears. Effectiveness of the bedding material in reducing moisture content of the high-moisture region is dependent also on the thickness and moisture distribution of the supporting bed; the optimum thickness is related to the height of the high-moisture region in the supporting bed.

These principles can better be understood by examining Fig. 14 for the effect of three different sizes of bedding material on the drainage of flotation product. The coarse supporting medium, buckwheat No. 4, does not affect the moisture distribution in the flotation coal. Both the fine coal and the coarse bed represent independent columns of coal in which a drainage pattern, typical of the size consist of that coal, is established. However, in the case of the 100x150 mesh or —200 mesh beds, both of which are considerably finer than the flotation coal, the high-moisture region in the flotation product is virtually eliminated, provided that the thickness of the supporting bed is greater than the high-moisture region in that bed. It should be noted that for the buckwheat No. 4 and the 100x150 mesh sizes, bed depths of about 14 and 36 in., respectively, would have given the same moisture distribution in the flotation coal. On the other hand, even a depth of 60 in. of —200 mesh coal was not great enough to allow the formation of a low-moisture zone in the supporting bed. Consequently, the flotation coal above the bed shows a small high-moisture region and slightly higher moisture values in the low-moisture zone. This increase in moisture values was probably also due to the low water permeability of the —200 mesh bed which retarded drainage sufficiently so that in this case equilibrium was not established in the flotation coal within 24 hr.

It is concluded that coarse beds do not affect the moisture distribution pattern of a column of draining coal, but may facilitate dewatering by permitting the drainage water to get away more readily. Also, it appears that beds of fine-sized material do not offer any particular advantage in dewatering and may actually inhibit drainage because of inherent low water permeability or percolation characteristics. The most logical choice of a bedding material, apart from foundation material or drain tile, is a suitable depth of the fine coal being dewatered, the minimum depth being limited by the high-moisture pattern in the coal.

Drainage Test at Settling Basin of Plant B: Flotation product is dewatered at Plant B in either of two basins about 125x125 ft and 15 ft deep, each having a capacity of 5000 to 6000 tons. Coal slurry from the

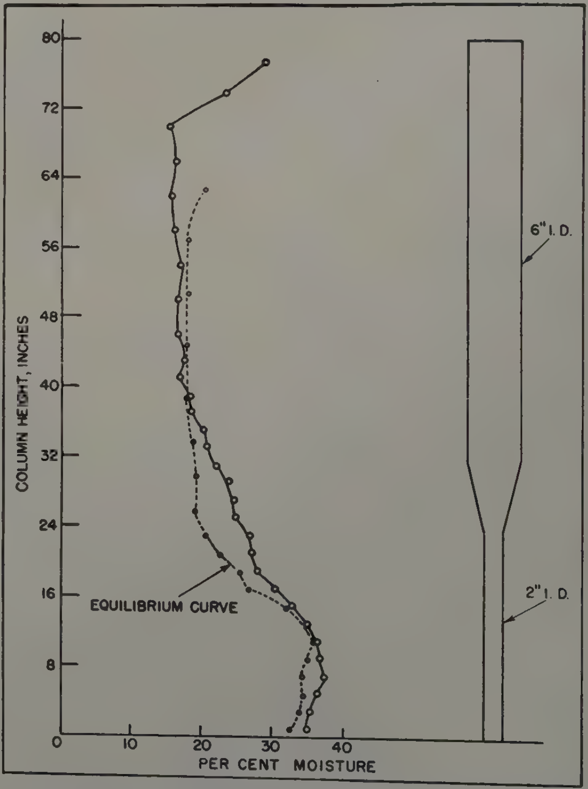

Fig. 13—Effect of drainage leg on moisture distribution of flotation product from plant B2, drainage time 24 hr.

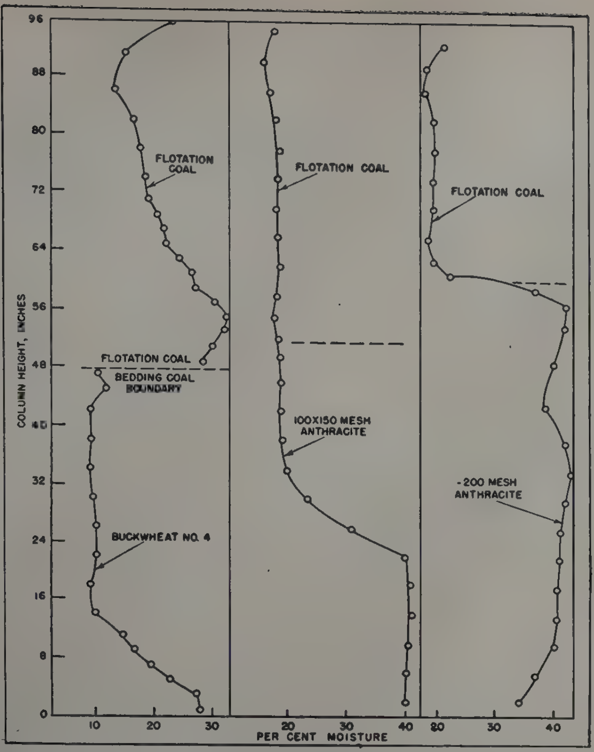

Fig. 14—Effect of bedding material on moisture distribution of flotation coal from plant B2, drainage time 24 hr.

flotation plant at about 25 to 35 pct solids is pumped intermittently for about 30 days, depending upon daily operating schedules, into the center of one of the basins. At the end of this time, the barricade at the portal is removed and the coal is unloaded mechanically while the other basin is being filled.

During the unloading of a basin, the staff members of the operating company removed samples for moisture and size analyses along a vertical face as the unloading machine advanced to three different positions in the basin. The moisture distribution results in Fig. 15 show the presence of moisture zones remarkably similar to those obtained on a laboratory scale. This is good agreement considering the intermittent manner of charging due to starting up and shutting down the flotation plant and to wide variations in solids content and flow rates causing segregation and stratification of material in the commercial basin; this stratification is seen when a vertical face is exposed during unloading.

The screen analyses also show a horizontal classification of the fine coal within the basin; the coarser sizes are found beneath the discharge pipe at the center while some of the fine sizes segregate toward the edge of the basin. It is important to note that the positions of the moisture distribution curves and the overall water percentages for the three sampling points are directly related to the particle size distribution at the respective station. These results give satisfactory evidence that laboratory drainage tests are applicable to plant operating conditions.

Effect of Wetting Agents on Drainage

If it is assumed that the high-moisture region represents the capillary rise of water in a complex bundle of capillaries formed by the packing of the fine coal, then it is an accepted fact that a decrease in the surface tension of the liquid should result in a lowering of the high moisture region. Experiments have been made along this line to demonstrate the existence of a capillarity effect in the lower part of a coal column and to investigate the effect of wetting agents on the drainage behavior of commercial fine coals.

These tests were performed by allowing the fine coal to soak overnight in solutions of the wetting agent and then charging to the column and draining for 24 hr; the drainage results obtained are compared with those from duplicate tests in which no wetting agent was used in the slurry water.

Tergitol NPG-10, experimental-grade, and Tergitol Dispersant NPG, commercial-grade, wetting agents furnished through the courtesy of the Carbide and Carbon Chem. Div., Union Carbide and Carbon Corp., were employed because of the high efficiency of these agents for surface tension reduction at low concentrations. Initial concentrations in solution of 0.005 pct or above will give the minimum surface tension, 35 dynes per cm, compared to distilled water, 75 dynes per cm, as measured by the Du Nouy method.

The results in Fig. 16 show that an initial concentration of 0.1 pct Tergitol NPG-10 in the slurry water decreased the height of the high-moisture region from about 32 to 16 in. and the total moisture content from 26.0 to 20.8 pct in a 4-ft column of flotation coal from plant B2. The surface tension of the drainage water was 40 dynes per cm, indicating that the concentration of wetting agent was only 0.002 pct and that 98 pct of the agent had been adsorbed by the fine coal. In a similar trial with flotation coal from plant E, using Tergitol Dispersant NPG, the high-moisture region was lowered from about 22 to 10 in. and the overall moisture content of the 4-ft column from 22.5 to 18.7 pct; the drainage water again showed less than 0.002 pct wetting agent in solution.

The effect of wetting agents on the drainage behavior of bituminous fines has been investigated briefly as shown previously in Fig. 9. Sample FC-96E was allowed to soak overnight in a 0.2 pct solu-

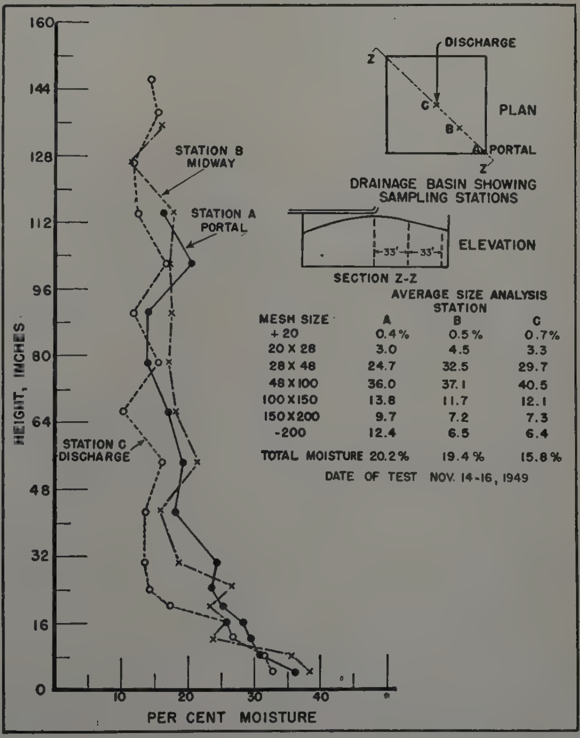

AVERAGE SIZE ANALYSIS

MESH SIZE	STATION A	STATION B	STATION C
+ 20	0.4%	0.5%	0.7%
20 X 28	3.0	4.5	3.3
28 X 48	24.7	32.5	29.7
48 X 100	36.0	37.1	40.5
100 X 150	13.8	11.7	12.1
150 X 200	9.7	7.2	7.3
-200	12.4	6.5	6.4
TOTAL MOISTURE	20.2%	19.4%	15.8%

DATE OF TEST NOV. 14-16, 1949

Fig. 15—Drainage tests at flotation settling basin of plant B.

tion of Tergitol NPG-10 and the moisture distribution pattern was determined after drainage for 24 hr. The initial concentration of wetting agent was sufficient to give the minimum surface tension, 35 dynes per cm, before and during drainage. The adsorption of the wetting agent by the bituminous fines was not determined.

Results for spiral plant product were equally encouraging in so far as moisture reduction was concerned, showing a decrease in the total moisture content of the coal from 17.9 pct with distilled water alone to 16.6 pct with 0.01 pct solution of the wetting agent, and to 13.8 pct with 0.1 pct solution, see Fig. 17. However, in the case of the test with 0.01 pct initial solution, considerable adsorption of the wetting agent by the coal was noted, as the surface tension increased from 35 to 66 dynes per cm; this change represented a decrease in concentration of the wetting agent from 0.01 pct to less than 0.0002 pct. It was observed that adsorption of the wetting agent by the fine coal occurred principally during the first few minutes of contact between the solution and the fine coal, and was not necessarily aggravated by allowing the mixture of fine coal and solution to stand overnight before charging to the column. This adsorption of wetting agent imposes a serious limitation on the use of such agents for lowering surface tension in coal slurries and thus for reducing the moisture content of a column of draining coal. Undoubtedly the degree of adsorption of the wetting agent is related to the nature of the agent and to the surface area of the fine coal. The adsorption may, therefore, be expected to vary markedly with size consist and probably also with the wetting agent used.

The drainage rate data for flotation and spiral plant products showed that the addition of a wetting agent does not materially alter the drainage rates during the early stage of a test, where most of the drainable water is removed and where the moisture distribution pattern is being established. However, wetting agents lower the moisture retention of the fine coal and do increase the rate at which the lower equilibrium moisture values are approached.

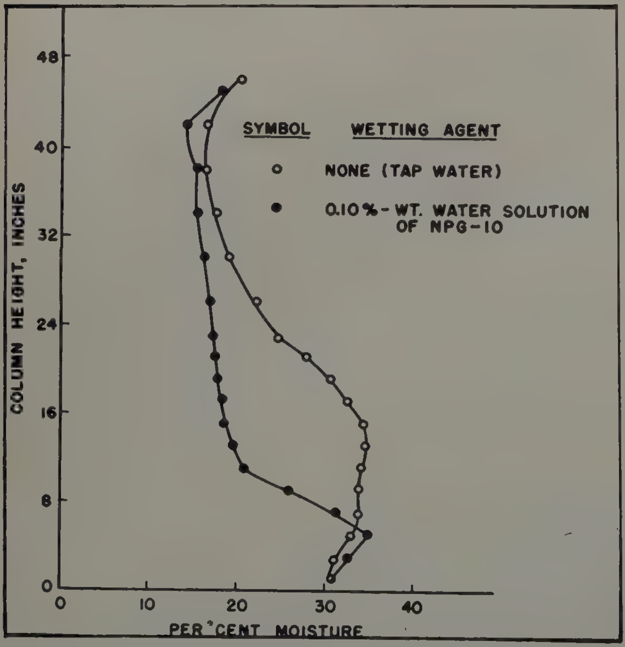

Fig. 16—Effect of wetting agent on drainage of flotation coal from plant B2.

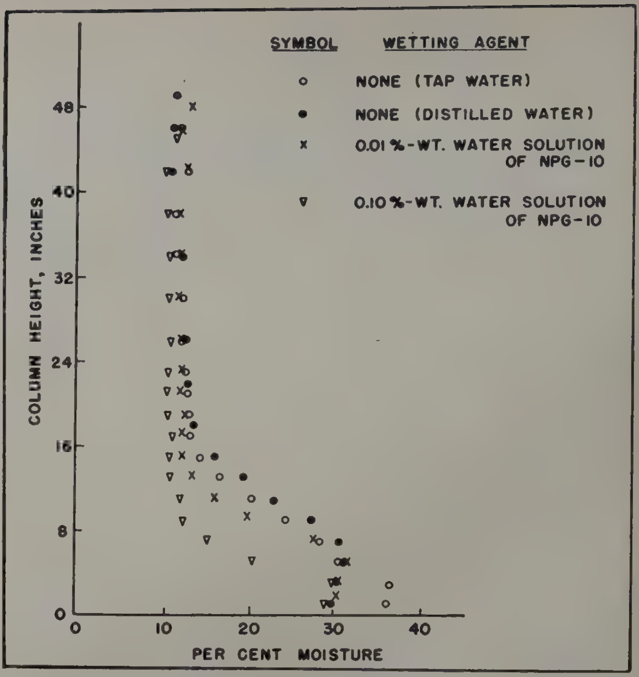

Fig. 17—Effect of wetting agent on drainage of spiral plant product, drainage time 24 hr.

For the particular size consist and wetting agent employed, an initial concentration of at least 0.1 pct wetting agent in solution is necessary, i.e., about 2 lb of agent per ton of dry coal, in order to offset the adsorption by the fine coal and still produce a low enough surface tension for lowering the moisture values of flotation coal. At the prevailing cost of about 35 cents per lb, the use of this wetting agent does not appear to be economically feasible. Dousing or spraying the top of a column of drained or draining flotation coal with solutions of wetting agent did not significantly alter the quantity of wetting agent required to effect a definite moisture reduction.

However, for coarse materials, where the surface area is only a fraction of that exposed by flotation coals, e.g., buckwheat No. 4 has about one-fifth the surface area of flotation coal per unit weight, the adsorption of the agent would be greatly reduced and the application of wetting agents might be more desirable. Also, the recycling of the drainage water would appear more feasible for the coarser sizes with the resulting saving in wetting agent required to maintain a low surface tension in the coal slurry. Nevertheless, it should be noted that the principal function of the wetting agent is to lower the height of the high-moisture region in the draining coal, and that the effectiveness of the wetting agent in lowering overall moisture contents would be greatly diminished for sizes which already show a low high-moisture region with water alone.

Acknowledgments

The authors are deeply indebted to J. D. Clendenin and H. J. Donald for many helpful suggestions and comments in the pursuance of the work, to G. W. Jones, M. Moul, A. J. Peterson, and J. H. Schalch for assistance in the experimental work, to E. L. Maloy and M. Ott for preparing the drawings, and to the Anthracite Research Advisory Committee for permission to publish the drainage results on anthracite fine coals.

Comparative Effectiveness of Coal Cleaning Equipment

by Orville R. Lyons

This paper presents a method whereby the amount of misplaced material and the difficulty of the separation can be used to compare coal cleaning equipment of all types, from effectiveness and capacity standpoints. The correlations presented do not include all types of equipment currently available, but the method can be used to evaluate any make or type of coal cleaning equipment, both old and new.

THE relative performance of coal washing equipment, or the effectiveness with which any type or make of equipment removes impurities from coal, has been most difficult to evaluate in the past. The most widely used yardstick is the Frazer and Yancey efficiency formula developed in 1922,[1] but Yancey in a later article states that "washers treating coals of different density composition or operating at different densities of separation cannot be compared directly on the basis of this criterion."[2] Prior to and since 1922, a variety of other methods has been used for comparison purposes, including the distribution curve, the error area, and the "ecart probable" or probable error. Yancey and Geer in discussing these methods conclude, "Performance can be evaluated in a number of different ways, with the choice of the proper method to use being dictated by the objectives of the investigation and the data available."[2]

It is true that performance can be evaluated in a variety of ways, but if the equipment is to be evaluated on an effectiveness basis, there should be only one universal comparison method. Varying methods have been used because one universal comparison method has not been found or developed.

In the article previously quoted, Yancey and Geer state in clear terms the primary concept for a universal comparison method: "One of the simplest, and certainly one of the most obvious evaluations of washery performance is the quantity of sink material in the washed coal and the float material in the refuse. If the washery products are tested at the density at which the washing unit is operated, the sink in the washed coal and the float in the refuse represent material that has been misplaced."

The quantity of misplaced material was used as a criterion of washery performance by Lincoln in 1913,[3] by the United States Bureau of Mines in 1938,[4] by Hancock in 1947,[5] and by the national French research agency Cerchar in recent years.[2] In 1950 Anderson[6] proposed the use of this criterion as an efficiency value to replace the Frazer and Yancey formula. However, none of the above-mentioned investigators used the misplaced material concept in a manner that would provide universal coal-cleaning equipment comparisons.

The Correlation Theory

The ideal coal cleaning process would treat all sizes and would make a perfect separation at any given specific gravity. All material lower in density than the desired value would report in the coal product and all material higher in density would report in the refuse product. Unfortunately, no known cleaning process achieves this goal and there seems little likelihood that any process yet to be invented will do more than approach it.

When coal is treated in volume under operating conditions, it is impossible to avoid mechanical entrapment, fluctuations in throughput and effective gravity of separation, and the creation of turbulent currents, even when a true heavy-liquid bath is used and the feed is closely sized and contains little intermediate gravity material. This being so, it is possible to appreciate the difficulties inherent in trying to obtain a perfect separation when treating a wide range of sizes and a feed containing high percentages of intermediate material, using turbulent currents to help create the effective separation gravity, under operating conditions which normally tend to be on the overload side.

When coal is separated from refuse in any coal cleaning equipment, some refuse always reports to the coal and some coal to the refuse; the writer therefore assumed that there should be a relationship between the total amount of misplaced material produced by any given piece of equipment and the difficulty of separation as represented by the percentage of near gravity material in the feed. With small amounts of near gravity or ±0.1 material in the feed there should be less misplacement of material than would occur with large amounts of near

---

ORVILLE R. LYONS, Member AIME, is with Republic Steel Corp., Cleveland, Ohio.

Discussion on this paper, TP 3390F, may be sent (2 copies) to AIME before October 31, 1952. Manuscript, Nov. 26, 1951. New York Meeting, February 1952.

Table I. Summary of Operating Data for a Variety of Coal Cleaning Equipment

Plant No.	Cleaning Unit		Coal Treated		Washed Coal		Refuse		Gravity of Separation	±0.1 Distribution Pct at Gravity of Separation*	Total Misplaced Material, in Washed Coal and Refuse, in Pct of Raw Coal
	Type	Make	Seam	Size, In.	Wt, Pct	Sink, Pct	Wt, Pct	Float, Pct			
1	Sand media	Chance	Illinois No. 6	6x1½	58.00	2.55	42.00	11.71	1.400	57.5	6.40
2	Sand media	Chance	Great Britain	5x1/16	78.50	1.19	21.50	2.60	1.425	24.0	1.49
3	Sand media	Chance	Elkhorn	4x¼	80.05	1.30	19.95	4.81	1.440	22.7	2.00
4	Sand media	Chance	Illinois No. 6	1½x5/16	86.00	0.60	14.00	0.90	1.450	14.7	0.65
5	Sand media	Chance	Lower Freeport	3½x⅜	88.00	0.50	12.00	0.50	1.450	15.5	0.50
6	Sand media	Chance	Upper and Lower Freeport	¾x⅛	65.00	0.50	35.00	2.25	1.450	25.0	1.12
7	Sand media	Chance	Thick Freeport	3½x¼	76.00	1.50	24.00	1.50	1.440	27.2	1.50
8	Bone media jig	Jeffrey	Upper Freeport	2x0	80.00	7.00	20.00	2.50	1.400	55.0	6.10
9	Bone media jig	Jeffrey	Upper Freeport	2x0	80.00	1.00	20.00	8.00	1.430	31.0	2.40
10	Bone media jig	Jeffrey	Pocahontas 3 & 5	7x⅝	80.00	3.50	20.00	6.75	1.475	33.0	4.15
11	Magnetite media	Link belt	Anthracite	4⅜x3/16	68.10	1.60	31.90	3.04	1.732	33.0	2.06
12	Fine iron media	Tromp	France	2x½	59.56	0.07	40.44	0.25	1.750	5.0	0.15
13	Magnetite media	Tromp	The Netherlands	3x¾	77.35	0.11	22.65	0.05	1.600	4.0	0.10
14	Magnetite media	Tromp	Great Britain		80.15	0.30	19.85	8.30	1.350	5.3	1.89
15	Fine iron media	Tromp	Great Britain		85.60	0.16	14.40	0.00	1.55	6.22	0.14
16	Fine iron media	Tromp	Great Britain		76.57	0.99	23.43	7.46	1.40	30.20	2.51
17	Fine iron media	Tromp	Great Britain		81.21	0.26	18.79	0.00	1.60	6.40	0.21
18	Pulsator jig	Elmore	Wilkeson	⅜x3/16	78.00	15.56	22.00	10.79	1.50	29.60	14.50
19	Pulsator jig	Elmore	Wilkeson	⅜x3/16	61.50	6.95	38.50	31.10	1.50	29.60	16.23
20	Classifier	R & S hydroseparator	Penna. Pittsburgh	5x1	68.75	1.53	31.25	17.95	1.50	9.40	6.66
21	Classifier	R & S hydroseparator	Penna. Pittsburgh	1x5/16	87.85	1.57	12.15	13.70	1.70	4.05	3.04
22	Classifier	Menzies hydroseparator	Pocahontas No. 4	2½x1	85.00	7.20	15.00	23.70	1.44	14.30	9.68
23	Classifier	Menzies hydroseparator	Penna. Pittsburgh	4x¾	87.30	0.75	12.70	10.75	1.60	2.60	2.02
24	Classifier	Menzies cone	Illinois No. 6	3x2	86.20	1.35	13.80	11.50	1.55	9.60	2.75
25	Classifier	Menzies cone	Illinois No. 6	1½x¾	89.28	3.10	10.72	12.81	1.50	9.85	4.15
26	Classifier	Menzies cone	Illinois No. 6	2x1½	81.90	3.50	18.10	13.60	1.50	13.60	5.32
27	Classifier	Menzies cone	Eagle	2¾x⅜	85.00	3.60	15.00	6.20	1.42	17.50	3.99
28	Classifier	Menzies cone	Pocahontas No. 3	2½x⅝	81.00	3.45	19.00	21.40	1.48	26.00	6.86
29	Classifier	Menzies cone	Eagle	5x1¼	85.00	0.50	15.00	6.20	1.55	5.50	1.36
30	Classifier	Menzies cone	Illinois No. 6	¾x⅜	91.30	1.20	8.70	15.80	1.70	4.55	2.47
31	Classifier	R & S hydrotator	Anthracite	13/16x28†	88.10	3.20	11.90	4.70	1.70	6.50	3.38
32	Classifier	R & S hydrotator	Miller	1½x⅛	71.00	1.14	29.00	1.49	1.60	4.00	1.24
33	Classifier	R & S hydrotator	Penna. Pittsburgh	⅛x48†	95.50	1.06	4.50	15.36	1.55	2.96	1.47
34	Classifier	R & S hydrotator	Penna. Pittsburgh	9/16x28	72.50	2.50	27.50	3.50	1.50	5.80	2.77
35	Wet table	Deister Conc. Co.	Island Creek	⅜x0	88.67	3.40	11.33	3.70	1.60	10.00	3.44
36	Wet table	Deister Conc. Co.	Penna. Pittsburgh	⅜x100†	91.60	11.84	8.40	5.75	1.35	45.50	11.32
37	Wet table	Deister Conc. Co.	Penna. Pittsburgh	⅜x100†	93.00	0.90	7.00	5.72	1.60	2.40	1.24
38	Wet table	Deister Conc. Co.	Ohio Pittsburgh No. 8	3/16x100†	77.90	3.50	22.10	4.70	1.50	14.60	3.77
39	Wet table	Deister Conc. Co.	Ohio Pittsburgh No. 8	3/16x100†	77.90	1.80	22.10	8.50	1.60	6.60	3.28
40	Wet table	Deister Conc. Co.	Pratt	¼x0	86.80	13.70	13.20	4.40	1.40	24.00	12.50
41	Wet table	Deister Conc. Co.	Pratt	¼x0	86.80	1.05	13.20	7.00	1.60	2.70	1.83
42	Wet table	Deister Conc. Co.	Penna. Pittsburgh	½x0	81.20	4.45	18.80	9.90	1.50	16.90	5.48
43	Wet table	Deister Conc. Co.	Penna. Pittsburgh	½x0	81.20	2.80	18.80	11.10	1.60	4.50	4.36
44	Wet table	Deister Conc. Co.	Upper & Lower Freeport	¼x0	91.20	1.40	8.80	12.90	1.60	6.10	2.41
45	Air table	Stump	Penna. Pittsburgh	⅜x0	67.80	11.02	11.11	32.20	1.60	4.60	15.41
46	Air table	Stump	Roslyn	⅜x0	91.00	9.20	9.00	68.70	1.60	3.14	14.54
47	Air table	Stump	Roslyn	⅜x0	91.00	15.50	9.00	59.10	1.40	40.60	19.42
48	Air table	Stump	Penna. Pittsburgh	⅜x0	67.80	12.57	32.20	22.62	1.50	9.00	15.80
49	Air table	Stump	Penna. Pittsburgh	⅜x0	67.80	9.40	32.20	26.98	1.70	4.40	15.05
50	Air table	Stump	Lower Elkhorn	¼x40†	82.70‡	15.90	17.30	46.20	1.44	12.50	21.12
51	Air table	American		½x¼	89.40	2.97	10.60	62.80	1.70	2.50	9.43
52	Air table	American	Roslyn	¼x0	93.53	16.00	6.47	37.90	1.40	32.80	17.45
53	Air table	American	Roslyn	¼x0	93.53	9.50	6.47	48.00	1.60	3.53	12.01
54	Barytes bentonite media	Dutch cyclone	Penna. Pittsburgh	14x35†	95.70	0.20	4.30	6.25	1.63	1.54	0.46
55	Magnetite media	Dutch cyclone	Penna. Pittsburgh	¼x0	88.92	1.12	11.08	5.47	1.55	2.63	1.60
56	Potash media	Dutch cyclone	European	5/16x16†	66.70	4.10	33.30	4.38	1.80	14.43	4.19
57	Loess media	Dutch cyclone	European	19/32x0	86.25	1.99	13.75	2.70	1.45	19.20	2.09
58	Roasted pyrite media	Dutch cyclone	European	5/16x32†	77.20	9.99	22.80	8.01	1.70	47.50	9.54
59	Loess media	Dutch cyclone	European	7/64x32†	88.30	2.28	11.70	2.59	1.45	32.60	2.31
60	Loess media	Dutch cyclone	European	19/32x0	86.25	5.78	13.75	1.34	1.40	81.00	5.17
61	Roasted pyrite media	Dutch cyclone	European	5/16x32†	77.20	1.19	22.80	21.76	1.80	14.00	5.88
62	Loess media	Dutch cyclone	European	7/64x32†	88.30	0.82	11.70	6.85	1.50	8.70	1.52
63	Barytes media	Dutch cyclone	Landau No. 3	¼x20†	41.30	20.30	58.70	10.90	1.35	72.60	14.78
64	Barytes media	Dutch cyclone	Landau No. 3	¼x20†	44.50	18.90	55.50	9.50	1.35	72.60	13.68
65	Barytes media	Dutch cyclone	Landau No. 3	¼x20†	60.00	13.40	40.00	17.30	1.40	70.20	14.96
66	Barytes media	Dutch cyclone	Coronation	¼x20†	41.00	14.40	59.00	33.00	1.40	84.00	25.37
67	Barytes media	Dutch cyclone	Spring-bok	¼x20†	26.70	19.30	73.30	23.80	1.35	76.60	22.60
68	Barytes media	Dutch cyclone	Spring-bok	¼x20†	45.40	32.50	54.60	8.60	1.35	76.60	19.45
69	Barytes media	Dutch cyclone	Phoenix	¼x20†	30.30	15.90	69.70	15.80	1.35	71.90	15.83
70	Barytes media	Dutch cyclone	Phoenix	¼x20†	63.00	11.70	37.00	7.40	1.40	74.40	10.11
71	Barytes media	Dutch cyclone	Phoenix	¼x20†	50.50	29.70	49.50	6.70	1.35	75.70	18.31
72	Spiral	Humphreys	Pocahontas No. 6	8†x0	96.30	3.10	3.70	52.60	1.60	1.75	4.93
73	Spiral	Humphreys	Clements	8†x0	96.50	3.20	3.50	42.10	1.60	0.74	4.56
74	Spiral	Humphreys	Roslyn	8†x0	85.3	7.70	14.70	27.60	1.60	6.3	10.63
75	Spiral	Humphreys	Kentucky No. 9	8†x0	94.3	14.90	5.70	21.20	1.60	5.8	15.26
76	Spiral	Humphreys	Raton & Trinidad	8x100†	77.7	60.30	22.3	3.10	1.38	67.5	47.49
77	Spiral	Humphreys	Raton & Trinidad	8x100†	77.7	14.20	22.3	14.70	1.60	8.7	14.28
78	Wet table	Deister Mach. Co.	Raton & Trinidad	½x0	86.95	15.60	13.05	4.70	1.38	27.5	14.21
79	Wet table	Deister Mach. Co.	Raton & Trinidad	½x0	86.95	4.10	13.05	13.20	1.60	6.53	5.32
80	Wet table	Deister Mach. Co.	Raton & Trinidad	½x0	93.08	9.20	6.92	4.50	1.38	21.90	8.87
81	Wet table	Deister Mach. Co.	Raton & Trinidad	½x0	93.08	1.90	6.92	12.50	1.60	3.60	2.64
82	Bone media jig	Jeffrey	Raton	6x⅜	82.00	0.45	18.00	5.20	1.60	5.66	1.31
83	Bone media jig	Jeffrey	Penna. Pittsburgh	4x¼	90.33	0.83	9.67	2.74	1.55	2.40	1.01
84	Pulsator jig	Vissac	Roslyn	3x1¼	78.00	4.50	22.00	17.50	1.45	25.00	7.36
85	Pulsator jig	Vissac	Roslyn	1¼x¼	92.56	1.50	7.44	18.00	1.69	3.00	2.73
86	Pulsator jig	Jeffrey	Routt	3x1¼	95.63	1.40	4.37	10.90	1.70	1.46	1.82
87	Pulsator jig	Jeffrey	Routt	3x1¼	95.63	1.80	4.37	8.10	1.60	2.29	2.07
88	Mill scale media	Ridley-Scholes	Great Britain	3x¼	86.00	1.79	14.00	0.40	1.45	10.00	1.60
89	Mill scale media	Ridley-Scholes	Great Britain	3x¼	89.00	0.59	11.00	0.50	1.60	4.46	0.56
90	Classifier	Menzies cone	Illinois No. 6	1½x¾	95.37	2.69	4.63	17.67	1.60	8.50	3.48

Table I. Summary of Operating Data for a Variety of Coal Cleaning Equipment (Continued)

Plant No.	Cleaning Unit: Type	Cleaning Unit: Make	Coal Treated: Seam	Coal Treated: Size, In.	Washed Coal: Wt, Pct	Washed Coal: Sink, Pct	Refuse: Wt, Pct	Refuse: Float, Pct	Gravity of Separation	±0.1 Distribution Pct at Gravity of Separation*	Total Misplaced Material, in Washed Coal and Refuse, in Pct of Raw Coal
91	Classifier	Menzies cone	Illinois No. 6	2x1½	88.80	5.31	11.20	4.53	1.40	21.00	5.23
92	Classifier	Menzies cone	Illinois No. 6	2x1½	88.80	0.42	11.20	16.50	1.50	13.40	2.22
93	Classifier	Menzies cone	Illinois No. 6	¾x⅜	91.67	1.70	8.33	10.58	1.60	5.47	2.44
94	Pulsator jig	Elmore	Wilkeson	3/16x3/32	69.30	11.43	30.70	24.10	1.50	25.00	15.34
95	Pulsator jig	Elmore	Wilkeson	1½x⅜	79.90	3.85	20.10	17.69	1.70	12.50	6.64
96	Pulsator jig	Elmore	Wilkeson	1½x⅜	56.10	10.96	43.90	26.35	1.50	31.40	17.69
97	Magnetite media	Link-Belt	Penna. Pittsburgh	3x⅜	96.10	1.20	3.90	1.90	1.60	9.70	1.22
98	Magnetite media	Link-Belt	Penna. Pittsburgh	4x⅜	52.80	0.40	47.20	1.10	1.60	9.60	0.73
99	Magnetite media	Link-Belt	Penna. Pittsburgh	4½x¼	68.30	0.70	31.70	1.70	1.55	4.75	1.02
100	Magnetite media	Link-Belt	Penna. Pittsburgh	4x5/16	29.50	9.50	70.50	6.50	1.35	61.00	7.40
101	Magnetite media	Tromp	The Netherlands	3⅛x⅝	48.3	0.40	51.7	0.40	1.535	20.00	0.40
102	Magnetite media	Tromp	The Netherlands	3⅛x⅝	57.0	0.50	43.0	0.50	1.835	8.00	0.50
103	Magnetite media	Tromp	The Netherlands	¾x¼	58.22	6.15	41.78	0.007	1.40	84.00	3.87
104	Magnetite media	Tromp	The Netherlands	¾x¼	58.22	0.14	41.78	1.31	1.45	55.00	1.40
105	Magnetite media	Tromp	France	2x5/16	46.78	1.10	53.22	1.01	1.75	46.50	1.05

* Corrected to allow for sink 2.0 sp gr material in raw coal.

† Mesh.

‡ 4 pct of raw feed was trapped by deduster and added to final washed coal; therefore, washed coal and refuse products shown here represent only 96 pct of raw feed.

gravity material. In both cases, naturally, the machine would need to be adjusted to provide a maximum separation of coal from refuse.

Such a relationship, if it could be developed, would include the three criteria listed by Yancey and Geer[2] as being essential to a comparison evaluation. The percentage of ±0.1 near gravity material in the raw coal at the gravity of desired separation would adequately represent the character of the raw coal and the density of the separation. The total amount of misplaced material, expressed as a percentage of the raw feed, would represent the effectiveness of separation between coal and impurity.

The Correlation Data

Table I contains a summary of data obtained for a total of 105 large scale tests on a great variety of coal cleaning equipment. These data were obtained from the literature,[7–20] from operators and equipment manufacturers,[21–27] and from tests conducted at preparation plants of Republic Steel Corp. The major portion of the data represents tests conducted at preparation plants under normal operating conditions. The remainder of the data is for tests conducted on a pilot-plant scale. In so far as could be determined, all the tests represent careful sampling and accurate analyses. All the raw coal float-and-sink data were replotted and the ±0.1 near gravity values adjusted to compensate for the amount of sink 2.0 specific gravity material in the feed, thus placing all of the data on a common basis.

Table II contains data showing the range of separating gravities at which separations were actually made by the various types and makes of coal cleaning equipment. No claim is made that the range of gravities shown in Table II is complete, as some of the equipment listed is being used to make separations at gravities lower and higher than shown.

Coarse Coal Cleaning Units: Figs. 1 and 2 present in graphical form correlations for coarse coal cleaning units or units used to treat coals having top sizes in excess of ½ in. with no limitation on the bottom size. The coarse coal units for which data were available include: 1—the Tromp process, 2—the Chance cone, 3—the Link-Belt drum, 4—the Ridley-Scholes bath, 5—the Jeffrey-Baum jig operated with a bone recirculation, 6—the Jeffrey diaphragm jig, 7—the Vissac pulsator jig, 8—the Menzies cone, 9—the Roberts & Schaefer-Menzies Hydroseparator, and 10—the Elmore pulsator jig. These data were plotted on two separate graphs to avoid overlapping and to show to best advantage the correlations obtained.

Of all the equipment for which test data were obtained, the Tromp dense-media bath is the most effective separator of coarse refuse from coal. The Chance cone is just as effective as the Tromp bath when treating feeds containing less than 7 pct ±0.1 near gravity material but is less and less effective as the difficulty of the separation increases.

The Link-Belt dense-media drum is slightly less effective than the Chance cone and Tromp process when treating feeds containing less than 20 pct near gravity material. It is just as efficient as the Chance cone but not so efficient as the Tromp bath when treating feeds containing from 20 to 50 pct near gravity material, and is slightly more effective than the Chance cone but not so effective as the Tromp bath when treating feeds containing in excess of 50 pct near gravity material.

The Ridley-Scholes dense-media bath is the least effective of the dense-media separators.

The two classifiers, the Menzies cone and the Hydroseparator, are less effective than the Ridley-Scholes bath and considerably less effective than the Tromp, Chance, or Link-Belt equipment. When com-

Table II. Separating Gravity Data for a Variety of Coal Cleaning Equipment

Cleaning Unit: Type	Cleaning Unit: Make	Range of Gravities Covered by Test Data
Sand media	Chance cone	1.40 to 1.45
Bone media jig	Jeffrey-Baum	1.40 to 1.60
Magnetite media	Link-Belt drum	1.35 to 1.732
Magnetite media	Tromp bath	1.35 to 1.835
Pulsator jig	Elmore	1.50 to 1.70
Pulsator jig	Jeffrey diaphragm	1.60 to 1.70
Pulsator jig	Vissac	1.45 to 1.69
Classifier	R & S & Menzies hydroseparator	1.44 to 1.70
Classifier	Menzies cone	1.42 to 1.70
Classifier	R & S hydrotator	1.50 to 1.70
Wet table	Deister Concenco No. 7	1.35 to 1.60
Air table	Stump	1.40 to 1.70
Air table	American	1.40 to 1.60
Magnetite media	Ridley-Scholes	1.45 to 1.60
Magnetite and misc. media	Dutch cyclone	1.35 to 1.80
Spiral	Humphreys	1.38 to 1.60
Wet table	Deister Machine Plat-O	1.38 to 1.60

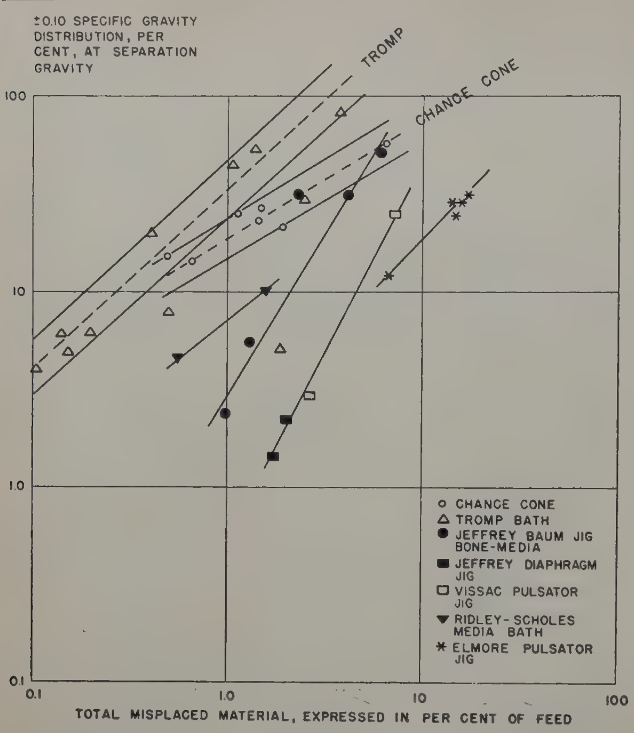

Fig. 1—Comparative effectiveness of coarse coal cleaning equipment.

pared with each other, the Menzies cone is more effective than the Hydroseparator.

The Jeffrey diaphragm and Vissac pulsator jig data plot on essentially the same line and are so plotted, although there undoubtedly will be some objections to such a procedure. When treating coals containing small amounts of near gravity material, the slow-speed pulsator jigs are less effective than the Hydroseparator. The jigs become progressively more effective as the amount of near gravity material increases, however, and in the range of 25 pct ±0.1 near gravity material they are just as effective as the Menzies cone. Extrapolation of the slow-speed pulsator jig data indicates that in the range of 80 to 90 pct ±0.1 the jigs would be just as effective as the Chance cone.

The Elmore high-speed pulsator jig is more effective than the Hydroseparator but less effective than the Menzies cone. Extrapolation of Elmore data indicates that in the range of 0 to 7 pct ±0.1 near gravity material the Elmore jig is more effective than the slow-speed Jeffrey and Vissac pulsator jigs.

The Jeffrey-Baum jig, and it should be emphasized that all of the test data are for jigs operated with a bone-media, is not so effective as the Menzies cone when treating coals containing from 0 to 3 pct ±0.1 near gravity material but is at least as effective and possibly more effective than dense-media equipment when treating coals containing 50 to 60 pct ±0.1 material. To a certain extent this conclusion is obscured by two factors. In every case the jigs were making a middling product which was being crushed, and either a portion or all of the crushed material was being returned to the jig feed. Since the difficulty of the separation or the percentage of ±0.1 near gravity material was determined from the raw coal float-and-sink data, the correlations obtained are bound to be somewhat in error. On the other hand, in two cases the Jeffrey-Baum jig was being used to treat all sizes down to zero, while all of the dense-media processes stopped short at some fairly coarse limiting size.

Intermediate and Fine Coal Cleaning Units: Fig. 3 presents in graphic form correlations developed for the intermediate and fine coal cleaning units or units used to treat: 1—coals having top sizes between ½ and ⅛ in., with no limitation on the bottom size, and 2—coals having top sizes of less than ⅛ in. The intermediate units for which data were available include 1—the Roberts & Schaefer Hydrotator, 2—the Deister-Concenco No. 7 wet table, 3—the Stump air table, 4—the American air table, 5—the Dutch cyclone dense-media process, both with and without the addition of a stabilizing material, and 6—the Deister Machine Co. Plat-O wet table. The only fine coal unit for which data were available is the Humphrey's spiral.

The Dutch cyclone using a stabilized media is the most effective separator in the intermediate group. Removal and control of the stabilizing material, whether Loess or Bentonite, is reported to require careful spraying and thickening steps and may require the use of froth flotation.

The Dutch cyclone using magnetite, roasted pyrites, or barytes without the addition of a stabilizing agent, the Deister Concenco No. 7 wet table, and the Roberts & Schaefer Hydrotator are all equally effective but are less effective than the Dutch cyclone operated with a stabilized media. It should be pointed out that the Dutch cyclone and Hydrotator tests were made on feeds sized or classified between 16 and 48 mesh, while the Deister table tests were made on relatively unsized feeds.

It might be argued that only the data for the Dutch cyclone and the No. 7 wet table cover the entire range of the correlation and that an unwarranted extrapolation is being made for the Hydrotator. However, in the range of separations for coals having small amounts of ± 0.1 near gravity material the three units are comparable and the

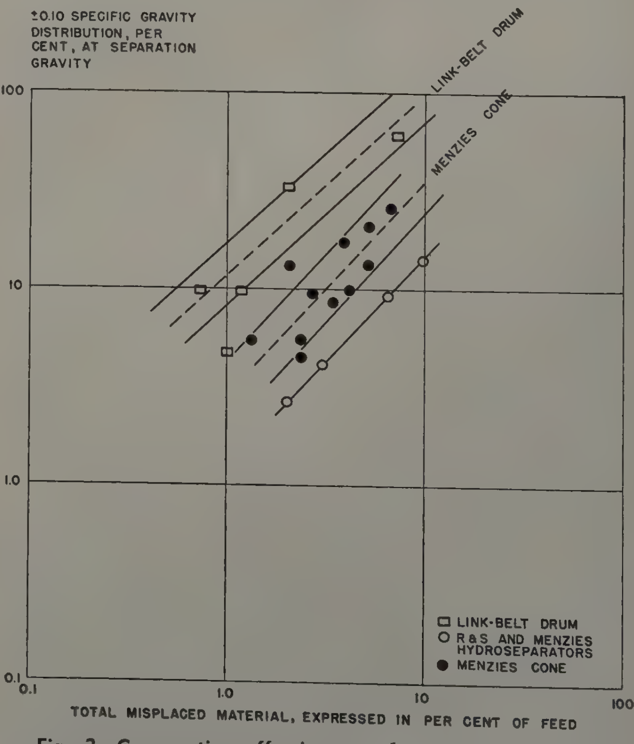

Fig. 2—Comparative effectiveness of coarse coal cleaning equipment.

Table III. Capacity Data

Test No.	Clean Coal Produced Tons Per Hr Per Sq Ft	±10 Distribution Pct at Gravity of Separation	Cleaning Unit Tested
1	0.68	57.5	Chance cone
3	0.85	22.7	Chance cone
4	0.90	14.7	Chance cone
5	1.68	15.5	Chance cone
6		25.0	Chance cone
7	1.37	27.2	Chance cone
8	1.60	55.0	Jeffrey-Baum jig
9	1.60	31.0	Jeffrey-Baum jig
10	1.60	33.0	Jeffrey-Baum jig
11	2.17	33.0	Link-Belt drum
14	0.91	5.3	Tromp separator
15	0.97	6.22	Tromp separator
16	0.87	30.20	Tromp separator
17	0.92	6.40	Tromp separator
18	0.27	29.60	Elmore jig
19	0.26	29.60	Elmore jig
22	1.89	14.30	Menzies hydroseparator
23	2.62	2.60	Menzies hydroseparator
27	1.78	17.50	Menzies cone
28	1.45	26.00	Menzies cone
29	2.28	5.50	Menzies cone
32	1.50	4.00	R & S hydrotator
33	1.13	2.96	R & S hydrotator
34	0.86	5.80	R & S hydrotator
54	5.46	1.54	Dutch cyclone
55	6.81	2.63	Dutch cyclone
56	7.34	14.43	Dutch cyclone
57	9.10	19.20	Dutch cyclone
58	6.40	47.50	Dutch cyclone
59	7.82	32.60	Dutch cyclone
60	9.10	81.00	Dutch cyclone
61	6.38	14.00	Dutch cyclone
62	7.82	8.70	Dutch cyclone
63	1.94	72.60	Dtuch cyclone
64	1.73	72.60	Dutch cyclone
65	2.70	70.20	Dutch cyclone
66	1.51	84.00	Dutch cyclone
67	1.09	76.60	Dutch cyclone
68	1.57	76.60	Dutch cyclone
69	1.31	71.90	Dutch cyclone
70	2.44	74.40	Dutch cyclone
71	1.85	75.70	Dutch cyclone
78	0.10	27.50	Deister Plat-O
79	0.10	6.53	Deister Plat-O
80	0.11	21.90	Deister Plat-O
81	0.11	3.60	Deister Plat-O
83	2.15	2.40	Jeffrey-Baum jig
84	2.97	25.00	Vissac pulsator jig
85	3.53	3.00	Vissac pulsator jig
94	0.28	25.00	Elmore jig
95	0.42	12.50	Elmore jig
96	0.26	31.40	Elmore jig
97	3.67	9.70	Link-Belt drum
101	0.48	20.00	Tromp separator
102	0.57	8.00	Tromp separator
103	0.58	84.00	Tromp separator
104	0.58	55.00	Tromp separator
105	0.47	46.50	Tromp separator

definite straight line correlations obtained for all of the sets of data indicate that the assumption is reasonable.

The Deister Machine Co. Plat-O table and some of the data for the Deister-Concenco No. 7 table show less effective separations than those for the Dutch cyclones, Hydrotators, and the bulk of the No. 7 tables. The variations of the No. 7 table can be explained as being inefficient operations and the lesser effectiveness of the Plat-O table could be explained as being inherent in the machine. However, it should be mentioned that the Plat-O data, while representing recent tests, are for old machines operated under irregular raw coal kind and size-consist conditions.

The air tables, and it should be noted that all of the tables were operated with a middling recirculation, are definitely the least effective of the intermediate group when treating coals containing small amounts of near gravity material. On the other hand, when treating coals containing between 30 and 45 per cent ± 0.1 near gravity material, the air tables are just as effective as the Plat-O table. Extrapolation of the air table data indicates that in the range of 70 to 90 per cent ± 0.1 material the air tables would be almost as effective as the Dutch cyclone, No. 7 table, Hydrotator group. The American table is slightly more effective than the Stump table in the lower ± 0.1 range but shows about the same effectiveness in the higher ± 0.1 range.

The only fine coal cleaning unit correlation shown in Fig. 3 is for the Humphrey's spiral treating 8-mesh × 0 or 8x100 mesh feeds. Since the Humphrey's spiral is alone in its class, as far as available operating data and correlations are concerned, it cannot be evaluated on a comparative basis.

Capacity Comparisons

An operating man is frequently more interested in the capacity of a unit than he is in its separating effectiveness and is willing to sacrifice effectiveness to some extent if by so doing he can materially increase capacity.

A line of reasoning similar to that presented under the section on the Correlation Theory suggested that there should be a correlation between the difficulty of a separation, or the amount of ± 0.1 material in the feed at the separating gravity, and the capacity for any make of coal cleaning equipment. Capacity was considered to be the tons of clean coal produced per hour per square foot of operating surface.

Table III contains a summary of the data available. Column 2 of Table III may be considered column 13 in Table I, thus eliminating duplications between Tables I and III.

Coarse Coal Cleaning Units: Fig. 4 presents in graphic form the capacity correlations obtained for coarse coal cleaning units, or units used to treat coals having top sizes in excess of ½ in. with no limitation on the bottom size. The coarse coal units for which data were available include 1—the Tromp process, 2—the Chance cone, 3—the Link-Belt drum, 4—the Jeffrey-Baum jig operated with a bone recirculation, 5—the Vissac pulsator jig, 6—the Menzies cone, 7—the Menzies Hydroseparator, and 8—the Elmore jig. Some of the relations show con-

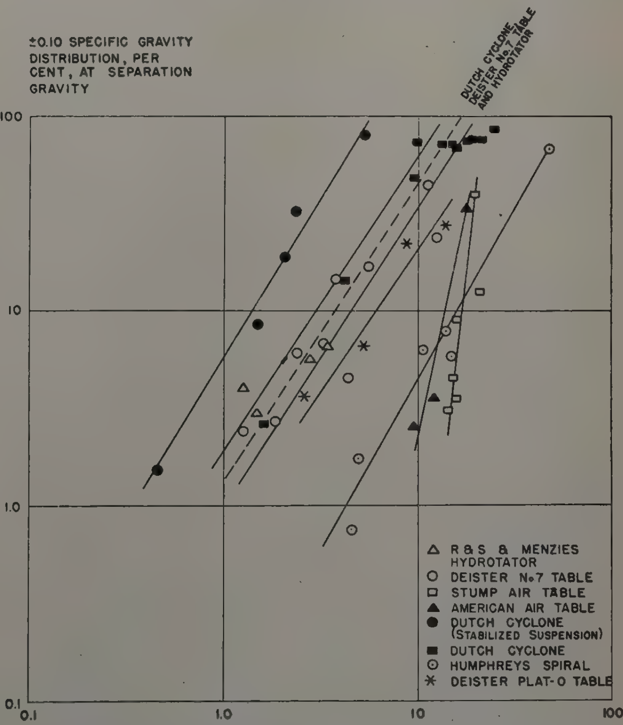

Fig. 3—Comparative effectiveness of intermediate and fine coal cleaning units.

siderable variation from an average condition; others are based upon only two or three points and are possibly in error, but all the data show trends and can be used for first approximation purposes.

The Vissac pulsator jig and the Link-Belt heavy-media drum have the greatest capacity per unit area of all the coarse coal cleaning units. The Vissac jig was used to treat sized feeds, and its high capacity can be explained on that basis.

The Jeffrey-Baum jig can produce just as much washed coal per unit area as the Link-Belt drum when treating coals containing 60 pct or more of near gravity material but has a relatively lower and lower capacity rating as the difficulty of the separation decreases.

So similar are capacity relationships of the Menzies cone and the Menzies Hydroseparator that they have been combined and plotted on the same line. The Menzies combination shows a lower capacity rating than the Jeffrey jig when treating coals containing more than 15 pct near gravity material, and a higher capacity rating than the Jeffrey jig, but not so high a capacity as the Link-Belt drum, when treating coals containing less than 15 pct near gravity material.

The Chance cone shows considerably less capacity than the Jeffrey jig or Menzies combination at difficult separations but a greater capacity than either when treating less difficult coals.

The Tromp process has the lowest capacity of all the heavy-density equipment. The Elmore jig has the lowest capacity of all of the coarse coal equipment for which data were available.

Intermediate Coal Cleaning Units: Fig. 5 presents capacity correlations obtained for intermediate coal cleaning units, or units used to treat coals with top sizes between ½ and ⅛ in., with no limitation on the bottom size. The intermediate coal units for which data were available are 1—the Roberts & Schaefer Hydrotator, 2—the Dutch cyclone dense-media process, and 3—the Deister Machine Co. Plat-O wet table. Paucity of available data leaves room for misrepresentation, but again, all the data show definite trends.

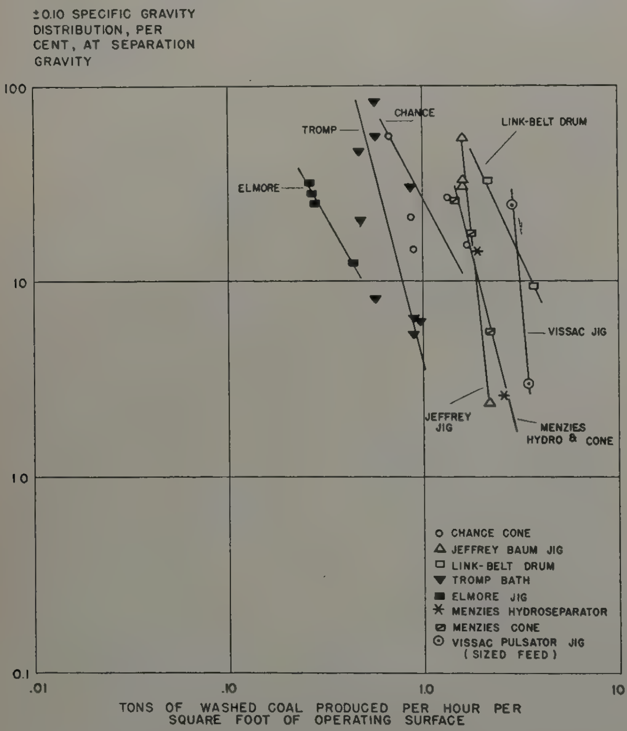

Fig. 4—Relationship between difficulty of separation and unit capacity for coarse coal cleaning units.

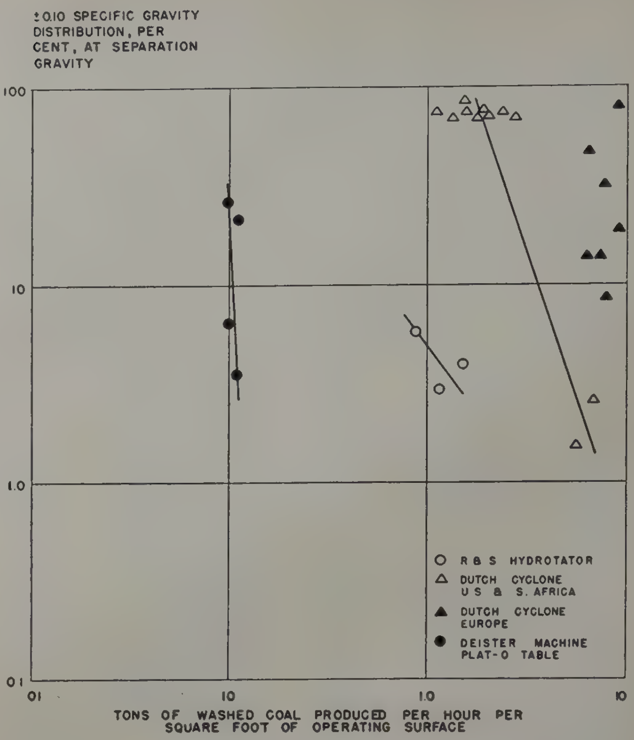

Fig. 5—Relationship between difficulty of separation and unit capacity for intermediate coal cleaning units.

The Dutch cyclone heavy-media process has tremendous capacity per unit area when compared with the R & S Hydrotator and the Deister Machine Co. Plat-O table. In this connection it is interesting that differences in capacity are reported by United States and South African investigators on the one hand and European investigators on the other. The European investigators reported considerably higher capacities and the values were approximately the same irrespective of the difficulty of the separation.

Conclusions

Conclusion No. 1: The total amount of misplaced material in washed coal and refuse products, as determined at approximate gravity of separation and expressed as percent of feed, is proportional to the percentage of ±0.1 near gravity material in the feed.

Each type and make of cleaning equipment has its own particular relationship, and to develop the separation characteristics of any particular piece of equipment it is necessary to obtain test data for several installations or for several tests at different separation gravities at the same installation.

Data for individual size fractions in composite feed may be used for correlation purposes, and will plot in the same way as composite size-consist data, if float-and-sink data are available for that particular size in the raw coal, washed coal, and refuse.

Data for both anthracite and bituminous coals provide the same relationships. The required specific gravity of the separation and the particle shape, i.e., the presence of thin, flat slate, may prevent the use of some piece of equipment for a specific washing job, but within the operating limits of the equip-

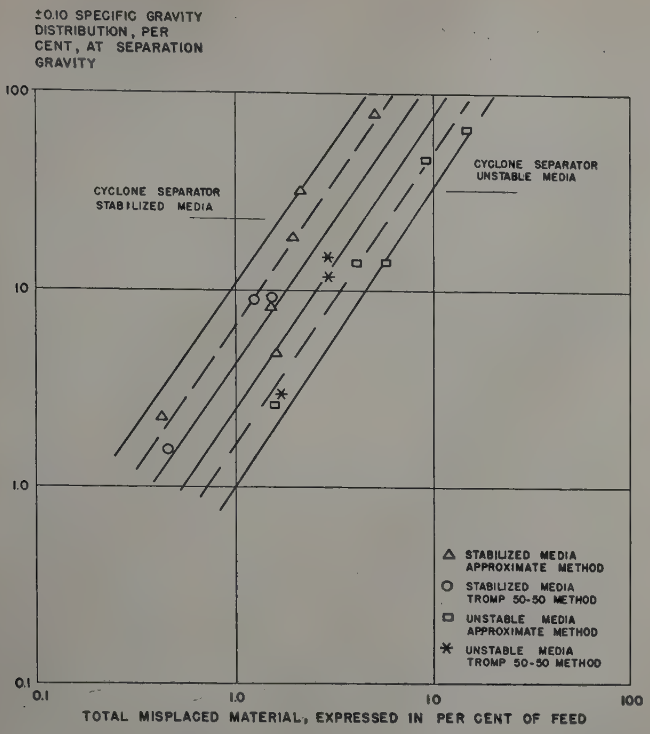

Fig. 6—A comparison of the correlations obtained when using the Tromp 50-50 method and the approximate method of determining gravity of separation.

ment, the specific gravity of the material has no influence on the correlations obtained.

To place all the data on a comparable basis, it is necessary to adjust the percentage of ±0.1 near gravity material to allow for the amount of sink 2.0 sp gr material in the feed.

Conclusion No. 2: To determine the effectiveness of a particular washing unit, it is necessary to have complete float-and-sink data for the composite raw coal. It should be emphasized that this data need be only for the composite size actually treated and not for each individual size fraction. It is not necessary to conduct exhaustive float-and-sink tests on the products of the washing unit. A one-gravity separation is all that need be used if it is approximately the gravity of the separation. However, it is preferable to conduct tests at a number of gravities to determine the separation gravity by the 50-50 method described by Yancey and Geer in 1938.[28]

Conclusion No. 3: The total amount of misplaced material, as determined at the approximate gravity of separation, expressed in percent of the feed, and representing a particular separation by a particular piece of equipment, may be distributed in varying proportions between washed coal and refuse, but its total remains essentially constant. Thus washing any coal with its constantly changing size consist and physical make-up in a given type and make of cleaning equipment at a given and approximately constant separation gravity normally results in a washed coal containing varying amounts of misplaced material; in consequence, the ash content of the washed coal will show considerable variance. It seems implied that regulation of the equipment used will allow more or less misplaced material to remain in the washed coal and that it is possible, speaking relatively, to obtain either a high ash or low ash washed coal while making a separation at essentially the same specific gravity.

Conclusion No. 4: The capacity of any given coal cleaning unit, when capacity is expressed as the tons of clean coal produced per hour per square foot of operating surface, is related to the percentage of ±0.1 near gravity material in the feed, or the difficulty of the separation.

Summary

The relative effectiveness ratings of most of the equipment discussed in this paper will not surprise any real student of coal preparation. Most preparation men have already independently arrived at the same or nearly the same conclusions by less direct methods of comparison. The misplaced material correlations merely corroborate conclusions already industry-wide, but do so on an exact basis. The capacity correlations likewise will surprise very few people. The correlations do provide reference points for future work, and use of the method will allow the evaluation of other makes and types of coal-cleaning equipment, both old and new.

The information presented in this paper indicates that certain machines are less effective separators of coal from refuse than others, and that some machines are capable of producing more tons of clean coal per hour per square foot of operating surface than others. This should not be construed as re-

Table IV. Cyclone Separator Data

Test No.	Media	Washed Coal		Refuse		Gravity of Separation, 50-50 Method	Gravity of Separation, Approx. Method	±0.1 Distribution at Gravity of Separation	Total Misplaced Material, Pct of Raw Coal
		Wt, Pct	Sink, Pct	Wt, Pct	Float, Pct				
54	Stabilized	95.70	0.20	4.30	6.25	1.63		1.54	0.46
54	Stabilized	95.70	1.70	4.30	0.60		1.50	4.93	1.65
54	Stabilized	95.70	0.30	4.30	3.40		1.60	2.36	0.43
55		88.92	1.30	11.08	5.00	1.54		2.96	1.71
55		88.92	1.12	11.08	5.47		1.55	2.63	1.60
56		33.30	7.50	66.70	0.80	1.52		15.00	3.03
56		33.30	4.38	66.70	4.10		1.80	14.43	4.19
57	Stabilized	86.25	2.50	13.75	6.50	1.49		9.25	1.32
57	Stabilized	86.25	1.99	13.75	2.70		1.45	19.20	2.09
58		77.20	1.80	22.80	7.50	1.79		15.30	3.10
58		77.20	9.99	22.80	8.01		1.70	47.50	9.54
59	Stabilized	88.30	0.80	11.70	7.20	1.505		9.20	1.55
59	Stabilized	88.30	2.28	11.70	2.59		1.45	32.60	2.31
57*	Stabilized	86.25	5.78	13.75	1.34		1.40	81.00	5.17
58†		77.20	1.19	22.80	21.76		1.80	14.00	5.88
59**	Stabilized	88.30	0.82	11.70	6.85		1.50	8.70	1.52
63		41.30	20.30	58.70	10.90	1.35	1.35	72.60	14.78
65		60.00	20.30	40.00	10.89	1.35		71.20	16.54
65		60.00	13.40	40.00	17.30		1.40	70.20	14.96

* Test 60 in original text.
† Test 61 in original text.
** Test 62 in original text.

flecting on the usefulness of some of the equipment. First cost and operating costs have not been taken into account in this evaluation, and since performance is only one factor among many in the selection of coal-cleaning equipment, other factors may outweigh the limitations of a slightly less efficient separation or a lower capacity.

Appendix

The term *gravity of separation* as used in this paper embraces two concepts for comparison purposes. The first concept is the one developed by Tromp in which *gravity of separation* is that gravity at which the distribution is 50 pct to clean coal and 50 pct to refuse. This is the only method the author would use if he wished to determine the gravity at which a separation is being made for a particular piece of equipment in a particular preparation plant. The second concept is one developed by the author in which *gravity of separation* is an approximate value as determined by scanning the float-and-sink data for washed coal and refuse produced by a particular piece of equipment. One or two such approximate values may be determined from a particular set of data. For example:

Specific Gravity	Washed Coal Wt, Pct	Refuse Wt, Pct
Float 1.30	30.0	1.0
1.30 x 1.35	45.0	1.0
1.35 x 1.40	22.0	2.0
1.40 x 1.50	2.0	3.0
1.50 x 1.60	1.0	8.0
1.60 x 1.70		35.0
Sink 1.70		35.0

With these data, approximate separations are indicated at 1.40 and 1.50 sp gr. These gravities and their corresponding amounts of misplaced material and percentage of near gravity material cannot be used to determine the actual gravity at which a separation is being made but may be used for comparison purposes, since either concept will provide essentially the same correlation between the amount of ±0.1 near gravity material and the total amount of misplaced material.

Table IV contains data for cyclone heavy-media separators in which the gravity of separation has been determined by the Tromp 50-50 method. The corresponding amounts of near gravity material and misplaced material are included. Table IV also contains data for the same tests in which the gravity of separation has been determined by the approximate method, only one gravity being indicated in some of the tests and two gravities in others. Corresponding amounts of near gravity material and misplaced material are also included. Fig. 6 shows a plot of these values, which should be compared to the initial plot shown in Fig. 3. Both sets of values provide essentially the same correlation relationship.

The bulk of the values listed under Gravity of Separation in Table I were determined by the approximate method. The method is rapid, presents two values at times when the Tromp method presents only one, and provides good values for comparison purposes.

References

[1] Thomas Fraser and H. F. Yancey: Interpretation of Results of Coal Washing Tests. *Trans.* AIME (1923) **69**, pp. 447-469.

[2] H. F. Yancey and M. R. Geer: Efficiency and Sharpness of Separation in Evaluating Coal-Washery Performance. Paper presented to AIME at St. Louis, February 1951.

[3] F. C. Lincoln: Coal Washing in Illinois. Engineering Experiment Stat., Univ. Ill., Bull. 69 (1913).

[4] H. F. Yancey, M. R. Geer, and R. E. Shinkoskey: Performance of a Pulsator-Type Coal-Washing Jig. U. S. Bur. Mines *R.I.* 3372 (1938).

[5] R. T. Hancock: Calculating Efficiencies from Washery Figures. *Colliery Engineering* (1947) pp. 140-142.

[6] W. W. Anderson: Quantative Efficiency of Separation of Coal Cleaning Equipment. *Trans.* AIME (1950) **187**, pp. 256-264.

[7] Byron M. Bird: Performance of the Chance Sand Flotation Process. *Mechanization* (May 1938).

[8] Anonymous: Sand Flotation Process Used in New Moss Creek Preparation Plant. *Mechanization* (May 1940).

[9] H. R. Randall and Edgar Schweitzer: Dense Media Separation Process. *Coal Mine Modernization,* 1949 Year Book, American Mining Congress.

[10] B. M. Bird and David R. Mitchell: Dense Media Processes. *Coal Preparation,* sec. ed., Chap. 14, AIME, 1950.

[11] John Griffen: Coal Washers of the Classifier Type. *Coal Preparation,* sec. ed., Chap. 10, AIME, 1950.

[12] R. E. Zimmerman: The Cleaning of Fine Sizes of Bituminous Coals by Concentrating Tables. *Trans.* AIME (1950) **187**, pp. 956-966.

[13] H. F. Yancey and M. R. Geer: Coal Cleaning Performance—Comparison of Pneumatic Jig, Pneumatic Table, and Baum-Type Jig. *Trans.* AIME (1946) **168**, pp. 208-223.

[14] M. R. Geer and H. F. Yancey: Preliminary American Tests of a Cyclone Coal Washer Developed in the Netherlands. *Trans.* AIME (1948) **177**, pp. 220-239.

[15] S. A. Falconer: Some Recent Investigations with the Dutch State Mines Cyclone Separator on Fine Coal Slurries. *Trans.* AIME (1950) **187**, pp. 790-800.

[16] Fuel Research Institute of South Africa: Recovery of the Coking Fraction from Witbank Fine Coal by Means of the Cyclone Washer. Report No. 10 (1948).

[17] M. R. Geer, H. F. Yancey, C. L. Allyn, and R. H. Eckhouse: Laboratory Performance Tests of the Humphreys Spiral as a Cleaner of Fine Coal. *Trans.* AIME (1950) **187**, pp. 1057-1067.

[18] W. M. Bertholf: Cleaning Table Middlings from a Coal Washery With the Humphreys Spiral Concentrator. *Trans.* AIME (1946) **169**, pp. 232-239.

[19] J. D. Price and W. M. Bertholf: Coal Washing in Colorado and New Mexico. *Trans.* AIME (April 1949) **184**, pp. 99-108.

[20] B. M. Bird and S. M. Marshall: Jigging, Classification, Tabling, and Flotation Tests of Coals from Pierce County, Washington. U. S. Bur. Mines *Bull.* 337 (1931).

[21] F. H. Coleman, Westmoreland Mining Co.: Private correspondence.

[22] W. B. Sweazy, C. H. Mead Coal Co.: Private correspondence.

[23] George Kennedy, Rochester & Pittsburgh Coal Co.: Private correspondence.

[24] J. D. Martin, United Engineers & Constructors: Private correspondence.

[25] R. C. Woodhead, McNally Pittsburgh Manufacturing Corp.: Private correspondence.

[26] J. M. Vonfeld, Pittsburgh Coal Co.: Private correspondence.

[27] M. G. Driessen: The Use of Centrifugal Force for Cleaning Fine Coal in Heavy Liquids and Suspensions with Special Reference to the Cyclone Washer. *Fuel* (December 1945) pp. 1-16.

[28] H. F. Yancey and M. R. Geer: Performance of a Baum-Type Coal-Washing Jig. U. S. Bur. Mines *R.I.* 3371, 1938.

[29] O. Schafer: Coal Preparation by the Tromp Dense-Liquor Process. *Colliery Engineering* (January 1939) pp. 18-22.

[30] K. Tromp: New Methods of Computing the Washability of Coal. *Colliery Guardian* (May 1937) pp. 955-959, 1009.

Solids Fluidization Applied to Lime Burning

by F. S. White and E. L. Kinsella

Solids fluidization utilized in two ways for the commercial production of lime is described. Crushed —6 mesh limestone is dried and dedusted in a single bed reactor, then calcined in a 5-stage reactor. Construction, operation, and results obtained with both processes are given.

THE solids fluidization process brought out by the Standard Oil Development Co. in the early forties for catalytic cracking of petroleum enabled rapid transfer of large quantities of heat from gases to solids under closely controlled temperature conditions. As the technique developed, it was natural that applications for the process outside the petroleum industry would be sought. The calcination of limestone to quicklime requires the transfer of a large quantity of heat at high and closely controlled temperatures. For these reasons, this possible application was one of the first to be investigated.

Laboratory work conducted by the Dorr Co. indicated that lime produced by solids fluidization would be of exceptional quality. Calculation of theoretical heat balances showed that savings in fuel could be expected. Accordingly, a pilot plant of 10 tons per day capacity was erected by the New England Lime Co. at Adams, Mass., to substantiate the process. Operation of the pilot plant, previously described,[1] showed that excellent lime could be produced with a saving in fuel. The work also indicated the necessity of preparing feed to remove the finer fractions if dust losses were to be held to a tolerable level. A single-stage fluidized solids drier-stripper was developed to accomplish this sizing.[2] Subsequently a commercial lime reactor was erected at Adams, beginning operation in June 1949, followed by air sizer facilities completed in November 1951. This paper will describe these two applications of solids fluidization.

The raw material for preparation of lime by the fluidizing process is a high calcium crystalline limestone having the approximate chemical composition shown in Table I. The stone is first prepared by crushing and grinding in conventional equipment to pass a 6-mesh sieve. After crushing, the material is sent to the FluoDry unit for drying and dedusting.

Fluidized Drying and Sizing

As shown in Fig. 1, the FluoDry unit consists of a ¼-in. cylindrical steel shell, 9-ft ID by 22-ft 6-in. overall height. Attached horizontally at the bottom is a 6-ft diam combustion chamber, approximately 7 ft 6 in. long. A refractory constriction dome, consisting of first-quality fire brick shapes, partitions the inside into two sections. The lower section is called the windbox and the upper the bed compartment. The vertical wall of the shell is lined with 6-in. first-quality rotary kiln blocks. In the bottom of the windbox a hoppered section is formed with castable refractory to permit the windbox to be readily cleaned via a 6-in. screw conveyor. The combustion chamber is similarly lined with refractory shapes. On the 6-in. diam section, 4½ in. of insulating brick, HW-26, are used. The inner combustion chamber is lined with 4½-in. Korundal brick to withstand the high flame temperatures encountered.

An 8-in. steel feed pipe, entering vertically through the top and fitted with an air-operated cone valve,

---

F. S. WHITE, Assistant to the President, and **E. L. KINSELLA** are with New England Lime Co., Adams, Mass.

Discussion on this paper, TP 3388H, may be sent (2 copies) to AIME before October 31, 1952. Manuscript, February 11, 1952. Revised June 19, 1952. New York Meeting, February 1952.

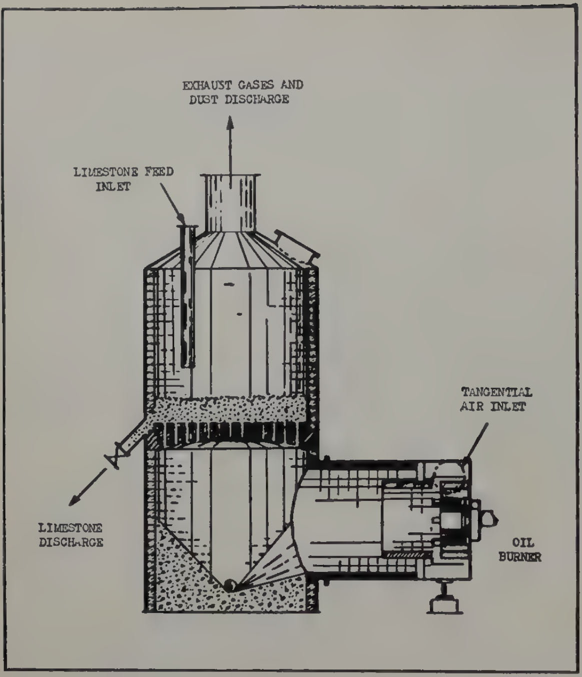

Fig. 1—Sectional view of FluoDry unit.

provides a means of introducing feed to the unit. The discharge consists of a 6-in. pipe at the top of the dome, running angularly to the outside and likewise fitted with an air-operated slide valve.

Air for fluidization and atomizing of the oil is supplied by two blowers. Primary air is supplied by a Buffalo blower rated 12,000 cfm at 2.0 lb gage and driven by a 150-hp motor. Air for the oil burner is provided by a Buffalo blower rated 600 cfm at 2 lb gage. Exhaust gases from the sizer are passed through a series-parallel combination of four cyclone collectors, then through a continuously cleaned felt bag collector of the Hersey type.

Table I. Approximate Analysis of Limestone Feed

Composition	Pct
SiO_2	1.2 to 2.5
R_2O_3	0.3 to 0.5
$CaCO_3$	95.0 to 97.0
$MgCO_3$	1.0 to 1.5

Table II. Operating Data, FluoDry Unit

Bed temperature	200° to 225°F
Air flow	12000 cfm
Feed rate	100 to 125 tons per hr
Oil required	50 to 60 gal per 100 tons limestone feed
Power required	98 kw-hr per 100 tons limestone feed
Split	100 lb feed = 86 lb coarse feed plus 14 lb fines

Control of the drying temperature is effected by a recording temperature controller sensing the temperature via a thermocouple immersed in the fluidized bed. The instrument regulates the flow of oil by positioning the oil burner valve with a diaphram motor valve. The bed level is similarly regulated by a recording controller measuring the differential pressure of the fluidized bed. The instrument positions an air-operated slide valve to allow material to discharge at a rate which will hold a constant bed level. Indicating instruments are also utilized to measure pressure drops throughout the system and temperatures in the combustion chamber and dust collectors. Safety devices to guard against flame and power failures have been incorporated.

The sizer is operated in conjunction with the crushing plant, the screen discharge being the feed to the sizer. The operation of the sizer from start to shutdown is simple. After the blowers are started, the oil burner, using Bunker C oil, is lighted by an electrically ignited gas torch. The inlet valve is then opened, permitting feed to enter. Finally, the discharge valve is opened when the bed reaches the desired level. When in balance the unit is switched to automatic control, the operator then monitoring the unit from the control panel. When it is not in operation, the feed and the burner are turned off, the bed drained out and the blowers shut down. While company experience with this FluoDry unit has thus far been limited, there has been enough operating time under winter conditions to make possible a compilation of data, shown in Table II, and to justify the following tentative conclusions.

1—Mechanical operation of the unit is simple, and very low maintenance costs are anticipated. 2—It is an efficient drier, capable of drying limestone with a moisture content of 2 to 3 pct while burning 60 gal of Bunker C fuel oil per 100 tons limestone. 3—It is, however, a less efficient sizer than desired. Inspection of Fig. 2, a plot of the screen analyses of the feed, product, and dust, will show that the sized product still contains about 7.0 pct −100 mesh. This represents about 1/3 of the original −100 mesh fraction fed to the unit. While an improvement has been noticed in operation of the rotary kilns on this quality-sized and dried feed, less of an improvement has been found in operation of the FluoSolids kiln. For the latter, it would be highly desirable to remove all of the −100 mesh fraction.

Fluidized Calcination

The crushed and sized limestone is next processed to lime in the FluoSolids reactor. In Fig. 3, a sectional view, the reactor is seen to consist of a vertical steel shell 13 ft 6 in. ID by 45 ft high, closed at the bottom by a windbox having a perforated steel constriction plate, and at the top by an insulated steel cover with a gas take-off to the dust collectors. The reactor is lined throughout with 9 in. of 2600°F

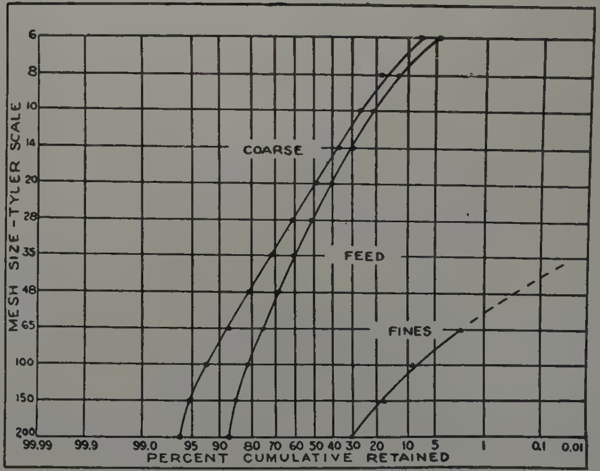

Fig. 2—Plot of screen analyses of FluoDry samples.

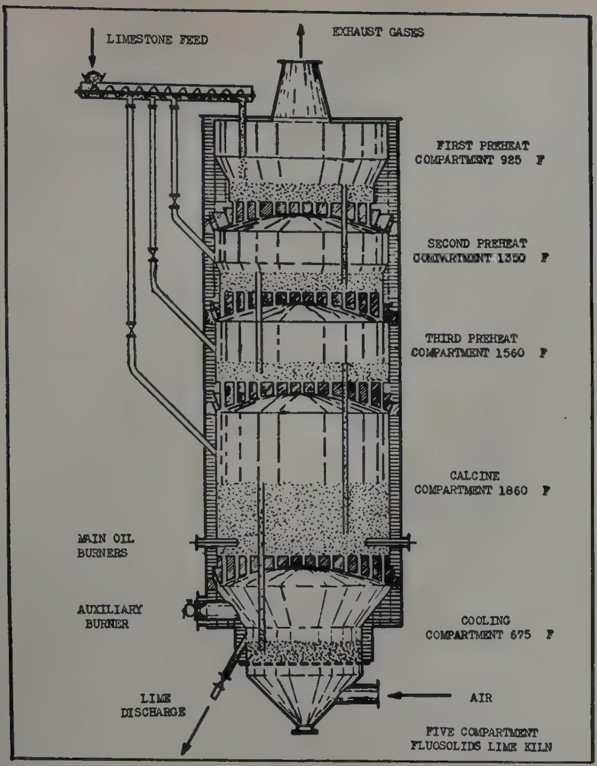
LIMESTONE FEED
EXHAUST GASES
FIRST PREHEAT COMPARTMENT 925 F
SECOND PREHEAT COMPARTMENT 1350 F
THIRD PREHEAT COMPARTMENT 1560 F
CALCINE COMPARTMENT 1860 F
MAIN OIL BURNERS
AUXILIARY BURNER
COOLING COMPARTMENT 675 F
LIME DISCHARGE
AIR
FIVE COMPARTMENT FLUOSOLIDS LIME KILN

Fig. 3—Sectional view of FluoSolids kiln.

series insulating firebrick. Four firebrick constriction domes divide the unit into five stages, the top three being devoted to preheating incoming stone, the fourth to calcination, and the fifth to cooling of the lime.

The firebrick domes are pierced with holes approximately 3 in. in diam for upward flow of gases. The upper ends of these holes are fitted with stainless steel orifices drilled with smaller holes of varying sizes adjusted to give a pressure drop which will insure fluidization across the bed. Each dome is also fitted with an alloy steel pipe for transferring solids downward to the next successive stage. Fig. 4 is a photograph of the interior of the calcining compartment showing some of these details.

The reactor in operation can best be visualized from a description of the startup procedure. With the reactor empty, the normal air blast is started followed by ignition of the auxiliary burner firing into the cooling compartment. After a period of preheating, limestone is fed directly to the calcining chamber via a "side feed" pipe until a 3½ to 4-ft bed of fluidized stone is established. Feed is stopped, allowing the temperature of the bed to increase slowly to 800°F, whereupon the regular burners are inserted into the calcining bed.

These burners, 12 in number, are lengths of extra heavy carbon steel pipe which are inserted through packing glands into an insulated, air-purged burner jacket projecting radially 15 in. into the bed at a height of 6 in. off the constriction plate. A positive displacement pump driven from a common shaft by a variable speed motor supplies each burner with 1/12 the total Bunker C oil flow. No effort is made to atomize the oil with air or to preheat it beyond pumping consistency.

When the regular burners are in operation, the auxiliary burner is shut down. Combustion then transfers entirely to the fluidized bed, rapidly raising its temperature until 1540°F is reached. At this point calcination starts, the temperature then rising only slightly until calcination is completed. While the calciner bed is being reduced to lime, the three preheat beds are successively established. By the time the top bed has been made, calcination is usually completed, the temperature once again rising rapidly. A flow of feed sufficient to stabilize the temperature at 1860°F is then started into the first preheater. As each preheater is filled to the level of the top of its transfer pipe, the incoming feed starts a flow of displaced material through the stages to the calciner. Thus new feed is preheated to temperatures of 925°, 1360° and 1560°F, utilizing the heat in the combustion gases and the CO_2 evolved from the calcining stone.

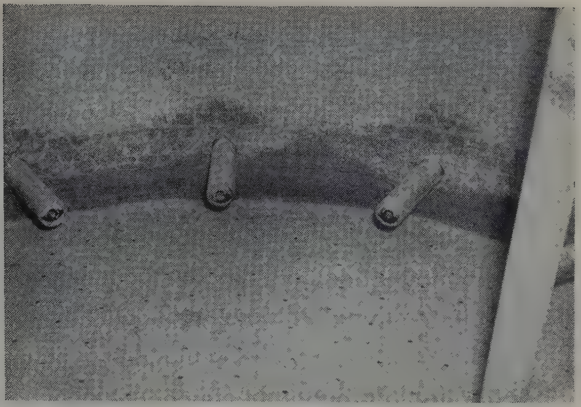

Fig. 4—Interior of calcining compartment.

Finally, when the calciner is filled to the overflow point, finished lime is allowed to flow to the cooler where the incoming air cools the lime to 700°F, and is itself preheated. Finished lime then discharges from the kiln through an automatically controlled slide valve similar to that previously described for the drier.

As shown in Fig. 5, the kiln is well instrumented. Production is controlled by manually setting the potentiometer which governs the speed of the oil pump motor. Air flow is also regulated manually to hold 3 to 5 pct excess air as determined by a recording oxygen instrument analyzing the stack gases. There are, in addition to the controlling instruments, indicating instruments which measure bed and constriction plate pressure drops, bed temperatures, and back pressures on the oil guns to warn of plugging.

With constant heat input the amount of limestone feed required would be uniform with homogenous feed. However, variations caused by segregation in the storage bins and varying chemical compositions

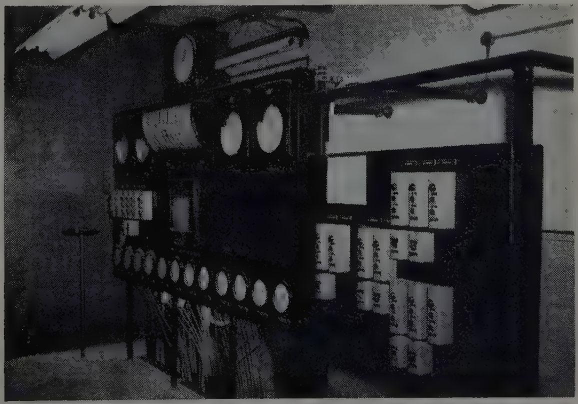

Fig. 5—Instrument panel for calciner.

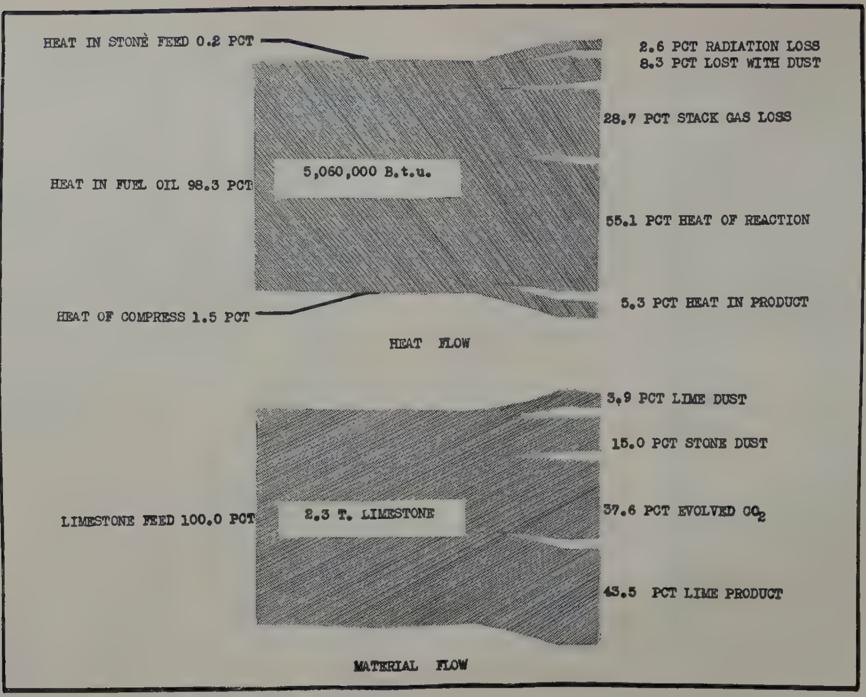

Fig. 6—Heat and material flow diagrams based on one ton of product.

cause temperature fluctuations. These are detected by a recording controller which measures the calciner temperature and then varies the speed of a constant weight belt feeder. Except for serious upsets, temperatures are controlled to ± 20°F of the desired values. Over a period of time ratios of stone fed to oil burned have been surprisingly constant. Typical data for a 24-hr period of operation are presented in Table III.

Table III. Data for Heat and Material Balances

Oil consumption	2907 gal per 24 hr
Oil temperature	160°F
Oil analysis	87 pct carbon 10 pct hydrogen 152,000 Btu per gal, gross
Lime produced	89.0 tons
Lime temperature	690°F
Stone used	204.0 tons
Stone temperature	70°F
Air flow	4,850,000 cf (stp)
Air temperature after compression	150°F
Stack gas temperature	900°F
Stack gas analysis	34.0 pct CO_2 1.0 pct O_2
Dust analysis	32.0 pct lime 68.0 pct limestone

By means of this data heat and material balances were calculated, the results being graphically shown in Fig. 6. Inspection of these balances will reveal a major advantage and a disadvantage of the fluidized process for burning lime.

The major advantage of the process is in the fuel economy. Approximately 5 million Btu of heat are required to produce one ton of recoverable lime. This figure compares favorably with a well-run modern shaft kiln and is lower than that required for a modern rotary kiln, where 7 to 8 million Btu will be used. In the New England area where fuel costs are high this is an important saving.

On the debit side is the fact that yield of lime from stone is only about 76 pct of theoretical, as compared to 100 pct in a shaft kiln and 90 pct or thereabouts in a rotary kiln. Recoveries obtained in the 3-stage pilot furnace, with feed quality only slightly better than that currently being processed, were of the order of 90 pct, which would be considered satisfactory. Reason for greater dust loss in the commercial unit has not yet been determined.

Quality of the fluidized product is excellent. Repeated analyses of the product show the residual CO_2 contents to be less than the 0.15 pct representing 99.8 pct removal of CO_2. To obtain this degree of calcination in a rotary or shaft kiln would require operating temperatures in excess of 2000°F, which would tend to flux the impurities with the CaO, thus lowering the available lime content of the finished product. Fluxing is not appreciable in the temperature range of 1800° to 1900°F employed in the fluidized process. As a result the available lime contents obtained in the fluidized product approach very closely those predicated by the stone analyses.

Reactivity of the lime with water can be made to vary by changing the burning temperature. Whereas the normal product has a reaction speed of 60 sec when slaked with 2½ parts water at 100°F, the rate can be advanced or retarded through a range of 25 to 400 sec by lowering or raising the temperatures from the normal operating point of 1860°F.

In summation, the first attempts to apply fluidized solids technique to the manufacture of lime burning have resulted in a new method for drying and sizing limestone on a large scale and an efficient method for calcining limestone to a quicklime of high quality.

Acknowledgments

We are indebted to the engineers of the Standard Oil Development Co. and the Dorr Co. who developed the fluidization technique, to C. C. Loomis of New England Lime Co., who encouraged these particular applications, and to W. J. Barrett for preparing the photographs.

References

[1] F. S. White: Operation of the Pilot Size FluoSolids Lime Reactor. *Pit & Quarry* (January 1948).

[2] C. J. Wall and W. J. Ash: Fluid-Solid Air Sizer and Dryer. *Industrial and Engineering Chemistry* (June 1949).

Economic Aspects of Sulphuric Acid Manufacture

by William P. Jones

THE consumption of sulphuric acid, one of the most important commodities in our modern industrial world, is often used as a barometer for industrial activity. The economics of acid manufacture are largely dependent upon the location of the place of consumption and the availability of raw materials in that locality.

Sulphuric acid is made from SO_2, oxygen from the air and water. Therefore the sulphur dioxide is the only raw material to be considered in an economic study. SO_2 can be obtained from almost any material containing inorganic sulphur, such as elemental sulphur, pyrites, coal, sour gas and oil, metallurgical gases, waste gases, or gypsum and anhydrite. Many tons of acid can also be reclaimed by the recovery and concentration of spent acids.

The aim of this paper is to present a guide to the economic aspects to be considered when the installation of an acid plant is contemplated. It must be remembered that 1 ton of elemental sulphur produces 3 tons of sulphuric acid and that the shipping of sulphuric acid by tank car is very costly. The size of the plant must also be given careful consideration. For instance, operation of a plant producing 5 tons of acid per day might be warranted in Brazil or Pakistan, whereas economics usually favor buying quantities up to 50 tons per day for use within the United States.

Elemental sulphur, when available at the low price of 1½¢ per lb delivered at an acid plant, has always been the raw material most frequently used for sulphuric acid. All conditions favor its use at this price.

The so-called sulphur shortage has been the subject of so many technical papers, magazine articles, and newspaper items during the past year that it hardly seems necessary to mention it again, but a very brief review of the matter will serve as a foundation for the discussion that follows.

There is no shortage of sulphur. Only a shortage of low-cost Frasch-mined brimstone exists today. Other more expensive sulphur-bearing materials are plentiful, both in the United States and abroad. The low cost of Frasch-mined brimstone has discouraged the development of higher cost sources. However, the approaching depletion of Gulf Coast dome deposits and the greatly increased demand for sulphur here and abroad have made it necessary for industry to prepare for conversion to utilize sulphur in other forms. For future planning this situation must be considered permanent and not temporary. This conclusion is based on the fact that although sulphur demand will continue to rise, the production of Frasch-mined sulphur probably will not increase greatly beyond its present level of about 5,000,000 long tons per year.

The International Materials Conference in Washington estimates 1952 requirements of the free world at nearly 7½ million long tons; and the Defense Production Administration has recently set a new goal for 8,400,000 long tons annual domestic production by 1955. The total sulphur equivalent produced in this country in 1950 was 6 million tons. What, then, are the alternatives for the manufacture of the vital chemical, sulphuric acid?

Today about 85 pct of this country's sulphur, and nearly 50 pct of the world supply, comes from our Gulf Coast salt domes and is extracted from the earth by Frasch's hot water process. The Gulf Coast salt dome deposits have been the most important known natural deposits in the world, producing 90 million tons of sulphur during the past 50 years. However, at the present rate of extraction these deposits cannot be expected to last indefinitely.

Pyrites

Pyrites are, and have been for many years, the source of more than 50 pct of the world's sulphur requirements. The principal use, of course, is in the manufacture of sulphuric acid. The use of pyrites in the United States has diminished greatly because of the availability of low cost native sulphur, but pyrites have continued a major source of sulphur in many other countries.

The most available pyrites for use in this country are in the form of lump pyritic ore and in mill tailings from flotation of other minerals such as lead, zinc, copper, gold, and silver. An important factor, when the use of pyrites for acid manufacture is being considered, is the disposal of calcine. A ton of sulphuric acid requires approximately ¾ ton of high-grade pyrite and results in ½ ton of calcine. If the calcine is a fairly pure oxide, free of harmful impurities, it can be used, after sintering, in an iron blast furnace burden. Its value might be as high as 15¢ per unit of Fe at the blast furnace; or possibly $10.00 per ton of sinter, if it assays 65 pct Fe. This might result in a credit of $4.00 per ton of acid if the sintering plant and blast furnace are both located adjacent to the acid plant. On the other hand, several factors must be considered before this credit can be realized, i.e., freight to blast furnace, availability of sintering facilities, methods of eliminating impurities, and the removal of valuable metal values. In some locations it would be most economical to dump the calcines.

W. P. JONES, Member AIME, is General Manager, Chemical Construction (Inter-American) Ltd., Toronto.

Discussion on this paper, TP 3418H, may be sent (2 copies) to AIME before Nov. 30, 1952. Manuscript, Feb. 20, 1952. Revised Aug. 28, 1952. New York Meeting, February 1952.

This page of Mining Transactions AIME follows p. 906. The intervening non-Transactions pages appeared in Mining Engineering.

Lump pyrite and pyrrhotite sometimes run as high as 49 pct S and 45 pct Fe. When this material contains no detrimental impurities it is ideal for the manufacture of sulphuric acid. It must be crushed and ground before it can be burned in a flash or flue-solids roaster, but the resulting calcine, after sintering, brings a premium as blast furnace burden. Lump material is easier to ship and can be stockpiled without appreciable loss due to oxidation.

On the other hand, lump pyrite is usually higher in cost per unit of sulphur, since the selling price must pay for the cost of mining, shipping, and profits. The higher credits for the calcine must be used to offset this additional cost.

The largest readily available source of pyrites in North America is in the form of flotation mill tailings. Most of the copper, lead, zinc, gold, and silver being mined and milled is associated with pyrite. The ore is treated by flotation for the metal values and usually the tailings contain from 20 to 35 pct sulphur in the form of iron pyrite. Because of the low market demand for pyrites during the past several decades, most of these tailings have been stockpiled. Such mill rejects can often be upgraded to 45 to 50 pct S content by another flotation treatment, as pyrite is an easily floated mineral. Capital investment is needed only for flotation equipment, thickeners, dewatering filters, and driers.

Although mill tailings can be purchased at a considerably lower price than lump pyrite and may be equally useful for making acid, the value of the calcines may be greatly decreased for blast furnace burden because of the presence of excess amounts of copper, lead, or zinc.

The capital investment for a pyrite-burning acid plant is approximately twice that for a brimstone plant. Naturally, operating, maintenance, and amortization costs are also higher, owing to the greater amount and complexity of the equipment necessary to produce clean SO_2 from pyrites. Pyrite roasters are required, and an extensive purification train as compared to a simple sulphur combustion chamber for converting brimstone into SO_2.

Pyrites Converted into Sulphur and SO_2

There are a number of places around the world where the supply of pyrites is abundant but where there is no source of elemental sulphur, and there are some uses where it is undesirable to convert sulphur into SO_2 as is done for the manufacture of acid. A process under development now by the Noranda Mines Ltd. of Canada is very interesting in that it converts about 1/3 of the total sulphur, the labile atom, in pyrites into elemental sulphur and the remaining 2/3 into SO_2 which can be converted directly into sulphuric acid. In this way pyrites are converted into three usable products, namely, elemental sulphur, sulphur dioxide, and iron oxide sinter. The successful development and demonstration of this process would be very important to the industrial economy of a number of locations throughout the world.

The greatest waste of sulphur in any form is probably that found in the presence of coal. Not only do huge amounts of sulphur go into the atmosphere from the combustion of coal, but undetermined quantities are deposited on the refuse piles found near coal washers. Many coals contain considerably more than 1.5 pct sulphur, and these must be cleaned before being used for metallurgical purposes. High sulphur coals are to be found across the main coal belt extending from western Pennsylvania through the middle west to Kansas. All through this region coal-cleaning plants are discarding refuse containing 3 to 12 pct sulphur.

To be of value as pyrite, refuse from these plants must be reconcentrated to upgrade the pyrite and reduce the carbon content. The pyrite concentrate should assay not less than 30 pct S and not more than 6 pct C for consideration as acid-plant raw material. Heavy media, tabling or flotation might be used for the concentration of coal brasses, depending upon the characteristics of the washing plant refuse. Coal brasses would be an economical raw material for sulphuric acid manufacture only when the market for the acid is in close proximity to a coal washer capable of producing a large tonnage of low carbon, high sulphur pyrite. The low sulphur values to be found in coal brasses prohibit shipping any great distance.

Spent Oxide

In Great Britain spent oxide from the many gas plants and coke oven plants provides a very significant amount of sulphur. In 1948, the sulphur from nearly 200,000 tons of spent oxide was converted into acid in Great Britain. One of the main phases of England's sulphur conservation program is for the utilization of spent oxide sulphur. However, in the United States the amount of spent oxide available is steadily decreasing to a point where it scarcely becomes a factor in the sulphur picture. The utility companies in New York City have the largest current production of spent oxide in the country. This product runs about 33 pct sulphur, and the total yearly tonnage amounts to only about 1,600 tons of sulphur. It is believed that all the spent oxide on the northeastern seaboard, from Washington to Boston, would total only 25 tons of sulphur per day. Although there are still a number of the larger cities in the West and Midwest that produce spent oxide, the amount available in any one locality is small. Increased use of natural gas throughout the country is causing the gradual decline of this material.

Sour Gases

The sulphur present as an undesirable impurity in many types of industrial gases represents an appreciable potential source of sulphur for sulphuric acid. Exploitation of this source has been started within the past few years. Among the gases which contain available sulphur are sour natural gas, refinery tail gas, manufactured or water gas, and coke oven gas, most of the sulphur being in the form of H_2S. Many problems are posed by the presence of one of the most toxic of gases, hydrogen sulphide, which is corrosive to pumps, pipelines, and other transmission equipment. Generally, therefore, the H_2S must be removed from these gases before they may be utilized, and to a much greater extent than would be economical for sulphur recovery alone.

Consequently, a considerable portion of the work necessary for the recovery of commercial grade sulphur from these varied gases has been accomplished, with the result that the cost of recovering sulphur will not be as great as would be initially imagined. However, the real economy of utilizing the sulphur in sour gases lies in large volume operations. If the source of sour gas is near a market for sulphuric acid, the H_2S can be removed from the gas and burned directly in an acid plant. This results in one of the most economical acid plants. Unfortunately, the source of large volumes is usually remote from large acid markets, and then the H_2S is partially burned to SO_2, which reacts with the remaining H_2S in the presence of a catalyst to form elemental sulphur.

Metallurgical Gases

The total sulphur emitted to the atmosphere from zinc, lead, copper, and nickel smelters is annually greater than the entire world's native sulphur production. A large quantity of this sulphur can be economically recovered in the form of sulphur or sulphuric acid. However, the big drawback is the location of such smelting operations in relation to the markets for sulphur and acid.

Two companies, Consolidated Mining & Smelting Co. in Canada and American Smelting & Refining Co., have pioneered the research and development of processes for the utilization of sulphur from smelter gases. Consolidated takes 400 tons of sulphur out of 500 million cu ft of waste gases. From these it produces 1,100 tons of sulphuric acid daily, which then is used in the production of fertilizers.[1] All gases from the lead sintering, zinc roasting, and even the acid plants are treated and about 90 pct of the total sulphur values removed and converted to acid.

The flue gases from the combustion of coal and tail gases from a large number of industrial operations contain a small amount, usually only a fraction of a percent, of SO_2, which has always been considered far too weak for economical recovery. An estimated 25 million tons of sulphur go into the atmosphere annually from the combustion of coal alone.

Sulphur dioxide is the most common source of air pollution in the world today. Municipalities and public opinion are becoming more and more conscious of the problem, and eventually utilities may be forced to remove the sulphur compounds from their stack gases. Recent studies[2] indicate that economical recovery of sulphur from such low concentration gases is a distinct possibility, and large quantities of acid could be made at competitive costs.

Gypsum and Anhydrite

Deposits of gypsum, $CaSO_4 \cdot 2H_2O$, and anhydrite, $CaSO_4$, are plentiful throughout the world, and these materials are being used, to a limited extent, as raw materials for the manufacture of sulphuric acid.

The Muller-Kuhne Process was developed in Germany during the first World War, and a commercial plant producing 500 tons of H_2SO_4 per day was later built at Wolfen, Germany, where an ideal combination of raw materials and market for acid and cement existed. In order to make such an operation practical, there must be a saleable lime or cement produced from the calcium in the gypsum. Imperial Chemical Industries have this same combination of circumstances at Billingham in the north of England. Other plants are now under construction for making acid from gypsum in both England and Austria. These developments were undoubtedly brought about by the world shortage of sulphur and sulphuric acid.

The process consists essentially of roasting ground gypsum, or anhydrite, in a rotary kiln, with clay and fuel, such as coke. The basic reaction is

$$CaSO_4 + \tfrac{1}{2} C = CaO + SO_2 + \tfrac{1}{2} CO_2$$

The clay combines with the CaO to form cement clinker, and the SO_2 gas goes off through a purification system and to a contact acid plant.

Although this process sounds extremely simple, it must be understood that considerable operating and control difficulties are encountered; it is doubtful that the process could be used to advantage in this country where so many other more favorable raw materials exist.

A plant producing 100 tons of acid per day would also produce 100 tons of cement. This is generally considered too small to be economical for a cement plant. Therefore, it seems more logical to build a cement plant of 500-ton capacity, or more, and make H_2SO_4 in quantity required, as a byproduct, from a kiln using gypsum as the raw material. The production of sulphuric acid from gypsum can be regarded as feasible only if cement, or lime, is the main product, the acid being produced as a valuable byproduct. In addition, the plant must be located near the site of the gypsum deposit and the market for the acid must be nearby.

Recovery of Spent Acids

In many cases, sulphuric acid is used in such a way that it is not destroyed and does not go into the product, but it is diluted with water and sometimes other contaminants. Acid used in the manufacture of alcohols, explosives, oils, gasoline, detergents, titanium, and steel, for example, can be recovered by concentration or by decomposition.

The U. S. oil refinery industry ranks high on the list of consumers of sulphuric acid, using about 1.5 million tons per year. This acid does not pass into the product, so that a large percentage is available for recovery. The spent acid is contaminated with petroleum sludge. A refinery must make provision for disposal of its acid sludge, and this is one of the industry's major problems. Some refineries dump this waste product on vacant land, some burn it with other fuel under boilers, and others have installed facilities for recovery and concentration.

Some refinery-spent acids, such as that from alkylation gasoline plants, are high enough in strength and low enough in impurities to be utilized in a number of ways without treatment, provided a suitable market is close to the refinery. This acid at 85 to 90 pct strength can be transported, since it is not viscous and does not attack steel. Alkylation spent acid is being used for the manufacture of fertilizers, and a number of other uses are being found for it. Where no market for such a product exists, alkylation acid must be regenerated into a clean acid. Other spent refinery acids can also be reconcentrated in plants designed especially to deal with various contaminating constituents. The initial cost of such plants is high for small tonnages.

Recovery of sulphuric acid from steel mill pickle liquor is also now feasible, since the cost of new acid is rising. Pickle liquor can readily be concentrated up to 60 pct acid and re-used in pickling baths.

Relative Costs

As previously stated, the largest single factor in any decision regarding raw materials for sulphuric acid is the cost and availability of the materials. Therefore, transportation costs play a very important part in the decision. Table I gives approximate investment and production costs for the various raw materials discussed, at production of 100 tons of H_2SO_4 per day. Both investment and production costs vary greatly per ton capacity with the size of plant. It must be noted that the raw material cost has a great effect on the total cost per ton of acid produced. Table I also shows that acid can be produced more economically by other materials than elemental sulphur, when that raw material is available at little or no cost.

Table I. Comparative Unit Costs Per Daily Ton H_2SO_4, Based on 100 Net Tons Per Day

Raw Material	Capital Investment		Raw Material Cost, $	Cost Per Net Ton 100 Pct H_2SO_4	
	Per Daily Ton Capacity, $	Factor		Raw Material	Total Cost, $
Weak acid, 52 pct	3,500	0.6		None	5.60
Sulphur	6,000	1.0	30.00*	9.20	15.10
Weak acid, 30 pct	6,000	1.0		None	10.00
Zn roaster gas	7,500	1.25		None	8.90
Hydrogen sulphide	8,000	1.33	22.00*	6.90	14.90
Alky. spent acid, 87 pct	11,000	1.84		None	12.40
Pyrites	12,000	2.0	20.00*	6.40	19.00†
Refinery sludge, 55 pct	15,000	2.5		None	17.80
Anhydrite	17,500	2.9	2.00**	3.20	25.70

* Per long ton of sulphur equivalent.
** Per ton of anhydrite.
† No credit for calcines.

The $30.00 sulphur cost is taken as an average cost of sulphur delivered, based on the present $22.00 f.o.b. Texas Gulf Mines. With this table as a guide, it requires little arithmetic to see that further increases in the price of sulphur will force more and more acid manufacturers to convert or initially construct for the use of other raw materials.

Every raw material listed, except anhydrite, is currently being used in this country for the manufacture or concentration of acid.

References

[1] R. A. King: Economic Utilization of Sulphur Dioxide from Metallurgical Gases. *Industrial Engineering Chemistry* (November 1950) **42**, pp. 2241-2248.

[2] H. F. Johnstone: Recovery of Sulphur Dioxide from Dilute Gases. Delivered at Canadian Pulp and Paper Association, Montreal, Jan. 24, 1952.

[3] Ralph H. Espach: Sources of Hydrogen Sulphide in Wyoming. *Industrial Engineering Chemistry* (November 1950) **42**, pp. 2235-2237.

[4] E. P. Fleming and T. C. Fitt: High Purity Sulphur from Smelter Gases. *Industrial Engineering Chemistry* (November 1950) **42**, pp. 2249-2253.

[5] W. T. Lundy: Known and Potential Sulphur Resources of the World. *Industrial Engineering Chemistry* (November 1950) pp. 2199-2201.

[6] *Oil and Gas Journal*, Special Report: Oil's Sulphur Boomlet. Jan. 14, 1952.

The Cement Industry of Mexico

by Luis Elek

DEVELOPMENT of the cement industry in Mexico began some 40 years ago. It has gradually reached great importance in the economic life of the country and has contributed greatly to the technical and economical advances which have been so noteworthy, particularly during the last 15 years.

From a modest start, the industry now comprises 18 cement-producing plants having a potential annual capacity of approximately 14 million bbl. About half the plants were built and equipped with second-hand machinery during the last world war when no new machinery could be procured. They will hardly attain full production before being modernized and reconditioned, a job now under way in several of the plants.

At present, the yearly consumption is only about 8 to 9 million bbl but is steadily increasing. This is only a fraction of the cement consumed in the U.S.A., which is about 250 million bbl per year, although on the basis of consumption per capita per year, the figure is 1/3 bbl for Mexico and 1 2/3 bbl for the U.S.A. Cement consumption in Mexico is well above the average of all other Latin American countries, with the exception of the Argentine, and considering the potentialities and undeveloped riches of Mexico, the road construction and irrigation works, it is fair to assume that the Mexican cement industry will still prosper and expand in spite of temporary setbacks in the future caused by local events of economic or political nature.

Portland cement is manufactured by burning a mixture of raw materials, one of which is mainly composed of calcium carbonates and the other of aluminum silicates. The most typical materials answering this description are limestone and clay, both of which occur in Mexico in many varieties. To be usable for cement manufacture limestone should contain at least 77 to 80 pct calcium carbonate. Lower grade limestone can be used for cement manufacture only if the lime content is increased by the beneficiation process, which has not yet been adopted by the Mexican cement industry. Most of the limestone used by Mexican cement plants has a calcium carbonate content of 90 to 95 pct and therefore requires addition of one or several correction materials. A typical composition of raw mix for cement manufacture is 85 pct limestone and 15 pct shale, clay or volcanic materials.

Occasionally it is necessary to add a smaller amount of sand or other siliceous material to increase the silica ratio in the raw mix. Likewise, it is sometimes necessary to add 1 or 2 pct iron ore to facilitate fusion in the kiln and to obtain proper relation between alumina and iron oxide. After calcining and

---

LUIS ELEK is Production Manager of La Tolteca, Compania de Cemento Portland S.A. and Cemento de Mixcoac, S.A.

Discussion on this paper, TP 3413H, may be sent (2 copies) to AIME before November 30, 1952. Manuscript, November 14, 1951. Mexico City Meeting, October 1951.

clinkering in the rotary kilns, the cement produced should have about the following composition:

Feed	Pct
SiO_2	21.5
Al_2O_3	5.1
Fe_2O_3	3.0
CaO	63.6
MgO	2.4
SO_3	1.8

The tendency in Mexico has been to locate the cement plants as near as possible to the consumption centers, such as Mexico City, Guadalajara, and Monterrey. As the limestone deposits, unfortunately, do not always follow the populated areas, it is sometimes necessary to haul the limestone over considerable distances from the quarries to the cement plants. Transport is generally by rail, and since the railroads are inadequate to meet the demands of the industry, severe difficulties are often encountered. Limestone for the cement plant in Guadalajara is brought in over 100 miles of railroad, and precrushed rock for the two cement plants on the outskirts of Mexico City is hauled for a stretch of 40 miles.

All the limestone quarries in Mexico are worked in open pit with drilling and blasting in the conventional manner. Blasted rock is generally handled by power shovel and transported in trucks to the crushing station; a typical installation consists of a pan feeder for uniform feed to the primary crusher, which normally is a jaw or gyratory crusher, followed by a vibrating screen from which the oversize material passes through a secondary crusher, often of the hammermill type. The rock is generally crushed to max 1-in. size and the tendency is to reduce it to ¾ in. or even less to improve the efficiency of the raw grinding mills in the cement plant.

The process of cement manufacture consists of grinding raw materials to form a fine homogeneous mixture, burning the mixture in a kiln to form a clinker, and grinding the clinker with the addition of a small proportion of gypsum to a fine powder. Either the wet or dry process is used, depending on local conditions, the nature of the raw materials, availability of water, and cost of fuel. In general it is considered that a more accurate control of the raw mix composition is possible with the wet process, but the fuel consumption is higher than in the dry process.

Regarding the raw grinding, most of the installations in Mexico are laid out in traditional manner, with preliminary grinding in a ball mill followed by final grinding in a tube mill, both working in open circuit. Lately some plants have adopted more modern closed circuit grinding in comparatively short mills using an airswept circuit and separator, thus obtaining high grinding efficiency and low power consumption, sometimes 2.5 kw-hr per bbl. Usually about 90 pct raw meal passes 200 mesh. These installations refer to plants employing the dry process, for various reasons used almost exclusively in Mexico. Of the 18 cement plants, only 3 are wet process plants, the raw material being ground together with water in ordinary compartment mills until about 90 pct of the slurry passes 200 mesh.

Since the composition of raw materials varies, there is considerable variation in the chemical composition of raw mix leaving the mills. As it is important, however, to obtain a uniform composition of raw mix entering the calcining kilns, a system of homogenization must be installed in connection with the storage silos for the ground material. Homogenization is normally performed by blending silos; sometimes a blending system is used with compressed air, thereby restraining variations of the calcium carbonate titration within very narrow limits.

Calcining and clinkering of the raw mix is performed in rotary kilns. In the 18 cement plants at present operating in Mexico, 46 rotary kilns are installed and 7 more are in the process of being installed. In Mexico the size of the kiln varies greatly, ranging from 6 ft in diam by 60 ft long, with a 24-hr production of 150 bbl, to the largest kiln 11 ft in diam by 350 ft long, with an output of 2400 bbl of clinker. The rotary kilns are fired with heavy fuel oil, or, in northern Mexico, by natural gas. During the passage of material through the kiln calcination takes place, and in the burning zone where the temperature is about 2200° to 2400°F, the chemical reactions between the lime, silica, alumina, and iron take place, resulting in a chemical compound which is Portland cement.

The clinker, which is comprised of small pellets, leaves the kiln and is cooled by air in a clinker cooler to recuperate the heat. This preheated air is afterwards used as secondary air for combustion in the rotary kiln. The fuel oil consumption in the rotary kiln is between 15 to 20 pct of the weight of the produced clinker, depending on the thermal efficiency of the kiln installation.

The clinker is finally ground in mills of the long compartment type, or in short ball mills, from whence it is turned into tube mills for additional grinding with about 3 pct gypsum until approximately 90 to 97 pct passes 200 mesh. Cement grinding in closed circuit with air separation is generally adopted to increase the grinding efficiency and capacity of the mill. The ground cement is stored in silos and ready for packing in paper bags or for distributing in bulk to larger consumers.

The cement is produced according to the official Mexican specifications, which in general are very similar to the ASTM specifications, and it can be stated that the chemical and physical properties of the cement produced in the Mexican cement plants complies with the ASTM specifications for Portland cement in the U.S.A. Recently some Mexican cement plants have also introduced the so-called high early strength cement, which is ground to extreme fineness for the purpose of obtaining the highest possible early compression and tensile strength.

The cement industry in Mexico has shown a tremendous expansion in the last fifteen years and suffers from many shortages due to this quick development. In some plants the power supply is insufficient, in others the railways cannot provide the necessary raw materials or transport the finished cement, and sometimes even the oil supply is limited, with the consequence that the industry in 1951 worked at about 80 pct of its capacity in spite of the ever growing demand for cement. Since low output very seriously increases the cost of production, many of the plants could not show a satisfactory profit. In view of the shortage, the price of the cement was fixed by the government with the usual result of this kind of intervention, a black market giving profits to racketeers rather than to the industry. It is hoped that time will cure these difficulties, and the industrialization program of the government augurs a good prospect for the future of the cement industry in Mexico.

Factors in the Economics of Heat-Treated Taconites

by Will Mitchell, Jr., C. L. Sollenberger, and Ford F. Miskell

Heat treatment of ore prior to comminution reduces power requirements for grinding, reduces grinding media wear, and improves recovery of iron values from a typical Minnesota magnetic taconite. Test data demonstrating this, as well as an analysis of the economics of commercial application of the technique, are presented.

THE taconites in general are hard, tough ores, difficult to grind. Liberation of iron mineral constituents usually is accomplished by grinding the ore through at least 100 mesh, and often it has been found necessary to grind substantially through 325 mesh to achieve satisfactory recovery and grade in the concentration process. Because of the fineness of grind required and the enormous tonnages of material contemplated for treatment in the future, costs resulting from grinding media wear and power consumption, together with capital investment required for comminution, approach astronomical figures. Economy in any one of these elements per ton of material ground could very well reflect a considerable saving to the ferrous industry in yearly costs. With this in mind, the Research Laboratories of Allis-Chalmers Manufacturing Co. have launched a program to discover means of effecting this economy. The initial phase of the work as described here deals with a heat treatment of crushed raw ore, followed by thermal shock in cooling, for the preparation of rod mill feed.

Several investigators[1-5] have noted an improvement in the grindabilities of ores treated in this manner. One investigator[2] subjected low grade iron ores to heat treatment in an electric furnace. Basing his conclusions on screen analyses of crushed products, he observed that treated ore was more easily crushed than the untreated. He reported that observation of the treated and untreated ore through a microscope revealed cracks following the grain boundaries in treated ore, whereas no cracks were present in untreated ore. However, few if any have quantified the improvement in terms of total hp hours saved, reduction of wear of grinding media, or reduction of capital costs of grinding equipment involved. By means of Bond rod mill and ball mill grindabilities[6] and by comparative wear tests, the conditions maintained during this investigation have been definitely evaluated.

Heat treatment experiments have been made on a batch scale in a muffle furnace, followed by continuous scale experiments in a rotary kiln under various conditions of temperature, atmosphere, retention time, and quenching to determine the combination that would give the greatest improvement in the grindability of a taconite without affecting adversely the magnetic susceptibility of the magnetite. From these data, relative costs have been calculated for grinding both untreated and heat-treated ore on a basis of plant capacity of 120 tons per hour. Heat requirements for a rotary kiln, as well as the kiln capacity required for the treatment, have been estimated.

Table I. Chemical Analysis of Lower Cherty Taconite, Erie Mining Co.

SiO_2	48.88
Al_2O_3	0.17
Fe_2O_3	27.79
FeO	15.31
MgO	1.64
CaO	0.94
CO_2	3.07
C (organic)	0.06
P_2O_5	0.067
H_2O (combined)	1.74
Total	99.67
Total Fe	31.32

Table II. Mineralogical Analysis of Ore Sample

Mineral	Wt, Pct
Magnetite	30
Siderite	4
Hematite	5
Silicates	18
Minnesotite	
Greenalite	
Stilpnomelane	
Chert	40

For these tests 50 tons of ore were obtained from the Aurora mine of the Erie Mining Co., Hibbing, Minn. The ore was reported[7] to have been selected from the magnetic portion of the lower chert horizons. An average chemical analysis of this portion is shown in Table I and an approximate mineralogical analysis is shown in Table II.

No attempt was made to differentiate between the various silicates because the compositions vary widely on the different horizons and depend on the degree of oxidation. Minnesotite, however, is the predominant silicate. The siderite grains were dispersed throughout the ore but were essentially associated with the rock-forming minerals.

In a series of preliminary tests in which batches of —6 mesh ore were heat-treated in a muffle fur-

WILL MITCHELL, JR., C. L. SOLLENBERGER, Members AIME, and F. F. MISKELL are with Basic Industries Laboratories, Allis-Chalmers Manufacturing Co., Milwaukee, Wis.

Discussion on this paper, TP 3412B, may be sent (2 copies) to AIME before November 30, 1952. Manuscript, Feb. 18, 1952. Revised Aug. 25, 1952. New York Meeting, February 1952.

nace at several temperatures, it was found that slight variations were obtained in the Bond grindability of the samples, determined at 200 mesh. However, it was noted that the circulating loads from the grindabilities became increasingly finer as the treatment temperature was increased. Also the slope of the size analysis curve of the product (Gaudin-Schuhmann plot) became noticeably steeper as this temperature was increased. The same effect was noted with both air and water-quenched products, except that the circulating loads were substantially finer when the treated ore was water-quenched.

It appeared that the grinding characteristics of the ore had changed during the heat treatment, but these changes were not manifested in the grindability value. Observation of the products by means of the petrographic microscope indicated that the grindabilities were being made at a size below the liberation size of many of the constituents of the ore. Fracture across-the-grain appeared to consume an unduly high proportion of the energy. It was obvious that if a conservation were to be made, across-the-grain fractures should be minimized and fracture along grain boundaries increased. A few of the experiments were repeated with grindabilities determined at 100 instead of 200 mesh, and the results substantiated this contention. With increased temperature, an increased grindability at 100 mesh was obtained with the air-quenched product, and an even greater improvement was obtained when the heated ore was water-quenched. Using as a guide the best conditions indicated by the batch experiments, investigators advanced the program to continuous tests in a rotary kiln.

Kiln Tests

The rotary kiln used consists of a cylindrical steel shell in three flanged sections with an overall length of 15 ft 4 in. and a diam of 26 in. The shell is lined with refractory brick, giving an effective inside diam of 16.25 in. It is mounted on a frame with adjustable supports which permit raising or lowering of the shell to any practical slope. The shell is driven by a variable speed motor and is fired with propane gas counter-current to the flow of material. A natural draft system is used. Temperatures can be recorded at 2 ft intervals along the length of the shell by platinum-13 pct rhodium thermocouples imbedded in the refractory lining. An optical pyrometer is used to obtain the temperature of the material being treated as it passes through the hottest zone of the kiln. Fig. 1 is a photograph of this kiln. Feed is introduced 4 in. inside the shell by a 3-in. pipe vibrated with a Syntron mechanism. A retaining ring with an inside diam of 10 in. keeps the feed from overflowing the feed end.

For air quenching, the discharge was collected in the calcine buggy shown in Fig. 1; for water quenching, it was collected in a buggy filled with water.

Retention time was predicted from the formula[8]

$$T = \frac{1.77\sqrt{\theta}\,L\,F}{S\,D\,N}$$

where θ is the angle of repose of the feed (40° for the taconite), L is the length of the shell in feet, S is the slope of the shell in degrees, D is the inside diameter of the shell in feet, N is the speed in revolutions per minute and T is the retention time in minutes. F is a factor required when constrictions are present in the tube. When no constrictions or obstructions are present, F is unity.

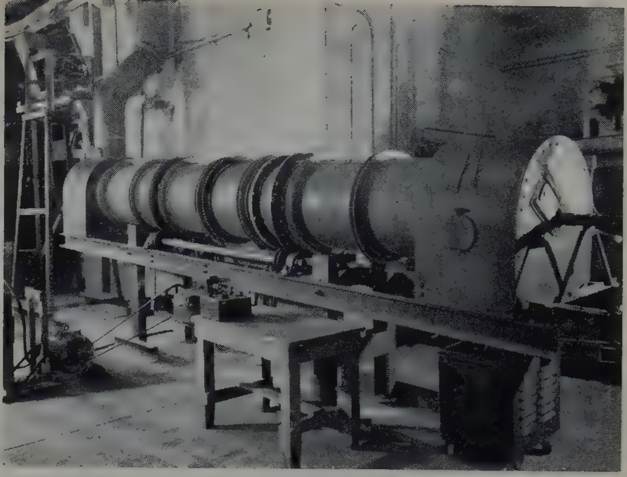

Fig. 1—Rotary kiln, 15 ft x 26 in.

In practice, the volumetric loading of a kiln is usually maintained between 6 and 12.5 pct and is calculated from the formula

$$\text{Loading} = \frac{(CFH)\ (100)}{(60)\ (FM)\ (A)}$$

where CFH is either the feed or product rate in cubic feet per hour, FM is the rate of travel of material through the shell in feet per minute, and A is the cross sectional area of the kiln inside the lining in square feet. In these tests the loading was maintained at 10 pct.

The feed was crushed in a jaw crusher to —3 in., then screened at ¾ in. The oversize was crushed in a Hydrocone crusher and the product, which was about 96 pct passing ¾ in., was combined with the screen undersize. Coke was crushed and screened to —4 +20 mesh for admixing with the taconite when reducing conditions were required.

Two runs were made at 1 hr retention with a hot zone temperature of 1800°F. In the first, no coke was mixed with the taconite, but in the second, 2 pct coke by weight was mixed with the feed. Both air and water-quenched products were collected for each run and rod and ball mill grindability tests made. From the grindabilities, the power required to grind from ¾ in. to 8 mesh in rod mills and from 8 mesh to 100 mesh in ball mills was calculated using Bond's work index formula.[9] The results obtained are shown in Table III.

These results show that practically the same grindability was obtained regardless of the atmosphere used. A considerably higher grindability, however, resulted from water quenching.

To determine whether or not sufficient residual coke remained in the kiln product to cause erroneous

Table III. Effect of Kiln Atmosphere and Type of Quench on Grindability of Product

Atmosphere	Quench	Rod Mill Grindability, 14M G per Rev	Power Requirement, Kw-Hr per Ton	Ball Mill Grindability, 100M G per Rev	Power Requirement, Kw-Hr per Ton
Untreated ore		5.96	2.74	1.15	10.7
Oxidizing	Air	12.1	1.77	1.76	7.38
Oxidizing	Water	24.3	1.15	2.27	6.03
Reducing	Air	12.1	1.77	1.89	6.95
Reducing	Water	22.3	1.22	2.25	6.06

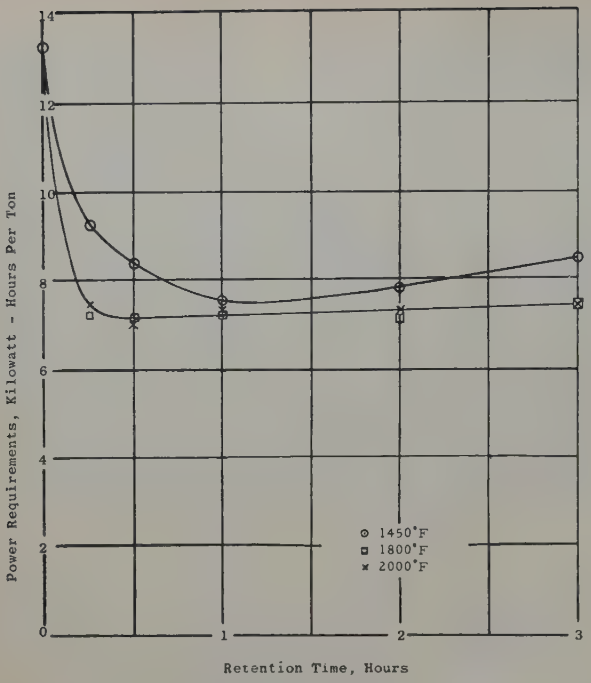

Fig. 2—Grinding power requirements versus retention time at three temperatures.

grindabilities, the —100 mesh grindability product from the run in which coke was used was analyzed for carbon content. It was found to contain only 0.35 pct; obviously any effect on the grindabilities due to carbon would be within the limits of error of the experimental methods used.

A series of runs was made to determine the effect of temperature and retention time on grindability. These were all made with 2 pct coke mixed with the feed, and the products were water-quenched. Runs were made at retention periods of 15, 36, 60, 120, and 180 min. and at burning zone temperatures of 1450°, 1800° and 2000°F as indicated by the optical pyrometer.

From rod and ball mill grindabilities on these products, the total power required to grind from 80 pct passing ¾ in. to 80 pct passing 100 mesh was calculated. The power requirements in kw-hr per ton versus retention time for each of the three temperatures investigated are shown on Fig. 2.

These data show that as the roasting temperature is increased to 1800°F, the power requirement necessary for grinding decreases. Minimum power requirement when a temperature of 1450°F was used was obtained with a 1-hr retention period, and at 1800° and 2000°F with a ½-hr retention period. In all cases power requirements increased slightly with retention periods greater than 1 hr. There appears to be no advantage in using temperatures greater than 1800°F. At 2000°F a black product having a glazed surface was obtained. At temperatures slightly higher than 2000° agglomerates were formed. These latter products were exceedingly friable in the rod mill, but were not so easy to grind in the ball mill as was ore treated at lower temperatures. An examination of Fig. 2 indicates that the greatest overall improvement in grindability was obtained with a burning zone temperature of 1800°F and a retention period in the kiln of ½ hr. It should be explained here that previous experience has demonstrated that the retention period required in a commercial size kiln is double that of the laboratory kiln.

A taconite —2 pct coke mixture was passed through the kiln at a burning zone temperature of 1800°F, and 1 hr retention. The product was water-quenched, then air-dried and passed through the kiln a second time using the same conditions as before, see Table IV. Products were both air and water quenched and the grindabilities determined.

These results show that an additional reduction in grinding power requirements can be obtained by passing the ore through the kiln a second time. However, for the economic comparisons which follow, it was assumed that the treatment of the taconite should consist of a 1-hr pass through a commercial size kiln having a burning zone temperature of 1800°F, followed by water quenching.

Character of Product

The taconite used in the tests contained about 4 pct siderite, $FeCO_3$. One of the advantages of heat treatment was the conversion of the siderite, in a reducing atmosphere, to the magnetic oxide which allowed subsequent recovery in the magnetic concentrate. The —100 mesh ball mill grindability products from the runs at 1450°, 1800°, and 2000°F, all at 1 hr retention, were tested for magnetic susceptibility in a Stearns magnetic tube tester. An increase in the recovery of iron from 86 to 95 pct was obtained, with little effect upon concentrate grade. Maximum recovery was obtained from material treated at a temperature of 1800°F.

Table IV. Effect of a Second Pass

Pass	Atmosphere	Quench	Rod Mill Grindability, 14M G per Rev	Power Requirement, Kw-Hr per Ton	Ball Mill Grindability, 100M G per Rev	Power Requirement, Kw-Hr per Ton
1	Reducing	Water	22.3	1.22	2.25	6.06
2	Reducing	Air	26.5	1.09	2.26	6.04
2	Reducing	Water	31.7	0.97	2.35	5.84

From size analyses of the grindability products as plotted on log-log paper, it was noted that as the grindability increased, the slope of the distribution curve increased. An example of this is shown in Fig. 3. The —100 mesh ball mill product from untreated taconite reported 60 pct passing 200 mesh whereas the heat-treated product reported only 48 pct passing 200 mesh.

This reduction in the amount of fines could well be significant and an advantage, especially in nonmagnetic ores where slimes might inhibit concen-

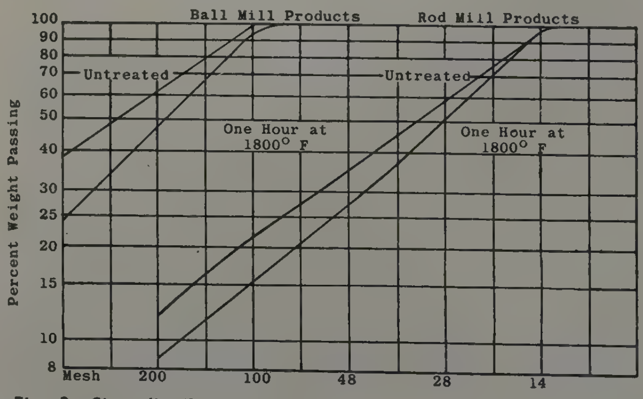

Fig. 3—Size distribution of untreated and heat-treated grinding mill products.

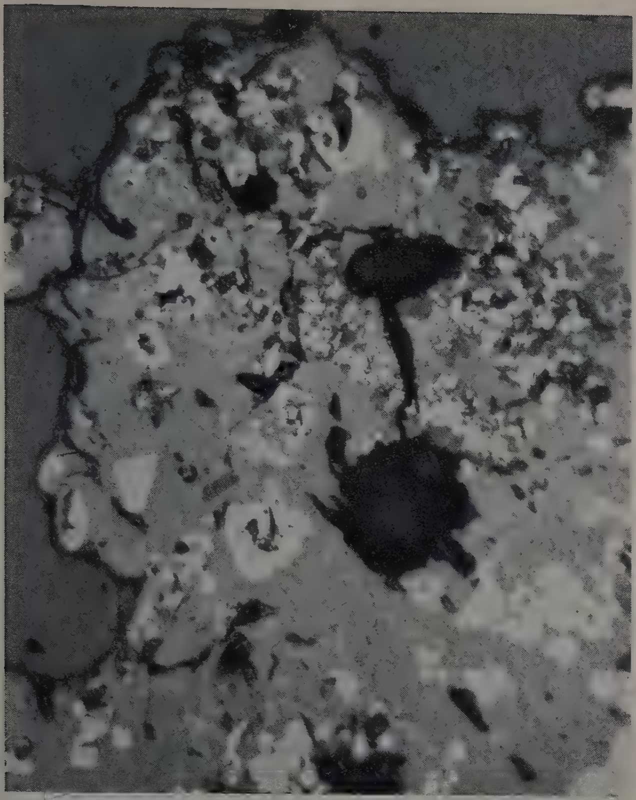

Fig. 4—Photomicrograph of polished section of taconite heated for one hour at 2000°F. Note the coalescense of the magnetite crystals. X250.

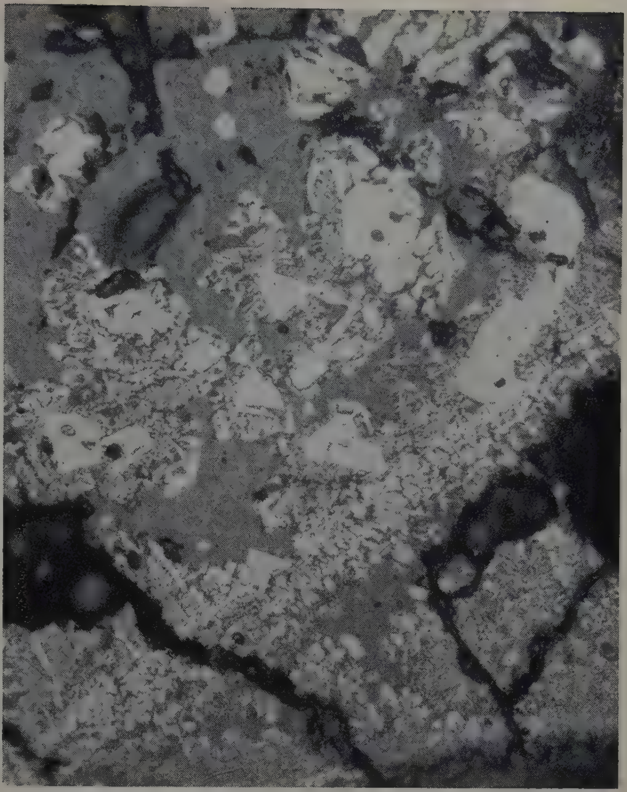

Fig. 5—The same specimen as shown in Fig. 4 illustrates the dendritic growth of magnetite crystals and the coalescense of these dendrites into larger euhedral crystals. X500.

tration. However, it is possible that reduction in fines content might have deleterious effects on pelletization properties of the magnetite concentrates.

Six thin sections and 14 polished sections of untreated feed and heat-treated products were examined microscopically for evidence of recrystallization or cracking which might account for the increases in grindability. No appreciable differences in grain size or crystal development were noted in any of the specimens treated for 1 hr or less below 1800°F, although there was slight evidence of bridging of magnetite grains in specimens treated for 2 hr at 1450°F. In specimens treated at 2000°F, there was abundant evidence of recyrstallization and coalescence of the magnetite. The magnetite had recrystallized into fine dendritic groups. Upon further growth, these dendrites coalesced and formed large euhedral crystals. Fig. 4 shows coalescence of anhedral to subhedral magnetite grains. Fig. 5 shows the dendritic structure as well as coalescence.

A thorough examination of the thin sections resulted in one possible explanation for the increase in grindability. The untreated feed contained siderite dispersed throughout the ore, whereas the heat-treated samples showed an absence of siderite. During the heat treatment, the siderite had been changed to iron oxide. With the chemical change there would be an acompanying decrease in volume from the original space occupied by the siderite to the space occupied by the oxide. The voids thus produced would tend to weaken the structure and increase the grindability. The increase in grindability can also be attributed to the creation of cracks or zones of weakness through differential thermal expansion of the various components of the ore during heating and differential contraction during the rapid cooling afforded by the water quench.

Heat treatment may be accomplished by several means such as the vertical shaft furnace, hearth roaster, sintering machine, fluosolids furnace, or rotary kiln.

From the test work reported here it can be seen that the substantial increase in grindability is, in the main, dependent upon the thermal shock resulting from a water quench of relatively high temperature products; hence a heat recuperating system is practically precluded.

The thermal efficiency of the vertical shaft furnace has been demonstrated by Fred D. DeVaney[10] but it should be noted that the treated product is discharged from the shaft at a temperature in the neighborhood of 300°F. A water quench applied at this temperature would probably not produce sufficient shock to a magnetic taconite. An improved grindability would not be realized, especially where no chemical change or little recrystallization is effected by the heat treatment.

Besides the inherent economic operating disadvantages of a hearth roaster, no thermal conservation over that enjoyed by kiln processing is obvious at this time.

The sintering machine, as well as the fluosolids furnace, operates most effectively on a sized feed, although in combination, one could handle rod mill feed with the fines removed, and the other, ball mill feed. This would assume a screening operation at perhaps 8 to 10 mesh of the raw rod mill feed. Again, a heat recuperating system could not very well be applied in the use of this apparatus for the reasons given above; hence the Btu content of the discharged product, accounting for a large proportion of the heat loss, would be similar to that of a rotary kiln. In view of these factors, the cost of heat treatment was estimated only for a rotary kiln plant.

To heat taconite 1 hr in a kiln having a burning zone temperature of 1800°F, at the rate of 120 tons per hour, an 11-ft 6-in. by 300-ft kiln would be required. Total equipment costs for a kiln plant including drive, controls, burning equipment, exhaust system, conveying equipment, and water quencher would be approximately $451,200.* About 700 installed hp would be required to operate this plant.

To heat one ton of taconite, having an assumed specific heat of 0.3, from 70°F to 1800°F, 1,040,000 Btu's are required. If it is assumed that the radiation loss will be 20 pct of the above figure and 10 pct moisture must be evaporated from the ore, a total of 1,548,000 Btu's are required. When one kiln is used to heat this tonnage of ore to 1800°F, the exit gas temperature may be as high as 1000°F, and fuel efficiency will be about 59 pct.[11] Total heat requirements then are 2,620,000 Btu's per short ton. If bituminous coal having a heat value of 13,800 Btu's per lb is used as fuel, at $0.30 per million Btu's, fuel costs per ton of taconite treated will be $0.79. A kiln plant estimate is shown on Table V.

Economies Effected

As previously noted, one of the advantages of heat treatment of the taconite was an increase in recovery of iron. The ore used in these experiments contained only about 4 pct siderite. For magnetite ores high in iron carbonates a much greater improvement in total iron recovery would be obtained.

Total power required to grind the untreated ore from 80 pct passing ¾ in. to 80 pct passing 8 mesh in rod mills and on down to 80 pct passing 100 mesh in ball mills was calculated from the grindability results and Bond's work index to be 13.44 kw-hr per ton. The power to grind heat-treated ore with the same reduction was 7.44 kw-hr per ton or a saving of 6.00 kw-hr per ton.

To determine the relative abrasiveness of heat-treated and untreated taconite, samples of each were passed through a hammer mill operating at 1800 rpm with two hammers and with grate bars spaced at ⅛ in. Approximately 90 lb of untreated feed were put through the mill to determine the feed rate which would properly load the mill and case harden the wearing surfaces of the hammers and grate bars. Then the samples listed on Table VI were passed through the mill. The hammers and grates were weighed before and after each test. The data obtained are shown on Table VI.

Table V. Estimated Operating Expenses for Kiln Plant Heating 120 Tons Per Hr at 1800°F for Retention Period of 1 Hr

Item	$ Per Ton
Power, estimated available at $0.011 per kw-hr	$0.048
Labor, 4 1/3 men per shift, $1.50 per hr avg	0.0541
Maintenance, 10 pct equipment cost annually, 330 days per year	0.0475
Write-off on installation,** taxes, depreciation at 20 pct of equipment cost annually	0.238
Fuel	0.79
Total	1.1776

** Assumed to be 2.5 times the equipment cost.

Table VI. Pulverator Wear Tests

Item	Untreated	Treated
Total weight of feed, lb	597	423
Feed rate, tons per hr	2.56	3.06
Avg kw demand	12.72	6.80
Power requirement, kw-hr per ton	4.98	2.22
Total wear on grates and hammers, lb per ton	1.697	0.448
Total wear in lb per hp-hr	0.254	0.151

Table VII. Relative Grinding Plant Costs, 120 Tons Per Hr

Item	Cost Per Ton Untreated Ore	 Heat-treated Ore
Power	0.148	0.082
Labor	0.021	0.021
Maintenance	0.034	0.021
Write-off	0.182	0.105
Ball and rod maintenance	0.189	0.062
Liner maintenance	0.019	0.006
Total	0.593	0.297

One rule of thumb states that ball and rod wear are directly proportional to the horsepower hours per ton required to grind an ore and that this wear is about 0.15 lb of metal per horsepower hour for magnetic taconite. This same rule states that liner wear is roughly 10 pct of the ball and rod wear. Using this rule and the same ratio of wear for untreated and treated ore obtained in the hammer mill tests, it was calculated that for untreated ore, ball and rod wear is 2.7 lb per ton and liner wear is 0.27 lb per ton. For treated ore, ball and rod wear is 0.88 lb per ton and liner wear is 0.088 lb per ton. By heat-treating the ore, a wear saving of 1.78 lb of metal per ton of ore milled should be possible.

For a basis of comparison of capital equipment costs, a convenient tonnage was 120 tons per hr or 2880 short tons per day. To grind this tonnage of untreated ore, one 10½x12-ft overflow rod mill and two 10½x12-ft overflow ball mills would be required. To grind heat-treated ore, one 9x12-ft overflow rod mill and one 10½x14-ft overflow ball mill would be required.

The omission of the one mill would probably make little difference in the number of men required to operate the grinding circuit with the tonnage used as a basis. Consequently labor costs should be essentially the same.

For a comparison of grinding plant costs, each plant handling 120 short tons per hr, the following assumptions were used. Metal replacement cost was assumed to be $0.07 per lb and power was assumed to be available at $0.011 per kw-hr. Labor requirements were assumed to be 1 2/3 men per shift at an average hourly rate of $1.50. Annual maintenance costs were assumed to be 10 pct of the equipment costs and the total installation was assumed to be 2.5 times the equipment cost. Write-off on the installation, taxes, and depreciation were assumed to be 20 pct of the equipment cost annually. A 330-day year was used. Total equipment costs for grinding untreated ore were estimated at $326,897. For grinding treated ore these costs were estimated at $200,119. The relative costs for grinding treated and untreated ore are shown on Table VII. Table VII shows that heat-treating the taconite ore makes possible a saving of $0.296 per ton in grinding costs.

Conclusion

At the present time, with the conventional apparatus available today for pyroprocessing, heat costs generally are high in comparison to power costs in comminution. It was found that on a basis of plant capacity of 120 tons per hr the saving in overall grinding costs would be $0.30 per ton, whereas heat treatment in a rotary kiln installation would cost about $1.18 per ton.

---

* Based on 1951 U.S. dollar.

The heat treatment of ores in general solely to reduce grinding costs probably cannot be justified on that basis alone at the present time. However, this technique does furnish the additional advantage of reducing grinding media wear, and in this particular case improves the recovery of iron brought about by the conversion of siderite to magnetite. The saving attained through increased iron recovery has not been included in the economic comparisons.

The substantial reduction in the percentage of slimes produced during grinding of heat-treated ore could enhance the applicability of the flotation process in nonferrous beneficiation, and coupled with the other advantages might justify the pyroprocessing.

Acknowledgments

Acknowledgment with thanks go to G. V. Woody for suggesting this problem to us and for his good advice, to J. A. Mandarino for the microscopy, to W. F. Hackett, J. T. Dingle, R. Norlander, and A. K. Boszhardt for their work on the preliminary tests, and to H. K. Ihrig for help with the manuscript.

References

[1] V. I. Karmazin: Combined Roasting and Magnetic Concentration of Iron Ore. *Gornyi Zhur.* **120,** No. 9/10 (1946) pp. 28-35.

[2] Maschinenbau-Anstalt Humboldt: Treating Iron Ores. British Pat. 234, 377 (Nov. 11, 1924).

[3] P. J. Holmquist: Influence of the Microstructure and Roasting on the Crushing Properties of Certain Iron Ores. *Jernkontorets Ann.* (March 1932) **116,** pp. 119-148.

[4] E. O. E. Tyden: Further Concentration of Previously Concentrated Iron Ore Slime. Swedish Pat. (April 16, 1935).

[5] L. E. Schiffman, C. S. Lawson, and J. T. Blakemore: Iron Ore Concentration. U. S. Pat. 2,240,718 (May 6, 1941).

[6] F. C. Bond: Standard Grindability Tests Tabulated. *Trans.* AIME (July 1947), MINING ENGINEERING (1949) **183,** pp. 313-329.

[7] Fred D. DeVaney: Personal communication.

[8] U. S. Bur. Mines TP 384 (1927).

[9] F. C. Bond: The Third Theory of Comminution. *Trans.* AIME (1952) **193,** pp. 484-494.

[10] Fred D. DeVaney: Magnetic Roasting of Lean Iron Ores. Presented Annual Meeting AIME. New York, February 1952.

[11] *Power.* (December, 1948) p. 116.

Technical Note

The Tromp Heavy Media Process

by John Griffen

THE distinguishing principle of the Tromp process is the use of a medium in the bath which is not stable, i.e., the solids will settle and the density of the medium increases with depth. A medium of uniform density can most easily be effected by agitation or by means which increase the viscosity of the medium. Either of these works against the sharpness of separation of coal from its impurities.

The Tromp process grinds the medium solids to relative coarseness, allows them to settle downward in the bath without hindrance, and introduces horizontal currents of medium at intermediate levels between top and bottom of the bath. This prevents any accumulation of particles denser than the upper layer of the medium from which the clean coal is conveyed away or an accumulation of particles lighter than the bottom layer or medium whence the refuse is removed. In a relatively shallow bath making a two-product separation, the intermediate horizontal currents sweep these intermediate gravity materials away to be discharged with the refuse removed by the conveyor. Such a system provides a number of advantages.

The gravity of separation can be changed simply by changing the density of the medium without changing particle size of medium solids or other conditions, as would be necessary with a system requiring uniform or stable density throughout the bath. Some installations in Europe separate at 1.40 sp gr on one shift, producing a superclean coal, and on the next shift reclean refuse from dry cleaning units and effect a separation at 1.80 sp gr.

Medium solids may be much coarser in size consist, which reduces the viscosity of the medium and promotes its fluidity and in turn the sharpness of separation. Coarser medium solids with a more rapid settling rate are much more easily recoverable from the dilute medium rinsed from the products.

The Tromp process is not limited to the use of medium solids having magnetic properties. Instal-

---

JOHN GRIFFEN, Member AIME, is a Chemical Engineer with McNally Pittsburgh Manufacturing Corp., Pittsburgh.

The subject of this paper, TN 131F, is discussed by the author at greater length in a paper scheduled for publication in the Blast Furnace, Coke Oven and Raw Materials Proceedings, AIME, 1952, Vol. 11. Manuscript, March 13, 1952.

lations in Europe use a variety of solids which have the required specific gravity to produce the desired bath densities having the desired fluidity. Magnetite is being used in some instances.

A particular method of recovery and reconditioning of the medium solids from the rinsings is not peculiar to the Tromp process. In its early development, some fifteen years ago, gravimetric methods of recovery were first used, even though a magnetite medium was employed. Magnetite has the advantage of being readily recoverable from the rinsings by fairly simple means, consisting of screening at 60 to 70 mesh to remove the coarser shale and coal impurities and afterward classifying in a simple conical tank to remove the slimes contamination from the raw coal treated.

Magnetic recovery and reconditioning can be used if magnetite or other magnetic solids are utilized. However, these operations, as employed in commercial enterprises, have been so successfully accomplished by the combination of screens and hydraulic classification that they seem preferable to magnetic methods.

As carried out in connection with the Tromp process gravimetric recovery offers some advantages, particularly when separations are made below 1.8 sp gr. With the bath medium at densities lower than this figure, the average density of the medium solids can be well below that of reasonably pure magnetite and yet have a relatively low percentage of solids by volume which will assure a fluid medium. For example, with separation at 1.45 sp gr, if the average density of the medium solids is 3.25, the percentage of solids by volume will be only 20 pct and the viscosity of the medium will be exceedingly low. These medium solids would contain only about 40 pct by volume of magnetite, sp gr 5.0, the balance being mainly coarser shale contaminating solids.

The amount of medium which must be removed from the bath is a function of the contaminating solids entering the bath with the feed. It is readily seen from the above paragraph that, with a given contamination, the amount of magnetite which must be handled in the recovery system is reduced when the solids in the rinsings contain only 40 pct by volume of magnetite.

Furthermore, a high recovery of magnetite is promoted by the fact that a high proportion of the recovered solids are the coarser portion of the contaminating solids. Tests on the solids in recovered medium show that the coarsest sizes consist of shale contaminated with a little coal while the intermediate sizes are largely shale and the finest sizes are magnetite with some shale. The following is an example:

Microns	Wt, Pct	Solids, Sp Gr
150	2.0	1.84
150 to 120	4.0	1.98
120 to 88	12.8	2.60
88 to 0	81.2	4.06
Total	100.0	3.57

The classification effected by the gravimetric recovery system makes the contaminating solids recovered and re-used as medium fairly coarse, which in turn reduces the viscosity of the medium. Experience has shown that these coarser shale particles do not build up in the recovered medium. This is seemingly due to their being less hard than magnetite so that they are degraded more rapidly than the magnetite and are continuously eliminated by the hydraulic classification in the recovery cone.

The Tromp process has been designed with automatic controls on the essential operations so that operator attention can be reduced to a minimum. An automatic density regulator controls the density of the recovered medium to that required for the separating density desired in the bath. The setting of this regulator can be readily changed.

To compensate for another variable which arises from variations in moisture content of the raw feed coal due to inevitable differences in size consist, a bath automatic regulator is also provided. Variations in feed moisture will dilute the bath medium and in turn the medium drained from the products and returned directly to the bath. The bath regulator measures the density of the returned medium, and when it drops below the desired figure diverts the required proportion to an auxiliary small settling cone which densifies the diverted stream to compensate for the water added with the feed.

Correction

In the September 1952 issue: TP 3382BH. Glass and Chemical Sand Manufacture in the Edwards Paddle Scrubber, by Will Mitchell, Jr., T. G. Kirkland, and R. C. Edwards. P. 875, col. 2, should read: Will Mitchell, Jr. and T. G. Kirkland, Members AIME, are with Research Laboratories, Allis-Chalmers Manufacturing Co., Milwaukee. R. C. Edwards is with the Processing Machinery Department. P. 876, par. 2, line 2, should read "feed rate of slurry." P. 876, par. 4 should read:

If the screening had been done wet, the sand was dewatered to 12 to 18 pct moisture by means of a rake classifier where the −200 mesh fraction was eliminated. When the feed was dry screened, it was necessary to add water by means of a spray at the feed end of the scrubber and the fines were allowed to pass through the scrubber to be removed later in the final classifier.

P. 879, Table VII, col. 3: line 3 should read 0.973; line 6 should read 1.924; line 12 should read 1.268; line 15 should read 3.190. P. 879, Table IX, col. 5, line 8, should read 6.3.

Professional Training of the Geophysical Engineer

by James B. Macelwane, S.J.

Historically whenever application of scientific results to a new problem required the special experimental background, the economic outlook and the practical knowledge characteristic of the engineer, a curriculum in that type of engineering based on the professional requirement grew up in the engineering colleges. This is precisely what is happening now in geophysical engineering.

THE Mineral Industry Education Division of AIME has long been interested in geophysical education. Organized in 1938, a Committee on Geophysical Education presented a number of reports in succeeding years. The AIME is an engineering society; hence it might be expected that the interest of the Mineral Industry Education Division would have centered about the relation of courses in geophysics to engineering education. However, this was not the case. The burden of the discussion held under the auspices of the Committee on Geophysical Education bore on geophysics in general and particularly on its relation to geology.

In the decade that has passed since those meetings much water has flowed under the bridge. Not only have the geophysical sciences developed at an extraordinarily rapid rate but the practical importance and the range of their applications have spread in ever widening circles and have even assumed a very prominent place in research programs of the military, the Army, the Navy and, particularly, the Geophysical Research Directorate of the Air Force at Cambridge, Mass. So enormously have the geophysical sciences as such grown in scope and in degree of specialization that no one man in a lifetime of study can hope to master the theoretical and experimental complexities or even to follow intelligently in the published literature all the varied accomplishments of basic research in these fields. As in the other sciences, most of the results of geophysical research have potential economic value and are being applied to a wider and wider range of human needs.

Here we see a parallel with the older sciences and their relation to engineering. Whenever the applications of scientific results required the special experimental background, the economic outlook, and the practical knowledge characteristic of the engineer, a curriculum in that type of engineering grew up in the colleges and universities. In the words of the "Report of the Committee on Adequacy and Standards of Engineering Education" in the January 1952 number of the *Journal of Engineering Education:* "Engineering education in America was not developed after a preconceived plan. It evolved in parallel with the needs of a growing country, a country engaged in the development of a vast industrialization. From the first it filled a practical need, and its design emanated largely from an evaluation of the professional requirement." The advent of the railroad created a need for scientifically trained engineers and the response was the curriculum in civil engineering. The development of steam power created the demand for a curriculum in mechanical engineering. Neither of these types of engineers was trained to cope with the requirements of electrical power, and so there came to be a curriculum in electrical engineering. The advent of radio communication and of electronics during the first World War and in the years that followed resulted in the establishment of electronics engineering, sometimes within the curriculum in electrical engineering and sometimes independent of it. The complexities of industrial management have created an ever increasing demand for industrial engineers and the consequent building up of a curriculum in industrial engineering. The wide industrial application of chemical processes required a type of engineer whose background was training in chemistry but who was able to design processes and plants on an industrial scale; hence we have the curriculum in chemical engineering. The advent of the airplane created an entirely new set of problems which were solved by the training of aeronautical engineers. Many of these have called for more and more science and mathematics. Such was the history of the older engineer-

---

JAMES B. MACELWANE, S.J., Member AIME, is Dean of the Institute of Technology, Saint Louis University, St. Louis, Mo.

Discussion on this paper, TP 3411JL, may be sent (2 copies) to AIME before November 30, 1952. Manuscript, Feb. 11, 1952. New York Meeting, February 1952.

Table I. Distribution of Subjects in a Curriculum* Leading to B.Sc. Degree in Geophysical Engineering, Saint Louis University, Accredited by ECPD

Humanities	Mathematics	Science	Engineering
Freshman English	Engineering mathematics	Freshman physics	Technical drawing
Report writing	Calculus (3 semesters)	Engineering physics	Descriptive geometry
Speech	Differential equations	Chemistry	Surveying
Philosophy	Vector analysis	Physical geology	Plane-table mapping
History	Potential theory	Historical geology	Machine tools
Business management	Managerial accounting	Minerals and rocks	Applied mechanics
		Structural geology	Thermodynamics
		Engineering astronomy	Hydraulics
			Electrical engineering
			Electronic circuits
			Strength of materials
			Structural and ground vibrations
			Force fields of the earth
			Exploration geophysics

* Physical education is included in this program.

ing curricula and such too is the history of geophysical engineering.

What is a geophysical engineer? What is an engineer in general? There would seem to be three characteristics of the professional engineer on which all can agree. In the first place, an engineer must be equipped with a store of fundamental scientific knowledge sufficient to enable him to solve the problems inexorably thrust upon him in the practice of his profession. In the second place, he must have acquired the technical skills required for planning and design of structures, apparatus, circuits, processes, or procedures in his field that will give the optimum performance at the least cost, and he must be capable of making a reliable estimate both of the performance and of the cost so as to obtain the most for the outlay that is justified by the foreseeable overall returns. Thirdly, he must be a capable manager and must know how to deal with men. These three general characteristics give at least a partial definition of a geophysical engineer. In the large and important class of geophysical problems that arise in prospecting for petroleum and other minerals, the geophysical engineer is immediately faced with the task of planning a program, and in his planning he must solve two problems: 1—He must decide what is the most effective procedure that can be applied in the given circumstances. 2—He must weigh the performance of the various methods against the economic limitations of the situation to secure the maximum of useful information at the lowest justifiable cost. Obviously, both the planning and the execution of such a project will require a thorough training in the geophysical sciences, and unless the geophysical engineer has this solid background of geophysical science, he cannot choose intelligently either the sciences to be applied or the method of their application. Without this solid background of geophysical science he will neither know the limitations of the method itself nor realize the pitfalls of instrumentation and interpretation. It is by no means enough for a geophysical engineer to know physics, geology, and electronics engineering. He must know geophysics. On the other hand, he must not be merely a scientist, however competent; he must be above all an engineer. He is applying physical principles verified in the laboratory to an uncontrolled medium, the earth. Unless he is able to superimpose on his thorough knowledge of geophysical science the practical economic outlook of the engineer, he cannot forecast intelligently either performance or cost.

Geophysical exploration is only one of the many fields that call for the special abilities and experience of the geophysical engineer. The Seismological Engineering Foundation on the Pacific Coast came into being because the problems which antecede and underlie the design of structures to resist the destructive action of earthquake motions transcend the potentialities of the civil and structural engineer. On the other hand they have too much of an engineering aspect to interest the geophysical scientists. The problems are seismological, but they call for the background and practical knowledge of geophysical engineers.

A further broad field into which geophysical engineering has expanded in the last few years is a study of the impact of vibrations on buildings and other structures, particularly in urban communities, caused by quarry and mine blasts, by trip hammer blows, by pile driving, by vibrating machinery, and by highway and railway traffic.

Again, in the quarrying and strip mining industry, the skills of an engineer are needed for the general application of geophysical methods in determining overburden and in mapping the topography of a buried rock surface. The services of a highly trained geophysical engineer are required in the foundation work connected with the construction of highways, dams, bridges, and similar structures, and he is called upon to deal with the closely related problem of locating water supplies and developing water resources by geophysical means. Most of these activities are illustrated by papers on the geophysical program of the AIME annual meeting, February 1952.

In view of these circumstances, what conclusions must be made concerning requirements for professional training of the geophysical engineer? As in all other branches of engineering education, the ideal curriculum will be expected to produce two results, professional attitudes and professional competence. The professional attitude of an engineer is that of a public servant who is conscious of his social responsibility not only to his client but to public welfare in general. Professional competence requires that he have the knowledge and skill to utilize geophysical science in an economic manner for the practical solution of any problem that is brought to him. His training, therefore, as shown in Table I, will be in four main areas. The first of these is the field of humanities. This type of training is the foundation of clear and forceful thinking, the ability to analyze a problem, to organize the subject matter of a report in correct perspective and to write a report in a telling and attractive style. The second area is mathematics. The third comprises the fundamental sciences, particularly physics, geophysics, and geology. The fourth, engineering, includes both general training and specialized geophysical engineering.

Titanium Dioxide Analysis of MacIntyre Ore by Specific Gravity

by Alan Stanley

THE MacIntyre Development of National Lead Co. is located at Tahawus, N. Y., in the heart of the Adirondack Mountains. Operations involve the mining and concentrating of a titaniferous iron ore to produce ilmenite and magnetite concentrates. A general description of the operation and metallurgy has been given by Frank R. Milliken.[1]

Pigment plant production demands that the MacIntyre mill produce a 44.7 pct TiO_2 ilmenite concentrate. To achieve the required ilmenite grade and tonnage it is important that the table concentrate grade be closely controlled. Unfortunately, however, the titaniferous orebody which feeds the MacIntyre mill is not uniform. Ore dressing characteristics vary from one end of the orebody to the other, and from one level to the next. The changeable nature of the mill feed precludes a single adjustment of the equipment for long periods of time. Thus the operators must constantly watch the equipment to insure a uniform concentrate from the fine and coarse tables and Wetherills, or dry magnetic separators.

Chemical assaying of mill products requires about 4 hr from the time the sample is taken until assay results are obtained, and this is available only on a two-shift basis. The ore may change rapidly, even several times during a shift, so that assay results lose most of their control value by the time they are reported to the mill operating crew. Members of the crew have therefore tried to evaluate the table and Wetherill concentrate by visual inspection, since through long experience the shift operators, under most circumstances, can gage closely the grade of the mill products. However, there are times when the physical nature of the ore is radically different from normal. Under these conditions visual inspection is of no value, and at such times final ilmenite as low as 43 pct TiO_2 has been produced and shipped before the assay results have been received. The specific gravity method of assaying for TiO_2 has been attempted to eliminate the shipping of ilmenite below normal grade as well as to help control day to day and hour to hour mill production.

Table I shows the minerals found in the MacIntyre ore along with their average weight proportions and specific gravities. The first two products considered for the specific gravity method were fine and coarse table concentrates. It was reasoned that these products were essentially ilmenite with the higher specific gravity gangue minerals. Since they were always produced the same way, and the desired grade of TiO_2 was always constant, the specific gravity of these materials would increase or decrease as the amount of ilmenite increased or decreased. Thus for table concentrates which assayed 40 pct TiO_2 a constant gravity would invariably be obtained, and as the TiO_2 value changed the specific gravity would change in direct proportion.

The third product considered was Wetherill ilmenite. It was assumed that a desired grade of 44.7 pct TiO_2 would also always contain the same amount and type of gangue minerals along with the ilmenite, and thus would always have the same specific gravity. As the TiO_2 value of the ilmenite concentrate changed so would its specific gravity.

Dr. Kenneth Vincent, chief metallurgist of the Baroid Division of National Lead Co. at Magnet Grove, Ark., ran specific gravity tests on 17 samples of the desired products. The lowest specific gravity reading assayed the lowest in TiO_2 and as the specific gravity increased the trend was for the TiO_2 assay to increase, see Fig. 1. Since these results warranted further investigation, a 500-g capacity Torsion balance and 250 ml Le Chatelier specific gravity bottles were obtained.

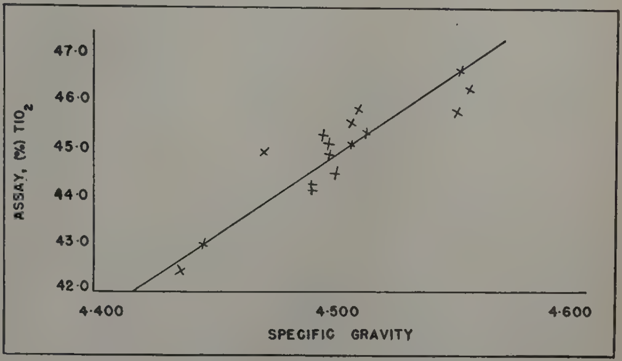

Fig. 1—Initial results, specific gravity assaying.

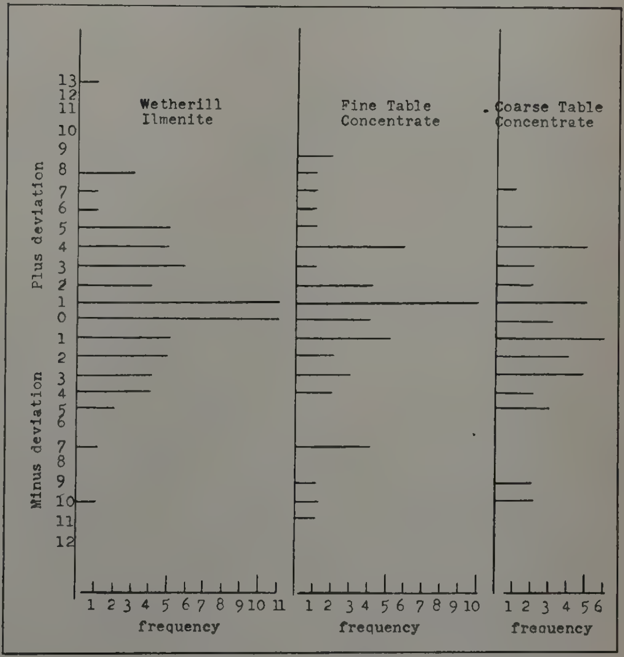

Fig. 2—Deviation vs frequency charts.

Shift samples of fine table concentrate, coarse table concentrate, and final ilmenite were tested. Each sample was split and 85 g weighed on the Torsion balance. The Le Chatelier bottle was filled with water to a zero mark. To avoid wetting the neck of the bottle it was found necessary to do this

---

ALAN STANLEY, Junior Member AIME, is General Engineer, National Lead Co., Tahawus, N. Y.

Discussion on this paper, TP 3410H, may be sent (2 copies) to AIME before November 30, 1952. Manuscript, Feb. 27, 1952. Revised July 23, 1952. New York Meeting, February 1952.

Table I. Specific Gravities and Average Proportions of Minerals in MacIntyre Ore

Mineral	Avg Wt, Pct	Specific Gravity
Magnetite	35.0	5.2
Ilmenite	32.0	4.5-5.0
Plagioclase	10.0	2.6-2.8
Garnet	8.0	3.8
Pyroxene and Hornblend	8.0	3.0-3.6
Biotite	4.0	2.5-3.0
Spinel	2.0	3.6
Pyrite	0.5	5.0
Calcite	0.3	3.0
Apatite	0.2	3.2

Table II. Specific Gravity Standards

Wetherill Concentrate		Fine Table Concentrate		Coarse Table Concentrate	
Ml	TiO_2, Pct	Ml	TiO_2, Pct	Ml	TiO_2, Pct
18.42	46.5	18.74	42.5	18.72	43.0
.52	46.0	.84	42.0	.82	42.5
.62	45.5	.94	41.5	.92	42.0
.72	45.0	19.04	41.0	19.02	41.5
.82	44.5	.14	40.5	.12	41.0
.92	44.0	.24	40.0	.22	40.5
19.02	43.5	.34	39.5	.32	40.0
.12	43.0	.44	39.0	.42	39.5
.22	42.5	.54	38.5	.52	39.0

by means of a funnel with a long stem. After the water was added a zero reading was taken. A short-stemmed funnel was then used to add the weighed sample. To remove dissolved air from the water and thus prevent a possibility of erroneous figures, all water used in the determinations was boiled and cooled prior to use.

When the sample was poured into the bottle some air was carried with it. It was necessary to shake all the air from the grains before the volume reading was taken. When the air was removed the water displacement was noted and the flask emptied into a pan. The sample was dried and sent to the laboratory for chemical analysis.

Several hundred determinations were completed on the three products under investigation. Results showed that each product must have a separate standard.

The specific gravity tables, see Table II, were drawn up in the following manner. The volume obtained from a sample assaying high in percent TiO_2 was subtracted from the volume obtained from a sample assaying low in percent TiO_2. This value, that is, difference in volume, was divided by the difference in pct TiO_2 to obtain a scale showing the correlation between the specific gravity and the chemical assay. Since the same weight of 85 g is used in all tests, difference in volume is directly proportional to difference in specific gravity. Volume differences were used to facilitate reading standard charts.

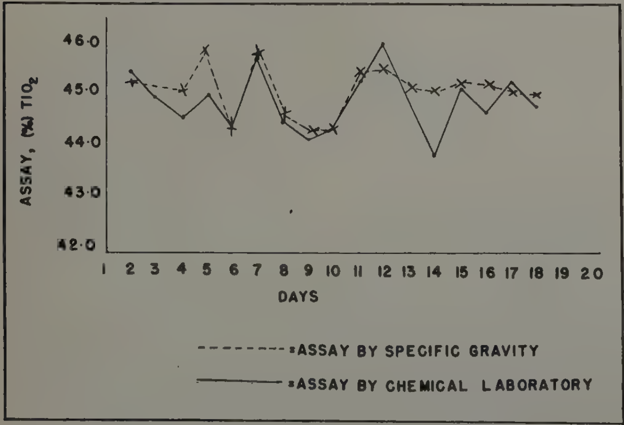

Fig. 3—Chemical vs specific gravity assaying.

The data shown below were used to determine the scale for Wetherill ilmenite, where each 0.1 pct difference in assay equals 0.02 ml volume difference.

TiO_2, Pct	Volume Per 85 G
45.7	18.85
44.3	18.58
1.4	0.27

$0.27/1.4 = 0.193$ ml per 1 pct TiO_2

$0.27/1.4 = 0.0193$ ml per 0.1 pct TiO_2

$0.27/1.4 = 0.02$ ml per 0.1 pct TiO_2

The 85-g samples used for the specific gravity tests were sent in for chemical assay. This chemical assay was presumed to be correct and the value obtained from specific gravity tables was recorded as either plus or minus the difference of the two values. If a value of 45.2 pct TiO_2 was obtained by specific gravity and the chemical assay was 44.8 pct TiO_2, the deviation was recorded as +4 units, each unit equaling 0.1 pct TiO_2. A check sample by specific gravity showing 44.7 pct TiO_2 would have a deviation of −1 unit.

The scale of 0.02 ml per 0.1 pct TiO_2 was used to draw up the standard table for Wetherill ilmenite. The plus and minus deviations were then found and the scale was shifted until the total plus and total minus deviations were as nearly equal as could be obtained. A summation of these data follows:

Product	Sum of Plus Deviations	Sum of Minus Deviations	Determinations, No.
Wetherill ilmenite	135	80	70
Fine table conc.	77	77	44
Coarse table conc.	52	88	43

Graphs of deviation vs. frequency were used to show the accuracy of determining pct TiO_2 by determining the specific gravity. Deviation-frequency charts for Wetherill ilmenite, fine table concentrate, and coarse table concentrate are shown in Fig. 2.

Conclusions

This paper is presented to show what has been accomplished by the specific gravity assay method at one mill, and to acquaint the mining industry with the possibility of a new tool for operational controls. It cannot replace chemical analysis but is a quick and convenient method for use of mill operators as a product control. It must be remembered that this method is used as a guide, and it forecasts the trends accurately enough to warrant its use. The results of a month's specific gravity analysis vs chemical analysis of actual plant control is shown in Fig. 3.

Each product to be analyzed by the specific gravity method must be individually tested and a separate standard table made.

The specific gravity method, as related to MacIntyre ore, is not infallible. Several times the results became too erratic for proper control.

Acknowledgments

The writer wishes to thank P. W. Allen, Plant Manager, J. J. Strohl, Mill Superintendent, W. P. Jenkins, Mill Foreman, and J. Bassarear, Junior Metallurgist, for their help and advice in evolving the specific gravity technique for TiO_2 analysis.

Reference

[1] Frank R. Milliken: Metallurgy at National Lead Company, MacIntyre Development. *Trans.* AIME (1949) **183**, p. 101.

Gravity Investigations In The Iron River-Crystal Falls Mining District of Michigan

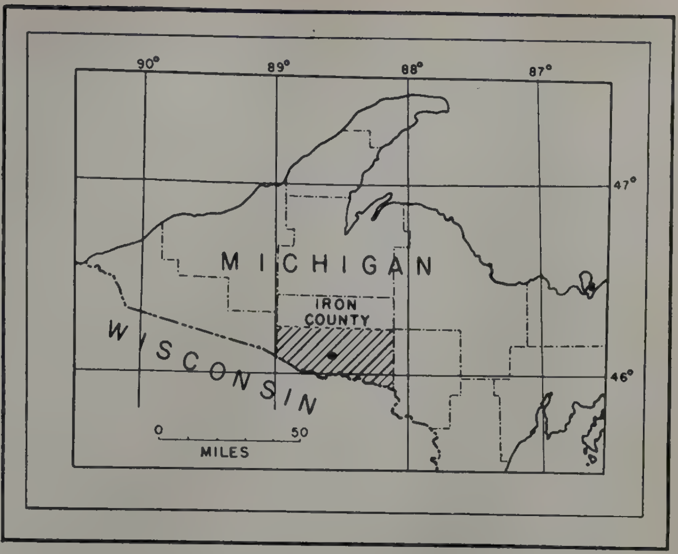

Fig. 1—Area covered in gravity investigations of Iron River-Crystal Falls mining district. Round Lake area in solid black.

by L. O. Bacon and D. O. Wyble

THERE has been considerable speculation among mining geologists and mining men in general as to the relative merits of gravity methods in iron-ore exploration. Most of the investigations which have been carried out in recent years have been done by mining companies, and few if any of the results have been published.

Three gravity surveys have been made in the Iron River-Crystal Falls area,[1,2] one by the U. S. Bureau of Mines, with inconclusive results, and the other two by Radar Exploration Co. for the Cleveland-Cliffs and the M. A. Hanna companies, with results not known to the writers. Both the last-mentioned surveys were detailed investigations, the stations being spaced as close as 10 ft along traverses,[1] and were made to determine the feasibility of locating iron ore by gravitational methods.

Because of the presence of a large body of ore already extensively drilled, Dr. Harold L. James of the U. S. Geological Survey, Iron River, Mich., suggested that a further test of gravitational methods of exploration be made in the Round Lake area of Iron County, see Figs. 1 and 2. This survey indicated a considerable regional gradient and led to a study of the surrounding gravity field and its relation to the major structural features of the syncline within which the iron formation lies.

The southwestern part of Iron County presents a series of hills and hollows elongated in a roughly north-south direction. The bedrock topography is of pre-glacial origin. Relief is moderate; a maximum elevation difference of approximately 350 ft was observed during the survey. Major drainage is dendritic with the larger streams: the Brule to the south, the Paint to the north, and the Iron in the central part. Hills are thickly grown with hardwoods, and lowland areas, not under cultivation, are usually covered by second-growth softwoods.

The area covered in this paper includes the southern half of Iron County, Mich., with a deep synclinal basin occupying the central part of the area, and the southeast corner of Gogebic County, immediately to the west of Iron County.

The upper Huronian iron formation, slates, and graywackes which form the synclinal basin rest upon a greenstone basement. The basin has not been completely outlined by exposures, drill records or other means, as outcrops are scarce and the thick mantle of glacial drift makes geological investigations extremely difficult.

Glacial drift varies in depth up to 300 ft or more. The drift is usually thickest under the hills and is thinnest in the depressions and along drainage courses where most of the bedrock exposures occur. The area over which gravity investigations were made is almost entirely covered by glacial material.

Bedrock of the basin consists of a complexly folded series of iron formation, slates, and graywackes. One of the series of slates has a high magnetic susceptibility due to the fine-grained magnetite it contains. This formation can be detected readily by magnetic methods and provides a marker horizon which can be easily followed. The magnetic slates are stratigraphically above the iron formation, and much of the geological interpretation of the area is based upon the magnetic anomalies they produce.

L. O. BACON and D. O. WYBLE are with Michigan College of Mining and Technology.

Discussion on this paper, TP 3383L, may be sent (2 copies) to AIME before November 30, 1952. Manuscript, Aug. 16, 1951. Revised June 20, 1952. New York Meeting, February 1952.

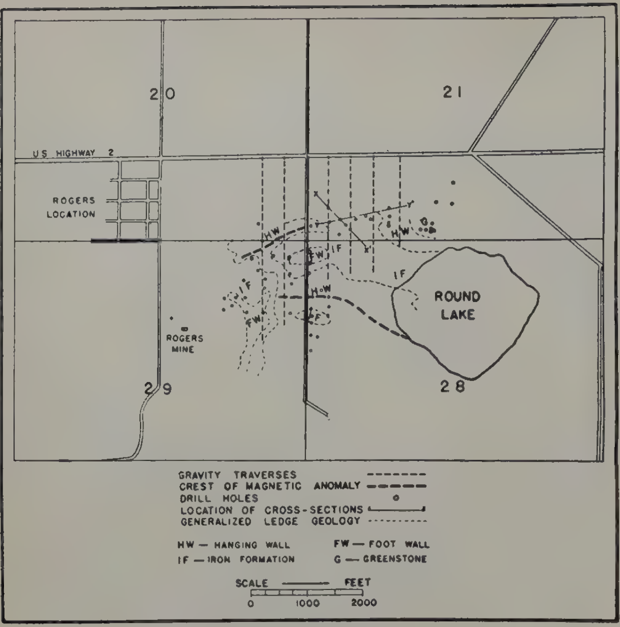

Fig. 2—Plan map of Round Lake area.

The iron formation, together with the slates and graywackes which occur in the basin, are considered to be Upper Huronian. This is younger than the major iron formation of the Marquette, Gogebic, and old Menominee Ranges. The age of the greenstone is in doubt. It has been suggested by Pettijohn[3, 4] that it might be equivalent to the volcanics of the Middle-Huronian Hemlock greenstone or the greenstone of the Keewatin series. The greenstone, where exposed, has been observed to be generally massive and commonly characterized by pillow and agglomerate structures. In some places the greenstone is strongly magnetic and in others it contains interbedded slate with some magnetic iron formation.

The term *iron formation* includes the ore, hematite and limonite, cherty iron ore, jasper, sideritic slates, and minor ferrignous slates.

Because of the extremely complicated cross folds, overturned folds, faulting, and shearing, it is almost impossible to follow the stratigraphical sequence in a single section. Major folds are complicated by minor ones; even folding within folds occurs, and the structural footwall is not always the stratigraphical one. Geological interpretations based upon underground mapping and drill data are often in error because of the extremely complex structure. The stratigraphical succession as outlined to date by members of the U. S. Geological Survey[5-8] follows.

The lower part of the footwall series of rocks between the greenstone and iron formations consists mostly of graywacke, above which lies a dark gray sericitic slate. Both rocks contain 6 to 12 pct iron, occurring primarily as siderite. The thickness of these two members has not been determined. Overlying the sericitic slate is a highly pyritic, graphitic slate. This slate is the footwall for the iron formation throughout the Iron River district. Near the base of the graphitic slate is a breccia, the so-called *speckled gray,* which forms a marker horizon. The observed iron content of the slate varies from 2 to 25 pct. The thickness of the pyritic, graphitic slate is given as 20 to 40 ft.

The iron formation rests conformably on the graphitic slate. Where the iron formation is unoxidized it consists of dark gray chert and gray siderite with occasional layers of sideritic slates. Oxidation has changed the siderite to hematite in places, yielding an oxidized iron formation. The average iron content of the unoxidized iron formation is about 24 pct, whereas when oxidized the iron content is nearly 35 pct and the ore generally contains 50 to 60 pct iron. In general most of the iron formation is oxidized. Since the iron formation is tightly folded, its true thickness is hard to determine. Estimates run from 100 to 300 ft, but it has been found to be as thin as 10 ft in some places.

The hanging wall series, composed of graywacke, gray slate, and magnetic slate, lies disconformably upon the iron formation in some areas. Because of this disconformity the lower part of the hanging

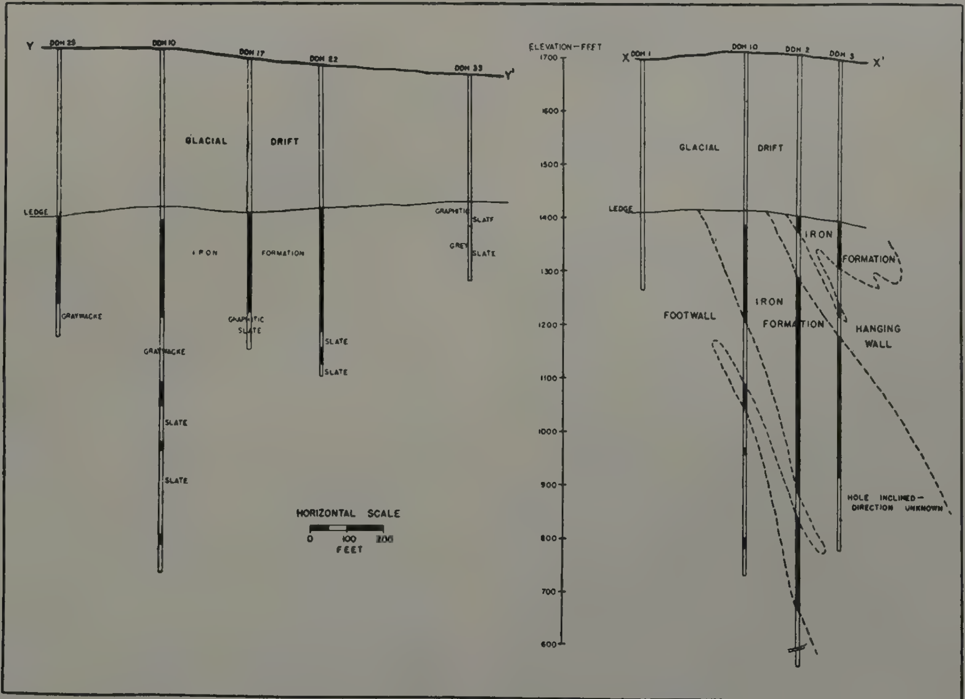

Fig. 3—Generalized geolgic cross section of Round Lake area.

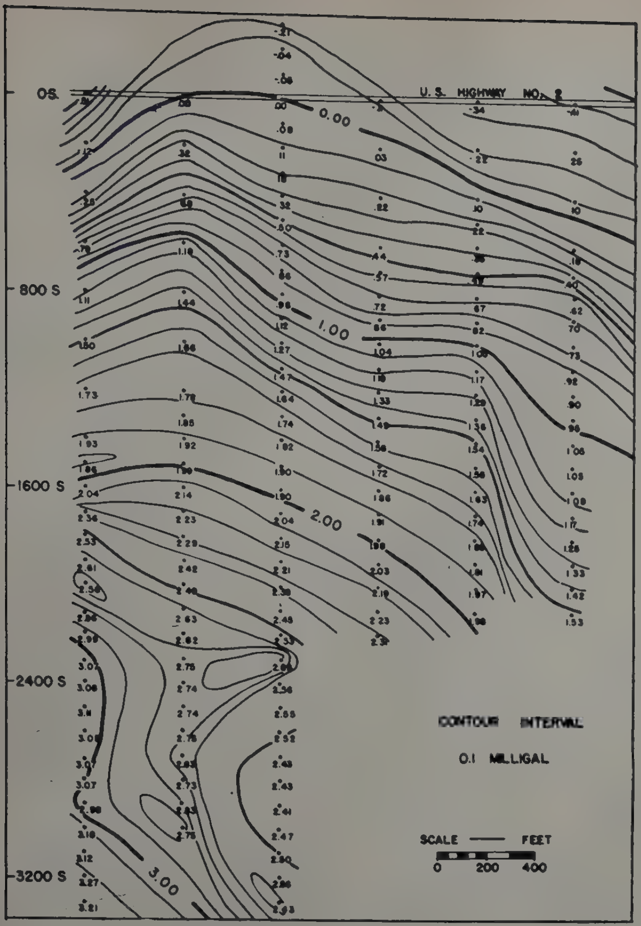

Fig. 4—Bouguer gravity map of Round Lake area.

wall series varies considerably in thickness and lithology. The contact between hanging wall and iron formation may vary from an extremely sharp demarcation line to a very slow gradational change. The graywacke and gray slate hanging wall members have a thickness of 100 to 400 ft.

Above the graywacke and gray slate members is a magnetic slate, the youngest rock in the area for which a description can be given. The lower portion of the magnetic slate is a gray, thinly-banded sideritic rock of cherty appearance quite often embodying finely disseminated crystalline magnetite, although some parts contain little or none. Above this occurs a dark, strongly magnetic rock composed mostly of a chlorite-like mineral, with a high percentage of minute crystals of magnetite scattered throughout. The iron content of this series runs from 15 to 25 pct and its thickness is estimated to be about 100 ft.

As previously mentioned, the ore deposits are mainly of soft red hematite and limonite with some hard hematite, the hematite being the more abundant. The orebodies are very irregular in shape and size, most of them occurring along the keels of synclines and apparently bearing a close relationship to the size of the associated folds. Some of the orebodies have been found immediately below the glacial drift and some have been drilled to a depth of nearly 2000 ft without being bottomed. The change from ore to iron formation of a percentage too low to be commercial is a gradual one.

The physical property of a rock of greatest importance in gravitational methods of exploration is density. Variation in the density of rocks causes a variation in the gravitational attraction which can be measured by a sufficiently sensitive instrument.

Densities of the rocks in the Iron River district according to Zinner[1] are given in Table I with the exception of the density of the greenstone, determined by Wyble[9] from 11 samples provided by the U. S. Geological Survey.

Table I. Densities of Rocks in the Iron River-Crystal Falls Area

Rock Samples	Density	No. of Samples from Density Profile	Average Density
Glacial drift			2.0
Magnetic slate	2.98		2.98
Graywacke	2.57-2.89	2	2.73
Iron ore	3.78,3.88,3.94	3	3.87
Cherty iron ore (jasper)	3.00,3.15,3.16	3	3.10
Black slate (footwall)	2.64-2.88	2	2.76
Graphitic slate	2.06-2.55	2	2.30
Greenstone	2.84-2.91	11	2.86

Density of the graphitic slate may be too low, as samples were taken from the dump where decomposition of the pyrite could have reduced the density materially. Because of the high pyrite content the rock in place has been estimated[1] to have a density of nearly 3.0.

Density of the iron ore is given from Table I as about 3.9, equivalent to 9.3 cu ft of ore per long ton. The mining companies, however, have found that 12 cu ft of ore per ton is more nearly correct.[1] If the density of the ore is computed on the basis of the above, the figure of 3.0 is arrived at. Since the composite density of the jasper, graywacke, and slates is also nearly 3.0, significant gravity anomalies over an orebody could not be expected. The cubic feet per ton factor is affected by a number of things besides the actual density. In arriving at this figure the following factors are also considered[2]: 1—Mining loss. 2—Rock occurrences in the orebody and the question of whether or not these are to be discarded in

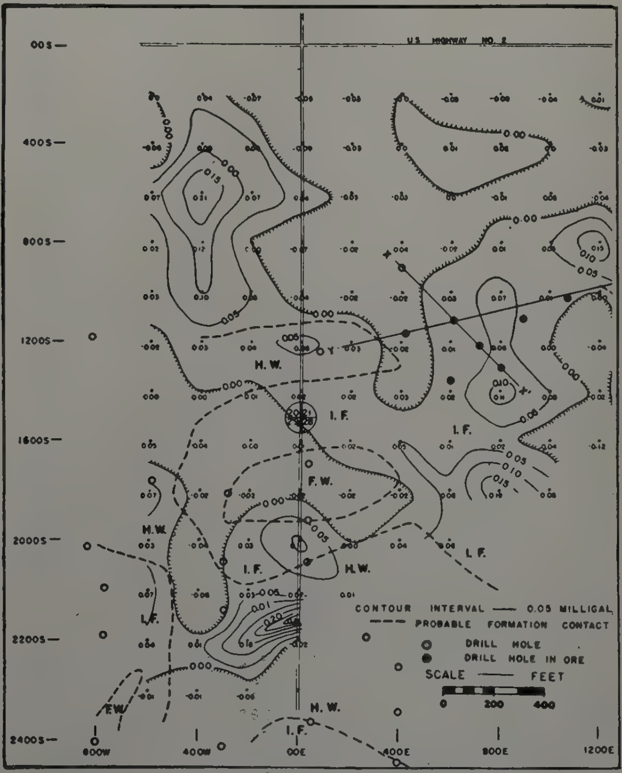

Fig. 5—Residual gravity map of Round Lake area.

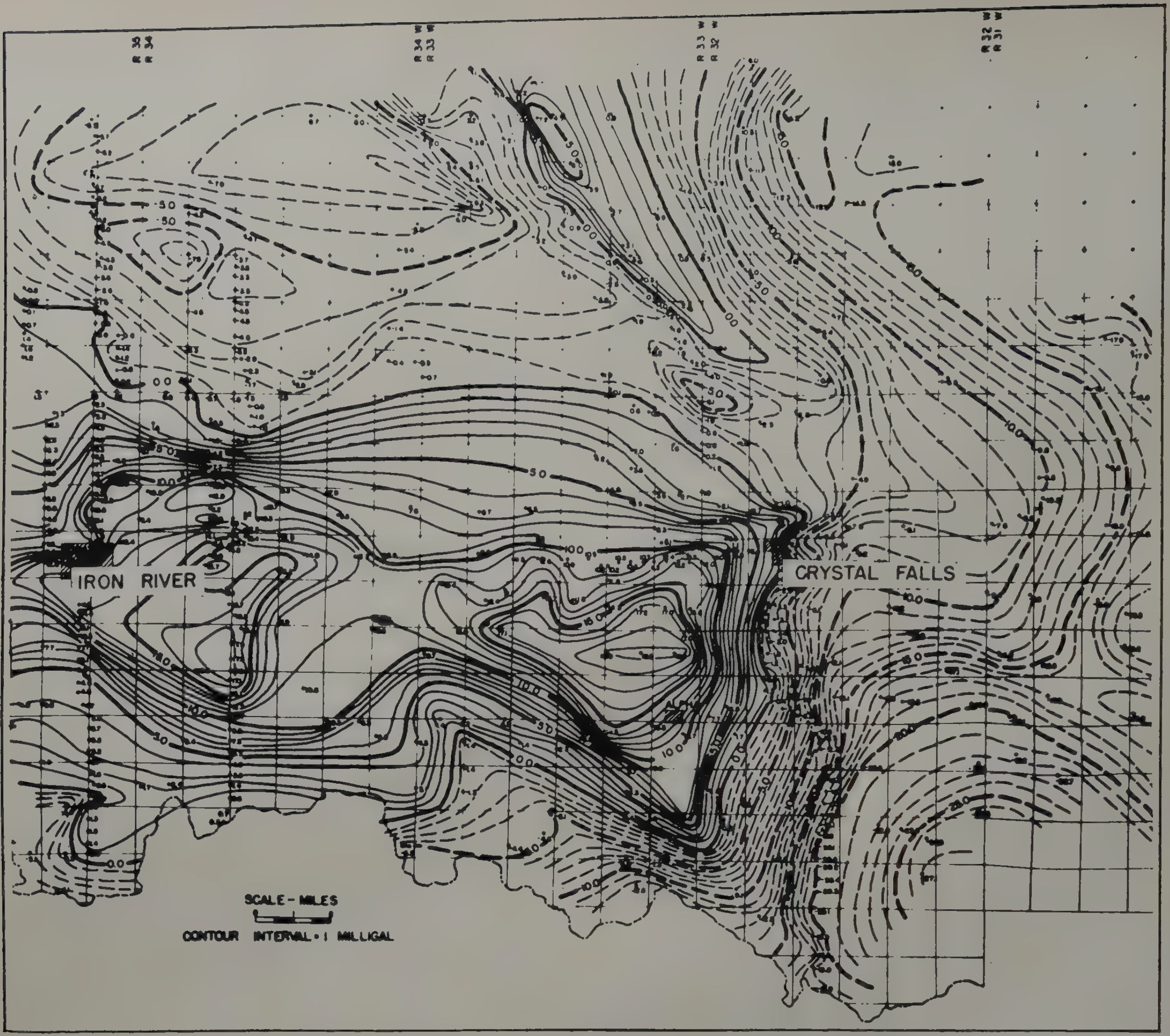

Fig. 6A—Bouguer gravity map of area between Iron River and Crystal Falls, Mich.

mining or go with the ore to increase the tonnage and adversely affect the grade. 3—Dilution with wall rock and/or material from the gob. 4—Occasional recovery of relatively clean ore from the gob resulting from mining loss in previous operations. 5—Gain or loss in moisture as a result of mining and subsequent handling.

Since a cubic factor of 12 takes into account the above items, it is obviously too high to use to calculate the ore density which probably lies, therefore, somewhere between 3.0 and 4.0. In view of the lack of data a figure of 3.3 has been assumed for the density of the iron ore. This results in a density contrast of 0.3 between iron ore and hanging wall-footwall series and of 0.2 between iron ore and cherty iron formation. The density of the latter is based upon only three samples. Royce[2] states that the density contrast of 0.3 seems reasonable as the ore encountered in their drilling was quite dense with apparently little porosity. The writers have assumed that there is a density contrast of 0.3.

The calculated gravity anomaly for Fig. 3 is 0.30 milligal, as determined by use of polar charts with end corrections applied for an orebody 1000 ft in length and for density contrast of 0.3. Residual anomalies smaller in magnitude are observed.

Field work was carried out with Worden Gravimeter No. 28, having a scale constant of 0.03483 milligals per scale division. The instrument has a fairly uniform drift which amounted to from one to two divisions per hr. Just prior to completion of the Round Lake survey, the instrument sustained damage in the field. After repairs were made the maximum drift had increased by a factor of three. The drift gradually decreased with time until it amounted to from 2 to 3 divisions per hr, or approximately 0.1 milligal per hr, near the end of the field season.

In the Round Lake survey, stations were set at 100-ft intervals along north-south traverses 400 ft apart, except along the northern edge of the area where the stations were 200 ft apart, see Fig. 2. Elevations were obtained with an accuracy of 0.1 ft relative to the gravity base station for which an elevation of 100 ft was assumed. Extreme care was taken to maintain the highest precision in the reduced data. The probable error of a single station is about ± 1 division, or ± 0.03 milligal, except in the southern portion where there is moderate relief. No terrain corrections were made on this survey.

In the regional survey, seven north-south traverses were laid out in the Iron River-Crystal Falls area with stations ¼ to 1 mile apart. Elevations for these traverses, to the nearest foot, were available from Michigan Dept. of Highway road profiles, or were obtained by leveling. Stations were also established at all points, usually road intersections,

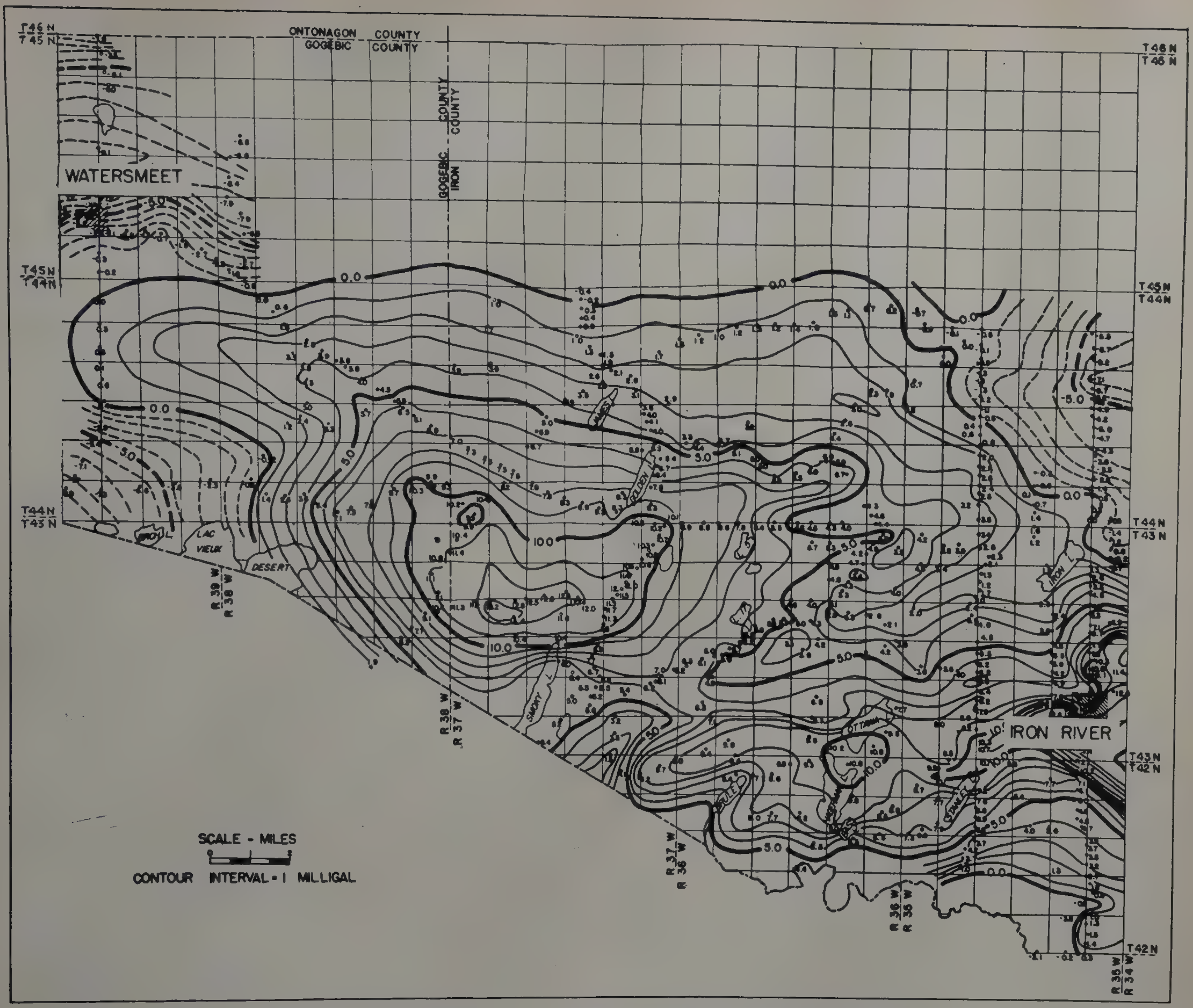

Fig. 6B—Bouguer gravity map of area between Iron River and Watersmeet, Mich.

which had an elevation given on the U. S. Geological Survey quadrangle maps.

In the Iron River-Watersmeet area about 150 station elevations were obtained by using an altimeter in conjunction with a station recording microbarograph to monitor barometric fluctuations. Elevation checks on U. S. Coast and Geodetic Survey bench marks up to 10 miles from the recording station indicated that 75 pct of the elevations were within ± 3 ft and that 95 pct were within ± 5 ft. A 5-ft error would cause about a 0.3 milligal error in the reduced data, a not too serious matter in a regional survey of this type. In all about 750 stations were occupied in an area of approximately 600 sq miles. This indicates a density of about 1 station per sq mile; however, this varies considerably, as much of the area is not readily accessible and has very low station density.

In reduction of the data, corrections were made for instrument drift, free-air effect, simple Bouguer effect, and latitude variation. No correction was made for terrain effects, since in the Round Lake area the terrain was relatively flat, while for the regional survey it was not necessary to make such a correction to maintain a precision of ±0.3 milligal in the reduced data.

All gravity stations in the Round Lake area were referred to a local base station which was later tied into the regional survey. The regional survey was referred to a base station established at the U. S. Coast and Geodetic Survey BM Iron River, elevation 1515 ft, in front of the Iron River High School, and assigned an arbitrary value of 10.0 milligals.

Interpretation of Results of Gravity Investigation

The Round Lake Area: After reduction of the gravity data the results were plotted on a map, Fig. 4. This shows the Bouguer gravity uncorrected for regional effects. There is a strong regional gradient which becomes increasingly positive to the south. This regional effect obscures any gravity anomalies which may be the result of ore. The anomalies which apparently are associated with the ore or iron formation are revealed by changes in the contour lines. There is an indication of a positive anomaly between 0 East and 800 West traverse at 2000 to 3200 South. Another indication occurs at 1200 E near 1400 S. These indications are slight, however, and more or less obscured by the effect of the regional gradients. It is thus desirable to remove as far as practicable the regional effect from the Bouguer gravity.

The regional effect was removed by forming the residual gravity value by the nine point system, where the residual is equal to the value of the station minus the average value of the station and the eight closest stations on a uniform grid, in this in-

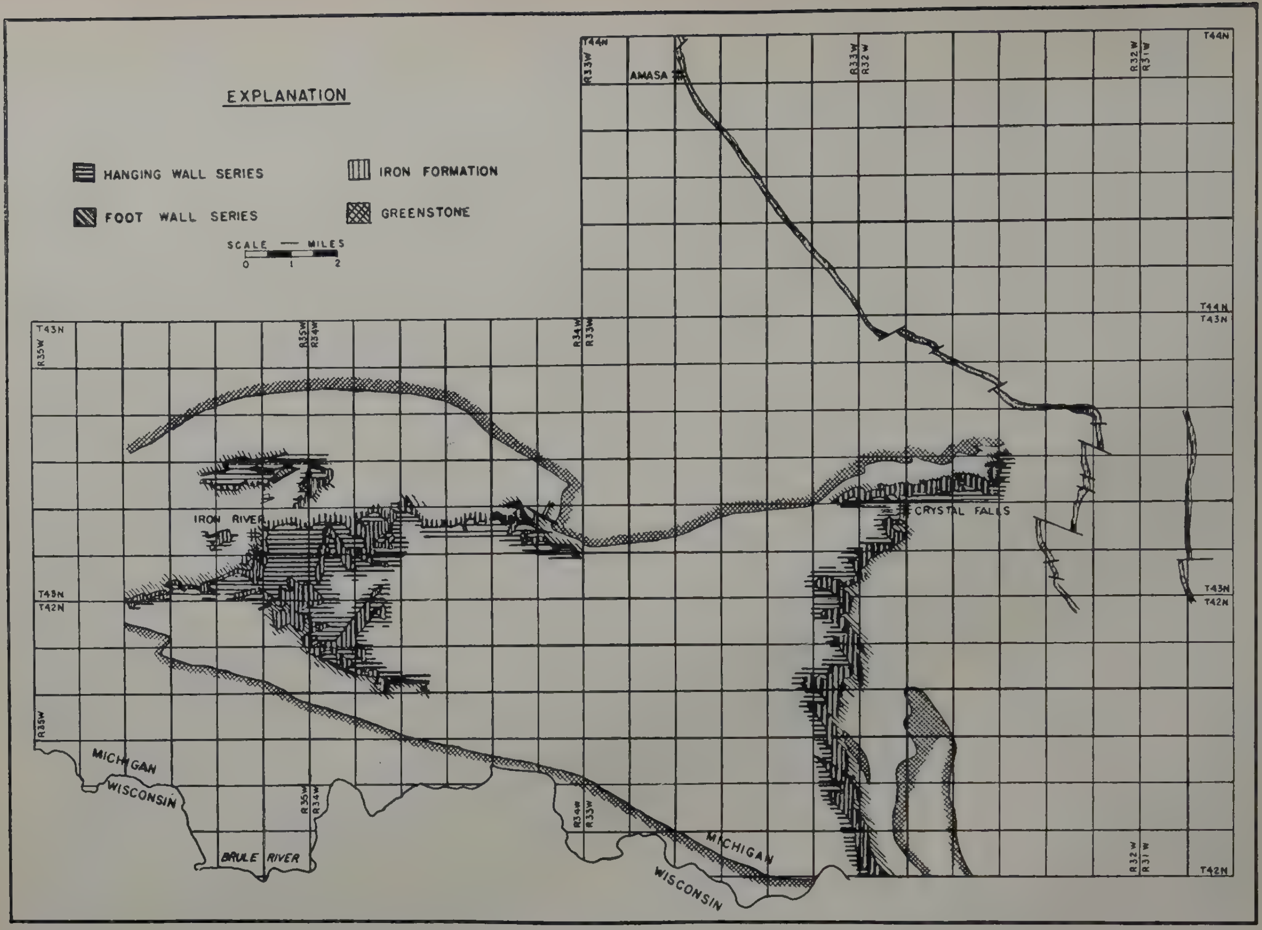

Fig. 7—Generalized geolgic map of Iron River-Crystal Falls District, Mich. After Dutton.[8]

stance a 200-ft grid system obtained by' interpolation between traverses 400 ft apart. The residual gravity map is shown as Fig. 5 with pertinent geological data superimposed.

Anomalies are now apparent in the southwest, northeast, and northwest portions of the area. This agrees fairly well with the geological features as revealed by available drill hole information, there being in general a positive residual over the areas underlain by iron formation. The only area in which ore is known to exist is along section Y-Y'. This shows a somewhat greater residual value than where no ore was encountered. The positive residuals at 600 S, 400 W, 1800 S, 800 E, and 2300 S, 0 E have not been drilled, or if so the records are not available to the writers.

Without more work it is impossible to say whether the residual gravity shown in Fig. 5 is caused by the density contrast between iron formation and ore or by the contrast between iron formation and the foot and hanging wall because of the lack of density data.

Regional Gravity Investigations: Results of the regional gravity surveys are shown as two contour maps, Figs. 6A and 6B, with a contour interval of 1A and B milligal. This interval is too large and the station spacing too great to show any small local anomalies, but it does reflect the major structural features.

The gravity anomalies encountered are extremely large. In the southeastern portion of the area, Fig. 6B, there is a change of 46 milligals in a distance of about 10 miles. The negative anomaly lies between two outcrops of Laurention granite,[10] not shown on Fig. 7, and probably is caused by the lower density of the granite. No density values are available on this rock. The outcrop of greenstone in the southwest corner of T. 42 N., R. 32. W. lies in the region southwest of Alpha where the gravity gradient is the greatest. Its effect on the gravity values apparently merges with the effect of the granite.

The highest positive gravity anomalies apparently occur where the structural basin is the deepest. Considering the magnitude of the gravity anomaly between the area southwest of Crystal Falls and the area about 3 miles southwest of Amasa, which is underlain by greenstone, we can obtain an estimate of the thickness of the Huronion sediments. Taking the average values of the anomaly to be 25 milligals, and for simplification applying the formula for the gravity effect caused by a body large in horizontal extent and of finite thickness, then the difference in thickness is given by

$$\Delta h = \Delta g / 2 \pi \gamma \, (\Delta \sigma)$$

where g = gravitational anomaly, γ = gravitational constant, $\Delta\sigma$ = density contrast, Δh = thickness of anomaly producing source. For a density contrast of 0.3 between Huronion sediments and greenstone and for the 25 milligal anomaly, a value of 6500 ft is obtained as the necessary amount of rock of a higher density to produce that large an anomaly. This is probably not an unreasonable figure.

Another striking feature of this map is the large positive anomaly in the south central portion, coinciding very well with the known syncline containing the iron formation, Fig. 7.

The gravity map, Fig. 6A, indicates that the syncline narrows with a southeast trend near the Michigan-Wisconsin border, south of Crystal Falls. At

Crystal Falls there is a narrowing of the anomaly and several miles east of Crystal Falls the gravity trend makes about a 120° turn northwestward toward Amasa. Comparison of the Generalized Geologic Map, Fig. 7, with the Bouguer Gravity map of the area shows a very excellent correlation.

The gravity map shows a large re-entrant along the southern limb of the major syncline, 5 miles west of Alpha. This may be the result of a major fold, a projection of the greenstone toward the central portion of the structural basin, or possibly a major fault.

One of the small local anomalies of interest is the one occurring at the northern half of Section 20, T 43 N., R 34 W. This is about one mile northwest of the Round Lake area. To the writers' knowledge, no drilling has been done within the area outlined by the closed 12.0 contour lines. This area is almost directly east of the Bates mine, located in the NW¼ of the NW¼ Section 19, T 43 N., R. 34 W., and could well be underlain by an eastward extension of the iron formation which occurs in the vicinity of the Bates mine. Folding or faulting may have interrupted the continuity of the formation.

Another explanation of the local anomaly mentioned above is possible. Since the anomaly has a magnitude of only 2 milligals it could conceivably be caused by a change in elevation of the bedrock topography. A difference of approximately 160 ft in the bedrock topography could cause a 2-milligal anomaly as the density contrast between bedrock and drift material is about 1.0. Even though variations in the bedrock topography could cause this anomaly, the writers believe that because of the spatial relationship further investigation in this area is warranted.

Fig. 7 shows iron formation to the north of Iron River apparently not reflected on the gravity map. The writers have no explanation for this other than the fact that the depth of the synclinal basin here may be quite shallow and the paucity of data does not allow for delineation of any anomaly.

Of primary importance are anomalies occurring in the western portion of Iron County and the southeastern portion of Gogebic County, where little is known of the subsurface geology. The gravity anomaly narrows to the south and westward of Iron River but extends to Brule Lake a distance of about 10 miles. This anomaly coincides with the known trend of the iron formation as shown in Fig. 7, which in this part of the area is based on drill records. The anomaly may extend into Wisconsin from T 42 N, R 36 and 37 W, the closed contours being based on very few points. Of primary importance is the large gravity anomaly occurring in T 43 and 44 N, R 37 and 38 W. This anomaly has a magnitude about equal to that southeast of Iron River and covers a large area. In view of the correlation between the synclinal basin and the gravity anomaly between Iron River and Crystal Falls, this westerly anomaly may well be associated with another synclinal basin which may in turn contain iron formation and associated rocks.

There is no geological information available on this area although some magnetic work has been done north and west of Smoky Lake. The results of this magnetic work are not known to the writers.

Dr. Harold James states that there is no known iron formation in the area in which this gravity anomaly occurs. Since the glacial drift is thick and there are no outcrops known to the writers, this area may be underlain by a structural basin and may well be a potential new iron-ore district.

To sum up briefly, there is some possibility that gravity methods may be able to differentiate between large iron ore bodies and the iron formation in the Iron River-Crystal Falls district, although further investigation along this line is necessary to substantiate the conclusion.

The regional gravity work outlines quite clearly the major structural features of the Iron River-Crystal Falls synclinal basin.

A large anomaly occurring about fifteen miles west of Iron River may well be associated with another structurally similar basin and consequently may be another potential iron ore district.

Acknowledgments

The authors express their appreciation to Dr. Harold L. James for his assistance and comments on the gravity investigations as well as to Messrs. Kenneth L. Weir and Waldon P. Pratt, all of the U. S. Geological Survey, Iron River District, for field assistance in the Round Lake area.

The authors are also indebted to Professor T. C. Sermon and Dr. A. K. Snelgrove for their suggestions and criticisms, to Miss Jean Feldscher for typing the manuscript, and to the Geophysics Committee of the Michigan College of Mining and Technology for permission to publish.

References

[1] Paul Zinner, Clyde L. Homberg, and Terry W. Owen: Investigation of the Iron-Bearing Formation of Iron County, Michigan Utilizing Geophysical and Other Methods. Bur. Mines *RI* 4583, U. S. Dept. of Interior (November 1949).

[2] Stephen Royce: Personal communication.

[3] F. J. Pettijohn: Magnetic and Geological Data of Parts of the Crystal Falls-Alpha Iron District, Iron County, Michigan. Michigan Dept. of Conservation Geol. Survey Div. Plate 1 (1948).

[4] F. J. Pettijohn: Geology of the Crystal Falls-Alpha Iron-Bearing District, Iron County, Michigan. U. S. Geol. Survey Strategic Mineral Investigation Preliminary Map No. 3-181, 1947.

[5] H. L. James and Kenneth L. Weir: Magnetic Survey and Geology of the Eastern and Southeastern Parts of the Iron River District, Iron County, Michigan. U. S. Dept. of Interior, Circular 26 (July 1948).

[6] Harold L. James, L. D. Clark, and L. E. Smith: Magnetic Survey and Geology of the Ice Lake—Chicago Creek Area, Iron County, Michigan. U. S. Geol. Survey Preliminary Report 3-213 (1947).

[7] C. E. Dutton, C. F. Parks, and J. R. Balsley, Jr.: General Character and Succession of Tentative Divisions in the Stratigraphy of the Mineral Hills District, Iron River, Iron County, Michigan. U. S. Geol. Survey Preliminary Report (1945).

[8] Carl E. Dutton: Geologic Work in Iron and Dickinson Counties, Michigan U. S. Geological Survey Circular 84 (September 1950).

[9] D. C. Wyble: A Study of the Regional Gravity of the Southwestern End of the Iron River Mining District, Michigan. Unpublished M. S. Thesis (1950) Michigan College of Mining and Technology.

[10] L. P. Barrett, F. G. Pardee, and N. Osgood, compilers: Geological Map of Iron County, State of Michigan. Dept. of Conservation (1929).

[11] Charles Richard Van Heise and Charles Kenneth Leith: The Geology of the Lake Superior Region. Monograph 52 (1910).

[12] R. C. Allen: The Iron River Iron-Bearing District of Michigan. Michigan Geol. Survey Publication 3, Geol. Series 2 (1910).

[13] Robert McArdle: Gravity Survey of the Round Lake Area, Iron County, Michigan, 1950. Unpublished report to the Geophysics Committee, Michigan College of Mining and Technology.

[14] H. L. James: Personal communication.

Periclase Refractories in Rotary Kilns

by Leslie W. Austin

ROTARY kiln operators will agree that some of the most severe conditions a refractory must stand occur in the hot zone of a kiln burning Portland cement, dead burn dolomite, magnesite, periclase, and similar materials. Frequently the operator is faced with factors beyond his control which drastically shorten the life of refractories. Shutdown due to mechanical failure can be serious if the period is of sufficiently long duration to cause the dropping of coating or the loosening of the lining. A change in slurry can affect the coating and cause ring buildup. A change in type of fuel and its effect upon the flame can cause a shift in location of the hottest zone. Weekend shutdowns or any other interruption can cause the operator trouble and may damage the refractories, since stopping and starting a rotary kiln is certainly more difficult than stopping and starting a motor. Some operators have tried to set an estimate of damage for each shutdown in equivalent days of running time.

Conditions affecting the refractory may be roughly grouped in four classes: chemical attack, mechanical stress, thermal shock, and abrasion.

Chemical Attack: The drive to obtain maximum production through a kiln demands maximum operating temperatures, temperatures which are limited more by the ringing up or melting of the clinker. This can cause interface temperatures at the junction of coating and refractory which require the use of a basic kiln block to withstand the chemical attack. Chemical changes take place within the refractory itself, especially in chemically bonded or unburned kiln blocks. These changes cause the formation of the ceramic or burned bond. Migrating liquids or fluxes from the kiln charge have an effect within the refractory and lead to mineral or glass formation. The alkalies, sodium and potassium, migrate into the refractory as silicates, chlorides, sulphates or other salts. They may move under capillary action or may be caused to move by volatilization with condensation in the cooler portion.

Mechanical Stress: Concentrated stress may be caused by several factors or combinations thereof. 1—The rings of refractories must be kept tight and rigid within the kiln, and this alone demands considerable force to hold the blocks in place. So that the force will not be concentrated, the blocks should fit the circle as perfectly as possible, with the faces in contact overall. 2—As the kiln is heated, thermal expansion takes place at the hot end of the kiln block. Since this disturbs the plane face it too can cause a concentrated stress at the two ends of the block, and shearing stress can be set up within the brick itself because of the difference in expansion between the two ends. 3—If a lining becomes loose and moves in the shell very severe stress can be set up, and as the kiln rotates this load changes and gives the effect of repeated loading. Permanent expansion of the refractory can also cause severe loading. 4—Not least important, flexing of the kiln is frequently the cause of concentrated stresses.

Thermal Shock: Thermal shock, the result of heating and cooling too rapidly, occurs on starting and stopping or when a large patch of coating drops, exposing the bricks. Again, its destructive effect is often the result of phase change, liquid to solid or the reverse; dense refractories loaded with glass-forming impurities are particularly susceptible. Thermal shock is a problem with refractories set in the wall or roof of a stationary furnace, and becomes even more serious in a rotary kiln, the tendency to spall being magnified with movement and concentration of stress. Uniform rate of feed and loading insures both better coating and a more uniform stress.

Abrasion: If the refractories do not take a coating, abrasion can become a most destructive factor. Movement of the lining in shell or movement of loose blocks causes abrasion, which is also most destructive if the refractories do not take a coating.

An analysis of the problem of basic lining for the hot zone reveals, therefore, a number of desirable characteristics: high refractoriness, basic chemical reaction, resistance to spalling, good strength at all stages, ability to take coating, true sizing, volume stability, and abrasion resistance. Increased demand

---

LESLIE W. AUSTIN is Director of Refractory Research, Kaiser Aluminum & Chemical Corp., Oakland, Calif.

Discussion on this paper, TP 3389H, may be sent (2 copies) to AIME before October 31, 1952. Manuscript, Feb. 2, 1952. New York Meeting, February 1952.

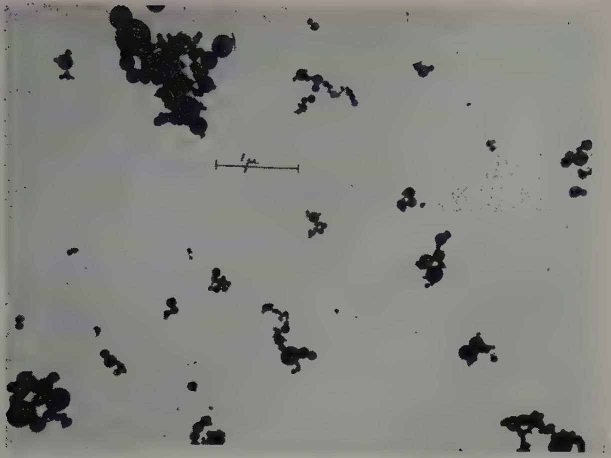

Fig. 1—Relative size of volatized silica as shown by electron microscope. X30,000. Average particle size approximately millimicrons.

for cement production and the improvement in basic kiln blocks have led to the substitution of basic refractories for fireclay and 70 pct alumina refractories in the hot zone of rotary cement. Although each kiln presents an individual problem, even in the same plant, there are basic characteristics inherent in all. If the clinker and the refractory lining react together to form a liquid slag at the operating, or clinkering temperature, the operation is in jeopardy if the kiln is overheated or the coating dropped. Much time and production can also be lost if the operation is necessarily controlled by the temperature of reaction between the lining and the kiln burden instead of the temperature for optimum production rate. Basic kiln blocks have been known for some years as the best solution to the problem. Burned magnesite brick were the first basic lining material and in some places still are. However, because of their moderate ability to stand load at high temperature and their tendency to spall, magnesite brick never became widely used for this purpose. Large scale use of *magnesite-chrome* brick, by far the most important type of basic refractory for this service, began about 20 years ago. Initially the magnesite was the dead-burned natural product, but eventually pure synthetic grades formed chiefly from high purity magnesium hydrate and known in the trade as *periclase* came to be used. These furnish ideal grain for the formation of the forsteritic bond.

It is possible to make a periclase from precipitated magnesium hydrate which will be of relatively higher purity and more uniform composition. Deleterious impurities are eliminated, desirable additives are made, and the mass is burned at higher temperature than possible with the ordinary natural magnesite. One method of making periclase is to treat calcined dolomite with sea water. The magnesium hydrate is derived from the magnesia inherent in the dolomite and magnesium chloride from the sea water. The lime is removed as soluble calcium chloride. The filter cake of magnesium hydrate receives desirable additive and is burned to 1700°C or more with a resultant grain of low porosity and high refractoriness. This periclase is used as source of magnesia in both chemically bonded and burned blocks with or without the addition of chromite. Periclase of this type contains about 91.5 pct MgO.

Except for kilns making white cement, refractory grade chromite is used as a component of most basic kiln blocks in combination with the periclase. The chromite is a desirable component since it results in low thermal expansion, lower rate of heat conductivity, increased resistance to thermal spalling, and greater control of volume stability.

Taking into consideration inherent characteristics of periclase and chromite, and conditions under which refractory kiln blocks must operate, research was concentrated upon developing highly refractory crystalline bonds which would develop at relatively low temperatures in chemically bonded refractories and would give strength, volume stability, and resistance to spalling. The result of this work was a crystalline forsterite bond which forms in place by solid phase reaction between fine magnesia and what research workers have called *volatilized silica*. This silica, formed as a byproduct of ferro-silicon manufacture, may be made synthetically and is especially adaptable for use in refractories. The electron microscope, see Fig. 1, shows the particles to be nearly perfect spheres with an average diam of about 1/6

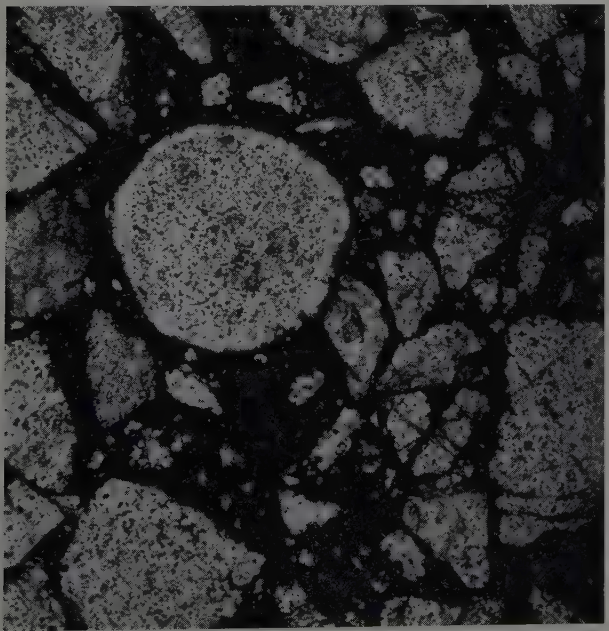

Fig. 2—The light-colored periclase grain is here clearly distinguishable from the dense bond.

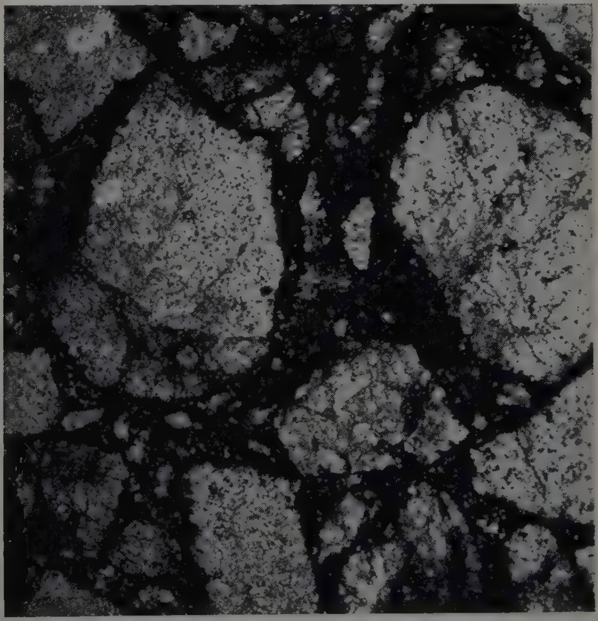

Fig. 3—After being fired to 1000°C the bond portion is lighter, but grain and bond are still sharply defined.

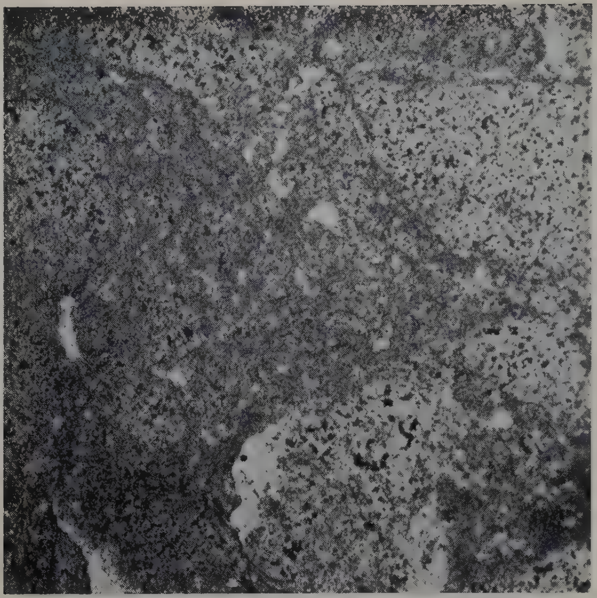

Fig. 4—After a burning temperature of 1500°C the periclase grains are surrounded by a well-developed crystalline forsteritic bond.

micron. The silica is mixed with fine magnesia in close approximation to the forsterite ratio, $2MgO \cdot SiO_2$, to form the bond.

Importance of the particle size of silica employed in the bond is shown in Table I, which correlates results of crushing tests on fired and unfired cubes cut from bricks similarly prepared except for the sizes of the silicas used. The notable improvements in bonding strength that accompany increase in the specific surface of silica used in the bond demonstrate the value of employing the finest silica economically feasible. As a basis for comparison, results are included in Table I for similar tests on a chemically bonded periclase brick using —200 mesh silica flour, note sample 6.

In Table I the sizing of silica is reported in terms of specific surface, as this presents a more readily understandable picture of the nature of materials so finely subdivided. For comparison, the specific surface of the finest Portland cement, an impalpable flour, is approximately 2800 sq cm per g.

Table I. Crushing Stress Developed by Test Specimen Made of Periclase Grain Bonded with Silica of Different Particle Size, Burned to Indicated Temperatures, Cooled, and Crushed. Values are Rounded Off to the Nearest 50 PSI

Sample	Specific Surface of SiO_2 in Bond, Sq Cm per Cm	Unfired	1000°C	1200°C	1450°C
1	67,500	17,500	6560	11,000	17,750
2	52,500	15,500	4850	8900	17,750
3	37,450	13,600	4100	7300	15,550
4	22,450	12,800	1400	4100	15,750
5	7410	11,200	1050	2890	13,600
6	(—200 mesh) under 2800	2600	1100	1400	3000

As stated above, the magnesia and silica are used in their combining ratio to form forsterite, that is, two mols of magnesia to one of silica, or for practical purposes, 134 parts magnesia to 100 parts silica. These ratios apply to the pure materials; when minor amounts of impurities are present it may be desirable to calculate from the analyses the additional amounts of magnesia required to convert these impurities to the higher temperature forms.

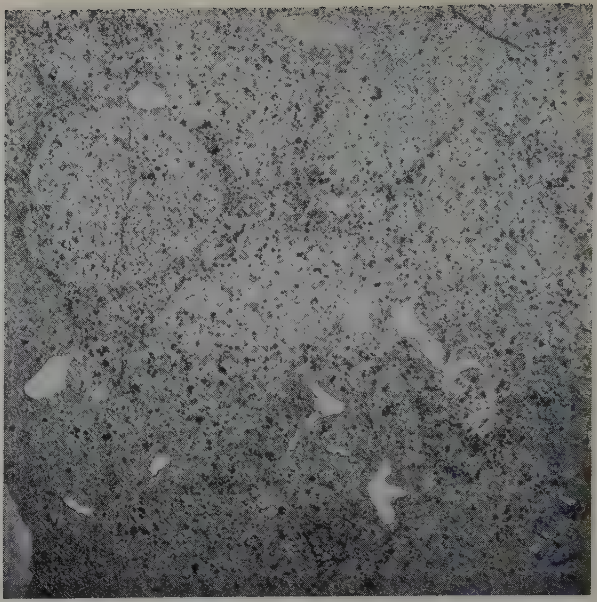

Fig. 5—Photomicrograph of a specimen of brick fired to 1800°C, illustrating high refractoriness of crystalline bond.

It is not necessary that the total magnesia or periclase in the brick bear a ratio to the silica which is in the forsterite ratio. Since there is no melting, the surface only of the periclase grains will be a source of magnesia to form the forsteritic bond. Magnesia over and above that required to form forsterite is not objectionable. Attention is called to the crushing strengths obtained by firing the specimens to intermediate temperature, cooling, and crushing. These tests show very clearly that even though the chemically bonded material loses some strength as it is heated, the specimens with the fine silica retain a much higher strength than those with coarser silica, when burned to intermediate temperature, and the strength increases rapidly to a high burned strength. This is of utmost importance in a chemically bonded kiln block.

Fig. 1 illustrates the relative size of the volatilized silica as shown by electron microscope. Figs. 2-5 are photomicrographs of thin sections made during the development of the forsteritic bond. These four slides were cut from a periclase brick bonded with fine silica and fine magnesia and burned to four different temperatures. The bond material contained a small amount of carbon and appears very dark in the chemically bonded or unfired specimen. Temporary bonds to give green strength for manufacturing and handling are obtained by the use of either magnesium sulphate or magnesium chloride.

Fig. 2 shows clearly the periclase grain as the light-colored portions. Each one of these periclase grains consists of many individual crystals. Attention is called to the close dense bond. The section shows a clear distinction between grain and bond. Fig. 3 is similar to Fig. 2 except that it was fired to 1000°C before the slide was made. The bond portion has lost much of the dark coloring, but the two-component system, grain and bond, is still clearly seen. Fig. 4 resembles the two preceding illustrations, with a difference in firing temperatures only. Here the burning temperature was 1500°C. It is much harder to distinguish between the grain and bond, but closer examination shows clearly the periclase grains which are now surrounded with well-developed crystalline forsteritic bond. Attachment of the bond to the crystals should be noted as well as the remarkable volume stability of the bond. Examination of such slides under crossed nicols shows more clearly the distinction between grain and bond. A few small voids are shown, but they are not connected and are unimportant. The last slide in the series, see Fig. 5, was made from the specimen of brick fired to 1800°C or 3272°F. Even after firing to this high temperature the grains and bond are still clearly apparent and show that the bond is a highly refractory crystalline mineral bond which did not melt. Here again there are a few small unconnected voids.

These slides demonstrate the volume stability, bonding power, and high refractoriness of this bond which forms within the chemically bonded and burned kiln block without a volume change.

Combustible shims to compensate for thermal expansion are important, as are the steel spacers binding the kiln blocks together. Extensive research was carried out to develop the proper use of chromite in the basic kiln block. In this development work it is necessary to use the steel shim between the blocks in a manner approximating as nearly as possible that used in the kiln, since the steel plate oxidizes and has a swelling influence upon the chromite. Trials showed the importance of percentage chromite used, screen size of the chromite grains, and the importance of placing strong forsteritic bond as a protective coating around the chromite grains. The effect of temperature in influencing the volume stability of the periclase-chromite kiln block is also very important. Best results have been obtained by using the same starting formulas and processing for both the chemically bonded and burned kiln blocks.

In summation, performance records obtained over the past eight years have proved the advantages of using high purity periclase and the crystalline forsterite bond.

Application of Coarse Coal Magnetite Separators In An Existing Circuit

by V. D. Hanson, W. K. Heinlein, and J. M. Vonfeld

TWO overfeed drum-type separators using a suspension of magnetite in water as the separating medium have been installed in the Champion No. 1 preparation plant of the Pittsburgh Coal Co., Division of the Pittsburgh Consolidation Coal Company. A simplified flow diagram of the Champion No. 1 coarse coal circuit is shown in Fig. 1. A railroad car rotary dump, capable of handling 20 cars per hr, discharges the coal into a hopper. Coal is fed from the hopper of the rotary dump to a 60-in. belt conveyor by two reciprocating pan-type feeders. The belt conveyor feeds the run of mine coal onto the main raw coal screen. The first deck is fitted with 3 in. round hole perforated plate which removes the 3x0-in. coal. The second deck of the screen is equipped with 6-in. lip screens which separate the remaining coal into +6 in. and 6x3 in. The +6 in. coal is transferred to a shaking picking table and then discharged onto the loading boom. The 6x3-in. coal is fed to the No. 2 dense medium vessel for cleaning. The clean coal from this unit flows to a vibrating screen where the medium is removed and the coal sized into 6x4 in. and 4x3 in. The 6x4-in. coal is transferred to the loading booms and the 4x3-in. is conveyed to the clean coal classifying screens to remove degradation.

The 3x0-in. raw coal is blended in a system composed of three storage bins having a total capacity of 400 tons. From these bins the coal is fed onto a 48-in. flight conveyor by three reciprocating feeders. This flight conveyor delivers the coal to the Rheo plant. The 3x0-in. coal is then cleaned in two 48-in. Rheolaveur launders each equipped with two Rheo boxes. The first set of boxes removes a primary refuse and the second set produces a middling product which is recirculated in the launders. The cleaned coal and water overflows from the primary launders to two sizing and dewatering shaker screens where the water and — ⅜-in. coal are removed for further cleaning in the Rheo fine coal plant. The 3x⅜-in. clean coal is combined with the 4x3-in. coal from the No. 2 vessel, sized into 4x2 in., 2x1¼ in., and 1¼x⅜ in., then sent to the loading booms.

The 3x0-in. refuse from the primary launders is normally fed to the No. 1 dense medium circuit, but any portion or all of this material can, as an alternate, be processed in the Rheo rewash launder. The primary refuse when fed to the dense medium circuit is screened into ⅜x0 which is cleaned in the fine coal plant and 3x⅜ for cleaning in the No. 1 vessel. The clean coal from this vessel is passed over a vibrating drainage and rinse screen, then sluiced to the rewash sizing shaker where it is dewatered and sized for loading.

The installation of a pilot plant separating vessel using a suspension of magnetite in water was pro-

---

V. D. HANSON, J. M. VONFELD, Members AIME, and W. K. HEINLEIN are Mechanical Engineer, Product Control Manager, and Superintendent, Champion No. 1 Preparation Plant, respectively, Pittsburgh Coal Co., Division of Pittsburgh Consolidated Coal Co., Library, Pa.

Discussion on this paper, TP 3385F, may be sent (2 copies) to AIME before November 30, 1952. Manuscript, April 14, 1952. New York Meeting, February 1952.

posed for the Champion No. 1 plant early in 1941. Rising labor rates, coupled with the difficulty of hand picking 6x4-in. raw coal, in which the percentage of impurities was increasing, made the investigation of this process attractive. Plans for a pilot plant, however, were not completed until early in 1945. Later in the same year a cooperative arrangement was entered into with the Link-Belt Co. for the erection of the first magnetite dense medium plant to clean bituminous coal in this country. Construction was completed and the plant was placed in operation in January of 1946.[1]

The primary objectives were to discover whether the drum-type vessel could make a satisfactory separation, to determine the operating characteristics of the vessel and its auxiliary units, and to obtain information which would be useful in the design of new plants.

The original No. 1 dense medium vessel was designed to make a three-product separation. It was divided into two compartments by a partition and the flow of medium could be controlled so that upward currents could be created on one side and downward currents on the other. The vessel when operated in this manner could produce a clean coal with approximately 1 pct sink at 1.60 sp gr and a refuse containing 1 pct float at the same gravity, but the middling product was mediocre, since it frequently contained over 50 pct of 1.60 sink material. In an effort to solve this problem, fluid flow studies were made using a transparent model of the vessel, and although valuable flow information was obtained, a solution was not found. After this unit had been operated for approximately one year, the partition was removed and the vessel was employed as a two-product separator.

The experimental vessel which had been in service for 6 years was rebuilt in January 1952. A phantom view of the present No. 1 unit is shown in Fig. 2. It consists of a cylindrical steel casing 15 ft in diam, 13 ft wide, and 6 ft long. The wheel, or drum, which has given the vessel its type designation, has an outside diam of 12 ft and an inside diam of 9 ft. Sixteen flights divide the inside of the drum into compartments each having an approximate capacity of 6½ cu ft. The drum, supported inside the casing on trunnions, is driven by a 10-hp motor and speed reducer through a roller chain drive. The roller chain engages hardened steel teeth which are inserted in slots and spot-welded on each side of the drum. Wear on the chain is minimized by keeping it well above the medium level, so that the drum speed of 1 1/10 rpm allows ample time for the suspension to drain from the sprocket teeth.

The feed is sluiced down the feed chute by a stream of medium and enters the vessel. Separation takes place rapidly, the float coal being transported across the vessel and over the weir by the overflowing medium, most of which is admitted through the bottom of the vessel. The coal and medium travel first across a stationary wedgewire screen where part of the medium is removed. The remainder goes on to the first section of the vibrating screen, where it is drained off. On the balance of the screen area, the magnetite adhering to the coal is rinsed off and the product dewatered. The material which sinks drops into the compartments of the drum and is transported over a curved plate to the top of the vessel and discharged into the refuse flume. From the refuse flume the material drops to a drain and rinse screen. Fig. 3 is a view of the original installation at the operating floor level. The drives for the clean coal and refuse screens are in the left foreground. The top of the vessel is shown on the right and the densifier for magnetite concentration and storage can be seen in the background.

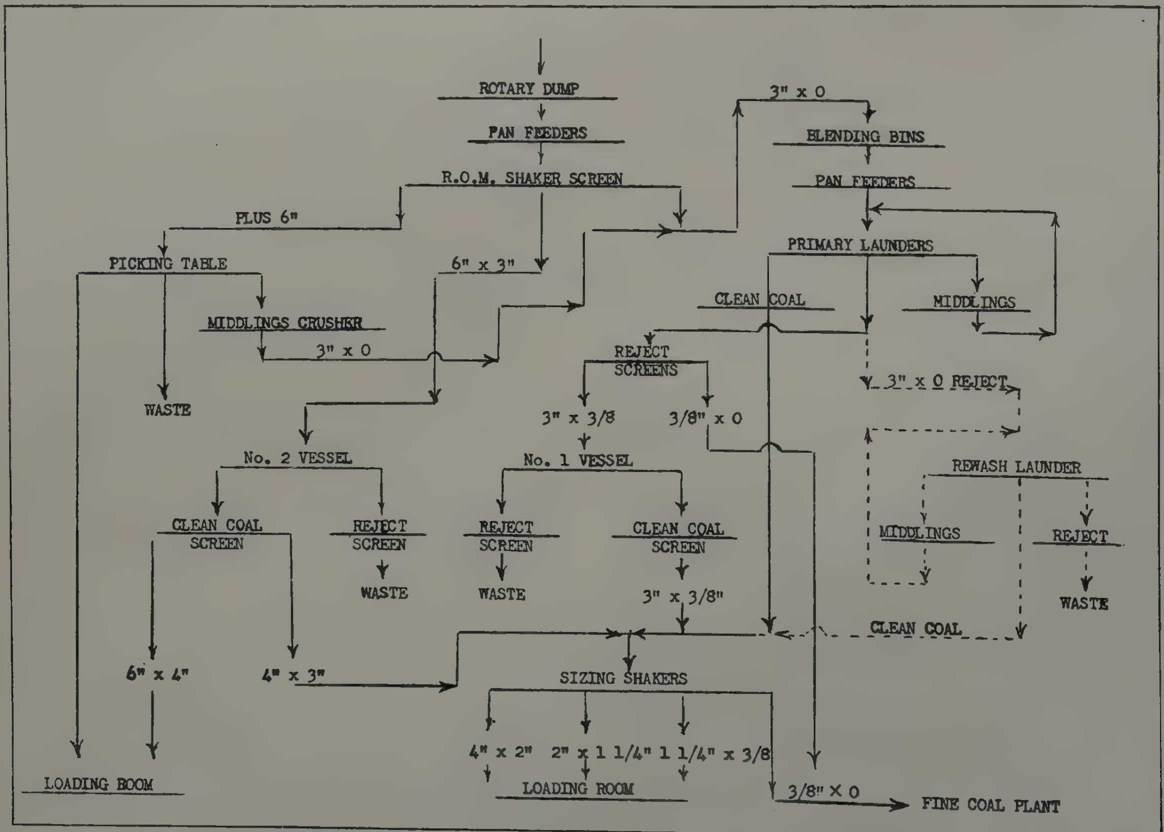

Fig. 1—Coarse coal flow diagram Champion No. 1.

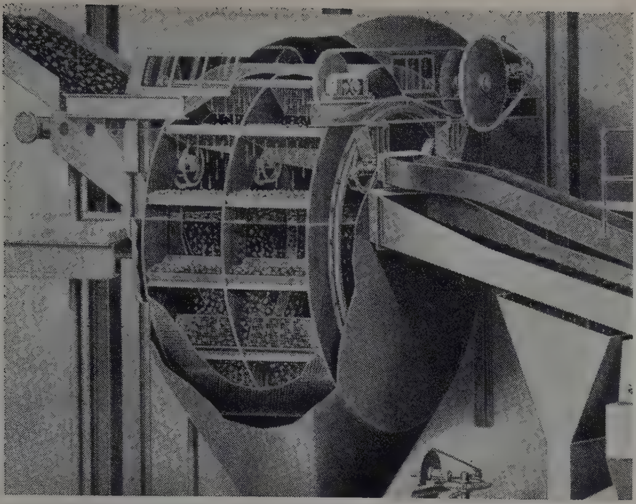

Fig. 2—Link-Belt float-sink concentrator vessel.

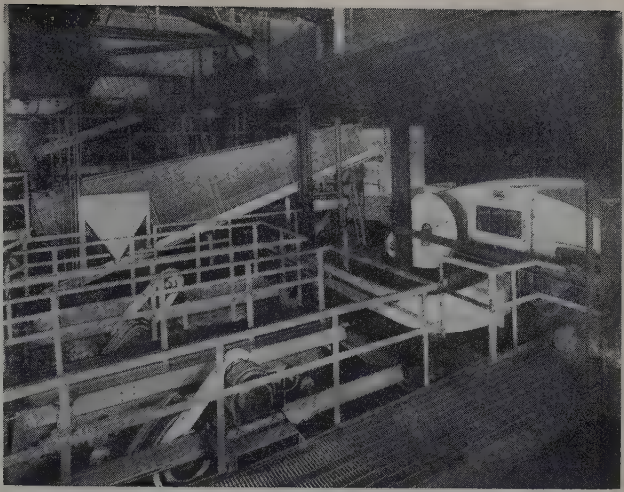

Fig. 3—Link-Belt heavy media coal washing equipment at the Pittsburgh Coal Co., Champion, Pa.

Fig. 4—A section of the +6-in. picking table.

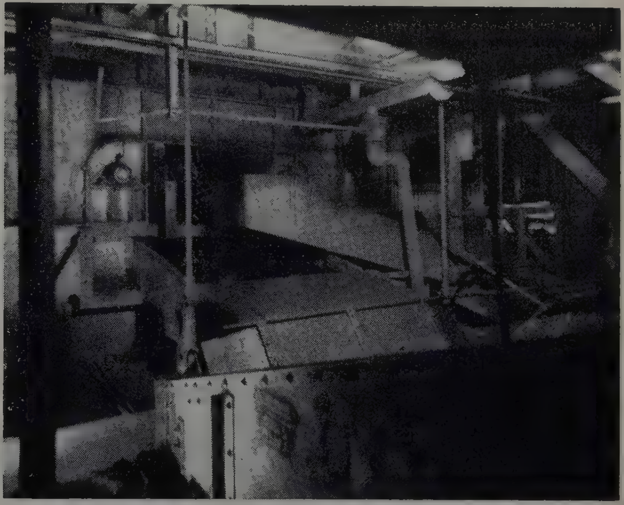

Fig. 5—Coal discharging from the No. 2 vessel onto a vibrating screen.

After two years' experience with the No. 1 vessel, test information proved that a second vessel for treating 6x3-in. raw coal would make a valuable addition to the plant circuit. In the original layout, two tables were required, one for picking the + 6-in. material, and the other for the 6x4-in. size. Fig. 4 gives a close-up view of the present + 6-in. picking table. In Fig. 5 float coal is shown discharging from the No. 2 vessel onto a vibrating screen. The reject material is discharged into the flume directly above the clean coal overflow and then transferred to the refuse screen.

The flow of medium in the vessels and recovery circuit is shown in Fig. 6. Each vessel is supplied with medium from a pump sump. The No. 1 vessel requires 1300 gpm and the No. 2 vessel 1900 gpm. This medium is constantly circulating and its specific gravity must be kept two-hundredths below that of the desired gravity of separation.

All fresh magnetite is added to the system by a vibrating dry feeder to the No. 2 vessel sump. The magnetite used at Champion is purchased in 100-lb bags ready for use and ground so that 100 pct passes 65 mesh, 90 pct passes 150 mesh, and 60 pct 325 mesh. This magnetite as received contains approximately 86 pct of magnetic material. It is important to add magnetite to the pump sump so that some benefit can be obtained from the 14 pct of non-magnetic material.

For adequate rinsing of the coal, 2 gpm of water per ton of feed per hr are required. In the Champion No. 1 circuit, this means that the magnetite must be recovered from 900 gpm of spray water. Three magnetic separators operated in parallel series are used for recovery. The two separators in series are fed the underflow from the thickener containing 6 pct of solids and the third separator has a feed containing 3 pct of solids. These solids contain 32 pct of magnetic material. From the separators the recovered magnetite flows to two screw-type classifiers for thickening and storage.

Each vessel operator checks the density of the circulating medium at 15-min intervals with a specific gravity bottle. To increase the density, he can lower the screw in the densifier, thus adding more magnetite to the system. For lowering the gravity, water is introduced into the circulating pump sump. The operators of this system can easily maintain the density of the medium within one one-hundredth of the specific gravity desired.

Magnetite consumption for 1951 at Champion was 8 to 10 lb per ton of feed, or, since the combined recovery is 53 pct, the consumption per clean coal ton was 1.5 lb.

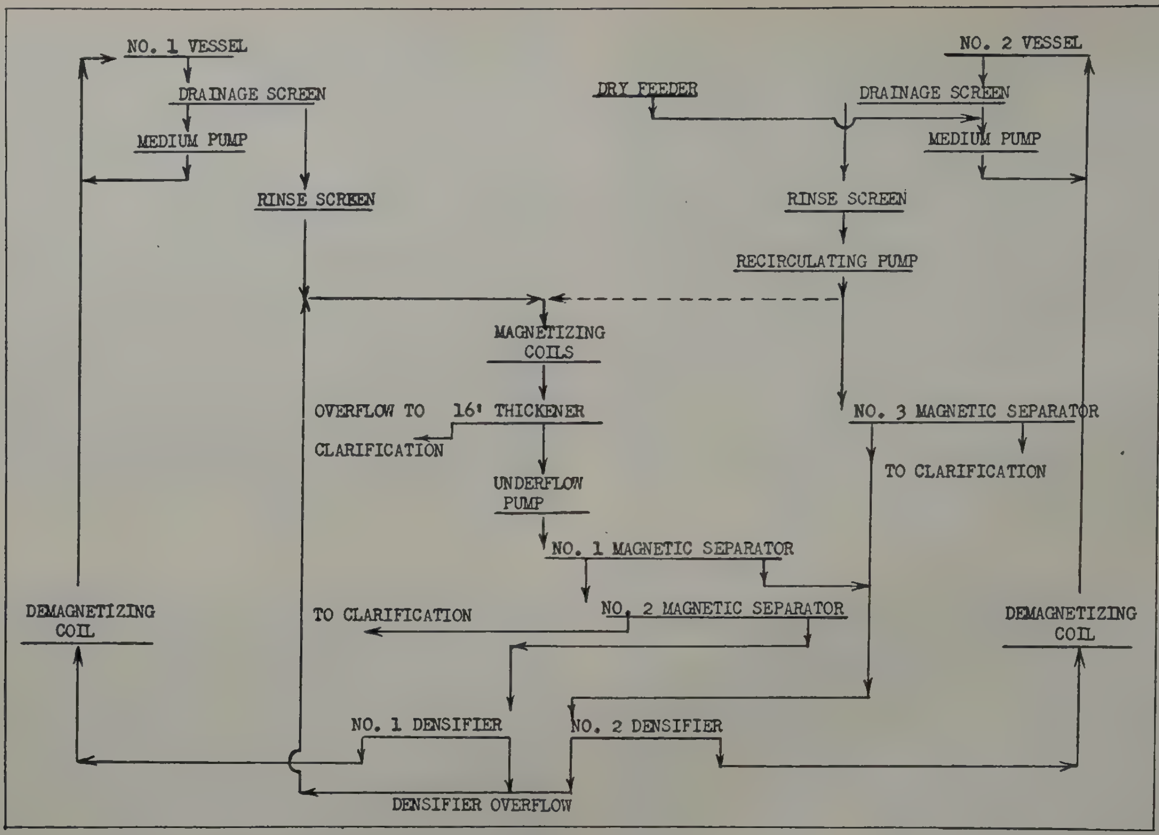

Fig. 6—Medium flow diagram.

Specific gravity analyses of the feed-washed coal and refuse from the No. 1 vessel when handling 300 tons of 3x⅜-in. primary refuse are shown in Table I. Calculated distribution of specific gravity fractions is shown at the bottom of the table. Efficiency for this test, calculated from the Fraser and Yancey formula,[2] was 95.8 pct. A distribution curve of the type developed by Yancey and Geer[3] is shown in Fig. 7. The curve crosses the 50 pct distribution line at 1.52 sp gr, which is, therefore, the gravity of separation.

This curve shows that none of the low gravity coal was lost in the refuse, but that some of the heavy gravity sink did report to the clean coal.

Table II shows specific gravity analyses for the No. 2 vessel when 175 tons of 6x3-in. feed are

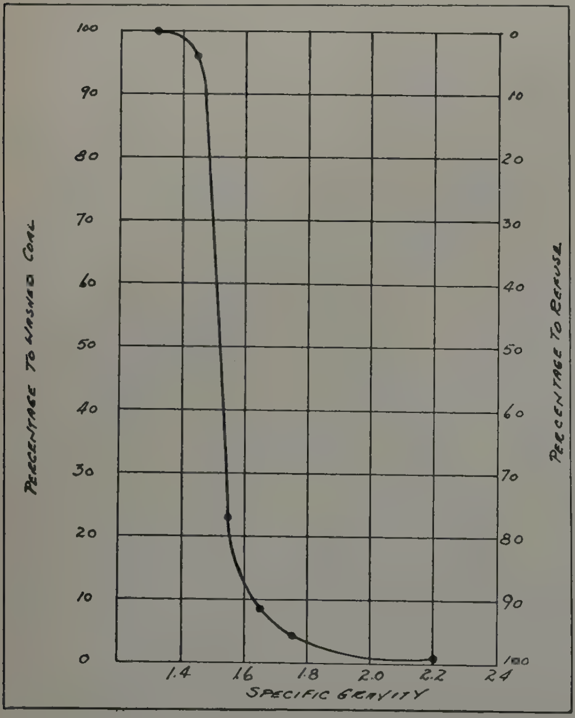

Fig. 7—Distribution curve for No. 1 vessel treating 3x⅜-in. primary refuse.

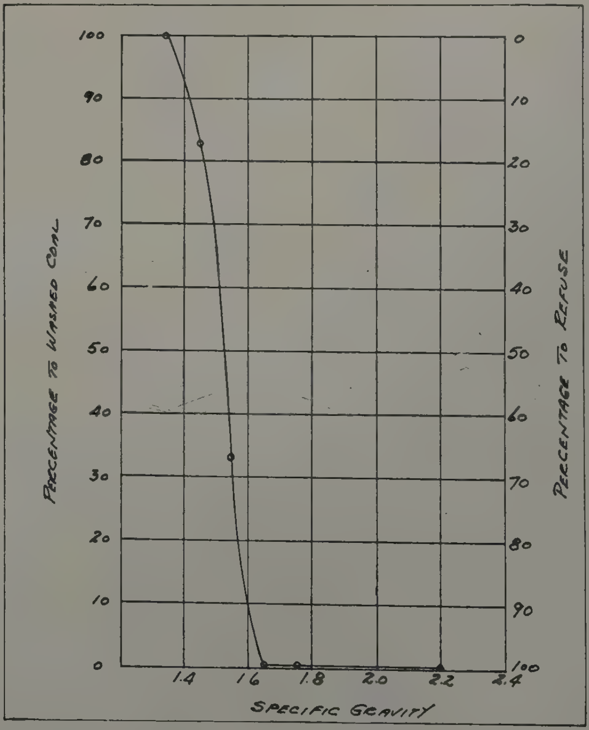

Fig. 8—Distribution curve for No. 2 vessel treating 6x3-in. raw coal.

Table I. Analyses of Feed, Washed Coal, and Refuse No. 1 Vessel Treating 3x⅜-In. Primary Refuse

Product	Sp Gr	Weight, Pct	Ash, Pct	Cumulative Weight	Cumulative Ash
Feed Calculated from Products	Under 1.40	34.7	6.9	34.7	6.9
	1.40 to 1.50	3.2	17.0	37.9	7.7
	1.50 to 1.60	2.2	22.2	40.1	8.6
	1.60 to 1.70	2.0	33.4	42.1	9.7
	1.70 to 1.80	1.8	38.3	43.9	10.7
	Over 1.80	56.1	77.9	100.0	48.5
Clean coal Weight 39 Pct	Under 1.40	89.0	6.9	89.0	6.9
	1.40 to 1.50	8.0	17.0	97.0	7.7
	1.50 to 1.60	1.3	24.0	98.3	7.9
	1.60 to 1.70	0.4	38.1	98.7	8.0
	1.70 to 1.80	0.2	47.0	98.9	8.1
	Over 1.80	1.1	74.2	100.0	8.9
Refuse Weight 61 Pct	Under 1.40	0.0	0.0	0.0	0.0
	1.40 to 1.50	.2	16.7	0.2	16.7
	1.50 to 1.60	2.8	21.6	3.0	21.3
	1.60 to 1.70	3.0	33.0	6.0	24.7
	1.70 to 1.80	2.8	37.9	8.8	28.1
	Over 1.80	91.2	77.9	100.0	74.4

Calculated Distribution of Specific Gravity Fractions

Sp Gr	Pct to Washed Coal	Pct to Refuse
Under 1.40	100.00	0.00
1.40 to 1.50	96.23	3.77
1.50 to 1.60	23.05	76.95
1.60 to 1.70	7.85	92.15
1.70 to 1.80	4.36	95.64
Over 1.80	0.77	99.23

Table II. Analyses of Feed, Washed Coal, and Refuse No. 2 Vessel Treating 6x3-In. Raw Coal

Product	Sp Gr	Weight, Pct	Ash, Pct	Cumulative Weight	Cumulative Ash
Feed Calculated from Products	Under 1.40	60.8	5.3	60.8	5.3
	1.40 to 1.50	4.1	16.7	64.9	6.0
	1.50 to 1.60	2.5	26.5	67.4	6.8
	1.60 to 1.70	.1	38.2	67.5	6.8
	1.70 to 1.80	.3	46.0	67.8	7.0
	Over 1.80	32.2	80.4	100.0	30.6
Clean coal Weight 65 Pct	Under 1.40	93.5	5.3	93.5	5.3
	1.40 to 1.50	5.2	16.4	98.7	5.9
	1.50 to 1.60	1.3	22.8	100.0	6.1
	1.60 to 1.70	0.0	0.0	100.0	6.1
	1.70 to 1.80	0.0	0.0	100.0	6.1
	Over 1.80	0.0	0.0	100.0	6.1
Refuse Weight 35 Pct	Under 1.40	0.0	0.0	0.0	0.0
	1.40 to 1.50	2.0	18.4	2.0	18.4
	1.50 to 1.60	4.6	28.4	6.6	25.4
	1.60 to 1.70	.4	38.2	7.0	26.1
	1.70 to 1.80	.9	46.0	7.9	28.4
	Over 1.80	92.1	80.4	100.0	76.3

Calculated Distribution of Specific Gravity Fractions

Sp Gr	Pct to Washed Coal	Pct to Refuse
Under 1.40	100.0	0.0
1.40 to 1.50	82.9	17.1
1.50 to 1.60	33.3	66.7
1.60 to 1.70	0.0	100.0
1.70 to 1.80	0.0	100.0
Over 1.80	0.0	100.0

Table III. Power Distribution

Item	Pct of Total
Pumping	57.2
Screening	20.1
Conveying	12.8
Vessel Drives	6.1
Magnetic Separation	2.0
Thickening	1.8
Total	100.0

treated. Calculated efficiency was 99.9 pct. The distribution curve, Fig. 8, crosses the 50 pct point at 1.52 sp gr. In this test, none of the coal lighter than 1.40 reported to the refuse and none of the material heavier than 1.60 entered the washed coal.

Three phase 60-cycle power is supplied at 440 v to the various motors in the plant. Direct current for the three magnetic separators and magnetizing coils is obtained from a motor generator set at 250 v. The total power consumed by the dense medium units is approximately 275 kw and is distributed as shown in Table III.

Accurate costs for the dense medium plant are difficult to determine since the men assigned to the units perform some work chargeable to other accounts. Table IV includes only the direct cost of operating the vessels and their auxiliary equipment.

The effect of the installation of dense medium drums in the Champion No. 1 circuit is shown in the following series of charts.

Fig. 9 shows the pct weight of the output tonnage produced by the two vessels and the effect of progressive steps taken to obtain the maximum benefit from these units. In 1946, during the pilot plant stage, only 1.6 pct of the tonnage was dense medium clean coal. In 1947 the No. 1 vessel became part of the Rheo circuit, but owing to difficulties in disposing of the vessel refuse, only 40 pct of the primary launder refuse could be handled. A refuse belt conveyor was installed in 1948 and the percentage of total clean coal from the dense medium circuit increased 2½ pct. The effect of the installation of the No. 2 vessel in March of 1949 is shown by the increase in the percent of clean coal in 1949 and 1950. Finally, by the addition of more screening capacity for the 3x0-in. primary launder refuse, the No. 1 vessel was able to handle all of the 3x⅜-in. size of this product and a peak of 29.2 pct of the clean coal tonnage was produced by the dense medium system.

An improvement in the quality of all clean coal sizes has resulted from the installation, and Fig. 10

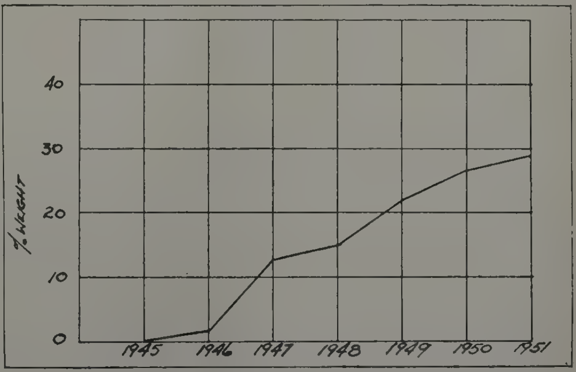

Fig. 9—Dense medium clean coal, percent of weight.

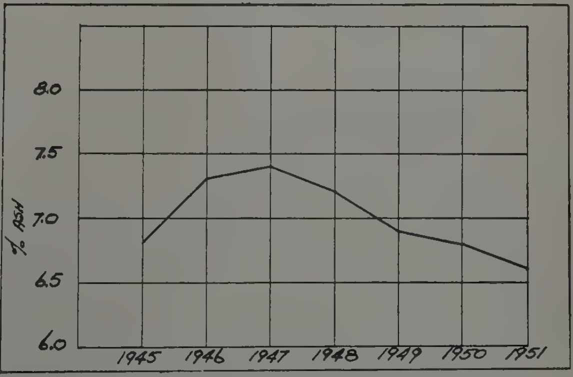

Fig. 10—Ash content of 4x2-in. clean coal.

Table IV. Cost of Operating Separators and Their Auxiliary Equipment

Item	$ Per Clean Ton
Operating Labor	.0488
Maintenance	.0323
Supplies	.0560
Power	.0117
Total	.1488*

* The above total does not include the royalty charge of $.01 per ton.

shows the change in ash content of the 4x2-in. size. This size was selected because it reflects the effect of both vessels. From 1946 to 1949, the No. 1 unit was recovering 4x⅜-in. coal from the refuse and from then on was handling the 3x⅜-in., while the No. 2 vessel produced 6x3-in. clean coal. The average ash content of the 4x2-in. for 1945 was 6.8 pct and rapidly increased with an increase in raw coal impurities to a maximum of 7.4 pct in 1947. In 1948 the trend was reversed and each successive year shows a gradual reduction toward the desired objective of 6.5 pct. The improvement in ash content is the combined result of the sharper separation in the dense medium vessels and better launder operation obtained by the reduction of the size and quantity of material fed to the primary Rheo units.

Fig. 11 shows the change in the feed and clean coal rates from 1945 to 1951. In 1945 the plant was handling raw coal at an average rate of 869 tons per hr and with a reject of 16.5 pct was able to produce 725 tons of clean coal. The chart clearly shows the increasing quantities of material that must be handled to maintain clean coal output.

In 1938 a production rate of 810 tons per hr was maintained with a feed rate of 888 tons; to attain the same rate in 1951, a feed of 1143 tons per hr was required.

The change in character of the raw feed is shown in Fig. 12. The reject from the raw coal of three of the mines supplying the bulk of Champion No. 1 tonnage has increased from 19.3 pct in 1945 to 32.3 pct in 1951. The increase in impurities in the raw feed is not, as might be supposed, the result of increased mechanical loading, but is instead the result of a change in the method of mining. The mines had found that it was economically more advantageous to load the slate with the coal rather than separately. The change in production rate resulting from this type of loading is shown in Fig. 13. From 1945 to 1951, there has been an increase of 46.3 pct in the clean coal produced per man hr. This increase in production has substantially reduced the labor cost per ton. It is believed that without the dense medium vessels this reduction could not have been made.

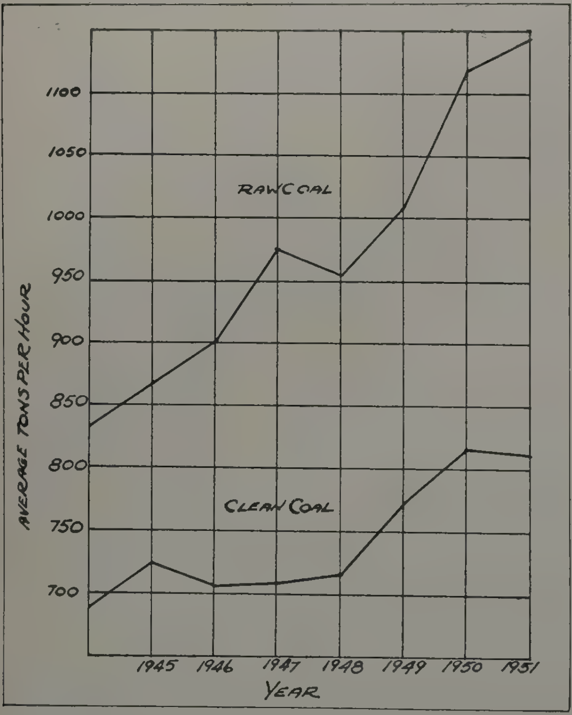

Fig. 11—Production curve for raw and clean coal, tons per hour.

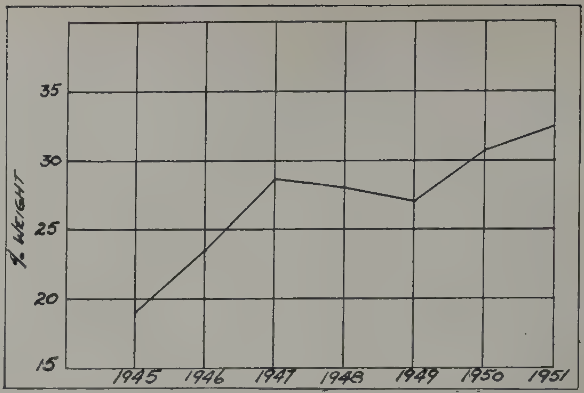

Fig. 12—Raw feed rejected from mechanically mined coal, percent of weight.

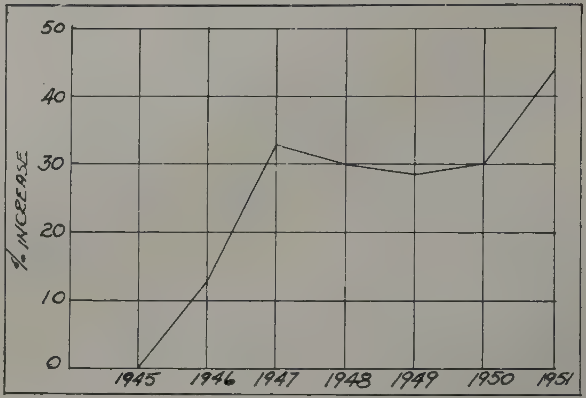

Fig. 13—Increase in clean coal produced per man-hour of mechanically mined coal.

Acknowledgment

The authors are indebted to H. C. Rose, President of the Pittsburgh Coal Co., Division of Pittsburgh Consolidation Coal Co., for permission to present this information and wish to thank the members of the present staff and also those formerly associated with the Pittsburgh Coal Co. who have contributed to the successful application of the dense medium units. We wish particularly to thank J. B. Morrow, whose pioneering and foresight have contributed so much to coal preparation knowledge.

References

[1] S. A. Miller and D. H. Davis: The Operation of a Heavy Density Unit Using Magnetite Suspension for Coal Cleaning. Pittsburgh Section AIME Fall Meeting, Nov. 7, 1947.

[2] Thomas Fraser and H. F. Yancey: Interpretation of Results of Coal Washing Tests. *Trans.* AIME (1923).

[3] H. F. Yancey and M. R. Geer: Performance of a Baum-Type Coal Washing Jig. U. S. Bur. Mines *RI* 3371 (1938).

Microstructures in Iron Ore Pellets

by Strathmore R. B. Cooke and Thomas E. Ban

The paper discusses the mineralogy, structure, and strength of magnetite pellets fired in air and in a neutral atmosphere at various temperatures. The information obtained from this investigation is used to explain the origin of the structures occurring in pellets produced by pilot-plant operation.

MUCH experimental work has been performed on the mechanism of agglomeration and pelletizing of moist ore and concentrates and on the process of firing agglomerates, but except for the work of Tigerschiöld and Ilmoni[1] much of the published information is empirical, and the literature contains no information concerning the structure of fired pellets. Results of a preliminary study of the microstructures occurring in pellets produced both in the laboratory and on a pilot-plant scale are presented in this paper. Most of the results were obtained from pellets prepared from Mesabi magnetic taconite, but through the courtesy of the staffs of the Minnesota Mines Experiment Station and the Bethlehem Steel Co., fired pellets produced from limonite and hematite ores and from Lebanon magnetite have also been examined. The work has been restricted almost entirely to pellets produced without additives, the exceptions being those in which coal was added to the filter cake before rolling.

Schwartz has described the microstructures occurring in ore sinters produced under reducing conditions.[2] Many of the structures and constituents he describes are common to fired pellets, but the constituents normally occur in markedly different proportions. His statement that "in all satisfactory sinter the amount of hematite is small, perhaps not over 2 or 3 per cent" is inapplicable to pellets produced by pilot plant operation or by any process in which air is not deliberately excluded. Pilot plant pellets contain over 90 pct by weight of hematite, and those produced in the smaller furnaces of the Minnesota Mines Experiment Station contain more than 80 pct of that constituent.

Preparation of Specimens

It is difficult to examine unfired pellets microscopically because of their insufficient coherency to withstand sectioning and polishing. Fired pellets sometimes lack coherency and frequently contain holes which are troublesome during polishing. Impregnation of both air-dried and fired pellets is readily accomplished by the use of methyl methacrylate monomer.[3] The dry pellets are covered in a test tube with excess monomer, to which a small amount of accelerator has been added. When the test tube is placed in a cooling bath and evacuated with an aspirator, most of the entrapped air is removed, and disruption of weak pellets by boiling of the monomer is reduced to a minimum. Polymerization is then effected by immersion of the test tube in a water-bath at about 45°C, this temperature being held for 4 or 5 days. The test tube may then be broken away from the solidified mass and the pellets sectioned by a carborundum wheel or a diamond saw. Where time is important, impregnation is carried out at a higher temperature by Meyer's method.[4]

Air-dried pellets must be impregnated with especial care; otherwise swelling occurs and the solids are displaced. It is more important to be certain that the monomer forms a reasonably complete network throughout the specimen than that all entrained air is removed, and for this reason the vacuum technique may be omitted.

Impregnated agglomerated products and pellets are extremely coherent, section well, and may be polished either by hand or by machine. Hand polishing is not satisfactory for the examination of conditions existing at the boundaries of grains, and for this machine polishing must be used. The Graton-Vanderwilt machine gives excellent results, provided that pressure on the specimen is considerably in excess of that recommended by the manufacturer.

Mineralogy of Fired Pellets

Only two opaque iron minerals, magnetite and hematite, have been recognized in pellets. The complete identity of these artificial minerals with their corresponding natural counterparts is shown by their mineralographic characteristics and their X-ray structures. Wüstite has not been found.

Slag is the most common transparent constituent of fired pellets. Occasionally conditions have been appropriate for the crystallization of fayalite from the slag, and at other times another crystalline sil-

---

S. R. B. COOKE, Member AIME, is Professor of Metallurgy and Mineral Dressing, School of Mines and Metallurgy, University of Minnesota, Minneapolis. THOMAS E. BAN, Junior Member AIME, is with the Cleveland-Cliffs Iron Co., Ishpeming, Mich.

Discussion on this paper, TP 3428B, may be sent (2 copies) to AIME before December 31, 1952. Manuscript, Feb. 20, 1951. Revised Sept. 2, 1952. St. Louis Meeting, February 1951.

This page of Mining Transactions AIME follows p. 988. The intervening non-Transactions pages appeared in Mining Engineering.

icate, unidentified, has been seen. Both Schwarz' eutectic structure between silicate and magnetite and his crystallographic intergrowth between these constituents may occur.

Structure of Air-Dried Pellets

Pellets were rolled in a drum 2 ft long by 2 ft in diam. Sectioning of green, or wet, pellets for microscopic examination is unsatisfactory; therefore they were dried at room temperature. Re-arrangement of the solids during drying seems to be of negligible importance, for the measured shrinkage during this process is less than 0.001 in. for pellets which are 0.75 in. in diam.

Fig. 1 shows part of an air-dried pellet which was impregnated as described above, sectioned and polished. It was prepared from an eastern Mesabi taconite concentrate, the size analysis and composition of which are given in Tables I and II. Most of the experimental results reported in this paper were obtained on pellets prepared from this material.

A pellet with 25 pct porosity, made from a concentrate containing 91 pct magnetite (65.9 pct total Fe) and 9 pct quartz will contain by volume 62.4 pct of magnetite and 11.6 pct of quartz. Because of this, the magnetite content appears disproportionately low in polished sections when compared with the high iron content of the concentrate. Fig. 1 shows the individual fragmented particles of magnetite and gangue, together with some interlocked particles of gangue and magnetite. Fig. 2, taken with the highest available resolving power, shows the irregular and fragmented nature of the magnetite. Particle size ranges down to 0.25 micron, the limit of resolution of the objective used. Because the objective was an oil immersion lens, both the plastic and the silicate gangue appear dark.

Structure of Magnetite Pellets Fired in a Neutral Atmosphere

Oxidation of magnetite occurs at low temperatures. Under the requisite conditions it will slowly oxidize to hematite at temperatures not materially different from those prevailing at the surface of the earth; in the laboratory marked oxidation occurs in half an hour at 200°C. To eliminate the variable of oxidation, pellets were heated to various temperatures in an electrically-heated tube furnace in an atmosphere of nitrogen or helium from which all traces of oxygen were removed. For this purpose the commercial gas was bubbled through absorption bulbs containing a solution prepared by reducing acidified potassium dichromate with zinc. The resulting blue chromous salt has great affinity for oxygen, changing color immediately when its absorptive powers are exhausted. The success of this treatment became obvious upon comparison of pellets heated in commercial nitrogen or helium with others heated in the de-oxygenated gases. The first-mentioned pellets contained relatively large quantities of hematite, the second, none, except that which could be attributed to the residual air in the pores of the pellets.

Table I. Size Analysis of Concentrates

Size		Wt, Pct
−28	+48 mesh	0.36
−48	+65 mesh	0.27
−65	+100 mesh	0.50
−100	+150 mesh	1.25
−150	+200 mesh	4.43
−200	+270 mesh	8.30
−270	+34 microns	9.88
−34	+24 microns	10.80
−24	+17 microns	15.31
−17	+12 microns	13.00
−12	+8.5 microns	11.38
−8.5	+6 microns	8.74
−6		15.78
	Total	100.00

Table II. Chemical Analysis of Concentrates

Constituent	Wt, Pct
Total Fe	63.25
Fe^{++}	19.00
SiO_2	8.84
Al_2O_3	1.45
CaO	0.08
MgO	0.57
TiO_2	0.08
Mn	0.12
S	0.01
P	0.025

The pellets were prepared from concentrates of the same composition and size distribution given in Tables I and II. Air-dried pellets were heated in an inert atmosphere at temperatures ranging from 100° to 1200°C by direct introduction into a fur-

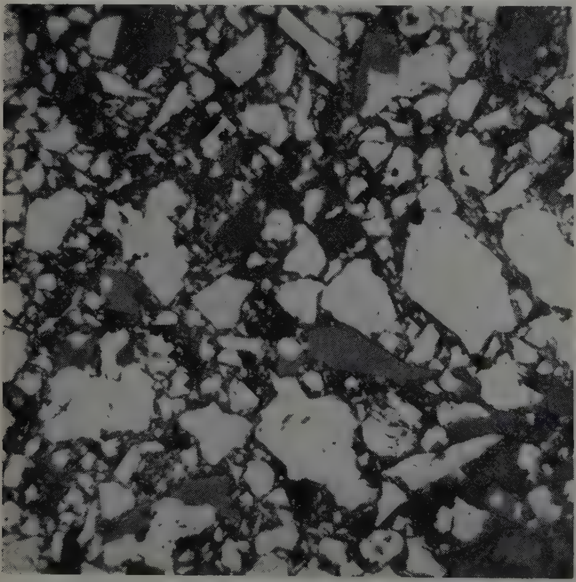

Fig. 1—Section of pellet rolled from eastern Mesabi taconite concentrate. Magnetite is white, quartz and siliceous gangue minerals are grey, and pores are filled with plastic. X250.

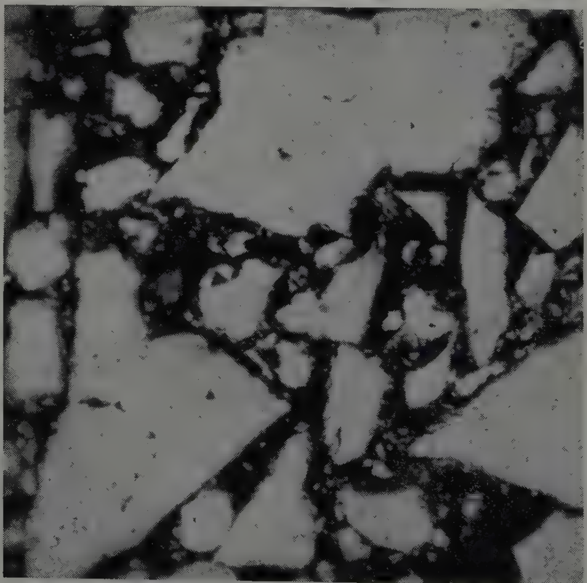

Fig. 2—Section of pellet shown in Fig. 1. X1200, oil immersion.

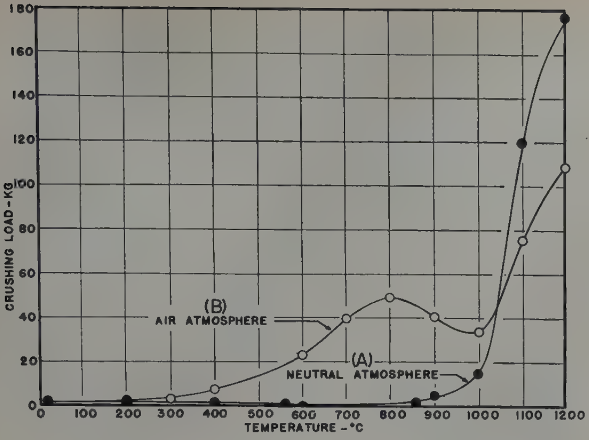

Fig. 3—Strength-temperature curves, 30 min.

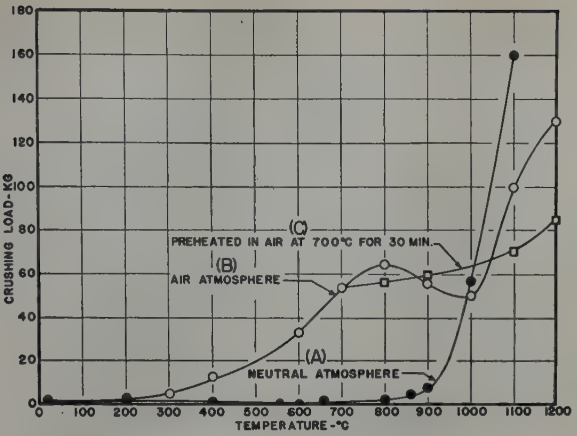

Fig. 4—Strength-temperature curves, 120 min.

nace already at temperature. Two periods of heating were employed for each temperature, 30 and 120 min, respectively. In addition to those pellets selected for microscopic examination, 10 or more pellets were treated at each temperature and their strengths determined in an Amsler testing machine. The arithmetic mean strengths are given in Figs. 3 and 4, curves A.

Air-dried pellets had a strength of 1.2 kg. A surprising feature, shown by both the 30 and 120 min firing tests, is the drop in strength between 200° and 660°C. This is accounted for by removal of the last of the adsorbed film of water responsible for the dry strengths of the pellets.

At 660°C the 120-min series has returned to the original dry strength, and the 30-min series shows a similar response. Between 800° and 900°C both series start gaining markedly in strength, and as shown by curves A in Figs. 3 and 4, the strength increases exponentially with temperature. For comparison, the strength of the best pilot-plant fired pellets is of the order of 200 or 250 kg.

Specimens fired in an inert atmosphere for 120 min at temperature intervals of 100° from 500° through 1200°C were impregnated and polished. The sections were examined microscopically, both at low powers for changes in general appearance and at high resolution to determine the existence of small changes, especially at the grain boundaries. Specimens fired below 800° show only a slight conversion of magnetite to hematite, due to entrapped air, with no structural changes except for a cracking of the hydrated silicates. On the other hand, all pellets fired up to 660°C disintegrated with considerable rapidity when immersed in water, and those fired at higher temperature remained intact indefinitely under the same conditions. The writers regard this as indicating that weak bonding commenced at this low temperature.

Examined microscopically, pellets fired at 800°C show no obvious change compared with the air-dried pellets. At high resolving powers occasional thin blades of hematite can be seen in the magnetite grains, its distribution being uniform throughout the pellet. Since much less hematite occurs, only sporadically, in the untreated pellets, it is assumed that this hematite originates from oxidation by the residual air in the pores, before the nitrogen has had time to sweep it out. Assuming that a ¾-in. pellet contains 25 pct porosity, and that all the contained oxygen is available for conversion of magnetite to hematite, then approximately 7 mg of hematite will be produced. This is of the order of magnitude observed.

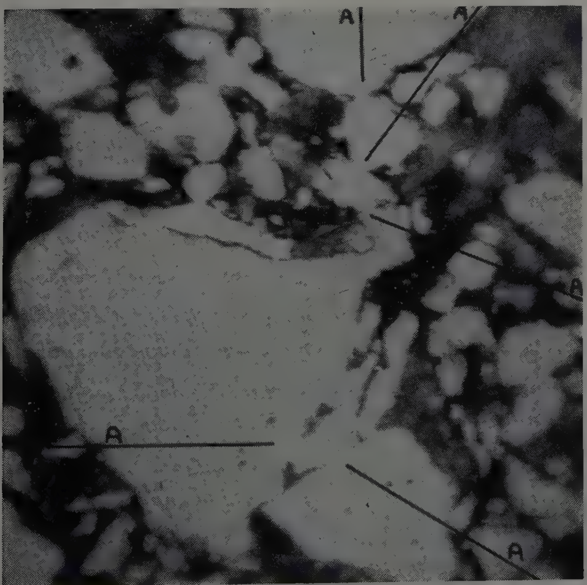

Fig. 5—Bridging of magnetite grains, A, at 900°C. X1000, oil immersion.

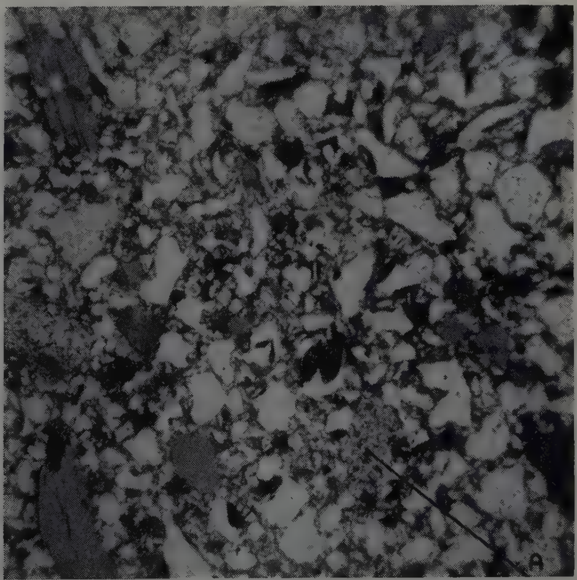

Fig. 6—Section of pellet fired at 1000°C, showing agglomeration of fine magnetite particles, A, and bridging of coarser magnetite. X250.

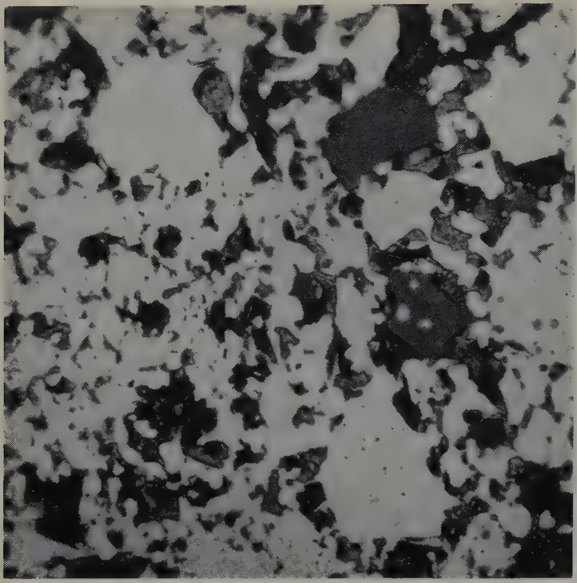

Fig. 7—Section of an iron ore pellet, showing continuous lattice of magnetite at 1100°C. X250.

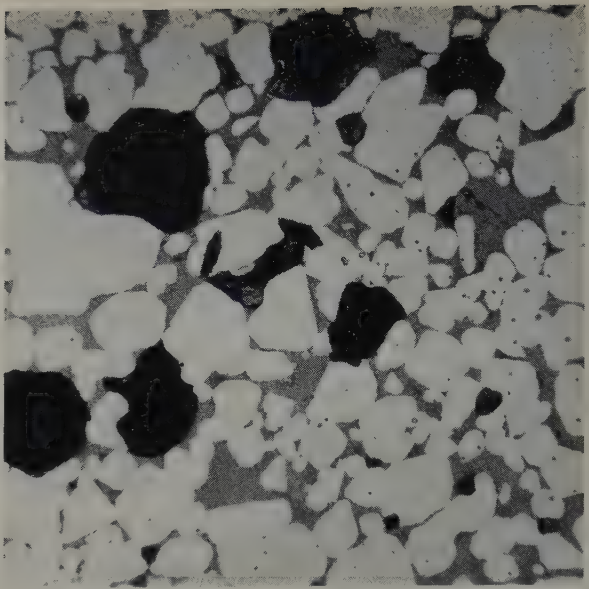

Fig. 8—Magnetite grains and continuous slag network at 1200°C. Compare this with Fig. 7 for changes in pore size. X250.

The 900°C pellets show slight but important differences compared with the 800°C pellets, but these are observable only at high powers. First, the hematite has entirely disappeared, presumably having entered into solid solution in the magnetite. Second, there is a distinct tendency for grains of magnetite which are in contact to join together and form short bridges, as shown in Fig. 5. Thirdly, there is a blunting of the cusps of the original magnetite grains. On the other hand, the distribution of the micron-size particles of magnetite appears the same as in the previous specimen, and there is no apparent change in the gangue.

At 1000°C there are marked changes. First, nearly all the smallest magnetite grains have agglomerated into relatively large sponge-like masses, shown in Fig. 6. Secondly, the bridging between adjoining magnetite particles has become very pronounced, an extension of the structure shown in Fig. 5. The larger gangue particles show no change except for blunting of the cusps, but smaller particles have begun to lose their identity and tend to yield to the forces causing the magnetite to grow.

At 1100°C the original microstructure of the pellets is almost unrecognisable, for in large measure the magnetite has recrystallized. Only the very largest magnetite and gangue particles preserve something of their former identity, and there is a continuous structure of the former from one edge of the pellets to the other. The spongelike masses of magnetite occurring in the pellets fired at 1000°C have become massive, with the internal structure broken only by fine lines of slag. The gangue has been largely converted to glassy slag, forming a discontinuous network between the magnetite grains and acting as a bond between adjacent particles. Fig. 7 shows a section of one of these pellets. It should be noted that attainment of this structure is coincident with a very marked increase in strength. There must be a very considerable mobility of both magnetite and slag at 1100°C, for the many fine pores have coalesced into a much smaller number of large pores.

Fig. 8 is a photomicrograph of a pellet fired at 1200°C. For all practical purposes the magnetite is monodisperse, the grains being surrounded by slag. The pores have been reduced greatly in number, and are now of a size comparable with the largest magnetite grains. Curiously, there is no bridge structure of the magnetite as in the 1100°C pellets and the slag has now assumed continuity of structure across the specimen.

From the preceding observations two inferences appear safe. 1—In a neutral atmosphere, magnetite grains will bond, when and where they touch, at least at 900°C, and possibly at still lower temperatures. Under these conditions there is no visible change in the gangue constituents except dehydration. 2—At somewhat higher temperatures the gangue plays an important part in the growth of the magnetite. At about 1000°C grain growth commences at the expense of the fine magnetite particles which are spacially separated. It seems improbable that such growth can occur unless there is actual transfer of magnetite through another medium, in this case the gangue or the slag which is forming from the gangue. In fact, it is probably no coincidence that marked grain growth of magnetite and increase in pellet strength are contemporaneous with the formation of conspicuous quantities of slag. It is noteworthy, however, that observed cementation of osculating particles of magnetite occurs some 700°C below the melting point of magnetite, suggesting high mobility in the solid state.

The gangue constituents apparently possess considerable mobility at 1000°C, possibly analogous to the softening of a siliceous slag, but seemingly more than 100° too low for melting to occur. Taking the probable slag-forming constituents of Table II, neglecting the small amount of TiO_2, and recalculating to 100 pct will give the results shown in Table III.

Table III. Slag-Forming Constituents in Taconite Concentrates

Constituent	Wt, Pct
SiO_2	70.8
Al_2O_3	11.6
CaO	0.6
MgO	4.6
MnO	12.4
	100

In slag formation, whatever amount of FeO is necessary for equilibrium will come from the complex iron silicates in the gangue and from the magnetite. From the available equilibrium diagrams, the melting point of a slag containing the listed oxides and FeO cannot be much below 1150°C.

Structure of Magnetite Pellets Fired in Air

For an investigation of the effect of oxidation on strength, pellets similar to those fired in inert atmospheres were heated at temperature for 30 and 120 min. Ten pellets were used to determine strength at each temperature for the two series, and the results are plotted as curves B in Figs. 3 and 4.

Strength increases with temperature, reaching a first maximum at 800°C. Thereafter it decreases to a minimum at about 1000°C, and then climbs to a second and undetermined maximum at higher temperatures. The minimum above 800°C was unexpected but is confirmed by similar tests made elsewhere on other magnetite concentrates. Pellets fired according to the schedule given were impregnated, sectioned, and semi-polished on 3/0 metallographic paper, but were not given a final polish because of their striking appearance at this stage. Pellets fired for 30 min at 400° and 600°C were red throughout and macroscopically were uniform from edge to edge. Those fired at 700°C contained a relatively small dark-grey core surrounded by a red shell. The 800°, 900° and 1000°C specimens had progressively larger cores and thinner shells. The cores of the 1100°C pellets approximated in size those of the 900°C specimens, those of the 1200°C pellets were similar in size to those of the 800°C pellets, and both the 1100° and 1200°C pellets contained marked contraction cracks separating cores from shells. All the 30-min pellets were magnetic, the 700° to 1200°C specimens especially so. The structures reported above are shown diagrammatically in the upper part of Fig. 9.

Of the pellets fired for 120 min, those from 400° to 1000°C were uniformly red. The 400°C pellets were magnetic, the 600° and 700°C pellets weakly so, the 800° to 1000°C specimens were non-magnetic, and the 1100° and 1200°C pellets were strongly magnetic. Those fired at the two highest temperatures possessed cores similar to, but smaller than, those of their 30-min counterparts, and the concentric crack between core and shell was well developed, see Fig. 9.

Examination showed that the dark-colored cores consist of unaltered or of very slightly oxidized magnetite, and that the red shells consist of slightly oxidized to completely oxidized coarse magnetite grains in a network of very fine hematite, see Fig. 10. This last-mentioned structure originates in the complete oxidation of the interstitial slime magnetite, a process occurring rapidly at relatively low temperatures. Internal reflection within this fine hematite gives a predominating red color to this part of the pellet, even though magnetite may be the more abundant mineral. For example, the 400° and 600°C pellets fired for 30 min are magnetic, even though megascopically they are red throughout. The cores of pellets fired at 700°C consist of coarse magnetite grains surrounded by a network of magnetite slimes in which there are only occasional areas of oxidation. The cores of the 800° to 1100°C pellets are similar, but the microscopic structures previously described for pellets fired in nitrogen are becoming evident. At 1100° and 1200°C the magnetite of the cores assumes the structures shown respectively in Figs. 7 and 8.

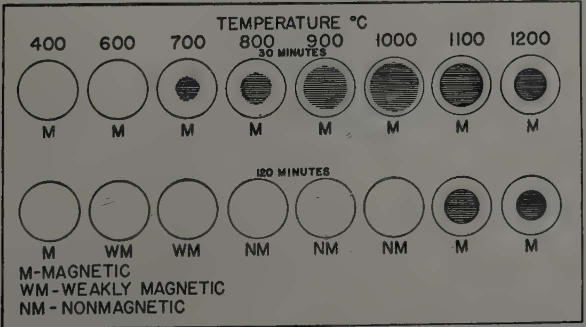

Fig. 9—Macroscopic structures of magnetite pellets fired in air.

Nearly all the magnetite in the 120-min specimens fired at 600° and 700°C has been oxidized, and there is no magnetite in those specimens fired at 800°, 900°, and 1000°C.

Although the rate of oxidation should increase with increasing temperature, in the case of the 30-min pellets the amount of magnetite converted to hematite actually decreases with increasing temperature, up to 1000°C. The authors regard this as due to a decrease in permeability. For example, at 400° to 600°C the pellets possess so loose a structure that oxygen readily penetrates the interstitial slimes and oxidizes the fine magnetite to the centers of the pellets. It is presumed that at higher temperatures the freshly-formed hematite is more mobile and bridges and seals the pores so that gaseous penetration is substantially reduced. Sealing is incomplete, however, because total oxidation occurs in 120 min at temperatures of from 800° to 1100°C, inclusive.

The formation of hard cores in both series of tests at 1100° and 1200°C is due to the fact that lowered permeability permits early slag formation and recrystallization of magnetite at these temperatures, just as in magnetite pellets fired in nitrogen. Once slag has formed and the grain size has coarsened, oxidation is necessarily slower.

Concentric shrinkage cracks at temperatures above 1100°C are due to condensation of the core. At these temperatures the slag has softened and pores have enlarged but have become less numerous; eventually they coalesce by surface tension, in the space between the rigid shell and the core. Significantly, no concentric cracks occur in pellets fired in neutral atmospheres, but a decrease in volume of 15 pct or more occurs in those fired at 1100°C or above.

Structure of Pilot Plant Pellets

The characteristics of laboratory-fired pellets have been discussed at considerable length, since they provide valuable information concerning the behavior of pellets fired in pilot plant furnaces. However, laboratory conditions are not identical with those of practice. In large-scale firing, wet pellets are loaded gently onto the charge, which in a matter of inches below the loading level passes through the maximum temperature in the furnace. Expulsion of water is extremely rapid, the pellets reach temperature very rapidly, and are soaked for a long period, measured in hours, in a heat-exchanging, oxidizing atmosphere. In practice, furnace temperatures are high, for heat liberated by the oxidation of the magnetite to hematite is available. Furthermore, coal is frequently added to the concentrates before rolling,

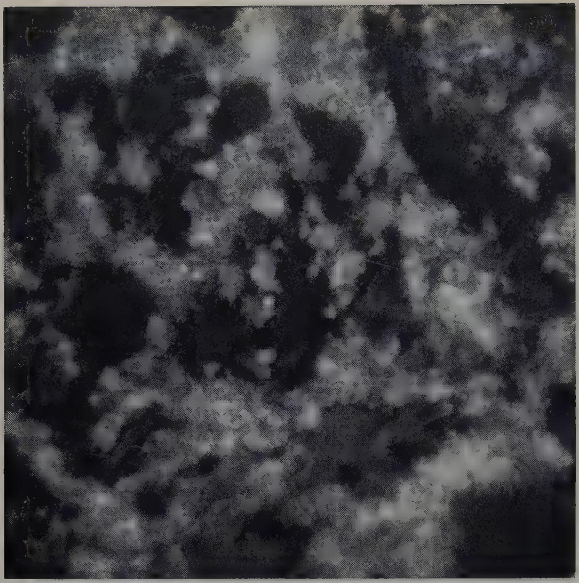

Fig. 10—Network of oxidized slime magnetite, white, surrounding larger grains of superficially oxidized magnetite, black. X1000, oil immersion, crossed nicols.

and this contributes additional heat as well as carbon monoxide, both of which may play a determining role in the mineralogy of the pellets.

Magnetite pellets with or without coal, fired in the Minnesota Mines Experiment Station shaft furnaces, possess structures almost identical with out pellets fired for 120 min at 1200°C in air. The shells contain hematite grains pseudomorphic after the original larger-fragmented magnetite particles, together with the slime network of hematite. The structure of the cores is identical with that shown in Fig. 8, even to the order of size of the recrystallized magnetite. In some cases the core magnetite is retained as such; in others it has been oxidized subsequently to hematite. With a larger amount of gangue present than in the concentrate used by the writers, the magnetite often attains singular perfection of crystal shape.

Pellets made in the large pilot plant furnaces consist almost entirely of hematite. Microscopic study clearly shows that prior to complete oxidation they have a binary structure identical with that previously described. The only apparent changes consist in the replacement of the recrystallized magnetite of the cores by hematite, and, in the highest-strength pellets, a coarsening of the grain of the shell. Oxidation of the core occurs without modification of the outlines of the magnetite polyhedra.

Thermal shock may cause radial cracking of the shell. If this occurs at sufficiently high temperature, the recrystallizing magnetite and fluid slag extrudes from the crack. Grate-fired pellets commonly show this effect, which may also occur in furnace products.

It is generally recognized that *red* pellets are weak and friable, but that dark *blue* pellets are strong and show little friability. There is a remarkable correlation between strength and microstructure. Red pellets may have a shell in which there is a great amount of slime hematite, best seen in polarized light, or may have no core, the entire pellet consisting of oxidized slime magnetite bonding more or less oxidized and unrecrystallized magnetite. Blue pellets, on the other hand, contain little or no slime hematite in the shell, and the cores consist of slag-bonded recrystallized magnetite or of slag-bonded hematite formed from the oxidation of that magnetite. It is certain that either through channelling or some other effect the red pellets have not been heated to a high enough temperature.

The authors' concept of the changes through which pellets proceed during pilot plant firing is as follows:

1—Moisture escapes from the pellet. Either during this operation or shortly following it the interstitial slime magnetite of the shell oxidizes, and by at least 300°C there is an appreciable increase in strength due to cementation and grain growth.

2—As the pellet moves into a hotter zone, oxidation of the slime proceeds inward, and the coarser magnetite of the shell oxidizes.

3—At 800°C the shell formation is almost completed. The shell has considerable hot strength and its permeability to the furnace atmosphere is greatly reduced. The pellet is now subject to appreciable load from overlying burden, but the shell prevents collapse of the dry, powdery magnetite core.

4—Marked changes in the core commence between 800° and 900°C and continue to high temperatures. The magnetite forms a network structure by cementation, and there is softening of the gangue. The hot strength of the core probably increases because the magnetite network is forming in the solid state.

5—At some temperature between 1100° and 1200°C the slag-forming constituents have become plastic and form a matrix in which the magnetite disperses as more or less equiaxed polyhedra. However, if the slag volume is small there is evidence that the magnetite network of item 4, above, is retained. The core presumably has little hot strength, and it is only the oxidized shell which prevents collapse. In many pellets much of the pore space rearranges into a concentric crack between shell and core.

6—In all pellets there has been complete recrystallization of the magnetite in the core prior to the start of oxidation. Oxidation commences at the outside of the core and slowly proceeds inward. In pellets which have been fired in small shaft furnaces oxidation does not necessarily proceed to completion, and the cold pellet may contain a substantial magnetite core. All pilot plant pellets examined, however, contain very little residual magnetite.

Addition of coal to magnetite pellets raises peak temperatures and probably permits formation of a larger core. Excess coal causes fusion and collapse of the pellet.

From the point of view of commercial production of pellets from magnetite concentrates, it is extremely fortunate that a shell containing slime hematite forms in the early stage of firing.

Acknowledgments

The writers wish to express their thanks to Professor E. W. Davis and to Mr. L. S. Taylor of the Minnesota Mines Experiment Station, to the former for the samples of fired pellets used in this investigation and to the latter for preparing the green pellets used in the firing experiments.

References

[1] M. Tigerschiöld and P. A. Ilmoni: Fundamental Factors Influencing the Strength of Green and Burned Pellets Made from Fine Magnetite-Ore Concentrates. AIME Preprint, Blast Furnace, Coke Oven, and Raw Materials Conference, Cincinnati, April 1950.

[2] G. M. Schwartz: Iron-Ore Sinter. *Trans.* AIME (1929) **84**, p. 39.

[3] James Forbes Bell: Notes on the Uses of Methyl Methacrylate 'Lucite' in a Geological Laboratory. *Economic Geology* (1939) **34**, p. 804.

[4] Charles Meyer: Notes on the Cutting and Polishing of Thin Sections. *Economic Geology* (1946) **41**, p. 166.

The Preparation of Low-Ash Coal

by Adam L. Wesner and A. C. Richardson

This paper describes the development of a continuous float-and-sink process to produce coal low enough in ash content to be suitable for production of electrodes. The cleaned coal had a combined iron and silicon content of 0.239 pct. The efficiency of recovery was 84 pct.

During World War II the demand for electrode carbon was greater than could be met by the supply of petroleum coke available for this use. It was believed that coke made from an extremely low-ash coal might be a suitable substitute for petroleum coke. Requirements for electrode carbon to be used for the production of aluminum are that the silicon plus iron content shall be not more than 0.14 pct of the coke. However, during the period when petroleum coke was in short supply, it appeared that relaxations of the specifications might be allowed to permit 0.4 pct iron plus silicon in the coke. For this work, the specifications were that the coal should contain less than 1 pct of ash, and the combined iron and silicon content of the coal should not exceed 0.28 pct.

Heavy-liquid separations made on a number of coals showed that if certain size fractions of some coals were separated at low specific gravities the resulting float products would meet the required specifications. The objective of this work was to develop a continuous, commercially feasible process for producing low-ash coal. After consideration of various processes, the method chosen was a float-and-sink separation using a solution of calcium chloride as the separating medium.

Eagle Seam coal was used for the experiments. The −10 +35 mesh fraction was found to be the most promising feed for producing the low-ash content coal. A batch of 30 tons of −3/8-in. coal was screened at 10 and 35 mesh; the yield of −10 +35 mesh was 20 pct of the feed. This fraction comprised the feed for the separation tests. In spite of the fact that this portion was screened a second time at 35 mesh, the coal still contained 16 pct that was finer than 35 mesh. Three-fourths of the undersize was in the −35 +48 mesh range.

Table I. Batch Float-and-Sink Separation of Raw Coal

Product				Cumulative	
Sink	Float	Wt, Pct	Ash, Pct	Wt, Pct	Ash, Pct
	1.25	4.61	0.82	4.61	0.82
1.25	1.26	27.67	0.73	32.28	0.74
1.26	1.27	33.76	0.83	66.04	0.79
1.27	1.28	11.53	1.44	77.57	0.88
1.28	1.32	10.27	3.96	87.84	1.25
1.32	1.59	9.64	11.90	97.48	2.30
1.59		2.52	60.30	100.00	3.76

Product	Wt, Pct	Ash, Pct	Fe, Pct	Si, Pct
Composite float 1.27	66.04	0.79	0.073	0.112
Composite sink 1.27	33.96	9.44	0.451	2.369
Composite heads	100.00	3.73	0.201	0.878
Feed		3.79	0.193	0.921

A representative portion of the −10 +35 mesh fraction was subjected to batch float-and-sink separations to determine the best gravity to be used in the continuous tests to obtain a high recovery of low-ash content coal. The heavy liquid used was a mixture of carbon tetrachloride and benzene which assured complete wetting of all of the particles. As usual in batch separations, adequate time was allowed for each separation so that even the near gravity particles had ample time to separate. The separations were made at increments of 0.01 sp gr from 1.25 to 1.28 and also at 1.32 and 1.59. Each specific-gravity increment was assayed for ash content. From these data it was concluded that 1.27 sp gr was best for the continuous separation of the coal.

The products from the batch separation were composited into float 1.27 and sink 1.27 sp-gr fractions; these were assayed for ash, iron, and silicon. Table I shows the results of the batch separations. The composite float 1.27 fraction contained 66.04 pct of the total weight, and had an analysis of 0.79 pct ash, 0.073 pct iron, and 0.112 pct silicon, or 0.185 pct iron and silicon combined. These data are indicative of the results possible if a perfect separation is made at 1.27 sp gr under static conditions. Inasmuch as the method under investigation is a dynamic system these results could not be obtained. It remained to be determined, however, just how close to the theoretical results the actual continuous separation would be.

A. L. WESNER and A. C. RICHARDSON, Members AIME, are Research Engineer and Supervisor of Minerals Processing Division, respectively, Battelle Memorial Institute, Columbus, Ohio.

Discussion on this paper, TP 3425F, may be sent (2 copies) to AIME before December 31, 1952. Manuscript, March 4, 1952. Revised Sept. 22, 1952. New York Meeting, February 1952.

Dry coal, especially fine dry coal, is highly resistant to wetting by water. In calcium chloride solution the resistance to wetting is even greater. As is shown later in this paper, thorough wetting is essential for a good separation. This made is necessary to develop a method which gave thorough wetting of the coal in calcium chloride solution.

Qualitative tests were made on a number of wetting agents in 1.27 sp-gr calcium chloride solution. Most of the wetting agents were eliminated because they formed precipitates immediately upon addition to the calcium chloride solution. Three wetting agents showed some promise, namely Tergitol Penetrant 4, Du Pont Reagent DP 243, and Invadine C. Comparative tests on these three wetting agents showed Tergitol Penetrant 4 to be far superior to the other two in calcium chloride solution. The amount required was 0.75 lb per ton of coal treated.

Having found a suitable wetting agent, the next step was to establish quantitatively how much the separation in calcium chloride solution is improved when a wetting agent is used. Two representative samples of coal were separated in 1.263 sp-gr calcium chloride solutions, one with 0.05 pct Tergitol Penetrant 4 and the other with no wetting agent. In each case a careful batch separation was made between the float product and the sink product. Table II shows the results obtained. With wetting agent, the float product comprised 54.6 pct of the weight and had an ash content of 0.74 pct. Without wetting agent, the float product contained 79.7 pct of the weight and assayed 1.16 pct ash. This experiment shows the necessity for complete wetting in order to prevent a substantial weight of refuse from reporting in the float coal.

Some of the continuous separation tests described later were made by feeding dry coal into the calcium chloride solution, but it was also desired to make some of the tests with coal which had been prewetted in water. Cold water, hot water, and steam were tried, but these did not give complete wetting of the dry coal. Several wetting agents were tried in water; the best wetting agent found was Wetsit. The required amount was about 0.25 lb per ton of coal treated, or about one-third the amount of Tergitol Penetrant 4 required to wet dry coal in calcium chloride solution. As the cost of both of the wetting agents was about 25¢ per lb, wetting in water with Wetsit would cost about 12¢ per ton less than wetting with Tergitol Penetrant 4 in calcium chloride solution.

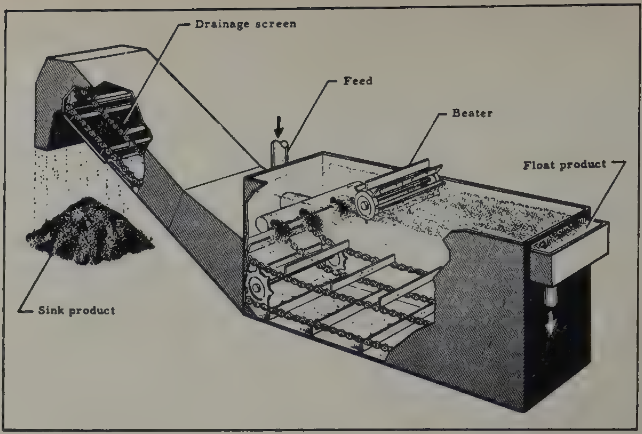

Fig. 2—Heavy-liquid separator.

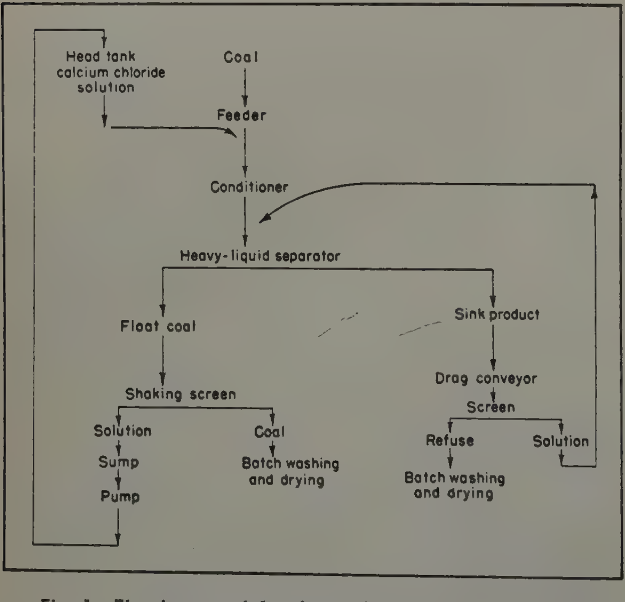

Fig. 1—Flowsheet used for the production of low-ash coal.

The flowsheet for the continuous-separation experiments is shown in Fig. 1. Calcium chloride solution served not only as the separating medium, but was also circulated through the system to provide a means of transporting the feed coal and the float product.

In the experimental plant, no provision was made for continuous washing and recovery of the residual calcium chloride solution retained on the products. Washing and drying were accomplished in batch operations.

A sketch of the separating vessel is shown in Fig. 2. This is a rectangular settling tank 2 ft wide, 8 ft long, and 3½ ft deep. A drag flight conveyor is provided to transport the sink product across the bottom of the vessel, up the inclined portion of the tank, over a stationary drainage screen, and then to discharge. A slow-speed multiblade paddle beater is provided to agitate the float coal gently to reduce occlusion of refuse in the float coal.

Table II. Batch Float-and-Sink Tests on Coal in Calcium Chloride Solution With and Without Wetting Agent

Product	Without Wetting Agent		With Wetting Agent	
	Wt, Pct	Ash, Pct	Wt, Pct	Ash, Pct
Float 1.263	79.7	1.16	54.6	0.74
Sink 1.263	20.3	12.95	45.4	6.85
Composite	100.0	3.65	100.0	3.51
Heads		3.79		3.79

In operation, the circulating solution and the coal are fed into a central standpipe of the conditioner, and then discharged from the top of the conditioner by gravity through the side or end of the tank about 1 ft below the liquid level. The feed is distributed evenly across the width of the tank by means of a manifold pipe. Besides the solution entering with the feed, calcium chloride solution is added to the inclined portion of the tank to prevent float coal from being trapped in this section. The calcium chloride solution is maintained at the desired density and volume by additions of either strong liquor or water to the pump sump as needed.

Procedure and Results of Continuous Separations

Preliminary experiments were made to establish the best operating procedure for the continuous separation. It was established that 1—a cleaner float product was made when the multiblade paddle beater was used, 2—a higher yield of float product was obtained when about one-fifth the circulating solution was added to the inclined portion of the tank, and 3—there was no difference in the results when the two methods of wetting described previously were tried.

In the final, large-scale test the coal was prewetted in water. A six-ton lot of coal was agitated in water containing Wetsit; then the coal was filtered on a pan-type vacuum filter. The moisture content of the filtered coal was 9 pct. The coal was fed to the separating vessel at a rate of 1000 lb of dry coal per hr. The total amount of calcium chloride solution circulated was 2700 lb per hr, 2200 lb with the coal, and 500 lb to the incline. It was necessary to add strong calcium chloride solution to the head tank in sufficient quantity to compensate for the water carried into the system by the wet coal. The specific gravity of the separating solution was maintained between 1.265 and 1.270 throughout the test. The products of the test were washed free of calcium chloride, then dried, weighed, and assayed.

The results showed the yield of float coal to be 66.4 pct of the total feed, the assay was 0.92 pct ash, 0.087 pct iron, and 0.152 pct silicon, or 0.239 pct total iron plus silicon. Using the ash content of 0.92 and interpolating in Table II, the float coal assay would indicate a separation at a gravity of about 1.284 and the yield at this gravity should be 78.7 pct. The yield actually obtained was 66.4 pct; therefore, the efficiency of recovery was 84.4 pct.

The ash content of the float product made in the continuous separation at sp gr 1.265 to 1.270 was slightly higher than that of the float 1.27 product made in the batch separation. The higher ash content is the result of a less perfect operation of a continuous system compared with a batch separation. This difference is to be expected, because in batch operations the near gravity particles have periods of undisturbed quiet in which to find their proper place, while the solution in a continuous separating tank is in constant motion even though precautions are taken to reduce turbulence and agitation to a minimum.

Acknowledgment

The authors wish to thank the Koppers Co., sponsor of the project under which this method was developed, for permission to publish this article.

Cementing in Deep Diamond Drill Holes

by Adrian E. Ross

Diamond drilling through caving formations at depths greater than 2000 ft has long presented serious difficulty, generally solved either by casing or cementing. Casing is permitted only when the resulting smaller hole is acceptable, and cementing is frequently a problem at depth. A new method that injects cement under pressure at the desired location is an aid in diamond drilling deep holes.

DRILLING through caving formations in diamond drill holes at depths greater than 2000 ft has long been a serious problem. These caving formations are normally passed only by casing the hole or by cementing the hole. Casing the hole is possible only when a resulting smaller hole is acceptable. In as much as only a limited number of reductions are economically practical, cementing is frequently considered the only method suitable for solving these problems. Cementing either by pumping a slurry into the hole or by dropping cylinders containing cement has proved satisfactory on holes under 2000 ft. In holes substantially deeper than 2000 ft these methods are not satisfactory, since during the pumping process cement *separates out*, whereas cylinders usually break before the bottom of the hole is reached. A new procedure, *the injector method*, apparently solves these problems.* With this method, cement is lowered in the hole in a cylinder, the cement being

---

* This cement injector device and procedure were developed by Robert R. Carver, Assistant Manager of Contract Department, Sprague & Henwood, Inc., Lewis W. Fetherman, Factory Engineer, Sprague & Henwood, Inc., and the author.

A. E. ROSS, Member AIME, is Assistant to the President and Chief Engineer, Sprague and Henwood, Inc., Scranton, Pa.

Discussion on this paper, TP 3423A, may be sent (2 copies) to AIME before Dec. 31, 1952. Manuscript, Dec. 5, 1951. New York Meeting, February 1952.

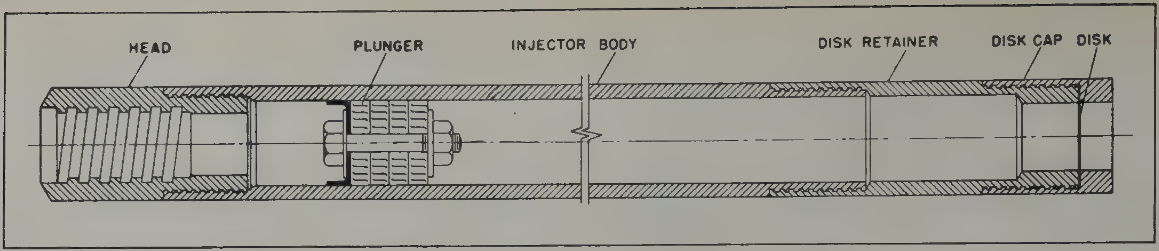

Fig. 1—Design of cement injector.

held in place by a disc in the bottom of the cylinder. When the caving formation is reached, sufficient hydraulic pressure is applied to a piston at the top of the cement cylinder to break the disc, causing the cement to be injected under pressure at the desired location in the hole. In this way, thick, properly mixed, quick-setting cement can be placed anywhere in the hole at the operator's discretion.

The Problem in Drilling

Drilling of deep diamond drill holes becomes an increasingly difficult problem when intermittent soft broken formations or faulted zones are encountered. Such formations or faulted zones cause caving, with the result that the hole is filled each time the core-barrel is withdrawn. The caved section is then redrilled at high bit cost. Furthermore, it is often difficult or even impossible to advance the hole beyond the caved area. The normal solution to such a problem is either to case the hole, thereby reducing it one size, or to cement it.

Consider first the problem of casing. If only one cave area is encountered, the hole could very readily be reduced one size. For example, assume a hole were being drilled with an NX bit, 2⅛-in. diam core, the largest of the four standard sizes. If the customer would accept a BX core, 1⅝-in. diam, then the hole could be reduced one size to BX and continued. In some instances the customer would accept an AX core, 1⅛-in. diam, which is the next smallest size, and if necessary the hole could be reduced a second time. If he were willing to accept an EX core, ⅞-in. diam, the size following AX, theoretically the hole could be reduced a third time. However, it is considered impractical to drill size EX in a hole 4000 to 5000 ft deep.

It might logically be assumed that a size larger than NX should be used in starting the hole if it is expected that numerous cave areas will be encountered, but at this point economics enter the situation. If holes larger than NX are drilled, the cost per foot is greatly increased. The exact amount varies with the formation and the depths being drilled, but it is safe to say that using the next size larger than NX would render the cost of the hole at least 25 pct greater than the cost of the NX hole. Two sizes larger than NX could very easily increase the cost over NX by 75 pct, and in some cases as much as 100 pct. Such increases in cost naturally limit the use of these larger sizes. Frequently the customer is unable or unwilling to pay the cost of starting larger size drill holes.

In one recent instance, several deep holes were drilled across a number of fault zones and zones of finely crushed mica schist. Each time the core barrel was withdrawn the hole immediately refilled. Two days of continuous washing failed to clean the hole, and casing it was considered economically impractical. Conventional methods of cementing were therefore tried, as described in the following paragraphs.

Conventional Cementing Practices

Conventional methods of cementing diamond drill holes range from pouring cement from a pail to dropping well prepared cardboard cylinders of carefully mixed cement down the drill hole. Two of the most commonly used methods are described below, with comments on their failure at depths greater than 2000 ft.

Pumping the cement mixture through the drill rods is a method now commonly used in deeper holes. One version of this procedure is described in detail by J. D. Cumming.[1] Drill rods with a special coupling attached to the bottom end are lowered into the drill hole. This coupling contains a small opening in the bottom end and other openings around its periphery. The peripheral openings are used to wash the cave from the wall of the hole. When the hole is properly cleaned, cementing is started. For this operation the intake of the pump is transferred from the water source to a container of cement mixed sufficiently thin to permit proper flow through drill rods and drill rod couplings. The required amount of cement is then pumped into the hole and the rods withdrawn and washed before the cement has time to set in the rods.

Attempts to apply this method failed. At depths greater than 2000 ft the cement apparently had a tendency to separate out or *drown,* thus preventing proper hardening. There may also have been a small flow of water in the cave area. This may have washed away the thin cement before it had a chance to set. Then too, at such depths the friction head developed was excessive, and standard high pressure

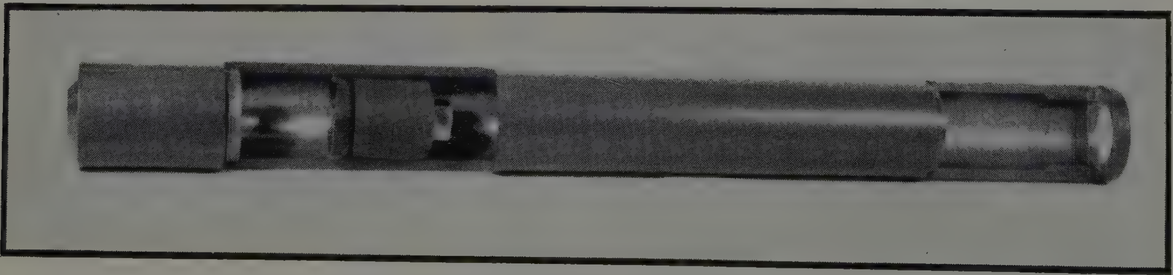

Fig. 2—Cement injector.

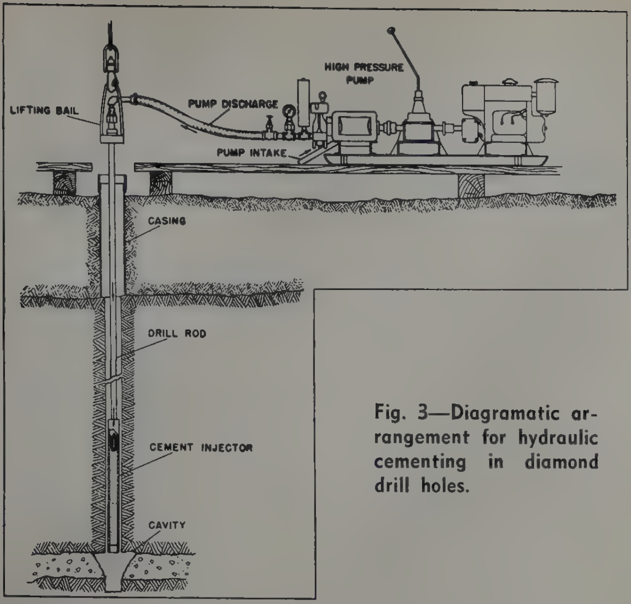

Fig. 3—Diagramatic arrangement for hydraulic cementing in diamond drill holes.

drilling pumps were neither suitable for such cementing work nor capable of developing adequate pressure. Special grout pumps would have been required before this method could have been given a further trial.

In the other procedure normally used for difficult cementing conditions, the cylinder method, cement is lowered to the cave area in a cardboard cartridge or paper cylinder. When this method is used it is customary first to drop a string of casing into the hole to permit the cement containers to reach the bottom without interference. The cartridge or cylinder is then filled with cement and dropped through the casing. If the cylinder does not break upon hitting the bottom of the hole, drill rods are lowered to break it, thus freeing the cement. With this method a fairly heavy mixture of cement may be used, permitting a quick set. It offers a distinct advantage over the pumping method if there is any movement of water in the cave area.

In deep holes, however, difficulty was experienced with this procedure. Apparently the hydrostatic pressure broke the cylinders at these depths, since paper and cardboard were found floating to the surface of the hole before any tamping process had been used.

Cement Injector Development

Trouble was encountered in one of the holes previously mentioned at a depth slightly over 2000 ft. The hole was washed for several days in an unsuccessful effort to clear the cave. Casing it was not practical, as this hole and several others were to go to a depth of between 4000 and 5000 ft. Cementing the cave area was considered the only suitable solution to the problem. The cementing methods described above were attempted without success. It was imperative, if the holes were to be completed at the specified size, that a simple and successful method be developed which would not necessitate costly grouting equipment, special high pressure grout pumps, or the hiring of special crews. Cycle time on deep holes is a major economic factor, so the procedure should require a minimum number of trips into the hole. The overall delay time from cessation of drilling to start of drilling should also be kept to a minimum, as labor costs for drilling crews are very high.

To meet these requirements, the cement injector shown in Fig. 1 was developed by Sprague and Henwood, Inc. It will be noted that most of the parts are made from equipment normally available at a drill or in a nearby small shop. The head is a standard AX-casing to B-rod substitute. The plunger is made from pump buckets, together with a bolt, nut, and washer. The injector body is made from flush-jointed casing. The disc retainer is made from solid stock or from tubing with an inside diameter somewhat smaller than the casing so that an internal shoulder will be provided to limit the travel of the plunger. The disc cap is made from material similar to the disc retainer and the disc is made from thin sheet brass or copper. The thickness of the disc may be varied according to the breaking pressure desired. For example, one disc made from .005 standard brass shim stock broke with water pressure on a laboratory test at approximately 350 lb pressure. This same disc broke at 500 to 600 lb pressure when it was used in the hole and the injector was charged with cement.

The injector body may be any required length. Normally Sprague & Henwood manufactures the injector body in 10-ft lengths, coupling 50 to 100 ft of body, depending upon the amount of cement required to fill any given cave area. Fig. 2 is a photograph showing the key parts of the cement injector. Two cut-away portions show the plunger and the disc. The flush-jointed casing is used so that there may be a smooth wall from top to bottom of the casing to permit the piston to move without interference.

Fig. 3 shows a diagramatic arrangement for hydraulic cementing in diamond drill holes. The high-pressure water pump normally used on a deep drill hole is suitable for this purpose. The pump intake is attached to a source of water. The pump discharge is attached to the drill rod, which in turn is held in place by the usual lifting bail. The bottom end of the drill rod assembly is attached to the head of the cement injector and the bottom of the cement injector is placed opposite the cave area to be cemented. Arrows show the flow of water through the pump intake and the pump, and out the pump discharge down the drill rod to the cement injector.

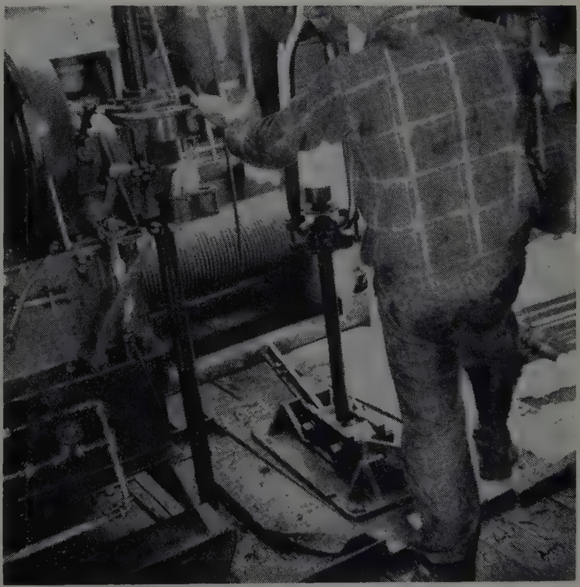

Fig. 4—Drill assembly in operation.

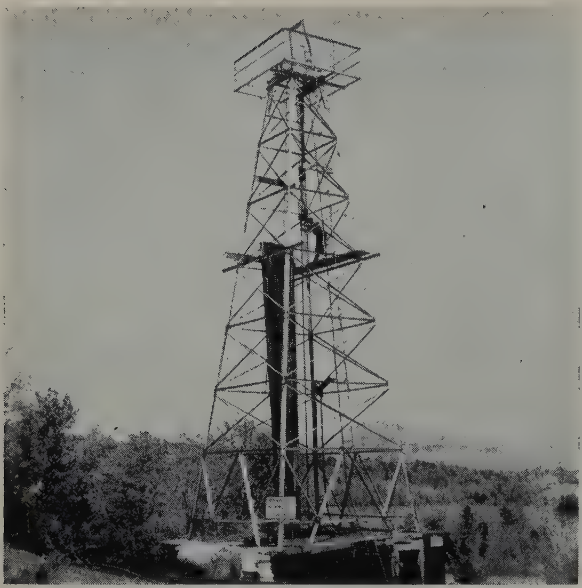

Fig. 5—Drill rig.

Fig. 4 shows a close-up of the drill operator lowering the assembly into the drill hole. The hoisting bail is shown under the operator's arm, and the foot clamp is shown in the bottom of the picture. Fig. 5 is a view of the drill shanty and derrick showing the general arrangement used in the operation described above.

The grout injector method of cementing has been used successfully many times during the past 10 months, usually without any supervisor on the job at the time of cementing. This method has proved successful for cementing cave areas in holes as deep as 4500 ft. It has failed during this development period only a few times, and each time the failure was traced to the operator, who had usually neglected to fill the drill rods with water. Failure to fill the drill rods resulted in excessive pressure under the disc of the cement injector, causing the disc to break prematurely. No other difficulty was encountered.

Cement Injector Practice

When the cement injector is used, the amount of cement required is first determined. In general it has been found that cement in 100 ft of AX casing will fill approximately 65 ft of a BX hole. These figures vary according to the extent of cave area encountered. After the amount of cement required is determined, the type of cement and the mixture are given careful consideration. Portland Cement, Hi-Early Portland Cement, Lumnite Cement, and mixtures of these various types have been tried, as well as admixtures including calcium chloride, plaster of paris, and several chemicals. Lumnite Cement is probably the most satisfactory. Usually the heaviest possible mixture of cement and water is used, with no gravel or sand. The exact mixture depends on the temperature of the day, the temperature of the water, and the time required to lower the cement injector into the hole. Tests are made with the cement mixture to avoid premature hardening of the cement. The operator must have time to insert the rods in the hole, apply pressure, and inject this cement into the cave area. At a shallow depth where little time is required to reach the bottom of the hole, 4 gal of water are used to a bag of Lumnite cement. Under normal conditions, this mixture will provide for 5 hr before the cement takes its initial set. Where the holes are deeper and more time is required to reach the bottom, thinner mixes are used. However, any consistency which is thinner than 7½ gal of water to a bag of cement should be avoided.

When the cement is ready, the disc, disc cap, disc retainer, and first 10-ft length of injector body are assembled and lowered into the hole. It will be noted that the disc retainer has a shoulder which prevents the plunger from passing that point. When this first length is lowered into the hole it is filled with the cement mixture described above. A second length of injector body is then attached, lowered in the hole and then filled with cement. The process is repeated until the correct number of injector bodies are connected to provide the desired quantity of cement. After the last length of injector body is added and filled with cement the piston is placed above the cement and the head is attached to the top end of the injector body.

Drill rods are then attached to the injector head and the tools lowered into the hole. Each section of drill rod is filled with water after it is attached to the string of tools and lowered to the drill platform. When a 40 or 50 ft length of drill rod is used as shown in Fig. 5 some difficulty is experienced in preventing air pockets, but this trouble is held to a minimum if care is exercised in filling each section with water so that pressures on the top and bottom of the disc are equalized. When the cement injector has reached the depth required, the string of tools is held by the foot clamp, a standard waterswivel is connected to the tools, and the tools are then held with the hoisting bail or other suitable means.

The standard high-pressure water pump used on the job is then connected with the string of tools in the hole and the water pressure increased until the disc is broken. It will be noted in Fig. 3 that a water pressure gage is shown on the left end of the high pressure pump. This gage is watched at all times during the operation because it is the key to the satisfactory operation of the cement injector. When the disc breaks, the tools are then pulled back slowly as the cement is being ejected from the injector body. The pressure gage on the pump shows a decrease when the disc is broken, and the pressure falls while the cement is being expelled. When the piston is pushed to the bottom of the casing and shoulders on the inward projection of the disc retainer, the pressure immediately builds up. If the action is too rapid, the relief valve which has been set at approximately 800 lb opens, signalling the operator to turn off the pump. The tools are then withdrawn from the hole and washed thoroughly. The cement is allowed to set approximately 16 hr.

Conclusion

The cement injector described herein has worked satisfactorily to depths as great as 4500 ft. There is no indication as yet that it has been employed at its maximum usable depth. In fact, it is believed that the injector should work satisfactorily at almost any depth, provided a method may be developed for placing it in the hole before the cement takes a premature set in the injector. Field experience alone will determine the ultimate limits of this deep-hole cementing device.

Reference

[1] J. D. Cumming: *Diamond Drill Handbook*, pp. 151-152. Havelock, Ontario, 1951.

Discussion*

Contents

AH—Metal Mining and Industrial Minerals

Pipeline Transportation of Phosphate. (Paper by I. S. Tillotson, R. B. Burt, and J. A. Barr, *Transactions* AIME, **193**, 273; *Mining Engineering*. March 1952. Discussion by Howard Howie.) 1066

B—Minerals Beneficiation

The Effect of Zinc Deleading Operations on Lead-Zinc Selectivity at the Parral and Santa Barbara Mines. (Paper by C. L. Boeke and G. C. Gunther, *Transactions* AIME, **193**, 495; *Mining Engineering*. May 1952. Discussion by I. M. Symonds, L. H. Lange, Norman Weiss, H. S. Wildman, C. F. Zeuch, E. H. Crabtree.) 1067

Jaw Crusher Capacities, Blake and Single-Toggle or Overhead Eccentric Types. (Paper by D. H. Gieskieng, *Transactions* AIME, **190**, 971; *Mining Engineering*. November 1951. Author's supplement.) 1069

Screened Ore Use for Fine Grinding at Lake Shore Mines. (Paper by Bunting S. Crocker, *Transactions* AIME, **193**, 499; *Mining Engineering*. May 1952. Discussion by Fred C. Bond, J. Myers, Norman Weiss, Harlowe Hardinge, Oscar Johnson, L. E. Djingheuzian.) 1069

The Third Theory of Comminution. (Paper by Fred C. Bond, *Transactions* AIME, **193**, 484; *Mining Engineering*. May 1952. Discussion by Milton C. Shaw and Donald R. Walker, R. J. Russell.) 1071

Flotation Rates and Flotation Efficiency.† (Paper by Nathaniel Arbiter, *Transactions* AIME, **190**, 791; *Mining Engineering*. September 1951. Discussion by Gregoire Gutzeit and Porter Clements.) 1074

F—Coal

The Formation of Acid Mine Drainage. (Paper by K. L. Temple and Arthur R. Colmer, *Transactions* AIME, **190**, 1090; *Mining Engineering*. December 1951. Discussion by E. W. Lyon, A. A. Berk.) 1075

Filter Cake Size-Consist and Moisture Relationships. (Paper by O. R. Lyons, *Transactions* AIME, **190**, 868; *Mining Engineering*. October 1951. Discussion by J. D. Clendenin.) 1078

Comparative Effectiveness of Coal Cleaning Equipment. (Paper by O. R. Lyons, *Transactions* AIME, **193**, 895; *Mining Engineering*. September 1952. Discussion by Judson S. Hubbard, G. B. Walker.) 1080

Using Electric Furnaces and Heaters to Determine the Free Swelling Index of Coal. (Paper by E. Swartzman and G. C. Behnke, *Transactions* AIME, **190**, 871; *Mining Engineering*. October 1951. Discussion by W. A. Selvig.) 1081

Frothing Characteristics of Pine Oils in Flotation. (Paper by Shiou-Chuan Sun, *Transactions* AIME, **193**, 65; *Mining Engineering*. January 1952. Author's correction.) 1082

I—Geology

Geology of the Silver-Lead-Zinc Deposits of the Avalos-Providencia District of Mexico. (Paper by W. H. Triplett, *Transactions* AIME, **193**, 583; *Mining Engineering*. June 1952. Discussion by John G. Barry.) 1083

---

* TP 3421

† For further discussion of this paper see *Transactions* AIME (November 1951) **190**, 991-992.

AH-Metal Mining and Industrial Minerals

Pipeline Transportation of Phosphate

by I. S. Tillotson, R. B. Burt, and J. A. Barr

DISCUSSION

Howard Howie *(Knoxville, Tenn.)*—The authors are to be congratulated on the presentation of a paper containing so much valuable information on the pipeline transportation of phosphate, as there is very little literature on the subject.

The writer is especially interested in the paper, as he conceived the arrangement of the Akin and Godwin plants and was in charge of the design work and the engineering incident to their construction.

The Akin and other phosphate deposits in the Tennessee phosphate area lie on beds of limestone that are very irregular. The limestone beds, after the phosphate matrix has been removed, are similar in appearance to land severely eroded by the action of water and denuded of top soil. Depressions in the limestone, called cutters, are irregular in depth with vertical or overhanging walls, having the general appearance of cracks in dried clay. They change abruptly in direction, width, and depth, and vary on the Akin tract from 1 to 25 ft in depth and from 1 to 50 ft in width. Pinnacles of limestone commonly occur in the cutters which appear, when exposed, like small clifflike islands in a river. Limestone floats also occur.

The phosphate matrix fills the cutters and covers the uncuttered areas, the thickness of the cover varying continually and sometimes rather abruptly. It occurs generally as stratifications of phosphate rock and clay of varying thickness.

The phosphate rock in the matrix varies in hardness and in percents of silica, lime, iron oxides, and fluorine, and the clay varies in toughness. In some places the deposit consists of narrow strata of rock almost devoid of clay streaks. In other nearby locations the clay will predominate. When it is excavated, the phosphate rock breaks into thin irregular lumps, locally known as plate rock. Limestone lumps are also excavated with the matrix. Akin plate rock is generally much softer than that occurring in other deposits in the area.

Because of the above described physical and chemical variations of the excavated material, the resultant slurry varies in size distribution, specific gravity, and percent of slimes. When the rock is soft or when there is an increase of clay, the slime fraction is greatly increased as it passes through pumps and pipelines, resulting in reduced pipe friction. It is obvious that the longer the pipeline the greater the reduction of coarse fractions into fines, causing a decrease in pipe friction that cannot be accurately evaluated.

The matrix is mined with a dragline that drops it into a hopper with a grid composed of 9-in. parallel bar spacings located above the hammer mill. The matrix on, and passing through the grid, is subject to the action of powerful sprays which wash it down to the hammer mill, together with any limestone lumps that are not removed before passing through the grid. The hammer mill reduces the feed to lumps of plate rock and clay, most of which will pass through the 8-in. pump suction. The mixture discharges into a pool containing the pump suction pipe. Water from a hydraulic nozzle moves the mixture to the pump suction intake. The pump, driven by a variable speed motor, is the same size as the pumps mentioned on p. 279. Provision is made to remove any lumps that lodge in a bend in the suction pipe in a manner similar to that used in the Florida phosphate fields.

The hammer mill and pump units are mounted on wide steel skids so that they can be moved as the mining operation progresses. The discharge from the pump flows through an abrasion-resistant spiral welded steel pipe 8¼ in. actual inside diam, 8 in. nominal diam, for a maximum distance of 2200 ft, which is the limiting pumping distance for one pump. This pipeline, referred to hereafter as pipeline A, discharges into a ball mill without balls, which in turn discharges into a rotary screen attached to it that separates the slurried matrix into 1¼-in. oversize and undersize fractions. The oversize is returned to the mill for further reduction; the undersize is pumped to a Dorrco washer and then flows into a hydroseparator 160 ft in diam. In spite of the size reduction in the hammer mill and the blunging and washing of the slurry in its passage through the pump, pipeline, mill, and washer, the discharge to the hydroseparator frequently contains mud balls almost perfectly spherical. Sometimes the discharge from the 16,000-ft pipeline at Godwin contains mud balls the size of bird shot and smaller. This pipeline will be referred to subsequently as line B. Liquid caustic is added to the slurry at the Akin plant before its passage through the hydroseparator, which decreases the size of particles in the overflow by dispersion. In passing through pumps 1, 2, and 3 and pipeline B, the slime fraction in the underflow is increased by abrasion and blunging and also by continuing dispersive action of the caustic.

The matrix for use in the experimental tests referred to on p. 279 was obtained from three small surface openings on the Akin tract that were made previous to the purchase of the tract by the Authority. Matrix used in the 2 and 4-in. experimental pipeline tests was taken from the three openings and proportioned to obtain a sufficient quantity that would be fairly representative of the average in the Akin deposits. Prospecting samples of matrix had been obtained from drill holes which showed no small variation in physical and chemical properties. Some of the physical variation is evident from the size distribution of solids in samples taken during the tests covering line B flows so thoroughly made by the Authority under the direction of Mr. Burt, see Table V, p. 280.

Hydraulic gradients for a pipe of 8-in. diam were derived from the 2 and 4-in. pipeline tests using the so-called representative matrix as above described, and plotted on the profile of pipeline B.

Gradients of other materials in slurry form passing through pipelines that bore some similiarity to the Akin matrix slurry were also plotted. After a study had been made of the hydraulic gradients plotted on the profile and the varying slurry flow that would probably occur during actual operation, three pumps were ordered, referred to as No. 1, 2, and 3 on p. 279.

No. 1 and 2 pumps were installed and the third kept in reserve should the operation of 1 and 2 pumps prove satisfactory, since installation of the third pump would require an attendant, as well as the laying of 5400 ft of pipe to supply it with seal-water from the Akin plant. Subsequently, it was found desirable to install the third pump to maintain capacity when the slime fraction was low and the coarse fractions were large.

Reference to Fig. 6 will show that the flow in B line goes upgrade in three locations. At the outlet at Godwin, the slurry flows between two 45° bends for an approximate distance of 18 ft to rise above the ground a sufficient height to discharge into a launder feeding the first classifier. This condition requires extra energy, which is taken care of by keeping the hydraulic gradient a sufficient distance above the high points.

Although there are rather heavy upgrades in the line, the choking condition that might occur at the low points is mitigated by the outlet's being 109 ft lower in elevation than the inlet.

Referring to Table V, p. 280, during test period 15 the heaviest head loss was 3.14 pct, which is the slope of the hydraulic gradient. If the elevation of the pump is 729 ft, see profile, Fig. 6, p. 278, and the equivalent head of pulp is 395 ft, the head elevation of the pulp would be 729 ft plus 395, or 1124 ft. The head loss in 16,000 ft was 160 times 3.14, or 502 ft, and the gradient elevation at Godwin was 1124 ft minus 502, or 622 ft. The outlet at Godwin is at elevation 620, so the pressure at the outlet was 2 ft, or about 1 lb. If the pipeline were on a level grade at elevation 729, the pressure would be zero at 12,580 ft from pump No. 2, which is located at the Akin plant.

When the pumps stopped operating the first time because of electric power failure, the Akin plant supervisor telephoned to inquire when electric service would be resumed and was informed that it would be an hour. He motored down the road roughly paralleling the line to close the automatically controlled dump valves and to view the results of the discharge through them. He found that they had not opened. When pumping was resumed without the feeding of any additional slurry for some time, the settled solids moved out of the line without mishap. At a later date 3 hr elapsed after an unscheduled stoppage of the pumps before pumping was resumed. The dump valves were not opened and no choking of the solids occurred that prevented subsequent normal operation.

The following sentence on p. 279 is quoted from the paper. "In actual practice, however, the automatic operation of the valves was not entirely successful so they are now manually operated, although dumping is not frequently necessary."

Wood stave pipe was selected for the following reasons: 1. Wood stave pipe had been successfully used for many years for moving tailings from nonferrous plants in the West.

One company had used a 12-in. wood stave pipeline for 4 years without a leak, the flow consisting of rather coarse tailings in a 4 to 1 pulp. The wear on the pipe was not known as it was buried. When the pipe line was laid, a piece of iron pipe was installed between the tailings discharge and the intake to the wood stave pipe. The iron pipe did not last a year.

2. The British escaped from Dunkerque on May 29, 1940, and on Jan. 6, 1941, President Roosevelt asked for billions for defense of Britain and Allies. The pipe was requisitioned some time between these dates when steel was in demand and deliveries uncertain. Abrasion resistant steel pipe was ordered for pipeline A and a sufficient amount for a comparative test with wood stave pipe in pipeline B.

3. The comparative merits of abrasion-resistant steel and wood stave pipe in transporting Tennessee phosphate slurry were unknown. The installation of some of both types would present an opportunity to ascertain which was the more desirable.

The wood stave pipe was made of wire-wound creosoted vertical grain Douglas fir strips 1½ in. thick, with a coat of asphalt on the exterior, the manufacturers claiming that pipe made of creosoted staves lasted longer and had a lower friction loss per 100 ft of length for equal rates of flow.

Abrasion occurred mostly in the bottom quarter of the pipe circumference. Laying the pipe on the surface permitted revolving it to present another nearly unworn surface. A dispersant was not used while the wood pipe was in service.

After about 4 months the wood stave pipe was disconnected and examined. The bottom quarter of the circumference was worn away to a depth of ¼ in. Places occurred for a foot or less in length where the wear was much deeper. Leakage occurred first in those places.

B-Minerals Beneficiation

The Effect of Zinc Deleading Operations on Lead-Zinc Selectivity at the Parral and Santa Barbara Mines

by C. L. Boeke and G. G. Gunther

DISCUSSION

I. M. Symonds, *(Cia. Minera de Penoles, Monterrey, N. L., Mexico)*—Messrs. Boeke and Gunther have written most interesting papers describing their zinc deleading operations. Mr. Gunther was kind enough to show me his operation last fall. Aside from the excellent results, I was most impressed by the ease of control. I had expected a difficult operation requiring careful control and supervision, but found one requiring little attention.

The only disappointing fact of the separation is the poor copper recovery in the concentrate of the deleading float. The final zinc concentrate still has about 3 pct chalcopyrite, assuming the copper is chalcopyrite, and adversely affects the zinc grade. If the copper mineral is free, the poor recovery is probably due to the high cyanide concentration. Fortunately, about 75 pct of the copper is recovered before the pulp goes to the zinc circuit.

Mr. Gunther's remarks about proper cyanide to zinc sulphate ratios cannot be overemphasized. Although our experience has been confined mostly to the conventional lead-zinc separation, we have found these ratios most important, and more important in the mill than in the laboratory. The laboratory appears to give optimum results over a wider range of reagent control than the mill, especially in regard to the effect of cyanide.

In handling relatively high grade ores in the mill we usually find that ratios of cyanide to zinc sulphate of 1 to 10 or 20 or higher work best. Where there is a substantial amount of chalcopyrite present it has been noted that cyanide in the range of 0.02 to 0.10 lb per ton of ore is often beneficial in zinc rejection and possibly in copper recovery in the lead concentrate, while larger amounts, say 0.20 to 0.25 lb per ton, will float more zinc and cause a serious rejection of chalcopyrite. On an ore with 15 to 20 pct zinc content we have had to use 0.8 to 1.2 pounds of zinc sulphate per ton of ore with the above cyanide to obtain optimum results.

Some time ago we made a laboratory study following Parral and Santa Barbara practice on an ore which had never a very satisfactory rejection of zinc in the lead concentrate. The results were not encouraging and a mill test was not run. Since then the study has been reopened using in the laboratory fresh zinc concentrate from the mill instead of one made in the laboratory. A reasonably clean lead float from the zinc concentrate was obtained. It has been checked several times and each time the zinc concentrate made in the mill responds and the one made in the laboratory does not. Although undoubtedly some reasonable explanations can be given, it is presented here only as an interesting observation that may be of use to others.

L. H. Lange *(The Galigher Co., Salt Lake City)*—I would like to add to this an experience of mine along the same lines, except a little more exaggerated, on a property in southwest Africa treating dumps which were very rich in copper, lead, and zinc. On a certain fraction of these dumps, some 200,000 tons, averaging about 4 pct copper, 6 pct zinc, and 10 to 12 pct lead, selective flotation was practically out of the question. A technique was developed for the treatment of these ores in which a bulk float of the sulphides was made, the cleaned bulk concentrate being treated with dichromate and American Cyanamid reagent 610 for the depression of the lead and copper sulphides. Dichromate alone had but little effect, but the combination of this reagent and 610 produced quite a satisfactory result. In the early work, selective flotation of some of the easier floating sulphides of lead and copper was attempted, but without much success. However, on some of the upper level mine ores this scheme is now being used before the bulk flotation of the sulphides of copper and lead, more difficult to float, and the easy floating zinc. Sufficient soluble copper is present in these dump ores so that no copper sulphate was needed to activate the zinc, the bulk flotation being carried out with soda ash, xanthate, and frother. This procedure does not make so high a grade zinc concentrate as is made at Santa Barbara, but the company had a very good contract for their zinc concentrates in Belgium, getting pay for the copper and lead in the concentrates. This scheme of treatment developed therefore paid off on these difficult oxidized sulphide ores.

Norman Weiss *(American Smelting & Refining Co., Salt Lake City)*—Since I know the Santa Barbara territory well, I am somewhat familiar with the deleading operations in that district. At Santa Barbara we started deleading in 1941 and 1942 when we ran into some oxidized ore from the Coyote mine. We found it difficult to float all the lead without floating zinc also.

At that time the zinc concentrate ran about 53.5 pct zinc and 3 pct lead. This product was not acceptable at the zinc-smelter because of its high lead content. Consequently, after some experimentation we put in a deleading section.

The zinc concentrate was first conditioned with cyanide and zinc sulphate, also a small amount of soda ash. Sodium bicarbonate and sodium hydroxide were also used as the alkaline reagent. After the concentrate had been conditioned a lead froth was made, and the resulting tailing, zinc concentrate, ran only 1.8 to 2 pct lead, which was satisfactory.

Very many lead-zinc mills now successfully separate lead from the zinc concentrate in some way or another, particularly in the Northwest. Some take a zinc flotation middling and refloat this for lead; others have filtered and dried the zinc concentrate before deleading.

However, the contribution that Mr. Gunther and Mr. Boeke have made to this art is very important, since for the first time they have deliberately permitted lead to escape from the lead circuit in order to improve selection there and have then picked it up out of the zinc concentrate. As far as I know, this is the first time that this has been done.

This seems to be a valuable technique for lead-zinc ores containing copper. On the normal lead-zinc ore containing little or no copper, the zinc content of the lead concentrate may be held below 3 or 4 pct without much difficulty. When the ore also contains copper the problem is more difficult, and the operator has the choice of accepting a lead concentrate containing 7 or 8 pct zinc or even more, or else of upgrading the lead concentrate and sacrificing precious metals and copper.

The method used in the Parral district and described by Mr. Gunther and Mr. Boeke, therefore, may be successfully used on other ores of this type.

H. S. Wildman *(A. S. & R. Co., Avalos, Chihuahua, Mexico)*—At the present time at the Santa Eulalia Mill we are treating the leasers' ore from the Santa Barbara district. As these ores are obtained at or near the surface they contain a great deal of the semi-oxidized or slow-floating lead which tends to report in the zinc concentrate.

Since we have not yet been able to install a zinc concentrate deleading unit like that at the Santa Barbara mill, we have resorted to the tabling of the lead tails prior to zinc flotation and have been able to recover a fair portion of this so-called slow floating lead. At the same time we were able to stabilize the lead float, as the previous tendency had been to add a surplus of collector agent to prevent so much lead passing over to the zinc float and at times lowering the grade below the shipping requirements.

C. F. Zeuch *(The Dow Chemical Co., California)*—In all this work, has anything been done in heating the zinc concentrate before attempting to delead it?

G. G. Gunther (author's reply)—No work has been done at Parral or Santa Barbara to investigate the effect and the possible use of heat in the zinc deleading operations, mainly because a cheap source of heat is not available at either plant.

E. H. Crabtree *(The Eagle Picher Co., Okla.)*—First, I might answer Mr. Zeuch's question on the effect of heat on differential separation. We have one operation now which is being conducted on an old slime pond. This slime pond resulted from muddy primary thickener overflows, which had accumulated many years because the thickeners were too small for the tonnage being handled. A couple of years ago we attempted to clean out this slime pond and retreat it. It contained several percent of combined lead and zinc. Since we were unable to make a satisfactory selective separation by conventional means, we assumed because the extremely fine sizes, we finally wound up by making a bulk lead-zinc concentrate which is cleaned and filtered and then conditioned in what we call our hot conditioner. We give this bulk lead-zinc concentrate a retention time at boiling temperature for approximately 1 hr with high concentration of sodium metasilicate. After this conditioning period, the material is passed through a hydroseparator for removal of the excess sodium silicate and the high caustic solution which we have there. The underflow from this hydroseparator then goes into a lead-zinc differential circuit and we are able to make a reasonably good separation. By that I mean that we make about a 65 pct lead concentrate and about a 58 pct zinc concentrate. This is, I think, a solution of a particular problem. We have attempted this hot conditioning with sodium silicate on other ores and it was not successful, but it is particularly successful on extremely slimy material, which, incidentally, has quite a bit of organic material in it resulting from the original ore.

There is another comment I want to make on Mr. Gunther's paper. As we all know, and as Mr. Weiss pointed out, the main virtue of zinc deleading is that we do not have to control our lead circuit so well. We can work more for lead grade and allow some of the lead to go into the zinc concentrate because we have an opportunity to recover it later. In all the lead-zinc operations I have had experience with, I have found that once the lead goes through into the zinc circuit, which is usually a high-lime circuit, the lead becomes very sluggish and floats there slowly. As a result a large portion of the lead floating in the zinc rougher circuit floats down toward the tail cells. At one of our operations in Arizona we have taken advantage of this. We pull off a zinc rougher concentrate which goes to the zinc cleaners and then to filtration, but the zinc scavenger concentrate, which contains the large portion of the lead, is reground in cyanide and then returned back to the head of the lead circuit. I think one virtue of this is that we can grind in quite a high cyanide strength there without fear of depressing chalcopyrite, since any chalcopyrite that is depressed along with the zinc we have an opportunity to recover again in the lead rougher circuit.

Jaw Crusher Capacities, Blake and Single-Toggle or Overhead Eccentric Types

by D. H. Gieskieng

SUPPLEMENT

D. H. Gieskieng (author)—Under the subject of Crushability-Capacity Effect, on page 972, reference is made to Dodge-type crusher data obtained with jaw strokes of 0.04 and 0.02 in. The latter figure was that employed by Hersam[3] and is the basis for much of the material under this subject in Taggart.[4] The jaw stroke of 0.04 in. was used by Mörtsell[5] in a similarly thorough investigation.

---

[3] E. A. Hersam: Factors Controlling the Capacity of Rock Crushers. *Trans.* AIME (1923) 68, p. 463.

[4] A. F. Taggart: Handbook of Mineral Dressing, Sec. 4, p. 12. John Wiley and Sons, New York, 1945.

[5] Sture Mörtsell, Bergsingenïör. Prof. Vid K Tekn. Hogskölan.

Screened Ore Used for Fine Grinding at Lake Shore Mines

by Bunting S. Crocker

DISCUSSION

Fred C. Bond *(Allis-Chalmers Manufacturing Co., Milwaukee)*—This is a very complete description of the screened ore fine grinding installation at Lake Shore. The only important data which might be desired are the operating screen analyses and power consumption in each stage.

The statement that the energy consumption, or kw-hr per ton, remains constant for all mill diameters is of great interest, but the opinion is widely held that the kw-hr per ton decreases as the mill diameter increases. More definite test work is needed to establish this point.

Screened ore fine grinding has been successful on hard Lake Shore ore and on about equally hard South African Rand ore. However, it is still not determined whether it would be successful on ores of average or less than average hardness. It is possible that with softer ores the consumption of ore pebbles might be exceedingly high, or might even exceed the available supply. Also, the softer feed might result in a rapid buildup of harmful intermediate sizes in the mill circuit. These factors can be determined only by a full scale or long pilot mill test. In any case the Lake Shore staff is to be congratulated for this pioneering work.

Bunting S. Crocker (author's reply)—As requested, the operating screen analyses and power consumption for each of the four stages of pebble milling are given, see Table XII. The first three stages are in series circuit; the last stage is in closed circuit. The primary circuit had rock feed averaging 124 g per piece and the final stages rock feed weighing 63 g. The intermediate stages had mixtures of the two.

Regarding Mr. Bond's statement that "the opinion is widely held that the kw-hr per ton decreases as the mill diameter increases," I would say that I have frequently been told this but have never yet been shown any evidence or seen any evidence published that would prove this statement. It may be true that some of the big mills recently installed have mechanical power savers such as micarta bearings and better lubrication, but as far as the power consumed inside the mill is concerned, we at Lake Shore think that it varies as $D^{2.6}$, and that is all. We published extensive information on this point in our 1939 paper. Recently Mr. Banks at Consolidated published the figures on his 10 ft 8 in. x 12 ft 0 in. rod mill. As reported in this discussion by the writer,[9] we calculated the power necessary to run this mill based on our 7x6-ft rod mill to within 1 pct of the actual power reported by Mr.

Table XII. Pebble Mill Screen Analysis, Feb. 19, 1952

	Primary Stage, P.M. No. 4* to 7 and 8, Total KW, 365		Secondary Stage, P.M. No. 9 and 11, Total KW, 253		Tertiary Stage P.M. No. 14, Total KW, 131		Final Stage, P.M. No. 12 and 13, Total KW, 261	
	Sand, 760 Tons		Sand, 540 Tons		Sand, 370 Tons		Sand, 310 Tons	
Mesh	Feed	Discharge	Feed	Discharge	Feed	Discharge	Feed	Discharge
6	0.2							
8	1.6	0.2	0.4					
10	6.7	0.4	1.1	0.2	0.3	0.2	0.2	0.1
14	16.5	1.2	3.0	0.2	0.5	0.1	0.1	0.1
20	16.0	1.4	3.3	0.2	0.4	0.1	0.3	0.1
28	12.8	2.0	4.0	0.2	0.4	0.1	0.3	0.1
35	12.0	3.9	6.9	0.6	1.0	0.2	0.4	0.1
48	7.8	5.0	7.8	1.2	1.9	0.3	0.8	0.3
65	6.5	7.1	11.4	3.0	4.8	0.9	2.5	0.4
100	5.0	9.7	13.4	7.5	12.2	3.2	6.5	1.4
150	3.8	11.0	14.1	13.3	20.7	10.0	13.3	3.5
200	1.7	8.5	11.5	9.4	16.9	15.8	20.1	2.9
270	2.5	7.7	6.9	15.5	18.2	14.7	23.9	17.9
325	1.7	9.3	8.2	15.1	14.2	17.7	19.1	22.9
—325	5.2	32.6	8.0	33.6	8.5	36.7	12.5	50.2
Cum + 3								
Cum + 10	8.5	0.6	1.5	0.2	0.3	0.2	0.2	0.1
Cum + 35	65.8	9.1	18.7	1.4	2.6	0.7	1.3	0.5
Cum + 150	88.9	41.9	65.4	26.4	42.2	15.1	24.4	6.1

* No. 4 P.M. is 6x16 ft, all others 6 ft 8 in. x 16 ft.
Rod mill tonnage, 940 tons per day.

Banks. Our formula was $D^{2.6}$! We feel that this point is established.

At the time the paper was given no work had been done on any ore except Lake Shore. The Rand ores are not nearly so hard as Lake Shore. However, recently the writer has had an opportunity to test six different ores, two of which were quite soft; one contained shale. In the preliminary tests these softer ores made much better looking pebbles, if this is important, than did the Lake Shore ore. They did not produce large intermediate sizes, and in fact they cleaned up the "chips" better than harder ores. The softer ores made much "rounder" pebbles and as a result pebble grinding could start at coarser stages than at present practiced at Lake Shore, where 8 mesh is the top size in the feed.

J. Myers *(Tennessee Copper Co., Copperhill, Tenn.)*—I was a reader on this paper and consequently had a chance to study some of the aspects of the work. There are three questions that I would like to ask. First, do you think that this means of comminution would apply to ores that are softer than the very hard ore of Lake Shore? The substance of this question is that while the rock from the ore might be softer, the work to be done is less. Secondly, you have laid a great deal of stress on getting the correct size of pebbles. Since you prepared this paper, has any further information developed that would be of aid to any of us who wished to make tests in this manner? Thirdly, have you any idea what the upper range of grinding might be? Many of us would not want to grind quite as fine as you are doing.

Norman Weiss *(American Smelting and Refining Co., Salt Lake City)*—Mr. Crocker kindly let me have a copy of his manuscript some months ago, and we immediately started work at our Neptune property, where it costs us about $60.00 a ton to fly balls into the property. Naturally, we have not made any progress commensurate with what Mr. Crocker has done. We have merely made a very small start, but even thus far the data show that we are going to check Mr. Crocker very closely. The ore at the Neptune property is likewise very hard and is primarily ground through two ball mills followed by grinding in a number of secondary ball mills, one of which has been converted to pebbles using ore. We believe we may be able to save up to 30¢ or 40¢ per ton. The ball consumption two years ago was about 4.8 to 5.1 lb per ton. By studying the ball sizes, ball rationing, and quality of balls, we have reduced that to 2.3. We are using the best ball we can get on account of the freight, but there is still much money to be saved.

I should like to ask Mr. Crocker a question. In the layout at Lake Shore, I believe, the classifiers are situated above the ball mills, so that the discharge from the ball mills is pumped to the classifiers. That simplifies the procedure, but what happens if the classifiers are set alongside the ball mills, preventing the enlargement of the latter, so that for each ball mill now working at 46 pct of its original capacity you have the same classifier that previously handled the whole tonnage?

Harlowe Hardinge *(The Hardinge Co., York, Pa.)*—This paper is very important to the mining industry because it brings out a feature of grinding long neglected. In the early nineteen hundreds nearly all grinding was done with pebble mills. Later, balls were tried. A gain was made in floor space, and a gain in capacity, but very little gain was made in efficiency. However, styles changed, people became interested in doing something different, and the pebble mill was no longer continued in general use in the wet grinding of ores except on the Copper Range in Michigan. We have almost forgotten the advantages of the pebble mill, and I believe Mr. Crocker's paper is valuable if it does no more than bring us back to some of the old fundamentals that were determined many years ago. He has done things somewhat differently from the way they were done then, but his methods are quite similar in some respects to the work in South Africa, where grinding is carried on at low cost. I was there last year and saw operations feeding pieces as large as 10 in. to the mill in the form of grinding media, as well as smaller sizes comparable to those discussed in the paper. This method will create substantial savings in operation costs where it applies, but it does not always apply. It is important in considering what has been done here that we do not assume that pebble mill methods of operation are the same as ball mills to accomplish the same work. By this I have in mind such factors affecting the overall economy of the two methods as mill speeds, pulp densities, liner forms, high or low pulp level discharge arrangements, and mill diameters. We must make calculations by considering these points individually and not try to make too many comparisons between what we would do with a pebble mill to make it operate like a ball mill.

Oscar Johnson *(The Mine and Smelter Supply Co., Denver)*—The Chilean mill in use at the Utah Copper was beginning to give way to pebble and ball mill grinding in 1914. This was about the time that the Marcy Mill was introduced experimentally at the Utah Copper.

Although flotation was known to be successful prior to 1912, the Utah ores were not entirely treated by this process until about 1923. During this period the fine grinding was taken over by the installation of 7x10-ft mills using 2-in. balls as a grinding media. By 1930 all grinding for flotation was done by 7x10-ft primary mills using about 2⅜-in. balls, and secondary mills of same size using 2-in. balls. I well recollect that during this early period the Mine and Smelter Supply Co. handled orders from the Utah Copper Co. for Danish and French pebbles and also secured considerable quantities of cobbed materials from quarries located in Iowa and Minnesota. Using these materials must have been a successful expedient until Utah Copper could get into production making iron balls. Evidently they gave maximum capacity, which was the main objective.

I am very much interested in Mr. Crocker's statement that Lake Shore is using low discharge mills, since in 1937 I interested Mr. A. L. Blomfield in our grate discharge arrangement; he gave us an order for one which I am sure started Lake Shore off on the operation of the low discharge mills. Canadian Institute of Mining and Metallurgy *Bulletin*, Vol. 43, carries an illustration of this low discharge screen with the 8 lifters which we suggested as proper for handling the discharge of the tube mill. I also recollect that when Mr. Francis Bosqui was going to South Africa we gave him data on the grate discharge, thinking he might wish to suggest it to the milling men in Africa. The Utah Copper Co. has applied low discharge grates to their 7x10-ft primary mills.

Bunting S. Crocker (author's reply)—Mr. Myers asked if this process would work on soft ores. Many people have asked that same question. Actually we have not tested soft ores, but we have many reasons for thinking that pebble grinding would work as well or even better with softer ores. The South African ores are much softer than those at Lake Shore, and pebble milling has been successful there for years. Their daily pebble consumption is about ten times ours. The equipment we put in to handle 30 tons of pebbles per day could easily handle 100 to 200 tons per day. Therefore on softer ores the savings on the amount of rock that bypasses the crushers is considerably greater. We save 1½¢ per ton by not having to crush 3 pct of our ore; plants with softer ores might save 4¢ to 5¢ per ton. The pebbles from softer ores also round up more quickly and make more spherical pebbles. There seems no reason why most ores should not be tested by this process. When we started work on this problem there appeared to be thousands of obstacles, but they nearly all resolved themselves; it did not turn out

---

[9] Canadian Institute of Mining and Metallurgy *Bull.* (July 1952).

to be half so complicated as we thought it was going to be.

Mr. Myers next asked if we had further information about correct pebble size. We have done a great deal of work on this subject since the paper was written, and as it is long and rather detailed, I think we will publish it separately in a second paper which will appear in the Canadian Institute of Mining and Metallurgy *Bulletin*. Since it is impractical to screen rock to exactly one size, pebble feeds are always similar to "rationed ball feeds," which is usually an advantage, and it is therefore necessary to make several calculations to arrive at a pebble load in the mill which will have the same weight per average piece as the previously determined correct size of steel ball.

The last question asked by Mr. Myers concerned the upper range of pebble grinding. Mr. Hardinge partly answered this question when he reviewed the South African practice. Over there they use pebbles that are up to 10 in. in size. We have tested pebbles up to 6 in. in size, equivalent to 4-in. steel balls, and are considering replacing our second stage ball mill with a rock mill. We would save an additional 2½¢ on this change. Our present pebble plant is handling 8 and 10 mesh material and I think pebble milling with 2-in. pebbles could be carried to 6 mesh in many plants. I might mention that Wright-Hargreaves has already put this process in and has run it successfully for the past two years. Their saving is 21¢ per ton as against our 28¢ because their ball milling section was stronger than ours and it was not convenient for them to do as much work in the pebble mills. We do 85 pct of our wet grinding in the pebble mills.

Mr. Weiss asked what would happen to auxiliary equipment such as classifiers, motors, etc., if a steel mill were converted directly, thus having only 47½ pct of the original capacity. We solved this point by expanding the diameter of the mill until it drew the same power and had the same capacity as the original mill. Therefore the motors, classifiers, etc., were in balance. The fact that our bowl classifiers were on the upper floor does not really make any difference.

There are two other points that have come up since the paper was first written: 1—Grinding with pebble media eliminates much of the chemical reducing action of iron. With 5x16 steel tube mills grinding in cyanide solution, the oxygen saturation of the solution in the discharge was 9 pct saturated. This is detrimental in cyanide work and we had to use three primary agitators to bring the oxygen back into the solution before thickening. Using pebble mills, the solutions are 67 pct saturated in the pebble mill discharge, and we only use one primary agitator now. Thus the "conditioning", in a chemical sense, that takes place in grinding mills is different with pebble mills from steel mills. Some flotation plants may even have to add fine iron as a reducing agent if that effect is desired. Cyanidation plants of course will benefit. 2—The stage grinding shown in this report gives a better sulphide distribution for flotation than the previous two-stage circuit. We now get less fine pyrite and less very coarse pyrite in the flotation feed. Most of the pyrite is in the 20 to 40 micron sizes, which is ideal for flotation recovery.

DISCUSSION

L. E. Djingheuzian *(Canadian Department of Mines and Technical Surveys, Ottawa)*—This paper summarizes the results of exceedingly useful work done at Lake Shore and presents some unusual data. By analyzing these data, I have obtained a few tentative figures which I believe might be of interest.

Before Lake Shore changed their fine grinding with steel to fine grinding with screened ore as pebbles, their steel consumption was 4.3 lb per ton of ore. After the changeover to grinding with pieces of ore as pebbles, the pebble consumption was determined to be 28 tons per 1000 tons of ore, or 56 lb of pebbles per ton. From this, the ratio of pebble consumption to steel consumption by weight works out at 13 to 1.

Total gross power input in fine grinding of 1000 tons at Lake Shore is $(182 \times 8) = 1456$ hp, or 26.1 kw-hr per ton. Assuming 20 pct frictional losses in the mills and the useful energy input from tumbling media in grinding hard siliceous ore at 15 pct, according to Schellinger's experiments,[10] the useful energy input per ton of ore at Lake Shore will be 12 pct of the energy input to the motor, or 3.13 kw-hr.

Since Lake Shore screened ore wears 13 times as fast as steel, the net energy required to wear a ton of steel, formerly used at Lake Shore, will be:

$$3.13 \times 13 = 40.69 \text{ kw-hr,}$$
$$\text{or } 161.7 \text{ joules per g steel.}$$

Since for unit weights the ratio of the surface of Lake Shore ore, sp g 2.70, to the surface of steel, sp g 7.80, is 3.094 to 1.525, the same volume of steel absorbs in grinding to the same mesh 13x3.094 to 1.525 as much energy as the same volume of Lake Shore ore.

The amount of surface energy stored in grinding quartz was determined by Schellinger[10] as 107,000 ergs per cm^2. Assuming that Lake Shore ore stores the same energy in grinding as quartz, the energy stored in steel in grinding will be

$$(107{,}000 \times 13)\ 3.094 \text{ per } 1.525 = 2{,}821{,}900 \text{ ergs per cm}^2$$

I would like to know how this figure checks with any determinations, if ever made, by physical metallurgists on surface energy stored in steel during work hardening before rupture.

Using this figure, the amount of new surface formed in grinding of 1 g of steel to 90 pct —325 mesh, Lake Shore grind, will be

$$(161.7 \times 10^7) \text{ per } 2{,}821{,}900 = 573 \text{ cm}^2$$

---

[10] A. K. Schellinger: Solid Surface Energy and Calorimetric Determinations of Surface Energy Relationships for Some Common Minerals. *Trans.* AIME (April 1952), pp. 369-374.

The Third Theory of Comminution

by Fred C. Bond

DISCUSSION

Milton C. Shaw and **Donald R. Walker** *(Massachusetts Institute of Technology)*—For many years the two empirical rules of comminution bearing the names of Rittinger and Kick have been applied to grinding processes to account for the energy required to crush brittle materials. The basis for Rittinger's rule was the thought that the energy to grind a substance went largely into supplying the additional energy associated with the new free surface, while Kick's law was prompted by the concept of dimensional similarity and is a special statement of the concept of constancy of strain energy to cause rupture. According to Rittinger the energy to grind a given volume varies as the change in the square of the mean particle size, $\upsilon \sim \Delta(D^2)$, while according to Kick this energy varies as the change in the cube of the mean particle size, $\upsilon \sim \Delta(D^3)$. These two rules at first appear to be incompatible, and considerable controversy is to be found in the literature concerning which of the rules is the true one.

The present author has contributed to this controversy by proposing that a rule intermediate between that of Kick and Rittinger be adopted. The energy required to grind a given volume of material is assumed to vary as the change in the 5/2 power of the mean particle size, $\upsilon \sim \Delta(D^{5/2})$. While it is inferred that a derivation for this intermediate relationship is presented, it would appear to be more accurate to refer to it as an assumed relationship, since it is not based on a clear-cut model or physical picture.

In more recent times it has become clear that a negligible part of the energy in comminution is associated with the production of new surface. Grinding efficiencies, based on surface energy, of the order of but 0.1 to 1 pct are normally reported. It is thus evident that the physical basis for Rittinger's rule is grossly in error. However, we are left with the fact that there is considerable experimental data in essential agreement with the Rittinger relationship. It would then appear that what is needed is a new physical basis for the old rule.

In recent metal cutting studies[12] the energy required to remove a given volume of metal was found to increase as the particle size was decreased. This trend was found to continue to a certain critical size, corresponding to a layer about 1 micron in thickness, beyond which the energy per unit volume remained constant.

All materials contain numbers of imperfections and inhomogeneities which affect the amount of shear stress necessary to yield or rupture the material. As the volume of the material subjected to stress is reduced, the probability of finding an inhomogeneity to act as a strength-reducing agent is decreased. The material appears to have higher strength than it does in bulk and the energy required to remove a given volume thus increases. When the energy ceases to rise with decreasing particle size, the material is exhibiting the theoretical strength of a perfect lattice structure, since it is being forced to shear in regions between inhomogeneities. The region in which the energy per unit volume is inversely proportional to the particle size is in full agreement with Rittinger's rule, while Kick's law precisely expresses the observed energy behavior in the region where full theoretical strength obtains.

It would thus appear that Rittinger's rule should hold for relatively large particles, larger than about 1 micron, while Kick's law should hold for smaller particles. The literature reveals that in the main the proponents of Kick's rule were dealing with fine grinding while the champions of Rittinger were engaged in relatively coarse grinding. It is to be noted that while each of the two rules appears to satisfy experimental data reasonably well, the reason they do is entirely different from the reasons originally advanced by Rittinger and Kick. The basis for the existence of two empirical rules is the size effect in materials associated with flaws and inhomogeneities. If materials had a single valued strength regardless of size, Kick's law would always hold. In practice Kick's law ceases to hold when the particle size becomes great enough to include inhomogeneities. It is a pure coincidence that in this latter region Rittinger's rule, which was originally derived from a false physical picture, is in general agreement with experimental results and the concept of a variation of particle strength with size.

While the aforementioned reasoning is based on results for ductile metals, it must be realized that brittleness is also a function of particle size. Materials are brittle only because they contain inhomogeneities sufficiently large to prevent them from being ductile. In crushing materials normally considered brittle in bulk, the major portion of the energy is associated with plastic flow. The observed negligible difference between the energy required to crush materials normally considered to be ductile and brittle is a further consequence of the size effect in materials.

Supporting data and a fuller treatment of the ideas set forth in the above discussion will soon be submitted in a paper on the theory of comminution.

---

[12] W. R. Backer, E. R. Marshall, and M. C. Shaw: The Size Effect in Metal Cutting. *Trans.* A.S.M.E. (1952) 74, p. 68.

R. J. Russell *(Hardinge Co., York, Pa.)*—The paper as originally written for presentation in Mexico City and as revised states that the Rittinger theory is not tenable mathematically because of the presumed lack of consideration of the distance factor. It also lists three assumptions presumed to be essential to the development of the Rittinger theory.

The Rittinger theory states simply, "The energy necessary for reduction of particle size is directly proportional to the increase of surface." A practical consideration does not require and cannot have a datum point of theoretical zero surface area.

A simple means to illustrate the Rittinger concept has been the breaking of a cube into smaller cubes. It is not required that this be done by compression. It is unimportant in the Rittinger concept how it is done. It may be by shear or tension. Regardless of the manner in which fracture is obtained, the deformation before fracture provides a distance factor and the Rittinger theory is not indefensible mathematically.

Attempts have been made to correlate work done in grinding to surface energy, but this is no part of the original Rittinger concept, even though it may be a valid concept.

It has not been proved in the paper that the Rittinger theory is not correct.

Recently there is a tendency to consider the Rittinger theory a too simple concept of a complicated phenomenon. Any lack of consideration on grounds of simplicity rules out logic. When any material is subdivided, surface is increased, but neither mass nor volume is changed. It is logical, then, that a relationship to surface exists.

During the past 20 years several competent investigators of crushing and grinding processes have provided confirmation that the Rittinger theory is substantially correct. The work of Gross and Zimmerley demonstrated the validity of the Rittinger theory, and despite the problems encountered in measuring surface areas other observers produced further substantiation.

In 1938[13] Bond and Maxson stated that their work on the grinding characteristics of ores conclusively establishes that "the useful work done in grinding is proportional to the new surface area produced; in other words, Rittinger's law is the correct expression of work done."

Difficulties encountered in obtaining absolute measurements of surface area do not in any way invalidate the Rittinger theory. The practical application of Rittinger is limited only if relative surface area data cannot be established, and these are as accurately and readily capable of establishment as diameters which must be approximated before application of formulae developed in the paper.

Assumptions no less questionable than those cited against Rittinger are made by the author in the derivations offered as well as the confirmations. Substantiation of Rittinger by tests on quartz ore are discounted, yet the author offers a confirmation based on crushing quartz crystals and glass spheres.

The Rittinger theory implies that size distribution of any given feed is unimportant so long as surface is known, and the same is true for the product. Therefore, tests made which confirm Rittinger and use a screened or sized feed are valid so long as areas of feed and product are known or related.

The Third Theory states that work useful in breakage is inversely proportional to the square root of the diameter of the product particles. If this is true, a scalped or sized feed should require no special treatment so long as particle diameters are determined.

Presumably the equivalence of a normal feed is determined in the section on Effect of Scalping Feed, and if so the work index value should not change. In fact, Mr. Bond states: "The work index is constant over all size ranges for a homogeneous material reduced at the same relative mechanical efficiency."

It is my opinion that the tabulated data from the laboratory tests and plants do not provide any proof of the stated Third Theory. These data are based upon empirical relationships established by Mr. Bond and as such may have practical application in approximating equipment size and power requirements for certain crushing and grinding requirements. Mr. Bond calls attention to the necessity for applying properly a judgment factor. This limits practical use of the procedure to benefit only those having experience in crushing and grinding.

Since according to the Third Theory the useful work is directly proportional to the square root of the surface area formed, an experimental proof should be established from surface area determinations. If this were to be done it would necessarily expose errors in work which has been done and which appears to confirm the Rittinger theory.

Fred C. Bond (author's reply)—The statement by Professor Shaw and Mr. Walker regarding Rittinger and Kick can be clarified to read: "According to Rittinger the energy to reduce a given particle to product particles of constant size and similar shape varies as the square of the given particle diameter, while according to Kick it varies as the cube of the given particle diameter." According to the present author the exponent should be 5/2. Under the Rittinger concept the useful energy input goes into the formation of new surface area, under the Kick concept it goes into the reduction of particle volume, and under that of the present author it goes into the formation of crack tips, which extend through the particle, resulting in breaks. Each of these three concepts is fundamentally an assumed relationship, and the correct one should be selected by its conformity with laboratory tests and commercial crushing and grinding installations. Other things being equal, the most accurate comparisons are those which involve the largest range of particle sizes.

The second form of the Rittinger theory is a logical development of the first form, and the commentator's statement: "It is thus evident that the physical basis for Rittinger's rule is grossly in error," which refers to the second form, is warmly applauded.

Inhomogeneities probably exist in practically all the materials subject to crushing and grinding. However, these inhomogeneities extend down to the supposed micelle structure at about one micron, far finer than the ordinary range of fine grinding, and the theoretical breakage of a perfect lattice structure has little bearing on ordinary crushing and grinding problems. Breakage cracks probably follow the micelle boundaries, and the effects of coarser inhomogeneities vary greatly with different materials, depending upon their relative strength, arrangement, and spacing. The coarse inhomogeneities are far too irregular and variable to permit the formulation of a rule covering their effect on the crushing and grinding of all materials. In fact their effect appears to be of little importance in many instances, especially in grinding. So-called natural grain sizes show up in the size distribution curves of some materials but are apparently completely absent in many cases.

In the literature of comminution it has generally been reported that the Kick theory agrees more nearly with the actual energy required in coarse crushing where the coarse inhomogeneities are presumably more effective, and the Rittinger theory with grinding. But neither theory agrees well with the facts when reduction over a large size range is considered.

The behavior of brittle materials under stress is very different from that of ductile metals because of the difference in strain energy flow after initial failure, and analogies between the manner of breakage of brittle rock and that of ductile metal are apt to be misleading.

Mr. Russell defends the Rittinger theory in its original form, but offers no defense of the application of the surface energy concept to it. The original Rittinger theory states that the energy necessary for reduction of particle size is directly proportional to the increase of surface, while according to the Third Theory it is directly proportional to the square root of the increase of surface. The numerical conflict between the two theories is whether the exponent of the new surface area should be 1 or ½.

However, there is a wide difference in the mental processes by which the theories were derived. The Rittinger advocates consider that the production of new surface is the direct object and the criterion of the work done in comminution, while the Third Theory implies that the production of active crack tips, which are extended and split the rock by the resident strain energy of the deformed body, is the immediate object and proper criterion of the work done. The Rittinger theory requires the measurement of surface areas alone, and entirely neglects the deformation or strain distance necessary to produce the new surface, thereby denying the definition of work as the product of force and distance. The work input can be calculated directly from easily obtained size distribution analyses by the Third Theory, while the Rittinger theory requires difficult, inaccurate, and often impossible surface area measurements.

John Gross states:[14] "Several investigators have determined the absolute efficiency of crushing on the assumption that the energy required in crushing is only that necessary to create new surface energy. Such calculations are of academic interest only and have no practicable significance, as they ignore the distance through which the crushing force must act before new surface is produced."

The use of any comminution theory without the concept of theoretically infinite particle size, or zero surface area, is analogous to the use of a portion of a thermometer scale on which the zero reading is unknown. The total energy input can be compared to the absolute temperature, which made the entropy concept possible.

The primary objection to the illustration of the theoretical breakage of cubes to demonstrate the Rittinger or Kick theory is that the shape is particularized; no matter whether compressive, tensile, or shearing forces are used. The cubical shape and the even distribution of stresses do not correspond to actual crushing and grinding conditions.

The experimental confirmations of the Rittinger theory by Gross and Zimmerley and others suffer from at least two defects which did not appear important when the theory was tacitly accepted before the tests were made, but which appear larger when it is challenged. The first of these is that the range of size reductions compared was so limited that the difference caused by the surface area exponents of 1 and ½ would be small and might be disregarded. It is only too natural to accept results which confirm what is expected and believed, and to reject readings which do not exactly conform as erroneous, especially when those readings cannot be explained by any known hypothesis. At present, comparison of the results of crushing to 1 in. with grinding to 200 mesh should confirm the Third Theory rather than that of Rittinger.

The second defect is that most of these tests were made with an artificial feed composed of particles of only one screen size, in order to simplify the surface area determinations. It is true that this should make no difference if the Rittinger theory is previously accepted as being correct, but it can make a large differ-

---

[13] Fred C. Bond and Walter L. Maxson: Grindability and Grinding Characteristics of Ores. *Trans.* AIME (1938) 134, pp. 296-317.

ence if the Third Theory is correct. The present author made this error in the 1938 paper,[13] in which —14 +20 mesh screened particles were reduced in the pendulum impact device to measure the surface area produced by impact, and results were obtained which appeared to substantiate the Rittinger theory.

The work index is valid only for a natural feed containing the normal fines resulting from crushing or grinding; the section headed Effect of Scalping Feed describes a method for obtaining the approximate natural feed size when a scalped feed of known size distribution and known hourly tonnage is used. In most cases where a crusher feed is scalped by passing through a grizzly ahead of the crusher it is more satisfactory to disregard the action of the grizzly entirely, since the hourly tonnage and size distribution of the material removed by the grizzly are usually not known.

When the plotted percent passing size distribution lines of the feed and product are parallel, the reduction ratio remains constant for all sizes, and the work index calculated from the convenient 80 pct passing size is equivalent to that calculated on the basis of any other selected passing size. If the lines are not parallel the work index will be affected, but the effect will be relatively small for small differences in slope of the plotted lines, and will be only the square root of the effect on the new surface area produced. However, scalping the feed produces a large effect on the work index which requires correction, and using feed particles of a single screen size requires a still larger correction.

Variations in the ratio of interior to outer surface in crushed quartz particles of different screen sizes may account for differences in the work indexes at these sizes. John Gross in Crushing and Grinding, Table 14,[14] shows that this ratio varies from 2.64 for 3x4 mesh particles to 0.11 for 150x200 mesh. Glass marbles have no interior surface.

Laboratory grindability tests yield work indexes which are valid only over the size range where the machine operates efficiently. When a hard ore is reduced in a fine grinding ball mill the efficiency begins to drop off with feed sizes larger than about 6 mesh, and such a mill fed with ½-in. ore will require more work input per ton than that calculated from the grindability test. Correction factors for oversize feed and other operating variable must be calculated from experience.

Many additional confirmations of the Third Theory which are not described in the paper have been obtained from commercial crushing and grinding installations, the most striking feature of which is the general agreement of the work index calculated from crushing plant results with that calculated from fine grinding and intermediate reduction stages in the same plant. Since the Rittinger theory is notoriously inconsistent in comparisons over a large size range the author is convinced that the Third Theory agrees better with the facts of comminution.

---

[14] John Gross: Crushing and Grinding. U.S. Bur. Mines *Bull.* 402, p. 7.

Flotation Rates and Flotation Efficiency

by Nathaniel Arbiter

DISCUSSION

Gregoire Gutzeit and **Porter Clements** *(General American Transportation Corp., Chicago)*—We find Professor Arbiter's paper especially interesting in view of rate studies we have conducted in our laboratories in connection with the recovery by flotation of fine coal from mine washery waste waters and river deposits. In an attempt to evaluate the effects of design and operating variables of a flotation machine developed by our company specifically for coal and for the purpose of scaling-up laboratory batch flotation results for plant design, an approach was made through a study of flotation kinetics.

Investigation of the (combustible) recovery-time variables showed that a plot of time/recovery vs time gave the simplest linear representation of the data, tests being conducted by preliminary conditioning with collector, followed by flotation with stagewise reagent addition. It is interesting to note that in this case, where the bulk of the feed is floated, the data may be graphically represented in the same manner as the data shown by Professor Arbiter for ores containing a relatively low proportion of floatable minerals.

In comparing data from two batch coal flotations run in the same laboratory machine by preparing t/R vs t plots and determining rate constants by extrapolation, Professor Arbiter's method is found to be extremely sensitive, since the t/R intercept is usually less than 1. A small difference between intercept values in this range becomes magnified when the reciprocals or A^2K values are calculated. For instance, two different anthracites, 28x200 mesh, of about the same ash content were batch-floated in the same laboratory machine under approximately the same conditions for 2.5 min, giving combustible recoveries of 0.936 and 0.976. The t/R vs t plots were reasonably linear. A^2K values were 1.5 and 4.1, respectively. It should be mentioned, however, that the first two points for each set of data, 0.25 and 0.50 min, fall above the line, probably because of incomplete conditioning, hence, lower initial recovery and higher t/R values. Unless all of the plotted points fall exactly on a straight line, the choice of the most representative line is at the discretion of the experimenter. As shown above, for almost the same average or overall rates, A^2K values differ considerably, the sensitivity being inversely proportional to the value of the intercept. Unfortunately, in the case of coal flotation, t/R vs t plot, the area of greatest importance to the extrapolation is characterized by somewhat scattered points. It would appear, then, that the use of this rate constant to evaluate floatability or flotation machine performance would have greater significance for the slower-floating minerals. However, the positions of the first few points seem to give a good indication of the effectiveness of the conditioning step.

In deriving a theoretical flotation rate equation, Volkova[20] attempted to show the influence of relatively nonfloatable material on the mineral being separated. His integrated rate equation contained both first and second order terms, having the form

$$Kt = (1\text{-}Z)\left(\frac{R}{1\text{-}R}\right) + Z \ln\left(\frac{R}{1\text{-}R}\right)$$

where K is the rate constant, t the time, Z the fraction of more floatable mineral initially present in the feed solids, and R the recovery of the mineral based on a maximum possible recovery of unity. It is indicated that for small values of Z the second order term would be dominant, while for large values or for the flotation of a single mineral ($Z = 1$), the first order term would be significant. Recovery-time data presented by Arbiter for ores where Z was small appear to give the second order hypothesis some foundation from the resulting linearity of the t/R vs t plots and from his Table II showing the dependence of recovery upon initial mineral concentration. It should be pointed out, however, that the presence of the same variable, time, in both terms tends to mask the true nature of the R-t function; since the second order expression is rearranged and plotted $\frac{R}{1-R}$ vs t, the points do not fall as close to a straight line. If Volkova's R-t data, calculated from the above equation for three barite-quartz mixtures, where Z was 0.2, 0.3, and 0.5 for barite, are plotted both as t/R vs t and $\ln \frac{1}{1-R}$ vs t, the latter graphs are found to be quite sensitive to changes in Z, giving rather widely separated nonlinear curves. The t/R vs t plots result in closely-spaced curves with linearity increasing with the increase in Z, a trend in opposition to what should be expected. The plot for the 0.5 barite mixture is perfectly linear, again showing the ability of the $\frac{t}{R}$ vs t plot to represent rather than characterize the data.

Sutherland's R-t data for glass spheres[21] and our own coal flotation results do not show linearity in directly plotting $\ln \frac{1}{1-R}$ vs t, but equations containing these terms may be made to fit the data by introducing constants to achieve linearity. Sutherland developed an equation fitting his glass sphere R-t data with an accuracy of ±1 pct, but his method does not constitute a practical approach to the problems of evaluating floatability and flotation machine performance.

To summarize, we believe that since any one of several types of equations can be made to conform to a set of R-t data by the incorporation of suitable constants in the chosen form, the multitude of variables influencing flotation rates will continue for the time being to resist efforts to describe the mechanism by a single generalized equation.

For the present, we are forced to consider flotation as a rate process of unknown order, basing our calculations and conclusions on graphical analyses of the R-t data.

---

[20] Z. Volkova: *Acta. Phys. Chim. U.R.S.S.* (1947) 22, p. 331.

[21] K. L. Sutherland: *Journal of Physical and Colloidal Chemistry* (1948) 52, p. 394.

F — Coal

The Formation of Acid Mine Drainage

by Kenneth L. Temple and Arthur R. Colmer

DISCUSSION

E. W. Lyon *(Bureau of Mines, Pittsburgh)*—Previous to the first World War James Campbell and E. C. Auld of the H. C. Frick Coke Co. carried out a successful large-scale pilot plant experiment on the treatment of mine drainage and patented certain features of the process. The writer's first serious contact with the acid mine drainage problem began when he was Managing Engineer for this plant and has been more or less continuous until the present time. As early as 1919, Powell and Parr in Bulletin No. 111, University of Illinois Experiment Station, indicated that biochemical action was probable in the oxidation of coal seam sulphides to sulphates in the absence of air. During the twenties and early thirties, Sayers and Leitch of the Bureau of Mines, with Van Zant and others of the Sanitary Engineering Bureau, Pennsylvania Department of Health, developed the principles of the method of abatement later known as mine sealing. Between 1935 and 1942, engineers of the U. S. Public Health Service and eight cooperating State Health Departments conducted a vast full-scale experimental application of the mine sealing process at 4000 mines, from Indiana to Maryland and from Pennsylvania to Alabama. Nearly all these workers agreed, in private conversations, that the reactions taking place in the mine were more variable and more complex than had been anticipated. Their repeated recommendations for specialized studies have motivated the current investigations which, while exploring new channels, confirm many earlier concepts.

The authors of this paper, Dr. Temple and Dr. Colmer, have contributed something new and vital to mine drainage technology. For this they are to be highly complimented. They have also made some statements, it is believed inadvertently, which are sure to arouse disagreement.

The introductory paragraph contends that acid mine drainage presents a "peculiarly difficult problem for two principal reasons."

1—The first is that the acid discharge increases in proportion to the expansion of the industry. In this respect the mining industry is not unique, since expansion is common to most pollution sources, both domestic and industrial. It *is* unique in that the pollution persists, or even increases, after mining operations have ceased and responsible ownership has abdicated. In justice the individual operator cannot be expected to underwrite a perpetual control, or do more for his drainage than is being done for the abandoned mine drainage. The difficulty here is political, and lies in establishing the equity between private and public responsibility.

2—It is stated secondly that "there is no method yet known that will appreciably alleviate the acid water problem except at totally prohibitive cost to the coal operator." On the contrary, it may be shown that there are two methods which will provide substantial improvement. These are chemical treatment and mine sealing.

Chemical treatment is admittedly expensive, but if full advantage is taken of present knowledge it is not necessarily as unthinkably expensive as many have claimed. In the upper Ohio River Valley the mines discharge approximately 3 million tons of acid per year—equivalent ton for ton to calcium carbonate or limestone. Over the same area the damages due to acid drainage have been variously estimated at $5 million to $30 million annually. At the present value of the dollar it is probably nearer the latter figure. It would be reasonable, then, to assess at least $5, and perhaps as much as $10 million dollars, against each ton of acid. In computing the total cost to the industry, it has usually been assumed that it would be necessary to treat *all* the acid. However, a large portion of the total imposed load on the streams is neutralized by the natural alkalinity of the surface runoff. Surveys also show that nine tenths of the acid load is discharged from about one third of the mines. The average production from this group of mines may be 700 to 1000 tons of acid per mine per year. If properly handled, about $3.00 worth of pulverized limestone and $3.00 worth of hydrated lime will neutralize each ton of such acid. Under certain favorable conditions, it is possible to recover both iron oxide and aluminum oxide in commercial quantities and possibly other byproducts. It may be deduced, therefore, that giving nature assistance at particular trouble spots may well be practical. Chemical neutralization of mine drainage is not a cureall, and is not universally applicable, but it has a place when used with discretion. Its main disadvantage, other than cost, is that most of the sulphate remains in solution as permanent hardness, forming compounds objectionable to water users.

The combination process of air and drainage control known as "mine sealing" has been demonstrated throughout eight states by a $10-million experiment carried out under the sponsorship of the U. S. Public Health Service and the several State Health Departments. Notwithstanding that the actual work was done under the limitations imposed by the use of relief labor, the favorable results were too widespread and too well authenticated to be disregarded.[4] As was to be expected from the state of the art, efficiency varied greatly from location to location. On the average, the overall discharge of acid sulphate salts from sealed mines was reduced 70 pct, usually accompanied by a simultaneous reduction in volume of drainage. Unfortunately, most of the operating data is still buried in the archives. Because of the restrictions imposed on the expenditure of public money, the program was limited to abandoned mine workings where it was considered that there was no responsible owner. The system is nevertheless readily applicable to worked-out sections of operating mines. If the mine projection has provided for sealing successive panels, the cost is very moderate and may frequently result in an overall saving due to reduced ventilation and drainage costs. Since over 80 pct of the total acid discharge comes either from abandoned mines or worked-out portions of operating mines, the remainder from truly active areas need give little concern. It can scarcely be said, therefore, that "there are no methods yet known that will alleviate the acid water problem except at exhorbitant cost. . . ." The fact that a process is not perfect does not preclude its being used until it can be improved or a better method found.

The contention that the roof shales and rider coals constitute the prime source of acid-forming minerals is most pertinent, and the observation that there is no substantial acid production until the strata is fractured and exposed to the mine atmosphere is equally valuable. The scientific determination and documentation of these facts is probably an even more useful contribution than the discovery that a specific form of bacteria is actively associated in the biochemical chain of reactions. Engineers engaged in the underground phases of mine drainage have long noted and verbally discussed the fact that acid conditions are not bad during first mining. Pipe lines from gathering pumps at the room faces are little affected. After pillar robbing has fractured the overburden the corrosivity and volume of the drainage both increase greatly. Thus these unrecorded observations support and extend the findings of the authors.

With regard to the sulphur oxidizing bacillus, the authors do not state whether an acid condition is first necessary for the growth of the bacteria or whether the bacteria can be found on neutral or alkaline surfaces containing sulphur compounds which they thereafter decompose with the production of acid. It is implied that moisture is necessary, but it would be interesting to know if the bacteria is aerobic or anaerobic, that is, whether or not the bacteria can exist and multiply if the sulphur-bearing slate is completely and continuously submerged in stagnant water. Other obvious questions might be asked, but it is presumed that the authors are already working on them.

In view of the statement that the source material producing mine acid has not been exactly identified, it is believed that more proof should be awaited before discounting the presence of free acid. It is true that there are many analyses in which the metallic ions are equivalent to the sulphate ions, but there are also many analyses that can only be balanced by counting the free hydrogen ions as evidenced by the pH determination. Theoretically the pyrite, iron sulphide FeS_2, should decompose to ferrous sulphate, $FeSO_4$, and sulphuric acid, H_2SO_4. As the iron changes valence by oxidation from ferrous to ferric ions, a portion of the free acid is recombined, $Fe_2(SO_4)_3$, to satisfy the added sulphur demand of the iron. Other portions of the free acid may dissolve aluminum compounds in transit and appear in the analysis as aluminum sulphate. If sufficient calcium carbonate is encountered in passage, all of the actively ionized acid is combined and will be found as calcium sulphate. From a variety of analyses it appears that any one of these conditions may prevail. There may be much free acid or no free acid, depending upon time and place. Incidentally, there is a surprising uniformity in the sulphate ratio in the mineral analysis of mine drainage which bears out the above presumption. Whether the particular discharge is acid, neutral, or alkaline, the sulphate radical, $SO_4=$, remains at a remarkably constant percentage of the total mineral content.

It is submitted that the load of polluting salts conveyed by mine drainage may eventually be traced to a leaching action upon the freshly broken rock, a rapid decomposition of iron sulphides by bacterial action as indicated in this paper, and a slower but possibly more sustained decomposition of the more stable pyrites and marcasites through chemical oxidation. The new evidence currently presented may be interpreted as confirming the main tenets of mine sealing, as developed and amplified through the demonstration program of the U. S. Public Health Service, and it is believed that mine sealing still offers the most promising, reasonably effective means of abating the nuisance at low cost.

We do need to know much more about the detailed behavior of acid mine drainage under varying conditions from earliest formation to final disposition before maximum efficiency and economy can be attained. It is to be presumed that an amount equal to the damages caused by acid mine drainage could be profitably expended to eliminate the damage. Such figures, the result of a thoroughgoing impartial appraisal by experienced valuation engineers, are not available. It would seem that any serious attempt to solve the problem should begin with a determination of this factor. Secondly, it is fairly certain that any method, mine sealing for instance, if applied to a mine would modify its layout and operating schedule, maybe for better and maybe for worse. Here, not research in its proper sense, but just plain engineering-management studies and experimentation on full-scale operating mines is needed. Just what is the effect, at representative mines, upon costs, drainage, ventilation safety, panel sequence, corrosion of rails and other equipment, and similar factors? The answers might be startling, either for or against the proposal. Prior to the determination of such facts it is quite probable that whenever the industry, either directly or indirectly through public agencies, expends upon mine-drainage-stream-pollution as much as 5¢ per ton of coal mined, the problem will no longer exist.

---

[4] Ohio River Pollution Control, House Document No. 266, 78th Congress, 1st Session.

Kenneth L. Temple (author's reply)—Mr. Lyon is quite correct in pointing out the contributions of earlier workers in the field of acid mine drainage. A complete list would contain many more names. Frank Haas, a practical mining man who was prominent in the development of the northern West Virginia coal field, had a deep interest in acid formation and a remarkably clear insight into the problem. The first accurate biological studies of acid water were carried out by J. B. Lackey. Many workers at West Virginia University and elsewhere have devoted much time to a study of acid mine drainage, its formation or treatment. In addition to those mentioned by Mr. Lyon, the names of L. V. Carpenter, L. K. Herndon, W. W. Hodge, D. B. Reger, E. T. Reetman, W. R. Downs, A. H. Davidson, and G. L. Hall are associated with earlier studies of acid drainage. In spite of the importance of the problem as indicated by these investigators, no full time studies were made until the inception of the BCR project at West Virginia University and the Mellon Institute project. For a short period there was also a full time project at the U. S. Bureau of Mines in Pittsburgh.

Mr. Lyon in his criticism of the opening paragraph stressing the importance of mine water pollution apparently missed the point, which is that since worked-out mines continue to make acid, the expansion of mining steadily decreases the amount of surface water that is free from acid mine drainage.

Chemical treatment is feasible only in the milder examples of acid mine water. It is not practical by any known method for the highly acid waters so widespread in the great bituminous coal area of northern West Virginia, southwestern Pennsylvania and eastern Ohio and of occasional occurrence elsewhere. The best study of chemical treatment applicable to the American soft coal fields is that by S. A. Braley of Mellon Institute in a report entitled *A Pilot Plant Study of the Neutralization of Acid Drainage from Bituminous Coal Mines,* published by the Pennsylvania Department of Health.

The mine-sealing program still has its adherents. Perhaps a good study of the results of the mine-sealing program should be made, if only to provide the data for settling arguments about its merits. Few of the early follow-up reports on mine sealing are worthwhile, inasmuch as the mines were still filling at the time of the reports and the low acidity measurements made at that time cannot be duplicated today. It is the opinion of the authors that mine sealing, so-called, as applied to the slope or drift mine, is an expensive and ineffectual procedure.

The question whether an acid condition is first necessary for the growth of the sulphur-oxidizing bacteria is practically meaningless. The reason is the small scale of the bacterial world. An acid spot accidentally produced, a few square microns in area, would be sufficient to allow one bacterium to start growing. The acid formed by this bacterium would spread out and make the surrounding area acid enough to allow more cells to grow. In order to inhibit bacterial growth through control of acidity it is necessary to have a buffered solution bathing all sulphuritic particles. This, of course, is not the case in the mine. Since the present paper deals primarily with the source of sulphuritic material from which acid is formed, the many aspects of bacterial action are not dwelt upon.

The statement that there is no free acid is based entirely upon analyses by M. E. Hinkle, formerly of this laboratory. His data seem to be conclusive for the type of waters studied, which include the most highly acid mine waters discharged from coal mines. The result is a balance between cations and anions, not including hydrogen ions, indicating that there is no net free sulphuric acid. The high titratable acidity is due to the hydrolysis of various salts, the principal one being ferrous sulphate. It is not inconceivable that samples of acid mine drainage containing some free sulphuric acid might be found; they have not been found in the local coal fields, and would not be expected under the local geological conditions. Perhaps pyrite in sandstone would give such a water sample containing ferrous sulphate and sulphuric acid, but in the authors' experience the water from a mine that has a roof of sandstone containing pyrite is only mildly acid and does not constitute the main problem.

A. A. Berk *(Bureau of Mines, College Park, Md.)*—The Bureau of Mines has been privileged to follow the West Virginia University work on coal-mine drainage through frequent progress reports. This summary paper by Temple and Colmer is based on careful observation in the field and painstaking research in the laboratory. Comments on this work by others in the field emphasizes the essential complexity of the problem, since the interpretation of the data is questioned and acceptance of the observations as fundamental data is disputed.

There is no doubt that Thiobacillus Thiooxidans may increase the rate at which sulphuric acid is formed from sulphides in roof strata, debris, and residual coal in the mines. Such chemical reactions generally occur in several steps and the overall rate is determined by the rate of the slowest step in the chain. The bacteria appear to accelerate the formation of acid by speeding up the rate-controlling reactions. A laboratory demonstration of this effect, including rate determinations, would make an excellent problem for a doctor's thesis at the University.

On the other hand, there is ample evidence that the formation of sulphuric acid does not require bacterial assistance. Elaborate tests at West Virginia University confirmed this basic fact. Thus, although the work of Temple and Colmer is a long stride from the observation of Carpenter and Herndon[5] 20 years ago that Thiobacillus Thiooxidans thrived in sewage made acidic by acid-mine water, it does not appear to present a practical method of coping with the pollution problem.

The one practical suggestion made by the authors is that coating an acid-producing surface to seal it from contact with air would stop acid formation. Such local sealing is impractical both because of the nature of the surfaces and because interference with the movement of seepage water would break surface seals quickly. In contrast, sealing off the air of abandoned mines, or abandoned areas of mines, with water-filled concrete traps should have the same desirable effect. Sulphuric acid formation is known to have been greatly decreased and even stopped in instances in which complete sealing was effected. The apparent success of the energetically conducted mine-sealing program in Pennsylvania is, however, no confirmation that bacteria are needed for the formation of sulphuric acid, since oxygen is a primary factor, without which the huge tonnages of sulphuric acid cannot be formed by any process.

Mine sealing is still the only practical method by which the output of naturally formed sulphuric acid can be reduced. Tonnage reductions achieved in Pennsylvania's program are most impressive. In many localities the output already can be tolerated because of the natural alkalinity of the watershed. Conditions should improve, as sources of incoming air, many located in adjacent active workings, are sealed. However, some form of neutralization or acid removal may be required before tolerably clean streams are restored in the coal country. A solution acceptable to both operators and State Authority is being sought by the Stream Pollution Research Laboratory of the Bureau of Mines.

---

[5] West Virginia University Research Bulletin No. 10, 1933.

Filter Cake Size-Consist and Moisture Relationships

by O. R. Lyons

DISCUSSION

J. D. Clendenin *(Bureau of Mines, Anthracite Research Laboratories, Schuylkill Haven, Pa.)*—In this paper and earlier ones, Mr. Lyons is to be commended for endeavoring to place coal dewatering on a more rational basis, thereby systematizing available information and providing better tools for estimating design or evaluating performance. The task requires much more effort than is generally appreciated. His contribution would be much more useful, however, if the spread in the relationship shown between average particle size and moisture content of the cake could be reduced, i.e., if he would present available data on other factors influencing the filtering operation and determine their effect on the relationship illustrated in his Fig. 1. In the present paper, the author appears to have abandoned consideration of some of the factors* he endeavored to appraise previously[3, 4] yet there is mounting evidence, as he has suggested, that satisfactory results in dewatering require attention to principles and details.

On the basis of the evidence presented here, I question, at least in part, the author's conclusions. For example, at average particle size 0.0035 to 0.0045 in., the moisture content range in Fig. 1 is from 22 pct to approximately 48 pct; at 0.03 to 0.04 in., it is 9 pct to about 22 pct. Any predetermination of moisture content from the relationship presented is useful only for estimating the range or variations that one might anticipate, certainly not for an average that has much significance. This is brought out more emphatically in Fig. 2 by an indication of these moisture ranges along with the corresponding average particle size range as taken from Fig. 1.

This contribution would have added value if the author had included a consideration of other factors affecting moisture content; hence the relationship he presents. He mentions some important factors and refers to "normal operating conditions," which, it is recognized, are different at different plants and often differ considerably in the same plant at different times. It would be helpful if any or all of the following data were available for each of the 26 tests listed for various coal filter cakes: 1—filter area and size of filter; 2—capacity levels at which unit was operated; 3—temperature; 4—solids density of slurry; and 5—vacuum on filter. Pertinent information for Test No. 8 and Nos. 10 through 18 has been reported previously[3, 4] by the author as Plant Nos. 1 to 10 inclusive. Data on other factors such as immersion doubtless merit consideration as he has indicated.

Fuhrmeister[20] has shown the effect of: 1—temperature on both the dryness of calcium carbonate cake and the cake rate in pounds per square foot per hour; 2—percent solids in the feed on the filter cake rate; and 3—percent of −200 mesh solids in a coal slurry of 45 pct solids on both the percent moisture in the cake and the filter cake rate. None of these effects is insignificant. The influence and interrelation of these and/or other factors on cake moisture in coal filtration have been investigated in the laboratory, and a few reports made available;[21–23] no doubt, much other unpublished work exists. In predetermining moisture contents the influence of other factors besides average particle size, as determined by the author, cannot be neglected.

If one plots percent surface moisture against percent of −200 mesh solids in the filter cake, as in Fig. 2, using all the author's data except Test Nos. 19, 22, 23 and 24,** the moisture content spread is no greater, perhaps even less, than that in the author's plot of surface moisture against average particle size. Thus, within limits, a determination of the −200 mesh in the cake, or slurry, should be all that is necessary to estimate moisture content in the finished cake. Besides, data reported by Fuhrmeister[20] for coal, and other data reported elsewhere[3, 4] by Mr. Lyons, also fit into the general pattern of Fig. 2 as shown. The three points above the upper dashed line in Fig. 2 are suspect because it looks as if the operations were scarcely "normal." One would not select the inside drum and disc combination on the basis of the degree of dewatering accomplished here.† Furthermore, the anomalous positions of the two points for the outside drum above 40 pct moisture suggest that the conditions of the tests represented merit closer scrutiny.

---

* For example, the presence of clays and slimes with their great power of water retention in coal filter cakes was assayed by determining the ash content of the −200 mesh material; surface moisture was plotted against the product of percent −200 mesh and the percent ash content of this material. Can details like the presence of clays and other subversive material be neglected? The presence of these subversive materials in fine-coal circuits is a common source of dewatering and cleaning problems. Their removal at the best spot is difficult. If feasible, however, suitable attention to pH may greatly assist[18,19] in controlling and minimizing water retention by the filter cake, either by removal of these fines and slimes early enough or by converting them into a less water-retentive form. One objective many operators strive for is the removal of these materials before they enter the fine-coal circuit.

** These are not included because no −200 mesh is present or it cannot be picked directly from the data.

† Comparison of the particle size consist of the coal in Test No. 25 on this filter with that for Test No. 26 on the Genter filter raises a question in regard to the conditions under which Test No. 25 operated. In both these tests the surface moisture reported is virtually equal. In contrast, the −200 mesh material in the Test No. 26 coal is 29.2 pct, or 10 times greater than the 2.8 pct in Test No. 25; 22.7 pct of −325 mesh makes up most of the through 200 mesh in the No. 26 coal, yet the average particle sizes given for the two coals are in the same range.

It is extremely doubtful whether the high proportion of 70x200 mesh, 53.4 pct, in the Test No. 25 coal, which is only 4 times greater than the corresponding fraction, 13.2 pct, 65x200 mesh, in Test No. 26, can account[21,24] for the water-retentive powers necessary in the Test No. 25 fine coal to give surface moisture equivalent to that in Test No. 26. The size characteristics of the No. 25 coal suggest that the surface moisture of the filter cake from the inside drum and disc combination should be appreciably lower than 21 pct.

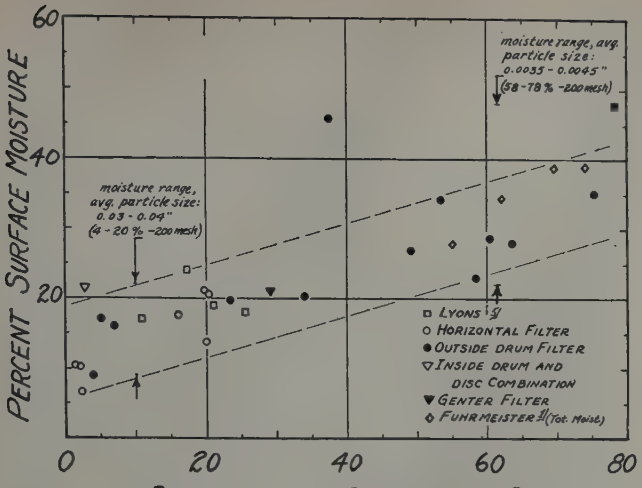

Fig. 2—Moisture range compared with average particle size range shown in Fig. 1.

Comparison of the conditions[3, 4] for these two tests in Table III with conditions in Table IV for the tests by Fuhrmeister shown in Fig. 2 are revealing. One might ask which group represents "normal operating conditions," and why there is such a discrepancy in filter cake rates for the conditions most nearly comparable in the two groups. Are the high-ash clay slimes present to the same extent in Table IV coal slurry as in Table III material, and to what extent do their water-retentive properties affect the latter results?

It would be interesting to compare the filter cake moisture reported for the relatively coarse coals in Test Nos. 22 through 24 with the moisture contents resulting from gravity drainage of the same coals for various lengths of time. In all probability, these could be drained to similar levels of moisture in a car or properly designed pocket within a reasonable time.[21, 23] Certainly, pressure filtering is hardly practical with these coals, and centrifuging would only be justifiable where a premium is placed on time and/or space, or where is shows the greatest overall economy.

It would seem that the author's conclusion relative to the comparative effectiveness of all filters from a moisture reduction standpoint needs to be qualified because the influence of other factors in the relationship he depicts must be included if he is to make the available information most useful. The author's conclusions will require one to exercise the utmost discrimination in predicting dewatering performance when coal slurry solids contain above 30 pct of —200 mesh material, because the test data for three of the four filters, from the author's present paper, shown in Fig. 2 are confined to the left of the 30 pct ordinate. Surely, there is little need for all the types and designs of filters that are available if "apparently all of the makes . . . are equally effective from a moisture reduction standpoint," which, after all, is the purpose of the filtering operation here. There most certainly are significant differences in dewatering ability of filters relative to requirements, conditions, and factors in an operation, else men would never have developed some of the filters now available.[20, 25]

Table III. Solids in Filter Feed, 50 to 55 Pct

Surface Moisture, Pct	—200 Mesh, Pct	Ash in —200 Mesh, Pct	Filter Cake Rate, Lb Per Sq Ft Per Hr
46.2	37.5	54.8	12
48.3	78.4	46.4	8

Table IV. Solids in Filter Feed, 45 Pct

Moisture in Cake, Pct	—200 Mesh, Pct	Filter Cake Rate, Dry, Lb Per Sq Ft Per Hr
38	74	58
38	69	65
34	62	78
28	55	93

O. R. Lyons (author's reply)—Mr. Clendenin has prepared a very good discussion and has brought up some points that should be clarified.

In the first place, the author has not abandoned the concept that the presence of clays and slimes increases the moisture content of a filter cake. The author merely wished to provide a method that would allow classified filter feeds to be compared with what might be called "normal" filter feeds. The method previously proposed by the author, plotting surface moisture against the product of the —200 mesh pct and the percent ash content of this material, is still valid but cannot be used to evaluate a filter cake containing very little or no —200 mesh material.

Any make of filter will operate at essentially the same vacuum and pull through a comparable volume of air when treating essentially the same size-consist coal. Bed-porosity is related to the size-consist of the material, the type of filter cloth, and the inches of vacuum. Size-consist adequately expresses all of these variables since the type of filter cloth primarily governs the size of the retained material and inches of vacuum depend primarily on the size-consist of the filter cake.

No mention was made of filter capacity in the paper because the author was not able to obtain sufficient operating data to provide more than the rather general conclusion that capacity is related primarily to feed pulp dilution and the size-consist of the feed material. Speed of rotation has an influence on capacity, but it can be neglected, since all filters operate at very slow speeds.

Wide fluctuations in the moisture contents of the filter cakes produced can be explained on the basis of: 1—the size of the filter installation and 2—the nature of the feed, whether classified or not. Large filter installations, where the elimination of blinding and cloth replacement is a continuous rather than an intermittant process, showed very little variation from the average. Small filter installations provided very good or very poor results depending on the degree of maintenance. Semi-classified or classified feeds provide erratic results as compared to "normal" feeds. Channeling can occur in cakes containing only a small amount of slimes; consequently the cake will be wet.

The author cannot agree with Mr. Clendenin's conclusion that there are basic mechanical advantages to be found in one type of filter as compared with another in so far as coal filters are concerned in moisture reduction. It may be true that some filters have decided advantages when compared on the basis of floor space required, ease of maintenance, ease of feeding, and even capacity, but these considerations are outside the scope of the paper.

---

[18] G. B. Dickey and C. L. Bryden: *Theory and Practice of Filtration*, pp. 48, 50. Reinhold Publishing Corp., New York, 1946.

[19] J. W. McBain: *Colloid Science*, pp. 378-379. D. C. Heath and Co., New York, 1950.

[20] Charles Fuhrmeister, Jr.: Improving Filtration and Filtration Rates. *Chemical Engineering Progress* (November 1951) 47, No. 11, pp. 550-554.

[21] D. W. Gillmore and C. C. Wright: Drainage Behavior and Water Retention Properties of Fine Coal. *Trans.* AIME (September 1952) 193, pp. 886-894.

[22] D. W. Gillmore and C. C. Wright: Further Studies on Drainage Behavior and Water Retention Properties of Anthracite Fine Coal. Unpublished report, Mineral Industries Experiment Station, The Pennsylvania State Coll., Nov. 10, 1950.

[23] W. T. Turrall: Anthracite Method of Coal Drying. *Coal Mine Modernization Year Book* (1950) pp. 276-294. American Mining Congress.

[24] J. M. Dalla Valle: *Micromeritics*. 2nd ed., p. 283. Pitman Publishing Co.

[25] H. P. Grace: What Type Filter and Why. *Chemical Engineering Progress* (October 1951) 47, No. 10, pp. 502-507.

Comparative Effectiveness of Coal Cleaning Equipment

by O. R. Lyons

DISCUSSION

Judson S. Hubbard *(The Humphreys Investment Co., Denver)*—In this very interesting paper several brief references are made to the Humphreys spiral, a device used for cleaning fine coal.

In Table I, Plants 76 and 77, data are given on spiral performance treating Raton and Trinidad coal. The fine coal, as fed to the spiral in these instances, is actually a table middling, hence the more easily treated material was previously removed and a large number of particles were present which were difficult to clean. Mr. W. M. Bertholf of the Colorado Fuel and Iron Co. presented a paper in February, 1946, *Cleaning Table Middlings from a Coal Washery with the Humphreys Spiral Concentrator,* from which I quote:

"In considering the results of our tests it should be noted that the feed was our table middling, and that any real separation is a 'moral victory' as there is little material that could properly be called coal and practically no heavy rock, the consequences being that previous attempts to clean the middling have not at all been successful."

Referring again to Table I, Plants 72, 73, 74, and 75, these data were obtained by Yancey and Geer and others and presented at the February 1950 Meeting, AIME, in a paper entitled *Laboratory Performance Tests of the Humphreys Spiral as a Cleaner of Fine Coal.*

Results shown for those tests involve all particles from 8 mesh through the colloids, which admittedly is not an ideal situation for spiral feed if much refuse is contained in the —80 mesh or —100 mesh size range.

As an illustration of the effect of treating too broad a size range, let us consider Plant No. 75, Kentucky No. 9 seam. Spiral feed was 8 mesh x 0. Now had this been 8x100 mesh the percentage of misplaced material would have been 8.0 pct instead of the reported 15.26 pct. Similar comparisons can be made on the other data presented with respect to the spiral.

Other types of equipment show a similar trend in that whenever too fine a size is treated in a given unit process the percentage of misplaced material increases. Since the spiral is working near the finer end of the size range, it will sometimes be advantageous to treat the entire range of —8 mesh material rather than to deslime and make a fair showing on, say, the +80 or +100 mesh. Desliming is subsequently done in any case in the dewatering or thickening operation.

Results obtained by spiraling any given coal depend on factors too numerous and complex to discuss here, but there are strong indications that proper preparation of feed to the spiral can improve results obtained on some of the raw coals tested. This is clearly pointed out at the end of the aforementioned paper by Yancey and Geer. "The spiral is an extremely simple device which involves no moving parts and is constructed almost entirely of unmachined castings. Since it is such an uncomplicated mechanism, operation is simple and virtually foolproof. These characteristics, which go far toward insuring low cost operation, are attractive attributes in any coal cleaning unit."

Certain equipment used in conjunction with the spiral has resulted in a decrease in the percentage of misplaced material, notably in actual practice the launder screen which is used to remove objectionable high ash fines from a spiral-washed coal product. Private correspondence with the U. S. Bureau of Mines has intimated that an additional yield of coal is possible by flotation of the spiral middling. Possible future improvements and developments may result from other methods now under consideration.

Finally, some compromise must be made between the best metallurgical performance and the best practical or economical results. Mr. Lyons emphasizes in his summary this objective of overall economy in selection of equipment.

G. B. Walker *(American Cyanamid Co., Stamford, Conn.)*—I had the pleasure of reviewing the draft of this paper and my curiosity was aroused by the data given for Tromp plants, in that all of the examples shown appeared to be 2-product separations, whereas all the Tromp plants with which I am familiar have been 3-product units.

The data given for plants No. 101 and 102 appear to be taken from Tromp's brochure on his process and represent the results obtained at the Dominale plant in Holland which was operated for many years by Mr. Tromp. The plant, which was designed to treat 58 tons per hr, was sampled while treating 35 tons per hr of 3¼x¾-in. coal. Example 101 appears to conform to what would result if the middling product were calculated into the refuse product, while Example 102 represents the calculation of the middling into the coal product. It is believed that Examples 103 and 104 represent the operation of the Willem-Sophie Mine in Holland recalculated on the same basis.

In checking the English examples given by numbers 14, 15, 16, and 17, the same procedure seems to have been followed. These results have, apparently, been taken from an article in *Colliery Engineering* in August 1941, describing the initial operation of the Williamthorpe Colliery of the Hardwick Colliery Co. Two vessels are employed in this plant, one to treat soft coal and one to treat hard coal. Example No. 14 presents the results that could be obtained from the soft coal bath if the middling were calculated into the refuse, and Example 15 the results when the middling is calculated into the coal. Examples 16 and 17 represent the same expedient in the case of the hard coal bath.

Of interest to this discussion is the fact that during the past year the Simon-Carves Engineering Co. in England has installed in the Williamthorpe plant their new "Sim-Car" medium cleaning system which is based on magnetic extraction and control and which is licensed under the Heavy-Media Separation Processes patents by the American Zinc, Lead and Smelting Co. This system has been described in the December 1951, issue of *Colliery Engineering.* It is reported that since the Williamthorpe Colliery was changed from the Tromp system of medium cleaning to the Magneto-Motive method of medium control the opera-

Table V. Comparative Effectiveness of Coal Cleaning Methods Employed by the Dutch State Mines

Type of Bath	Media	Type of Coal	Grain Size, In.	Separation, Sp Gr	Washed Coal		Refuse		± 0.1 Distribution, Pct, at Gravity of Separation	Total Misplaced Material in Washed Coal and Refuse in Pct of Raw Coal
					Wt Pct	Sink Pct	Wt Pct	Float Pct		
Shallow	Slime tailings	Bituminous	3½x⅝	1.455	49	0.6	51	0.5	9	0.55
Deep	Barytes	Anthracite	4½x⅝	1.475	76	0.5	24	2.5	30	0.98
Deep	Crushed shale	Anthracite	1x⅝	1.60	75	0.4	25	0.5	4	0.43
Deep	Barytes	Bituminous	1¾x⅜	1.50	86	0.45	14	0.4	15	0.45
Deep	Barytes	Bituminous	1x5/16	1.59	76	0.5	24	1.1	8	0.74

tion of the plant has been greatly simplified in that the viscosity and specific gravity of the medium can be more easily controlled. In addition, we are advised that the medium loss at the Williamthorpe Colliery has been reduced to 40 pct of the figure experienced under the Tromp system. It is our understanding that the National Coal Board is planning on a conversion of the other Tromp plants in England to the "Sim-Car" magnetic recovery and control system.

Example 13 has been identified by Dr. Kriegsman of the Dutch State Mines as being the results obtained in a Tromp washer at the Moritz Mine. This plant was dismantled some 8 years ago and has been replaced by the Dutch State Mines Slate Tailing Process. Dr. Kriegsman has kindly supplied me with the following data, relating to some of the cleaning plants operated by the Dutch State Mines, as a contribution to illustrate the results that can be obtained on Dutch coals with various types of dense medium, including crushed shale, barytes, and slime tailings.

In a survey of this sort it is extremely difficult to cover all phases of the field, and it is my personal feeling that Mr. Lyons has treated the heavy-media system very fairly, although I would like to point out that all his examples are predicated on Link-Belt separatory vessels and appear to be limited to the Champion and Park Breaker installations. While the Link-Belt vessel is one of the best available for use in heavy-media plants, I think it would be only fair to consider some of the other six types of satisfactory vessels which are in operation in the coal industry. There are now 54 heavy-media plants in operation or under construction for the treatment of coal. These 54 plants have a combined capacity of over 25 million tons a year and employ a total of 71 separatory vessels, of which 17 are Link-Belt.

Using Electric Furnaces and Heaters to Determine the Free Swelling Index of Coal

by E. Swartzman and G. C. Behnke

DISCUSSION

W. A. Selvig *(Bureau of Mines, Pittsburgh)*—Considerable difficulty has been experienced by different laboratories in meeting the temperature specifications of the standard A.S.T.M. method, which specifies a gas burner for heating. At the Pittsburgh Station of the Bureau of Mines, where natural gas is used for the test, the gas pressure available is not quite high enough to meet the temperature requirements of the standard method. This difficulty was solved by installing in the gas line a gas booster pump equipped with a diaphragm-valve pressure control. An electric furnace obviously permits easier temperature control than does the standard gas burner.

The degree of swelling of a caking coal, when heated in a crucible, is influenced considerably by the characteristics of the heat input into the coal. In the standard gas-burner method much of the heat is concentrated at the bottom of the crucible, a condition that appears to be duplicated by the conical-style electric heater used by the authors.

The A.S.T.M. standard method for volatile matter in coal specifies platinum crucibles of not less than 10 or more than 20-cc capacity. As the Bureau of Mines has standardized on platinum crucibles of 10-cc capacity, these were used to determine if they would give results for free swelling comparable to those obtained by Swartzman and Behnke, who found 15-cc platinum crucibles to be satisfactory. In these tests the same type of electric furnace and method of procedure recommended by the authors were used. These tests showed that a 10-cc crucible is too small to give results checking those of the standard A.S.T.M. gas-burner method.

The 10-cc crucibles gave buttons that did not conform in shape to the standard profiles, so the free-swelling indexes could not be estimated by matching the shape of the coke buttons with the standard profiles as described in the standard method. It was found, however, that, for coals with relatively low free-swelling indexes of 5 or less, satisfactory agreement with the standard method could be obtained by measuring the profile area or the volume of the coke buttons. For highly swelling coals, satisfactory agreement with the standard method could not be obtained by these methods, as low results were obtained. Apparently, the 10-cc-capacity crucible is too small for satisfactory agreement with the standard gas-burner method for coals having free-swelling indexes greater than 5.

Frothing Characteristics of Pine Oils in Flotation

by Shiou-Chuan Sun

DISCUSSION

Shiou-Chuan Sun (author's correction)—Too late for revision, the author realized that the data on stability of froth presented in this paper were not based on the same height of froth column. It is recommended herein that the stability of froth is better calculated by dividing the time elapsed until the froth disappeared by the volume (in cu cm per sq cm) or height of the froth column, and is expressed in sec per cm. The stability data in Tables I, II, and III of this paper were recalculated, in accordance with this recommendation, and the results are shown respectively in the accompanying Tables VII, VIII, and IX.

Compared with Tables I, II, and III of the paper, the stability data of Tables VII, VIII, and IX are more reliable in disclosing the persistence of froth of various frothers having different frothabilities. For example, the conclusion given in the paper that the stability of froth is generally proportional to the volume of froth becomes invalid when the stability of froth is expressed in sec per cm, as shown in Tables VII, VIII, and IX. Table VII shows that both the stability and volume of froth increase with the addition of small amounts of n-hexyl alcohol, and that further additions of n-hexyl alcohol decrease the stability but increase the volume of froth. Table VIII indicates that the stability of different types of frothers is governed by their chemical composition and is difficult to predict from their frothability. Table IX shows that the stability of different frothers with similar nonpolar groups tends to increase with a decrease of the hydrophilic property of their polar groups, and consequently with the decrease of their solubilities. This is further substantiated by the fact that the stability of frothers, as listed in Table IX, is generally lowered by the solvent effect of absolute ethyl alcohol. Table IX shows also that the stability of froth tends to increase with the decrease of the volume of froth, provided the frothers used have similar nonpolar groups and dissimilar polar groups.

Table VII. Stability of Froth Produced by Various Concentrations of Pure n-Hexyl Alcohol at 7.0 pH Value, and 71.6 CC Per Sq Cm Per Min Rate of Aeration

Test	Conc. of n-Hexyl Alcohol, Mg per L	Volume of Froth, CC per Cm^2	Stability of Froth, Sec per Cm
1	9.63	1.1	5.36
1a	9.63	1.1	5.45
2	19.26	1.3	5.84
2a	19.26	1.3	5.77
3	28.89	1.7	5.82
3a	28.89	1.7	5.77
4	48.15	2.1	4.91
5	77.04	3.0	3.70
5a	77.04	3.0	3.67
6	105.93	3.8	3.68
7	144.45	5.8	2.83
7a	144.45	5.8	2.84
8	288.90	6.7	2.69
8a	288.90	6.7	2.69

Table VIII. Stability of Froth Produced by Various Frothers, Tested at 7.0 pH Value, 19.2 ± 0.5 Mg Per Liter Concentration, and 71.6 Cc Per Sq Cm Per Min Rate of Aeration

Test	Frother	Stability of Froth Sec per Cm	Stability Index, Using n-Hexyl Alcohol as Standard	Frothability Index, Using n-Hexyl Alcohol as Standard
1	Pure n-hexyl alcohol	5.77	100.0	100.0
2	Tergitol wetting agent 7	<6.00	<104.0	>1153.0
3	Tergitol penetrant 4	6.83	118.2	262.0
4	Ethyl silicate, tetraethyl orthosilicate	3.18	55.2	169.0
5	Methyl Amyl acetate, 4-methyl-pentyl acetate-2	3.39	58.8	138.4
6	Methyl amyl alcohol	4.43	77.0	123.0
7	Pine oil 302, Hercules	5.57	96.5	107.7
8	Cresylic acid 1B, Koppers	2.86	49.6	107.7
9	Cresylic acid No. 1, Reilly	2.92	50.7	100.0
10	Pine oil F, Hercules	5.17	89.7	92.4
11	Cresylic acid D2A	2.42	41.9	92.4
12	DuPont frother B-23	4.83	83.8	92.4
13	Tergitol penetrant 08	7.25	125.7	92.4
14	Butyl carbitol solvent, diethyl glycol monobutyl ether	4.17	72.3	92.4
15	Cresylic acid — English, American Cyanamid	4.08	71.0	84.6
16	Pure n-octyl alcohol	5.27	91.6	84.6
17	Frother 60, American Cyanamid	8.30	144.0	76.9
18	Pine oil GNS. No. 5, American Cyanamid	4.50	78.1	76.9
19	Cresylic acid EE, Oronite	4.42	76.7	73.1
20	Cresylic acid 4020, American Cyanamid	8.22	142.6	69.2
21	Pine oil 302W, Hercules	4.88	84.8	69.2
22	Frother HTT, American Cyanamid	5.00	86.8	61.5

Table IX. Stability of Froth Produced by the Principal Constituents of Pine Oil, Tested at 7.0 pH Value, 19.2 ± 0.5 Mg Per Liter Concentration, and 71.6 Per Sq Cm Per Min Rate of Aeration.

Principal Constituents of Pine Oil	Polar Group	Solubility, Gm per L	Stability of Froth Sec per Cm	Stability** Index, Using n-Hexyl Alcohol as Standard	Frothability Index, Using n-Hexyl Alcohol as Standard
Beta terpineol	C-OH	2.2	3.85 (3.31)*	66.7	100.0
Alpha terpineol	C-OH	1.98	4.36 (4.00)	75.7	84.6
Fenchyl alcohol	C-OH	sl.	3.54 (2.89)	61.4	100.0
Borneol	C-OH	0.64	3.45 (1.78)	59.9	84.6
Camphor	C=O	1.6	3.36 (3.84)	58.3	84.6
Dihydro-terpineol	C-OH	—	4.57 (3.22)	79.3	53.7
Fenchone	C=O	i	7.25 (3.40)	125.5	30.8
Anethole	C-O-C	v.sl.	8.33 (3.36)	144.2	23.3
Methyl chavicol, estragol	C-O-C	i	10.0 (4.33)	173.5	15.4
Terpinolene	none	i	(3.25)		tr.
Dipentene	none	i	(4.17)		tr.
Camphene	none	i	(2.89)		tr.
Beta pinene	none	i	(3.13)		tr.

* Data in parentheses were determined by first dissolving reagent in equal volume of absolute ethyl alcohol.
** Stability of froth of n-hexyl alcohol used for calculation was 5.77 sec per cm.

I—Geology

Geology of the Silver-Lead-Zinc Deposits of the Avalos-Providencia District of Mexico

by W. H. Triplett

DISCUSSION

John G. Barry *(Mexico)*—"The Nerinea limestone," writes W. H. Triplett, p. 584, "is . . . medium-bedded (0.5 to 1.0 m). . . ." This is the Zuloaga formation. It has always been described as thick-bedded (1.0 to 3.0 m). "Whether the marls and shales were less amenable to replacement," he goes on to say, ". . . is a matter of opinion." In general, it is probable that the thinner-bedded formations were less competent than the nearby thicker-bedded, so that the latter produced premineral breccias when all were subjected to flexing stresses.

With reference to Mr. Triplett's analysis, p. 584, under *Lower Cretaceous*, in the Taraises and Cupido formations some few horizons should be considered as possibly containing hidden orebodies. In the Potrero camp, shown on the general map in the northwestern part of Fig. 4, p. 587, several mineralized beds are known; they are found throughout the whole thickness of the Cuesta del Cura formation.

With regard to intrusive rocks, p. 585, the general map, Fig. 4, shows that the Potrero and Noche Buena camps are near a third, monzonitic intrusive. It seems doubtful that the Aranzazú was any hotter than the Providencia camp. However, the former does contain large deposits of exogenetic silicates, which in large part occur within the Zuloaga limestone, as shown by Bergeat[9] in a stereogram. At the Aranzazú camp the La Caja formation was only slightly changed, whereas it was altered highly at the Providencia, possibly endogenetically. That the temperatures at the Providencia camp were relatively high at one time is also shown by the tourmaline veinlets and lenses in the monzonite and by the garnets on Temeroso peak; high temperature mineralization has possibly been eroded.

Maps and sections show that the Concepción del Oro—Temeroso stock occupies the original locus of some 40 km^3 of sedimentary rocks. The remains of large roof pendants at Carmen and Animas indicate that stoping was active. Whether all the sedimentaries were stoped and assimilated presents a lively problem, a correlative of which would be an estimate of the original constitution of the invading instrusive rock.

As to extrusive rocks, see p. 585, there is also a large thick area of the extrusives left near Noche Buena in the "La Caja" intramontane valley of the La Caja range. This place gave its name to the range. The volcanics are also said to occur in considerable amount in the Mazapil valley.[10]

Turning now to the remarks under Regional Structure, p. 586, as partly indicated on the general map, Fig. 4, the Mazapil Mountains of the Mazapil region are a continuous, U-shaped range including a northern leg of some 24 km, a southern leg of similar length, and a uniting base which lies to the East and which measures some 10 km in a S 20 E direction. Thus the U-shaped mountains are continuous through a length of 58 km and also contain one continuous anticline, the adjacent valleys being synclinal. The northern leg of the U is called the La Caja range, the base is called the Concepción del Oro range, and the southern leg the Santa Rosa range.

The ranges in northeastern Zacatecas and southern Coahuila contain anticlines and the valleys contain synclines, which where thin are necessarily highly compressed isoclines with very steep dips. Many of the anticlines also have isoclinal components which are overturned, original mushroom tops being indicated. The anticline in the base of the U of the Mazapil Region, Concepción del Oro range, is a recumbent anticline, over to the ENE, with a necessarily subjacent recumbent syncline.

Table IV. Recast of Table II

						Contents, Pct				Contents, Pct			
			Assays			Gold		Silver		Lead		Zinc	
Level	Tons	Au, G	Ag, G	Pb, Pct	Zn, Pct	Diff.	Cum.	Diff.	Cum.	Diff.	Cum.	Diff.	Cum.
11-12	10,493	0.82	339	11.0	20.8	5.7	100.	3.8	100.	3.8	100.	2.4	100.
12-13	60,496	0.44	240	8.2	22.1	17.6	94.3	15.6	96.6	16.6	96.2	14.6	97.6
13-14	91,431	0.31	199	6.2	20.7	18.5	76.7	18.8	80.6	18.8	79.6	20.9	83.0
14-15	88,422	0.31	201.5	6.0	19.4	18.5	58.2	20.4	61.8	18.3	60.8	19.2	62.1
15-16	80,343	0.31	195.5	6.6	17.9	16.4	39.7	16.4	41.4	17.8	42.5	15.6	42.9
16-17	71,993	0.29	185	6.0	18.6	13.3	23.3	13.7	25.0	13.7	24.7	14.1	27.3
17-18	41,522	0.25	160	5.3	17.6		10.0		11.3		11.0		13.2
18-19	28,157	0.21	160.1	4.5	19.4								

Table V. Recast of Table III

						Contents, Pct				Contents, Pct			
			Assays			Gold		Silver		Lead		Zinc	
Level	Tons	Au, G	Ag, G	Pb, Pct	Zn, Pct	Diff.	Cum.	Diff.	Cum.	Diff.	Cum.	Diff.	Cum.
7-8	9,905	1.33	381.1	14.7	18.5	2.7	100.0	1.6	100.0	1.5	100.	1.2	100.
8-9	39,855	1.11	454.6	14.3	19.5	9.3	97.3	7.6	98.4	5.9	98.5	5.2	98.8
9-10	84,080	0.86	355.6	13.3	17.9	14.4	88.0	12.1	90.8	11.2	92.6	9.9	93.6
10-11	144,125	0.69	310.5	13.7	17.1	20.4	73.6	18.3	78.7	20.1	81.4	16.6	83.7
11-12	109,781	0.45	265.8	12.4	16.9	10.3	53.2	12.2	60.4	14.1	61.3	12.7	67.1
12-13	96,744	0.44	210.1	9.4	16.9	8.8	42.9	8.4	48.2	9.3	47.2	11.0	54.4
13-14	110,544	0.42	216.3	9.9	16.1	9.5	34.1	9.8	39.8	11.2	37.9	12.0	43.4
14-15	152,110	0.52	241.1	9.2	16.5	16.0	24.6	14.8	30.0	14.0	26.7	16.6	31.4
15-16	131,430	0.38	339.0	11.8	19.3		8.6		15.2		12.7		14.8
16-17	5,927	0.27	184.3	4.6	19.9								

The map prepared by Dill, Fig. 5, is similar to one prepared by the writer in 1950, King's map having been used as a base in both cases. It will be seen that a prominent axis of horizontal flexure of the anticlines in the "kingdom" will pass through the Mazapil region, which thus becomes a prominent structural focus in an extremely large area of the Mexican geosyncline.

The Potrero and Noche Buena Camps occur in the western part of the La Caja range. In general, the Providencia Camp is near the curve of the northern leg into the base of the U. The Concepción del Oro Camp is in the base of the U. The La Laja Camp is at the swing of the base of the U into the southern leg, while the Santa Rosa Camp is west of the last and in the Santa Rosa range.

The Santa Rosa rhyolites to which Mr. Triplett refers, p. 586, were called by Burckhardt, following determinations by H. Rosenbusch, a highly altered porphyry which was not exactly determinable. The writer believes that is may represent a chilled facies of the monzonitic rocks.

The vertical beds referred to under Local Structure, p. 586, are necessarily seen in passing from the recumbent anticline to the subjacent recumbent syncline.

The occurrences at Noche Buena and San Francisco del Alto are another structural story, but the latter place is centrally located in the La Caja range and not far from a central synclinal flexure in the anticline.

"Shrinkage of the intrusives," see pp. 586-587, probably did not cause openings in the limestone beds; rather these were due to brecciation caused by small horizontal flexures. It seems likely to the writer that in the deeper levels the flexures broke to form the fractures, or veins, mentioned.

If on the maps of Fig. 7 a series of lines are drawn parallel to the sedimentary markers and contacts, it will be seen that many widely separated bodies are aligned. This indicates deposition in conjunction with favorable beds. The writer knows of several identifiable favorable beds in the Zuloaga limestone.

The writer believes that the facts presented under Zoning, p. 591, are a contribution of very great importance from all points of view, and he further believes that much credit should be given to Manager E. A. Manderfield for his constant and careful statistical work during the past 28 years. This collection is extraordinary, and Peñoles should be congratulated. Furthermore, it will be desirable to collect similar facts from many large mines, but with additional details such as the variations in contents of pyrite and other minerals.

For the two best-known and deepest orebodies the facts are noted in Tables II and III, which show tonnages between equally spaced levels, and the corresponding assays and metal ratios. These data have been drawn in rectilinear graphs. From the viewpoint of genesis the writer believes that it might be helpful to calculate the total contents of each metal and its vertical distribution from the bottom up.

When plotted ón rectilinear charts, Tables IV and V show almost straight and parallel lines; other methods of plotting would possibly be better. The greatest spread between gold and zinc is in the case of Table V, between Levels 13 and 10, lead and silver lying between them.

Table IV shows that the increments of gold are less than the others up to Level 13, and greater above. The increments of silver and lead are closely related, and they are relatively large between Levels 16 and 13. The increments of zinc are larger than the others up to Level 16, and between Levels 15 and 13.

Table V shows relatively large increments of gold up to Level 14, and between Levels 12 and 9. The increments of silver and lead are closely related, but they show relatively large increases between Levels 16 and 14, and between Levels 12 and 9. Increments of zinc materially exceed others up to Level 12, above which they are not much less than those of silver and lead.

The writer concurs with the author in the belief that the collection and study of similar data in many other cases will in the future be a great aid to an understanding of ore deposition and stabilities, and to predictions resulting therefrom.

The general map, Fig. 4, is similar to a part of one prepared by the writer in February 1950, which was widely circulated among mining persons and companies in the Mazapil region. One important correction should be noted. There is no lobe of intrusive at Potrero, and the eastern point of the intrusive does not extend so far to the east of Noche Buena. The northern and eastern parts of the boundary of the San Francisco del Alto-Noche Buena monzonitic intrusive should run as follows: from 9980 N-14,000 W to 9975 N-12,700 W, and thence southerly. The Cuesta del Cura-Indidura contact is at the Potrero Adit (19), the latter formation lying to the north.

It is important to emphasize that the sedimentary column compiled by the present writer, see Fig. 1, is still subject to use and checking lithologically. C. L. Rogers, U. S. Geological Survey, and his associates from Recursos Minerales who are studying phosphate occurrences are using a column about as follows:

Cretaceous	Caracol	Plus	1000 M	
	Indidura		180	(two members)
	Cuesta del Cura		270	
	La Peña		140	(two members)
	Cupido		300	
	Taraises		140	
Upper Jurassic	La Caja	Avg	100	
	Zuloaga	Plus	400	(six units)

It is even more important to note that the hiatus at the top of the upper Cretaceous is one of extensive time. It represents the Laramide Revolution during which the sediments were uplifted and lithified, and compressed and folded intensely. The uplifting permitted the fusion and welling up of those intrusive rocks which are now seen as monzonites. Erosion was probably continuous and intense. The Laramide Revolution probably began in the late upper Cretaceous and continued into the Eocene. It is interesting also to take into account some approximate secular times which have been reported as measured by radioactivity:

Appalachian Revolution	210,000,000 B.C.
End of Triassic	150,000,000
End of Cretaceous	60,000,000
Laramide Revolution	
Miocene	10,000,000

Successive disturbances of equilibrium produced openings through which flowed differentiates from the magmatic depths; from them successive stages of mineralizations were deposited. The writer believes that there were *zones* which developed mechanically outward from certain centers of resistance and reinforcement. He would also prefer to think of differences found in fairly uniform deposits, such as those at Providencia, as *segregations*.

Much careful work on collections and laboratory studies remains to be done before the several stages of mineralizations can be competently discussed. However, at the present time the writer believes that there were some seven stages of mineral aggregates deposited during the Laramide Revolution and that the principal stage found at Providencia was mesothermal and one of the last.

The much later andesitic and rhyolitic rocks of the Miocene, dikes at San Pedro de Ocampo as well as the volcanics noted, were followed by mineralizations which deposited siliceous-silver, siliceous-gold, and calcitic-gold ores. Still later disturbances in the Tertiary were probably responsible for the sparse and scattered deposition of minerals related to manganese, fluorite, mercury, antimony, barite, and various carbonates.

---

[9] Alfred Bergeat: La Granodiorita de Concepcion del Oro en el Estado de Zacatecas y sus Formaciones de Contacto. Bol. Inst. Geol. de Mexico (1910) No. 27, p. 109.

[10] Personal communication from C. L. Rogers, U.S. Geol. Survey.

Magnetic Roasting of Lean Ores

by Fred D. DeVaney

DURING the past few years a radically new process for the magnetic roasting of iron ores has been investigated and developed by Pickands Mather & Co. and the Erie Mining Co. in the Erie laboratory at Hibbing, Minn. This process, originally devised by Dr. P. H. Royster of Washington, D. C., involves the use of a roasting technique quite different from older methods. It has now been demonstrated that iron-bearing materials can be roasted as effectively as by any previously known method, and at a much lower cost.

The increasing shortage of highgrade iron ores in this country has accelerated the search for new methods that would permit low grade materials to be utilized. The concept of magnetically roasting low grade nonmagnetic ores such as the oxidized taconites and then separating such material magnetically has always had considerable appeal. The magnetic concentration idea is attractive because of the sharpness of the separations and cheapness of the method. Heretofore, however, the equipment and the processes available for the magnetizing-roasting step have left much to be desired. The customary equipment available for reduction roasting has been: 1—multiple hearth furnaces, 2—rotary kilns, and 3—shaft type kilns. In addition, it is understood that some work has been done in magnetically roasting fine ores by a process using the FluoSolids principle, but little information on this process is available. The multiple hearth kiln has been used the most but first costs and operating costs have been high because of low capacity, high maintenance, and poor gas utilization. Magnetic roasting can be done in a rotary kiln, but the radiation losses are high and the conversion to magnetite is usually unsatisfactory because of poor contact between the gases and the solids. Of the shaft-type furnaces, probably the most efficient yet developed is that designed by E. W. Davis of the Minnesota Mines Experiment Station. This furnace was operated at Cooley, Minn., during 1934-1937 but was abandoned in 1937 because the operation was uneconomic.

Heretofore the basic concept behind most magnetic roasting processes has been the idea of heating iron ore to a temperature of 800° to 1100°F in a strong reducing atmosphere, preferably either carbon monoxide or hydrogen. Temperatures under 800°F were undesirable since excessive roasting time was required. Temperatures over 1100°F were avoided because of the danger of converting part of the iron to ferrous oxide which is nonmagnetic.

In the new roasting process, the operation is carried on in a shaft furnace using a controlled atmosphere containing a low percentage of reducing gas. The temperature in the roasting zone is considerably higher than with the usual reducing gas and this speeds up the reduction time. Portions of the spent furnace gases are cooled and recirculated and this together with the good contact between ore and gas makes for high reducing gas utilization. High heat economy is secured by recuperating heat from the roasted ore by passing the cold reducing gases countercurrent to flow of ore. The heat transfer principle is similar to that employed in a pebble stove and to that used in the Erie Mining Co. furnace at Aurora, Minn., for pelletizing fine magnetite concentrates derived from taconite.

The theory of controlled atmosphere during the roasting operation can best be appreciated by inspecting the equilibrium diagram of the Fe-C-O system shown in Fig. 1. An inspection of this diagram shows that in certain areas magnetite, Fe_3O_4, is the only stable form of iron. A further inspection of this table shows that if the proper ratio is maintained between carbon dioxide to carbon monoxide, such a gas will be reducing with respect to hematite, Fe_2O_3, and will be oxidizing with respect to both ferrous oxide, FeO, and iron, Fe. It should be kept in mind that the formation of ferrous oxide in a roasting operation is harmful, since this oxide is nonmagnetic; if it forms in any quantity, it will cause substantial loss of iron in the ensuing magnetic separation step. If a ratio of approximately three parts carbon dioxide to one of carbon monoxide is maintained, the resulting operation can be carried on at a relatively high temperature without fear of over-reduction. Specifically, most of the tests in the Erie furnace have been made at a temperature of 1500° to 1600°F, with an entrant gas containing approximately 5 pct carbon monoxide and 15 pct carbon dioxide, with the remainder largely nitrogen. It should be remembered that the ratios of carbon monoxide to carbon dioxide shown in Fig. 1 hold even though the bulk of the gas is an inert gas such as nitrogen. It may surprise many to learn that a gas containing as low as 3 pct carbon monoxide, and 12 pct carbon dioxide with the remainder nitrogen is an extremely effective reducing gas in the 1000° to 1600°F temperature range. The reducing gas is not limited to carbon monoxide, and mixtures of hydrogen and carbon monoxide may be used effectively, provided that a similar ratio is maintained between the reducing gases and carbon dioxide and water vapor. For a more detailed explanation of the theory involved, the reader is referred to U. S. patents 2,528,552 and 2,528,553.

From a safety standpoint, the weak reducing gas used in the furnace offers an advantage. Its composition is such that it is well below the limits of explosion should air enter a hot furnace. This condition is not true with the usual reducing furnace, in which a gas rich in carbon monoxide or hydrogen is used.

The general furnace design and method of operation may best be understood by an inspection of

---

F. D. DEVANEY, Member AIME, is Chief Metallurgist, Pickands Mather & Co., Hibbing, Minn.

Discussion on this paper, TP 3414B, may be sent (2 copies) to AIME before January 31, 1953. Manuscript, March 20, 1952. New York Meeting, February 1952.

This page of Mining Transactions AIME follows p. 1084. The intervening non-Transactions pages appeared in Mining Engineering.

Figs. 2 and 3. Fig. 2 shows a cross-section of the magnetic roasting furnace system at Hibbing. This furnace is circular and has an ID of 2½ ft. It is capable of roasting from 1 to 1¼ long tons of iron ore per hr. In practice, the furnace is charged with crushed ore and is fed through either a double bell arrangement such as is used on blast furnaces or by the hopper-like device shown. The shaft of the furnace is filled completely with ore, which moves down the shaft as the material is discharged from the bottom. Basically, the furnace consists of an upper and lower stove with a middle chamber in between. A mixing chamber and combustion chamber are also provided. An optional furnace design is to have two stoves in parallel and operate them intermittently, as in the manner of a pebble heater. Since two stoves are superimposed one upon the other in the present installation, it is called a tandem furnace. In the upper stove, the cold moist ore is heated up to the desired temperature by uprising gases. The gases are of such composition, to be discussed later, that the descending ore is reduced and the iron oxides converted to magnetite. Ore from the upper chamber travels through the middle zone of the furnace where the area of discharge into the lower stove may be restricted. Weak reducing gas is blown up through the lower stove, cooling the hot descending roasted ore. The purpose of the middle stove is to make it easier for gases from the lower stove to pass through the combustion chamber than to travel up through the central part of the shaft. Because of the lesser resistance to the flow of gas to and through the combustion chamber, a greater portion of the gas follows such a path, and in the mixing chamber these gases are brought up to the desired temperature by a mixture of gases from the combustion chamber. A separate combustion chamber is provided so that the fuel added can be burned completely with little or no excess of oxygen. It is very desirable that the amount of air to be used for combustion be held to a minimum since an excess would tend to cause combustion of the gases used for reduction. As usually operated, the temperatures of the gas leaving the mixing chamber are held at 1500° to 1600°F. This heated gas passes up through the ore and comes off the top of the furnace at a temperature of 180° to 300°F. The ore is discharged from the bottom of the furnace at a temperature of 150° to 250°F. With some ores, it is desirable to water-quench this material to prevent oxidation.

The gases blown through the furnace serve a twofold purpose, to reduce the iron oxides and also to act as a carrier gas or heat exchange media. For a carrier gas, the amounts must be closely regulated so that sufficient cooling gas is supplied at the bottom of the furnace to abstract the heat from the discharged ore. Likewise, the volume of heated gas must be such that it supplies the necessary heat to the raw ore fed to the furnace. This amount of carrier gas can be calculated readily from the specific heats of the gases and ore, and in operation the amount so blown conforms closely to the theoretical. The amount of gas blown is usually from 10 to 12 cu ft per lb of ore roasted. To obtain a suitable amount of carrier gas of the proper analysis and to secure reducing gas efficiency, a major portion of the exit gases from the top of the furnace is scrubbed and cooled and then recirculated. The amount of gas wasted from the top of the furnace is equal only to the products of combustion from burning the oil or gas necessary to supply heat for the process in addition to water vapor coming from the ore. In the Hibbing furnace, reducing gas is produced in a slagging-type gas producer. This gas has a composition of approximately 34 pct carbon monoxide, 1.8 pct hydrogen, 0.6 pct carbon dioxide, 0.4 pct water, and 62 pct nitrogen. It has been found that an efficient roasting procedure can be achieved if the carrier gas entering the bottom of the furnace contains 6 pct carbon monoxide. This carrier gas is made up of the spent exit gas from the top of the furnace, which will normally carry from 1½ to 3 pct carbon monoxide and an amount of new gas from the gas producer to bring the average to 6 pct carbon monoxide. The composition of this gas is easily set and maintained by means of a combustible gas recorder and by instrument-actuated valves. The combustible gas indicator analyzes the gases continuously, and through interlocking controls varies the amount of rich gas admitted to the system to hold the gas composition constant.

The basic reducing reaction that takes place in the roasting zone is: $3Fe_2O_3 + CO$ to $2Fe_3O_4 + CO_2$.

This reaction is exothermic and liberates 88 Btu's per pound of magnetite formed. This heat is liberated in the upper stove and contributes substantially to the heat economy of the system. The mass of ore in the constricted area in the middle stove serves a useful purpose other than a heat recuperator in that it insures that a greater portion of the gas from the lower stove will pass through the mixing chamber and be brought up to the desired temperature. This permits a close control of the temperatures in the roasting zone. The control temperature of the operation is the temperature of the gases leaving the mixing chamber. The maximum temperature in the furnace, however, is in the upper stove about a foot down from the stockline where much of the heat of reaction is liberated. The peak temperature at this point is usually 150°F higher than the control temperature. This peak temperature can be indirectly controlled by adjusting the control temperature in the mixing chamber by varying the amount of fuel burned. By use of the carrier gas principle and the burning of fuel in a combustion chamber, the temperature in any part of the furnace can be held constant within 20°F. This insures optimum roasting conditions.

Fig. 3 is a schematic drawing of the furnace and of the auxiliary equipment. The gas at Hibbing is

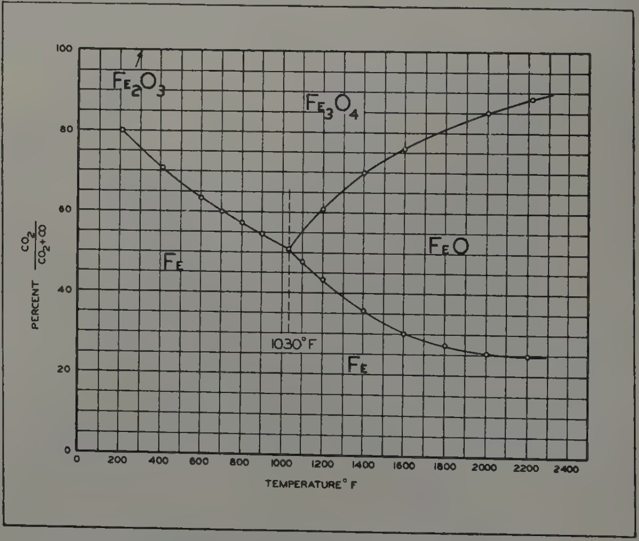

Fig. 1—Equilibrium diagram, ternary system Fe-C-O.

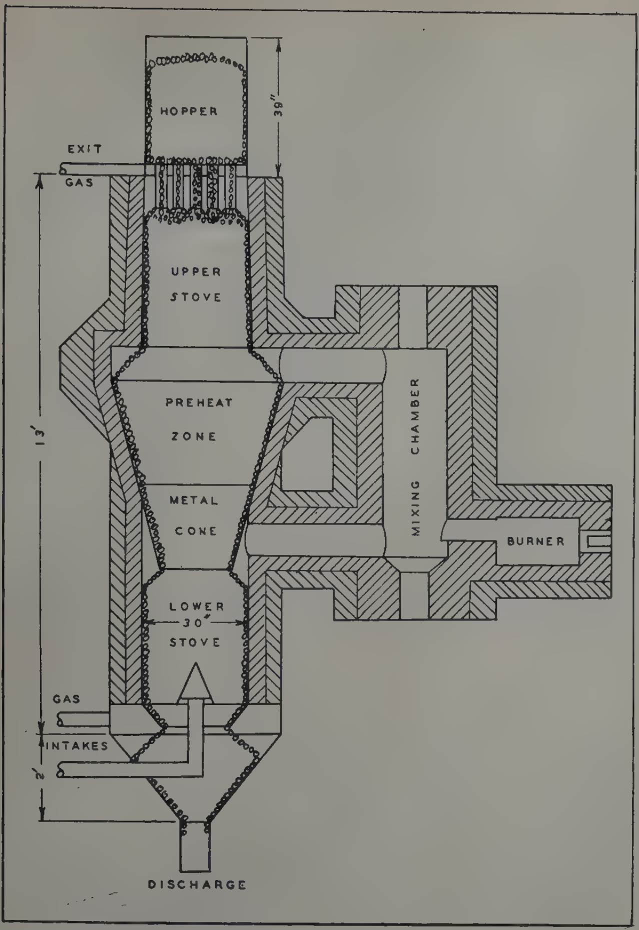

Fig. 2—Tandem magnetic roasting system.

supplied by a slagging-type gas producer, D. This gas, after being cooled and scrubbed, C, joins with a portion of the exit gases from the furnace and is compressed in a blower, E, and blown into the bottom of the furnace, A. The amount blown is adjusted to the feed rate to the furnace. The heat to the system is supplied by burning oil or gas in a Dutch oven, H. Air for the combustion of this fuel is furnished in stoichiometric quantity by blower, G. An amount of exit gas is vented equal to the volume of gas formed by burning fuel and water vapor from the ore. The entire system is under pressure and the amount vented takes care of itself automatically if the vent is made small enough so that there is a positive pressure at this point. The remainder of the top gas is scrubbed and cooled in the scrubber, C, and then joins gas from the gas producer.

During the past five years, in the development of the process, many low grade iron ores from the Lake Superior district have been roasted. Such materials as oxidized taconite and low grade ores from the Minnesota, Wisconsin, and Michigan ranges have been tested. In general, the optimum roasting technique, as far as temperature of roast and gas composition are concerned, is similar for all. However, structural differences such as density, porosity, and distribution of fines have a great effect on the roasting operation.

For purposes of illustration, a typical test on an oxidized Minnesota taconite will be reported in detail. The ore used was a banded oxidized taconite from the lower cherty horizon in the Hibbing area. The iron content was 29.64 pct. Hematite was the predominant iron mineral. The amount of magnetite in the crude ore was small, and the recovery by magnetic concentration alone on a finely ground sample was less than 3 pct. The ore was crushed to pass a 1-in. sq opening, and this was fed to the furnace without screening. Screening at 8 mesh is required on ores that contain many fines, but many of the oxidized taconites can be crushed and few fines formed. The rate of feed to the furnace was 1 long ton per hr on a dry basis. The feed rate is set by adjusting the variable discharge mechanism at the bottom of the furnace to discharge at a given rate and by keeping the hopper at the top of the furnace full. For this test, the amount of carbon monoxide in the entrant gas was set at 6 pct. This setting is made on the Bailey combustible meter, and the meter continuously analyzes the gas going to the bottom of the furnace and actuates a valve from the new gas supply so that the gas composition is kept constant. The same meter continuously measures and records the amount of combustibles in the gases at the top of the furnace.

The amount of carrier gas blown is calculated from the feed rate, which was 2240 lb per hr, or 37.4 lb per min. The amount of carrier gas required was from 10 to 12 cu ft per lb of ore. The initial amount of gas blown was 410 cu ft per min, but it was found that to maintain the best operating conditions it was necessary to increase the gas to 450 cu ft per min, or 12 cu ft per lb of ore. The volume is varied by adjusting a valve between the blower, E, in Fig. 3 and the bottom of the furnace. The rate of blow determines the position of the heat line in the upper stove and also the temperature of the discharged ore. It should be remembered that the heat line in the upper stove is determined by the rate at which the ore descends and the heat wave rises. When in balance, the heat line is static. If the rate of blow is excessive, the heat line will be close to the stock line, the exit gas will be hot, and heat will be wasted in the exit gases. If the rate of blow is too low, there will be an inadequate quantity of carrier gas to take the heat from the ore being discharged and heat will be lost in the ore discharge. This is also undesirable because, if ore is discharged too hot, oxidation of the roasted ore may occur. The

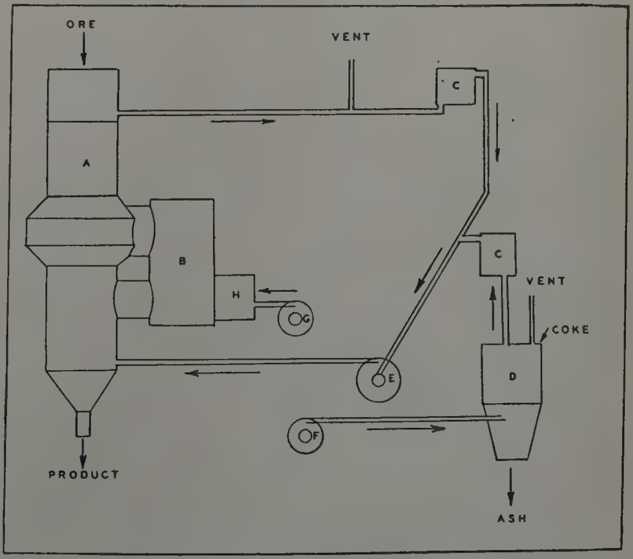

Fig. 3—Ore roasting circuit. The key letters on the figure refer to the following:

A.	Tandem furnace.	E.	Multistage blower.
B.	Mixing chamber.	F.	Positive displacement blower.
C.	Gas scrubbers.	G.	Positive displacement blower.
D.	Gas producer.	H.	Combustion chamber.

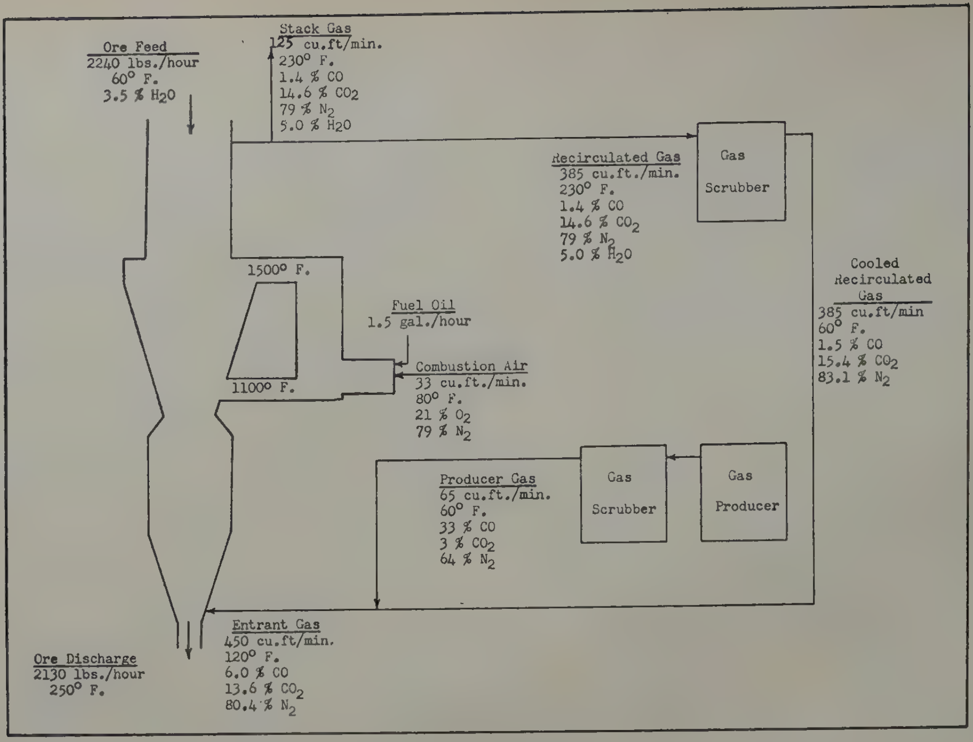

Fig. 4—Diagram showing gas flow, temperature, and composition. Note: All volumes at standard conditions.

position of the heat line is readily controlled manually by varying the rate of blow so that the temperature of the exit gases at the top furnace is held at an optimum. This can also be controlled closely by instruments which regulate the rate of blow so that the exit gases are held within narrow temperature limits. In the example cited, the temperature of the gases leaving the mixing chamber was held at 1500°F. This heat was secured by burning oil with closely controlled quantities of air in a small combustion chamber. After the furnace had reached a state of balance, the amount of oil required was found to be 1.50 gal per hr, or 1.50 gal per long ton of ore roasted. The amount of carbon monoxide required to reduce a pound of iron in the form of hematite to magnetite is 1.12 cu ft. In the example given, 65 cfm of producer gas containing 33 pct carbon monoxide was used per min. Of this amount 8.4 pct was wasted with the exit gases, 59 pct was used to reduce the ore, and because of air leakages 32.6 pct of the gas was burned in the furnace. The gas burned, which has a heating value of 100 Btu per cu ft, contributed a total of 126,600 Btu per hr to the system. The total heat supplied to the roasting operation, from the burning of oil and a portion of the reducing gas, was 327,000 Btu per hr or 327,000 Btu per long ton of ore roasted. In a properly designed large furnace with good insulation the heat requirements for roasting a similar ore should not exceed 200,000 Btu per long ton.

This low fuel consumption is made possible because of the excellent recovery of heat from the roasted ore by the carrier gases coming up through the lower stove. An 1100°F preheat of this carrier gas is secured, and the only additional heat that need be supplied is an increase of temperature to 1500°F. A peak temperature of 1637°F was reached about 18 in. down from the stock line in the upper stove where the exothermic reaction of hematite to magnetite takes place.

Most of the pertinent data for this test, relative to feed rates, gas volumes, gas analyses, and furnace temperatures, are shown graphically in Fig. 4.

After the ore was roasted, magnetic concentration tests were made on ore ground to 150 mesh. This fine grinding was required on this particular ore to give sufficient liberation to make acceptable grade concentrates. These results are shown in Table I, where it may be noted that a weight recovery of 43.77 pct was made of a concentrate having a grade of 63.25 pct iron and 7.56 pct silica.

The overall iron unit recovery was 90.63 pct. It should be remarked in passing that the magnetic roasting step, in addition to putting the ore into a form that can be readily and cheaply concentrated, usually makes it much more amenable to grinding. The power required to grind a roasted taconite is about half that needed to grind unroasted taconite.

The physical characteristic of the ore to be roasted greatly affects its preparation for roasting. Some porous ores need be crushed to only 2 in. and a good roast can be secured. Other dense ores require crushing to ⅜ in. to secure good penetration of the reducing gas, or the roasting time must be increased. In general, a decrease in feed size is more effective than an increase in roasting time. The amount of fines in the ore to be roasted is very important, as the fines greatly affect the resistance to the flow of gas. An increase in fines increases the pressure the furnace blower must operate against, and thereby increases the horsepower requirements. The

Table I. Magnetic Concentration Test on Roasted Taconite Ground to 150 Mesh

Product	Wt, Pct	Iron	Silica	Total Iron, Pct
Crude ore		29.64		
Roasted ore	100.00	30.54		100.00
Magnetic concentrate	43.77	63.25	7.56	90.63
Nonmagnetic tailing	56.23	5.08		9.37

amount of —10 mesh material that can be tolerated is about 20 pct. Without question, the furnace works best on a charge containing no —10 mesh material. With such a charge, the power requirements are minimum and heat transfer is more uniform.

With unscreened material, dust collectors must be provided in the flues between the lower stove and the mixing chamber, or at the bottom of the mixing chamber itself. The temperature of both these points is well below the fusion point of any of the ore constituents, so that there are no slagging problems.

With most ores, the solution of the fines problem is to screen and then briquette the fines with a cheap binder, such as waste sulphite liquor, and charge these briquettes into the furnace with the coarse material. Such briquettes hold together well during the roasting operation and are sufficiently porous so that the conversion to magnetite is excellent. An alternative method applicable to some ores is simply to roll the fines in a balling drum and charge the balled fines into the furnace with coarse material.

The furnace may be used for purposes other than the magnetic roasting of iron ores. It may be used for reduction roasting of nickel, manganese, and other ores by varying the temperature of the roast and the gas composition to suit the particular application. This has been checked on several ores.

The capacity of the furnace on iron ores is from 5 to 6 long tons per sq ft of shaft area per 24-hr day. The mechanical maintenance on the furnace is low, as there are no moving parts in the furnace. The feeder and the discharge mechanism are both outside the furnace. Radiation losses can be held to a minimum because of the ease with which a shaft furnace can be insulated. The utilization of reducing gases and roasting efficiency both are excellent. Labor requirements are small, as feeding and discharging the furnace is done mechanically. Metallurgical control is taken care of by instruments which hold the temperature of the furnace, the rate of blow, and the composition of the gases within close limits. In conclusion, it may be said that the tandem furnace offers an entirely new approach to the reduction roasting of ores, particularly iron ores, and the results of extended tests on a 1 ton per hr furnace justify the statement that with this furnace reducing roasting can now be done cheaply and effectively.

The Effect of Heat Treatment and Certain Additives On the Strength of Fired Magnetite Pellets

by Strathmore R. B. Cooke and William F. Stowasser, Jr.

The most important factor responsible for the development of strength in fired magnetite pellets containing no additive is the oxidation of the magnetite to hematite and the subsequent recrystallization and grain-growth of this constituent. In the laboratory, pellets having the highest strength and the greatest uniformity of structure were obtained by oxidation at a relatively low temperature and firing between 1300° and 1400°C. Effects of a number of inorganic additives are also reported.

RESULTS presented in a previous paper[1] have shown that the strength of fired pellets made from eastern Mesabi magnetite concentrates containing 8 to 9 pct SiO_2 as quartz and silicates is due to several processes which occur during firing. These are: 1—recrystallization and cementation of the fragmented magnetite grains; 2—formation of slag from reaction between the quartz, silicates, and available ferrous iron, followed by slag-bonding of the magnetite grains; and 3—oxidation of the magnetite to hematite and subsequent recrystallization and grain growth of this constituent.

Microscopic examination of all magnetite pellets fired in one operation in small and large-scale pilot plant furnaces and possessing normal strengths shows that the processes 1, 2, and 3 have taken place; where strengths are low and the pellets are otherwise subnormal, one or more of the processes has not occurred. For example, soft and friable *red* pellets may contain a central core of slag-bonded recrystallized magnetite which is strong enough in itself, but the shell contains only slightly recrystallized hematite, indicating that the maximum temperature reached was too low.

Processes 1 and 2 can occur only under reducing conditions, as for example, when coal is intentionally added to the original pellets; under neutral conditions, when pellets are fired in an inert atmosphere; or when pellets are brought so rapidly to temperature in an oxidizing atmosphere that oxygen diffusion to the core lags behind the recrystallization and slagging effects. This last-mentioned process has occurred in all pilot-plant shaft fur-

---

S. R. B. COOKE, Member AIME, is Professor of Metallurgy and Mineral Dressing, School of Mines and Metallurgy, University of Minnesota, Minneapolis. W. F. STOWASSER, JR., Junior Member AIME, is with Allis-Chalmers Manufacturing Co., Milwaukee.

Discussion on this paper, TP 3429B, may be sent (2 copies) to AIME before January 31, 1953. Manuscript, Dec. 26, 1951. New York Meeting, February 1952.

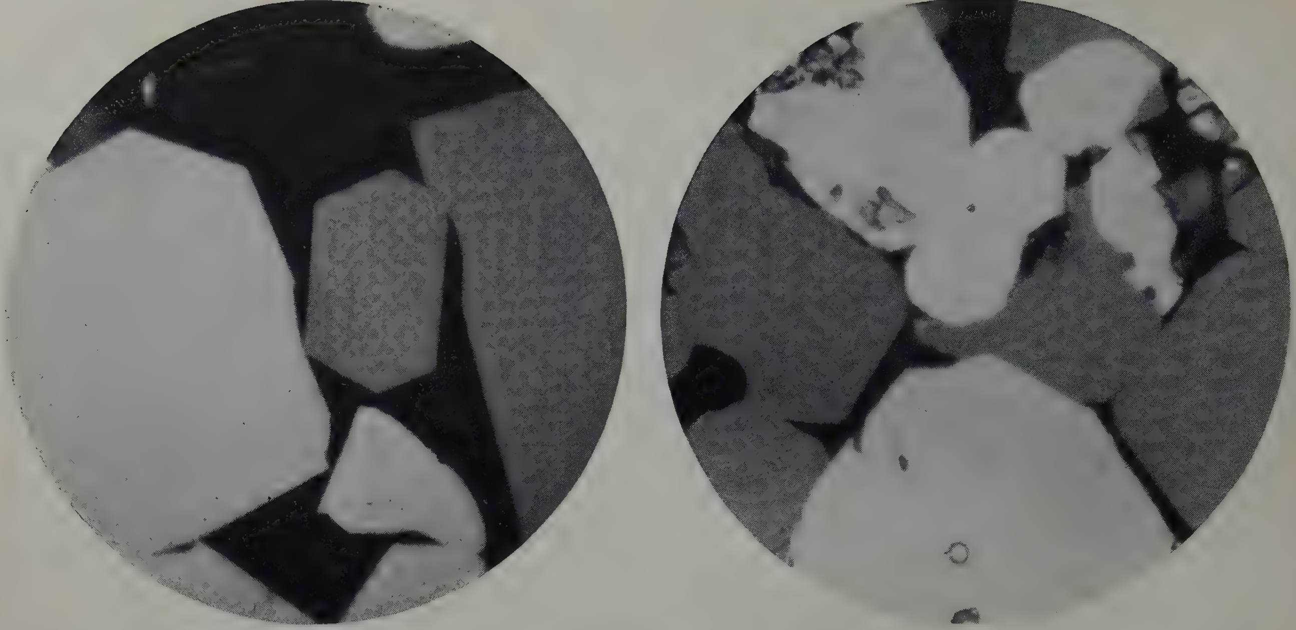

Fig. 1 (Left)—Idiomorphic grains of magnetite (grey) and subhedral hematite in a pellet containing added lime and fired at 1400°C. X1770. Fig. 2 (Right)—Partial conversion of hematite to magnetite in a pre-oxidized pellet fired at 1400°C. X1770.

nace products which the writers have examined, even though oxidation during the heat-exchanging operation subsequent to firing may have removed all but insignificant quantities of magnetite. Hematite concentrates which have been balled with an addition of coal and fired in an oxidizing atmosphere cannot be differentiated structurally or mineralogically from similarly fired magnetite pellets containing no coal.

Factors Responsible for the Development of Strength in Fired Magnetite Pellets

It seems easy to account for the cold strength of a fired pellet when slag has been formed. Prior to firing, a pellet consists of a heterogeneous mass of pores, magnetite, and quartz bonded by relatively weak surface forces. In a substantially neutral atmosphere and at sufficiently high temperature, silicate slag forms in which the magnetite seems to have appreciable but undetermined solubility. The slag wets the solid magnetite and upon cooling functions as a reasonably strong adhesive between the magnetite grains. Strength is further increased by the consolidation of the interstitial pores into a few large holes, so that a much greater surface of the solid constituents is in contact.

On the other hand, it is more difficult to explain the apparently beneficial effect that recrystallization and grain growth of the iron oxides contribute to pellet strength. With both magnetite and hematite there appears to be very considerable mobility at moderate temperatures. In the case of magnetite and just below temperatures at which slag begins to form, small grains are absorbed into larger ones, and a network of this constituent readily develops throughout the pellet. There is a concomitant increase in pellet strength. At higher temperatures growth of the magnetite is accelerated, and provided that there is an appreciable amount of slag, idiomorphic crystals of magnetite appear, see Fig. 1. With only small amounts of slag the crystals are subhedral to anhedral, with much greater areas of contact between neighboring grains. Accompanying the development of idiomorphic magnetite there is a marked decrease in strength of the pellet. It seems that magnetite-to-magnetite bonding is stronger than magnetite-to-slag bonding, and that slag is the weakest constituent developed in pellets. This statement should not be interpreted to mean that slag formation is always undesirable, for the cold strength of a slag-bonded pellet can be higher than that of one in which slag bonding and recrystallization of the metallic oxides is absent. Furthermore, the strength of slag should be increased by the keying action of numbers of idiomorphic grains of magnetite.

Process 3 occurs in normal pelletizing sequence, and cognizant of its importance in heat economy, the writers are also beginning to realize its physical importance in the production of pellets. First, oxidation of magnetite commences below 600°C, so that a relatively tough shell is formed on all pellets before much load comes on to the bed, and deformation of the pellets and consequent extrusion of the viscous cores is prevented when slagging temperatures are reached. Secondly, the freshly-formed hematite does not combine or slag with silica or silicates, so that there is no deformation of pellet shape even at relatively high temperatures, and adhesion between adjacent pellets is normally nonexistent. Above 1300°C, however, significant amounts of hematite transform to magnetite, see Fig. 2, permitting formation of a sticky fayalite slag or of an eutectic between magnetite, silica, and silicates. It is probable that some of the not infrequent formation of lumps of agglomerated pellets in zones of localized and excessive temperature in pelletizing furnaces is due to this thermal decomposition of hematite, although much is due to the extrusion of liquid matrix from broken balls. Thirdly, the higher the firing temperature, the coarser the grain size of the hematite. During the oxidation of magnetite pellets the hematite is formed from the magnetite by a process of grain refinement. There is no physical disintegration, but as certain crystallographic directions within any one magnetite crystal are preferentially oxidized, a single crystal

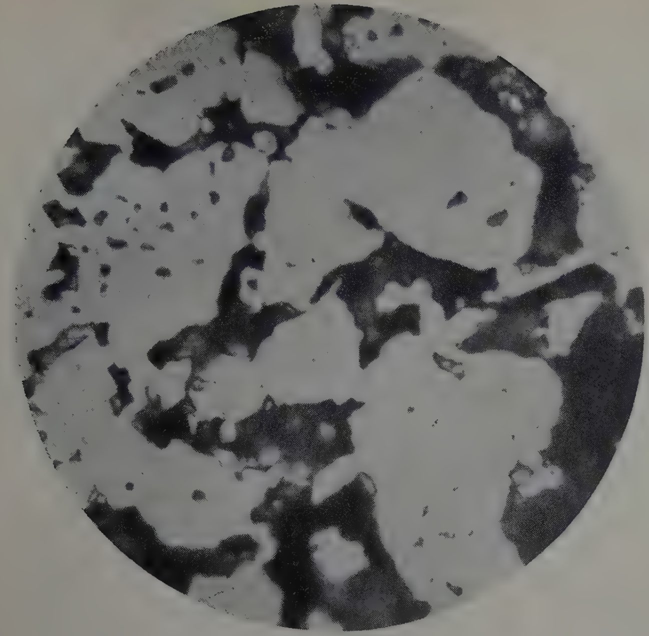

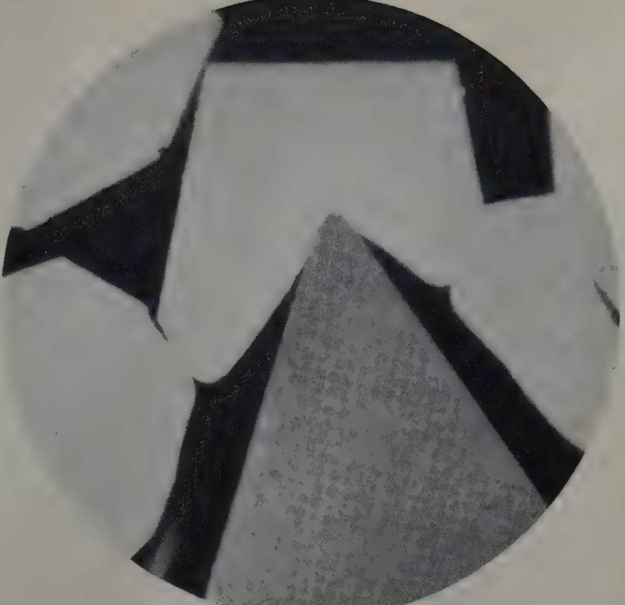

Fig. 3 (Left)—Disappearance of fine hematite to form a network of equiaxed grains. Pellet fired at 1200°C for 30 min in air. X750. Fig. 4 (Right)—Portion of a large magnetite grain (grey) and idiomorphic hematite. This pellet contained added lime and was fired at 1300°C after oxidizing at 800°C. X1770.

of magnetite eventually becomes a number of independently oriented grains of hematite.

At temperatures around 500° or 600°C the resulting structure is relatively stable, and prolonged heating does not change the orientation or size of the hematite grains. At higher temperatures, however, the hematite grains commence to grow, and what was originally a single crystal of magnetite becomes a single crystal of hematite. Just as grain growth occurs within a grain of this type, so also does grain growth occur throughout the mass of the pellet, the small grains being absorbed by the larger, until a network of equiaxed hematite grains is established throughout the pellet, see Fig. 3. With the coarsening of the grain size, there is a concomitant increase in strength. Because no slag is formed below 1300°C, there can be no transfer of iron atoms through a second constituent, and hematite grain growth below that temperature is dependent only upon the mobility of the iron atoms in that mineral. That the mobility is a real phenomenon is substantiated by carefully controlled laboratory experiments in which magnetite pellets have developed an outer coating of needle-like and radially directed hematite crystals between 1 and 2 mm in length.

The structure developed within the pellet by these mechanisms is analogous to that developed by magnetite in a neutral atmosphere, and the strength of the pellet increases greatly to a maximum at about 1300°C. Between 1300° and 1400°C, however, the quartz and silicate grains which have hitherto preserved their individuality disappear and form slag.

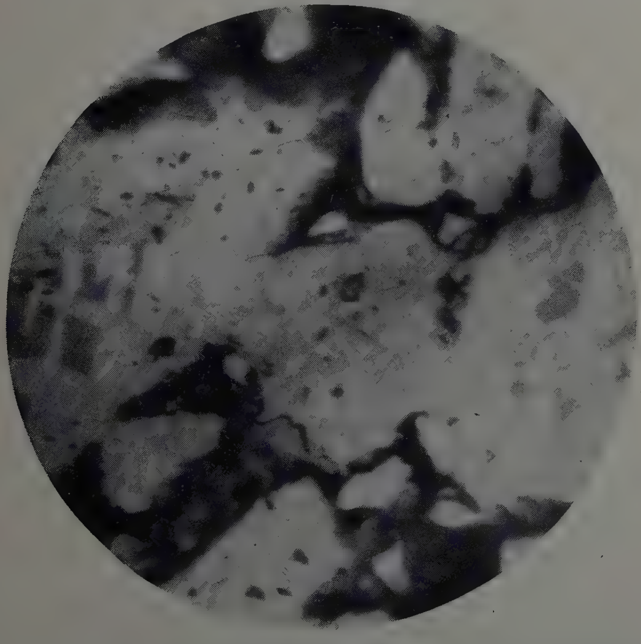

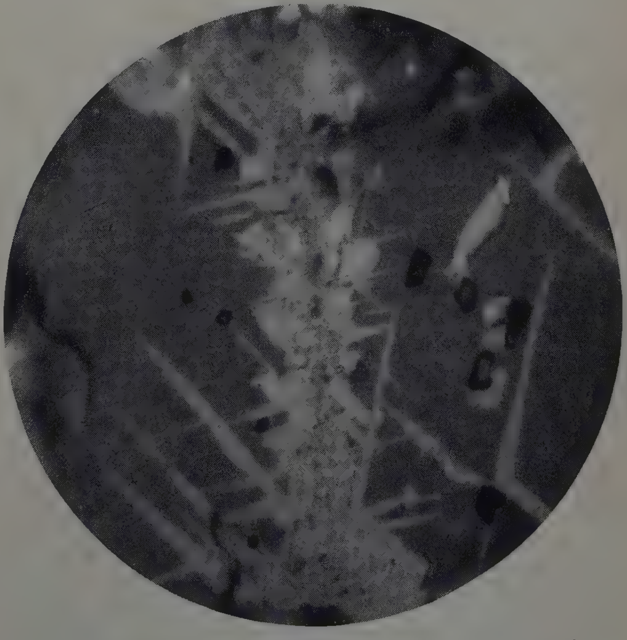

Fig. 5 (Left)—Cementation of three neighboring grains obtained by heating a magnetite pellet to 800°C in air. The same phenomenon, although less pronounced, can be observed in pellets oxidized at 600°C. X2000. Fig. 6 (Right)—Line of cementation between two magnetite blocks clamped together, heated to 800°C in air for 2 hr, and subsequently furnace-cooled. X2000.

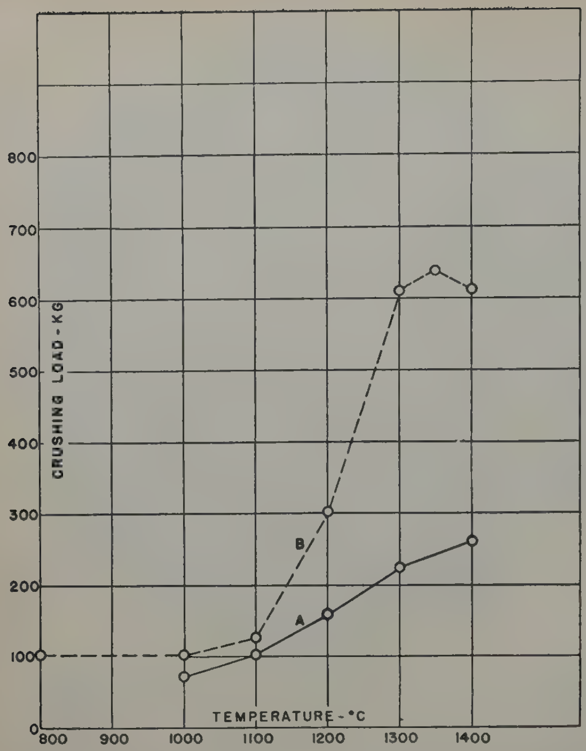

Fig. 7—Cold strength vs firing temperatures for magnetite pellets without additives. Curve A represents strength of single fired pellets and Curve B strength of pellets pre-fired at 800°C in air, 2 hr, and refired at temperatures indicated.

At the same time the continuous hematite network breaks up, and large, idiomorphic, and disconnected crystals of hematite and magnetite appear, see Fig. 4. A decrease in pellet strength accompanies this change. The strongest pellets made from magnetite are those in which there is a continuous network of coarsely crystalline hematite in a matrix of unaltered quartz grains, with a very small quantity of interstitial slag interlocked with the hematite.

Previous work[1] has shown that at firing temperatures between 300° and 1000°C magnetite pellets, compared with identical pellets fired in a neutral atmosphere, are superior in strength if they are fired in air. The strength appears to be due to cementation of contiguous oxide grains at the instant of oxidation, the iron atoms at that time having such high mobility during the lattice transformation that free exchange and rearrangement is possible. Once cementation is effected, further transfer occurs in the normal process of grain growth, the larger areas of crystal contact giving an overall increase in pellet strength. Microscopically, this initial cementation can be observed at temperatures as low as 600°C, see Fig. 5. It will be noted from the photomicrograph that the orientation of adjacent grains which have bridged is different, thus removing the condition of like crystallographic orientation of the original magnetite grains as a requirement for cementation.

A simple experiment illustrates this cementation during oxidation. Two small blocks of coarsely crystalline magnetite were cut and ground to flat surfaces. The blocks were placed with their plane surfaces in contact and held together under considerable pressure with a screw clamp, the area of surface contact being approximately ½ sq in. The assembly was heated in air for 2 hr at 800°C and then furnace-cooled. The magnetite blocks adhered to each other when removed from the clamp and were sectioned across their plane of contact and polished. Fig. 6 shows the contact area. Obviously air has had access to the faces in contact, but oxidation within the mass of the blocks was minor. It is noteworthy that hematite blocks and crystals subjected to the same treatment do not cement together, and likewise individual grains of magnetite resting loosely in contact with each other do not cement when heated to the same temperature. From these experiments it is concluded, first, that oxidation of magnetite to hematite results in a temporary state of disorganization with accompanying enhanced mobility of iron atoms so that particle-to-particle bridging occurs, and, secondly, that high unit pressures are required to make the bridging process effective.

There is a further and most important gain from oxidizing the pellet throughout at moderate temperatures, at least to the extent of forming a superficial layer of hematite on all magnetite grains, before firing at high temperatures. The pellets resulting from this double firing procedure are very homogeneous, for on testing for strength they break in two to four pieces without the production of fines. In contrast, a pellet fired directly at high temperature and without pre-oxidation possesses a duplex structure in which the core has shrunk from the shell, and fractures, upon breaking, into pieces and fines.

In the earlier work by Cooke and Ban[1] eastern Mesabi magnetite pellets approximately ¾ in. in

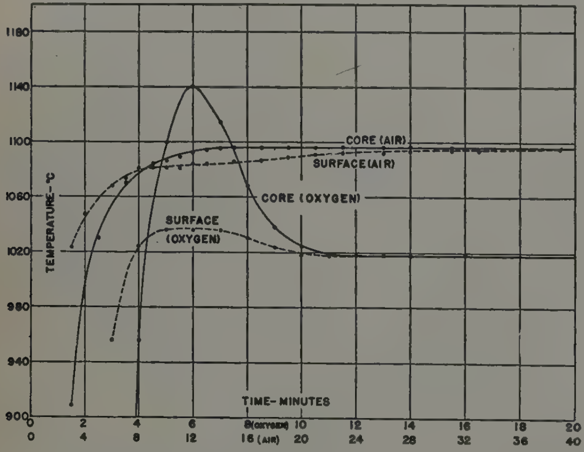

Fig. 8—Temperature differential between surface and core of eastern Mesabi magnetite concentrate pellets fired in air, 5 cu cm per min per g, and in oxygen.

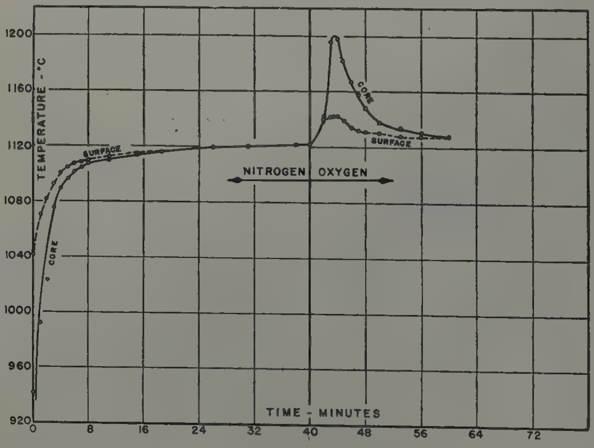

Fig. 9—Time-temperature relationship during heating of a magnetite pellet in nitrogen and subsequent oxidation.

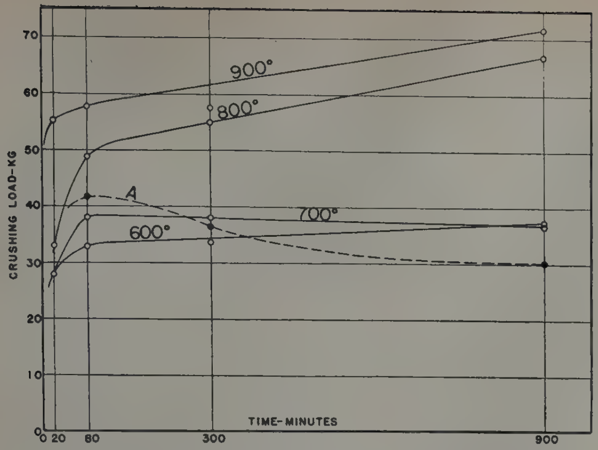

Fig. 10—Strength-time isotherms for ferric oxide pellets heated in air.

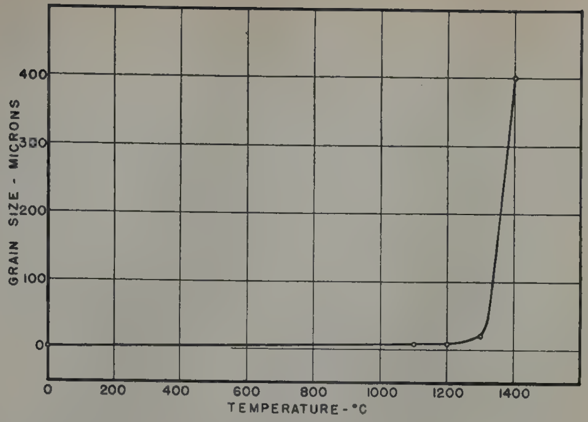

Fig. 11—Grain size-temperature curve for ferric oxide.

diam were heated in air at 700°C for 30 min. After cooling, the pellets were then re-fired in air at various temperatures up to 1200°C, higher temperatures being unattainable with the equipment then available. There was no particular virtue in cooling before re-firing except that the step facilitated laboratory procedure.

Since then the double firing experiments have been performed on identical pellets to a maximum temperature of 1400°C, in a muffle furnace, however, instead of the original tube furnace.

The cycle of heat treatment consisted in heating dried pellets for 2 hr in air at 800°C to obtain at least superficial oxidation of all magnetite particles through to the centers of the pellets. The pellets were then cooled, and subsequently batches were reheated for 30 min at 100° intervals from 1000° to 1400°C. These double-fired pellets were then tested for strength at room temperature. Since the Amsler machine had a limiting compressive load of 300 kg, the higher strength pellets were tested on an hydraulic compression machine.

Microscopic examination of the pellets treated at 800°C showed the oxidation to extend uniformly to the centers. Slime magnetite was completely oxidized, but the larger grains of magnetite were incompletely transformed to hematite. The strength of the pellets was 102.2 kg.

Double firing did not change the strength at 1000°C, but this increased at successively higher temperatures to a maximum, at 1350°C, at which temperature the cold strength was 637.8 kg. At 1400°C the strength decreased to 612.5 kg, see curve B, Fig. 7.

In contrast to these results, identical pellets fired in a single stage to the indicated temperature, i.e., without the pre-firing stage at 800°C, gave a maximum cold strength of only 260 kg at 1400°C, see curve A, Fig. 7.

Pellets fired in pilot-plant furnaces all possess a shell produced by a process analogous to double-firing. As the cold pellet is heated, a wave of oxidation proceeds into the pellet, and initial cementation takes place in the shell. Because of the heat liberated by the strongly exothermic reaction and the decrease in permeability effected by the cementation, after a short period diffusion of oxygen lags behind heat transfer, with the result that the cores are slagged and magnetite is recrystallized before complete oxidation of the pellet occurs. Normally this gives an undesirable duplex structure. Occasionally, however, conditions arise in pilot-plant furnaces which are not well understood, and so-called *blue* pellets are produced in which there is no megascopic appearance of a duplex structure. However, microscopic examination of polished sections of such pellets always shows that slagging of the siliceous constituents and recrystallization of the magnetite has occurred in the centers, the magnetite eventually having been oxidized to hematite. These blue pellets are rated the best by practical operators.

Thermal Differentials in Pellets During Firing

Much discussion has centered about the magnitude of the temperature differential between core and shell of a pellet during firing. Because pellets occasionally cracked during furnace firing and extruded a more or less liquid mass, it has been assumed that core temperatures are considerably above shell temperatures. Actually, under the oxidizing conditions prevailing in a pilot-plant furnace, the cores possess a lower melting point than the already oxidized shells, and the above argument loses a good deal of its weight.

Ban[2] has shown that during firing the core temperature of magnetite pellets rises above the temperature of the surface. This is true for pellets both with and without included coal, although the temperature differential is greater when coal is present. Fig. 8 shows the measured temperatures of the cores and surfaces of coal-free pellets fired in air and oxygen respectively. For example, the surface temperature of a ¾-in. pellet charged into the 1020°C zone of an electric furnace through which oxygen was passing required 4 min to reach furnace temperature. Both core and surface temperatures then rose to maxima after a total of 6 min in the furnace, when they were respectively 120° and 15° above furnace temperature. Both then dropped to furnace temperature after about 11 min total firing time. A pellet fired in air at somewhat higher furnace temperature than in the last example also exhibited a temperature gradient between core and surface, with a smaller differential, 10°, than with oxygen, 104°. Peak and furnace temperatures were reached after 21 and 40 min, respectively.

Fig. 9 shows the effect of bringing a pellet up to furnace temperature in an inert atmosphere and then admitting oxygen. In nitrogen the core lags behind the surface temperature until equilibrium is reached; then with admission of oxygen both core and surface exceed the furnace temperature, although the gain in both cases is less than when the pellet is inserted directly into oxygen, and the differential is only 56°. Presumably this last is due to a slower rate of magnetite oxidation, brought about by the recrystallization of that mineral in the nitrogen and also by the lowered permeability effected by slag formation. It seems probable that the temperature differential existing in pilot-plant furnaces is closer to that shown by the air-fired pellet of Fig. 8 than by the pellet fired in oxygen, first because the pellets are brought to temperature more slowly in practice, and second, because partial pressure of oxygen in furnace gases is probably not very different from that employed in this laboratory experiment.

The Effects of Heat Treatment and of Additives on Ferric Oxide

Since the foregoing discussion indicates that the recrystallization and grain growth of hematite is one of the controlling factors in the formation of a strong pellet, an investigation was made to determine the effects of temperature and of selected addition agents on the behavior of this mineral. The initial experiments employed chemical grade ferric oxide, but a closer approach to the practical aspect consisted of an investigation of the combined effects of additives and heat treatment on pellets prepared from the same magnetite concentrates used previously. The selection of the additives was dictated in part by the results obtained with the ferric oxide and in part by a consideration of the requirements of economics and of the reduction process to which the pellets would eventually be subjected.

The material used was Baker's analyzed ferric oxide. Particle size was fairly uniform, averaging 0.8 μ. The material contained 99.704 pct Fe_2O_3, 0.170 pct SiO_2, 0.050 pct SO_4, 0.040 pct Mn, and minor amounts, 0.010 or less, of Cu, Zn, NO_3, PO_4, and As.

Reproducible spherical pellets, ¾-in. in diam, were hand-rolled from the dampened oxide, and air-dried prior to firing. Drum pelletizing was difficult to manage, exhaustive of patience and prodigal of time, while briquetting, using either cylindrical or spherical moulds, failed to give unflawed shapes.

The temperatures at which these pellets were fired ranged from 600° up to and including 1200°C, but only those fired below 1000°C could be used for measurement of cold strength, for at 1000° the pellets shrank very considerably and cracked regardless of the heating and cooling rates employed. The effect of holding for various times at temperature was also investigated up to 900°C, with strengths determined after 20, 80, 300, and 900 min firing time. Dry, unfired pellets had strengths ranging from 3 to 4 kg.

The data for this series of experiments are given in Fig. 10, which shows a strength-time isotherm for each temperature investigated. It would have been interesting to obtain grain size measurements for each temperature, but this was impossible below 1100°C because the excessive internal reflection of the small hematite crystals masked the grain boundaries. However, other pellets were heated from 1100° to 1400°C for 30 min, and although it was impossible to measure their strengths because of spalling, measurements of grain size were made and are given in Fig. 11. Figs. 12 to 15 show the striking increase in grain size at these higher temperatures.

When hand-rolled pellets, prepared from a technical grade of ferric oxide, were fired at 1000°C, the strengths were markedly different from those obtained with the purer oxide. They did not stress-crack on cooling, and the shrinkage was much less. As shown by Curve A, Fig. 10, their maximum strength was considerably less than that of the purer pellets fired at 900°C, and at longer firing times the strength actually diminished. Since the particle diameter of both oxides was originally the same, it appeared that the technical grade contained either an additional impurity or more of a specific impurity. Spectrographic analysis showed both oxides to contain the same metallic impurities in about the same quantities with the exception of barium and silicon, which were in larger amounts in the technical grade material. Subsequent chemical analysis gave 3.57 pct Ba, 8.69 pct SiO_2, and 0.069 pct PO_4.

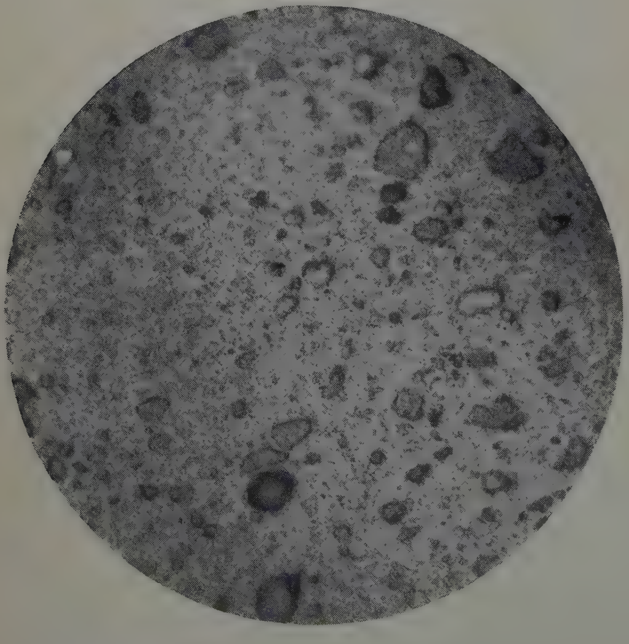

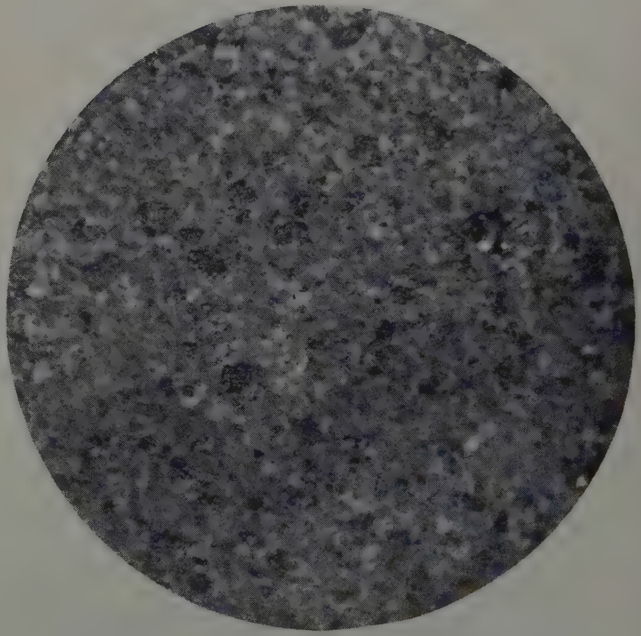

Fig. 12 (Left)—Crossed nicols. Analytical grade ferric oxide compacted and heated for 30 min at 1100°C. Average grain size of hematite, 6 microns. X200. Fig. 13 (Right)—Crossed nicols. The same material shown in Fig. 12, heated for 30 min at 1200°C. Average grain size, 7 microns. X200.

Analytical ferric oxide pellets and similar pellets to which 1 pct $BaCO_3$ was added were fired at 800°C for 300 min. The former had a strength of 53.4 kg, the latter a strength of 8.4 kg. Tests made under identical conditions but with the substitution of 6 pct −200 mesh quartz for the barium carbonate gave a strength of 51.8 kg. These tests indicate that silica, within the limits of the quantity given, has little effect on the pellet strength, but that barium has an extraordinary effect in lowering strength.

Although the writers have not investigated this matter further, it appears that relatively small amounts of certain additives, or even impurities occurring naturally in the ore, might exert a deleterious effect on pellet strength.

A number of inorganic additives were considered which might improve strength of pellets. Those finally selected were calcium oxide, magnesium oxide, sodium fluoride, and sodium carbonate. It was hoped that these additives would improve the physical properties of the pellets, either by accelerating grain growth or by reducing the temperature at which optimum strength could be obtained.

Hand-rolled pellets were prepared from analytical grade oxide containing 1 and 5 pct of the selected additives, and were fired in air for 30 min in an electric muffle furnace at temperatures ranging from 800° to 1400°C at 100° intervals.

At 800°C pellets containing borax cracked and spalled, and those with sodium fluoride explosively disintegrated. At 900°C the only pellets remaining intact were those containing lime and magnesium oxide. At 1000°C the lime and magnesia-containing pellets showed evidence of surface cracking, and at higher temperatures all pellets showed the fissures which occurred in ferric oxide pellets fired to corresponding temperatures without an additive. Since this was normal under the circumstances, the tests were considered capable of furnishing useful information, and it was decided to investigate further the effect of adding lime and magnesia to eastern Mesabi magnetite pellets.

The Effect of Firing on Magnetite Pellets Containing Added Lime and Magnesia

Six sets of drum-rolled magnetite pellets were prepared. The first two sets contained 5 pct calcium oxide added during rolling. One set was used for direct firing, and the other for re-firing at elevated temperatures following an oxidizing heating at 800°C for 2 hr. The third set contained 10 pct added lime and was direct-fired.

The fourth and fifth contained 5 pct magnesium oxide added during rolling, and the sixth contained 10 pct added magnesia. Originally the intention was to fire the magnesia-containing pellets according to the same procedure outlined above for the lime-bearing pellets, but it was found that they required careful heating up to 500°C to prevent them from explosively disintegrating upon being heated to 800°C or above. The procedure was accordingly modified to meet these requirements. This initial treatment undoubtedly permitted partial oxidation and therefore tended to minimize the differences between single-fired and double-fired pellets.

Figs. 16 and 17 show the strengths of pellets containing lime and magnesia respectively and fired according to the procedure given above. They should be compared with Fig. 7.

Single-fired pellets containing lime showed no significant difference in strength compared with straight magnetite pellets fired in the same way. The maximum strength was obtained with pellets pre-oxidized at 800°C and refired at 1300°C, but it was only about 2/3 the maximum strength shown by Curve B of Fig. 7. Abrasion resistances of pellets were compared qualitatively by means of rubbing pellets together, an insufficient number being available for a tumbling test. On the basis of this crude test the abrasion resistance of those pellets containing 5 pct lime, pre-oxidized at 800° and fired at 1300°C, was markedly superior to that of pellets without lime, pre-oxidized at 800° and fired at 1200°, 1300°, and 1400°C.

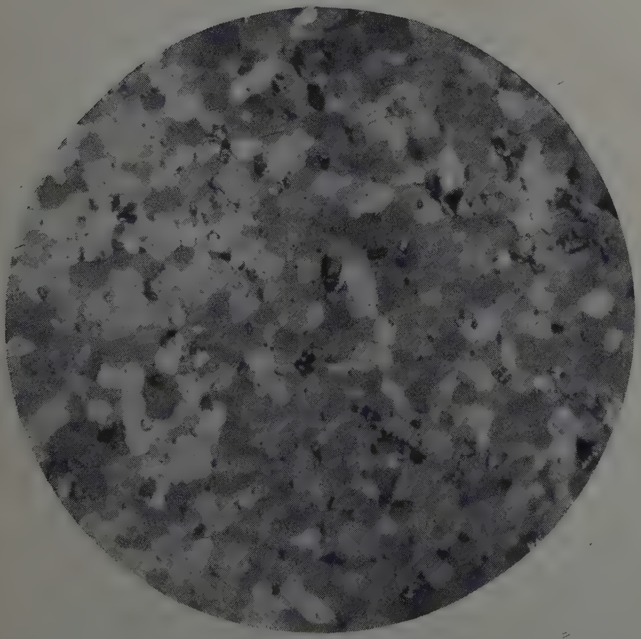

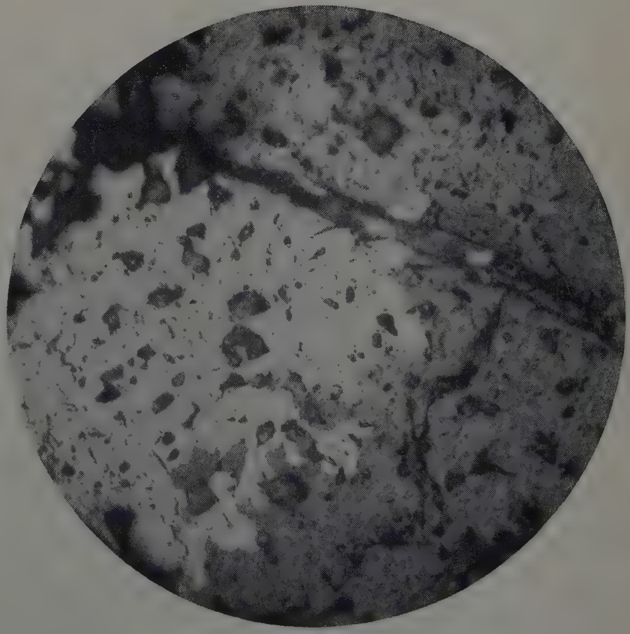

Fig. 14 (Left)—Crossed nicols. The same material shown in Fig. 12, heated for 30 min at 1300°C. Average grain size, 20 microns. X200. Fig. 15 (Right)—Crossed nicols. The same material shown in Fig. 12, heated for 30 min at 1400°C. Average grain size, 400 microns. X200.

Calcium oxide does not react with magnetite, but it unites with ferric oxide to form calcium ferrites. According to the equilibrium diagram[3] for the system CaO-Fe_2O_3, for 5 pct and 10 pct by weight of CaO, calcium ferrite, CaO Fe_2O_3, is in equilibrium with hematite below 1200°C. The presence of silica complicates the situation because this reacts at high temperatures with both lime and ferrite to form silicates. Above 1250°C hematite forms magnetite.

Microscopic examination of the fired pellets containing lime showed that oxidation of the magnetite occurred more readily at low temperatures than in the absence of lime, presumably because the additive preserved the original permeability. Ferrite formation was rapid at 1000° and complete at 1100°C, but at 1200°C and higher the silicates reacted with ferrite to form slag and hematite.

Magnesium oxide does not react with magnetite, but it unites with ferric oxide to form a spinel which is isomorphous with magnetite. As earlier work indicated that magnetite exhibited grain growth commencing at about 800°C and becoming pronounced at 1000°C, it was thought possible that the spinel structure could be maintained in an oxidizing atmosphere by the introduction of magnesium oxide, the assumption being that the magnesium spinel would exhibit grain-growth properties similar to those of magnetite.

Experimentally, however, it was found that the temperature required to replace hematite by magnesium spinel was so high, 1000°C or more, and the rate of replacement so slow that nothing was gained by using this additive. As shown by Fig. 17, the maximum strengths were not high, and simple tests showed that the abrasion resistance of these pellets was inferior to those of both the lime-magnetite and the magnetite pellets.

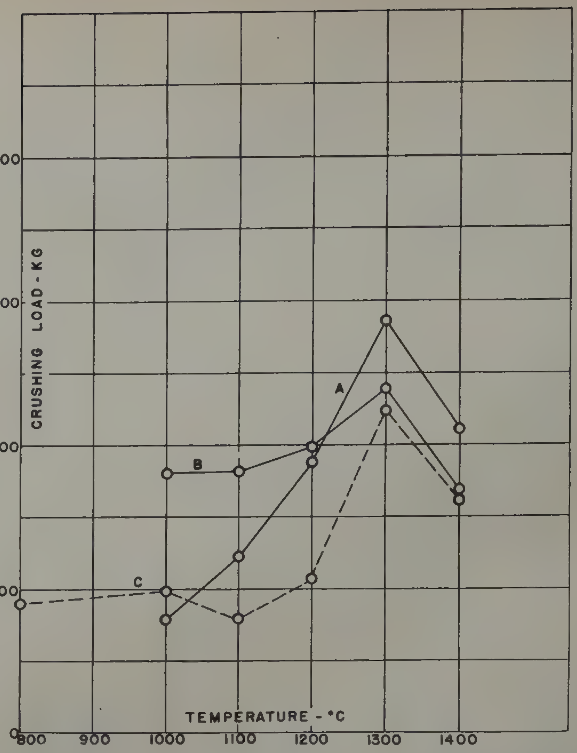

Fig. 17—Strength-temperature curves for magnetite pellets containing added magnesium oxide. Curve A: 5 pct MgO, preheated in air at 500°C and reheated to the temperatures indicated. Curve B: 10 pct MgO, preheated in air at 500°C and reheated to the temperatures indicated. Curve C: 5 pct MgO, preheated in air for 2 hr at 800°C and refired at the temperatures indicated.

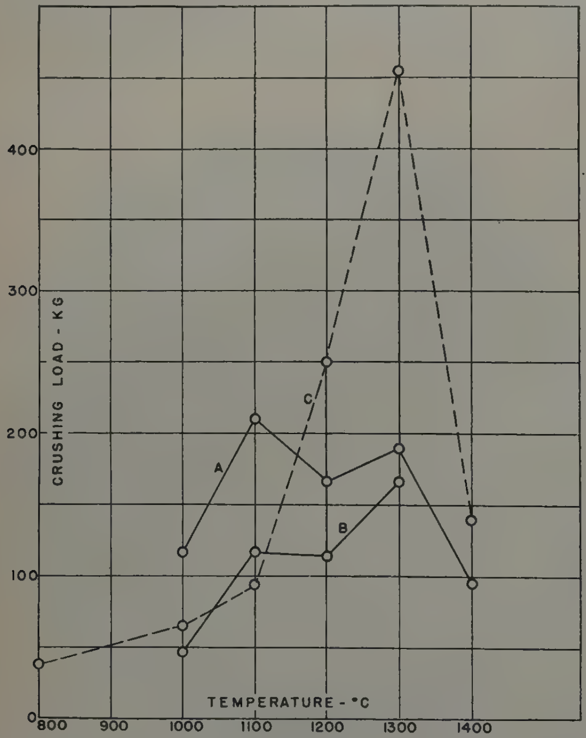

Fig. 16—Strength-temperature curves for magnetite pellets containing added calcium oxide. Curve A: 5 pct CaO, single-fired. Curve B: 10 pct CaO, single-fired. Curve C: 5 pct CaO, oxidized in air for 2 hr at 800°C and refired at the temperatures indicated.

Summary

Under laboratory conditions, maximum cold strength was obtained from magnetite pellets first by a superficial oxidation of all included magnetite grains at moderate temperatures and then by an increase of the firing temperature to promote grain growth of the resulting hematite. Such treatment affects uniformity of grain size and homogeneity of structure, the contraction crack between core and shell, so characteristic of pellets which have been brought rapidly to temperature in an oxidizing atmosphere, being subordinated or entirely eliminated. Excessive firing temperature was deleterious to strength because of thermal decomposition of the hematite, accompanied by slagging, breakdown of the continuous oxide network, and creation of blowholes due to the liberation of oxygen.

Neither calcium nor magnesium oxides added during rolling gave fired strengths comparable to those obtained from the unadulterated magnetite concentrate pellets, although calcium oxide conferred a measure of abrasion resistance.

Acknowledgments

The authors' thanks are extended to Dean Thomas L. Joseph for his continued interest and help, to Dr. Wladimir Philippoff for many suggestions made during the progress of this work, and to the Allis-Chalmers Manufacturing Co. for donating equipment and for sponsoring a fellowship for the junior author through which a major part of this work was accomplished.

References

[1] Strathmore R. B. Cooke and T. E. Ban: Microstructures in Iron-Ore Pellets. *Trans.* AIME (November 1952) **193**.

[2] T. E. Ban: Unpublished Master's Thesis, The Agglomeration of Fine Taconite Concentrates by Pelletizing. Univ. Minn. June, 1951.

[3] R. B. Sosman and H. E. Merwin: Preliminary Report on the System Lime-Ferric Oxide. *Journal Washington Academy Sciences* (1916) **6**, pp. 532-537.

Effects of Alkalinity on the Flotation of Lead Minerals

by Marston G. Fleming

General theories of alkali depression are disproved by this paper, which shows that its operation depends upon the nature of the mineral-collector system involved. Three mechanisms of alkali depression are examined and limitations of critical pH as a fundamental factor in flotation are discussed.

CRITICAL pH has been defined by Wark[1] as that pH value below which a mineral will float and above which it will not float in solutions containing a given concentration of collector but free from other depressants or activators. The relationship between mineral, collector concentration, and pH is expressed in the form of a critical pH curve determined by the captive bubble method and is generally regarded as being fundamental to the system involved. The mechanism of alkali depression is currently in dispute, two general theories having received authoritative support. The view expressed in Taggart's chemical theory of flotation[2] is that in the presence of a critical concentration of hydroxyl ions, all the metal ions available at the surface of the mineral are present as anions of the form $[M(OH)_x]^{-y}$. The formation of the necessary metal xanthate is thus precluded and, furthermore, any metal xanthate coating previously formed, at a lower pH, will be dissolved. Gaudin[3, 4] and the Melbourne school under Wark[5] hold that alkali depression is caused by the preferential adsorption of hydroxyl ions by the mineral surfaces.

This paper describes an investigation of the mechanism of alkali depression in each of the three systems: cerussite-aqueous carbonate-xanthate, cerussite-xanthate, and galena-xanthate.

Alkali Depression of Cerussite by Control of Carbonate Ion Concentration

Wark and Cox[6] have shown that in the presence of Na_2CO_3, a higher concentration of xanthate is required to effect bubble contact with a cerussite surface than in carbonate-free solutions. To examine this depression of cerussite by sodium carbonate, a series of captive bubble tests was carried out on cerussite specimens in solutions containing 100 mg per liter of potassium ethyl xanthate and varying concentrations of sodium carbonate. The pH was adjusted by the addition of dilute hydrochloric acid. For purposes of comparison a standard critical pH curve was determined for cerussite with potassium ethyl xanthate in solutions containing no added carbonate. In the latter case pH adjustment was made with sodium hydroxide. The experimental method employed in both series was broadly similar to that described by Wark and Cox;[7-9] a number of refinements suggested by Sutherland[10] were adopted, and the procedure was further developed and modified to suit the particular requirements of the investigation.

The relationship between pH and the concentration of potassium ethyl xanthate necessary to induce bubble contact at cerussite surfaces is shown in Fig. 1. The relationship between pH and the concentration of sodium carbonate necessary to prevent bubble contact at cerussite surfaces in the presence of 100 mg per liter of potassium ethyl xanthate is shown in Fig. 2. Comparison of the two curves shows that at a collector concentration of 100 mg

Table I. Composition of Solutions Containing Na_2CO_3 Just Sufficient to Prevent Contact at Cerussite Surfaces in the Presence of 100 Mg Per Liter. Potassium Ethyl Xanthate

	Concentration in Mols Per Liter			
pH	Na^+	Cl^-	HCO_3^-	$CO_3^=$
8.1	0.0303	0.0155	0.0146	0.71×10^{-4}
8.2	0.0265	0.0135	0.0128	0.78×10^{-4}
8.3	0.0232	0.0114	0.0116	0.89×10^{-4}
8.4	0.0200	0.0095	0.0103	1.00×10^{-4}
8.5	0.0166	0.0075	0.0089	1.08×10^{-4}
8.6	0.0134	0.0060	0.0072	1.10×10^{-4}
8.7	0.0110	0.0052	0.0056	1.08×10^{-4}
8.8	0.0088	0.0043	0.0044	1.04×10^{-4}
8.9	0.0072	0.0037	0.0035	1.07×10^{-4}
9.0	0.0060	0.0032	0.0026	1.00×10^{-4}
9.1	0.0050	0.0027	0.0021	1.02×10^{-4}
9.2	0.0038	0.0022	0.0014	0.87×10^{-4}
9.3	0.0029	0.0017	0.0010	0.80×10^{-4}
9.4	0.0022	0.0012	0.0008	0.81×10^{-4}
9.5	0.0015	0.0009	0.0005	0.59×10^{-4}
9.6	0.0008	0.0003	0.0004	0.59×10^{-4}

M. G. FLEMING, Member AIME, is Senior Lecturer in Mineral Dressing, The Royal School of Mines, The Imperial College of Science and Technology, London.

Discussion on this paper, TP 3424B, may be sent (2 copies) to AIME before January 31, 1953. Manuscript, April 8, 1952. Los Angeles Meeting, February 1953.

per liter KEX, the presence of 0.02 molar Na_2CO_3 lowers the critical pH from 9.7 to 8.0.

The carbonate solutions contained Na^+, K^+, Pb^{++}, H^+, OH^-, Cl^-, $CO_3^=$, HCO_3^- and EX^- and, at the concentrations used, dissociation may be assumed to be complete. Na, K, H, Cl, and EX were measured quantities. By introducing these known values into the statement of electrical neutrality for the system and combining this with the second dissociation constant of carbonic acid and the ionic product of water, it is possible, with a little algebraic manipulation, to calculate the missing factors. In Table I are listed the concentrations of the various ions present in the solutions which correspond to selected points along the curve in Fig. 2. The quantities tabulated are, therefore, the concentrations present when just sufficient sodium carbonate has been added to prevent the contact of an air bubble at the surface of cerussite in the presence of 100 mg per liter of potassium ethyl xanthate. With the exception of the carbonate ion itself, the concentrations of the ions vary widely along the length of the curve. The concentration of $CO_3^=$ is, however, remarkably constant and the curve, in effect, is a line of constant carbonate ion concentration, solutions to the right of the curve having a greater concentration and solutions to the left a smaller concentration of this ion than the constant. Variations at high pH may be explained by the fact that these solutions are approaching the point where alkalinity itself is the critical agent. The curve becomes almost asymptotal at pH 8 and variations at low pH are probably due to magnification of small errors by the steep slope of the curve.

The critical carbonate ion concentration for air-cerussite contact in the presence of 100 mg per liter of potassium ethyl xanthate may, then, be taken as $1.0x10^{-4}$ mols per liter at 25°C.

Interpretation of Results: Latimer[11] gives the following value for the solubility product of lead carbonate at 25°C:

$$(Pb^{++})(Co_3^{=}) = 1.5x10^{-13} \qquad [1]$$

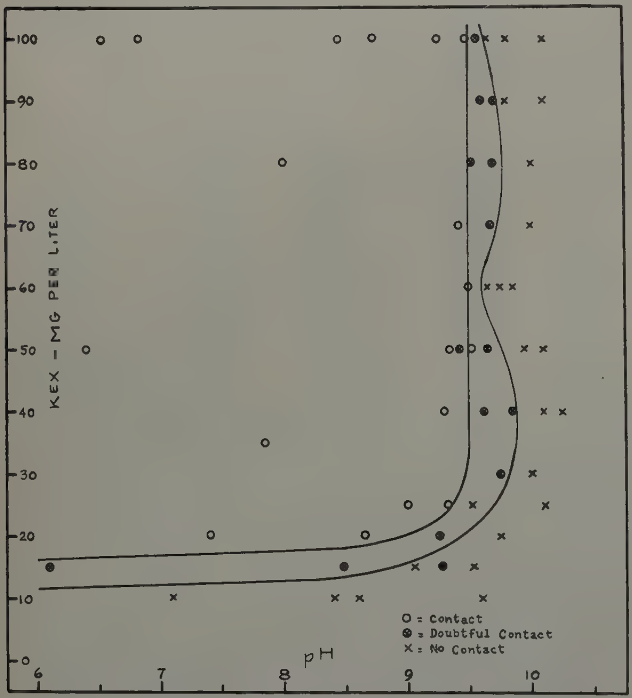

Fig. 1—Relationship between pH and the concentration of potassium ethyl xanthate necessary to induce contact at cerussite surfaces.

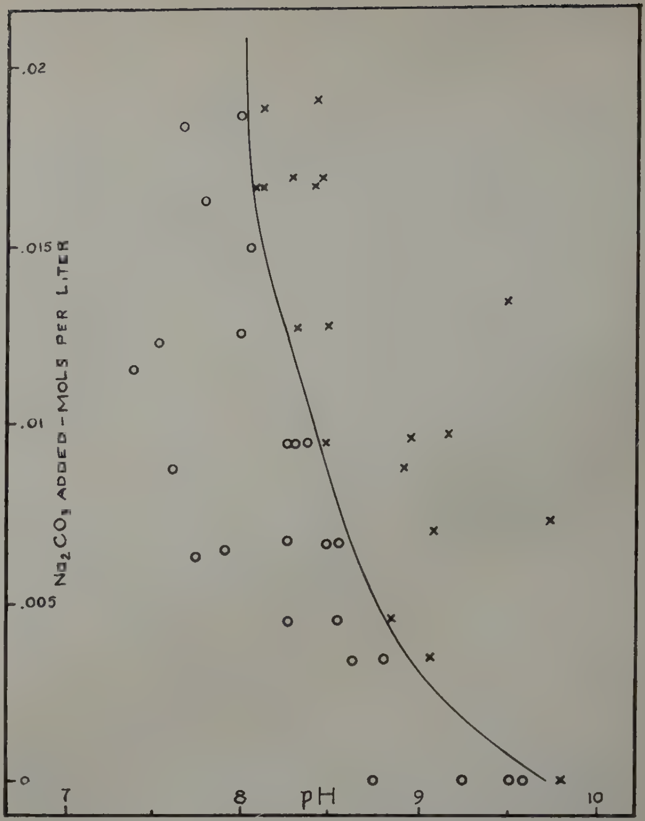

Fig. 2—Concentration of sodium carbonate necessary to prevent contact at cerussite surfaces.

In the presence of the critical carbonate ion concentration determined above the solubility of the lead ion becomes

$$(Pb^{++}) = \frac{1.5x10^{-13}}{1.0x10^{-4}} = 1.5x10^{-9} \text{ mols per liter}$$

Taggart and Hassialis[12] have determined the solubility product of lead ethyl xanthate to be $6.7x10^{-16}$

$$(Pb^{++})(EX^-)^2 = 6.7x10^{-16} \qquad [2]$$

Potassium ethyl xanthate to the amount of 100 mg per liter corresponds to a xanthate ion concentration of $6.25x10^{-4}$; by a substitution of this value in the solubility product, the saturation value for lead ion in the xanthate solutions tested may be obtained.

$$(Pb^{++}) = \frac{6.7x10^{-16}}{(6.25x10^{-4})^2} = 1.7x10^{-9}$$

This figure is in close agreement with the lead ion concentration present in aqueous carbonate solutions that contain the critical carbonate ion concentration. Therefore, there is strong justification for stating that in the system xanthate-aqueous carbonate-cerussite, the carbonate ion is the controlling factor in determining the critical pH above which an air bubble cannot make contact with the mineral surface and the function of the carbonate is to reduce the solubility of the cerussite to a point at which the concentration of lead ions is equal to or less than the saturation value for lead xanthate in the solution.

Alkali Depression of Cerussite by Mineral Decomposition

To study the reaction between cerussite and alkali a galvanic cell capable of registering small changes of lead ion concentration was employed:

$$Pb \mid Pb^{++}\ (aq) : KCl\ (aq\ saturated), HgCl_2 \mid Hg.$$

The lead electrode was specially purified rod, 99.9988 pct Pb, supplied by Johnson Matthey & Co. The test solution vessel contained a mechanical stirrer and a glass electrode which, by a special switching arrangement, could replace the lead electrode in the circuit so that EMF and pH could be measured alternately. The complete cell was suspended in a thermostatic bath at 25°C. The lead ion concentration was measured in aqueous solutions in contact with solid, freshly ground cerussite and the alkalinity of the solution was progressively increased by additions of potassium hydroxide. After each addition of alkali the mixture was left for 55 min with the glass stirrer producing a gentle agitation. At the end of this time the pH and EMF were recorded and the next addition of alkali was made.

The results are shown in Fig. 3 where lead ion concentration is plotted against hydrogen ion concentration on a negative logarithmic basis. There is very little change in lead ion concentration until the pH approaches 9 when there is a sharp inflection; thereafter, the lead ion concentration decreases rapidly as the alkalinity is increased. The results do not represent true equilibrium conditions for either hydrogen or lead ion concentrations, as these could only have been obtained with intervals of 2 to 3 weeks between KOH additions. However, the 1-hr interval allowed for the establishment of partial equilibrium was, as the work showed, sufficient to smooth out the initial instability brought about by the addition of alkali and was actually more representative of the conditions obtaining in flotation test work than would have been the case had full, stable equilibrium been established.

Interpretation of Results: It has already been shown that, in cerussite flotation, the lead ion concentration is a controlling factor in determining the critical pH. The sharp inflection point which occurs near pH 9 in the curve shown in Fig. 3 is, therefore, undoubtedly significant. It is suggested that this point marks the pH at which, under the conditions of the test, the formation of basic lead carbonate begins. Thus:

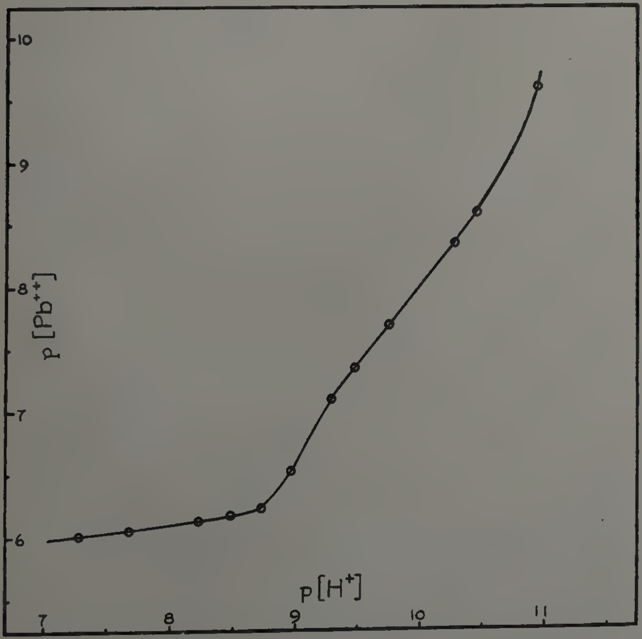

Fig. 3—Cerussite. Relationship between lead ion concentration and hydrogen ion concentration.

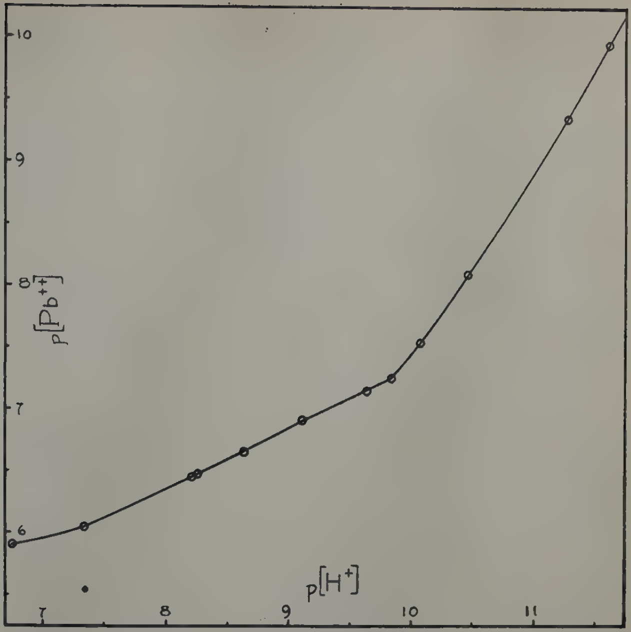

Fig. 4—Lead ethyl xanthate. Relationship between lead ion concentration and hydrogen ion concentration.

$$3Pb\,CO_3 + 2\,OH^- = Pb_3\,(CO_3)_2(OH)_2 + CO_3^= \quad [3]$$

In alkaline solutions, basic lead carbonate does not dissociate to yield free lead ions but, as Randall and Spencer have shown,[13] reacts with more hydroxide in the following manner:

$$Pb_3(CO_3)_2\,(OH)_2(solid) + 7\,OH^- = 3HPbO_2^- + 2CO_3^= + 3H_2O \quad [4]$$

The presence of excess $CO_3^=$ over and above that produced by the dissociation would repress these reactions and, indeed, in carbonate solutions at low alkalinity, basic lead carbonate is dissociated with the formation of Pb^{++} and HCO_3^-[14]:

$$Pb_3\,(CO_3)_2(OH)_2\ (solid) + 4H_2\,CO_3\ (aq) = 3Pb^{++} + 6HCO_3^- + 2H_2O \quad [5]$$

Carbonate ion thus acts in two ways to control the concentration of lead ion and the formation of the desired hydrophobic coating of lead xanthate on the surface of cerussite. 1—As has been shown, it has direct influence on the dissociation:

$$PbCO_3\ (S) = Pb^{++} + CO_3^= \quad [6]$$

2—It represses the formation of basic lead carbonate. In solutions to which no carbonate salt has been added the critical pH for cerussite flotation would correspond to the conversion of a limiting proportion of the mineral surface to basic lead carbonate. In solutions containing added carbonate ion, critical pH might represent the formation of basic lead carbonate as described above or it might represent the point at which the dissociation of cerussite has been reduced, through the mechanism of eq 6, until the concentration of lead ions is equal to or less than saturation value for lead xanthate in the solution.

Alkali Decomposition of Lead Xanthate

Using the galvanic cell and experimental procedure previously described, the influence of increasing concentrations of potassium hydroxide

Table II. Captive Bubble Tests with Galena

Test	Preconditioning KEX Mg per Liter	pH	Time, Min	Rinse Prior to Transfer	Test Solution KEX Mg Liter — pH	Min After Pre-Conditioning	Captive Bubble Reaction
1	25	7.15	30	Water	0 — 6.7	0 — 120	Strong contact continuing
2	25	7.15	30	Water	0 — 6.7	0 — 2	Strong contact
				None	0 — 12.2	2 — 3	Sticking
				Not transferred	0 — 12.2	3 — 4	No contact
				Water	0 — 6.7	4 — 10	No contact
				None	25 — 6.7	10 — 12	Strong contact in ½ min
				Water	0 — 12.2	12 — 14	Sticking
				Not transferred	0 — 12.2	14 — 15	No contact
				Water	0 — 6.7	15 — 30	No contact
3	25	7.15	30	Water	0 — 7.0	0 — 2	Strong contact
				None	0 — 11.9	2 — 4	Sticking
				Water	0 — 7.0	4 — 6	Sticking
				None	0 — 11.9	6 — 8	Sticking
				Not transferred	0 — 11.9	8 — 34	No contact
				Water	0 — 7.0	34 — 150	No contact
4	100	7.2	30	Water	0 — 6.5	0 — 2	Strong contact
				None	0 — 11.7	2 — 9	Contact
				Not transferred	0 — 11.7	9 — 10	Sticking
				Water	0 — 6.5	10 — 11	Sticking
				None	0 — 11.7	11 — 12	Sticking
				Not transferred	0 — 11.7	12 — 13	No contact
				Water	0 — 6.5	13 — 30	No contact
5	100	7.2	30	Water	0 — 6.8	0 — 2	Strong contact
				None	0 — 10.7	2 — 25	Contact
				Not transferred	0 — 10.7	25 — 62	Sticking
				Not transferred	0 — 10.7	62 — 64	No contact
				Water	0 — 6.8	64 — 100	No contact
6	25	7.26	30	Not transferred	25 — 7.26	0 — 2	Strong contact
				None	25 — 11.8	2 — 4	Contact
				Not transferred	25 — 11.8	4 — 21	Sticking
				Not transferred	25 — 11.8	21 — 31	No contact
				Water	0 — 6.9	31 — 41	No contact
				None	25 — 7.26	41 —	Strong contact after 1 min
7	25	11.83	30	Not transferred	25 — 11.83	0 — 2	No contact
				Water	0 — 6.7	2 — 22	No contact
				None	25 — 7.1	22 —	Strong contact after 1 min

upon the lead ion concentration of aqueous solutions in contact with solid lead ethyl xanthate was measured. The results are shown in Fig. 4 where p (Pb^{++}) is plotted against p(H^{+}). The curve indicates a gradual decrease in lead ion concentration up to pH 10 which marks an inflection and, thereafter, a sharp reduction of (Pb^{++}) as the alkalinity is further increased.

During these experiments it was observed that upon the addition of KOH which raised the pH from 9.82 to 10.07, the solution, which had hitherto been colorless, assumed a distinctly yellow shade and the solid lead xanthate became tinged with brown. Further additions of alkali accentuated this change and, at the end of the test, the liquid was distinctly yellow and the solid residue had turned dark brown. This was confirmed by a series of tests in which solid lead ethyl xanthate was placed in solutions of varying alkalinity and changes were observed over a period of 20 hr. These left no doubt that the decomposition of lead ethyl xanthate is a gradual process the rate of which depends upon the concentration of alkali in the solution. Some of the solid, dark brown reaction product was prepared by a method which removed all soluble matter but avoided the loss of any solids. Analysis showed this to be pure lead sulphide.

Interpretation of Results: These results show that under conditions similar to those in which flotation testing is carried out, lead ethyl xanthate is decomposed by alkali with the formation of lead sulphide as a reaction product. The curve in Fig. 4 is, in effect, a record of this decomposition. Below pH 10 the reaction is slow and, under the usual conditions of flotation research, probably not critically important. Above pH 10 the reaction becomes more rapid and apparently proceeds to completion. Although complete conclusions cannot be established from the available data, the following three-stage reaction is suggested:

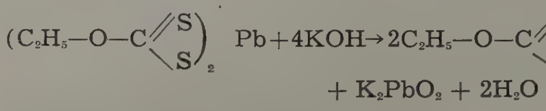

$$\left(C_2H_5{-}O{-}C\begin{smallmatrix}\diagup\!\!\diagup S\\ \diagdown S\end{smallmatrix}\right)_2 Pb + 4KOH \rightarrow 2C_2H_5{-}O{-}C\begin{smallmatrix}\diagup\!\!\diagup S\\ \diagdown S{-}K\end{smallmatrix} + K_2PbO_2 + 2H_2O \qquad [7]$$

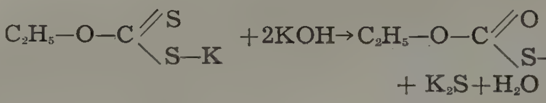

$$C_2H_5{-}O{-}C\begin{smallmatrix}\diagup\!\!\diagup S\\ \diagdown S{-}K\end{smallmatrix} + 2KOH \rightarrow C_2H_5{-}O{-}C\begin{smallmatrix}\diagup\!\!\diagup O\\ \diagdown S{-}K\end{smallmatrix} + K_2S + H_2O \qquad [8]$$

$$K_2PbO_2 + K_2S + 2H_2O \rightarrow \underline{PbS} + 4KOH \qquad [9]$$

In the first stage the lead ethyl xanthate is decomposed by alkali into soluble plumbate, alkali xanthate, and water. An alteration of alkali xanthate into monothiocarbonate, potassium sulphide, and water is known to occur in alkaline solutions, but this reaction would not be favored were it not for removal of potassium sulphide from solution by interaction with the plumbate and precipitation of lead sulphide as shown in eq 9. Under the circumstances, however, reactions eq 8 and eq 9 can proceed until the plumbate is used up, and simultaneous production of hydroxide from eq 9 will help to maintain the alkalinity of the system.

Alkali Decomposition of Collector Coatings at Galena Surfaces

A series of captive bubble tests were carried out in which galena was first conditioned in neutral potassium ethyl xanthate solutions and then transferred to solutions of varying pH. In transferring from one solution to another the specimen was held face down in glass tongs while 50 ml of solution was poured over it as a rinse. While they were immersed in the test solutions, the mineral specimens were tested for bubble contact at very short intervals, usually every 30 to 60 sec. Results are given in

Table II. The time required for rinsing and transferring the specimens was probably never longer than 10 sec and is omitted from the timetable which refers only to the period in which the specimens were immersed in the test solution. Temperature was maintained at 25°C.

Interpretation of Results: The results of these captive bubble tests may be summarized as follows:

1—The collector coating formed by potassium ethyl xanthate on galena surfaces is stable in neutral solutions, Test 1. This fact is well known to flotation investigators.

2—A preformed xanthate coating on galena loses its hydrophobic character in alkaline solutions, Tests 2 to 5.

3—The alteration of such a preformed coating by alkaline solutions is gradual, the rate being proportional to the alkalinity of the solution, Tests 2 to 5. In strongly alkaline solutions, the mineral surface becomes hydrophilic very quickly, Test 2. In solutions whose pH is close to the critical pH for galena, the change to a wettable surface may take as much as 1 hr, Test 5.

4—A collector coating which is formed by preconditioning in 100 mg per liter KEX solution appears to be more resistant to alkaline solution than one formed in 25 mg per liter KEX solution, Tests 3 and 5.

5—Failure to effect bubble contact with a precoated galena surface in alkaline solutions is due to a definite alteration of the coated surface and not simply to the concentration of hydroxyl ions at the solid-liquid interphase. At every stage in the alteration of the surface the same degree of wettability is found when the mineral is removed from the alkaline solution, washed in running distilled water, and tested in water such as existed in the alkaline solution immediately before its transfer, Tests 2 to 7.

6—The presence of alkali xanthate in the solution retards but does not prevent the alteration of a preformed xanthate coating by alkaline solutions, Tests 3 and 6.

7—The action of alkaline solutions on a galena surface, whether precoated with xanthate or not, does not prevent its ready acceptance of a new xanthate coating when it is transferred to a neutral xanthate solution, Tests 1, 6, and 7.

These observations suggest that the collector coated surface of galena is, in effect, lead xanthate and that the depressant action of high pH in flotation is due to the decomposition of that surface as described in this paper under Alkali Decomposition of Lead Xanthate. The relation of items 1 to 5, above, to this hypothesis is self-evident. Item 6 is explained by reference to eq 7, from which it can be seen that the decomposition of lead ethyl xanthate by alkali will be repressed by the presence of alkali xanthate in the solution. Item 7 derives clearly from the fact that the decomposition results in the deposition of fresh lead sulphide upon the surface of the mineral, which is thus well conditioned for collector-coating in a neutral or slightly alkaline solution.

Summary and Conclusions

The tests described show that no general theory of alkali depression is tenable, for the mechanism of depression depends upon the nature of the mineral-collector system concerned. It has been shown that the action of carbonate-free alkaline solutions in preventing the flotation of cerussite may be independent of the collector and may be due entirely to decomposition of the mineral surface. This type of alkali depression is not necessarily confined to cerussite but may operate in any case where the basic product does not yield simple metal ions. When the xanthate collection of cerussite is carried out in solutions containing an appreciable amount of soluble carbonate, the alkali has been shown to exert its depressant effect indirectly through control of the carbonate ion concentration. In this case there is no true alkali depression, for the formation of a collector coating is prevented by solubility-product control of a metathetical reaction. A third type of alkali depression which has been studied in this research operates through the decomposition of the collector coating by alkaline solutions. This is almost certainly a critical influence in the xanthate flotation of galena and, possibly, in the flotation of other metal sulphides with anionic collectors. It would be extremely dangerous, however, to draw general conclusions from results based entirely on experiments with lead xanthate and galena, for the behavior of the other principal sulphide minerals, those of copper, iron and zinc, in xanthate flotation is considerably more complicated than that of galena. With other mineral-collector systems alkali depression may operate through an entirely different mechanism from any described above.

When alkali depression is caused by decomposition of collector coatings it is apparent from an examination of the curve in Fig. 4 that the term *critical pH* can be relative only. The slope of this curve together with the results given in Table II show that decomposition of the metal xanthate is a continuous process which, although accelerated above a certain pH, proceeds slowly even in weakly alkaline solutions. Time, as well as hydroxyl ion concentration, is thus an essential factor, and the correlation of different critical pH curves is dependent, to some degree at least, upon the conditioning period. The close standardization of conditions for captive bubble testing by investigators at Columbia and Melbourne Universities and the almost universal adoption of their methods by other workers has tended to hide this effect.

The standard method in such tests employs a conditioning period of 30 min. Where the agency of alkali depression is decomposition of the metal xanthate, it would be expected that under standard conditions the critical pH curve corresponds to the locus of the points at which accelerated decomposition begins. With conditioning periods shorter than standard the position of the curve would probably remain much the same. With longer conditioning periods, however, it would be expected that critical pH would be lower and that the resultant curves would probably lie inside, or slightly to the left of the standard curve.

Similarly, it would be reasonable to expect that the rate of decomposition would be influenced by temperature in such a way that for a given xanthate concentration the critical pH would vary inversely as the temperature of the test. Wark[15] has shown this to be the case with critical pH values for galena, pyrite, and chalcopyrite in 25 mg per liter potassium ethyl xanthate solutions. For galena, the critical pH value is given as 10.8 at 10°C and 9.7 at 35°C.

The time required for the destruction by alkaline solutions of the metal-xanthate coating on mineral surfaces would depend upon the thickness of that coating. With cerussite and anglesite, both relatively soluble minerals, there is strong evidence, supported by the results given above under Alkali Depression of Cerussite by Control of Carbonate Ion Concentration, that the collector coating is produced metathetically and may have an appreciable thickness. Similarly, it might be expected that the oxidized surfaces of sulphide minerals would react with xanthates to form a heavier layer of metal xanthate than would be the case with fresh, unoxidized surfaces. If the equilibrium were not complicated by other factors, such as decomposition of the oxidized mineral surface itself by alkali as in the case of lead carbonate, it is reasonable to suppose that a mineral surface capable of forming a heavy coating of metal xanthate would be less susceptible to alkali depression than one which would normally form a monomolecular film. In this connection it is interesting that Sutherland and Plante[16, 17] found that oxidizing the surface of a sulphide mineral changed its response to ethyl xanthate and led to greater tolerance to the depressant action of cyanide and alkalis.

References

[1] I. W. Wark: *Principles of Flotation*, p. 186. Australasian Institute of Mining and Metallurgy, Melbourne (1938).

[2] A. F. Taggart: *Handbook of Mineral Dressing*, pp. 12-30. John Wiley and Sons, New York, 1945.

[3] A. M. Gaudin: *Flotation*, p. 78. McGraw-Hill Book Co., New York, 1932.

[4] A. M. Gaudin: *Principles of Mineral Dressing*, p. 388. McGraw-Hill Book Co., New York, 1939.

[5] I. W. Wark and A. B. Cox: *Trans.* AIME (1934) **112**, p. 299.

[6] I. W. Wark and A. B. Cox: *Trans.* AIME (1939) **134**, p. 12.

[7] I. W. Wark and A. B. Cox: *Trans.* AIME (1934) **112**, p. 189.

[8] A. B. Cox and I. W. Wark: *Engineering and Mining Journal* (1936) p. 641.

[9] Reference 1, pp. 74-80.

[10] K. L. Sutherland: Private communication, 1948.

[11] W. M. Latimer: *Oxidation Potentials*, p. 313. Prentice-Hall, New York, 1938.

[12] A. F. Taggart and M. D. Hassialis: *Trans.* AIME (1946) **169**, p. 260.

[13] M. Randall and H. M. Spencer: *Journal of American Chemical Society* (1928) **50**, p. 1572.

[14] International Critical Tables (1930) **7**, p. 250. McGraw-Hill Book Co., New York.

[15] Reference 1, p. 187.

[16] E. C. Plante and K. L. Sutherland: *Trans.* AIME (1949) **183**, p. 160.

[17] E. C. Plante: *Trans.* AIME (1949) **183**, p. 189.

Theory, Scale-Up, and Operating Variables of the Peterson Top Feed Reservoir

by R. J. Piros, R. A. Brusenback, and D. A. Dahlstrom

DEWATERING fine coal has been a serious problem to many operators who desired to wet-wash finer sizes and maintain high recovery. Centrifugal driers have become popular for this purpose for sizes between ⅜ in. and 14 mesh. Below 14 mesh the perforated screen centrifuges lose a large percent in the effluent solid bowl types that do retain —14 mesh coal, produce excessive degradation, tend to retain the highest ash fraction in any size fraction, and are subject to abrasion, which results in higher maintenance.

In 1949 Truax-Traer Coal Co. planned a cyclone installation at their Ceredo preparation plant to recover coal down to 150 mesh with approximately a 14-mesh top size. Since available centrifugal equipment was not considered satisfactory, an investigation of rotary vacuum filters was begun in cooperation with the Peterson Filters and Engineering Co. to determine the suitability of the Peterson Top Feed Reservoir (TFR) filter. This investigation, which is described below, has resulted in a highly satisfactory installation of two 6x10-in. Peterson TFR filters that have been in operation over a year.

After some preliminary laboratory batch vacuum filter tests, a pilot plant double-drum Peterson TFR filter was installed at Ceredo to prove the feasibility of vacuum filtration and determine optimum conditions. The full scale units were then installed on the basis of the pilot plant results. This was followed by an extensive research program on vacuum filtration in the laboratory at Northwestern University to investigate basic design and operating variables and their influence on final moisture content of the filter cake. A method of scale-up from laboratory batch tests to the full-size unit was also proposed and proved. Because of the importance of dewatering fine coal today, it was felt that the results of the three steps should be made available for the use of others facing this problem. The work at Northwestern is given in a theoretical section following the discussion of the pilot plant and full-scale operation.

Fig. 1 is a flow diagram of the cyclone and filter installation. The feed is drawn from below the

---

R. J. PIROS, Junior Member AIME, formerly with the Truax-Traer Coal Co., Chicago, is now with International Minerals and Chemical Corp., Mulberry, Fla. D. A. DAHLSTROM, Member AIME, is with Northwestern University, Evanston, Ill. R. A. BRUSENBACK is with the University of Colorado, Boulder, Colo.

Discussion on this paper, TP 3422F, may be sent (2 copies) to AIME before January 31, 1953. Manuscript, May 15, 1952. New York Meeting, February 1952.

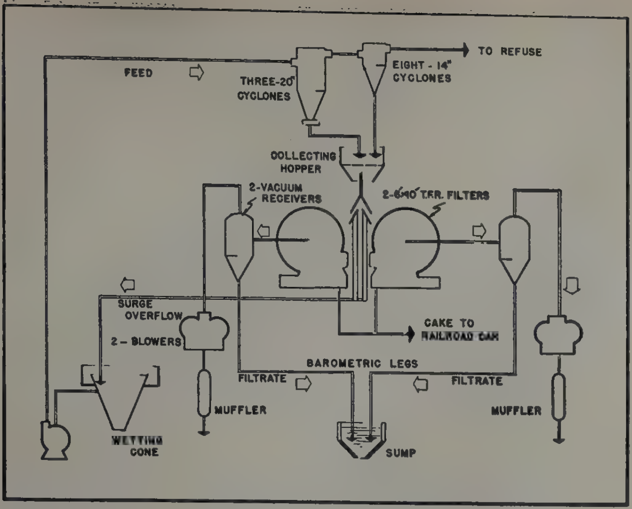

Fig. 1—Flow diagram of cyclone and filter installation.

surface of two raw coal wetting cones and pumped to a battery of three 20-in. and eight 14-in. cyclones arranged so that the overflow of the 20-in. forms the feed for the 14-in. cyclones. No intermediate pump is used. The underflow from the eleven cyclones discharges into a collecting hopper which splits the feed to the two filters or applies it to either one when desired. The solids content of the filter feed is regulated by a back-pressure valve on the overflow from the 14-in. cyclones and by adjustable underflow nozzles on the 20-in. units. The thickened slurry drops into a top feed reservoir formed by the filter drum and a slightly off-vertical steel sheet. A seal is made at the horizontal centerline of the drum by a heavy rubber pad and a bed of coal. The filter cake is formed in this reservoir by the application of vacuum and is carried on the filter screen as the drum revolves toward the scraper. The filter valve bridge is adjusted so that the cake is discharged under vacuum. Moisture is removed by the pressure differential across the cake and by the intense vibration generated by electro-magnetic vibrators mounted on the inside of the drum. The drum is set on rubber pads and is composed of an inner stainless steel drum deck with a stainless steel B-Z tri-rod screen with ¼-mm slot. The space between the drum deck and the screen is divided into narrow channels through which the filtrate and air are withdrawn. These two phases are separated in a 4-in. diam vacuum receiver with a barometric leg for filtrate removal. Vacuum is created by two 18x27 RCD Roots-Connersville positive displacement blowers.

Operating Results

Initial operation of the filter installation was begun in December 1950. Since that time only one minor part, the Micarta valve bridge, has been replaced, owing to abrasive or structural failure. Several minor changes have been made to improve the operation, e.g., new scrapers have been designed and tension springs for the scrapers have been installed. These improvements are now standard equipment on all models. The only maintenance work that has been done is to tighten the stainless steel hold-down bolts on the screen to the deck to prevent air leakage. This was done after about three months of operation. The screen itself shows little sign of wear, and the scrapers, which are the points of greatest abrasion, are in good condition. No trouble is expected or has occurred at any other point. The relatively slow movement of all parts has overcome the high maintenance problem of most mechanical dewatering devices.

The fine coal circuit is subject to wide fluctuations in feed rate and size distribution because of the variety of coal processed by the plant. For this reason, it is necessary to employ an operator for the filter and cyclones, although he has been able to perform considerable clean-up and general plant maintenance when feed conditions are uniform. Because of these wide fluctuations, the units have handled over 100 tons per hr for short periods. However, best moisture results are obtained at solid rates under 80 tons per hr. Table I gives operating data for several tests under varying conditions.

The average surface moisture for 23 tests on West Virginia No. 2 gas was 14.73 pct at an average capacity of 59.2 tons per hr for the two 6x10's. The average size-consists of the filter cake for these 23 tests is given in Table II. Samples of the filtrate exhibit a very low solids content and contain pri-

Table I. Operating Data for Two 6x10-Ft Peterson TFR Filters, West Virginia No. 2 Gas Coal, Truax-Traer Coal Co., Ceredo, West Va.

Date	Surface Moisture, Pct	Dry Ash, Pct	Vacuum, In. Mercury	Drum Speed, Min Per Rev	Cake Thickness, In.	Air Rate Standard, Cfm	Calculated Solids, Tons Per Hr*	—200 In. Cake, Pct	Vibration Intensity, Pct
12-15-50	15.61	7.98	8	2.0	2⅞	4900	39.4**	5.6	75
12-19-50	15.33	8.02	11	2.0	2	4040	53.0	4.9	75
12-21-50	14.09	8.80	12.5	3.0	3	3600	54.0	5.4	100
12-21-50	16.49	8.90	10.5	2.5	2¾	4160	60	7.2	0
12-21-50	16.55	8.12	11.75	2.21	3	3820	51.9**	5.2	100
12-23-50	14.06	8.01	11.5	2.1	2¾	3900	71	5.2	100
12-29-50	14.33	7.59	10.0	2.0	2½	4300	47	4.5	100
1-3-51	12.45	8.81	13	1.67	2¼	3500	55	6.5	100
4-7-51	13.37	7.75	10	1.67	1¼	4300	48	4.8	80
4-7-51	14.27	7.34	10	1.87	2	4300	56	4.8	80
4-7-51	18.94	7.72	10	1.73	3	4300	92.4	4.1	80
4-7-51	13.67	7.00	10	1.83	1½	4300	43	4.9	80
4-7-51	15.50	6.60	10	2.07	2½	4300	65	6.9	80
4-7-51	13.20	7.70	10	2.00	2½	4300	68	5.3	80
4-7-51	15.03	7.07	10	2.00	3	4300	80	4.5	80
4-7-51	13.89	6.72	10	1.73	2	4300	61	4.4	80
8-3-51	14.73	5.86	9.5	1.89	2½	4450	74.5		75
8-7-51	14.17	9.22	9.25	2.70	2¾	4530	56		75
8-8-51	14.62	8.58	10	2.67	2¾	4300	55.5		75
8-17-51	13.84	7.53	9.25	3.6	2¾	4530	40.0		75
8-23-51	14.00	6.50	10.25	2.4	3	4230	69.0		75
9-21-51	16.3	7.48	10.5	2.85	2½	4160	24	9.0	75
9-28-51	14.3	5.75	12.5	2.13	3	3600	38	6.0	75
							59.2 Wet weight 50.5 Dry weight		
Average	14.73 Pct								

* Based on drum speed, cake thickness, and bulk density.
** Weighed total cake discharge over time interval.

Table II. Average Size Consist of West Virginia No. 2 Gas Filter Cake, 6x10-Ft Peterson TFR Filter, Truax-Traer Coal Co., Ceredo, West Va.

U.S. Standard Mesh	Wt, Pct	Cumulative Pct On	Range—Wt, Pct
+14	6.1	6.1	3.4- 9.1
14x30	26.3	32.4	17.3-51.0
30x50	39.6	72.0	24.5-52.8
50x100	15.8	87.8	7.4-23.2
100x200	6.6	94.4	3.3-10.2
−200	5.6	100.0	3.0- 7.2

Table III. Typical Filtrate Solids Analysis, 6x10-Ft Peterson TFR Filter, Truax-Traer Coal Co., Ceredo, West Va.

	1.45 Pct Solids		2.46 Pct Solids	
U.S. Standard Mesh	Wt, Pct	Ash, Pct	Wt, Pct	Ash, Pct
+30	5.3	2.92		
30x50	9.6	2.75	3.1	
50x100	15.1	4.12	9.4	
				4.19
−100	70.0	22.90		
100x200			9.4	7.02
−200			78.1	45.76

marily −200 mesh particles, the ash content of which is very high. Loss of this fine slime material further aids in the desliming process which is largely obtained in the cyclones. The amount of loss can be regulated by the choice of slot opening for the tri-rod screen. Table III illustrates a typical analysis of the filtrate.

One of the important features of the Peterson TFR filter is the installation of electro-magnetic vibrators on the inside of the filter drum to create an intense vibration of the cake as it is formed and dried. A denser cake is formed which aids in squeezing out more of the water. A series of three tests at different levels of vibration were made on the same day with the units. Fig. 2 shows the reduction of 3.6 pct in final moisture content when the intensity of vibration was increased from 0 to 85 pct of full load amperage. In addition to making possible a higher moisture removal, the vibrators aid in operation by maintaining a uniform cake thickness. Furthermore, vibration appears to have a greater effect on moisture reduction when the tonnage is high, thereby effectively increasing the capacity of the filters.

The top feed reservoir feature has several advantages over conventional filter design for dewatering coal. 1—Coarse coal can be fed to the unit without a build-up in the feed reservoir. 2—The reservoir is designed especially for rapid-settling, fast-filtering products. 3—When the filter cake is formed, a more uniform size-distribution throughout the cake results than with the underfeed filter. The latter type tends to pull the finer sizes to the filter screen first, thereby reducing the filtration rate and increasing final moisture. In most cases, this deslimed material cannot be handled on underfeed filters. 4—The top feed units at Ceredo operate with a very short cake formation period, usually with a pool 1 ft deep, permitting a much longer drying time: 75 pct of the total filter area as compared to about 45 pct for the underfeed type. This gives further assistance to improved moisture percentages and tonnage rates.

It is particularly important in designing a TFR installation to provide good control and distribution of the filter feed. Proper solids to liquids ratio is essential, as well as correct size distribution. Coals with extremely high air permeability will give difficulty in priming the filter and in maintaining the cake. Locating the feed reservoir on other installations at a higher level on the drum has overcome this difficulty.

Pilot Plant Work

Laboratory tests by Peterson Filters and Engineering Co. indicated that the following variables were of prime importance in determining filtration rate and final moisture: 1—inches Hg of vacuum, 2—air rate through the cake, expressed as cu ft per min or cfm/ft^2 at the vacuum, 3—size consist of feed, 4—type of cake discharge from drum, 5—percent solids in feed, 6—vibration, 7—drum speed or minutes per revolution, mpr.

To present a better idea of the effect of these variables, a pilot plant unit was installed, consisting of a 10-sq ft, double-drum TFR filter supplied by the Peterson Filters and Engineering Co. The unit was fed by the underflow from a 14-in. cyclone thickener. Any proportion of the discharge from the cyclone could be bled to the filter. An oversize Roots-Connersville positive displacement blower was furnished by the manufacturer to permit any desired vacuum. The filter cake discharge was collected on a 9-in. belt and transferred to a flight conveyor carrying clean coal. This product was collected during test runs and weighed to give accurate tonnage figures. Samples for moisture analysis were taken as the coal was scraped from the drum. Table IV gives representative data for the pilot plant unit.

It was apparent as soon as operation of the unit began that the underflow from the cyclone could be thickened to the point where uniform feed to the

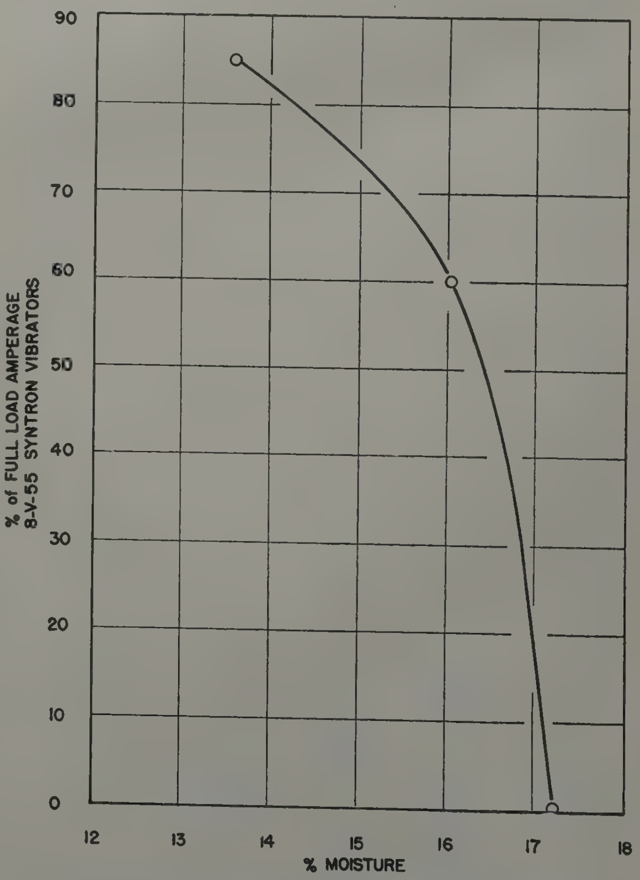

Fig. 2—Vibration intensity vs filter cake moisture. Test date, Jan. 9, 1950. Two-inch cake. Drum speed, 2 mph.

Table IV. Pilot Plant Data, 10-Sq Ft Peterson TFR Double-Drum Filter, Truax-Traer Coal Co., Ceredo, West Va.

Test No.	Filter Cake, Tons Per Hr Per 100 Sq Ft	Standard Cfm Per Sq Ft	Drum Speed, Min Per Rev	Vacuum, In. Mercury	Cake Thickness, In.	Total Cake Moisture, Pct*	Vibration	—200 Mesh in Cake, Pct
5	16.9	25.1	1.8	10.5	1.75	19.2	Off	5.5
8	39.7	15.4	1.1	13.0	2.5	26.0	Off	8.2
9	23.0	16.9	2.05	11.5	2.7	22.3	Off	9.2
10	12.9	14.6	1.8	5.1	1.3	18.9	Off	5.0
11	12.9	14.6	1.8	5.1	1.3	18.3	Off	
12	9.2	21.8	2.67	7.0	1.4	18.4	Off	4.7
13	17.1	23.7	1.8	7.0	1.8	21.5	On	
17	15.7	10.1	1.58	6.0	1.4	21.8	On	
18	15.7	10.1	1.58	6.0	1.4	23.1	Off	1.8
19	6.45	21.2	5.33	13.5	2.0	17.4	Off	4.6
20	16.2	23.0	2.07	12.75	1.9	19.9	On	
21	16.2	23.0	2.07	12.75	1.9	18.3	Off	
22	10.6	14.0	3	5.4	1.8	21.2	On	
23	10.6	14.0	3	5.4	1.8	21.0	Off	6.2
24	10.6	17.5	3	15.0	1.8	14.6	On	
25	10.6	17.5	3	15.0	1.8	19.0	Off	6.2
28	10.7	27.7	1.5	11.0	1.4	25.2	Off	14.9
29	16.7	27.7	1.5	11.0	1.4	19.1	On	
31	27.7	22.1	1.08	11.0	2.2	29.1	Off	14.9
32	5.07	28.5	3.67	10.8	1.1	19.8	On	
33	5.07	28.5	3.67	10.8	1.1	22.4	Off	
34	10.14	25.0	1.92	12.0	1.1	20.4	On	
35	10.14	25.0	1.92	12.0	1.1	23.6	Off	16.6

* Surface moisture pct equals total moisture pct — 1.8. (1.8 is U.S. Bureau of Mines published seam moisture for No. 2 gas.)

filter was impossible. This was the feature which limited thickening ahead of the filter, and it was found that maintaining feed solids concentration at about 50 pct gave best results on the pilot plant unit.

Effect of CFM/Ft^2, MPR, and TPH/100 Ft^2

Because of the great amount of interaction between filtration variables, it is impossible to determine quantitatively the individual influences by the classic experimental method of varying only one factor at a time. Consequently it was decided to attempt a correlation based on an empirical combination of the variables. Observation of the data in Table IV suggested that the surface moisture was dependent on the variables as follows: 1—Surface moisture decreased with higher cfm/ft^2. 2—Surface moisture decreased with lower drum speed. 3—Surface moisture increased with higher tonnages. 4—Surface moisture increased as size-consist became smaller.

From the above, a plot of final surface moisture as a function of (cfm/ft^2) (0.65 mpr)/(tph/100 ft^2) was compiled as illustrated in Fig. 3. The factor 0.65 mpr was indicative of the time that air would be actually passing through the cake. A reasonable correlation appeared to exist. The significance and restrictions of the correlation will be discussed in the following paragraphs.

Test work was done on two different types of feed. Runs 1 through 27 were on material drawn from the raw coal cones through the single 14-in. cyclone. This yielded a feed similar to that expected in the full-scale operation. The remaining tests were conducted on the same type of material with the coarse fraction scalped off. Since the size-consist of the individual runs for the same feed did not vary greatly, it was decided to correlate on the basis of the average size consist or surface area. In Fig. 3 the upper curve refers to the finer coal, while the lower curve relates to the coarser material. The two curves have the same slopes and shape but are displaced from each other to give higher surface moisture for finer cakes, or higher specific area.*

The shape of the curve is very important and indicative of the operation which can be expected. The point of sharp break is considered the location of optimum operation. To the left of this point the moisture increases rapidly. Thus overloading the filter causes a significant increase in surface moisture as insufficient air volume is drawn through the cake. To the right of the optimum, the curve is quite flat, indicating that little can be gained by drastic reduction in tonnage or overdesign of vacuum pumps. Attention should also be directed towards the necessity of obtaining a fully deslimed feed so that full efficiency of the filter can be utilized in yielding minimum moisture percent and maximum rate.

Laboratory tests indicated that substantial improvement in moisture could be expected when high frequency vibration was applied to the cake. The preliminary pilot plant data was not conclusive, as both negative and positive results were experienced. This was finally attributed to improper mounting of the vibrators in the pilot plant unit. They were bolted rigidly to the drum, which was in turn rigidly mounted to its framework. If care was taken always to sample the product at a point where vibration was a maximum, that is, over the vibrator, sub-

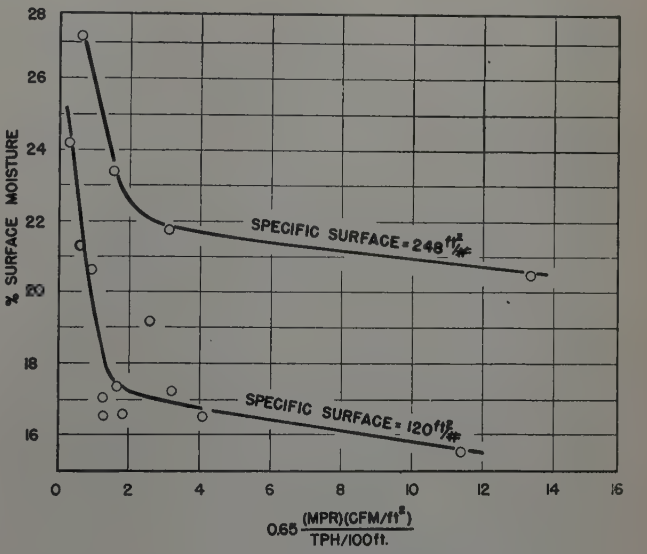

Fig. 3—Pilot plant filter tests, no vibration, showing effects of tonnage, tons per hour per 100 sq ft; air volume, cfm per square feet; drum speed, mpr; size consist; and specific surface.

---

* Specific area is defined as the surface area of cubes whose dimensions are the average of the dimensions of the size fractions measured in square feet per pound.

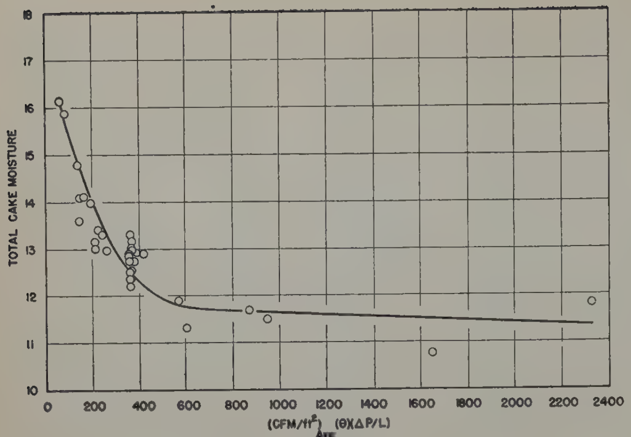

Fig. 4—Total moisture as a function of $(\text{cfm/ft}^2)_{\text{Avg}}$ (θ) $(\Delta P/L)$. Experimental vacuum filtration data. No vibration. Slurry temperature, 80°F.

stantial decreases in moisture content were obtained. The reduction varied from 2.2 to 6.1 pct. Although results were not consistent, they were encouraging enough to indicate that the 6x10-ft filters should be equipped with vibrators. Therefore the filter deck on the large units was rubber-mounted to achieve proper application of the vibration. Further proof of the actual dewatering efficiency with vibration will be found in the theoretical section to follow.

One of the most important characteristics of this type of filter, soon evident in the pilot plant, was its capacity for dealing with wide fluctuations in tonnage without interruption of production. The drum speed could be rapidly controlled to adjust for tonnage changes. In addition, the Top Feed Reservoir fluid level automatically increased with the higher feed rates. This increases the pickup time and therefore cake thickness and capacity. An overflow weir is provided for extreme overload.

From the curve of Fig. 3 it was now possible to design the full-scale unit with respect to filter area and vacuum pump requirements. Accordingly the flow sheet and filters, as indicated in Fig. 1, were recommended to handle up to 100 tons of dry solids per hour.

Theoretical Vacuum Filtration Studies

To obtain a more quantitative analysis of the influence of filtration variables on capacities and final moisture contents, an experimental investigation was undertaken at Northwestern University. A small vacuum unit was constructed, similar to the one used by Peterson Filters and Engineering Co., consisting of a gasket-sealed receptacle which accommodated a 4-in. sq stainless steel B-Z tri-rod filter screen. A Syntron vibrator was also attached to the unit so that vibration intensity could be studied. All filtrates were collected in a receiver beneath the screen, and the unit was connected to a vacuum system that permitted both control of vacuum and accurate measurement of the air drawn through the filter cake. A large batch of coal from Eastern Gas and Fuel Co. was thoroughly mixed to yield a uniform size-consist throughout. This was checked by periodic wet screen analyses on different runs. An average size-consist for the experimental coal is given below in Table V.

In the performance of all tests, a prepared 60 pct solids concentration slurry was made up, thoroughly mixed, and poured onto the filter deck. The valve to the unit was opened to allow the desired vacuum, and the filtration time was recorded after the disappearance of water from the top of the cake. This would correspond to the drying arc time on the TFR filter. The vacuum was immediately broken at the end of the run and measurement was made of the cake thickness. Samples were then taken for size and moisture analysis.

It was decided that the following should be studied in an analysis of filtration variables: 1—air rate and quantity, 2—vacuum level, 3—drying time, 4—cake thickness, 5— −200 mesh content, 6—feed slurry temperature, 7—vibration intensity, 8—tri-rod screen slot opening. Accordingly an experimental program was proposed to investigate these factors.

Influence of Air Rate and Quantity, Vacuum Level, Drying Time, and Cake Thickness

It is impossible to study individually the influence of air rate and quantity, vacuum level, drying time, and cake thickness, as they are all interacting. Accordingly it was necessary to perform a large number of runs at varying conditions so that empirical correlations could be tested. All runs were made on the same type of coal at constant slurry temperature, −200 mesh content, screen slot opening ¼ mm, and zero vibration. Results are shown in Table VI.

To obtain a correlation of final moisture content as a function of these four variables, a theoretical approach is necessary. Moisture removal in vacuum filtration is primarily obtained by the drawing of air through the filter cake. As the amount of air, temperature, and contact time are relatively small, it would appear that evaporation would play an insignificant part. Rather, moisture removal will be largely a function of entrainment or propelling of water by the moving air. From these considerations, water removal or final moisture content should be primarily a function of air velocity, length of time the air passes through the cake, and cake permeability. As air velocity through the cake will increase as the air expands, it was decided to base air velocity at the average cake pressure, i.e., atmospheric pressure minus one-half the vacuum level. Air velocity through the interstices of the cake, which is impossible to measure, will be a function of air quantity at the average cake pressure per square foot of filter surface. Finally, pressure drop per unit length of cake is a function of cake permeability and accordingly can be used as a more convenient measure.

From this theoretical reasoning, a correlation for final moisture content as a function of $(\text{cfm/ft}^2)_{\text{avg}}$ (θ) $(\Delta P/L)$ was attempted where:

$(\text{cfm/ft}^2)_{\text{avg}}$ = Cubic feet of air per minute per square foot of filter area at average cake pressure.
θ = Drying time in minutes.
ΔP = Pressure drop in inches of mercury.
L = Thickness of filter cake in inches.

Table V. Average Size Consist, Experimental Vacuum Filtration Coal

U.S. Standard Mesh	Wt, Pct
+6	0.3
6x8	9.1
8x12	11.9
12x20	21.0
20x40	16.7
40x60	11.2
60x100	8.7
100x200	7.0
−200	14.1

Table VI. Experimental Vacuum Filtration Tests, Slurry Temperature 80°F, Laboratory Coal

Test No.	Vibration, Pct Full Intensity	Standard Cfm Per Sq Ft*	Vacuum, In. Mercury	Filtration Time, Min	Cake Thickness, In.	Total Cake Moisture—Wt, Pct
1	48	10.65	27.10	1.31	1.01	13.76
2	48	2.45	23.63	4.06	1.01	12.53
3	48	0.314	19.66	21.10	1.00	11.73
4	48	3.854	19.36	2.40	0.98	14.43
5	48	4.24	15.81	2.25	0.99	16.05
6	48	1.354	17.37	10.10	0.97	13.96
7	48	2.835	17.17	4.92	0.94	15.92
8	48	0.943	17.38	14.35	0.95	13.60
9	0	3.300	17.50	4.10	1.07	12.76
10	0	3.054	17.47	4.48	1.10	12.44
11	0	3.255	17.54	4.20	1.05	12.95
12	0	3.667	17.45	3.73	1.13	12.87
13	0	2.955	12.61	4.58	1.10	13.19
14	0	2.897	17.43	4.72	1.12	12.91
15	0	3.377	17.56	4.05	1.12	13.04
16	0	2.735	17.45	5.00	1.07	12.76
17	0	2.339	17.52	5.85	1.10	12.55
18	0	1.960	17.45	6.91	1.11	12.23
19	0	3.059	17.57	4.47	1.10	13.20
20	0	2.660	17.72	5.14	1.11	13.32
21	0	2.094	17.49	2.64	1.11	14.11
22	0	2.546	17.40	1.14	1.10	15.89
23	0	3.020	17.43	2.70	1.09	13.43
24	0	2.683	17.66	8.24	1.11	11.85
25	0	3.959	17.47	9.07	1.13	11.54
26	0	3.030	17.74	19.18	1.08	10.77
27	0	3.220	27.60	4.29	1.12	11.83
28	0	2.438	23.91	5.67	1.13	11.73
29	0	2.281	20.76	6.12	1.09	11.89
30	0	3.472	13.81	3.98	1.13	13.34
31	0	2.768	10.74	4.94	1.14	14.14
32	0	3.013	7.84	4.54	1.13	14.83
33	0	2.247	4.73	6.02	1.14	16.15
36	0	6.17	17.61	2.24	0.66	12.93
37	0	2.867	12.52	4.77	1.10	13.04
38	0	2.064	17.59	6.70	1.58	13.01
39	0	1.777	17.50	7.70	2.09	14.00
40	0	1.237	17.51	11.05	2.85	13.63
45	0	3.213	17.62	4.26	1.14	12.76
46	0	3.886	17.53	3.52	1.13	13.00
47	0	3.209	17.62	4.31	1.11	13.99
48	0	4.04	17.53	3.38	1.12	13.51
49	0	3.331	17.69	4.15	1.15	12.52
50	0	3.372	17.53	4.10	1.15	12.62
51	0	2.634	17.55	5.25	1.14	12.40
52	10	1.230	17.65	11.23	1.03	11.67
53	33	0.575	17.53	24.01	0.97	12.39
54	70	0.820	17.47	16.84	0.97	13.94

* Standard conditions 14.7 psia and 80°F.

Fig. 4 illustrates the reasonable correlation obtained. Other methods were also tried, but none yielded as good an agreement.

Several important concepts can be derived from the resultant curve. The decided break in the curve is again apparent as in Fig. 3, indicating the importance of designing the filter to operate at or slightly beyond this point. Overdesign merely results in wasted filter capacity or unnecessary power costs on the vacuum pumps. The important interactions of the four variables should be stressed. If cake thickness is increased too far, air rate through the cake will be reduced, resulting in insufficient air velocities to perform the potential economic moisture removal of vacuum filtration. Drying time can be increased by use of greater area, but this will automatically require greater amounts of air per square foot of area. If sufficient care is not exercised, oversizing of the filters may result.

Vibration Intensity

In order to prove the value of the correlation method, the pilot plant data of Table IV are also plotted in the same manner in Fig. 5. Again a reasonable correlation exists. Data for the pilot plant vibration tests were not plotted, as they definitely exhibited anomalies indicating that vibration was displaying a random effect. Undoubtedly, as will be later shown, this was caused by improper application of vibration.

Vibration tests on the experimental vacuum unit are also listed in Table VI. However, results were random, as with the pilot plant unit, and good agreement was not obtained. Two reasons are considered to have caused this effect. First, the filter cake in the experimental unit is formed under static conditions, and this necessitates a small pickup time, which may permit segregation to occur. With no vibration, this did not occur, but segregation did result upon application of vibration. Secondly, the high −200 mesh content, 14.1 pct, in combination with the segregation effect with vibration undoubtedly caused excessive plugging of the interstices within the cake. With lower slime feed slurries, segregation would not occur, because of the shorter pickup time; thus vibration effects could be reliably ascertained.

One quantitative indication of the effect of vibration can be obtained from the experimental data of Table VI. With equal feed slurry volumes and solids concentrations, cake thickness without vibration averaged 1.11 in., whereas with vibration this value was 0.98 in. A 12 pct decrease in cake thickness is thereby obtained by vibration, which undoubtedly aids in moisture removal when it is correctly applied.

As proof of the beneficial advantages of vibration, the operating data for the full-scale unit have been plotted in the same correlation manner in Fig. 6. The smooth curve for the pilot plant data of Fig. 5 is also indicated. It will be observed that the values lie below the smooth curve from 2 to 5 pct. The advantages of vibration become self-evident when displayed in this manner. It should also be noted that the full-scale data cluster about the correlating factor region where the break point occurs in the smooth pilot plant curve. This indicates that the filter has been correctly scaled-up for the installation.

Feed Slurry Temperature

As filter cake temperature increases, air velocity through the cake will also increase at the same standard cfm/ft² rate because of the temperature expansion effect on the air. Further, viscosity and surface tension of the water will also decrease, thus improving the permeability of the cake. Theoretically, therefore, feed temperature should have a quantitative effect on final moisture content.

A series of tests were made at varying feed temperatures as reported in Table VII. Comparing final water contents of the runs, it is apparent that moisture definitely decreases with an increase in temperature. Furthermore, it will be observed that all runs were made at essentially the same correlating coefficient, offering proof of temperature influence.

Table VII. Experimental Vacuum Filtration Tests, Varying Feed Slurry Temperatures, Laboratory Coal

Slurry, Degrees F	Standard Cfm Per Sq Ft	Vacuum, In. Mercury	Filtration Time, Min	Cake Thickness, In.	Total Cake Moisture—Wt, Pct	$(\text{Cfm/Ft}^2)_{\text{Avg}}\ (\theta)\ (\Delta P/L)$
40	2.787	17.66	4.96	1.09	13.34	384
58	2.620	17.55	5.22	1.10	12.43	372
100	2.680	17.77	5.16	1.14	12.51	373
120	2.520	17.60	5.43	1.13	12.13	364

C. Fuhrmeister in an earlier paper[1] listed industrial data for vacuum filtration indicating an increase in filtration rate, expressed as pounds of cake per square foot per hour, of 1 pct per degree Fahrenheit. Furthermore, he observed a 1.6 pct drop in final moisture content for an 80°F temperature increase which closely parallels this work.

Mr. R. L. Sutherland of the Truax-Traer Coal Co. has noted[2] that there is a close correlation between final moisture content of the finished coal at the Ceredo plant and the circulating water temperature. In the winter months when water temperatures are approximately 40°F, average moisture content of the loaded coal is 5.8 pct. When water temperatures reach 79°F in the summer months, moisture content is only 4.75 pct. This points to the possible advantages of a closed water system wherein water temperatures can be maintained at 70° to 80°F to obtain approximately a 1 pct decrease in final moisture contents. When thermal drying installation and operating costs are considered, it may be more economical to maintain water temperatures at 70° to 80°F and blend the filter cake with the coarse coal. Studies are worthwhile to ascertain not only how much water would be removed by the two methods, but also exactly how much each pound of water removal costs.

Tri-Rod Slot Openings

Referring to Table IV, runs 46 and 50 were made with 0.001-in. B-Z tri-rod screen, runs 45 and 49 with 0.005-in. B-Z tri-rod screen, and runs 47 and 48 with 0.020-in. B-Z tri-rod screen. The remainder were all made with 0.010-in. B-Z tri-rod. No appreciable effect on the final moisture content could be observed. However, there was a decided influence, as would be expected, upon the loss of solids in the filtrate. Table VIII gives a summary of these effects; special attention should be paid to the —200 mesh removal.

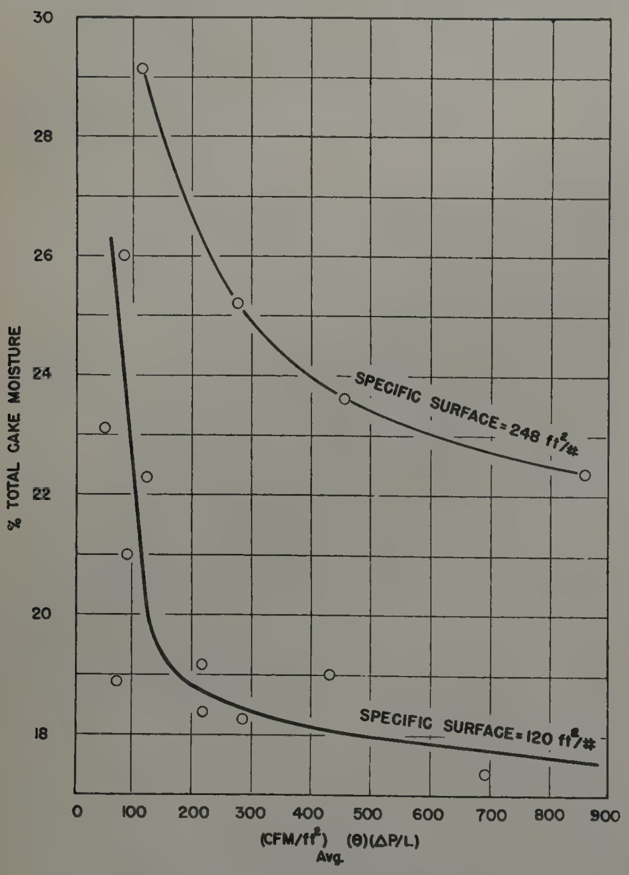

Fig. 5—Percent final moisture as a function of $(\text{cfm}/\text{ft}^2)_{\text{Avg}}(\theta)$ $(\Delta P/L)$, from Truax-Traer pilot plant data. No vibration applied.

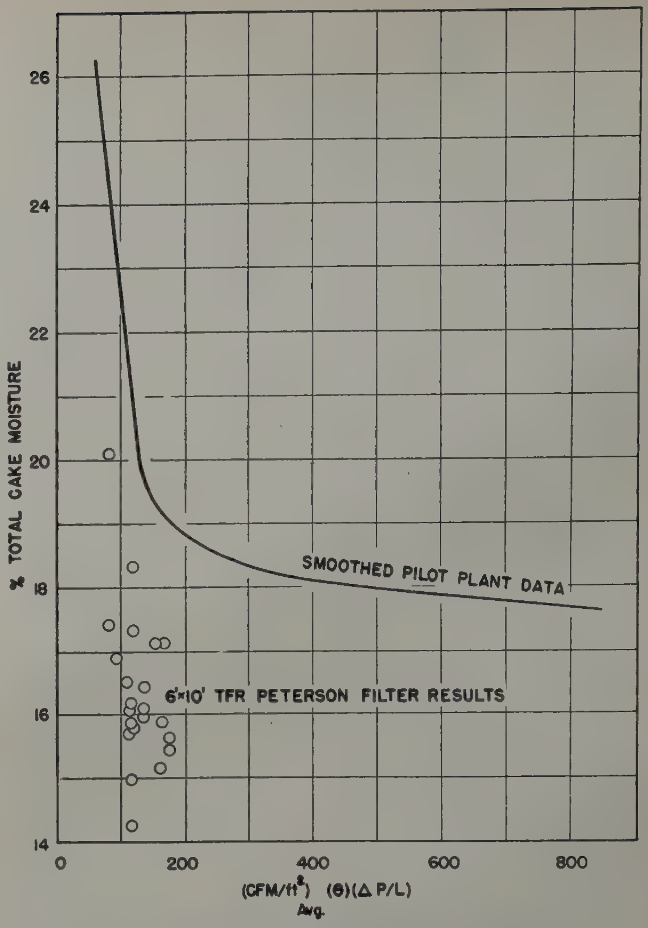

Fig. 6—Comparison of 6x10-ft TFR Peterson Filter results with vibration and smoothed pilot plant data without vibration.

It will be observed that slime removal increases steadily with opening. However, loss of desirable solids is probably excessive for the 0.020-in. size. Thus it is apparent that appreciable removal of high ash slimes can be effected in the filter but will be limited to the coarse solids loss that can be tolerated. However, 10.3 pct slime removal obtained with the 0.010-in. screen would represent a desirable decrease in final ash content of the filter cake. Naturally, the percentage amount of slime removed will also vary with cake thickness.

—200 Mesh Content

The influence of slimes upon final moisture content and filtration capacity has been stressed in many articles. Undoubtedly this is a prime factor in filter operation. Most authors emphasize the importance of desliming in increasing filtration rates and moisture removal. Fuhrmeister indicated data in his paper where a 25 pct increase in —200 mesh content decreased filter cake tonnage rate 30 pct and increased moisture content 38 pct. The economics of such unwanted inclusions are self-evident. Similar evidence is presented in the two curves of Fig. 3, where appreciable increases in moisture content and lowered rates were experienced with higher slime content coal.

A series of runs were made on the experimental coal with varying amounts of —200 mesh pct. Results are given in Table IX. Upon investigation of the data, it will be apparent that filtration time decreases rapidly with a decrease in —200 mesh content, indicating the sizable increase in filtration capacity that results. Furthermore, there is a definite decrease in final moisture content, although not as marked. It should be noted that air rate becomes excessive at slime contents below 2 pct. This is definite proof of the serious influence of slime percent on cake permeability. However, it should be apparent that some slime content is probably necessary for vacuum filtration. If the cake becomes too permeable, it will be difficult to prime the filter and hold a cake. As previously mentioned, this can be overcome by modification of filter design.

Filtration installation and operation costs are high, while desliming costs due to the advent of the cyclone are very low. Thus the economics certainly justify the inclusion of desliming equipment when necessary in any filtration flowsheet.

Filter Scale-Up

To prove that filters can be scaled-up by the experimental tests and correlation methods outlined in this paper, runs were made on the vacuum unit at Northwestern on sample material from the feed to the full-scale units at Ceredo. Complete operating data and moisture tests were recorded at the plant on the day each sample was taken. The correlation between the tests is indicated in Table X. Excellent agreement was obtained, as attested by the similarity of the data. It is feasible, therefore, first to run simple filtration tests, taking the recommended data, and thus scale up the unit so that operation will result at maximum economy.

Summary

Successful application of the Peterson Top Feed Reservoir vacuum filter to mechanical dewatering of 14x150 mesh coal has been achieved at the Truax-Traer Coal Co., Ceredo, West Va. Surface moistures will range from 13 to 17 pct, and capacities up to 100 tons per hr of dry solids have been handled on the two 6x10-ft units. Maintenance and repair have been negligible, while operation is uniform and relatively simple, in spite of the large surges in solids rate of this fine coal. Vibrators are also utilized on the filters where they serve to compact the resultant smoother cake, and thus squeeze out more of the water. The pilot plant studies to obtain feasibility and scale-up information are discussed and special emphasis is placed on correct full-scale design. Care must be taken so that filtration equipment is not overdesigned, causing excessive power costs and inefficiently used capacity.

An experimental program on vacuum filtration investigated all important variables under closely controlled conditions. A reasonable correlation for final moisture as a function of air rate, drying time, and cake permeability ($\Delta P/L$) for a specific coal was obtained, which also appeared theoretically sound. This method can be used on any fine solids for filter scale-up by making a few simple vacuum filtration tests as indicated with such data being measured.

Vibration was proved to be beneficial for the Truax-Traer installation, as it lowers final moisture by 2 to 5 pct. Tri-rod screen size appeared to have little effect on total water content, although small but important desliming was achieved with little loss of +200 mesh coal up to 0.010-in. slot opening. Slurry feed temperature increase will decrease water content as well as increase filtration rate. Special studies should be made of the economics of heating circulating water as against the high expense of thermal drying. Finally, the importance of desliming has been stressed, as slime inclusions exert a pronounced effect by raising moisture and lowering filtration capacities. In most applications of vacuum filtration to coal solids, desliming will be mandatory to eliminate this troublesome material, as economics will more than justify it.

Table VIII. Influence of Slot Opening on Slime Removal and Solids Loss

B-Z Tri-Rod, Nominal In. Slot Opening	Feed Solids in Filtrate, Pct	—200 Mesh in Filtrate Solids, Pct	Loss +200 Mesh to Filtrate, Pct*	—200 Mesh Removal in Filtrate, Pct
0.001	0.80	70.4	0.28	4.0
0.005	1.75	61.1	0.79	7.6
0.010	2.50	58.1	1.22	10.3
0.020	5.60	46.4	3.50	18.4

* Based on 14.1 pct —200 mesh in feed.

Table IX. Influence of —200 Mesh Content on Filtration Results, Laboratory Experimental Coal

—200 Mesh, Pct	Standard Cfm Per Sq Ft	Vacuum; In. Mercury	Filtration Time, Min	Cake Thickness, In.	Total Cake Moisture—Wt, Pct
14.1	3.020	17.43	2.70	1.09	13.43
7.7	8.91	17.66	1.55	1.13	13.00
5.1	13.82	17.50	0.98	1.07	13.36
1.8	115	7.00	0.24	1.11	11.75
0.7	251	17.08	0.11	1.07	9.47

Table X. Comparison of Actual and Experimentally Predicted Results

	Test 1		Test 2	
	Actual	Experimental	Actual	Experimental
Total cake moisture, pct	18.1	18.85	16.1	16.31
Standard cfm/ft²	17.1	17.24	14.8	20.63
Vacuum, in. mercury	10.5	10.7	12.5	12.45
Cake thickness, in.	2.5	2.27	3.0	2.80
Drying time, min.	1.85	1.81	1.39	1.39

Acknowledgments

The authors wish to thank the Truax-Traer Coal Co. and its personnel for their consideration and constant cooperation. Special appreciation is due Mr. R. L. Sutherland of that company for his help, thoughtfulness, and valuable advice.

References

[1] C. Fuhrmeister: Improving Filtration and Filtration Rates. *Chemical Engineering Progress*, November 1951.

[2] R. L. Sutherland: Recovering and Desliming Fine Coal with Cyclones, Cincinnati Meeting, American Mining Congress, April 1950.

[3] D. A. Dahlstrom: Low-Cost Industrial Desliming of Fine Solids. Joint Fuels Conference, AIME, ASME, Oct. 10 and 11, 1951, Roanoke, Va.

[4] J. L. Lewis: The Treatment of Slurries. *Colliery Guardian*, Sept. 3, 1948.

[5] O. R. Lyons: Filter Cake Size-Consist and Moisture Relationships. *Trans.* AIME (1951) **190**, pp. 868-870.

[6] D. R. Mitchell, ed.: *Coal Preparation.* AIME, 1950.

[7] A. F. Taggert: *Handbook of Mineral Dressing.* John Wiley and Sons, New York, 1945.

[8] A. F. Taggert: *Elements of Ore Dressing.* John Wiley and Sons, New York, 1951.

Features Incorporated in the Design of Lone Star's Two New Dry Process Cement Plants

by Claiborne C. Van Zandt

THE heavy postwar demand for Portland Cement has created shortages that are gradually being overcome by increases in plant capacity. In the postwar period, the Lone Star Cement Corp. has expanded several of its existing 15 plants and has built 2 new plants, now in operation, with a third new plant under construction in Brazil, of design somewhat different from that of the two preceding ones.

The new domestic plants are located at Lone Star, Va., near Roanoke, and at Maryneal, Tex., near Sweetwater, and went into operation during 1951. Each plant is equipped with two rotary kilns and has an initial capacity of 1,500,000 bbl per year, or 6,000,000 sacks. The total cost of each plant was about $10,500,000, and on this basis $7.00 in 1951 money are required per bbl of annual capacity; at 376 lb per bbl, this corresponds to $37.00 per ton of output. The investment corresponds to approximately $80,000 per hourly-wage earner employed.

The purpose of this paper is to describe the most interesting design features of the two new and almost identical Lone Star plants.

Why the Dry Process Was Chosen

The two new domestic Lone Star mills employ the dry process because: 1—The raw materials at both properties are particularly suitable and can be dried very readily. 2—The Maryneal, Tex., plant does not have water available for slurry. 3—Very substantial kiln fuel savings can be obtained. 4—Dry raw grinding reduces ball and liner wear and general maintenance, without any sacrifice in power.

Operating costs to date have more than justified the choice of the dry process for these two plants.

Raw Materials

The chemical composition of Portland Cement raw material after crushing, grinding, and mixing, but before burning, is about as follows:

Item	Pct	
$CaCO_3$	75-78	Limestone, marl, and shell
$MgCO_3$	1-3	
SiO_2	13-15	Shale, clay, and blast furnace slag
Al_2O_3	3-5	
Fe_2O_3	2-4	

Shales and clays generally do not contain sufficient SiO_2 and Fe_2O_3, and these components must, therefore, be added in the form of sand, iron ore, and sometimes tailings from an iron ore concentrating plant. Certain objectionable materials occur in raw mix: magnesia, limited in cement to 5 pct, in excessive amounts; alkalies, as sodium and potassium; phosphorous; and sulphur, generally present in coal and oil.

The Roanoke raw materials are dense limestone and shale. The Maryneal materials are soft limestone and a hard brittle clay that can be handled much like shale. Sand and iron ore are required in small quantities.

General Plant Layout and Construction

The two plants are so similar that one joint description will cover both, with such exceptions as will be especially indicated.

The crushing plant is located in the quarry, and raw material is conveyed by belt to the storage building, where all materials are stored and handled. Fig. 1 identifies the various structures of the Roanoke plant. The large storage building is used for the storing and handling of all materials, including limestone, shale, sand, iron ore, coal, clinker, and gypsum. Directly adjoining the storage building is a structure under a similar arched roof, containing the raw and clinker grinding departments and the electrical substation. The discharge ends of kilns and coolers, and coal or gas burning equipment are also placed at one end of the mill building. The 340-ft long kilns extend away from the main buildings to form the long leg of an L, at the end of which is the feeding and kiln dust collecting equipment, and the raw blending silos are conveniently located adjacent to the feed end of the kilns.

The machine shop, storeroom, electrical shop, foremen's office, service rooms, and meeting hall are combined in one structure in the center of the plant, and the office and laboratory are close by.

The cement silos and packhouse do not have to be tied directly into the manufacturing process and are therefore located at a point convenient to the railroad tracks.

C. C. VAN ZANDT, Member AIME, is Vice President, Lone Star Cement Corp.

Discussion on this paper, TP 3426H, may be sent (2 copies) to AIME before January 31, 1953. Manuscript, March 21, 1952. New York Meeting, February 1952.

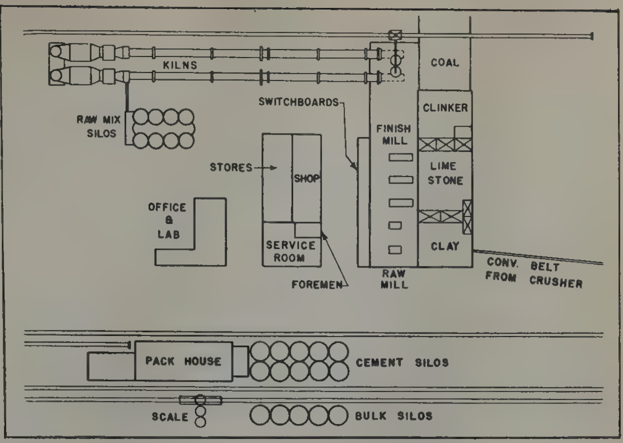

Fig. 1—General plant layout, Roanoke.

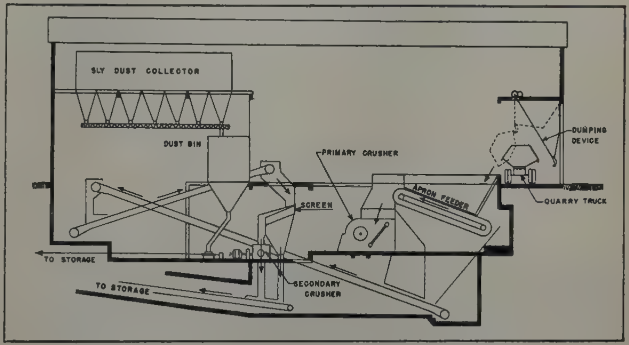

Fig. 2—The crushing plant.

The compact arrangement with centralized service, shop, offices, and laboratory has greatly simplified maintenance and supervision. Full provision has been made within the existing buildings to install additional equipment for increasing plant capacity at Roanoke by 50 pct and at Maryneal by 100 pct. Electrical power systems, pipelines, conveyors, and shipping facilities are also installed for these higher ultimate capacities.

Operations are on a 24-hr, 365-day basis except at packhouse, quarry, and crushing plant, where a 40-hr work week is normally observed.

Almost the entire plant is constructed of reinforced concrete, including the two continuous barrel roofs covering the storage, burning, and grinding buildings. Other concrete or portland cement products are also employed, such as concrete block and Transite siding and roofing. Aside from the use of the company's product, it is found that concrete construction results in a much more attractive structure, which is free of vibration and remains much cleaner than a fabricated steel structure. Painting is required only on machinery items. Corrulux translucent siding has been widely employed at Maryneal with very satisfactory results, building interiors being very well lighted during the daytime.

Quarrying and Crushing

Bucyrus No. 27-T well drills are used for blast holes at Roanoke, and limestone and shale are removed from the quarry by two Marion 3 cu yd type 492 electric shovels and Mack tractors equipped with Easton 16-ton side-dump trailers.

Primary crushing is done at Roanoke in a 42-in. Allis-Chalmers gyratory driven by a 200-hp motor followed by a CF-15-50 Pennsylvania reversible impactor driven at 900 rpm by a 400-hp motor. The impactor is operated in closed circuit with two 5 ft 0 in. x 11 ft 6 in. rod-deck Ripl-Flo screens with rod spacing of ⅝ in. At the Sylvester quarry, about 35 miles from Maryneal, a hard clay resembling shale is dug with a 1½-yd Marion diesel drag line and transported by rail to the plant, where it is crushed in a Pennsylvania roll crusher. At Maryneal a Joy Model 225 rotary drill is mounted on a Ford chassis and is used for drilling both the limestone deposit at the plant and the clay deposit at Sylvester. A 4-cu yd Bucyrus No. 100-B electric shovel and Mack tractors with 16-ton Easton trailers supply limestone to a Pioneer 72-in. x 21 ft 6 in. apron feeder.

Fig. 3 is a diagram of the crushing plant at Maryneal. The primary crusher, a No. 7260 Dixie Hammermill, is followed by a 6 ft x 12 ft Ripl-Flo scalping screen and a No. HM-05 Hammermills, Inc. crusher for oversize.

An Eriez Metal Detector is installed at the belt conveyor leading from the primary to the secondary crusher. It consists of a detector coil which circles the belt, and an electronic control cabinet. When a

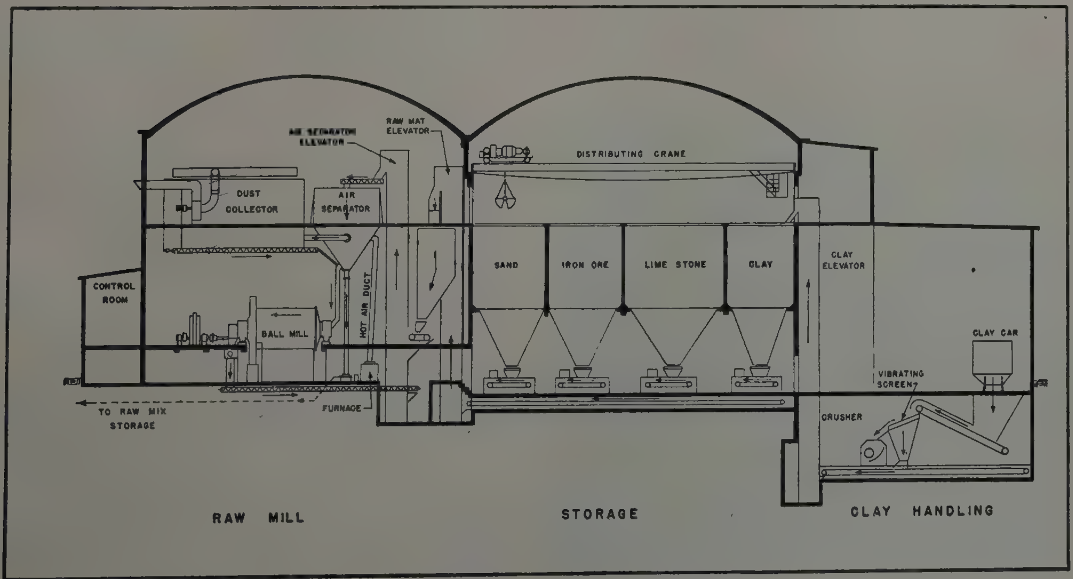

Fig. 3—Raw grinding and clay handling system.

piece of tramp metal, magnetic or nonmagnetic, passes through the coil, the belt and primary feeder are stopped and a horn is blown. The operator then knows the spot where he will find the tramp metal, and after its removal he restarts the equipment. This device and a similar detector which has been in use for about 18 months at a Lone Star crushing plant in Alabama have resulted in the discovery and removal of much objectionable metal that would otherwise have caused extensive damage.

Storage Buildings

The storage building is a reinforced concrete structure 75 ft wide and 340 ft long, served by two 10-ton Bedford cranes with 3-cu yd Blaw-Knox clam shell buckets. The various raw material components and cement clinker are stored where designated by the Chief Chemist and are transferred to the feed bins as required. A Merrick Feed-O-Weight is located under each feed bin, so that materials can be accurately withdrawn at a predetermined rate.

The thin concrete barrel roofs represent a type of construction rapidly gaining favor. They are economical, require only a small movable form, and present a very cleancut, pleasing appearance.

Drying and Raw Grinding

Fig. 3 shows the flowsheet of the raw material drying and grinding system, as well as the clay crushing plant installed only at Maryneal.

Raw materials are delivered by bucket crane to the raw feed hoppers. Merrick Feed-O-Weights measure out each material in the required proportions and the mixture is then delivered to the raw ball-mill feed bins. From here it is withdrawn as required; the feed rate is manually controlled by the operator who occasionally checks the recording ammeter connected to the air separator elevator motors. A circulating load of 500 pct is maintained.

Two completely separate raw grinding units are employed. Each unit is composed of a 9½-ft diam by 15-ft single compartment Allis-Chalmers ball mill driven by a 700 hp motor, operated in closed circuit with a 16-ft Sturtevant air separator driven by a 100-hp motor. A mill with motor is shown in Fig. 4. The raw material is fed directly to the air separators, which are supplied with hot air for drying by means of oil or gas fired air heaters. Each air heater automatically supplies the amount of heat required to drive off the moisture. These heaters are fired with oil at the Roanoke plant and natural gas at Maryneal. Each air separator discharges tailings to its respective ball mill, the mill output being returned to the air separator. The moisture-laden gases leaving the air separator are held to a maximum temperature of 200°F and are exhausted through a 35-ft long, 18,000 cfm Northern Blower dust collector and fan driven by a 50-hp motor. No hot air is passed through the mills, as all the drying is done in the air separators. Separators, duct work, conveyors, and elevators are all thoroughly insulated to retain as much heat as possible in the system and prevent condensation. The heat of grinding within the ball mills is thus maintained and assists materially in the drying. It is believed that these raw grinding and drying installations are the first to employ ball mills in closed circuit having air separators with raw material fed first to the separators, and the results have far exceeded expectations.

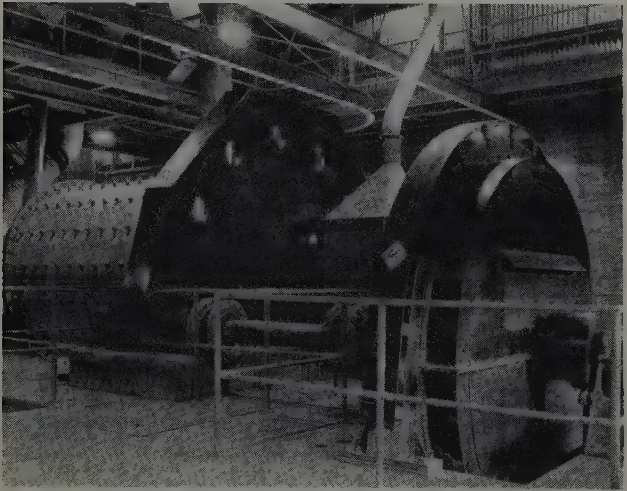

Fig. 4—Allis-Chalmers ball mill and motor.

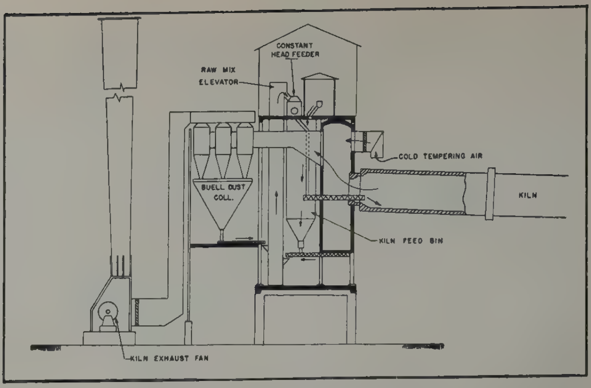

Fig. 5—Kiln feed arrangement.

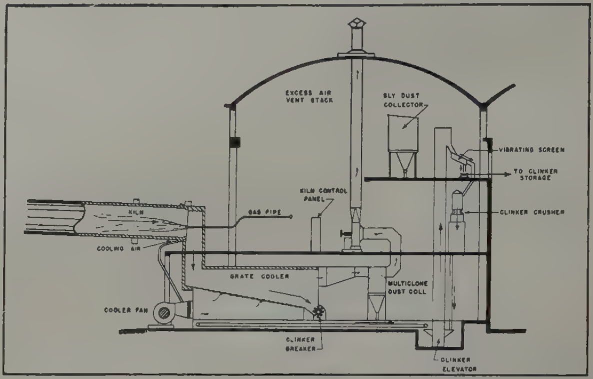

Fig. 6—Kiln department, burning and cooling system.

The actual performance data at Roanoke is given in Table I. The figures represent a monthly average and are not for test periods. On some days the output greatly exceeds the overall average. The output is much higher than required and the mills have never been fully charged to determine their ultimate capacity.

The raw grinding system operates without trouble, even though at Maryneal the moisture content of the feed has averaged 5.9 pct, with periods of 8 pct.

The heat delivered to the separators is adjusted automatically to take care of moisture fluctuations in the raw material. Approximately 15,000 cfm of hot gases are drawn through each Sturtevant separator. Exit temperature is kept at 180° to 200°F, while the inlet gases from the air heater will vary from 400° to 850°F maximum. Moisture-laden air

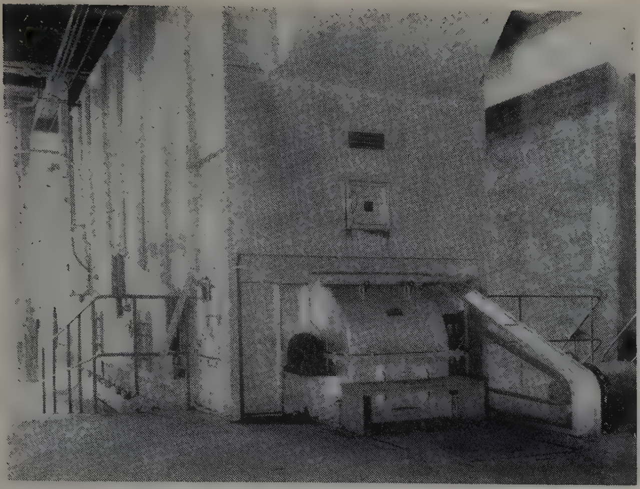

Fig. 7—Air quenching cooler.

from the separators is exhausted through a collector. The separator fines run less than 1 pct moisture, and are conveyed by a Fuller-Kinyon system to the raw blending silos located near the feed end of the kilns. Every part of each raw grinding system is under suction and is connected to the Norblo unit which handles the gases from the air separator. The raw mill department is therefore entirely dust-free.

Table I. Typical Data for Two Raw Grinding Units Operated in Parallel, Lone Star Plant, Roanoke, Va., and one Unit, Lone Star Plant, Maryneal, Texas

ROANOKE, VA.	
Output, monthly average	70 to 80 net tons per hr
Fineness	91 to 93 —200 mesh
Moisture in feed, 30-day average	Dry months 2.8 pct Wet months 4.3 pct
Moisture in product, 30-day average	.15 to .30 pct
Typical Power Requirements	**KW**
Two 9½x15 ft ball mills	1000
Two 16-ft air separators	129.6
Two air separator elevators	33.8
Two Norblo exhaust fans	48.6
Two oil furnaces	18.2
All feeders and conveyors	41.7
	1271.9
Fuller-Kinyon system raw mill to silos	139.1
Kw-hr per ton mills only	12.5
Kw-hr per ton auxiliaries	3.4
	15.9 kw-hr per ton
Requirement for the Fuller-Kinyon system	1.74 kw-hr per ton
Heat Requirements	
Fuel oil per ton	.55 to .85 gal
Btu per ton of material dried	80,000 to 131,000
Btu per bbl of equivalent cement	23,000 to 38,000
Gross heat required per lb water evaporated	1700 Btu
MARYNEAL, TEXAS	
Moisture in feed, 8-month avg	5.9 pct
Moisture in feed, 30-day avg	8.0 pct (in wet months)
Moisture in product	.65 pct
Gross heat required per lb water evaporated	1730 btu

Raw Mixing and Blending

The blending system includes 11 silos 85 ft high, each with a capacity equivalent to 3000 bbl of cement. A Fuller rotary feeder is placed under each silo discharge cone, and each feeder has an individual adjustable speed drive. The conveying system permits blending, re-blending, and transferring, as required. A passenger elevator connects the various working floors.

Table II. Typical Kiln and Cooler Operating Data, Lone Star Plant, Roanoke, Va.

Kiln output, monthly avg	2000 bbl each
Coal consumption, as received	70 lb per bbl
Heat consumption at 13,600 btu	954,000 btu
Kiln exit gas temperature	1200° to 1400°F
Temperature of exit gas, cold air mixture	650°F
Kiln speed, actual	40 to 50 rph
Kiln motor input, normal	25 kw
Coal fineness	87 pct —200 mesh

Fig. 5 shows the kiln feed and equipment. Kilns are 10 ft in diam and 340 ft long and are placed on a slope of 7/16 in. per ft. The refractory lining is 6 in. thick. The actual power normally required to drive a kiln at 50 rph is 25 hp. The main gears encircling the kilns, of Falk single helical design, are driven by matching pinions which in turn are driven by Falk herringbone speed reducers. There is no vibration at any kiln speed such as frequently occurs with kilns equipped with straight spur gearing. The kilns are equipped with auxiliary gasoline engine drives for use in the event of power failure; these have been used many times.

Burning and Cooling

Each kiln is nominally rated at 2000 bbl output per day, and the burning zone temperature is about 2700°F, see Table II. They are fired at the lower end, the fuel being coal in Virginia and natural gas in Texas. Feeders are synchronized with drives to maintain a constant bed depth within the kilns.

Raw material is fed into the upper end of the kilns with horizontal screw conveyors, and the short drop from screw to kiln lining results in little dusting. This method is recommended as a great improvement over the conventional long inclined feed spout so often used. Fine raw mix drops from such a spout with a splash, and much material is then airswept out of the kiln.

The kiln exit gases pass through a Buell dust collector and then through a Prat-Daniel fan. At the Roanoke plant, the collector is followed by a Koppers Elex electrical dust precipitator which collects the very fine fractions. All dust is returned to the feeding system and thus back to the kilns.

Since the dust collectors and fans are constructed of ordinary steel, a maximum gas temperature of 700°F must not be exceeded. This is provided for by mixing cold air with 1300°F gases from the kiln.

Fig. 6 shows the cooling and burning arrangement at the discharge end of the kiln. The hot clinker dis-

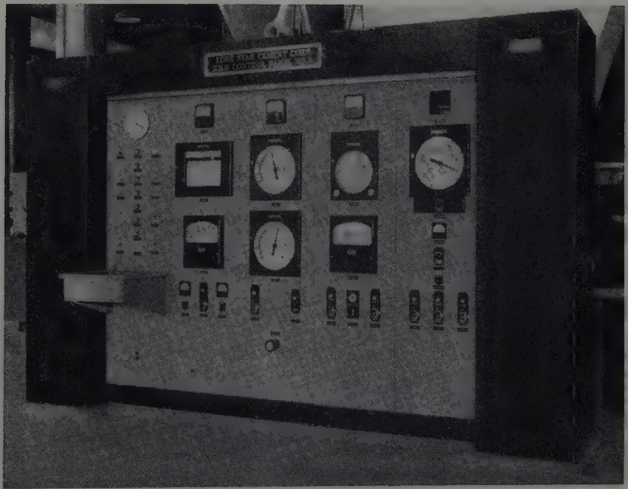

Fig. 8—Kiln control panel.

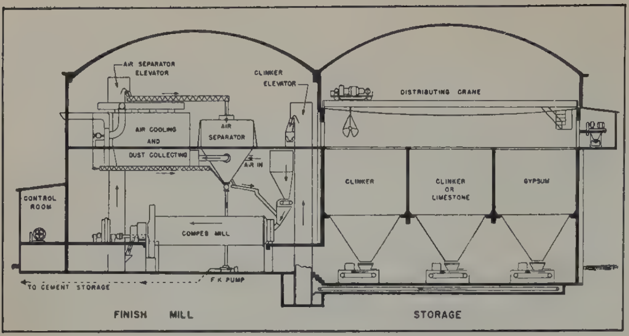

Fig. 9—Clinker grinding system.

charges to a Fuller grate-type air quenching cooler. Cold air is blown up through the clinker grates, and the hottest portion of the resulting heated air is returned to the kilns as combustion air. In order to bring the temperature of the clinker down to approximately 150°F, it is necessary to use considerably more air than is required for combustion. Excess air is vented through Multiclone dust collectors and fans, at a temperature varying from 200° to 300°F. The dust collectors recover the coarse clinker dust that would otherwise accumulate on the roofs and adjacent machinery.

Fig. 6 also shows an interesting feature developed by the Lone Star Cement Corp. now used on all grate-type cooler installations at company plants. It consists of a small hammermill which crushes all +1½-in. material and returns it to the inside of the cooler. Approximately 7 hp is consumed in this crushing operation. Since the oversize clinker is hot, it is given a second opportunity to cool when thrown back upon the grate.

Hammer wear is so slight that the clinker breakers need only be given attention once a year.

Although the clinker breakers reduce the material to −1½ in. in size and insure complete cooling by breaking up the hot chunks, much of the material is nevertheless too large for efficient grinding. All clinker is therefore sent over Aero-Vibe screens and the tailings recrushed in a No. 330 Hydrocone crusher to −⅜ in.

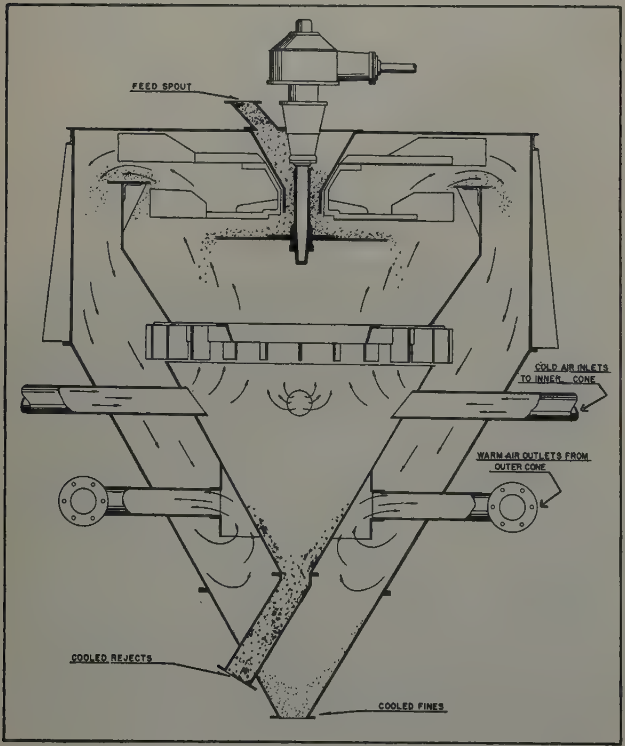
FEED SPOUT
COLD AIR INLETS TO INNER CONE
WARM AIR OUTLETS FROM OUTER CONE
COOLED REJECTS
COOLED FINES

Fig. 10—Air separator arranged for Norblo cement cooling system.

Fuel Firing

Raymond bowl mills serve as unit pulverizers for each of the Roanoke kilns. The coal mills are placed in the cooler rooms so that coal feeders can be on the burning platform where they can be watched by the kiln operator. The Maryneal natural gas burning system involves a 15-in. gas manifold automatically kept under 35-lb pressure. Burners are 3-in. pipes with 2-in. tips, and the tip pressure is about 5 lbs.

The kiln control panel illustrated on Fig. 8 carries instruments affecting the operation of the kilns and coolers, and a few essential controls that have been found by experience to be very useful. These include kiln exit gas temperature recorder, mixed kiln exit gas-air temperature recorder and warning horn, kiln speed recorder, natural gas flow meter, or coal feed controller, damper regulators, draft gages, feeder and kiln revolution counters, overgrate cooler pressure control, cooler grate speed control, kiln speed controller, and ammeters.

Clinker Grinding

Fig. 9 shows the clinker grinding department. The three main feed bins are placed within the storage building, one being reserved for clinker, one for limestone, and one for gypsum. Materials are drawn from the bins by means of totally enclosed Feed-O-Weights discharging into a drag conveyor, which in turn delivers the material to an elevator discharging to a second drag which fills the individual bins feeding each mill.

To prevent segregation, the individual mill bins are small, and individual feeders deliver feed to the mills at a rate determined by the power consumption of the elevator feeding the air separator. If the circulating load, which normally amounts to, say, 300 pct, increases or decreases below the desired value, a corresponding response appears on a recording ammeter and an adjustment is made manually by the operator.

Table IV. Typical Operating Data for Three 8x32-Ft Clinker Mills Operated in Parallel, in Closed Circuit with 16-Ft Air Separators*

Net output per mill	112 bbl per hr
Cement fineness	95 to 96 pct −325 mesh
Cement surface area	1750 to 1800 Wagner
Circulating load	About 400 pct
Mill motor input	640 Kw
Kw-hr per bbl, mill only	5.7
Kw-hr per bbl, auxiliaries	1.1
	6.8 kw-hr
Cement temperature	150°F

* Power figures do not include Fuller-Kinyon system.

The grinding equipment consists of three 8x32-ft two-compartment Allis-Chalmers Compeb Mills equipped with Lorain liners and operated in closed circuit with 16-ft air separators. Each mill is driven by an 800-hp motor, and each air separator by a 100-hp motor.

Each grinding unit is equipped with a 30-ft dust collector which keeps the entire grinding operation under suction and also draws about 10,000 cfm through each air separator to cool the cement. Fig. 10 illustrates the general method by which cold air is drawn into the inner cone of the separator and hot air removed from the space between the inner and outer cones. Table IV gives the actual operating performance. This system of cooling is very effective in that it cools the tailings as well as the finished cement and thus maintains the temperature of the grinding mill much lower than would otherwise be the case.

Cement ground without air cooling is generally discharged at a temperature between 230° and 270°F, sometimes higher. With the Norblo cooling system pictured, the temperature of the cement runs about 140° to 160°F as it leaves the grinding system, and cools considerably more by the time it reaches the packhouse. One test shows that 64 pct of the mechanical energy consumed by a Compeb mill is ultimately recovered as heat from the cooling air.

Ten clinker grinding units operated by Lone Star are now aircooled in this manner. This system is a great improvement over the conventional method of spraying the outside of the mill shells with water. It is interesting to note that the cement cooling system and the raw material drying system are alike, hot air being supplied to the air separator for drying and cold air for cooling.

Cement Storage

One group of silos is set aside for cement to be packaged, a second group exclusively for bulk cement.

Through the use of Fuller-Kinyon pumps, piping, valves, and hose switches, complete flexibility is maintained and cement from any silo can be delivered to any packing point. A passenger elevator serves the silos.

Bulk and Package Shipments

As about 65 pct of all cement is now shipped in bulk, one set of silos was set aside solely for this purpose, and cement is loaded directly from the side of each silo as shown in Fig. 11. A special bulk loading station and track scale are also provided, and cement for any silo can be pumped to this point. Fig. 11 shows a cross-section of the packhouse, where four packing stations are installed. One station is set aside solely for Masonry cement, and since there is no interconnection of equipment, contamination cannot take place. Another packing station is set aside for Incor, either air-entraining or plain. The two remaining stations are reserved for various types of standard cement. A unique feature of all the Lone Star packing plants is the circulating system employed. A constant head is maintained over the packing machines at all times, resulting in uniform and very accurate weights. Circulating tanks are provided so that a quick switch can be made from one type of cement to another.

The packing plants are kept immaculately clean, and working conditions are attractive.

General Dust Suppression

Many engineers have expressed surprise at the extensive use of drag conveyors in these new plants. Drags are often considered outmoded equipment never to be used where belt conveyors could be employed. There is no question about the low cost of belt conveyor operation, and this has been used where warranted. Belt conveyors, on the other hand, are dusty, and being a constant source of spill, they require continual cleanup. Properly designed drag conveyors are entirely self-contained and com-

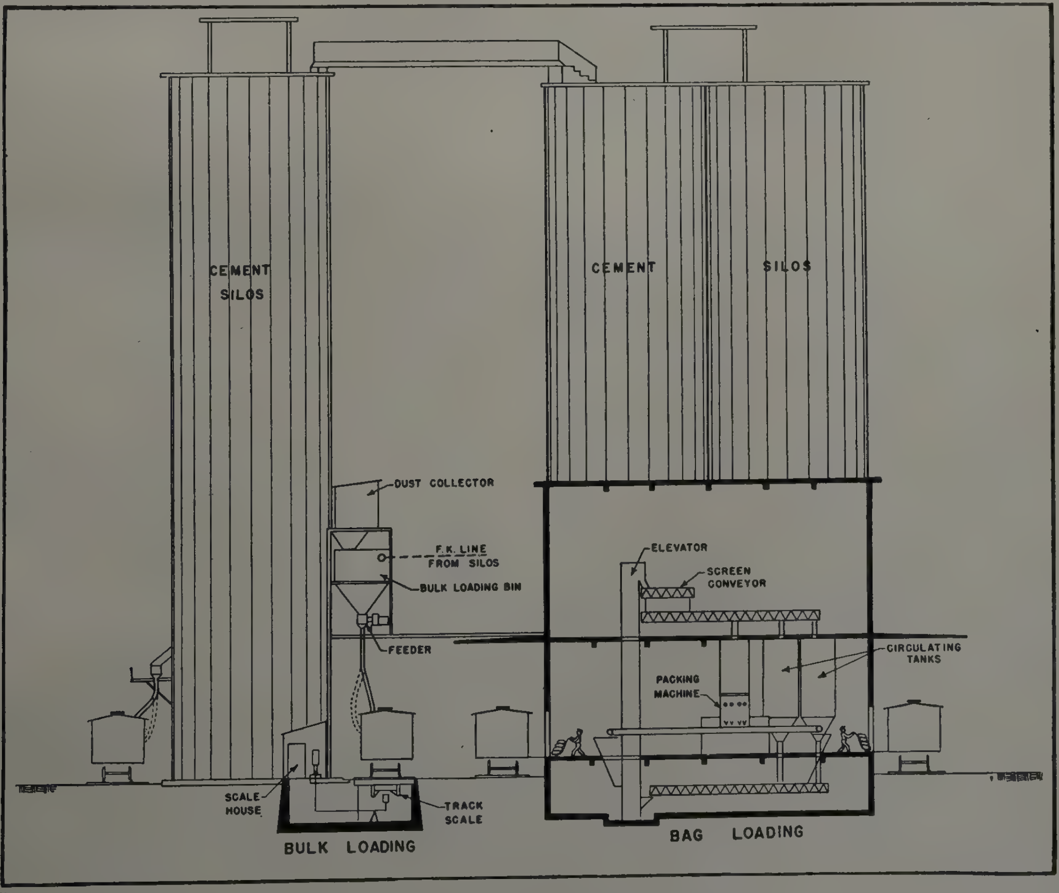

Fig. 11—Cement storage and shipping department.

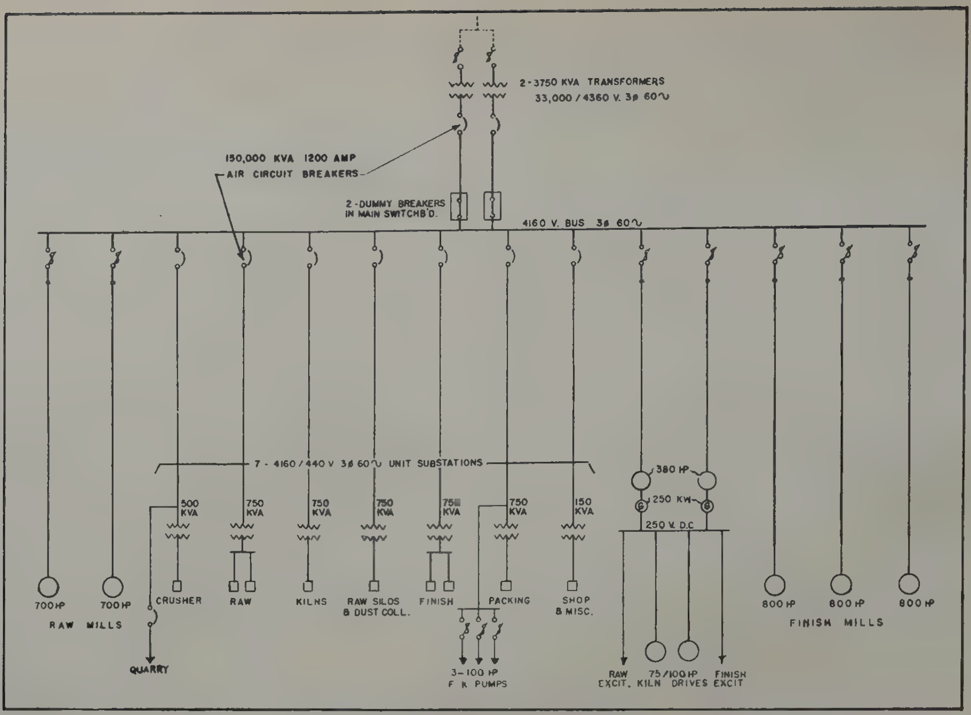

Fig. 12—Electrical distribution system.

pletely dustless. They require no cleanup whatsoever. The essential wearing parts are made of mangananese steel, and maintenance is very moderate. All the drag conveyors have tight covers, and one small dust pipe connection serves to keep an entire drag system clean.

Every machine, hopper, and silo in each plant is kept under suction, and this feature, together with good housekeeping, results in a well-swept appearance. The most serious dust problem at Maryneal is to keep the buildings tight enough to prevent dust entering from without during occasional dust storms.

Shops, Offices, Storeroom, and Laboratory

A concrete building 82x182 ft long is used for machine shop, storeroom, electrical shop, foremen's office, locker rooms, and washrooms. On the second floor of the building there is also a room that is used for safety meetings and for many other purposes. A serving kitchen with stove and refrigerating equipment is provided.

The office and laboratory is an L-shaped concrete building, completely air-conditioned, with superintendent's office in the center of the L, the assistant superintendent's office and drafting room at one side, and a meeting room with special ventilating equipment at the other. Foremen's meetings are held every morning, and the room also serves to take care of special meetings which frequently occur. The remainder of one wing of the L houses the laboratory, and the other wing takes care of the clerical and timekeeping office. Washroom and locker room facilities are centrally located.

Electrical System

Fig. 12 is a one-line diagram prepared for the Roanoke plant. The electrical shop is located at one end of the machine shop, in the most central part of the plant. Typical power requirements at Roanoke are as follows:

Item	Pct
Quarry	.28
Crushing	.65
Raw drying and grinding	5.70
Blending	1.20
Burning and cooling, and kiln dust collecting	3.90
Coal burning*	1.07
Clinker storage and grinding	8.10
Packing and shipping	.58
Total	21.48 kw-hr per bbl

* The Maryneal, Tex., plant has no coal burning charge, as gas is used for fuel.

A 4360-v distribution system supplies all the General Electric unit substations, the quarry shovels, and all motors 300-hp and larger, including Ball and Compeb Mill synchronous motors and synchronous M-G sets. The synchronous motors are 80 pct power factor machines and the system power factor is kept near unity.

All motors 300-hp and larger are wound for 4000/2300 volts so they can be transferred to any Lone Star plant operating at 2300 volts if the need should arise. These large motors and the main switchboard were supplied by Allis-Chalmers. All motors 250-hp and smaller and all gearmotors were supplied by General Electric. Each mill motor is equipped with inching equipment used for spotting the mills for inspection or charging.

The main switchboard, all synchronous motor starters, M-G sets, raw and finish unit substation, raw and finish grinding multi-unit control centers, and D.C. distribution equipment are placed in the substation lean-to adjacent to the mill building. A General Electric 4160/480-v unit substation is installed in each department of the plant to handle the 440-v load. All main circuit breakers are rated at 150,000-kva interrupting capacity and 1200 amp.

The main substation and where possible other substations are supplied with filtered air to eliminate the costly maintenance resulting from dust and moisture.

INDEX

Transactions, Mining Branch

American Institute of Mining and Metallurgical Engineers

January-December 1952, Vol. 193

PAGES IN EACH ISSUE

January	49-80	July	677-708
February	177-208	August	775-806
March	273-304	September	875-906
April	369-400	October	957-988
May	477-508	November	1053-1084
June	573-604	December	1219-1250

A

Acid mine drainage 1075
Adsorption of Sodium Ion on Quartz 683
Adsorption on Quartz, from Aqueous Solution, of Barium and Laurate Ions 193
Allis-Chalmers Manufacturing Co.: *Effect of Heat Treatment and Certain Additives on the Strength of Fired Magnetite Pellets* 1223
  Factors in the Economics of Heat-Treated Taconites 962
  Glass and Chemical Sand Manufacture in the Edwards Paddle Scrubber 875
  Third Theory of Comminution 484
American Cyanamid Co.: *Radiotracer Studies of the Action of Dithiophosphate in the Selective Flotation of Galena and Sphalerite Using $CuSO_4$ and NaCN* 375
Anaconda Copper Co.: *Deep Hole Prospect Drilling at Miami, Tiger, and San Manuel, Arizona* 682
Anhydrite, source of sulphuric acid 959
Application of Coarse Coal Magnetite Separators in an Existing Circuit 983
Ash, R. L., Boddorff, R. D., Butler, C. T., and Kay, W. W.: *Drilling and Blasting Methods in Anthracite Open-Pit Mines* 884
Atlas Powder Co.: *Drilling and Blasting Methods in Anthracite Open-Pit Mines* 884
Augers, underground mining 677
Austin, Leslie: *Periclase Refractories in Rotary Kilns* 980

B

Bacon, L. O. and Wyble, D. O.: *Gravity Investigations in the Iron River—Crystal Falls Mining District of Michigan* 973
Ball mills: grinding costs 499
Ball shape, tests in grinding 500
Ban, Thomas E. and Cooke, Strathmore, R. B.: *Microstructures in Iron Ore Pellets* 1053
Barium and laurate ions, adsorption on quartz 193
Barr, James A., Burt, R. B., and Tillotson, I. S.: *Pipeline Transportation of Phosphate* 273
  discussion 1066
Barry, John G.: *Discussion on Geology of the Silver-Lead-Zinc Deposits of the Avalos-Providencia District of Mexico* 1083
Bartlett, Z. W., Lee, C. O., and Feierabend, R. H.: *Development and Operation of Sulphur Deposits in the Louisiana Marshes* 775
Battelle Memorial Institute: *Preparation of Low-Ash Coal* 1059
Belts, conveyor: control of acceleration 49
  deceleration 51
  fluid couplings 52
  protective magnetic equipment 61
  vertical curve determination 52
Berk, A. A.: *Formation of Acid Mine Drainage*. Discussion 1075
Bits: drill, diamond orientation in 177
Blasting: anthracite open-pit mines 884
  primary, Chile 300
  Swedish iron ore mines 189
  underground 189
Boddorff, R. D., Ash, R. L., Butler, C. T., and Kay, W. W.: *Drilling and Blasting Methods in Anthracite Open-Pit Mines* 884
Boeke, C. L. and Gunther, G. G.: *Deleading Zinc Concentrate at the Parral and Santa Barbara Mills* 495
  discussion 1067
Bond, Fred C.: *Discussion on Screened Ore Used for Fine Grinding at Lake Shore Mines* 1069
  The Third Theory of Comminution 484
  discussion 1071
Booth, R. B., Judson, C. M., Lerew, A. A., Kennedy, J. S., and Simard, G. L.: *Radiotracer Studies of the Action of Dithiophosphate in the Selective Flotation of Galena and Sphalerite Using $CuSO_4$ and NaCN* 375
Braden Copper Co., Chile 573
Brown, Albert, Pearson, Frederick C., and Ermert, Emil R.: *Power Facilities at a Modern Anthracite Open-Pit Mine* 578
Brusenback, R. A., Piros, R. J. and Dahlstrom, D. A.: *Theory, Scale-Up, and Operating Variables in the Peterson Top Feed Reservoir* 1236
Burt, R. B., Tillotson, I. S., and Barr, James A.: *Pipeline Transportation of Phosphate* 273
  discussion 1066
Butler, C. T., Ash, R. L., Boddorff, R. D., and Kay, W. W.: *Drilling and Blasting Methods in Anthracite Open-Pit Mines* 884

C

Cadwell, Donald E., Philippoff, W., and Cooke, S. R. B.: *Contact Angles and Surface Coverage* 283
Calorimeter, grinding 370
Calorimetric determinations of surface energy of minerals 369
Carbamate solutions, extraction of manganese 55
Carbonization, Disco low temperature process 287
Carbonization, Wisner process, departure from 290
Carne, J. L.: *Ore Control Methods at Inspiration Consolidated Copper Company* 685
Cement Industry of Mexico 960
Cement plants, Lone Star Cement Co. 1244
Cementing in Deep Diamond Drill Holes 1061
Central Pennsylvania Quarry Stripping & Construction Co.: *Drilling and Blasting Methods in Anthracite Open-Pit Mines* 884
Chain Belt Co.: *Control of Conveyor Belt Acceleration* 49
Chang, C. S. and Gaudin, A. M.: *Adsorption on Quartz, from an Aqueous Solution, of Barium and Laurate Ions* 193
Chemical Construction (Inter-American) Ltd.: *Economic Aspects of Sulphuric Acid Manufacture* 957
Chemicals from Coal Hydrogenation 381
Chile Exploration Co.: *Primary Blasting Practice at Chuquicamata* 300
Christopher Coal Co.: *Some Effects of Sewickley Seam Mining on Later Pittsburgh Seam Mining* 687
Chuquicamata, primary blasting practice 300
Cia. de Cemento Portland S.A.: *Cement Industry of Mexico* 960
Cia. de Real del Monte y Pachuca: *Surface Expression of Veins in the Pachuca Silver District of Mexico* 594
Cia. Minera Asarco, S.A.: *Deleading Zinc Concentrate at the Parral and Santa Barbara Mills* 495
Cia. Minera de Penoles, S.A.: *Geology of the Silver-Lead-Zinc Deposits of the Avalos-Providencia District of Mexico* 583
Clements, Porter and Gutzeit, Gregoire: *Flotation Rates and Flotation Efficiency*. Discussion 1074
Clendenin, J. D.: *Filter Cake Size-Consist and Moisture Relationships*. Discussion 1078
Coal: anthracite open-pit mines 884
  auger mining 677
  classifiers 896
  cleaning equipment, comparative effectiveness 895
  coarse, application of magnetite separators 983
  desliming 788, 1242
  dewatering of 1078, 1236
  fine, drainage behavior and water retention properties 886
  flotation 1074
  free swelling index 1081
  geology research, bibliography 202
  hydrogenation 381
  separation, Tromp heavy media process 967
  Sewickley and Pittsburgh seam mining 687
  thermal metamorphism 392
  wetting agents 893, 1060
Comminution: Kick theory 484
  Rittinger theory 484
  Third theory 484
  discussion 1071
Comparative Effectiveness of Coal Cleaning Equipment 895
  discussion 1080
Consolidation Coal Co. (Ky.): *Experiments with an Underground Auger* 677
Contact Angles and Surface Coverage 283
Control of Conveyor Belt Acceleration 49
Conveyor belts. See belts
Cooke, Strathmore R. B. and Ban, Thomas: *Microstructures in Iron Ore Pellets* 1053
Cooke, Strathmore R. B. and Stowasser, William F., Jr.: *Effect of Heat Treatment and Certain Additives on the Strength of Fired Magnetite Pellets* 1223
Cooke, S. R. B., Philippoff, W., and Cadwell, Donald E.: *Contact Angles and Surface Coverage* 283

Cooke, Strathmore R. B., Schulz, Norman F., and Lindroos, Emert: *Effects of Certain Starches on Quartz and Hematite Suspensions* 697
Copper-lead concentrate, flotation of 495, 1067
Copper-sulphide, ore control methods 685
Copper mining: drill performances 682
  methods at Braden Copper Co., Chile 573
Copper-nickel deposits 699
Corn Products Refining Co.: *Effect of Certain Starches on Quartz and Hematite Suspensions* 697
Crabtree, E. H.: *Discussion on the Effect of Zinc Deleading Operations on Lead-Zinc Selectivity at the Parral and Santa Barbara Mills* 1068
Crocker, Bunting S.: *Screened Ore Used for Fine Grinding at Lake Shore Mines* 499
  discussion 1069
Cross, Aureal T.: *Recent Coal Geology Research* 202
Crushers, Blake and single-toggle 1069
Cyclones, liquid-solid 788

D

Dahlstrom, D. A.: *High-Efficiency Desliming by Use of Hydraulic Water Additions to the Liquid-Solid Cyclone* 788
Dahlstrom, D. A., Piros, R. J., and Brusenback, R. A.: *Theory, Scale-Up, and Operating Variables of the Peterson Top Feed Reservoir* 1236
Dale, C. O. and Rundle, W. J.: *Illinois Operations of the Eagle Picher Mining and Smelting Co.* 72
Davidson, D. M. and Schwartz, G. M.: *Geologic Setting of the Copper-Nickel Prospect in the Duluth Gabbro* 699
Dean, Reginald S.: *Manganese Extraction by Carbamate Solutions and the Chemistry of New Manganese-Ammonia Complexes* 55
Decrepitometric method 703
Deep Hole Prospect Drilling at Miami, Tiger, and San Manuel Arizona 682
Deleading Zinc Concentrate at the Parral and Santa Barbara Mills 495
  discussion 1067
Desliming, liquid-solid cyclone 788
Determination of the Temperature and Pressure of Formation of Minerals by the Decrepitometric Method 703
DeVaney, Fred: *Magnetite Roasting of Lean Ores* 1219
Development of a Mining Operation from Diamond Drill Data 784
Development and Operation of Sulphur Deposits in the Louisiana Marshes 775
Diamond Orientation in Drill Bits 177
Dimension Stone in Minnesota 77
Disco process, low temperature carbonization 287
Discussion: Metal Mining and Industrial Minerals 1066
  Minerals Beneficiation 1067
  Coal 1075
  Geology 1083
Dithiophosphate, in flotation of galena and sphalerite 375
Djingheuzian, L. E.: *Discussion on Screened Ore Used for Fine Grinding at Lake Shore Mines* 1071
Donath, E. E.: *Chemicals from Coal Hydrogenation* 381
Drainage: acid mine 1075
  lead-zinc mining in Illinois 73
Drainage Behavior and Water Retention Properties of Fine Coal 886
Drilling: anthracite open-pit mine operations 884
  augers in coal mining 677
  bits, diamond orientation 177
  cementing in deep diamond drill holes 1061
  churn 75
  core sampling for oil shale 601
  deep hole prospecting 682
  development of a mining operation from diamond drill data 784
  floating equipment, sulphur mining 777
  mobile unit 799
  Swedish iron ore mines 188
  well 72
Drilling and Blasting Methods in Anthracite Open-Pit Mines 884

E

Eagle Picher Mining and Smelting Co.: *Illinois Operations of the Eagle Picher Mining and Smelting Co.* 72
Economic Aspects of Sulphuric Acid Manufacture 957
Edwards paddle scrubber 875
Edwards, R. C., Mitchell, Will, Jr., and Kirkland, T. G.: *Glass and Chemical Sand Manufacture in the Edwards Paddle Scrubber* 875
Effect of Certain Starches on Quartz and Hematite Suspensions 697
Effect of Heat Treatment and Certain Additives on the Strength of Fired Magnetite Pellets 1223
Effects of Alkalinity on the Flotation of Lead Minerals 1231
E. I. du Pont de Nemours & Co.: *Drilling and Blasting Methods in Anthracite Open-Pit Mines* 884
Electro-magnetic vibrators, dewatering of fine coal 1238
Elek, Luis: *Cement Industry of Mexico* 960
Erie Mining Co.: *Magnetic Roasting of Lean Ores* 1219
Ermert, Emil, Brown, Albert, and Pearson, Frederick C.: *Power Facilities at a Modern Anthracite Open-Pit Mine* 578
Ertl, Tell: *Prospecting the Piceance Creek Basin for Oil Shale* 601
Experiments with an Underground Auger 677

F

Factors in the Economics of Grinding Heat-Treated Taconites 962
Features Incorporated in the Design of Lone Star's Two New Dry Process Cement Plants 1244
Feierabend, R. H., Bartlett, Z. W., and Lee, C. O.: *Development and Operation of Sulphur Deposits in the Louisiana Marshes* 775
Filter Cake Size-Consist and Moisture Relationships 1078
Fleming, Marston G.: *Effects of Alkalinity on the Flotation of Lead Minerals* 1231
Flotation: adsorption of sodium ion on quartz 683
  adsorption on quartz, from an aqueous solution, of barium and laurate ions 193
  adsorption theory 199
  contact angles and surface coverage 283
  deleading zinc concentrate 495, 1067
  dynamic phenomena 386
  effect of certain starches on quartz and hematite suspensions 697
  frothability of pine oils 65
    author's supplement 1082
  galena and sphalerite by dithiophosphate 375
  lead minerals 1231
Flotation rate, a function of particle size 794
Flotation Rates and Flotation Efficiency. Discussion 1074
Fluorspar, optical, photoelectric sorting of 803
Formation of Acid Mine Drainage. Discussion 1075
Freeport Sulphur Co.: *Development and Operation of Sulphur Deposits in the Louisiana Marshes* 775
Frothability, pine oils in flotation 65, 1082
Frothing Characteristics of Pine Oils in Flotation 65
  author's supplement 1082

G

Gaudin, A. M. and Chang, C. S.: *Adsorption on Quartz, from an Aqueous Solution, of Barium and Laurate Ions* 193
Gaudin, A. M., Spedden, H. R., and Laxen, P. A.: *Adsorption of Sodium Ion on Quartz* 693
Geology and geophysics: coal research 202
  copper-nickel deposits, Duluth gabbro 699
  decrepitometric indicator 703
  dimension stone, Minnesota 77
  geothermometer, pyrite 880
  gravity investigations, Michigan 973
  iron ore deposits, Michigan 973
  lead, southeast Missouri 477
  lead-zinc mining, Illinois 72
  lead-zinc-silver deposits, Avalos-Providencia district, Mexico 583, 1083
  nickel-copper deposits, Duluth gabbro 699
  oil shale, Colorado 601
  silver deposits, Pachuca district, Mexico 594
  silver-lead-zinc deposits, Avalos-Providencia district, Mexico 583, 1083
  thermal metamorphism and ground water alteration of coking coal 391
  thermo-electric properties of pyrite 880
  zinc-lead mining, Illinois 72
  zinc-lead-silver deposits, Avalos-Providencia district, Mexico 583, 1083
Geology of the Hayden Creek Lead Mine, southeast Missouri 477
Geology of the Silver-Lead-Zinc Deposits of the Avalos-Providencia District of Mexico 583
  discussion 1083
Geologic Setting of the Copper-Nickel Prospect in the Duluth Gabbro Near Ely, Minnesota 699
Geophysical engineer, professional training of 969
Geothermometer, pyrite 880
Giesking, D. H.: *Jaw Crusher Capacities, Blake and Single Toggle or Overhead Eccentric Types.* Author's supplement 1069
Gillmore, D. W. and Wright, C. C.: *Drainage Behavior and Water Retention Properties of Fine Coal* 886
Glass and Chemical Sand Manufacture in the Edwards Paddle Scrubber 875
Graham-Snyder mine, Eagle Picher Mining and Smelting Co. 72
Gravity Investigations in the Iron River-Crystal Falls Mining District of Michigan 973
Griffen, John: *The Tromp Heavy Media Process* 967
Grinding, fine, screened ore used for 499, 1069
Gunther, G. C. and Boeke, C. L.: *Deleading Zinc Concentrate at the Parral and Santa Barbara Mills* 495
  discussion 1067
Gutzeit, Gregoire and Clements, Porter: *Flotation Rates and Flotation Efficiency.* Discussion 1074
gypsum, source of sulphuric acid 959

H

Hanson, V. D., Heinlein, W. K., and Vonfeld, J. M.: *Application of Coarse Coal Magnetite Separators in an Existing Circuit* 983
Hardinge, Harlowe: *Discussion on Screened Ore Used for Fine Grinding at Lake Shore Mines* 1070
Heinlein, W. K., Hanson, V. D., Vonfeld, J. M.: *Application of Coarse Coal Magnetite Separators in an Existing Circuit* 983
Hematite and quartz suspensions, effect of starches upon 697
Hercules Powder Co.: *Drilling and Blasting Methods in Anthracite Open-Pit Mines* 884
High-Efficiency Desliming by Use of Hydraulic Water Additions to the Liquid-Solid Cyclone 788
Hjortzberg-Nordlund, Borje: *Underground Mining Trends in the Great Swedish Export Iron Ore Mines* 187
Howe Sound Exploration Co.: *Development of a Mining Operation from Diamond Drill Data* 784
Howie, Howard: *Discussion on Pipeline Transportation of Phosphate* 1066
Hubbard, Judson S.: *Discussion on Comparative Effectiveness of Coal Cleaning Equipment* 1080
Hydraulic transportation system 279
Hydraulic water cyclone tests 792
Hy-Mac hydraulic drill unit 177

I

Illinois: Graham-Snyder lead-zinc mine 72
Illinois Operations of the Eagle Picher Mining and Smelting Co. 72
Imperial College of Science and Technology: *Effects of Alkalinity on the Flotation of Lead Minerals* 1231
Industrial minerals, Saskatchewan 396
Inspiration Consolidated Copper Co.: *Deep Hole Prospect Drilling at Miami, Tiger, and San Manuel, Arizona* 684
  Ore Control Methods at Inspiration Consolidated Copper Company 685
Iron ore: economics of heat-treated taconites 962
  gravity investigations, Iron River-Crystal Falls, Michigan 973
  magnetic roasting, pellets 1219
  microstructure in pellets 1053
  underground mining trends in Sweden 187

J

Jaw Crusher Capacities, Blake and Single-Toggle or Overhead Eccentric Types. Author's Supplement 1069
Johnson, Oscar: *Discussion on Screened Ore Used for Fine Grinding at Lake Shore Mines* 1070
Johnson, Vard H.: *Thermal Metamorphism and Ground Water Alteration of Coking Coal Near Paonia, Colorado* 391
Jones, William P.: *Economic Aspects of Sulphuric Acid Manufacture* 957
Judson, C. M., Lerew, A. A., Booth, R. B., Kennedy, J. S., and Simard, G. L.: *Radiotracer Studies of the Action of Dithiophosphate in the Selective Flotation of Galena and Sphalerite Using* $CuSO_4$ *and NaCN* 375

K

Kaiser Aluminum and Chemical Corp.: *Periclase Refractories in Rotary Kilns* 980
Kay, W. W., Ash, R. L., Butler, C. T., and Boddorff, R. D.: *Drilling and Blasting Methods in Anthracite Open-Pit Mines* 884
Kennecott Copper Corp.: *Mining Operations at the Teniente Mine of the Braden Copper Company, Rancagua, Chile* 573
  Mobile Drill Unit in Use at the Utah Copper Pit 799
Kennedy, J. S., Judson, C. M., Lerew, A. A., Booth, R. B., and Simard, G. L.: *Radiotracer Studies of the Action of Dithiophosphate in the Selective Flotation of Galena and Sphalerite Using* $CuSO_4$ *and NaCN* 375
Kilns, rotary, periclase refractories in 980
Kinsella, E. L. and White, F. S.: *Solids Fluidization Applied to Lime Burning* 903
Kirkland, T. G., Mitchell, Will, Jr., and Edwards, R. C.: *Glass and Chemical Sand Manufacture in the Edwards Paddle Scrubber* 875
Koppers Co.: *Chemicals from Coal Hydrogenation* 381

L

Lake Shore Mines, Ltd.: *Screened Ore Used for Fine Grinding at Lake Shore Mines* 499
Lange, L. H.: *Discussion on The Effect of Zinc Deleading Operations on Lead-Zinc Selectivity at the Parral and Santa Barbara Mills* 1068

Laxen, P. A., Gaudin, A. M., and Spedden, H. R.: *Adsorption of Sodium Ion on Quartz* 683
Lead: effects of alkalinity on flotation of 1231
  geology of Hayden Creek mine in southeast Missouri 477
  Illinois operations of the Eagle Picher Mining and Smelting Co. 72
  recovery from zinc concentrate 495, 1067
Lead-zinc-silver deposits 583, 1083
Lee, C. O., Bartlett, Z. W., and Feierabend, R. H.: *Development and Operation of Sulphur Deposits in the Louisiana Marshes* 775
Lerew, A. A., Judson, C. M., Booth, R. B., Kennedy, J. S., and Simard, G. L.: *Radiotracer Studies of the Action of Dithiophosphate in the Selective Flotation of Galena and Sphalerite Using $CuSO_4$ and NaCN* 375
Lesher, C. E.: *Development of the Disco Process of Low Temperature Carbonization* 287
Lime burning, solids fluidization 903
Lindroos, Emert W., Cooke, Strathmore, R. B., and Schulz, Norman F.: *Effect of Certain Starches on Quartz and Hematite Suspensions* 697
Lipsey, George C.: *Development of a Mining Operation from Diamond Drill Data* 784
Liquid-solid cyclones 788
Loading, Swedish iron ore mines 189
Lone Star Cement Co.: *Features Incorporated in the Design of Lone Star's Two New Dry Process Cement Plants* 1244
Longyear Rotobore hydraulic drill 178
Lyon, E. W.: *Formation of Acid Mine Drainage.* Discussion 1075
Lyons, Orville: *Comparative Effectiveness of Coal Cleaning Equipment* 895
  discussion 1080

M

Macelwane, James B.: *Professional Training of the Geophysical Engineer* 969
Magnetite pellets: effect of heat treatment on 1223
  microstructures in 1053
Magnetic Roasting of Lean Ores 1219
Manegold, R. L.: *Super High Intensity Magnetic Equipment for Protecting Conveyors* 61
Manganese-ammonia complexes, chemistry 55
Manganese Extraction by Carbamate Solutions and the Chemistry of New Manganese-Ammonia Complexes 55
Massachusetts Institute of Technology: *Adsorption of Sodium Ion on Quartz* 693
  Adsorption on Quartz, from an Aqueous Solution, of Barium and Laurate Ions 193
  Photoelectric Sorting of Optical Fluorspar 803
McNally Pittsburgh Manufacturing Corp.: *The Tromp Heavy Media Process* 967
Measurement and Evaluation of the Rate of Flotation as a Function of Particle Size 794
Mexico: cement industry 960
  geology of silver-lead-zinc deposits 583, 1083
  silver deposits, Pachuca district 594
Miami Copper Co.: *Deep Hole Prospect Drilling at Miami, Tiger, and San Manuel, Arizona* 682
Michigan College of Mining and Technology: *Gravity Investigations in the Iron River-Crystal Falls Mining District of Michigan* 973
Microstructures in Iron Ore Pellets 1053
Mills. See pebble mills
Mine sealing 1076
Mining methods: anthracite open-pit mines 884
  auger 677
  Braden Copper Co. 573
  development from diamond drill data 784
  mobile drill unit 799
  Swedish iron ore mines 187
Mining Operations at the Teniente Mine of the Braden Copper Company, Rancagua, Chile 573
Minnesota: copper-nickel deposits 699
  dimension stone 77
Minnesota Mines Experiment Station 1219
Minnesota taconite, roasting test 1221
Mississippi sulphur deposits, development 775
Missouri, southeast lead mines 477
Missouri School of Mines: *Measurement and Evaluation of the Rate of Flotation as a Function of Particle Size* 794
Miskell, Ford F., Mitchell, Will, Jr., and Sollenberger, C. L.: *Factors in the Economics of Heat-Treated Taconites* 962
Mitchell, Will, Jr., Kirkland, T. G., and Edwards, R. C.: *Glass and Chemical Sand Manufacture in the Edwards Paddle Scrubber* 875
Mitchell, Will, Jr., Miskell, Ford F., and Sollenberger, C. L.: *Factors in the Economics of Heat-Treated Taconites* 962
Mobile Drill in Use at the Utah Copper Pit 799
Morris, T. M.: *Measurement and Evaluation of the Rate of Flotation as a Function of Particle Size* 794
Mutch, A. D.: *Variation of Thermo-Electric Properties of Pyrite in Association with Gold Ore* 880
Myers, J.: *Discussion on Screened Ore Used for Fine Grinding at Lake Shore Mines* 1070

N

National Lead Co.: *Titanium Dioxide Analysis of MacIntyre Ore by Specific Gravity* 971
Newall, J. P. and Storey, R. W.: *Experiments with an Underground Auger* 677
New England Lime Co.: *Solids Fluidization Applied to Lime Burning* 903
Nickel-copper deposits 699
Northwestern University: *High-Efficiency Desliming by Use of Hydraulic Water Additions to the Liquid-Solid Cyclone* 788
  Theory, Scale-Up, and Operating Variables of the Peterson Top Feed Reservoir 1236

O

Ohio State University: *Prospecting the Piceance Creek for Oil Shale* 601
Ohle, Ernest L.: *Geology of the Hayden Creek Lead Mine, Southeast Missouri* 477
Oil shale, prospecting 601
Open-pit mining: drilling and blasting methods 884
  power facilities 578
Ore Control Methods at Inspiration Consolidated Copper Company 685

P

Pachuca silver district of Mexico 594
Paddle scrubber, Edwards 875
Pearson, Frederick C., Brown, Albert, and Ermert, Emil R.: *Power Facilities at a Modern Anthracite Open-Pit Mine* 578
Pebble mills: grinding 499, 1069
  operating screen analysis 1069
  soft ores 1070
Pennsylvania State College: *Drainage Behavior and Water Retention Properties of Fine Coal* 886
  Frothing Characteristics of Pine Oils in Flotation 65
Periclase Refractories in Rotary Kilns 980
Peterson Top Feed Reservoir 1236
Pett, L. F. and Snow, L. E.: *Mobile Drill Unit in Use at the Utah Copper Pit* 799
Pfleider, E. P.: *Diamond Orientation in Drill Bits* 177
Philippoff, W.: *Some Dynamic Phenomena in Flotation* 386
Philippoff, W., Cooke, S. R. B., and Caldwell, Donald E.: *Contact Angles and Surface Coverage* 283
Phosphate, pipeline transportation of 273
Photoelectric Sorting of Optical Fluorspar 803
Piceance Creek basin, oil shale 601
Pickands Mather & Co.: *Magnetic Roasting of Lean Ores* 1219
Pine oils in flotation 65, 1082
Pipeline Transportation of Phosphate 273, 1066
Piros, R. J., Brusenback, R. A., and Dahlstrom, D. A.: *Theory, Scale-Up, and Operating Variables of the Peterson Top Feed Reservoir* 1236
Pittsburgh Consolidation Coal Co.: *Application of Coarse Coal Magnetite Separators in an Existing Circuit* 983
  Development of the Disco Process of Low Temperature Carbonization 287
Porter, D. and Turrall, W. T.: *Photoelectric Sorting of Optical Fluorspar* 803
Power Facilities at a Modern Anthracite Open-Pit Mine 578
Preparation of Low-Ash Coal 1059
Primary Blasting Practice at Chuquicamata 300
Professional Training of the Geophysical Engineer 969
Prospecting the Piceance Creek Basin for Oil Shale 601
Pulleys, magnetic head, extraction of tramp ore from conveyor 61
Pumping, solids in water suspension 273
Pyrite: source of sulphur 957
  thermo-electric properties in association with gold ore 880

Q

Quartz and hematite suspensions, effect of starches upon 697

R

Radiotracer Studies of the Action of Dithiophosphate in the Selective Flotation of Galena and Sphalerite Using $CuSO_4$ and NaCN 375
Recent Coal Geology Research 202
Reed, E. F.: *Deep Hole Prospect Drilling at Miami, Tiger, and San Manuel, Arizona* 682
Refractories, periclase, in rotary kilns 980
Republic Steel Corp.: *Comparative Effectiveness of Coal Cleaning Equipment* 895
Richardson, A. C. and Wesner, Adam L.: *Preparation of Low-Ash Coal* 1059
Ross, Adrian: *Cementing in Deep Diamond Drill Holes* 1061
Rundle, W. J. and Dale, C. O.: *Illinois Operations of the Eagle Picher Mining and Smelting Co.* 72
Russell, R. J.: *Discussion on The Third Theory of Comminution* 1072

S

Safety: copper mining 576
Saint Louis University: *Professional Training of the Geophysical Engineer* 969
Sand cleaning 875
San Manuel Copper Corp.: *Deep Hole Prospect Drilling at Miami, Tiger, and San Manuel, Arizona* 682
Saskatchewan's Industrial Minerals 396
Schellinger, A. Kenneth: *Solid Surface Energy and Calorimetric Determinations of Surface-Energy Relationships for Some Common Minerals* 369
Schulz, Norman F., Cooke, Strathmore R. B., and Lindroos, Emert W.: *Effect of Certain Starches on Quartz and Hematite Suspensions* 697
Schwartz, G. M. and Davidson, D. M.: *Geologic Setting of the Copper-Nickel Prospect in the Duluth Gabbro Near Ely, Minnesota* 699
Schwartz, G. M. and Thiel, G. A.: *Dimension Stone in Minnesota* 77
Screened Ore Used for Fine Grinding at Lake Shore Mines 499
  discussion 1069
Selvig, W. A.: *Using Electric Furnaces and Heaters to Determine the Free Swelling Index of Coal.* Discussion 1081
Separation, coal washing 983
Separators, magnetic 63
Shaw, Milton C.: *Discussion on The Third Theory of Comminution* 1071
Shen-Penn Production Co.: *Power Facilities at a Modern Anthracite Open-Pit Mine* 578
Silver deposits, Mexico 594
Silver-lead-zinc deposits 583, 1083
Simard, G. L., Judson, C. M., Lerew, A. A., Booth, R. B., and Kennedy, J. S.: *Radiotracer Studies of the Action of Dithiophosphate in the Selective Flotation of Galena and Sphalerite Using $CuSO_4$ and NaCN* 375
Smith, F. Gordon: *Determination of the Temperature and Pressure of Formation of Minerals by the Decrepitometric Method* 703
Snavely, W. J.: *Control of Conveyor Belt Acceleration* 49
Snow, L. E. and Pett, L. F.: *Mobile Drill Unit at the Utah Copper Pit* 799
Solids Fluidization Applied to Lime Burning 903
Sollenberger, C. L., Miskell, Ford F., and Mitchell, Will, Jr.: *Factors in the Economics of Heat-Treated Taconites* 962
Some Dynamic Phenomena in Flotation 386
Some Effects of Sewickley Seam Mining on Later Pittsburgh Seam Mining 687
Spedden, H. R., Gaudin, A. M., and Laxen, P. A.: *Adsorption of Sodium Ion on Quartz* 693
Sprague and Henwood, Inc.: *Cementing in Deep Diamond Drill Holes* 1061
St. Joseph Lead Co.: *Geology of the Hayden Creek Lead Mine, Southeast Missouri* 477
Stanley, Alan: *Titanium Dioxide Analysis of MacIntyre Ore by Specific Gravity* 971
Starches, effect on quartz and hematite suspensions 697
Storey, R. W. and Newell, J. P.: *Experiments with an Underground Auger* 677
Stowasser, William F. and Cooke, Strathmore R. B.: *Effect of Heat Treatment and Certain Additives on the Strength of Fired Magnetite Pellets* 1223
sulphur deposits, Louisiana marshes 775
Sulphur, transportation, liquid sulphur barges 781
Sulphuric acid: economic aspects of manufacture 957
  recovery of spent acids 959
Sun, Shiou-Chuan: *Frothing Characteristics of Pine Oils in Flotation* 65
  author's supplement 1082
Super High Intensity Magnetic Equipment for Protecting Conveyors 61
Surface Expression of Veins in the Pachuca Silver District of Mexico 594
Sweden, underground mining trends in iron ore mines 187
Symonds, I. M.: *Discussion on The Effect of Zinc Deleading Operations at the Parral and Santa Barbara Mills* 1067

T

Taconites, heat-treated, economics of 962
Tandem magnetic roasting system for iron ores 1220
Teniente mine, Braden Copper Co., Chile 573
Theory, Scale-Up, and Operating Variables of the Peterson Top Feed Reservoir 1236
Thermal Metamorphism and Ground Water Alteration of Coking Coal Near Paonia 391

- Thiel, G. A. and Schwartz, G. M.: *Dimension Stone in Minnesota* 77
- *Third Theory of Comminution*. Discussion 1071
- Thornburg, C. L.: *Surface Expression of Veins in the Pachuca Silver District of Mexico* 594
- Tillotson, I. S., Burt, R. B., and Barr, James A.: *Pipeline Transportation of Phosphate* 273
  - discussion 1066
- *Titanium Dioxide Analysis of MacIntyre Ore by Specific Gravity* 971
- Triplett, W. H.: *Geology of the Silver-Lead-Zinc Deposits of the Avalos-Providencia District of Mexico* 583, 1083
- *Tromp Heavy Media Process* 967
- Truax-Traer Coal Co.: *High-Efficiency Desliming by Use of Hydraulic Water Additions to the Liquid-Solid Cyclone* 788
  - *Theory, Scale-Up, and Operating Variables of the Peterson Top Feed Reservoir* 1236
- Tube mills, comparative efficiency 499
- Tungsten carbide balls, tests in grinding 500
- Turrall, W. T. and Porter, D.: *Photoelectric Sorting of Optical Fluorspar* 803
- Turton, F. E.: *Mining Operations at the Teniente Mine of the Braden Copper Company, Rancagua, Chile* 573

U

- *Underground Mining Trends in the Great Swedish Export Iron Ore Mines* 187
- University of Minnesota: *Contact Angles and Surface Coverage* 283
  - *Diamond Orientation in Drill Bits* 177
  - *Effect of Certain Starches on Quartz and Hematite Suspensions* 697
  - *Microstructures in Iron Ore Pellets* 1053
  - *Some Dynamic Phenomena in Flotation* 386
- University of Toronto: *Determination of the Temperature and Pressure of Formation of Minerals by the Decrepitometric Method* 703
  - *Variation of Thermo-Electric Properties of Pyrite in Association with Gold Ore* 880
- *Using Electric Furnaces and Heaters to Determine the Free Swelling Index of Coal*. Discussion 1081
- U. S. Geological Survey: *Thermal Metamorphism and Ground Water Alteration of Coking Coal Near Paonia, Colorado* 381

V

- Van Zandt, Claiborne: *Features Incorporated in the Design of Lone Star's Two New Dry Process Cement Plants* 1244
- *Variation of Thermo-Electric Properties of Pyrite in Association with Gold Ore* 880
- Vibrators, electro-magnetic, dewatering of fine coal 1238
- Vonfeld, J. M., Hanson, V. D., and Heinlein, J. M.: *Application of Coarse Coal Magnetite Separators in an Existing Circuit* 983

W

- Walker, Donald R.: *Discussion on The Third Theory of Comminution* 1071
- Walker, G. B.: *Discussion on Comparative Efficiency of Coal Cleaning Equipment* 1080
- Wesner, Adam L. and Richardson, A. C.: *Preparation of Low-Ash Coal* 1059
- West Virginia Geological Survey: *Recent Coal Geology Research* 202
- Weiss, Norman: *Discussion on The Effect of Zinc Deleading Operations on Lead-Zinc Selectivity at the Parral and Santa Barbara Mills* 1068
  - *Discussion on Screened Ore Used for Fine Grinding at Lake Shore Mines* 1070
- White, F. S. and Kinsella, E. L.: *Solids Fluidization Applied to Lime Burning* 903
- Wildman, H. S.: *Discussion on the Effect of Zinc Deleading Operations on Zinc-Lead Selectivity at the Parral and Santa Barbara Mills* 1068
- Williams, A. J.: *Saskatchewan's Industrial Minerals* 396
- Wisner process of carbonization, departure from 290
- Wright, C. C. and Gillmore, D. W.: *Drainage Behavior and Water Retention Propetries of Fine Coal* 886
- Wyble, D. O. and Bacon, L. O.: *Gravity Investigations in the Iron River-Crystal Falls Mining District of Michigan* 973
- Wyman, Glenn S.: *Primary Blasting Practice at Chuquicamata* 300

Z

- Zachar, F. R.: *Some Effects of Sewickley Seam Mining on Later Pittsburgh Seam Mining* 687
- Zeuch, C. F.: *Discussion on The Effect of Zinc Deleading on Lead-Zinc Selectivity at the Parral and Santa Barbara Mills* 1068
- Zinc: deleading concentrate of 495, 1067
  - Illinois operations of the Eagle Picher Mining and Smelting Co. 72
- Zinc-silver-lead deposits 583, 1083